



European Commission

Euratom

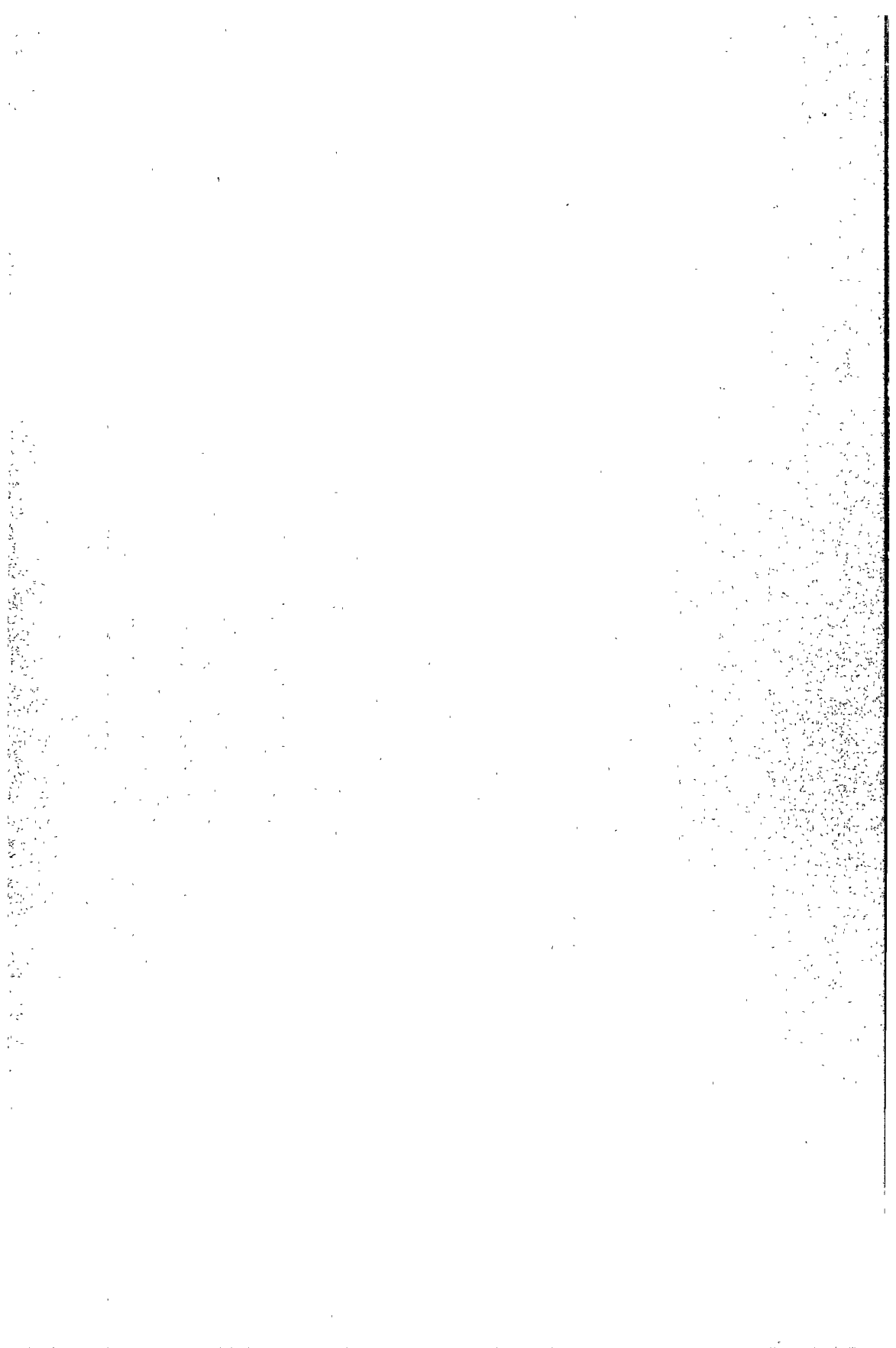
RADIATION PROTECTION

PROGRAMME

1990-91

Final report

Volume 1



**Comisión Europea
Europa-Kommissionen
Europäische Kommission
Ευρωπαϊκή Επιτροπή
European Commission
Commission européenne
Commissione europea
Europese Commissie
Comissão Europeia**

Euratom

Relación de actividades
Programa
PROTECCIÓN RADIOLÓGICA

Beretning
Program
STRÅLINGSBESKYTTELSE

Tätigkeitsbericht
Programm
STRAHLENSCHUTZ

Έκθεση πεπραγμένων
Πρόγραμμα
ΠΡΟΣΤΑΣΙΑ ΑΠΟ ΑΚΤΙΝΟΒΟΛΙΕΣ

Progress report
RADIATION PROTECTION
Programme

Rapport d'activité
Programme
«RADIOPROTECTION»

Rapporto d'attività
Programma
RADIOPROTEZIONE

Verslag van de werkzaamheden
Programma
STRALINGSBESCHERMING

Relatório de actividades
Programa
RADIOPROTECÇÃO

1990-91
Volume 1

**Published by the
EUROPEAN COMMISSION
Directorate-General XIII
Telecommunications, Information Market and Exploitation of Research
L-2920 Luxembourg**

HINWEIS

Weder die Europäische Kommission noch Personen, die im Namen dieser Kommission handeln, sind für die etwaige Verwendung der nachstehenden Informationen verantwortlich.

LEGAL NOTICE

Neither the European Commission nor any person acting on behalf of the Commission is responsible for the use which might be made of the following information

AVERTISSEMENT

Ni la Commission européenne ni aucune personne agissant au nom de la Commission n'est responsable de l'usage qui pourrait être fait des informations ci-après.

Bibliographische Daten befinden sich am Ende der Veröffentlichung.
Cataloguing data can be found at the end of this publication.
Une fiche bibliographique figure à la fin de l'ouvrage.

Luxembourg: Office for Official Publications of the European Communities, 1994

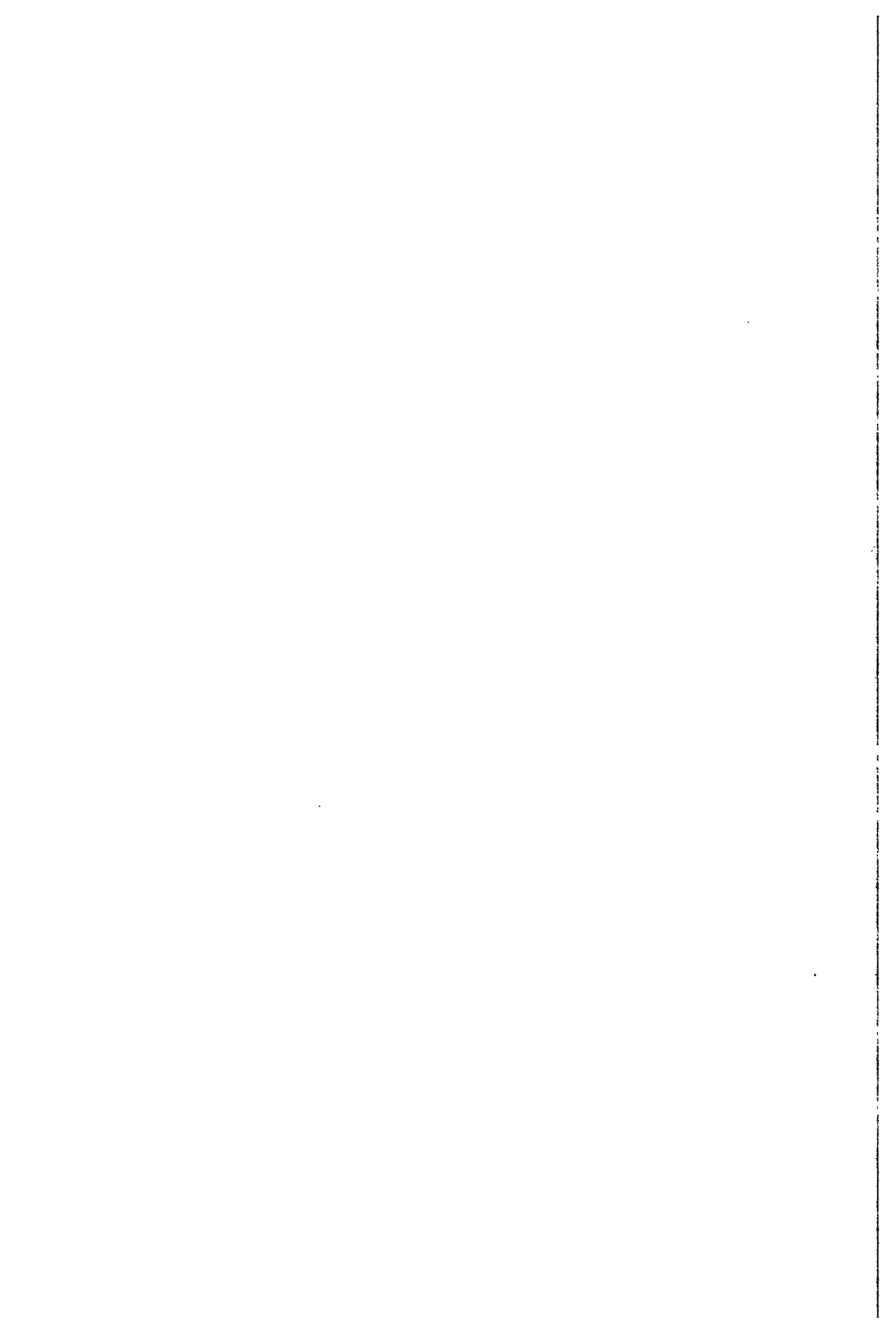
ISBN 92-826-8683-3 (Volume 1)

ISBN 92-826-8682-5 (Volumes 1 and 2)

© ECSC-EC-EAEC, Brussels • Luxembourg, 1994

Printed in Belgium

INTRODUCTION



Diese zwei Bände sind ein umfassender Bericht über den wissenschaftlichen Fortschritt während des siebten mehrjährigen Forschungs- und Ausbildungsprogramms auf dem Gebiet des Strahlenschutzes, das die Kommission der Europäischen Gemeinschaften (KEG) 1990 und 1991 im Rahmen des Euratom-Vertrags durchgeführt hat.

Dieses Programm ist für die europäische Strahlenschutzforschung nach wie vor wichtig, da es die Zusammenarbeit zwischen nationalen Forschungseinrichtungen und somit die optimale Nutzung der begrenzten materiellen und personellen Möglichkeiten fördert. Das Programm 1990-1991 kündigte die Einführung multinationaler Mehrpartnerverträge mit Instituten verschiedener Mitgliedstaaten an, die in koordinierter Weise zusammenarbeiten und auf der Grundlage eines Vertrags eine konkrete Forschungsaufgabe erledigen. Aus dem Programm wurden 116 multinationale Mehrpartnervorschläge mit 306 Einzelprojekten finanziert, wofür 21,1 Millionen ECU zur Verfügung standen. Aufgrund der Beteiligung Schwedens an diesem Programm arbeiteten schwedische Wissenschaftler an mehreren multinationalen Projekten mit. Diese multinationalen Mehrpartnerverträge sind äußerst erfolgreich, stärken die Zusammenarbeit, festigen das Vertrauen zwischen den Partnern, fördern den informellen Gedanken- und Datenaustausch und verleihen der Forschung neuen Schwung. Die Verträge haben den zusätzlichen Vorteil, daß sie die Struktur des Forschungsprogramms sichtbarer und für die Programm-Manager überschaubarer machen.

Das Programm 1990-1991 war in drei Hauptteile gegliedert:

- Strahlen- und Radioaktivitätsexposition des Menschen:
Messungen der Strahlendosis und ihre Interpretation
Transfer und Verhalten von Radionukliden in der Umwelt
- Folgen der Strahlenexposition des Menschen; ihre Abschätzung, Verhütung und Behandlung:
Stochastische Wirkungen von Strahlen
Nichtstochastische Wirkungen von Strahlen
Strahlenwirkungen auf den sich entwickelnden Organismus
- Risiken der Strahlenexposition und ihre Bewältigung:
Abschätzung der Strahlenexposition des Menschen und ihrer Risiken
Optimierung und Durchführung des Strahlenschutzes

Die Schlußberichte sind nach diesen Teilen gegliedert. Die Berichte selbst unterscheiden sich von früheren Schlußberichten, da sie über jeden multinationalen Mehrpartnervertrag einen eigenen Bericht enthalten und einen Überblick über die geleistete Arbeit mit den Ergebnissen jedes einzelnen Gruppenmitglieds bieten. Dies soll das Verhältnis zwischen den einzelnen Vertragspartnern klären und einen Hinweis auf die Zusammenhänge zwischen den einzelnen Verträgen jedes Programmteils liefern. Weil die Berichte jedes Abschnitts in numerischer Folge geordnet sind, ist die Gesamtstruktur jedes Teils nicht immer eindeutig, aber durchaus erkennbar.

Der Beginn der Verträge hat sich 1990 leider um einige Monate verzögert, weshalb es nicht möglich war, die Zwischenberichte wie bisher zum Jahresende zusammenzustellen. Stattdessen wurden alle Verträge abgewickelt und die Berichte Ende September 1992 zusammengestellt. Auch wenn Verträge aus dem Programm 1985-1989 in einigen Fällen als Einzelverträge verlängert wurden, sind die entsprechenden Berichte doch in diesen Schlußbericht aufgenommen worden.

Die bisherige Programmpolitik wurde fortgesetzt, den Informationsaustausch und die Zusammenarbeit zwischen Wissenschaftlern durch die Veranstaltung von 86 Arbeitsgruppensitzungen mit Vertragspartnern und geladenen Sachverständigen und von 22 internationalen Seminaren und Workshops zu fördern. Die 10 Protokolle dieser Sitzungen und die Veröffentlichungen aufgrund dieser Vertragsarbeiten sind der Beweis dafür, welch große Bedeutung der europäischen Forschung auf dem Gebiet des Strahlenschutzes zukommt.

Die Kommission hat im Rahmen dieses Programms weiterhin die Vereinbarungen mit den USA und Kanada durchgeführt und die Kontakte mit internationalen Organisationen und anderen Drittländern gepflegt. Ein Briefwechsel zwischen der KEG und der Stiftung für Strahlenforschung (RERF) in Hiroshima hat die Möglichkeit zu einer umfassenderen Zusammenarbeit mit japanischen Kollegen eröffnet.

Ein neuer Schwerpunkt der Programmarbeit ist die Entwicklung einer koordinierten Bildungspolitik im Rahmen der europäischen allgemeinen und beruflichen Bildung auf dem Gebiet des Strahlenschutzes (ERPET), um ein breites Spektrum von Fachwissen zu erhalten und den beruflichen Aufstieg von Nachwuchswissenschaftlern auf dem Gebiet des Strahlenschutzes zu fördern. In den letzten 24 Monaten sind 15 Ausbildungslehrgänge über allgemeinen Strahlenschutz und über Spezialgebiete wie Dosimetrie, molekularbiologische Verfahren, Radioökologie und Beherrschung von nuklearen Notfällen veranstaltet worden.

Herbert Allgeier
Direktor GD XII.F
Energie

Sergio Finzi
Hauptberater GD XI.A
Umwelt, Nukleare Sicherheit
und Katastrophenschutz

Jaak Sinnaeve
Referatsleiter GD XII.F.6
Forschungsaktion Strahlenschutz

These 2 volumes present a comprehensive account of the scientific progress achieved during the seventh multi-annual research and training programme on Radiation Protection which was carried out in the period from 1990 to 1991 under the Euratom Treaty of the Commission of the European Communities (CEC).

The programme continues to play an important role in European radiation protection research by stimulating the collaboration between the different national research organisations to optimize the use of the limited institutional and manpower resources. The 1990-1991 programme heralded the introduction of multi-national, multi-partner contracts with several institutes from different Member States working together in a coordinated fashion to investigate a specific problem in each contract. The programme funded 116 multi-national, multi-partner proposals involving 306 individual projects from a budget of 21.1 MEcu. Sweden was associated with the programme and Swedish scientists have been integrated in several of the multi-national proposals. These multi-national, multi-partner contracts have been most successful, have strengthened cooperation, developed confidence between the partners, stimulated informal exchange of ideas and data, and increased the momentum of the research. The contracts have also had the added advantage of making the structure of the research programme more visible and transparent for the programme managers.

The 1990-1991 programme was reorganised into three main sections, namely:

- Human Exposure to Radiation and Radioactivity, which includes
Measurement of Radiation Dose and its Interpretation
Transfer and Behaviour of Radionuclides in the Environment
- Consequences of Radiation Exposure to Man; Assessment, Prevention and Treatment, which includes
Stochastic Effects of Radiation
Non-Stochastic Effects of Radiation
Radiation Effects on the Developing Organism
- Risks and Management of Exposure, which includes
Assessment of Human Exposure and Risks
Optimization and Management of Radiation Protection

The Final Reports have been grouped into these sections but the reports differ from previous Final Reports as each multi-national multi-partner contract presents a single report giving an overview of the work carried out followed by the individual results from each member of the group. This should clarify the inter-relationship of the different partners in a contract and provide some indication of the association between the different contracts in each section of the programme. However, because the reports in each section are presented in numerical order the total structure of each sector is not totally clear although it can certainly be discerned.

La mise à exécution des contrats a malheureusement été retardée de quelques mois en 1990, de sorte qu'il n'a pas été possible de réunir les rapports d'activité à la fin de l'année, comme cela avait été le cas auparavant. On a attendu que tous les contrats aient été menés à leur terme pour rassembler les rapports à la fin du mois de septembre 1992. Quelques contrats remontant au programme 1985-1989 ont été prorogés à titre individuel, mais, dans la mesure du possible, les rapports afférents à ces contrats ont été regroupés conformément à la nouvelle structure.

Dans le cadre de ce programme, on a continué à suivre une politique de promotion des échanges d'informations et de coopération entre les scientifiques en organisant 86 réunions de groupes d'étude auxquelles ont participé des contractants et des experts et 22 séminaires et ateliers internationaux. Les 10 comptes rendus de ces réunions et les publications issues des travaux prévus dans les contrats témoignent de l'importance du rôle joué par la recherche européenne dans le domaine de la radioprotection.

De même, on a poursuivi la mise en oeuvre des déclarations d'intention signées avec les Etats-Unis et le Canada et maintenu les contacts avec les organisations internationales et d'autres pays non communautaires. Un échange de correspondance entre la CCE et la Fondation pour la recherche sur les effets des rayonnements (RERF) d'Hiroshima a ouvert la voie à une collaboration plus intense avec les Japonais.

Un nouvel aspect important des activités liées au programme a été le développement d'une politique de formation coordonnée dans le cadre d'ERPET (European Radiation Protection Education and Training), pour maintenir un éventail de compétences et promouvoir les perspectives de carrière des jeunes scientifiques qui se destinent à la recherche en radioprotection. 15 cours de formation couvrant la radioprotection en général et des domaines plus spécialisés, tels que la dosimétrie, les méthodes de la biologie moléculaire, la radioécologie et la gestion des situations d'urgence créées par un accident nucléaire, ont été organisés pendant les 24 derniers mois.

Herbert Allgeier
Directeur de la DG XII.F
Energies

Jaak Sinnaeve
Chef de l'unité DG XII.F.6
Activité de recherche sur la radioprotection

Sergio Finzi
Conseiller de la DG XI.A
Environnement, Sécurité nucléaire
et protection civile

Ces deux volumes contiennent un exposé complet des progrès scientifiques réalisés dans le cadre du septième programme pluriannuel de recherche et de formation en radioprotection exécuté en 1990 et 1991 en vertu du traité Euratom de la Commission des Communautés européennes (CCE).

Le programme continue de jouer un rôle prépondérant dans la recherche européenne en radioprotection en stimulant la collaboration entre les organismes nationaux de recherche, afin d'optimiser l'utilisation de ressources institutionnelles et humaines limitées. Le programme 1990-1991 a inauguré les contrats multinationaux à partenaires multiples, c'est-à-dire comportant la participation de plusieurs instituts de différents Etats membres qui, dans le cadre de chaque contrat, étudient conjointement et de façon coordonnée un problème particulier. Le budget du programme (21,1 millions d'écus) a permis de financer 116 propositions multinationales à partenaires multiples couvrant 306 projets individuels. La Suède s'est associée au programme et les scientifiques suédois ont participé à la réalisation de plusieurs propositions multinationales. La plupart de ces contrats multinationaux à partenaires multiples ont été couronnés de succès, ils ont renforcé la coopération, développé la confiance entre les partenaires, stimulé les échanges informels d'idées et d'informations, et accéléré le rythme de la recherche. Un autre avantage de ces contrats a été de rendre la structure du programme de recherche plus apparente et plus transparente pour ses gestionnaires.

A cet effet, le programme 1990-1991 a été divisé en trois grandes sections :

- Exposition de l'homme aux rayonnements et à la radioactivité
 - Mesure des doses de rayonnement et interprétation des résultats
 - Transfert et comportement des radionuclides dans l'environnement
- Conséquences pour l'homme de l'exposition aux rayonnements; évaluation, prévention et traitement
 - Effets stochastiques des rayonnements
 - Effets non stochastiques des rayonnements
 - Effets des rayonnements sur les organismes en cours de développement
- Risques et gestion de l'exposition
 - Evaluation de l'exposition de l'homme et des risques
 - Optimisation et gestion de la radioprotection

Les rapports finals suivent cette structure. Ils diffèrent des rapports finals précédents, en ce que, pour chaque contrat multinational à partenaires multiples, un rapport unique présente une vue d'ensemble des travaux effectués, suivie des conclusions individuelles de chaque membre du groupe. Cette présentation devrait faire apparaître les liens existant entre les différents partenaires dans le cadre d'un contrat, et fournir des indications sur le lien entre les différents contrats relevant de chaque section du programme. Néanmoins, comme les rapports correspondant à chaque section sont présentés par ordre numérique, la structure globale de chaque secteur n'est pas absolument évidente, bien qu'on puisse certainement la discerner.

The start of the contracts was unfortunately delayed for some months in 1990 and it has therefore not been possible to collect the progress reports at the end of the year as has been the practice previously, instead all the contracts have been allowed to finish and the reports have been collected at the end of September 1992. In some cases contracts from the 1985-1989 programme were extended as individual contracts but where possible the reports from these contacts have been grouped for presentation here.

The programme has continued its policy of promoting the exchange of information and cooperation between scientists by organising 86 study group meetings with contractors and invited experts and 22 international seminars and workshops. The 10 proceedings of these meetings and the publications originating from the contract work testify to the important role played by European research in the field of radiation protection.

The programme has continued to implement the Memoranda of Understanding with the USA and Canada, and has continued its contacts with international organisations and other countries outside the Community. An exchange of letters between the CEC and the Radiation Effects Research Foundation (RERF) at Hiroshima has opened the possibility for more extensive collaboration with Japanese colleagues.

One important new facet of the programme's activities has been the development of a coordinated training policy under ERPET (European Radiation Protection Education and Training) to maintain a cross-section of expertise and promote the career prospects of young scientists entering the field of radiation protection. 15 training courses have been organised during the past 24 months covering general radiation protection as well as more specialised areas such as dosimetry, molecular biological methods, radioecology and nuclear emergency management.

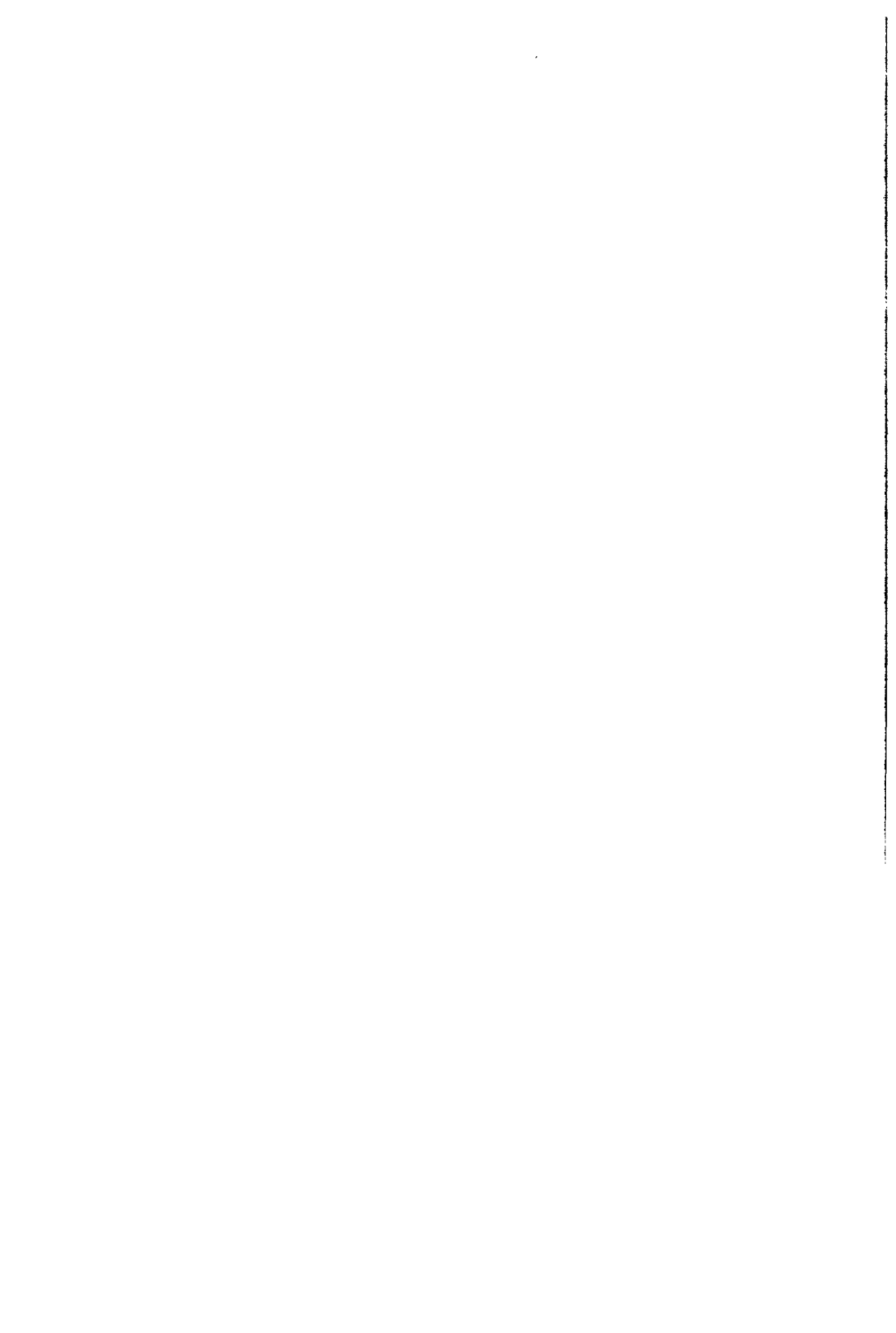
Herbert Allgeier
Director DG XII.F
Energy

Sergio Finzi
Chief Adviser DG XI.A
Environment, Nuclear Safety
and Civil Protection

J.Sinnaeve
Head of Unit DG XII.F.6
Radiation Protection Research Action

MEMBERS AND EXPERTS 1991-92

**Management and coordination advisory
committee "Radiation Protection"**



Mitglieder und Experten 1991-92
Beratender Verwaltungs- und Koordinierungsausschuss "STRAHLENSCHUTZ"

Members and Experts 1991-92
Management and Coordination Advisory Committee "RADIATION PROTECTION"

Membres et Experts 1991-92
Comité consultatif en matière de Gestion et de Coordination "RADIOPROTECTION"

Belgique - België

S. Hallez °
N. Henry °
R. Kirchmann
O. Vanderborght

Bundesrepublik Deutschland

W. Gössner °
A.M. Kellerer
H.H. Landfermann °

Danmark

A. Aarkrog °
H.L. Gjørup °
K.A. Jessen
N.O. Kjeldgaard °

Elliniki Dimokratia

S. Danali-Cotsaki °
D. Glaros °
A. Kappas
D. Maintas °
E.G. Sideris °

España

L. Arranz Carrillo °
J.L. Butragueño Casado
E. Iranzo
F. Mingot Buades °
G. López Ortiz

France

D. Blanc
C. Feltin
H. Jammet
B. Jampsin
J. Lafuma °
H. Métivier

Ireland

T. Colgan
J.D. Cunningham ° (Chairman 1989-)
C.P. O'Toole °

Italia

A. Cigna °
V. Covelli
F. Di Mauro
F. Morselli °

Luxembourg

P. Kayser °

Nederland

B. Bosnjakovic °
M.J. Frissel °
H.R. Leenhouts
P.H.M. Lohman
A.T. Natarajan
D.W. Van Bekkum

Portugal

M. Brites Santos Patricio °
E. Mendes Magalhaes †
J. Pistacchini Galvão °

United Kingdom

G.E. Adams
J.A. Dennis °
A. Eggleton
D.T. Goodhead
J.W. Stather °
H. Walker °

Commission

H. Eriskat
G. Gerber
J.M. Mousny secretariat
H. Schibilla

° Member of CGC

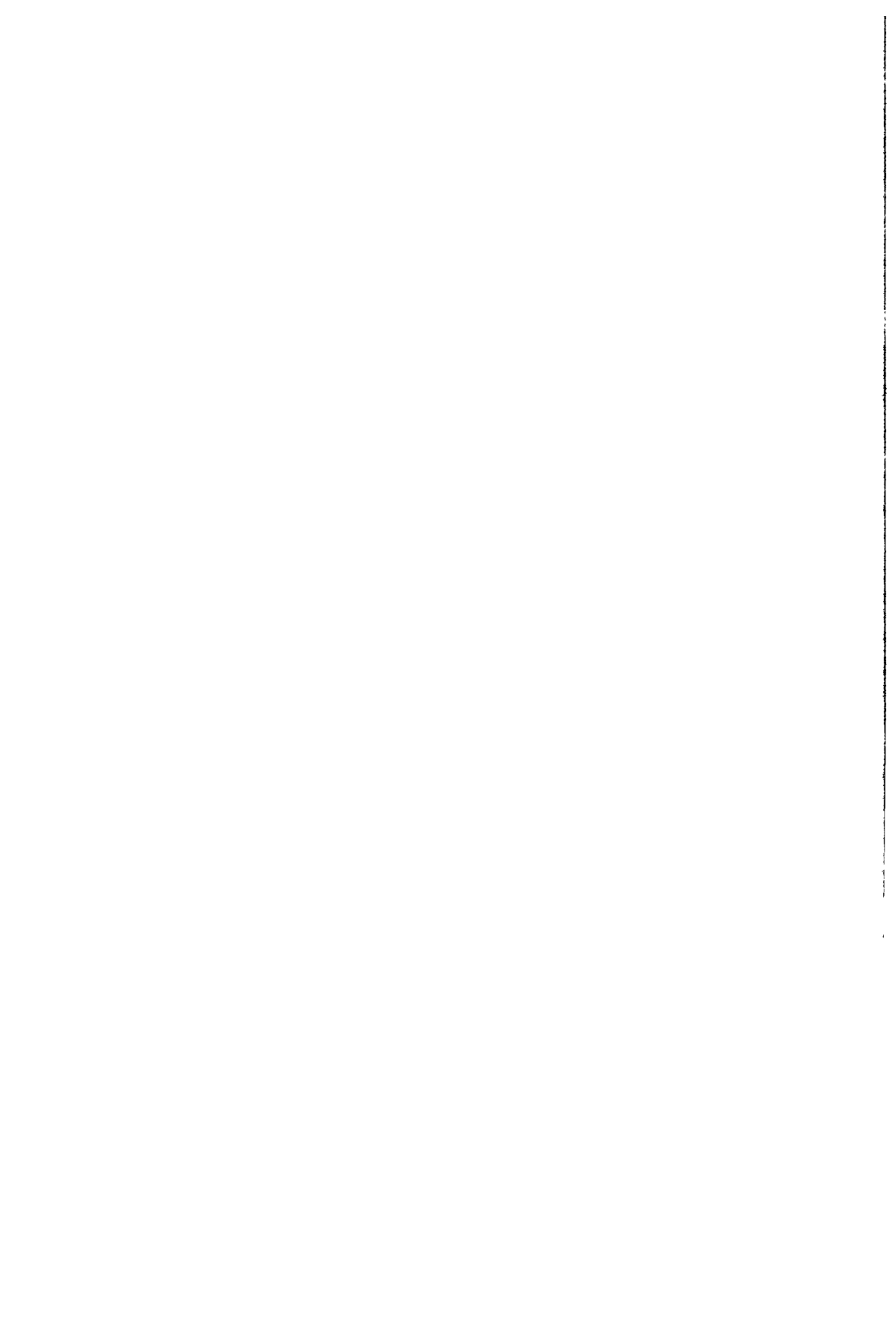


TABLE OF CONTENTS



TABLE OF CONTENTS

EINLEITUNG, INTRODUCTION, INTRODUCTION	III
Vorwort	V
Préface	VII
Preface	IX
MEMBERS AND EXPERTS 1991-92: Management and coordination advisory committee "radiation protection"	XI
TABLE OF CONTENTS	XV
RESEARCH IN RADIATION PROTECTION - VOLUME I	1
Summary	3
Contents of volume I	5
PART I - HUMAN EXPOSURE TO RADIATION AND RADIOACTIVITY	29
Measurement of radiation dose and its interpretation	31
COLLABORATION ON RESEARCH AND DEVELOPMENT CONCERNED WITH THE METHODOLOGY AND DATA IN RADIATION DOSIMETRY	33
Contract Bi6-026 - Sector A11	
1) <i>Dietze</i> , EURADOS	
QUANTITIES, UNITS AND MEASUREMENT TECHNIQUES FOR IONIZING RADIATION ..	61
Contract Bi6-322 - Sector A11	
1) <i>Allisy</i> , Bureau Intern.des Poids et Mesures	
THE IMPLEMENTATION OF THE OPERATIONAL DOSE QUANTITIES INTO RADIATION PROTECTION DOSIMETRY (NRPB ASSOCIATION)	67
Contract Bi6-347a - Sector A11	
1) <i>Clark</i> , NRPB - 2) <i>Marshall</i> , AEA Technology Harwell Laboratory	
3) <i>Lembo</i> , ENEA - 4) <i>Chartier</i> , CEA-FAR	
STUDY AND DEVELOPMENT OF AN INDIVIDUAL ELECTRONIC NEUTRON DOSIMETER	87
Contract Bi7-020 - Sector A12	
1) <i>Vareille-Decossas</i> , Univ. Limoges - 2) <i>Tommasino</i> , ENEA	
3) <i>Zamani-Valasiadou</i> - Univ. Thessaloniki - 4) <i>Barthe</i> , CEA-FAR	
5) <i>Fernades Moreno</i> , Universidad Autonoma de Barcelona	
USE OF THE VARIANCE-COVARIANCE METHOD IN RADIATION PROTECTION	107
Contract Bi7-025 - Sector A12	
1) <i>Kellerer.</i> , Univ. München - 2) <i>Jessen</i> , Univ. Aarhus Hospital	
3) <i>Lindborg</i> , Nat. Inst. of Rad. Protection	

THE MEASUREMENT OF ENVIRONMENTAL GAMMA DOSES	121
Contract Bi7-027 - Sector A12	
1) <i>Bøtter-Jensen</i> , Risø National Laboratory - 2) <i>Lauterbach</i> , PTB	
3) <i>Delgado Martínez</i> , CIEMAT	
DOSIMETRY OF BETA AND LOW-ENERGY PHOTON RADIATION USING EXTRAPOLATION CHAMBERS AND THIN SOLID STATE DOSIMETERS	145
Contract Bi7-028 - Sector A12	
1) <i>Christensen</i> , Risø National Laboratory - 2) <i>Chartier</i> , CEA-FAR - 3) <i>Herbaut</i> , CEA-Grenoble	
4) <i>Francis</i> , NRPB - 5) <i>Gasiot</i> , Univ. Sciences Technologiques du Languedoc	
6) <i>Scharmann</i> , Justus-Liebig-Universität	
THE USE OF MICRODOSIMETRIC METHODS FOR THE DETERMINATION OF DOSE EQUIVALENT QUANTITIES AND OF BASIC DATA FOR DOSIMETRY	183
Contract Bi7-030 - Sector A12	
1) <i>Grillmaier</i> , Univ. Saarlandes - 2) <i>Brede</i> , PTB - 3) <i>Zoetelief</i> , TNO-ITRI	
4) <i>Schmitz</i> , KFA Jülich GmbH - 5) <i>Ségur</i> , ADPA	
DETERMINATION AND REALISATION OF CALIBRATION FIELDS FOR NEUTRON PROTECTION DOSIMETRY AS DERIVED FROM SPECTRA ENCOUNTERED IN ROUTINE SURVEILLANCE	207
Contract Bi7-031 - Sector A12	
1) <i>Klein</i> , PTB-Braunschweig - 2) <i>Thomas</i> , NPL-Teddington	
3) <i>Chartier</i> , CEA-Fontenay-aux-Roses - 4) <i>Schraube</i> , GSF-Neuherberg	
CALCULATION AND MEASUREMENT OF DOSES FROM PARTICULATE RADIOACTIVE SOURCE	231
Contract Bi7-021 - Sector A13	
1) <i>Charles</i> , Nuclear Electric - 2) <i>Herbaut</i> , CEA-Grenoble - 3) <i>Patau</i> , Univ. Toulouse III	
INHALATION AND INGESTION OF RADIONUCLIDES (NRPB ASSOCIATION)	243
Contract Bi6-347b - Sector A14	
1) <i>Bailey</i> , NRPB 2) <i>Kendall</i> , NRPB - 3) <i>Stahlhofen</i> , GSF Frankfurt	
4) <i>Roy</i> , CEA-FAR - 5) <i>Patrick</i> , MRC Radiobiological Unit	
6) <i>Kaul</i> , Bundesamt für Strahlenschutz - 7) <i>Taylor</i> , KfK Karlsruhe	
ASSESSMENT OF INTERNAL DOSE FROM RADIONUCLIDES USING STABLE ISOTOPE TRACER TECHNIQUES IN MAN	273
Contract Bi7-029 - Sector A14	
1) <i>Roth</i> , GSF Frankfurt - 2) <i>Molho</i> , Università degli Studi di Milano	
3) <i>Hislop</i> , AEA Technology Harwell Laboratory	
4) <i>Taylor</i> , KfK Karlsruhe - 5) <i>Henrichs</i> , GSF Neuherberg	
Transfer and behaviour of radionuclides in the environment	309
PROMOTION OF FORMATION AND EXCHANGE OF INFORMATION IN RADIOECOLOGY - International Union of Radiologists	311
Contract Bi6-052 - Section A21	
1) <i>Myttenaere</i> , Univ. Cathol. Louvain-la-Neuve	

MODELLING THE TRANSPORT OF RADIONUCLIDES THROUGH THE FRESHWATER ENVIRONMENT	317
Contract Bi7-008 - Sector A21	
1) <i>Hilton</i> , NERC - 2) <i>Galvão</i> , LNETI - 3) <i>Cremers</i> , Univ/ Leuven (KUL)	
4) <i>Foulquier</i> , CEA - Cadarache - 5) <i>Pieri</i> , Univ. Nantes - 6) <i>Belli</i> , ENEA	
7) <i>Vanderborght</i> , Univ. Antwerpen - 8) <i>Serrano</i> , Univ. Malaga	
9) <i>Hambuckers-Berhin</i> , Univ. Liège - 10) <i>Comans</i> , Netherlands Energy Research Found	
RADIOECOLOGY OF TRANSURANICS IN THE MARINE ENVIRONMENT	393
Contract Bi7-042 - Sector A21	
1) <i>Mitchell</i> , University College Dublin - 2) <i>Iranzo</i> , CIEMAT	
3) <i>Guéguéniat</i> , CEA-Cherbourg - 4) <i>Damiani</i> , ENEA	
BEHAVIOUR OF POLONIUM-210 AND LEAD-210 IN EUROPEAN MARINE ENVIRONMENTS. APPLICATION OF BIOINDICATORS	423
Contract Bi7-006 - Sector A22	
1) <i>Köster</i> , RIVM - 2) <i>Guéguéniat</i> , CEA - Cherbourg	
3) <i>Duursma</i> , NIOZ - 4) <i>Galvão</i> , LNETI	
BIOGEOCHEMICAL PATHWAYS OF ARTIFICIAL RADIONUCLIDES	449
Contract Bi6-339 - Sector A23	
1) <i>Plocq</i> , SCOPE-RADPATH	
TRANSFER AND CONVERSION MECHANISMS OF H-3 AND C-14 COMPOUNDS IN THE LOCAL ENVIRONMENT	455
Contract Bi6-345 - Sector A23	
1) <i>Bunnenberg</i> , Niedersächs. Inst. Radioökologie	
THE BIO-AVAILABILITY OF LONG-LIVED RADIONUCLIDES IN RELATION TO THEIR PHYSICO-CHEMICAL FORM IN SOILS	461
Contract Bi7-011 - Sector A23	
1) <i>Lembrechts</i> , RIVM - 2) <i>Wilkins</i> , NRPB	
3) <i>Sandalls</i> , AEA Technology Harwell Laboratory - 4) <i>Cremers</i> , Univ. Leuven (KUL)	
FACTORS AFFECTING RADIOCAESIUM TRANSFER TO RUMINANTS	481
Contract Bi7-018 - Sector A24	
1) <i>Howard</i> , ITE - 2) <i>Vandecasteele</i> , CEN-SCK	
3) <i>Mayer</i> , McAulay Land Use Research. Inst. - 4) <i>Belli</i> , ENEA	
5) <i>Stakelum</i> , Agric. and Food Develop. Authority - 6) <i>Colgan</i> , NEB	
7) <i>Assimakopoulos</i> , Univ. Ioannina - 8) <i>Unsworth</i> , Univ. Nottingham	
9) <i>Jones</i> , Univ. Uppsala Agricult. Sciences	
DEPOSITION OF RADIONUCLIDES ON TREE CANOPIES AND THEIR SUBSEQUENT FATE	525
Contract Bi7-009 - Sector A25	
1) <i>Minski</i> , ICSTM - 2) <i>Belot</i> , CEA - FAR	
3) <i>Rauret</i> , Univ. Barcelona - 4) <i>Ronneau</i> , Univ. Cathol. Louvain-la-Neuve	

BEHAVIOUR OF Cs AND Sr IN NATURAL ECOSYSTEMS AND THE POTENTIAL RADIATION EXPOSURE OF THEIR EXTENSIVE USE	547
Contract Bi7-016 - Sector A25	
1) <i>Wirth</i> , Bundesgesundheitsamt - 2) <i>Guillite</i> , Univ. Liège	
3) <i>Palo</i> , Univ. Umeå Agricultural Sciences - 4) <i>Nimis</i> , Univ. degli Studi di Trieste	
5) <i>Bergamn</i> , Swedish Defense Res. Establ. - 6) <i>Wickman</i> , Univ. Umeå	
7) <i>Melin</i> , Nat. Inst. of Rad. Protection (SSI)	
RADIOECOLOGY OF SEMI-NATURAL ECOSYSTEMS	579
Contract Bi7-044 - Sector A25	
1) <i>Colgan</i> , RPII - 2) <i>Horrill</i> , NERC - 3) <i>Aarkrog</i> , Risø National Laboratory	
4) <i>Johanson</i> , Univ. Agricult. Sciences, Uppsala - 5) <i>Veresoglou</i> , Univ. Thessaloniki	
TRANSFER OF ACCIDENTALLY RELEASED RADIONUCLIDES IN AGRICULTURAL SYSTEMS (TARRAS)	617
Contract Bi7-046 - Sector A26	
1) <i>Cancio</i> , CIEMAT - 2) <i>Maubert</i> , CEA-Cadarache - 3) <i>Rauret</i> , Univ. Barcelona	
4) <i>Colle</i> , CEA-Cadarache - 5) <i>Cawse</i> , AEA Technology Harwell Lab.	
6) <i>Grandison</i> , Univ. Reading - 7) <i>Gutierrez</i> , CIEMAT	
PART II - CONSEQUENCES OF RADIATION EXPOSURE TO MAN; THEIR ASSESSMENT, PREVENTION AND TREATMENT	655
Stochastic effects of radiation	657
BIOPHYSICAL MODELS FOR THE EFFECTIVENESS OF DIFFERENT RADIATIONS	659
Contract Bi7-032 - Section B11	
1) <i>Paretzke</i> , GSF Neuherberg - 2) <i>Goodhead</i> , MRC Radiobiological Unit	
3) <i>Terrissol</i> , ADPA - 4) <i>Leenhouts</i> , RIVM	
SPECIFICATION OF RADIATION QUALITY AT THE NANOMETRE LEVEL	675
Contract Bi7-040 - Sector B11	
1) <i>Colautti</i> , INFN-Legnaro - 2) <i>Watt</i> , Univ. St. Andrew	
3) <i>Harder</i> , Georg-August Univ. - Göttingen - 4) <i>Leuthold</i> , GSF	
5) <i>Izzo</i> , Univ. degli Studi di Roma	
LATE SOMATIC EFFECTS OF IONIZING RADIATION ON THE MAMMALIAN ORGANISM	691
Contract Bi6-099 - Sector B12	
1) <i>Maisin</i> , Univ. Cathol. Louvain à Woluwe	
INDIVIDUAL RADIOSENSITIVITY AND ITS RELATION TO COLO-RECTAL CANCER	711
Contract Bi7-022 - Sector B12	
1) <i>Dutrillaux</i> , Institut Curie - 2) <i>Léonard</i> , Univ. Cathol. Louvain à Woluwe	
3) <i>Rueff</i> , New University of Lisbon	
THE GENETIC AND BIOCHEMICAL BASIS OF HUMAN DNA REPAIR AND RADIOSENSITIVITY	727
Contract Bi7-026 - Sector B12	
1) <i>Lohman</i> , Univ. Leiden, Sylvius Labor. - 2) <i>Bridges</i> , MRC Cell Mutation Unit	
3) <i>Bootsma</i> , Erasmus University Rotterdam - 4) <i>Moustacchi</i> , Institut Curie	
5) <i>Thacker</i> , MRC Radiobiological Unit - 6) <i>Backendorf</i> , Goriaeus Laborat.	

EVALUATION OF THE FREQUENCIES OF CHROMOSOMAL ABERRATIONS INDUCED IN HUMAN BLOOD LYMPHOCYTES BY LOW DOSES OF NEUTRONS	759
Contract Bi6-225 - Sector B13	
1) <i>Lloyd</i> , NRPB (Bi6-225) - 2) <i>Natarajan</i> , Univ. Leiden Sylvius Lab. (Bi6-166)	
3) <i>Obe</i> , Univ. Essen (Bi6-223) - 4) <i>Verschaeve</i> , Cen-SCK (Bi6-146)	
5) <i>Palitti</i> , Univ. degli Studi della Tuscia (Bi6-171)	
EVALUATION OF EXISTING AND DEVELOPMENT OF NEW HUMAN EPITHELIAL CELL TRANSFORMATION SYSTEMS AND DETERMINATION OF THEIR POTENTIAL IN RADIATION PROTECTION STUDIES	771
Contract Bi7-023 - Sector B13	
1) <i>Seymour</i> , NEB - 2) <i>Riches</i> , St Andrews University - 3) <i>Pertusa</i> , Valencia University	
CELLULAR AND MOLECULAR STUDIES ON RADIATION QUALITY: A COMPARISON BETWEEN GENETICALLY RELEVANT DAMAGE AND CELL INACTIVATION	785
Contract Bi7-033 - Sector B13	
1) <i>Kraft</i> , GSI - 2) <i>Sideris</i> , NCRS "Demokritos"	
3) <i>Lloyd</i> , NRPB - 4) <i>Natarajan</i> , Univ. Leiden	
RADIATION INDUCED PROCESSES IN MAMMALIAN CELLS: PRINCIPLES OF RESPONSE MODIFICATION AND INVOLVEMENT IN CARCINOGENESIS	805
Contract Bi7-034 - Sector B13	
1) <i>Van der Eb</i> , Univ. Leiden Sylvius Labo. - 2) <i>Sarasin</i> , CNRS	
3) <i>Devoret</i> , CNRS - 4) <i>Rommelaere</i> , Université Libre de Bruxelles	
5) <i>Bertazzoni</i> , Consiglio Nazionale delle Ricerche	
6) <i>Thomou-Politi</i> , Greek Atomic Energy Commission	
METHODOLOGY FOR THE ANALYSIS OF RADIATION CARCINOGENESIS STUDIES AND APPLICATION TO ONGOING EXPERIMENTS	829
Contract Bi7-035 - Sector B13	
1) <i>Broerse</i> , Academisch Ziekenhuis Leiden - 2) <i>Chmelevsky</i> , GSF Neuherberg	
3) <i>Masse</i> , CEA - FAR - 4) <i>Morin</i> , CEA - FAR	
5) <i>Zurcher</i> , TNO - 6) <i>van Bekkum</i> , TNO-ITRI	
STUDY OF RADIOBIOLOGICAL EFFECTS AT LOW DOSES	851
Contract Bi6-004 - Sector B13	
1) <i>Coppola</i> , ENEA-CRE Casaccia	
LATE EFFECTS IN RHESUS MONKEYS AFTER WHOLE-BODY IRRADIATION WITH W-RAYS AND FISSION NEUTRONS	859
Contract Bi6-075 - Sector B13	
1) <i>Broerse</i> , TNO-ITRI	
MOLECULAR AND CELLULAR EFFECTS OF PROTONS, DEUTERONS AND ALPHAPARTICLES	865
Contract Bi7-0036 - Sector B13	
1) <i>Moschini</i> , Istituto Nazionale di Fisica Nucleare - 2) <i>Goodhead</i> , MRC Radiobiological Unit	
3) <i>Belli</i> , Istituto Superiore di Sanità - 4) <i>Michael</i> , CRC-Gray Laboratory	
CELLULAR AND MOLECULAR MECHANISMS OF RADIATION-INDUCED MYELOID LEUKAEMIA IN THE MOUSE	889
Contract Bi7-037 - Sector B13	
1) <i>Janowski</i> , CEN-SCK - 2) <i>Cox</i> , NRPB	

AUTOMATED DETECTION OF RADIATION INDUCED CHROMOSOME ABERRATIONS BY SLIT-SCAN FLOW CYTOMETRY	897
Contract Bi7-038 - Sector B13	
1) <i>Barendsen</i> , Univ. Amsterdam - 2) <i>Green</i> , MRC Human Genetics Unit	
3) <i>Nüsse</i> , GSF Neuherberg - 4) <i>Bauchinger</i> , GSF Neuherberg	
5) <i>Aubele</i> , GSF Neuherberg	
STUDIES ON BASIC AND APPLIED ASPECTS OF RADIATION-INDUCED CHROMOSOMAL ABERRATIONS IN HUMAN CELLS	931
Contract Bi7-0039 - Sector B13	
1) <i>Natarajan</i> , Univ. Leiden Sylvius Lab. - 2) <i>Savage</i> , MRC Radiobiological Unit.	
3) <i>Olivieri</i> , Università di Roma "La Sapienza" - 4) <i>Cortés-Benavides</i> , Univ. Sevilla	
5) <i>Bryant</i> , Univ. St. Andrews - 6) <i>Ahnström</i> , Univ. Stockholm	
7) <i>Baverstam</i> , Nat. Inst. of Rad. Protection - 8) <i>Feinendegen</i> , KFA Jülich GmbH	
9) <i>Johanson</i> , Univ. Uppsala Agricult. Sciences - 10) <i>Ehrenberg</i> , Univ. Stockholm	
11) <i>Palitti</i> , Univ. degli Studi della Tuscia - 12) <i>Laurent</i> , Univ. Liège Sart Tilman	
13) <i>Pantelias</i> , NCSR "Demokritos" - 14) <i>Jorge</i> , Inst. Portug. Oncol. Francisco Gentil	
15) <i>Pereira-Luis</i> , LNETI	
MEASUREMENT OF TRANSFORMATION OF C3H 10T1/2 CELLS BY LOW DOSES OF IONIZING RADIATION	985
Contract Bi7-043 - Sector B13	
1) <i>Morgan</i> , AEA Technology Harwell Laboratory - 2) <i>Mill</i> , Nuclear Electric	
3) <i>Kellerer</i> , GSF Neuherberg - 4) <i>Frankenberg</i> , GSF Frankfurt	
5) <i>Tallone Lombardi</i> , Università degli Studi di Milano	
6) <i>Saran</i> , ENEA Casaccia Roma	
RADIATION-INDUCED MUTATIONS IN MAMMALS	1019
Contract Bi6-156 - Sector B14	
1) <i>Ehling</i> , GSF Neuherberg	
MUTATION STUDIES UPON SPERMATOGONIAL STEM CELLS OF MAMMALS AND GENETIC TESTS FOR NON-DISJUNCTION IN THE MOUSE	1025
Contract Bi6-143 - Sector B14	
1) <i>Cattanach</i> , MRC Radiobiological Unit	
RADIATION-INDUCED GENETIC EFFECTS IN GERM CELLS OF MAMMALS	1033
Contract Bi6-166 - Sector B14	
1) <i>Van Buul</i> , Univ. Leiden Sylvius Lab.	
RADIATION-INDUCED GENETIC EFFECTS IN GERM CELLS OF MAMMALS	1035
Contract Bi6-069 - Sector B14	
1) <i>Jacquet</i> , CEN/SCK Mol	
RADIATION-INDUCED GENETIC EFFECTS IN GERM CELLS OF MAMMALS	1039
Contract Bi6-077 - Sector B14	
1) <i>Streffer</i> , Universitätsklinikum Essen	
RADIATION-INDUCED GENETIC EFFECTS IN GERM CELLS OF MAMMALS	1045
Contract Bi7-048 - Sector B14	
1) <i>Van der Schans</i> , TNO-Medical Biological Lab.	

RADIOBIOLOGICAL PROPERTIES OF SPERMATOGONIAL STEM CELLS IN C3H/101 HYBRID MICE AND EVALUATION OF THE MODEL FOR INDUCTION OF GENETIC DAMAGE IN SPERMATOGONIAL STEM CELLS	1051
Contract Bi7-052 - Sector B14	
1) <i>De Rooij</i> , Univ. Utrecht	
STUDIES ON SPONTANEOUSLY-ARISING GENETIC AND PARTIALLY GENETIC DISORDERS IN MAN WITHIN THE FRAMEWORK OF THE EVALUATION OF GENETIC RADIATION HAZARDS	1055
Contract Bi6-226 - Sector B14	
1) <i>Lohman</i> , Univ. Leiden, Sylvius Labor.	
MOLECULAR BIOLOGY OF PATERNAL ONCOGENESIS	1061
Contract Bi7-068 - Sector B14	
1) <i>Höfler</i> , GSF Neuherberg	
OSTEOSARCOMA AND TUMOURS OF THE HAEMOPOIETIC SYSTEM BY LOW-DOSE IRRADIATION	1065
Contract Bi7-002 - Sector B15	
1) <i>Höfler</i> , GSF Neuherberg - 2) <i>Höfler</i> , Univ. München - Technische	
3) <i>Erfle</i> , GSF Neuherberg - 4) <i>Skou Pedersen</i> , Aarhus Universitet	
5) <i>Schoeters</i> , CEN - SCK - 6) <i>Bentvelzen</i> , TNO - ITRI	
THE DOSIMETRY AND METABOLISM OF INCORPORATED RADIONUCLIDES	1085
Contract Bi6-089 - Sector B15	
1) <i>Harrison</i> , NRPB	
STUDIES ON MYELOID LEUKAEMIA AND OSTEOSARCOMA INDUCED IN MICE BY RA-224	1091
Contract Bi6-064 - Sector B15	
1) <i>Humphreys</i> , MRC Radiobiological Unit	
RESEARCH IN RADIATION PROTECTION - VOLUME II	1097
Summary	1099
Contents of volume II	1101
Non-stochastic effects of radiation	1123
IMPAIRMENT OF THE HEMO-LYMPHOPOIETIC CELL SYSTEM AND ITS MICRO ENVIRONMENT BY IONIZING RADIATION. PATHOGENESIS OF NON-STOCHASTIC AND NEOPLASTIC EFFECTS AND CONDITIONS FOR A LONG TERM RESTORATION	1125
Contract Bi6-061 - Sector B21	
1) <i>Fliedner</i> , Univ. Ulm	
NON-STOCHASTIC EFFECTS OF IRRADIATION IN MAN: DIAGNOSIS, PROGNOSIS AND TREATMENT OF ACUTE RADIATION INJURY	1143
Contract Bi6-065F - Sector B21	
1) <i>Jammet</i> , CIR	

DEVELOPMENT OF CONDITIONS ALLOWING RESTORATION OF HAEMOPOIESIS BY ALLOGENIC PURIFIED AND <i>IN VITRO</i> MULTIPLIED HAEMOPOIETIC STEM CELLS	1147
Contract Bi6-079 - Sector B21	
1) <i>van Bekkum</i> , TNO-ITRI	
RADIATION DAMAGE AND RECOVERY OF THE IMMUNE SYSTEM	1155
Contract Bi6-059 - Sector B21	
1) <i>Doria</i> , ENEA	
THE REDUCTION OF THE RISKS OF LATE EFFECTS FROM INCORPORATED RADIONUCLIDES	1167
Contract Bi6-347e - Sector B22	
1) <i>Stradling</i> , NRPB - 2) <i>Volf</i> , KfK Karlsruhe - 3) <i>Métivier</i> , CEA-FAR	
4) <i>Burgada</i> , ADFAC (Univ. Pierre et M. Curie) - 5) <i>Archimbaud</i> , CEA-Pierrelatte	
EARLY AND LATE EFFECTS OF RADIATION ON SKIN	1187
Contract Bi6-063 - Sector B23	
1) <i>Hopewell</i> , Univ. Oxford	
PROBLEMS RELATED TO SKIN AND UNDERLYING TISSUES AFTER ACCIDENTS INVOLVING LOCAL IRRADIATION. EXPERIMENTAL STUDY IN THE PIG.....	1197
Contract Bi6-058 - Sector B23	
1) <i>Daburon</i> , CEA-FAR	
RADIATION EFFECTS ON THE SKIN AND SUBCUTANEOUS TISSUES: IMPLICATION FOR PROTECTION CRITERIA AND TREATMENT OF LOCALIZED ACCIDENTAL OVER-EXPOSURE	1203
Contract Bi7-056 - Sector B23	
1) <i>Coggle</i> , Med. Coll. St. Bartholomew's Hosp.	
EUROPEAN CLINICAL RESEARCH ON PRACTICAL PROTOCOLS FOR THE DIAGNOSTICS AND TREATMENT OF LOCALIZED OVEREXPOSURE	1209
Contract Bi7-049 - Sector B23	
1) <i>Góngora</i> , Institut Curie - 2) <i>Strambi</i> , ENEA	
3) <i>Herránz-Crespo</i> , Hospital General Marañón	
IRRADIATION AND THYROID DISEASE	1217
Contract Bi7-005 - Sector B24	
1) <i>Dumont</i> , Univ. Libre de Bruxelles (ULB) - 2) <i>Malone</i> , St James Hospital	
3) <i>Smyth</i> , Univ. College of Dublin, Belfield	
Radiation effects on the developing organism	1231
EFFECTS OF RADIATION ON THE DEVELOPMENT OF THE CENTRAL NERVOUS SYSTEM	1233
Contract Bi7-003 - Sector B31	
1) <i>Reyners</i> , CEN-SCK - 2) <i>Ferrer</i> , Hospital Principer de España	
3) <i>Coffigny</i> , CEA - Bruyères-le-Châtel	

DYSFUNCTION AND NEOPLASIAS OF HAEMOPOIETIC AND OSTEOGENIC TISSUE FOLLOWING EXTERNAL IRRADIATION OR BONE-SEEKING RADIONUCLIDE CONTAMINATION <i>IN UTERO</i> OR DURING NEONATAL DEVELOPMENT	1249
Contract Bi7-001 - Sector B32	
1) <i>Humphreys</i> , MRC Radiobiology Unit - 2) <i>Vandenheuvel</i> , CEN-SCK	
3) <i>Lord</i> , Paterson Institute Cancer Research - 4) <i>van Bekkum</i> , TNO-ITRI	
5) <i>Tejero</i> , Universidad Complutense de Madrid - 6) <i>Bueren</i> , CIEMAT	
THE DOSIMETRY AND EFFECTS OF FETAL IRRADIATION FROM INCORPORATED RADIONUCLIDES (NRPB ASSOCIATION)	1281
Contract Bi6-347d - Sector B33	
1) <i>Harrison</i> , NRPB - 2) <i>Henshaw</i> , Univ. Bristol - 3) <i>Coffigny</i> , CEA-FAR	
PART III - RISKS AND MANAGEMENT OF RADIATION PROTECTION	1303
Assessment of human exposure and risks	1305
THE RISKS OF RADIATION WORK: ANALYSIS OF REGISTRY DATA	1307
Contract Bi6-213 - Sector C11	
1) <i>Stather</i> , NRPB	
STATISTICAL RESULTS OF THE PERSONAL DOSIMETRY SERVICE AT THE GSF	1311
Contract Bi7-0053-D - Sector C11	
1) <i>Regulla, Schraube</i> , GSF Neuherberg	
PROCEDURES TO ASSESS INTAKES OF RADIONUCLIDES FROM SAMPLES OF AIRBORNE RADIOACTIVITY AND STATISTICAL STUDIES OF RADIATION RISKS	1315
Contract Bi6-116 - Sector C11	
1) <i>Stather</i> , NRPB	
RADON SOURCES AND MODELS (NRPB ASSOCIATION)	1325
Contract Bi6-347f - Sector C12	
1) <i>Miles</i> , NRPB - 2) <i>de Meijer</i> , Univ Groningen (KVI)	
3) <i>Damkjær</i> , Univ. Denmark-Tech - 4) <i>Majborn</i> , Risø National Laboratory	
5) <i>Wouters</i> , CSTC/WTCB - 6) <i>de Jong</i> , TNO-Arnhem	
7) <i>Ball</i> , NERC (BGS) - 8) <i>Hubbard/Enflo</i> , Nat. Inst. of Rad. Protec. (SSI)	
9) <i>Proukakis</i> , Univ. Athens - School of Medicine	
ASSESSMENT AND MANAGEMENT OF RADIATION EXPOSURE AND RISKS FROM NATURAL AND MAN-MADE RADIATION SOURCES	1361
Contract Bi6-114 - Sector C12	
1) <i>Kollas</i> , NCRS "Demokritos"	
NATURAL EXPOSURE FROM RADON AND RADON PROGENY IN SPANISH HOUSES ...	1367
Contract Bi6-314 - Sector C12	
1) <i>Quindós Poncela</i> , Universidad de Santander	

EVALUATION OF THE POPULATION EXPOSURE TO RADON IN THE VICINITY OF URANIUM MINING FACILITIES	1379
Contract Bi6-208 - Sector C12	
1) <i>Galvão</i> , LNETI	
RETROSPECTIVE ASSESSMENT OF RADON EXPOSURE FROM LONG-LIVED DECAY PRODUCTS	1387
Contract Bi7-013 - Sector C12	
1) <i>Samuelsson</i> , Lund University - 2) <i>Jonassen</i> , Technical University of Denmark	
3) <i>Falk</i> , Swedish Radiation Protection Institute - 4) <i>Poffijn</i> , Univ. Gent	
5) <i>Vanmarcke</i> , CEN-SCK - 6) <i>McLaughlin</i> , University College Dublin	
CHARACTERISTICS OF RADON- AND THORON DAUGHTERS AEROSOLS	1411
Contract Bi7-047 - Sector C12	
1) <i>Porstendörfer</i> , Georg-August-Universität - 2) <i>Poffijn</i> , Univ. Gent	
3) <i>Vanmarcke</i> , CEN-SCK - 4) <i>Akselsson</i> , Univ. Lund	
5) <i>Tymen</i> , Univ. Brest - 6) <i>Falk</i> , Nat. Inst. of Rad. Protection	
7) <i>Ortega</i> , Univ. Politècnica de Catalunya	
ASSESSMENT OF THE GEOLOGICAL FACTORS INFLUENCING THE OCCURRENCE OF RADON HAZARD AREAS IN A KARSTIC REGION	1439
Contract Bi7-059 - Sector C12	
1) <i>O'Connor</i> , Geological Survey of Ireland	
2) <i>Madden</i> , Radiological Protection Institute of Ireland (formerly Nuclear Energy Board)	
3) <i>McLaughlin</i> , University College, Dublin - 4) <i>McAulay</i> , Trinity College, Dublin	
5) <i>Brock</i> , University College, Galway	
6) <i>Van den Boom</i> , Bundesanst. Geowissenschaften	
CONSEQUENCES OF IRRADIATION OF POPULATION AND WORKERS (CEA ASSOCIATION)	1463
Contract Bi6-122 - Sector C13	
1) <i>A. Després</i> , CEA-FAR - 2) <i>J. Brenot</i> , CEA-FAR	
3) <i>H. Maubert</i> , CEA-Cadarache	
COMPARATIVE ASSESSMENT AND MANAGEMENT OF THE HEALTH AND ENVIRONMENTAL IMPACT OF ENERGY SYSTEMS AND STUDIES RELATED TO THE EXPRESSION OF THE DETRIMENT ASSOCIATED WITH RADIATION EXPOSURE	1475
Contract Bi7-004 - Sector C13	
1) <i>Lochará</i> , CEPN - 2) <i>Wrixon</i> , NRPB - 3) <i>Kemp</i> , Univ. East Anglia	
4) <i>Friedrich</i> , Univ. Stuttgart - 5) <i>Anguenot</i> , CEA-FAR	
QUANTIFICATION OF RADIATION RISKS, OPTIMISATION OF PROCEDURES AND ANALYSIS OF OCCUPATIONAL EXPOSURE	1489
Contract Bi6-111 - Sector C14	
1) <i>Jacobi</i> , GSF Neuherberg	
STATISTICAL METHODS FOR THE ANALYSIS OF GEOGRAPHICAL CORRELATIONS, APPLICATION TO THE ANALYSIS OF THE CORRELATION BETWEEN POPULATION RADIATION EXPOSURE AND CANCER MORTALITY	1491
Contract Bi6-126 - Sector C14	
1) <i>Hémon</i> , INSERM	

EPIDEMIOLOGICAL STUDIES OF RADIATION CARCINOGENESIS AND ITS BIOPHYSICAL BASIS Contract Bi6-221 - Sector C14 1) <i>Gössner</i> , GSF Neuherberg - 2) <i>Spiess</i> , Universität München - 3) <i>Kellerer</i> , GSF	1497
HEALTH EFFECTS OF CHRONIC EXPOSURE TO LOW DOSE IONIZING RADIATION ON WORKERS OF THE SPANISH NUCLEAR ENERGY INSTALLATIONS Contract Bi6-229 - Sector C14 1) <i>Artalejo</i> , CIEMAT	1505
THOROTRAST: INVESTIGATIONS TO EVALUATE THE LONG-TERM EFFECTS CAUSED BY ARTIFICIAL RADIATION IN MAN (THOROTRAST PATIENTS FOLLOW-UP STUDY IN GERMANY AND DENMARK) Contract Bi6-298 - Sector C14 1) <i>Van Kaick</i> , Deutsches Krebsforsch.Zent.Heidelberg	1509
LATE EFFECTS OF THOROTRAST AMONG DANISH PATIENTS Contract Bi6-333 - Sector C14 1) <i>Storm</i> , Danish Cancer Society	1515
SURVEY ON CHILDHOOD LEUKAEMIA Contract Bi6-319 - Sector C14 1) <i>Kaldor</i> , IARC	1545
EPIDEMIOLOGICAL STUDIES OF RADIATION RISKS (NRPB ASSOCIATION) Contract Bi6-347h - Sector C14 1) <i>Muirhead</i> , NRPB - 2) <i>Kellerer</i> , Univ. München - 3) <i>Chmelevsky</i> , GSF Neuherberg 4) <i>Oberhausen</i> , Univ. Saarlandes - 5) <i>Holm</i> , Karolinska Hospital 6) <i>Becciolini</i> , Università degli Studi di Firenze	1547
RADON AND LUNG CANCER IN THE ARDENNES AND EIFEL REGION Contract Bi7-007 - Sector C14 1) <i>Poffijn</i> , Univ. Gent - 2) <i>Tirmarche</i> , CEA - FAR - 3) <i>Wichmann</i> , Univ. Wuppertal 4) <i>Kayser</i> , Dir. de la Santé Div. Radioprot. - 5) <i>Darby</i> , Imperial Cancer Research Fund. 6) <i>Tirmarche</i> , CEA-FAR	1569
MORTALITY AROUND FRENCH NUCLEAR SITES IN THE POPULATION AGED 0 TO 24 Contract Bi7-066 - Sector C14 1) <i>Hill</i> , Inst. G. Roussy	1629
Optimization and management of radiation protection	1633
DEVELOPMENT OF FUNDAMENTAL DATA FOR RADIATION PROTECTION Contract Bi6-324 - Sector C21 1) <i>Smith</i> , ICRP	1635

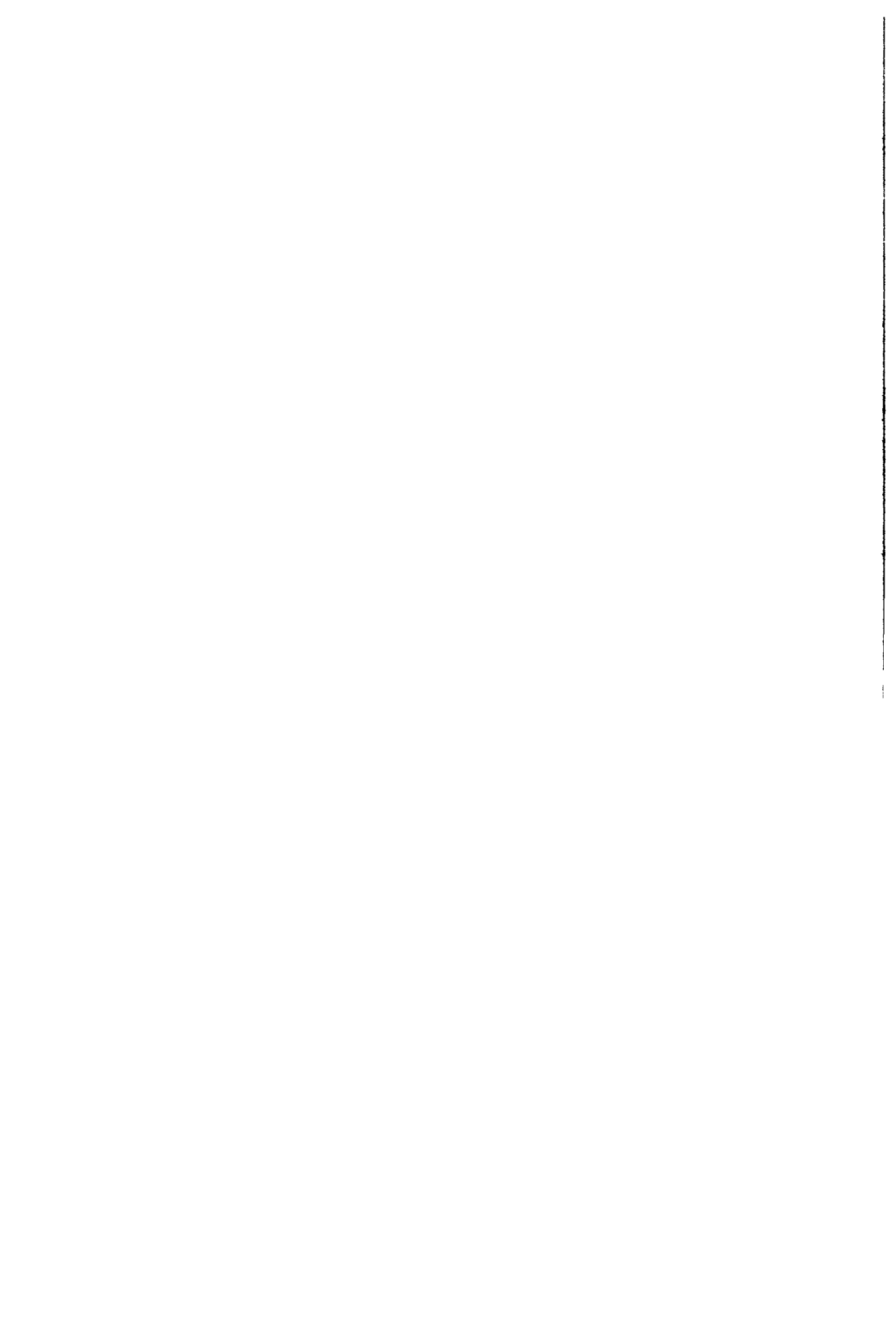
APPLICATION OF ALARA IN COMPLEX DECISION-MAKING SITUATIONS (NRPB ASSOCIATION)	1639
Contract Bi6-347i - Sector C21	
1) <i>Wrixon</i> , NRPB - 2) <i>Lochard</i> , CEPN - 3) <i>Meggitt</i> , SRD-AEA Technology	
REDUCTION OF DOSE IN X-RAY DIAGNOSTICS BY THE CHOICE OF THE OPTIMAL SCREEN-FILM COMBINATION	1649
Contract Bi6-316 - Sector C22	
1) <i>Hoeschen</i> , PTB	
REDUCTION OF PATIENT EXPOSURE IN MEDICAL DIAGNOSTIC RADIOLOGY. DOSIMETRY AND RISK (NRPB ASSOCIATION)	1657
Contract Bi6-347g - Sector C22	
1) <i>Wall</i> , NRPB - 2) <i>Drexler</i> , GSF Neuherberg	
3) <i>Kramer</i> , PTB - 4) <i>Broerse</i> , TNO-ITRI	
QUALITY CRITERIA, TOLERANCES, LIMITING VALUES, DOSIMETRY AND OPTIMIZATION IN A NUMBER OF FLUOROSCOPIC, DIGITAL FLUOROSCOPIC, DSA AND DIGITAL RADIOLOGICAL SYSTEMS	1677
Contract Bi7-014 - Sector C22	
1) <i>Malone</i> - FDVH/St. James's Hospital/TCD	
2) <i>Boddy/Faulkner</i> - Regional Radiation Physics-Newcastle	
3) <i>Busch</i> - Univ. Heidelberg Klinikum Mannheim	
THE EFFECTIVE DOSE EQUIVALENT DUE TO X-RAY DIAGNOSTIC EXAMINATIONS AND THE IMPACT OF QUALITY CONTROL ON MEDICAL EXPOSURE	1693
Contract Bi6-343 - Sector C22	
1) <i>Schmidt</i>	
QUALITY ASSURANCE AND REDUCTION OF PATIENT EXPOSURE	1699
Contract Bi7-019 - Sector C22	
1) <i>Fagnani</i> , CAATS - INSERM - 2) <i>Moore</i> , Integr. Radiological Services Ltd	
3) <i>Alm Carlsson</i> , Univ. Linköping - 4) <i>Dance</i> , The Royal Marsden Hospital	
5) <i>Flioni-Vyza</i> , Greek Anti-Cancer Institute - 6) <i>Rimondi</i> , Univ. Ferrara	
THE PRINCIPLES AND THE PRACTICABILITY OF QUALITY CONTROL AND QUALITY ASSURANCE IN PAEDIATRIC RADIOLOGY	1735
Contract Bi6-211 - Sector C22	
1) <i>Schneider</i> , Univ. München Kinderklinik	
OPTIMISATION OF PROTECTION IN MEDICAL DIAGNOSTIC RADIOLOGY	1745
Contract Bi6-214 - Sector C22	
1) <i>Vano Carruana</i> , Universidad Complutense de Madrid	
REFINEMENT OF METHODS FOR THE ASSESSMENT OF ORGAN DOSES, AND POSSIBLE REDUCTION OF PATIENT EXPOSURE	1751
Contract Bi6 -136 - Sector C22	
1) <i>Padovani</i> , Unità Sanitaria Locale N. 7 Udinese	

DIAGNOSIS RELATED DOSES: A COMPARATIVE INVESTIGATION IN SOME EUROPEAN HOSPITALS.....	1755
Contract Bi7-054 - Sector C22	
1) <i>Van Loon</i> - Univ. Hospital VUB - 2) <i>Thijssen</i> - Univ. Nijmegen Acad. Hospital	
PATIENT DOSE FROM RADIOPHARMACEUTICALS	1767
Contract Bi7-057 - Sector C22	
1) <i>Mattsson</i> , Univ. Lund - 2) <i>Smith</i> , MRC Clinical Research Centre	
3) <i>Henrichs</i> , GSF Neuherberg	
QUALITY CRITERIA AND DOSE REDUCTION IN COMPUTED TOMOGRAPHY	1783
Contract Bi7-067 - Sector C22	
1) <i>Jessen</i> , Univ. Aarhus Hospital - 2) <i>Galvão</i> , LNETI	
METHODOLOGY FOR EVALUATING THE RADIOLOGICAL CONSEQUENCES OF RADIOACTIVE MATERIALS RELEASED IN ACCIDENTS INCLUDING UNCERTAINTY ANALYSIS AND ECONOMIC IMPACT	1793
Contract Bi6-128 - Sector C24	
1) <i>Kessler</i> , KfK Karlsruhe	
METHODOLOGY FOR EVALUATING THE RADIOLOGICAL CONSEQUENCES OF RADIOACTIVE EFFLUENT RELEASED IN ACCIDENTS	1799
Contract Bi6-127 - Sector C24	
1) <i>Cooper</i> , NRPB	
METHODOLOGY OF PROBABILISTIC UNCERTAINTY ANALYSIS OF COMPUTATIONAL ASSESSMENTS	1807
Contract Bi6-125 - Sector C24	
1) <i>Hofer</i> , GRS	
OPTIMIZATION OF OFF-SITE RECOVERY ACTIONS FOLLOWING NUCLEAR REACTOR ACCIDENTS.....	1821
Contract Bi6-227 - Sector C24	
1) <i>Alonso</i> , Universidad Politécnica de Madrid	
DEPOSITION OF RADIONUCLIDES AND THEIR SUBSEQUENT RELOCATION IN THE ENVIRONMENT FOLLOWING AN ACCIDENTAL RELEASE TO THE ATMOSPHERE	1827
Contract Bi7-010 - Sector C24	
1) <i>Underwood</i> , SRD AEA Technology - 2) <i>Roed</i> , Risø National Laboratory	
3) <i>Paretzke</i> , GSF Neuherberg - 4) <i>Nixon</i> , UKAEA-SRD	
RADE-AID, THE DEVELOPMENT OF A RADIOLOGICAL ACCIDENT DECISION AIDING SYSTEM	1847
Contract Bi7-012 - Sector C24	
1) <i>Wagenaar</i> , TNO - 2) <i>Ehrhardt</i> , KfK Karlsruhe - 3) <i>Morrey</i> , NRPB	
INDOOR DEPOSITION AND RELATIONSHIP BETWEEN INDOOR AND OUTDOOR AIR CONCENTRATION	1859
Contract Bi7-015 - Sector C24	
1) <i>Roed</i> , Risø National Laboratory - 2) <i>Goddard</i> , ICSTM	

VALIDATION-TRAINING AND UNCERTAINTY-STUDY EXPERIMENTS FOR REAL-TIME ATMOSPHERIC DISPERSION MODELS	1871
Contract Bi7-017 - Sector C24	
1) <i>Mikkelsen</i> , Risø National Laboratory - 2) <i>Werner</i> , Deutche Forsch.anst.Luft Raumfart	
DEVELOPMENT OF A COMPREHENSIVE DECISION-AIDING SYSTEM FOR THE OFF-SITE EMERGENCY MANAGEMENT	1885
Contract Bi7-045 - Sector C24	
1) <i>Ehrhardt</i> - KfK Karlsruhe 2) <i>Robeau</i> - CEA-FAR	
3) <i>Bartzis</i> - NCSR "Demokritos" 4) <i>Caracciolo</i> - ENEA	
5) <i>ApSimon</i> - ICSTM 6) <i>Thykyer-Nielsen</i> - Risø National Laboratory	
7) <i>Paretzke</i> - GSF Neuherberg 8) <i>Persson</i> - Inst. Meterological and Hydrolog.	
REAL-TIME UNCERTAINTY HANDLING AND DEVELOPMENT OF A COMPUTER BASED TRAINING SYSTEM FOR THE MANAGEMENT OF OFF-SITE NUCLEAR EMERGENCIES	1921
Contract Bi6-106 - Sector C24	
1) <i>Govaerts</i> , CEN -SCK	
EMPIRICAL AND FRACTAL DESCRIPTION OF RADIOLOGICAL DATA DETECTED AFTER CHERNOBYL ACCIDENT	1925
Contract Bi7-062 - Sector C24	
1) <i>Ratti</i> , Univ. Pavia	
COORDINATION ACTIVITIES	1931
A. Meetings of study groups	1935
B. Meetings organised or co-organised by the Commission	1955
C. Meetings of experts	1965
ERPET - EUROPEAN RADIATION PROTECTION EDUCATION AND TRAINING	1979
Activities, Period: June 1991 - End 1992	
SELECTION OF PUBLICATIONS ISSUED ON THE INITIATIVE OF THE COMMISSION	1991
Publications, Period: 1 June 1991 - 31 December 1992	
Proceedings	1995
Monographs	2005
Other publications	2013
LIST OF ACRONYMS AND ABBREVIATIONS	2015
LIST OF RESEARCH GROUP LEADERS	2019

**RESEARCH IN RADIATION
PROTECTION**

VOLUME I



Radiation Protection Programme 1990-1991 - Final Report
Volume 1
Summary

The final report of the 1990-1991 period of the radiation protection programme outlines the research work carried out during the whole contractual period under all contracts between the Commission of the European Communities and research groups in the Member States. More than 450 scientists collaborated on this programme.

Results of more than 350 projects are reported. They are grouped into three sectors:

1 Human Exposure to Radiation and Radioactivity, which includes:

- 1.1 Measurement of Radiation Dose and its Interpretation*
- 1.2 Transfer and Behaviour of Radionuclides in the Environment*

2 Consequences of Radiation Exposure to Man; Assessment, Prevention and Treatment, which includes:

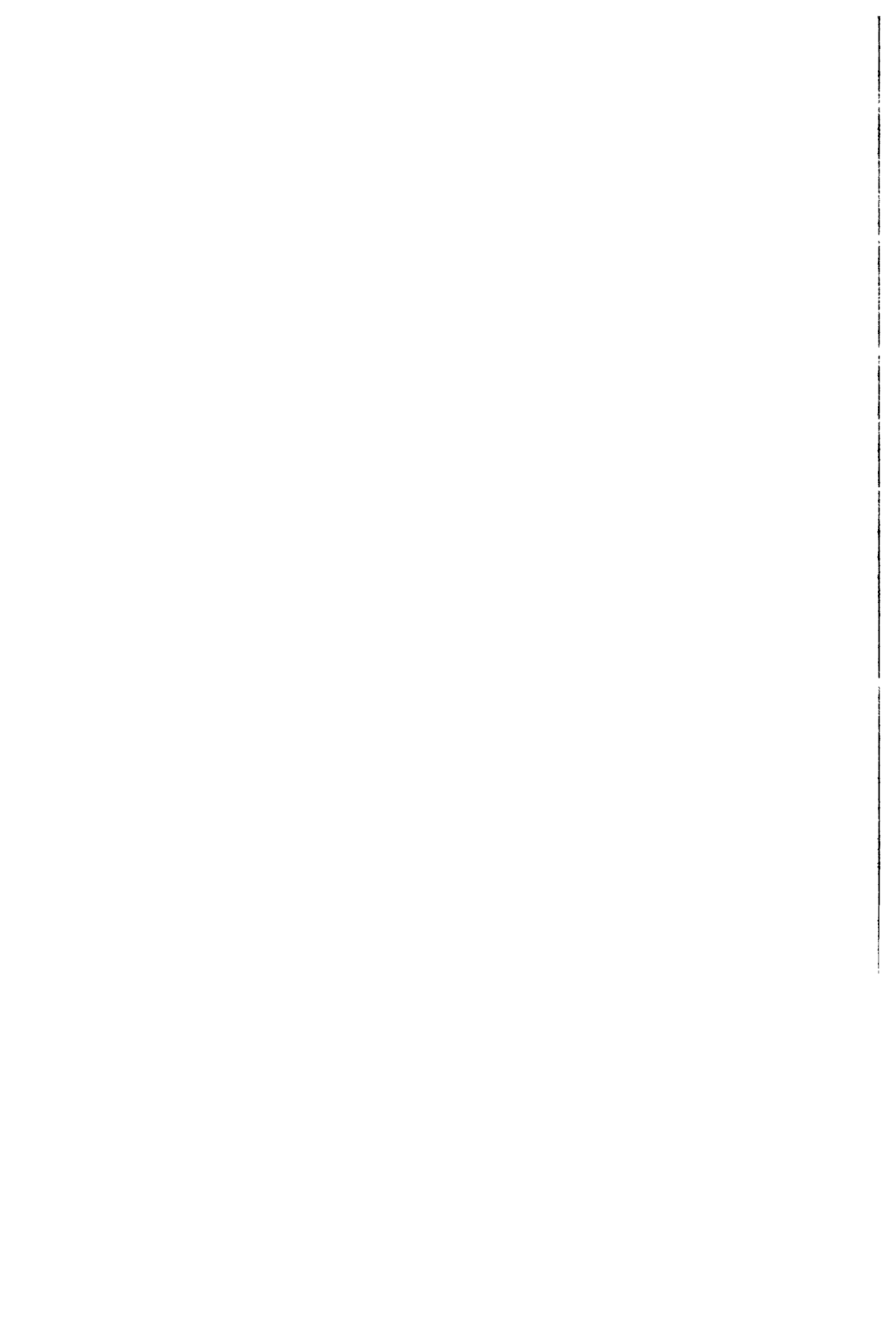
- 2.1 Stochastic Effects of Radiation*
- 2.2 Non-Stochastic Effects of Radiation*
- 2.3 Radiation Effects on the Developing Organism*

3 Risks and Management of Exposure, which includes:

- 3.1 Assessment of Human Exposure and Risks*
- 3.2 Optimization and Management of Radiation Protection*

Within the framework programme, the aim of this scientific research is to improve the conditions of life with respect to work and protection of man and his environment and to assure safe production of energy, i.e.:

- (i) to improve methods necessary to protect workers and the population by updating the scientific basis for appropriate standards;
- (ii) to prevent and counteract harmful effects of radiation;
- (iii) to assess radiation risks and provide methods to cope with the consequences of radiation accidents.



CONTENTS OF VOLUME I

Summary	3
PART I - HUMAN EXPOSURE TO RADIATION AND RADIOACTIVITY	29
Measurement of radiation dose and its interpretation	31
COLLABORATION ON RESEARCH AND DEVELOPMENT CONCERNED WITH THE METHODOLOGY AND DATA IN RADIATION DOSIMETRY	
Summary of project global objectives and achievements	33
Working group 2: Skin dosimetry: M. W. Charles, P. Christensen (until 1991)	
Objectives for the reporting period and progress achieved	35
Publications	38
Working group 4: Numerical dosimetry: B.R.L. Siebert	
Objectives for the reporting period	39
Progress achieved	39
Publications	41
Working group 6: Assessment of internal dose: J.A.Gibson	
Objectives for the reporting period	42
Progress achieved	42
Publications	46
Working group 7: Radiation spectrometry in working environments: H. Klein	
Objectives for the reporting period	48
Progress achieved	48
Publications	50
Working group 8: To develop and improve techniques for the individual dosimetry of ionising radiation: J.R. Harvey	
Objectives for the reporting period	51
Progress achieved	51
Publications	53
Working group 9: Criticality accident dosimetry: R. Médioni	
Objectives for the reporting period	54
Progress achieved	54
Publications	56
Working group 10: Basic physical data and characteristics of gas ionisation devices: P. Pihet	
Objectives for the reporting period	57
Progress achieved	57
Publications	60
QUANTITIES, UNITS AND MEASUREMENT TECHNIQUES FOR IONIZING RADIATION	
Summary of project global objectives and achievements	61

Project 1: Prof. Allisy	
Objectives for the reporting period	65
Progress achieved	65
THE IMPLEMENTATION OF THE OPERATIONAL DOSE QUANTITIES INTO RADIATION PROTECTION DOSIMETRY (NRPB ASSOCIATION)	
Summary of project global objectives and achievements.....	67
Project 1: Dr. Clark	
Objectives for the reporting period	69
Progress achieved	69
Project 2: Dr. Marshall	
Objectives for the reporting period	72
Progress achieved including publications	72
Publications	73
Project 3: Dr. Lembo	
Objectives for the reporting period	76
Progress achieved including publications	76
Publications	76
Annex: Montecarlo calculation of field parameters for the ICRU sphere with reference photon beams	77
References	78
Project 4: Dr. Chartier	
Objectives for the reporting period	81
Progress achieved including publications	81
Bibliography.....	83
STUDY AND DEVELOPMENT OF AN INDIVIDUAL ELECTRONIC NEUTRON DOSIMETER	
Summary of project global objectives and achievements.....	87
Project 1: Dr. Vareille - Dr. Decossas	
Objectives for the reporting period	89
Progress achieved	89
Publications	94
Project 2: Dr. Tommasino	
Objectives for the reporting period	95
Progress achieved including publications	95
Publications	95
Project 3: Dr. M. Zamani-Valassiadou	
Objectives for the reporting period	96
Progress achieved including publications	96
Publications	97
Project 4: Dr. J. Barthe	
Objectives for the reporting period	99
Progress achieved including publications	99
References	101

Project 5: Prof. F. Fernández Moreno	
Objectives for the reporting period	102
Progress achieved	102
USE OF THE VARIANCE-COVARIANCE METHOD IN RADIATION PROTECTION	
Summary of project global objectives and achievements.....	107
Project 1: Prof. Kellerer	
Objectives for the reporting period	108
Progress achieved including publications	108
Publications	112
Project 2: Dr. K.A. Jessen	
Objectives for the reporting period	113
Progress achieved	113
Project 3: Dr. Lindborg	
Objectives for the reporting period	116
Progress achieved	116
THE MEASUREMENT OF ENVIRONMENTAL GAMMA DOSES	
Summary of project global objectives and achievements.....	121
Project 1: Dr. Bøtter-Jensen	
Objectives for the reporting period	125
Progress achieved including publications	125
Publications	131
Project 2: Dr. Lauterbach	
Objectives for the reporting period	132
Progress achieved including publications	132
Publications	136
Project 3: Dr. Delgado Martínez	
Objectives for the reporting period	139
Progress achieved including publications	139
Publications	142
DOSIMETRY OF BETA AND LOW-ENERGY PHOTON RADIATION USING EXTRAPOLATION CHAMBERS AND THIN SOLID STATE DOSIMETERS	
Summary of project global objectives and achievements.....	145
References	150
Project 1: Dr. Christensen	
Objectives for the reporting period	151
Progress achieved including publications	151
Publications	156
References	156

Project 2: Dr. Chartier	
Objectives for the reporting period	157
Progress achieved including publications	157
Publications	159
Bibliography	160
Project 3: Dr. Herbaut	
Objectives for the reporting period	161
Progress achieved	161
References	167
Project 4: Dr. T. M. Francis	
Objectives for the reporting period	168
Progress achieved including publications	168
References	172
Publications	172
Project 5: Prof. Gasiot	
Objectives for the reporting period	173
Progress achieved including publications	173
Publications and bibliography	175
Project 6: Dr. Prof. Scharmann	
Objectives for the reporting period	179
Progress achieved including publications	179
References	182
Publications	182
THE USE OF MICRODOSIMETRIC METHODS FOR THE DETERMINATION OF DOSE EQUIVALENT QUANTITIES AND OF BASIC DATA FOR DOSIMETRY	
Summary of project global objectives and achievements	183
Project 1: Dr. Grillmaier	
Objectives for the reporting period	186
Progress achieved including publications	186
Publications	190
Project 2: Dr. Brede	
Objectives for the reporting period	191
Progress achieved including publications	191
Publications	194
Project 3: Dr. Zoetelief	
Objectives for the reporting period	196
Progress achieved including publications	196
Publications	199
Project 4: Dr. Th. Schmitz	
Objectives for the reporting period	200
Progress achieved including publications	200
Publications	202

Project 5: Dr. Ségur	
Objectives for the reporting period	203
Progress achieved including publications	203
Publications	206
DETERMINATION AND REALISATION OF CALIBRATION FIELDS FOR NEUTRON PROTECTION DOSIMETRY AS DERIVED FROM SPECTRA ENCOUNTERED IN ROUTINE SURVEILLANCE	
Summary of project global objectives and achievements	207
References	213
Publications	214
Project 1: Dr. H. Klein	
Objectives for the reporting period	215
Progress achieved	215
Project 2: Dr. D.J. Thomas	
Objectives for the reporting period	219
Progress achieved including publications	219
References	222
Project 3: Dr. J. L. Chartier	
Objectives for the reporting period	223
Progress achieved	223
Project 4: Dr. H. Schraube	
Objectives for the reporting period	227
Progress achieved including publications	227
References	230
CALCULATION AND MEASUREMENT OF DOSES FROM PARTICULATE RADIOACTIVE SOURCE	
Summary of project global objectives and achievements.....	231
Project 1: Dr. H. Charles	
Objectives for the reporting period	232
Progress achieved including publications	232
References	234
Project 2: Dr. Herbaut	
Objectives for the reporting period	235
Progress achieved including publications	235
References	236
Project 3: Dr. Patau	
Objectives for the reporting period	238
Progress achieved	238
INHALATION AND INGESTION OF RADIONUCLIDES (NRPB ASSOCIATION)	
Summary of project global objectives and achievements.....	243

Project 1: Dr. Bailey	
Objectives for the reporting period	247
Progress achieved including publications	247
Publications	249
Project 2: Dr. Kendall	
Objectives for the reporting period	251
Progress achieved including publications	251
Publications	253
Project 3: Dr. H. Stahlhofen	
Objectives for the reporting period	255
Progress achieved including publications	255
Publications	257
Project 4: Dr. Roy	
Objectives for the reporting period	260
Progress achieved including publications	260
Publications	264
Project 5: Dr. Patrick	
Objectives for the reporting period	265
Progress achieved including publications	265
Publications	267
Project 6: Dr. Kaul	
Objectives for the reporting period	268
Progress achieved	268
Project 7: Dr. Taylor	
Objectives for the reporting period	271
Progress achieved including publications	271
Publications	272
ASSESSMENT OF INTERNAL DOSE FROM RADIONUCLIDES USING STABLE ISOTOPE TRACER TECHNIQUES IN MAN	
Summary of project global objectives and achievements	273
Project 1: Dr. P. Roth	
Objectives for the reporting period	277
Progress achieved including publications	277
Publications	283
References	284
Project 2: Prof. N. Molho	
Objectives for the reporting period	285
Progress achieved including publications	285
Publications	290
Project 3: Dr. J. Hislop	
Objectives for the reporting period	292
Progress achieved including publications	293
Publications	301

Project 4: Dr. Prof. D.M. Taylor	
Objectives for the reporting period	302
Progress achieved including publications	302
References	304
Publications	305
Project 5: Dr. K. Henrichs	
Objectives for the reporting period	306
Progress achieved	306
Transfer and behaviour of radionuclides in the environment	
	309
PROMOTION OF FORMATION AND EXCHANGE OF INFORMATION IN RADIOECOLOGY	
International Union of Radiologists	
Summary of project global objectives and achievements.....	311
Project 1: Dr. Myttenaere	
Objectives for the reporting period	313
Progress achieved including publications	313
Publications	316
MODELLING THE TRANSPORT OF RADIONUCLIDES THROUGH THE FRESHWATER ENVIRONMENT	
Summary of project global objectives and achievements.....	317
Project 1: Dr. Hilton	
Objectives for the reporting period	320
Progress achieved including publications	320
References	323
Publications	324
Project 2: Dr. Galvão	
Sub-project 1: Physico-chemical behaviour of radionuclides in freshwater sediments	329
Sub-Project 2: Co-60 transfer in a freshwater ecosystem	331
References	343
Project 3: Prof. Cremers	
Objectives for the reporting period	344
Progress achieved	344
Project 4: Dr. Foulquier	
Objectives for the reporting period	350
Progress achieved including publications	350
Publications	358
Project 5: Prof. Pieri	
Objectives for the reporting period	359
Progress achieved including publications	359
References	363

Project 6: Dr. Belli	
Objectives for the reporting period	364
Progress achieved including publications	364
References	367
Project 7: Prof. Vanderborght	
Objectives for the reporting period	368
Progress achieved including publications	368
Publications	371
Project 8: Prof. Serrano	
Objectives for the reporting period	372
Progress achieved including publications	372
Publications	377
Project 9: Dr. Hambuckers - Berlin	
Objectives for the reporting period	378
Progress achieved including publications	378
Publications	381
Project 10: Dr. Comans	
Objectives for the reporting period	385
Progress achieved including publications	385
References	391
Publications	391
RADIOECOLOGY OF TRANSURANICS IN THE MARINE ENVIRONMENT	
Summary of project global objectives and achievements.....	393
Project 1: Dr. Mitchell	
Objectives for the reporting period	398
Progress achieved including publications	398
Publications	405
Project 2: Dr. Gascò	
Objectives for the reporting period	407
Progress achieved including publications	407
Publications	412
Project 3: Dr. Guéguénat	
Objectives for the reporting period	414
Progress achieved including publications	414
Publications	416
Project 4: Dr. Damiani	
Objectives for the reporting period	418
Progress achieved including publications	418
Publications	421
BEHAVIOUR OF POLONIUM-210 AND LEAD-210 IN EUROPEAN MARINE ENVIRONMENTS. APPLICATION OF BIOINDICATORS	
Summary of project global objectives and achievements.....	423

Project 1: Dr. Köster	
Objectives for the reporting period	428
Progress achieved including publications	428
References	433
Project 2: Dr. Guéguéniat	
Objectives for the reporting period	435
Progress achieved including publications	435
References	438
Project 3: Prof. Dr. Duursma	
Objectives for the reporting period	439
Progress achieved including publications	439
Publications	443
Project 4: Dr. Galvão	
Objectives for the reporting period	444
Progress achieved including publications	444
References	447
BIOGEOCHEMICAL PATHWAYS OF ARTIFICIAL RADIONUCLIDES	
Summary of project global objectives and achievements.....	449
Report on project activities	450
TRANSFER AND CONVERSION MECHANISMS OF H-3 AND C-14 COMPOUNDS IN THE LOCAL ENVIRONMENT	
Summary of project global objectives and achievements.....	455
Project 1: Dr. Bunnenberg	
Objectives for the reporting period	457
Progress achieved including publications	457
Publications	459
THE BIO-AVAILABILITY OF LONG-LIVED RADIONUCLIDES IN RELATION TO THEIR PHYSICO-CHEMICAL FORM IN SOILS	
Summary of project global objectives and achievements.....	461
Project 1: Dr. J. Lembrechts	
Objectives for the reporting period	465
Progress achieved including publications	465
Publications	468
Project 2: B.T. Wilkins - A.F. Nisbet	
Objectives for the reporting period	469
Progress achieved including publications	469
Publications	472
Project 3: Dr. Sandalls	
Do plants differentiate between K and C _s in root uptake?	473
The relative uptake of C _s and K by three different plant species	474
References	474

Project 4: Dr. A. Cremers	
Objectives for the reporting period	475
Progress achieved including publications	475
Publications	478
FACTORS AFFECTING RADIOCAESIUM TRANSFER TO RUMINANTS	
Summary of project global objectives and achievements.....	481
Project 1: Dr. Howard	
Objectives for the reporting period	486
Progress achieved including publications	486
Publications	489
Project 2: Dr. Vandecasteele	
Objectives for the reporting period	491
Progress achieved including publications	491
Publications	495
Project 3: Dr. Mayes	
Objectives for the reporting period	497
Progress achieved including publications	497
Publications	500
Project 4: Dr. Belli	
Objectives for the reporting period	501
Progress achieved including publications	501
Publications	503
Project 5: Mr. Stakelum	
Objectives for the reporting period	504
Progress achieved including publications	504
Publications	507
Project 6: Dr. Colgan	
Objectives for the reporting period	508
Progress achieved including publications	508
Publications	511
Project 7: Dr. Assimakopoulos	
Objectives for the reporting period	512
Progress achieved including publications	512
Publications	514
Project 8: Dr. Unsworth	
Objectives for the reporting period	516
Progress achieved including publications	516
Publications	521
Project 9: Prof. Jones	
Objectives for the reporting period	522
Progress achieved including publications	522
Publications	524

DEPOSITION OF RADIONUCLIDES ON TREE CANOPIES AND THEIR SUBSEQUENT FATE

Summary of project global objectives and achievements..... 525

Project 1: Dr. G. Shaw, Miss M.J. Minski

Objectives for the reporting period 526
 Progress achieved including publications 526
 Publications 530

Project 2: Dr. Belot

Objectives for the reporting period 531
 Progress achieved including publications 531
 Publications 534

Project 3: Dr. Rauret

Objectives for the reporting period 535
 Progress achieved including publications 535
 Publications 539

Project 4: C. Ronneau

Objectives for the reporting period 540
 Progress achieved including publications 540
 Publications 541
 Publications 543
 Publications 545

BEHAVIOUR OF Cs AND Sr IN NATURAL ECOSYSTEMS AND THE POTENTIAL RADIATION EXPOSURE OF THEIR EXTENSIVE USE

Summary of project global objectives and achievements..... 547

RADIOECOLOGY OF SEMI-NATURAL ECOSYSTEMS

Summary of project global objectives and achievements 579

Project 1: Dr. Colgan

Objectives for the reporting period 587
 Progress achieved including publications 587
 Publications 592

Project 2: Dr. A.D. Horrill, Dr. V.H. Kennedy

Objectives for the reporting period 594
 Progress achieved including publications 594
 Publications 602

Project 3: Dr. Aarkrog

Objectives for the reporting period 603
 Progress achieved including publications 603
 Publications 606

Project 4: Prof. Johanson

Objectives for the reporting period 607
 Progress achieved including publications 607
 Publications 608

Project 5: Dr. Veresoglou	
Objectives for the reporting period	610
Progress achieved	610
TRANSFER OF ACCIDENTALLY RELEASED RADIONUCLIDES IN AGRICULTURAL SYSTEMS (TARRAS)	
Summary of project global objectives and achievements	617
Project 1: Dr. Cancio	
Objectives for the reporting period	620
Progress achieved	620
Project 2: Dr. Maubert	
Objectives for the reporting period	625
Progress achieved	625
Project 3: Dr. Rauret	
Objectives for the reporting period	629
Progress achieved including publications	629
Publications	634
Project 4: Dr. Colle	
Objectives for the reporting period	636
Progress achieved	636
Project 5: Dr. Cawse	
Objectives for the reporting period	640
Progress achieved including publications	640
Publications	642
Project 6: Dr. Grandison	
Objectives for the reporting period	645
Progress achieved including publications	645
Publications	648
Project 7: Dr. Gutiérrez	
Objectives for the reporting period	649
Progress achieved	649
PART II - CONSEQUENCES OF RADIATION EXPOSURE TO MAN; THEIR ASSESSMENT, PREVENTION AND TREATMENT	
	655
Stochastic effects of radiation	657
BIOPHYSICAL MODELS FOR THE EFFECTIVENESS OF DIFFERENT RADIATIONS	
Summary of project global objectives and achievements	659
Project 1: Dr. Paretzke	
Objectives for the reporting period	660
Progress achieved including publications	660
Publications	663

Project 2: Dr. Goodhead	
Objectives for the reporting period	664
Progress achieved including publications	664
Publications	667
Project 3: Dr. Terrissol	
Objectives for the reporting period	669
Progress achieved	669
Project 4: Dr. Leenhouts	
Objectives for the reporting period	672
Progress achieved including publications	672
Publications	673
SPECIFICATION OF RADIATION QUALITY AT THE NANOMETRE LEVEL	
Summary of project global objectives and achievements.....	675
Project 1: Dr. Colautti	
Objectives for the reporting period	677
Progress achieved including publications	677
Publications	678
Project 2: Dr. D.E. Watt	
Objectives for the reporting period	679
Progress achieved including publications	679
Publications	682
Project 3: Theoretical foundations for the specification of radiation quality at the nanometre level: Prof. Dr. D. Harder	
Objectives for the reporting period	683
Progress achieved including publications	683
Publications	684
Project 4: Dr. Leuthold	
Objectives for the reporting period	685
Progress achieved	685
Project 5: Dr. Izzo	
Objectives for the reporting period	687
Progress achieved including publications	687
Publications	690
LATE SOMATIC EFFECTS OF IONIZING RADIATION ON THE MAMMALIAN ORGANISM	
Summary of project global objectives and achievements.....	691
Project 1: Dr. Maisin	
Objectives for the reporting period	692
Progress achieved including publications	692
Publications	708
INDIVIDUAL RADIOSENSITIVITY AND ITS RELATION TO COLO-RECTAL CANCER	
Summary of project global objectives and achievements.....	711

Project 1: Dr. Dutrillaux	
Objectives for the reporting period	713
Progress achieved including publications	713
Publications	715
Project 2: Prof. Léonard	
Objectives for the reporting period	717
Progress achieved including publications	717
Publications	718
Project 3: Dr. Rueff	
Objectives for the reporting period	721
Progress achieved including publications	721
Publications	726
THE GENETIC AND BIOCHEMICAL BASIS OF HUMAN DNA REPAIR AND RADIOSENSITIVITY	
Summary of project global objectives and achievements.....	727
Project 1: Prof. Dr. Lohman	
Objectives for the reporting period	732
Progress achieved including publications	732
Publications	734
Project 2: Prof. Bridges	
Objectives for the reporting period	737
Progress achieved including publications	737
Publications	739
Project 3: Prof. Bootsma	
Objectives for the reporting period	741
Progress achieved including publications	741
Publications	744
Project 4: Dr. Moustacchi	
Objectives for the reporting period	748
Progress achieved including publications	748
Publications	749
Project 5: Dr. Thacker	
Objectives for the reporting period	752
Progress achieved including publications	752
Publications	755
Project 6: Dr. Backendorf	
Objectives for the reporting period	756
Progress achieved including publications	756
Publications	758
EVALUATION OF THE FREQUENCIES OF CHROMOSOMAL ABERRATIONS INDUCED IN HUMAN BLOOD LYMPHOCYTES BY LOW DOSES OF NEUTRONS	
Summary of project global objectives and achievements.....	759

Project 1: Dr. Lloyd	
Objectives for the reporting period	760
Progress achieved	760
Project 2: Prof. Natarajan	766
Project 3: Prof. Dr. Obe	767
Project 4: Dr. Verschaeve	768
Project 5: Dr. Palitti	769
EVALUATION OF EXISTING AND DEVELOPMENT OF NEW HUMAN EPITHELIAL CELL TRANSFORMATION SYSTEMS AND DETERMINATION OF THEIR POTENTIAL IN RADIATION PROTECTION STUDIES	
Summary of project global objectives	771
Summary of global achievements	772
Project 1: Dr. Seymour	
Objectives for the reporting period	774
Progress achieved including publications	774
Publications	777
Project 2: Dr. Riches	
Objectives for the reporting period	779
Progress achieved including publications	779
Publications	781
Project 3: Prof. Pertusa	
Objectives for the reporting period	782
Progress achieved	782
CELLULAR AND MOLECULAR STUDIES ON RADIATION QUALITY: A COMPARISON BETWEEN GENETICALLY RELEVANT DAMAGE AND CELL INACTIVATION	
Summary of project global objectives and achievements	785
Project 1: Dr. Kraft	
Objectives for the reporting period	787
Progress achieved including publications	787
Publications	794
Project 2: Dr. Sideris	
Objectives for the reporting period	796
Progress achieved including publications	796
Publications	798
Project 3: Dr. Lloyd	
Objectives for the reporting period	800
Progress achieved including publications	800
Publications	801
Project 4: Prof. Natarajan	
Objectives for the reporting period	802
Progress achieved	802

RADIATION INDUCED PROCESSES IN MAMMALIAN CELLS: PRINCIPLES OF RESPONSE MODIFICATION AND INVOLVEMENT IN CARCINOGENESIS

Summary of project global objectives and achievements 805

Project 1: Prof. Dr. Van der Eb

Objectives for the reporting period 806
 Progress achieved including publications 806
 Publications 807

Project 2: Dr. Sarasin

Objectives for the reporting period 809
 Progress achieved including publications 809
 Publications 810

Project 3: Dr. Devoret

Objectives for the reporting period 814
 Progress achieved including publications 814
 Publications 815

Project 4: Prof. Rommelaere

Objectives for the reporting period 816
 Progress achieved including publications 816
 Publications 819

Project 5: Dr. Bertazzoni

Objectives for the reporting period 820
 Progress achieved including publications 820
 Publications 822

Project 6: Dr. Thomou-Politi

Objectives for the reporting period 824
 Progress achieved including publications 824
 References 827
 Publications 828

METHODOLOGY FOR THE ANALYSIS OF RADIATION CARCINOGENESIS STUDIES AND APPLICATION TO ONGOING EXPERIMENTS

Summary of project global objectives and achievements 829

Project 1: Dr. Ir. J. Davelaar, Prof. Dr. J.J. Broerse

Objectives for the reporting period 830
 Progress achieved including publications 830
 Publications 833

Project 2: Dr. Chmelevsky

Objectives for the reporting period 834
 Progress achieved including publications 834
 Publications 835

Project 3: Dr. R. Masse

Objectives for the reporting period 836
 Progress achieved 836

Project 4: Dr. M. Morin	
Objectives for the reporting period	840
Progress achieved including publications	840
Publications	841
Project 5: Dr. C. Zurcher	
Objectives for the reporting period	843
Progress achieved	843
Project 6: Prof. Dr. D.W. van Bekkum	
Objectives for the reporting period	849
Progress achieved including publications	849
Publications	850
STUDY OF RADIOBIOLOGICAL EFFECTS AT LOW DOSES	
Summary of project global objectives and achievements.....	851
Project 1: Prof. Coppola	
Objectives for the reporting period	853
Progress achieved including publications	853
Publications	856
LATE EFFECTS IN RHESUS MONKEYS AFTER WHOLE-BODY IRRADIATION WITH W-RAYS AND FISSION NEUTRONS	
Summary of project global objectives and achievements.....	859
Project 1: Dr. Broerse	
Objectives for the reporting period	860
Progress achieved including publications	860
Publications	864
MOLECULAR AND CELLULAR EFFECTS OF PROTONS, DEUTERONS AND ALPHAPARTICLES	
Summary of project global objectives and achievements.....	865
Project 1: Prof. Moschini	
Objectives for the reporting period	870
Progress achieved including publications	870
Publications	873
Project 2: Dr. Goodhead	
Objectives for the reporting period	875
Progress achieved including publications	875
Publications	878
Project 3: Dr. M. Belli	
Objectives for the reporting period	879
Progress achieved including publications	879
Publications	883

Project 4: Dr. B.D. Michael	
Objectives for the reporting period	884
Progress achieved including publications	884
Publications	888
CELLULAR AND MOLECULAR MECHANISMS OF RADIATION-INDUCED MYELOID LEUKAEMIA IN THE MOUSE	
Summary of project global objectives and achievements.....	889
Project 1: Dr. Janowski	
Objectives for the reporting period	891
Progress achieved including publications	891
Publications	893
Project 2: Dr. Cox	
Objectives for the reporting period	894
Progress achieved including publications	894
Publications	896
AUTOMATED DETECTION OF RADIATION INDUCED CHROMOSOME ABERRATIONS BY SLIT-SCAN FLOW CYTOMETRY	
Summary of project global objectives and achievements.....	897
Project 1: Prof. Dr. Barendsen	
Objectives for the reporting period	901
Progress achieved including publications	901
Publications	904
Project 2: Dr. Green	
Objectives for the reporting period	907
Progress achieved including publications	907
Publications	910
References	910
Project 3: Dr. Nüsse	
Objectives for the reporting period	911
Progress achieved including publications	911
Publications	913
Project 4: Prof. Bauchinger	
Objectives for the reporting period	917
Progress achieved including publications	917
Publications	921
Project 5: M. Aubele, G. Burger	
Objectives for the reporting period	922
Progress achieved including publications	922
Publications	928
STUDIES ON BASIC AND APPLIED ASPECTS OF RADIATION-INDUCED CHROMOSOMAL ABERRATIONS IN HUMAN CELLS	
Summary of project global objectives and achievements.....	931

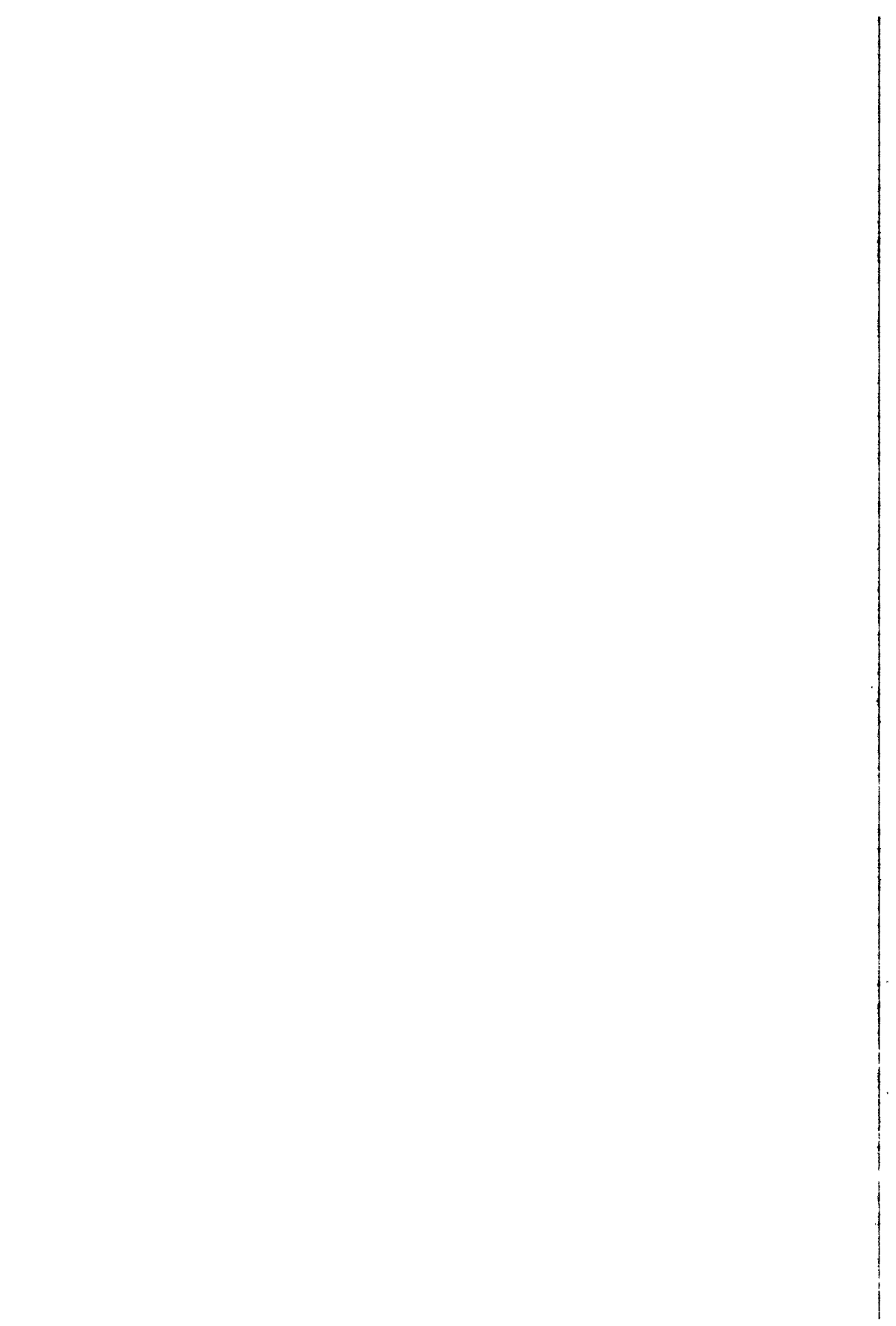
Project 1: Prof. Natarajan	
Objectives for the reporting period	935
Progress achieved including publications	935
Publications	939
Project 2: Dr. Savage	
Objectives for the reporting period	940
Progress achieved including publications	940
Publications	942
Project 3: Prof. Olivieri	
Objectives for the reporting period	943
Progress achieved including publications	943
Publications	944
Project 4: Dr. Cortés-Benavides	
Objectives for the reporting period	948
Progress achieved including publications	948
Publications	949
Project 5: Dr. Bryant	
Objectives for the reporting period	950
Progress achieved including publications	950
Publications	953
Project 6: Prof. Gunnar Ahnström	
Objectives for the reporting period	954
Progress achieved	954
Project 7: Dr. M. Harms-Ringdahl	
Objectives for the reporting period	957
Progress achieved	957
Project 8: Prof. L.E. Feinendegen	
Objectives for the reporting period	958
Progress achieved including publications	958
Publications	961
Project 9: Prof. Johanson	
Objectives for the reporting period	962
Progress achieved including publications	962
Publications	963
Project 10: Prof. L. Ehrenberg	
Objectives for the reporting period	965
Progress achieved	966
Project 11: Dr. Palitti	
Objectives for the reporting period	967
Progress achieved including publications	967
Publications	968

Project 12: Dr. Laurent	
Objectives for the reporting period	970
Progress achieved	970
Project 13: Dr. Pantelias	
Objectives for the reporting period	973
Progress achieved including publications	973
Publications	976
Projects 14 - 15: Dr. Jorge, Dr. Pereira-Luis	
Objectives for the reporting period	977
Progress achieved	977
MEASUREMENT OF TRANSFORMATION OF C3H 10T1/2 CELLS BY LOW DOSES OF IONIZING RADIATION	
Summary of project global objectives	985
Summary of project global achievements	985
Project 1: Dr. Morgan, Mr. Roberts	
Objectives for the reporting period	994
Progress achieved including publications	994
Publications	996
Project 2: Dr. Mill, Dr. Hall	
Objectives for the reporting period	997
Progress achieved including publications	997
Publications	998
Project 3: Prof. Dr. Kellerer, Dr. Hieber	
Objectives for the reporting period	1001
Progress achieved including publications	1001
Publications	1003
Project 4: Dr. Frankenberg	
Objectives for the reporting period	1005
Progress achieved including publications	1005
Publications	1006
Project 5: Prof. Talloni Lombardi, Dr. Bettega	
Objectives for the reporting period	1008
Progress achieved including publications	1008
Publications	1009
Project 6: Dr. Saran	
Objectives for the reporting period	1014
Progress achieved including publications	1014
Publications	1015
RADIATION-INDUCED MUTATIONS IN MAMMALS	
Summary of project global objectives and achievements	1019

Project 1: Dr. Ehling	
Objectives for the reporting period	1020
Progress achieved including publications	1020
Publications	1022
 MUTATION STUDIES UPON SPERMATOGONIAL STEM CELLS OF MAMMALS AND GENETIC TESTS FOR NON-DISJUNCTION IN THE MOUSE	
Summary of project global objectives and achievements.....	1025
 Project 1: Dr. Cattanaach	
Objectives for the reporting period	1028
Progress achieved including publications	1028
Publications	1031
 RADIATION-INDUCED GENETIC EFFECTS IN GERM CELLS OF MAMMALS	
Summary of project global objectives and achievements.....	1033
 Project 1: Dr. Van Buul	
Objectives for the reporting period	1034
Progress achieved including publications	1034
Publications	1034
 RADIATION-INDUCED GENETIC EFFECTS IN GERM CELLS OF MAMMALS	
Summary of project global objectives and achievements.....	1035
 Project 1: Dr. Jacquet	
Objectives for the reporting period	1036
Progress achieved including publications	1036
Publications	1038
 RADIATION-INDUCED GENETIC EFFECTS IN GERM CELLS OF MAMMALS	
Summary of project global objectives and achievements.....	1039
 Project 1: Prof. Streffer	
Objectives for the reporting period	1041
Progress achieved including publications	1041
Publications	1044
 RADIATION-INDUCED GENETIC EFFECTS IN GERM CELLS OF MAMMALS	
Summary of project global objectives and achievements.....	1045
 Project 1: Dr. Van der Schans	
Objectives for the reporting period	1046
Progress achieved including publications	1046
Publications	1048
 RADIOBIOLOGICAL PROPERTIES OF SPERMATOGONIAL STEM CELLS IN C3H/101 HYBRID MICE AND EVALUATION OF THE MODEL FOR INDUCTION OF GENETIC DAMAGE IN SPERMATOGONIAL STEM CELLS	
Summary of project global objectives and achievements.....	1051

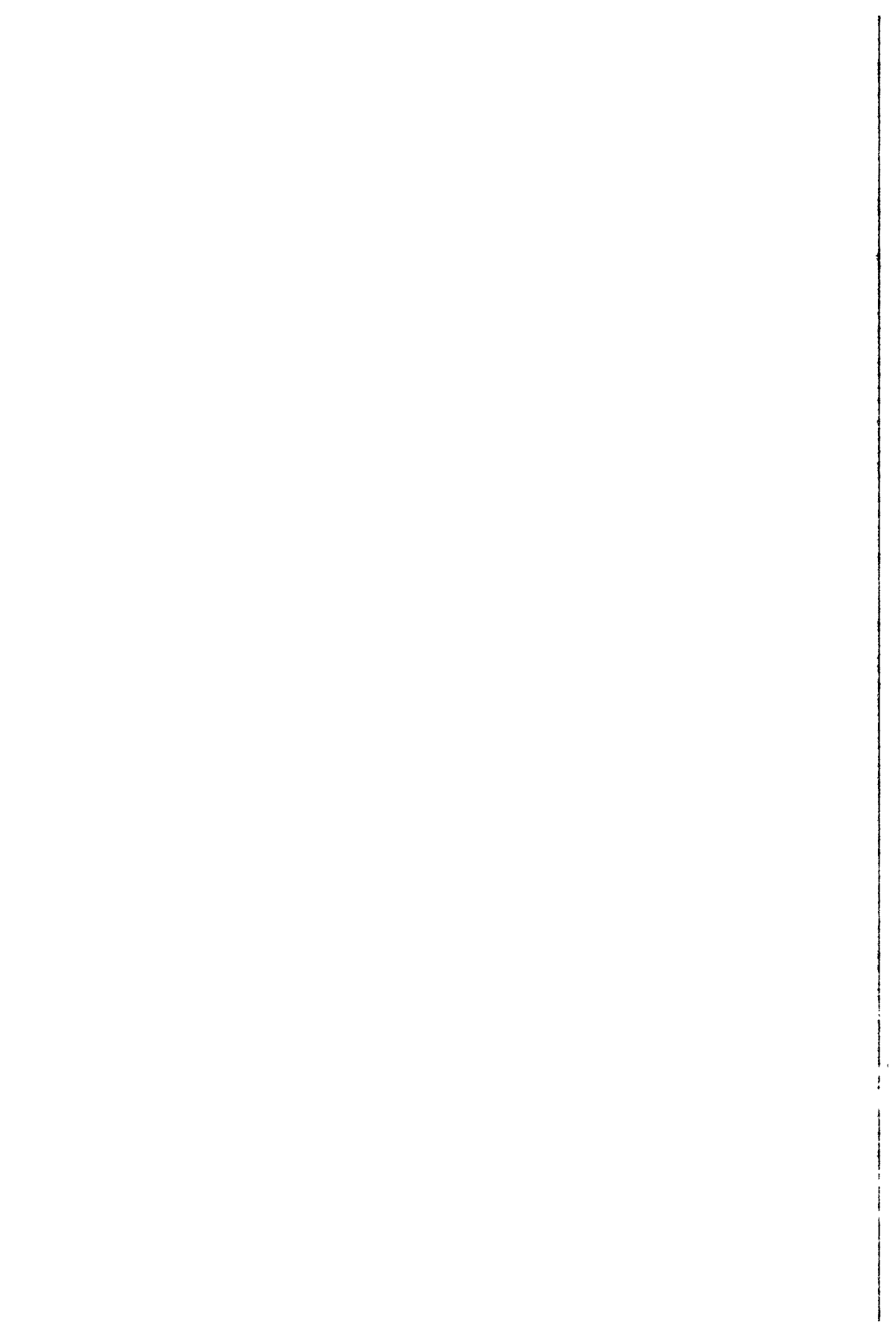
Project 1: Dr. De Rooij	
Objectives for the reporting period	1052
Progress achieved including publications	1052
Publications	1054
 STUDIES ON SPONTANEOUSLY-ARISING GENETIC AND PARTIALLY GENETIC DISORDERS IN MAN WITHIN THE FRAMEWORK OF THE EVALUATION OF GENETIC RADIATION HAZARDS	
Summary of project global objectives and achievements.....	1055
 Project 1: Prof. Dr. Lohman, Prof. Dr. K. Sankaranarayanan	
Objectives for the reporting period	1056
Progress achieved including publications	1056
Publications	1058
 MOLECULAR BIOLOGY OF PATERNAL ONCOGENESIS	
Summary of project global objectives and achievements.....	1061
 Project 1: Dr. Höfler	
Objectives for the reporting period	1062
Progress achieved	1062
 OSTEOSARCOMA AND TUMOURS OF THE HAEMOPOIETIC SYSTEM BY LOW-DOSE IRRADIATION	
Summary of project global objectives and achievements.....	1065
 Project 1: Dr. Höfler	
Objectives for the reporting period	1068
Progress achieved including publications	1068
Publications	1069
 Project 2: Dr. Höfler	
Objectives for the reporting period	1071
Progress achieved including publications	1071
Publications	1072
 Project 3: Dr. Erfle	
Objectives for the reporting period	1073
Progress achieved including publications	1073
Publications	1075
 Project 4: Dr. F. Skou Pedersen	
Objectives for the reporting period	1077
Progress achieved including publications	1077
Publications	1079
 Project 5: Dr. Schoeters	
Objectives for the reporting period	1081
Progress achieved including publications	1081
Publications	1082

Project 6: Dr. Bentvelzen	
Objectives for the reporting period	1083
Progress achieved	1083
 THE DOSIMETRY AND METABOLISM OF INCORPORATED RADIONUCLIDES	
Summary of project global objectives and achievements	1085
 Project 1: Dr. Harrison	
Objectives for the reporting period	1086
Progress achieved including publications	1086
References	1089
 STUDIES ON MYELOID LEUKAEMIA AND OSTEOSARCOMA INDUCED IN MICE BY RA-224	
Summary of project global objectives and achievements	1091
 Project 1: Dr. Humphreys	
Objectives for the reporting period	1093
Progress achieved including publications	1093
Publications	1095
Other references	1096

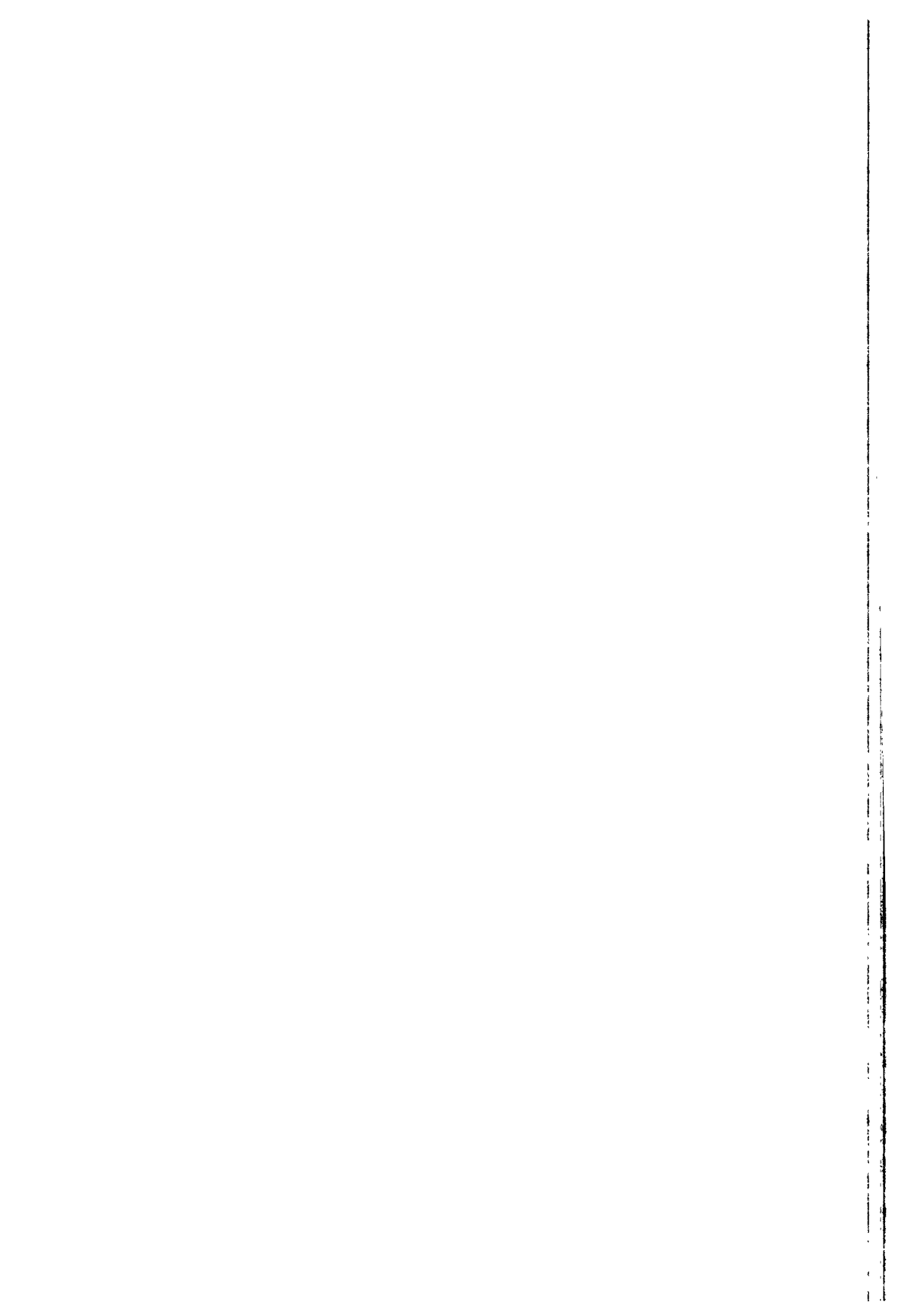


I

**HUMAN EXPOSURE TO
RADIATION AND RADIOACTIVITY**



Measurement of radiation dose and its interpretation



COLLABORATION ON RESEARCH AND DEVELOPMENT CONCERNED WITH THE METHODOLOGY AND DATA IN RADIATION DOSIMETRY

Contract Bi6-026 - Sector A1

1) *Dennis* , EURADOS-CENDOS

Summary of project global objectives and achievements

The global objectives of EURADOS and its project in the terminated programme period 1990-1992 were:

1. The stimulation of collaborative research and technical developments concerning the measurement and evaluation of exposures to and risks of ionizing radiation.
2. The harmonisation of methods for assessing radiation exposures by means of intercomparisons, workshops and active collaboration between laboratories in Europe.
3. The collection and evaluation of physical data relevant to dosimetry and the assessment of occupational, accidental and environmental exposures of the population in the European Communities.

To date, about 180 scientists from 65 laboratories in Western Europe participate in the work of EURADOS. The work of EURADOS is to a large extent performed by Working Groups of about 10 to 15 scientists from different European laboratories. Usually additional corresponding members and observers participate in the work and the meetings of the Groups. Each Working Group is set up by the EURADOS Council to meet defined objectives and once these are achieved a Working Group is disbanded. During the period 1990-1992 the following Working Groups have been active:

WG 1: Development and Implementation of Microdosimetric Instruments for Radiation Protection

This Group worked since 1983 and after successfully completing its tasks, the project was terminated in 1990.

WG 2: Skin Dosimetry

WG 4: Numerical Dosimetry

(Previous title: Dissemination and Development of Computer Programs for Dosimetric Problems)

WG 6: Assessment of Internal Dose

WG 7: Radiation Spectrometry in Working Environments

This Group has been started in 1991

WG 8: Development of Individual Dosimeters for External Penetrating Radiations

WG 9: Criticality Accident Dosimetry

This Group has been started in 1989/90.

WG 10: Basic Physical Data and Characteristics of Gas Ionization Devices

This Group has been started in 1990, partially taking over tasks from the former WG 5 which has been terminated in 1990.

The detailed objectives and achievements of the Working Groups are described in the following sections except those of Working Group 1 which has been given in the final report of the foregoing research period.

Every year EURADOS has organized a general meeting with all Working Groups together. In a common session the Working Groups presented their programmes and further actual topics were discussed. The last two meetings were performed in Lisboa (1990) and Dublin (1991). Protocols of the meetings are published in the yearly reports of the EURADOS chairman.

Within this project, EURADOS has mainly funded the meetings of the Working Groups and partially workshops and intercomparison measurements, while the individual research work at the participating laboratories and the preparation of those meetings have been funded by the contributing laboratories.

Working group 2: Skin dosimetry

Chairman: *M. W. Charles, P. Christensen* (until 1991)

Objectives for the reporting period and progress achieved

The working group has been involved in 7 main work areas listed below. The results of the group had a major influence on the revised recommendations of the ICRP (ICRP Publications 59 and 60). The group was closely involved with the organisation of a Skin Dosimetry Workshop held in May 1991 in Dublin. This meeting had excellent international representation and much of the work of the group has been presented. Proceedings of the workshop have been published in *Radiat. Prot. Dosim.* 39 (1-3).

The activities of the working group are:

1. Theoretical and experimental study of hot particle dosimetry
(*Charles* (coordinator), *Darley, Patau, Herbaut*)

This project is concerned with the problems of measuring and calculating doses from small beta radioactive sources. Sources below 1mm in diameter are commonly referred to as 'hot particles'. Renewed interest in the biological effect and dosimetry of such sources has been shown as a result of the Chernobyl reactor accident and as a result of practical problems on aging US PWR reactors (2). Dosimetry studies of a 1mm diameter $^{90}\text{Sr}/^{90}\text{Y}$ beta source have been carried out using a scanning small-electrode extrapolation chamber and radiochromic dye films (3,4). Radiochromic dye measurements were carried out in collaboration with Dr. Baum and Soares of the BNL and the NIST who are corresponding members of WG 2. It was found that the extrapolation chamber response was non-linear and tended to underestimate doses to small areas by a factor in excess of two compared to radiochromic dye films. A theoretical model was developed to explain the non-linear response and as a result good agreement was found between the two techniques. Radiochromic dye film measurements were carried out at Berkeley using manual and preliminary image analysis densitometry. This compared favourably with a more sophisticated and rapid method of laser scanning densitometry used by Dr Soares. These measurements have now been extended to neutron activated ^{60}Co and good agreement has again found between Dye film and extrapolation chamber (using a non-linear fit). The initial Monte-Carlo codes produced by Dr. Patau at the University of Toulouse (5) have proved to be user-friendly and reasonably fast and have produced dose estimates for spherical ^{60}Co test sources. These have been compared with semi-empirical calculations of beta doses utilised in a recently developed American code VARSKIN II. The doses calculated by various methods, over areas of 1mm^2 and 1cm^2 , are in reasonable agreement but are lower by a factor of 2 than data from measurements.

2. Study of extrapolation chamber measurement method

(*Böhm, Chartier, Christensen (coordinator), Francis*)

An intercomparison of extrapolation chambers and measurement procedures used for characterising low energy beta radiation fields has been organized among four European laboratories (CEA, France; NRPB, UK; PTB, FRG and RNL, Denmark) in order to standardise procedures for determining dose rates using extrapolation chambers. All participants used ^{147}Pm extended area sources (4 cm x 4 cm) constructed to the same specifications in identical holder and supplied by one manufacturer from the same batch. Different types of extrapolation chambers were used and measurement procedures and evaluation methods differed between the laboratories. Sources were exchanged between the laboratories to enable measurements on the same source to be carried out with different types of chambers. Due to the low penetrability of low energy beta radiation, a number of sources of uncertainty involved with the extrapolation chamber measurement method became more significant for measurements with low energy beta sources (e.g. ^{147}Pm) than with high energy sources (e.g. $^{90}\text{Sr}/^{90}\text{Y}$). In particular, three components of measurement could lead to major differences in the final results: absorption in air between source and detector, the evaluation of depth dose in tissue by the measurement of dose absorption in the front window and the evaluation of ionisation current under Bragg-Gray conditions. Some results were presented at the Workshop on Skin Dosimetry (6). A final report is in preparation.

3. Study of individual dosimeters

(*Christensen (coordinator), Francis, Gasiot, Herbaut, Kriegseis*)

Recent progress obtained in the development of individual dosimeters for the measurement of skin doses was reported in some papers presented at the Skin Dosimetry Workshop in Dublin (1). Monitoring of skin doses requires a personal dosimeter capable of measuring $H_p(0.07)$ with satisfactory accuracy. It has been suggested that in the case of high accidental exposures of the skin it may also be worth-while to make an assessment of a depth dose profile to enable a prognosis to be made either of the early or late effects that may follow. There are several thin detectors available based on the TL and TSEE techniques, which enables to assess the dose to the skin at different depths (7). However, further developments are still needed to adapt these detectors for practical routine applications of monitoring weakly penetrating photon radiations (8,9).

4. Benchmark experiment on the determination of dose rates from a $^{90}\text{Sr}/^{90}\text{Y}$ source

(*Böhm (coordinator), Patau, Herbaut*)

Dose rates at different distances from from a 6 cm diameter $^{90}\text{Sr}/^{90}\text{Y}$ source have been measured using extrapolation chambers. Measurements were performed by CEA (Grenoble) and PTB. The final evaluation of the data is not yet finished, because experiences from the study of extrapolation chambers (see section 2) should be considered before stating the final results. Due to the delay in the preparation of the final report on extrapolation chambers, the final evaluation of the PTB was also delayed. It is planned to exchange and discuss the data at least during the EURADOS meeting in Paris in november 1992. Final results will be available at the end of 1992.

5. Study of workplaces
(Heinzelmann)

A survey has been made of weakly penetrating radiation in German nuclear power plants and during fuel element fabrication. The dose equivalent rate from weakly penetrating radiation may be up to 100 times as great as that from strongly penetrating radiation. The radiation fields in nuclear power plants differ greatly. K capture emitters have to be taken into consideration. The radiation is frequently well shielded by radiation protection clothing and the skin dose from weakly penetrating radiation is, therefore, often small. During fuel element fabrication the dose equivalent rate is mainly caused by high energy beta radiation. This radiation is only slightly attenuated by radiation protection clothing. Therefore, the beta skin doses are often larger than the dose equivalent from strongly penetrating radiation. Hot particles do not appear to be a problem in Germany. The review of workplaces in Germany (10,11) is complete and was presented at the Skin Dosimetry workshop. On this basis recommendations on the dosimetry of external weakly penetrating radiation have been drawn up.

6. Rewiew of survey instruments for the measurement of skin dose rates
(Burgess, Christensen (coordinator), Marshall, Paretzke, Piesch)

Work has continued in analysing the present situation with respect to requirements and capabilities of survey instruments for the measurement of skin dose rates from external radiations at workplaces with the purpose of giving guidance to manufacturers as well as users of these instruments. Evaluations have been made of implications of the new recommendations by ICRP and ICRU for the design and performance criteria of the instruments. Survey instruments for measuring skin dose rates should be designed to measure the directional dose equivalent, $H'(0.07)$. As the radiation fields at the workplaces normally contain both weakly and strongly penetrating radiations, it will be practical, if the instruments in addition can also measure dose rates for evaluating doses to the deeper organs, i.e. they should be designed also to measure the ambient dose equivalent, $H(10)$. A review document describing the present situation of survey instruments for the measurement of skin dose rates is under preparation.

7. Collaboration with EULEP on biological effects of skin irradiation

The evaluation of the biological effects of various sizes of several energy beta radiation sources has been carried out in pig and mouse skin under the auspices of EULEP. EURADOS Working Group 2 provides radioactive source construction, dosimetry and analysis expertise as part of this collaborative project. An investigation of skin cancer in mice following spatially uniform and non-uniform sources has shown that uniform exposure is more carcinogenic than non-uniform exposures. This has provided important evidence against a 'hot particle' enhancement factor. An investigation of early and late deterministic effects (eg moist desquamation, ulceration, atrophy etc.) in pig skin has provided information on the dose response for these effects which has provided the basis for the recent revisions of ICRP basic recommendation (13). The information on the target position of cells in the skin for the various effects provides important data for the design of skin dosimeters for chronic and acute, routine and accident situations (14). Further radiobiological studies are

currently investigating the effect of radioactive particles of Co-60 which are commonly found in power reactors. The implications for practical beta dosimetry are being considered by an ICRU task group which has strong representation from EURADOS Working Group 2.

Publications

1. Proceedings of EURADOS Workshop on Skin Dosimetry. Dublin 1991 (Eds: H.G. Menzel, P. Christensen, J.A. Dennis). Radiat. Prot. Dosim. 39 (1-3) (1991).
2. M.W. Charles. The hot particle problem. Proceedings of EURADOS workshop on skin dosimetry. Radiat. Prot. Dosim. 39 (1-3) 39-47, (1991).
3. P.J. Darley, M.W. Charles, C.D. Hart, J. Wells and M.S.E. Coleby. Dosimetry of planar and punctiform beta sources using automated extrapolation chamber and radiochromic dye films. Proceedings of EURADOS workshop on skin dosimetry. Radiat. Prot. Dosim. 39 (1-3), 61-66 (1991).
4. C.G. Soares, P.J. Darley, M.W. Charles and J.W. Baum. Hot particle dosimetry using extrapolation chamber and radiochromic foils. Proceedings of EURADOS workshop on skin dosimetry. Radiat. Prot. Dosim. 39 (1-3), 55-60 (1991).
5. J.P. Patau. Monte Carlo calculations of the depth dose distribution in skin contaminated by hot particles. Proceedings of EURADOS workshop on skin dosimetry. Radiat. Prot. Dosim. 39 (1-3), 71-74 (1991).
6. T.M. Francis, J. Böhm, J.L. Chartier and P. Christensen. Experience gained on extrapolation chamber measurement techniques from an intercomparison exercise conducted with a 147 Pm source. Radiat. Prot. Dosim. 39, 109-114 (1991).
7. W. Kriegseis, H. Kessler, K. Rauber, A. Scharmann, J.L. Chartier, C. Itie and M. Petel. Response of TSEE dosimeters of foil-covered Beo thin films to beta radiation. Radiat. Prot. Dosim. 39, 127-130 (1991).
8. E. Piesch, B. Burgkhardt, S. Goldbach and M. Vilgis. The effect of secondary electrons on the photon energy response of TL and TSEE detectors used for beta and photon dosimetry. Radiat. Prot. Dosim. 39, 187-190 (1991).
9. P. Christensen, L. Botter-Jensen, K. Ennow and B. Majborn. Dosimeter configurations for the measurement of $H_s(0.07)$ and $H_p(10)$ from photons. Radiat. Prot. Dosim. 34, 111-114 (1990).
10. M. Heinzlmann. Experiences and problems of skin irradiation at workplaces in Germany. Radiat. Prot. Dosim. 39, 173-181 (1991).
11. M. Heinzlmann, G. Hallfarth, D. Regulla, G.H. Schepell and U. Welte. Recommendations on dosimetry of weakly penetrating radiation in nuclear power plants. Radiat. Prot. Dosim. 39, 183-186 (1991).
12. P.H. Burgess, T.O. Marshall and E.K.A. Piesch. The design of ionisation chambers for the measurement of Weakly penetrating radiations. Radiat. Prot. Dosim. 39, 157-160 (1991).
13. R.J.M. Fry, M.W. Charles, T.F. Gesell, J.W. Hopewell and R.E. Shore. The biological basis for dose limitation in the skin. ICRP Skin Task Group Report. ICRP Publication 59. The biological basis of skin dose limitation. Annuals of the ICRP 22 (2) (1991).
14. M.W. Charles. A Generation consideration of the choice of dose limits, averaging areas and weighting factors for the skin in the light of revised skin cancer risk figures and experimental data on non-stochastic effects. Intern. Journal of Radiat. Prot. 57(4) 841-858 (1990).

Working group 4: Numerical dosimetry

Chairman: *B.R.L. Siebert*

Objectives for the reporting period

The main objectives of the Working Group were

- to study and test computer codes developed for applications in radiation transport and dosimetry,
- to coordinate and assist in the use of computer codes in the field of radiation transport and dosimetry,
- to stimulate and coordinate the calculation of fluence-to dose conversion factors and dose distributions in phantoms and,
- to intercompare detector response functions calculated by different computer codes.

Progress achieved

An intercomparison of Bonner sphere unfolding codes was performed. It concentrated on the unfolding problem, ignoring response function uncertainties by assuming the responses to be known precisely. It was a 'blind' intercomparison, in that no spectral information was available beforehand, except for the energies of any monoenergetic component. 12 sets of solutions were presented by 8 participants. A detailed report on the work is available (1). A mathematical analysis of the results has been published in addition (2). The group especially acknowledges the effort of its consultant A. Alevra who organized the intercomparison.

The intercomparison was followed up by a benchmark study on response functions for Bonner spheres. The study concentrated on a particular set consisting of a spherical ^3He detector at the center of moderating polyethylene spheres of different sizes. Two polyethylen densities (0.92 g cm^{-3} and 0.95 g cm^{-3}) are considered. First results are available from six different authors using ANISN, MCNP, MCBEND and own codes. ANISN has the advantage of needing negligible computing times and the disadvantage of being restricted to spherical geometry. The other codes employed are full scale Monte-Carlo codes and therefore need long run times. They, however, allow other geometries (e.g. cylindrical counters) and the detailed study of resonance effects which at higher neutron energies become quite important for larger spheres. For thermal neutron energies discrepancies have been found which may be due to the use of different data. In order to analyze these discrepancies and to gain physical insight the computed neutron fluences were studied in addition to the response functions. One member of the working group prepared a new set of thermal neutron group cross sections for polyethylene which in part deviate significantly from those presently used. A report is available upon request. The collated results of the first part of the intercomparison have been published (ref. 3) and a final report is presently being prepared. The intercomparison of calculated and measured Bonner sphere responses was the next logical step. First results have been published (4). Obviously smaller spheres afford a more realistic model of the central detector (sphere and stem are to be described!). For larger spheres it could be shown that the

partial pressure of ^3He in the detector can in principle be determined by comparing measured with calculated responses.

Two WG members contributed to the numerical study of external radiation dose from Cs ground contamination. In calculations for a number of isotopes an agreement of about 2% was found. In more detailed calculations of organ doses some differences have been found. Some of these may be due to interpretational rather than calculational problems. This, once again, demonstrated the need of agreement upon phantoms for external and internal dosimetry.

In addition, two WG members agreed on a benchmark problem for photon and electron transport at interfaces. They studied the influence of the air gap in a calorimeter. One uses the code EGS and the other his own code. The main problem in this work is the extreme long computing time needed for achieving acceptable uncertainties. Hence final results have not yet been achieved.

The analytic code from Coyne and Caswell (NIST, Gaithersburg), which allows the energy deposition by secondary charged particles to be computed analytically is now available within Europe. An authorized version can be obtained from PTB.

In order to meet the increasing need for standardizing phantoms for external and internal dosimetry a subgroup has been founded. Discussions of this subgroup concentrated on the shortcomings of the MIRD phantom. The MIRD phantom is essentially a reference body for the mass and volume of man and his organs. It does not represent the range of human sizes, and it does not include a representation of the form or age of organs. Its chemical composition is not specified and it is not representative of children. A better approach to providing a phantom may be in terms of a voxel model where the body is represented in terms of voxels each of which has a number which identifies its position and material composition. The main problem with this approach, however, is seen with the considerable computer storage needed and the slow access time. Some voxel phantoms are already being studied, e.g. at GSF, Neuherberg.

Of again increasing importance are calculations and evaluations of fluence-to-dose equivalent conversion functions. An example of an evaluation is given in ref. 5. In addition to conversion functions a knowledge of albedo from calibration phantoms is needed for individual dosimetry in practice. A report on neutron albedo from phantoms and simple models of man has been published (6). The results can be summarised as follows:

The shape and the material of the phantom used in calibrations have some influence on the albedo and hence on the response of dosimeters which utilise this albedo in the detection process. In routine radiation protection, however, differences in readings due to this effect may be tolerated.

Encouraged by the EURADOS council, new emphasis has been given to the computation of neutron fluence-to-dose equivalent conversion factors, in order to meet new requirements put forward by ICRP Publication 60. A workshop on this topic based on the recommendations of the ICRP took place at the PTB in February 1992. The group agreed to provide the needed new conversion functions and to include to the calculations also perspex as material for calibration phantoms.

The working group discussed new efforts to develop and improve computer codes which include secondary radiation. One member and his coworkers extended the MCNP code in order to treat photon produced secondary electrons.

A general discussion on the dissemination and development of computer programs for dosimetric problems showed the need of more guidance for common users and the group tried to respond to this need. A questionnaire on the use of computer codes in applied numerical dosimetry which has been worked out. While the response was, however, up to now scarce, the efforts will be continued aiming to activate more users.

The group enforced the direct collaboration with other groups, especially Working Group 7 and 10. A first contribution in support of the objectives of Working Group 7 has been presented (7). Working Group 10 is supported by helping to collect *W*-values. An evaluation of *W*-values for protons in methane based TE-gas will be published.

Publications

1. A.V. Alevra, B.R.L. Siebert, A. Aroua, M. Buxerolle, M. Greccescu, M. Matzke, M. Mourges, C.A. Perks, H. Schraube, D.J. Thomas, H.L. Zabarowski. Unfolding Bonner Sphere Data: A European Intercomparison of Computer Codes. Laborbericht PTB-7.21-1990-1 (Braunschweig, 1990)
2. A.V. Alevra, M. Matzke, B.R.L. Siebert, Findings of an International Unfolding Intercomparison with Bonner Spheres. 7th ASTM-Euratom Symposium on Reactor Dosimetry (Strasbourg 1990)
3. C.A. Perks, D.J. Thomas, B.R.L. Siebert, S. Jetzke, G. Hehn and H. Schraube. Comparison of Response Function Calculations for Multispheres. VII-th Symposium on Neutron Dosimetry, Berlin 1991 (Proceedings to be published in Radiat. Prot. Dosim.)
4. B.R.L. Siebert, E. Dietz, S. Jetzke. Comparison of Measured and Calculated Bonner Spheres Responses for 24 and 144 keV Incident Neutron Energies. VII-th Symposium on Neutron Dosimetry, Berlin 1991 (Proceedings to be published in Radiat. Prot. Dosim.)
5. B.R.L. Siebert, A. Morhart. A Proposed Procedure for Standardising the Relationship Between the Directional Dose Equivalent and Neutron Fluence. Radiat. Prot. Dosim. 28 (1989) 47-51
6. B.R.L. Siebert, W.G. Alberts, B.W. Bauer. Computational Study of Phantoms for Individual Neutron Dosimetry. PTB Report N-6 (Braunschweig, 1990)
7. B.R.L. Siebert, H. Schraube, D.J. Thomas. Catalogue of Neutron Fields in Radiation Protection Environments and Programmes to obtain Appropriate Calibration Factors for Neutron Dosimeters. VII-th Symposium on Neutron Dosimetry, Berlin 1991 (Proceedings to be published in Radiat. Prot. Dosim.)

Working group 6: Assessment of internal dose

Chairman: *J.A.Gibson*

Objectives for the reporting period

1. monitor a research programme on stable isotope metabolic studies which are funded by the CEC in the 1990-94 Euratom RP Programme;
2. organise an intercomparison of assessment methods used in Europe, using data from actual exposures, so that dose records of internal doses can be confidently used across national boundaries;
3. monitor a study contract with CEC DGXII to propose European Registries of Internal Dosimetry (ERID) to include assessment data, autopsy data and models used in assessments;
4. cooperate with EULEP through a joint task group on 'Deposition and Clearance of Inhaled Particles in the Human Respiratory Tract (Human Lung) to assess the implications of the new ICRP and NCRP lung models on dose assessments including an assessment of the sensitivity of predicted doses to variations in the model parameters;
5. propose new research programmes and intercomparison studies to both CEC DGXI and DGXII.

Progress achieved

The whole Working Group 6 met twice during the period in Lisboa and Dublin at the EURADOS General Meetings. The contract to study stable isotope metabolism was started and progress is discussed below; the results of the intercomparison have been analysed and are in press; a study contract to determine the feasibility of the establishment of European registries of dose assessment, autopsy data and models for the assessment of internal dose has been completed; a joint task group with EULEP on Human Lung dynamics has been set up and met in Chilton in 1990 and in Reisenburg and Edinburgh in 1991; and a proposal was submitted to DG XI for an intercomparison involving an exposed individual.

1. Stable Isotope Studies

The principal objective of the programme is to investigate the use of stable isotope tracers to improve source terms for models of internal dosimetry from environmental exposure to radioactive materials. Stable isotope tracers are being used directly as markers (e.g. Sr), and as analogues (lanthanide series elements as actinide analogues). The use of stable isotopes tracers allows the extension of this principle to critical groups, where radiotracers cannot be used. This project has attracted partial CEC funding for collaborative work with groups in Germany and Italy.

Analytical methods have been successfully set up for the determination of lanthanide series elements in foodstuffs, urine and faeces. Excretion data have been determined for four male volunteers, and dietary intake estimated from analysis of a standard diet excluding beverages. These data have shown the relative abundances of the lanthanide series elements in diet and excreta to follow the naturally occurring relative abundances, suggesting that similar mechanisms of gut uptake apply for all elements in the series. The data for dietary intake and faecal excretion for each element are comparable, as would be expected. However, daily urinary excretion is typically around 10% that of faecal excretion, implying gut uptake factors to be greater than 3×10^{-4} , as quoted by ICRP. The absolute values of urinary excretion for the lanthanides is equivalent to data recently produced by alternative analytical methods at the CEC Joint Research Centre, Ispra. This has important implications for internal dose estimates from environmental exposure.

The results obtained have been used to design a dual isotope administration experiment for a number of lanthanide series elements, and barium (an analogue for radium). Ethical permission has been granted for a simultaneous administration of these elements, by ingestion and injection, in two volunteers and this is proceeding currently to determine f_1 values for the respective elements. Ethical permission has also been granted for a dual isotope administration for strontium, to measure f_1 values and faecal excretion in a group of five volunteers, as part of the CEC programme, and this is also proceeding currently. A similar experiment is being carried out at GSF, Frankfurt using alternative measurement techniques.

Discussions with a group at the University of Liverpool over the proposed administration of strontium stable isotope to a group of neonates, have proved fruitless as their facilities and staff were not geared to the sample collection required. Further discussions are now taking place with a neonatal research group at a London teaching hospital, who have experience in and a current programme of administration of tracer compounds to neonates. It is hoped that ethical permission will be sought and a study carried out over the remainder of this financial year.

The results of the preliminary study of lanthanide absorption currently being carried out will be used to design a larger study of gut uptake of the lanthanides and barium, in up to twenty volunteers of both sexes. Experimental design will be carried out in conjunction with GSF, Neuherberg to obtain relevant source terms for input to internal dosimetry models. The experiment will be designed to yield information on gender differences and age-related differences in fractional gut absorption. It is known that dietary status can affect the fractional gut absorption of metals and metal complexes, and this will be investigated in a separate experiment on the same group of volunteers.

The data obtained at Harwell will be complemented by volunteer studies at GSF, Frankfurt on fractional gut absorption using extrinsically and intrinsically labelled foodstuffs. Animal studies at KfK, Karlsruhe of body distribution of these elements, will also be carried out to further assess the validity and limitations of their use as actinide and radium analogues. GSF Neuherberg will analyse the experimental data to assess their implication to current dosimetry conventions.

The data obtained from this work and the CEC collaboration will demonstrate the use of the technique for the consideration of many of the variables which may be encountered in population dosimetry.

The techniques developed can then be used to provide source term data for radium and actinide analogues in critical population groups. At the same time, it would be proposed that the techniques be applied to other elements of radiological significance, such as cerium, ruthenium and zirconium or other analogues such as hafnium (a potential analogue for plutonium).

2. Intercomparison of Assessment Methods

A draft report on the intercomparison involving 9 European laboratories was produced and a final report will be published in Radiation Protection Dosimetry (15) with detailed methodology in a CEC document (14). Differences between laboratories have been largely eliminated and the results give confidence that dose records of internal doses should be transferable between countries taking part in the intercomparison.

3. European Registry for Internal Dosimetry (ERID)

This proposal was designed to establish the basis for setting up a European Registry for Internal Dosimetry, ERID, divided into three parts:

- a. ERIDA, a European registry of internal dose assessments using information supplied by European laboratories and obtained from the literature;
- b. ERAD, a European registry of autopsy data using information obtained by individual laboratories in each European country;
- c. ERMID, a European registry of mathematical models used for internal dose assessments in European laboratories and in the literature.

A study contract has been used to establish protocols, in consultation with European laboratories through EURADOS Working Group 6 and with the US Uranium and Transuranium Registries, in order to produce compatible databases for ultimate exchange of information. An intercomparison of dose assessment methods, organised by WG 6, is essentially complete and has formed the basis of the protocols. The ultimate objective is to ensure compatibility of internal dose records within Europe in the context of 1992.

ERIDA Protocols have been established for collecting data for the assessments registry and a prototype database using Superbase 4 in a Microsoft Windows environment has been produced. Further development will depend upon the availability of funds.

ERAD At the instigation of BNFL, the UK has established a management group to devise a protocol for a UK registry of autopsy data from former workers. When this protocol is agreed then European participation will be considered and some further funding will be required.

ERMID A proposal to use an Expert System for internal dose assessments was made in order to provide a computer tool for rationalising the approach

to this difficult problem within Europe. Experience with the approach proposed for criticality accident dosimetry has demonstrated validity for a similar problem involving sparse data with many variables and we are confident that, with appropriate funding, a computer program can be prepared of general applicability within Europe.

4. Joint EULEP/EURADOS Task Group on the Human Lung

The objective of the group is to produce improved respiratory tract models used to relate intakes by workers to organ doses and bioassay measurements, and to calculate the distribution of doses, particularly among the general population, resulting from any given exposure.

Assessment of radiation doses incurred when radioactive materials are inhaled requires knowledge of breathing rates; the dependence of regional deposition on particle size and physiological parameters; clearance kinetics from each respiratory tract region and for different materials; and morphometric parameters on which to calculate doses to tissues at risk. The deposition and clearance of inhaled particles have been extensively studied, because of the importance of the inhalation route, and significant advances have been made, resulting in the current revision of the ICRP lung model, but important gaps in knowledge remain. There are few data on submicron or hygroscopic particles, and major uncertainties about clearance kinetics in each region of the respiratory tract. Most human inhalation studies have been conducted on small groups of healthy men, but there is a need to quantify the effects of age, sex, disease, ethnic type etc.

The Task Group is addressing areas where existing models used in radiation protection are known to be weak. Experimental studies are quantifying parameters for the human respiratory tract and elucidating deposition and clearance mechanisms. Particular emphasis is placed on determining the extent to which particles deposited in, or cleared through, the bronchial tree may be retained in proximity to the bronchial epithelium, which is considered to be of relatively high radiosensitivity. Models are being developed to interpret and extrapolate the limited data available, identify research needs, and calculate deposition, retention and doses resulting from inhalation of radionuclides.

Two proposals before the group are:

- I. an analysis of the sensitivity of doses predicted by the new ICRP lung model to the uncertainty in the parameters; and
- II. the integration of the new ICRP lung model with other biokinetic models to produce a general model for dosimetry and bioassay.

Whilst proposal (I) is clearly within the remit of the task group the second proposal will require cooperation with other task groups within EULEP.

5. Intercomparison Study Proposal using Exposed Persons

An outline proposal has been submitted to DG XI and was discussed in detail in Dublin in May 1991. The idea is to use a person adventitiously contaminated

with ^{60}Co or gamma-ray emitting radionuclides (e.g. ^{133}Ba could well be a better test in that Harwell has subjects with well-known body contents).

The person chosen would need to be fit and available over an extended period of at least 12 and up to 24 weeks and be willing to travel and accept being in up to 12 countries for about 4 nights at a time. Unless the subject were of sufficient seniority, they would need to be accompanied by a knowledgeable researcher to act as guide, interpreter and possibly control subject. He should preferably, have had a single intake on a known date or chronic intake over a well-defined period. The activity level would need to be stable or reducing slowly and predictably and easily detectable in well-shielded counters.

The first and last visit would be to the organising laboratory for detailed tests similar to tests at other laboratories. Body monitoring could be carried out at more than one laboratory in a country if it could all be scheduled within the week. The schedule would include time at home but some weekends may be spent away in transit between laboratories.

It is envisaged that the intercomparison would be of the main nuclide, e.g. ^{60}Co or ^{133}Ba plus ^{137}Cs (and ^{134}Cs) from Chernobyl (if significant) and ^{40}K in the subject with the control obtained from measurements on the guide. Whole body monitoring and/or body scans would be made on two separate days at each laboratory with measurement at the start and finish of the intercomparison at the organising laboratory. Four daily urine samples would be taken during each visit, divided in two with half analysed by the test laboratory and half by the organising laboratory. (Pairs of samples may be bulked and divided to give the equivalent of 2 daily samples for each laboratory).

DG XI would select one test laboratory in each EC country capable of performing all the measurements and be willing to organise other intercomparisons within their own country.

The objective of the intercomparison is to establish a common basis of whole body measurements, urine analysis and internal dose assessments within the European Community so that internal dose records transferred with workers moving between member states can be recognised as valid in the host country with an appropriate degree of confidence.

Publications

1. Bailey, M. R. The Third International Workshop on Respiratory Tract Dosimetry, Albuquerque. J. Soc. Radiol. Prot. 10, 305-307 (1990)
2. Bailey, M.R. and Birchall, A. New ICRP dosimetric model for the respiratory tract: A progress report. Radiol. Prot. Bull. No. 119 (1991)
3. Bailey, M.R., Birchall, A., Cuddihy, R.G., James, A.C. and Roy, M. Compartment models for the mechanical clearance of particles from the respiratory tract of humans and laboratory animals (abstract). Proceedings of the Symposium on Particle-Lung Interactions: "Overload" Related Phenomena, Rochester, J. Aerosol Medicine 3, 68 (1990)

4. Bailey, M.R., Birchall, A., Cuddihy, R.G., James, A.C. and Roy, M. Respiratory tract clearance model for dosimetry and bioassay of inhaled radionuclides. Proceedings of the Third International Workshop on Respiratory Tract Dosimetry, Albuquerque. Radiat. Prot. Dosim. 38 (1/3) 153-158 (1991)
5. Birchall A. Uncertainty in bioassay determinations of plutonium intakes. Chilton, NRPB-M207 (1990)
6. Birchall, A. Reply to Coleman: "First-order compartmental models and the matrix of mean residence times". Health Phys. 59. 360 (1990)
7. Birchall, A., Bailey, M.R., and James, A.C. LUDEP: A lung dose evaluation program. Proceedings of the Third International Workshop on Respiratory Tract Dosimetry, Albuquerque. Radiat. Prot. Dosim. 38 (1/3) 167-174 (1991)
8. Birchall, A., James, A.C., and Muirhead, C.R. Adequacy of personal air samplers for monitoring plutonium intakes. Radiat. Prot. Dosim. 37, 179-188 (1991)
9. Bradley, E.J. and Prosser, S.L. The measurements of polonium and plutonium in human foetal tissues. In: Proceedings of CEIR Forum on Radionuclides and External Radiation: Implications for the Embryo and Foetus. (1990)
10. Bull, R.K. and Morrison, R.T. Calculation of annual limits of intake, excretion and retention of mixed fission products. BNES Conference on Occupational Radiation Protection, Guernsey (1991)
11. Dorrian, M-D. and Etherington, G. Radiocaesium in NRPB staff following the Chernobyl Accident. Radiol Prot. Bull. No. 110 (1990)
12. Etherington, G. and Dorrian, M-D. Radiocaesium levels, intakes and doses in a group of adults resident in southern England. Proceedings of the International Symposium on Environmental Contamination following a Major Nuclear Accident, IAEA, Vienna, Vol. 2, 327-338 (1990)
13. Gibson, J.A.B. and Bull, R.K. The Interpretation of Bioassay and In-vivo Data with the Proposed ICRP Lung Model and the Establishment of European Registries of Internal Dose Assessments, Models and Autopsy Data. Third International Workshop on Respiratory Tract Dosimetry, Albuquerque. Radiat. Prot. Dosim. 38 (1/3), 105-112 (1991)
14. Gibson, J.A.B., Birchall, A., Bull, R.K., Henrichs, K., Iranzo, C.E, Lord, D.J., Piechowski, J., Sollett, E., Tancock, N.P. and Wernli, C. European Intercomparison of Methods Used for the Assessment of Systemic Burdens of Internally Deposited Radionuclide. (CEC, DG Telecommunications, Information Industries and Innovation, Luxembourg). Radiation Protection Report EUR 14195 EN (1992)
15. Gibson, J.A.B, Birchall, A., Bull, R.K., Henrichs, K., Iranzo, C.E, Lord, D.J., Piechowski, J., Sollett, E., Tancock, N.P. and Wernli, C. European Intercomparison of Methods Used for the Assessment of Systemic Burdens of Internally Deposited Radionuclide. Radiat. Prot. Dosim., in press (1991)
16. Inn, K.G.W., Liggett, W.S., Volchok, H.L., Feiner, M.S., McInroy, J.F., Popplewell, D.S. et al. Interlaboratory comparison of actinides in human tissue: ^{239}Pu and ^{240}Pu . J. Radioanal. Nucl. Chem. 138, 219-229 (1990)
17. James, A.C., Gehr, P., Masse, R., Cuddihy, R.G., Cross, F.T., Birchall, A., Durham, J.S. and Briant, J.K. Dosimetry model for bronchial and extrathoracic tissues of respiratory tract. Proceedings of the Third International Workshop on Respiratory Tract Dosimetry, Albuquerque. Radiat. Prot. Dosim. 37, 221-230 (1990)
18. Parker, R.C., Bull, R.K., Stevens, D.C. and Marshall, M. Studies of aerosol distributions in a small laboratory containing a heated phantom. Ann. Occup. Hyg. 34, 35-44 (1990)
19. Popplewell, D.S., Harrison, J.D. and Ham, G.J. The gastrointestinal absorption of neptunium and curium in humans. Health Phys. 60, 797-805 (1991)
20. Ramsden, D., Birchall, A., Bull, R.K., Foster, P.P., Gibson, J.A.B., Strong, R., Taylor, N.A., Tylor, G.R. and Wraight, J. Laboratory intercomparison of methods used for the assessment of systemic burdens of plutonium. Rad. Prot. Dosim. 30, 95-99 (1990)

Working group 7: Radiation spectrometry in working environments

Chairman: *H. Klein*

Objectives for the reporting period

The determination of dose equivalent quantities in mixed neutron/photon fields is still a problem because of the strong neutron energy dependence of the dose equivalent response of commonly used monitors. Instruments with spectrometric properties, however, are assumed to solve this problem. In recent years different (trans)portable spectrometers have been developed for application in radiation protection practice.

The main objectives of EURADOS Working Group 7 are:

- to review the different systems available at European laboratories,
- to discuss their properties particularly those relevant to applications in working environments,
- to intercompare the systems by performing measurements in well specified calibration fields or working environments and
- to investigate the use of spectrometric measurements in the interpretation of area and individual dosimeter readings for the assessment of organ doses and effective doses.

Recommendations will be elaborated concerning the applicability of the different systems, the procedures for determining and verifying response functions and the unfolding methods.

Progress achieved

The objectives, the programme and the list of members proposed for the new WG7 were discussed by the EURADOS General Assembly and approved by the Council in May 1991. The first meeting (13 WG7-members plus 12 consultants and observers) was held in November 1991 at the PTB in Braunschweig. The status, problems and future developments of neutron and photon spectrometry were discussed separately.

1. Neutron spectrometry

To provide reliable risk estimates for workers exposed to neutrons, details of the radiation field must be known and spectrometric measurements are necessary, because no presently available dosimeter measures the required area or individual dose equivalent correctly. Various requirements for measurement systems are:

- they should provide both the energy and directional dependence of the neutron fluence,
- the energy resolution must be reasonable, particularly in the energy region between 10 keV and 1 MeV where the fluence-to-dose equivalent conversion factor varies strongly, or information on the mean quality factor must be provided alternatively,
- an overall uncertainty of 10 % is required for integral fluence values (15 % for dose equivalent) in the entire or selected energy regions,

- considering the recent ICRP recommendations dose equivalent rates of a few Sv/h should be measurable,
- the instruments must be portable, preferably battery powered and easy to decontaminate and
- short term and averaging long term measurements should be possible.

The spectrometers used by WG7-members for radiation protection applications have been checked with respect to these requirements. All spectrometers were designed to provide isotropic response in order to meet the requirements for ambient dose equivalent monitors. Indeed, the construction of a portable neutron spectrometer with a specific directional response over the entire energy range seems to be impossible. A rough estimate of the directional distribution may be derived from the reading of 4 to 6 monitors mounted on different sides of a phantom.

Nearly all establishments have now access to Bonner sphere systems. They cover the energy range from thermal to about 20 MeV, can be employed at dose rates from 10 nSv/h to 10 mSv/h depending on the central detector used and are insensitive to photons. The energy resolution of this spectrometer, however, is very limited. A benchmark exercise (organised by WG4) of the few-channel unfolding procedures most frequently used demonstrated that the integral fluence and dose equivalent can be evaluated with the desired uncertainty of 10 and 15 %, respectively, provided that the response matrix is reasonably well specified. Most calculated response functions have to be adjusted to experimental calibration data.

Other neutron spectrometers are in use at some institutes of WG members. They are:

- proton recoil proportional counters (10 keV - 1.5 MeV)
- organic liquid scintillation detectors (> 0.5 MeV)
- He-4 filled proportional counters (1.5 - 15 MeV).

These detectors show a much better energy resolution and reasonable n/ γ -discrimination properties. They, however, cover only a limited energy range. Various combinations often including a reduced set of Bonner spheres have therefore been used, but up to now no procedure is generally accepted for the simultaneous unfolding of data from different instruments. Working Group 7 deals some efforts on this task in close cooperation with EURADOS WG 4.

2. Radiation fields for intercomparison measurements

For tests of spectrometers the working group intends to perform intercomparison measurements in different reference radiation fields:

- the "realistic" neutron field realised at the 14 MeV neutron generator in Cadarache/CEA. At this calibration facility the field contains thermal, 1/E and fission neutron spectra contributions similar to those encountered at working places. The spectrum has been optimized by MCNP simulations. A small scale intercomparison has already been carried out and its analysis is in progress.
- the direct and room scattered neutrons from radionuclide sources (Cf-252, D₂O-moderated Cf-252, Am/Be(γ ,n)) available at the PTB,
- specially moderated fission spectra available at the ASPIS facility of the NESTOR test reactor at Winfrith,
- real working environments where a considerable fraction of the dose equivalent is due to neutrons.

The possibilities of comprehensive measurements have been investigated and the planning of first detailed intercomparisons are going on.

3. Other spectrometric and dosimetric systems

Commonly used area and individual dosimeters, the latter mounted on a phantom, will be included in the intercomparison. Tissue equivalent proportional counters (TEPC) have proved to be reasonable dosimeters by using γ -spectrum information. While their response functions show an energy dependence which results in the ambient dose equivalent of soft neutrons being considerably underestimated, attempts have already been made to overcome this problem by a suitable admixture to the filling gas. This will further be studied and the intercomparison measurements will also be used to investigate how the spectral information can in addition be used to reduce the energy dependence of the dose equivalent response.

4. Photon spectrometry

The situation in operational photon dosimetry is much better than for neutrons. In general, the commonly used instruments are able to measure the photon dose also in the presence of a considerable neutron dose fraction. The new phantom-related quantities, ambient and directional dose equivalent, now require some attention, because their fluence-to-dose equivalent conversion functions deviate from those to air kerma strongly in the energy range between 10 keV and 150 keV. For that reason there is some interest in photon spectrometry. Above 3 MeV there is also little known about the energy dependence of the response of commonly used dosimeters.

Some photon spectrometers, e.g. NaI(Tl) and BGO scintillation detectors or Ge semiconductor diodes, are well suited preferably in pure photon fields because its neutron and photon responses cannot be separated. Some organic scintillation detectors, e.g. NE213, allow however a separate measurement of neutron and photon induced pulse height spectra simultaneously. The versatile electron/photon transport code EGS4 has been used to calculate the photon response matrix of an NE213 spectrometer. The response functions simulated will be further checked by experimental data. After calibration the fully specified spectrometer will be intercompared in the described fields.

Publications

Due to the late start of the Working Group no publication has been finished up to the end of this research period

Working group 8: To develop and improve techniques for the individual dosimetry of ionising radiation

Chairman: *J.R. Harvey*

Objectives for the reporting period

The introduction of new operational quantities in individual monitoring as proposed by the ICRU and the assumed implementation of the new ICRP recommendations into practice obviously underlines the necessity of developing and improving techniques for individual dosimetry of ionising radiation. This was the main objective of the EURADOS Working Group 8. While the efforts during 1990/91 has been concentrated on individual dosimetry for neutron radiation, it has been decided at the EURADOS Council Meeting in Dublin, 1991, to extend the scope of the Working Group also to photon radiation with special view on the consequences of the ICRU and ICRP recommendations.

Progress achieved

The activities of the Working Group 8 has been focussed on three different areas.

1. Track-etch detectors

While track-etch detectors have been investigated and used for applications in neutron dosimetry since more than 20 years, there remains even today many problems for routine use of such detectors in radiation protection monitoring. The various types of plastic materials used give rise to differences in counted background and sensitivity. Each group using track-edge detectors applies its own etching procedures and no standardization has been achieved until today. The aim of the group was to interchange the experience obtained with different types of plastic material and to discuss the different etching techniques. During the Working Group meetings in 1990 and 1991 the participants presented results of their investigations performed at home. These presentations provided also the basis for the various intercomparisons organized by the Working Group.

A joint study has been carried out on the background and sensitivity characteristics of etch plastic from various sources. The results have been carefully analysed and will be published by the NRPB, UK, in the near future.

2. Intercomparison measurements

Intercomparison measurements are a very important task in the development, investigation and testing of individual dosimeters because it checks not only the quality of the detector itself but also that of the evaluation procedure. The Working Group has in the past organized four international intercomparisons the last of which was performed in 1990/1991 (5). Dosimeters of 14 participating laboratories were irradiated in monoenergetic neutron fields with energies of 0.114 keV, 0.565 keV, 5.3 MeV and 14.7 MeV and in neutron fields from Cf-252. In view of the potential weakness of track-edge dosimeters for obliquely incident neutron radiation, the irradiating laboratories, the GSF (Neuherberg) and the PTB

(Braunschweig), kindly agreed to include some none-normal irradiations. Hence irradiations were carried out at 0, 30 and 60 degrees and in addition for a range of doses at 5.3 MeV.

The following laboratories participated in the intercomparison:

1. Batelle Pacific Northwest Labs., Richmond, USA
2. Berkeley Nuklear Laboratories, Berkeley, England
3. Bureau of Radiation and Medical Devices, Ottawa, Canada
4. Dresden Technical University, Dresden, Germany
5. ENEA, Rome, Italy
6. ENEA, Bologna, Italy
7. KFK, Karlsruhe, Germany
8. Laboratoire de Dosimetrie, Alger, Algeria
9. NRPB, Chilton, England
10. Paul Scherrer Institute, Villigen, Switzerland
11. PTB, Braunschweig, Germany
12. Riso National Laboratory, Riso, Denmark
13. University of Barcelona, Barcelona, Spain
14. University of Thessaloniki, Thessaloniki, Greece
15. GSF, Neuherberg, Germany (irradiation laboratory only)

As can be seen this latest joint irradiation programme has beside members from CEC countries also incorporated groups from continental America and Algeria. The results which have been subject to a critical analysis, have once again provided a unique guide to the current performance of track-etch neutron dosimetry systems.

As a result of this intercomparison the group has decided to organize another intercomparison measurement in 1992 which should concentrate on specific tasks. In particular the directional dependence and the linearity of the dose equivalent response will be investigated at a range of energies. In addition, the PSI laboratory has kindly agreed to perform irradiations at 46 MeV and 66 MeV neutron energies. This unique irradiations will provide valuable information about the applicability of track-edge neutron detectors for dosimetry in aircrafts and around high-energy accelerators.

3. ICRP and ICRU recommendations

Following the approval of the EURADOS Council the work of the group has now been extended. The group's proposal to hold a workshop on the practical aspects of personal dosimetry, particularly with regard to the implications of the recent recommendations of the ICRU and the ICRP was accepted and a workshop titled

"Individual Monitoring of Penetrating Radiation - the Impact of Recent Recommendations of the ICRU and the ICRP"

will be held at PSI, Villigen, Switzerland from 5th to 7th of May, 1993. A small subgroup has been established to discuss the detailed programme.

Publications

1. Schraube, H. Response of Proton-Sensitive Etched-Track Detectors to Fast Neutrons. GSF-Bericht 22/90 (1990)
2. Luszik-Bhadra, M., Alberts, W.G., Dietz, E. and Guldbakke, S. A Track-Etch Neutron Dosimeter with Flat Response and Spectrometric Properties. Nucl. Tracks Radiat. Meas. 19, 485-488 (1991)
3. Harvey, J.R. A three Element track-edge Neutron Dosimeter with good Angular and Energy Response. Symp. on Neutron Dosimetry, Berlin 1991 (to be published in Radiat. Prot. Dosim.)
4. Luszik-Bhadra, M., Alberts, W.G., Dietz, E., Guldbakke, S. and Matzke, M. A wide-range Neutron Dosemete Based on a CR-39 Track Detector. To be presented at the 16th Conf. on Nuclear Tracks in Solids, Beijing 1992.
5. Alberts, W.G. International Study of CR-39 Track-Etch Neutron Dosimeters (EURADOS-CENDOS 1990). Symp. on Neutron Dosimetry, Berlin 1991 (to be published in Radiat. Prot. Dosim.)

Working group 9: Criticality accident dosimetry

Chairman: *R. Médioni*

Objectives for the reporting period

The main task of the Working Group in the reporting period (1990-1992) was to plan an intercomparison of criticality accident dosimetry systems at the SILENE reactor (Valduc, France) and to develop a complete protocol to be used during the intercomparison. For this objective it has been necessary to establish a reference dosimetry and to perform spectrometric measurements in the different leakage radiation fields from the SILENE reactor source available when using shields of different materials. A characterisation of these radiation fields is required before they can be used for the proposed international intercomparison of the criticality accident dosimetry systems.

It was planned to carry out spectrometric and dosimetric measurements at one reference location and to investigate the uniformity of the radiation field around the source for two configurations (the bare source and the source shielded by lead). These data shall provide the basis for the detailed protocol to be set up for the intercomparison of accident dosimeters.

Progress achieved

During the period 1990 - 1992 four meetings were held in order to discuss the programme of the investigations, the contribution of the various groups to this work and the more detailed schedule.

All discussions and arrangements for the intercomparison have been performed in close cooperation with the CEC, DG XI (Dr. Schnuer) and DG XII (Dr. Menzel), with the IAEA (Dr. Griffith) and the CEA group operating the SILENE reactor at Valduc. Because of the high costs for the use of the SILENE research reactor, its use could not be funded within the EURADOS budget. In order to be able to perform the full intercomparison, a close collaboration with DG XI was achieved and the further dosimeter irradiations at the SILENE reactor will be funded by a contract with DG XI of the CEC.

As a first step in the preparation of the intercomparison, the leakage radiation fields from the SILENE reactor were investigated by performing dosimetric and spectrometric measurements. In summary, the following measurement techniques have been applied for the investigation of the radiation fields.

1. For neutron radiation:

- Proton and alpha recoil proportional counters together with a Bonner sphere spectrometer were used for high resolution neutron spectrometry.
- Activation detectors and fission chambers were used for fluence and spectrometric measurements.
- Twin ionisation chambers (tissue-equivalent and aluminum chambers) were applied for the measurement of absorbed dose due to neutrons and photons.

- A tissue-equivalent proportional counter (TEPC) was used to measure dose equivalent and to determine the mean quality factor of the radiation.
 - Silicon diodes have been used mainly for relative fluence and dosimetric measurements.
2. For photon dosimetry, a Geiger-Müller (GM) counter and various thermoluminescent dosimeters (LiF₂(Tl), alumina) were applied.

Neutron spectrum and neutron dose measurements were carried out at one reference position on an arc of 4 m radius from the reactor axis using all available techniques. The photon dose was determined separately. The results of these measurements will be used to provide the best "reference values" of neutron and gamma-ray doses for the forthcoming intercomparison.

During the intercomparison a large area will be required to irradiate accident dosimeters from many participants, both in free-air conditions and on phantoms, simultaneously. This is necessary in order to reduce the expensive irradiation time. For that reason measurements have been performed also at other positions around the 4 m arc in order to establish and check the uniformity of the radiation field. Activation detectors, silicon diodes and TLDs have been used.

Two different radiation fields have been investigated. The first field is the leakage field from the bare unshielded experimental reactor source (the SILENE reactor core is a compact annular stainless steel vessel with an outer diameter of 36 cm containing the fissile solution with ²³⁵U-enriched uranium). The other field investigated stems from the same source which in this case is surrounded by a cylindrical lead shield of 10 cm in thickness. The shielding reduces the photon component of the field and decreases the mean energy of neutrons at 4 m distance from the source. Both radiation fields are of interest in accident dosimetry.

Most measurements were carried out by R. Médioni (CEA, Fontenay aux Roses) and H.J. Delafield (AEA, Harwell). Supporting measurements were contributed by D.J. Thomas and A.G. Bardell (NPL, Teddington) with a Bonner sphere spectrometer, by P. Pihet (Universität Homburg/Saar) with an LET-spectrometer (TEPC) and by scientists from CEA/Cadarache.

In order to perform a true and realistic intercomparison measurement it has been decided, not to publish the final results of the dosimetric and spectrometric measurements at the reference position before the intercomparison is carried out and the participants have presented their uncorrected results. Some general statements, however, can be given as a result of the measurements:

1. both neutron and gamma-ray measurements performed at the 4 m-radius arc show that the radiation field is generally uniform within 5 % for more than 6 m arc length around the circumference. This will allow the exposure of dosimeters on 2 or 3 anthropomorphic phantoms and in free air simultaneously.
2. The various independent measurements of the neutron and photon dose components are in good agreement and the results can therefore be used to define "reference values" for the intercomparison.

A next meeting is planned on 3rd of November 1992 in Paris and the final planning

and arrangements for the intercomparison measurements, which will be performed in June 1993, has been started.

With the results of this intercomparison it is aimed to hold a workshop on accident dosimetry in 1994.

Publications

1. Medioni, R. Silène: Source de Rayonnements de Référence. Proc. IRPA 8 Conference, Vol I (1992)
2. Medioni R. Working Group 9: Criticality accident dosimetry. In: EURADOS-CENDOS Chairmens Report 1990-1991 (ed. J. Dennis) (1992)
3. Delafield, H. International intercomparison of criticality accident dosimetry systems at Silène. Presented on Meeting at Fontenay aux Roses, May 1991
4. Barbry, F. and Medioni, R. SILENE, a Source of Reference Radiation Fields. Symp. on Neutron Dosimetry, Berlin 1991 (to be published in Radiat. Prot. Dosim.)
5. Medioni, R., Buxerolle, M., Delafield, H.J. and Perks, C.A. Reference Measurements of the Leakage Radiation Field from the SILENE Reactor (Lead shield) for an International Intercomparison of Criticality Accident Dosimetry Systems. Symp. on Neutron Dosimetry, Berlin 1991 (to be published in Radiat. Prot. Dosim.)

Working group 10: Basic physical data and characteristics of gas ionisation devices

Chairman: *P. Pihet*

Objectives for the reporting period

The Working Group 10 was initiated in Lisboa (Eurados General Assembly, 1990) with the aim to exchange information and to collaborate with respect to the following topics:

- the study of basic physical data (electron collision cross sections, W -values, stopping powers) relevant for gas ionisation devices,
- the modelling and experimental study of proportional counters with the aim to improve the knowledge of detector basic properties and search for the best characteristics of the detectors to meet the requirements of specific applications,
- the study of gas ionisation devices (e.g. low pressure proportional counters) for providing experimental data (ionisation-, dose-, radial distributions) relevant to the understanding of basic mechanisms of radiation action in biological systems,
- the improvement of computer codes and calculations for micro- and nanodosimetry applications in order to support new trends in detection methods.

Progress achieved

The first meetings were focused on reviewing knowledge recently improved with regard to the understanding of electrical discharge processes in cavities filled at low pressure and of energy transfer processes in irradiated matter. This knowledge includes basic collision cross section data as well as average interaction quantities such as kerma and W values. After setting priorities to specific tasks the Working Group concentrated the programme of the second year on the following subjects:

1. The improvement of electron molecule cross sections in organic gases and their application to detector modelling and basic research of W

Electron collision cross sections with molecules in organic gases are the primary quantities required to improve the knowledge of W and gas gain in cavities filled with tissue-equivalent (TE) gas. The methods developed several years ago at the University of Toulouse to determine such cross section data in methane and methane-based TE gas were applied to determine the corresponding cross sections in propane and isobutane. No such data were available although these gases are widely used in experimental microdosimetry. The current research is directed towards combined theoretical and experimental works aimed at verifying the consistency of cross section data tables and providing quantitative assessment of the accuracy which can be achieved.

2. A comprehensive evaluation of W values for neutrons and their uncertainty as a function of energy

The basic quantity required to convert the ionisation yield into energy deposition, the "average energy required to create an ion pair", W , is of fundamental interest for dosimetry and microdosimetry. W values for charged particles and average W values for the spectra of secondary charged particles are of practical relevance for the interpretation of ionisation yield spectra measured with PCs and for the determination of the accuracy achievable for mixed field dosimetry using gas detectors. A study was started to evaluate the consequences of recent W data for charged particles, especially protons, on the average W values for neutrons (W_n) as a function of energy. The work is aimed at reporting on :

1. a critical assessment of fitted curves for proton W values in the energy intervals 0.5 keV to 10 keV, 5 keV to 100 keV and 50 keV to 500 keV;
2. an update of mean W values for neutrons including new data for neutron energies above 20 MeV;
3. quantitative assessments for the uncertainties of neutron W values depending on the method used, the uncertainty of W values and kerma data for the secondary charged particles.

The evaluation of W values for protons is in progress and will be presented soon. W_n values at high neutron energies were assessed using the results of recent kerma experiments with low pressure proportional counters (Pihet et al., 1992). These data will be improved using the best fits of $W(E)$ for charged particles and improved kerma calculations at high neutron energies (Taylor et al., 1992). The emphasis will be placed upon the uncertainty of W_n with regard to the accuracy requirement of various types of applications and the neutron energy range. The work took into account the comprehensive review of W values for charged particles in preparation by an IAEA Committee and an earlier report on W_n prepared at the GSF, Neuherberg (1987).

3. The study of gas gain in low pressure proportional counters

Two collaborations have been initiated aimed at comparing experimental and theoretical determination of gas gain in microdosimetric counters (KFA Jülich, Univ. of Toulouse) and verifying the accuracy of gas gain modelling in non-equilibrium situations for PCs using an ion probe as experimental set-up (INFN Legnaro, Univ. of Toulouse).

The suitability of PC techniques is well recognised for various applications in dosimetry and microdosimetry, e.g. for operational radiation protection instruments, for investigation of radiation quality in radiobiology and for neutron kerma measurements. The knowledge of basic detector properties, however, remained poor namely due to the lack of reliable electron-molecule cross section data and appropriate simulations of charge collection processes. The progress achieved recently allows now to improve the response of PCs and to extend their range of applicability. A difficulty commonly encountered consists, however, when reducing the gas pressure leading to the enlargement of the avalanche region and the deterioration of equilibrium conditions between electron mean free path and electrical field gradient.

A modelling of PC's is achieved by combining different methods:

1. the determination of electron molecule cross sections and related swarm parameters (drift velocity, ionisation coefficients) for the full energy range of secondary electrons;
2. the calculation of the electrical field distribution taking into account precisely the counter geometry and its electrical design;
3. macroscopic calculation of gas gain for high and intermediate pressures using the solution of coupled continuity and Poisson equations;
4. microscopic calculations for low pressures using Monte-Carlo calculations.

The programme is concentrated on the consistency of the gas gain calculations and cross section data by initiating combined experimental and theoretical works and the application of modelling techniques to simulate the response of different kinds of detectors in comparison with experimental results. A collaboration with Columbia University (New York) was initiated to investigate the potential properties of ultra-miniature counters operated at variable pressures.

4. The preparation of a detailed report on the design and the construction of low pressure proportional counters

A large effort was made to settle the edition of a report on the design and the construction of low pressure tissue equivalent proportional counters (TEPC). The work was strongly motivated by the research programme of the participating groups and the urgent need to provide detectors with good performance. The participants indeed encounter in general large difficulties to get reliable detectors especially to meet the requirements of operational instruments for radiation protection applications and some groups are tentatively developing their own sensors. No commercial alternative exists to date. The work enables the exchange of scientific and technical information of relevance. The report is aimed at providing a condensed information of the experience gained on how to design and construct this type of instrument and formulating practical recommendations. The scope of the report includes seven sections dedicated to:

- the design of PCs and their limitations in size,
- the gas gain and microdosimetric modelling of PCs,
- the electrical design of PCs,
- the materials used and related engineering techniques,
- the mechanical and electrical construction of PCs,
- the counter operation and
- the applications of PCs.

Each section is covered by several papers under the coordination by a major contributor. From outside scientists and engineers well known for their experience in the field of detector development were asked to contribute. In particular, a collaboration was established with colleagues from USA who intend to actively contribute to the report. A complete draft of the report is scheduled for the end of 1993.

The work of the Group was organised in small task groups. Particularly, with regard to the application of detector modelling calculations, direct collaborations between the participating laboratories were initiated by contributing towards the progress of several university graduate works. Recently the programme was further discussed in a full Working Group meeting held at Toulouse.

Publications

1. Barthe, J., Mourgues, M., Bordy, J.M., Boutruche, B., Lahaye, T., and Portal, G. Etude de compteurs miniatures pour la dosimétrie individuelle des neutrons. Proc. IRPA 8 Conference, Vol I, 479-482 (1992)
2. Bordy, J.M. Caractérisation d'un compteur proportionnel équivalent tissue à dérive, Memoire CNAM, Paris (1992)
3. Colautti, P., Conte, V., Talpo, G., Tornielli, G., and Bouchefer, M. A method to investigate the working characteristics of new microdosimetric detectors which use low gas pressures. Nucl. Inst. Meth. submitted (1992)
4. Peres, I. Modelisation de la cinétique électronique et ionique dans les compteurs proportionnels cylindriques. Thesis, Univ. Toulouse (1990)
5. Pihet, P., Gerdung, S., Grillmaier, R.E., Kunz, A. and Menzel, H.G. Critical assessment of calibration techniques for low pressure proportional counters used in radiation dosimetry. Symp. on Neutron Dosimetry, Berlin 1991 (to be published in Radiat. Prot. Dosim.)
6. Pihet, P., Guldbakke, S., Menzel, H.G. and Schuhmacher, H. Measurement of kerma factors for carbon and A-150 plastic: neutron energies from 13.9 to 20.0 MeV, Phys. Med. Biol., in press (1992)
7. Schrewe, U.J., Brede, H.J., Gerdung, S., Kunz, A., Meulders, J.P., Nolte, R., Pihet, P. and Schuhmacher, H. Determination of kerma factors of A-150 plastic and carbon at neutron energies between 45 and 66 MeV, Symp. on Neutron Dosimetry, Berlin 1991, Radiat. Prot. Dosim. in press (1992)
8. Schuhmacher, H., Brede, H.J., Henneck, R., Kunz, A., Meulders, J.P., Pihet, P. and Schrewe, U. J. Measurement of neutron kerma factors for carbon and A-150 plastic at neutron energies of 26.3 and 37.8 MeV, Phys.Med.Biol. in press (1992)
9. Verma, P.K. and Waker, A.J. Optimisation of the electric field distribution in a large volume tissue equivalent proportional counter. Phys. Med. Biol. in press (1992)
10. Waker, A.J., Eivasi, M.T. and Williams, T.T. Low energy X-ray dosimetry in standard fields using low pressure proportional counters. Phys. Med. Biol. in press (1992)
11. Wang, J., Segur, P., Bordage, M.C. Determination of low energy electron-molecule cross sections in Silane. Proc. XX ICPIG, Pisa 1991, Vol 2, 446 (1991)

QUANTITIES, UNITS AND MEASUREMENT TECHNIQUES FOR IONIZING RADIATION

Contract Bi6-322 - Sector A11

1) *Allisy*, Bureau Intern. des Poids et Mesures

Summary of project global objectives and achievements

Objectives of the project

The development of internationally acceptable recommendations regarding:

- (1) Quantities and units of radiation and radioactivity,
- (2) Procedures suitable for the measurement and application of these quantities in radiation protection as well as in clinical radiology and radiobiology,
- (3) Physical data needed in the application of these procedures, the use of which tends to assure uniformity in reporting.

The ICRU considers and makes recommendations in the field of radiation protection.

Progress achieved

During the period 1 January 1990 - 30 April 1992, important progress was achieved on the development of ICRU reports related to significant problems in radiation protection, radiology and radiobiology. This included completion of the work on a number of reports, the advancement of drafting work on other documents, and the initiation of important new activities.

Work was essentially completed on the following ICRU Reports which have been approved by the ICRU for publication:

ICRU Report 46, *Photon, Electron, Proton, and Neutron Interaction Data for Body Tissues*

ICRU Report 47, *Measurement of Dose Equivalents from External Photon and Electron Radiations.*

ICRU Report 48, *Phantoms and Computational Models in Therapy, Diagnosis and Protection*

ICRU Report 49, *Stopping Power and Ranges for Protons and Alpha Particles.*

ICRU Report 50, *Prescribing, Recording and Reporting Photon Beam Therapy*

ICRU Report 46, *Photon, Electron, Proton and Neutron Interaction Data for Body Tissues*, is a companion volume expanding on the material covered in ICRU Report 44, *Tissue Substitutes in Radiation Dosimetry and Measurement*. The new

report provides specific information on representative sets of tissues that illustrates the effects of tissue composition variation on the pertinent radiation interaction quantities. It includes photon, electron, proton and neutron interaction data for body tissues, covering the age interval from fetus to adult. Soft tissues, skeletal tissues and calculi are considered. Soft tissues include adipose tissues, brain, breast (including component tissues), heart, liver and muscles (skeletal), which includes the connective tissue, blood vessels, blood, lymph, etc., generally associated with striated muscle. Skeletal tissues and calculi include cortical bone, breast calcification, cholesterol gallstones and various types of urinary (renal) stones. The first tabulation in the report provides elemental compositions, mass and electron densities of the complete set of body tissues. This is followed by a tabulation (184 pages) of the photon, electron, proton, and neutron interaction data. These include mass attenuation coefficients, electron mass stopping powers, electron mass scattering powers, proton stopping powers and neutron kerma factors. (A copy of the Report is enclosed.)

The ICRU has initiated a new program to make available on computer disks the bodies of data contained in ICRU Reports. The first release in this category, ICRU Report 46D, will provide all photon, electron, proton and neutron interaction data for body tissues as set out in ICRU Report 46.

The work on measurement of dose equivalent has resulted in the development of ICRU Report 47, *Measurement of Dose Equivalents from External Photon and Electron Radiations*. The report is now in press. It is the third report in the series treating determination of dose equivalent. The first report of the series, ICRU Report 39, *Determination of Dose Equivalents from External Radiation Sources*, provided definitions of quantities to be employed in radiological protection monitoring. ICRU Report 43, *Determination of Dose Equivalents from External Radiation Sources -- Part 2*, provided the grounds for the Commission's selection of the quantities and the basis for their definition. ICRU Report 47 provides guidance on the design, calibration and use of instruments required to implement the recommended system of dose determination. Covered in the new report are principles of measurement, operational quantities, characteristics of instruments, calibrations and the impact of the new operational quantities on the design of future instrumentation. Among the instruments characterized are ionization chambers, proportional counters, scintillation detectors, semiconductor detectors, photographic film, thermoluminescent dosimeters, thermally stimulated exoelectron emission detectors and photoluminescent detectors. An appendix provides conversion factors for dose equivalent quantities.

ICRU work on phantoms has resulted in the development of ICRU Report 48, *Phantoms and Computational Models in Therapy, Diagnosis and Protection*. This report is also in press. The development of realistic body phantoms and computational modes

is strongly dependent on the availability of comprehensive human anatomical data. Yet this information is often missing, incomplete or not easily available. In recognition of this, Report 48 emphasizes organ and body masses and geometries. The influence of age, sex and ethnic origins on human anatomy is considered. Existing types of phantoms and computational models used with photons, electrons, protons and neutrons are reviewed. Detailed specifications of more than ninety phantoms and computational models are provided in the report.

Current ICRU work on stopping powers is part of a broad program that encompasses stopping powers for electrons and positrons (Report 37), protons and alpha particles, and heavy ions. The work on the report on protons and alpha particles is now nearing completion with the printers' manuscript now in preparation. This will be published as ICRU Report 49, *Stopping Power and Ranges for Protons and Alpha Particles*. The report includes discussion of the stopping power formula and various corrections. It covers electronic (collision) stopping powers and nuclear stopping powers. Provided in the report is a comparison of tabulated and experimental stopping powers. Energy loss straggling and methods for stopping power measurement are treated in Report 49. In tables covering 148 pages, the report provides, for materials of interest in radiological physics and biomedical dosimetry: (1) electronic, nuclear and total stopping powers, (2) ranges, and (3) detour factors.

At its last meeting, the ICRU approved another report, *Prescribing, Recording, and Reporting Photon Beam Therapy*. This will be published as ICRU Report 50. The preparation of the printers' manuscript is now underway. The report was prepared in recognition of the fact that in the decade since its predecessor (Report 29) was published, it has become clear that further interpretation of the concepts relating to prescribing, recording and reporting therapy is required, as well as guidelines for application of ICRU recommendations in this area. These are provided in the new report, which also recognizes the expanding use of computers in radiotherapy.

In connection with the work on radiation quantities and units, the ICRU took an important step in connection with recommendations relating to radiation protection. The ICRU specified that the draft material on this subject, prepared for ultimate inclusion in the Commission's overall report on quantities and units, should be published in draft form in the ICRU NEWS. Through this mechanism, the Commission is seeking input from all of those interested in this important subject. (See enclosed copy of ICRU NEWS of December 1991.) Work on the more general set of fundamental quantities and units continues with a considerable portion of the drafting work already complete.

Substantial progress has also been achieved in other ICRU activities as reflected in the following status report on work underway in report committees engaged in the preparation of reports:

Advanced Drafting Stage:

- Fundamental of Particle Counting Applied to Radioactivity Measurements
- Dose Specification for Reporting Interstitial Therapy
- Performance Assessment in the Digital Representation of Images

Development Stage:

- Absorbed Dose Standards for Photon Irradiation and Their Dissemination
- Secondary Electron Spectra Resulting from Charged Particle Interactions
- Clinical Dosimetry for Neutrons (Specification of Beam Quality)
- In Situ Gamma Spectrometry in the Environment.
- Stopping Power for Heavy Ions

Recently Initiated:

- Beta-ray Dosimetry for Radiation Protection
- Determination of Body Burdens for Radionuclides
- Hyperthermia
- Proton Therapy
- Statistical Aspects of Environmental Sampling
- Tissue Substitutes, Characteristics of Biological Tissue and Phantoms for Ultrasound.

New Activities:

- Prescribing, Recording and Reporting Electron Beam Therapy
- ROC Analysis
- Medical Application of Beta Rays.

Project 1

Head of project: *Prof. Allisy*

Objectives for the reporting period

The development of ICRU reports on:

- (1) Fundamental quantities and units
- (2) measurement of dose equivalent for radiation protection purposes
- (3) absorbed dose standards for photon irradiation and their dissemination
- (4) fundamentals of particle counting applied radioactivity measurement
- (5) stopping powers for protons, alpha particles and heavy ions
- (6) phantoms for therapy, diagnosis and radiation protection
- (7) calculated photon, electron, proton and neutron interaction data for body tissues
- (8) secondary-electron spectra

Initiation of new work, particularly in relation with radiation protection, in areas where significant progress will be facilitated by the availability of ICRU recommendations.

Progress achieved including publications

ICRU Report 46, *Photon, Electron, Proton, and Neutron Interaction Data for Body Tissues*

ICRU Report 47, *Measurement of Dose Equivalents from External Photon and Electron Radiations (in press)*

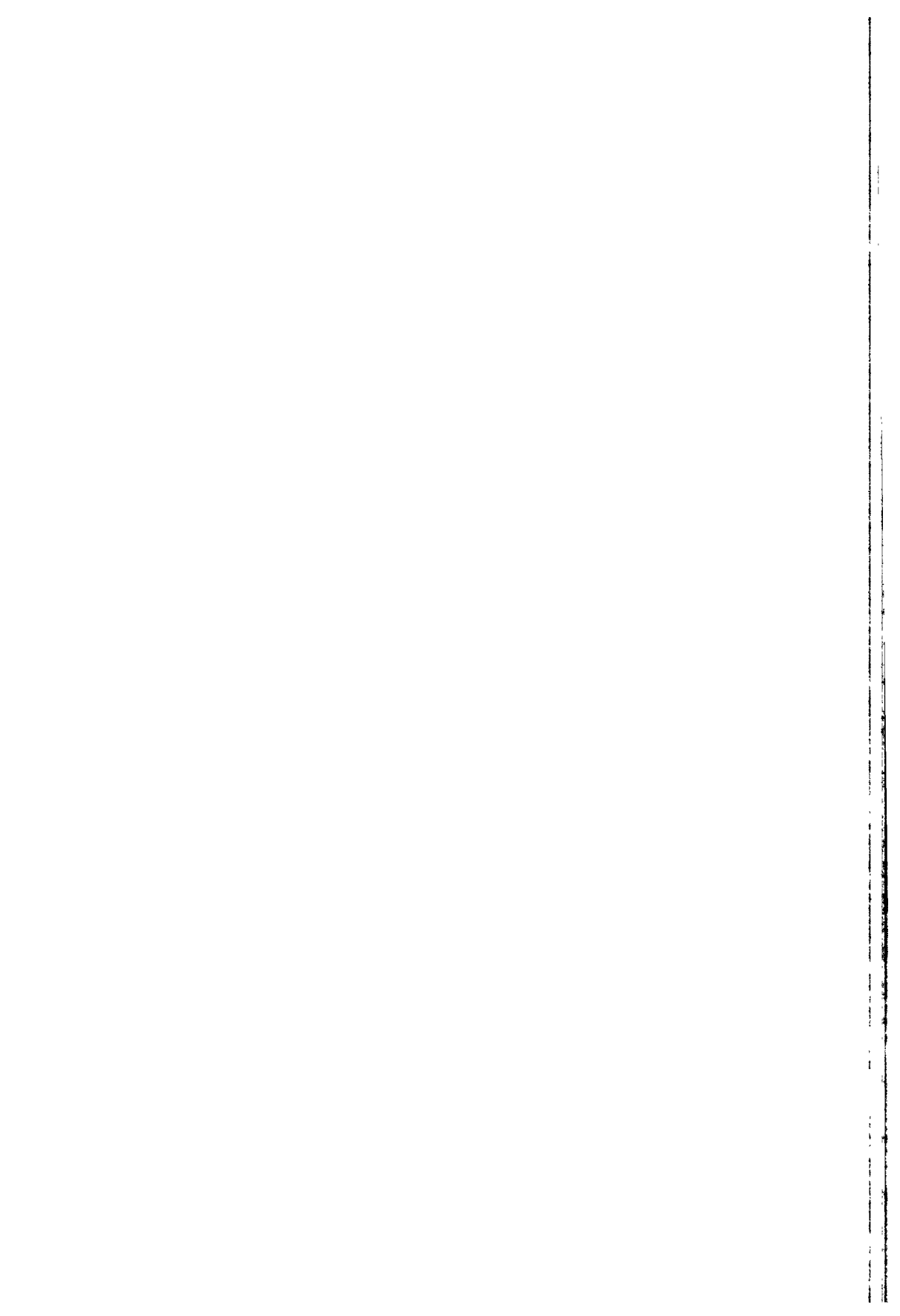
ICRU Report 48, *Phantoms and Computational Models in Therapy, Diagnosis and Protection (in press)*

ICRU Report 49, *Stopping Power and Ranges for Protons and Alpha Particles (preparing printer's manuscript)*

ICRU Report 50, *Prescribing, Recording and Reporting Photon Beam Therapy (preparing printers manuscript)*

"Quantities and Units for Use in Radiation Protection -- A Draft Report,"

ICRU NEWS 2/91, 5-9 (1991)



THE IMPLEMENTATION OF THE OPERATIONAL DOSE QUANTITIES INTO RADIATION PROTECTION DOSIMETRY (NRPB ASSOCIATION)

Contract Bi6-347a - Sector A11

- 1) *Clark* , NRPB - 2) *Marshall* , AEA Technology Harwell Laboratory
- 3) *Lebo* , ENEA - 4) *Chartier* , CEA-FAR

Summary of project global objectives and achievements

Objectives

The main objectives of the project are:

To investigate new methods of measuring the spectral and angular distribution of external radiations in the workplace, particularly for photons.

To improve current methods for measuring the spectra of neutron radiations in the workplace and prepare a compilation of measured neutron spectra.

To investigate the implications of spectral and angular distribution measurements for personal dosimetry, including methods of calibration of personal dosimeters and individual dose assessments in the workplace.

To improve methods of calculating photon and electron transport in phantoms, particularly the ICRU sphere and slab, to support practical calibration techniques for personal dosimeters.

To calculate backscatter factors for the ICRU sphere and to compare results with measurements in calibration laboratories.

To define procedures for calibrating personal dosimeters in terms of operational dose equivalent quantities in calibration laboratories.

To evaluate the performance of personal dosimeters (film and TLD) when measuring operational dose equivalent quantities in calibration beams.

Achievements

The main achievements of the project have been as follows:

To complete a thorough review of practical methods for measuring photon spectra in the workplace, and to construct a novel spectrometer using a sodium iodide detector, capable of giving spectral and angular distributions.

To carry out basic measurements of photon radiations using the custom built spectrometer and to compare with predictions obtained using a Monte Carlo simulation code.

To complete a compilation of measured neutron spectra in the workplace and to improve

techniques for measuring spectra.

To carry out a comprehensive set of Monte Carlo calculations of field parameters for the ICRU sphere with reference to photon beams, and prepare a paper on the work for publication in the scientific literature.

To establish by calculation and measurement that the synthetic material RS-1 has the same characteristics as ICRU tissue equivalent material.

To evaluate the ability of film and thermoluminescence dosimeters to measure personal dose equivalent $H_p(d)$ and establish a calibration method for this quantity using a 30 x 30 x 15 cm PMMA slab phantom.

Project 1

Head of project: *Dr. Clark*

Objectives for the reporting period

- i) To refine the design of a spectrometer based on a sodium iodide detector capable of obtaining energy spectra and angular distribution of photon radiations.
- ii) To construct and commission the spectrometer to the specified design and carry out some measurements of photon spectra in calibration laboratories.
- iii) To compare the measured spectra with the results of Monte Carlo calculations for the detector response.

Progress achieved including publications

The design of the spectrometer to obtain energy and angular spectra of photon radiation was finalised (Figure 1), achieving a compromise between portability in the workplace and the degree of resolution of angular data. The detector is a 17 mm x 25 mm sodium iodide crystal with a photomultiplier tube surrounded by lead shielding and a collimator. The weight of the complete assembly was limited to a maximum of 15 kg, to allow for the practical demands of making measurements in the workplace. The design of the lead shielding has been optimised within this constraint. The complete spectrometer is shown in the photograph in Figure 2, with the portable PC used to power the detector and process the data. The PC is a Toshiba T2000 SXe fitted with a Tennelec/Nucleus PCAP pulse height analysis and high voltage supply card. The assembly is battery powered and can be protected from contamination in the workplace.

The spectrometer has been commissioned following measurements of various photon energies at different angles of incidence. For typical x-ray energies, the spectrometer only responds to radiation incident at 0° on the detector shield cone acceptance angle (see Figure 1) with very little penetrating the lead shielding from other angles. As shown in Figure 3a virtually all the interactions fall into the photopeak. As expected, the spectra from higher energy photon radiations, such as ¹³⁷Cs and ⁶⁰Co sources is more complicated with Compton interactions and backscatter peaks from the lead shielding. A typical measured spectrum is given in Figure 3b for a ¹³⁷Cs source incident at 0°, and there is also significant penetration through the lead shield from radiation incident at other angles (see Figure 3c). The next phase of the development will be to devise methods suitable for use on the PC to unfold complicated spectra, in collaboration with AEA Harwell. The first steps have been taken, showing that the response of the equipment agreed with the predicted spectra using a Monte Carlo code EGS4 - see the progress report from Project 2.

Some practical aspects of making spectral measurements in workplaces have been investigated. In many areas where photon radiation measurements are required, there may be significant contamination problems. Although the spectrometer and PC can be protected from contamination, the mount equipment used to obtain angular data (eg., a tripod) can easily become contaminated. A novel solution to this problem has been found by using

lightweight laboratory stools which are disposable and can be adapted to ensure accurate angular measurements.

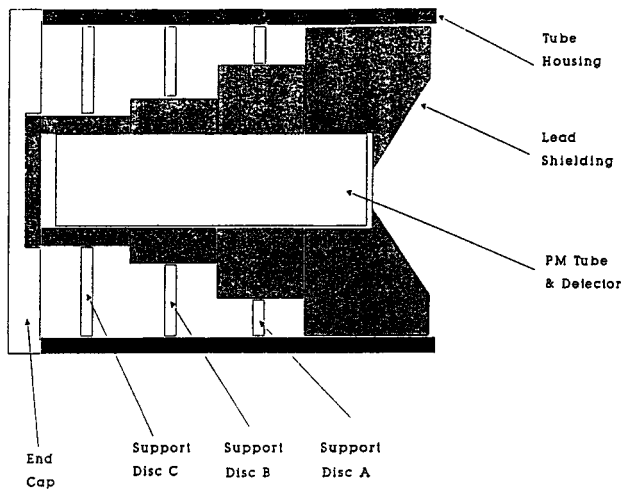


Figure 1. The outline design of the detector and shielding

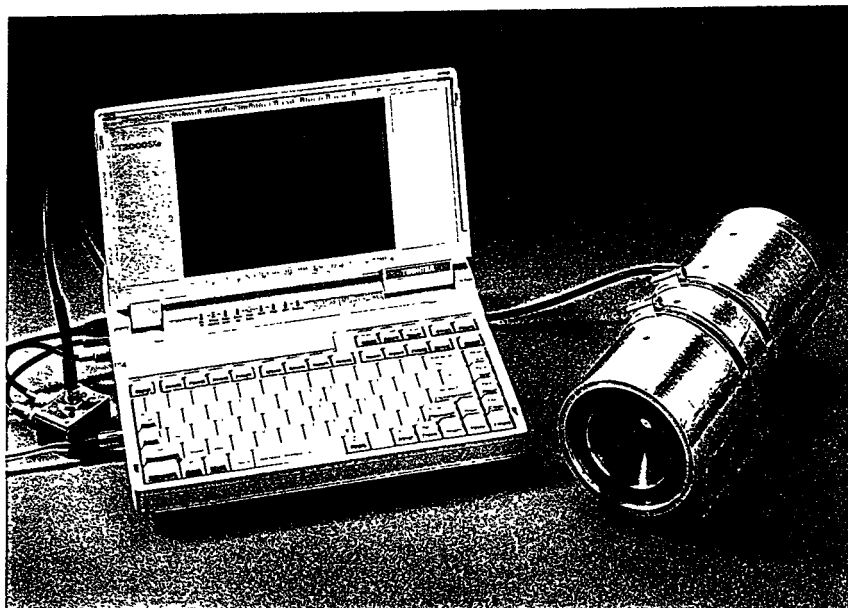


Figure 2. Photograph of complete assembly of the spectrometer

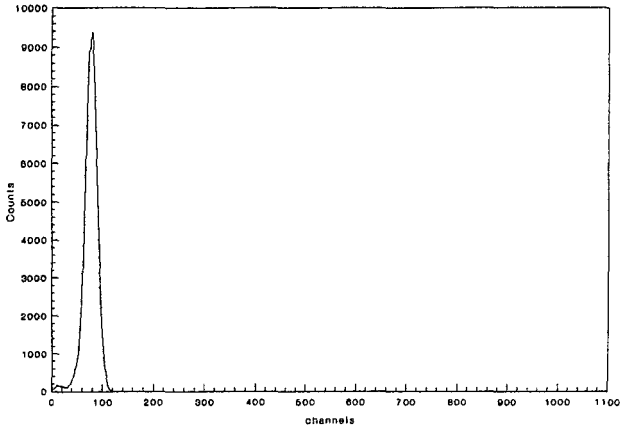


Figure 3a. Measured spectra from ISO low 109 keV photons incident at 0°

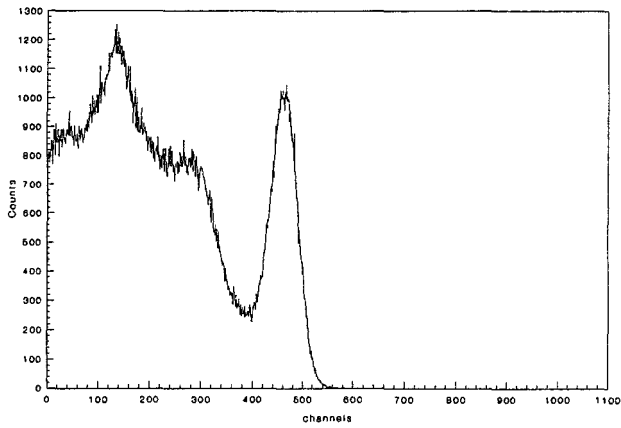


Figure 3b. Measured spectra from ^{137}Cs incident at 0°

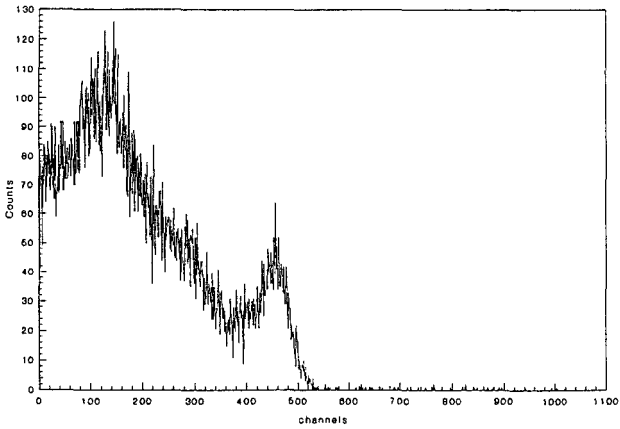


Figure 3c. Measured spectra from ^{137}Cs incident at 90°

Project 2

Head of project: *Dr. Marshall*

Objectives for the reporting period

- (i) To develop the ESG4 Monte Carlo computer code to determine theoretically the response of the photon spectrometer, developed by NRPB, as a function of energy and angle.
- (ii) To examine unfolding techniques developed for X-ray and neutron spectroscopy and adapt them to obtain energy and angular information.
- (iii) To make operational improvements to the Harwell neutron spectrometry system.
- (iv) To prepare a compilation of neutron spectra measured with the Harwell neutron spectrometer system and assess the implications of these spectra for the calibration of personal dosimeters used in the workplace.

Progress achieved including publications

1. Theoretical support for the development of a workplace gamma-ray spectrometer

The Radiation Dosimetry Department has developed a Monte Carlo computer model of the shielded sodium iodide detector developed by the NRPB. The model is based around the EGS4 suite of sub-programs which are able to simulate the transport of both electrons and photons through matter. The model has been used to produce spectra for the detectors placed in an infinite parallel beam of photons at different energies and the beam at different angles, which have been compared to experimental results produced by the NRPB. Good agreement between experimental and calculated response functions have been achieved. An example is shown in figure 1 and 2, which show spectra recorded by the spectrometer for a broad, parallel beam of Caesium 137 photons at normal incidence to the detector. Features which reduce the time required to run the model have been introduced and additional code has been added which will stimulate fluorescence produced by the K edge photoelectric effect in lead. Fluorescence produced in the sodium iodide crystal will be included at a later stage. The effect of detector resolution will also be included in the model, which will broaden full energy peaks and smooth Compton edges.

Salford Fortran 77 is now fully implemented which has improved program development facilities and increased the speed at which the model runs. Both the program development and running time have been improved by the acquisition of new computer hardware. A large number of problems in the EGS4 source code due to non standard FORTRAN and programming errors have been resolved.

An unfolding program developed a number of years ago at Harwell (The measurement of Spectra from X-ray machines. L H J Peaple, A K Burt, Phys Med Biol, 1969 14 (1) pp 73-85) has been identified and adapted to run on IBM compatible personal computers. This will be used to investigate the feasibility of unfolding three dimensional practical radiation spectra.

2. Neutron spectrometry

A number of operational improvements has been made to the neutron spectrometry system developed at Harwell. These have involved transferring the computer programs used to unfold the raw data collected by the counters, from an IBM mainframe to a personal computer. The ease of use has also been increased. These improvements considerably reduce the time required to unfold neutron spectra from the raw data.

Previous measurements of neutron spectra made at nuclear power stations (Gosgen, Switzerland, 2 locations; Dungeness 'A', UK, 3 locations; Hinkley Point, UK, 2 locations; and Trawsfynydd, UK, 1 location) have been collected together in a standard form and results were published at the 7th Symposium on Neutron Dosimetry⁽¹⁾. These spectra were also used to derive dosimeter responses and to compare the effect on calculated dose of changing the neutron quality factor, according to recommendations in ICRP 60. The neutron spectra collected to date have been made available for the compendium of workplace spectra being prepared by the EURADOS-CENDOS Working Group 7 'Radiation Spectrometry in Working Environments'.

During the period of this work the neutron spectrometry system developed at Harwell was used to measure the spectrum at the SILENE reactor facility in France, with the reactor shielded with 10 cm of lead and unshielded. For both sets of measurements simultaneous measurements were made with multispheres (NPL, UK) and a tissue equivalent proportional counter (Universität des Saarlands, Homburg). For the reactor shielded with lead there was generally good agreement between these measurements but a comparison has not yet been made for the measurements with the reactor unshielded. Open reports will not be published until the completion of an international intercomparison of criticality accident dosimetry systems to be held in June 1993. These measurements were made with separate CEC funding but in due course the data will be compared with the field measurements described above.

Publication

'Neutron Spectrometry and Dosimetry Measurements made at Nuclear Power Stations with Derived Dosimeter Responses'

H J Delafield and C A Perks

Accepted for Publication in Proc. 7th Symp. on Neutron Dosimetry, Berlin, 14-18 October 1991.

To be published in Radiation protection Dosimetry.

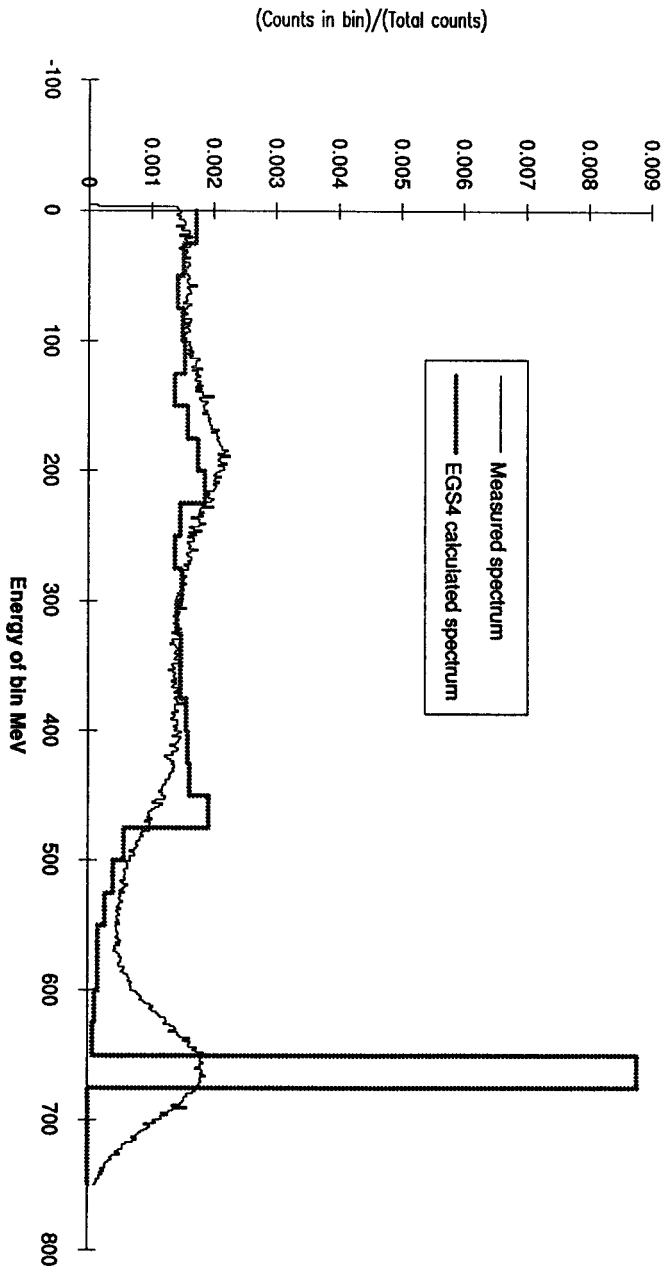


Figure 1
Calculated and measured energy spectra for a normal, parallel beam of Cs 137 photons,
incident on a 17mm diameter shielded NaI crystal.

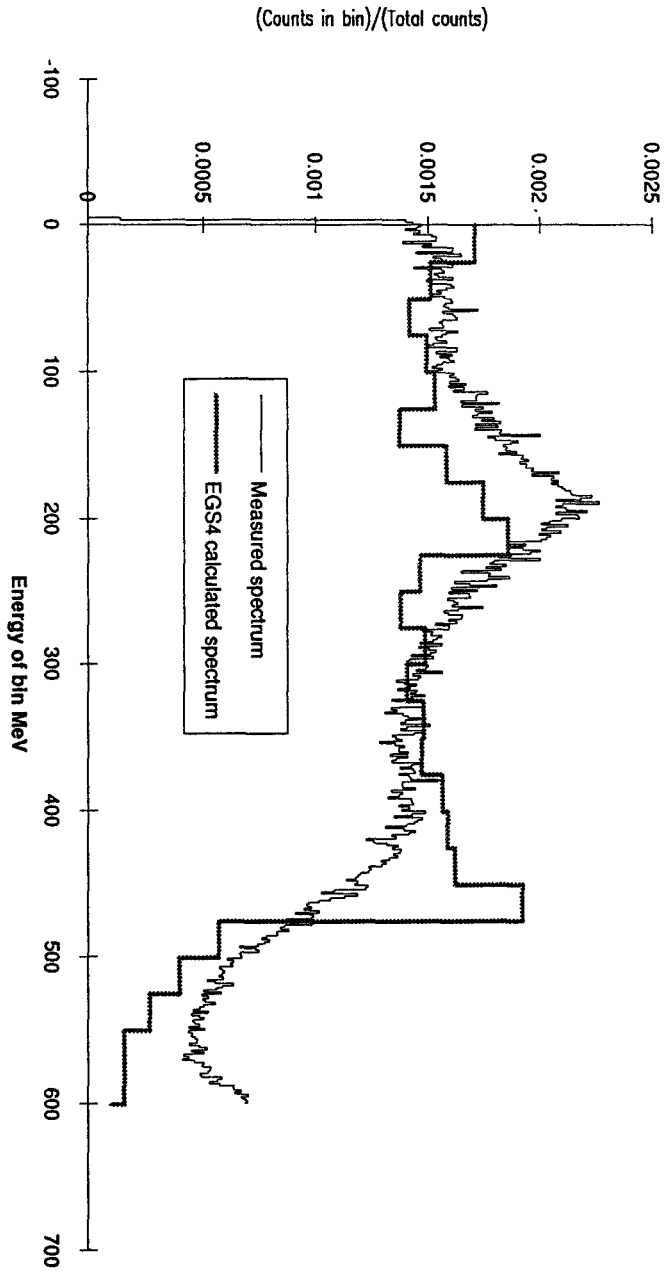


Figure 2

Calculated and measured energy spectra for a normal, parallel beam of Cs 137 photons, incident on a 17mm diameter shielded NaI crystal. Full energy peak omitted.

Project 3

Head of project: *Dr. Lembo*

Objectives for the reporting period

The contribution of ENEA dealt mainly with the calculation and measurement of backscatter factors in the presence of the ICRU sphere irradiated with ISO and B.I.P.M. reference photon beams.

The characterization of the radiation fields had to be completed with the calculation of the backscattered spectra and the backscattered mean energy angular distribution.

Computational evaluations of backscatter factors and their angular dependence had also to be compared with experimental values obtained using the X and gamma irradiation facility of the ENEA Bologna Secondary Standard Dosimetry Laboratory.

Progress achieved including publications

At the end of the reporting period three different investigations were completed which contributed to the characterization of the photon radiation field in the presence of the ICRU sphere:

- 1) Monte Carlo Calculations of angular distribution of backscatter factors: the ICRU sphere was chosen as a suitable phantom. The calculations were carried out for four ISO X-ray radiation series, one B.I.P.M. X-ray radiation series (with tube voltages ranging from 10 to 300 kV), with the addition of ^{137}Cs and ^{60}Co /1/, /4/. The MCNP Monte Carlo code was employed.
- 2) Monte Carlo Calculations of backscattered spectra and backscattered mean energy angular distribution: the spectral characterization of the backscattered radiation field was one of the main objectives reached. The real field in the presence of the ICRU sphere was determined combining the Monte Carlo results for backscatter spectrum and the source uncollided spectrum using the fluence backscatter factor as weighting factor /2/, /4/.
- 3) Experimental and computational analyses on the tissue substitute material RS-1: a series of measurements was carried to validate the MCNP code in the energy range of interest. The analysis confirmed that the RS-1 material behaves in the same way as the ICRU material in the same energy range /3/, /4/.

Publications

- /1/ G.F. Gualdrini " Field Parameters and Operational Quantities for the ICRU Sphere with Reference Photon Beams. PART 1° Monte Carlo Calculations of Angular Dependence of Backscatter Factors " ENEA RT/AMB/92/12/ in press.
- /2/ G.F. Gualdrini, F. Padoani and B. Morelli " Field Parameters and Operational Quantities for the ICRU Sphere with Reference Photon Beams. PART 2° Monte Carlo Calculations of Backscattered Spectra and Backscattered Mean Energy Angular Distribution " ENEA REPORT 1992 in press.
- /3/ G.F. Gualdrini, F. Monteventi and I. Sermenghi " Field Parameters and Operational Quantities for the ICRU Sphere with Reference Photon Beams. PART 3° Experimental and Computational Analyses on the Tissue Substitute Material RS-1 " ENEA REPORT 1992 in press.
- /4/ G.F. Gualdrini, L. Lembo, F. Monteventi, F. Padoani "Monte Carlo Calculations of Field Parameters for the ICRU Sphere with Reference Photon Beams" Paper accepted for publication in Rad. Prot. Dosim.

Montecarlo calculation of field parameters for the ICRU sphere with reference photon beams

1. Computational approach

The code employed in the calculation of the investigated field parameters was the general purpose Monte Carlo code MCNP (Monte Carlo for Neutron and Photons) /1/ developed at the Los Alamos Scientific Laboratory (USA). The code, which makes use of a point-wise cross section library for photons with data derived from Hubbell /2/ is provided with a very powerful geometry package, allowing to describe complex geometries and with a large variety of variance reduction techniques; in particular Cell splitting and russian roulette are the most commonly used.

The gamma transport was treated taking into account the modification of Thompson and Klein Nishina differential cross sections by appropriate form factors allowing for electron binding effects and fluorescent emission.

The problem mock-up was simplified in the computational model neglecting the presence of air. Furthermore the problems were solved in the so-called kerma approximation, i.e. the secondary electron transport was not taken into account. A more sophisticated treatment, allowing both for the presence of air and for secondary electron transport could have been important in conditions where electronic equilibrium is not fulfilled.

From the point of view of source description, each bremsstrahlung spectrum was taken from the Seelentag Catalogue /3/, which have been used in other papers for the same kind of applications. More recently a new set of X-ray spectrum data have been published by Laitano et al. /4/. A first comparison demonstrated that this new set of data is generally in good agreement with that by Seelentag, whilst in some cases the spectrum mean energy shows differences up to 3%. Nevertheless some preliminary calculations showed that these differences on mean energy have a small effect on backscatter factors.

2.1 Backscatter factor calculation

The first quantity investigated was the air kerma backscatter factor, defined as the ratio of the kerma in air on the center line of the photon beam at various angles and distances from the phantom surface and the collision kerma at the same point with the phantom absent. The ICRU sphere was chosen as a suitable phantom, however ICRU is now going to propose different phantom for calibration purposes. The values of distances equal to 0 cm, 0.5 cm and 1 cm, from the surface of the sphere have been here investigated in order to obtain factors applicable to typical operational and calibration geometry conditions.

The responses were calculated using boundary crossing estimators. Scoring areas were selected using spheres centered on the ICRU sphere center with radii of 15, 15.5 and 16 cm. and one-sheet cones with angles increasing by five degrees at a time.

In this way a series of spherical shells was described. The flux (the quantity to be scored) is defined as

$$\Phi = J/\mu$$

where J is the current and μ is the average cosine of the angle between the normal to the surface and the direction of the incident particle.

Air kerma has been evaluated using conversion coefficients from photon fluence to air kerma reported by ICRP Publication 51 /5/.

The air kerma backscatter factors are plotted in fig. 1 against the mean energy of the incident beam.

2.2 Calculation of fluence backscattered spectra and backscattered mean energy versus angle of incident radiation

A second computational study was concerned with the calculation of the angular dependence of the backscattered mean energy as well as the backscattered radiation spectrum in presence of the ICRU sphere.

a) Backscattered mean energy versus angle of incident radiation.

The quantity to be calculated in terms of MCNP tallies was the mean energy of

backscattered radiation E_B ,

$$E_B = \frac{E_{min} \int_{E_{min}}^{E_{max}} J(E) E dE}{\int_{E_{min}}^{E_{max}} J(E) dE}$$

where E_{\min} and E_{\max} are the minimum and maximum energies of the photon spectrum, $J(E)$ is the photon current and E is the photon energy.

The quantities have been scored for eighteen angles, with five degree angular bins, as for the previous calculations of backscatter factors, producing a complete set of backscatter mean energies versus angle. In fig. 2 the angular distribution of the backscattered mean energy for ^{137}Cs is reported.

b) Energy distribution of backscattered radiation

The energy distribution of the backscattered radiation has been accurately evaluated accuracy, bearing in mind the problem of obtaining results with reasonable standard deviation, when backscattered photons were scarce. The goal being a flux distribution in energy bins as narrow as possible, a particular facility supplied by MCNP had to be employed.

The incident X-ray spectra as obtained from the Seelentag catalogue have been merged with the corresponding Monte Carlo calculated backscattered spectrum, using the fluence backscatter factor as normalization coefficient. An example of plot for the 300 kV Narrow Spectrum ISO incident beam is reported in fig.3. About 500000 source particles were used for each calculation obtaining percentage standard deviations of the order of 2-3% in the most important energy bins.

3. Experimental validation

The principal aim of the experimental activity was the validation of the computational procedure, which has been applied to the calculation of dosimetric quantities, through the comparison of both front and angular backscatter factors for reference photon beams.

The RS-1 material /6/ phantom was adopted taking into account its optimum characteristics in simulating the ICRU material in the energy domain of interest. The experimental setup has been prepared in order to minimize the scattered radiation produced from sources different from the spherical phantom.

The accuracy is better the higher is the beam strength as in the case of B.I.P.M. series and the High Kerma Rate series; the total errors are usually within +/- 1%. This comparison shows that the percentage deviations between the experimental and calculated values are generally less than + or - 1% .

Furthermore some measurements were carried out in order to measure the angular variation of the backscatter factors, and the results were compared with corresponding Monte Carlo calculations, obtaining a good agreement .

References

- /1/ MCNP - A General Monte Carlo Code for Neutron and Photon Transport
LA-7396 Rev. 2 Los Alamos (1986)
- /2/ J.H. Hubbell , et. al. "Atomic Form Factors, Incoherent Scattering Functions, and Photon Scattering Cross Sections." J. Phys. Chem. Ref. Data 4, 471 (1975)
- /3/ W. W. Seelentag , W. Panzer , G. Drexler, L. Platz and F. Santner "A Catalogue of Spectra used for the Calibration of Dosemeters."
GSF-Bericht S-560 March 1979
- /4/ F. Laitano et al. " Energy Distributions and Air Kerma Rates of ISO and B.I.P.M.Reference Filtered X-Radiations." ENEA REP. December 1990
- /5/ ICRP Publication 51 "Data for Use in Protection Against External Radiation." Pergamon Press (1987)
- /6/ K.P. Hermann and D. Harder "Production and Use of a Polyethylene-based Tissue-equivalent spherical Phantom Substituting the ICRU Sphere for Photons." Rad. Prot. Dosim.(28) 1989

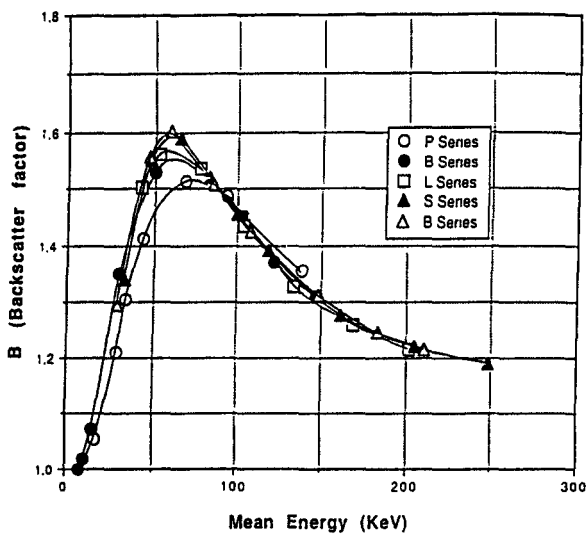


Fig. 1: Air kerma backscatter factors at the surface of the ICRU sphere versus mean energy of the incident X-ray beams for ISO and B.I.P.M. reference radiations.

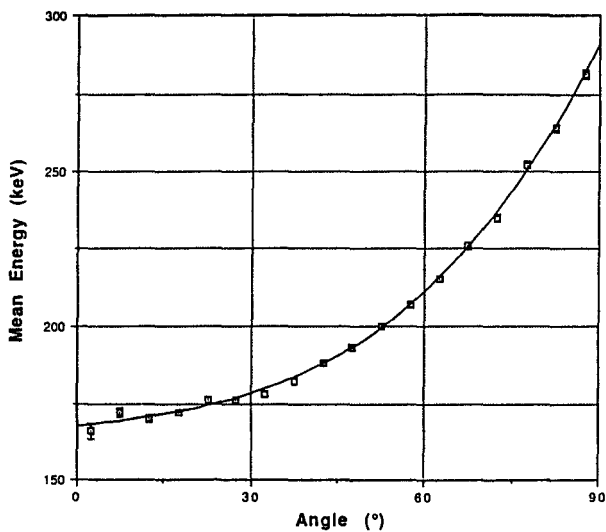


Fig. 2: Mean energy of backscattered radiations versus angle of incident beam for ¹³⁷Cs.



Fig. 3: Photon spectrum at 1 cm. from the ICRU sphere surface. Narrow spectrum 300 kV ISO incident beam

Project 4

Head of project: *Dr. Chartier*

Objectives for the reporting period

The CEA experimental program, presented in the conclusions of the previous report, has been carried out during the reporting period. The general objective consists of defining procedures for calibrated individual dosimeters used in radiation protection which should be compatible both with other methods currently in operation in the routine Dosimetry Services and with the implementation of dose-equivalent operational quantities as defined in the ICRU Reports 39, 43 and 47. This realistic process relies on the experimental study of dosimetric systems currently available to test their ability to evaluate the operational quantity $H_p(d)$, taking into account their characteristics and uncertainties. Furthermore, this study should contribute to the determination of the calibration factors of individual dosimeters used at specified work-places, where the photon radiation spectrum has been measured (NRPB and AEA Harwell projects).

Progress achieved including publications

1. Introduction

In the previous report, diagrams have clearly shown large differences between the results derived from the different dosimetric systems. The specific program of the relevant period was intended:

- a) to repeat partly the previous irradiations,
- b) to extend it in order to investigate other characteristics of dosimeters, in particular the angular response.

Four French Dosimetry Services have participated to this work by providing batches of 100 dosimeters and results concerning 3 types of dosimeters will be discussed here: 2 thermoluminescent [TL] and 1 photographic film [PF] dosimeter.

2. Experimental program

The irradiation program is described hereafter:

- Photon energies: ISO 4037 Photon Reference Radiations "Narrow Series"
23 keV (X-ray fluorescence), 48 keV, 83 keV, 118 keV, 205 keV, (60-Co).
- Calibration conditions:
 - Irradiation free-in-air ; Incidence 0°
 - Irradiation on PMMA slab phantom ; Incidence 0°
 - Irradiation on PMMA slab phantom ; Incidence 30°

- 6 types of dosimeters: PFD(3), TLD(3)
- For each energy and each calibration condition: irradiation of 5 samples.

3. Results

1) Influence of the calibration phantom

A plot of the response of dosimeters irradiated in front of a PMMA slab phantom relatively to the response "free-in-air" is shown in Figure 1. A good agreement with similar results of the previous report for a radiation incidence of 0° gives a check of the satisfactory reproducibility of current dosimetric systems. For the different experimental points plotted in the figures of this report, uncertainties are ranging in the 5 to 8 per cent interval.

2) Reference operational quantity

According to ICRU Report 47, the operational quantity for the calibration of personal dosimeters is $H_p(d)$ in the slab phantom (30 x 30 x 15 cm) of ICRU tissue material. The recommended values of d are either 10 mm or 0.07 mm. By using a PMMA phantom, the radiation field near the surface of the calibration phantom is different from that field in front of a ICRU tissue phantom. Therefore, taking $H_p(10)$ in the PMMA slab as the calibration quantity should compensate for the increase of scattering which is observed for the PMMA material. This assumption should be verified through other irradiations of dosimeters in front of a water slab phantom.

In figures 2 and 3, the ordinates scale represents the values of $I/H_p(d)$ for ICRU tissue and PMMA with:

- I : dose indicated by the dosimeter
- $H_p(10)$: personal dose equivalent at depth 10 mm in the phantom for 2 types of dosimeters. Conversion factors are taken from references (1) and (2).

For TL dosimeters, a systematic underestimation of doses is observed for photon energies higher than 200 keV. This may be due to the insufficient thickness of the plastic material (about 300 mg/cm²) placed in front of the TL material. This trend is representative of the lack of electron equilibrium for the specified energy range. As to PF dosimeters, an overestimation is apparent over the whole energy range (up to 1.25 MeV). Such a conservative behaviour can be corrected by applying a justified scaling factor or by reconsidering the dose evaluation procedure.

These results show that, in the case of calibration beams, (collimated geometry), current routine dosimeters should enable the individual monitoring in terms of dose equivalent operational quantities without performing drastic modifications.

3) Angular response

Irradiations of dosimeters performed according to an incidence angle of 30° have given results plotted in Figure 4. The order of magnitude of the variations agrees with the calculated values.

4) Future developments of the program

Up to now, the experimental program has dealt exclusively with conventional situations encountered at the level of calibration conditions. A more realistic step should be the case of the irradiation of dosimeters placed in front of a rotating phantom. This technique is generally accepted to simulate the movement of an individual moving at a workplace. This study should be completed by using a "wide spectrum" radiations reproducing the scattering component in the radiation field of a laboratory or workplace environment.

Bibliography

- 1 B Grosswendt Rad. Prot. Dos., Vol. 35, No 4, pp. 231-235 (1991)
- 2 B Grosswendt Rad. Prot. Dos., Vol. 40, No 3, pp. 169-184 (1991)

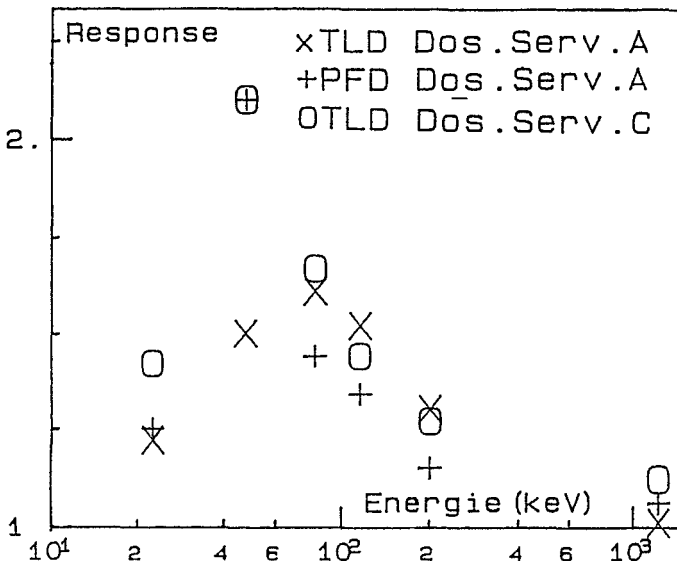


Figure 1

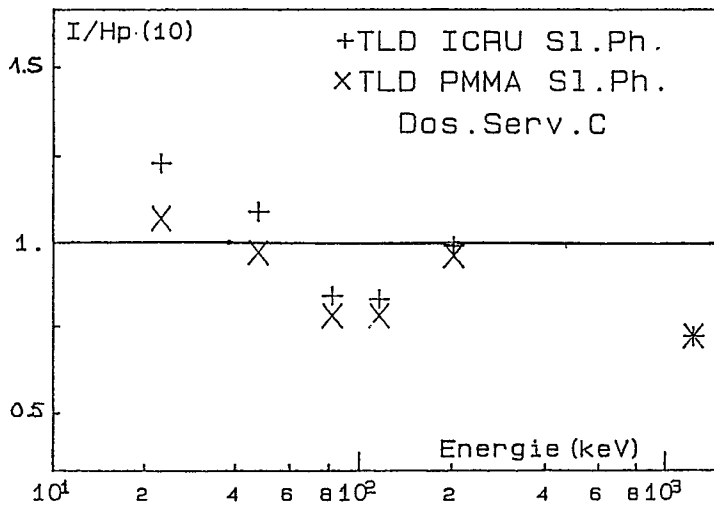


Figure 2

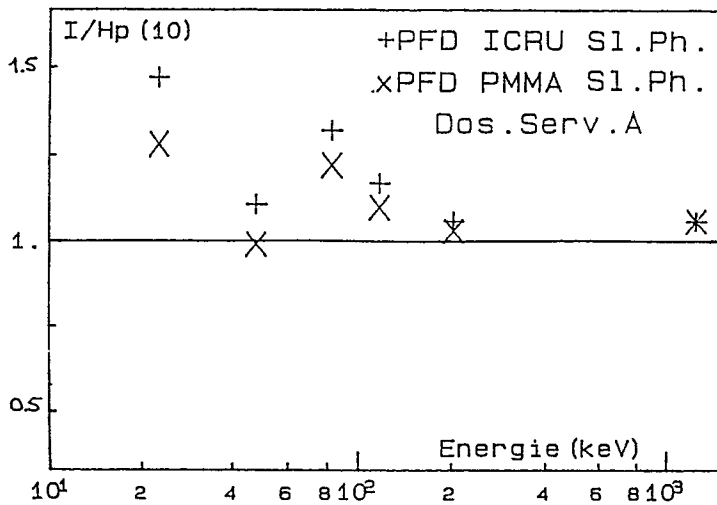


Figure 3

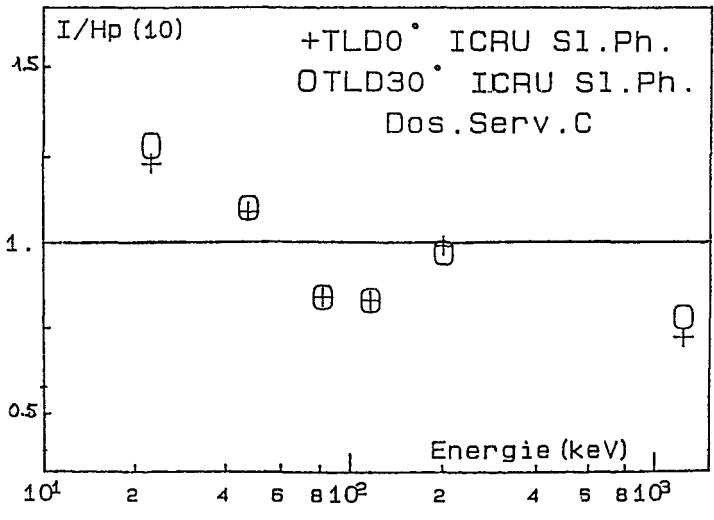
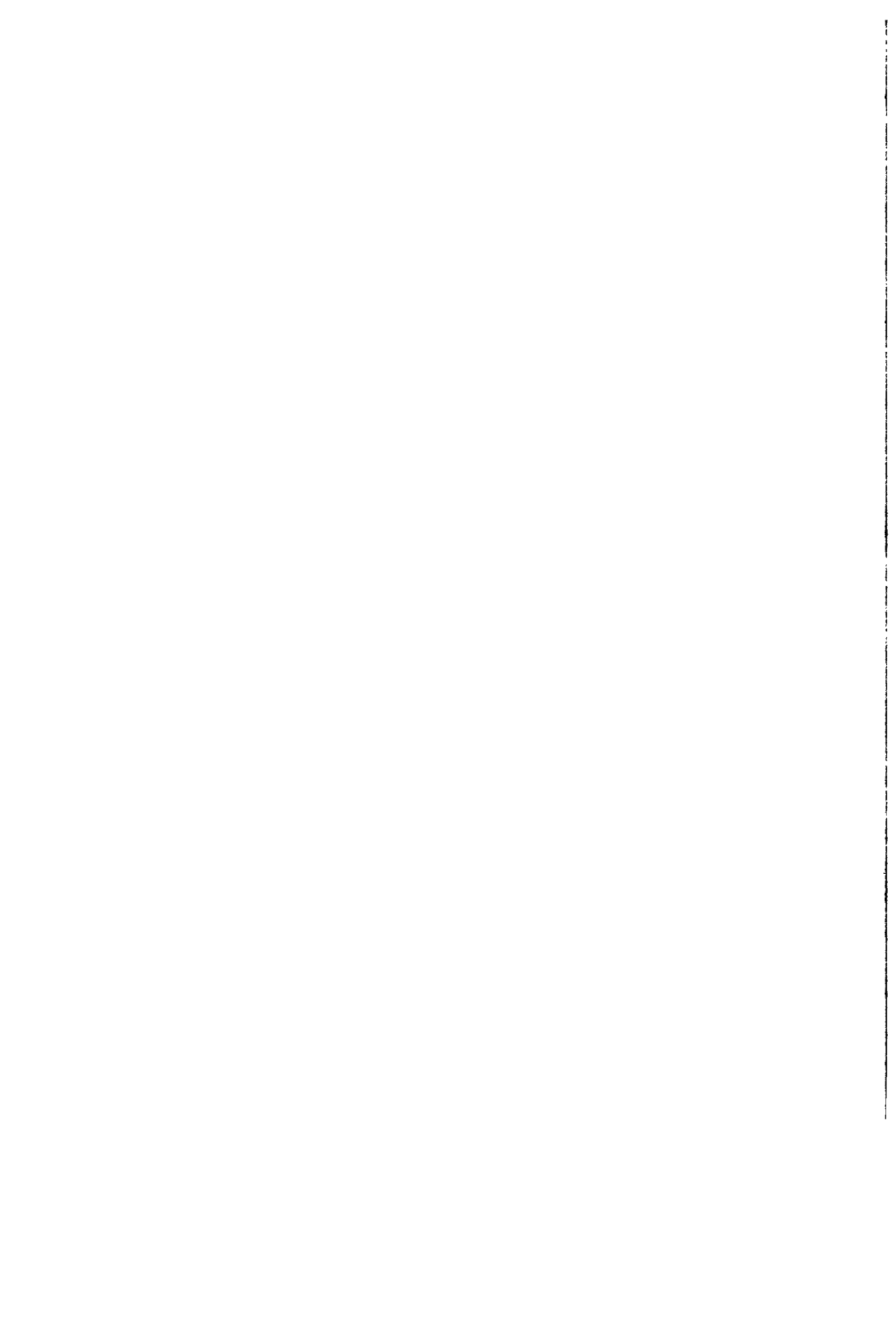


Figure 4



STUDY AND DEVELOPMENT OF AN INDIVIDUAL ELECTRONIC NEUTRON DOSIMETER

Contract Bi7-020 - Sector A12

- 1) *Vareille -Decossas* , Univ. Limoges - 2) *Tommasino* , ENEA
- 3) *Zamani-Valasiadou* , Univ. Thessaloniki - 4) *Barthe* , CEA FAR
- 5) *Fernández Moreno* , Universidad Autónoma de Barcelona

Summary of project global objectives and achievements

Summary of project and global objectives

This research proposal concerns the study and development of an individual electronic dosimeter working as a real time dosimeter, which has been compared with optimized H.E.C.E., E.C.E. and C.E. track etch dosimeters, which optimization was carried out by different laboratories.

LEPOFI (LIMOGES University) and S DOS (C.E.A. Fontenay aux Roses) work on the electronic system, the principle of which is to detect the secondary particles from a polyethylene converter using a PIPS (passived implanted Silicon) detector and to convert the pulses in term of dose equivalent in real time mode. A differential method is used in order to eliminate background contribution.

ENEA (ROMA), NPD (TESSALONIKI) and SFR (BARCELONA) are concerned with the optimization of different types of track etch detectors, with the objective to start using electronic devices as well.

Different investigations were proposed :

- calculations which take into account incidence angle and energy of neutrons, γ - n discrimination, background
- experiments, concerning the optimization of all the dosimeter devices and finally joint irradiations for the overall intercomparison taking into account calculations.

Thanks to the results obtained, new proposals have been identified with special regard to the device response intercomparison.

Achievements

During this contract each laboratory improved its own device through background studies (material background for etched track detector, electronic background and interfering quantities for diode device), in particular modelization by computer codes (EGS4, PNEDIOD,...) have been carried out for the diode investigation (LEPOFI-S DOS). For track detectors Monte-Carlo calculations have been realized for the response evaluation (SFR). In these conditions it was possible to have joint irradiations in the framework of the contract. Irradiation facilities for monoenergetic neutron beams (Bruyères-le-Chatel) as well as for realistic fields (CEN Cadarache) were obtained from S DOS CEA which also defined dosimetric references.

The results obtained with each device (track etched detector as well as electronic sensor) are explained in the following contributions of each participant. In this introductory report the conclusions achieved using the joint irradiations are described. The dose equivalent conversion factors used to evaluate the responses are from ICRP 21.

* The common work on the electronic device by S DOS and LEPOFI leads to a better understanding of the role of energy threshold of the electronic background and of γ contribution (experiments and calculations).

* When "classical converters" are used (polyethelene, makrofol,...) the response (tracks or pulses $\text{cm}^{-2} \text{mSv}^{-1}$) lies under 1000 counts $\text{cm}^{-2} \text{mSv}^{-1}$, smaller for etched track detectors, twice or more higher for electronic devices. For example, with a 1.2 MeV neutron beam, at normal incidence, the mean etched track detector response (C.E.C) is 302 tracks $\text{cm}^{-2} \text{mSv}^{-1}$ (obtained by SFR), the mean electronic device response is 754 pulses $\text{cm}^{-2} \text{mSv}^{-1}$ (obtained by LEPOFI) and 600 pulses $\text{cm}^{-2} \text{mSv}^{-1}$ (obtained by S DOS). For the two latters the response value depends on the energy threshold (cf. report of S DOS and LEPOFI). But in all cases a rather flat response as a function of neutron energy is shown for energy higher than 500 keV for the electronic device and higher than 144 keV for the track detector.

In the case of realistic neutron fields used during this contract, both detector responses (track etched and electronic) decrease because of the contribution of neutrons with energies lower than one hundred keV.

* When a more elaborated converter is used (polyethylene and a thin layer of ^6LiF evaporated on CR 39) it is possible to appreciably increase the response (5 tracks $\text{cm}^{-2} \mu\text{Sv}^{-1}$ at 1.2 MeV for example) (NPD). The response as a function of neutron energy is rather flat but not as good as that for the other devices for energies higher than 500 keV. On the other hand the response remains at high value when realistic fields are used.

* One of the participants (ENEA) has used the joint irradiations to investigate novel types of track detectors, such as electrochemical etched thin film of polycarbonate and cellulose nitrate. The results obtained cannot be compared with those from CR 39 and silicon detectors. These somewhat different investigations have made it possible the development of a new detector for fission induced neutrons which can be highly valuable for the registration of high energy neutrons.

Presentation of the device

In brief, the following conclusions can be drawn :

a - the two diodes system proposed for this contract (LEPOFI and S DOS) makes it possible the dosimetry of neutron beams, in spite of the relatively high energy threshold needed to compensate γ contribution.

b - The comparison between the different types of doseimeters (SFR - LEPOFI/S DOS) has shown that the silicon detectors are more sensitive than track etch devices. Both the electronic devices and track detectors present a similar angular response. Responses are in the two cases drastically decreasing when realistic fields are used.

c - New converter used with CR 39 and chemical etching (NPD) shows a higher response both for thermal and fast neutrons than the one obtained with other devices.

d - From these results and because of the advantages of electronic devices (real time doseimeter...) further investigations need to be concentrated on :

- choice of better converter
- improvement of silicon sensor
- better discrimination between neutron and γ photons
- effects of exposure on phantom.

Thanks to the two joint irradiations (Bruyères-le-Chatel and CEA Cadarache) a common paper is in preparation which points out comparisons between the various devices used by the teams involved in this contract.

Project 1

Heads of project: *Dr. Vareille - Dr. Decossas*

Objectives for the reporting period

The electronic dosimeter already proposed by LEPOFI had to be tested in various irradiation conditions and to be compared with other systems during joint irradiations in the framework of the contract.

Furthermore, some calculations on neutron response (thanks to Monte-Carlo computer code proposed by LEPOFI) and γ response (thanks to EGS4 code) had to be performed for a comparison with experimental results.

Progress achieved including publications

1. 1 - Presentation of the device

Differential method is used thanks to the two channels defined in figure 1. One diode is covered by a polyethylene converter implanted with boron and the other one is free of converter.

The response R_T of a channel can be expressed as :

$$R_T = S_n H_n + S_{ni} H_n + S_\gamma H_\gamma + B \quad (1)$$

where S_n is the response per unit of neutron dose equivalent due to converter from which protons, α and Li are emitted.

S_{ni} the response per unit of neutron dose equivalent due to neutron interactions on Si and other materials around the detector.

S_γ the response per unit of γ dose equivalent due to the dosimeter taken as a whole.

B the background.

Each contribution can be modified by bias voltage, geometry of sensor and surrounding materials, thickness and implantation of converter. The differential method leads to a response which is the difference of the two channel responses which have been simultaneously studied in order to optimize the dosimeter.

2. Diode test and calibration of the device

We realized :

* a comparison of the two diodes through :

- measurements of the reverse current which give values about 10 nA and show a good symmetry of the two diodes

- measurements of junction capacity as a function of bias voltage

* adjustments and linearity tests which lead to optimize the two channels.

The polyethylene thickness and boron implantation characteristics have been well defined, and the small dissymmetries between the two diodes reduced through electronic adjustments.

3. Experimental results

Some of these were obtained in collaboration with CEA-FAR. All the results lead to intercomparisons between the staffs involved in the contract.

3 - 1 - Responses in various neutron fields

In order to determine the dosimeter response three kinds of neutron fields were used:

- monoenergetic neutron fields (from thermal neutrons to 14 MeV) : GSF Munich ; Bruyères-le-Chatel ; CEN Cadarache ;
- polyenergetic neutron fields (AmBe, PuC) ;
- realistic neutron fields at CEN Cadarache : $^{252}\text{Cf} + \text{D}_2\text{O}$; $^{252}\text{Cf} + \text{D}_2\text{O} + \text{Cd}$; Canel (+) + Fe ; Canel (+) + Fe + H_2O .

In each case we tried to point out the device characteristics and its limitations. An example of pulse spectra is given on figure 2. Electronic background and "interfering quantities" (i.e. quantities to which the device is not intentionally sensitive : γ contribution, direct neutron interactions with silicon atoms of the diode ...) disturb spectra at low energies. In these conditions an energy threshold must be introduced. For monoenergetic beams its optimum value, determined from statistical studies and from the response curve plotted on figure 3, is about 125 keV. For the realistic fields studied in which the γ component is much higher, the threshold is as high as 550 keV. Table 1 summarizes the experimental results : for different neutron fields it presents the values of energy threshold and response (pulses $\text{mSv}^{-1} \text{cm}^{-2}$).

Table n° 1 : Summary of results obtained in various neutron fields by the electronic device

Beam	Threshold (keV)	Response (pulses- $\text{mSv}^{-1} \cdot \text{cm}^{-2}$)
570 keV	125	550
1,2 MeV	125	750
2,5 MeV	125	1075
5,3 MeV	500	1030
14,8 MeV	125	600
Thermal	600	1000
AmBe	350	750
PuC	350	660
$^{252}\text{Cf} (\text{D}_2\text{O})$	550	815
$^{252}\text{Cf} (\text{D}_2\text{O} + \text{Cd})$	550	560
CANEL+ (Fe)	550	330
CANEL+ (Fe + H_2O)	550	170

For 570 keV, 1.2 MeV, 2.5 MeV the lower dose equivalent which can be registered is about $50 \mu\text{Sv}$ and for thermal neutrons the lower dose equivalent rate about $57 \mu\text{Svh}^{-1}$. The relative angular response has also been studied (fig. 4).

3 - 2 - What is the γ contribution ?

In a first step, experiments in (n, γ) fields have been realized. The γ component has been measured using a G.M. counter. Our silicon detectors had been previously calibrated with ^{60}Co and ^{137}Cs sources so that the number of pulses due to γ rays would be evaluated. The expression (1) can be written :

$$R_T = S_{n_t} H_n + S_\gamma H_\gamma$$

where $S_{n_t} = S_n + S_{n_i}$. B can be neglected. R_T can be expressed as :

$$R_T = S_\gamma \frac{H_\gamma}{H_n} H_n + S_n H_n = (S'_\gamma + S_n) H_n$$

Table n° 2 clearly shows a decrease of the ratio S'_γ/S_n as the neutron energy increases.

Table n° 2 : Comparison between γ response and neutron response

NEUTRON ENERGY (keV)	H_n (mSv)	N_n (pulses) threshold at channel 15	H_γ (mSv) (mGy)	N_γ G.M.* (counts)	N_γ S.C.** (pulses) threshold at channel 15	H_γ/H_n %	N_γ^{SC}/N_n " $S'\gamma/S_n$
73	482.10^{-3}	1036	$4.2.10^{-3}$	2311	2024	0,88	1,95
159	1678.10^{-3}	1780	8.10^{-3}	4400	3856	0,48	2,17
593	11247.10^{-3}	9110	11.10^{-3}	6009	5302	0,1	0,58
1270	11786.10^{-3}	13224	$7.1.10^{-3}$	3908	3422	0,06	0,26
2624	11680.10^{-3}	19038	$13.3.10^{-3}$	7269	6411	0,11	0,34

4. Calculations

4.1 1 - γ contribution

The need of a threshold and the related sensitivity decrease is mainly due to γ contribution. In order to understand it, calculations were done using EGS4 computer code with a sensor model composed of 15 different parts. In this way, the role of the depth of the depleted zone, γ energy and angle of incidence, components of the sensor has been studied. As an example, fig. n° 5 shows the dosimeter response with and without any metallic part for a given irradiation. From this result it clearly appears that the structure of the sensor must be modified.

4.2 Neutron response

Using Monte-Carlo method, we developed a code (PNEDIOD) which takes into account the interactions of neutrons in the converter, as well as in the silicon diode, and gives the corresponding pulse spectra. The dosimeter model is the same as previously described. The pulse spectra and response were calculated as a function of various parameters : neutron energy (monoenergetic and AmBe), neutron angle of incidence, converter thickness, depth of the depleted zone. Figure n° 6 gives an example of the results for 1.2 MeV neutron beam.

5. Conclusion

The 2 diodes system used for this contract allows a dosimetry of neutron beams but an energy threshold is needed. For accelerator beams which have a low γ component the response is about $800 \text{ pulses mSv}^{-1} \text{ cm}^{-2}$ with a 125 keV threshold. For neutron spectra in which the γ component is more important (simulated realistic spectra) the threshold must be higher (550 keV for instance) and the response to neutrons decreases ($170 \text{ pulses mSv}^{-1} \text{ cm}^{-2}$). For the future, the structure of the dosimeter must be modified in order to reduce or discriminate as much as possible the γ response. The new dosimeter will have to be tested and the final characteristics to be determine thanks to on phantom irradiations.

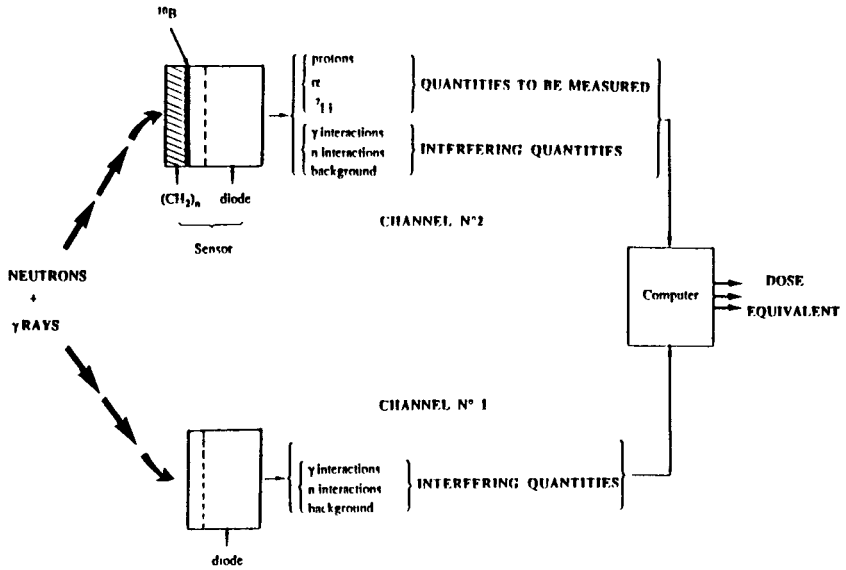


Figure 1: Schematic diagram of electronic neutron dosimeter.

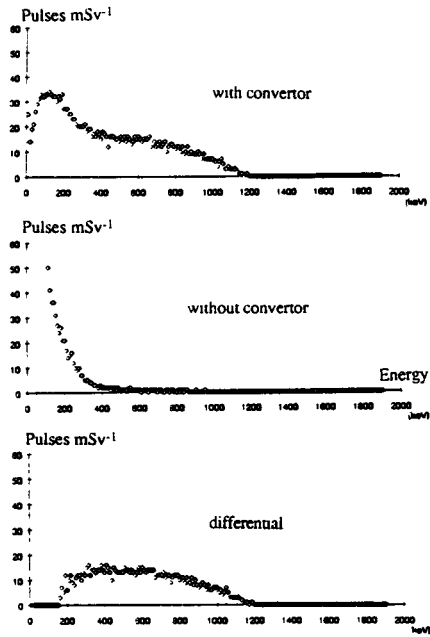


Figure 2: Device response to 1.2 MeV neutrons.

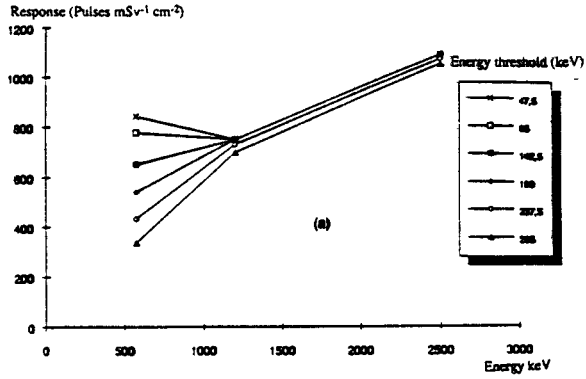


Figure 3: Response as a function of neutron energy, for various energy thresholds.

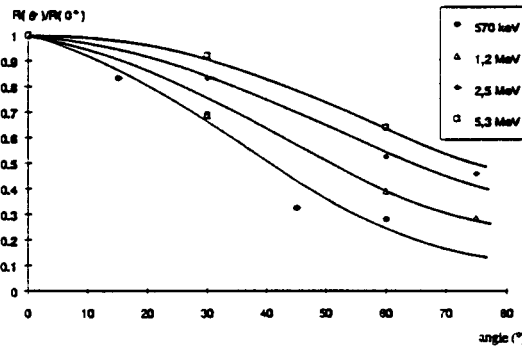


Figure 4: Relative response as a function of neutron incidence angle.

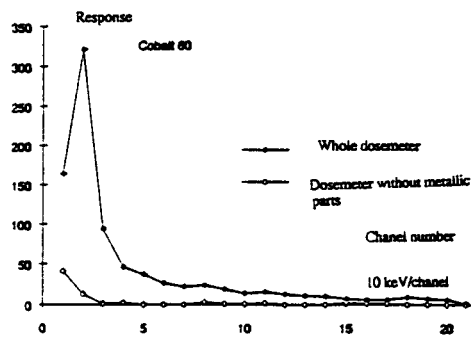


Figure 5: Calculated modification of the ^{60}Co pulse spectrum by the metallic parts of the sensor.

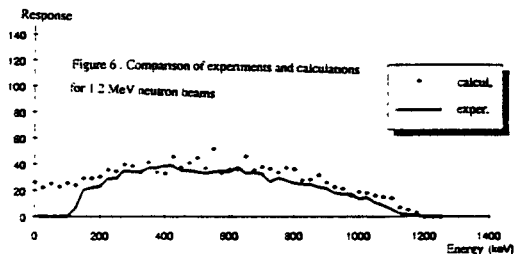


Figure 6: Comparison of experiments and calculations for 1.2 MeV neutron beams.

Publications

- * Radioprotection, 26, 2, (1991).
- * 3 communications 7th symposium on neutron dosimetry, Berlin - Oct. 14th - 18th 1991, to be published in R.P.D.
- * RADECS 91. 1st European conf. on radiation and its effects on devices and system, Montpellier - September 1991, to be published in I.E.E.E.
- * Thesis. D. Paul (May 1992), University of Limoges.
- * B. Dubarry-Chabanais, (September 1992), University of Toulouse.

Project 2

Head of Project: *Dr. Tommasino*

Objectives for the reporting period

The major mission goal of this project was the development of the new electrochemical etching (hereafter referred to as NECE), which exploits the advantageous characteristics of both the spark counter and the electrochemical etching for the scanning of large detector areas. In the case of fission fragment registration, successful results have been obtained. In the second reporting period a systematic investigation has been undertaken to study the NECE registration for alpha particles and neutron recoils.

Progress achieved including publications

The investigations of alpha particle registration in thin polycarbonate films by the NECE processes has shown limited success, essentially because the alcohol-based etchant resulted in poor self-healing characteristics.

For this reason, investigations have been limited to cellulose derivatives, such as cellulose nitrate, cellulose acetobutyrate and cellulose triacetate. Among these three detectors, cellulose nitrate has proved to be the most convenient specially for its relatively high sensitivity and fast NECE processes required for track breakthrough.

Cellulose nitrate films with a thickness of 20 microns and no additives was custom-made by Kodak.

When compared with LR-115, this film has a thickness greater than the etchable range of alpha particles.

The NECE parameters used were the same of those used for thick film electrochemical etching. In particular this 20-micron-thick cellulose nitrate film has been etched with 10% NaOH in water by applying an electric field in the range from 20 to 30 kv/cm RMS at 2 kHz.

To improve the self-healing processes, the thin Al electrode was kept at the positive polarity by superimposing to the AC field a DC bias of 40 volt.

Under these conditions, the spot formation is very rapid in the case of fission fragments tracks in polycarbonate, where the Al spots can be seen by naked eye, while it is difficult to see the etched-through tracks even at high magnification.

However the Al-spot formation in the case of alpha particles in cellulose nitrate is less rapid.

Furthermore the signal-to-noise ratio is no better than that which can be achieved by conventional electrochemical etching.

Finally the registration of neutron-induced recoils in polycarbonate has been investigated using the same NECE conditions described above.

Polycarbonate foils with thickness up to 30 microns have shown limited success respectively because:

- the long time required for the track breakthrough and the formation of the Al-spot;
- the less preferential electrolyte breakthrough along the tracks.

With the experience accumulated to date it is possible to conclude that the NECE processes, while very successful for fission fragment registration, appear less attractive for the registration of alpha particles and neutron induced recoils.

Publications

L. Tommasino, G. Torri and M. Notaro (1991) - Unique characteristics of thin films electrochemical etching. Nucl. Tracks Rad. Meas. 19, 223

L. Tommasino, - The importance of track detectors in radiation protection dosimetry, Proceedings of 16th Int. Congr. on SSNTD, Beijing 7-11 nov. 1992.

Project 3

Head of project: *Dr. M. Zamani-Valassiadou*

Objectives for the reporting period

The study of a CR-39 fast neutron detecting system based on (n- α) (n-p) converter. The purpose was to study and choose optimum parameters like polyethylene moderator thickness, etching development etc. in order to use this system as a fast neutron dosimeter. The work includes tests of the response over wide range of neutron energy.

Calculations as well as measurements at 2.5 MeV neutrons have been made and a part of the results is already published [1] [2].

The linearity of the system is also studied. Finally the dosimeter response under special neutron irradiation fields is discussed. Intercomparison with other neutron dosimeters is made in the frame of a common work under this contract.

Progress achieved including publications

The use of a certain detection system as a neutron dosimeter requires special response characteristics under a wide range of energy, various neutron doses, angles of neutron incidence etc. Many experiments have been performed in the frame of Eurados-Cendos Joint Irradiations [3] as well as during this project. The results we present here have been taken by a combination of polyethylene neutron moderator of 0.5 cm in thickness and a thin layer of ^6LiF (1-2 μm) evaporated on the one surface of the CR-39 detector which is in contact with the moderator. Chemical etching was performed at 70 °C in 20% NaOH solution for a time interval of about 6h in order to develop proton recoils and alpha particles from $^6\text{Li}(n, \alpha)t$ reaction. Details on the neutron dosimeter structure and preliminary results are given in refs [2] and [3].

The neutron detecting systems used as neutron dosimeters have, in general, an optimum response for a more or less wide range of neutron energy i.e. at thermal neutrons or a region of fast neutrons [4]. The proposed system is an attempt to obtain continuous response from thermal region up to 14.7 MeV. In fig. 1 we give the response for 0.144, 0.565, 1.2 MeV and 2.5 MeV¹. The observed response has a continuous behaviour for all the range of energies studied. The curve falls versus energy as it was expected from the cross section behaviour of $^6\text{Li}(n, \alpha)t$ reaction. Proton recoils give a constant level contribution in fast neutrons while protonic equilibrium is achieved. The superposition of proton recoils component to that of alpha particles helps the overall response behaviour versus energy, especially for neutron energies above 1 MeV. The results satisfy the requirement for flatness versus energy, which is valid for all types of neutron dosimeters. An other advantage of the system studied is that below 500 KeV we obtain continuously high response, without special additional combinations of other converters or development etc. which is the usual case of SSNTD neutron dosimeters based on proton recoils.

Another point of interest is to test response angular dependence of the detecting system. Preliminary results were obtained during irradiations at 2.5 MeV neutrons in the

¹ Irradiations were performed in Bruyeres le Chatel

Thessaloniki Nuclear Physics Laboratory [2]. The experiment was repeated for various energies in the frame of Eurados-Cendos Joint Irradiation programme 1990. In Fig. 2 we present results of this experiment. Irradiations were made at the same neutron dose of 2mSv. The angular behaviour is expected to be flat if only alpha particles are counted (including a part of tritons which are detectable also). The response angular dependence of all systems based on proton recoils falls as the irradiation angle increases (relative to the neutron beam) [5]. In Fig. 2 we can see that alpha particle behaviour dominates to that of proton recoils. We obtain almost the same curve, independently on neutron energy, which is also an advantage of the system studied.

Concerning the linearity of the system versus neutron dose, fig. 3 shows the results for 1.2 MeV neutrons. The system is linear versus dose [6]. The response, defined as the track reading per unit dose, is founded to be depended on neutron energy.

However, the same result can be concluded from response behaviour versus energy (fig. 1). Any other influence on linearity is not observed although low dose region must be examined in more detail.

An important parameter is also the thickness of (n, α) converter as it is experimentally improved [3]. The data of this experiment were obtained with 1 μ m layer of ⁶LiF converter.

Finally, test of the detecting system under various neutron fields have been made² in a joint irradiation programme in the frame of the present contract.

References - Publications

- [1] M. Zamani-Valassiadou, Progress Report (contract B170020C)
- [2] E. Savvidis, M. Zamani, D. Sampsonidis and St. Charalambous, Nucl. Tracks and Rad. Meas. 19 (1991) 527-530
- [3] W.G. Alberts, Joint Neutron Irradiation Programme, Eurados Cendos Report, 1991
- [4] E. Piechsh, S.A.Al-Najjar and K. Ninomiya, Rad. Prot. Dos. 27 (1989) 215-230
- [5] M. Luszik-Bhadra, W.G. Alberts, S. Guldbakke and H. Kluge, Rad. Prot. Dos. 38 (1991) 271-277
- [6] E. Savvidis, D. Sampsonidis and M. Zamani, Rad. Prot. Dos. (in Press)

² Irradiations were performed in Cadarache, France

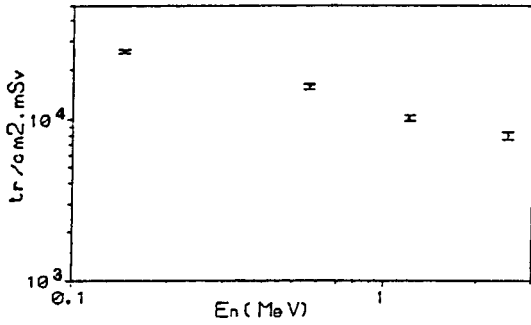


Figure 1. Fast neutron dosimeter response versus neutron energy.

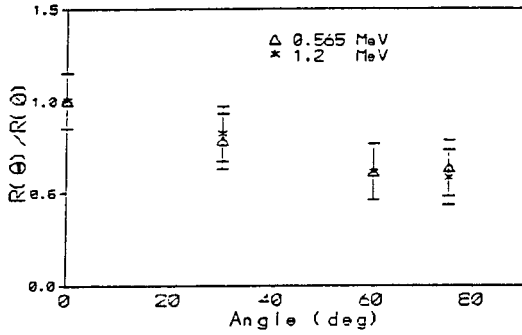


Figure 2. Response angular dependence.

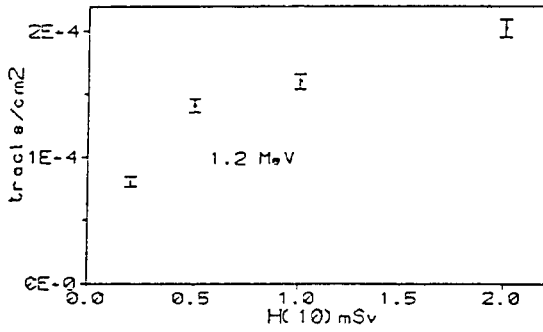


Figure 3. Linearity test of the fast neutron dosimeter.

Project 4

Head of project: *Dr. J. Barthe*

Objectives for the reporting period

The main objectives, envisaged for the final reporting period, are the performance of dosimetric tests of the double diode dosimeter with different radiation fields. For these studies neutron reference sources, accelerator or reactor facilities were used.

Progress achieved including publications

Principle

Many authors have studied the response of solid track detectors with neutron radiations, using a hydrogenous converter and/or a lithium borate converter. Theoretical and experimental studies with CR39 performed by Makovica show a quasi-linear proportionality between neutron dose equivalent and secondary charged particle fluence within $\pm 30\%$ of the normalised response for neutron energies between the thermal region and 10 MeV neutron energy. Barelaud and coll. replaced the solid track detector by a spectrometric diode detecting secondary particles emitted from the converter. The main secondary particles detected are recoil protons emitted from elastic scattering between fast neutrons and hydrogen atoms, alpha particles produced in nuclear reactions between thermal neutrons and boron-10 and electrons from interactions between gamma photons and the surrounding materials. To obtain a response more independent of the gamma component, a differential measurement is made using a second bare diode. The structural materials close to the diodes can strongly modify the gamma response of the detection system.

Experimental set-up

The double diode detector consists of two diodes from canberra having an effective area of 1.5 square centimetres and a bulk resistivity of about 600 Ω .cm. Intertechnique preamplifiers and amplifiers are used; two PC compatible multichannel analyser cards (2048 channels) from ortec are used with an amstrad PC compatible computer (386/387 DX processor).

The neutron source used for general tests is an Am-Be source. Mixed fields (neutrons and gammas) were obtained using at the same time an Am-Be source and a complementary Cobalt-60 source. Monoenergetic neutrons, 0.144, 0.530, 1.44 and 2.5 MeV, were obtained from the Van de Graaf accelerator located at the Bruyère le Chatel nuclear research centre. 14 MeV monoenergetic neutrons and realistic fields,

simulating those observed at different power plant locations, are obtained from the canal+ facility, thermal energy neutrons from sigma thermalized source assembly; these latter facilities are located in Cadarache nuclear research centre.

Measurements, in monoenergetic photon beams, have been performed to determine the behaviour of the photon diode responses in a mixed neutron gamma field. All experiments have been performed without the use of a phantom. In some cases, an automatic device is used to orientate the detecting devices in the neutron beam. Dosimetric references are defined by Chartier and coll. [4] from SDOS.

Experimental results

Three very important points have been studied for obtaining a correct determination of the double diode dosimeter behaviour in mixed neutron gamma fields:

1/ the sensitivity to neutron radiation in terms of counts per microsievert and per square centimetre. Due to the small cross section of the reaction between neutrons and hydrogen nuclei, this point seems to be one of the most important,

2/ the sensitivity to gamma radiations. All diode detectors are sensitive to photon radiations. In the case of differential measurements, a good discrimination between gamma and neutron radiations can only be obtained if the two diodes present exactly the same sensitivity to photons. The difference in sensitivities leads, mainly for low energy neutrons, to an over-estimation of the neutron dose equivalent if the most sensitive diode associated with the converter.

3/ the background noise signal. As described, unbalanced background signal leads to a wrong determination of the real dose equivalent and an abnormal increase in the detection threshold.

The response of both diodes is determined for two types of radiation: ^{60}Co photons of about 1 MeV for low energy loss and alpha particles of about 5 MeV from an ^{241}Am source for high energy loss.

In order to minimize the gamma contribution to neutron signal, the depleted layer of the diodes is reduced to a few tenth of a micrometer. Under these conditions, high energy particles traverse the depleted layer so that the diode does not work as a spectrometer does. Spectra obtained with high energy recoil protons show a peak corresponding to the maximum detectable energy.

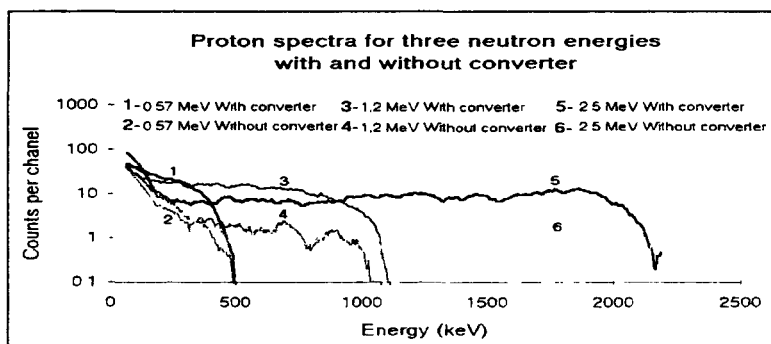


Figure 1. Spectra obtained for different neutron energies with and without converter
0.57 - 1.2 - 2.5 MeV, "CV" means with converter

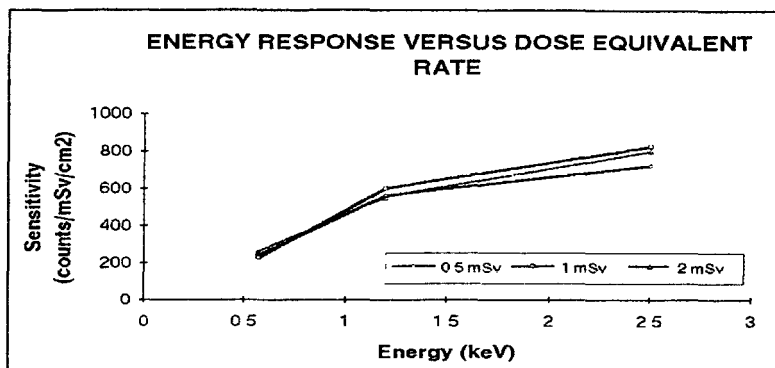


Figure 4: Dosemeter energy response.

Figure 4 shows the dosimeter energy response for 3 dose equivalent rates, 0.5, 1 and 2 mSv. A decrease in response versus neutron energy is seen. This effect is due to the reduction of the secondary proton emission which reaches the depleted diode layer. Indeed the mean path length of secondary protons decreases with initial neutron energy and only protons produced from a thin layer close to the converter surface can be counted. For a 0.144 MeV neutron energy a ratio inversion between the integrated counts of the 2 diode signals is observed. This effect is probably due to the absorption of low energy electrons from metallic surroundings in this hydrogenous converter.

Conclusion

The double diode dosimeter has, in terms of counts, a low sensitivity for low energy neutrons and a high sensitivity for photons. These two effects leads to an increase in neutron detection threshold and limits the minimum energy detection range for fast neutrons. Such a dosimeter does not record intermediate energy neutrons between 10 keV (albedo effect and boron doping) and 200 keV. Nevertheless, this dysfunction is not a redhibitory effect in realistic mixed field dosimetry encountered in nuclear power plants.

References

J. BARTHE, M. MOURGUES, J.M. BORDY, B. BOUTRUCHE, T. LAHAYE, P.SEGUR et G. PORTAL:

"Etude de compteurs miniatures pour la dosimétrie individuelle des neutrons", IRPA8, Montréal 18-22 mai, Compte-rendus Vol 1, pp 479 - 482 (1992).

J. BARTHE, T. LAHAYE, T. MOISEEV and G. PORTAL:

"Personal neutron diode dosimeter", Internationam Symposium on Solid State Dosimetry, Washington - USA, July 13-17, (1992), to be publish in RPD.

Project 5

Head of project: *Prof. Francisco Fernández Moreno*

Scientific staff: *Dr. Francisco Fernández Moreno, Dr. Carlos Domingo Miralles, Dra. Carmen Baixeras Divar*

Objectives for the reporting period

- Development of the ECE dosimeter for automated measurements
- Simultaneous experiments in neutron fields
- Intercomparison with other groups

Progress achieved including publications

1. Development of the ECE dosimeter for automated measurements

The work carried out consists of three main points:

- I Optimisation of the electrochemical etching conditions and of the reading technique for the CR-39 detector.
- II Optimisation of a fast neutron dosimeter in the energy range 140 keV - 5 MeV using polyethylene converter and Cr-39 detectors.
- III Proposal of a new neutron dosimeter and calibration experiments taking into account the results obtained.

- I Optimisation of the electrochemical etching conditions and of the reading technique for the CR-39 detector.

In this stage, results already published by our group about proton irradiation of CR-39 at the Strasbourg CRN 7MV Van-de-Graff accelerator at different angles and energies, have been used for this optimisation.

"Radiation Protection Dosimetry" Vol. 23 N° 1/4 175-178 (1988)

- II Optimisation of a fast neutron dosimeter using a polyethylene converter and Cr-39 detectors (Monte-Carlo method)

We have simulated the passage of a fast neutron beam (monoenergetic or coming from a neutron source) through an hydrogenated material at several incidence angles.

The dose equivalent response obtained from this estimation has been compared with the values obtained in the last EURADOS - CENDOS irradiations.

The results obtained have been published in:

- Seventh Symposium on neutron dosimetry. October 1991, Berlin
- Eurados-Cendos Report: 1991
- Radiation Protection Dosimetry (to be published)
- VIII Congreso Nacional de Física Medica Sep. 1991, Sevilla

A good agreement between the measured and the calculated values, with exception of the point at 14.8 MeV, has been obtained for the dose equivalent response, as shown in Figure 1.

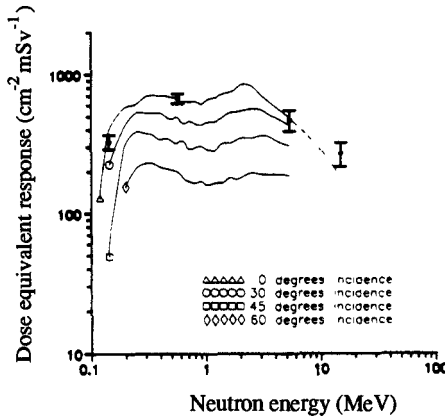


Figure 1 - Dosemeter dose equivalent response estimated from Monte-Carlo method as a function of the incident neutron energy for different incident angles. Also shown are our experimental results for normal incidence

- The poor statistics for 30° and 60° does not allow to verify the Monte-Carlo method estimation for these incidence angles
- The mean dose equivalent response values were:
 - 341 ± 194 (cm².mSv⁻¹) for 250 μm samples
 - 448 ± 127 (cm².mSv⁻¹) for 600 μm samples
- The dose minimum detection limit were found to be:
 - 136 μSv for 250μm samples
 - 261 μSv for 600 samples

III Proposal of a new neutron dosimeter and its calibration

Taking into account the given results we suggest to study the following points with other irradiations:

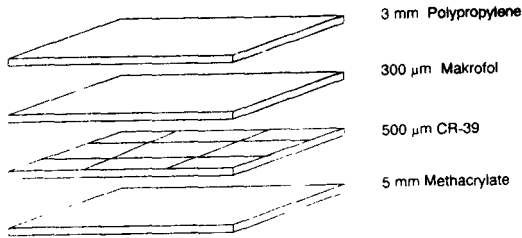
- Background reduction in order to improve the dose detection limits.
- Neutron irradiations at several incidence angles to verify the Monte-Carlo method estimations.
- Extension of our dosimeter to the lower neutron energy regions.

2. Simultaneous experiments in neutron fields

With this aim we have started the study of this points with irradiations in:

- Bruyère-le-Chatel
- Cadarache
- Bruyère-le-Chatel irradiations

CR-39, 500 μm thick and 32 hours curing time, manufactured by Pershore Moulding in November 1991 has been used for irradiations. $6 \times 6 \text{ cm}^2$ samples have been assembled in 16 cards and irradiated in the 4 MV Van-de-Graaf accelerator at the CN, Bruyère-le-Chatel (France) for several incidence angles, energies and doses. The dosimeter configuration was:



Each irradiated sample was cut in nine (2×2) cm^2 plates before etching. The plates have been electrochemically etched in the routine cells with a 6N KOH aqueous solution at 60° and $(20 \pm 1) \text{ kVcm}^{-1}$ for 5h at 50 Hz and 1h at 2 kHz, with 15 minutes post-etching. Tracks have been counted with an image analyzer in an area of about 0.69 cm^2 .

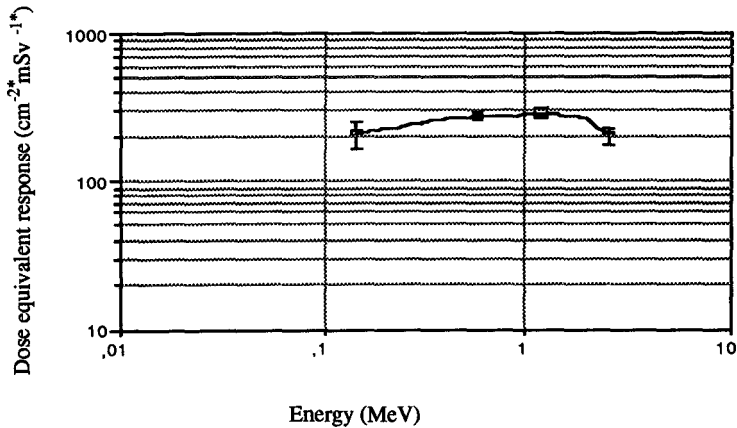


Figure 2 - Measured dose equivalent response as a function of neutron energy for normally incidence neutrons

The use of a 300 μm thick Makrofol converter explains the slight reduction in response at 2.5 MeV in comparison to the one obtained when a polyethylene radiator is used. A flatter dose equivalent response is observed in the considered energy range.

- Background values were similar for the different plates and its mean value was: 44 ± 13 ($\text{tracks} \cdot \text{cm}^{-2}$)
- The mean dose equivalent response for normal incidence was: 274 ± 17 ($\text{cm}^{-2} \cdot \text{mSv}^{-1}$)
- The dose minimum detection limit was found to be: 142 μSv

Our results are in reasonable agreement with those obtained by other authors.

- Cadarache irradiations

CR-39, 500 μm thick and 32 hours curing time, manufactured by Pershore Moulding in February 1992 has been used for irradiation. Samples of $6 \times 6 \text{ cm}^2$ have been assembled in 12 cards and irradiated at the CN Cadarache (France) for several energies and doses.

We have used the same dosimeter configuration, etching conditions and track counting system than those for the Bruyère-le-Chatel irradiation.

In Table I the main results are shown

Table I - Experiment: Cadarache

N° of samples	Experiment Code	Reference Dose Equivalent H* (mSv)	Counts	Background	Net Counts	Dose Equivalent Response
			$N \pm \text{SD}^{-1}$	$N' \pm \text{SD}^{-1}$ (cm^{-2})	$N'' \pm \text{SDM}$ (cm^{-2})	$R \pm \text{SDM}$ ($\text{cm}^{-2} \cdot \text{mSv}^{-1}$)
9	Canal plus	3.21 ± 0.01	861 ± 103	43 ± 5	818 ± 34	255 ± 11
18	Canal plus +	10.5 ± 0.3	150 ± 16	40 ± 7	110 ± 4	10 ± 1
15	Canal plus +	2.37 ± 0.05	76 ± 16	45 ± 8	31 ± 5	13 ± 2
16	Californium	1.3 ± 0.05	582 ± 37	28 ± 4	554 ± 9	426 ± 7
25	Californium	1.3 ± 0.05	473 ± 56	39 ± 6	434 ± 11	334 ± 9
13	Californium	1.32 ± 0.05	409 ± 92	65 ± 7	344 ± 26	261 ± 19
15	Sigma	2.32 ± 0.05	246 ± 57	54 ± 9	192 ± 15	83 ± 6

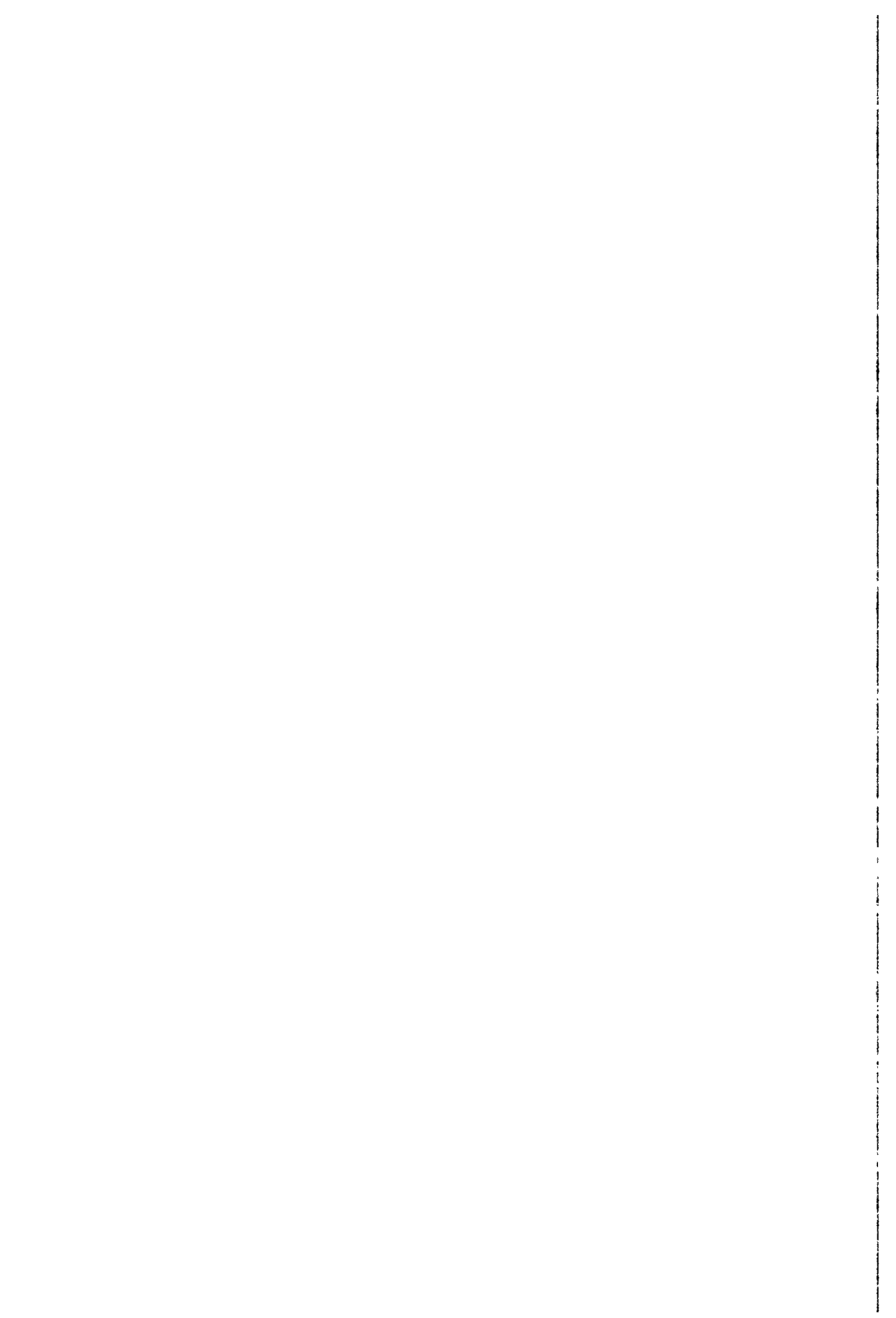
Background values are very similar for the different irradiation situations and its mean value was: $44 \pm 11 \text{ tracks} \cdot \text{cm}^{-2}$, consistent with the Bruyère-le-Chatel results.

The dose equivalent response values of $(255 \pm 32) \text{ cm}^{-2} \cdot \text{mSv}^{-1}$ for CANAL + (14,7 MeV) and $(430 \pm 9) \text{ cm}^{-2} \cdot \text{mSv}^{-1}$ for Californium source are in good agreement with those published by our group in the EURADOS-CENDOS 1992 intercomparisons. These results show the reproductibility of our electrochemical etching system.

The dose equivalent response decrease in the CANAL + and in the Californium exposures is due to the production of thermal neutrons that our dosimeter configuration is not able to detect, as expected.

The main component of the SIGMA exposure were thermal neutrons, but there was a small component of 1.5 MeV neutrons. The dose equivalent response of $(81 \pm 29) \text{ cm}^{-2} \cdot \text{mSv}^{-1}$ is consistent with this situation.

In view of these results we are at present optimizing, with our Monte-Carlo method, a dosimeter configuration, including an air converter, that would allow to record neutrons with energies between several keV and $\sim 100 \text{ keV}$. Some irradiations, carried out in the PTB laboratory, indicate the feasibility of this dosimeter.



USE OF THE VARIANCE-COVARIANCE METHOD IN RADIATION PROTECTION

Contract Bi7-025 - Sector A12

- 1) *Kellerer*, Univ. München - 2) *Jessen*, Univ. Aarhus Hospital
- 3) *Lindborg*, Nat. inst. of Rad. Protection

Summary of project global objectives and achievements

Microdosimetry was originally conceived as a fundamental tool of radiobiology to improve the understanding of the primary mechanisms of radiation action. However its applications in radiation protection and in clinical radiology are of increasing importance. Standards of increased accuracy in radiation protection dosimetry require the quantitative assessment of radiation quality.

In radiation protection the quality factor is defined as a function of the linear energy transfer. If the spectral distribution of the radiation field is known, the quality factor can be calculated. In fields with incompletely known spectra, radiation quality needs to be determined by measurement of the dose averaged lineal energy which is closely related to linear energy transfer.

Microdosimetric measurements in single event technique are restricted to low dose rate fields; they are time consuming or even impracticable, for instance, at installations for diagnostic radiology. The common variance technique is applicable in high dose rate fields, but it requires constant dose rate. Variance-covariance measurements however can be performed in high dose rate fields as well as in time varying radiation fields. The potential of the variance-covariance technique for the suppression of various disturbances is essential for instance in the vicinity of accelerators where electric noise is a common problem.

The three groups in the coordinated project are cooperating towards the further development of the variance-covariance technique, in the development of twin-proportional counters and twin ionisation chambers and in the optimisation of signal processing. The applications have been focused on the pulsed radiation fields of diagnostic x-ray installations and therapeutic accelerators. There is a need for such applications, for example in radiological quality control, and there is a lack of previous experimental data.

Project 1

Head of project: *Prof. Kellerer*

Objectives for the reporting period

Within the framework of project 1, instrumentation and methods for microdosimetric measurements with the variance-covariance method have been developed.

The inherent potential of the variance-covariance method for the suppression of various interfering disturbances have been analyzed in theoretical evaluations and in computer simulations

As a basis for the development and calibration of tissue equivalent proportional counters, the first Townsend ionisation coefficient for methane based tissue equivalent gas has been determined for a broad range of the reduced field strength.

Typical diagnostic x-ray fields and therapeutic electron beams have been assessed in terms of microdosimetric measurements. In contrast to the single event measurement technique, the variance-covariance measurements can be performed without technical manipulations that are necessary to reduce the intensity of the radiation fields, furthermore the variance-covariance measurements are substantially faster.

Progress achieved including publications

1. Development of instrumentation for microdosimetric measurements with the variance-covariance method

A tissue equivalent twin-proportional counter has been developed. The cylindrical shaped sensitive volume is defined by guard tubes; it is sized 20mm in height and 20mm in diameter. The outer cylinder is made of A-150 plastic. To make precision measurements possible, the twin detector is permanently connected to a gas flow system with automatically operated control of gas flow and gas pressure. Methane based tissue equivalent gas is used.

The outer cylinders of the detectors are connected to negative high voltage. The charges collected at the central anode wire are integrated in the feedback capacitors of electrometers; these are operational amplifiers which act as compensation circuits, clamping the central wire to zero potential. In the most advanced version of the equipment, the voltages at the integration capacitors are digitized simultaneously by high speed voltmeters. The results are transmitted to a personal computer. Measurements with a repetition rate of 100 kHz and with a depth of 14 bit can be performed. This fast signal processing is a prerequisite for measurements in high dose rate fields.

2. Calibration of the measuring device and determination of the first Townsend ionisation coefficient for methane based tissue equivalent gas

For calibration purposes an Am-241 α -spectrometer calibration source enclosed in a gas tight capsule can be attached to the detector (see Fig. 1). The α -particles enter the detector as a narrow collimated beam directed towards the central wire. Before the calibration measurements, the energy distribution of the α -particles emerging from the collimator and their energy loss within the sensitive volume have been determined in their dependence on gas pressure. The measurements were performed with a semiconductor spectrometer positioned in a vessel that was connected to the gas flow system (see Fig. 2). The most probable energy of the particles as a function of the path length in tissue equivalent gas is given in Fig. 3. The results of the measurements are indicated by points, whereas the solid line represents the Bethe theory.

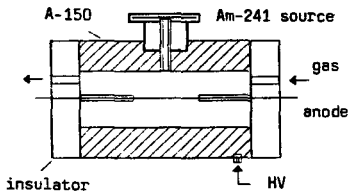


Fig. 1. Diagram of the detector with attached α -source.

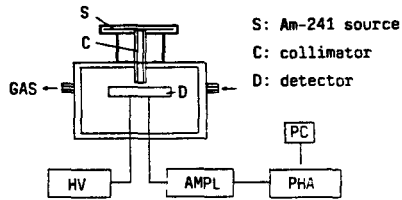


Fig. 2. Experimental set-up for measurement of the energy loss in tissue equivalent gas.

From the calibration measurements at various anode voltages and gas pressures the first Townsend ionisation coefficient was evaluated for a broad range of the reduced field strength. In Fig 4 the gas multiplication is given in its dependence on the inverse of the reduced field strength. The deviations from the Townsend theory at high reduced field strength are well known for other gas mixtures and are attributed by Segure to " non equilibrium conditions". For methane based gas our findings are in line with results of Waker.

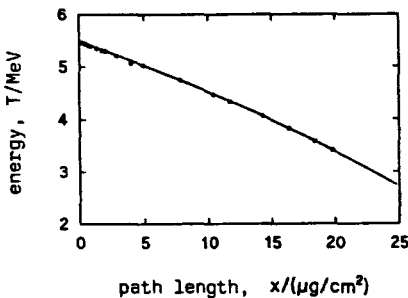


Fig. 3. Energy loss of the α -particles in its dependence on path length (solid line Bethe theory).

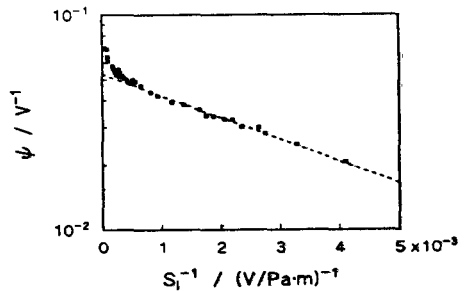


Fig. 4. Reduced gas multiplication in its dependence on reduced field strength.

3. Suppression of disturbances in variance-covariance measurements

There are two types of disturbances affecting the signals of both detectors simultaneously, i.e. in a correlated manner. The first type are disturbances which correspond to multiplying the signals with a factor that varies in time. An example are variations of the gas gain caused by variations of the high voltage; such variations can cause correlated disturbances if both detectors are connected to the same high voltage supply. This type of disturbance is entirely eliminated in variance-covariance measurements, in the same way as this method eliminates any distortions due to varying dose rates.

A second type are additive disturbances, such as electronic pick-up of a signal in both measuring channels. This kind of disturbance is not fully eliminated, but its influence is substantially reduced by the variance-covariance method; at equal mean output of the two channel the correction is precise. If there is a fixed ratio of the mean output, the correction is also perfect provided the results are computed from a suitable adjusted form of the basic equation that is symmetric relative to the two detectors.

The inherent possibilities of the variance-covariance technique for suppression of various interfering disturbances facilitate microdosimetric measurements and enhances their precision and accuracy.

4. Microdosimetric measurements in diagnostic X-ray fields

Microdosimetric measurements in diagnostic beams of x-rays have been performed. The anode voltages were varied between 30 and 125 kV. In these pulsed radiation fields microdosimetric measurements are possible only by application of the variance-covariance technique. In such fields the variance method is not applicable, and measurements in single-event technique are possible only if the dose rate is reduced greatly. However the substantial reduction of the tube current or the increase of the source to detector distance would change radiation quality. Furthermore measurements with the single-event technique are impracticable in duration.

The dose averaged lineal energy at different anode voltages and at different diameters of the simulated volume are given in Tab. 1. All measurements were performed with a two-pulse generator and with a filter equivalent to 2 mm of aluminum.

Tab. 1. The dose averaged lineal energy (keV/μm) at different anode voltages (kV) for two-pulse x-ray generator.

Voltage	0.2 μm	0.5 μm	1 μm	8 μm
30			3.42 ± 0.25	1.98 ± 0.03
35	5.89 ± 0.60	4.55 ± 0.24	3.35 ± 0.11	2.17 ± 0.12
42				1.84 ± 0.07
48	5.37 ± 0.54	4.30 ± 0.28	3.21 ± 0.09	
51				1.50 ± 0.02
60	5.98 ± 0.48	4.27 ± 0.25	3.19 ± 0.16	1.41 ± 0.06
75	5.82 ± 0.48	4.38 ± 0.13	2.94 ± 0.05	1.46 ± 0.06
90	5.86 ± 0.10	4.36 ± 0.19	2.97 ± 0.03	1.47 ± 0.08
110	6.10 ± 0.62	4.37 ± 0.27	2.94 ± 0.04	1.47 ± 0.09
125	5.93 ± 0.44	4.38 ± 0.35	2.99 ± 0.04	1.35 ± 0.04

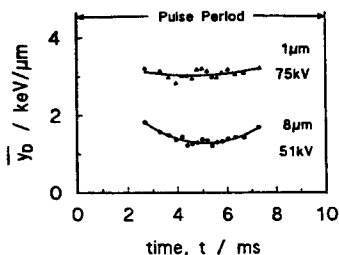


Fig. 5. Variation of the dose averaged lineal energy with the pulse phase of the periodic x-ray fields. (Δ) $1\mu\text{m}$, 75 kV; (\bullet) $8\mu\text{m}$, 51 kV.

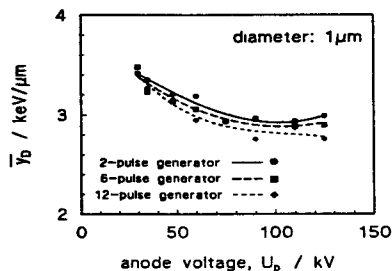


Fig. 6. Dose averaged lineal energy as a function of anode voltage for the (\bullet) 2-pulse, (\square) 6-pulse, and (\diamond) 12-pulse generator. The simulated diameter is $1\mu\text{m}$.

Using the temporal information in the measured data, one can determine the dose averaged lineal energy for any phase within the radiation pulse; for this purpose, one needs to extract from the full series of measurements the subsegments that correspond to the chosen phase intervals. Examples of phase dependences are given in Fig. 5 for a simulated volume of diameter $1\mu\text{m}$ and an anode voltage of 75 kV.

Data for the 6-pulse or 12-pulse generators that are commonly used today can be derived from the measurements with a 2-pulse generator using once more the temporal information. Values of the dose mean lineal energy, as a function of anode voltage, for different generators are shown in Fig. 6.

In further investigations variations of radiation quality with depth in the absorber have been examined. Different depths in tissue were simulated by the use of acrylic phantoms that were sufficiently equivalent to tissue for the radiations in question. The measurements were performed with anode voltages of 42 kV and 70 kV and with a filter that was equivalent to 1 mm of aluminum. The dose averaged lineal energy decreases with depth, and this is shown in Fig. 7 for a site of $0.5\mu\text{m}$. The decrease reflects the hardening of the radiation field with increasing absorber thickness.

5. Microdosimetric measurements in the electron beam of a therapeutic linear accelerator

The measurements in the electron beams that are used for radiation therapy have in the past predominantly been performed in the conventional single-event technique. For these measurements it was necessary to reduce the dose rate very substantially. The reduction can only be achieved by technical manipulations that exclude measurements in clinic routine. With the variance-covariance method, on the other hand measurements are possible at appreciable dose rates of 0.1 Gy/min or even more. Although one may want to avoid the high typical dose rates in radiation therapy of about 5 Gy/min moderate dose rate reductions are sufficient that can usually be achieved without complications. The

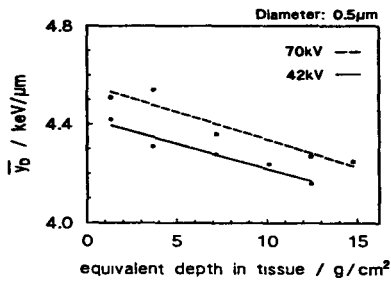


Fig. 7. Depth dependence of the dose averaged lineal energy for anode voltages of (—) 42 and (---) 70 kV.

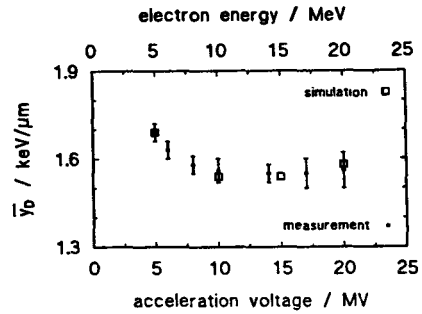


Fig. 8 Dose averaged lineal energy at different acceleration voltages for a simulated diameter of 500 nm (measurements and computer simulations).

measurements were performed in the beams of a therapeutic linear accelerator at acceleration voltages between 5 MV and 20 MV. The dependence of dose averaged lineal energy on the acceleration voltage is given in Fig. 8. The full dots give the mean values of three measurements and the standard errors. The open squares show the results of computer simulations. In addition to the experimental investigations computer simulations have been performed to assess the influence of the detector wall thickness and that of the diameter of the simulated site.

Publications

J. Chen, J. Breckow, H. Roos, and A.M. Kellerer, Further development of the variance-covariance method. *Radiat. Prot. Dosim.* 31, 171-174 (1990).

J. Chen, Microdosimetry of time varying radiation fields; development of the variance-covariance method. Thesis, University of Würzburg (1991).

J. Chen, H. Roos, and A.M. Kellerer, Microdosimetry of diagnostic x rays Applications of the variance-covariance method. *Radiat. Res.* 132, 000-000 (1992).

J. Chen, K. Hahn, H. Roos, and A.M. Kellerer, Microdosimetry of therapy electron beams; measurements and Monte-Carlo simulations. To be published in *Radiat. Prot. Dosim.* (1993).

Project 2

Head of project: *Dr. K.A. Jessen*

Objectives for the reporting period

To modify and improve existing equipment used for variance-covariance measurements in pulsed therapeutic radiation beams of high dose rate in order to extend the use of the method to "continuous" radiation fields as *fx.* used in diagnostic radiology. Development and testing of suitable detectors and the necessary electronics applicable for variance-covariance measurements in such beams using the ionisation mode. Adjust and extend computer programs for data processing in this mode and perform measurements of different beam qualities.

Progress achieved

The variance-covariance method is a measuring technique designed especially for measurements of the microdosimetric dose averaged lineal energy \bar{y}_D in fluctuating radiation beams. The advantage of this technique is due to the employment of two detectors instead of only one. In previous research equipment for the variance-covariance method has been developed. Two commercially available detectors were used and results were obtained for pulsed therapeutic x-ray and electron beams (H.B. Honoré et al, 1990). The situation in a continuous beam is somewhat different. The measurements must be based on integration of the signal from the detectors and this was not possible in the commercial detectors without radical changes in their construction. To make a successful charge integration in the variance-covariance-technique, integration of charge from both detectors in separate integrators in simultaneous intervals must be possible.

A new detector-pair of cylindrical shape made of A-150 tissue-equivalent conductive plastic has been produced with suitable guard electrodes and placed in a vacuum housing with shielded wire connections at ground potential to prevent charge pile-up in the wires. The final version was designed after experience gained from a cylindrical detector-pair made of solid-water coated inside with Aquadac. In the recognition, that the spherical shape is not needed because of the non-isotopic beams (the beams investigated have always a well defined beam-direction) the cylindrical shape was chosen in preference to the spherical and in addition, the cylindrical chambers are easier to manufacture, and are more suitable for module construction. The experimental arrangement is shown in Figure 1.

The charges produced in the detectors are fed directly into two computer controlled electrometers (Keithley 617 programmable). After appropriate amplification the analog signals pass on to a multifunction data acquisition board with simultaneous sample - and - hold capabilities (DATA TRANSLATION 2818). The values are digitised by an analog-digital-converter on the acquisition board and transferred by Direct-Memory-Access (DMA) to the computer for further data processing.

Measurements have been performed using the electrometers as A/D-converting instruments. The integration time given by the A/D-conversion rate of the electrometers were fixed at the highest level in order to obtain the highest possible resolution of the varying signals.

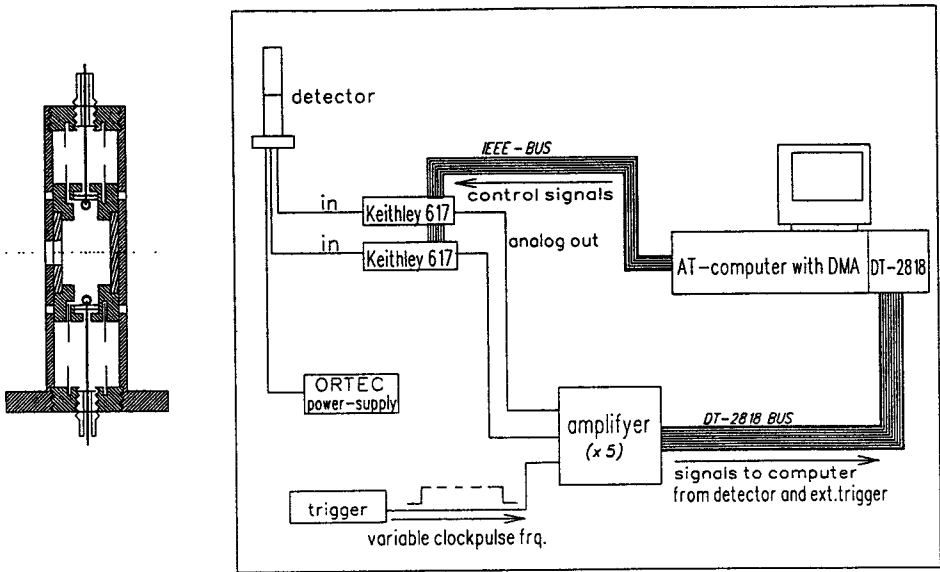


Fig. 1 The experimental arrangement for measurements in continuous radiation beams

Unfortunately this integration period is quite high (780 msec) resulting in a unrealistically long overall measuring time especially for diagnostic equipment if a statistically sufficient number of datapairs is to be collected.

The method of measurements has to be changed to much shorter integration intervals in the order of 5 msec giving smaller signals and shorter total data collecting time. Shortening the integration time results in increasing noise on the data. The noise appears as "ripples" overlaying the "real" variance of the consecutive sequences of data-pairs, and in fact shows negative pulses indicating loss of charge. A computer program has been developed making it possible to choose over a broader dynamic range of integration time and at the same time collect very large samples of data-pairs. The negative datapulses can be eliminated either by increasing the integration time adequately to an optimized level or by running a noise reduction algorithm designed to identify and remove the noise pulses. The later approach is very delicate because one must be able to distinguish between noise and "real" variance. The former approach involving optimizing of integration time has improved the quality of the data considerably, but has to be further optimized before final calibration. Measurements showing the tendency in the beam quality range from 150 kV to 250 kV have been performed and the results are shown in Fig. 2 (H.B. Honoré et al, 1992).

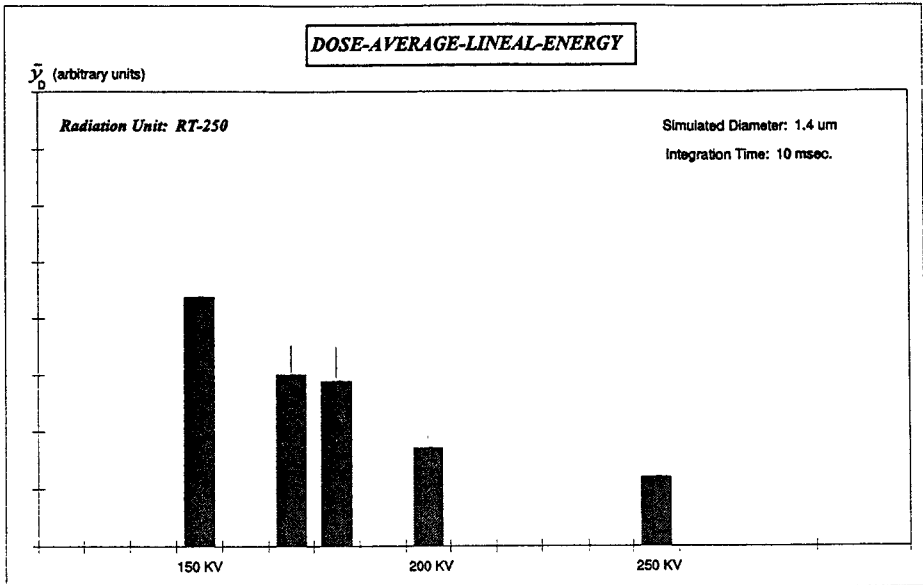


Fig. 2 The dose mean lineal energy for conventional X-ray beams in arbitrary units

Discussion: The experience gained by performing measurements in the proportional mode in pulsed undisturbed radiation beams from a linear accelerator has been used to modify and extend the variance-covariance microdosimetric measuring technique to the use of ionisation mode in "continuous" therapeutic and diagnostic radiation beams. The fact that there seems to be a narrow range for optimal operation has made the experimental method more difficult than originally expected. The compromise between lowering the signal to decrease integration time and increase the signal to obtain an acceptable variance has to be optimized very carefully. It will probably still be necessary to operate a noise reduction algorithm in order to eliminate negative data pairs. Before that it is necessary to investigate the noise profile on the signals very carefully. Essential parameters are also the charge collection in the detectors and the determination of the collection volume. A final test of the method and the measured dose mean lineal energy values of therapeutic and diagnostic radiation beams could be measurements with detectors operating in the proportional mode. Development of less sensitive detectors of smaller sizes has then to be performed.

H.B. Honoré, K.A. Jessen and H.H. Nielsen. Variance-Covariance measurements of the Dose Mean Lineal Energy in Beams for Radiotherapy. *Rad.Prot.Dosim.*, 31, 453-455 (1990).

H.B. Honoré, L.C. Jensen, K.A. Jessen and H.H. Nielsen. Variance-Covariance Measurements in Therapeutic and Diagnostic Radiation Beams of different Qualities, Submitted to *Rad.Prot.Dosim.* 1992.

Project 3

Head of project: *Dr. Lindborg*

Objectives for the reporting period

The objects were :

- To compare the two different electrometer types (capacitor and resistor feed-back respectively) concerning there electronic noise characteristics.
- To investigate the dependence of y_D with radiation quality and with object size in X-ray beams.
- To complete measurements in water with ionization chambers to be able to calculate the absorbed dose both from a ^{60}Co calibration and from calibration in X-rays.
- To simulate the measurements with Monte Carlo calculations.

Progress achieved

The construction of the electrometer amplifiers, i.e. an amplifier with very low input leakage current, have been completed. For comparison two types were constructed: charge integrating and current measuring amplifiers. For covariance measurements both channels were equipped with electrometers of the same type.

The integrating amplifier (charge-to-voltage converter) had a feed-back capacitor as shown in Figure 1. Samples were taken on the increasing output voltage at known time intervals, ΔT , defining the integration time of a single measurement. The time intervals were normally set between 0,1 and 10 seconds. The digital voltmeter had the ranges 20 V, 2 V or 200 mV full scale with $4\frac{1}{2}$, $5\frac{1}{2}$ or $6\frac{1}{2}$ digits, giving a resolution of 1 mV to 100 nV. With a feed-back capacitor value of 100 pF this corresponds to a resolution of 100 fC to 10 aC per digit. A low leakage reed relay was used to discharge the feed-back capacitor, to avoid amplifier saturation. A special relay connection reduces the leakage current and virtually eliminates the stray capacitance parallel to the feed-back capacitor.

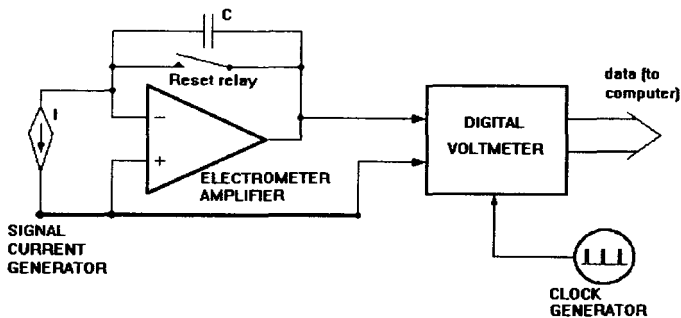


Figure 1. Integrating amplifier

The current amplifier (current-to-voltage converter) had a feed-back resistor as shown in Figure 2. It is followed by a voltage-to-frequency converter (U/f-converter), which in practice makes it integrating. The U/f-converter has one output for each voltage polarity. The scale factor can be set to 10 V/MHz, 1 V/MHz, 100 mV/MHz or 10 mV/MHz. The zero crossing error is low (less than 5 Hz). The feed-back resistor value is approx. 10 G Ω . The combination of electrometer and U/f-converter gives a total resolution adjustable from 1 fC per pulse (or 1 fA/Hz) to 1 aC per pulse (1 aA/Hz). The integration time intervals, defined by the gate time for the counters, were chosen between 0,1 and 10 seconds. The counters had each eight decimal digits (max. 10⁸ pulses). For covariance measurement with the resistor feed-back electrometers the stray capacitances parallel to the resistors had to be adjusted to get equal time constants for the two channels (11 ms, i.e. much shorter than the integration time intervals).

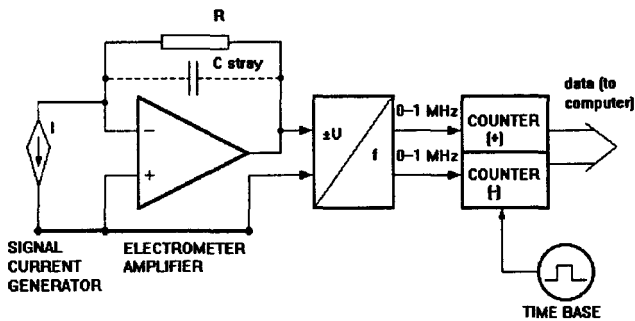


Figure 2. Current amplifier

The charge as well as the current amplifier has a MOS input operational amplifier, type CA3420 (Harris) as input stage. It is supplied with a minimum allowable voltage (2,0 V single supply) to assure low leakage current (10 fA). It is cascaded with a MC1436 (Motorola) as output amplifier to give a wide output range (with ± 24 V supply voltage). Shielded separation between the two stages gives virtually zero stray capacitance between input and output.

The main noise sources have been recognised as the following:

- Thermal resistor noise (for a 10 G Ω resistor this gives a standard deviation in the current equal to $1,26 \text{ fA}/\sqrt{\text{Hz}}$).
- Shot noise (due to the standard deviation of a limited number of electrons collected).
- Amplifier input voltage noise applied over the resistor at the input and over the input capacitance (specified by the manufacturer).
- Resolution of the read-out instruments (volt meters and counters, respectively).
- Hum and disturbances from power supplies and other equipment.

Figure 3 and Figure 4 show the theoretical variance of the noise current for the different noise sources and their sum (called total noise). In the figures the variance is plotted as a function of the integration time in a single measurement. The figures also show the measured noise variance (called leakage variance). The measurements were made with detectors connected to the amplifiers but without irradiation. The cable length between the detector and the amplifier were 3,3 m for the integrating and 0,7 m for the current amplifier. The measured current

(leakage current) was about 20 fA and the theoretical value for the shot noise variance in Figure 3 and 4 was calculated for this value. For the integrating amplifier a feed-back capacitor of 100 pF was used. The resolution was 5 ½ digits and the range 0,1 V corresponding to 1 μ C in the last digit. The current amplifier was used with the range 10 mV corresponding to 1 aC per pulse. In the figures it can be seen that the measured noise variance is a factor of 3 higher than predicted by the theory for the current amplifier and a factor of 100 higher for the integrating amplifier and an integration time of 0,1 s. The difference is less with longer integration time.

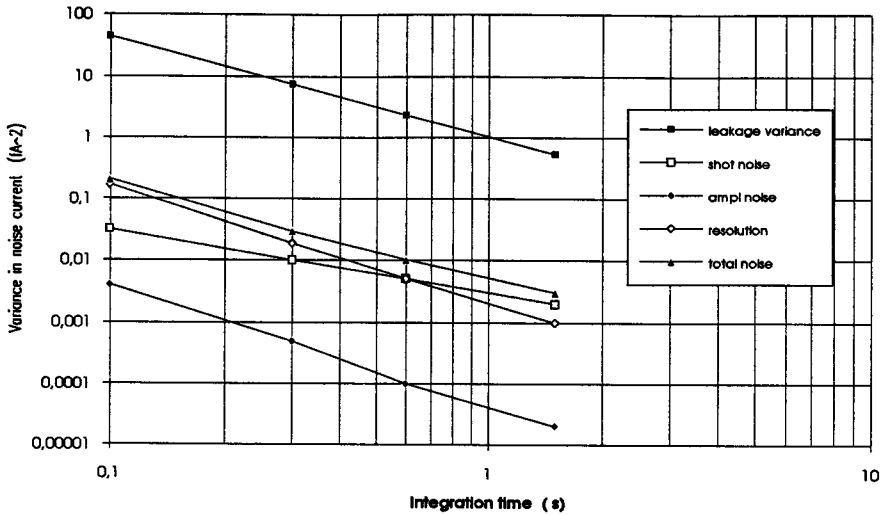


Figure 3. Integrating amplifier

At this current and for the current amplifier the total noise variance is dominated by the thermal noise (in the Figure 4 these two curves are overlapping). For the integrating amplifier at this current the shot noise and the resolution is approximately the same. Comparing the two amplifier techniques it can be seen that there is no significant difference in the measured noise variance at the overlapping time interval. The difference between the measured and the theoretical variance for the current amplifier seems to be acceptable. For the integrating amplifier the large difference is not yet understood.

To investigate the possibility to measure y_D for small object sizes with the variance-covariance method measurements were done with two spherical chambers. Model A4 has an inner diameter of 38,1 mm and model A5 has an inner diameter of 57,2 mm. The wall of the detectors were made of C-552 plastic. The detectors were placed in a cylindric plastic container filled with air. The detectors were both placed on the central beam line, separated 50 mm, with the smallest detector closest to the X-ray tube. The measurements were made with pressures from 0,015 kPa to 3 kPa corresponding to object diameter between 6 nm and 2 μ m. The preliminary results of the measurements are given in Figure 5, where the results for both chambers are plotted. The result marked A has not been corrected for the variance in the leakage, while in the result marked B a leakage variance has been subtracted. The figure shows

that down to around 20 nm the leakage variance is small, but becomes quickly dominating below that point. The way to treat this correction is not yet fully understood.

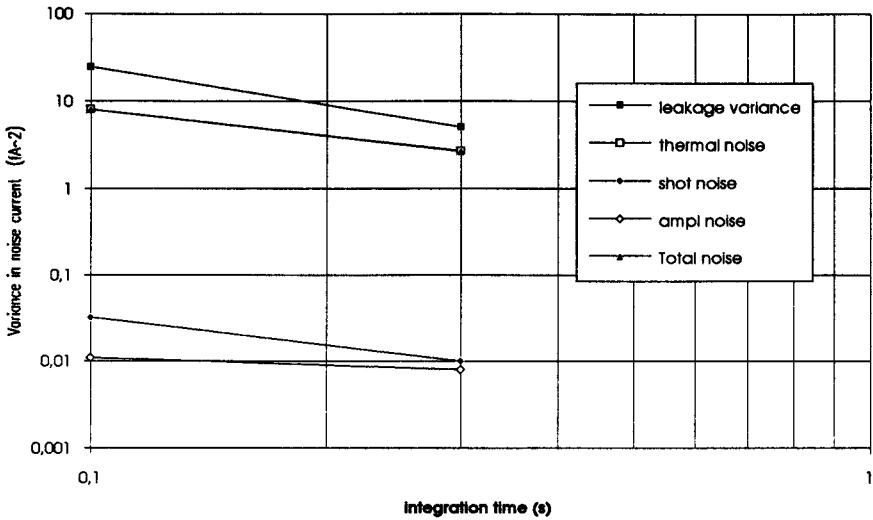


Figure 4. Current amplifier

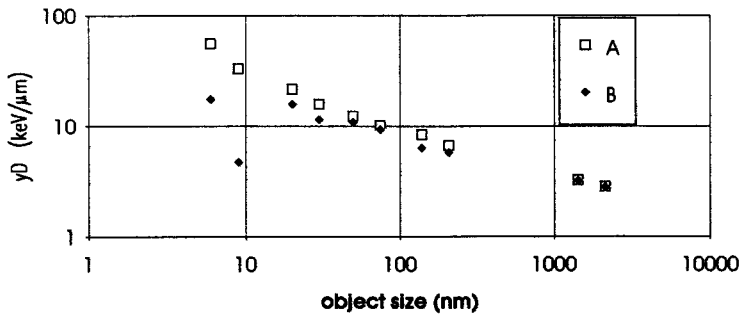


Figure 5. Dose mean lineal energy as function of the object size



THE MEASUREMENT OF ENVIRONMENTAL GAMMA DOSES

Contract Bi7-027 - Sector A12

- 1) *Bøtter-Jensen* , Risø National Laboratory -
- 2) *Lauterbach* , PTB
- 3) *Delgado Martínez* , CIEMAT

Summary of project global objectives and achievements

The aim of this project was mainly to determine and analyse the response of different active doserate meters and passive integrating TL dosimeters for measuring the environmental background photon radiation and to establish reference calibration procedures to enable an international intercomparison of measuring results. To ensure that measurements can be made with sufficient accuracy, it is necessary to determine the detector responses to cosmic and terrestrial radiations and to take into account the inherent instrument/dosimeter background and linearity at low dose rates.

Studies of instrument/dosimeter calibration methods included free-field and shadow-shield calibrations using certificated ^{137}Cs , ^{60}Co and ^{226}Ra gamma sources where the ground albedo, air build-up and room scatter components for a variety of source-detector geometries and surroundings were calculated by the Monte Carlo code MCNP. Calculated doserate values compared very well with those obtained from field calibrations using a variety of environmental dose rate meters. Field measurements were further performed at Risø to determine the detector/dosimeter responses to terrestrial and cosmic radiation.

The determination of instrument/dosimeter linearity, angle- and temperature dependence and inherent background were performed in the newly established low-level underground measurement laboratory (PTB/UDO) at 925 m depth in the Asse saltmine facility where the radiation background is less than 1 nGyh^{-1} . The photon energy responses were determined using different gamma sources in addition to 6 MeV photons provided by an accelerator installation at the PTB laboratories.

Environmental monitoring with integrating TL dosimeters were improved by introducing a new-developed evaluation method based on numerical analysis of the glow curves which especially has proved to be important for assessing the individual dosimeter background for the initial dose readout. Glow curve analysis computer programmes were successful developed at CIEMAT both for linear and non-linear heating of TL dosimeters. The Asse underground laboratory formed a unique basis for studies of self dose and temperature effects of different TL dosimeter materials normally used for environmental monitoring.

Special emphasis from all the participants was laid on studies of long term air-kerma rate measurements around the Hinkley Point Nuclear Power Station (UK) to assess how different detector types respond to small variations of the background due to the release of ^{41}Ar plumes and the direct 6 MeV ^{16}N radiation. The integrated air kerma values from each of the radiation components were evaluated from the measurements and compared with those from TL dosimeters placed on each active detector.

Four monitoring systems equipped with different types of detectors were used over the period 6 November 1990 to 7 March 1991. The two systems from Physikalisch-Technische Bundesanstalt (PTB) used a proportional counter and a plastic scintillation detector and recorded the photon dose equivalent rate every 10 minutes. Both the monitors supplied by Risø National Laboratory, which used a high pressure ionisation chamber (Reuter Stokes RSS-111), and the Geiger-Müller detector system from the GEC, UK recorded the air-kerma rate every 5 minutes.

Over the period 6 November, 1990 to 7 March, 1991, the four detectors were located approximately 200 metres S.W. of Hinkley Point, a Power Station which operates two Magnox reactors. In addition to the kerma rate measurements, coincident records of the wind speed, wind direction and reactor operation history were obtained. Over the four month period of the measurements both the two reactors, R1 farthest from the measurement location and R2 nearest to the detectors, operated at power levels in the range from 0 to 943 MW(t).

Over a shorter 2 month period 11th January to 7th March, 1991, TLD dosimeters supplied by CIEMAT, Spain were also exposed at the same position as the active detectors. Two types of TL dosimeters were used. A non-discriminating LiF TLD-100 dosimeter for dose measurements and a discriminating dosimeter based on the Panasonic UD-802 combining $\text{Li}_2\text{B}_4\text{O}_7:\text{Cu}$ and $\text{CaSO}_4:\text{Tm}$ detectors under different plastic and lead filters.

At the measurements location there are two contributions to the photon air-kerma rate from the power station. The 1.29 MeV photons from the ^{41}Ar discharge plume, which is present when the wind direction is from the station and the direct radiation predominately due to the 6.13 MeV (approximately 68%) gamma ray emissions of the 7.13 second half-life ^{16}N isotope. This is produced in the CO_2 coolant gas via the $^{16}\text{O}(\text{n,p})^{16}\text{N}$ reaction.

On the last day of the experiment the photon spectrum of this radiation was confirmed by measurements made with a portable intrinsic Ge spectrometry system of the PTB.

At the measurement location the measured air kerma rate \dot{K}_{total} of a detector at any instant time is given by the following equation

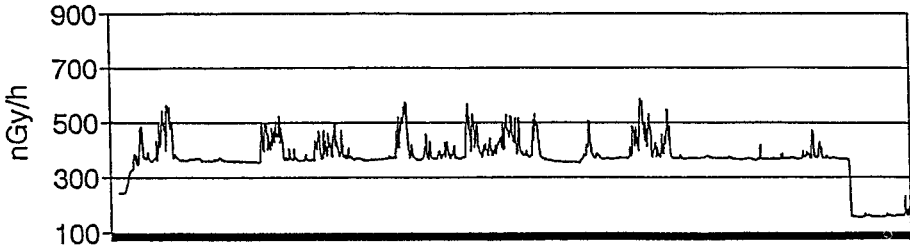
$$\dot{K}_{\text{total}} = [k_c (\dot{K}_c) + k_t (\dot{K}_t) + k_{\text{Ar}} (\dot{K}_{\text{Ar}}) + k_{\text{dir}} (\dot{K}_{\text{dir}})] - R_i$$

where k_c , k_t , k_{Ar} and k_{dir} are the response of the detectors to cosmic radiation, terrestrial gamma radiation, ^{41}Ar and the direct radiation from the power station respectively;

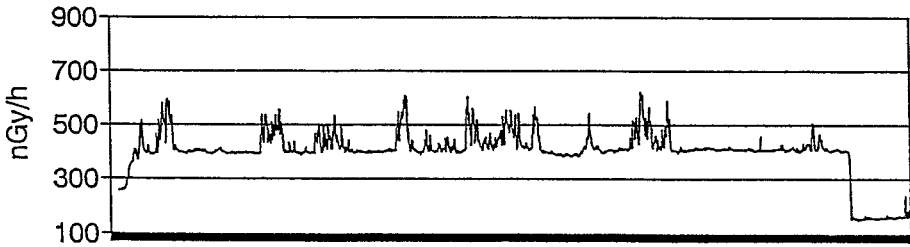
\dot{K}_c , \dot{K}_t , \dot{K}_{Ar} and \dot{K}_{dir} are the air kerma rates from cosmic radiation, terrestrial gamma radiation, ^{41}Ar and the direct radiation from the power station respectively. R_i is the contribution to the reading of the instrument from internal radioactive contamination and/or electronic noise.

The measured, uncorrected variations in air kerma rate as measured by three of the four active detector systems over the TL integration period 11th January to 7th March 1992 are shown in Fig. 1.

RS-SYSTEM (RISØ)
1991



GM-SYSTEM (U.K.)
1991



RM-SYSTEM (P.T.B.)
1991

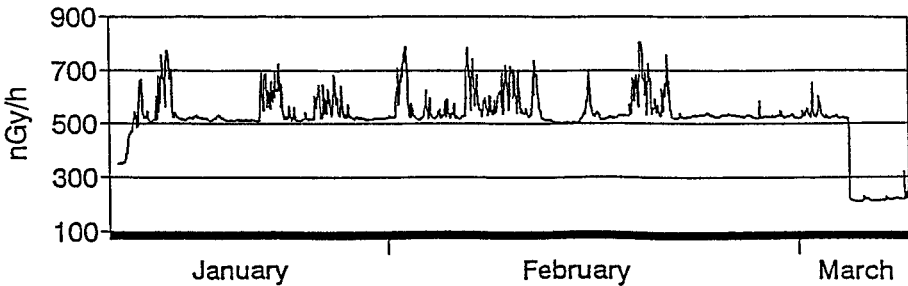


Fig. 1. The measured, uncorrected variations in air kerma rate as measured by three of the four active detector systems over the TL integration period 11th January to 7th March 1992.

A more detailed analysis was made of the results over the two month period that the TLD's were exposed. By comparing the power levels and the measured air kerma rates for each system sample period it is possible to separate the responses of the instruments to various components of the radiation field. From this information the integrated air kerma over the 2 months for these radiation components were calculated for three of the four active dose rate meters used (one system malfunctioned during the period) and the TL dosimeters. These results are shown in Table 1.

Table 1 - Integrated Air Kerma in μGy from the Different Radiation Components

Detector System	Air Kerma (μGy)			
	Background $K_b + K_c$	^{41}Ar	Direct (6 MeV)	Total
Proportional Counter	144.7	36.3	494.2	675.2
High Pressure Ionisation Chamber	117.4	31.4	340.3	489.2
Geiger Müller Counter	98.4	27.1	409.8	535.3
LiF TLD-100	----	----	----	422
$\text{CaSO}_4 : \text{Tm}$	----	----	----	408
Discriminating Dosimeter	----	----	----	407

The results were corrected by response factors for the three detector systems and for the TLD's. The values of K_{Ar} can be taken to be equal to the response to Co-60 radiation. The values of K_c were determined from measurements of the cosmic radiation on the Roskilde Fjord at Risø and the values of R_i were determined in the Asse salt mine. The values of K_t can be assumed to be numerically equal to the response to ^{226}Ra for detectors whose response varies significantly over the photon energy range 0.5 MeV to 1.25 MeV, whilst for those detectors whose response varies little over this range their response to Cs-137 is used. The results corrected for these response values are shown in Table 2.

Table 2 - Values of Air Kerma Corrected for the Detector's Response

Detector Type	Air Kerma (μGy)				Total
	K_t	Cosmic	^{41}Ar	K_{dir} 6MeV	
Proportional Counter	66.1	44.4	28.9	301.9	441.3
High Pressure Ionisation Chamber	70.5	43.2	31.4	282.5	427.6
Geiger Müller Counter	58	43	26.4	253.3	381
LiF TLD-100	68	48	28	259	403
$\text{CaSO}_4 : \text{Tm}$	67	51	29	256	403
Discriminating Dosimeter					377

There is a very good agreement of the estimations of the air kerma arising from the ^{41}Ar radiation, in spite of this being the smallest contribution to the total dose at the measurement location. The different detectors also give consistent estimations of the highest dose component from the 6 MeV photon radiation.

Project 1

Head of project: *Dr. Bøtter-Jensen*

Objectives for the reporting period

- A.1 Monte Carlo calculations of the air kerma rates for different free-field calibration geometries using certificated ^{137}Cs , ^{60}Co and ^{226}Ra sources.
- A.2 Monte Carlo Calculations of the scattered air kerma radiation for different shadow shield calibration geometries using certificated ^{137}Cs , ^{40}Co and ^{226}Ra sources.
- A.3 Refinement of Monte Carlo calculations of free-field calibration geometries where surrounding buildings and detector energy responses etc. were taken into account.
- A.4 Free-field and shadow-shield calibrations of different detector types using certificated ^{137}Cs , ^{60}Co and ^{226}Ra sources and the determination of detector responses from terrestrial and cosmic radiations.
- B.1 Long term measurement studies at Hinkley Point Nuclear Power Station of the variation of the ambient radiation due to ^{41}Ar plumes and the ^{16}N 6 MeV radiation.
- B.2 Detailed analysis of the Hinkley Point long term measurements using precise calibration data and detector response information obtained from free-field and 6 MeV (accelerator) calibrations.
- C Implementation of the CIEMAT glow curve analysis technique in Risø TL environmental monitoring procedures (non-linear heating).
- D Final report to be presented to the CEC and publications.

Progress achieved including publications

1. Studies of calibration methods and field measurements

Instrument/dosemeter calibration studies included free-field and shadow-shield geometries where ground albedo, air build-up and room scatter components for a variety of source-detector geometries were determined using Monte Carlo calculations (MCNP code). Field experiments included the determination of the detector responses to terrestrial and cosmic radiations.

1.1 Monte Carlo calculations of the air kerma rate for open free-field geometries

The MCNP code has been used to calculate the air kerma rate from sources of ^{137}Cs , ^{60}Co and ^{226}Ra in different source-to-detector distances in a free-field geometry on a flat ground (open field). The elemental comparison of soil, air and source material which are needed for these calculations can be extended to more complex geometries including surrounding buildings, trees etc.

At the detector point the air-kerma rate, \dot{K} , has three components: the uncollided kerma rate, \dot{K}_{uncol} , from photons emerging from the source; the scattered kerma rate from the

ground, \dot{K}_{ground} , originating from photons leaving the ground surface into the detector point after one or more scattering reactions in the air/ground media; and finally the scattered kerma rate from air, \dot{K}_{air} , originating from photons leaving the air into the detector point after one or more scattering reactions in the air/ground media.

From special features in the MCNP code regarding photon importance and photon energy distribution it is possible to separate these components:

$$\dot{K} = \dot{K}_{uncol} + \dot{K}_{ground} + \dot{K}_{air} = \dot{K}_{uncol} + \dot{K}_{scatter} \tag{1}$$

For a given radionuclide the energy distribution of the air kerma rate from scattered photons at the detector point will depend on the measurement geometry, viz. the source-to-detector distance and the distance of the source/detector above the ground. Such a distribution is shown in Figure A.1.1. for a ^{137}Cs source. The source-to-detector distance, D , is here 3 metres and both source and detector are elevated 1 metre above ground. The total scattered air kerma for this geometry has been calculated as: $\dot{K}_{scatter} = 0.12 \cdot \dot{K}_{uncol}$. Consequently, the total air kerma rate, \dot{K} , can be expressed by the uncollided air kerma rate, \dot{K}_{uncol} :

$$\dot{K} = \dot{K}_{uncol} + \dot{K}_{scatter} = 1.12 \cdot \dot{K}_{uncol} \tag{2}$$

which implies that uncollided photons contribute with approximately 88% of the total air kerma rate, \dot{K} , and scattered photon with the remaining 12% for which the energy distribution is shown in Figure A.1.1.

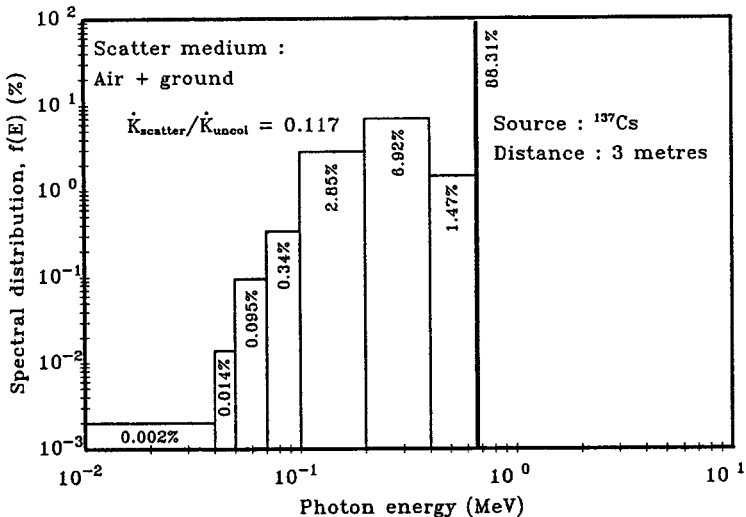


Figure A.1.1. Energy distribution of the relative free-field air kerma rate from a ^{137}Cs source at a distance of 3 metres.

If the response of a given detector as a function of the photon energy, E , is $r(E)$, the instrument response, R , to the total air kerma rate, \dot{K} , having a spectral distribution, $k(E)$, as shown in Figure 1, can be calculated as:

$$R = \sum_{i=1}^n \dot{K}(E_i) \cdot r(E_i) \quad (3)$$

where n is the number of photon energy intervals used in the spectral calculation.

In Figure A.1.2. the MCNP calculated ratios of total scattered to uncollided air kerma rates are shown for the three sources ^{137}Cs , ^{60}Co and ^{226}Ra as a function of the source-to-detector distance (D) and with the source and detector elevated 1 metre above ground.

The material composition of the soil specified in the calculations is that for dry "Risø-soil": O (53.5%), Si (34.3%), Al (3.8%), Fe (1.8%), K (1.7%), Ca (1.65), Mg (1.4%) and remainder (1.9%). The density of the soil is assumed to be 1.37 g cm^{-3} .

The results shown in Figure A.1.2. of the scattered air kerma rates have been separated in contributions from air and ground. The scattered photons from the source material have been accounted for as unscattered photons. Detailed calculated values are published elsewhere (see publication list) for source-to-detector dosimeters from 0.5 to 50 metres.

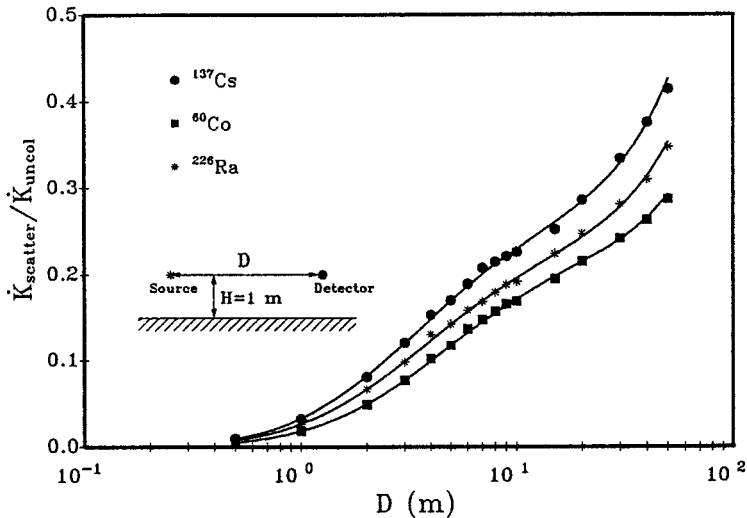


Figure A.1.2. Relative scattered free-field air kerma rates from ^{137}Cs , ^{60}Co and ^{226}Ra sources as a function of distance.

1.2 Monte Carlo calculations of the air kerma rate for shadow-shield geometries

Relative values of the air kerma rates from scattered photons have been calculated for the radionuclides ^{137}Cs , ^{60}Co and ^{226}Ra in a shadow-shield facility at Risø for source-to-detector distances of 3, 4 and 5 metres. The actual calibration room is made of concrete (walls, floor and ceiling) and the dimensions are 12 x 6 x 2.2 m. The shield was of lead and dimensions 16x16x10 cm. The relative scattered air kerma rates without the lead shield contribute with 20-60% of the uncollided air kerma rate depending on distance and nuclide.

1.3 Monte Carlo calculations of the air kerma rate for free-field geometries in an enclosed garden environment

To see how buildings and other objects affect the scattered radiation, relative values of the air kerma rate from scattered photons have been calculated for the nuclides ^{137}Cs , ^{60}Co and ^{226}Ra in free-field calibration geometries inside an enclosed rectangular garden environment (30 x 90 metres). The garden containing plants and trees is surrounded by laboratory buildings on four sides.

On comparing the MCNP calculated values with measured values it is concluded that surrounding buildings and trees, if not closer to the source and detector than 10 - 15 metres, will have insignificant influence on the total air kerma rate. Details are published elsewhere (see publication list).

1.4 Comparison of calculated and experimental results

The Monte Carlo calculated air kerma rate values have been compared with values measured by a variety of environmental dose rate meters during previous CEC sponsored intercomparison studies of free-field calibration experiments using certificated ^{137}Cs , ^{60}Co and ^{226}Ra sources.

The mean values of the ratios of measured to calculated total air kerma rates, $\dot{K}_{\text{meas}}/\dot{K}_{\text{cal}}$, obtained in the free-field calibrations from three groups of environmental dose rate meters that comprised 8 ionisation chambers, 5 plastic scintillators and 4 energy-compensated GM and proportional detectors are presented in Table A.4. As can be seen from the ratios in Table A.4 very good agreement was found between the calculated and measured air kerma rates.

A paper containing detailed descriptions of the Monte Carlo calculated scattered contributions to the total air kerma rates in different free-field and shadow-shield calibration geometries has been submitted to Radiation Protection Dosimetry (by 14. April 1992) for publication.

Table A.4. Mean values of measured-to-MCNP-calculated ratios of total air kerma rates, $\dot{K}_{meas}/\dot{K}_{cal}$, obtained for three different groups of environmental dose rate meters in free-field calibration experiments at source-to-detector distances of 3, 5 and 10 metres using certificated ^{137}Cs , ^{60}Co and ^{226}Ra gamma sources.

Mean values of measured-to-MCNP calculated total air kerma rates, $\dot{K}_{meas}/\dot{K}_{cal}$				
Detector	No. of instruments	Free-field		
		^{137}Cs	^{60}Co	^{226}Ra
Distance: 3 metres				
Ion chambers (mean)	8	1.004 ± 0.024	1.001 ± 0.021	0.982 ± 0.021
Plastic scint. (mean)	5	1.007 ± 0.009	0.993 ± 0.060	0.961 ± 0.054
GM + prop. detec. (mean)	4	0.988 ± 0.034	1.006 ± 0.027	0.994 ± 0.025
Total instruments (mean)	17	1.001 ± 0.023	1.000 ± 0.036	0.979 ± 0.035
Distance: 5 metres				
Ion chambers (mean)	8	1.000 ± 0.013	0.995 ± 0.014	0.989 ± 0.018
Plastic scint. (mean)	5	1.020 ± 0.033	1.002 ± 0.069	0.969 ± 0.052
GM + prop. detec. (mean)	4	0.990 ± 0.022	1.002 ± 0.014	0.978 ± 0.042
Total instruments (mean)	17	1.004 ± 0.024	0.999 ± 0.036	0.981 ± 0.035
Distance: 10 metres				
Ion chambers (mean)	8	0.989 ± 0.016	0.991 ± 0.029	0.979 ± 0.037
Plastic scint. (mean)	5	1.001 ± 0.042	0.987 ± 0.075	0.960 ± 0.067
GM + prop. detec. (mean)	4	0.963 ± 0.046	0.997 ± 0.017	0.944 ± 0.090
Total instruments (mean)	17	0.986 ± 0.034	0.991 ± 0.043	0.965 ± 0.059

2.1 Long term measurements at the Hinkley Point Power Station (UK)

Continuous measurements of the air kerma rate at the Hinkley Point Power Station were successfully completed partly under a Risø subcontract with I.M.G. Thompson (UK) using four different designs of active monitoring systems in addition to passive integrating TL dosimeters. Details are given in section I of this report and in a paper being submitted for publication in Radiation Protection Dosimetry.

2.2 Analysis of the Hinkley Point Power measurements

Comparison of results from the four active detectors shows that though they all very closely followed the variations in air kerma rate with time, they did not give agreement on the magnitude of the different radiation components. Figure B.2 shows an example of the air kerma rate variations for a period during January 1991 as measured by the high pressure ionisation chamber as provided by Risø National Laboratory and by the UK GM counter.

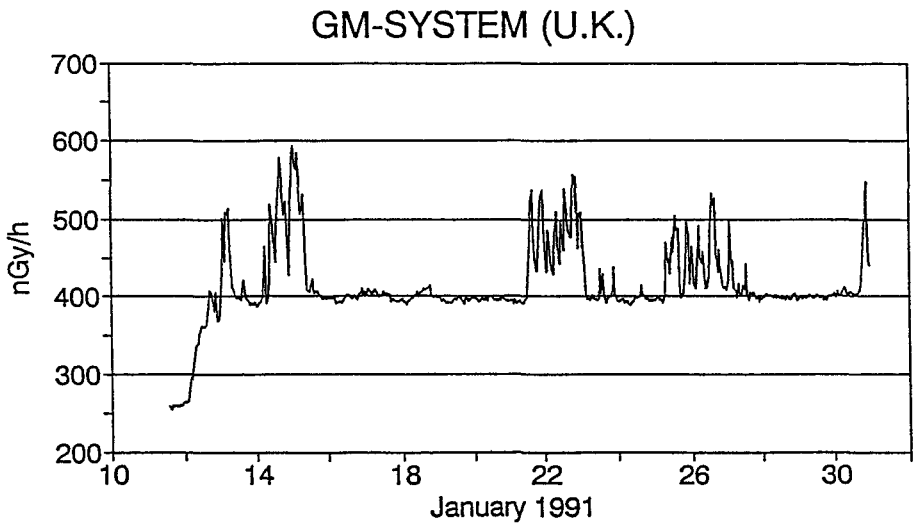
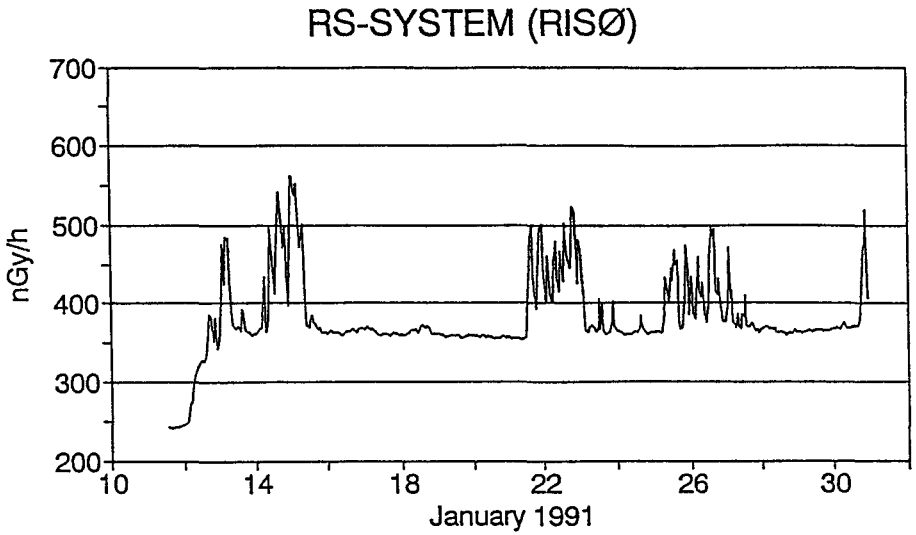


Figure B.2. The air kerma rate variations at the Hinkley Point Power Station in January 1991 as measured by a Reuter Stokes high-pressure ionisation chamber (RS-system) and a GEC GM counter (GM-system).

The Hinkley Point experiments clearly demonstrated that accurate measurements of doses in the environment arising from a nuclear facility can only be obtained if continuous measurements are made and the detectors response to the different natural and man made radiation components at that location are accurately evaluated.

3. Implementation of glow curve analysis technique (CIEMAT) in the Risø TL environmental monitoring procedures

The Implementation of the glow curve analysis technique developed at CIEMAT into the routine environmental TL monitoring at Risø was successfully completed under a collaboration between RISØ and CIEMAT by creating a new computer programme fitted to a special non-linear hot gas heating system. The results are described in a paper accepted for presentation at the 10th Solid State Dosimetry Conference in Washington July 1992 (Proceedings to be published in Radiation Protection Dosimetry).

Publications

Bøtter-Jensen, L and Hedemann Jensen P.
Determination of Scattered Gamma Radiation in the Calibration of Environmental Dose Rate Meters. Submitted for publication (by 14 April 1992) in Radiation Protection Dosimetry.

Gomez Ros, J.M., Muñoz, J.L., Delgado A., Bøtter-Jensen, L and Jørgensen, F.
A Glow Curve Analysis Method for Non-Linear Heating Hot Gas Readers. Accepted for presentation at the 10th Solid State Dosimetry Conference, Washington DC July 1992 (Proceedings to be published in Radiation Protection Dosimetry).

Thomson, I.M.G., Bøtter-Jensen, L., Lauterbach, U., Pessara, W., Delgado, A. and Saez-Vergara, J.C., The Assessment of External Photon Dose Rate in the Vicinity of Nuclear Power Stations; An Intercomparison of Different Types of Monitoring Systems. To be submitted to Radiation Protection Dosimetry.

Project 2

Head of project: *Dr. Lauterbach*

Objectives for the reporting period

1.1 The measuring facilities in UDO

1.2 The 6 MeV calibration facility

2.1 Measurements in UDO

- Inherent background of the dose rate meters
- Linearity at low air kerma rates
- Angle dependence of the detector responses at low air kerma rates
- Energy dependence of the detector responses at low air kerma rates

2.2 Measurements at the 6 MeV facility

- Calibration measurements
- Build-up measurements

2.3 Analysis of Hinkley Point measurements

Progress achieved including publications

1. Facilities for the measurements

1.1 The new Asse low level laboratory "UDO" of the PTB

In 1991 the low level laboratory "UDO" of the Physikalisch-Technische Bundesanstalt (PTB) was established in the Asse salt mine near Braunschweig.

The laboratory is made of a special construction material with a very low content of radionuclides (below 1.5 Bq/kg) which consists of a resin coated laminated paper. The temperature in this facility is controlled by an air condition system and is stabilized at a value of 22.5° C.

Recent measurements using a proportional counter have shown a value of 0.6 nGy/h for the background radiation level.

Measurements of the radon concentration inside the laboratory will be performed in the near future.

A collimated beam irradiation facility produced photon fields from various radionuclides with air kerma rate levels from 10 nGy/h up to 250 nGy/h. The radionuclides with the appertaining air kerma rates at a distance of 1.79 m from the sources are given in Table 1.

The air kerma rates of the various sources are determined by a secondary standard ionisation chamber of the PTB.

The photon beam of this facility hits only the back wall of the calibration room thus avoiding backscatter from the ceiling and the floor.

The background radiation level is further reduced by a factor of 10 in a lead shielded box in this room which has the size 50 cm x 50 cm x 80 cm. This facility is mainly provided for the determination of the inherent background of environmental dose rate meters.

A turntable is available for measurements of the dependence of the response on the angle of the incident radiation. More details are given in [1].

Table 1

Radionuclide	Air kerma rate at a distance of 1.79 m* nGy/h
¹³⁷ Cs	9.99
¹³⁷ Cs	19.1
¹³⁷ Cs	46.3
¹³⁷ Cs	89.8
¹³⁷ Cs	178
²⁴¹ Am	88.5
⁵⁷ Co	145
¹³⁷ Cs	192
⁶⁰ Co	223

* related to 04.03.1992

1.2 6 Mev calibration facility at the PTB

High energy photons for the calibration of dose rate meters are produced by the reaction $^{19}\text{F} (p, \alpha \gamma) ^{16}\text{O}$ using accelerated protons with an energy E_p of 2.7 MeV irradiating a target of CaF_2 . To reduce the contamination of the photon beam by electrons the target is shielded by a cap made of perspex. The air kerma rates in this field are determined by the spectral photon fluence measured by a $\text{Ge}(\text{Li})$ - spectrometer and by measurements with a 0.5 cm^3 ionisation chamber with a total wall thickness of 2.5 g/cm^3 .

The energies of the photons lie mainly in the 6 - 7 meV range. The properties of this photon field for calibration are described in detail elsewhere [2].

Dosimetric measurements of the air kerma rate in the 6 - 7 MeV photon field with build-up caps for increasing the wall thickness of the detector have shown a decrease of the reading. The reason for this effect is the contamination of the photon field by high energy electrons. The source of the electrons is the decay of the first excited state of ^{16}O which has the same spin and parity as the ground state (0^+), i.e. a photon transition is impossible. This state is de-excited by means of pair production. The emitted electrons have an energy of about 2.5 MeV. There is no influence on the measured air kerma rate if sufficient thick build-up caps with 2.5 g/cm^2 are used for these photon energies. The range of the electrons in the perspex is

only in the order of 1.2 g/cm².

The angular distribution of the air kerma rate is constant within 2% within an angle range of $\pm 5^\circ$ for an incident proton energy of 2.70 MeV.

This calibration facility for high energy photons is established in the low-scatter area of the accelerator plant of the PTB[3].

2. Results

During this intercomparison four detector types for environmental dose rate meters were involved:

- High pressure ionisation chamber (HPC)
- Scintillation detector (SCI)
- Proportional counter (PC)
- GM counter (GMC)

2.1 Measurements in "UDO"

The following properties of these detectors were determined during this intercomparison programme:

- Inherent background for HPC, PC, GMC
- Linearity for PC
- Angle dependence for HPC and PC
- Energy dependence for PC

There were various technical problems to operate the "Funksonde" with the scintillation detector at very low air kerma rates especially due to the built-in software which was developed for another purpose. Therefore not all measurements could be taken in the laboratory "UDO" with this instrument.

In Table 2 are presented values of the inherent background in nGy/h which were determined in the lead shielded box.

The measured value of the proportional counter FHZ 600 A corresponds very well with the background reported by the manufacturer. It amounts about 15% of the normal natural background. The indicated inherent background of the high pressure ionisation chamber RSS-111 seems to be more than 12 times lower than those of the PC.

Inherent contamination of the construction material by radionuclides and leakage currents as well as dark currents are the main sources of the indicated inherent background of these instruments.

Table 2

HPC	SCI	PC	GMC
1.0	< 5	12.4	-

The linearity of the indication of the PC at low air kerma rates was investigated with the set of ¹³⁷Cs sources producing radiation levels from 10 nGy/h up to 180 nGy/h. In Fig. 1 the readings are presented versus the applied radiation fields. The offset with 13.4 nGy/h of the linear relationship corresponds fairly good with the background reading of the PC with 13.2

nGy/h in the calibration room. The slight difference may be caused by scattered radiation from the back wall of the calibration room.

Figures 2 and 3 demonstrate the dependence of the response on the angle of the incident radiation for the HPC and PC. Fig. 3 shows clearly that for the PC the dependence on the angle is also dependent on the photon energy. In this case the preferred direction is perpendicular to the axis of the cylindrical detector. As mentioned in [4] this must be also taken into account for calibration measurements with the shadow shield method. The detector must be irradiated in its preferred direction. Otherwise the calibration is in error.

The energy dependence of the response of the PC was investigated with the 4 photon energies $E\gamma$ of the ^{241}Am -, ^{57}Co -, ^{137}Cs - and ^{60}Co - sources of Table 1. The dependence of the response on the photon energy can be approximated by the third order polynom

$$E(E\gamma) = 1.398 [\lg(E\gamma)]^3 - 9.767 [\lg(E\gamma)]^2 + 22.35[\lg(E\gamma)] - 15.74$$

using the 4 measured values. The comparison with the dependence measured by 12 different photon energies yields a fairly good approximation by the polynom. This shows that the energies of the 4 photon sources are sufficient to investigate the energy dependence of the response of this kind of detectors.

2.2 Measurements at the 6 MeV calibration facility

- Calibration measurements
- Build-up measurements

The calibration measurements were performed at three different distances from the high energy photon source: 2 m., 3 m. and 4 m. In Table 3 are presented the reference values and readings of the dose rate meters in the calibration photon field.

Table 3

Dist. m	Ref. Val. nGy/h	HPC nGy/h	Ref. Val. nGy/h	SCI nGy/h	Ref. Val. nGy/h	PC nGy/h	Ref. Val. nGy/h	GMC nGy/h
2	665.2	786.4	-	-	682.3	1202.6	-	-
3	312.1	357.7	-	-	305.0	523.0	-	-
4	176.2	196.5	171.7	162.8	176.2	294.5	-	-

Due to problems with the software only measurements at 4 m distance could be evaluated for the "Funksonde" with a scintillation detector.

Table 4 shows the mean values of the responses for 3 of the 4 investigated detectors calculated from the values at the three distances.

Table 4

HPC	SCI	PC	GMC
1.148	0.95	1.716	-

Build-up measurements were performed with the GMC and the PC. The GMC showed the same behaviour as the measurements described in [2] a decreasing reading with increasing wall thickness up to the point where all electrons are absorbed (up to 6 g/cm²). In the contrary such effect could not be observed for the measurements with the PC. Taking into account the attenuation of the photons in the build-up slabs of perspex (up to 6 g/cm²) no decrease of the reading was found. Due to the construction of this detector the electrons are absorbed in its wall.

2.3 Analysis of Hinkley Point measurements

A detailed analysis of the long term measurements at Hinkley Point nuclear power station was performed under consideration of the calibration measurements, of the detector responses for terrestrial-, cosmic- and high energy radiation and of the inherent background.

A common publication of all participants has been prepared [5].

References

- [1] Lauterbach, U., Peßara, W., "Die Kalibrier- und Meßeinrichtung der Physikalisch-Technischen Bundesanstalt für extrem niedrige Strahlungspegel", PTB-Bericht in preparation
- [2] Guldbakke, S, Schäffler, D., "Properties of high-energy photon fields to be applied for calibration purposes", Nucl. Instr. and Meth. A299 (1990) 367
- [3] Strzelczyk, H., "Experimentelle Einrichtungen für Kalibrierungen am Dosimetriemeßplatz der Gruppe 6.5 'Neutronendosimetrie' der Physikalisch-Technischen Bundesanstalt", PTB-Bericht, PTB-ND-27 (1986)
- [4] "The measurement of environmental gamma doses", CEC Contract Bi7-027, Progress report (1991)
- [5] Boetter-Jensen, L., Delgado, M., Lauterbach, U., Peßara, W., Sàez-Vergara, J.C., Thompson, I.M.G., "Long term air kerma rate measurements at Hinkley Point nuclear power station", to be published

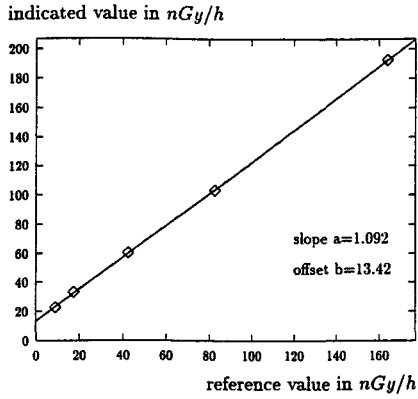


Figure 1 - Dependence of the readings of the PC FHZ 600 A on low air kerma rates

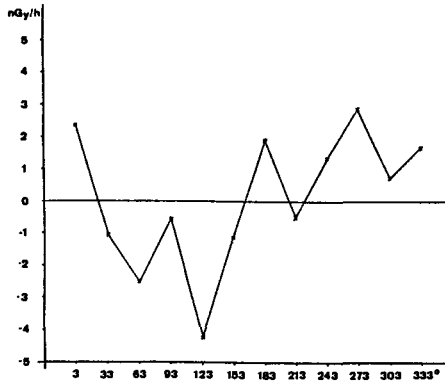


Figure 2 - Angle dependence of the reading on the incident direction of photons for the HPC RSS-111 presented as differences from the mean value of 147 nGy/h for ^{137}Cs

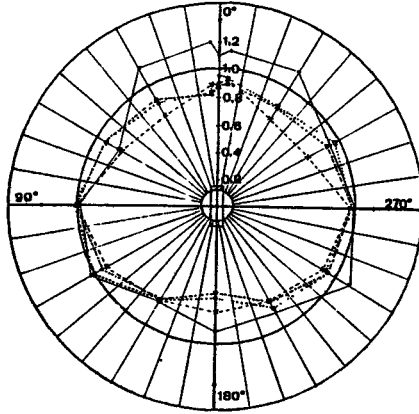


Figure 3 - Angle dependence of the response on the incident direction of photons from various radionuclides for the PC FHZ 600 A; ^{241}Am —, ^{57}Co ---, ^{137}Cs ···, ^{60}Co -·-·-

Project 3

Head of project: *Dr. Delgado Martínez*

Objectives for the reporting period

- a) Refinement of computer programmes for the evaluation of glow curves obtained with linear and non linear (hot gas) heating methods. Determination of the TLD-100 operational performance for low dose measurements (10-100 μ Gy) (CIEMAT-RISØ).
- b) Study of the modifications experienced by LiF TLD-100 glow peaks in severe ambient conditions. Characterization of temperature effects during long exposure intervals. (CIEMAT).
- c) Estimation of dose using several types of TL dosimeters at Hinkley Point Power Station (RISØ-PTB-CIEMAT).
- d) Determination of self-dose characteristics of TLD materials (Asse Mine). Study of the influence of non-radiation induced TL peaks.
- e) Support with TL measurements to be carried out as part of the common research project with RISØ and PTB.

Progress achieved including publications

- a) The integrity of the CIEMAT Simplified Glow Curve Analysis (SGCA) programme for LiF TL dosimeters was proved in field conditions. Improvements in the reliability and operational quality in the lower dose range for TLD-100 were appreciated, extending the conventional lower detection limit. After including some new programme utilities with the purpose of facilitating its use, the SGCA is fully operative.

Further improvements have been introduced in the CIEMAT analysis programmes resolving complex glow curves into individual peaks. In particular, new and highly accurate approximations for different kinetic orders together with an elegant and rapid procedure for peak area calculation. The purpose of this research line is to refine as much as possible peak resolving type programmes, preparing them for future uses in practical dosimetry.

A paper on this subject was published in Radiation Protection Dosimetry in 1990. A review paper on TL glow curve analysis was presented to the CEC seminar "Dosimetry in Diagnostic Radiology" and will also be published in Radiation Protection Dosimetry.

During the period now reported an intensive collaboration has taken place between the CIEMAT and RISØ groups in order to develop a new computer code for the analysis of the glow curve produced by non-linear hot gas readers. This programme applying the principles of the SGCA method is now operative. A CIEMAT-RISØ communication reporting the essential features of this computer programme has been accepted for presentation in the 10th Solid State Dosimetry Conference (10th SSD) (Washington, July 1992).

- b) The study of the individual evolution of the TLD-100 glow peaks during prolonged exposures at normal and elevated ambient temperatures (20-70°C) has been completed. From this study, it has been concluded that Randall-Wilkins fading (spontaneous leakage of trapped charges), cannot explain the detected variations in the TL yield during ambient exposures. These variations are due to changes in the trap structure and to their distribution which occur in the material.

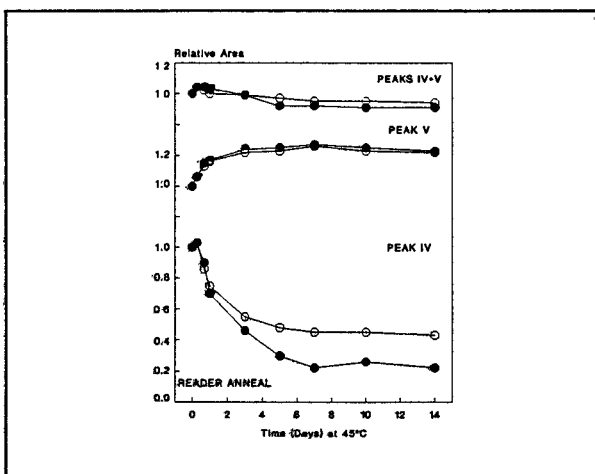


Figure 1 shows the evolution of the TLD-100 peaks IV and V and their sum with storage time at 45°C. Black dots represent the evolution during storage of unirradiated dosimeters and white dots the irradiated dosimeters. The unstable character of peak IV should be noted, as should the fact that this peak is more intense when storage follows irradiation relative to irradiation following storage.

During 1990 and 1992 four papers have been published on temperature effects or related topics in scientific journals and two more were accepted for presentation at a scientific symposium (Natural Radiation Environment, Salzburg 1991) and conference (10th SSD, Washington 1992).

It is to be noted that previous papers published on TL temperature effects by the CIEMAT group are the cause of an active controversy on the peak evolution features. As a direct consequence of the interest of the subject, the CIEMAT group

has been asked to co-organize (CIEMAT and TU Delft, Holland) the First International Intercomparison of Glow Curve Analysis Methods. The results will be presented during the 10th SSD Conference.

- c) CIEMAT provided TL dosimeters which were exposed along with active doserate meters from UK, RISØ and PTB, at a location near to the Hinkley Point Nuclear Power Station. The TLDs were exposed during two months (January and February 1991) and evaluated at CIEMAT after completion of the integration period. Transit control dosimeters were include together with the set of field dosimeters.

Two types of dosimeter were used. A non-discriminating LiF TLD-100 dosimeter for dose measurements and a discriminating dosimeter based on the Panasonic UD-802 combining $\text{Li}_2\text{B}_4\text{O}_7:\text{Cu}$ and $\text{CaSO}_4:\text{Tm}$ detectors under different plastic and lead filters.

The TL evaluation, using for the TLD-100 detectors the SGCA programme, produced consistent satisfactory results, the measurements all agreeing within 3%. The discriminating dosimeters showed the existence of high energy photon radiation. The energy was estimated by the dose calculation algorithm as being in the high limit of its range.

- d) During 1991, the first set of selfdose measurements were carried out in the UDO Laboratory (Asse salt mine, GSF operated). The aim of this first experiment was to collect basic data on the selfdose properties of the most common TL phosphors. Four TL materials from Harshaw ($\text{LiF}:\text{Mg},\text{Ti}$, $\text{CaF}_2:\text{Dy}$, $\text{CaF}_2:\text{Mn}$, $\text{CaSO}_4:\text{Dy}$) and two from Panasonic ($\text{Li}_2\text{B}_4\text{O}_7:\text{Cu},\text{Ag}$ and $\text{CaSO}_4:\text{Tm}$) were stored in different groups and conditions inside the UDO Laboratory. Additional groups were irradiated to known doses in the old gallery for calibration purposes.

With the considerable amount of information collected, a preliminary report was written and a more detailed one is now under preparation. The most striking results were the abnormally high dose results obtained, after one month storage in the virtually radiation free UDO Laboratory from one batch of UD-814 Panasonic badges, revealing a very important selfdosing. This fact is even more significant considering that this badge model was specifically developed for environmental monitoring. The origin of this effect as determined by Panasonic was due to contaminated lead filters incorporated in the badges.

The results obtained from Harshaw and Panasonic TLDs, though preliminary, are interesting enough and call for the continuity of this line of work.

- e) In order to facilitate the comparison between TLD and active detectors obtained in the Hinkley Point experiment, several activities were developed to establish the response of TLD used to the different components found in the radiation field (cosmic, terrestrial, ^{41}Ar plume and 6 MeV photons from ^{16}N).

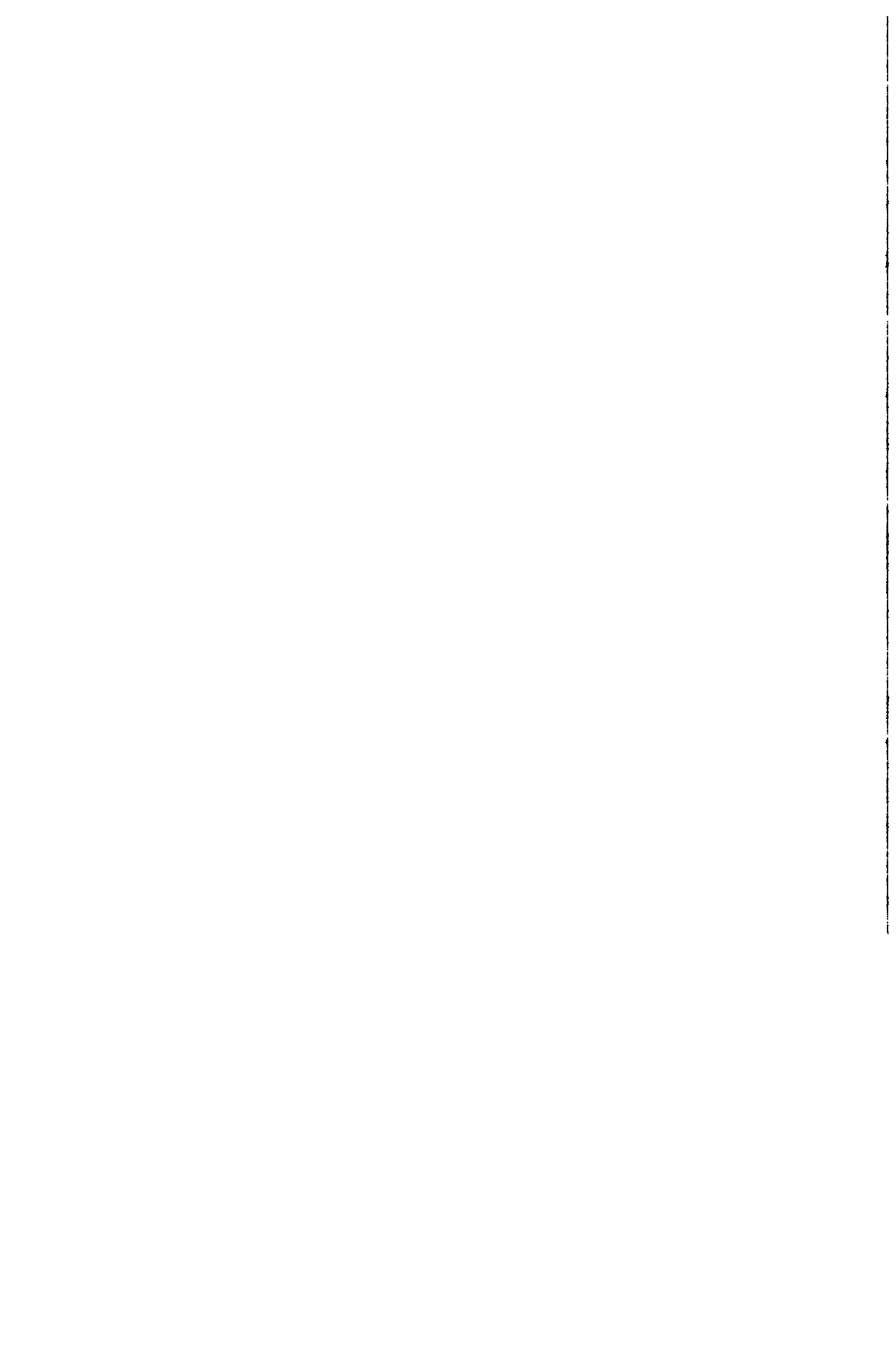
Different TLD badges were exposed during three months in Roskilde Fiord (wooden post in deep sea for cosmic, seaborder for terrestrial, the same place for the free field calibration celebrated in May 1991). This experiment has provided correction factors for the response of the TL materials to the cosmic and terrestrial components of the natural radiation background.

Studies of the response of different TL materials to high energy photons (6 MeV) were performed. TLD badges were irradiated at the PTB accelerator facility, with different plastic filtration (up to 4.0 cm PMMA). The study was completed with gamma irradiations (^{137}Cs and ^{60}Co) at the CIEMAT irradiation facility. Results and conclusions of this experiment will be presented at the 10th SSD Conference (Washington, July 1992).

Complete list of publications which have appeared or were accepted during the reporting period.

1. A simple method for glow curve analysis improving TLD-100 performance in the dose region below 100 μGy ". A. Delgado and J.M. Gómez Ros. Radiation Protection Dosimetry 34, 357 (1990).
2. Evolution of TLD-100 glow peaks IV and V at elevated ambient temperatures. A. Delgado and J.M. Gómez Ros. J. Phys. D: Appl. Phys. 23, 571 (1990).
3. Modifications induced in the TLD-100 trap distribution during exposures at different ambient temperatures. A. Delgado and J.M. Gómez Ros. Radiation Protection Dosimetry 34, 233 (1990).
4. Glow Curve Analysis: a method for improving TLD performance. A. Delgado and J.M. Gómez Ros. To be published in Radiation Protection Dosimetry (1992). Proceedings of the CEC Seminar on Dosimetry in Diagnostic Radiology.
5. A glow curve analysis method for non linear hot gas readers. J.M. Gómez Ros, J.L. Muñiz, A. Delgado, L. Bøtter-Jensen and F. Jørgensen (CIEMAT-RISØ). Accepted for presentation in the 10th Solid State Dosimetry Conference. Washington, July (1992).
6. High ambient temperature effects in LiF TLD-100. A. Delgado, J.M. Gómez Ros and J.L. Muñiz. J. Phys. D: Appl. Phys. 24, 1126 (1991)
7. On the hole character of LiF TLD-100 peak IV. A. Delgado. J. Phys. D: Appl. Phys. 25, 295 (1992).
8. Confirmation of the evolution of TLD-100 glow peaks 4 and 5 during storage at ambient temperatures. A. Delgado, J.M. Gómez Ros, J.L. Muñiz, A.J.J. Bos and T. Pijters (CIEMAT-TU Delft). Accepted for presentation in the 10th Solid State Dosimetry Conference. Washington, July (1992).

9. Temperature effects in LiF TLD-100 based environmental dosimetry. A. Delgado, J.M. Gómez Ros and J.L. Muñiz. Presented in the Fifth International Symposium on the Natural Radiation Environment. Salzburg, September (1991).
10. TL Response to high energy photons. J.C. Saez-Vergara, A. Delgado and J.M. Gómez Ros. Accepted for presentation in the 10th Solid State Dosimetry Conference. Washington, July (1992).



DOSIMETRY OF BETA AND LOW-ENERGY PHOTON RADIATION USING EXTRAPOLATION CHAMBERS AND THIN SOLID STATE DOSIMETERS

Contract Bi7-028 - Sector A12

- 1) *Christensen*, Risø National Laboratory - 2) *Chartier*, CEA-FAR
- 3) *Herbaut*, CEA-Grenoble - 4) *Francis*, NRPB
- 5) *Gasiot*, Univ. Sciences Technologiques du Languedoc
- 6) *Scharmman*, Justus-Liebig-Universität

Summary of project global objectives and achievements

Objectives

For accurate dosimetry of beta and low-energy photon radiations, a large number of specific requirements on measurement techniques have to be defined and appropriate calibration facilities realised because of the low penetrability of these radiations. This project has been aimed at identifying such requirements and realising facilities and measurement methods for determining doses due to weakly penetrating radiations with greater accuracy and consistency than has been possible previously. A particular goal of the project has been to contribute to the achievement of beta calibration beams with high dose rates and thereby satisfying an urgent requirement for calibration of dosimeters and dose rate meters for radiation protection purposes.

The work of the contract has comprised the following main objectives:

- Establishment of a regimen for beta calibrations based on extended area sources that comply with ISO Series 2 specifications.
- Study and refine the extrapolation chamber measurement techniques for beta dosimetry.
- Characterisation of beta radiation fields in terms of directional dose equivalent rate, $\dot{H}'(d; \alpha^\circ)$.
- Development and characterisation of thin solid state dosimeters for weakly penetrating radiations.
- Development of dosimetry of low-energy photon radiation.

Achievements

1. Establishment of beta calibration facilities

Beta calibration facilities using extended area sources capable of irradiating dosimeters and dose rate meters at different irradiation angles and distances have been established in four laboratories of the participants. Two types of sources have been used, namely the French CEA type (circular, 42 mm diameter, active area) and the type used at NRPB (square, 40 mm x 40 mm, active area). Results have been obtained for 42 mm diameter $^{106}\text{Ru}/^{106}\text{Rh}$, $^{90}\text{Sr}/^{90}\text{Y}$, ^{204}Tl , and ^{147}Pm sources and square, 40 mm x 40 mm, $^{90}\text{Sr}/^{90}\text{Y}$ and ^{147}Pm sources. Furthermore measurements have been initiated to acquire data from a 1-mm thick, 200 mm x 200 mm, sheet of perspex containing ^{14}C incorporated in the acrylic material. Also the Büchler-PTB secondary standard $^{90}\text{Sr}/^{90}\text{Y}$, ^{204}Tl , and ^{147}Pm sources are available for making intercomparisons between "point" sources and extended area sources. The sources have been positioned in different holder constructions with different backing materials (aluminium, tufnol and perspex). The type of backing material used for the source may have some influence on the beta-energy spectrum of the radiation beam. Plans have been made for a further study of this influence.

Results obtained for a few sources on dose rate homogeneity and residual beta energy of the radiation beams indicate that the types of extended area sources applied are capable of providing appropriate calibration fields that comply with specifications setup by the ISO for Series 2 beta calibration sources. Improvement of the dose rate homogeneity can be obtained by using beam-flattening filters; however this improvement is obtained at the expense of a decrease in dose rate. Thus the use of a beam-flattening filter resulted in a reduction of the dose rate to about 60% of the value measured without filter for the ^{204}Tl [1] source and 25% for the ^{147}Pm source. Based on half life measurements and gamma spectroscopy analyses combined with dose rate measurements it was found that the $^{106}\text{Ru}/^{106}\text{Rh}$ source contained a significant amount of a different beta radioisotope, and therefore this source can not fulfil the ISO requirement of radiochemical purity. The problem has been addressed to the producer of the source. If it is a general problem to obtain a pure $^{106}\text{Ru}/^{106}\text{Rh}$ source it should be considered, also in view of the short half live (372 days) of ^{106}Ru whether this source could be replaced by another high-energy beta source for the ISO Series 2 type sources. In Table 1 typical dose rate values for the established beta calibration sources are presented.

Table 1. Typical dose rates, $\dot{D}_i(0.07;0^\circ)$, in $\text{mGy}\cdot\text{h}^{-1}$ obtained for the established beta sources. Source-detector distance, in cm, are indicated below each dose rate value.

	$1\ ^{106}\text{Ru}/^{106}\text{Rh}$	$^{90}\text{Sr}/^{90}\text{Y}$	^{204}Tl	^{147}Pm	^{14}C
Area sources	100 (30)	100-200 (30)	100 (30)	25 (20)	0.25 (10)
"Point Sources" (Büchler/PTB)		a) 10 b) 250 (30)	1 (30)	1.5 (20)	

- a) "2mCi" source with beam-flattening filter
 b) "50mCi" source without beam-flattening filter

2. Study of extrapolation chamber measurement method

The extrapolation chamber measurement method is the basic standard dosimetry measurement method applied to beta dosimetry. As the method is tedious requiring a great number of operations to obtain a single dose rate measurement considerable efforts has been put in the development and realisation of fully computerised automated measurement procedures. Important parameters of the evaluation procedures, e.g. the evaluation of extrapolation curves, depth-dose profiles and uncertainties, have been extensively studied and procedures and computer programs have been developed to facilitate an optimal and consistant evaluation of the measurement data [2,3]. Important design parametre of the extrapolation chamber, e.g. the thickness of the entrance window, and dimension of electrode have been studied. To obtain an accurate estimate of zero-depth dose rates, $\dot{D}_i(0;\alpha^\circ)$, entrance windows with a small thickness are required. Results obtained for electrodes with different diameters ranging from 10 mm to 40 mm indicate that there is some influence of size of electrode on the measurement result. Important knowledge of the extrapolation chamber measurement method has been gained through intercomparison exercises. These are seperately reported in sect. 6.

3. Characterisation of beta radiation fields

The beta radiation fields have been characterised in terms of absorbed dose rate to tissue, $\dot{D}_i(d;\alpha^\circ)$, which can be considered to be numerical equal to the quantity used for radiation protection purposes, namely the directional dose equivalent rate; $\dot{H}^*(d;\alpha^\circ)$. From the measured depth-dose data, conversion

factors $G(d; \alpha^n) = \dot{D}_e(d; \alpha^n) / \dot{D}_e(d; 0^n)$ can be evaluated.

Analyses of the depth-dose data have shown that the initial parts of the absorption curves including the electron scattering build-up phase with good accuracy can be represented by polynomial expressions.

4. Development and characterisation of thin solid state dosimeters for dosimetry of weakly penetrating radiations

For dosimetry of weakly penetrating radiations there is a need for thin detectors with a sufficient low mass per area to avoid a significant attenuation of the radiation during passage through the detector. The low mass of such detectors necessitates the use of highly sensitive detector materials. The work has been concerned with: development and study of tissue-equivalent (e.g., LiF) TL dosimeters, development and study of TLD techniques and dosimeters based on laser heating and development and study of tissue-equivalent TSEE dosimeters.

Results from measurements of beta-ray responses of 0.13 mm (28 mg.cm⁻²) LiF teflon discs showing responses for the measurement of H_p(0.07) of 0.70 and 0.23 for exposure to beta rays from ²⁰⁴Tl and ¹⁴⁷Pm sources, respectively, emphasise the need for thin detectors. The LiF:Mg,Cu,P TL material is an interesting material for this purpose because it combines a high sensitivity (about 25 times that of normal LiF:Mg,Ti) with good energy response characteristics for exposure to photons. It should be noted that a dosimeter intended for the measurement of skin doses usually will be exposed to both beta rays and strongly penetrating photons. Thin detectors have been prepared from different products of LiF:Mg,Cu,P TL powders and their dosimetric characteristics have been studied. The results show that the LiF:Mg,Cu,P TL material exhibits good characteristics for application as a thin detector for individual monitoring for weakly penetrating radiations [4]. A disadvantage of the material is that the sensitivity decreases when it is treated at temperatures above 240°C which complicates the annealing procedure required for its re-use.

The laser heating TLD technique is interesting for dosimetry of weakly penetrating radiations because it can operate with small detector thicknesses combined with a fast reading. Besides for individual dosimetry purposes the TLD laser heating method is particular useful for scanning of radiation fields [5]. A fully automated computer-controlled laser heated TLD reader has been designed and realised. The reader allows dosimeter plates of sizes up to 200 mm x 200 mm to be scanned with an resolution of about 100 microns. CaSO₄:Dy TL dosimeters suited for laser heating have been developed and tested. The reproducibility of measurement of a dose of 4 mGy from a ⁹⁰Sr/⁹⁰Y source for these dosimeters is below 1%. Work is in progress of developing dosimeter constructions suitable for individual monitoring, in particular for beta doses.

The TSEE dosimetry technique fully meets the requirement of thin detectors and high sensitivity for individual monitoring for weakly penetrating radiations. Dosimeter constructions based on BeO thin film detectors consisting of an oxidised 100 nm beryllium layer on a circular graphite substrate of 12.5 mm diameter have been analysed for energy and angular responses for exposure to photons and beta rays. Due to the small thickness of the BeO detectors the responses are mainly determined from scattered electrons from the surrounding materials. By adjusting holder design as well as filter materials dosimeter constructions with nearly ideal responses have been achieved [6].

5. Development of dosimetry of low-energy photons

An X-ray facility operating at potentials ranging from 10 to 30 kV has been established. The facility is provided with an extrapolation chamber for the measurement of absorbed dose rate to tissue and a free air chamber for determining air kerma rate. Computer programs have been developed for remote controlling the various operations involved in the measurements procedure.

The facility is available for experimental determination of conversion coefficients, converting from air kerma to absorbed dose to tissue and for studying responses of dosimeters and dose rate meters for exposure to low-energy photons in the range from 5 to 15 keV.

6. Intercomparison of extrapolation chamber measurement methods used by the participating laboratories

An intercomparison of the extrapolation chamber measurement methods in use at four laboratories of the participants of the contract (NRPB, CEA-Fontenay-aux-Roses, CEA-Grenoble and RISØ) has been initiated with the main purpose of ensuring consistency of the standard beta dosimetry exercised by the participants. Objectives of the intercomparison exercise were to cooperate in identifying and solving problems involved with the extrapolation chamber measurement method and especially in evaluating on the measurement uncertainty valid for the method. Parallel with this intercomparison exercise the participants have taken part in a similar intercomparison using a different source (^{147}Pm). That intercomparison was exercised in collaboration with PTB, Braunschweig and organised under the regi of EURADOS [2].

Table 1. Main characteristics of the extrapolation chambers used for the intercomparison.

Laboratory	Chamber Type	Entr. window		Electrode		Electrom. Lower range (A)
		Thickness (mg.cm ⁻²)	Material	Diam. (mm)	Material	
RISØ	PTW 23392	2.6	Mylar	30	Perspex	10 ⁻¹⁷
CEA/FAR	PTW 23392	2.6	Mylar	30	Perspex	10 ⁻¹⁶
NRPB	NRPB design	0.85	Mylar	≈ 32	MS20	10 ⁻¹⁷
CEA, Grenoble	PTW 23391	7.05	Polythene	30	A.150	10 ⁻¹⁷

An extended area ^{204}Tl source (active diameter 42 mm) was applied for the intercomparison. Two holders were used for the source: the standard French CEA type [1] and a modified version of the type used at NRPB (see the report by NRPB of this report). The essential dosimetric difference between the two holders is the use of different backing materials (Al and "Tufnol", respectively) for the source.

The measurement programme comprised the determination of the dose rates at distances of 15, 20 and 30 cm from the source and at the radiation angles 0° and 45°. The results should be given in terms of $\dot{D}_r(0.07; \alpha)$ and furthermore depth-dose data should be acquired for the range from the thickness of the entrance window of the extrapolation chamber and up to at least 10 mg.cm⁻². Uncertainties on the reported dose rate values should be evaluated in accordance with procedures proposed by Chartier [3]. It was agreed that a number of systematic uncertainties would essentially be equal for all systems and could therefore be combined to a single value that could be used by all participants. The main uncertainty component to be assessed by each participant would be that related to the determination of the slope of the extrapolation curve.

Table 2. Measured dose rates, $\dot{D}_i(0.07; \alpha^\circ)$, from the ^{204}Tl source at distances 15, 20 and 30 cm from the source and at irradiation angles $\alpha = 0^\circ$ and 45° . Estimated uncertainties ($\pm 1\text{S.D.}$) are indicated below each dose rate value.

Laboratory	$\dot{D}_i(0.07; \alpha^\circ)$ in $\text{mGy}\cdot\text{h}^{-1}$.					
	15 cm distance		20 cm distance		30 cm distance	
	$\alpha=0^\circ$	$\alpha=45^\circ$	$\alpha=0^\circ$	$\alpha=45^\circ$	$\alpha=0^\circ$	$\alpha=45^\circ$
RISØ	382 $\pm 2\%$	368 $\pm 2\%$	211 $\pm 2\%$	198 $\pm 2\%$	84.3 $\pm 2\%$	76.6 $\pm 2\%$
CEA/FAR	383 $\pm 2.6\%$	398 $\pm 2.2\%$	207 $\pm 2.1\%$	207 $\pm 2.7\%$	87.9 $\pm 1.9\%$	81.6 $\pm 2.2\%$
NRPB	384.6 $\pm 2\%$	378.2 $\pm 2\%$	207.6 $\pm 2\%$	202.4 $\pm 2\%$	84.5 $\pm 2\%$	80.5 $\pm 2\%$

*) Due to a delay of the intercomparison programme caused by unforeseen long periods of time used for the transportation of the source between the laboratories of the participants results are sofar only available from three of the four participants of the intercomparison.

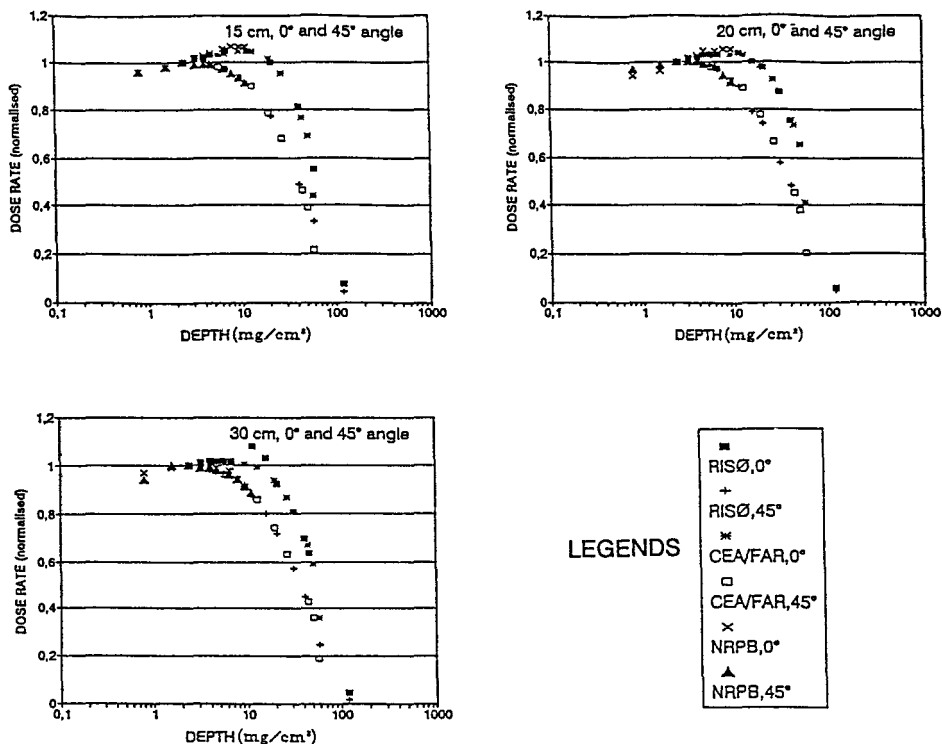


Figure 1. Results of measurement of depth-dose profiles for the ^{204}Tl source obtained at distances of 15, 20 and 30 cm from the source and for irradiation angles $\alpha = 0^\circ$ and 45° . All data are normalised to depth: $2.4 \text{ mg}/\text{cm}^2$

The results of the intercomparison are generally in good agreement. Some of the differences of the results shown in Table 2 may be due to the use of different holders for the source which will be further studied.

References

1. Chartier, J.L., Cutarella, D. and Itié, C. Characterisation of the Radiation Field of Beta Secondary Standards with Extended Area Sources. Radiat. Prot. Dosim. 39 (1/3), 115-118(1991).
2. Francis, T.M., Böhm, J., Chartier, J.L. and Christensen, P., Experience Gained on Extrapolation Chamber Measurement Techniques from an Intercomparison Exercise Conducted with a ^{147}Pm Source, Radiat. Prot. Dosim. 39(1/3),109-114,(1991).
3. Chartier, J.L. and Cutarella, D. Proposal for a simplified procedure to evaluate the uncertainties in EC measurements. Internal CEA/FAR report(1991).
4. Christensen, P., Study of LiF:Mg,Cu,P TL Detectors for Individual Monitoring for Weakly Penetrating Radiations, 10th Intern. Conf. on Solid State Dosimetry, Washington D.C. USA, July 13th-17th, 1992. (In press).
5. Servière, H., Vignolo, C., Prévost, H. and Gasiot, J. Laser Heating of TL Dosimeters: Application to Beta Dose Mapping. Radiat. Prot. Dosim. 39 (1/3), 145-148 (1991).
6. Kriegseis, H., Kessler, H., Rauber, K., Scharmann, A., Chartier J.L., Itié, C. and Pétel, M. Response of TSEE Dosimeters of Foil-Covered BeO Thin Films to Beta Radiation. Radiat. Prot. Dosim. 39 (1/3), 127-130 (1991).

Project 1

Head of project: *Dr. Christensen*

Objectives for the reporting period

Risø National Laboratory contributes to the joint research project by establishment and characterisation of standard beta calibration fields, analyses and refinement of the extrapolation chamber measurement method and development and characterisation of thin solid state detectors for dosimetry of weakly penetrating radiations.

More specific objectives for the working programme are:

- establishment of calibration facilities using extended $^{106}\text{Ru}/^{106}\text{Rh}$ and ^{14}C sources.
- analyses and refinement of the extrapolation chamber measurement method, in particular, by participating in intercomparison programmes carried out among the participants.
- characterisation of beta radiation fields in terms of $\dot{D}_f(d;\alpha^\circ)$ with emphases put on $^{106}\text{Ru}/^{106}\text{Rh}$ and ^{14}C sources.
- development and analyses of thermoluminescent materials for application as thin detectors for individual dosimetry of weakly penetrating radiations.

Progress achieved including publications

1. Establishment of beta irradiation facilities

1.1 Experimental set-up

The set-up established for beta irradiations and dose rate measurements has been described in the 1990-91 CEC progress report. It allows instruments and dosimeters (e.g. extrapolation chamber and TL detectors) to be irradiated at different irradiation angles and distances from the source. The source holder allows different source constructions to be used including the French CEA type, the NRPB type and the Büchler/PTB secondary standard type.

Two sources have been acquired for this project, a $^{106}\text{Ru}/^{106}\text{Rh}$ source with a total diameter of 58 mm and an active area of diameter of 42 mm, and a ^{14}C source consisting of a 200 mm x 200 mm, 1 mm thick perspex sheet containing ^{14}C incorporated in the acrylic material. The $^{106}\text{Ru}/^{106}\text{Rh}$ activity is positioned on silver material and covered by a 50 mg.cm⁻² layer of silver. To facilitate the handling of this source it has been fixed in a 60 mm diameter, 1mm deep depression in a 100 mm x 100 mm x 20 mm perspex block. The activity of the $^{106}\text{Ru}/^{106}\text{Rh}$ source was stated by the producer (Amersham) to 3.7 x 10⁸ Bq and that of the ^{14}C source to 18,5 MBq.g⁻¹ perspex or 2x10⁴.s⁻¹.cm⁻² beta particles (2π geometry) emitted from the surface of the source. For the ^{14}C source, 1 mm thick perspex shields with holes of different diameters have been constructed enabling different sizes of this type of source to be studied.

1.2 Compliance with ISO specifications for series 2 sources

The radiation field from the $^{106}\text{Ru}/^{106}\text{Rh}$ source was studied for dose rate homogeneity and residual maximum beta particle energy and the results were compared with the ISO requirements for these characteristics specified for Series 2 sources [1]. Furthermore results were obtained on the radiochemical purity of the source.

Dose rate homogeneity.

The homogeneity of the radiation field was studied by irradiating 255 TL detectors placed on a perspex plate in depressions equally distributed over an area of approximately 100 mm x 90 mm. Measurements were made for the distances 20, 30 and 40 cm from the source. The measurements were made with 0.9 mm thick, 0.5 mm diameter, TLD-700 LiF detectors from the Harshaw Chemical Co. The response of these detectors is essentially constant for the range of angles from 0° to 15° [2] and they can therefore be used for distances down to at least 20 cm. For smaller distances detectors with a smaller thickness should be chosen.

The results of the measurements are shown in Figure 1. It can be seen that the ISO requirement of $\pm 5\%$ for the dose rate homogeneity is fulfilled for areas of 100 mm x 90 mm for all three distances. The uncertainty of the measurements were approximately 1% (1 S.D.) and therefore the isolated peaks observed in the figures can be explained by uncertainties of the measurement method.

Residual maximum beta particle energy.

Residual maximum beta particle energy, E_{res} , was determined at the calibration distances, 20, 30 and 40 cm by using the extrapolation chamber for the measurement of dose rates behind absorbers of perspex sheets. The evaluation of E_{res} from the measured depth-dose data is described in Sect. 1.3 in the report by NRPB of this report.

From the results presented in Table 1 it can be seen that the ISO requirement of $E_{\text{res}} \geq 2.80$ MeV is fulfilled for all three calibration distances.

Table 1. Measured residual maximum beta particle ranges and the values of residual maximum beta particle energy evaluated from them for distances = 20, 30 and 30 cm.

Source to detector distance cm	Residual maximum beta range R_{res} mg.cm^{-2}	Residual maximum beta energy, E_{res} MeV
20	1500	3.1
30	1500	3.1
40	1470	3.0

Radiochemical purity.

From dose rate measurements performed in May 1991, December 1991 and July 1992, respectively, the half life of the $^{106}\text{Ru}/^{106}\text{Rh}$ source was determined to 734 days for the decay during the first period and 962 days for the second period which is not in agreement with the half life, 372.2 days, stated for the ^{106}Rh radionuclide [1]. It was found from analyses of the photon spectrum of the source that

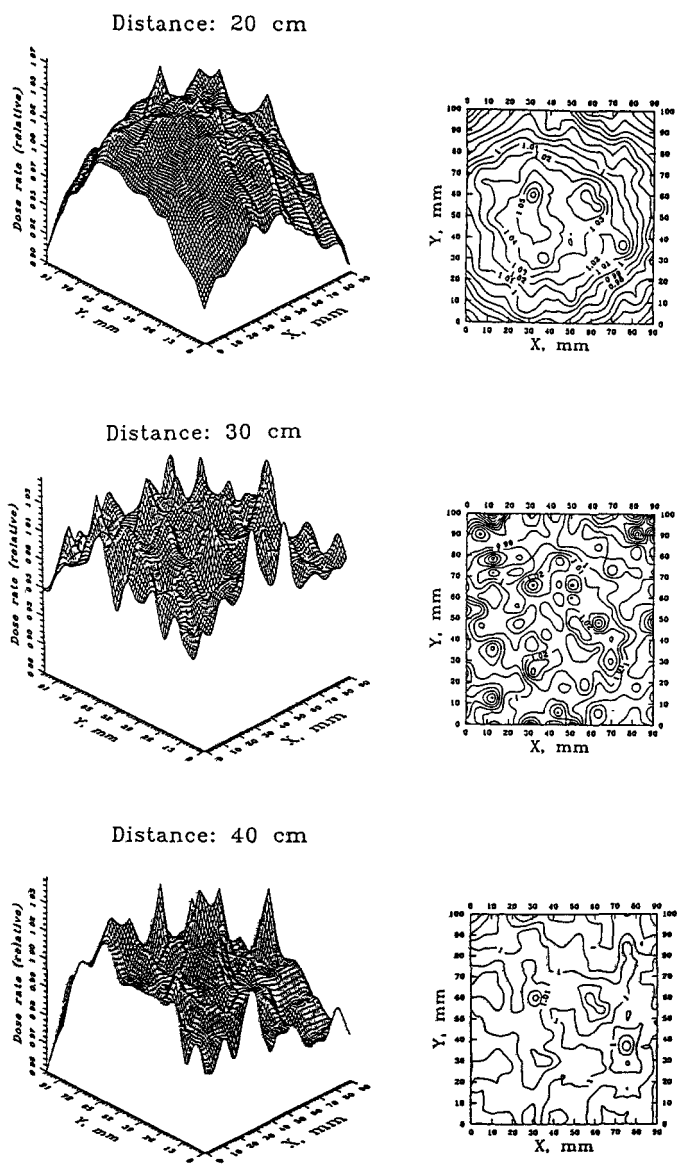


Figure 1. Results of measurement of dose rate homogeneities at three distances from the $^{106}\text{Ru}/^{106}\text{Rh}$ source. The measurements were made with, 0.9 mm thick, 5mm diameter, LiF TLD-700 TL detectors.

only photon energies belonging to the ^{106}Rh radionuclide were present in the spectrum. On the basis of the measured photon emission from the source the activity of the ^{106}Rh radionuclide could be determined to approximately 6×10^7 Bq and using calculated data by Cross et. al. [3] for broad normally incident beams of beta rays from ^{106}Rh , the dose rate to tissue corresponding to this activity at a distance of 30 cm from the source was determined to 6.5 mGy.h^{-1} . As the actual, measured dose rate value was 39 mGy.h^{-1} it can be concluded that only about 17% of the exposure from the source can be referred to ^{106}Rh . As the dose rate determined from measurements with 0.9 mm thick TL LiF detectors is nearly equal to that measured with the extrapolation chamber, mainly high-energy beta particles seem to be involved also in the remaining 83% of the exposure [2].

It can be concluded that the source does not meet the ISO requirement of radiochemical purity. The problem has been addressed to the producer of the source with the intension to acquire a new pure $^{106}\text{Ru}/^{106}\text{Rh}$ source.

2. Analyses and refinement of the extrapolation chamber measurement method

Experimental set-up.

Two PTW type 23392 extrapolation chambers with different thickness of the entrance window, i.e. 2.6 and 0.8 mg.cm^{-2} carbon-coated mylar foils, respectively, have been established. Work has progressed in achieving fully automated, computer-controlled measurement and dose-rate evaluation procedures.

Results.

Results of intercomparison exercises, one concerned with an extended ^{147}Pm area source and carried out between three of the laboratories participating in this contract and PTB, Braunschweig [4], and another one concerned with an extended ^{204}Tl area source and carried out as part of the work of this contract, have been used to identify specific problems of the extrapolation chamber measurement method and to work out standard evaluation procedures including the determination of uncertainties of the method. Results of the intercomparison exercises are reported in section 6 of the general report on the joint project.

Initial studies have been made of the possibilities of achieving ultra-thin entrance windows of thicknesses in the range of 0.1 to 0.2 mg.cm^{-2} using ultra-thin VYNS foils which have been prepared at Risø for other purposes [5]. Ultra-thin entrance windows are of particular interest for dosimetry of low-energy beta radiation, e.g. that of ^{63}Ni and ^{14}C .

3. Characterisation of beta radiation fields in terms of \bar{D}_t ($d:\alpha$)

$^{106}\text{Ru}/^{106}\text{Rh}$ source.

Depth-dose distributions have been measured for the $^{106}\text{Ru}/^{106}\text{Rh}$ source at distances of 20, 30 and 40 cm from the source and at different irradiation angles up to 60° . Although the data are not representative for a pure $^{106}\text{Ru}/^{106}\text{Rh}$ source they may be of interest as an example of a source containing a mixture of high-energy beta radionuclides. The measurements were carried out with an extrapolation chamber with entrance window thickness 2.4 mg.cm^{-2} tissue-equivalent material. Mylar foils and perspex sheets were used as absorbers and scaling factors given by Cross [6] were used for converting to tissue-equivalent thicknesses.

Results from some of the measured depth-dose profiles are presented in Figure 2. All experimental data have been normalised to the thickness of the entrance window of the extrapolation chamber, i.e. 2.4 mg.cm^{-2} tissue. In addition to the experimental values also curve fits (lines) using a 3. degree polynomial fit are shown. It can be seen that for depths up to about 200 mg.cm^{-2} the experimental data can be represented by a 3. degree polynomial with good accuracy. From the measured depth dose data, factors $G(d; \alpha^\circ) = D_i(d; \alpha^\circ)/D_i(d; 0^\circ)$ can be obtained. Preliminary results indicate that also these factors can be represented by a 3. degree polynomial with good accuracy for irradiation angles up to 60° .

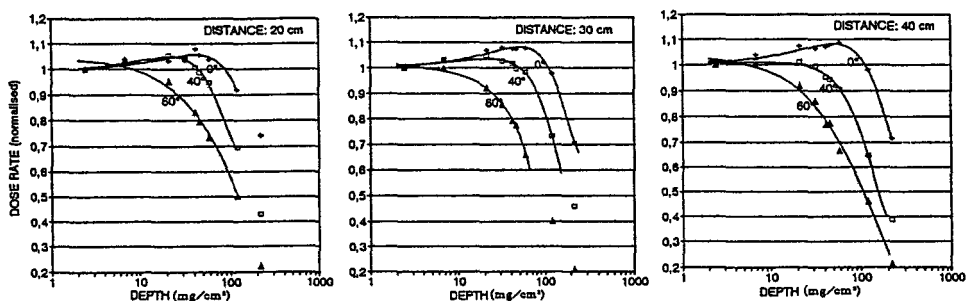


Figure 2. Depth-dose profiles obtained for the $^{106}\text{Ru}/^{106}\text{Rh}$ source for three distances from the source. Symbols indicate experimental data normalised at 2.4 mg.cm^{-2} and lines the corresponding 3. degree polynomial fits.

^{14}C source.

Depth-dose data have been obtained for the ^{14}C source at distances of 10 and 15 cm from the source and at different irradiation angles. The evaluation of the acquired data is in progress.

4. Development and study of thin TL detectors

An appropriate dosimeter for individual monitoring for weakly penetrating radiations can be achieved from a simple dosimeter construction consisting of a thin tissue-equivalent TL detector covered with a thin tissue-equivalent filter. The detector must be sufficiently thin (a few mg.cm^{-2}) to avoid significant attenuation of the radiation during the passage through the detector. The low mass of the detector implies the need for a highly-sensitive tissue-equivalent detector material. The LiF:Mg,Cu,P TL material is interesting because it combines a high sensitivity with good photon energy response characteristics. The work has therefore been concentrated on this material.

Three commercial products of LiF:Mg,Cu,P TL powders (Solid Dosimetric Detector and Method Laboratory, Beijing, China, Nemoto & Co., Tokyo, Japan and Moscow State University, Moscow, Russia) were studied. The Chinese material is also available as thin detectors consisting of a layer of, about 5 mg.cm^{-2} , TL powder fixed on a polyimid (kapton) tape [7]. Similar detectors were prepared from the three powder materials.

A general problem of the LiF:Mg,Cu,P material is that the TL sensitivity decreases during heat treatments at temperatures above 240°C and that short-period annealings at temperatures below 240°C are not satisfactory for removing the residual TL signal belonging to traps with glow peaks in the temperature range from $260\text{-}300^\circ\text{C}$. In Figure 3 glow curves are shown for the three materials given different heat treatments before the irradiations. The Figure clearly illustrates that all three materials are highly sensitive to heat treatments at temperatures in the range of $270\text{-}300^\circ\text{C}$ and also that significant parts of the glow curves are located at temperatures above 240°C . It can be seen that the

Russian material is more resistant to annealings at 270 °C than the two other materials.

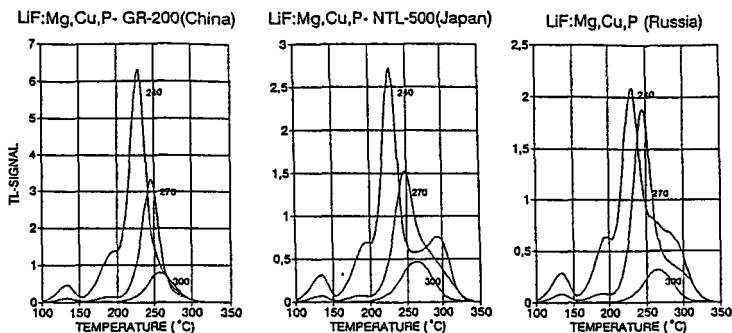


Figure 3. Glow curves from 10-mg samples of three LiF:Mg,Cu,P TL materials, pre-irradiation annealed for 15 minutes at 240, 270 and 300 °C, respectively.

Various dosimetric properties of the thin detectors were investigated. The results have been reported in ref. [8]. It can be concluded from this study that the LiF:Mg,Cu,P TL material shows good dosimetric characteristics for application as thin detectors for individual monitoring for weakly penetrating radiations. Considerable improvement of the material would be achieved if its resistance to heat treatments could be improved.

References

1. ISO. Reference Beta Radiations for Calibrating Dosimeters and Doserate Meters and determining their Response as a Function of Beta Radiation Energy. ISO 6980. First Revision 1990-11-01.
2. Christensen, P., Böhm J. and Francis, T.M. Measurement of Absorbed Dose to Tissue in a Slab Phantom for Beta Radiation Incident at Various Angles. In: Fifth Information Seminar on the Radiation Protection Dosimeter Intercomparison Programme, Bologna, 1987. Report EUR 11363, (Luxembourg:CEC) (1988).
3. Cross, W.G., Wong, P.Y. and Freedman, N.O. Dose Distributions for Electrons and Beta Rays Incident Normally on Water. Radiat. Prot. Dosim. 35(2) 77-91 (1991).
4. Francis, T.M., Böhm, J., Chartier, J.L. and Christensen, P., Experience Gained on Extrapolation Chamber Measurement Techniques from an Intercomparison Exercise Conducted with a ^{147}Pm Source, Radiat. Prot. Dosim. 39(1/3),109-114,(1991)
5. Chen, Q.J., and Nielsen, S.P. Preparation of Thin Alpha Sources by Electro spraying for Efficiency Calibration Purposes. J. Radioanal. Nucl. Chem., Letters 135 (2) 117-123 (1989).
6. Cross, W.G., Variation of Beta Dose Attenuation in Different Media. Phys. Med. Biol.,13, 611-618 (1968).
7. Wu Fang, Zha Ziyang, Li Jian and Zhu Zhongmei, LiF:Mg,Cu,P, A New Material for Thermoluminescence Dosimetry, Radiat. Prot. Dosim.,34, 331-334 (1990).
8. Christensen, P., Study of LiF:Mg,Cu,P TL Detectors for Individual Monitoring for Weakly Penetrating Radiations, 10th Intern. Conf. on Solid State Dosimetry, Washington D.C. USA, July 13th-17th, 1992. (In press).

Publications

1. Francis, T.M., Böhm, J., Chartier, J.L. and Christensen, P., Experience Gained on Extrapolation Chamber Measurement Techniques from an Intercomparison Exercise Conducted with a ^{147}Pm Source, Radiat. Prot. Dosim. 39(1/3),109-114,(1991)
2. Christensen, P., Study of LiF:Mg,Cu,P TL Detectors for Individual Monitoring for Weakly Penetrating Radiations, 10th Intern. Conf. on Solid State Dosimetry, Washington D.C. USA, July 13th-17th, 1992. (In press).

Project 2

Head of project: *Dr. Chartier*

Objectives for the reporting period

The achievement of the tasks of the CEA/IPSN/SDOS, in the frame of radiation protection dosimetry, is directly dependent on the availability of radiation facilities enabling to perform the study and the calibration of dosimeters and dose rate meters. In the specific field of weakly penetrating radiations (beta and low energy photon radiations), a complementary action has to be undertaken to establish dosimetric references in CEA. On the basis of these general demands, the contribution of the CEA/SDOS deals with:

- a) the realisation and the characterisation of intense beta radiation fields and the participation in the revision of the ISO Standard 6980.
- b) the methodology for evaluating the measurement data obtained with extrapolation chamber.
- c) the realisation and the characterisation of low energy X-radiation beams (energy range: 5-15 keV) for studying and type-testing dosimetric instruments.
- d) the intercomparison of dosimetric references with those of other laboratories involved in similar activities.

Progress achieved including publications

1. Beta radiations

1.1 Experimental set-up

The experimental set-up has been extensively described in the 1990-1991 report, in particular the computer-controlled operation of the extrapolation chamber. Modifications have been carried out on the initial version. In particular, the extrapolation curve file $[I; kI(l); s(I)]$ where l stands for the chamber depth, is automatically provided at the end of the measurements for performing the fitting.

1.2 Computational procedures

The evaluation of results, both for extrapolation and depth-dose curves has been performed through Fortran programs, namely XTCREGR.FOR and DDCREGR.FOR, enabling a weighted least-squares fit to a polynomial function. Both programs have been transmitted to other laboratories for being tested and applied. In addition, an estimation of uncertainties on the calculated results is given by determining the standard deviations on the fitting coefficients.

1.3 Evaluation of uncertainties

A detailed procedure for combining the uncertainties involved in extrapolation chamber measurements has been proposed (1) and discussed. It is based on an extensive analysis of uncertainties as developed in (2), applied to the guidelines and concepts recommended in (3) and (4).

The implementations for extrapolation and depth-dose curves are explicitly described up to the final values of the overall uncertainties on the calculated quantities.

1.4 (204-Tl) measurements

An extended area (204-Tl) source (active diameter 42 mm) has been circulated for calibration by the 4 contractors. The intercomparison results are discussed in the general part of the report. But an extensive series of data, obtained by the SDOS laboratory has been given in the 1990-1991 report, with associated uncertainties for both configurations, with and without flattening filters. Different calibration distances, 15, 20 and 30 cm, and several incidence of angles, 0°, 15°, 30° and 45°, have been considered, enabling to derive the values of the conversion factors $F(0.07; \alpha^\circ)$.

1.5 (147-Pm) measurements

In a similar way, an extended area (147-Pm) source (active diameter 42 mm) has been characterised for the following conditions: Calibration distances 15, 20 and 30 cm, and incidence angles 0°, 15°, 30° and 45°. Additional data with flattening filters are available for 20 cm (ISO 6980). Nevertheless, the complete series of data will not be included in this report because it has appeared that the analytical expression chosen for fitting the depth-dose curves (DDC) modifies notably the calculated quantity, in particular when the entrance window of the chamber is rather thick: 2.4 mg/cm² (PTW model). A final decision is still under discussion. Such a question is clearly demonstrated by the content of the following table in which the DDC is represented

- either by an exponential absorption law: $\text{Ln}D(x) = (\mu/\rho)\rho x$

- or by a composite law as : $\text{Ln}D(x) = \text{Ln}D_0 + a_1\rho x + a_3(\rho x)^B$,

where $D(x)$ is the dose at depth x .

Table 1. Results from measurements of dose rates from the (147-Pm) Source. Distance: 20 cm. Dose in $\mu\text{Gy/s}$. Reference date: (01/01/92)

	WITHOUT FILTERS			WITH FILTERS		
	REGRES	REGRES	RATIO	REGRES	REGRES	RATIO
	1	1+3	1/1+3	1	1+3	1/1+3
Dt (0)	26.72	24.39	1.09	6.69	6.46	1.04
Dt (0.02)	17.96	17.71	1.01	4.24	4.24	1.00
Dt (0.07)	6.65	7.21	0.92	1.36	1.40	0.97

Depending on the irradiation conditions, a difference of 8% is observed for the ratio of $D_t(0.07; 0^\circ)$ values (without filters), whereas the increase is only 3% with filters. This effect is due to the change in the energy spectrum when flattening filters are used. But it has been stated that a (degree 1+3) polynomial gives generally a much better fit of (147-Pm) DDC for depth ranging from 2 to 10 mg/cm². Furthermore, it appears that the use of $D_t(0.00, \alpha^\circ)$ as a reference quantity should not be maintained.

2. Low energy photon radiations

2.1 Measurement of photon dose with an extrapolation chamber

For photon radiations generated at potential between 5 and 30 kV, an extrapolation chamber (EC) is a suitable reference instrument for the measurement of the absorbed dose at a point in a medium (6). From the measurement of the ionisation in the cavity of the chamber, the "exposure inside the phantom" (ICRU Report 19) J_a can be determined. Then the required absorbed dose D_m can be derived by the relation:

$$D_m = \frac{W (\mu_{en}/\rho)_m}{e (\mu_{en}/\rho)_{air}} J_a \quad J_a = \frac{\Delta I}{\Delta m}$$

Practically, from the extrapolation curve $I(l)$, where l stands for the chamber depth, a differentiated curve $(\Delta I/\Delta l)$ is plotted and extrapolated to depth 0. The linear part of this curve corresponds to the values of $(\Delta I/\Delta m)$ for SEE condition in the air cavity, i.e. for chamber depths larger than the maximum range of the electrons generated in the entrance foil.

2.2 Experimental arrangement

The photon radiation beams of the initial project, fluorescence x-rays, have been replaced by the filtered beams produced by an X-ray unit operating at potentials ranging from 10 to 30 kV with additional filters (energetic resolution: 15 to 20%). A series of diaphragms enables to master the beam cross-section and to irradiate only the collecting electrode. A monitor chamber (transmission type PTW 7861) connected to a Keithley 617 electrometer provides an information to correct the EC current for the photon flux variations. The different actions will be remote-controlled by a 386 Compaq PC. A specific program has been implemented and is currently tested.

2.3 Measurement procedures

The calibration quantity, $D_m(0.07;\alpha^\circ)$ or $H'(0.07;\alpha^\circ)$, derives from the measurements achieved with the extrapolation chamber, the (μ_{en}/ρ) ratio being averaged over the calculated photon spectrum in the cavity. The determination of the kerma in air is performed with a free air chamber placed at the same reference point.

Publications

1. J.L. Chartier, D. Cutarella, C. Itié. Characterisation of the Radiation Field of Beta Secondary Standards with Extended Area Sources. Rad. Prot. Dos. Vol. 39 N°1/3 p. 115-118 (1991).
2. T.M. Francis, J. Böhm, J.L. Chartier, P. Christensen. Experience Gained on Extrapolation Chamber Measurement Techniques from an Intercomparison Exercise Conducted with a (147-Pm) Source. Rad. Prot. Dos. Vol. 39 N°1/3 p. 109-114 (1991).
3. W. Kriegseis, H. Kessler, K. Rauber, A. Scharmann, J.L. Chartier, C. Itié, M. Pétel. Response of TSEE Dosimeters of Foil-covered BeO Thin Films to Beta Radiation. Rad. Prot. Dos. Vol. 39 N°1/3 p. 127-120 (1991).

Bibliography

1. Proposal for a simplified procedure to evaluate the uncertainties in EC measurements. J.L. Chartier, D. Cutarella (1991).
2. PTB Report Dos 13. J. Böhm (1986).
3. WECC Doc. 19 (1990).
4. CIPM Recommendation (CI-1981) Metrologia 19 (1982).
5. PTB Mitteilungen 89 (3/79). J. Böhm, K. Hohlfeld, H. Reich.

Project 3

Head of project: *Dr. Herbaut*

Objectives for the reporting period

- Establishment of beta radiation fields incorporating suitable extended circular ^{147}Pm and $^{90}\text{Sr} + ^{90}\text{Y}$ sources.
- Establishment of computer controlled automatized extrapolation chamber measurement set up.
- Characterization of the radiation fields of the above beta sources in term of $D_t(d, \alpha)$ for different values of d and α and evaluation of conversion factors $G(0,07, \alpha)$ for different values of α and different calibration distances of the sources.

The measurement will be performed with and without use of beam flattening filters.

- Determination of conversion factors $G(0,07, \alpha)$ for different values of α for the above sources and for point sources of ^{147}Pm and $^{90}\text{Sr} + ^{90}\text{Y}$ from the PTB/Büchler secondary standards using :
 - a) two different designs of extrapolation chamber (FWT and PTW type) with different sizes of collecting electrodes ;
 - b) thin and ultra thin thermoluminescent dosimeters ;
 - c) TSEE dosimeters based on BeO or LiF.

Progress achieved

1. Design and realization of calibration devices

At Grenoble, the Büchler facility for point sources and the CEA irradiation facility for beta (^{147}Pm and $^{90}\text{Sr} + ^{90}\text{Y}$) extended circular sources ($\phi = 42$ mm) are in use.

Different rotating devices have been designed and built for the both facilities, for extrapolation chambers and TL dosimeters.

2. Extrapolation chamber

2.1 General description and characteristics

The reference detector is a PTW extrapolation chamber model 23391, whose cavity has a thickness varying between 0,6 mm and 2,5 mm, with a variable spacing of 10 μm increments. The collecting electrodes (10, 15, 20, 30, 40 mm in diameter) and the guard ring are made of A 150 tissue equivalent plastic material. The entrance window is made of polythene 7,05 $\text{mg}\cdot\text{cm}^{-2}$ thick, corresponding to the thickness for the determination of the

dose to the skin. The cavity of the chamber is filled with air.

The electric field for the PTW chamber is constant and equal to $50 \text{ V}\cdot\text{mm}^{-1}$. The PTW chamber is connected to a Keithley electrometer (model 642) with a measuring limit of 10^{-17}A .

An on-line HP. Vectra ES 12 computer carries out the data acquisition (including ambient parameters), the data processing and the computation of the dose and of its uncertainty.

2.2 Influence of collecting electrode areas

To study the influence of this parameter, we have determined the area of each collecting electrode (Table 1) according to the Böhm's method /1/.

Table 1 - Collecting electrode areas

Nominal area cm^2 (diameter)	Experimental area cm^2	Standard deviation %
0.785 (10 mm)	0.9	0.8
1.77 (15 mm)	1.89	0.3
3.14 (20 mm)	3.31	0.3
7.07 (30 mm)	7.4	0.15
2.57 (40 mm)	13.01	0.2

The results of this influence for the ^{147}Pm and $^{90}\text{Sr} + ^{90}\text{Y}$ beta extended sources, without filter are presented in Fig. 1a and 1 b.

This influence seems to be the same for the two beta radionuclides and is only a function of the electrode diameter.

We think that this effect is related to the homogeneity of the beam on the one hand /2/ and on the value of the curvature of the entrance window on the other hand.

This effect will be studied more thoroughly.

Nevertheless, it has no influence on the determination of the G (0,07, α) conversion factor but it has a great importance (4 % for the 30 mm diameter collecting electrode) in the computation of the absorbed dose rate in tissue.

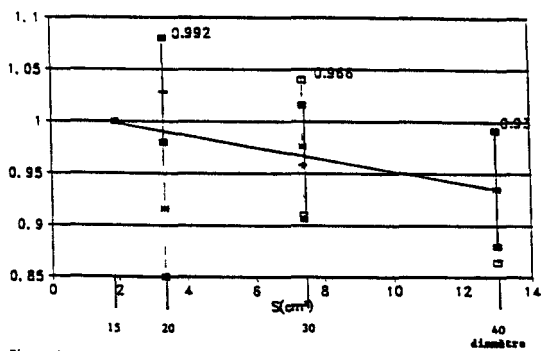


Figure 1a

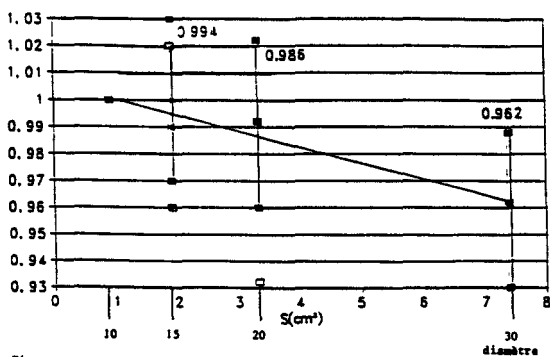


Figure 1b

Figures 1a and 1b present the values of absorbed dose rate in tissue normalized to the value obtained for the smallest area of the collecting electrode (left scale), for the ^{147}Pm source (1a) and $^{90}\text{Sr} + ^{90}\text{Y}$ source (1b) ($\alpha = 0^\circ$, * $\alpha = 45^\circ$).

The limits of the uncertainties (2σ) are noted (■ for $\alpha = 0^\circ$, □ for $\alpha = 45^\circ$)

2.3 Characterization of beta ray beams in term of absorbed dose rate in tissue

The determination of the absorbed dose rate in tissue $\dot{D}_t(0,07, \alpha = 0)$ at the specified depth of tissue of 0,07 mm is obtained by the classical method /1/.

The characteristics of some beams and our corresponding experimental results $[\dot{D}_t(0,07, \alpha = 0)]_m$ compared with reference values $[\dot{D}_t(0,07, \alpha = 0)]_r$ are presented in Tables 2 and 3.

Table 2 - Beams characteristics

Radionuclide E_{max}	Source diameter (mm)	Filter yes or no	Irradiation Facility	Calibration distance (cm)	Beam Number
^{204}Tl $E_{max} = 0.763 \text{ MeV}$	42	no	CEA	30	1
$^{90}\text{Sr} + ^{90}\text{Y}$ $E_{max} = 2.274 \text{ MeV}$	42	no	CEA	30	2
$^{90}\text{Sr} + ^{90}\text{Y}$ $E_{max} = 2.274 \text{ MeV}$	8	no	Büchler	30	3

Table 3 - Experimental results (reference date : 01.01.1990) the uncertainties are given for one standard deviation.

Beam Number	Absorbed dose rate (mGy.h ⁻¹)		$\frac{\overset{\circ}{D}_t(0,07, \alpha = 0)_m}{\overset{\circ}{D}_t(0,07, \alpha = 0)_r}$
	Measured value $\overset{\circ}{D}_t(0,07, \alpha = 0)_m$	Référence value $\overset{\circ}{D}_t(0,07, \alpha = 0)_r$	
1	46.9 ± 1.00	47.8 ± 0.8 (a)	0.981 ± 0.03
2	197 ± 1.2	196 ± 2.1 (b)	1.005 ± 0.02
3	226 ± 1.3	228 ± 2 (c)	0.991 ± 0.01
(a) FWT.EIC 1 chamber /3/ - (b) LMRI value - (c) PTB value			

In Table 3, our results are in good agreement with the reference values.

2.4 Conversion factors $G(0,07, \alpha)$

The conversion factors $G(0,07, \alpha) = \frac{\overset{\circ}{D}_t(0,07, \alpha)}{\overset{\circ}{D}_t(0,07, \alpha = 0)}$ have been determined for ^{147}Pm and $^{90}\text{Sr} + ^{90}\text{Y}$ extended sources and ^{204}Tl and $^{90}\text{Sr} + ^{90}\text{Y}$ point sources. The results are presented for the ^{147}Pm and $^{90}\text{Sr} + ^{90}\text{Y}$ sources in Figure 2.

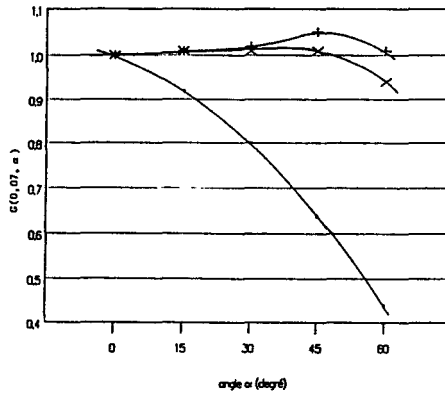


Figure 2: Conversion factors $G(0,07, \alpha)$ for different beta sources [+ $^{90}\text{Sr} + ^{90}\text{Y}$ Büchler point sources, without filter, 30 cm.; $^{90}\text{Sr} + ^{90}\text{Y}$ extended circular source (42 mm in diameter without filter, 30 cm); • ^{147}Pm extended circular source (42 mm in diameter without filter, 20 cm)].

3. Thermoluminescent dosimeters

The applicability of thermoluminescent (TL) detectors for the determination of the factors $G(0,07, \alpha)$ for different beta particle fields was investigated.

TL detectors have the following main characteristics :

- geometry : disk
- material : LiF embedded in Teflon
- thickness : 0,13 mm

They are covered by a mylar foil corresponding to a tissue thickness of 0,07 mm and positioned on a perspex slab (20 mm thickness) which can be tilted to measure $G(0,07, \alpha)$. The results obtained for $\alpha = 0$ are presented in Table 4 and Figures 3 and 4 show results for different angles.

Table 4 - The ^{147}Pm , ^{204}Tl , and $^{90}\text{Sr} + ^{90}\text{Y}$ sources are point source from the irradiation Büchler facility. R is the response par unit $D_t(0,07)$ normalised to that for ^{60}Co radiation

Source	R	Standard deviation %
^{60}Co	1.0	/
$^{90}\text{Sr} + ^{90}\text{Y}$	0.95	4
^{204}Tl	0.70	4,5
^{147}Pm	0.23	5

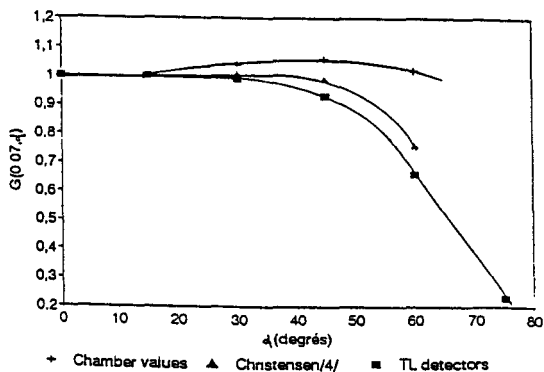


Figure 3: Represents the values of $G(0.07, \alpha)$ as a function of the angle α for $^{90}\text{Sr} + ^{90}\text{Y}$ point source (Büchler) without filter, at a 30 cm distance.

- 0,13 mm LiF dosemeter (this work)
- + extrapolation chamber (this work)
- Δ 0,4 mm LiF dosemeter (Christensen /4/).

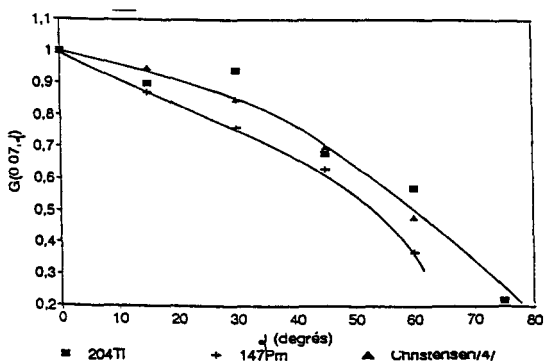


Figure 4: Represents the values of $G(0.07, \alpha)$ as a function of the angle α for $^{204}\text{Tl} + ^{147}\text{Pm}$ point sources (Büchler) with filter.

- 0,13 mm LiF dosemeter for ^{204}Tl at a 30 cm distance (this work)
- Δ 0,4 mm LiF dosemeter for the same conditions (Christensen /4/)
- + 0,13mm LiF dosemeter for ^{147}Pm at 20 cm distance (this work).

Measured values are smaller than those obtained with the extrapolation chamber and similar to 0,4 mm LiF ones. Very thin detectors are needed ; we are working now on LiF mixed with graphite TL detectors, manufactured by Vinten.

4. Conclusion

The PTW 23391 extrapolation chamber available with several diameters of collecting electrode allowed to show the influence of the diameter on the measurement of the absorbed dose rate in tissue ; nevertheless this effect does not perturb the computation of the $G(0,07, \alpha)$ conversion factor.

The results obtained with 0,13 mm LiF detectors show marked difference from those obtained with extrapolation chamber, but are in good agreement with those presented by Christensen with 0,4 mm LiF dosimeters. Nevertheless the 0,13 mm dosimeters are not thin enough and the results reinforce the view that very thin detectors are needed to measure absorbed dose from low energy beta radiations.

References

- [1] BÖHM, J. - The National Primary Standard of the PTB for Realizing the Unit of the Absorbed Dose Rate to Tissue for Beta Radiation - PTB.DOS.13 (1986).
- [2] CHARTIER, J.L.
IPSN/DPT n° 89-135 du 19.12.1989.
- [3] HERBAUT, Y. - HEEREN DE OLIVEIRA, A. VIVIA, R. LEROUX,
J.B.DELAHAIE, M.
Characteristics of an Extrapolation Chamber FWT Type EIC1 in Beta Radiation Fields.
Radiat. Prot. Dosim. 14(2) - 187 - 191 (1986).
- [4] CHRISTENSEN, P. BÖHM, J. FRANCIS, T.M.
Measurement of absorbed dose to tissue in a slab phantom for beta radiation incident at various angles.
Beta dosimetry - Report EUR 11363 (1988).

Project 4

Head of project: *Mr. T.M. Francis*

Objectives for the reporting period

1. Participation in intercomparison exercises conducted among the European laboratories with a view to standardising extrapolation chamber measurement techniques and establishing a protocol for such measurements.
2. Acquisition of an extended area $^{90}\text{Sr}/^{90}\text{Y}$ source that will conform to the physical characteristics specified by the ISO⁽¹⁾ for a Series 2 secondary standard source.
3. Design and construction of a holder for that source.
4. Measurements required for characterising this source in terms of the metrological aspects of the above specification. This entails measurement of beta radiation field from that source in terms of directional dose equivalent rate, $\dot{H}'(d;\alpha^\circ)$ at the calibration distances of interest and the determination of residual maximum beta particle energy of the spectrum at those distances. In addition, measurement of depth-dose distribution in tissue and determination of conversion factors from $\dot{H}'(0.07;0^\circ)$ to $\dot{H}'(0.07;\alpha^\circ)$ for several values of α at the calibration distances were planned.

Progress achieved including publications

1. Methodology

1.1 Preliminary work

The results of an intercomparison⁽²⁾ carried out between three of the laboratories collaborating in the current contract and PTB, Braunschweig were used for the standardisation of measurement procedures and evaluation techniques with extrapolation chambers. An extended area ^{147}Pm source of similar construction to the sources under development in this programme (described in section 1.2 below) was used for this intercomparison. A further intercomparison among the participants of the current contract utilising a circular ^{204}Tl foil source (being developed by CEA, France under the current contract) was also carried out. A protocol based on the principles agreed among all participants was established for the measurements to be carried out in this programme.

1.2. Source and source holder

An extended area $^{90}\text{Sr}/^{90}\text{Y}$ ($E_{\text{max}}=2.27$ MeV) source was acquired. The source has the activity (nominally, 370 MBq) incorporated in a rolled silver foil, the face thickness of the inactive silver layer covering the sources being 0.5 ± 0.1 kg.m⁻²; the uncertainty refers to one standard deviation. The source (overall thickness ≈ 0.3 mm) is square in shape (overall dimension 60 mm x 60 mm) with the activity confined to a central area of 40 mm x 40 mm. A special holder was designed for the source. The holder is made from a block of Dural measuring 75 mm x 75 mm x 28 mm thick with a centrally placed recess 60 mm x 60 mm x 18 mm deep. A block of low atomic number material (phenolic laminated 'Tufnol' BS 2572: 1976) measuring 60

mm x 60 mm x 17.7 mm thick was placed in the recess of the Dural block over which the source foil was positioned. It is held in position on the backing material by means of a 2.25 mm thick sheet of tufnol with a 40 mm x 40 mm window through which the active area of the source is exposed. The holder has a threaded stud on one of its sides into which a rod can be screwed to enable positioning of the source in front of the extrapolation chamber. Figure 1 shows a cross-section of the source holder. A shielded container for use with storage or transportation was designed and fabricated in brass.

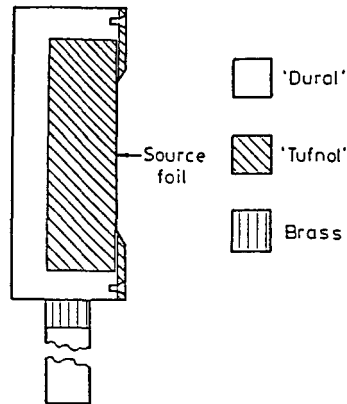


Figure 1. Cross section of source holder

1.3. Measurements

The main features of the extrapolation chamber that was used for these measurements have been described previously⁽³⁾. All measurements reported here have been carried out in accordance with the procedures agreed among the participants and have been outlined as recommendations in a previous publication⁽²⁾. Measurements of dose equivalent rate, $\dot{H}'(d;\alpha)$, at source to chamber distances of 0.2 and 0.3 m and for $d = 0.008$ and 0.07 kg.m^{-2} and $\alpha = 0^\circ, 15^\circ, 30^\circ, 45^\circ$ and 60° have been completed. Each measurement was repeated at least 25 times.

For the determination of depth-dose distributions the extrapolation chamber was not operated in its normal mode. Instead, ionisation currents were measured for different window thicknesses by adding layers of absorber over the chamber window and maintaining a fixed chamber gap, small enough ($\leq 1000 \mu\text{m}$) to be considered as a Bragg-Gray cavity, but consistent with the sensitivity of the measuring equipment. Under these conditions, ionisation current is proportional to absorbed dose rate and the depth-ionisation current distribution so obtained will have the same shape as the depth-dose distribution. The shallowest tissue depth at which such a measurement could be carried out was 0.008 kg.m^{-2} , this being the tissue equivalent thickness of the entrance window of the chamber. For the measurements under greater thicknesses, further layers of material were added to the window. Up to a thickness of approximately 0.3 kg.m^{-2} sheets of mylar (polyethylene terephthalate) were used. For thicknesses greater than about 1 kg.m^{-2} , sheets of perspex (polymethyl methacrylate) were used. In both cases, the measured thicknesses were converted to their

equivalent thicknesses in tissue using the scaling factors given by Cross⁽⁴⁾.

Residual maximum beta particle energy, E_{res} , was evaluated at the calibration distances, 0.2 and 0.3 m, from the measurement of the residual maximum beta particle range, R_{res} , for those distances as recommended by the ISO⁽¹⁾. For the measurement of R_{res} , the signal from a thin-window GM detector (Philips ZP 1482) connected to a scaler ratemeter (type 6-90) was determined as a function of absorber thickness. The detector was positioned with the window facing the source at the appropriate calibration distance. All surfaces of the GM detector except the window were shielded with lead bricks to reduce scattered radiation reaching the detector. Perspex absorbers of various thicknesses were placed directly over the detector window measuring count rate with each thickness in place. Count rates with several absorbers with thickness greater than the maximum range of beta particles from $^{90}\text{Sr}/^{90}\text{Y}$ (≈ 10 mm of perspex) were measured to assess the residual photon background. A plot of the logarithm of signal (count rate) versus absorber thickness in $\text{kg}\cdot\text{m}^{-2}$ was made. R_{res} is defined as the thickness corresponding to the intersection of the extrapolated linear portion of the measured signal versus thickness graph with the lower level signal due to the residual photon background. E_{res} was then evaluated from the following relationship⁽¹⁾:

$$E_{res} = \{[(0.91 \times R_{res} + 1)^2 - 1]/22.4\}^{1/2}$$

where E_{res} is in MeV and R_{res} is the residual maximum beta particle range in $\text{kg}\cdot\text{m}^{-2}$.

2. Results and conclusions

Table 1 gives measured values of directional dose equivalent rate, $\dot{H}'(d;0^\circ)$, at two tissue depths (0.008 and 0.07 $\text{kg}\cdot\text{m}^{-2}$) for the calibration distances 0.2 and 0.3 m. This table also gives results for other angles having normalised at $\alpha=0^\circ$. The dose rate available from this source is approximately an order of magnitude greater than that delivered by the largest of $^{90}\text{Sr}/^{90}\text{Y}$ sources from series 1 at the calibration distance (0.3 m). Table 2 gives values for percentage depth-dose distribution in tissue at source to detector distances of 0.2 and 0.3 m. The depth-dose distributions at 0.3 m are also graphically illustrated in Figure 2. The shape of initial part of the depth-dose distribution obtained with the extended area source is not very dissimilar to that obtained with a series 1 source previously⁽⁵⁾. However, the magnitude of "build up" is somewhat greater with this source than that obtained with series 1 source. This could be due to the absence of the filter with this source.

Table 1: Directional dose equivalent rates at two tissue depths and for two distances and their variation with orientation (normalised at 0°).

Distance m	Tissue depth, d kg/m^2	$\dot{H}'(d;0^\circ)$ mSv/h	$\dot{H}'(d;\alpha)/\dot{H}'(d;0^\circ)$				
			$\alpha=0^\circ$	$\alpha=15^\circ$	$\alpha=30^\circ$	$\alpha=45^\circ$	$\alpha=60^\circ$
0.2	0.008	224	1.00	1.02	1.06	1.13	1.20
	0.07	239	1.00	1.02	1.06	1.12	1.12
0.3	0.008	98	1.00	1.02	1.05	1.11	1.16
	0.07	104	1.00	1.02	1.07	1.09	1.08

Table 2: Percentage depth-dose distribution in tissue at source to detector distances = 0.2 and 0.3 m.

Tissue depth kg/m ²	$\{\dot{H}'(d;\alpha)/\dot{H}'(0.008;\alpha)\} \times 100$									
	Source to detector distance=0.2 m					Source to detector distance=0.3 m				
	$\alpha=0^\circ$	$\alpha=15^\circ$	$\alpha=30^\circ$	$\alpha=45^\circ$	$\alpha=60^\circ$	$\alpha=0^\circ$	$\alpha=15^\circ$	$\alpha=30^\circ$	$\alpha=45^\circ$	$\alpha=60^\circ$
0.008	100	100	100	100	100	100	100	100	100	100
0.024	102	102	102	102	101	102	102	103	102	101
0.039	105	104	104	104	101	103	103	103	102	101
0.055	106	106	105	105	101	105	104	104	104	100
0.071	107	107	106	105	100	105	105	104	104	100
0.087	107	108	106	106	99	105	106	105	104	99
0.118	107	110	106	106	97	107	105	105	104	95
0.150	108	110	106	105	94	108	107	105	104	93
0.181	109	111	107	104	92	109	107	104	101	90
0.212	109	110	107	101	88	109	107	104	101	88
0.244	109	110	107	100	86	108	106	104	100	85
0.275	109	110	107	99	84	109	107	103	98	82
0.307	108	109	106	98	81	109	106	102	97	79
1.085	91	90	81	64	39	93	89	81	63	39
1.651	76	73	62	45	25	77	72	62	44	25
1.753	73	70	60	42	23	74	70	59	41	23
2.365	57	52	43	28	14	56	52	42	27	14
3.215	36	32	25	15	6.6	35	32	24	14	6.5
3.442	32	29	22	13	5.5	31	28	21	12	5.4
4.009	22	20	14	8.0	3.3	22	19	14	7.7	3.6
4.111	18	15	11	6.2	2.4	20	19	12	7.2	2.9
4.859	12	10	7.2	3.7	1.3	11	10	6.8	3.4	1.2
5.573	7.1	5.7	3.8	1.8	0.6	6.2	5.3	3.5	1.6	0.5
6.468	3.0	2.4	1.5	0.6		2.7	2.3	1.4	0.6	
6.615	2.5	2.0	1.3			2.3	1.9	1.2	0.5	
7.692	0.6	0.5	0.3			0.5	0.5	0.3		

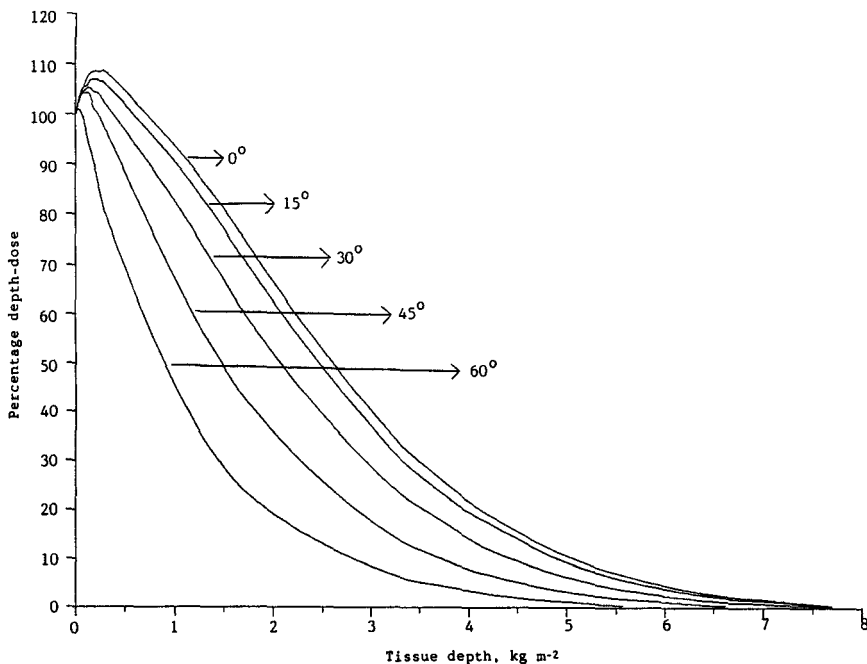


Figure 2. Depth-dose distribution in tissue from a ⁹⁰Sr/⁹⁰Y extended area source at a distance of 0.3 m for various incident angles (normalised to 100% at 0.008 kg m⁻² depth).

The values obtained for the residual maximum beta particle energy, E_{res} , at the calibration distances are given in table 3. The values obtained for both the distances are in conformity with the specifications laid down by the ISO(1).

Table 3: Measured residual maximum beta particle ranges and the values of residual maximum beta particle energy evaluated from them for distances = 0.2 and 0.3 m.

Source to detector distance m	Residual maximum beta range, R_{res} kg/m ²	Residual maximum beta energy, E_{res} MeV
0.2	9.10	1.95
0.3	8.65	1.86

References

1. ISO. Reference Beta Radiations for Calibrating Dosimeters and Doserate Meters and for Determining their Response as a Function of Beta Radiation Energy. ISO 6980. (Geneva: International Organisation for Standardisation) (1984).
2. Francis, T.M., Böhm, J., Chartier J.-L. and Christensen, P. Experience gained on extrapolation chamber measurement techniques from an intercomparison exercise conducted with a ¹⁴⁷Pm source. Radiat. Prot. Dosim., 39(1/3), 109-114(1991).
3. Francis, T.M. The development of a reference instrument for the direct determination of dose equivalent from beta radiation at various depths in tissue. Radiat. Prot. Dosim., 12, 219-222 (1985).
4. Cross, W.G. Variation of Beta Dose Attenuation in Different Media. Phys. Med. Biol., 13, 611-618 (1968).
5. Christensen, P., Böhm, J. and Francis, T.M. Measurement of Absorbed Dose to Tissue in a Slab Phantom for Beta Radiation Incident at Various Angles. In: Fifth Information Seminar on the Radiation Protection Dosimeter Intercomparison Programme, Bologna, 1987. Report EUR 11363, (Luxembourg: CEC) (1988).

Publications

1. Francis, T.M., Böhm, J., Chartier J.-L. and Christensen, P. Experience gained on extrapolation chamber measurement techniques from an intercomparison exercise conducted with a ¹⁴⁷Pm source. Radiat. Prot. Dosim., 39(1/3), 109-114(1991).

Project 5

Head of project: *Prof. Gasiot*

Objectives for the reporting period

The general objective is a contribution to the dose measurement of weakly penetrating radiations using laser heating of a two dimensional thin thermoluminescent solid state dosimeter. In the case of thin dosimeters, laser heating can be effectively fast and efficient because short reading times, in the order of the millisecond, are associated with high TL intensity [1,2]. The laser heating requirements meet the general recommendations that for beta radiation dosimetry the ideal dosimeter should be thin [3,4]. A schematic view of the previous generation of reader is described in ref. [5].

The present work concentrates on:

- Building and testing a new high sensitivity laser heating TLD reader adapted to beta dosimetry. This includes: a control of the experiment (positioning the dosimeter; heating and laser power control; command of various apparatus and remote configuration) and a data acquisition and processing software.
- Developing and testing new dosimeters adapted to laser heating and beta dosimetry. This includes adjusting the dosimeter-filter-support assembly.
- Comparing the performances of the laser system with those of a conventional reader.

Progress achieved including publications

1. Design and building of a TLD reader

The new TLD reader is equipped with a RF 125 type laser. The experimental set up is presented in fig. 1. The main improvements on the reader features are:

-Electronic laser power control. We use an electronic control of the laser power by varying the low frequency modulation of the R. F. laser excitation.

The control of the laser output allows a stability of the laser power better than 0.2%. This power stability should allow a reproductibility better than 2% on the reading of the thermoluminescence of large plates. The signal fluctuation is therefore mainly dependent on the dosimeter preparation.

-Positioning the dosimeter is computer controlled, ensuring that the origin of the detector to be read is always in the same position.

-To improve the sensitivity, a new optical design has been developed. The system is under test. This new system allows us to read with the same sensitivity different TLD materials ($\text{CaSO}_4:\text{Dy}$ as well as Al_2O_3 , for instance), deposited on different supports, including glass, polyimides ...

-Heating and control functions of the new reader have been improved to assure a continuous heating on a line, in addition to the traditional point by point reading. This set up allows us to read both, large plates (200mmx200mm) and dosimeters as small as 20mmx20mm. The resolution has been improved and is now of the order of 100 microns at the minimum.

Data acquisition and software has been developed to insure the following features:

- Acquisition of sample and irradiation characteristics.
- Determination of the experimental reading conditions, i.e.:
- Control and measurement of the laser parameters.
- Reading of a dosimeter with the associated data acquisition.
- Data processing.

The actual development has included several new features such as the control, the visualisation and the analysis of the laser heating and of the TL curve. The data processing system allows for transfer of the data to an ASCII file.

2. Testing the reader

A comparative study of the performance of the laser reader and that of a conventional reader has been performed with the team of Prof. F. Fernandez (Servicio de Fisica de las Radiaciones, Universidad Autonoma de Barcelona, Spain)[6]. We have developed a facility to produce the large amount of $\text{CaSO}_4:\text{Dy}$ powder required in the preparation and optimisation of the dosimeter, using a method previously described [7]. Samples with concentration of dopant ranging from 0.05 to 2.5 mole% Dy were prepared. The samples were irradiated using a 50 kV X-ray source and a $^{90}\text{Sr}/^{90}\text{Y}$ source. We studied the influence of the dopant concentration and the pre-annealing temperature on: crystal size and shape prior to irradiation; intensity and position of the the low and high temperature peaks of the glow curves; sensitivity and fading. We observed that the crystal size decreases strongly with the dopant concentration (for dysprosium contents): above 1 mole% we observed clusters of very tiny thin crystals without any well defined shape. Fig. 2 and 3 show the influence of the annealing temperature after preparation (1 hour at 350°C plus 3.30 hours at 400°C) on the glow curves of $\text{CaSO}_4:\text{Dy}$ 0.1 mole%. Samples with annealing exhibit stronger intensity of the high temperature peak leading to higher sensitivity. On the other hand these samples showed a lower ageing than those which were not annealed. Fig.4 and 5 show reproductibility of the TL output as a function of readings.

3. Developing new dosimeters adapted to laser heating and to beta dosimetry

Steps 3 are still in progress. The work is related to the conception, the simulation and finally the test of dosimeters adapted to the new TLD reader and for radiation metrology of low energy radiations. The skills and the tools accumulated in this field during the past few years [8] have been applied to develop dosimeters to measure doses, in particular,

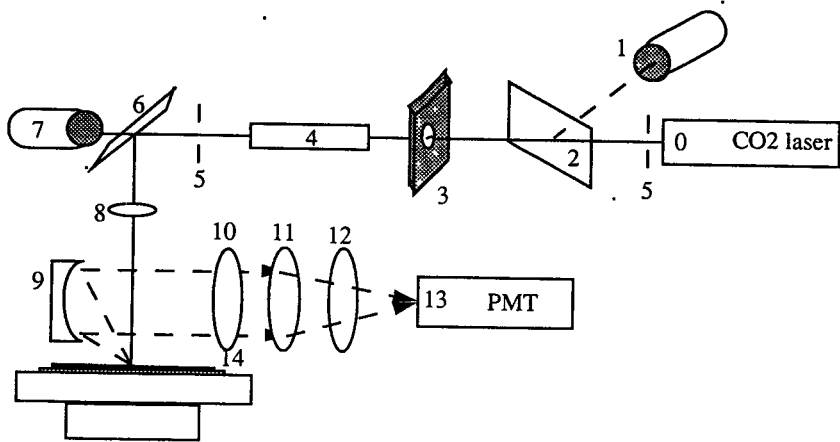
from beta rays ($^{90}\text{Sr}/^{90}\text{Y}$, ^{147}Pm , ^{204}Tl). Improvements of the dosimeters have been achieved by varying the kind of support and the TL material. Concerning the TL material, we have still some problems with respect to the preparation and the reading of thin tissue equivalent sensitive materials.

The dosimeter response with respect to the filter-support-detector arrangement has been investigated. Computational simulations allow for the determination of the energy deposited in the TL material and around the detector.

Actually the reproducibility of the reading of the thermoluminescence of small plates (20mmx20mm) is better than 5%; for large plates (200mmx200mm) typical values are within 5 to 10%.

Publications and bibliography

1. Gasiot, J., Fillard, J. P. and Bräunlich, P. Laser Heating in Thermoluminescent Dosimetry. *J. Appl. Phys.* 53, 5200-5208 (1982).
2. Bräunlich, P., Tetzlaff, W., Gasiot, J. and Jones, S. C. Development of a Laser Heating TLD Reader. In: *Proc. Int. Beta Dosimetry Symp.* Washington DC. February 15-18, 293-305 (1983).
3. Christensen, P. and Prokic, M. S. Energy and Angular Response of TL Dosimeters for beta ray Dosimetry. *Radiat. Prot. Dosim.* 17, 83-87 (1986).
4. Christensen, P., Herbaut, Y. and Marshall, T. O. Personal Monitoring for external sources of beta and low Energy Photon Radiations. *Radiat. Prot. Dosim.* 18, 241-260 (1987).
5. Servièrre, H., Vignolo, C. Prévost, H. and Gasiot, J. Laser Heating of TL dosimeters: Application to beta Dose Mapping. *Radiat. Prot. Dosim.* 39, 145-148 (1991).
6. Luguera, E., Fernandez, F. and Gasiot, J. Thin $\text{CaSO}_4:\text{Dy}$ for Beta Dosimetry. Grain size and Energy dependence. *Radiat. Prot. Dosim.* 33, 207-209 (1990).
7. Prévost, H., Gasiot, J. *et al.* UV Emission in the TL Peaks of $\text{CaSO}_4:\text{Dy}$; Origin and Application to High Temperature Dosimetry. 10th International SSD Conference, Georgetown, Washington DC, July 13-17, 1992.
8. Gasiot, J. Convention N° B 16* 231-F (EDB) December 1988.



- | | | |
|-----------------|--------------------|-------------------------------|
| 0 CO2 LASER | 5 Beam shaper | 10 filter |
| 1 wattmeter | 6 mirror | 11 lens (visible) |
| 2 reflector | 7 joulemeter | 12 Visible calibration source |
| 3 shutter | 8 ZnS lens | 13 PMT |
| 4 Beam expander | 9 Parabolic mirror | 14 TLD plate |

Figure 1: Configuration of the new Laser TLD reader

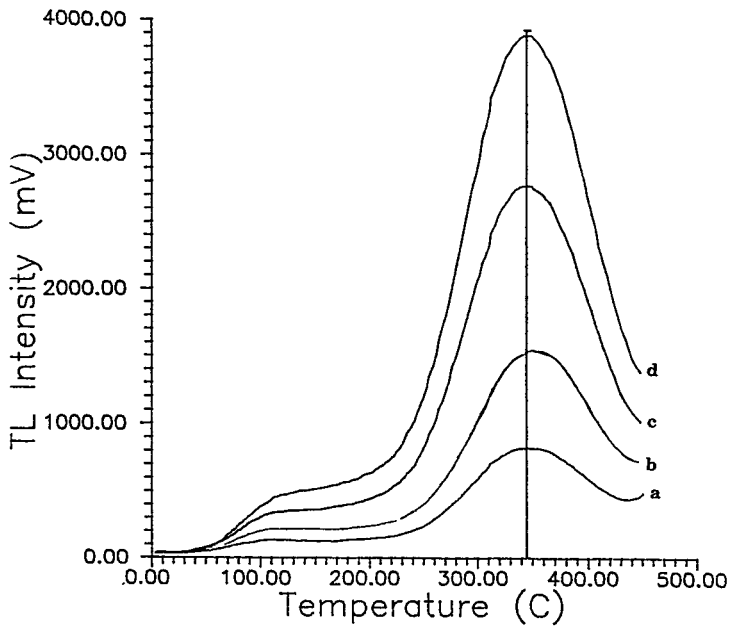


Figure 2: Glow curves of $\text{CaSO}_4:\text{Dy}$ without annealing
Dose (mGy) = 1.5 (a); 3 (b); 6 (c); 9 (d)

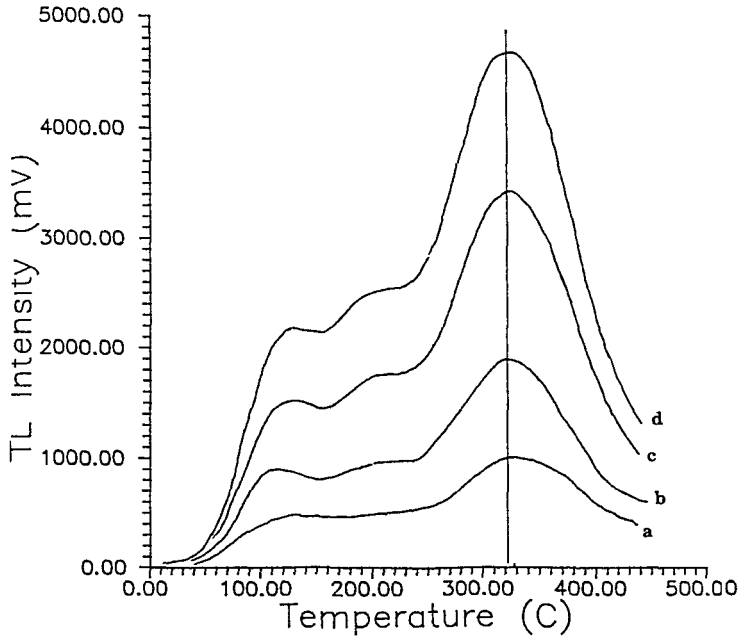


Figure 3: Glow curves of $\text{CaSO}_4:\text{Dy}$ with annealing
Dose (mGy) = 1.5 (a); 3 (b); 6 (c); 9 (d)

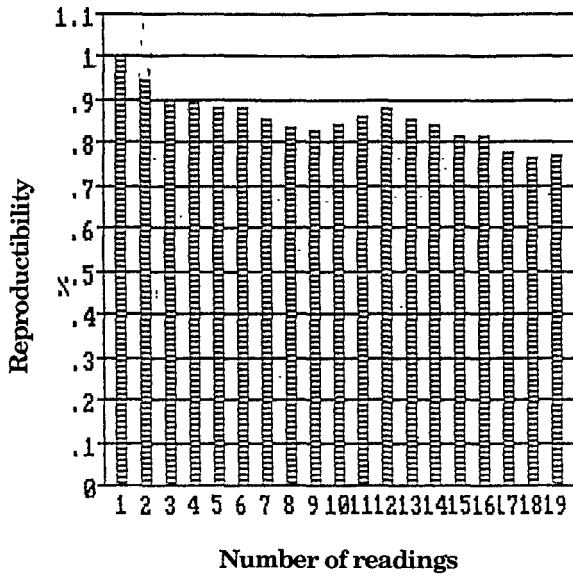


Figure 4: Reproducibility test of TL dosimeter without annealing.
Irradiated to 4 mGy with a $^{90}\text{Sr}/^{90}\text{Y}$ source.

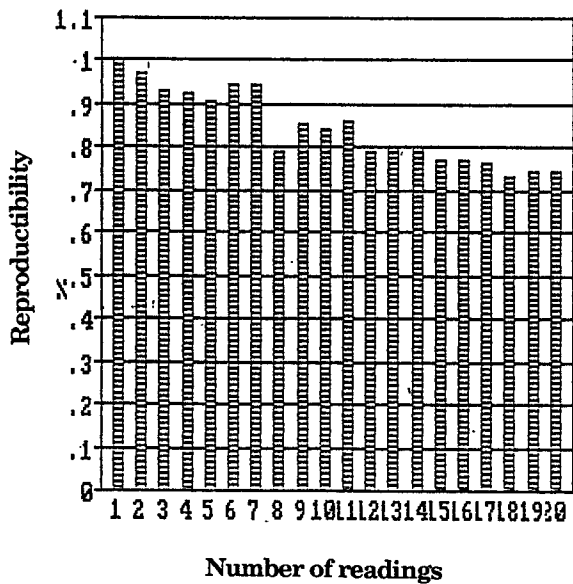


Figure 5: Reproducibility test of TL dosimeter with annealing. Irradiated to 4 mGy with a $^{90}\text{Sr}/^{90}\text{Y}$ source.

Project 6

Head of project: *Prof. Scharmann*

Objectives for the reporting period

The TSEE method is particularly suited for the dosimetry of weakly penetrating radiation because it employs an extremely thin sensitive layer. In a co-operation between the CEA institute in Fontenay-aux-Roses and the I. Physikalisches Institut of the University of Giessen the capability of exoelectron emitting BeO thin films dosimeters for the measurement of personal dose equivalent $H_p(0.07)$ in beta radiation fields was tested and optimized. Measurements were carried out with respect to

- Improvement of the detector geometry
- Reproducibility of the dose response
- Optimization of covering foils
- Development of an optimised dosimeter badge
- Comparison with the results obtained by extrapolation chambers for different beta radiation sources
- Determination of the ratio beta/gamma of the dosimeter sensitivity.

Progress achieved including publications

1. Experimental conditions

BeO thin film detectors produced by the Battelle Institute in Frankfurt were studied which consisted of a 100 nm BeO layer on a circular graphite substrate of 12.5 mm diameter. Irradiations were performed with ^{60}Co and the beta radiation sources of the Buchler secondary standard in Fontenay-aux-Roses. In Giessen a $^{90}\text{Sr}/^{90}\text{Y}$ source of type F according to the notation by Christensen et al. (1) was applied. For all exposures to beta radiation the detectors were placed on a Plexiglass slab (polymethyl methacrylate) of a thickness ≥ 10 mm. The experimental results are mean values from 4 - 8 detectors with standard variations between 2 - 8 %. Foils of $7.2 \text{ mg}\cdot\text{cm}^{-2}$ ($50 \mu\text{m}$) Hostaphan (polyethylene terephthalate) and $8.4 \text{ mg}\cdot\text{cm}^{-2}$ ($60 \mu\text{m}$) Makrofol, a conducting black polycarbonate material with soot additions were used as tissue equivalent cover materials. Makrofol was taken because it protects against optical fading and avoids charging effects, however, foils of $7 \text{ mg}\cdot\text{cm}^{-2}$ were not available. The TSEE measurements were carried out with a proportional counter of stabilized gas multiplication in Giessen (2) and a multi-needle counter in Fontenay-aux-Roses (3).

2. Energy dependence of the TSEE response

Detectors covered by $7.2 \text{ mg}\cdot\text{cm}^{-2}$ Hostaphan had an almost correct response for normal radiation incidence, independent of beta radiation energy (Table 1). The too thick Makrofol covers produced a significant undersensitivity in the case of ^{147}Pm irradiations. In the future a very recently developed black polypyrrole foil shall be used which is intrinsically conducting. Sheets of a thickness of $7 \text{ mg}\cdot\text{cm}^{-2}$ were particularly produced for our needs.

Table 1: Relative response of BeO thin film detectors covered by Hostaphan and Makrofol per unit absorbed dose to tissue $D_t(0.07)$

Radionuclide	Mean energy (MeV)	Relative response	
		50 μm Hostaphan	60 μm Makrofol
^{60}Co	1.25	1.00	1.00
$^{90}\text{Sr}/^{90}\text{Y}$	0.8	1.05	1.10
^{204}Tl	0.24	1.04	0.97
^{147}Pm	0.06	0.96	0.77

3. Angular response

Corresponding to the factors $F(0.07, \varphi)$, which have been established with extrapolation chambers (1) a factor $F' = R(0.07, \varphi)/R(0,0)$ can be defined where R denotes the TSEE response. The factors $F'(0.07, \varphi)$ were determined for beta radiation from the sources of the Buchler standard. They were in close agreement to the values of $F(0.07, \varphi)$ (Fig. 1).

In order to prevent the sensitive BeO layer of the detectors from mechanical contact with covering materials it is evaporated into a 0.5 mm deep recess of the substrate. A comparison with flat detectors of 19 mm substrate diameter showed that the side walls of 12.5 mm standard detectors cause shading and decrease the TSEE response at angles $> 60^\circ$ of radiation incidence (Fig. 2). The measured deviations were corresponding to the computed shadow area on the sensitive BeO layer.

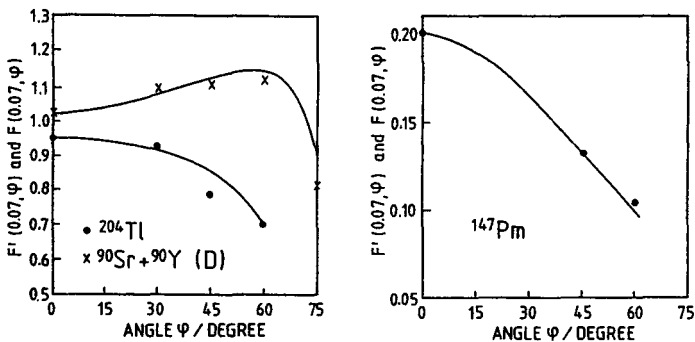


Figure 1. Angular response of Hostaphan covered BeO thin film detectors to $^{90}\text{Sr}/^{90}\text{Y}$, and of Makrofol covered detectors to ^{204}Tl and to ^{147}Pm in comparison to the factors $F(0.07, \varphi)$ (curves).

If the detectors are placed in a badge care has to be taken that the upper part of the badge does not additionally affect the angular response. The badge formerly used in Giessen (4) raised the value of $F'(0.07, \varphi)$ by more than 10 % due to scattering at angles of incidence $0^\circ - 30^\circ$, while $F'(0.07, 75^\circ)$ was only 0.4. For this reason a new badge was designed consisting of a holder of black perspex with an extended window diameter. It produced the same results as in Fig. 2 for exposures to $^{90}\text{Sr}/^{90}\text{Y}$.

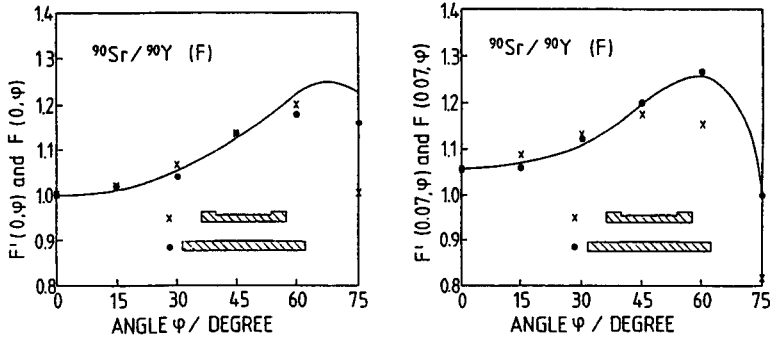


Figure 2. Angular response of uncovered detectors and detectors covered by $7.2 \text{ mg}\cdot\text{cm}^{-2}$ Hostaphan to $^{90}\text{Sr}/^{90}\text{Y}$ (source F, distance 30 cm) in comparison to the factors $F(0,\varphi)$ and $F(0.07,\varphi)$ for two different detector geometries.

4. Depth dose determination by TSEE

The dependence of the TSEE response of BeO thin film detectors exposed to $^{90}\text{Sr}/^{90}\text{Y}$ on the thickness of covering Hostaphan foils was exactly in accordance with the transmission factors $T(d)$ for tissue in the Buchler calibration report (Fig. 3). Similar measurements were also carried out with detectors covered by Makrofol, aluminium, copper and gold. The results obtained with Makrofol slightly deviated from those of Fig. 3 in a manner typical for a material of a too low atomic number. These deviations are caused by the high concentration of soot additions to the polycarbonate base of Makrofol.

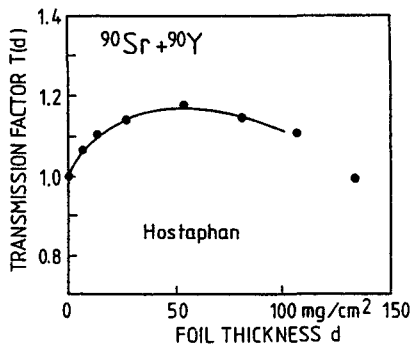


Fig. 3. Dependence of the TSEE response of detectors exposed to $^{90}\text{Sr}/^{90}\text{Y}$ (source F, distance 30 cm) on the thickness of covering Hostaphan foils in comparison to the transmission factors in tissue (curve).

5. Influence of wet atmosphere on the reproducibility of the dose response

It is known from previous measurements (5) that the dose response can increase by 10 - 15 % if irradiated BeO thin film detectors are stored in water for several hours and subsequently dried in air. In order to understand this effect such detectors and other insulating exoelectron emitters were studied under vacuum conditions with TSEE excitation by a computer controlled scanning electron

gun and exoelectron detection by a channeltron (6). Extremely strong surface charging of the detectors could be achieved and modified by variation of primary electron energy and dose and the exhaustion of secondary electrons. Water vapour was admitted through a leak valve to a partial pressure of 4 hPa. This study showed that the increase of the TSEE response by humidity can be attributed to surface neutralization which is caused by intense water adsorption on charged insulating surfaces. Without neutralization emitted exoelectrons are partly deflected to adjacent surface sites because of inhomogeneous charge distributions.

However, such effects could not be observed on BeO thin films which were in the usual manner exposed to beta or gamma radiation in air and read-out with the counting tube equipment. A set of 48 dosimeters from different preparations by the Battelle Institute in Frankfurt and the Staatliches Materialprüfungsamt in Dortmund, was repetitively exposed to $^{90}\text{Sr}/^{90}\text{Y}$ (1 mSv) and prior to the TSEE measurement either stored in saturated water vapour, vacuum or normal laboratory atmosphere. The different storage conditions had no influence on the dose response. The standard deviations for the detectors varied between 1 and 5 %.

References

1. Christensen, P., Böhm, J., and Francis, T.M. Measurement of Absorbed Dose to Tissue in a Slab Phantom for Beta Radiation at Various Angles. In: Beta Dosimetry - Fifth Information Seminar on the Radiation Protection Dosimeter Intercomparison Programme, Bologna, May 1987. EUR 11363, (Luxembourg: CEC) pp. 39-75 (1988).
2. Kriegseis, W., Scharmann, A., Senger, W. and Woerner, B. Equipment for Fast Automatic Readout of TSEE Dosimeters Employing a Wide Range Proportional Counter. Japan. J. Appl. Phys. 24, Suppl. 24(4), 60-64 (1985).
3. Petel, M., Comby, G., Quidort, J. and Barthe, J. Multineedle Counter with Cathode Focusing (MNCF) Used for TSEE Dosimetry. Radiat. Prot. Dosim. 4(3/4), 171-173 (1983).
4. Petel, M., Chartier, J.L., Itié, C., Kessler, H., Kriegseis, W. and Scharmann, A. Dependence of the TSEE of Beta Irradiated BeO Thin Film Detectors on the Properties of Surrounding Materials. Radiat. Prot. Dosim. 33(1/4), 307-310 (1990).
5. Kriegseis, W., Scharmann, A., Senger, W., Weiss, A., Wieters, C.U. and B. Woerner. Dosimetric Properties of Exoelectron Emitting BeO Thin-Film Detectors. Atomkernenergie-Kerntechnik 46, 264-271 (1985)
6. Woerner, B., Kriegseis, W. and Scharmann, A. The Influence of H_2O Adsorption on the Thermally Stimulated Exoelectron Emission (TSEE) of BeO Thin Films. Phys. Stat. Sol. (a) 128, 419-426 (1991).

Publications

Kriegseis, W., Kessler, H., Rauber, K., Scharmann, A., Chartier, J.L., Itié, C and Petel, M. Response of TSEE Dosimeters of Foil-Covered BeO Thin Films to Beta Radiation. Radiat. Prot. Dosim. 39(1/3), 127-130 (1991).

THE USE OF MICRODOSIMETRIC METHODS FOR THE DETERMINATION OF DOSE EQUIVALENT QUANTITIES AND OF BASIC DATA FOR DOSIMETRY

Contract Bi7-030 - Sector A12

- 1) *Grillmaier*, Univ. Saarlandes - 2) *Brede*, PTB
- 3) *Zoetelief*, TNO-ITRI - 4) *Schmitz*, KFA Jülich GmbH
- 5) *Ségur*, ADPA

Summary of project global objectives and achievements

1. Development of radiation protection dosimeters based on microdosimetric principles:

The project was aimed at the development of detectors using microdosimetric methods for the measurement of dose equivalent in neutron-photon fields. The methods include low pressure tissue-equivalent proportional counters (TEPC) and high pressure ionisation chambers (HIPC) for area monitoring, and a semiconductor detector (SCD), as microdosimetric device, for individual dosimetry. The objectives were to improve the performance of TEPCs and to study the feasibility of HIPCs and SCDs with regard to their implementation for radiation protection dosimetry.

The studies included the investigation of various technical problems, and the determination of the dose response of the detectors and their properties as LET spectrometer. The work included measurements in reference radiation fields. Depending on the stage of development reached, some dosimeters could also be tested in environments of practical relevance for radiation protection enabling the assessment of their effective capabilities in work conditions. The investigations required theoretical studies using radiation transport and energy deposition calculations. Furthermore the knowledge of basic characteristics of the detectors (swarm parameters, gas gain, recombination, dead layer) were improved by using computer simulation.

The performance and specifications of the TEPC were improved and criteria for the optimisation of their energy response and the required research work were identified. The programme is intended to be continued with the aim to reduce the simulated diameter down to several hundred nanometers and to determine the response of the TEPC in reference radiation fields with realistic spectra.

The feasibility study of HIPCs revealed that large size detectors are required to meet sufficient sensitivity implying to solve complex technical problems related to their electrical design. The determination of their energy response requires more investigation.

To develop SCD dosimeters, buried charged coupled devices were first developed and experimentally tested in comparison with random access memory chips. Based on these preliminary investigations and using simulation calculations, the construction of chips with suitable characteristics to be used as microdosimetric devices were started. First samples are expected soon enabling prototypes to be developed and tested during the next period.

2. Basic data for dosimetry :

The work with microdosimetric devices on one hand requires but also provides basic information for dosimetry. Different problems were investigated including :

2.1 Electron collision cross sections and related interaction quantities in gases :

The research on electrical discharge modelling in gas cavities is aimed at a better understanding of charge collection processes in ionisation gas devices, in particular gas amplification in low pressure proportional counters. This work has therefore within the frame of the present project a direct impact for the development of operational dosimeters based on TEPC techniques. In fact the study includes primarily the determination of the required electron collision cross sections in the relevant organic vapours such as TE gas compounds. The methods to determine these cross sections are indirect being based on deconvolution calculations using gas gain modelling and experimental swarm parameters. During the contractual period, these cross sections were determined for propane, isobutane and related TE mixtures of direct relevance for microdosimetric counters. A critical question remains the accuracy achievable in gas gain calculations requiring to compare experimental and calculated gas gain data in well defined conditions. Such work involves a larger collaboration and was initiated within Working Group 10 of EURADOS. Within this cooperation, the application of these cross section tables to derive W values in the gases of interest is investigated.

2.2 Neutron kerma factors :

Radiation protection dosimetry covers specific environments such as research accelerators, space and civil aircrafts where high energy radiation, in particular high energy neutrons, dominates. The investigations of high energy neutron fields were within the present project directed toward (1) the determination of kerma factors in different materials and (2) providing reference fields with well defined spectral characteristics for the calibration of radiation protection dosimeters.

Within the present partnership, a long term collaboration existed to perform accurate measurements of neutron kerma factor based on combined neutron spectral fluence and kerma measurements. PCs are specially well suited for kerma measurements in fast neutron fields. Fluence measuring techniques are well established below 20 MeV. During this period these techniques were improved to be applied in the neutron energy range between 30 and 70 MeV. The whole kerma measurements actually performed so provided a consistent set of experimental kerma factors for A-150 plastic and carbon for neutron energies from 14 to 70 MeV. The current work is continued to determine the corresponding data for oxygen material. These results are of direct relevance for the improvement of nuclear models for the interaction of neutrons with light nuclei.

The kerma experiments required accurate knowledge of neutron spectral fluence. To obtain this information, spectrometry methods had to be substantially modified and improved for these high neutron energies. The work allowed in turn to extend the reference fields available for calibration of radiation protection dosimeters to the high energy range. No such facility existed so far. Calibration experiments in collaboration with other contracts were performed at the PSI in Switzerland. The characterisation of high energy fields with different characteristics is being investigated also in Louvain-la-Neuve. High energy neutron dose equivalent conversion factors were evaluated and the dose equivalent response of TEPCs was for the first time systematically investigated at these high energies.

2.3 Dose calculations in phantom :

Dose calculations in phantoms were investigated with two endpoints.

A correct interpretation of the dose equivalent response of the dosimeters requires to take into account the influence of radiation scattered in the phantom and the definition of operational quantities in radiation protection. For microdosimetric devices this investigation can be achieved by combining radiation transport and energy deposition calculations. The calculations performed also served to design the operational detectors and to investigate a reference dosimeter based on TEPC as transfer device for the calibration of other instruments.

Dose calculations were also applied to derive organ dose in humanoid phantoms with the aim to investigate the consequences of the new recommendations by the ICRP, in particular the meaning of quality factors based on LET compared with the new radiation weighting factors.

Project 1

Head of project: *Dr. Grillmaier*

Scientific staff: *S. Gerdung, A. Kunz, T. Lim, P. Pihet*

Objectives for the reporting period

To improve the dose equivalent response of low pressure tissue-equivalent proportional counters (TEPCs) for low and intermediate energy neutrons by optimising TEPC characteristics (gas pressure and composition, wall thickness) by mean of calculations and experiments in reference fields. To assess the influence of ambient temperature on the stability of gas gain to improve the practical performance of TEPCs for radiation protection work.

To continue measurements at research facilities and radiation protection environments, using in particular the HANDI survey meter (Homburg Area Neutron Dosimeter).

To complete in close collaboration with the PTB the determination of kerma factors in A-150 and Carbon for neutrons from 14 to 70 MeV by using PCs to measure absolute kerma. To investigate accuracy of PC measurements with regard to the calibration techniques used.

Progress achieved including publications

1. Optimisation of the HANDI radiation protection dosimeter

The development of the ambient dose equivalent meter HANDI based on a low pressure tissue equivalent proportional counter (TEPC) was continued in collaboration with the Bundes Minister für Umwelt Naturschutz und Reaktorsicherheit (2)(5). An operational version of the HANDI system was produced in a limited series to be tested by expert institutes in order to assess the capability of the instrument for radiation protection dosimetry. The instrument was namely given to perform radiation protection measurements in civil aircrafts, the continuation of this work being planned for the next period within the frame of another contract. Furthermore, it was used successfully at different radiation protection environments, e.g. to measure the dose equivalent distributions in intense neutron-photon fields around a cyclotron specially built for radioisotope production and dedicated for clinical use (Fig. 1) (2)(3).

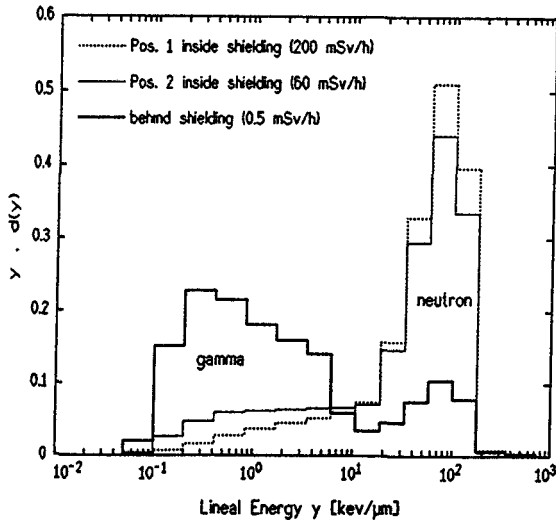


Figure 1. TEPC measurements at different locations around a 3 MeV compact medical cyclotron made by I.B.A. Louvain-la-Neuve for P.E.T. The TEPC measurements served to characterise the radiation fields close to the cyclotron in the absence of reliable spectrometry information. The spectra were systematically measured inside and outside the concrete shielding providing detailed neutron-photon dose equivalent mappings around the accelerator (2).

The work was focused on improving the performance of the TEPC for mixed fields dosimetry, in particular the improvement of the dose equivalent response for neutrons with low and intermediate energies. The reading of a TEPC for neutrons with energies below several hundred keV is considerably lower than the ambient dose equivalent due to the combined effects of short range particles in the cavity and neutron transport in the detector wall (1). An additional experiment was performed in the 144 keV filtered neutron beam of the Research and Measurement Reactor (FRMB) at the PTB to investigate more precisely the influence of these effects (6). The results compared with those of earlier experiments confirmed that the solution depends on a difficult compromise for the choice of the wall thickness, the gas pressure and the gas composition, the main difficulty remaining to increase the response at neutrons energies around 10-100 keV. To search for the optimum parameters, the experimental investigations were completed by mean of computational methods. The MCNP 3B3 code was used at the PTB to simulate neutron transport in the detector wall and combined with the Caswell and Coyne code to calculate the energy deposition distribution in the cavity (Fig. 2).

Although the "ideal" energy independent curve was not found, a response in the order of $\pm 40\%$ seems feasible in an energy range already considerably larger than for conventional radiation protection instruments. To reach this objective the best compromise would be to use : (1) lower diameters than those commonly used to achieve a significant improvement in the 100 keV region; (2) detector wall thickness not exceeding 1 cm; and (3) ^3He to enhance the response to thermal neutrons however in very small amounts ($<1\%$) due to the fast increase of the response below 1 keV and at thermal energies. Adding ^3He does not influence the determination of the photon component and the response of the TEPC to fast neutrons.

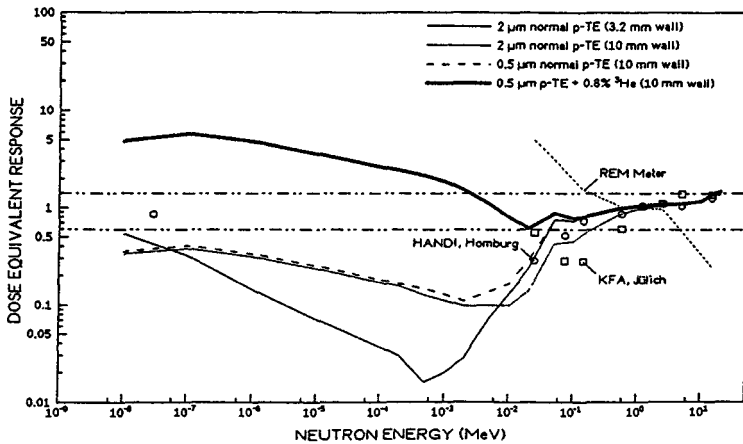


Figure 2. Dose equivalent response of a TEPC as a function of neutron energy as calculated by varying the counter characteristics. Theoretical curves are compared with experimental data (HANDI, 2.8 mm wall; KFA, 18 mm wall). The response of a rem-meter using thick moderator is added for comparison. In the range from high energies down to about 5 keV, the calculations show that an adequate response for the TEPC can be achieved. At lower energies the decision for the best compromise depends on the spectrometry information available for practical fields.

Other properties of TEPCs were investigated to increase their technical performance (6). Namely, in practical environments, TEPCs must be used in ambient temperatures varying from about 15 to 40 °C. The temperature dependence of gas amplification was studied by testing the stability of the alpha source calibration peak for counters maintained in a thermostatically controlled chamber. For various TEPCs filled with propane TE gas a decrease in gas gain of 0.7 %/°C was observed for temperature increasing from 10 to 50 °C. Furthermore, no significant variation was observed for counters filled with pure isobutane leading to associate the effect of temperature with the CO₂ content. A counter with metal walls and filled with propane based TE gas also did not show significant variation leading to assume the effect as due to the interaction of A-150 plastic wall and CO₂. Isobutane appears therefore a relevant alternative to propane based TE gas. It also offers better gas gain properties enabling to operate the detector at lower voltage and reduced gas pressure.

Possible improvements of the TEPC characteristics places the instrument as a relevant alternative to conventional detectors using thick moderators. In particular, an adequate response is feasible in the 10-500 keV and thermal regions which are the dominant neutron components in reactor environments. This and the good performance of TEPCs in high energy fields motivated the continuation of the programme to search for the solution of two remaining problems: (1) what is, and how to improve, the operation of TEPCs at low pressures simulating volumes in the order of 0.5 μm, especially TEPCs with large sizes; and (2) what is the effective response of the instrument in realistic fields similar to those encountered in radiation protection practice taking into account the relative weight of the different energy components.

2. Dosimetry research using PCs

Kerma measurements were performed using PCs made of carbon and A-150 plastic in neutrons fields with energies from 30 to 70 MeV at the Paul Scherrer Institute (CH). These experiments aimed at the determination of kerma factors for carbon and A-150 were performed in collaboration with the PTB and the Université Catholique de Louvain to combine PC and neutron fluence measurements. They completed similar experiments performed at the PTB in the range from 14 to 20 MeV (7). The whole set of kerma experiments was revised by improving calibration techniques with emphasis put on the basic physical data required and the influence of experimental uncertainties (5). The overall uncertainty of the kerma measurements using a TEPC and a CPC was found ranging from 4 to 7 % in the neutron energy range of 14 to 20 MeV, from 4 to 15 % in the range of 30 to 70 MeV (see Project 2 for publications).

Taking advantage of the combined TEPC and spectral fluence information available, the TEPC measurements served as a preliminary investigation for the dose equivalent response of the TEPC to high energy neutrons, of relevance in high energy radiation environments such as around research accelerators, in space and civil aviation.

3. Microdosimetric investigations of various radiation fields at research facilities

TEPCs were used at the research reactor Silène within the frame of spectrometry measurements around the bare and the shielded source to support a reference dosimetry for an intercomparison of criticality accident dosimeters. Preliminary measurements were performed in moderated neutron fields with "realistic" spectra simulated at Cadarache. Furthermore the laboratory continued to support investigations of radiation quality at different facilities : (1) comparison of two different irradiation geometries used for biological experiments at the research reactor TAPIRO; (2) comparison of lineal energy distributions for 14 MeV neutron therapy beams in fixed and moving beam configurations in Heidelberg; (3) comparison of y-distributions for 80 MeV proton therapy beams in correlation with radiobiological experiments to assess the use of biological weighting functions in microdosimetry.

Scientific staff:

S. Gerdung, A. Kunz, T. Lim, P. Pihet

Other research group(s) collaborating actively to this project:

Centre de Protonthérapie d'Orsay (Dr. A. Mazal) (F)

Centro Ricerche Energia Casaccia, ENEA, Lab. di Patologia (Prof. M. Coppola) (I)

Commissariat à l'Energie Atomique, CEA Fontenay aux Roses (Dr. J. Barthe) (F)

Contract BI70051F "Dosimetry and spectroscopy measurements of the leakage radiation fields from the Silene reactor (CEA, Valduc)" (Dr. R. Medioni, Dr. H.J. Delafield) (CEC)

Deutsches Krebsforschungszentrum, DKFZ, Heidelberg (Dr. K.H. Höver) (D)

Univ. Catholique de Louvain-la-Neuve, Unit. Phys. Nucl. (Prof. J.P. Meulders) (B)

Paul Scherrer Institute, PSI Villigen (Dr. R. Henneck, Dr. P. Schmelzbach) (CH)

Publications

- 1) Kunz, A., Pihet, P., Arend, E. and Menzel, H.G. An easy-to-operate portable pulse-height analysis system for area monitoring with TEPC in radiation protection. Nucl. Instr. and Meth. Phys. Res., A229, 696-701 (1990)
- 2) Pihet, P., Arend, E., Conard, E., Grillmaier, R.E. and Kunz, A. Survey of dose equivalent distributions around a medical isotope producing cyclotron using a TEPC ambient dosimeter. Proc. 23rd Int. Symp. Radiat. Prot. Phys. (Gaussig, 1990), in preparation.
- 3) Kunz, A., Menzel, H.G., Pihet, P., Schuhmacher, H. and R.E. Grillmaier. Messungen der Neutronen-Photonen Äquivalentdosis mit einem TEPC Monitor in der Umgebung von medizinischen Beschleunigern. Proc. "Strahlenschutz im medizinischen Bereich und an Beschleunigern" (Göttingen, 1990), Strahlenschutz in Forschung und Praxis, C. Reiners, D. Harder and O. Messerschmidt, eds., 32, 267-274 (1992)
- 4) Kunz, A. Entwicklung eines Meßgerätes zur Dosimetrie in gemischten Neutronen-Photonenstrahlenfeldern unter Anwendung eines gewebeäquivalenten Niederdruckproportionalzählers. Universität des Saarlandes (FRG), Thesis (1992).
- 5) Pihet, P., Gerdung, S., Grillmaier, R.E., Kunz, A. and Menzel, H.G. Critical assessment of calibration techniques for low pressure proportional counters used in radiation dosimetry. Symp. Neutron Dosimetry (Berlin, 1991), Rad. Prot. Dosim. in press (1992)
- 6) Kunz, A., Arend, E., Dietz, E., Gerdung, S., Grillmaier, R.E., Lim, T. and Pihet, P. The Homburg area monitor HANDI : characteristics and optimisation of the operational instruments. Symp. Neutron Dosimetry (Berlin, 1991), Rad. Prot. Dosim. in press (1992)
- 7) Pihet, P., Guldbakke, S., Menzel, H.G. and Schuhmacher, H. Measurement of kerma factors for carbon and A-150 plastic : neutron energies from 13.9 to 20.0 MeV, Phys.Med.Biol. in press (1992)

Project 2

Head of project: *Dr. Brede*

Scientific staff: *R. Dangendorf, R. Nolte, U.J. Schrewe, H. Schuhmacher, B.R.L. Siebert*

Objectives for the reporting period

Investigation of reference neutron fields between 20 MeV and 70 MeV

Determination of neutron kerma factors in A-150 plastic and carbon ($20 \text{ MeV} < E_n < 70 \text{ MeV}$) combining low-pressure proportional counter measurements with time-of-flight techniques and spectral neutron fluence determination with a scintillation detector and neutron fluence measurements with a proton recoil telescope.

Development of a transfer device for dose equivalent quantities.

Progress achieved including publications

1. Investigation of reference neutron fields

The upper end of the neutron energy range previously at 20 MeV for various dosimetry applications has shifted to higher energies as many radiation fields exist in which persons may receive a significant fraction of dose from neutrons with energies above 20 MeV, e.g. at particle accelerators, in aircraft and spacecraft.

The determination of the response of neutron dosimeters used in radiation protection in this energy region is therefore essential. At $E_n < 20 \text{ MeV}$, adequate reference radiation fields are available and calibration procedures for radiation protection instruments are well established. Above 20 MeV neutron energy however, neither calibrated beams nor calibration protocols are available (11). In order to establish a calibration facility for survey and personal dosimeters at neutron energies higher than 20 MeV, reference neutron fields have been characterised and made available at the Paul Scherrer Institute (PSI), Villigen, Switzerland.

Using the pulsed proton beam of the PSI cyclotron and a 2 mm thick Be target for the neutron production, time-of-flight (TOF) spectrometry has been applied with NE213 scintillation detectors. Fig. 1 shows five different neutron spectra which have been measured with TOF techniques. The absolute neutron fluence in the high-energy peak has been measured with a recoil proton telescope (PRT) (9).

The consistency of spectral neutron fluence determination with a liquid scintillation detector using TOF techniques and fluence measurements with a proton recoil telescope (9) has been investigated in the energy range between 20 MeV and 70 MeV. The inclusion of events due to neutron reactions with carbon nuclei, in addition to n-p scattering events in the scintillator, caused deviations of up to 15 % from measurements (2) with a PRT which is based purely on n-p scattering. Fig. 2 shows the response of the NE213 scintillation detector to almost monoenergetic neutrons of 60.6 MeV. Good agreement between calculations and measurements has been found if only events due to the n-p scattering are used for the analysis of the scintillation detector.

In order to monitor the neutron fluence of the collimated beam, the $^{107/109}\text{Ag}(n,3/5n)^{105}\text{Ag}$ reaction cross section for $20 \text{ MeV} < E_n < 70 \text{ MeV}$ has been determined (5). Due to the neutron energy thresholds of approximately 18 MeV and 35 MeV, these reactions are well suited to determine the total neutron fluence of high-energy neutrons without being sensitive to the low-energy component of the beam.

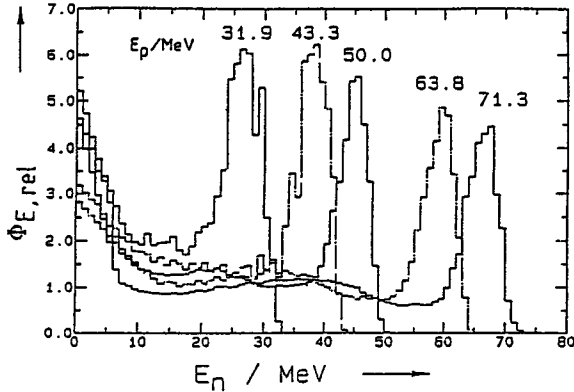


Figure 1. Relative spectral neutron fluence $\Phi_{E,rel}$ as a function of neutron energy E_n for five radiation fields at PSI produced with different proton energies E_p on a 2 mm thick Be target.

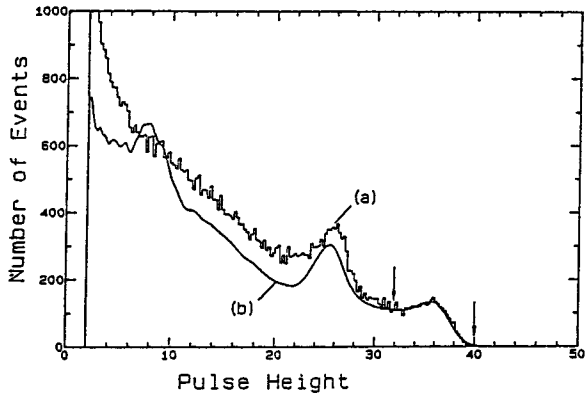


Figure 2. Response spectrum of the scintillation detector for incident neutrons with an energy of $(60.6 \pm 0.8) \text{ MeV}$. (a) experimental spectrum, (b) calculated with the modified SCINFUL code 1 and normalised to (a) in the region indicated by the arrows.

¹ Dickens, J. K., SCINFUL. A Monte Carlo Based Computer Program to Determine a Scintillator Full Energy Response to Neutron Detection for E_n between 0.1 and 80 MeV: Program Development and Comparison of Program Predictions with Experimental Data. Oak Ridge National Laboratory Report ORNL 6463 (1988)

2. Determination of kerma factors

Kerma factors of A-150 plastic and carbon were determined for neutron energies between 20 MeV and 70 MeV. The neutron kerma were measured in the quasi-monoenergetic collimated neutron beam at PSI, with low-pressure proportional counters with walls made of A-150 plastic and carbon. The neutron fluence of the beams was determined with a PRT (9).

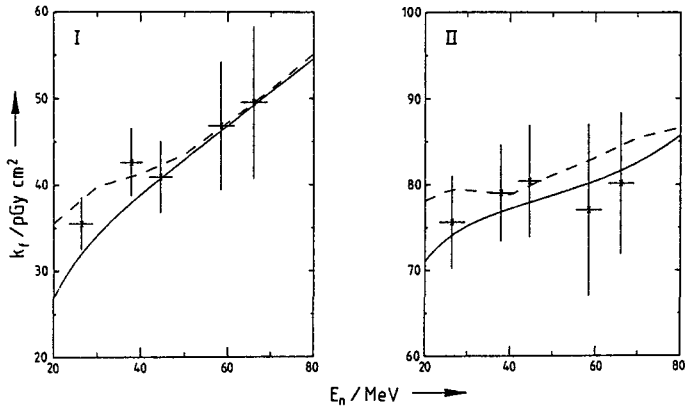


Figure 3. Kerma factor k_f for carbon (I) and A-150 plastic (II) versus neutron energy E_n . Data points of Schrewe et al. (6,7), calculations of Brenner 2 solid line and of Wells 3 broken line.

The experimentally determined kerma factors of A-150 plastic and carbon (6,7) are compared with data obtained with models and calculations in Fig. 3. In the energy range between 40 MeV and 70 MeV the calculations of Brenner and Wells agreed best with our results.

3. Development of a transfer device

The calculational studies of a 'transfer instrument' for ambient dose equivalent have been continued. The device consists of a combination of a tissue-equivalent proportional counter (TEPC) and a phantom. Preliminary results, already published (8) showed an energy dependence of the system of less than $\pm 20\%$ within the energy range between thermal and 20 MeV. Influenced by the new ICRP 60 recommendation of a new relationship for the quality factor as a function of linear energy transfer, the new fluence-to-ambient dose equivalent conversion factors were calculated (12). The aim of the present calculations is the investigation of the dose equivalent response of a TEPC in a spherical and a slab phantom with respect to the angular dependence of the incoming irradiation.

2 Brenner, D.J.: Neutron Kerma Values above 15 MeV Calculated with a Nuclear Model Applicable to Light Nuclei., *Phys. Med. Biol.* 29 (1983) 437-441

3 Wells, A.H.: A Consistent Set of Kerma Values for H, C, N and O for Neutrons of Energies from 10 to 80 MeV. *Radiat. Res.* 80 (1979) 1-9

Scientific staff:

R. Dangendorf, R. Nolte, U.J. Schrewe, H. Schuhmacher and B.R.L. Siebert

Other research group(s) collaborating actively to this project:

Univ. Basel (Dr. R. Henneck) and Paul Scherrer Institute Villigen (Dr. P. Schmelzbach) (CH)

Université Catholique de Louvain-la-Neuve, Unit. Phys. Nucl. (Prof. J.P. Meulders) (B).

Universität Göttingen, 2. Physikal. Institut (Prof. F. Smend) (D).

University of Birmingham (Prof. M. Scott) (UK)

University of Wisconsin-Madison, (Prof. P.M. DeLuca, Jr.) (USA)

Publications

- (1) Brede, H.J., Beverung, W. and Böttger, R. An External Pulsing System for the Louvain-la-Neuve Cyclotron. Internal PTB-Report: PTB 7.31-90-1 (1990).
- (2) Nolte, R., Schuhmacher, H., Brede, H.J. and Schrewe, U.J. Measurement of High-Energy Neutron Fluence with Scintillation Detector and Proton Recoil Telescope, submitted to Radiat. Prot. Dosim.
- (3) Pihet, P., Gerdung, S., Brede, H.J., Menzel, H.G., Schrewe, U.J., Schuhmacher, H.: Low Pressure Proportional Counter Technique to Determine Kerma in Various Materials for Neutrons between 14 and 60 MeV. Gemeinsame Jahrestagung 1990. Strahlenschutz im medizinischen Bereich und an Beschleunigern, Göttingen, 19.-22. September, ISBN 3-88585-860-6 (1990) 344-345
- (4) Schrewe, U.J., Brede, H.J., Langner, F. and Schuhmacher, H. The Use of Microdosimetric Detectors Combined with Time-Of-Flight Techniques, Nucl. Instrum. Meth. A299 (1990) 226-230
- (5) Schrewe, U.J., Brede, H.J., Matzke, M., Nolte, R. Meulders, J.P., Schuhmacher, H. and Slypen, I.: $^{107/109}\text{Ag}(n,3/5n)^{105}\text{Ag}$ Reaction Cross Section for $20 \text{ MeV} < E_n < 70 \text{ MeV}$. Contr. Nucl. Data for Science and Technology, Jülich, Germany, May, 13th - 17th, 1991.
- (6) Schrewe, U.J., Brede, H.J., Henneck, R., Gerdung, S. Kunz, A., Menzel, H.G., Meulders, J.P., Pihet, P., Schuhmacher, H. and Slypen, I.: Determination of Kerma Factors for A-150 Plastic and Carbon for Neutron Energies above 20 MeV. Contr. Nucl. Data for Science and Technology, Jülich, Germany, May, 13th - 17th, 1991.
- (7) Schrewe, U.J., Brede, H.J., Gerdung, S., Nolte, R., Pihet, P., Schmelzbach, P. and Schuhmacher, H.: Determination of Kerma Factors of A-150 Plastic and Carbon at Neutron Energies between 45 and 66 MeV, submitted to Radiat. Prot. Dosim.
- (8) Schuhmacher, H. and Dietze, G. Zur Realisierung der neuen Meßgrößen im Strahlenschutz in gemischten Photon-Neutron Feldern. Gemeinsame Jahrestagung 1990, Strahlenschutz im medizinischen Bereich und an Beschleunigern (ed. D. Harder), ISBN 3-88585-860-6 (1990) 106-107.
- (9) Schuhmacher, H., Siebert, B.R.L. and Brede, H.J. Measurement of Neutron Fluence for Energies between 20 MeV and 60 MeV Using a Proton Recoil Telescope: Proc. of Specialists' Meeting on Neutron Cross Section Standards for the Energy Region above 20 MeV, Uppsala, Sweden, Report NEANDC-305 (1991)

- (10) Schuhmacher, H., Brede, H.J., Henneck, R., Kunz, A., Meulders, J.P., Pihet, P. and Schrewe, U.J.: Measurement of Neutron Kerma Factors for Carbon and A-150 Plastic at Neutron Energies of 26 MeV and 38 MeV, submitted to Phys. Med. Biol.
- (11) Schuhmacher, H. and Alberts, W.G. Reference Neutron Fields with Energies up to 70 MeV For the Calibration of Radiation Protection Instruments. submitted to Radiat. Prot. Dosim.
- (12) Schuhmacher, H. and Siebert, B.R.L.: Quality Factors and Ambient Dose Equivalent for Neutrons Based on the New ICRP Recommendations. Radiat. Prot. Dosim. 40 (1992) 85-89.

Project 3

Head of project: *Dr. Zoetelief*

Scientific staff: *Dr. J.J. Broerse, F.S. Draaisma (until September 1991)*

Objectives for the reporting period

To perform measurements with high-pressure ionisation chambers (HPIC) around a Van de Graaff accelerator producing 15 MeV neutrons and neutrons of other energies and to analyse the results in terms of cavity size effects and ion recombination theory. To use the Caswell and Coyne code to perform calculations of energy deposition, ion yield and cavity size effects and compare the results with the HPIC measurements. To study ion recombination theories to allow future analysis in terms of columnar recombination (Jaffé theory) or cluster recombination (Kara-Michailova-Lea theory).

Progress achieved including publications

1. Feasibility of high pressure chambers for radiation protection dosimetry

High pressure ionisation chamber systems might provide an alternative to TEPC instruments as dose equivalent meters in mixed fields. The experimental and signal processing system is less complex and HPIC provide a better spatial resolution without losing sensitivity. Previous studies revealed that at elevated gas pressures an increased sensitivity is obtained for various filling gases. The amount of initial recombination as well as the pressure dependence of the reading at fixed voltages can be used to determine radiation quality.

In the present project emphasis was placed on developing a field instrument for measurement of dose equivalent in mixed neutron-photon fields based on TE and Al HPIC using Ar and methane as filling gases. Measurements were carried out at various positions around a Van de Graaff generator producing 15 MeV neutrons and at the maze entrance of the neutron generator hall to simulate irradiation conditions more relevant for radiation protection than used in previous studies.

In our first progress report within the present contract it is indicated that the leakage currents were too large, i.e., in the order of 10^{-13} A at a collecting potential of 600 V. The contribution to the total current measured at 600 V for positions 2 m, 0° (i.e. 2 m distance from the target on the axis of the ion beam) and 2 m, 45° varied from about 3 per cent to 50 per cent for pressures varying from 8 MPa to 0.01 MPa. It can be seen from Table 1 that for positions in the maze entrance the dose rate is reduced by factors ranging from about 18 to 500. Consequently, a reduction in leakage current in the order of at least a factor of 100 should be achieved to allow measurements at all positions at increased (about 1 MPa) pressures. In first instance, leakage was reduced by drying the chambers inside an exsiccator, but this provided only a short term solution. The chambers were therefore modified by replacing several insulators. This was particularly difficult since the previous construction included insulators which appeared to have a worse electrical resistance but good properties to provide gas tightness up to 10 MPa. Eventually, the

leakage currents were reduced to 10^{-15} A, which is of the same order of magnitude as that of common ionisation chambers. Measurement at position A with the Al HPIC filled with Ar (photon dosimeter) at 5 MPa and 600 V collecting potential are about 5×10^{-15} A. It has therefore to be concluded that also in view of the recent ICRP recommendations the present system will not be sensitive enough for practical radiation protection purposes. This might be achieved by using chambers of larger dimensions.

Table 1 Relative absorbed doses for different positions in the primary field and maze entrance for d(1)+T neutrons

<i>measuring position</i>	<i>DT</i> (10^4 Gy/C)	<i>DN</i> (10^4 Gy/C)	<i>DG</i> (10^4 Gy/C)	<i>H*</i> (10^4 Gy/C)
2 m, 0°	9.1 ± 0.6	8.0 ± 0.6	1.1 ± 0.1	120 ± 10
2 m, 45°	9.0 ± 0.6	7.9 ± 0.6	1.1 ± 0.1	120 ± 10
2 m, 90°	4.2 ± 0.3	3.5 ± 0.2	0.77 ± 0.08	59 ± 2
6 m, 45°	1.7 ± 0.1	1.36 ± 0.09	0.34 ± 0.03	25 ± 1
pos C	0.53 ± 0.06	0.40 ± 0.05	0.13 ± 0.02	7.2 ± 0.3
pos B	0.17 ± 0.05	0.13 ± 0.04	0.04 ± 0.01	2.0 ± 0.3
pos A	---	---	---	0.07 ± 0.01

* From Studsvik rem-counter

In Table 2 for 15 MeV neutrons a comparison is shown of the mean quality factor previously obtained from measurements with proportional counters and a recombination parameter, i.e., the ratio of the readings at 500 V to the readings at 100 V at a gas pressure of about 5 MPa. The recombination parameter of the measurements with the Al high pressure ionisation chamber is not significantly different for the various measuring positions as expected since this chamber has a low kU value, i.e., about 6 per cent. The recombination parameters using methane as filling gas are also not significantly different for the two chamber types, although the uncertainties in the results obtained with the TE HPIC are large since these measurements were made with too high leakage currents. The recombination in the HPIC with methane as filling gas are approximately a factor of 10 lower than those obtained from proportional counter measurements. Measurements at lower neutron energies will be performed to study whether this relationship is more generally valid. As soon as the program for 15 MeV neutrons with the TE HPIC is completed measurements will be made for d(2.3)+D neutrons at the same measurement positions.

The Caswell and Coyne code for calculation of energy deposition and ion yield has been installed on a work station and can be used for calculations of the contributions from crossers insiders, starters and stoppers. A comparison with experimental results with different wall and gas compositions has not yet been performed.

Table 2 Mean quality factor from microdosimetric measurements and recombination parameters (relative reading $R(500V)/R(100V)$ at 5 MPa gas pressure) from HPIC

<i>measuring position</i>	\bar{Q}	<i>TEHPIC</i>		<i>AlHPIC</i>	
		<i>methane</i>	<i>methane</i>	<i>methane</i>	<i>Ar</i>
2 m, 0°		1.53 ± 0.02	1.47 ± 0.02	1.13 ± 0.02	
2 m, 45°	15.2 ± 0.8	1.47 ± 0.02	---	1.11 ± 0.02	
2 m, 90°	15.2 ± 0.8	1.8 ± 0.2	---	---	
6 m, 45°	15.8 ± 0.8	1.9 ± 0.4	1.38 ± 0.05	1.16 ± 0.05	
pos C	15.0 ± 0.8	---	1.4 ± 0.1	1.15 ± 0.05	
pos B	14.2 ± 0.8	---	11.2 ± 0.	1.18 ± 0.05	
pos A	---	---	---	1.3 ± 0.3	

2. Columnar recombination theory in high pressure cavities

The columnar recombination theory of Jaffé has been introduced into a computer program and was used to fit ion recombination as a function of voltage at various pressures. The theory requires various constants including ion pair density inside a column electron and ion mobilities, recombination rate constants, diffusion parameters some of which are dependent on pressure. Values of these parameters are generally not well known. The computer code has to be modified for at least two reasons, i.e., the central facility at our institute obtained different types of computers with differing operating systems and with the present program results at different pressures can not be jointly fitted with the present version. It is promising that we recently became aware of work of Hatano and colleagues from the Tokyo Institute of technology on free-ion yields, electron mobilities and recombination rate constants in various gases including methane and argon.

Scientific staff

Prof. Dr. J.J. Broerse, F.S. Draaisma (until September 1991).

Other research group(s) collaborating actively to this project

Institute of Atomic Energy, Swierk (Dr. N. Golnik), Poland.

U.S. Super Collider project (Dr. J.J. Coyne), U.S.A.

Publications in the total contract period

- (1) H.M. Gerstenberg, J.W. Hansen, J.J. Coyne, J. Zoetelief. Calculations of the relative effectiveness of alanine detectors for neutrons with energies up to 17.1 MeV. Radiat. Prot. Dosim. 31, 85-89, 1990.
- (2) J.J. Coyne, R.S. Caswell, J. Zoetelief, B.R.L. Siebert. Calculations of microdosimetric spectra for low energy neutrons. Radiat. Prot. Dosim. 31, 217-221, 1990.
- (3) D.R. Schleger-Bickman, H.J. Brede, S. Guldbakke, V.E. Lewis, and J. Zoetelief. Measurements of k_u values of argon-filled magnesium ionization chambers. Phys. Med. Biol. 35, 717-730, 1990.
- (4) T.M. Piters, A.J.J. Bos, J. Zoetelief. Thermoluminescence dosimetry in mixed (g, n) radiation fields using glow curve superposition. Accepted by Radiat. Prot. Dosim.

Project 4

Head of project: *Dr. Th. Schmitz*

Scientific staff: *D. Barthmann, L.E. Feinendegen, M. Kopec, Th. Schmitz, O. Schröder, K. Morstin, (AGH Krakau)*

Objectives for the reporting period

- Experimental investigations of semiconductor detector properties in neutron fields, using SRAMS (static random access memory) chips as microdosimetric detector.
- Optimisation of the detector design with respect to the thickness of tissue equivalent layers for neutron radiations.
- Investigation on the relation of microdosimetric spectra measured with semiconductor detectors and tissue equivalent counters.

- Calculation of energy deposition spectra in organs for radiation fields of different composition and with different geometrical properties.
- Collection of relevant biological data to enable an investigation on the correlation between energy deposition spectra and biological effects.

Progress achieved including publications

1. Development of a semi-conductor dose equivalent meter as microdosimetric device

The final design of a semiconductor detector, which is suited for the application as a microdosimetric detector, was worked out in collaboration with the Institute for Semiconductor Physics (IHP). Due to the short period of time available for the production of a first prototype, it was decided to modify an existing buried channel charge coupled device structure (BCCD).

The advantage of a buried structure lies in a reduction of noise in connection with an increase of detectable energy. The active layer of the chip will be sheltered by means of a potential wall against signals which are created in the substrate of the semiconductor chip. The dead layer on top will be reduced to an electrically necessary minimum (i. e. less than 100 nanometers).

With the help of simulation calculations, the operation of the designed chip was verified. Thereafter, the production of the chips was started. First samples of the chips were expected at the end of 1991, but due to technical delays, the chips will not be available before the end of June 1992. The delay offered the possibility to check the chip design completely and to introduce improvements of the noise characteristics. Furtheron, all the necessary electrically data and timing information is available, so that the preparation of the experimental set up for measurements with the BCCD chip could be started.

In addition to the development of the BCCD chip experiments with static random access memory (SRAM) chips with 4, 16 and 64 kByte of memory had been planned and built up. For the experiments a collimated fast neutron beam is used, which is produced by the bombardment of a thick Beryllium target by 14 MeV deuterons from the compact cyclotron at the KFA.

The interpretation of these experiments is under way as well as the comparison to microdosimetric dose distributions measured with a low pressure proportional counter in the same neutron field.

The calibration procedure is based on the measurement of alpha particles from a ^{241}Am source within a vacuum chamber. The setup for these measurements was specially prepared for the purpose of calibration. However, the measurements with the alpha source will also be used to gain more information about the structure of the chips and consequently to help in the interpretation of experiments.

2. Energy deposition and radiation transport calculations in organs and consequences of the ICRP60 recommendations

The work on biological response functions was continued. Within the framework of these studies, advanced Monte Carlo transport calculations have been performed in the male phantom, which has been developed on the basis of the ADAM phantom. The ADAM phantom was modified in the sense that it contains all organs, for which weighting factors are given in the last ICRP recommendations, i.e.: gonads, red bone marrow, colon, lung, stomach, bladder, liver, oesophagus, thyroid, skin, bone surface, and remainder. The phantom is composed of 4 different tissues: skin tissue, lung tissue, skeletal tissue, and soft tissue. The material composition comprises the following elements: H, C, N, O, Na, Mg, P, S, Cl, K, Ca, Fe, Zr, and Pb.

The calculations have been performed with the code MCNP-3A. The nuclear data required for these calculations were taken from BMCCS, MCPL and TMCCS nuclear data libraries. Three different irradiation geometries were investigated: anterior-posterior, posterior-anterior, and lateral, for broad parallel beams of monoenergetic neutrons impinging from the front, back, and a side of the phantom, respectively. In each case calculations have been done for 33 different neutron energies, from thermal up to 20 MeV.

The results of these calculations have been used to study the consequences of the recommendation of the ICRP, which were forwarded in its report No. 60. In this report, it is suggested that the dose equivalent to a tissue or organ should be determined from the product of the absorbed dose in that tissue and a radiation weighting factor, which is characteristic for the radiation incident on the body. The concept of weighting factors is seen by the ICRP as a simplification against the concept of using a LET dependent quality factor, which is characteristic for the radiation at the location of the organ. The dose equivalent derived with the new concept is named effective dose, E , whereas the quality factor based dose equivalent was called effective dose equivalent, H_E .

The new quantity effective dose has been calculated and compared to the effective dose equivalent, H_E . For the latter, the new formulation of the quality factor, also proposed in ICRP report 60, has been used. The achieved results indicate that the simplified concept of assigning radiation weighting factors to an undisturbed field, and thus of neglecting quality variations within the human body, is highly incompatible with the LET-based quality factor concept. The discrepancy between the effective dose equivalent and the effective dose depends on the energy of the incident neutrons. For energies below 10 keV both quantities differ by a factor of 2, while between 10 keV and 100 keV this factor changes between 7 and 2. Generally the new quantity

gives the higher values, with exception of the region 2 to 4 MeV, where it is slightly lower than H_E .

In the last months, additional modifications have been introduced to the phantom. They follow suggestions of C.A.Lewis and R.E.Ellis and introduce two additional organs: trachea and bronchi. In addition the location of the stomach has been changed. Furtheron, a female phantom, which is based also on the GSF publication has been developed. The modifications mentioned above have been introduced also in this case. This phantom is currently being tested, and transport calculations are expected to start shortly.

Scientific staff

D. Barthmann, L.E. Feinendegen, M. Kopec, Th. Schmitz, O. Schröder
K. Morstin (AGH Krakau)

Other research group(s) collaborating actively to this project

Members of EURADOS working Committee 10
Institut für Halbleiterphysik GmbH, Frankfurt/Oder
P. Olko, Institute of Nuclear Physics, Krakau Poland

Publications

- (1) Olko, P., Booz, J. Photon Induced Microdosimetric Distributions in Nanometer and Micrometer Regions, Radiat. Prot. Dosim 31, Nos. 1-4, pp. 205-209 1990.
- (2) Schmitz, Th., Morstin, K., Olko, P., Booz, J. The KFA Counter: A Dosimetry System for Use in Radiation Protection. Radiat. Prot. Dosim 31, Nos. 1-4, pp. 371-375 1990.
- (3) Schmitz, Th. Microdosimetry Health Physics Instrumentation. In: Advances in Radiation Protection, Oberhofer, M. (ed.), Kluwer Academic Publisher, London, pp. 171-197 1991.
- (4) Schmitz, Th., Booz, J., Feinendegen, L.E. Das Problem der Risikoabschätzung im Bereich der Umweltbelastung mit ionisierenden Strahlen. AGF-Tagung 'Umwelt und Krebs', Gockel, E., Schulte-Hostede, S. (ed.), Arbeitsgemeinschaft der Großforschungseinrichtungen (AGF), Thenée Druck Bonn, pp. 52-55 1990.
- (5) CCD-Sensormatrix für ionisierende Strahlung. Application for a patent at the German Patent-Office on January 07. 1992
- (6) Pierschel, M., Ehwald, K.-E., Heinemann, B., Januschewski, F., Schmitz, Th., Schröder, O. A BCCD-based Dosimeter for mixed Radiation Fields. Sixth European Symposium on Semiconductor Detectors, 24th - 26th February 1992, Milano, Italy, IEEE Trans. Nucl. Instr. Meth. (in press).
- (7) Kopec, M., Morstin, K., Schmitz, Th., Feinendegen, L.E. Calculations of Microdosimetric Spectra in Humanoidal Phantoms. 9-th International Congress of Radiation Research, Toronto, 7-12 July 1991.
- (8) Morstin, K., Kopec, M., Schmitz, Th. Equivalent Doses vs. Dose Equivalents for Neutrons Based on New ICRP Recommendations. Proceedings of the 7-th Symposium on Neutron Dosimetry, Berlin, 14-18 October 1991. Radiat. Prot. Dosim. (in press)
- (9) Booz, J., Morstin, K., Kopec, M., Olko, P., Schmitz, Th., Feinendegen, L.E. Bidimensional Microdosimetry as a Tool for Evaluating Biological Response and Target Structure. Proceedings of the Workshop on Biophysical Modelling of Radiation Effects, Chadwick, K., Menzel, H.G. (eds.), IOP Publishing Ltd, Bristol, England.

Project 5

Head of project: *Dr. Ségur*

Scientific staff: *A. Alkaa, D. Blanc, A. Chouki, J. Y. Gosselin, C. Moutarde*

Objectives for the reporting period

Our main objective for the present period was the determination of electron-molecule collisions cross-section in propane. Furthermore, some preliminary calculations were made of the electric field and the corresponding gaseous gain in counters with complex geometries. Non-equilibrium behaviour of the ionisation coefficient in low pressure cylindrical tissue equivalent proportional counter was also investigated.

Progress achieved including publications

The determination of electron-molecule cross-sections in organic vapours is of paramount importance not only for modelling the motion of electrons in proportional counters, but also for the determination of energy losses and consequently the W values in particular gases of relevance for dosimetry and microdosimetry techniques. Furthermore, the theoretical study of the slowing down of electrons from very high (a few MeV) to very low (a few eV) energies cannot be made without a good knowledge of the cross-sections for all interaction processes involved in electrical discharge mechanisms (ionisation, excitation, vibration, attachment), for the whole range of energies and for the gas of interest.

Unfortunately, knowledge of the cross-sections for organic vapours is actually very poor. The only gas whose cross-sections are well known is methane (see our previous report, contract n° B16-A-292-F). But in the case of propane and generally for most organic vapours, a little information is available. In the case of propane, very few experimental determinations of these cross-sections have been made so far and no theoretical determination is for the moment available. Furthermore, with respect to theoretical determination, a quantum mechanical approach is still unable, at low electron energies (lower than 100 eV) to give valid data since the interaction potential between electrons and these molecules is not well known due to the complex structure of the molecule.

In our opinion, the only approach to determine these cross-sections at present is to use information from the experimental determination of swarm parameters (i.e. drift velocities, diffusion coefficients, ionisation coefficients, etc...). All these data depend (in so-called equilibrium conditions) on the ratio of the electric field E divided by the pressure P (E/P or E/N where N is the density of the background gas). The various swarm parameters being defined by quadrature over the distribution function of electrons and the electron-molecule cross-sections, it follows that the knowledge of the variation versus E/N of these parameters allows, through an unfolding procedure, the energy variation of the cross-sections to be determined.

This unfolding procedure does not usually provide a unique set of cross-sections, but, if the number of data derived from experimental determination of swarm parameters are large enough (determined in pure gas and in several mixtures for example), the results obtained are at least as accurate as those from direct measurements of the cross-sections due to the very high accuracy of measurements in swarm experiments (experimental errors are less than 3% in most cases).

Figure 1 shows the electron-molecule cross-sections that we obtained using our unfolding procedure.

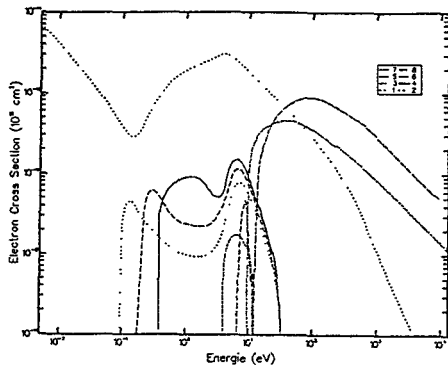


Figure 1. Electron-molecule cross-sections in propane determined with our unfolding procedure.

- 1 Elastic momentum transfer cross-section;
- 2-4 Cross-sections for various vibrational levels;
- 5 Cross section for excitation of optical levels;
- 6 Total ionisation cross-section;
- 7 Attachment cross-section.

It is well known in the literature that the occurrence of a Ramsauer minimum in the elastic momentum transfer cross-sections together with some vibrational cross-sections induces a very characteristic variation of the drift velocity as a function of E/N . In this case, the drift velocity, which is shown in figure 2 for propane and some propane-argon mixtures, first increases and then decreases. The importance and the location of these maxima and minima are strongly connected to the variation of elastic and vibrational cross-sections, and a small change in these cross-sections induces a large variation in the drift velocity. In these conditions, if many experimental data are available in propane and in mixtures of propane with some other gases (whose the cross-sections are well known), these data may be used to determine elastic and vibrational cross-sections. The experimental set of data shown in figure 2 was then used to unfold these cross-sections.

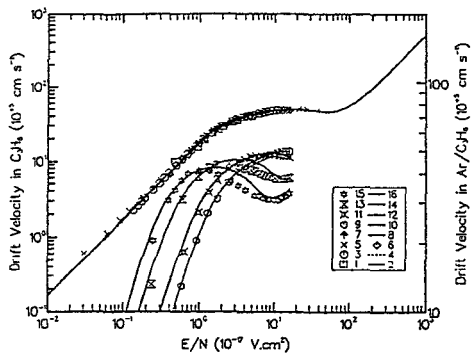


Figure 2. Electron drift velocity in propane and in propane-argon mixtures. Propane: 1-7 experimental data, 8 our calculations; Propame-argon mixtures: 90% C_3H_8 (9 exper. data (e.d.), 10 our calculations (o.c.)), 80% C_3H_8 (11 e.d., 12 o.c.), 50% C_3H_8 (13 e.d.,14 o.c.),20% C_3H_8 (15 e.d., 16 o.c)

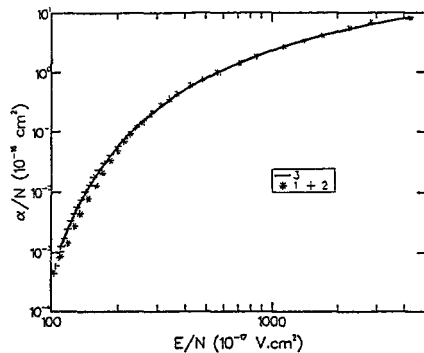


Figure 3. Ionisation coefficient in propane (1-2 exper. data, 3 our cross-section)

The use of drift velocity and characteristic energy to determine cross-sections is not sufficient to make these cross-sections consistent with the ionisation coefficient. To do that, it is necessary to take into account, during the unfolding procedure, experimental data of the ionisation coefficient together with ionisation cross-sections. In figure 3, we show the ionisation coefficient in propane tissue equivalent mixtures for which few or no data exist at the moment in the literature.

With these new electron cross-sections, it is easy to calculate many different parameters of great interest in the field of dosimetry or microdosimetry. The first important data are the various swarm parameters (drift velocity, characteristic energy, ionisation coefficient) in propane tissue equivalent mixtures for which few or no data exist at the moment in the literature.

The variation as a function of E/N of these quantities is shown in figure 4 and 5 for ionisation coefficients, drift velocity and characteristic energies.

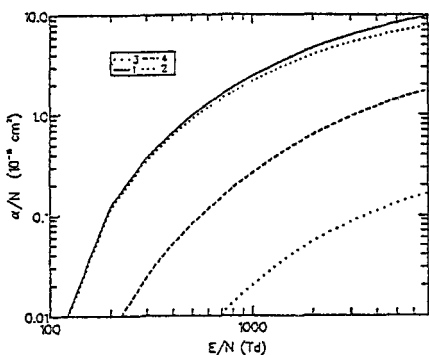


Figure 4. Electron ionisation coefficient in propane based tissue-equivalent gas. 1 total ionisation coefficient, 2 C₃H₈ partial ionisation coefficient, 3 N₂ partial ionisation coefficient, 4 CO₂ partial ionisation coefficient

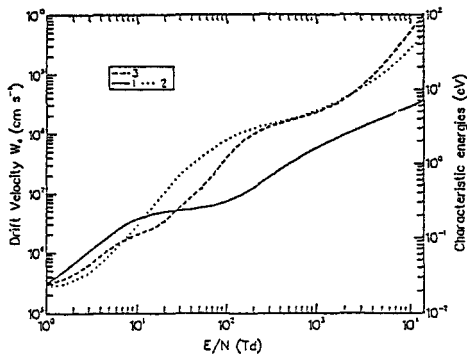


Figure 5. Swarm parameters in propane based tissue-equivalent gas. 1 Drift velocity, 2 Transverse characteristic energy, 3 Longitudinal characteristic energy

No comparison with experimental results can be made for these calculations because no corresponding experimental data is, for the moment, available. Comparisons were only possible with gas gain measurements in cylindrical or spherical proportional counters.

To conclude, we may note that our propane electron-molecule cross-sections were determined for a large range of energies, between thermal to 10 keV. For energies higher than the ionisation threshold, the unfolding procedure based on swarm parameters can no longer be adopted. Fortunately quantum mechanical calculations can now be used for elastic and ionisation cross-sections. However, a check of the validity of cross-sections at high energies could be made by comparing experimental and calculated W values for propane or propane tissue equivalent.

Scientific staff

A. Alkaa, D. Blanc, M. C. Bordage, A. Chouki, J. Y. Gosselin, S. Laffont, C. Moutarde.

Other research group(s) collaborating actively to this project

Commissariat à l'Energie Atomique, Fontenay aux Roses (Dr. J. Barthe) (F.)

Istituto Nazionale di Fisica Nucleare, Laboratory di Legnaro (Dr. P. Colautti) (I)

Publications in the total contract period

- (1) P. Ségur, I. Pérès, J. P. Boeuf and J. Barthe, Modelling of the electron and ion kinetics in cylindrical proportional counters, Proc 10th Symp. on Microdosimetry (Rome, 1989), J. Booz, J. A. Dennis and H.G. Menzel, eds., CEC, EUR 12864, Radiat. Prot. Dosim., 31, 107 (1990).
- (2) I. Pérès, Modélisation de la cinétique électronique et ionique dans les compteurs proportionnels, Thèse d'Université, April 1990, Toulouse.
- (3) I. Pérès, M. C. Bordage, P. Ségur, Determination of methane cross sections and calculation of electron hydrodynamic parameters in argon-methane mixtures, ESCAMPIG (Orléans) (Aug 1990).
- (4) P. Ségur, A. Chouki, M. C. Bordage, J. Y. Gosselin, Determination of electron-molecule cross sections in propane and calculation of swarm parameters in propane based mixtures, XI Symp. Microdos. Gatlinburg, Ten., USA (Sept. 1992).
- (5) J. Barthe, M. Mourgues, J. M. Bordy, P. Ségur, B. Boutruche, G. Portal, Study of mini-counters for personal dosimetry, IRPA 8, Montréal, Vol I, p. 479 (17-22 May 1992).
- (6) D. Blanc, P. Ségur, J. Barthe, J. M. Bordy, Tissue equivalent proportional counters in health physics, IRPA 8, Montréal, Vol I, p. 459 (17-22 Mai 1992).
- (7) P. Colautti, V. Conte, G. Talpo, G. Tornielli, P. Ségur, C. Moutarde, A. Alkaa, Experimental and theoretical determination of the space variation of the gas gain inside low pressure TEPC, XI Symp. Microdos. Gatlinburg, Ten., USA (Sept. 1992).
- (8) S. Gerdung, R. Grillmair, M. Lim, P. Pihet, H. Schuhmacher, P. Ségur, Performance of TEPCs at low gas densities and their dose equivalent response to low energy neutrons, XI Symp. MicroDos. Gatlinburg, Ten., USA (Sept. 1992).
- (9) M. C. Bordage, J. Y. Gosselin, A. Chouki, P. Ségur, Electron collision cross sections in Propane. Swarm parameters in propane and argon-propane mixtures, ESCAMPIG, St Petersburg, (Aug 1992).

DETERMINATION AND REALISATION OF CALIBRATION FIELDS FOR NEUTRON PROTECTION DOSIMETRY AS DERIVED FROM SPECTRA ENCOUNTERED IN ROUTINE SURVEILLANCE

Contract Bi7-031 - Sector A12

- 1) *Klein* , PTB-Braunschweig - 2) *Thomas* , NPL-Teddington
3) *Chartier* , CEA-Fontenay-aux-Roses - 4) *Schraube* , GSF-Neuherberg

Summary of project global objectives and achievements

The main objective of this collaborative project was to produce in the laboratory a few well characterised neutron fields that replicate typical spectral neutron fluence distributions encountered in radiation protection practice. These fields are needed for the calibration of neutron area and personal dosimeters which generally do not have the energy response required to determine dose-equivalent quantities. The project consists of four distinct parts, namely

- (1) the measurement of the spectral neutron fluence typically encountered in practice,
- (2) the preparation of a catalogue of all measured spectra in an agreed format including the calculation of relevant dose-equivalent quantities and the response of commonly used neutron dosimeters
- (3) the inspection of this catalogue in order to extract a few representative spectra and their expansion in terms of the calibration spectra already available or, if necessary, newly defined ones, and finally
- (4) the computational prediction of configurations consisting of the usual neutron sources (accelerator, reactor or radionuclide-based) and appropriate moderators in order to produce these reference fields in the laboratory.

The spectrometric measurements were performed independently by each laboratory, chiefly in the respective country, and are briefly described in their reports, which also include improvements of the spectrometers, the calculation and experimental calibration of the response functions.

A total of 17 recently measured or re-analysed previous data have been added to the catalogue which was so far chiefly based on catalogues recently compiled. However, a set of programs have been developed to set up and update the catalogue, to analyze and order the spectra and to calculate relevant dosimetric quantities and detector responses. Details are given in section 2. of this summary.

Although the catalogue has not yet been made use of to find a few basic spectra which should then be replicated in the laboratory for calibration purposes, various moderator assemblies have been simulated by means of the MCNP code for a 14 MeV neutron generator. Among several available spectral configurations, one was selected which associates features of neutron spectra encountered at nuclear facilities and additional characteristics (a monoenergetic radiation at 14 MeV) to check the capabilities of the spectrometric systems and unfolding procedures. This configuration was realized at the CEA Cadarache facility and investigated in the frame of a small-scale intercomparison with various spectrometers and dosimeters. The results are summarized in section 3.

The list of publications related to the project and printed or submitted in the reporting period is added as part 4.

1. A computer library and a program package for the handling of neutron spectra encountered in radiation protection practice

The problem of individual neutron dosimetry for external irradiation can be summarized by the following two equations /1/:

$$H = \int_{\Omega} \int_{E_n} d\Omega dE_n \Phi_{E_n}(\Omega, E_n) h_{\Phi}(\Omega, E_n) \quad (1)$$

and

$$M_r = \int_{\Omega} \int_{E_n} d\Omega dE_n \Phi_{E_n}(\Omega, E_n) R_{\Phi_r}(\Omega, E_n) \quad (2)$$

where H is the dose equivalent to be measured, $\Phi_{E_n}(\Omega, E_n)$ is the neutron fluence distribution in relation to direction and energy, M_r is the value indicated by a dosimeter of kind r and $R_{\Phi_r}(\Omega, E_n)$ is the neutron fluence response of such a dosimeter. The term "of kind r " is used for different components of one dosimeter, e.g. areas under different radiators in an etched track dosimeter or combinations of dosimeters, such as etched track and albedo dosimeter.

The problem of dosimetry is then to determine a function $f(M_1, \dots, M_R)$ such that

$$H = f(M_1, \dots, M_R) \quad (3)$$

There are one or more such functions for any neutron field and any set of R dosimeters. Unfortunately, these functions generally depend on the neutron fluence distribution and on the dose-equivalent quantity considered.

One possible approach is the search for an ideal dosimeter /1/, which is implicitly defined by:

$$h_{\Phi}(\Omega, E_n) = \sum_r u_r R_{\Phi_r}(\Omega, E_n) \quad (4)$$

Such an ideal dosimeter would indicate H in any neutron field. In practice, however, ideal dosimeters do not exist.

Another possible approach is to use spectrometric methods. If the neutron fluence distribution is known, then eqs. (1) and (2) can be used to derive H and the set of M_r . For a dosimeter with one component, eq. (3) is reduced to the standard calibration relation:

$$H_{\text{exp}} = (H_c/M_c) M_{\text{exp}} \quad (5)$$

where the subscript "exp" indicates the actual use and the subscript "c" the derived values under calibration conditions. This approach can be generalized for a dosimeter with many components, i.e. $R > 1$ /1/.

In practical neutron dosimetry neither the approach via eq. (4) nor via eq. (5) may be possible and a combination of both methods is needed.

In trying to find an appropriate combination of these methods it is necessary:

- a) to know the fluence response functions of dosimeters (dosimeter components) and neutron fluence distributions encountered in radiation practice and in calibration fields,
- b) to create algorithms to model relations as defined in eq. (3) or for specific applications as in eqs.(4,5) and, see below, eq. (6) and, last but not least,
- c) to visualize (i.e. represent numerically and graphically) the results of such combined methods.

In order to fulfill these three requirements a simple and portable FORTRAN program package has been written, which will help to find optimal calibration procedures. The package consists of a catalogue program to handle spectra, conversion and detector response functions, and of additional programs for the analysis of the spectra in terms of dosimetry.

- In particular, the programs allow
- spectra and responses found in the literature or communicated privately to be put in a standard form
 - the data base for dosimetric quantities, spectra and response functions to be generated
 - groups of spectra to be selected using appropriate keywords
 - various dosimetric quantities and the reading of selected detectors to be computed

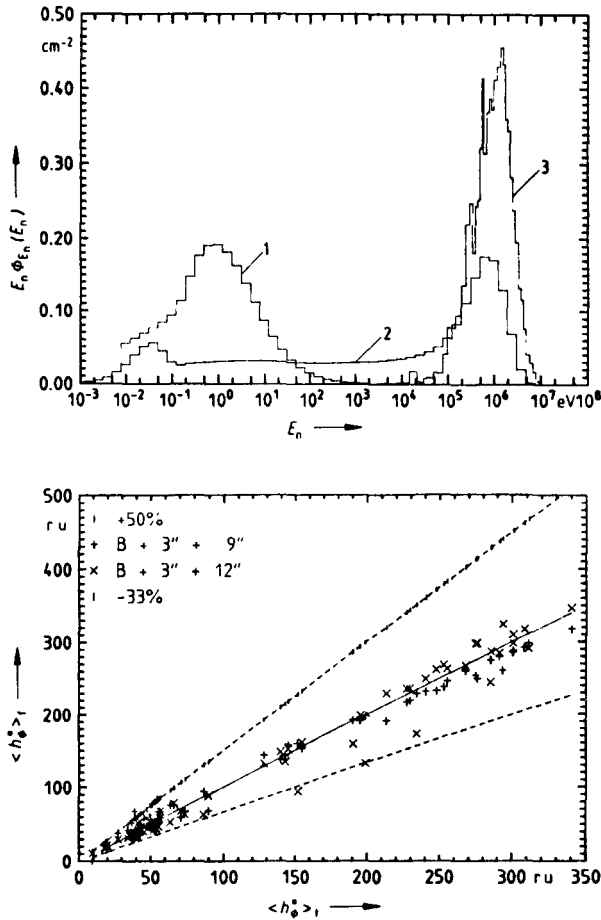


Fig. 1: Examples of the application of the program package
 1a) Three neutron spectra representative of fission environments are depicted as a function of neutron energy. Their values for $\langle h_{\Phi}^* \rangle_1$, 9.68, 143 and 311 μSvcm^2 for spectra 1, 2, and 3, respectively encompass the range met in fission working fields.
 1b) The bare counter (B), a 7.62 cm (3") and either a 30.48 cm (12") (x) or a 22.86 cm (9") (+) sphere, are combined to act as a "nearly ideal dosimeter in fission environments". The solid line pertains to an ideal dosimeter and the dashed lines indicate the true value multiplied or divided by 1.5, respectively. The abscissa indicates the true mean neutron fluence to dose equivalent conversion factor and the ordinate the value indicated by the dosimeters.

- spectra to be ordered in terms of dosimetric quantities, e.g. mean energy or fluence to dose equivalent conversion factors
- spectra to be analyzed differentially by defining energy regions and integrating in these energy regions over products of fluence and dosimetric quantities
- least-squares methods to be used to compute optimal combinations of detectors for a selected group of spectra or optimal linear combinations of calibration spectra in order to closely approximate environmental spectra
- additional user-written subroutines to be easily implemented

All programs can communicate by standardized input and output and support all relevant steps by on-line and off-line graphical display.

The catalogue contains at present 315 spectra and various detector response functions. Most of the spectra have been taken from existing compendia /2,3,4/. Spectra measured within this project have been included in addition.

In order to demonstrate the capabilities of the program package, the possibility of determining dose equivalent in fission environments is examined. By this example a method will be introduced, which combines the search for an ideal dosimeter with spectrometric methods.

Using the keywords "fission" and "PWR" 64 spectra are found. The spectrum averaged fluence to dose equivalent conversion factors, $\langle h_{\Phi}^* \rangle_t$, range from 9.65 to 340 pSvcm². Spectra with low and high values of $\langle h_{\Phi}^* \rangle_t$ are shown in Fig. 1a. A set of n_r Bonner spheres /publ. I.4.1/ is selected and the readings in all 64 spectra are computed. The results together with the values of $\langle h_{\Phi}^* \rangle_t$ are then sorted according to increasing values of $\langle h_{\Phi}^* \rangle_t$. The sorted data are then used to try out possible combinations of Bonner spheres. Finally, the following set of eq. (6) is solved by simple least squares methods:

$$\langle h_{\Phi}^* \rangle_{i,t} \cong \sum_{r=1}^{n_r} w_r \frac{M_{ir}}{\Phi_i} \quad (6)$$

where i indicates the spectra and, in this example runs from 1 through 64. The w_r are the weight factors and the M_{ir} the readings of the r -th Bonner sphere in the i -th spectrum. Results are depicted in Fig. 1b, where the fitted values of $\langle h_{\Phi}^* \rangle_{i,f}$ (right hand side of eq. (6)) are plotted as a function of the true values of $\langle h_{\Phi}^* \rangle_{i,t}$. Results obtained in this way are subject to scrutiny and especially to statistical analysis not described here.

The same procedure can be used to study possible combinations of personal dosimeters. This procedure can also be used to decompose environmental spectra in terms of calibration spectra, or more generally, to study the similarity of groups of spectra with respect to their dosimetric properties.

In summary, the program package developed within this project allows measured and calculated results to be combined in order to optimize practical determinations of dosimetric quantities.

2. The realistic neutron calibration field at the CEA Cadarache 14 MeV neutron facility

From measurements in nuclear power and fuel (re)processing plants it is well known that the spectral neutron fluence encountered at working places can usually be represented by a superposition of a thermal distribution ($E_n \leq 1$ eV), an intermediate $1/E$ part and a fission neutron distribution ($E_n > 10$ keV) with the energy parameters depending on the shielding material used.

The assembly composed of a neutron multiplier and shielding and moderating materials surrounding a 14 MeV neutron source enables to produce several neutron fields. The relative fraction of the basic distributions can to some extent be adjusted by varying the shape, dimensions and the type of materials employed (publ. I.4.8). This set-up was simulated by means of the general Monte-Carlo Neutron Transport code MCNP-3A in order to study the possible fluence distributions in a measurement area.

Intercomparison measurements with different neutron spectrometers and various types of area and personal dosimeters were performed in one of the available spectra. The criteria which led to the choice of the intercomparison spectrum were to take into account the entire energy range of realistic neutron spectra (10^{-9} to 15 MeV), to check the energy resolution of the detectors used (narrow structures due to the iron shield) and the capability of the unfolding codes to reconstitute a separate "monoenergetic" line (14 MeV leakage component). This mixed field allowed also to operate the existing neutron-photon discrimination techniques. All measurements had to be performed at the same point. Three detectors for associated α -particles, symmetrically positioned at backward angles inside the beam tube, served as monitors for normalization.

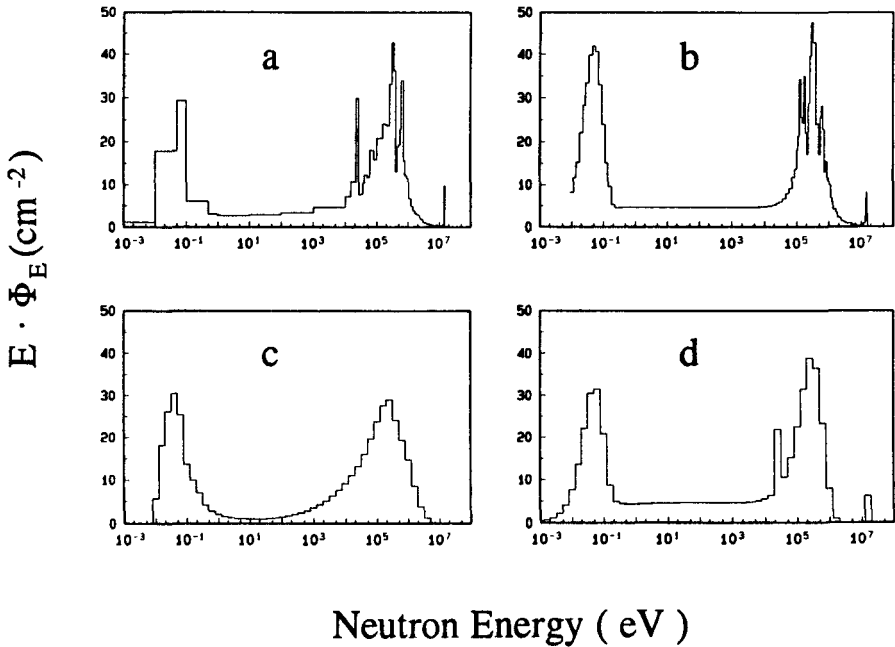


Fig. 2: Spectral neutron fluence at the point of measurement in front of the moderator assembly calculated with MCNP-3A (a) and measured with spectrometers of CEA (b), GSF (c) and PTB (d), all normalized for one α -monitor count.

Various neutron spectrometers from CEA, GSF and PTB were employed. Each participating institute was asked to evaluate from its data only one neutron spectrum for comparison. In Fig. 2 the calculated spectral fluence, normalized for one α -monitor count, is shown together with experimental data obtained with

- a set of Bonner spheres with a small cylindrical ^3He counter in combination with spherical proton recoil proportional counters and an NE213 scintillation detector (CEA, see publ. I.4.10),
- a set of Bonner spheres with a LiI(Eu) detector (GSF, see publ. I.4.5) and
- a set of Bonner spheres with a spherical ^3He counter (PTB "C"-system, see publ. I.4.5)

The unfolded spectral neutron fluences are in reasonable agreement with the calculated distribution in shape and integral fluence. The arithmetic mean of the dose equivalent values derived from the CEA and PTB spectra is in the following used for reference.

Various area and personal dosimeters were employed for comparison. As shown in Table 1 and Fig. 3, the moderating-type area monitors (CRAMAL, STUDSVIK, HARWELL and a Leake-type sphere used with the PTB spectrometer) generally overestimate the corresponding dose equivalent reference value, while the TEPC systems underestimate the dose equivalent. This behaviour can be explained by the imperfect dose-equivalent response, particularly in the low energy region ($E_n \leq 200$ keV). The low fluence averaged mean energy $\langle E_n \rangle \approx 250$ keV of this field already indicates that calibration factors obtained in the field of a D₂O-moderated Cf source should be applied, instead of bare Cf or Am-Be sources. The large overestimation by the DINEUTRON is not as easily understandable because this dual sphere system was specially designed for measurements in similar neutron fields.

Table 1:
Integral neutron fluence Φ , fluence averaged mean energy $\langle E_n \rangle$ and dose equivalent quantities \hat{H} and H^* as determined by calculation (1), spectrometry (2-4) or by means of various dosimeters (5-13). H_r is the arithmetic mean of the dose equivalent values determined by CEA and PTB spectrometers and served as a reference.

N r	Data Name	Φ_{total} (cm^{-2})	$\langle E_n \rangle$ (keV)	\hat{H}_{tot} (nSv)	H^*_{tot} (nSv)	\hat{H}/H_r	H^*/H_r^*
1	MCNP-CALCUL	199	217.8	12.6	14.5	0.93	0.91
2	CEA-SPECTR.	210	219.5	13.1	15.2	0.97	0.95
3	PTB-BON-SP.	222	329.4	14.0	16.7	1.03	1.05
2+3	2 SPECTROM	216 <=REF=>	274.5	13.55	15.95	1.00	1.00
4	GSF-BON-SP.	193	200.7	13.9	15.6	1.03	0.98
		Org	Calibration				
5a	DINEUTRON	CEA	Am-Be + bCf	27.6	—	2.04	—
5b	DINEUTRON	CEA	Moder. 252Cf	18.1	—	1.34	—
6	CRAMAL	CEA	2 MeV mono	16.7	—	1.23	—
7	STUDSVIK	CEA	Am-Be	12.5	—	0.92	—
8	HARWELL-MON	PTB	Am-Be	18.2	—	1.34	—
9a	LEAKE REM-C	PTB	Bare 252Cf	20.0	—	1.48	—
9b	LEAKE REM-C	PTB	Moder. 252Cf	14.3	—	1.06	—
10	TEPC GSF	GSF	Am-Be	11.9	—	0.88	—
11a	TEPC HANDI	PTB	60Co-gamma	—	9.7	—	0.61
11b	TEPC HANDI	PTB	Moder. 252Cf	—	13.6	—	0.85
12	TLD-ALBEDO	PTB	Bare 252Cf	—	10.9	—	0.68
13	TRACK-ETCH	PTB	Bare 252Cf	—	12.4	—	0.78

The results obtained with different personal dosimeters irradiated on a spherical phantom (polyethylene, 30 cm in diameter) are in reasonable agreement with the reference value. In addition, the simultaneous irradiation of four personal dosimeters at different positions of the phantom confirmed that the neutron fluence is strongly directional. Also the rough energy information (three intervals) deduced from the response of the PTB track-etch dosimeter is in reasonable agreement with the theoretical predictions and the experimental data.

The results of these comprehensive investigations will be discussed in detail elsewhere, including all spectrometric data, calculated and measured photon doses and estimates of the uncertainties.

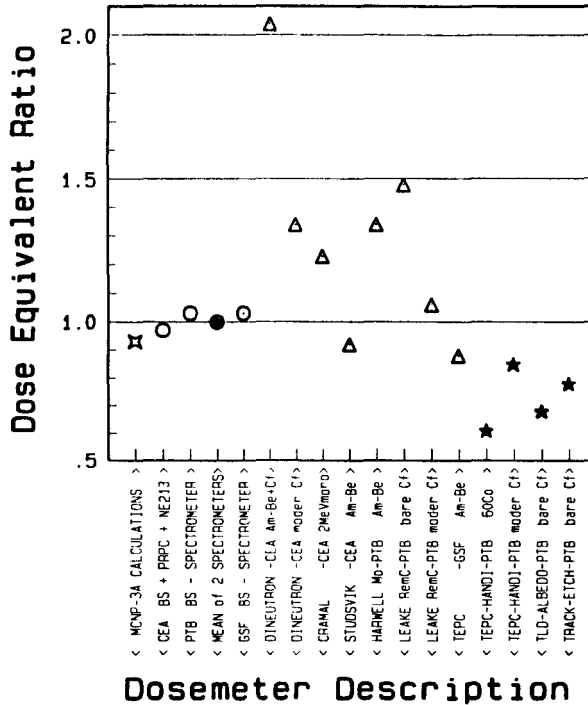


Fig 3: Dose equivalent measured with spectrometers (circles, indicating \hat{H} results) and dosemeters (triangles for H and stars for H') with reference to the arithmetic mean of the CEA and PTB spectrometric data.

References

- 1) Siebert, B.R.L., Hollnagel, R. and Jahr, R. *A theoretical concept for measuring doses from external radiation sources in radiation protection.* Phys. Med.Biol.(1983) 28, p 521-533.
- 2) Griffith, R.V., Palfalvi, J. and Madhvavath, U. *Compendium of neutron spectra and detector responses for radiation protection purposes.* IAEA Technical Report Series No. 318 (Vienna,1990)
- 3) Ing, H. and Makra, S. *Compendium of neutron spectra in criticality accident dosimetry.* IAEA Technical Report Series No. 180 (Vienna,1978)
- 4) Britvitch G.I., Makagnov A.V. and Flyamer, G.V. *Typical neutron spectra in work and auxiliary environments of reactors, accelerators and installations with isotopes* (in Russian). Rep. Inst. of High Energy Physics, Dept. of Radiat. Research, (Serpouchow USSR), 1985)

Publications

1. V. Mares, G. Schraube, H. Schraube
Calculated neutron response of a Bonner sphere spectrometer with ^3He counter
Nucl. Instrum. Meth. A307 (1991) 398 - 412
2. K. Weise, M. Weyrauch, K. Knauf
Neutron response of a spherical proton recoil proportional counter
Nucl. Instrum. Meth. A309 (1991) 287 - 293
3. G. Leuthold, V. Mares, H. Schraube
Calculation of the neutron ambient dose equivalent on the basis of the ICRP revised quality factors
Radiat. Prot. Dosim. 40 (1992) 77 - 84
4. D.J. Thomas, A.G. Bardell
Neutron spectrometry in working environments
In: Proceedings of the International Conference on Occupational Radiation Protection, British Nuclear Energy Society, London 1991
5. A.V. Alevra, M. Cosack, J.B. Hunt, D.J. Thomas, H. Schraube
Experimental determination of the response of four Bonner sphere sets to monoenergetic neutrons (II)
Radiat. Prot. Dosim. 40 (1992) 91 - 102
6. D.J. Thomas
Use of the program ANISN to calculate response functions for a Bonner sphere set with ^3He detectors
NPL report RSA (EXT) 31, Teddington March 1992
7. A.V. Alevra, H. Klein, K. Knauf, J. Wittstock
Neutron field spectrometry for radiation protection purposes
Radiat. Prot. Dosim. (in press)
8. J.L. Chartier, F. Posny, M. Buxerolle
Experimental assembly for the simulation of realistic neutron spectra
Radiat. Prot. Dosim. (in press)
9. S. Jetzke, H. Kluge, R. Hollnagel, B.R.L. Siebert
Extended use of a D_2O -moderated ^{252}Cf source for the calibration of neutron dosimeters
Radiat. Prot. Dosim. (in press)
10. F. Posny, J.L. Chartier, M. Buxerolle
Neutron spectrometry system for radiation protection measurements at working places and in calibration fields
Radiat. Prot. Dosim. (in press)
11. B.R.L. Siebert, E. Dietz, S. Jetzke
Comparison of measured and calculated Bonner sphere responses for 24 and 144 keV incident neutron energies
Radiat. Prot. Dosim. (in press)
12. B.R.L. Siebert, H. Schraube, D.J. Thomas
A computer library of neutron spectra for radiation protection environments
Radiat. Prot. Dosim. (in press)
13. D.J. Thomas, A.J. Waker, J.B. Hunt, A.G. Bardell, B.R. More
An intercomparison of neutron field dosimetry systems
Radiat. Prot. Dosim. (in press)
14. M. Weyrauch, K. Knauf
Absolute neutron fluence determination with a spherical proton recoil proportional counter
Radiat. Prot. Dosim. (in press)

Project 1

Head of project: *Dr. H. Klein*

Scientific staff: *A.V. Alevra, Dr. K. Knauf, J. Wittstock, Dr. M. Luszik-Bhadra, Dr. S. Jetzke, Dr. B.R.L. Siebert, Dr. M. Weyrauch*

Objectives of the reporting period

1. Development of computer programs to improve the calculation of response functions of Bonner spheres and proton recoil proportional counters used for neutron spectrometry in radiation protection practice.
2. Measurement of the spectral neutron fluence in "realistic" calibration fields and at working places.
3. Development of computer programs to set up the catalogue of neutron spectra encountered in radiation protection practice, to expand these spectra in terms of basic spectra and to evaluate dosimetric quantities.

Progress achieved including publications

1.1 Experimental and calculated response of Bonner spheres

The fluence response matrix of the PTB "C" set of Bonner spheres presently in use was obtained by fitting ANISN calculations (publ. I.4.6) to experimental data for monoenergetic neutrons (publ. I.4.5) in the energy region from 1.2 keV to 14.8 MeV. The fit factors are shown in Fig. 1. At lower energies a remarkable shape adjustment was necessary in order to meet thermal calibration data. Very recently a complete set of MCNP calculations became available (publ. I.4.1) which fit in with the experimental data in the entire energy region for the bare ^3He detector and for all spheres with diameters larger than 12.7 cm ("5") as also shown in Fig. 1.

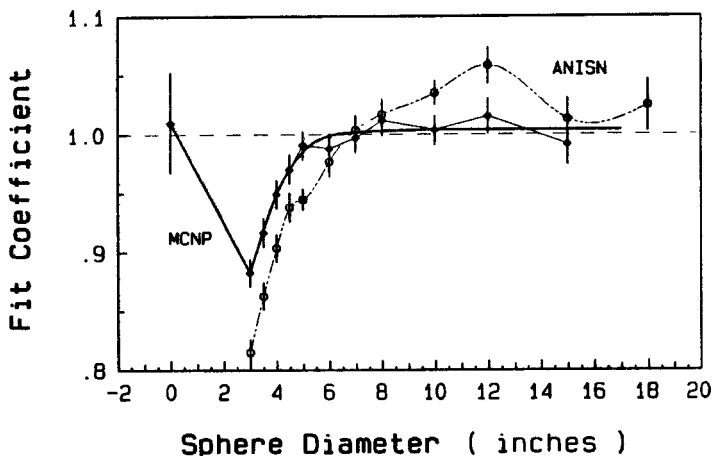


Fig. 1: Fit factors required to adjust the response of Bonner spheres calculated with the ANISN and MCNP code to experimental data (see publ. I.4.6, I.4.1 and I.4.7).

Systematic deviations are obvious for the smaller spheres indicating that the simplified model used in these calculations is not adequate. Indeed, more realistic simulations confirmed the influence of the steel capsule and the stem (Fig. 2). While the capsule reduces the response by about 5% independent of the neutron energy, the angle of incidence and the sphere diameter, the stem causes a slight anisotropy of the response and reduces the response for energies ≥ 1 keV by up to 10% for the smallest sphere experimentally investigated (3"). This influence is almost negligible for a 5" sphere. It can be concluded that these details must be taken into account for reliable response calculations.

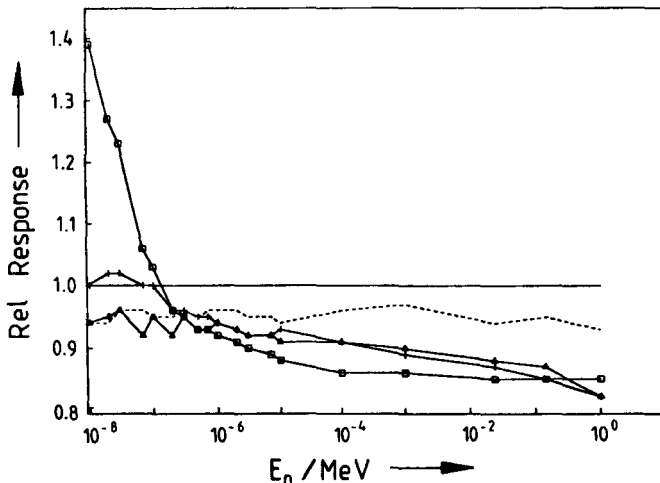


Fig. 2: Response of a 3" Bonner sphere calculated with MCNP for a realistic detector model including the steel capsule (dotted) and the stem of the ^3He detector for irradiation along the stem (\square), perpendicular to it (Δ) and from the opposite side ($+$) of the stem in comparison with the response obtained for the simplified model (see also publ. I.4.1).

1.2 Calculation of the response of spherical proton recoil proportional Counters

Because of its isotropic response a spherical proton recoil proportional counter is especially suited for neutron spectrometry in fields of unknown directional distribution and usually covers the energy region from 10 (50) keV to 1.5 MeV. In the ideal case the response function has a rectangular shape, but two effects chiefly reduce the proton energy really registered:

- a) the wall effect which is considered in all algorithms used, and
- b) the non-uniform gas amplification since the electric field in a spherical counter is not constant along the wire.

The latter electric effect had to be accounted for by empirical corrections of the slope of the trapezoidal distribution to fit experimental data. Both effects have recently been taken into account in Monte Carlo simulations (publ. I.4.2). The electric field was calculated numerically using the method of virtual charges, and the gas amplification was then obtained from classical Townsend theory. The calculated and the measured response of the 144 keV neutrons of a Si-Ti-filtered reactor beam are in complete agreement (publ. I.4.2). Hence, the calculated response matrix was used for the absolute determination of the spectral neutron fluence applying unfolding procedures if necessary (publ. I.4.14).

2. Neutron spectrometry in the field

Various neutron fields have been investigated covering a dynamic range of dose equivalent from a few nSv/h to some mSv/h (publ. I.4.7). The measurement of the natural

neutron background induced by cosmic rays demonstrated the stability of the ^3He detector system. The determination of the spectral neutron fluence corresponding with a dose equivalent rate of as low as 3 nSv/h took a measurement time of about 8 weeks.

Furtheron, three different calibration fields have been investigated. A rather soft neutron spectrum similarly encountered in radiation protection practice was produced at the neutron facility in Cadarache and served for an intercomparison exercise (see section I.3). A very similar neutron field (Fig. 3) can be achieved if a Cf source and the point of measurement are situated in opposite corners of a bunker room used at the Nuclear Research Center in Karlsruhe for the calibration of personal dosimeters, in particular the official German Albedo dosimeter.

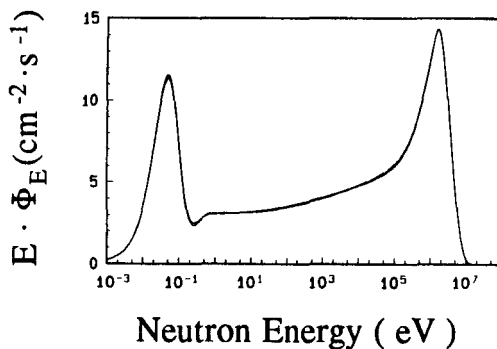


Fig. 3: Special neutron fluence measured with a bare Cf source and the Bonner spheres situated in opposite corners of the KfK bunker room

Different calibration fields were obtained in the PTB bunker if only the room return neutrons of a bare or a D_2O -moderated Cf source were considered (Fig. 4). The Bonner spheres were completely shielded from direct neutrons by appropriate shadow cones. The unfolded neutron spectra are in reasonable agreement with the MCNP simulations, also at absolute scale, except for the thermal energy region, indicating that the albedo of neutrons thermalized in the concrete is clearly underestimated in the calculation.

3. The catalogue of neutron spectra

All measured and calculated neutron spectra are included in the new catalogue. The programs developed for updating, ordering and inspecting this computer library are described in section I.2.

Publications: see summary, page 214.

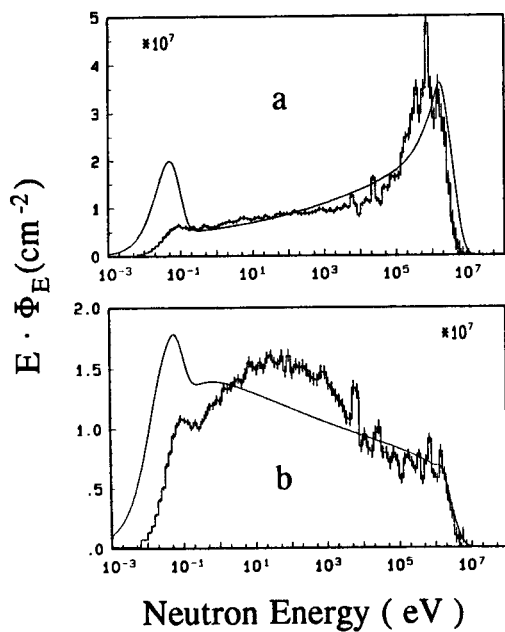


Fig. 4: Spectra of room return neutrons of a bare(a) and a D_2O -moderated (b) Cf source situated in the centre of the PTB bunker. The experimental spectra (smooth lines) measured with Bonner spheres behind appropriate shadow cones and MCNP calculations (histograms) are compared at absolute scale

Project 2

Head of project: *Dr. D.J. Thomas*

Scientific staff: *A.G. Bardell, G.C. Taylor, O.F. Naismith*

Objectives for the reporting period

The main objective was to identify and characterise the types of neutron fields to which radiation workers are exposed. It involved establishing a data base of such fields using all available experimental and calculated data, from all sources worldwide, and presenting this in a unified representation. NPL was actively involved in preparing the data base by gathering the spectra and developing the handling routines necessary to manipulate the spectra and extract the required information. All the collaborators, including NPL, are engaged in the business of neutron field spectrometry and part of the objective was to perform additional measurements in relevant sites, and also to improve the spectrometry systems.

Progress achieved

1. Spectrometer developments

NPL has a Bonner sphere (BS) spectrometry system, and this provides spectral information over the full neutron energy range of interest in most field measurements i.e. thermal to about 20 MeV. Work has continued on improving the sphere response functions¹⁻³), most recently by employing MCNP calculations to supplement the earlier ANISN calculations, particularly in the low energy region where MCNP provides much better agreement with experiment. The computer code STAY'SL was used to optimize the response functions, and provide uncertainty estimates, by incorporating all the available data, both experimental and calculational, in a consistent way.

A BS system will only provide low resolution, and this fact is of greatest consequence for the region above about 10 keV where the majority of the dose occurs for most spectra, and where the fluence to dose equivalent conversion factors vary most markedly with energy thus making calculation of the total dose from a measured spectrum dependent on the spectral details. To provide improved resolution in the high energy region (about 0.5 to 20 MeV) a new NE-213 scintillator spectrometer has been built and is now available for use.

Two different size scintillators are available, both right cylinders, of diameters 2 and 5 cm respectively. To separate the photon and neutron signals from the detector, a dual-parameter system is used to analyze the rise time and energy signals from the photomultiplier using a technique first suggested by Owen⁴). The data acquisition and analysis system is based on a personal computer, and with this it is possible to perform a preliminary spectrum unfolding at the measurement site. This provides an invaluable check of the measurements at a time before the equipment is dismantled and when repeat measurements can still be made if problems are identified. The NE-213 has already been used successfully for field measurements.

2. Field measurements

2.1 Source fabrication plant

A set of measurements was performed at a radionuclide neutron source fabrication plant. The BS spectrometer was used to measure the neutron fields in the vicinity of four different types of sources and the spectra have been incorporated in the data base for the catalogue. Measurements of the dose equivalent were also made at the same locations using two area survey instruments, the Harwell model 0949 and the Dineutron, see Table 1 for an intercomparison, and, for three of the locations, using a microdosimetric counter.

Agreement between the BS system and the microdosimetric system was good for the quantity dose equivalent, although there was a discrepancy for the quality factor.

Data for the three locations where microdosimetric measurements were made have already been reported⁵⁾. At the fourth location the source was ²⁴¹Am incorporated in a ceramic. The total activity was of the order of 7 TBq, and the spectrum is shown in figure 1. This was measured at a distance of 50 cm from the source in an area where scattering of the neutrons was not negligible. The results are therefore a reasonable representation of the spectrum which would be seen by a person handling such a material in a working environment.

Table 1. Comparison of neutron dose equivalent rates ($\mu\text{Sv h}^{-1}$) measured around four different sources located in working environments.

Source	Bonner sphere system			Harwell	Dineutron
	MADE*	ICRP51 ⁺	Wagner [§]	0949	
AmO ₂	4.41	4.29	4.40	4.65	3.46
²⁴⁴ Cm	20.5	20.9	21.1	22.1	16.8
Am-Be	28.8	28.2	29.1	29.1	-
Am ceramic	15.4	15.9	16.0	16.6	17.7

* fluence to dose equivalent conversion factors from ICRP 21.

+ fluence to dose equivalent conversion factors from ICRP 51.

§ fluence to dose equivalent conversion factors from Wagner et al. Radiat. Prot. Dosim. 12 231-235 (1985).

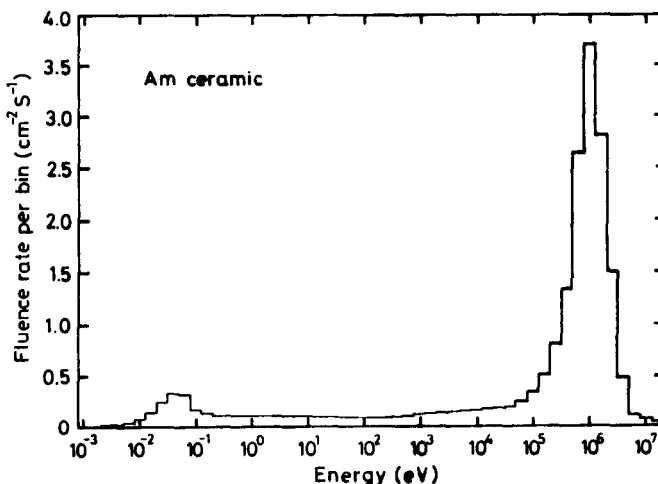


Fig. 1 Neutron spectrum at 50 cm from a source of approximately 7 TBq of ²⁴¹Am incorporated in a ceramic material.

2.2 Research reactor

In 1993 an intercomparison of criticality accident dosimetry systems will be undertaken, with CEC support, at the Silene reactor housed on the CEA site at Valduc, France. To provide the reference dosimetry for this exercise, teams from CEA, AEA Technology Harwell, and NPL performed measurements for the two configurations which will be used in the intercomparison. These are: the reactor shielded by 10 cm of lead, and the bare reactor. Neutron spectrum measurements were made by the Harwell and NPL teams. The results provide an extremely useful benchmark for comparing with calculations, e.g. those of Ing and Makra⁶). The calculations provide estimates of the free field spectra ie with no scatter or room return. The measurements will give insights into the extent to which these scatter effects modify the spectra and the extent to which the calculated spectra can be relied upon as true estimates of the types of field to which workers might be exposed.

The normal measurement technique with BSs is to use a single central detector and to irradiate one sphere at a time. Because of access restrictions at Silene this was not possible, and the measurements were performed with five spheres at a time relying on the cylindrical symmetry of the field to ensure that all spheres were exposed to the same spectrum.

A report of the lead shielded reactor measurements has been prepared and submitted to the CEC (DG XI and DG XII), however, neither of the measured spectra can be made available publicly until after the criticality accident dosimetry intercomparison, planned for June 1993, has taken place. This is because, in the first instance, it is intended that participants in this exercise should analyze their dosimeter readings without knowledge of the neutron spectrum. Immediately the exercise is complete the results can be included in the data base for the catalogue.

3. The data base and catalogue

A large amount of data is available for both measured and calculated neutron spectra; not all of it is directly relevant to radiation protection situations, and critical judgement is necessary to derive conclusions from it about the performance of dosimeters used in protection level measurements. There exist two good compendia of spectra, that by Ing and Makra⁶), which contains only calculated data, and that by Griffith, Palfalvi, and Madhvanath⁷) which contains both calculated and measured spectra. The most recently available data are not, however, included (none since about 1982). This is important since improvements in spectrometer design etc. give the more recent data greater reliability. The dosimetric quantities used in the above documents have also been superseded by more recent recommendations from the ICRP and the ICRU.

Although the above documents are very useful, there is also a need to be able to access the data easily, to be able to search through it for related data, and to be able to calculate any dosimetric quantity or detector response of interest. This is best achieved by having the spectra in a computer data base with programs to access the data and extract the required information.

A suite of computer codes has been developed at PTB and these have been investigated and used at NPL who have provided feedback to develop and improve the codes.

Spectra from the two compendia described above have been included in the data base and, in order to extend it, a questionnaire was prepared and circulated to all groups known to be involved in neutron spectroscopy. About 30 questionnaires were distributed by NPL worldwide, in addition to those distributed by PTB and CEA in Germany and France, and replies are continuing to be received. This data has been, and will continue to be, incorporated into the data base. All data measured by the four participants in the present contract have been included.

References

1. A V Alevra et al., Radiat. Prot. Dosim. **23** (1988) 293-296; *Experimental determination of the response of four Bonner sphere sets to monoenergetic neutrons.*
2. A V Alevra et al., Radiat. Prot. Dosim. **40** (1992) 91-102; *Experimental determination of the response of four Bonner sphere sets to monoenergetic neutrons (II).*
3. D J Thomas, NPL Report RSA(EXT)31, March 1992; *Use of the program ANISN to calculate response functions for a Bonner sphere set with a ³He detector.*
4. R B Owen, Nucleonics **17** (1959) 92.
5. D J Thomas et al., To be published in Radiat. Prot. Dosim.; *An intercomparison of neutron field dosimetry systems.*
6. H Ing and S Makra, IAEA Technical Report Series No. 180, Vienna, 1978; *Compendium of neutron spectra in criticality accident dosimetry.*
7. R V Griffith, J Palfalvi and U Madhvanath, IAEA Technical Report Series No. 318, Vienna, 1990; *Compendium of neutron spectra and detector responses for radiation protection purposes.*

Project 3

Head of project: *Dr. J. L. Chartier*

Scientific staff: *F. Posny, J. Kurdjian, G. Pelcot, G. Audoin, C. Itié*

Objectives for the reporting period

1. Measurements of neutron fluence distributions encountered in practical situations with proton recoil (PR) detectors in association with a multisphere (MS) system.
2. Improvement of the spectrometric system.
3. Production of neutron fields which could replicate typical radiation protection spectra: computational predictions using the MCNP-3A code and realisation of the assembly at CEA Cadarache.
4. Participation in the CEA Cadarache intercomparison exercise.

Progress achieved including publications

1. New data for the neutron spectra catalogue

The measurements campaigns in French nuclear installations have been performed at work-places where neutron hazards are present. The multisphere system and proton-recoil spectrometry unit have both been used:

- at Fontenay-aux-Roses (CEA) in front of a glove-box in which Am-Be neutron sources are manufactured. The spectrum shown in figure 1 presents the general shape of an Am-Be source modified at low energies by the neutrons scattered due to the walls of the glove-box and to the local environment,

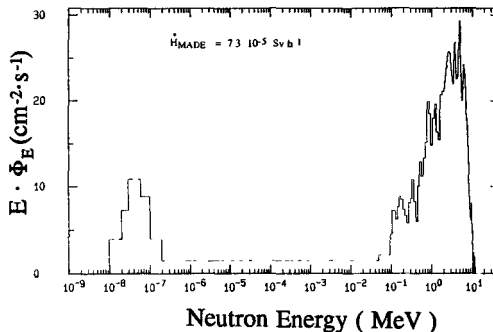


Figure 1: Neutron spectrum at an AM-Be source manufacturing work station: CEA Fontenay-aux-Roses.

- at the processing plant of La Hague (COGEMA) near a transportation container of irradiated fuel. In figure 2 the spectrum obtained shows structures in the MeV energy region, probably due to the shielding materials inside the container (steel, lead, wood, resin ...),

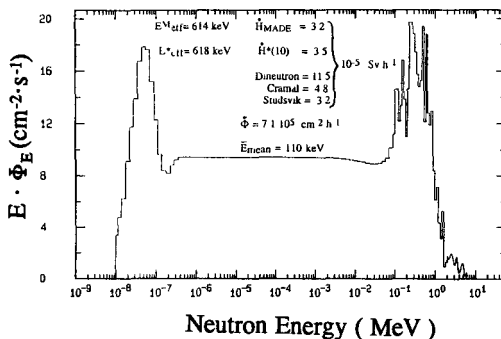


Figure 2: Neutron spectrum near a transportation container of irradiated fuel: Cogema La Hague.

at Valduc (CEA-DAM) in a Pu chemistry laboratory. The measured point was located in front of a glove-box in which PuF_4 is handled. The spectrum presented in figure 3 shows neutrons from the PuF_4 mixed with traces of PuO_2 moderated and scattered by the various surrounding materials.

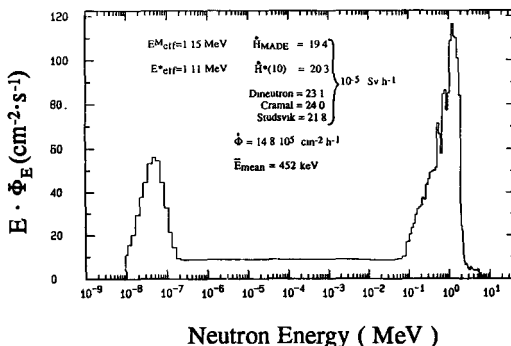


Figure 3: Neutron spectrum at a Pu chemistry work station: CEA Valduc.

In the last two cases and in the intercomparison exercise, additional measurements were performed at the same locations with three radiation protection devices: Cramal, Dineutron and Studsvik. The results are reported in section 3. The discrepancies with respect to the spectrometric results clearly show that the dose-equivalent response of such devices strongly depends on the fluence distributions and therefore on the field in which they have been calibrated.

2. Association of MS and PR techniques

Up to 1991 the MS and PR complementary techniques had consisted in two independent evaluations of data, showing a systematic discrepancy between the two results in the common energy range. The overevaluation by PR detectors was attributed to the oversimplified unfolding of the NE213 detector data and to the underestimated efficiency of the SP2 counters.

The previous unfolding code has been replaced by the code MATXUFCORR, which takes into consideration the shape of the experimental response functions before applying the mathematical process recommended by JOHNSON (folding product). This new code

was used to unfold the spectra measured in the reference fields (ISO 8529) of calibrated Am-Be and ^{252}Cf sources. Good agreement was found for the shape as well as for the fluence value (Fig. 4 and 5). If the measured spectrum shows a component at the 14.6 MeV neutron energy, a particular data processing is applied to subtract the parasitic contributions due mainly to the $\text{C}(n,n')\alpha$ and $\text{C}(n,n')3\alpha$ reactions and the edge effects.

The characteristics of the PR detectors between 120 keV and 3 MeV were determined with monoenergetic neutrons at the research center of Bruyères-le-Châtel (Van de Graaff 4 MeV): response functions (shape and energy calibration), energetic resolution and efficiency variation versus the neutron energy. In order to estimate the absolute efficiency value for each counter, a measurement was performed with the same ^{252}Cf reference source (Fig. 5). The PR and MS systems are now in good agreement in terms of fluence, and the link between them is made by a simple juxtaposition of the two parts: 0.01 eV - 100 keV (MS) and 100 keV - 20 MeV (PR).

3. Computational predictions of neutron spectra

An irradiation facility composed of the following elements: [14.6 MeV neutrons] + [^{238}U converter] + [Fe shield] + [polyethylene duct] + [shields (optional)] is expected to be able to replicate several spectral shapes similar to those measured. In order to optimize the numerous parameters of such an assembly, Monte Carlo calculations were performed by using the 3D general code MCNP to calculate the neutron and photon spectra in a "calibration zone".

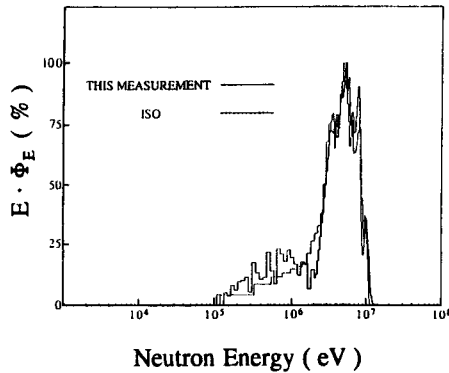


Figure 4: Neutron spectrum of an Am-Be source. The two spectra have been normalized to the maximum value.

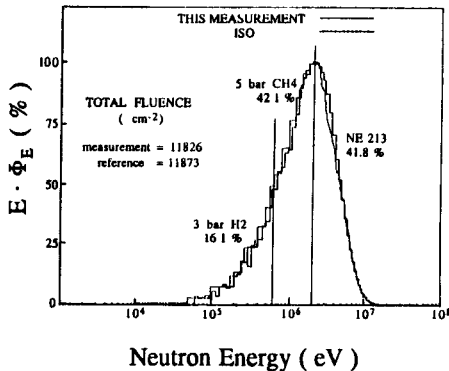


Figure 5: Neutron spectrum of a ^{252}Cf . The percentages indicate the contribution to the total fluence

Several modifications of the MCNP input file were considered: the use of ENDFBV library data, angular and energetic distributions of the emission neutron spectrum, absorption and scattering of "14 MeV" neutrons in the copper target backing, in the cooling water flow, in the aluminium target assembly container and in the environment of the beam line, and the influence of thermal treatment $S(\alpha, \beta)$ for H in the polyethylene of the duct.

In addition, the photon component was calculated in order to obtain information on its relative contribution in the calibration zone: 21.4% and 1.8% respectively of the total fluence and dose equivalent.

Another set of results has been obtained by changing the primary neutron energy from 14.6 MeV to 2.8 MeV. These neutron energies which are produced by (D,T) and (D,D) reactions with small accelerators ($HV \leq 400$ kV) seem to be rather easier to use than intense neutron sources. In addition, with 2.8 MeV neutrons, the drawback of the leakage of a residual 14.6 MeV component and the hazards inherent in the handling of Ti(T) targets are avoided. The calculations have given a first evaluation of possible realistic spectra and associated dose rates (publ. 4.8).

4. The intercomparison exercise

The first element of the assembly is a 150 kV accelerator which produces the 14.6 MeV neutron field via the (D,T) reaction. In order to compare the measurements performed during the two weeks of the exercise, special care was taken with the monitoring system. By means of the associated particle technique, three semiconductor detectors recorded the α particles emitted backwards (176°). Between the measurements, a series of periodic checks was carried out with a movable ^{241}Am source: the pulse distribution of each diode and its energetic resolution checked that the detectors were operating correctly and the recorded counting showed a reproducibility better than 1%. During the measurements, the mean value of the three count rates was taken as the monitoring reading. The fluctuations of the ratios of each count rate with respect to the mean value indicated good stability. In addition, the purity of the Ti(T) target was controlled by the check of the recorded pulse distributions.

The results of the measurements are presented in section 3 together with the MCNP-calculation.

Publications: see summary, page 214.

Project 4

Head of project: *Dr. H. Schraube*

Scientific staff: *J. Jakes, G. Leuthold, V. Mares, G. Schraube*

Objectives for the reporting period

1. Calculation of the response matrix of a Bonner sphere spectrometer set with spherical ^3He -counter as the basis for unfolding of Bonner sphere data which had been experimentally determined at working places.
2. Collating and sifting of published data for their aptitude of being included into the envisaged spectra catalogue.
3. Calculation of the operational dose equivalent quantity $h^*(10)$
4. Adaption of the calculated response matrix to a BS system with $^6\text{Li(Eu)}$ detector
5. Unfolding of own experimental data as measured at working places. Completion of the spectra catalogue with these data and data from literature examinations.

Progress achieved including publications

1. Calculation of Bonner sphere matrix

During the calculation of the Bonner sphere matrix three items were studied: i) the pressure dependence of response, when the gas pressure of the ^3He counter is varied, ii) the influence of the polyethylene density of the spheres to the response, and iii) the possibility of representing of the whole matrix in the sphere diameter domain by a log-normal distribution (Zaborowski-technique).

The Monte Carlo calculations of BSS response were performed for a commercially available ^3He spherical proportional counter with a diameter of 3.2 cm and a reference pressure of 172kPa placed in the center of the polyethylene moderating spheres with different diameters in the range of 2 inch to 15 inch.

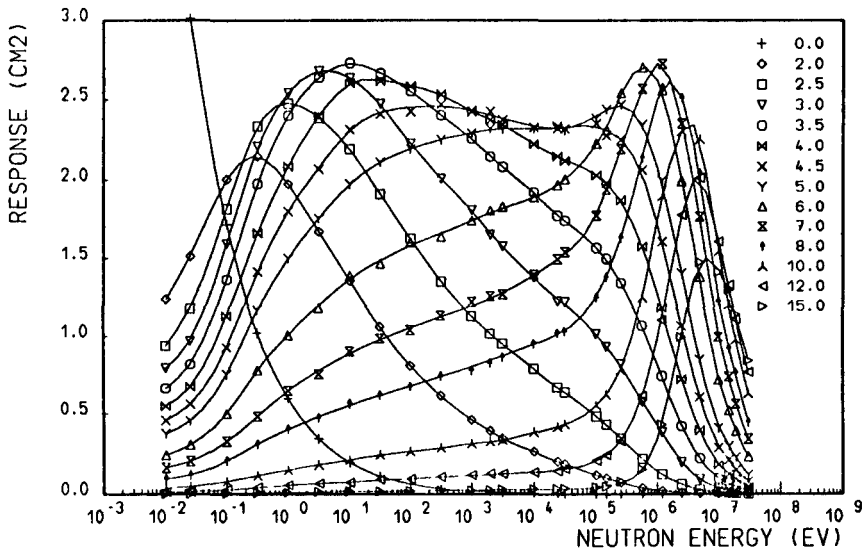


Figure 1 Energy response of BSS for MCNP calculated spheres (data points). The lines connect the responses at the 49 energies of the final matrix.

The response data obtained from the MCNP calculation were then interpolated to generate the response matrix with 49 energy points in log-equidistant intervals (i.e. 5 per decade) from 0.01 eV to 30 MeV for spheres from 2 to 15 inch in diameter steps of 0.5 inch. The responses for the additional Bonner spheres were interpolated in the sphere diameter domain for each respective neutron energy using the cubic spline interpolation method which smoothes out the estimated statistical uncertainties at the same time. The same method was then used for the interpolation in the (logarithmic) energy domain for all response data obtained both from MCNP calculation and from the sphere diameter interpolation.

2. Spectra catalogue

An extensive collection of nearly 90 neutron spectra in Russian language was translated and all Bonner sphere data extracted and transferred into the format of the new catalogue.

3. Ambient dose equivalent conversion function $h^*(10)$

The basic operational quantity to be determined in realistic radiation fields is the ambient dose equivalent which is defined at 1cm depth of the ICRU sphere for parallel incident radiation field. As the LET dependence of the quality factor was recently changed by the ICRP, this quantity had to be recalculated in the frame of this project. The MCNP Monte Carlo programme was employed for this purpose, too. The chemical binding energy of the molecules in water was taken into account to simulate the conditions as encountered in tissue equivalent material, and the respective cross sections applied. The resulting conversion function $h^*(10)$ is shown in figure 2 together with a fitted analytical expression for practical applications.

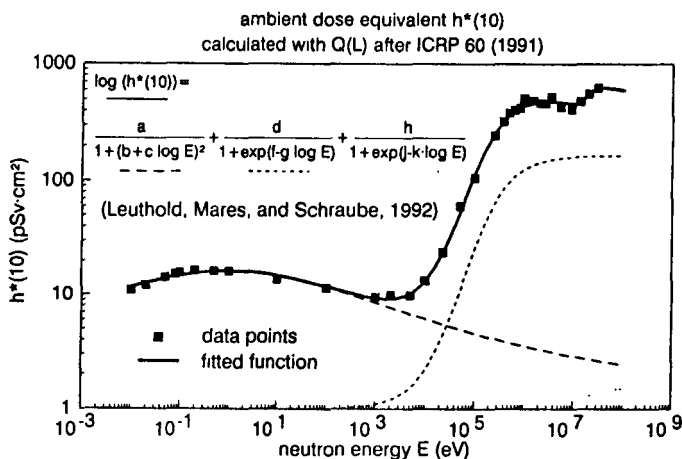


Figure 2 Fluence-to-ambient dose equivalent conversion function $h^*(10)$ for the ICRP60 revised quality factors, and the components of the analytical representation ($a=1.210$, $b=3.035 \cdot 10^{-3}$, $c=0.1830$, $d=2.218$, $f=10.85$, $g=2.281$, $h=0.1751$, $j=100$, $k=13.75$).

4. Bonner sphere responses for the ${}^6\text{LiI}(\text{Eu})$ -system

For the BS spectrometer with spherical ${}^3\text{He}$ counter an excellent agreement between the calculations (Mares et al., 1991) and the experimental data (Alevra et al., 1992) has been achieved. Therefore, it was tried to extend the experiences to a BS spectrometer with ${}^6\text{LiI}(\text{Eu})$ scintillator, as it was used to study the radiation fields in working environments, and as it is still a widely used device. The system was modelled with a simplified arrangement of the scintillator and the surrounding constructive materials, and again calculated by

the aid of the MCNP programme as done already successfully with the ^3He system. It appeared that the results still differ to the latest available ANISN calculations for this system of Hertel and Davidson (1984) as well as to the experimental data. It may be concluded that there are physical conditions which are not yet taken properly into account in the calculations.

5. Neutron spectra at survey fields

Measurements with the BS spectrometer with $^6\text{Li(Eu)}$ scintillator were analyzed to receive the neutron spectra and the essential integral data. All data were evaluated by using i) the original Hertel and Davidson matrix and ii) the improved matrix taking into account the experimental results of Alevra et al. (1992).

Several guess spectra were used as start data in the iterative unfolding process which is described by Alevra et al. (1990). It was generally observed that the improvement of the response matrix had a much larger effect to the results than the application of different guess spectra (see figure 3). As the largest correction in the matrix had to be applied to the largest spheres, the high energy part of the spectrum was affected largest by the change in the response matrix. The inverse of the correction factor to the 12" sphere corresponds approximately with the increase of the integral dose equivalent.

Cadarache facility. The spectrum at the Cadarache facility was studied in the frame of the joint interlaboratory exercise. In a first step, the original H&D matrix and three starting spectra were used which consisted of two components with 3 different relative contributions: an 1/E slowing down part, and a fast Maxwellian. The energies where the two contributions were equal was chosen at $E''=0.2, 0.5$ and 1MeV (guess spectra #1 to 3), respectively. In a second step the improved matrix was used. As starting spectra one of the above mentioned spectra was used (#2), further one with a thermal Maxwellian distribution (see figure 2c in the summary chapter I.3) and finally the spectrum from the MC-calculation of Chartier et al. (1992) for the actual irradiation arrangement. While the integral data differ only little with the change of the start spectra, the resulting unfolded spectra do show the more details the more a-priori information is used in the start spectra, e.g. the knowledge of 14MeV source term, 24keV iron-resonance, etc..

Neutron spectra at working environments. At several places in the nuclear power circle, i.e. during handling of MOX elements, inside two PWR reactors, and inside the containment of a BWR were unfolded in the same way as above. The data are provided for the spectra catalogue.

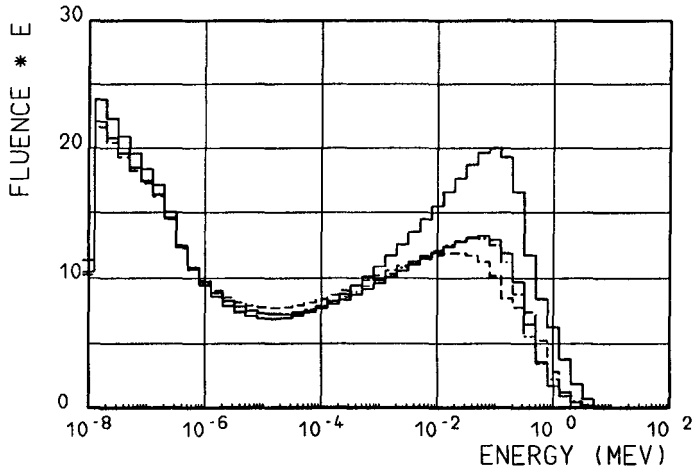


Figure 3 Spectral results inside the containment of a BWR for the unfolding using the improved Hertel and Davidson matrix (guess spectrum#2, upper curve), and the original H&D matrix, respectively, starting with guess spectra #1 to #3 (lower 3 curves)

References

- A.V.Alevra et al.: Unfolding Bonner sphere data: A European intercomparison of computer codes. PTB Report PTB-7.22-90-1 (1990)
 N.E.Hertel and J.W.Davidson, Nucl.Instr.Meth. A238(1985)509
 V.Mares et al.(1991), G.Leuthold et al.(1992), A.V.Alevra et al.(1992), and Chartier et al. (1992): see publication list at the end of the summary chapter

CALCULATION AND MEASUREMENT OF DOSES FROM PARTICULATE RADIOACTIVE SOURCE

Contract Bi7-021 - Sector A13

- 1) *Charles*, Nuclear Electric - 2) *Herbaut*, CEA - Grenoble
- 3) *Patau*, Univ. Toulouse III

Summary of project global objectives and achievements

The evaluation of the hazard posed to the skin by very small radioactive sources (diameter < 1 mm) has become popularly known as the 'hot particle' problem. The 'problem' arises from the difficulty of calculating or measuring the magnitude of the spatially non-uniform exposure and the difficulty of evaluating the potential biological response. Concern regarding the hazard of hot particles on the skin and in the lungs has been raised in consideration of the environmental impact and plant clean-up problems following the Chernobyl reactor accident. They are also an operating problem on US PWR reactors. Recent NCRP and ICRP reports have provided criteria for skin dose limitation including recommendations for limiting effects from 'hot particles'. The NCRP criteria is however a factor of 10 more relaxed than the ICRP recommendation of a dose limit of 0.5 Sv over an area of 1 cm^2 at a depth of $70 \mu\text{m}$. As well as this continuing controversy regarding the limitation of hot particle risks both committees point out that more dosimetry and radiobiology data are necessary for poorly penetrating low energy radiations such as beta radiation from Co-60 (an important constituent of radioactive contamination in nuclear power reactors). The objectives of this project are to develop and validate methods for the measurement and calculation of doses from radioactive particulates. This is being done by producing a range of standardised 'hot particle' radiation sources so that measurements can be directly compared with calculations for well characterised radioactive sources. The project also involves the development and use of novel dosimetry techniques for dose evaluation (scanning small electrode extrapolation chamber and radiochromic dye films) and the development of a dedicated Monte-Carlo code for 'hot-particle' dose calculations for various source sizes and geometries.

The production and dosimetry of radioactive particles (particularly Co-60) has proved to be far more difficult than envisaged. Radiochromic dye film has been developed as a new and successful technique for hot particle dosimetry. Problems of using the extrapolation chamber have been found to be due to non-uniform chamber exposure and this has been overcome by mathematical modelling and fitting data using non-linear regression analysis. Final agreement between dosimetry techniques is good. A Monte-Carlo code has been successfully developed for Co-60 and Tm-170 sources and there appears to be reasonable agreement between this and the widely used semi-empirical computer code VARSKIN. However the measured doses are about a factor of 2 greater than calculated. This is thought to be due to self absorption in the source and deviations from ideal source design. This will be rectified and studied further in the next extended contract period.

Project 1

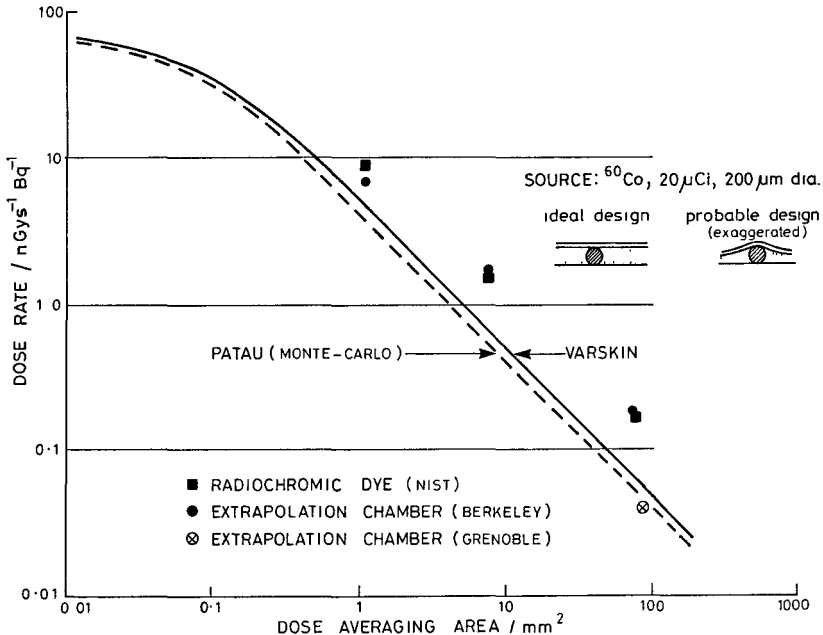
Head of project: *Dr. Charles*

Objectives for the reporting period

A comparison will be made of dose measurements using radiochromic dye film and extrapolation chamber methods for standard 'hot particle' sources of Co-60 and Tm-170. Doses are to be measured over various areas from 1 - 100 mm² and at various depths between 20-150 µm, to facilitate comparison with recommendations of the ICRP and for use in related animal experiment studies. The measured doses will be compared with calculated doses using Monte-Carlo code and semi-empirical methods. If necessary revisions will be made to source construction and calculation methodologies to provide a valid comparison of measurements and calculations. Advice will be formulated on the most appropriate methods for dose calculation and measurement for 'hot particles'.

Progress achieved including publications

This contract commenced on 1 October 1990. A report of progress was provided in April 1991 and several papers related to the project were presented at a EURADOS skin dosimetry workshop held in Dublin in May 1991 and these have recently been published⁽¹⁻⁴⁾. At that time dosimetry studies of a 1 mm diameter Sr/Y-90 beta source had been carried out using a scanning small-electrode extrapolation chamber and radiochromic dye films. It was found that the extrapolation chamber response was actually non-linear and the use of linear fitting routines tended to under-estimate doses to small areas by a factor in excess of two compared to radiochromic dye films. A theoretical model was developed to explain the non-linear response. The use of non-linear regression analysis for the evaluation of the extrapolation chamber data provided good agreement between the two techniques. Radiochromic dye film measurements were carried out at Berkeley using manual and image analysis densitometry. This compared favourably with a more sophisticated and rapid method of laser scanning densitometry used by Dr Soares at the National Institute of Standards and Technology in Washington DC. These measurements have since been extended to neutron activated Co-60 particles produced, after some early difficulties, at the high flux reactor in Petten. The initial Monte-Carlo codes produced by Dr. Patau at University of Toulouse, as part of this contract, have proved to be user-friendly and reasonably fast and have produced dose estimates over various averaging areas for spherical Co-60 test sources. These have been compared with semi-empirical calculations of beta dose utilised in a recently developed American code VARSKIN 2. The doses calculated by various methods, over areas from 1 mm² to 1 cm², are in reasonable agreement but are lower by a factor of 2 than measurements (Figure 1).



The difference between the measured and calculated doses for Co-60 is currently under investigation. The difference may be due to small deviations from an ideal geometry in the test sources (schematically illustrated in figure 1). The aim was to produce an ideal parallel geometry with a spherical source sandwiched between parallel aluminium foils, with a unit density glue between the sandwich. If the foil is actually curved around the sphere, rather than tangential to it, then the reduced absorption through the material overlying the source may give rise to the discrepancy. Modifications to the calculational models have been made in an attempt to mimic the reduced beta absorption. The results support this possibility in that they predict significantly higher doses than the ideal geometry. Figure 1 indicates results of calculations and measurement. The calculations using a VARSKIN 2 model are for a source ($200\mu\text{m}$ diameter, $20\mu\text{Ci}$) sandwiched between an aluminium base and aluminium foil window with air as the medium between the sandwich. The Monte-Carlo code calculation assumes a low density (0.1 g cm^{-3}) glue. Both of these models to some extent simulate the more likely curved geometry which gives a smaller absorption of beta radiation in the surrounding material.

Doses have been measured using various methods:

1. An automated scanning extrapolation chamber with various electrode diameters down to 1 mm. Contact doses were measured.
2. Radiochromic dye film, measuring the change in optical density with a scanning laser read-out system (Dr. Soares, NIST, Washington DC). Contact doses were measured.
3. A larger area (0.9 cm^2) extrapolation chamber at a short distance from the source has been carried out by Dr. Herbaut in Grenoble as part of this contract.

In order to further investigate the discrepancy between measurements and calculations various changes are being made to the protocol which is the subject of an extended contract. We have produced a modified design of Co-60 source with a more rigidly defined planar geometry.

Neutron activation is to take place at Brookhaven National Laboratory high flux reactor in early 1993. Dose measurements will be repeated using radiochromic dye and extrapolation chamber methods. We are also making measurements and calculations for a rather higher energy beta emitter where self absorption is not so pronounced ($Tm-170$; $E_{max} \sim 1$ MeV) and the source construction will not be so critical. The Monte-Carlo code has been modified to include this additional beta source and to accommodate its cylindrical geometry. The Monte-Carlo code will also be extended to simulate the extrapolation chamber geometry of the Grenoble group. The use of thermoluminescence (TL) dosimetry is also planned. This will utilise a scanning laser heating system at Montpellier as part of an extended contract.

Progress on this project has been slow due to difficulties of obtaining high flux neutron exposures and because of the unforeseen necessity to tightly specify the Co-60 source design. Overcoming these problems however has led to a greater understanding of the important factors in hot particle dosimetry and has led to useful links with American laboratories who are now assisting with neutron irradiations and are involved in dosimetry comparison studies. As a result of these inter comparisons it should be possible to recommend methods for the measurement of hot-particle doses using various techniques, including extrapolation chamber, radiochromic dye films and TL. It should also be possible to provide advice on the range of applicability and precision of both Monte-Carlo and semi-empirical methods of dose calculation.

References

1. P.J. Darley, M.W. Charles, C.D. Hart, J. Wells and M.S.E. Coleby. Dosimetry of planar and punctiform beta sources using automated extrapolation chamber and radiochromic dye films. Proceedings of EURADOS workshop on skin dosimetry. Dublin 13-15 May 1991. Radiation Protection Dosimetry. 39 (1/3) 61-66, 1991.
2. M.W. Charles. The hot particle problem. Proceedings of EURADOS workshop on skin dosimetry. Dublin 13-15 May 1991. Radiation Protection Dosimetry. 39 (1/3) 39-47, 1991.
3. C.G. Soares, P.J. Darley, M.W. Charles & J.W. Baum. Hot particle dosimetry using extrapolation chamber and radiochromic foils. Proceedings of EURADOS workshop on skin dosimetry. Dublin 13-15 May 1991. Radiation Protection Dosimetry. 39 (1/3) 55-60, 1991.
4. J.P. Patau. Monte Carlo calculations of the depth dose distribution in skin contaminated by hot particles. Proceedings of EURADOS workshop on skin dosimetry. Dublin 13-15 May 1991. Radiation Protection Dosimetry, 39 (1/3) 71-74, 1991.

Project 2

Head of project: *Dr. Herbaut*

Objective for the reporting period

Experimental measurements of the tissue dose rate in the proximity of a ^{60}Co "hot particle" source will be made by means of a PTW extrapolation chamber (electrode surface area of 100 mm^2) and thermoluminescent lithium fluoride dosimeters charged with graphite. The results will be compared with dose rates obtained by Monte-Carlo codes and other semi-empirical methods.

Progress achieved including publications

This contract commenced in October 1990. An interim progress report was provided in May 1991^[1]. The first spherical ^{60}Co source was supplied by Dr. Charles in May 1991, which explains why the experimental work to determine absorbed doses from this source is still in progress at the present day. Consequently, only part of the results are provided in this report.

1. Measurements using an extrapolation chamber

The use of a tissue-equivalent extrapolation chamber is a standard method for measuring dose rates from beta-emitting sources. An in-depth study of the characteristics of a PTW model 23391 extrapolation chamber was performed. This ionisation chamber was equipped with electrode diameters of 10, 15, 20, 30 and 40 mm of A150 tissue-equivalent material. The chamber entrance window was of 7.05 mg.cm^{-2} polythene, which corresponds with the recommended thickness for skin dose measurements. The collecting surfaces of the electrodes were determined using the method presented by J. Böhm^[2].

Beam measurements were made for sources of ^{147}Pm , ^{204}Tl , $^{90}\text{Sr}+^{90}\text{Y}$ calibrated by PTB and LMRI in order to verify the methodology used to determine absorbed tissue doses. The results compared well.

The extrapolation chamber was used to determine tissue dose rates from a spherical ^{60}Co source (diameter $175\text{ }\mu\text{m}$, with an activity of $8.5 \times 10^5\text{ Bq}$ on 1.10.91) supplied by Dr. Charles. The chamber was fitted with an electrode of diameter 10.7 mm (surface area 90 mm^2), and dose rates were taken at a tissue depth of 7 mg.cm^{-2} , and at various distances (0.5, 1, 2 and 3 mm) from the source.

The table below gives the total dose rates due to β and γ rays ($\dot{D}_{\beta+\gamma}$) normalised to 1 Bq. An assessment of the ratio of dose rates $\dot{D}_{\gamma} / \dot{D}_{\beta+\gamma}$ has also been performed.

Distance from the source (mm)	$\dot{D}_{(\beta+\gamma)}$ nGy.s ⁻¹ .Bq ⁻¹	Standard deviation (%)
0.5	3.13×10^{-2}	23
1	3.04×10^{-2}	12
2	2.44×10^{-2}	7
3	1.92×10^{-2}	5

The above results, associated with measurements currently in progress at a distance of 0.2 mm, should make it possible to assess the dose rate upon contact with the source, and compare this value with the one given by the Monte-Carlo code of Dr. Patau [3].

2. Measurements using thermoluminescent dosimeters

Thermoluminescent Lithium Fluoride VINTEN dosimeters mixed with graphite (disc diameter of 12.7 mm) were placed on a perspex support and covered by a layer of mylar of thickness 7 mg.cm⁻². These dosimeters were used to determine the absorbed dose rate of the ⁶⁰Co source. An in-depth study of their dosimetric characteristics (linearity, energy-response function) under the reference β -ray beams of the Büchler irradiator (¹⁴⁷Pm, ²⁰⁴Tl, ⁹⁰Sr+⁹⁰Y) showed that the dosimeters were well adapted for measuring weakly penetrating rays, and consequently those emitted by ⁶⁰Co ($E_{\beta\text{max}} = 318$ keV).

Measurements of the absorbed dose rates at a distance of 2 mm from the ⁶⁰Co source, and a study of the variation in the dose as a function of tissue depth (7 - 100 mg.cm⁻²) are currently in progress.

3. Comparison with theoretical calculations

Our experimental results (extrapolation chamber) show a satisfactory agreement with the results obtained using the VARSKIN 2 model [4] (supplied by Dr. Charles). See Figure 1.

References

1. Contract Bi.7.021. Progress report (25/4/91)
2. Böhm, J., PTB-DOS 13 (1986)
3. Patau, J.P., *Radiat. Prot. Dosim.* **39**, 71-74 (1991)
4. Durham, J.S., *Radiat. prot. Dosim.* **39**, 75-78 (1991).

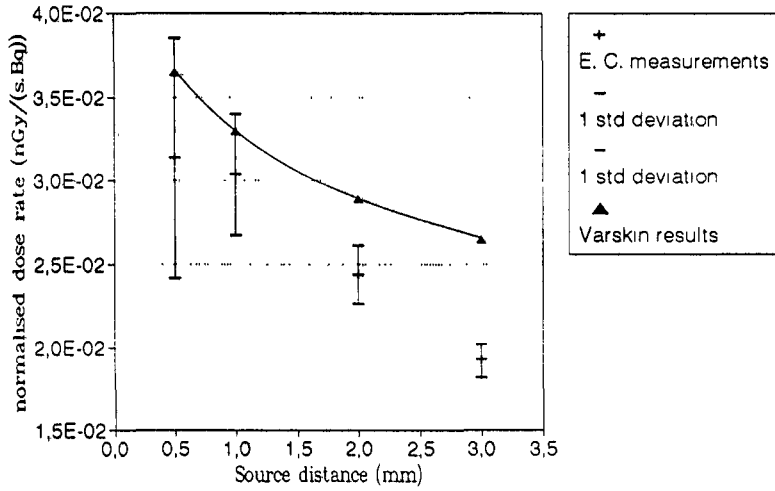


Figure 1 - ^{60}Co source (175 μm , 23 μCi at 1/10/91)

Project 3

Head of project: *Dr. Patau*

Objectives for the reporting period

In order to evaluate biological risks to the skin irradiated by hot particles a package of computer programmes was to be developed in our laboratory. The problems were to tackle by Monte-Carlo simulations of particle transport. These methods are perfectly suited to feature with good resolution the spatial distributions of high gradient energy deposition in the vicinity of such small radioactive sources. Moreover these methods are able to exactly take into account all particles releasing energy, all effects of geometrical configuration as well as the chemical composition of the system irradiated whatever its complexity. We had to deal with configurations such as those which are used for dose measurements by the other contracting parties.

Progress achieved

Processing:

We were interested in beta radiations emitted from ^{60}Co and ^{170}Tm radionuclides because experiments have to be performed with them. Injuries caused by such sources laid on the skin are almost exclusively due to beta ray slowing down. The first configuration looks like the one which was previously taken (Patau, Radiat. Prot. Dos. 39, 1/3, 71-74, 1991), but the pure cobalt spherical sources and the pure aluminium support were replaced by actual blended materials. In the second configuration the sources were pure thulium discs. In both cases energy spectra were calculated according to Fermi's beta decay theory for allowed (^{60}Co) or first-forbidden (^{170}Tm) transitions. For the ^{60}Co , only the first beta transition ($E_{\text{max}} = 317.9$ keV) was taken into account, while for ^{170}Tm both beta transitions were considered according to their relative intensity. Depth distributions of absorbed energy are calculated in a polystyrene cylinder with a resolution of 0.001 cm for the ^{60}Co sources and 0.0036 cm for the ^{170}Tm sources. Experimental measurements with extrapolation chambers are assumed to be made inside the same polystyrene cylinder. In the case of ^{60}Co irradiation the contribution of gamma rays to energy deposition can be simply evaluated to less than 0.01% in each slice. In the case of ^{170}Tm the other emissions, particularly 73.8 and 81.8 keV electrons, may very lightly influence depth energy curves, in the first slice. A specific programme considering these electrons allowed to estimate their contribution to less than 0.5%. In the second slice their contribution is practically non-existent. However, these electrons could have a less negligible influence in the first slices if a finer resolution is taken. It may be the same if a hot particle is directly on the skin. The energy deposited in the first slice by all low energy photons emitted from ^{170}Tm is roughly estimated to less than 5.10^{-5} times the energy deposited by beta rays.

Programmes were executed for a given set of cobalt sphere and thulium disc diameters (Co: 122, 143, 175, 190, 193 μm . Tm: 400, 650, 1200, 2000 μm); Thulium discs are 100 μm thick; a 4 mg.cm⁻² thick aluminium foil is overlaying the sources. All geometrical parameters are adjustable on user's requirement. While waiting for experimental results we have compared our results for the Tm sources with those obtained for the same configuration by EGS4 programme. The latter uses Moliere multiple scattering angle distribution instead of Goudsmit and Saunderson's. Coulomb energy loss is described by restricted stopping power

between two ionisations considered as discrete interactions. These are simulated with Möller scattering cross section, while we use Landau's pathlength energy straggling distributions.

Results

In any case our programmes simulated 200,000 primary electron histories and their secondaries while EGS4 was run for 50,000 histories.

Depth distributions of energy deposition are shown on figure 1 in semi-logarithmic scale for ^{60}Co sphere sources, on figure 2 for ^{170}Tm disc sources. In the latter case results given by EGS4 on figure 3 can be seen very close to ours.

Energy spectra of electrons leaving the source and entering the cylinder of polystyrene are calculated (fig. 4) as well as the number of primary or secondary electrons entering the polystyrene cylinder (named "useful electrons").

Conclusion

The distributions of energy deposition vary appreciably with the diameter of the sources whatever their shape. So, one must be fully aware that little inaccuracy on dimensions, composition or density of each part of the configurations could give rise to discrepancies between calculations and experiments. The accuracy of fittings that can be made in scattering distributions is conditioned by the preciseness of all experimental parameters. The present programmes can easily be executed for other dosimeters such as TLD instead of extrapolation chambers.

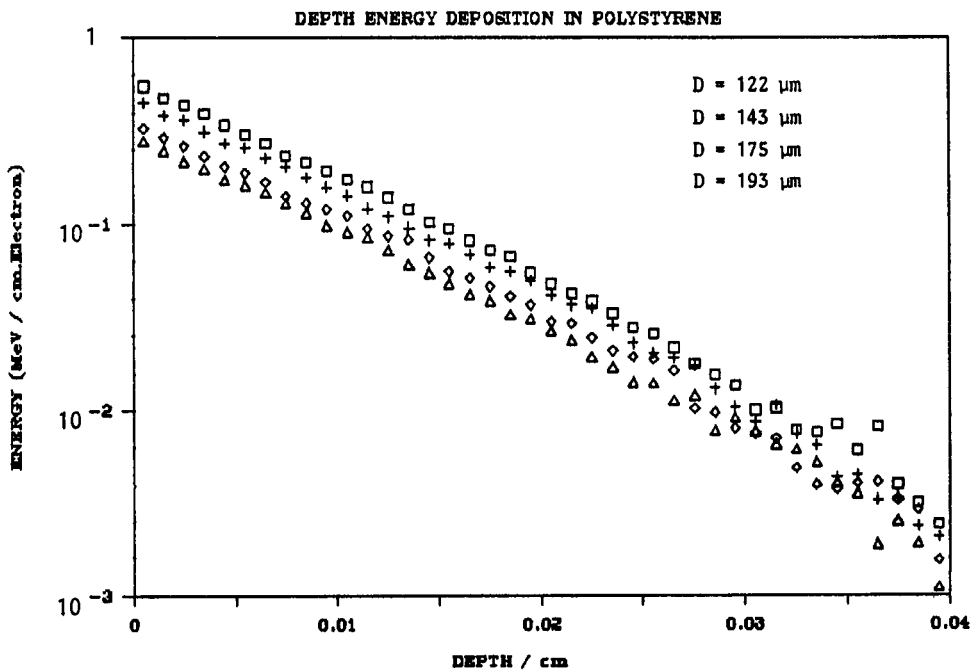


Figure 1 - Cobalt sphere samples

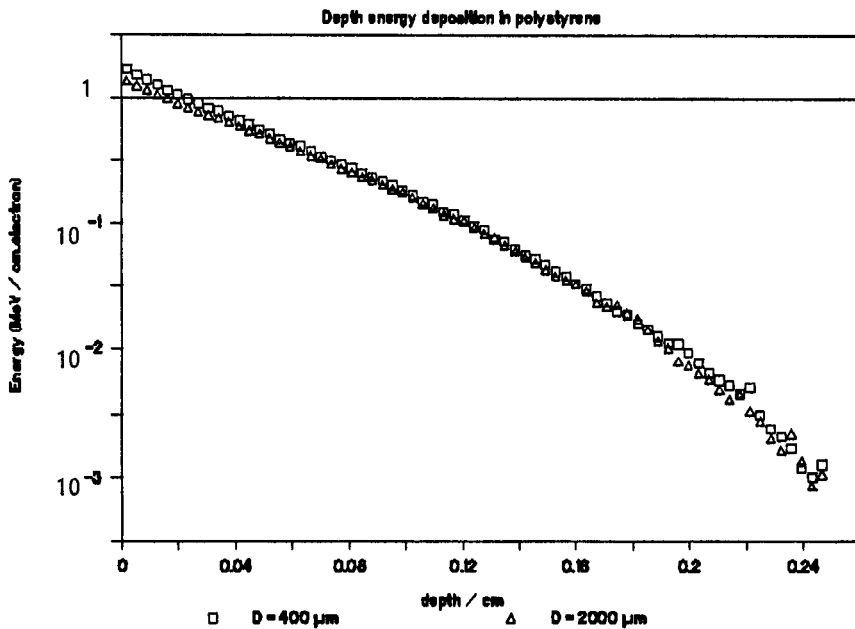


Figure 2 - Thulium disc samples

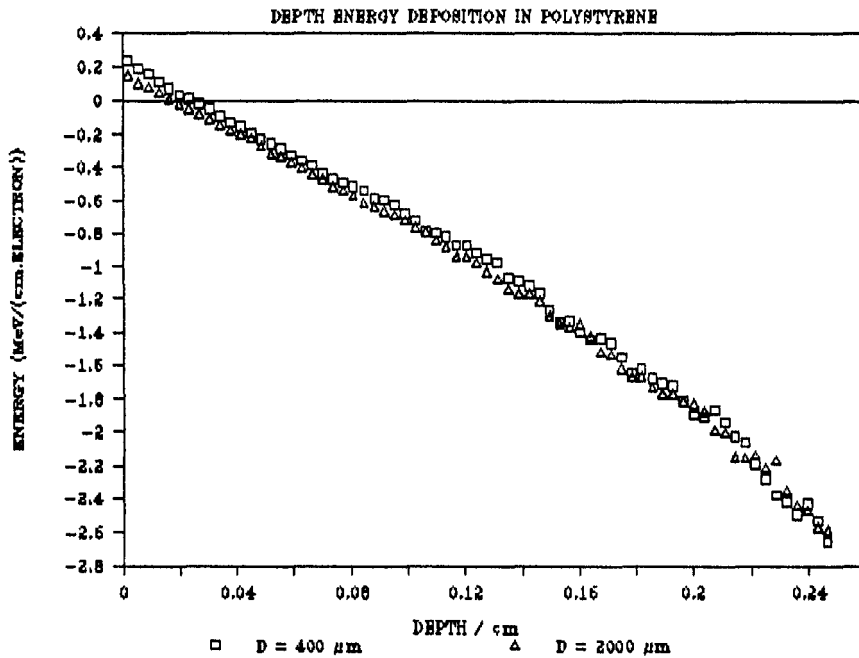


Figure 3 - EGS4: Thulium disc samples

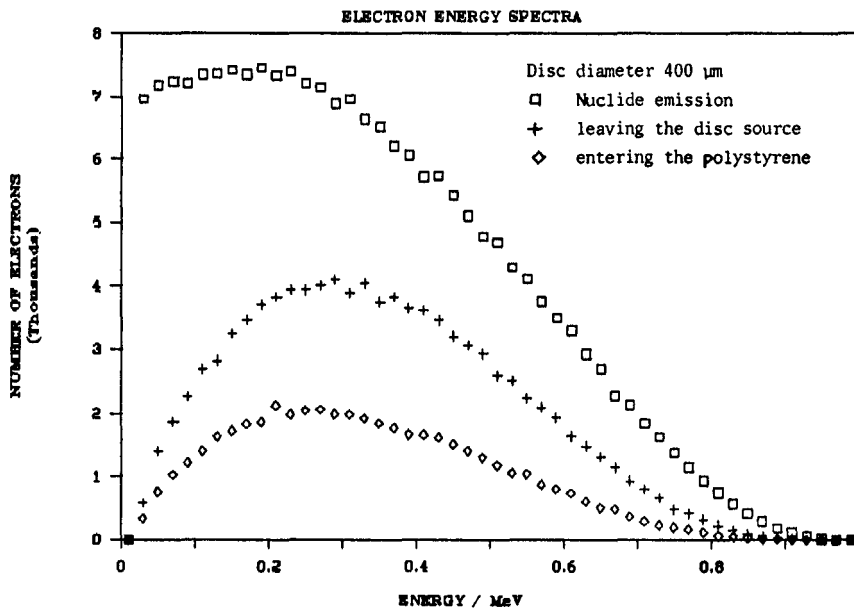


Figure 4 - Thulium disc samples

INHALATION AND INGESTION OF RADIONUCLIDES (NRPB ASSOCIATION)

Contract B16-347b - Sector A14

- 1) Bailey, NRPB - 2) Kendall, NRPB - 3) Stahlhofen, GSF Frankfurt
4) Roy, CEA-FAR - 5) Patrick, MRC Radiobiological Unit
6) Kaul, Bundesamt für Strahlenschutz - 7) Taylor, KfK Karlsruhe

Summary of project global objectives and achievements

This co-ordinated project was formed from three proposals submitted to the CEC Radiation Protection Programme: 890029 "Modelling and experimental studies of inhaled radionuclides in the human respiratory tract" involving NRPB (Bailey); GSF; CEA and MRC; 890082 "The calculation of doses from intakes of radionuclides by inhalation and ingestion" involving NRPB (Kendall) and BfS, and 890333 "Calculations on committed dose equivalents for internal exposures: Consequences of new ICRP recommendations" (KfK/IGT).

The project is thus concerned with the development and implementation of models for evaluating doses from intakes of radionuclides, by both inhalation and ingestion. For the inhalation route it also includes experimental studies designed to provide data required to improve models. Much of the work is linked to the development of ICRP models and recommendations relating to the dosimetry of internally deposited radionuclides. This is a particularly active area at present and will continue to be for the next several years, with the revision of the respiratory tract model, reference man, biokinetic models for individual elements (in conjunction with age-dependent models), and possible new models for bone and GI Tract. These are expected to lead to a full revision of ICRP Publication 30. Several of the participants are members of the relevant Task Groups of ICRP Committee 2:

- Human Respiratory Tract Models for Radiological Protection (Bailey, Roy, Stahlhofen);
- Age-Dependent Dosimetry and Dose per Unit Intake for Members of the Public, AGDOS, (Nosske, Bailey, Kendall);
- Dose Calculations (Kendall, Nosske);
- Reference Man (Roy);

Professor Taylor, as a member of ICRP Committee 2 itself, contributed to all of these, but especially AGDOS.

Following the dissemination in 1990 of proposed changes to the ICRP recommendations, the implications for doses per unit intake and ALIs were explored: *ie.*, changes in tissue weighting factors, w_T , and in the limit on committed effective dose. Consideration was given to whether there was a continuing need for additional limits on individual organ doses. Subsequently, the NRPB's compendium of dose per unit intake factors was updated to take account of the new w_T s in ICRP Publication 60, and other recent information, particularly the NEA review of gastro-intestinal absorption fractions (f_1 values). A detailed investigation of the effect of the new ICRP w_T s, for intakes of over 300 radionuclides in various chemical forms, was produced. On average, committed effective doses (CED) are higher than committed effective dose equivalents (CEDE) by 7% and 20% for intakes by inhalation and ingestion, respectively, but with considerable variation.

Uniformly distributed radionuclides have almost identical CEDs and CEDEs. The greatest reductions are for long-lived bone seekers because of the reduction in bone surface w_T , and the greatest increases are for short-lived ingested nuclides.

A report prepared by the ICRP Task Group on Age-Dependent Dosimetry (AGDOS), covering biokinetic models for a further 13 elements was accepted by ICRP. Age-dependent biokinetic models were implemented for a number of important radionuclides, and results compared between BfS, NRPB and Oak Ridge. A general review of f_1 values was also completed and in some cases revised values proposed. The updating of literature reviews on the biokinetics of those elements not being considered by AGDOS continued, with particular attention to the alkali metals. Work began on the development of generic biokinetic models for those actinides and lanthanides for which little or no direct human information is available.

Uncertainties in dose resulting from variability in biokinetic parameters are being determined. To establish a database and evaluate published biokinetics studies, an application program, based on a fulltext retrieval system, was developed at BfS. A detailed review of biokinetic data relating to cobalt was carried out, with emphasis on factors causing inter-subject differences. Intersubject variations in doses from cobalt intakes were then evaluated. The biokinetic database was modified, following addition of data on thorium.

Consideration was given to developments in computer programs needed to take account of: the proposed new respiratory tract model; radioactive decay products with biokinetic behaviour different from the parent; and age-dependent parameters. Effort was applied to developing methods for calculating doses to the fetus from maternal intakes; implementing models that take account of exchange between blood and organs of deposition (recycling); and providing organ doses as functions of time after intake.

Considerable effort went towards the work of the ICRP Task Group on Human Respiratory Tract Models for Radiological Protection. Extensive reviews were carried out of information relating to respiratory tract physiology, and to particle deposition and clearance. Models were developed to predict aerosol deposition in each respiratory tract region, and particle clearance kinetics. Reference values were recommended and consideration given to associated uncertainties and intersubject variations. A microcomputer program was developed to examine the practical application and radiological implications of the proposed model. A draft report was reviewed by ICRP Committee 2 and the Main Commission in 1991. Revisions were subsequently made to the model, its supporting documents and software, to take account of their comments, and to incorporate new information.

The ICRP Task Group has identified the bronchial epithelium as being of particularly high sensitivity to radiation among the respiratory tract tissues. It has traditionally been assumed that particles were cleared from this region within a few hours, but recent studies, notably at GSF and MRC, have indicated that a large fraction, of the order of 10%, may be cleared much more slowly. This has been included in the proposed new ICRP model, and calculations have shown that it can be the dominant factor in the contribution to effective dose from irradiation of the respiratory tract from long-lived α -emitters. However, it is acknowledged that there are major uncertainties associated with this phenomenon.

Further human studies to investigate this were conducted at GSF. Subjects inhaled radiolabelled particles as a small bolus at the end of a breath. Gamma camera images following inhalation of ^{99m}Tc -labelled Fe_2O_3 particles suggested that the deposit was mainly central, and only about 50% of the deposited activity cleared within a day. After inhalation of sub-micron ^{111}In -oxide the fraction cleared rapidly was even less. Measurements of the dispersion and recovery of inhaled boluses also supported the view that the phenomenon is due to slow bronchial clearance rather than penetration of the bolus to alveoli.

Complementary animal studies were conducted at MRC to address the problem. The use of animals enables the amounts of activity associated with the trachea to be determined directly. Lung clearance and retention were followed, after inhalation of ^{57}Co -labelled fused aluminosilicate particles by rats. The amounts of activity on the surface of the trachea and first bifurcation were greater than expected if all clearance from these areas were rapid. The amounts sequestered in the walls of these airways were similar to earlier findings at MRC. The important question of the extent of delayed bronchial clearance of particles cleared from alveoli was addressed by determining the distribution of particles deposited directly into the sub-pleural alveoli of rats. Results suggest that under these conditions intra-pulmonary airway retention is predominantly peribronchial, mediated by lymphatic drainage, with smaller components resulting from particles remaining on the epithelial surface and possibly from others crossing the airway epithelium into the connective tissue beneath. The histological and image analysis procedures needed for a study to determine the proportion of the airway epithelium covered by ciliated cells were developed. Results of measurements on rat trachea indicate that approximately 50% of the surface is non-ciliated.

Human experimental studies were also carried out to measure:

- Breathing patterns and respiratory parameters, at rest and during exercise, in adults and children.
- Total respiratory tract and nasal deposition of particles in the size range 0.7 - 3 μm inhaled by healthy adults and children, and by two groups of adults with respiratory disease (restrictive and obstructive). Deposition was compared for spontaneous and controlled breathing.
- Total and regional deposition, using sub-micron, monodisperse ^{111}In -labelled indium oxide.
- Long-term (300 d) lung retention of monodisperse Fe_3O_4 particles by magnetopneumography. In six healthy non-smokers, lung retention was characterised by a half-time of 110 days, in agreement with data in the literature.
- Aerosol bolus dispersion and pulmonary function in smokers and non-smokers.

Meetings of participants

A full meeting of the Project Scientific Co-ordinating Committee was held at NRPB Chilton on 22 October, 1990. In 1991, meetings were held in conjunction with the Seventh International Symposium on Inhaled Particles, (Edinburgh, UK, 16-20 September) for those involved in inhalation studies; and the Workshop on Age-Dependent Factors in the Biokinetics and Dosimetry of Radionuclides (Schloss Elmau, FRG, 5-8 November), for those involved in internal dosimetry. Participants also met during meetings of the EULEP-EURADOS Task Group on Deposition and Clearance of Inhaled Particles in the Human Respiratory Tract, and the ICRP Task Groups on Human Respiratory Tract Models for Radiological Protection (Richland, WA., USA 10-15 May, 1990) and on Age-Dependent Dosimetry and Dose per Unit Intake for Members of the Public (Hungerford, UK, 22-26 April, 1991);

The participants submitted a joint proposal to the CEC Nuclear Fission Safety Programme 1991-1994 "Radiation Protection Research Action 1992-1993", to extend and develop the work carried out under this Contract. All submissions were proposed for funding, but two projects will be formed: one concentrating on inhalation studies, and the other on development and implementation of internal dosimetry models in general.

Project 1

Head of project: *Dr. Bailey*

Objectives for the reporting period

- (i) To develop models for respiratory tract clearance and dosimetry of inhaled radionuclides, focussing on the development and implementation of the proposed new ICRP lung model.
- (ii) To carry out experimental studies to characterise the clearance of inhaled particles from the human nasal passage.

Progress achieved including publications

1. Model development

As a contribution to the work of the ICRP Task Group on Human Respiratory Tract Models for Radiological Protection, an extensive review of the literature relating to particle clearance from the human respiratory tract was carried out. Documents were completed on: justification of the approach and assumptions in the proposed clearance model; particle clearance from the extrathoracic airways; particle clearance from the tracheo-bronchial region; particle clearance from the alveolar-interstitial region; and particle retention in the thoracic lymph nodes. These documents formed the basis of the Particle Clearance Annex to the ICRP Task Group Report.

While there have been numerous measurements of mucociliary clearance in the posterior nasal passage, from which inter-subject variation and the effects of various factors can be quantified, data on clearance from the anterior nasal passage are sparse. There is thus a clear need for further experimental studies.

Many studies have been reported on particle clearance from the tracheo-bronchial region. The mucociliary transport rate has been measured in the trachea, but rates in the remaining airways have to be predicted from model calculations. The effects of many factors on lung mucociliary clearance have been investigated: physiological factors (*eg.* age, sleep); diseases; pharmacological agents; pollutants. However, evaluation and comparison of the effects is complicated by interactions, the inhomogeneity of the organ, and the wide variety of end-points measured by different researchers. Experiments have suggested that a significant fraction of material deposited in these airways is not cleared rapidly by mucociliary transport, but there remains great uncertainty about the extent and duration of delayed clearance from the bronchi, and also about whether delayed clearance affects material in transit from more distal airways (See Projects No. 3 and 5). Recent experiments at GSF Frankfurt have indicated that the slow-cleared fraction depends on physical particle size, and model parameters have been set so that this fraction decreases from 50% at 2 μm and below, to a few percent at 7 μm .

Alveolar clearance has been quantified in experimental studies up to a year after inhalation. Measurements following accidental intakes are difficult to interpret, but suggest a component of much longer retention in the lung than assumed in the ICRP Publication 30 model. Similarly, autopsy measurements indicate some very long term (tens of years) lung retention in man.

Reference values for the model parameters describing particle transport from each region of the respiratory tract were specified. Estimates were made of inter-subject variation and uncertainties in the reference model parameter values. Where information was available, modifying factors were recommended for specific population groups. For bronchial and bronchiolar clearance, the ratio of clearance rate in the study group to that in controls was obtained for a number of important factors including sleep, several lung diseases, drugs, and cigarette smoking. For alveolar clearance, it was considered that at present only cigarette smoking had a significant effect that could be quantified.

A revised draft of the Task Group Report has been prepared and will be re-submitted to the ICRP Main Commission in late 1992. The model proposed by the Task Group is more comprehensive than that used in ICRP Publication 30, and is intended for both dosimetry and bioassay calculations. The most fundamental difference is that target cells have been identified in each respiratory tract region, and the doses to these are evaluated directly, instead of simply the mean lung dose. These factors in turn require deposition, clearance and dosimetry to be treated in more detail than in the ICRP Publication 30 model. The new model also relates intake (Bq) to exposure (concentration x time), according to the age and level of physical activity of the subject (See Project No. 4), and taking account of the size-dependent difference between the concentration in the ambient air and that entering the respiratory tract, caused by inertial effects at aerodynamic diameters greater than about 5 μm . In order to examine the practical application and radiological implications of the proposed model, a microcomputer program, LUDEP (Lung Dose Evaluation Program), has been developed. It is a user-friendly menu-driven program which runs on IBM-compatible personal computers. It calculates doses to each region of the respiratory tract; doses to all other specified body organs; and excretion rates and retention curves for bioassay purposes.

The program was used to investigate the implications of the proposed new ICRP model for a range of radionuclides. Doses arising from inhalation of ^{239}Pu in the form of a 1 μm AMAD aerosol in either a relatively insoluble form (eg. oxide) or in a moderately soluble form (eg. nitrate) were determined. An important finding was that an important contribution to the effective dose from irradiation of the respiratory tract arises from the dose to the bronchial epithelium. This results from (i) the assumption that a large fraction of the material (about 50% for a 1 μm AMAD aerosol) deposited in the bronchial region is cleared slowly ($t_{1/2}$ about 20 d); and (ii) the relatively high sensitivity, and hence weighting, attributed to the bronchial epithelium. Doses to other organs are similar to those calculated with the ICRP Publication 30 model for ^{239}Pu -nitrate, because a similar fraction of the inhaled activity eventually reaches the blood, but are lower for ^{239}Pu -oxide, because of lower deposition in the alveolar region.

Similar calculations were performed for several other radionuclides with a range of half-lives and decay emissions. For alpha-emitters, ^{210}Po , ^{234}U , ^{239}Pu , ^{241}Am , ^{242}Cm and ^{244}Cm were used; and for beta-gamma emitters, ^{32}P , ^{59}Fe , ^{57}Co , ^{60}Co , ^{106}Ru - ^{106}Rh , ^{140}Ba - ^{140}La and ^{144}Ce - ^{144}Pr . These doses were compared with the corresponding doses calculated using the ICRP Publication 30 lung model, and the results were incorporated into the Task Group

report.

Model parameters describing absorption into blood for a number of compounds of radiologically significant radionuclides were derived from the time-dependent absorption rates determined by the NCRP Task Group on Respiratory Tract Dosimetry Modeling. However, these were for a limited range of elements and drew only on data obtained in man or large animal species. A clear need was identified to extend this work to utilise the extensive information available from rodent studies.

2. Experimental studies

Because of unforeseen commitments in other work areas, substantially less effort than anticipated could be allocated to experimental studies of the clearance of inhaled particles from the human nasal passage. Nevertheless, some progress has been made. Methods for generation of monodisperse aerosols have been developed further. A vibrating orifice aerosol generator is used to generate the larger ($> 5 \mu\text{m}$) particles required by the study, while a spinning disc aerosol generator is used to generate smaller particles. Equipment has been set up for the calibration of the sodium iodide detector array which will be used for *in vivo* measurements of initial deposition of the aerosol in the inhalation laboratory. Work has also continued on upgrading the low background *in vivo* measurement facilities, with the commissioning of a new array of high resolution germanium detectors, and replacement of the data acquisition and analysis system. Although development of these low background facilities was not carried out under this contract, they will be used for the inhalation studies, and for future human biokinetics experiments.

Publications

Bailey, M.R., Birchall, A., Cuddihy, R.G., James, A.C. and Roy, M. Compartment models for the mechanical clearance of particles from the respiratory tract of humans and laboratory animals (abstract). Proceedings of the Symposium on Particle-Lung Interactions: "Overload" Related Phenomena, Rochester, New York, May 17-18, 1990. *J. Aerosol Medicine*. 3, 68 (1990).

Bailey, M.R., Birchall, A., Cuddihy, R.G., James, A.C. and Roy, M. Respiratory tract clearance model for dosimetry and bioassay of inhaled radionuclides. IN Proceedings of the Third International Workshop on Respiratory Tract Dosimetry, Albuquerque NM, July 1-3, 1990. *Radiat. Prot. Dosim.* 38, 153-158 (1991).

Birchall, A., Bailey, M.R. and James, A.C. LUDEP: A lung dose evaluation program. *ibid.* 38, 167-174.

James, A.C., Gehr, P., Masse, R., Cuddihy, R.G., Cross, F.T., Birchall, A., Durham, J.S. and Briant, J.K. Dosimetry model for bronchial and extrathoracic tissues of the respiratory tract. *ibid.* 37, 221-230.

Bailey, M.R. and Birchall, A. New ICRP dosimetric model for the respiratory tract: A progress report. *Radiol. Prot. Bull.* No. 119, February 1991, 13-20.

James, A.C. and Birchall, A. Implications of the ICRP Task Group's proposed lung model for internal dose assessments in the mineral sands industry. Proceedings of an International Conference on Occupational Health and Safety in the Minerals Industry, Perth, Western Australia, September 10-14, 1990. Perth Chamber of Mines and Energy of Western Australia pp 201-222 (1991).

Bailey, M.R. and Birchall, A. The ICRP Task Group respiratory tract model - an age-dependent dosimetric model for general application. Proceedings of the Workshop on Age-Dependent Factors in the Biokinetics and Dosimetry of Radionuclides, Schloss Elmau, FRG, 5-8 November, 1991. Radiat. Prot. Dosim. 41, 99-100 (1992).

Stahlhofen, W. Scheuch, G. and Bailey, M.R. Measurement of the tracheobronchial clearance of particles after aerosol bolus inhalation. Proceedings of the Seventh BOHS International Symposium on Inhaled Particles, Edinburgh, 16-20 September 1991 (in press).

Project 2

Head of project: *Dr. Kendall*

Objectives for the reporting period

Validate the RAPID database of dose per unit intake factors. Conduct an intercomparison of dose per unit intake factors derived at NRPB with those derived at BfS (Bundesamt für Strahlenschutz).

Provide calculations and comments during the development of ICRP tissue weighting factors for ICRP 60. Explore the consequences for internal dosimetry of the final recommendations.

Assist in dose calculations for forthcoming parts of ICRP 56 on age-dependent and fetal dosimetry. Continue quality assurance on previously published results.

Progress achieved including publications

An intercomparison of dose per unit intake factors was carried out between NRPB and BfS. Agreement for adult values was generally very good (97% of nuclides agreeing to within 10%). No serious disagreements were found for important nuclides and differences could usually be traced to specific features of the modelling. For children, agreement was still good, though the differences were larger than for adults. This is, in part, due to the use of different growth functions and different ways of dealing with the age dependence of Specific Effective Energies. A number of discrepancies were found, many of which could be traced to different assumptions in the modelling.

A good deal of work was carried out to explore the implications for internal dosimetry of the draft recommendations of the ICRP (NRPB-M242). The proposals of February 1990 led to a number of difficulties, most of which were overcome in the final version. However, the low weighting factor recommended for bone surfaces still allows a dose of 1 Sv to this tissue from one year's intake of certain nuclides. However, this is unlikely to be a serious problem in practice:

- a) The old organ dose limit was designed to protect against non-stochastic (deterministic) effects. Many of the nuclides involved are α emitters for which a radiation weighting factor of twenty has been used. This is the value recommended for stochastic effects; for deterministic effects a lower value may be more appropriate.
- b) Many of the nuclides are fairly uncommon (eg. ^{93}Zr) and, in practical situations they are likely to be encountered in mixtures with other materials which do not preferentially irradiate bone surfaces.
- c) We considered committed doses, ie. doses received in the fifty years after intake. If a material has a long physical and biological half life then a substantial fraction of the dose may be incurred decades after exposure and, perhaps, not within the lifespan of

the individual.

A detailed investigation of the effect of the final ICRP tissue weighting factors, w_T , was published (NRPB-R245 and others). In this the new quantity, committed effective dose, was compared with the old committed effective dose equivalent, based on the old tissue weighting factors of ICRP Publication 26, for intakes by inhalation and ingestion of over 300 radionuclides in various chemical forms.

It was found that, on average, committed effective doses were higher than committed effective dose equivalents by 7% for intakes by inhalation and by 20% for intakes by ingestion. The former increase is due largely to the fact that the 10% rule is not applied to the calculation of the new quantity. The larger increase for intakes by ingestion is because of the extra weight now given to organs of the GI tract (stomach and lower large intestine) whose tissue weighting has effectively doubled.

There are, of course, considerable differences between different radionuclides. Those which are uniformly distributed throughout the body give values for committed effective dose almost identical to those for committed effective dose equivalent (eg. ^3H , ^{14}C and ^{137}Cs), since the sums of the two sets of w_T values are equal to one. The most notable reduction in tissue weighting factor is for bone surfaces and for long-lived bone seekers there is a reduction in effective dose, although by less than the reduction in bone surface weighting factor, because there is a contribution to effective dose from the dose to the red bone marrow. As is well known, actinides are bone surface seekers, and for several nuclides of practical importance (eg. some chemical forms of ^{239}Pu and ^{241}Am) committed effective dose is lower than committed effective dose equivalent by a factor approaching two. A similar reduction is seen for ^{210}Po because of the reduced weighting now given to the remainder organs, kidney and spleen, and for ^{235}U where bone surfaces and kidneys receive the highest doses.

Iodine isotopes, and nuclides with iodine daughters, show an increase of about 60% as a result of the increase in the thyroid weighting factor. The greatest increases in committed effective dose are seen for ingestion of nuclides which preferentially irradiate the gastrointestinal tract, particularly those which are short lived. In these cases the increase can almost match the change in weighting factor for stomach, a factor of about two (eg. ^{106}Ru). A similar increase is seen for ^{99}Tc which gives high doses to both gut and thyroid.

A program for deriving retention expressions for recycling compartmental models was successfully ported from the VAX cluster and further developed on a 486 Personal Computer. This enables us to reduce recycling models to a form which is compatible with our existing internal dosimetry programs. It also provides some degree of quality assurance by giving a second means of calculating integrated activities. Using this program the recycling bone model for actinides proposed in ICRP Publication 56 has been incorporated into PEDAL2, the NRPB's established program for calculating doses per unit intake. Initial comparisons with doses published in ICRP Publication 56 are very encouraging. Some discrepancies were found, but these are attributable to known differences in input parameters.

A generalised method for calculating doses to the fetus based on maternal intakes both during gestation and in previous years was developed. Dose to the fetus from activity

in maternal tissues is approximated by the dose to the maternal uterus. Doses resulting from activity in the fetus are estimated using a placental discrimination factor derived from experimental work. This work is included in the first draft of ICRP Publication 56, Part 4.

Software has been written which gives a breakdown of internal doses by year from a series of acute intakes of a mixture of radionuclides. Amongst other things, this enables age dependent risk factors to be applied.

A program for calculating radiation detriment (SPIDER) has been written by another group at the Board. A large set of internal dose data has now been generated so that the detriment associated with external and internal exposures can be assessed using the same measures of risk.

Publications during period

NRPB (1990). "The calculation of doses from internal emitters using a new computer program: Quality control on the RAPID database". Chilton. NRPB-M215 (London, HMSO).

NRPB (1990). "Effectance, Committed Effective Dose Equivalent and Annual Limits on Intake: Some comments on the implementation of the ICRP proposals". Chilton. NRPB-M242 (London, HMSO).

NRPB (1991). "Committed Equivalent Organ Doses and Committed Effective Doses from Intakes of Radionuclides". Chilton. NRPB-R245 (London, HMSO).

G M Kendall, J W Stather, A W Phipps (1990). "Effectance, Committed Effective Dose Equivalent and Annual Limits on Intake: What are the changes". J. Radiol. Prot. 10 (2), 83-93.

J W Stather, J D Harrison, G M Kendall (1992). "Uptake and Distribution of Radionuclides in the Embryo and Fetus - Implications for Dosimetry". In: "Radiation Research: A Twentieth-Century Perspective". Eds: W C Dewey, M Edington, R J M Fry, E J Hall, G F Whitmore. Academic Press (USA).

A W Phipps, G M Kendall, T P Fell and J W Stather. "Revised estimates of dose from internal emitters and implications for ALIs". Radiol. Prot. Bull. 123, 9-14 (1991).

NRPB (1991) "Committed Equivalent Organ Doses and Committed Effective Doses from Intakes of Radionuclides". Chilton, NRPB-M288 (London, HMSO).

NRPB (1991). "Committed Effective Doses at Various Times after Intakes of Radionuclides". Chilton, NRPB-M289 (London, HMSO).

B W Kennedy, A W Phipps, T P Fell and G M Kendall. "The calculation of doses from internal emitters using a new computer program: Quality control on the RAPID database". Chilton 1990, NRPB-M215 (London, HMSO).

A W Phipps, G M Kendall and J W Stather. "Effectance, Committed Effective Dose Equivalent and Annual Limits on Intake: Some comments on the implementation of the

ICRP proposals". Chilton 1990, NRPB-M242 (London, HMSO).

J W Stather, G M Kendall and A W Phipps. "Implications of the ICRP draft recommendations for ALIs". Radiol. Prot. Bull. 113, 9-14 (1990).

T P Fell, G M Kendall and T J Silk (1992). "A Comparison of Age Dependent Specific Effective Energies for the Determination of Internal Doses." IN: "Age-dependent Factors in the Biokinetics and Dosimetry of Radionuclides", Eds: D M Taylor, G B Gerber, J W Stather. Rad. Prot. Dos. Vol 41 Nos 2-4 245-249.

J W Stather, J D Harrison, G M Kendall (1992). "Radiation Doses to the Embryo and Fetus Following Intakes of Radionuclides by the Mother" IN: "Age-dependent Factors in the Biokinetics and Dosimetry of Radionuclides", Eds: D M Taylor, G B Gerber, J W Stather. Rad. Prot. Dos. Vol 41 Nos 2-4 111-118.

Project 3

Head of project: *Dr. H. Stahlhofen*

Objectives for the reporting period

- (i) Investigations of the effect of convective dispersion and cardiogenic mixing on bolus recovery and Effective Airway Diameter measurements.
- (ii) Investigation of human tracheobronchial clearance by measuring lung retention of radio-labelled particles inhaled as a bolus.
- (iii) Measurements of total and regional deposition of ultrafine ($<0.1\mu\text{m}$) particles.
- (iv) Development of an improved statistical and algebraic model of regional deposition in the human respiratory tract: Mathematical formulation of the variability of regional deposition data, and of mass deposition of polydisperse aerosols.
- (v) Magnetometric measurements of long-term retention, macrophage activity and intracellular viscosity.

Progress achieved including publications

(i) With a newly developed inhalation device it was possible to generate small volumes of aerosol (boluses) which could be inhaled by human volunteers during a controlled inhalation of clean air. The inhaled and exhaled aerosol distribution and particle number concentration could be measured. In humans, the effects of breath hold periods (t_b) up to 1 minute on aerosol dispersion and particle recovery have been studied. With boluses applied to volumetric lung depths $>50\text{ cm}^3$, there was a marked increase, followed by a subsequent decrease, in dispersion of the exhaled bolus with increasing t_b . By conducting experiments at increased heart rate it was shown that this effect is a result of cardiogenic mixing of aerosol particles in human airways. The increase in dispersion led also to increased deposition of inhaled particles in inhalation studies with higher heart rates and smaller aerosol particles. This effect of cardiogenic mixing was observed for aerosol particles having aerodynamic diameters (d_{ae}) $<2\text{-}3\ \mu\text{m}$. Particles with smaller d_{ae} are transported to greater lung depths than larger ones during breath holding periods. Similarly the results of sedimentation-derived Effective Airway Diameter (EAD) measurements were found to depend on particle size. By comparing bolus recovery data to model calculations, assuming three different lung models, and both still and stirred settling, it could be shown that aerosol boluses inhaled to lung depths $<50\text{ cm}^3$ do not reach alveolar structures during inhalation.

Aerosol bolus dispersion was measured in smokers and non-smokers after in- and exhalation. No significant differences were found between non-smokers and healthy young smokers (aged between 20 and 30 years). In smokers aged between 40 and 60 years bolus dispersion was significantly greater when boluses were inhaled into volumetric lung depths $>$ about 400 cm^3 . No differences between the smokers and non-smokers were found in parameters of conventional pulmonary function tests.

(ii) The retention of ^{111}In -labelled iron oxide and fused aluminosilicate (FAP) aerosol particles deposited from small boluses in the conducting airways has been measured for particles of different d_{ae} . The slowly-cleared fraction was found to decrease from about 60%

for 1.6 μm particles to about 25% for 6 μm d_{ae} particles. Fe_2O_3 particles were produced labelled with $^{99\text{m}}\text{Tc}$ with sufficient activity to obtain gamma camera images after inhalation of small aerosol boluses. These images showed very central deposition patterns when the boluses were inhaled at the very end of an inhalation. Measuring lung retention with these particles gave similar results to those with the ^{111}In -labelled aerosols: only about 50% of 3.5 μm particles cleared within one day.

(iii) A method was developed to produce monodisperse submicron radioactive particles. Particles of ^{111}In -labelled indium chelate obtained from controlled condensation of APDC vapour are degraded to stable indium oxide particles in a high temperature furnace. This aerosol has been used for human inhalation studies. Regional deposition of the particles was studied in three subjects by measuring clearance from the lungs by scintillation counting. The results showed a very small fraction of rapidly cleared particles (about 5%). The fast-cleared fraction was lower than predicted tracheobronchiolar deposition, and the slow-cleared fraction was higher than predicted alveolar deposition. This indicates that a slow-cleared component of tracheo-bronchiolar clearance also exists for submicron particles.

(iv) The algebraic regional deposition model was based on a statistical analysis of the available data. For extrathoracic and nasal aerodynamic deposition the model could be completely based on experimental results. For tracheo-bronchial and alveolar deposition, theoretical results have also been used. The model was extended to include dependence on age and sex, and natural biological variability. Deposition is expressed as a function of semi-empirical parameters which reflect particle transport and the respiratory data of the subject group considered. Scaling factors account for the dependence on sex, age and for natural biological variability. The mean, and the upper and lower 95% confidence limits, are obtained with the same function. Mass deposition of polydisperse aerosols was included in the model by numerical integration of the model functions. As a result, mass deposition of lognormally distributed aerosols is given explicitly as a function of the geometric standard deviation and mass median diameter.

As a contribution to the work of the ICRP Task Group on Human Respiratory Tract Models for Radiological Protection, a review of the literature on particle deposition in the human respiratory tract was carried out. A deposition model was developed and reference values for the model parameters specified. Following review of the Task Group Report by ICRP Committee 2 and the Main Commission, the model and its supporting documents were revised.

(v) An improved spinning top aerosol generator was used to produce spherical monodisperse Fe_3O_4 particles. These particles have remanent magnetic properties, and can be detected with a SQUID system. Using these particles and the SQUID, the intracellular viscosity and the cell activity of lung macrophages were studied *in vivo*. The macrophage activity has been characterized as a randomization process with a randomization energy of 6.7×10^{-18} J. Thermal energy can be neglected in studying the particle behaviour since it is about three orders of magnitude lower. Viscosity measurements using secondary magnetisation showed a non-Newtonian behaviour of the cytoplasmic viscosity. At shear rates of 0.01 s^{-1} an apparent viscosity of 130 Pa s was measured, which rose to above 1000 Pa s at a shear rate of 0.001 s^{-1} . In a study of the lung retention of these iron oxide particles with 6 healthy non-smokers using the magnetopneumographic method over 300 days, the half-time of long-term retention was determined as about 110 d.

The *in vivo* magnetopneumographic investigations with magnetic Fe₃O₄-particles were extended to *in vitro* studies, with mouse peritoneal macrophages (cancer cell-line J774) or lavaged pulmonary macrophages. Magnetic micro-particles were added to the cells, prepared as adhered monolayers in standard medium. After one day, more than 80% of the particles were phagocytized by the cells. Relaxation, cell motility and intracellular viscoelastic properties were measured and showed results comparable with our *in vivo* studies. This allows us to have an *in vitro* model for the macrophages, where cell function can be influenced by chemical agents and drugs, in order to obtain a deeper understanding of cellular function.

Publications

James, A C, Stahlhofen, W, Rudolf, G, Egan, M J, Nixon, W, Gehr, P, and Briant, J K (1991). The respiratory tract deposition model proposed by the ICRP Task Group. Proceedings of the Third International Workshop on Respiratory Tract Dosimetry, Albuquerque, July 1-3 1990. Radiat. Prot. Dosim., 38 (1-3) 159-165.

Möller, W, Roth, C, and Stahlhofen, W (1990). Improved spinning-top aerosol generator for the production of highly concentrated ferromagnetic aerosols. J. Aerosol Sci. 21(Suppl. 1) S657-S660.

Roth, C, and Stahlhofen, W (1990). Radioactively labelled ultrafine particles for clearance measurements. J. Aerosol Sci. 21(Suppl. 1) S443-S446.

Rudolf, G, Köbrich, R, and Stahlhofen, W (1990). Modelling and algebraic formulation of regional aerosol deposition in man. J. Aerosol Sci. 21(Suppl. 1) S431-S434.

Scheuch, G, and Stahlhofen, W (1990). Dispersion of aerosol boluses in the human tracheobronchial tract. J. Aerosol Sci. 21(Suppl. 1) S431-S434.

Stahlhofen, W and Möller, W (1990). Magnetic measurement of macrophage activity in human lungs. In: Environmental Hygiene II, Eds. N H Seemayer and W Hadnagy, Springer, Berlin, FRG, 213-216.

Stahlhofen, W and Scheuch, G (1990). Messung der menschlichen Mukoziliarclearance. Pneumologie 44, 422-432.

Stahlhofen, W, Möller, W, and Godleski, J (1990). Relaxation measurements with spherical magnetic particles in the human lungs. J. Aerosol Sci. 21(3), 355-362.

Stahlhofen, W, Rudolf, G, and Scheuch, G (1990). Short-term and long-term clearance of particles in the human respiratory tract as function of particle size. J. Aerosol Sci. 21(Suppl. 1) S407-S410.

Stahlhofen, W and Möller, W (1990). Using spherical magnetic particles for testing the intracellular viscosity. J. Aerosol Sci. 21(Suppl. 1) S43S-S438.

Stahlhofen, W (1990). Über die Ablagerungswahrscheinlichkeit von Aerosolteilchen im menschlichen Atemtrakt. In: Lokalthherapie von Luftwegsinfektionen, Eds. H Ganz and E Grill, Georg Thieme, Stuttgart, FRG, 40-44.

Hlawa, R., Wönne, R., Schiller-Scotland, C. F., Gebhart, J., Heyder, J. and Hofmann, D. Untersuchungen zur Totaldeposition monodisperser Aerosole im Atemtrakt von Schulkindern bei verschiedenen Atemmustern. 13. Jahrestagung der Gesellschaft für Pädiatrische Pneumologie, 21.-23.3.1991, Dresden, FRG. (1991)

Köbrich, R., Rudolf, G., Stahlhofen, W. A statistical model of aerosol deposition in the human airways. *J. Aerosol Med.* 4, 34 (1991).

Möller, W., Stahlhofen, W. *In vivo* measurements of hydrodynamic properties and activity of alveolar macrophages. 8th Int. Conf. on Biomagnetism, 18-24 August, Münster, FRG (1991).

Stahlhofen, W. and Möller, W. Magnetopneumography with spherical monodisperse ferrimagnetic particles. *ibid.*

Rudolf, G., Köbrich, R., Stahlhofen, W. Optimum conditions for aerosol inhalation. *J. Aerosol Med.* 4, 34 (1991).

Scheuch, G. and Stahlhofen, W. The effect of heart rate on aerosol recovery and dispersion in human conducting airways after periods of breathholding. *Exp. Lung Res.* 17, 763-787 (1991).

Scheuch, G. and Stahlhofen, W. Deposition and dispersion of aerosols in the airways of the human respiratory tract: the effect of particle size. *Exp. Lung Res.* 18, 343-358 (1992).

Scheuch, G., Schiller-Scotland, C. F., Stahlhofen, W. Evaluation of airway dimensions by means of aerosols using two different particle sizes. *J. Aerosol Med.* 4, 43 (1991).

Scheuch, G., Schiller-Scotland, C. F., Stahlhofen, W. The effect of particle size on the evaluation of aerosol-derived effective airway dimension (EAD). *J. Aerosol Med.* 5, 1-9 (1992).

Schiller-Scotland, C.F., Gebhart, J., Kronenberger, H., Lintl, H., Siekmeier, R.: Effective airway dimensions of healthy smokers and non-smokers derived from aerosol inhalation studies: effect of age. *J. Aerosol Med.* 4, 43 (1991).

Schiller-Scotland, C.F., Hlawa, R., Gebhart, J., Heyder, J., and Wönne, R. Total deposition of monodisperse aerosols in the respiratory tract of children. *J. Aerosol Med.* 4, 42 (1991).

Stahlhofen, W., Möller, W. The behaviour of inhaled spherical iron oxide particles in human lungs: magnetometric studies. In: *Environmental Hygiene III* (Eds.: N.H. Seemayer, W. Hadnagy). Berlin: Springer Verlag, 1-4 (1991).

Köbrich, R., Rudolf, G., and Stahlhofen, W. An algebraic model of mass deposition in man. Proceedings of the Seventh BOHS International Symposium on Inhaled Particles, Edinburgh, 16-20 September 1991 (in press).

Roth, C., Scheuch, G., and Stahlhofen, W. Radioactively labelled ultrafine particles for clearance measurements. *ibid.* (1991).

Rudolf, G., Köbrich, R., Stahlhofen, W., and James, A.C. Regional aerosol deposition in man - a statistic and algebraic model. *ibid.* (1991).

Scheuch, G., and Stahlhofen, W. Effect of settling velocity on particle recovery from human conducting airways after breathholding. *ibid.* (1991).

Schiller-Scotland, C.F., Hlawa, R., Gebhart, J., Wönne, R., and Heyder, J. Particle deposition in the respiratory tract of children during controlled and spontaneous mouth breathing. *ibid.* (1991).

Stahlhofen, W. Scheuch, G. and Bailey, M.R. Measurement of the tracheobronchial clearance of particles after aerosol bolus inhalation. *ibid.* (1991).

Stahlhofen W. New results on magnetopneumography. *J. Aerosol Med.* 4, 41 (1991).

Project 4

Head of project: *Dr. Roy*

Objectives for the reporting period

The development of dosimetric modelling of respiratory tract is under revision by the International Commission for Radiological Protection. The revised model will use recent knowledge in deposition and retention of inhaled aerosols, and should apply to all members of the population, therefore considering the dependence of parameters upon age and influence of disease. As a contribution to such work, the aims of this project were :

Experimental study of total and nasal deposition of inhaled inert particles :

-Nasal deposition of particles in the size range 0.5-10 μ m, inhaled through the nose by healthy adults and patients suffering from rhinitis.

-Total deposition of particles in the size range 0.8-3.3 μ m, inhaled through the mouth by healthy adults, healthy children and two groups of patients with airway obstruction and lung volume restriction, as determined by both clinical examination and respiratory function explored by spirometry : vital capacity (VC), forced expired volume in one second (FEV1) and by plethysmography : residual volume (RV), total lung capacity (TLC) and functional residual capacity (FRC). All these subjects were asked to inhale at the same breathing rate, to better point out the effects of age and disease upon deposition data. These studies were performed in volunteers, with the approval of the Ethical Committee of the hospital Pitié-Salpêtrière Paris.

Data collecting for the choice of recommended values concerning lung volumes, ventilation rates and time budgets of population categories, according to their age, gender and occupation, all parameters that determine the amount of gases and particles inhaled and deposited in the airways.

Progress achieved including publications

1. Experimental deposition studies

An aerosol exposure device with a constant flowrate allowed on-line inspiration, expiration and measurement by laser velocimetry of aerosols concentrations; monitoring of flowrates by a single Fleisch tube and integration of tidal volumes over the breathing period controlled the required ventilation parameters. Particle deposition was calculated from the variations of aerosol concentrations and flowrates downstream the subjects. This methodology improved the data reliability by avoiding sedimentation and impaction during inhaled and expired aerosol storage as was possible in our previous studies.

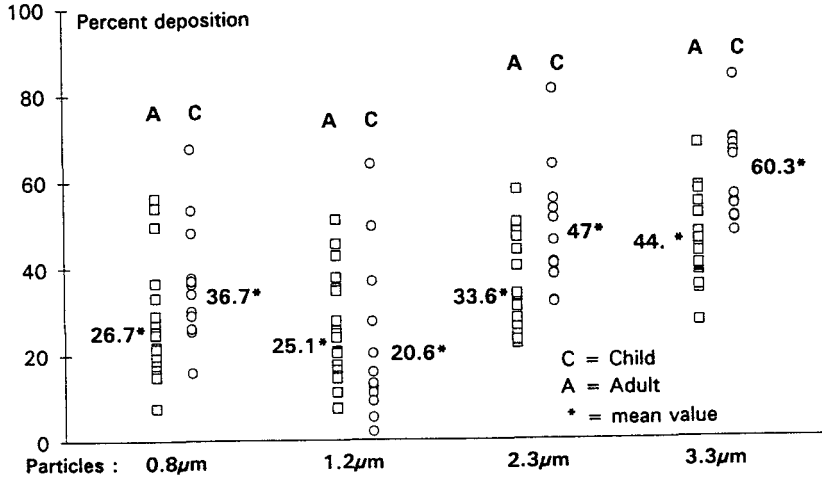
1/. Total deposition of an aerosol containing four sizes of monodisperse particles: 0.8, 1.2, 2.3, and 3.3 μ m aerodynamic diameter, (Dae), inhaled through the mouth was measured, with the same required ventilation rate, tidal volume = 0.5 litre, inspiratory time = 1.5 to 2 second in all the subjects .:

-15 healthy children from 6 to 15 years old;

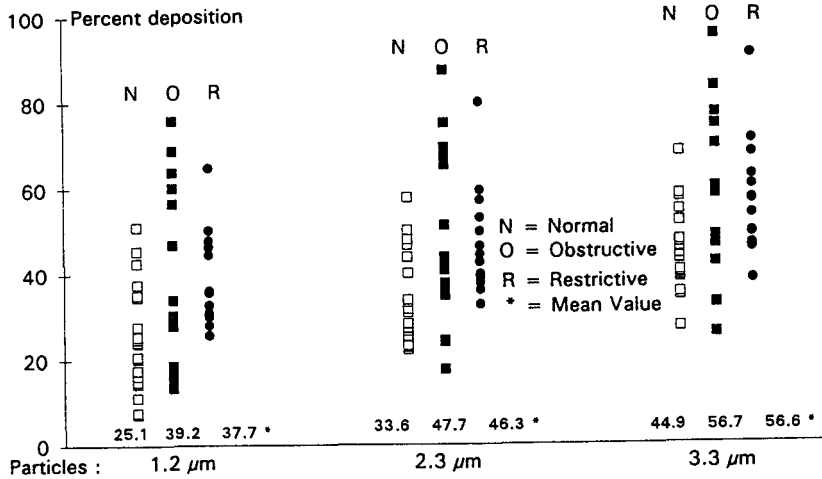
- 20 healthy adults, men and women;

-15 adults suffering from interstitial lung disease, with restrictive lung function;

-15 adults suffering from chronic obstructive pulmonary disease, with obstructive lung function..



Oral deposition in normal adults and children



Oral deposition in normal adults, obstructive and restrictive patients

Deposition data were found higher, in children than in adults: the mean values were respectively in children and in adults: 36.7 ($\sigma=13.4$) and 26.7 ($\sigma=13.2$) for 0.8 μm ; 20.6 ($\sigma=18.9$) and 25.1 ($\sigma=12.5$) for 1.2 μm ; 47 ($\sigma=13.8$) and 33.6 ($\sigma=10.5$) for 2.3 μm ; 60.3 ($\sigma=10.6$) and 44 ($\sigma=9.4$) for 3.3 μm and significantly different by the nonparametric Wilcoxon test, except for 1.2 μm . The smaller particle, (0.8 to 2.3 μm) deposition correlated with FRC.

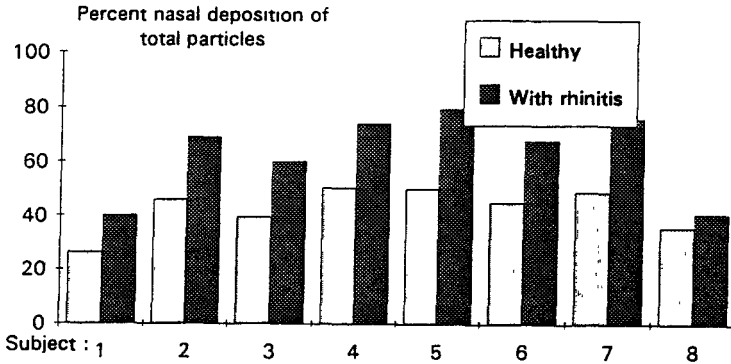
In patients with both diseases the mean values were all found significantly, higher than the normal subjects', except for the 0.8 and 3.3 μm particles in obstructive patients.

This increase in total deposition in children as well as in restrictive patients indicated an effect of the lung volume dimensions smaller in both cases than the healthy adults'. This

was less clear for deposition in obstructives, with reduced airway calibers.

2 / Nasal deposition of a polydisperse aerosol ($0.5 < D_{ae} < 10 \mu\text{m}$) inhaled through the nose was measured in 22 healthy subjects and 21 suffering from infectious rhinitis. Anterior rhinomanometry was measured in each subject. Percent mass deposition, measured by comparing inhaled and expired aerosol concentrations, once by nose, once by mouth controlled breathing, was found higher in subjects with rhinitis, than in the healthy ones. The mean values were respectively in rhinitis and in healthy subjects: 54.5 ($\sigma = 13.4$) and 44.7 ($\sigma = 12.2$) for the total mass; 40.8 ($\sigma = 13.4$) and 27.3 ($\sigma = 9.9$) for the $0.5 < D_{ae} < 3 \mu\text{m}$, mass fraction; 77.3 ($\sigma = 13.7$) and 71.7 ($\sigma = 14.4$) for the $3 < D_{ae} < 6 \mu\text{m}$ mass fraction; they were significantly different, except for the 3 to 6 μm fraction.

Eight subjects who were studied twice: while healthy and while suffering from the disease, showed constantly clear differences in nasal resistances, pressure drop and aerosol deposition, before and during rhinitis; their data were less scattered than the ones observed in the two latter groups, suggesting that nose deposition during disease shows individual variability but is rather constant in one subject.



Particle deposition (total particles) in subjects before and during rhinitis

Subject	Sex	Healthy							Rhinitis					
		Age y	Weight kg	Height cm	Nasal resistance at 0.3l.s-1 kPa.l-1.s	DP kPa 10-3	N.D. 0.5-3 μ %	N.D. 3-6 μ %	N.D. Total %	Nasal resistance at 0.3l.s-1 kPa.l-1.s	DP kPa 10-3	N.D. 0.5-3 μ %	N.D. 3-6 μ %	N.D. Total %
RO	2	26	57	163	0.154	80	19	41	26.5	0.189	87	28	62	40
AN	1	31	64	175	0.165	102	38	62	46.0	0.229	113	55	91	69
BO	1	31	64	165	0.093	100	24	68	39.5	0.144	163	48	77	60
RY	2	53	58	156	0.128	93	32	85	50.5	0.350	207	58	98	74
PH	2	22	58	164	0.196	159	39	72	50.0	0.202	193	70	93	80
GI	2	27	53	160	0.101	23	31	71	45.0	0.110	68	53	89	68
BR	1	48	83	191	0.082	48	30	83	49.0	0.088	33	68	96	76
MHB	2	36	55	166	0.103	34	31	66	36.0	0.221	114	29	64	41
Mean		34	61.5	168	0.128	79.9	30.5	68.5	42.8	0.192	122.3	51.1	83.8	63.4
S.D.		11	9.5	10.9	0.040	44.2	6.6	13.7	8.3	0.082	61.1	15.8	14.3	15.3
Min		22	53	156	0.082	23	19.0	41.0	26.5	0.088	33	28.0	62.0	40.0
Max		53	83	191	0.196	159	39.0	85.0	50.5	0.350	207	70.0	98.0	79.5

2. Data for use in respiratory tract modelling

1/ Reference values for the most relevant physiological parameters to be included in model calculations were reviewed and choices were made for adults and children (newborn, 3 months, 1, 5, 10, 15 years) concerning:

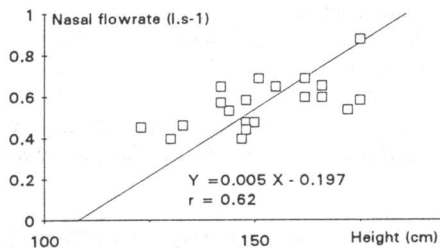
- lung volumes: TLC, VC, FRC, and dead space (V_D)
- ventilation rates:tidal volume (TV) and respiratory frequency (F_R) at rest, at light and at heavy exercise;
- time-budgets and residences of population groups, according to their age, gender and exercise level.

Reference values were thus recommended for lung modelling in several ethnic groups for whom there was sufficient information: Caucasians, Chinese, Japanese, Africans, Afro-Americans, Native Americans, etc...

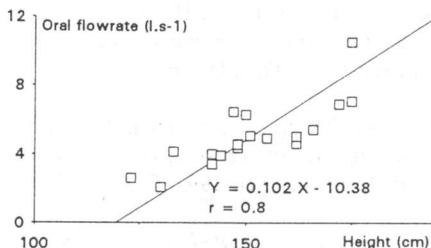
2/Measurement in healthy adults and children of breathing parameters for use in respiratory tract modelling :

Breathing cycle at rest and at light exercise: inspiratory and expiratory times and pauses values, as a function of age.

Comparison of oral and nasal peakflow in children of various ages.

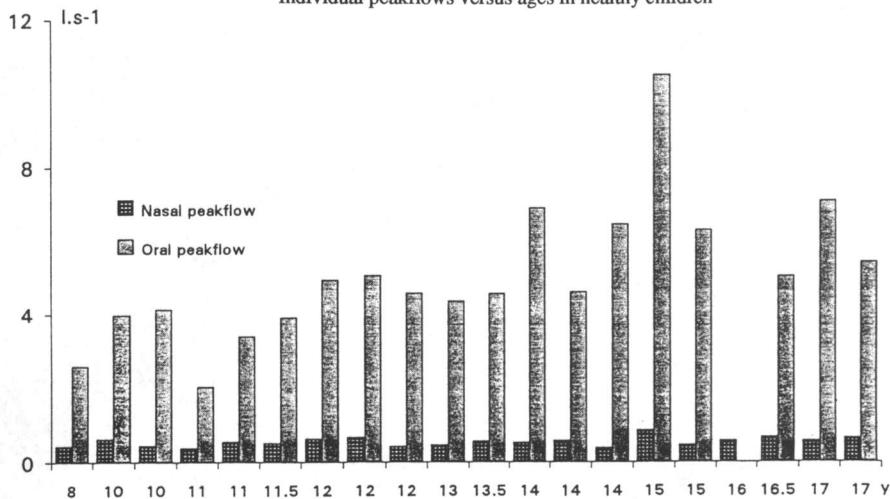


Nasal peakflow versus body size in healthy children



Oral peakflow versus body size in healthy children

Individual peakflows versus ages in healthy children



Publications during the reporting period

Roy M and Courtay C. *Daily activities and breathing parameters for use in respiratory tract dosimetry*. Radiat. Prot. Dosim. 1991, 35, n°3, 179-186.

Becquemin M.H., Swift D.L., Bouchikhi A., Roy M., Teillac A. *Particle deposition and resistance in the noses of adults and children*. Eur. Respir. J. 1991, 4, 694-702.

Bailey M.R., Birchall A., Cuddihy R.G., James A.C. and Roy M. *Respiratory tract clearance model for dosimetry and bioassay of inhaled radionuclides*. In Proceedings of the Third International Workshop on Respiratory Tract Dosimetry. Radiat. Prot. Dosim. 1991, 38, 153-158.

Becquemin M.H., Yu C.P., Roy M.. *Total deposition of inhaled particles related to age; comparison with age-dependent model calculations*. In Proceedings of the Third International Workshop on Respiratory Tract Dosimetry. Radiat. Prot. Dosim. 1991, 38, 23-28.

Roy M., Becquemin M.H. and Bouchikhi A. *Ventilation rates and lung volumes for lung modelling purposes in ethnic groups*. In Proceedings of the Third International Workshop on Respiratory Tract Dosimetry. Radiat. Prot. Dosim. 1991, 38, 49-56.

Yu C.P., Zhang L., Becquemin M.H., Roy M. and Bouchikhi A. *Semi-empirical algebraic modeling of total and regional deposition of inhaled particles in the human lung of various ages*. J. Aerosol Sci. 1992, 23, n°1, 73-79.

Roy M. *Age -related aspects of physiology in respiratory tract modelling*. In: Age-Dependent Factors in the Biokinetics and Dosimetry of Radionuclides. Radiat. Prot. Dosim. 1992, 41, n°2-4, 93-98.

Project 5

Head of project: *Dr. Patrick*

Objectives for the reporting period

- (i) By means of animal studies, to elucidate the physiological basis of the slow (delayed) clearance of inhaled particles from the conducting airways of the respiratory tract.
- (ii) To investigate aspects of the functional morphology of the airway epithelium, in order to explore further the possible reason for the slow clearance of particles.

Progress achieved including publications

1. Particle clearance studies

Two lines of investigation have been followed to study the mechanism of the slow clearance of particles from the large airways of rats.

In the first place particles were administered by inhalation: Fischer rats were exposed to an aerosol of fused alumino-silicate particles labelled with ^{57}Co . From 3 days after inhalation the animals were regularly monitored in a small animal whole body counter. Animals were sacrificed at 1, 7, 28 and 112 days after inhalation, measurements of ^{57}Co excretion having been made during 3-7 days before killing. A measured length of trachea was defined *in situ*, then removed from the carcass and washed repeatedly with saline. The region of the first bifurcation was similarly removed and washed. The ^{57}Co content in the washings and the airway wall were determined by scintillation counting.

From this data the retention of particles in the trachea was analysed into three functional compartments: T_f = material being rapidly cleared by the muco-ciliary mechanism; T_s = slow-moving or stationary material remaining on the surface of the epithelium for an extended period; and T_w = particles sequestered in the airway wall. Expressed as a fraction of the whole-body retention at 1 day after inhalation, multiplied by 10^5 and normalised to a measured tracheal length of 20 mm, T_f decreased from 22 at 7 days to 0.6 after 112 days. Such a large decrease was to be expected for rapid muco-ciliary clearance. In contrast, T_s was 39 at 7 days but only fell to 37 by 28 days and to 7.0 by 112 days. T_w remained between 10 and 15 throughout the experiment. Thus the fraction of the inhaled particles estimated to be slow-moving or to remain stationary on the epithelial surface was the largest of the three compartments at 7 and 28 days after inhalation, and was approximately an order of magnitude greater than the rapidly cleared component at 28 and 112 days. The fraction of particles sequestered in the tracheal wall was similar to earlier findings in this laboratory. The tracheal washings were examined as autoradiographs of cytospin preparations. At the later times it was found that nearly all the ^{57}Co was within macrophages.

This study in the rat has demonstrated that long-term retention of inhaled particles on the surface of large airways is possible, and suggests that such retention involves macrophages which are resident there.

In the second line of investigation particles were deposited in sub-pleural alveoli by microinjection. Of special interest was the extent to which radioactive particles deposited specifically in the alveolar region of the lung could be retained long-term at sites close to the epithelium of the conducting airways.

Approx. 0.05 μ l ^{195}Au -labelled gold colloid was administered by microinjection into the subpleural alveoli of the left lung of 32 rats. The fate of this material was studied for up to 15 months with serial sacrifices at 1, 7, 30, 112, 280 and 462 days. 2-mm slices of fixed lung were prepared and assayed for ^{195}Au . The slice containing the most radioactivity, which was therefore presumed to include the deposition site, was dissected into 2-mm cubes and these were also radio-assayed. Autoradiographs of lung sections were prepared from these and from adjacent slices.

The distribution of ^{195}Au at sacrifice showed that nearly all the gold colloid which was retained in the body was within the respiratory tract. Radioassay of the 2-mm slices indicated that the particles were not appreciably redistributed throughout the lung volume, so that most of the material not cleared from the lung remained close to the deposition site. At the later times after microinjection much of the gold colloid was associated with thickened pleura and adjoining septae. Autoradiography revealed small amounts of ^{195}Au on the surface of the bronchiolar epithelium at all times up to 462 days after microinjection. No penetration to the interstitium was seen by 1 day after microinjection, by which time practically all the particles had been phagocytosed by alveolar macrophages. At all times from 7 to 462 days the largest amounts of ^{195}Au were to be found at peribronchiolar sites. ^{195}Au was also sometimes seen in the connective tissue immediately beneath the airway epithelium. Particles were observed in the vicinity of the hilum after 7-112 days, both in lymphoid as well as in peribronchial tissue.

An approximate estimate has been derived of the amount of colloidal gold associated with the intra- and extra-pulmonary airways after deposition in peripheral alveoli: relative to the contemporary content of the whole respiratory tract this increased to 5% by 30 days and then decreased to 2% up to 462 days. At the same time the thoracic lymph node content increased steadily to 8%. The amount of gold colloid in the extrapulmonary bronchi and the trachea never exceeded 0.2%.

It is suggested that for particles deposited in alveoli, retention associated with airways is predominantly peribronchial, mediated by lymphatic drainage; less retention results from particles either remaining on the epithelial surface or crossing the epithelium into the connective tissue beneath. The significant levels of retention on the surface of the airway epithelium after inhalation, as was seen in the first investigation reported here, would of course include the retention of particles deposited directly on the airways.

2. Functional morphology

A study of the functional morphology of the large airways has commenced to explore the possible basis for the delayed bronchial clearance of particles. Histological and image analysis procedures were established for a quantitative study of the proportion of epithelium in the conducting airways which is not covered with cilia.

Measurements have been made on the trachea of 12 Fischer rats. The circumference of the epithelial surface in transverse sections was determined, together with the sum of the segments of the circumference which are devoid of cilia. Sections from each animal were taken from

proximal, middle and distal trachea. For comparison, each section was divided into 4 quadrants: dorsal, ventral and two lateral.

Analysis of the data revealed a statistically significant variation among the 12 animals studied. For the 4 quadrants of the proximal trachea, the mean \pm standard deviation for the percentage of epithelium that is *non*-ciliated were: dorsal = $45 \pm 13\%$, right-lateral = $51 \pm 8\%$, ventral = $53 \pm 5\%$, left-lateral = $56 \pm 11\%$. These differences were not statistically significant, which was perhaps surprising in view of the generally different anatomical appearance of the ventral segment. Taking all 4 quadrants together, the percentages for the three regions of trachea were: proximal = $52 \pm 7\%$, middle = $60 \pm 6\%$, distal = $51 \pm 8\%$. Again these differences were not statistically significant. The studies will be continued to compare different animal strains and species.

Publications

Patrick G & Stirling C (1992) The transport of particles of colloidal gold within and from rat lung following local deposition by alveolar microinjection, *Environmental Health Perspectives* 97, 47-51.

Patrick G & Stirling C (in press) The redistribution of colloidal gold particles in rat lung following local deposition by alveolar microinjection, *Annals of Occupational Hygiene*.

Project 6

Head of project: *Dr. Kaul*

Objectives for the reporting period

1. Beginning of the development of a computer code to calculate dose coefficients using very general biokinetic compartment models.
2. Development of a fulltext retrieval system to evaluate literature on biokinetics.
3. Study of the uncertainty in doses for isotopes of cobalt due to the variability of biokinetic parameters published in the literature.
4. Study of the effect of the dose limitation system of ICRP Publication 60 on the ALLs of the German Radiation Protection Ordinance.

Progress achieved

1. Development of a computer code to calculate dose coefficients

Work has started to develop a computer code to calculate dose coefficients, the activity content of several organs or tissues and the excretion ratios using very general biokinetic compartment models with an exponential retention function. At present the number of nuclear transformations of the mother nuclide in the various compartments can be calculated if there is no recycling of activity between the compartments.

2. Development of a fulltext retrieval system to evaluate literature on biokinetics

To evaluate literature studies in biokinetics, especially to evaluate uncertainties in dose resulting from the variability in biokinetic parameters published in the literature, an application program based on a fulltext retrieval system has been developed.

For each analyzed element (evaluation of the element thorium with this fulltext retrieval system has been started) two specific databases have been developed, describing the analysis of the activity distribution within the body, and the proposed biokinetic models for systemic activity (including the gastro-intestinal absorption) and their parameters.

For each of the two databases the first part, which consists of three sections, is identical:

- Section 1: Bibliography
names of authors, title, year and type of publication, keywords, etc.
- Section 2: Survey
information such as name and chemical form of the analyzed element, type of study, analyzed species, paths and frequency/duration of exposure, methods of analysis and detection.

- Section 3: Specifications
all the information for each analyzed chemical form of the element and each kind of individual studied (sex and age group, status of health and nutrition), incorporated activity, etc.

After this common part there is a part specific to each of these data bases:

- Analysis data base:
number of samples, activity in various tissues, statistical values, etc.
- Biokinetic data base:
the f_1 value, half-times for the blood, uptake factors and names of compartments to which activity leaving blood is transferred, biological half-times in these compartments and uptake factors and names of the following compartments; the same information is stored for these following compartments.

The structure of the biokinetics data base will be similar to that of the input file to our computer code. It is planned to write a transformation routine to get input files from entries to these data bases.

3. Analysis of the biokinetics of cobalt

The biokinetics of cobalt, an element with some radioactive isotopes important for radiation protection purposes due to their production by activation of neutrons in nuclear power plants, have been investigated.

It is known that in some species cobalt incorporated in its pure inorganic form can also become an organic compound, e.g. by synthesis of vitamin B12. In this form, the retention period of cobalt in the organism is far longer than that of the inorganic form. For this reason, ways to model the biokinetics of cobalt in its organic or inorganic forms have been examined.

In the present report, the f_1 -value was re-evaluated. In ICRP Publication 30, the f_1 -value of cobalt was recommended to be 0.3, but this value is only valid for reference man, a healthy male caucasian of 70 kg. According to literature studies it was found, however, that the gastro-intestinal absorption of cobalt depends on many parameters, e.g. on sex, age and the state of health of the person. One example is the increased uptake of cobalt by persons with iron deficiency. Due to the antagonism of cobalt and iron, such populations (anemic patients, children, women during menses) take up more cobalt than others. For this reason it is recommended, not to consider only one f_1 -value applicable to all groups of the population, but more individual values. In this approach, both the qualitative and quantitative differences of radioactive cobalt, and the individual preconditions of the respective persons should be considered.

The uptake of cobalt is also increased when vitamin C or cobalt in the organic form are involved. The f_1 -value may then rise to 1.

Most of the studies in this field were made through animal experiments. Unfortunately, because the results are very variable and the metabolism is different from one species to another it is very difficult to make analogies from animals to humans.

The influence of more individual biokinetic parameters, developed as described above, on doses has been studied.

4. Effect of ICRP Publication 60 on the ALIs of the German Radiation Protection Ordinance

The effect of the new dose limitation system recommended by ICRP Publication 60 on the annual limits on intake (ALI) of the German Radiation Protection Ordinance has been studied. Because of the lower organ or tissue limits on which the ALIs of the German Radiation Protection Ordinance were based, these limits in almost all cases were determined by organ or tissue doses rather than the effective dose equivalent. For this reason these ALIs were often smaller than those recommended by ICRP Publication 30.

The examination showed that for the most restrictive ALI of each radionuclide and each path of intake the quotient of the German ALI and the ALI according to ICRP Publication 61 which is based on ICRP Publication 60 was in the range between 0.2 and 4, with geometric means of 1.26 for inhalation and 1.13 for ingestion, i.e. on average the German ALIs were larger than the ALIs of ICRP Publication 61. This effect was greatest in those cases where the German ALIs were already based on the effective dose equivalent limit.

Project 7

Head of project: *Dr. Taylor*

Objectives for the reporting period

- a. To review the ICRP biokinetic models for the uptake and retention of elements in the human body with reference to recently published information.
- b. To consider the published information on biokinetic parameters for the elements within well-defined chemical families in the light of the chemical and biochemical properties of the elements in order to provide a sound scientific basis for the prediction of relevant parameters for those elements for which such biokinetic information is not available.
- c. The formulation of revised and improved biokinetic models for adults which will be used in the revision of ICRP Publication 30 which is now necessary in the light of the 1990 Recommendations of the ICRP.

Progress achieved including publications

In the period since this contract began on 1 April 1991, work has continued, in collaboration with the ICRP Task Group on Age-Dependent Dosimetry, on the review of the biokinetic models for the elements sulphur, cobalt, nickel, zinc, strontium, molybdenum, technetium, silver, tellurium, barium, lead, polonium and radium. A report containing revised and age-dependent biokinetic models for these elements, together with calculations of dose per unit intake following ingestion of their most important radionuclides has been adopted for Publication as ICRP Publication 56 Part 2.

In collaboration with Dr J D Harrison of NRPB, the absorption of all elements, except nitrogen, oxygen and the noble gases, from the human gastrointestinal tract has been completed. The previously recommended values for transfer from gastrointestinal tract to blood f_1 have been re-assessed and, in a number of instances, revised estimates have been proposed. This work, which provides the most comprehensive survey available of the information on the absorption of elements from the human gastrointestinal tract, is intended to form a chapter in the new edition of the ICRP publication on reference man.

Work has begun on the development of generic models to predict and describe the biokinetics of members of families of chemically closely-related elements for which little or no direct human information is available. The initial work has been concerned with the actinide and lanthanide series and part of this work will be published in Part 2 of ICRP Publication 56.

In an attempt to identify chemical parameters which could be helpful in the prediction of biokinetic parameters for those elements for which human or animal data are not available, the chemistry, biochemistry and biokinetics of the alkali metal series have been reviewed and compared. The ionic polarizability of the four metals shows an

approximately linear relationship to the longest term component of their biological retention in man. Using only the comparative data on the retention of ^{82}Rb and ^{137}Cs measured in human subjects by Lloyd et al (Lloyd et al., *Radiation Research* 54, 463-478, 1973) a linear regression line with a slope of 0.031 ± 0.007 is obtained which yields predicted values for the half-times of retention of sodium and potassium of 7-11 days and 29-37 days, respectively; these values are in good agreement with those currently assumed by ICRP for the latter two metals. This preliminary study suggests that carefully selected chemical parameters may be helpful in predicting half-times of retention of elements in the human body when direct information is not available, or cannot ethically be obtained.

Publications

International Commission on Radiological Protection (1993) Age-dependent Doses to Members of the Public from Intakes of Radionuclides. Part 2. *Annals of the ICRP in press*.

Taylor, D M (1992). Why is age-dependent dosimetry important? *Radiation Protection Dosimetry* 41, 51-54.

Taylor, D M and Bligh, P H (1992). The transfer of ^{45}Ca , ^{85}Sr and ^{140}Ba from mother to newborn in rats. *Radiation Protection Dosimetry* 41, 143-145.

ASSESSMENT OF INTERNAL DOSE FROM RADIONUCLIDES USING STABLE ISOTOPE TRACER TECHNIQUES IN MAN

Contract B17-029 - Sector A14

- 1) *Roth*, GSF Frankfurt - 2) *Molho*, Università degli Studi di Milano
- 3) *Hislop*, AEA Technology Harwell Laboratory
- 4) *Taylor*, KfK Karlsruhe - 5) *Henrichs*, GSF Neuherberg

Summary of project global objectives and achievements

1. Global objectives of the project

The global objective of this project was to evaluate the use of stable isotopes as tracers in metabolic investigations in humans to meet the accepted and continuing need for more realistic biokinetic data of radionuclides of relevance in radiation protection. The transfer of some relevant radionuclides into the human body via the food chain was to be investigated by experimental studies in man, with particular attention to the reliability and variability of transfer parameters under realistic conditions. Additional investigations on the internal distribution and excretion patterns should improve the metabolic and dosimetric models and consequently the dose assessments of internal exposure.

Elements identified as being of interest were strontium, tellurium, ruthenium, barium, plutonium and other actinides.

Human metabolic data are generally obtained either from measurements after accidental exposure or from experimental studies where radioactive isotopes are used as tracers. Human studies with radioactive tracers, however, whilst very valuable, are becoming increasingly difficult to perform, particularly when healthy persons or especially when children are involved. A promising possibility for metabolic studies in man seems to be the use of isotopically enriched stable elements as tracers.

The metabolic behaviour of strontium, tellurium, ruthenium and barium can be studied by substituting the radioactive isotopes by stable isotopes of the same element as tracers. For plutonium and other highly toxic radioelements, where no stable isotopes exist, stable analogues can be used in metabolic studies. Selected elements of the lanthanide series seem to be promising candidates as actinide analogues in stable element tracer studies, since they show similar chemical properties as the actinides. Therefore, this approach can provide valuable information which is not otherwise obtainable by planned systematic investigations.

2. Tasks involved in the project

The proposed work involved four major tasks:

1. Development and validation of methods.
 - Development of techniques for determination of stable isotopes in biological samples.
 - Exchange of biological samples for the optimisation of analytical methods and of samples from *in vivo* studies to evaluate the reliability of biokinetic parameters as determined by different measuring techniques.
 - Validation of the use of lanthanide series elements as surrogates for plutonium and other actinides.
2. Metabolic investigations.
 - For the elements under study, intestinal uptake, internal kinetics and excretion patterns should be investigated in animals and man. Before stable analogues for the actinides can be applied to humans, it has to be shown that they exhibit essentially the same biokinetics as the actinides they are to model.
3. Improvement of metabolic models.
 - The biokinetic data obtained should help to improve the metabolic and dosimetric models for some of the elements investigated.
4. Dose assessments.
 - On the basis of the obtained data and models, new calculations of internal dose was to be performed for these elements.

This project was not intended to complete all these tasks for all of the elements under study because of the short period of this contract (two years) and the limited resources. Especially for stable actinide analogues, much basic research work is necessary, whereas the state of knowledge and the development of techniques is more advanced for the other elements of interest. However, the expected achievements during this period should provide a valuable basis for further projects in this field.

The goals of this project required the close collaboration of several laboratories to contribute with their special expertise and experience in the different aspects involved. The work of each of the laboratories requires the results obtained by the other ones.

3. Summary of achievements

3.1 Tellurium

Analytical methods for the determination of tellurium and specific tellurium isotopes in solutions and biological materials were successfully developed and applied (Project 1 and Project 2). The occurrence of tellurium in dietary constituents was evaluated and a daily intake between 1 and 10 μg estimated. The feasibility of stable tellurium isotopes for biokinetic investigations was verified by intra-individual comparison with standard radioactive tracer methods in animal experiments (Project 1 and Project 2). Organ distribution of tellurium after oral and intravenous administration was also

evaluated in animal experiments (Project 1). It could be shown that different chemical forms of tellurium (tellurite, tellurate) have significantly different biokinetics in animals. Therefore, although the structure of the metabolic model for tellurium may be the same for different chemical forms, the parameter values are definitely not (Project 1 and Project 2). These differences were also shown in *in vitro* studies with human blood cells (Project 1). Oral administration of tellurium in different forms (tellurite, tellurate, metallic colloid, intrinsically bound in cress) to human volunteers showed significant differences in the excretion patterns and in the f_1 values (Project 1). Since the main chemical form of tellurium in fission products is TeO_2 , we propose from the results of these investigations a f_1 value of 0.3 for radiation protection considerations. This value is somewhat higher than the f_1 value of 0.2 proposed by the ICRP.

In summary: the observations described here verify the ICRP dosimetric model for tellurium isotopes but also show a considerable variability of intestinal absorption and excretion rates in man which should be taken into account in the context of monitoring occupationally exposed persons.

3.2 Ruthenium

Proton nuclear activation analysis (PNA) was successfully developed as a suitable analytical method for determination of stable ruthenium isotopes ^{99}Ru and ^{101}Ru (Project 2). It was proven in animal experiments that the amount of stable ruthenium used in tracer experiments does not perturb significantly the metabolic processes to be evaluated (Project 2).

3.3 Strontium

Mass spectrometric methods have been shown to be suitable for the determination of strontium in biological material. Inductively coupled plasma - mass spectrometry (Project 3) or thermal ionization mass spectrometry (Project 1) can be used to measure isotope concentrations and isotope ratios. ICP-MS was applied to estimate the range of strontium and calcium intake from infant formulae (Project 3). A volunteer study was carried out to investigate the uptake and excretion kinetics of strontium in six male and six female volunteers (Project 3). The uptake pattern between men and women was found to be significantly different. The f_1 values were found to be greater than the value of 0.3 currently used by ICRP. To evaluate strontium metabolism following the uptake of contaminated materials, strontium in different forms (aqueous solution, in milk, in cress, intrinsically or extrinsically labelled) was administered to human volunteers (Project 1). The f_1 values obtained show considerable variations with the form and amount of strontium administered but are generally higher than the ICRP- values, in agreement with the findings of Project 3.

The experiments reported here reveal a strong dependence of the intestinal absorption from the amount administered. The results derived show that for activities which are realistic for the possible case of environmental pollutions, the intestinal absorption is possibly substantially higher than assumed by ICRP. This means that the corresponding

dose coefficients for ingested strontium isotopes may be higher by a factor of up to three as compared to the ICRP values (Project 5).

3.4 Lanthanides (as analogues for actinides)

The validity of the use of europium and gadolinium as surrogates for americium and curium was assessed by comparison of their binding to plasma proteins *in vivo* and *in vitro* (Project 4). The results obtained so far suggest that europium and gadolinium, like americium and curium, bind to transferrin *in vivo* and *in vitro*, although the binding is weak and it seems unlikely that transferrin is the major transport species for any of these four metals *in vivo*. The tissue distribution of europium and gadolinium following injection into rats was compared with previously published data for americium and curium (Project 4). The observed differences between lanthanides and actinides in the uptake and retention patterns do not seem to be significant. The tissue distribution of europium and gadolinium is essentially identical (Project 4). On the basis of these results, europium and gadolinium appear to be acceptable surrogates for americium and curium, at least for studies of the overall biokinetics of these elements in humans.

ICP-MS was successfully used to measure all lanthanide series elements simultaneously in a single sample. Investigations in human volunteers on the daily intake, urinary and faecal excretion of the lanthanide elements showed a close similarity in the form of the abundance curve and the intake and excretion curves, indicating that little or no differentiation is seen between each of the elements across the rare earth group (Project 3). The results showed that the uptake of actinides and lanthanides may be greater than hitherto supposed. In a volunteer study, several lanthanide elements were used as analogues for the behaviour of actinide series elements, and barium as a chemical analogue for radium. For barium, fractional absorption was greater than the recommended ICRP f_1 value of 0.1. For the lanthanide elements, a number of results are in excess of the f_1 value of $3 \cdot 10^{-4}$ reported by ICRP (Project 3).

The results obtained so far from these investigations indicate that possibly a severe revision of the current biokinetic and dosimetric models may be necessary. Until now the data only allow the derivation of upper limits. Further investigations are necessary to provide the data for precise dose calculations..

4. Conclusions

The results of this joint research project, funded partly by the CEC Radiation Protection Research Programme, are very encouraging. A close and fruitful collaboration has been established among the participating laboratories from Germany, the United Kingdom and Italy. It was this cooperation that enabled the progress achieved which in turn provides the basis for the continuation and extension of these studies.

Project 1

Head of project: *Dr. P. Roth*

Objectives for the reporting period

1. Development of analytical methods for measurements of tellurium in biological materials.
2. Investigations on tellurium biokinetics in animals as a prerequisite for human studies.
3. Evaluation of the variability in the intestinal absorption and excretion of tellurium in man.
4. Measurement of strontium uptake following intake of contaminated biological materials and variation with strontium doses.

Progress achieved

1. Tellurium
 - 1.1 General

Tellurium is a rare non-essential element with a natural abundance in the earth's crust of a few micrograms per kilogram [1]. Tellurium can enter the environment of man either due to its increasing use in industry [2] or as radioactive isotopes after a potential nuclear event [3]. Particularly, ^{132}Te and its daughter nuclide ^{132}I contribute up to 8% to the activity release in the first 2 weeks following a slow neutron fission event [4]. This has been proven after the reactor accident at Chernobyl [5,6]. Therefore, a better understanding of the biokinetics of tellurium is required for risk assessment.

Few data are available on the metabolism of tellurium in man. Most of the knowledge of the biokinetics of tellurium has been obtained from animal experiments or from a few accidents with tellurium incorporation in man [7]. Studies on tellurium in humans are therefore highly desirable. In the past, the biokinetics of trace elements has commonly been derived from experiments involving radioactive tracers. Due to the increasing restrictions limiting the in vivo use of radioactive substances in human studies there is a need for methods based on the application of stable isotopes as tracers.

1.2 Analytical

Analytical methods for the determination of tellurium in solutions and in biological materials were successfully developed. Tellurium concentrations in solutions were measured by means of atomic absorption spectrometry (AAS) using the hydride generation technique (spectrometer PE 2380 with hollow cathode lamp and hydride generation system MHS 20; all Perkin Elmer). Tellurium concentrations in biological materials were measured by means of graphite furnace atomic absorption was extracted with MIBK. The reproducibility was $\pm 20\%$ and detection limits of $10 \mu\text{g}/\text{kg}$ of Te wet weight for cress and $0.2 \mu\text{g}/\text{l}$ of Te for urine was achieved. The details of this method are described in Publication 1. The method was successfully applied for the determination of tellurium in blood plasma of rabbits (Publication 2). An analytical method for the measurement of particular stable tellurium isotopes was developed using Secondary Ion Mass Spectrometry (SIMS). The SIMS measurements were carried out by using the dual-beam raster scanning ion microprobe DORAMIS (Doppelstrahl-Rasterionenmikroskopie), an improved version of the DIDA ion microprobe described elsewhere [8]. Details of the optimization

procedure of sample preparation for SIMS analysis are given in Publication 1. About 10 ng of ^{124}Te and ^{126}Te contained in 1 ml of blood plasma are well detectable under these conditions. Analysis of stable tellurium isotopes by proton nuclear activation (PNA) was developed by the University of Milan (See Project 2).

1.3 Tellurium ingestion with foodstuffs

The occurrence of tellurium in various foodstuffs and beverages was investigated. A detailed table of the results obtained is given in Publication 3. The measured tellurium concentrations in vegetables, lettuce, and fruits (i.e. edible plants) is of the order of 1 $\mu\text{g}/\text{kg}$ or below. Only some root vegetables have significantly higher concentrations. This value is about 2 orders of magnitude lower than previously published data [9]. From the ICRP estimates of food supplies for different geographical regions [10], a daily intake of tellurium between 1 and 10 μg can be estimated. This again is at least a factor of 10 lower than previous estimates [11,12]. The main uptake of tellurium occurs with the consumption of edible roots, while beverages do not contribute significantly.

Tellurium concentrations were also measured in body fluids (whole blood, erythrocytes, blood plasma, saliva, urine), hair and fingernails of 8 healthy human volunteers. These values are in broad agreement with previously published data. A detailed table is given in Publication 3.

1.4 Animal experiments

The feasibility of stable tellurium isotopes for biokinetic investigations was verified by an intra-individual comparison with standard radioactive tracer methods in rabbits. Tracer solutions containing enriched ^{124}Te and ^{126}Te (stable) and radioactive tellurium tracers ($^{121\text{m}}\text{Te}$ or $^{123\text{m}}\text{Te}$) were administered simultaneously by gavage and/or intravenously. Blood samples were drawn during the first 2 days after application. The activity of the separated blood plasma was measured by standard gamma ray spectroscopy. After wet ashing and solvent extraction with MIBK the samples were analyzed for stable tellurium by GFAAS and SIMS. The results obtained by applying stable isotopes were found to be in good agreement with the data acquired by using radioactive tracers. These results clearly proved that tellurium metabolism can be investigated applying stable isotopes as tracers. (see Publication 1).

In order to investigate the organ distribution of tellurium after its application, Te was administered orally and intravenously to three swine. These investigations, which were performed in collaboration with GSF Neuherberg (Project 5), served also as a preliminary step before studies in humans. (Publication 4).

The metabolic and dosimetric models for tellurium proposed so far [11] do not assume different biokinetic parameters for different chemical forms of tellurium. This, however, seems to be important, since the toxicity of different chemical forms of tellurium varies considerably. For example, tellurites have been shown to be about 10 times as toxic as tellurates in rats [13]. In an animal experiment with rabbits, stable tellurium was applied as tracer to evaluate the biokinetics of tellurite and tellurate. Tellurium was administered intravenously to four rabbits as sodium tellurite (Na_2TeO_3) or sodium tellurate (Na_2TeO_4). Two rabbits received an additional dose of tellurium perorally. For validation of the methods applied, the intravenous tellurium dose and the oral tellurium dose were labelled with radioactive tellurium isotopes ($^{123\text{m}}\text{Te}$ and $^{121\text{m}}\text{Te}$ respectively). Details of the study are given in Publication 5. The time courses of Te in plasma are shown in Figure 1a and 1b, illustrating the different kinetics of the two chemical forms. The time course of the ratios of Te in plasma and red blood cells (Figure 2) also shows that the valency state of Te seems to be an important factor that determines the passage of Te through cell membranes.

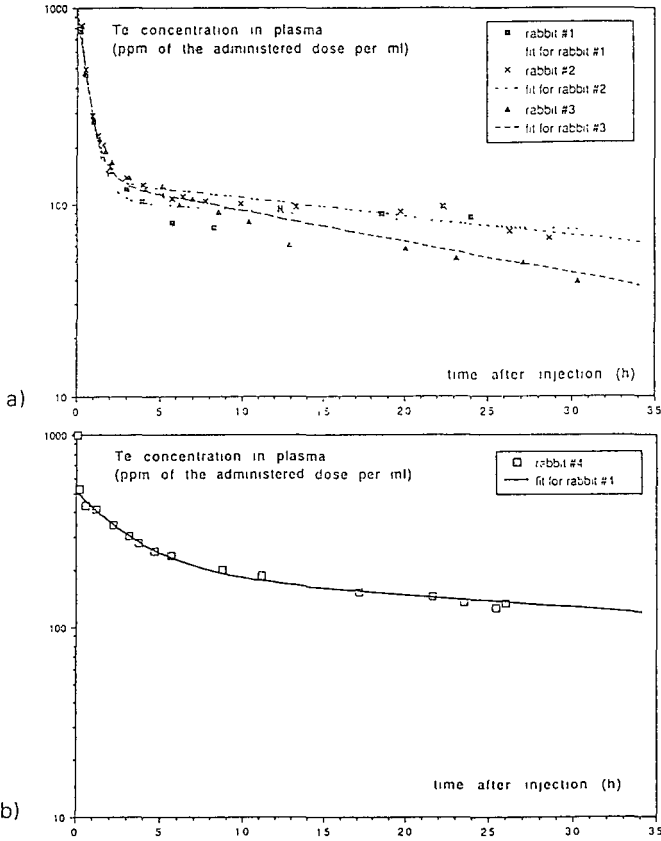


Figure 1: Tellurium concentration in the blood plasma of rabbits after the intravenous administration of sodium tellurate (a) or sodium tellurite (b). The symbols represent the measured values and the curves the best fits to them as obtained from the proposed metabolic model shown in Figure 3 with the model parameters given in Table 1.

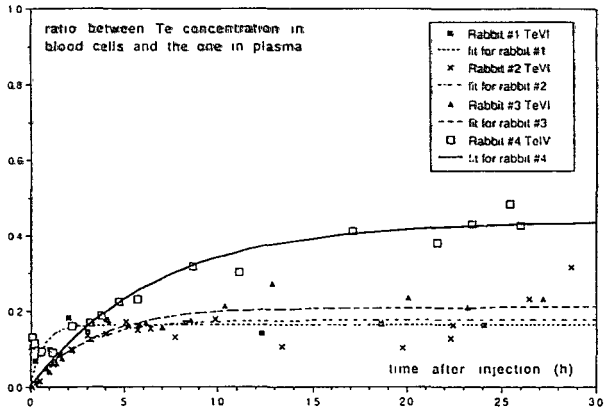


Figure 2: In vivo distribution of tellurium in the blood of rabbits after the intravenous administration of sodium tellurate (Rabbits #1 to #3) and sodium tellurite (Rabbit #4), expressed as the ratio of tellurium in blood cells to tellurium in plasma.

From the tracer data, the compartmental model shown in Figure 3 was postulated and the model parameters as shown in Table 1 were derived. Details of the study are presented in Publication 5.

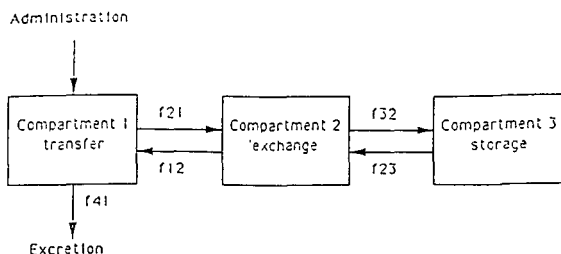


Figure 3 Compartmental model for the metabolism of tellurium.

Table 1 Volumes of the transfer compartment and fractional transfer coefficients for the metabolic model of tellurium as shown in Figure 3

Animal #	Rabbit 1	Rabbit 2	Rabbit 3	Rabbit 4
Chemical form of administered Te	Na ₂ TeO ₄			
Volume of transfer compartment (ml)	980	850	1040	1940
Fractional transfer coefficients (min ⁻¹)				
f ₂₁ (1 → 2)	2.3 E-2	2.5 E-2	2.0 E-2	2.3 E-3
f ₁₂ (2 → 1)	3.0 E-3	4.0 E-3	4.4 E-2	2.2 E-3
f ₂₃ (2 → 3)	4.9 E-6	9.5 E-6	1.7 E-5	9.7 E-6
f ₃₁ (3 → 1)	1.3 E-3	2.9 E-3	3.8 E-3	6.6 E-4

Additional animal experiments were performed in collaboration with the University of Milan to evaluate intestinal tellurium absorption (See Project 2).

1.5 *In vitro* studies

To aid in extrapolating the results of animal experiments to humans, *in vitro* studies with human blood cells were performed. In two experiments, 16 and 20 blood samples from healthy human volunteers were incubated with tellurium as sodium tellurite or tellurate labelled with ^{123m}Te. These incubation studies showed a similar cellular uptake pattern as found *in vivo* in the rabbits, with tellurite being much faster incorporated into cells than tellurate. (For details see Publication 5).

1.6 Volunteer studies

To evaluate the metabolic behaviour of tellurium in man, tellurium in different forms was administered perorally to healthy male volunteers.

A total of 12 investigations were performed in 5 subjects. Te was given as sodium tellurate, sodium tellurite, metallic colloid, and intrinsically bound in cress. For the latter, cress was cultivated with tellurium-containing water in order to provide Te for ingestion in a form which is more equivalent to foodstuffs. (Details are given in Publication 6).

The excretion patterns for these experiments are presented in figure 4, showing that hexavalent Te is more readily excreted than the tetravalent form. Table 2 gives the fractions of Te which were excreted in urine during the first three days after administration.

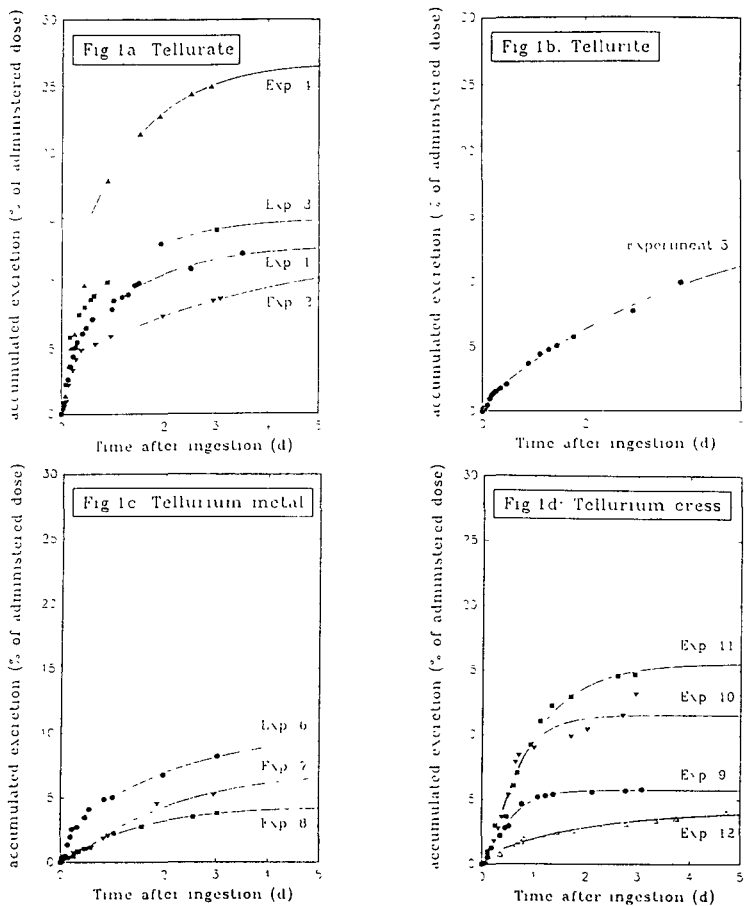


Figure 4. Cumulated renal excretion of tellurium after peroral administration of tellurium in different forms to human volunteers, expressed as percentage of the given dose. a) sodium tellurate (experiments 1 to 4); b) sodium tellurite (experiment 5); c) metallic tellurium (experiments 6 to 8); d) cress intrinsically labelled with tellurium (experiment 9 to 11); raw cress; experiment 12: cress salad with dressing).

Table 2: Results of 12 experiments performed on 5 healthy male volunteers with the peroral administration of tellurium in different forms.

N ^o	volunteer	body mass (kg)	administered Te		3 day excretion (% of dose) ¹	intestinal absorption ² (%)
			(μg) ¹	form		
1	A	65	31 \pm 2	Na ₂ TeO ₃	11.7 \pm 3.0	17.5
2	A	67	57 \pm 3	Na ₂ TeO ₄	8.8 \pm 2.2	18.0
3	B	68	28 \pm 1	Na ₂ TeO ₃	14.1 \pm 3.5	20.0
4	C	76	26 \pm 1	Na ₂ TeO ₄	25.2 \pm 5.4	35.5
5	A	68	15 \pm 1	Na ₂ TeO ₄	7.9 \pm 2.3	21.5
6	A	66	40 \pm 4	Te metal	9.0 \pm 3.0	14.0
7	D	65	25 \pm 2	Te metal	5.2 \pm 1.5	10.0
8	E	90	36 \pm 3	Te metal	3.8 \pm 1.1	6.0
9	A	67	30 \pm 4	Te cress	5.8 \pm 1.7	7.5
10	B	67	18 \pm 3	Te cress	13.3 \pm 3.3	15.5
11	C	76	23 \pm 3	Te cress	15.8 \pm 3.5	21.0
12	A	65	55 \pm 15	Te cress salad	3.2 \pm 1.0	5.5

¹ the range of uncertainty given reflects mainly the reproducibility of the sample preparation and of the AAS tellurium determination
² all values have been rounded to the nearest half percent

Table 2 also shows the values for the intestinal absorption (f_1 -values). For tellurate the mean percentage absorption was 23% with a standard deviation of 9%. This inter-individual variation is larger than the variation expected from the analytical method. The intestinal absorption of tetravalent tellurium was found to be 21.5%. There seems to be no substantial difference in the fractional absorption of the two tellurium salts. For metallic tellurium the absorbed fraction was $10\% \pm 4\%$. The excretion of tellurium after ingestion of Te in cress is delayed as compared to tellurate, indicating also a delayed intestinal uptake. The f_1 -values for Te in cress are also lowered ($14.5\% \pm 7\%$). Addition of a salad dressing to the cress in one volunteer decreased the absorption from 7.5% to 5.5%.

Since the main chemical form of tellurium in fission products is TeO_2 , we propose from the results of these investigations a f_1 -value of 0.3 for radiation protection considerations. This value is somewhat higher than the f_1 -value of 0.2 proposed by the ICRP (11).

2. Strontium

2.1 Analytical

At GSF laboratory in Frankfurt, graphite furnace atomic absorption spectrometry (GFAAS) has been used to measure strontium concentrations in biological materials. For the determination of particular stable isotopes of strontium, thermal ionization mass spectrometry was applied. This method provides the most accurate and precise values of isotope ratios. However, as the element to be analyzed has to be present in the sample in a very pure form, usually a very extensive sample preparation procedure is required, especially to remove interfering alkaline metals. Considerable work capacity had to be used for the development of optimum sample work-up procedures. After wet ashing under pressure and precipitation with ammonium oxalate, no reproducible concentration measurements with GFAAS were achievable. Therefore, a special extraction chromatographic material (Sr-Spec, EICrom, Darien, IL60559, prepacked columns) for the selective sorption of Sr from acidic media was used. Sr-Spec is specific for strontium and is free from interferences by most other metal ions. Biological samples containing Sr to be analyzed (1 ml of urine or 0.2 to 1.0 ml of blood plasma) were dried in a teflon container and wet ashed in a pressure bomb system with 0.8 ml of concentrated nitric acid. To the ashed solution about 2 ml of H_2O were added to obtain 3-molar HNO_3 . This acidic solution was then loaded to the column. Then the column was rinsed three times with 3-molar HNO_3 , and Sr is eluted with up to 6 fractions of 1 ml of H_2O . To avoid contamination with natural Sr, HNO_3 was purified by subboiling distillation and deionized water (Millipore) was used for all the preparatory steps. The whole sample preparation procedure was carried out in a clean bench. Strontium concentrations are determined in each eluted fraction to provide the total Sr amount in the sample. Those fractions with the highest Sr content (usually No.2 to 4) were then mixed together and dried. For mass spectrometric measurements, this residue was redissolved with 5 ml of H_2O and 2 μl of this samples were prepared on the evaporation filaments in the thermal ion source. The analytical recovery of the separation for GFAAS measurements was verified using radioactive ^{85}Sr and was found to be 99.9%.

2.2 Volunteer studies

To evaluate strontium metabolism following the uptake of contaminated materials, strontium in different forms was administered to human volunteers. Oral administration of strontium was either in aqueous solution, in milk, or with cress. Cress was labelled with strontium either extrinsically or intrinsically. For the latter, cress was cultivated with strontium-containing water. The intrinsic labelling provides strontium for ingestion in a form which is more equivalent to foodstuffs. Details of the experimental design are shown in Table 3.

Table 3 - Experimental design of the volunteer studies.

Number of subjects	Isotope	Quantity (μg)	Form	Route
1	Sr-84	270	Carrier free	Injection
	Sr-86	1000	In 100 ml of milk	Oral
2	Sr-86	1000	In aqueous solution (100 ml)	Oral
	Sr-86	100	In aqueous solution (100 ml)	Oral
3	Sr-84	600	300 μg in cress (as intrinsic marker)	Oral
	Sr-86		300 μg in cress (as extrinsic marker)	Oral

Urine was collected for up to 7 days after administration. Blood drawings were performed at different times. After 24 hours, 11.1% of the injected strontium is excreted via urine. In patients, who received radioactive ^{85}Sr for diagnostic purposes, the mean value for 24-hour excretion in urine was 11.8%. The results of this study are presented in Table 4.

Table 4 - Variations of f_1 -values for strontium in man with the form and amount of strontium administered

Quantity (μg)	Form of administration	f_1 -value
1000	In 100 ml of milk	0.27
1000	In 100 ml of aqueous solution	0.52
		0.37
100	In 100 ml of aqueous solution	1.00
300	In cress (intrinsic)	0.68
		0.74
		0.49
300	In cress (extrinsic)	0.47
		0.63
		0.51

The f_1 -values reported here are higher than those currently accepted by the ICRP [11] but are in agreement with those obtained by another analytical approach in Harwell Laboratory as part of this project (See Project 3).

Publications

- [1] Kron, T., Wittmaack, K., Hansen, Ch., Werner, E.: Stable Isotopes for Determining Biokinetic Parameters of Tellurium in Rabbits. *Anal Chem* 63, 2603-2607 (1991).
- [2] Kron, T., Hansen, Ch., Werner, E.: Bestimmung von Tellur im Blutplasma von Kaninchen, In: 5. *Colloquium atomspektrometrische Spurenanalytik* (Ed.: B. Welz). Überlingen: Perkin-Elmer GmbH, 809-814 (1990).
- [3] Kron, T., Hansen, Ch., Werner, E.: Tellurium ingestion with foodstuffs. *J Food Comp Anal* 4, 196-205 (1991).

- [4] Kron, T., Voigt, G., Hansen, Ch., Werner, E.: Tellurium distribution in the tissue of swine after peroral and intravenous administration of potassium tellurite. *In: 6th Intern. Trace Element Symposium. As, B, Br, Co, Cr, F, Fe, Mn, Ni, Sb, Sc, Si, Sn, and other Ultra Trace Elements* (Eds.: M. Anke et al.). Leipzig: Eigenverlag Karl-Marx-Universität, 1342-1347 (1990).
- [5] Kron, T., Roth, P., Hansen, Ch., Ewald, U., Werner, E.: A Metabolic Model for Tellurite and Tellurate. *Trace Elem Med*, in press, (1992).
- [6] Kron, T., Hansen, Ch., Werner, E.: Renal Excretion of Tellurium After Peroral Administration of Tellurium in different Forms to Healthy Human Volunteers. *J Trace Elem Electrolytes Health Dis* 5, 239-244 (1991).
- [7] Hansen, Ch., Kron, T., Werner, E.: Renal Excretion after Peroral Administration of Tellurium to Humans. *Phosphorus, Sulfur, and Silicon* 67, 429-434 (1992).

References

- [1] Kabata-Pendias, A.: *Trace Elements in Soils and Plants*. CRC Press, Boca Raton, (1984).
- [2] Einbrodt, H.J., Michels, S.: Tellur. *In: Metalle in der Umwelt* (Ed. E. Merian), Verlag Chemie, Weinheim, 561-569 (1984).
- [3] Boddy, K., Mathems, R.F., Weller, F.H.: Calculation of tellurium and iodine fission product activities. *Nucleonics* 22, 130-140 (1964).
- [4] Wright, P.L., Bell, M.C.: Comparative metabolism of selenium and tellurium in sheep and swine. *Am J Physiol* 210, 6-10 (1966).
- [5] Smith, F.B., Clark, M.J.: Radionuclide deposition from the Chernobyl cloud. *Nature* 322, 690-691 (1986).
- [6] Strahlenschutzkommission: Auswirkungen des Reaktorunfalls in Tschernobyl auf die Bundesrepublik Deutschland. *Veröffentlichungen der Strahlenschutzkommission*, Band 7, Fischer, Stuttgart (1987).
- [7] Blackadder, E.S., Manderson, W.G.: Occupational absorption of tellurium: a report of two cases. *Br J Ind Med* 32, 59-61 (1975).
- [8] Wittmaack, K.: Design and performance of quadrupole-based SIMS instruments: A critical review. *Vacuum* 32, 65-89 (1982).
- [9] Schroeder, H.A., Buckman, J., Balassa, J.: Abnormal Trace Elements in Man: Tellurium. *J Chronic Dis* 20, 147-161 (1967).
- [10] International Commission on Radiological Protection (ICRP): Report of the Task Group on Reference Man. *ICRP Publication 23*, Pergamon, Oxford (1975).
- [11] International Commission on Radiological Protection (ICRP): Limits for Intakes of Radionuclides by Workers. *ICRP Publication 30*, Pergamon, Oxford (1979).
- [12] Tsalev, D.L., Zaprianov, Z.K.: *Atomic Absorption Spectrometry in Occupational and Environmental Health Practice*, CRC Press, Boca Raton, Vol. 1, 194-196 (1983).
- [13] Franke, K.W., Moxon, A.L.: The Toxicity of Orally Ingested Arsenic, Selenium, Tellurium, Vanadium and Molybdenum. *J Pharmacol Exp Ther* 61, 89-102 (1937).

Project 2

Head of project: *Prof. N. Molho*

Objectives for the reporting period

The main objective for our group was the development of analytical techniques for the quantitative measurement of trace stable isotopes (Ce, Ru, Zr, Te) in biological tissues and the subsequent application to biokinetic studies.

To this aim the project and construction of a new facility for the proton activation of isotopes producing short living radionuclei was foreseen and the optimization of the irradiation parameters for the isotopes of interest was planned. Moreover some biokinetic studies on animals were taken into consideration.

Unfortunately, in consequence of the reduced funding obtained for the project we were in the need to reduce the proposed program; in this view we chose to pay attention predominantly to Te and Ru.

Progress achieved

The mechanical construction of the irradiation chamber has been completed together with the computer controlled driving system. A specific program has been written for the driving system in order to allow a very flexible use of the irradiation setup.

Up to 40 samples can be mounted in the irradiation chamber and every sample can have different and specifically programmed irradiation times. Moreover every sample can be dismantled by means of a mechanism activated from the control room: in this way it is possible to take out the samples from the irradiation room without any direct intervention.

1. Optimization of parameters for stable isotopes determination

With the old irradiation facility the optimization of the proton activation methodology for the specific determination of stable tellurium and of stable ruthenium isotopes in plasma samples has been performed.

A preliminary study of the possible nuclear reactions induced by protons on the stable Te isotopes included in the natural isotopic mixture shows that ^{124}Te and ^{126}Te are the most suitable isotopes to be used as tracers. In fact, via (p,n) reactions they produce radioactive nuclei with half lives (4.18 d and 13.02 d) that allow an off-line detection and a significant reduction of the matrix background. Moreover the decay characteristics of these radionuclei are suitable for the detecting system.

In order to optimize the measurement conditions, the yields of the induced reactions were measured. The data obtained allow to choose the best incident proton energy of 11.2 MeV. Moreover the same data show that at this energy there is no cross interference in the production of the two radionuclides. Interfering nuclear reactions on nuclei of the plasma matrix which can produce the same radioisotopes as those of interest were investigated.

Another important test was performed to check the linear relationship between the intensities of the specific gamma rays and the amounts of ^{124}Te and ^{126}Te present in the samples. The measured ^{124}Te and ^{126}Te content values in samples doped with different known amounts of the isotopes show a very good correspondence with the added values. This fact implies that all the procedure is not affected by hidden systematic errors and in particular there are no problems of volatilization of radioactive products from the sample.

To check the presence of interferences with the gamma transitions of interest the half lives were measured by means of the same lines. The values so determined (4.35 ± 0.3 D and 13.04 ± 0.2 D respectively for ^{124}I and ^{126}I) are in very good agreement with the values reported in literature (4.18 D and 13.20 D).

To determine the detection limits of PNA for ^{124}Te and ^{126}Te , plasma samples enriched with known amounts of these isotopes have been analyzed. Assuming as minimum detectable quantity the amount corresponding to a peak area equal to three times the subtended background statistical fluctuation, we obtained as minimum measurable concentration in plasma the values of 4 ng/ml for ^{124}Te and 6 ng/ml for ^{126}Te .

On the basis of the natural isotopic composition of Ru, of the possible nuclear reactions induced by proton on the Ru stable isotopes and of the decay characteristics of the radioactive isotopes obtainable from such reactions, ^{99}Ru and ^{101}Ru are convenient for our purpose.

In fact the obtained radioisotopes, ^{99}Rh and ^{101}Rh have gamma decay transitions with energy and intensity (353 keV 31.6 %, 544.8 keV 40.1 % relative intensity) suitable for detection and half lives (16 D, 4.34 D) sufficiently long to allow an off-line detection and a significant reduction of the biological matrix background. Vanadium was chosen as reference element for quantitative analysis.

In order to optimize the condition of measurement the proton energy corresponding to the maximum yield of the chosen reactions was determined. To this aim a stack of thin identical targets enriched with the isotope of interest, separated by aluminium foils of appropriate thickness, was irradiated. The ^{99}Ru enriched targets and likewise the ^{101}Ru enriched targets were prepared adding a ^{99}Ru or ^{101}Ru enriched solution to a gel substance to obtain, after drying, a thin layer of the order of 2 mg/cm² with a concentration of Ru isotope of 2 $\mu\text{g}/\text{mg}$. The energy of the incident proton beam was 20.5 MeV and the energy incident on each successive target was calculated. The data obtained allow us to choose the best incident proton energy of 13 MeV; moreover the same data show that no cross interference in the production of the two radionuclides is induced at this energy.

In order to check the response linearity of the method a series of measurements on samples doped with known quantities of ^{101}Ru and ^{99}Ru were performed. The correlation coefficient obtained were $r = 0.9997$ and $r = 0.9999$ respectively.

To determine the detection limits in plasma of PNA for ^{99}Ru and ^{101}Ru , plasma samples enriched with known amounts of these isotopes were analyzed. The minimum detectable concentration in plasma is 2 ng/ml for ^{99}Ru and 4 ng/ml for ^{101}Ru .

2. Biokinetic studies

A study concerning tellurium intestinal absorption was accomplished. The experiments have been performed in animals by stable tracer administration, using the double tracer technique.

Rabbit 1 was given 167 μg of ^{126}Te intravenously and 1.39 mg of ^{124}Te orally and rabbit 2 was given 169 μg of ^{124}Te intravenously and 1.16 mg of ^{126}Te orally. Eleven blood samples were drawn from each rabbit within 480 minutes after the injection.

The concentrations of the tracers ^{124}Te and ^{126}Te in plasma samples withdrawn at different times after administration were determined by PNA analysis. Fig.1 shows the concentrations of the injected and of the orally given tracer in plasma for one rabbit.

By double tracer method, which involves the measurement of the concentrations in plasma of both tracers, the fractional tellurium intestinal absorption of $(4.7 \pm 0.4)\%$ and $(4.0 \pm 0.3)\%$ respectively for the two rabbits was determined.

With the aim to test in animals the feasibility of ruthenium metabolism studies by double tracer technique we needed experimental evidence that the amount of stable tracers involved in the procedure does not perturb significantly the mechanism investigated. The most critical point seems to be the intravenous injection. We carried out experiments on rabbits in order to study the Ru disappearance in plasma after intravenous injection of different amounts of natural Ru in comparison with the Ru disappearance after intravenous injection of radioactive ^{106}Ru .

Four male rabbits were given an intravenous injection of 1 μCi of radioactive ^{106}Ru and about 120 minutes later, except rabbit 1, the three remaining rabbits were given another intravenous injection. The second administration was the following: 2 μCi of ^{106}Ru to rabbit 2, 50 μg of natural Ru to rabbit 3 and 250 μg to rabbit 4.

Fig. 2 shows, as a function of time from the first injection, the specific activity of ^{106}Ru expressed as percent of the administered activity and moreover for rabbits 3 and 4 the figure shows the concentration of natural Ru expressed as percent of the administered quantity.

From the behaviour of the data we can see that injected tracer has a clearing pattern that cannot be reproduced by a single exponential: it is possible to assume that a least two single clearing mechanism with different velocities are active in the time interval considered.

A comparison of the ^{106}Ru clearance obtained for rabbits 3 and 4 with the ^{106}Ru clearance in rabbit 1 show that the administration of a large amount of stable Ru does not introduce any appreciable change in the clearance process.

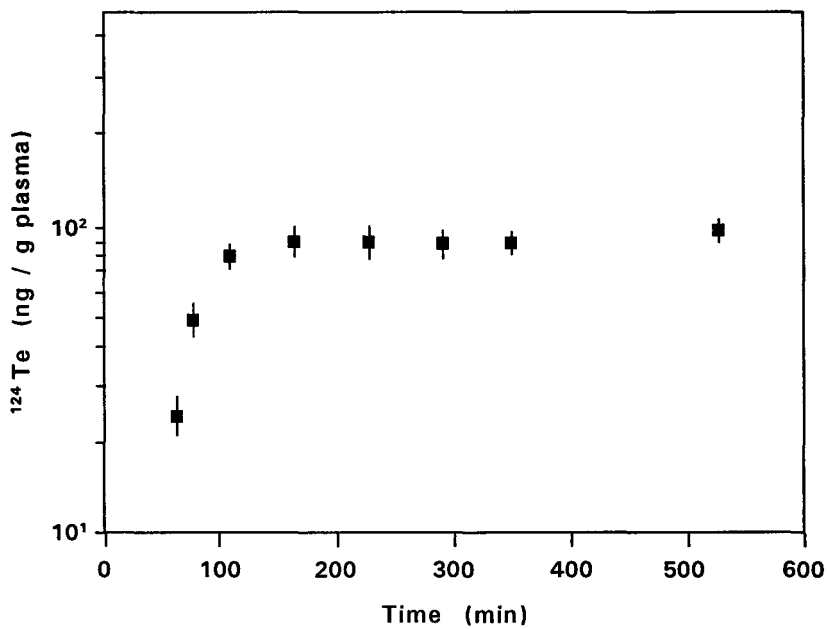
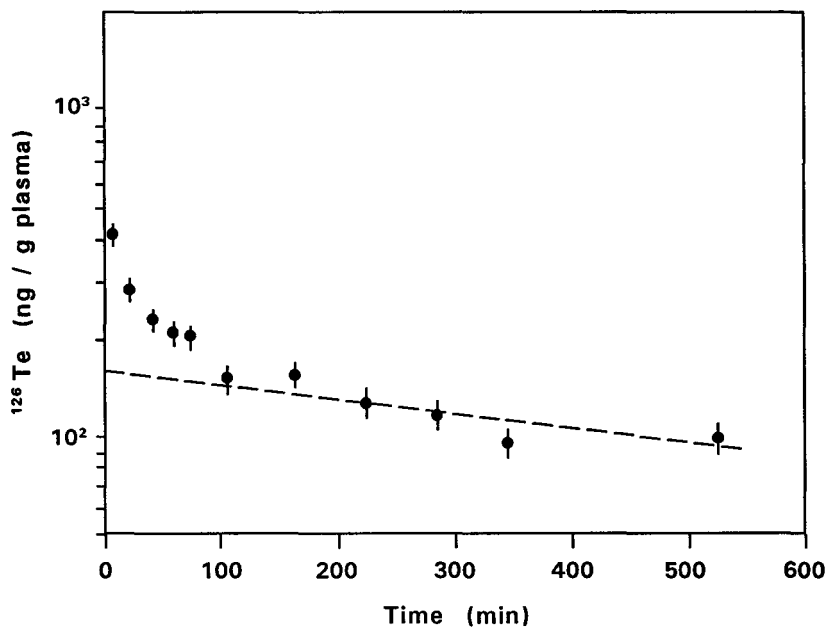


Fig. 1: Concentrations of the injected (^{126}Te) and orally given (^{124}Te) tracer in plasma of one rabbit.

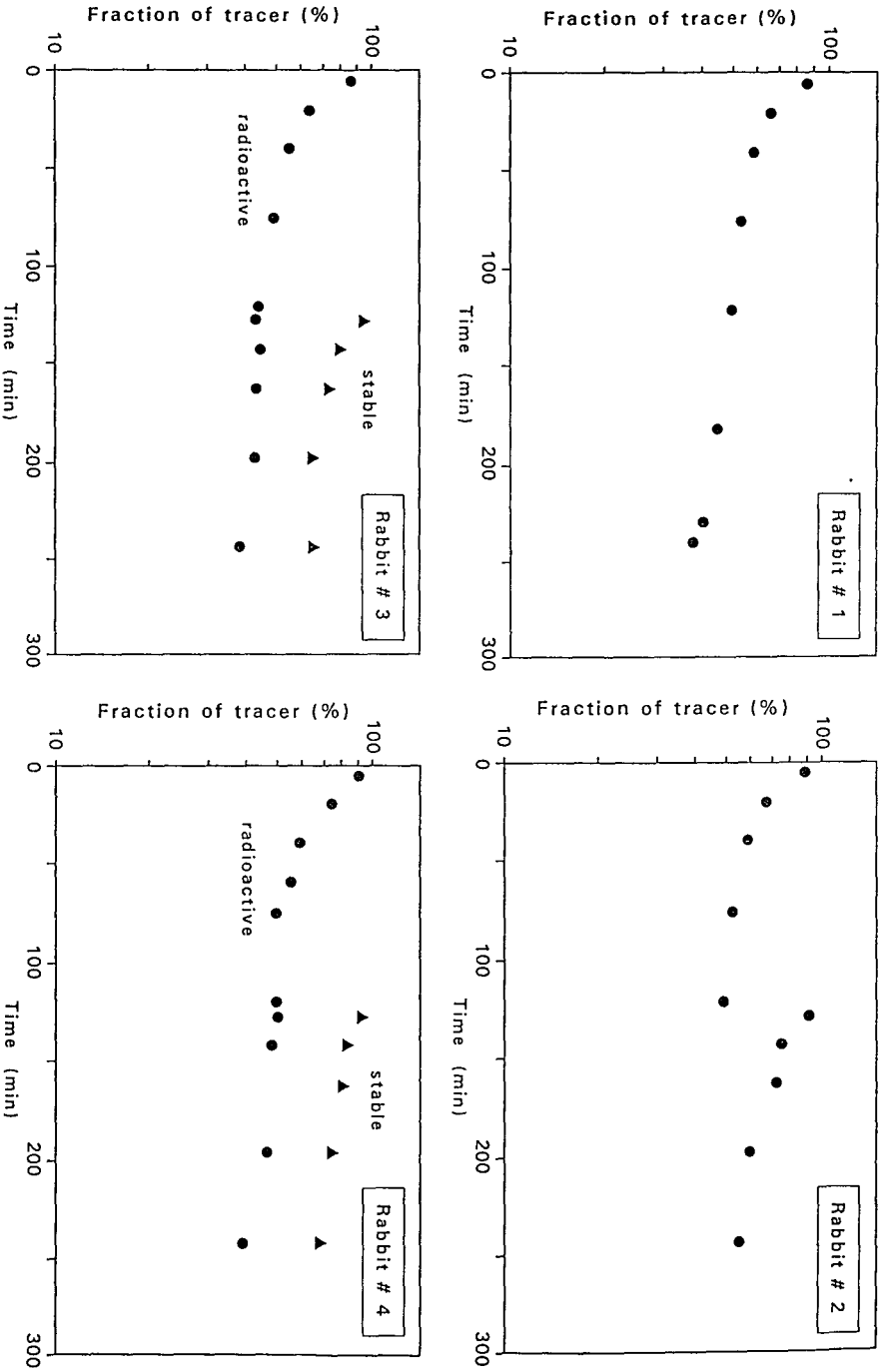


Fig. 2: Time course of intravenously administered ruthenium in four rabbits: Rabbit #1: 1 μ Ci of radioactive ^{106}Ru ; Rabbit #2: 1 μ Ci of radioactive ^{106}Ru ; 2 hours later 2 μ Ci of radioactive ^{106}Ru ; Rabbit #3: 1 μ Ci of radioactive ^{106}Ru ; 2 hours later 50 μ g of natural Ru; Rabbit #4: 1 μ Ci of radioactive ^{106}Ru ; 2 hours later 250 μ g of natural Ru.

Publications

- M.C. Cantone, D.de Bartolo, G.Gambarini, N.Molho, L.Pirola, Ch.Hansen, P.Roth, E.Werner
Tannin influence on iron metabolism studied by means of stable isotopes as tracers.
Phys. Med. 5, 79-82 (1989)
- M.C. Cantone, G.Gambarini, N.Molho, L.Pirola, Ch.Hansen, P.Roth, E.Werner
Studies of elemental metabolism by stable tracers.
European Congress of Med. Phys., Oxford 13-15 Sept. 1990
- A.Giussani, M.C.Cantone, D.de Bartolo, G.Gambarini, N.Molho, L.Pirola, Ch.Hansen, P.Roth, E.Werner
A preliminary study on Te intestinal absorption with stable tracers.
Istituto Nazionale Fisica Nucleare INFN Rapporto TC-91/11, 1991
- M.C.Cantone, D.de Bartolo, G.Gambarini, N.Molho, L.Pirola, Ch.Hansen, P.Roth, E.Werner
Molybdenum metabolism studied by means of stable tracers.
Med. Phys. 19, 2 1992
- Ch.Hansen, P.Roth, E.Werner, M.C.Cantone, G.Gambarini, N.Molho, L.Pirola
Assessment of intestinal iron absorption by means of stable isotopes and proton nuclear activation analysis.
VII Int. Symp. Trace Elements in Man and Animals. Dubrovnik (Yugoslavia), 20-25 May 1990
- Ch.Hansen, P.Roth, E.Werner, M.C.Cantone, D.de Bartolo, G.Gambarini, N.Molho, L.Pirola
Intestinale Eisenaufnahme beim Menschen: Messung mittels stabiler Isotope und Protonenaktivierungsanalyse.
Medizinische Physik 148-149 (1991)
- M.C.Cantone, D.de Bartolo, G.Gambarini, F.Groppi, N.Molho, L.Pirola
Activities of the Medical Physics Laboratory at the Physics Dept. of Milan University, Italy
Applications of Nuclear Techniques. Edited by G.Vourvopoulos and T.Paradellis.
World Scient. Publ., 131-136 (1991)
- N.Molho
Studies of metabolism using stable isotopes as tracers and charged particle activation as analytical method.
Applications of nuclear Techniques. Edited by G.Vourvopoulos and T.Paradellis.
World Scient. Publ., 87-101 (1991)

- M.C.Cantone, D.de Bartolo, G.Gambarini, N.Molho, L.Pirola, Ch.Hansen, P.Roth, E.Werner
Use of stable Ru in assessing Ru clearance: experiments in animals.
VII Congresso Associazione Italiana Fisica Biomedica,
Monteconero 8-12 June 1992

Project 3

Head of project: *Dr. J. Hislop*

Objectives for the reporting period

1. Development of measurement procedures for barium and lanthanide series elements in human excretion samples.
2. Uptake and excretion of lanthanide series elements and barium following oral and intravenous administration to humans.
3. Kinetics of excretion of strontium by oral and faecal routes following oral and intravenous administration.

1. Project background (UK)

The principal objectives of this work in the UK stem from the recommendations of the report by Sir Douglas Black on "Investigation of the possible increased incidence of cancer in West Cumbria" particularly with respect to increased leukaemia and lymphoma diagnosed in young people. This was centred principally around the areas of the UK's nuclear fuel reprocessing plants. Included under the heading of health implications of radioactive discharges were recommendations that more work should be carried out on :

- a) the gut transfer factors at present used, especially for children, with special attention being paid to radionuclides, where this factor is believed to be low, and to organic forms of radionuclides.
- b) the metabolic differences between adults and children with a view to improving the models used.

The lanthanide series of elements are of interest as they show similar chemical properties to the actinide series. Relative retention in bone and liver has been shown to be related to ionic radius for the actinide and lanthanide series of elements (from the data of PW Durbin, in Uranium Plutonium Transplutonic Elements, HC Hodge et al., Eds., Springer-Verlag, Berlin (1973)). Thus, the lanthanides offer potential for use as actinide analogues, to better quantify model source terms.

A number of lanthanide materials have been evaluated for use as actinide analogues in both animals and man, with this work concentrating on the measurement of fractional absorption following oral and intravenous administration, as well as information on relative routes and rates of excretion. This has been carried out for neodymium and dysprosium, each of which has two suitable isotopes. The uptake of samarium, gadolinium and europium has been measured following oral adminis-

tration alone. In addition, work has been carried out using strontium and barium, which are also of significance in environmental radiological protection, especially in critical population groups such as children and pregnant women.

Progress achieved

1. Analytical

1.1 General

Inductively coupled plasma - mass spectrometry (ICP-MS) has been used for measurement of biological samples, with measurement of isotope concentrations and isotope ratios possible down to sub- part per billion (ppb) levels with minimal sample pre-treatment. Preparation typically involves ashing of the samples to remove organic matter, followed by dissolution in a mixture of hydrochloric, nitric and hydrofluoric acid, with silica removed as H_2SiF_6 . Although this has proven adequate for strontium and barium sample preparation, the lanthanide series elements require further separation and pre-concentration on ion-exchange columns, prior to ICP-MS analysis. Analytical recoveries using these ion exchange procedures have been verified using ^{152}Eu , a γ -emitting lanthanide radiotracer.

Having developed the analytical methods required for studies of uptake and metabolism of these elements of interest, a series of studies were carried out to produce relevant background knowledge of the natural occurrence of these elements before proceeding to studies in volunteers.

1.2 Natural occurrence of lanthanides in the diet

A series of measurements were carried out on total excretion samples from a group of six male subjects, and on samples from a Total Diet (excluding beverages). The data obtained in this study are shown in Table 1 and summarised in Figure 1, which shows the rare earth abundance levels (g/tonne crust), intake (mean of 6 whole diet samples in mg), faecal excretion (mean of 6 individuals in mg) and urinary excretion (mean of 6 individuals in mg).

The absolute data in Figure 1 are similar to data in a recent publication (Minoia *et al*, *Sci. Total Environ.* 95 (1990) 89-105), which lends support to the validity of the analytical approach adopted. Data from the current study by ICP-MS for urine are shown compared in Table 2 with data from Minoia *et al*, by neutron activation or atomic absorption analysis, where values are available.

Three conclusions are apparent from Figure 1; the close similarity in the form of the abundance curve and the intake and excretion curves shows that little or no differentiation is seen between each of the elements across the rare earth group. This confirms that the human uptake and excretion mechanisms are likely to be insensitive to the slight chemical differences across the rare earth group of ele-

ments, and therefore possibly, to the small differences between the rare earths and the actinides, their intended analogues. Secondly, absolute faecal excretion levels are very similar to those found in the standard diet samples. The final point which emerges is that the urinary excretion is about 10% of the intake and faecal excretion levels, implying that the uptake of actinides and lanthanides may be greater than hitherto supposed.

Table 1 - Lanthanide excretion and estimated daily intake

Element	Daily Intake (μg)	Urine Excretion ($\mu\text{g} / 24\text{h}$)	Faecal Excretion ($\mu\text{g} / 24\text{h}$)
La	4.7 ± 1.9	0.36	5.2
Ce	8.6 ± 3.6	1.21	9.5
Pr	0.91 ± 0.34	0.09	1.3
Nd	2.9 ± 1.0	0.53	5.3
Sm	0.51 ± 0.19	0.03	0.7
Eu*	-	0.11	0.4
Gd	0.72 ± 0.32	0.07	1.1
Tb	0.08 ± 0.03	0.01	0.1
Dy	0.45 ± 0.16	<0.04	0.8
Ho	0.09 ± 0.03	0.01	0.2
Er	0.26 ± 0.10	0.04	0.5
Tm	0.03 ± 0.01	0.004	0.1
Yb	0.28 ± 0.11	0.04	0.7
Lu	0.04 ± 0.02	<0.01	0.1

* No value given for Eu intake as added ^{152}Eu used as recovery standard

Table 2 - Lanthanides - urine excretion

Element	Urine (ng / 24h) Harwell ¹⁾ ICP - MS	Urine (ng / l) Minoia et al. ²⁾ NAA/ICP-AES/GFAAS
Eu	126 ± 128	110 ± 80
Gd	75 ± 23	< 1000
La	400 ± 149	730 ± 55
Lu	< 9	50 ± 40
Nd	540 ± 87	3840 ± 190
Sm	30 ± 13	55 ± 38
Yb	37 ± 11	28 ± 20

Notes

- 1) Mean of six replicates (four subjects), plus or minus one standard deviation.
- 2) Mean of six to twenty eight subjects, plus or minus one standard deviation.

Abundance, Intake and Excretion of RE's in μg

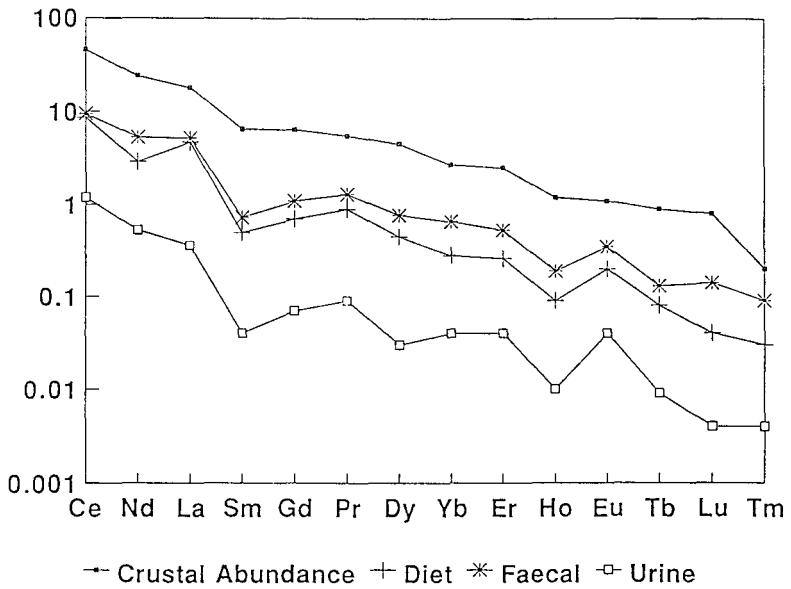


Figure 1 Abundance in g/tonne, and human intake and excretion levels in $\mu\text{g}/\text{day}$ absolute, measured by inductively coupled plasma mass spectrometry, following chemical separation and preconcentration

1.3 Elemental intake from infant formulae

It has already been noted that critical groups, such as children are likely to be at greater risk from environmental radioactivity, especially bone-seeking radionuclides, due to rapid growth. It is hoped that stable isotope tracer studies can be extended to these groups with supplemental doses of enriched calcium and strontium stable isotopes. It would be more scientifically valid if oral intakes to children can be maintained within their normal levels of intake, and hence measurements have been carried out of a number of different milk based infant formulae to estimate the range of strontium and calcium intake which can be found. All formulations were purchased from a retail source. The results are based on a 30 fluid ounce daily intake, with the formulation prepared as per the manufacturers' instructions. The results obtained are shown in Table 3 :

Table 3 - Estimated Ca and Sr intake in 2 month infant

Product	Ca Intake per day (mg)	Sr Intake per day (μ g)
Wysoy	595	402
SMA Gold	457	134
Cow & Gate Premium	576	359
Cow & Gate Soya	452	367
Cow & Gate Plus	676	234
SMA White	517	105
Ostermilk 2	489	131
Local Water (840 ml)	70	347

It can be seen that for milk based infant formulae, daily calcium intake ranges between 450 and 680 mg and that daily strontium intake ranges between 100 and 400 μ g. In addition, known variation in water hardness across the UK will yield at least a factor of 5 in variations of calcium and strontium intake from water. This is borne out by a UK nationwide survey of the strontium content of milk teeth removed for orthodontic reasons, being carried out currently by the Harwell Laboratory. Preliminary results have shown strontium content to vary by as much as a factor of four (unpublished data). This preliminary study has also looked at total daily excretion of calcium and strontium from two infants, with values found to be consistent with the calculated intakes.

Thus, supplementary doses of enriched Ca and Sr can be proposed within this natural variation in intake. The proposed use of calcium and strontium chlorides matches the form in which they are already found as ingredients in the infant formulae.

A protocol for the study of calcium and strontium uptake in neonates has been agreed with the paediatricians at the Institute of Child Health, St. Georges Hospital, London and been approved by the hospital ethical committee.

2. Volunteer studies

2.1 Strontium uptake in male and female volunteers

In order to demonstrate the use of stable isotope techniques, a volunteer study was carried out to investigate the uptake and excretion kinetics of strontium in six male and six female volunteers. Each subject was given a 2 mg oral dose of enriched ^{86}Sr with blood and urine samples taken over the next 30 days.

The uptake pattern between men and women was found to be significantly different; three days after the oral ingestion, mean levels of the ^{86}Sr tracer in plasma were 5.8 times higher in the female volunteers compared with the male volunteers, and urinary excretion was found to be 2.2 times that for the males. In both cases, the subsequent rate of loss of Sr from the blood and excretion via the urine, showed the same biological half-time of wash-out as would be expected. In blood plasma, the mean excess level of the ^{86}Sr tracer was $0.33 \pm 0.11 \text{ ng ml}^{-1}$ for men, and $1.93 \pm 1.47 \text{ ng ml}^{-1}$ for women on Day 3. In urine, the mean excess urinary excretion of the ^{86}Sr tracer on Day 3 was $18.6 \pm 7.5 \text{ ng ml}^{-1}$ for men, and $41.3 \pm 34.9 \text{ ng ml}^{-1}$ for women. Salivary levels of ^{86}Sr were also measured and showed the same trend as for plasma Sr, but with higher relative error.

2.2 Isotope uptake in volunteers (dual administration studies)

An experiment was carried out with two volunteers to determine the fractional gut absorption, and relative urinary and faecal excretion and their kinetics, of stable isotope tracers of lanthanide series elements and barium following dual administration by ingestion and injection. A number of lanthanide elements were used to determine whether problems exist for specific isotopes, with a view to designing a larger study in men and women. Dual isotope administrations of strontium and barium were also carried out at the same time. Quantities of isotopes administered in each case were consistent with levels found in the body for the injection, and consistent with normal daily intakes for ingestion. Details of isotopes administered are given in Table 4. Concentrations of all elements were measured pre-administration by inductively coupled plasma - optical emission spectrometry (ICP-OES). Results for this feasibility study suggested that Nd was the most appropriate lanthanide to measure, and thus Nd and Ba were subsequently administered to a group of 4 men and 4 women, with intakes again shown in Table 4. The main study involved two administrations; one following an overnight fast, the other following a standard breakfast.

Table 4 - Isotopes administered - Feasibility and main studies

Element	Isotope	Natural Abundan (%)	Enriched Abundan (%)	Route	Intake (µg) (Feas)	Intake (µg) (Main)
Strontium	Sr-84	0.56	80.86	Injection	110	25
	Sr-86	9.86	95.80	Oral	1800	1830
Barium	Ba-135	6.59	60.7	Injection	19	12
	Ba-134	2.42	86.22	Oral	69	165
Neodymium	Nd-145	8.30	80.64	Injection	1	9
	Nd-143	12.18	91.06	Oral	19	150
Dysprosium	Dy-160	2.34	69.49	Injection	1	-
	Dy-163	24.9	94.1	Oral	7	-
Samarium	Sm-147	15.0	96.5	Oral	13	-
Europium	Eu-151	47.8	98.91	Oral	12	-
Gadolinium	Gd-157	15.65	99.70	Oral	6	-

Pre-intake samples of blood, urine (24hour) and faeces (24hour) were collected from each volunteer. Following an overnight fast of 12 hours, the volunteers ingested a mixture of enriched stable isotopes as listed above, added to a 300 ml glass of water. At the same time, they were injected with a further mixture of enriched stable isotopes, also listed above, dissolved in 10 ml isotonic saline. The fast was then continued for a further four hours. The volunteers then gave 24 hour collections of urine and faeces for the next 7 days, with further blood samples 24, 72 and 168 hours after isotope administration.

2.2.1 Faeces

Twenty four hour samples were bulked and wet weight recorded. Samples were then ashed to dryness and dry weights recorded. 1g of ash was further oxidised with a mixture of HNO₃ and HF, and ashed to dryness, prior to resuspension with HCl. Samples for lanthanide measurement were then transferred to an ion-exchange column for separation, prior to analysis by ICP-MS.

2.2.2 Urine

Twenty four hour urine samples were bulked and volumes noted. 250 ml aliquots were removed prior to the remainder being boiled down, oxidised and ashed. 1g of ash was further oxidised with a mixture of HNO_3 and HF, and ashed to dryness, prior to resuspension with HCl. Samples for lanthanide measurement were then transferred to an ion-exchange column for separation.

The fractional uptakes of strontium from the gut of the five male volunteers are shown in Table 5. The f_1 data following an overnight fast are greater than those reported by Spencer et al (*Metabolism*, **9**, 916-925 (1960)) and Fujita (1963) who reported fractional uptake figures of 0.22 and 0.14 using radioactive ^{85}Sr in elderly patients following standard diets. The f_1 data are also significantly higher than the adopted ICRP value of 0.3, and in broad agreement with results from GSF Frankfurt. The relative excretion to faeces and urine from the injected dose is given as a F/U ratio, with significant excretion via both routes. The proportion of the injected dose retained in the body after 7 days has also been shown to remain high.

Table 5 - Strontium uptake

Subject		f_1	F / U	Retention
A	Fasted	0.72	1.26	0.58
B	Fasted	0.52	1.98	-
C	Fasted	0.58	0.20	0.57
D	Fasted	0.38	0.47	0.52
E	Fed	0.11	1.13	0.78
Spencer (1960)	Fed Patients	0.22		
Fujita (1963)	Fed Patients	0.14		
ICRP		0.30		

Fractional absorption data for barium are shown in Table 6a for men and Table 6b for women. Again, under fasting conditions, the fractional absorptions are greater than the adopted ICRP f_1 value of 0.1, although those following a standard meal are consistent with the ICRP value. The ratios of faecal / urine excretion for the two subjects were in general agreement with data reported by Newton et al (*Health Physics*, **61**, 191-201 (1991)), who reported ratios of 5-16 following injection of radioactive ^{133}Ba . A greater degree of variation is observed for the data reported from this study. In most cases, the proportion of the injected dose retained in the

body after 7 days remains high. However, some of the female subjects show rapid excretion of the barium dose. This may be related to gender differences in calcium metabolism, which is known to be affected in women prescribed the contraceptive pill or undergoing Hormone Replacement Therapy, and this merits further investigation.

Table 6a - Barium uptake (Male)

Subject		f_1	F / U	Retention
A	Fasted	0.20	0.0	0.99
B	Fasted	0.43	16.5	0.17
C	Fasted	0.29	2.6	0.86
D	Fasted	0.41	1.3	0.86
A	Fed	0.04	3.2	0.86
B	Fed	-	-	-
C	Fed	0.01	6.7	0.72
D	Fed	0.08	6.3	0.67
ICRP 30		0.10		
Newton (1991)			4 - 16	

Table 6b - Barium uptake (Female)

Subject		f_1	F / U	Retention
A	Fasted	0.55	1.6	0.70
B	Fasted	-	-	-
C	Fasted	0.36	200	0
D	Fasted	0.10	4.8	0.35
A	Fed	0.65	8.8	0.23
B	Fed	-	-	-
C	Fed	0.03	25	0
D	Fed	0.13	29	0
ICRP 30		0.10		
Newton (1991)			4 - 16	

For the lanthanides, all showed rapid excretion to urine rather than faeces which is consistent with data from Evans (1990), Biochemistry of the Lanthanides. In the feasibility study, isotopes of Nd and Dy were administered by both routes, but results were inconclusive for Dy due to analytical interferences. Single isotopes of Sm, Gd and Eu were ingested only. A number of f_1 results for Nd in the main study are shown in Table 7. It can be seen that a number of results for the fasted state are in excess of the f_1 value of 3×10^{-4} adopted by ICRP, although again, results for administration following a standard meal are consistent with the ICRP value.

Table 7 - Neodymium uptake

Subject		f_1	F / U	Retention
C	Fasted	1.7×10^{-4}	3.3×10^{-2}	0.85
D	Fasted	2.2×10^{-3}	2.8×10^{-3}	0.86
E	Fasted	5.7×10^{-4}	8.0×10^{-3}	0.92
G	Fasted	4.0×10^{-3}	1.6×10^{-2}	0.93
C	Fed	$< 6 \times 10^{-3}$	5.6×10^{-1}	0.95
H	Fed	5.9×10^{-4}	2.75×10^{-2}	0.90
ICRP		3.0×10^{-4}		

In conclusion, preliminary results suggest that fractional absorption of strontium, barium and neodymium can be enhanced when the metals are taken in the fasted state, which may have significant implications for population radiological protection from environmental radionuclide exposure.

Publications

Dalgarno BG, Brown RM and Pickford CJ
 Strontium metabolism - A study of uptake using the stable isotope ^{86}Sr as a tracer
 Journal of Trace Elements in Experimental Medicine (in press)

Project 4

Head of project: *Prof. D.M. Taylor*

Objectives for the reporting period

To assess the validity of the use of europium and gadolinium as surrogates for americium and curium by comparison of their binding to plasma proteins *in vivo* and *in vitro*, and of the tissue distribution of europium and gadolinium following injection into rats in comparison with previously published data for americium and curium.

Progress achieved

In the first stage of the work gel chromatographic studies, using Sephacryl S-300, DEAE-Sepharose and Blue Sepharose, established that both ^{152}Eu and ^{153}Gd were bound to the iron transport protein transferrin in rat serum. The binding pattern was identical following the labelling of serum either *in vivo*, by intravenous injection of the metal-citrate complexes, or *in vitro* by addition of the radionuclides, as the nitrilotriacetate complexes, to rat serum. The separation of the ^{152}Eu - and ^{153}Gd -transferrin complexes on the ion-exchange medium DEAE-Sepharose suggested that the complexes dissociated on the gel, however, affinity chromatography on Blue Sepharose CL-6B established that about 20% of the total serum radioactivity was associated with transferrin after both *in vivo* and *in vitro* labelling. This latter finding is in good agreement with observations of Cooper and Gowing [1] with americium and curium.

Spectroscopic studies of lanthanide binding to human transferrin using UV-difference spectroscopy, with either nitrilotriacetic acid or, better, iminodiacetic acid as carrier chelator, showed that for both europium and gadolinium a maximum of two atoms of the metal could be bound to each molecule of transferrin. Other studies in which the binding of ^{152}Eu and ^{153}Gd to human transferrin *in vitro* was studied by centrifugal ultrafiltration, using Millipore *Ultrafree MC* filters to separate protein-bound from non-protein-bound metal, also established that a maximum of two lanthanide atoms could be bound per transferrin molecule. Saturation of ^{152}Eu - or ^{153}Gd -labelled transferrin with non-radioactive iron resulted in the release of the bound lanthanide. All these results suggest that the iron binding sites on the transferrin molecule are probably involved in binding the lanthanides.

The data from the spectroscopic and ultrafiltration studies were used together with the computer speciation programmes PHREEQE and GOALSEEK to derive values for the conditional stability constants for the Eu- and Gd-transferrin complexes. The calculations yielded the following values for the overall stability constants:

Europium-transferrin $\log \beta = 9.10 \pm 0.09$ (n=9)

Gadolinium-transferrin $\log \beta = 9.37 \pm 0.10$ (n=9)

These constants are somewhat greater than the log K_1 values of 6.8 for the Gd-, 6.3 ± 0.7 for the Am- and 6.5 ± 0.8 for the Cm-transferrin complexes which were calculated by Harris [2]. More work is needed to refine the calculations of the stabilities of the Eu- and Gd-transferrin complexes, but the present data do suggest that the binding of the trivalent lanthanides and actinides to transferrin is much weaker than that of Fe(III) or Pu(IV), for which values of $\log \beta \approx 22$ have recently been derived using similar methods [3]. The relatively weak binding of Eu(III), Gd(III), Am(III) and Cm(III) to transferrin suggests that this protein is probably not the major carrier for any of the four metals *in vivo*.

In a small scale animal study, ^{152}Eu and ^{153}Gd were administered simultaneously as the chlorides to 4 to 6 months old female Sprague-Dawley rats by intravenous injection. Groups of three animals were sacrificed at 1, 2, 4, 8, 16, 32 and 64 days post injection and the content of the two radionuclides in the various organs was determined using differential γ -ray spectroscopy. The results for the uptake and retention in liver and skeleton are listed in Table 1 which also presents similar data for ^{241}Am and ^{244}Cm , taken from unpublished studies carried out in male August-Marshall hybrid rats of approximately the same age [Taylor, D. M., unpublished data 1960-1975].

Table 1

The distribution of europium, gadolinium, americium and curium in the liver and skeleton of rats

Time [days]	Liver				Skeleton			
	Eu	Gd	Am	Cm	Eu	Gd	Am	Cm
1	17.0	13.2	40.3	32.2	59.6	61.8	48.2	36.3
2	16.6	12.0			62.7	65.4		
4	10.8	10.8	17.4	22.9	61.6	61.6	47.8	40.8
7-8	6.9	4.4	22.9		58.4	60.4	48.6	32.0
16	3.2	2.1			54.1	57.0		28.8
28-32	1.0	0.7	3.6	3.6	53.5	55.0	51.4	34.8
64	0.4	0.3	1.7	2.5	45.4	49.2	44.9	35.8

Errors are not shown but were generally <10% of the mean value

The data in Table 1 show that for all four metals the total deposition in liver and skeleton was 70-80% of the activity entering the blood. Retention of europium and gadolinium in the skeleton was virtually constant over the whole period of

observation, a finding which is consistent with the half-times of ≈ 1600 - 1700 days previously reported for the retention of americium and curium in the skeleton of August-Marshall rats [4]. The initial deposition of americium and curium in the liver was higher than that of europium or gadolinium, but these variations probably reflect differences in the age, gender and strain of the rats used. Similarly the deposition of americium and curium in the skeleton appears to be lower than that of the two lanthanides. However, despite the differences in the organ uptake, the retention pattern of the four elements studied is essentially similar.

Gel chromatographic analysis, on Sephacryl S-300 of the distribution of ^{152}Eu and ^{153}Gd amongst the proteins of the liver cytosol, at 2 days after intravenous injection of the radionuclides, showed that the vast majority of the radioactivity was associated with ferritin, an observation in full accord with those made previously for ^{241}Am and ^{244}Cm [5].

On the basis of the information gained from this study, europium and gadolinium appear to be acceptable surrogates for americium and curium, at least for studies of the overall biokinetics in humans. The more detailed studies of the mechanisms of binding in cells and tissues and of the speciation of the trivalent actinides and lanthanides in the body fluids and tissues, which will form the extension of this contract, should identify any areas of difference which might lead to serious difficulties in using lanthanides as surrogates to predict the detailed biochemical and biokinetic behaviour of the trivalent lanthanides within specific organs or tissues.

References

- [1] Cooper, J.R. and Gowing, H.S., *International Journal of Radiation Biology*, **40**, 569-572, 1981.
- [2] Harris, W. R., *Inorganic Chemistry*, **25**, 2041-2045, 1986.
- [3] Yule, L., A comparison of the binding of plutonium and iron to transferrin and citrate. PhD Thesis, University of Wales, Cardiff, UK, 1991, p. 126.
- [4] Taylor, D.M., *Health Physics*, **45**, 768-772, 1983.
- [5] Popplewell, D.S., Boocock, G., Taylor, D.M. and Danpure, C.J., The subcellular distribution of americium and curium in rat liver. In *Radiation Protection Problems relating to Transuranium Elements.*, Commission of the European Communities, EUR 4612 d-f-e, pp 203-333, 1971.

Publications

Taylor, D. M., Duffield, J. R., Williams, D. R., Yule, L., Gaskin, P. W. and Unalkat, P. Binding of f-elements to the iron-transport protein transferrin. *European Journal of Solid State and Inorganic Chemistry*, 28 (Suppl.) 271-274, 1991.

Yule, L., Quinn, G. W., Taylor, D. M. and Williams, D. R. Speciation of rarer metals in biological systems. in *Metal Compounds in Environment and Life 4, (Interrelations between Chemistry and Biology)*, Science and Technology Letters Northwood, UK/ Science Reviews Inc, Wilmington, DE, USA, pp. 421-428, 1992.

Yule, L., Quinn, G. W., Taylor, D. M. Ultrafiltration and spectroscopy of plutonium transferrin. in *Metal Compounds in Environment and Life 4, (Interrelations between Chemistry and Biology)*, Science and Technology Letters Northwood, UK/Science Reviews Inc, Wilmington, DE, USA,, pp. 39-45, 1992.

Unalkat, P., Miller, L. E., Quinn, G. W., Taylor, D. M., Williams, D. R. Eu-Transferrin and Gd-Transferrin Complexes. Poster presented at "*Metal ions in Biological Systems*", Royal Society of Chemistry, Newcastle upon Tyne, UK 8-12 July 1992.

Unalkat, P., The use of europium and gadolinium as analogues for americium and curium respectively, M.Phil Thesis, University of Wales, UK, submitted September 1992.

Project 5

Head of project: *Dr. K. Henrichs*

Objectives for the reporting period

- Review of the available data base for the elements relevant for the project (Sr, Te, Ce, Ru, Pu and higher actinides).
- Preparatory investigations for the calculation of age dependent dose coefficients on the basis of the newly measured data.
- Evaluation of the measured data aiming to improve the biokinetic data base (models) suitable for dosimetric purposes.
- Calculate dose conversion factors for the radionuclides of interest, taking into account dependencies on age and on chemical characteristics as well as influences of the nutritional composition as far as investigated experimentally.

Progress achieved

By means of a literature review the scientific basis for the biokinetic models and data of all radionuclides tabled in ICRP Publication 30 was checked. Based on the results of this review and on the results of the German Reactor Safety Study (Phase B), those elements were identified which are of importance for the protection of the general public (in case of an accident in nuclear facilities) but for which relevant dosimetric data and their variabilities are not sufficiently well known. These elements were strontium, cerium, barium, ruthenium, tellurium, zirconium, plutonium and higher actinides.:

1. Strontium

Although many data have been published on the biokinetics of Sr in man, the importance of Sr isotopes in the context of possible reactor accidents makes it necessary to quantify the variability of biokinetic parameters with regard to the dosimetry with special emphasis on children;

2. Zirconium and cerium

One of the most important parameters, the fractional uptake (f,) of ingested activity from the gastro-intestinal tract to the blood, is very uncertain for those elements;

3. Ruthenium and tellurium

The biokinetic data available are only taken from a few animal experiments, and

excretion patterns in humans are completely unknown. For the interpretation of monitoring data reliable biokinetic information is urgently needed;

4. Transuranium elements

Their high dose factors, their importance in nuclear industry, and the public concern of these elements urge the need to improve the comparatively poor data base for the assessment of monitoring data as well as for the calculation of dose coefficients for various ages. Especially, the influence of uptakes with food on the fractional absorption into blood are nearly unknown.

Based on these results, the most important parameters to be investigated within this project were identified as the f_1 -factors for the nuclides mentioned as functions of age taking into account the influences of food constituents.

In cooperation with another CEC funded project (coordinated by the University of Lund, Sweden) and as a preparation for the future calculations of dose coefficients for children, radiation transport simulations were performed on the basis of a phantom representing a 5-week old baby. This baby phantom was developed by means of computer tomography pictures of a real child; so this phantom gives a better description of the anatomy for this individual. The results of the simulations however, do not deviate significantly from those derived by using a standard anthropomorphic mathematical phantom, which simplifies the real anatomy substantially. This result is to be confirmed by another similar calculation for a 7 year old child.

The evaluation of the biokinetic data derived from the experiments of this project mainly consists in the improvement of existing biokinetic models and data bases. In this context, a sensitivity analysis of the dosimetric models is needed, requiring very high computer power. Therefore, a specially designed computer code was developed, optimized for the solution of very complex and rather stiff systems of differential equations. This code was implemented on a parallel computer system (consisting of 32 high speed processors) thus enabling the very fast calculation of retention functions.

The first evaluation of the biokinetic data derived until now from the experiments described before, gave the following results:

5. Tellurium

- The f_1 -values measured in humans in this project show a considerable variability but agree sufficiently well with the value adopted by the ICRP.
- Although the ICRP assumptions for the dosimetric model are mainly based on few animal studies, the excretion rates which may be derived from the ICRP model agree well with the observations made for humans in this project.
- Further metabolic investigations in humans are necessary to quantify the doses of incorporated tellurium isotopes to the skeleton.

- In summary: the observations described here verify the ICRP dosimetric model for tellurium isotopes but also show a considerable variability of intestinal absorption and excretion rates in man which should be taken into account in the context of monitoring occupationally exposed persons.

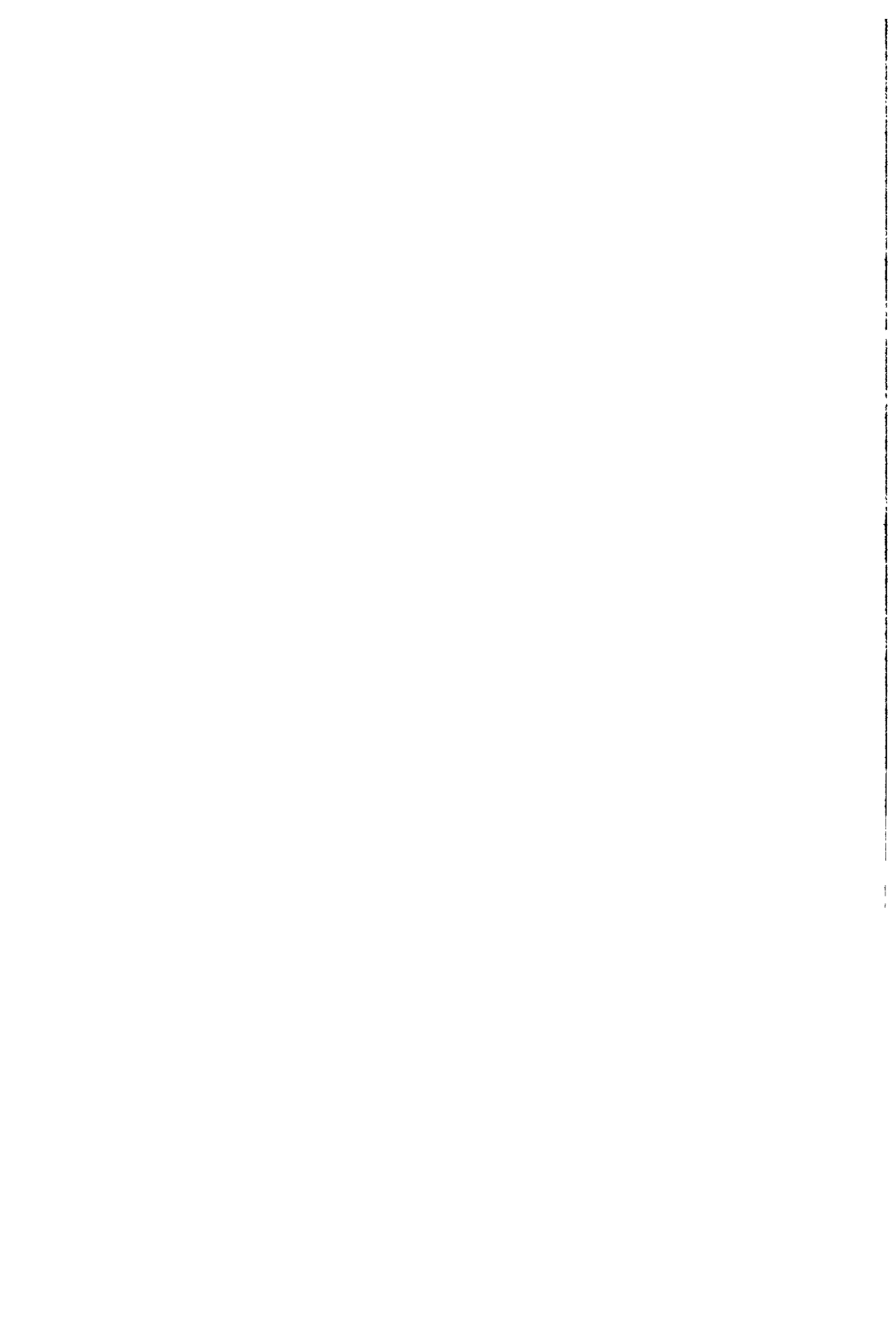
6. Strontium

The experiments reported here revealed a strong dependence of the intestinal absorption from the amount administered. The results derived show that for activities which are realistic for the possible case of environmental pollutions, the intestinal absorption is possibly substantially higher than assumed by ICRP. This means that the corresponding dose coefficients for ingested strontium isotopes may be higher by a factor of up to three as compared to the ICRP values.

7. Lanthanides

The experiments do not yet give a clear picture, but the preliminary results indicate that possibly a severe revision of the current dosimetric model may be necessary. Until now the data only allow the derivation of upper limits; for a useful dosimetric calculation more precise information is needed.

Transfer and behaviour of radionuclides in the environment



PROMOTION OF FORMATION AND EXCHANGE OF INFORMATION IN RADIOECOLOGY (INTERNATIONAL UNION OF RADIOLOGISTS)

Contract Bi6-052 - Section A21

1) *Myttenaere*, Univ. Cathol. Louvain-la-Neuve

Summary of project global objectives and achievements

- 1) Cooperation and exchange of information between radioecologists, in particular those from countries outside the European community, in order to stimulate interactions that would increase our understanding of problems in radioecology.

Missions:

- a) USSR, 5 IUR representatives - 10 days (7-17 May 1990)
- b) W-Europe, 9 IUR Soviet members - 10 days (October 1990)

Co-organization of Seminars, with financial assistance by IUR

Kiev 27 April - 4 May 1991 on "Radioecology and Countermeasures", organized by IUR Soviet Branch; 68 participants (18 non -Soviet)

Cooperation to International Projects

International Chernobyl Project. 1 IUR representative participated to task 3 mission 2 - USSR 12-25 August 1990 IUR Working Group Meetings

- a) "Plant-to-Animal Transfer" W.G. Neuherberg (GSF), 23-25 April 1990; 22 participants from 15 Res. Inst. + CEC and IAEA representatives
 - b) "Soil-to-Plant Transfer" W.G. Uppsala, 27-29 September 1990, 20 contributions
 - c) "Environmental Assessment Modelling" W.G., 6 March 1991, Vienna 36 participants from 17 countries + CEC and IAEA
 - d) WG Meeting of MARECO, in the framework of RADSTOMP 91, Norwich (UK) 9-14 September 1991
 - e) WG Meeting of "Plant- to-Animal Transfer" on Countermeasures, Uppsala (Sweden) 16-19 September 1991
- 2) Training of young scientists. This will remain a major objective, the best practical means being the organization of summerschools at regular intervals of time.

Organization of a summerschool : Mol 8-20 July 1990.
 - 3) Development of a curriculum for a Radioecology Textbook, contacts are in progress with the Publishers Chapman and Hall.
 - 4) Co-organization of international scientific seminars
 - a) Luxembourg 1-5 October 1990 on "Seminar on Comparative Assessment on the Environmental Impact of Radionuclides released during three Major Nuclear Accidents: Kyshtym, Windscale, Chernobyl" 200 participants (46 Soviet Scientists)

- b) Cadarache 7-11 October 1991, CEC-IUR Seminar on "Intervention Levels and Countermeasures"
 - c) Znojmo 12-16 October 1992, CEC-IUR-SCSR Seminar on "Chemical Speciation - Hot Particles".
- 5) Cooperation with other international organizations (i.e. IAEA, SCOPE, FAO/IAEA, IUPAC) in order to introduce the IUR expertise to their respective projects
- a) SCOPE-RADPATH Lancaster Mtg. 26-30 March 1990, financial support to 10 IUR members
 - Colchester Edit: Mtg. 12-20 April 1991, financial support to 3 IUR members
 - b) VAMP Mtg. 1 IUR representative, Vienna Dec 1990, March 1991, plus grants
 - c) BIOMOVS Mtg. Stockholm 8-12 October 1990, plus grants

Project 1

Head of project: *C. Myttenaere*

Objectives for the reporting period

- 1) Cooperation and the exchange of information between radioecologists in particular Soviet Scientists and those from countries outside EC and from countries which are not associated with the Radiation Protection Research Programme, in order to stimulate interactions that would increase our understanding of Radioecology problems;
- 2) Training of young scientists will be emphasized in the IUR new programme, in particular through organization of summer schools;
- 3) IUR will develop a curriculum for a basic course in radioecology;
- 4) Furthermore IUR will play various roles in the field of informing the Public, i.e., "Information packages" and individual experience of IUR members previously involved in this difficult area.

Progress achieved including publications

1. Promotion of the formation of young scientists

The first Summer School on Radioecology was organized in Mol from the 8th to the 20th of July 1990 by the International Union of Radioecologists.

The realisation of such a project was made possible thanks to the financial support of the European Communities (DG XI and DG XII) and the Belgian Nuclear Research Centre Mol.

The course was designed to fulfil the need of qualified scientists in the environmental radioactive protection areas of research centers, universities and industry.

Twenty-nine people having different classes of age have participated assiduously to the lecture given by 23 different eminent lecturers.

The lectures and an evaluation Report were sent previously to Dr. G. Gerber.

2. Development of Cooperation with the Soviet Scientists

The creation of a Soviet Branch of IUR increased tremendously the contacts and was one of the main reasons of the success of the Seminar on "Comparative Assessment of an Environmental Impact of Radionuclides released during the major accidents: Kyshtym, Windscale and Chernobyl" held in Luxembourg 1-5 October 1990 and organized by CCE (DG XI, DG XII) and IUR with the cooperation of SCOPE-RADPATH.

The Seminar was attended by about 200 participants of whom 46 were Soviet Scientists.

At the Soviet invitation, 5 IUR representatives (A. Aarkrog, C. Myttenaere, M. Frissel, L. Foulquier and H. Dahlgaard) spent 10 days (7-17 May 1990) in USSR. A Mission Report has been attached to the previous Progress Report.

In the framework of the "Mutual Agreement" 9 Soviet Scientists visited various radioecological laboratories (Belgium, France, United Kingdom, Denmark) in October 1990.

A Seminar on "Radioecology and Countermeasures", organized by IUR Soviet Branch, was held in Kiev 27 April - 4 May 1991. 68 scientists attended this scientific meeting. The publication of the proceedings is in progress.

3. Contribution of IUR to International Programmes

- SCOPE RADPATH:

- a) The first case study Meeting, which comprised a technical workshop (focusing particularly on Sellafield discharges and Soviet radionuclide releases) was held from 26-30 March 1990 at University of Lancaster, U.K. In total 43 participants from some twelve nations, were present at the meeting. IUR supported the participation of 10 IUR members as IUR officially cooperates to the SCOPE-RADPATH programme.
- b) An editorial Meeting took place in Colchester (U.K.) from 12 to 20 April 1991. IUR supported financially three participants.

- BIOMOVIS:

The IUR "Environmental Assessment Modelling Working Group" has provided partial support for the attendance of several IUR members to the BIOMOVIS final meeting in Stockholm (8-12 October 1990). A young scientist received a grant which allowed his attendance.

- VAMP (IAEA):

The IUR supported the attendance of members to two VAMP meetings in Vienna as IUR is formally involved in the IAEA/CEC Environmental Model Validation Study. (Dec. 1990 and March 1991).

- IAEA - IUR:

CRP set up in order to produce a Handbook of Transfer Parameter Values to Tropical and Sub-Tropical Environments. M. Frissel, IUR Representative, attended a two days meeting organized in Vienna, May 1990.

4. Working Groups Activities (in brief)

In the new CEC Radiation Protection programme, the cooperation between the European Countries is very important. But it is also important to assure contacts and exchange of information between those groups of European Laboratories and other European and especially non-European Scientists in the same fields.

The WG under IUR can act as an international forum for such contacts.

- a) The WG "Radioecology of Continental Waters" (Leader: L. Foulquier) has continued the inventory and the updating of information in this field. A Report "Synthèse des travaux relatifs à l'impact de Tchernobyl sur écosystèmes aquatiques" has been issued and distributed during the CEC-IUR Luxembourg Seminar (Contract with CEC-DG XI).

- b) WG "Marine Radioecology" (MARECO) Leader H. Dahlgaard, has represented MARECO at the second research coordination meeting of the CRP on "Sources of Radioactivity in the Marine Environment and this relative Contributions to Overall Dose Assessment from Marine Radioactivity" organized under IAEA in Risø 28 May - 1 June 1990.

The next MARECO Meeting will be held in Norwich (UK) 9-14 September 1991, in the framework of RADSTOMP 91.

- c) WG "Soil-to-Plant Transfer" (Leader: M. Frissel)
The WG organized a Workshop in Uppsala (27-29 September 1990) on "The contamination of crops because of Soil Adhesion". About 20 contributions were presented (see Annex 1).

The WG's Data Bank received somewhat less data than last year, a relatively large fraction of them contained in so-called "Post-Chernobyl data on the uptake of Cs and Sr". Recently also TF values from the Chernobyl area were received from IUR Soviet members.

- d) WG "Plant-to-Animal Transfer" (Leader: J. Van den Hoek)

The 3rd meeting of the WG took place at the Institut für Strahlenhygiene, Bundesamt für Strahlenschutz (Neuherberg, FRG) from 24-26 April 1990.

Twenty-two scientists from 15 Research Institutes, a representative of CEC (DG XII) and from IAEA, participated to this meeting. Furthermore 6 young scientists from four countries were invited to participate and to make a contribution.

The summaries of the contribution as well as the discussions and the areas of future research are given in the Report of this WG meeting (see Annex 2).

It must be also mentioned that there WG members have contributed to the Summer School on Radioecology (Mol, July 1990).

The next WG Meeting, to be held in Uppsala (Sweden) 16-19 September 1991, will deal with the Countermeasures in Plant-to-Animal Transfer.

- e) WG "IUR Environmental Modelling" (Leader: G. Linsley)

Activities 1989-90.

One of the main objectives of this Working Group has been to contribute to the validation of environmental assessment models. To this end it was proposed that IUR be one of the co-sponsoring organizations for the international BIOMOVS study.

This was accepted and IUR has had this role since 1986. Similarly, the IUR is formally involved in the IAEA/CEC Environmental Model Validation Study (VAMP) and sends delegates to the Research Coordination Meetings of that study. The IUR has been represented at all meetings of the two international model validation studies.

The environmental Assessment Modelling Working Group has provided partial support for the attendance of several IUR members to meetings of both BIOMOVS and VAMP. In the period 1989-90 the IUR supported the attendance of members to the VAMP meeting in Vienna (December 1989) and to the BIOMOVS final meeting in Stockholm (1990).

In 1989/90 there were no formal meetings of the Working Group, but many of the members are in regular contact through their involvement in the BIOMOVS and VAMP studies.

In April 1990, the leader of the Environmental Assessment Modelling attended an international seminar of the new recommendations of the International Commission on Radiological Protection (ICRP) organized by CEC in Luxembourg and offered comments on the recommendations from the standpoint of environmental protection.

On 6 March 1991, a WG Meeting was held in Vienna in which 36 scientists from 17 countries + CEC and IAEA took part (see Annex 3).

5. Exchange of Information

An Information Bulletin is issued periodically, the last issue (N° 12) is attached as Annex 4. It must be also mentioned that a Newsletter will be issued on a quarterly basis, the first one is given in Annex 5.

List of relevant publications

- a) IX IUR Annual Meeting, Madrid Sept: 15-19, 1986. Seminar CEC-JEN, Chernobyl, Posters session, extended Summaries.
- b) XIII IUR Annual Meeting, Luxembourg October 1-5, 1990.
Seminar CEC-IUR on comparative Assessment of the Environmental impact of Radionuclides released during Three Major Nuclear Accidents: Kyshtym, Windscale, Chernobyl-Proceedings EUR 13574 (vol I,II), 1991.
- c) I IUR Soviet Branch Meeting, Kiev 27 April - 2 May, 1991.
Proceedings of Seminar on Radioecology and Countermeasures DOC UIR 1992.
- d) Kirchmann, R. Radioecological aspects of the Chernobyl accident.
Ann. Ass. Belge Rad. Vol 16, n° 2, 65-95, 1991 (in French).
- e) Myttenaere, C., Consequences of the Kyshtym nuclear accident on Man and his environment.
Ann. Ass. Belge Rad. Vol 16, n° 2, 97-110, 1991 (in French).
- f) Kirchmann, R. and Demin, V.F., Agricultural Countermeasures taken in the Chernobyl Region and Evaluation of the Results. In Radiation Research, A Twentieth Century Perspective-Proc. 9th ICRR Toronto, Academic Press, inc., vol. II, 449-453, 1991.
- g) XIV IUR Annual Meeting, Cadarache October 7-11, 1991.
Intern. Seminar CEC-CEA-IUR on Intervention Levels and Countermeasures. Proc. in Press.

MODELLING THE TRANSPORT OF RADIONUCLIDES THROUGH THE FRESHWATER ENVIRONMENT

Contract Bi7-008 - Sector A21

- 1) *Hilton* , NERC - 2) *Galvão* , LNETI
- 3) *Cremers* , Univ/ Leuven (KUL) - 4) *Foulquier* , CEA - Cadarache
- 5) *Pieri* , Univ. Nantes - 6) *Belli* , ENEA
- 7) *Vanderborgh* , Univ. Antwerpen - 8) *Serrano* , Univ. Malaga
- 9) *Hambuckers-Berhin* , Univ. Liège - 10) *Comans* , Netherlands Energy Research Found

Summary of project global objectives and achievements

The programme was designed to identify areas of our understanding of the transport of radionuclides through aquatic environments and uptake by fish which limit the general applicability of the present generation of mathematical models. The initial programme concentrated on four areas:

- 1) Chemical processes underlying adsorption onto particles.
- 2) The processes involved in the enhanced transport of radiocaesium from some catchments.
- 3) Processes of remobilisation in sediments and at the seawater/ freshwater interface.
- 4) Effects of water chemistry and the ecology of aquatic organisms on the uptake, storage and excretion of radionuclides.

During the initial stages of the programme, studies at Univ. Liège and ECN, the Netherlands were included within the original programme by the CGC.

Significant advances have been made in all areas:

- 1) Chemical processes underlying adsorption onto particles.

Measurements suggest that a maximum of 1% of the radiocaesium in sediment samples is in regular ion-exchange sites and that almost all the simple ion exchange sites of Cs are on organic matter. K_d values can be predicted, within a factor of 2, from a knowledge of $[K_d, m_K]$, $[K_d, m_N]$ and the potassium and ammonium concentration in the water. As a result it can be inferred that Ca and Mg have no direct effect on the adsorption properties of sediment particles.

A new methodology has been devised to study desorption behaviour. Using this technique it can be shown that desorption efficiency decreases with increasing contact time between the solid and the radiocaesium and that the desorption behaviour is not related to the initial sorption characteristics. This suggests that there are structural differences in exchange pools between the different sediments. The presence of higher levels of Ca and Mg during adsorption decrease the desorption recovery efficiency. Both sorption and desorption kinetics can be modelled by a three component system (frayed edge sites, high affinity sites; liquid phase). However it is not possible to predict the fitting parameters from more fundamental properties at the present.

- 2) The processes involved in the enhanced transport of radiocaesium from some catchments.

Field measurements have shown that peat bogs in a lake catchment will continue to supply radiocaesium to the lake at a rate of about 3% of the initial catchment inventory per annum. This maintains the lake water at higher activities than would be predicted by normal models where long term losses of 0.01-0.1% per annum are typical. The rate of transport is a function of flow in the streams leaving the peat bogs and reduces with time. Loss rates for a number of streams in the catchment of a single lake could be modelled by an equation of the form $\text{Activity} = C_0 \cdot \exp(-kt) \cdot \text{flow}^a$, where C_0 , a and k are constants. C_0 could be predicted from the proportion of the catchment consisting of peat bog and the initial deposition of

radiocaesium. The universality of this equation is unknown. However the work suggests that lakes and reservoirs containing peat bogs will be more susceptible to radiocaesium remobilisation than formerly expected.

3) Processes of remobilisation in sediments and at the seawater/ freshwater interface.

A field study has shown that, within the saline wedge, the quantity of small particles increases as the salinity increases and that the K_d of small (0.1-5 μm) particles is a factor of 2 higher than the K_d of larger (5-100 μm) particles. The total, weighted mean, K_d reduced by an order of magnitude from 1.17×10^5 to 0.13×10^5 for an order of magnitude change in conductivity.

4) Effects of water chemistry and the ecology of aquatic organisms on the uptake, storage and excretion of radionuclides.

Kinetic parameters have been measured for the uptake of Co-60 through a water-algae-zooplankton-fish pathway and for Ag-110m for a more complex pathway of algae-daphnia, gammarus, chironomid- carp, trout. Ecological constraints were included in the Ag-110m model such as the seasonal cycles of food source availability and fish growth patterns. Model runs for a Chernobyl type contamination were carried out.

Analysis of data collected after the Chernobyl deposition showed that about 54% of the variability in the activity of individual perch and trout were caused by differences in size. The mechanism of this effect is not known but some data suggest that differences in food sources of different size fish are not the cause. Introduced fish showed very low accumulation of radiocaesium for a given size suggesting that food is the major uptake pathway.

Using molecular biological methods it has been possible to show that radiocaesium shows ionic behavior in the cytosolic fraction of the liver and diffuses to the muscle. Americium, on the other hand, is linked to proteins in the cytosol of the liver and is probably eliminated rather than diffusing to the muscle. Since cadmium, and probably metal inducers of metallothioneins can inhibit the linking of Americium to Cytosolic proteins, the external, environmental conditions become more important in determining americium's effect on the food chain. Models of radionuclide transfer will have to take this into account.

In a model system Co uptake was determined by the concentration of free ion in solution and the hydrogen ion concentration. Uptake of Co increased with decreasing H^+ concentration. In addition the uptake of Co by brine shrimp reduced with increasing salinity. However acclimation to increasing salinity prior to each experiment resulted in increased uptake of Co. The uptake also increases with temperature of exposure but decreases with an increase in the temperature of acclimation. These results indicate the importance of both chemical and biological processes in controlling the uptake of radioactive Co by the brine shrimp. The basic understanding concerning these mechanisms provides a preliminary framework for the development of conceptual models of radionuclide uptake.

Uptake by plants of inorganic ions, including radionuclides, is achieved by the passage of the ions through the cell wall via channels. An understanding of the way in which the channels operate for the radionuclide of interest and/ or any other comparable ions would improve the models of radioactivity accumulation in algae and vascular plants. The flow of ions is a function of the potential difference across the membrane and the amount of time the channel is open. The former is controlled by the external pH, temperature and the concentration ratio of the stable isotope inside and outside the cell. Whereas the opening and closing of the channel is a function of the external concentration of related ions e.g. K^+ in the case of Cs^+ , and the external concentration of a trigger ion, e.g. Ca^{2+} controls the K^+ channel.

In addition the observed concentration factor is a function of the amount of growth, which is controlled by light, temperature and nutrient concentrations. More detailed understanding of these properties would lead to a conceptual model which would introduce a normalised parameter, equivalent to the concentration factor, which would show much less variability between sites and between species.

A laboratory study of radionuclide uptake by bacterial communities showed that they could sorb or incorporate significant quantities of radiocobalt and radiocaesium within a 24 hour period. This uptake could be modelled by a Michelis -Menten type model. At 20°C radionuclide loss showed two kinetic rates; the first described by a half life of the order of a minute and the second of the order hours to days. At 13°C no loss was observed. Radionuclide loss at 20°C was faster at pH 8 and reduced at higher or lower pHs. Given that the mean temperature in the river Meuse is 13°C with a pH of 8, bacteria are likely to act as radionuclide sinks for much of the time but, when the temperature increases in summer they could act as sources.

Laboratory and modelling work by ECN has shown that there is a strong interrelationship between the kinetics of radiocaesium sorption and the reversibility of the process. A slow uptake process is believed to represent a migration of radiocaesium to illitic interlayer sites from which the radionuclide is not easily released. The rate of this migration depends strongly on the major competing cation in the ion exchange process and is very relevant for the evaluation of the risk of radiocaesium remobilisation from contaminated sediments. In-situ studies in sediments of lake Esthwaite (ECN/IFE) and laboratory diffusion tube experiments have indicated that virtually all Chernobyl radiocaesium is sorbed on the sediments with in-situ K_d 's of the order of 10^4 - 10^5 mL/g and that probably only a minor fraction is exchangeable (i.e. available for remobilisation in the short term). It is suggested that research should be directed towards determination of the reverse rates of radiocaesium uptake in order to determine the potential for remobilisation on the longer (months-years) time scales. Moreover, a distinction is needed between K_p 's for total and exchangeable radiocaesium in order to accurately model radiocaesium transport in sediments and to follow changes in the in-situ exchangeability of the radionuclide.

The studies in this programme have demonstrated that many of the processes involved in the transport of radionuclides through aquatic systems are controlled by definable, underlying principles. A deeper understanding of these principles will lead to mathematical descriptions which can be incorporated into the present generation of models to reduce the between site and between species variability of the present descriptive parameters.

Project 1

Head of project: *Dr. Hilton*

Objectives for the reporting period

The programme of work has been split into two main parts a) transport processes from catchments to water bodies and the processes of transport within water bodies; b) uptake of radionuclides by fish, in particular the incorporation of ecological knowledge into improved mathematical models.

a) Catchment losses and transport processes.

- 1) to elucidate the causes of, and processes driving the large releases of radiocaesium observed in some upland catchments.
- 2) to study the variation with time of the adsorption properties of particles settling in a eutrophic lake.

b) radionuclide uptake by fish.

- 1) to incorporate emerging results on the effects of biochemical and ecological processes on the uptake of radionuclides (particularly radiocaesium) by fish into mathematical models.

Progress achieved including publications

Significant progress has been made on sections a1 and b1. Practical sampling problems have limited progress on section a2.

a) Catchment losses and transport processes.

- 1) to elucidate the causes of, and processes driving the large releases of radiocaesium observed in some upland catchments.

Radiocaesium activity was measured in 26 lakes (figure 1) in the English Lake District (north west England) in 1988 and in 1990. Contrary to observations made in most lakes, several lakes in our study showed measurable Cs activity at these times, 2 years and 4 years respectively after the Chernobyl accident. Calculation showed that even if the only loss process operating was hydraulic flushing then radiocaesium levels should have been below the limit of detection in all, except two lakes by 1988. Analysis of ancillary data showed that the residual activity was not caused by inhomogeneous deposition of radioactivity and that it was unlikely to be caused by remobilisation from the sediments. A simple correlation analysis showed that the lakes which retained the highest levels had very low levels of clay minerals, particularly illite and chlorite, in their sediments. Conversely, lakes which showed no significant retention of radiocaesium in the water column had very high levels of clay minerals in their sediments. However, between these two extremes there was no apparent correlation between retained radiocaesium in the water column and sediment clay content.

Because there were no internal sources of supply within the lakes the retained radiocaesium must have been released by the catchment. However, the lack of correlation between sediment clay mineral content (as an integrator of catchment soil properties) and radiocaesium retention showed that the relationship was not simple. A study of the lakes with

the highest retention showed that catchment loss rates were very high, at about 2-3% of the total catchment inventory per annum. The lack of relationship between soil types (as indicated by the sediment properties) and residual radiocaesium could be explained if only a part of the catchment were losing radiocaesium to the lake at these high rates, ie only one, specific soil type experienced these losses.

In order to elucidate more detail on the processes involved, a catchment which had retained a high activity level in the lake water was studied in depth. Seven streams flow into Devoke Water (figure 1). Changes in activity with time in six of these streams are shown in figure 2 for the three years following the Chernobyl deposition. Activity levels in streams 1 and 2 were consistently higher than in the lake, whereas streams 3, 4 and 6 were consistently lower. In addition, the sample to sample variation was much greater in streams 1 and 2 than in either the lake or the other streams and was considerably larger than observable, systematic variations with time.

A multiple regression analysis showed that data for streams 1-4 was well fitted by the relationship:

$$\log A = -0.001064 t + 0.302003 \log F + \text{constant}$$

where A is the activity in each stream (mBq/l); t is the time in days since the deposition and F is the stream flow in cumecs (m³/s). Streams 5, and 6 obey the same equation but the effect of flow is reduced so that the second coefficient equals zero. The constant can be estimated from a regression with the area of fibrous peat (peat bog) in the sub-catchment of each stream as the independent variable.

$$\text{constant} = 0.0473 \text{ \%fibrous peat} + 4.383$$

Using these equations it was possible to estimate the cumulative loss from the different sub-catchments. Sub-catchments of streams 1 and 2, which contained the largest fibrous peat (peat bog) areas maintained loss rates between 3 and 4% of the inventory per annum, whereas the other catchments showed loss rates of typically less than 1% per annum. The latter are consistent with long term losses reported for other catchments but the former, higher values are exceptional and are consistent with the rates of loss observed in the large survey of lakes reported earlier. In Devoke Water the radiocaesium is lost in quantity only from the peat bog areas. This is consistent with the previous survey, where the lakes with the highest radiocaesium residuals are almost completely surrounded by peat bogs, whereas peat bogs are absent from the low residual lakes. Intermediate lakes have partial cover of the catchments by peat bogs. These findings suggest that water supply reservoirs containing peat bogs within their catchments are at a greater risk from radiocaesium deposition than was previously realised.

The previous studies highlighted the importance of peat bogs in maintaining high residual radiocaesium in lakes after a deposition event. However no indication of the processes involved in the release were obtained. In order to shed more light on the situation a study was made of the changes in radiocaesium levels in two streams in the Devoke Water catchment which occurred during a rain storm.

Three processes have been proposed as possible mechanisms of Cs release from flooded peat catchments. One possibility is that these soils contain no clay minerals so that the Cs is bound by simple ion exchange to the organic material.

A second is suggested by analogy with the observations of Comans (1990), Cremers (1989), Evans (1983) and others. Illite has sites around its mineral grains which are specially size selective for Cs. Cremers (1989) has shown that these sites are about 100 times more selective for Cs than for K. If very small amounts of illite are present in the soils then they could selectively sorb the Cs, concentrating it at the illite frayed-edge sites (FES) rather than on ordinary ion exchange sites where open competition with other metal ions would take place. It is possible that, even though the FES constitute a very small component of the soil matrix, they could dominate the chemistry of Cs release because of their selectivity. Comans (1990) has shown that, in lake sediments, the K_d of Cs reduces significantly in the presence of ammonia. This is due to the similarity in size of the non-hydrated Cs and NH_3 ions. As a result they compete on equal terms for the Cs selective adsorption sites in the frayed edges of illite mineral grains (Cremers, 1989) and Cs is released into solution in the presence of ammonia in solution.

A third possibility has been proposed by Hasanen and Meittinen (1963) and Carlsson and Liden (1978) who suggested that in humus rich catchments Cs could be kept in solution by chelation to dissolved or colloidal humic substances.

Dominance of the release process by simple ion exchange would suggest a relationship between the major competitive ion exchanger and dissolved Cs; dominance of the illite mechanism would suggest a relationship with ammonia concentrations and dominance by the chelation of Cs by humic materials would suggest a relationship with dissolved organic carbon. Neither ammonia nor DOC concentration changes bore any relationship to dissolved Cs-137 in either stream. However a strong relationship was observed between calcium (and alkalinity and pH) and dissolved Cs in the stream emanating from the peat bog, although no relationship was found in the other stream. The data suggest that, in peat bogs, radiocaesium is sorbed by simple ion exchange and that high concentrations of other cations will induce desorption and subsequent wash-out of the radiocaesium. This raises the possibility that in other situations where simple ion exchange is the dominant sorption mechanism, e.g. silica sand soils, remobilisation from the catchment could be a significant means of maintaining high radiocaesium levels in the water column.

2) to study the variation with time of the adsorption properties of particles settling in a eutrophic lake.

The properties of settling particles in eutrophic lakes change with time during the year, from mainly catchment derived material in the winter to mainly algal particles in the growing season. This suggests that the K_d of the larger settling particles may change significantly throughout the year. (As smaller particles remain in suspension semi-permanently, measurement of the suspended population of particles by simple filtration may provide a biased estimate of K_d for use in transport models.) In conjunction with KUL a field sampling programme was devised to obtain samples of settling solids from a well studied lake. As the programme developed from a desk study to a reality it became clear that very large samples (2-5g dry solid) would be required to carry out the analyses. In order to obtain quantitative flux estimates a large volume sediment trap (0.3m diameter, 2.1m high) was designed and built. The design worked well and one or two samples were collected in early spring. However, when summer anoxia developed, oxidation of the hypolimnetic water during the separation of the particles from the 10 l of water retained in the bottom of the trap created large quantities of ferric oxide which would have significantly altered the particle sorption properties. After trying many technical solutions, all of which failed, the simple expedient of relocating the trap in the epilimnion solved the problem. However, as a result there was no time left to make the measurements over an annual cycle. It is hoped to carry out these measurements at a later date.

b) radionuclide uptake by fish.

1) to incorporate emerging results on the effects of biochemical and ecological processes on the uptake of radionuclides (particularly radiocaesium) by fish.

Data on the activity of radiocaesium in fish (perch, trout and pike) after the Chernobyl accident showed enormous variability. A detailed study of the data sets from two lakes was made in order to define the sources of this variability.

Detailed notes taken at the time of sampling identified several individuals as stocked trout by their colour. The activity levels in this group were much lower than in native fish. Levels ranged from 10 to 200 Bq/kg in this group compared to 100 to 2000 Bq/kg in the total trout sample. This is consistent with other data which show that farmed trout are less susceptible to the effects of radiocaesium and that food is the most important vector in the uptake of radiocaesium. Removal of these data points reduced the variability considerably but, at the upper end of the stocked trout activity level the activities overlapped with the trout which were not identified by colour as stocked. In order to identify stocked fish more quantitatively in the future, stable carbon ratios were measured on the fish flesh. Preliminary results suggest that stocked fish, having been fed on food derived from marine fish, show higher ^{13}C : ^{12}C ratios than native or semi-wild fish (ie fish released a long time ago).

The remaining data points for trout and perch, in one lake, and trout only in a second lake showed a power relationship with fish size (figure 3 and 4). The variability due to size accounted for 53% of the variability in individual trout. Analysis of a subsample of these fish showed that there was no difference between the gut contents of fish of different size. Although this suggests that different food sources are not the cause of observed variations with size, it may be an artifact from the sampling methods used.

Removal of the variation between sizes by normalisation to a common size produced the time series plots shown in figure 5 for trout in the two lakes. Trout in Loweswater lost radiocaesium at a much faster rate ($t_{1/2}=103$ days) than fish in Devoke Water ($T_{1/2}= 825$ days). This was due to the continuing inputs from the catchment which occurred in Devoke water but not in Loweswater. As a result the biological half life observed in Loweswater was close to the typical value of 100 days observed in laboratory studies whereas the decay rate in Devoke Water was controlled by the reduction of radioactivity in the water column and was thus better termed an ecological half-life.

This study highlighted the relationship between radioactivity levels and fish size. This appears to be a phenomenon which is associated with the dynamic nature of the Chernobyl release. Other studies, post Chernobyl have now been reported which show this same relationships. However similar effects were not observed from the pseudo-steady state deposition of weapons fallout. A full understanding of this dynamic effect will be required before models of transfer into fish can be improved significantly.

References

- Carlsson, C and K.Liden. (1978) Cs-137 and potassium in fish and littoral plants from a humus-rich oligotrophic lake 1961-1976. *Oikos* v.30; 126-132.
- Comans, R.N.J., J.J.Middleburg, J.Zonderhuis, R.J.W.Woittiez, G.J.DeLange, A.K.Das and C.H.Van der Weijden. (1989) Mobilisation of radiocaesium in pore water of lake sediments. *Nature* v.339, 367-369.
- Cremers, A., A.Elsen, P.M.De Preter and A.Maes. (1988) Quantitative analysis of radiocaesium retention in soils. *Nature* v.335, 247-249.

Evans, D.W., J.J.Alberts and R.A.Clark (1983) Reversible ion-exchange fixation of cesium-137 leading to mobilisation from reservoir sediments. *Geochim. Cosmochim. Acta* v.47, 1041-1049.

Hasanen, E. and J.K.Miettinen. (1963) Caesium-137 content of freshwater fish in finland. *Nature* v.200; 0118-1019.

Papers published or in press resulting from this work

Hilton, J., R.S.Cambray, and N.Green. (1992) Chemical fractionation of radioactive caesium in airborne particles containing bomb fallout, Chernobyl fallout and atmospheric material from the Sellafield site. *J. Environ. Radioactivity*. v.15; 103-111.

McDougall, S.,J.Hilton and A.Jenkins. (1991) a Dynamic model of caesium transport in lakes and their catchments. *Water Res.* v.25; 437-445.

Elliott, JM., J.Hilton, E.Rigg, PA.Tullett, D.Swift, P.Leonard. Radioactivity in fish from two Cumbrian lakes after Chernobyl: sources of variability within the data. *J.Appl. Ecol.* v.29; 108-120.

Hilton,J., F.Livens, P.Spezzano, and P.Leonard. The retention of radioactive caesium by different soils in the catchment of a small lake. *Sci. Tot. Environ.* in press.

Spezzano, P., J.Hilton, J.P.Lishman and T.R.Carrick (1992). The variability of Chernobyl Cs retention in the water column of lakes in the English Lake District, two years and four years after deposition. *J. Environ. Radioactivity.* in press.

Hilton, J. and P.Spezzano. An investigation of possible processes of radiocaesium release from organic upland soils to water bodies. *Wat. Res.* Submitted for publication.

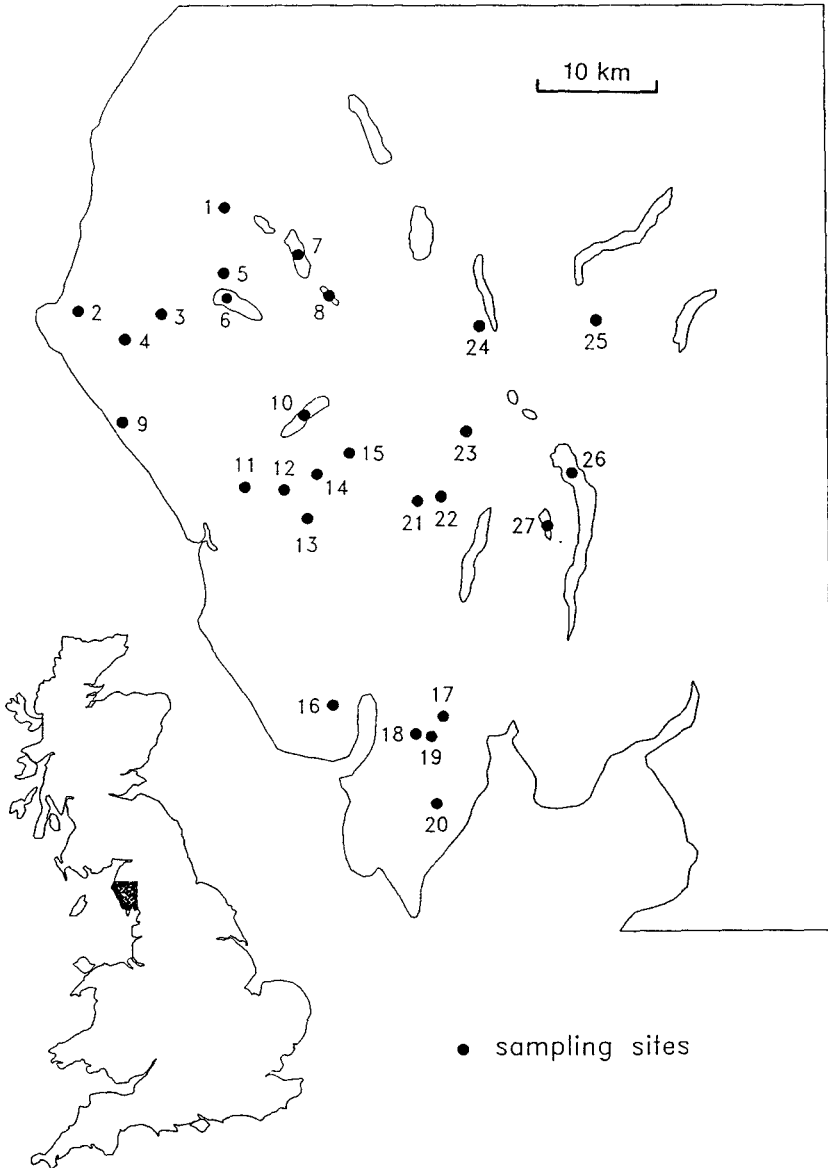


Figure 1: Location of the sampling sites. Ordnance Survey grid references in brackets.

1) Mockerin Tarn (NY083231); 2) Mirehouse (NX980150); 3) Meadley Reservoir (NY050145); 4) Longlands Lake (NY013127); 5) Cogra Moss (NY095196); 6) Ennerdale Water (NY110150); 7) Crummock Water (NY160180); 8) Buttermere (NY180160); 9) Braystones (NY005060); 10)Wastwater (NY145002); 11) Parkgate Tarn (NY118006); 12) Eskdale Green (NY145002); 13) Devoke Water (NY160970); 14) Eel Tarn (NY189019); 15) Stoney Tarn (NY199024), 16) Gricecroft (Baystone Bank) Reservoir (NY172859); 17) Knottalow Tarn (NY272802); 18) Harlock Reservoir (NY247792); 19) Pennington Reservoir (NY257788); 20) Urswick Tarn (NY270745); 21) Seathwaite Tarn (NY253987); 22) Levers Water (NY280993); 23) Blea Tarn (Langdale), (NY293044); 24) Harrop Tarn (NY312137); 25) Brotherswater (NY402128); 26) Windermere (north basin) (NY382010); 27) Esthwaite Water (NY360970).

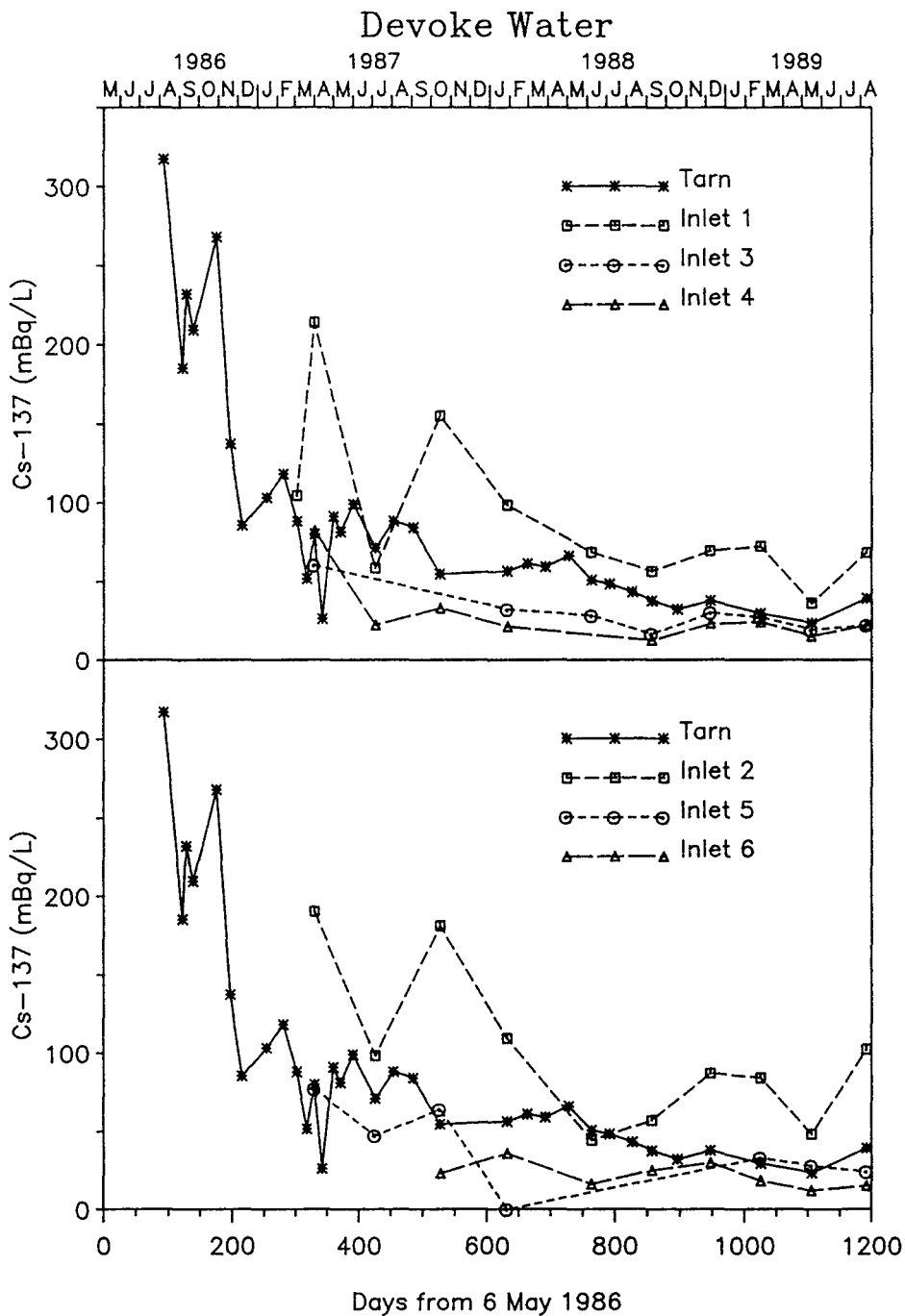


Figure 2: Plots of concentration against time for lake water and (a) streams 1, 3 and 4; (b) streams 2, 5 and 6.

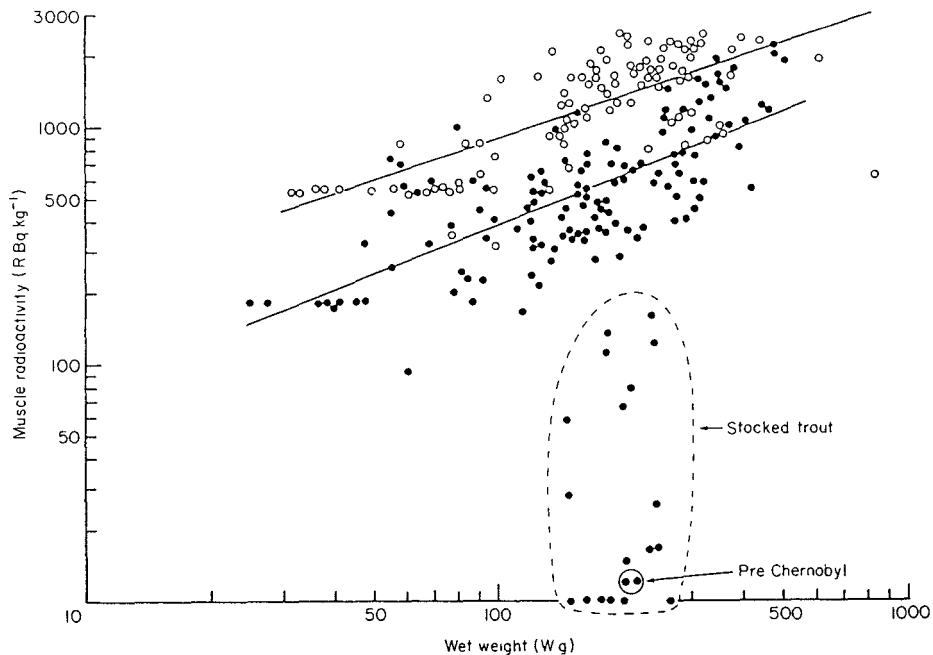


Figure 3: Relationship between muscle radioactivity ($R \text{ Bq kg}^{-1}$) and wet weight (Wg) for individual brown trout (\bullet) and perch (\circ) from Devoke Water; regression lines: brown trout, $\log_{10} R = 1.22 + 0.68 \log_{10} W$ ($n = 140$, $r^2 = 0.525$, $P < 0.001$), values for 18 stocked trout and two pre-Chernobyl trout omitted from analysis (points enclosed by broken lines); perch, $\log_{10} R = 1.80 + 0.57 \log_{10} W$ ($n = 104$, $r^2 = 0.508$, $P < 0.001$).

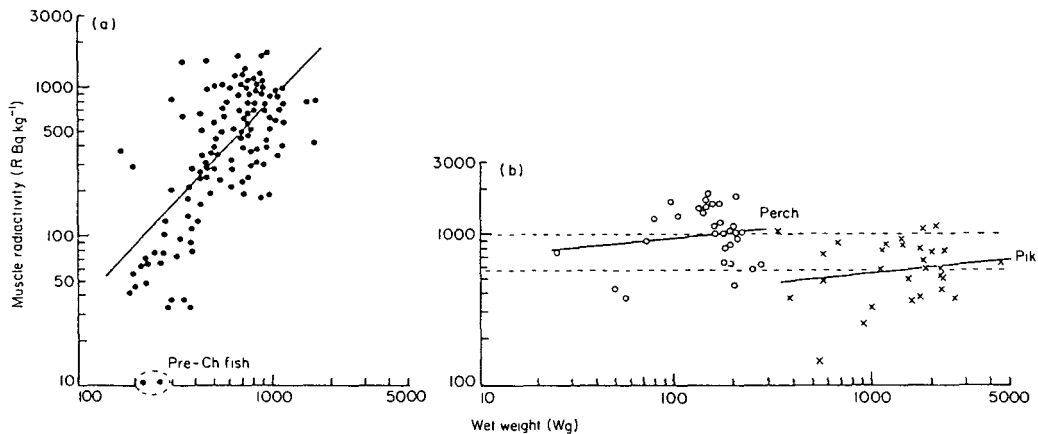


Figure 4: Relationship between muscle radioactivity ($R \text{ Bq kg}^{-1}$) and wet weight (Wg) for:
 (a) individual brown trout from Loweswater; regression line: $\log_{10} R = -1.28 + 1.40 \log_{10} W$ ($n = 143$, $r^2 = 0.495$, $P < 0.001$), values for two pre-Chernobyl (Pre-Ch) trout omitted from analysis (points enclosed by broken line);
 (b) individual perch (\circ) and pike (\times) from Loweswater; regression lines: perch, $\log_{10} R = 2.73 + 0.12 \log_{10} W$ ($n = 34$, $r^2 = 0.020$, $P > 0.05$, NS); pike, $\log_{10} R = 2.35 + 0.13 \log_{10} W$ ($n = 29$, $r^2 = 0.029$, $P > 0.05$, NS); horizontal lines are geometric means of 988.8 Bq kg^{-1} for perch and 567.6 Bq kg^{-1} for pike.

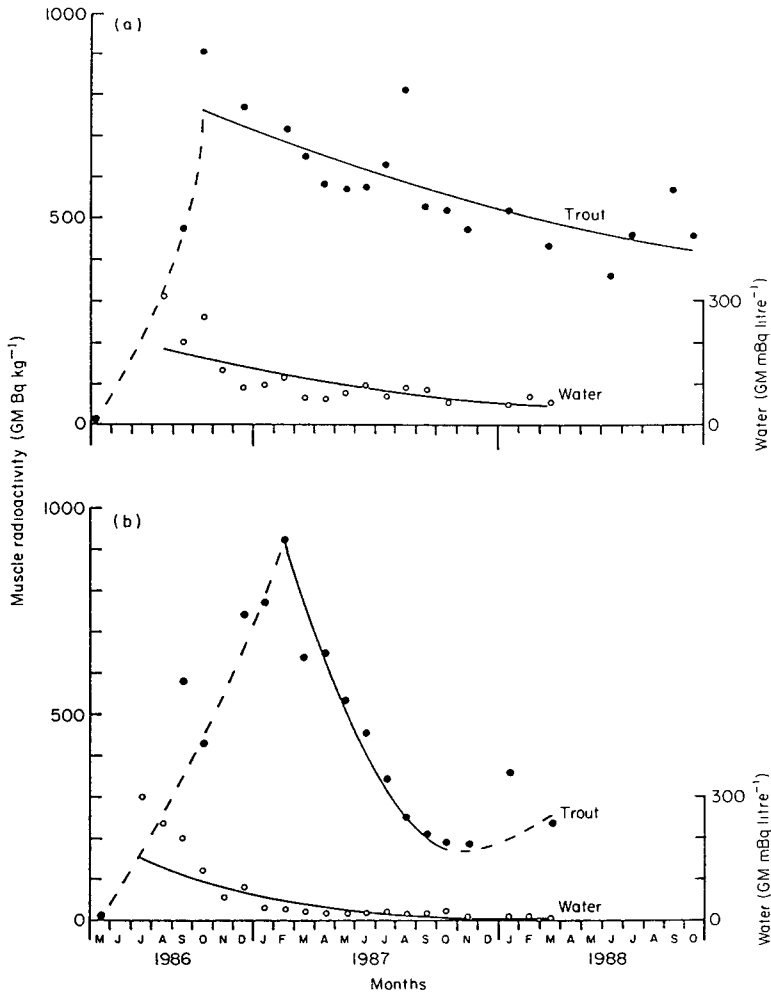


Figure 5: Relationship between Geometric Mean (GM) radioactivity in brown trout (GM Bq kg^{-1}) or in water ($\text{GM m Bq litre}^{-1}$) and time (t months from May 1986) for (a) Devoke Water, (b) Loweswater; broken lines simply show trends, solid lines are exponential curves given by:
 (a) Devoke Water trout, $\text{GM} = 862.8 \exp(-0.0252t)$ ($n = 18, r^2 = 0.605, P < 0.01$); water, $\text{GM} = 229.2 \exp(-0.0725t)$ ($n = 18, r^2 = 0.662, P < 0.01$);
 (b) Loweswater trout, $\text{GM} = 5596.6 \exp(-0.202t)$ ($n = 9, r^2 = 0.976, P < 0.001$); water, $\text{GM} = 212.0 \exp(-0.173t)$ ($n = 20, r^2 = 0.810, P < 0.01$).
 (Each GM for trout is for values that were first scaled to a standard fish weight: 167 g for Devoke, 597 g for Loweswater; these values being GM wet weight for all trout in the samples).

Project 2

Head of project: *Dr. Galvão*

Sub-project 1: Physico-chemical behaviour of radionuclides in freshwater sediments

1. Introduction

In what concerns the physico-chemical behaviour of radiocesium in Tejo River sediments (Fratel dam), a study was developed to quantify the sediments properties, keeping in view the radiocesium sorption. In particular, sediments were characterized in terms of specific sites numbers and selectivity pattern of cesium towards potassium and ammonium ions.

The radiocesium sorption behaviour might be predicted since it is well known that radiocesium is very selectively adsorbed on sediments and the sorption processes are essentially governed by the liquid phase concentrations of the poorly hydrated cations potassium and ammonium. However, in order to assess the long term effects, it is important to quantify the cesium processes of desorption and remobilization, once, with longer equilibrium times, a redistribution of cesium towards the most selective sites occurs, making it less and less extractable.

On this basis new methodologies were applied to Tejo River sediments, which allow radiocesium transfer rate measurements from a sediment to an ion exchange resin, under a quite mild liquid phase concentration, 10^{-7} M, which is representative of natural conditions. The contact time or aging time effect on radiocesium desorption was quantified.

2. Methods

The methods used for the characterization of Tejo River sediments ($T1 < 63\mu\text{m}$ and $T2 < 500\mu\text{m}$) are described in Madruga and Cremers, Progress Report 1990.

Radiocesium desorption yield determinations with potassium and ammonium salt solutions and the study of aging time effects, were carried out using the experimental procedures described in Madruga and Cremers, Progress Report 1991.

3. Results

The sediments characterization data, cationic exchange capacity (CEC), frayed edges sites (FES) numbers and selectivity coefficients $K_e(\text{Cs}/\text{K})$ and $K_e(\text{Cs}/\text{NH}_4)$ are presented in Table 2.1. $K_e\text{M}_k$ as well as $K_e\text{M}_{\text{NH}_4}$ plotted versus different K and NH_4 concentrations are shown in Figures 2.1 and 2.2 respectively.

Table 2.2 presents the simulation parameters of the Cs/K selectivity pattern in the FES, using a simulation model with three different sites of increasing Cs selectivity.

Some examples of the aging time effect on the radiocesium desorption yields, for T1 sediment, using the experimental protocol (B) (see Madruga and Cremers, Progress Report 1991), are presented in Figures 2.3 and 2.4.

4. Discussion

Figures 2.1 and 2.2 show that from 0.008 to 0.01 meq/ml, at high potassium and ammonium concentrations, the $K_d \cdot m_K$ and $K_d \cdot m_{NH_4}$ products are constant, what means that the frayed edge sites (FES) are homionically saturated in these ions. The selectivity coefficients (NH_4/K) in the specific sites, calculated from the ratio $K_d \cdot m_K / K_d \cdot m_{NH_4} \text{ max.}$, are higher than 1 (Table 2.1), therefore ammonium ions are more selective than potassium ions in the FES.

For carrier-free conditions, knowing field values of m_K and evaluated FES, "in situ" K_d predictions can be made. Therefore, from "zero" cesium loading K_c (164), FES value (Table 2.1) and $m_K = 0.1$ meq/l, the "in situ" K_d prediction is approximately 9×10^3 ml/g for T2 (<500 μ m sediment (considered as total sediment)). However, this value is higher than "in situ" K_d obtained from Cs-137 concentration in Tejo sediments and water ($\approx 3.5 \times 10^3$ ml/g), due to the effect of other competitive cations, such as NH_4^+ .

From the simulation parameters presented in Table 2.2, it can be seen that the FES can be divided into exchange sites exhibiting very high Cs/K selectivity (sites I and II), and exchange sites with Cs/K selectivity not substantially differing from planar exchange sites (site III, in $K_c \approx 2$).

All the results presented in Tables 2.1 and 2.2 are in good agreement with those found for other substrata by several authors.

In what concerns the aging time effects on the radiocesium desorption, Figures 2.3 and 2.4 show that desorption yields decrease as aging times increase, and after a short contact time (3 days), a very pronounced fraction, about 50% of adsorbed, is irreversibly bound to the sediment. The rate of such rapid fixation process, must be more related to structural differences between specific site groups, than to a diffusion into the sediment crystal lattice.

The cesium desorption values for shortest contact times, indicate a higher decontamination efficiency of ammonium relatively to potassium.

Sub-Project 2: Co-60 transfer in a freshwater ecosystem

1. Introduction

Fratel Dam, in Tejo River, was the subject of an anterior study concerning the radiocesium transfer in a freshwater trophic chain of that ecosystem (Contract CEC n^o BI6-0245-P), and is again the objective of the present Contract CEC n^oBI7-0008, due to its particular characteristics. Actually, Tejo River, has origin in Spain, and the first dam in the river, for hydroelectric power generation, is at Fratel, a few kilometers from the border. In the Spanish sector of Tejo River there are three Nuclear Power Plants (NPP), one at Zorita upstream and NE of Madrid, another one far upstream (Trillo), and the third at Almaraz about 120 km from the border. Therefore, we have a strong interest on studying the radioecology of the Fratel dam, because, in spite of periodic water discharges, there is a certain retention time and therefore the artificial radionuclides released by Almaraz NPP may eventually be accumulated in the dam.

Co-60 was never detected in the portuguese sector of the river, however its amount in the liquid effluents of NPP's is not negligible. From a biological standpoint, cobalt's importance is due to the fact of being a component of the vitamin B12 molecule, which is essential for all mammals including man.

In the present report, the results of the modalitiés of contamination and elimination in a simplified freshwater trophic chain, including sediments, are shown.

2. Methods

The characterization of the dam from the physico-chemical, biological, and radiological points of view was already done, however the main characteristics of Fratel dam water are still being determined, for instance, Ca²⁺, K⁺, Na⁺, Mg²⁺.

Based on the main metal elements data measured in water, sediments and biota, during the period 1987-1989 (Carreiro, to be published), stable cobalt average values are available for the compartments of the ecosystem studied, Table 2.3.

The experimental study was performed considering the following trophic chain: Selenastrum capricornutum Printz (cl. Chlorophyceae), Daphnia magna Straus (cl. Crustacea) and Chondrostoma polylepis polylepis Steindachner (cl. Osteichthyes, fam. Cyprinidae) in Fratel dam water, always previously filtered through 0.45µm membranes. Temperature was kept at about 20 °C.

The experiments concerning the water-sediments interaction, were carried out with sediments and water from Fratel dam. Co-60 was used under the form of CoCl₂ and during the experiments its physico-chemical forms were determined.

The detection system consists on a well-type NaI (Tl) detector connected to a multichannel analyser. The detector size is 4"x4" and the well is 1¼ diameter and 2½ deep.

3. Results

3.1 First trophic level: *Selenastrum capricornutum*

3.1.1 Accumulation

The uptake experiments were carried out in a confined medium, with a Co-60 concentration of about 20 Bq ml⁻¹. Three replicates of the experiment in water from Fratel dam were done: in one of them cell concentration was constant, during the 7 days of the experiment, and in the other two there was an increase of cell concentration towards an equilibrium situation.

The concentration factor (Bq kg⁻¹ of dry algae / Bq kg⁻¹ of water) obtained was CF = (2.3 ± 0.6) 10³.

3.1.2 Retention

The decontamination was carried out in a confined medium: following the contamination period, after the microalgae resuspension in non radioactive Fratel water, seven fractions were prepared to be measured, one by one, at different time intervals, 5m, 1h, 4h, 1d, 2d, 4d, and 7d. Four replicates of the experiment were done, being the retention (in percentage) expressed by the function:

$$R_t = 42 e^{-2.73t} + 58 e^{-0.333t} \quad (t \text{ in days})$$

The biological half-lives are Tb₁=6h and Tb₂=2 days.

3.2 Second trophic level: *Daphnia magna*

3.2.1 Accumulation

3.2.1.1 Contamination through the water pathway

Transfer of Co-60 from water to *Daphnia magna* was studied during a period of 28 days. The experiment was started with 200 ovigerous females weighing 3.2 mg indiv.⁻¹ (w.w), in 2 liters of Fratel water with an initial radioactivity of 39 Bq ml⁻¹.

During the first three days of the experiment, eclosions have occurred. At the 4th day, neonates weighed 0.14 mg indiv.⁻¹ (w.w) and at the 28th day the weight was 0.38 mg indiv.⁻¹.

Concentration factor in neonates has shown a maximum CF = 148 at the 7th day, then started to decrease to stabilization. At the equilibrium, the arithmetical mean of all measures taken between the 11th and the 28th day was:

$$CF_{eq} = 53.1 \pm 6.2 \quad (\text{w.w.})$$

3.2.1.2 Contamination through water and food pathways

A short experiment was undertaken, in order to evaluate the trophic transfer factor (TTF) and the relative contribution of

water and food (microalgae Selenastrum) on the contamination of D. magna with Co-60.

Two-hundred mature females weighing 3.0 mg indiv.⁻¹ (w.w) were introduced into flask A, with 2 liters of Co-60 labelled Fratel water, with an initial radioactivity of 22 Bq ml⁻¹. Daphnids received no nutrients. A similar group of crustaceans was introduced into flask B, with 2 liters of Fratel water and unicellular microalgae Selenastrum capricornutum. Initially, algal biomass was 54.3 mg l⁻¹ (dry weight) and its radioactivity was 65903.5 Bq g⁻¹ (d.w.). Radioactivity in water was 19 Bq ml⁻¹.

After three days, daphnids in flask B have reached a concentration factor CF = 88 (w.w.). According to this value, the relative contribution of water on the contamination of daphnids in flask A was 85%, the remaining 15% being attributed to the transfer of Co-60 from microalgae. Trophic transfer factor reached a very low value:

$$TTF_{sd} = 4.4 \times 10^{-2}$$

3.2.2 Retention

Retention of Co-60 by Daphnia magna was studied following: i) uptake from water and ii) uptake from water and food (Selenastrum capricornutum).

One hundred daphnids contaminated through the water, weighing 2.7 mg indiv.⁻¹ (w.w.) and whose radioactivity was 1418 Bq g⁻¹, were kept in 500 ml of non radioactive Fratel water, flask C. Another group of 100 individuals contaminated by water and food, weighing 3.6 mg indiv.⁻¹ (w.w.) and whose radioactivity was 1586 Bq g⁻¹, was set up into flask D, in similar conditions.

Water was changed every 24h during the first 8 days and then 5 times a week, till the end of the experiment, 20 days. After 3 days microalgae were added to the water, to serve as nutrient.

During this experiment neonates have eclosed and deaths have occurred among the initial individuals. For measuring purposes only the latest were considered.

In flask C, 38 individuals weighing 4.5 mg indiv.⁻¹ (w.w.) have remained after 19 days, while in flask D, only 17 individuals weighing 7.0 mg indiv.⁻¹ (w.w.) remained after 21 days. In both cases retention has followed a three - compartmental kinetics expressed (in percentage) respectively by:

$$R = 43.2 e^{-0.910t} + 54.4 e^{-0.673t} + 2.4 e^{-0.073t} \quad (C)$$

$$R = 18.6 e^{-37.7t} + 65.9 e^{-0.426t} + 15.5 e^{-0.080t} \quad (D)$$

with t referred to days, and the following biological periods:

$$Tb_1 = 18.2 \text{ h}, Tb_2 = 1.03 \text{ d} \text{ and } Tb_3 = 8.9 \text{ d} \quad (C)$$

$$Tb_1 = 0.44 \text{ h}, Tb_2 = 1.6 \text{ d} \text{ and } Tb_3 = 8.7 \text{ d} \quad (D)$$

3.3 Third trophic level: *Chondrostoma polylepis polylepis*

3.3.1 Accumulation

3.3.1.1 Contamination through the water pathway

Transfer of Co-60 from water to fish has been performed during a period of 64 days, with 9 specimens initially weighing 3.1 g indiv.⁻¹ (w.w.). Fishes were kept in 40 liters of Fratel water, having an initial radioactivity of 24.5 Bq ml⁻¹. They were put inside suspended baskets, so they could not reach the bottom of the aquarium and eat their own fecal pellets.

Frozen daphnids and fish dry food were given to the specimens, in a different batch into which they were daily transferred (except during the weekend) for a short period of time (2-3 hours).

The concentration factor reached a maximum value, CF = 7.1 ± 4.3, at the 8th day and then decreased and stabilized at the 40th day. Arithmetical mean of all the values verified at the equilibrium was:

$$CF_{eq} = 3.6 \pm 0.4$$

3.3.1.2 Contamination through the food pathway

Co-60 trophic transfer from *Daphnia magna* to *Ch. p. polylepis* was performed during 6 weeks. A group of 6 fishes, weighing initially 2.2 g indiv.⁻¹ (w.w.), received a total amount of 9.8 kBq/8.3 g (w.w.) of Co-60 labelled frozen daphnids. Fishes were maintained together in the same aquarium, with 6 liters of water, which was changed 5 times a week and a radioactive meal was furnished 4 times a week. A complementary diet was guaranteed by adding fish dry food, in order to maintain a daily diet representing 5% of total initial fish weight.

After 10 days in which fishes received 7 radioactive meals, the trophic transfer factor (TTF) has reached the equilibrium. Kinetics is expressed by the function:

$$TTF_t = 0.0464 (1 - e^{-0.1658t}) \quad (t \text{ in days})$$

While TTF was in equilibrium, the retention factor, meaning the ratio between total radioactivity in fish and total radioactivity of all ingested meals, has shown a tendency for decreasing. Maximum value during the growth phase of TTF kinetics was 2.3x10⁻¹. At the end of the experiment, the retention factor was 7.3x10⁻².

3.3.2 Retention

The retention experiment following the contamination through the water revealed only one biological half-life, T_b = 64 days, the retention expression (in percentage) being:

$$R_{t,t} = 100 e^{-0.0107t} \quad (t \text{ in days})$$

Following the contamination through the food pathway, the

retention showed two biological half-lives, $T_{b1} = 3.6$ and $T_{b2} = 54$ days. The retention (in percentage) is expressed by:

$$R_{(t)} = 9.5 e^{-0.19t} + 90.5 e^{-0.13t}$$

3.4 Water - sediments interaction

3.4.1 Effect of sediment concentration on the distribution coefficient (k_d)

All the experiments were carried out with dry river sediments from Fratel Reservoir (grain size $< 500 \mu m$), the sediment concentrations ranging from 500 to 2000 $mg l^{-1}$. An inverse relationship between the k_d and the sediment concentration was found, described by the equation:

$$k_d = 2211 - 2001 \ln C_s$$

being C_s the sediment concentration ($r^2=0.973$ for $p<0.05$), Fig. 2.5.

3.4.2 Kinetic analysis of Co-60 uptake and release by sediments

Uptake

The uptake study with a sediment concentration of $1g l^{-1}$, was carried out following the radioactivity decrease in water. The numerical analysis leads to the following relationship:

$$C_t = 49.4 e^{-0.384t} + 46.3 e^{-0.014t} \text{ (in percentage) (1)}$$

showing two components and two periods, 1.2 and 50 days.

Release

The desorption experiments showed no variation with different sediment concentrations, in an open system (with water renewal). The radioactivity retained in the sediments in function of time is expressed by the following exponential:

$$C_t = 17 e^{-3.083t} + 83 e^{-0.0155t} \text{ (in percentage) (2)}$$

There are two components and the corresponding half-lives are 5 h and 45 days.

4. Discussion

4.1 Trophic chain

In what concerns the experiments with the microalgae Selenastrum capricornutum it is noticed that there is a very fast and high initial accumulation, which, in spite of being different in all replicates, tends to an equilibrium at 7 days. The CF = $(2.3 \pm 0.6)10^3$ obtained is within the range of reported values in the literature for microalgae Chlorophyceae.

The retention study showing two biological half-lives suggests

that, besides the surface adsorption, there is an active metabolic process.

In relation to the planktonic crustacean Daphnia magna, from the accumulation experiments carried out - direct contamination through the water and contamination through water and food -, the relative contributions of water and food on the contamination of D. magna are respectively 85% and 15%.

The retention study, following both kinds of accumulation experiments, shows three biological half-lives, therefore three compartments, although it remains difficult to specify them with accuracy. The elimination of the radioisotope, goes along with molting and eclosions, both occurring with high frequency during the first week. Surface desorption is recognised by the presence of Co-60 in solution, with strongest intensity after the first 24 hours and becoming negligible after 4 - 6 days. Retention after contamination through water and food, shows an initial rapid decrease ($T_{b1} = 0.44$ h), which must be attributed to the renewal of the digestive tract.

The CF and the TTF evaluated to the fish Chondrostoma polylepis polylepis, lead to the conclusion, that the relative contributions of water and food to the contamination of the fish, are respectively 59% and 41%, although the food retention factor is 7.3×10^{-2} .

The study of the Co-60 retention shows only one biological half-life, 64 days, in the case of contamination through the water, and two, about 4 days and 54 days, when the contamination pathway is the food. In this case the compartment of higher retention, might correspond to the incorporated Co-60, just as in the first case.

All these values concerning fish experiments are in good agreement with other ones found in the literature.

The CF evaluated through the stable cobalt values, Table 2.4, is 1.7×10^2 , i.e., two orders of magnitude higher than the experimental one. The explanation for this low CF might be a certain isotopic competition, not studied in this work, but it should be noticed as well, that the stable cobalt concentrations in water and in fish are in natural equilibrium.

4.2 Sediments

The inverse relationship between the distribution coefficient and the concentration of adsorbing solids has been found by several authors, and may be attributed to either a solid-solid interaction which mediates the adsorption process, the dissolution of the sediment and water soluble organic matter, or the progressive blocking of sorption sites of the agglomerating granular sediments.

The K_d is a function of sediment properties, but also of the physico-chemical water properties. Fratel Reservoir sediments have a high percentage of large grain size particle, a BET surface area of $4.1 \text{ m}^2 \text{ g}^{-1}$ and low cationic exchange capacity, characteristics that might explain the low Co-60 K_d values.

However, *in situ*, the K_d value evaluated through the stable cobalt in natural equilibrium in water and sediments, Table 2.4, is 3.3×10^4 .

Comparing the equations (1) and (2) we observe two components which might correspond to different Co-60 sorption mechanisms in the sediments: the first faster component might involve the exchange of ions between the bulk solution and the chemisorbed layer, while the lower one might involve the exchange between this layer and the solid surface; the longer $T_{1/2}$, actually very similar, are respectively 50 and 45 days.

5. Conclusions

The conclusions are summarized in Figure 2.6, representing the main radioecological parameters evaluated for the simplified ecosystem studied.

Table 2.1 - Characterization of sediments in terms of FES numbers and cesium selectivity pattern to potassium and ammonium ions

Sed.	CEC $\mu\text{eq/g}$	FES $\mu\text{eq/g}$	[Kd.mK] meq/g	Ln Kc (Cs/K)	[Kd.mNH ₄] meq/g	Ln Kc (Cs/NH ₄)	Kc (NH ₄ /K)
T1	143	6.7	1.42	5.4	0.36	4.0	3.9
T2	75	5.5	0.60	4.7	0.19	3.5	3.2

Table 2.2 - Simulation parameters of the Cs/K selectivity pattern in the FES

Sediments	SITE I		SITE II		SITE III	
	Kc	Ln Kc	Kc	Ln Kc	Kc	Ln Kc
T1	107559	11.6 (0.2%)	6021	8.7 (1.04%)	9.5	2.3 (98.8%)
T2	91062	11.4 (0.14%)	3428	8.1 (0.9%)	5.4	1.7 (98.9%)

Table 2.3 - Stable Cobalt concentration in several compartments of Fratel Dam ecosystem

Year	Water mg l ⁻¹	Sediments mg kg ⁻¹ (dry)	Hydrophytes mg kg ⁻¹ (dry)	Fish Cyprinidae mg kg ⁻¹ (wet)
1987	(1.5±0.7)E-4	(2.1±0.1)E+0	(8.1±2.2)E+0	(8.3±3.0)E-3
1988	(1.0±0.2)E-4	(4.4±0.2)E+0	(3.7±0.6)E+0	(4.4±0.5)E-2
1989	(1.2±0.1)E-4	(7.8±3.1)E+0	(7.1±3.5)E+0	(3.5±1.5)E-2
Average of all results	(1.2±0.3)E-4	(3.9±1.2)E+0	(6.4±0.2)E+0	(2.0±0.9)E-2

Table 2.4 - Comparison of CFs and K_ds for stable cobalt (in situ) and for radiocobalt (experiments)

Element	CF(fish, w.w.)	K _d (sediments, d.w.)
Stable Co	1.7 10 ²	3.3 10 ⁴
Co-60	3.6	2.0 10 ³ *

* experiments with a sediment concentration of 1g l⁻¹

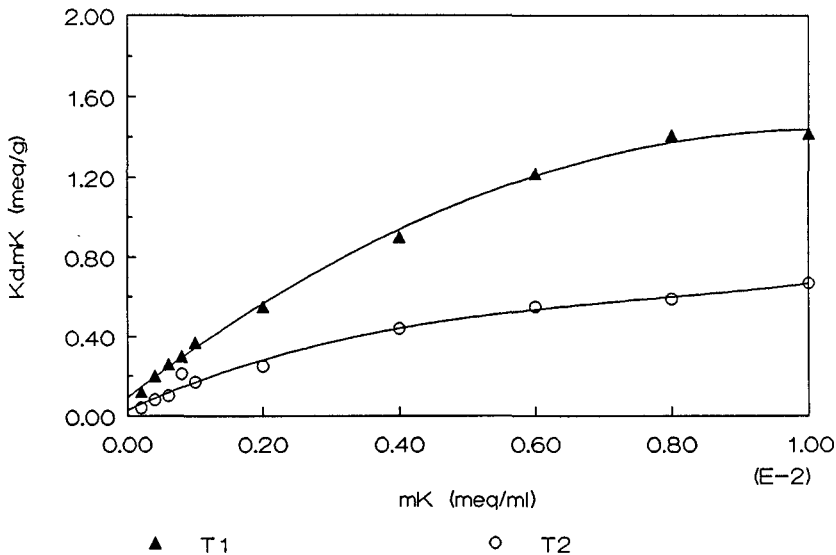


Figure 2.1 - m_K dependence on the $K_d \cdot m_K$ product for T1 and T2 sediments, in presence of 0.012N AgTU.

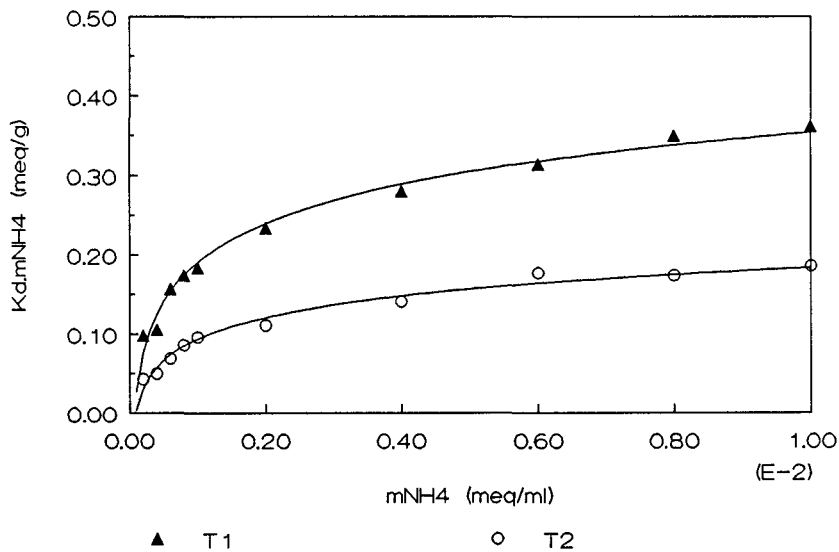


Figure 2.2 - m_{NH_4} dependence on the $K_d \cdot m_{NH_4}$ product for T1 and T2 sediments, in presence of 0.015N AgTU.

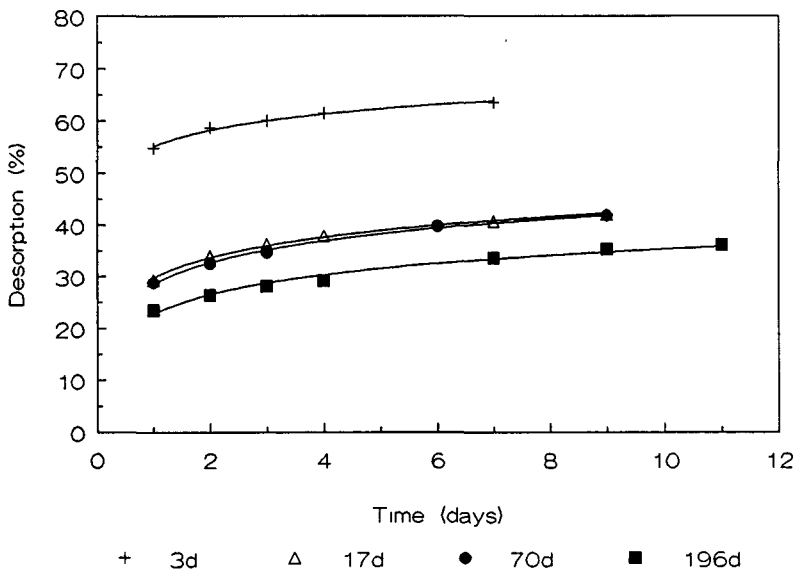


Figure 2.3 - Time dependence of cesium desorption for T1 sediment (0.5g) with Dowex 50W-x8 resin $10^{-3} M$ NH_4Cl form. Aging times 3, 17, 70 and 196 days.

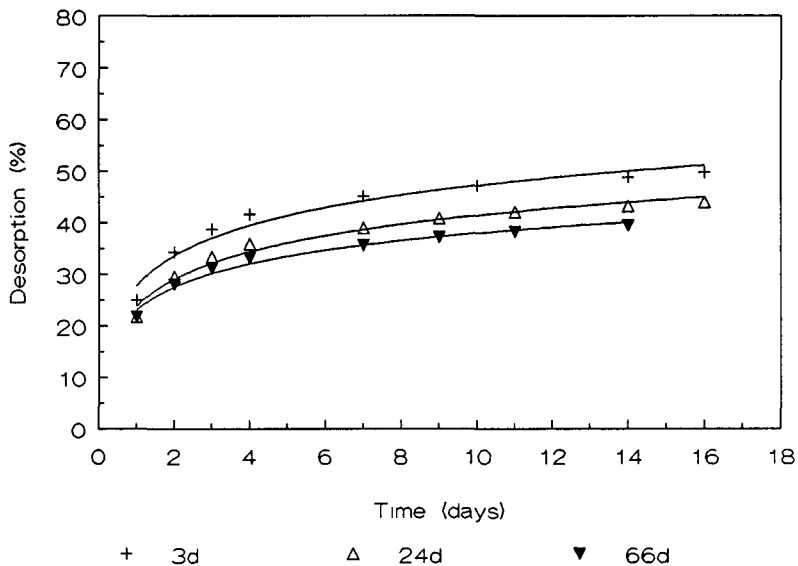


Figure 2.4 - Time dependence of cesium desorption for T1 sediment (0.5g) with Dowex-x8 resin $10^{-3} M$ KCl form. Aging times 3, 24 and 66 days.

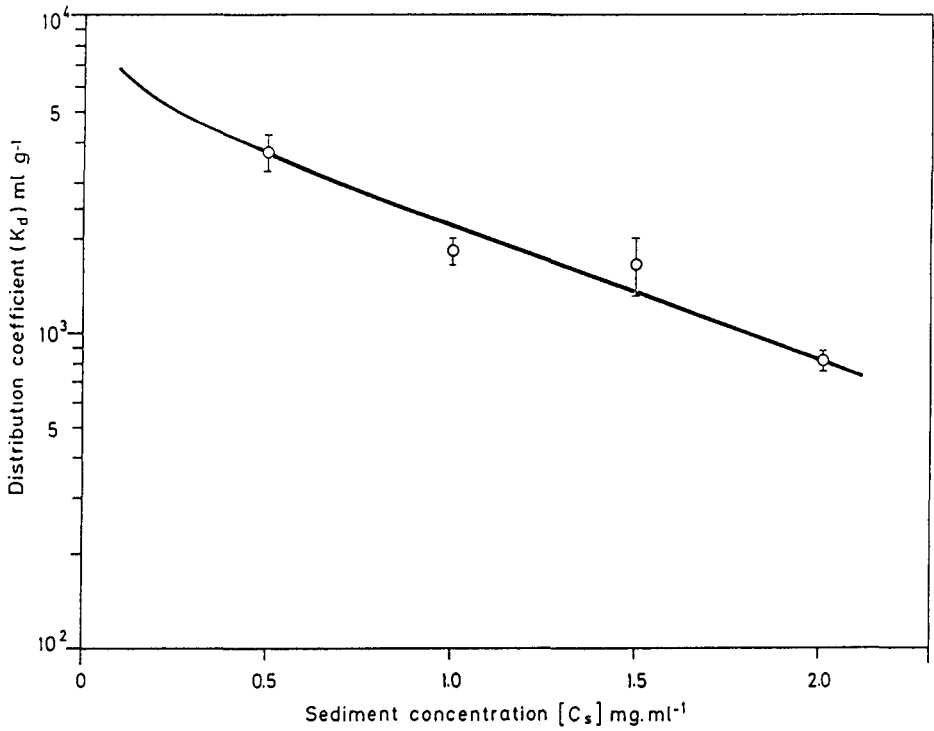
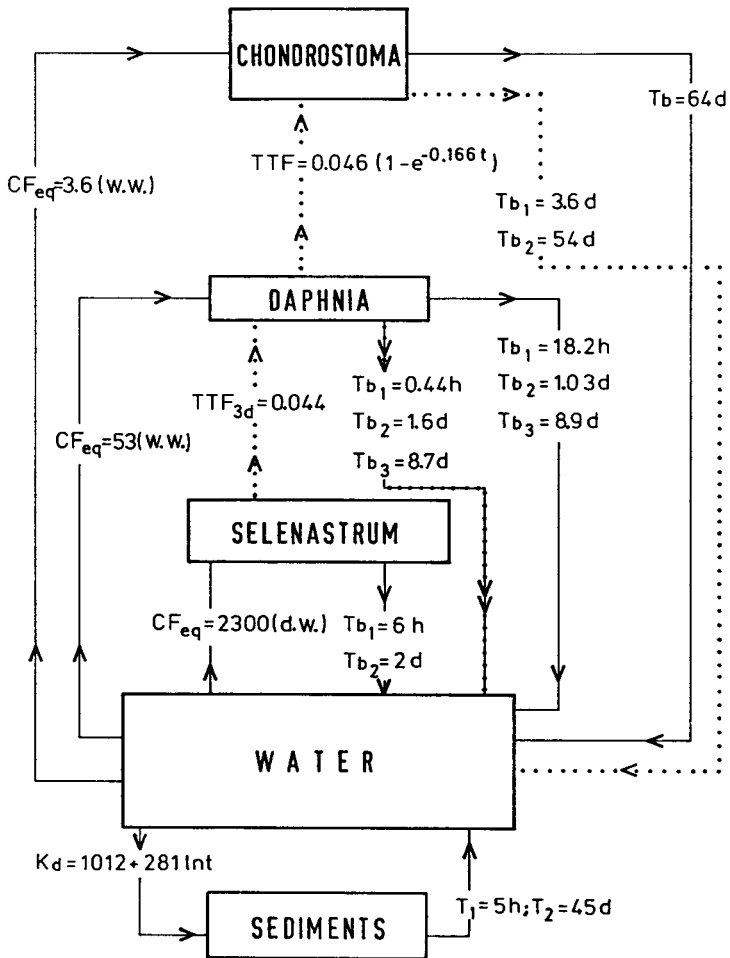


Figure 2.5 - Evolution of Co-60 K_d in function of sediment concentration.



TRANSFER OF Co-60 IN AN
EXPERIMENTAL FRESHWATER ECOSYSTEM

Figure 2.6 - Experimental model of Co-60 transfer in a simplified freshwater ecosystem.

References

- Carreiro, M.C.V. (1990)
Ecological Study of three Sampling Stations in Tejo River.
LNETI/DPSR-B-n24 (III série)
- Madruga, M.J. and Cremers, A.
Physico-Chemical Behaviour of Cs-137 in Tejo River Sediments.
Progress Report (May-December 1990)
K.U. Leuven, Belgium 1990
- Madruga, M.J. and Cremers, A.
Physico-Chemical Behaviour of Cs-137 in Tejo River Sediments.
Progress Report (January-June 1991)
K.U. Leuven, Belgium 1991
- Carreiro, M.C.V. (1991)
Transfer of Artificial Radionuclides in a Freshwater Environment.
Progress Report for the Period May 1990 - March 1991. SRA-n25/91.
- Madruga, M.J., Carreiro, M.C.V. (1991)
Experimental Study of Co-60 Behaviour in Tejo River Sediments,
Hydrobiologia, 0,1 - 8, 1991
- Carreiro, M.C.V.
Concentrations of Stable Elements in Water, Sediments and Biota
of Tejo River (to be published)
- Corisco, J.A.G., Carreiro, M.C.V.
Co-60 Transfer in a Freshwater simplified Trophic Chain. I
Accumulation and Retention by the Planktonic Algae Selenastrum
capricornutum Printz (to be published)
- Corisco, J.A.G., Carreiro, M.C.V.
Co-60 Transfer in a Freshwater simplified Trophic Chain. II
Relative Contribution of Water and Food in the Accumulation and
Retention by the Planktonic Crustacean Daphnia magna Straus (to
be published)
- Corisco, J.A.G., Carreiro, M.C.V.
Co-60 Transfer in a Freshwater simplified Trophic Chain. III
Relative Contribution of Water and Food in the Accumulation and
Retention by the Fish Chondrostoma polylepis polylepis
Steindachner (to be published)

Project 3

Head of project: *Prof. Cremers*

Objectives for the reporting period

1. Characterization of sediments in terms of parameters relevant for the short-term prediction of solid/liquid partitioning of radiocaesium.
2. The study of the long-term behaviour of radiocaesium in sediments in terms of remobilization potential and the effect of aging fixation.
3. The study of the kinetics of sorption and desorption of radiocaesium in sediments.

Progress achieved

1. Sediment characterization

A broad range (eighteen samples) of fresh water and estuarine sediments originating from various locations were considered in the program. The study includes sets of samples from the Lake District, UK (Loweswater, Wastwater, Devoke, Esthwaite, Windermere), the Ravenglass estuary (UK), the Chernobyl area, Tejo river (P) Hollands Diep and Ketelmeer (NL). All samples were characterized in terms of overall cation exchange capacity (CEC), organic matter content (OM), the number of micaceous frayed edge sites (FES) responsible for the specific sorption of radiocaesium, $[K_{D,m_K}]$ and (K_{D,m_N}) values. These quantities are defined as the radiocaesium specific sorption potentials in a K and NH_4 scenario respectively and correspond to the product of FES capacity and the trace Cs-to-K and Cs-to- NH_4 selectivity coefficient, respectively, in the specific sites. All parameters relevant to the specific sorption of radiocaesium (FES, K_{D,m_K} , K_{D,m_N}) were measured by making use of the silver thiourea masking technique, described in earlier reports. CEC values cover a range of 7.1 to 31 mE/100g and O.M. contents vary in the range of 4 to 33% OM is nearly exclusively responsible for the reversible ion exchange sorption properties of the sediments studied. This is evidenced from normalizing the sediment CEC values w.r.t. OM content. The average result is 1.49 (± 0.45) mE/g, a value which is typical for OM in sediments.

FES capacities cover a range 3-40 $\mu E/g$ representing on average 7% (± 3) of overall CEC values. This value is significantly higher than for soils, a result which is not unexpected and can be explained by the fact that it is predominantly the fine fractions which are not being deposited. $[K_{D,m_K}]$ values cover a wide range of 0.4 to 5 mE/g whereas $[K_{D,m_N}]$ values cover a range of 0.12 to 1 mE/g. The ratio of these two quantities varies in the range of about 4 to 6.5 and corresponds to the NH_4 to K selectivity coefficient in the specific sites. Such ratio has also been found for reference micaceous clays and demonstrates the action of such minerals in these systems.

On the basis of these results, some important conclusions can be drawn. The first one relates to the partitioning of radiocaesium between the FES and the regular CEC pool. Such partitioning can be calculated on the basis of a comparison of $[K_{D,m_N}]$ values and the

radiocaesium interception potential of the CEC pool. This quantity corresponds to the product [CEC] $Z_K \cdot K_c(Cs/K)$ in which Z_K refers to the K occupancy in and $K_c(Cs/K)$ to the Cs-K selectivity for exchange complex.

In general, $Z_K < .05$ and $K_c = 1$ of OM. Calculations show that (taking $Z_c = .05$) for all sediments studied, at most 1% ($0.53 \pm .25\%$) of radiocaesium can be expected to be present in the regular ion exchange sites. These estimates were backed up experimentally by the finding that bulky ions (such as bisquaternary ammonium) showing very high selectivity for regular exchange sites are not able to displace radiocaesium from sediments.

As a consequence, it would appear that sorption K_D values should be solely describable in terms of $[K_D \cdot m_K]$ and $[K_D \cdot m_N]$ values and water composition (i.e. K and NH_4). On the basis of the range of $[K_D \cdot m_N]$ values reported above a range of 4000 to 40000 (using $K=0.1$ mE/L can be predicted for freshwater scenarios. Including a NH_4 at a concentration of 0.1 mE/L would reduce these values by a factor of about 5. Experimental studies on various sediments have shown that, with rare exceptions, sorption K_D values can be predicted within a factor of about 2 using the equation

$$K_D = \frac{[K_D \cdot m_K]}{m_K + m_N K_c(N/K)}$$

Such result shows that, as far as the water composition is concerned, Ca and Mg have no direct effect on radiocaesium sorption in the sediment.

2. Long term effects and radiocaesium desorption

The characterizations presented in section 1 are of limited relevance to long-term effects and to the potential of a sediment to act as a future source term for radiocaesium release upon a change in geochemical scenario (e.g. in anoxic sediments and lake destratification). The key issues in this process are radiocaesium desorption capability and the effect of aging thereon.

The kinetic limitations inherent to the use of concentrated solutions of K or NH_4 for measuring desorption led us to develop a new methodology based upon an "infinite bath" scenario. In short, the method is as follows: a Cs-contaminated sediment is dialytically equilibrated with an ion exchanger showing significantly higher Cs-sorption properties as compared to the sediment. As a result, the sediment-solution equilibrium is disrupted, thus generating a radiocaesium desorption flux into a liquid phase with virtually zero levels in radiocaesium (hence the term infinite bath). Such equilibration is usually carried out in a 10^{-3} M NH_4 (or K concentration). After 24 hours the ion exchanger is replaced by a fresh sample and the procedure may be continued any desired number of times until a well-defined desorption plateau is obtained. Usually a one week desorption period is sufficient although in some cases, longer desorption periods are used. The process is monitored by counting the activity collected on the ion exchanger and the residual activity left in the sediment at the end of the experiment. The amount of ion exchanger to be used is critical. To establish proper boundary conditions it is required that $K_D \cdot m^e > 10 K_D \cdot m^e$ (m referring to mass, e to ion

exchanger, s to sediment). In general the ratio of the two quantities is 50 to 100. Various options can be used for the ion exchanger. In the early phases, either illitic clay or sulphonic acid resins were used as caesium sorbents. More recently, use was made of cyanoferrates exhibiting exceedingly high Cs-K_D values (5.10⁴ ml/g). The method is now developed into a routine procedure and has been scaled up for application to field-contaminated samples opening new perspectives for studying long-term aging effects.

Figure 1 shows some typical examples of radiocaesium desorption plots, characterized by well-defined plateau values. All sediments have been submitted to such desorption tests. Desorption levels for short aging times (days) may vary anywhere between about 50 to 90%. This finding is similar to what was found for soils (10-90%). Most significant however is the finding that the desorption behaviour bears absolutely no relationship whatever to sorption characteristics of the systems. It would therefore appear that we have to accept some structural differences within the FES pools of different sediments.

For all sediments, tests were carried out in which desorption yields were monitored as a function of aging time. In all cases aging effects could be demonstrated corresponding to a decrease in desorption yields, ranging from 10-40% for aging times of about 11 weeks. Again, no link could be made with specific sorption properties of the system.

The coherence of radiocaesium sorption behaviour in the various sediments is in sharp contrast with their erratic fixation behaviour. So far we have adopted the view that the FES pool represents some structural entity quite similar in the various systems but which is unrelated to the water composition. Recent findings have however demonstrated some significant effects. Three systems (illite, Po and Loire sediment) were allowed to age for several months in three different ionic scenarios: 1mM K, 1mM K + 100mM Mg and 1 mM K + 100mM Ca. They were then labelled with Cs-137 and allowed to age for 1 and 24 days. Desorption yields were measured using the infinite bath methodology. The results are shown in table 1. All values are averages of two measurements differing by 2% at most.

It is seen that for one day aging time, nearly quantitative desorption (93-98) can be accomplished. After 24 days desorption yields drop by some 10-15% in the homoionic potassium scenario. In contrast, desorption yields in the K-Mg and K-Ca scenarios are some 20-45% lower than in the K scenario. It thus appears that strongly hydrated ions may influence some structural property of the FES, leading to an accelerated fixation process.

Exactly similar results were obtained in soils at much lower ionic strengths and it appears that the key factor is the Potassium Adsorption Ratio (PAR) of the water:

$$m_K / \sqrt{m_{Ca} + m_{Mg}}$$

Consequently, depending on water composition of lakes (low or high K levels) significant differences in long-term behaviour may be expected. These aspects need utmost attention in future studies.

Table 1 Radiocaesium desorption yields (%) obtained in three ionic scenarios

	aging	K	K+Mg	K+Ca
Po	1day	97	95	94
	24 days	82	61	49
Loire	1 day	97	98	97
	24 days	88	66	65
Illite	1 day	97	95	93
	24 days	84	44	39

3. Adsorption kinetics

A kinetic three box model for describing the solid-liquid sorption dynamics has been developed using only three parameters. The boxes are: the liquid phase (L), the regular frayed edge sites (FES) and the high affinity sites (HAS). The model postulates a direct initial adsorption on the FES and a relatively slow and reversible redistribution process of radiocaesium from those FES towards the HAS, hereby passing through the liquid phase (L). Interaction between L and FES is characterized by an equilibrium constant K_D ; partitioning of radiocaesium between L and HAS is assumed to be governed by two first-order rate constant k_1 and k_2 . The model is defined by the following two equations:

$$dC_s(\text{HAS})/dt = k_1 \times C_s(\text{L}) - k_2 \times C_s(\text{HAS})$$

and a mass balance.

Analytical solutions for the changing partitioning of radiocaesium between L, FES and HAS with time have been obtained using Laplace transformations.

The adsorption process was experimentally followed by monitoring the radiocaesium activity in the liquid phase for two Po sediments, three Loire sediments, four Tejo river sediments and suspended material from the Meuse, in two solutions of 10^{-3}M and 10^{-4}M potassium chloride respectively.

The experimental data could adequately be described using our kinetic model. The half-life for the adsorption processes ranges between half a day and four days for a S/L ratio of 1/1000 and is, for each substrate, longer in a 10^{-3}M KCl solution compared to a 10^{-4}M KCl solution. This is in qualitative agreement with the decreasing desorption yields for adsorption in KCl solutions of decreasing concentrations: the longer the half-life the slower the translocation from the easily accessible FES to the kinetically controlled HAS and the higher the apparent desorption yield.

The partitioning of radiocaesium between FES and HAS at equilibrium is highly dependent on the substrate under study and varies between 35 and 75 percent.

4. Desorption kinetics

The study of desorption kinetics in a finite volume of solution is always hampered by the by the build-up of radiocaesium levels in the liquid phase causing the desorption to slow down and stop very quickly - depending on the S/L ratio making it very difficult to obtain statistically significant fittings of the kinetic parameters. An 'infinite: bath' scenario seemed more adequate to give a kinetic explanation of the experimental desorption patterns.

Essentially the model was not altered: only the boundary conditions changed, since the level of radiocaesium in solution L is kept near zero during the whole desorption run. Although the three boxes remained, one of the parameters changed: the upgoing rate constant k_2 from L to HAS disappeared and the fraction of the total amount of radiocaesium on the sediment associated with the HAS at the start of the desorption, $\text{fracC}_i^{\text{HAS}}$, had to be taken into consideration.

Desorption patterns as a function of desorption time could be fitted very well for the five substrates under study: two lake sediments (Devoke and Esthwaite) from Cumbria, UK, one estuarine sediment from Ravenglass, UK one river sediment (Hollands Diep) and one reservoir sediment (Ketelmeer) from the Netherlands. Desorption experiments were carried out for three different adsorption times: 2, 36 and 76 days. An example of the desorption data and matching simulations on Hollands Diep for the three aging times is given in figure 2.

Since the desorption of radiocaesium continues, although very slowly even after three weeks of desorption, a true desorption plateau is never reached. The differences in apparent desorption yield for the three aging times can entirely be explained on the basis of our reversible kinetic model. Only one of the simulation parameters varies with adsorption time: $\text{fracCs}^{\text{HAS}}$. For the simulations in figure 2, $\text{fracCs}^{\text{HAS}}$ raises from 20% after 2 days over 25% after 36 days to 45% after 76 days of adsorption. Since the desorption out these HAS is kinetically controlled - with half-lives varying between 10 and 70 days, the apparent desorption plateaus decrease with aging time.

When comparing the backward rate constants k_2 for the different sediments, the relatively narrow range wherein they vary is striking and leads us to the hypothesis that important differences in desorption behaviour between sediments is mainly due to different adsorption rates k_2 . These rates cannot be deduced directly from 'infinite bath' desorptions. Further desorption experiments for a broader range of aging times - and accordingly more values for $\text{fracCs}^{\text{HAS}}$ as a function of time - should enable us to get a hold on the rate of the apparent fixation process.

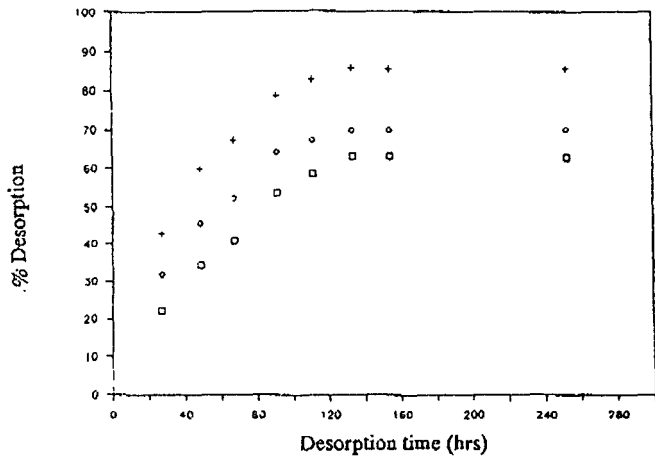


Figure 1. Desorption of radiocaesium for (top to bottom): Devoke, Ravenglass and Esthwaite sediments. Aging time is 10 days.

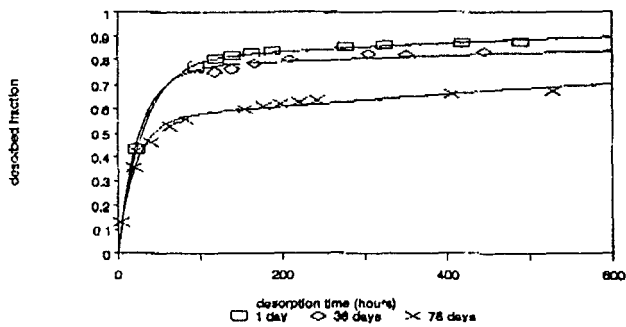


Figure 2: Experimental and simulated desorption patterns for Hollands Diep sediment after three different aging times: 1, 36 and 76 days.

Project 4

Head of project: *Dr. Foulquier*

1. A comparative study of the impact on the Rhone River of liquid effluents from nuclear installations and fallout from the Chernobyl accident (A. Lambrechts)

Because of the density of nuclear plants installed along its banks, the Rhône is a particularly valuable terrain for investigation. Over 300 km, 17 power stations and three fuel cycle plants are installed along this river (Figure 1). These nuclear plants discharge after treatment liquid effluents according to the national legislation.

Our laboratory studies the radioecology of the Rhône river, collecting, both upstream and downstream of nuclear installations samples of water, sediment, aquatic vegetation and fish which are treated before making measurements of radioactivity by gamma spectrometer or by radiochemical methods for alpha and beta emitters. The results of these measurements are stored in a computer data base.

Natural radioactivity (due to K 40, Be 7, and to elements of the uranium and thorium families) is constant over the whole river with mean values given in table 1.

From Creys-Malville to Marcoule, 12 artificial radionuclides were observed before may 1986 when the Chernobyl accident occurred (table 2).

Aquatic vegetation is a good indicator of radioactivity, particularly moss which responds quickly to fluctuations of radioactivity in the water. Levels of radioactivity in fish, although lower in concentration, still reflect the composition of the power station effluent.

Artificial radioactivity (mainly tritium) in compartments of the Rhône are 10 to 50 times lower than natural radioactivity levels. They are characterized by the presence of fission products ($^{134,137}\text{Cs}$, ^{90}Sr) and products from either activation or corrosion of materials within the reactors ($^{58,60}\text{Co}$, $^{110\text{m}}\text{Ag}$, ^{54}Mn , ^{65}Zn , ^{95}Zr ...).

Downstream from the fuel reprocessing plant of Marcoule, new radionuclides appear and those that existed upstream increase mainly (table 3).

After 30 years of the fuel reprocessing plant operation, the artificial radioactivity of the river compartments is inferior or equal to their natural radioactivity.

The accident of Chernobyl occurred on 26 April 1986. The radioactive plume passed over the east of France during the first week of May 1986. The radionuclides were deposited essentially as wet deposition, either during rain or by the washing out of aerosols. 19 radionuclides have been detected in the fallout but only 5 (after the rapid disappearance of ^{131}I and ^{132}Te) were observed to be significant in the compartments of the Rhône during May (table 4).

The impact of Chernobyl was more important in the upper part of the Rhone river where no nuclear liquid effluent existed. From Creys to Marcoule the radioactivity from the Chernobyl fallout added up with this from liquid effluents. Downstream from Marcoule the

impact of Chernobyl was less obvious because the liquid effluent from the reprocessing plant had the highest radioactivity.

After May 1986, a decrease in the radioactivity was observed in all the compartments of the river. The speed of the reduction depended of the effective half-life of the radionuclide. By the end of 1988 the levels of radioactivity were the same order of magnitude as those measured before the accident.

2. Mechanisms of transfer of ^{110m}Ag in a simplified aquatic food chain (J. Garnier-Laplace, J.P. Baudin)

Radioecological field studies showed the presence of ^{110m}Ag in the principal compartments of freshwater ecosystems receiving liquid effluents from nuclear installations. The presence of this radionuclide in the natural environment results principally from liquid effluents from pressurised water reactors under normal operation. Since May 1986, the frequency of detection has increased as a result of the atmospheric fallout following the Chernobyl accident. As a result of these two source terms, on the river Rhône for example, ^{110m}Ag was measured in a number of field samples, particularly in sediments and fish (table 5). In all cases, field studies have shown that the sediments integrate ^{110m}Ag pollution, forming in the ecosystem the most concentrated physical reservoir which represents a source of secondary contamination for food chains.

Series of laboratory experiments were enterprised under simplified ecological conditions in order to understand and interpret the values of ^{110m}Ag concentration collected in the Rhône river and other aquatic ecosystems. The purpose of such experimental study was to quantify each radionuclide transfer between one compartment to the other and to measure the exchange kinetics. The final objective was to create a mathematical model simulating the ^{110m}Ag distribution in a trophic chain after a chronic or acute contamination.

The trophic chain was constituted with 4 levels:

- a primary productor which was the alga *Scenedesmus* chosen according to its ecological importance, its universal repartition and its easy culture conditions in laboratory.
- 1st order consumers: *Daphnia* which is a pelagic crayfish, *Gammarus* which is a pelagic crayfish and the *Chironomus* larva which is a limnic insect larva. They are natural preys for omnivorous fish.
- 2nd order consumer: the carp (*Cyprinus carpio*) was chosen for its presence in all the french rivers and its pelagic way of life linked to sediment.
- 3rd order consumer: the trout (*Salmo trutta*) was chosen for its carnivorous diet (with the presence of small fish), its universal repartition and its consumption by man.

In this experimental ecosystem, every possible transfer of ^{110m}Ag from a compartment to the other was studied, direct transfers from water or sediment, trophic transfers from food to consumer.

Each transfer was divided in two steps:

- the accumulation phase where the organism was in relation with the radionuclide,
- the depuration phase where the organism was taken off from the radioactive environment and put in an inactive medium.

Each transfer was quantified by an equation based on the compartmental models theory. Figure 2 give the maximum values of the radioecological parameters obtained in this experimental ecosystem.

From these parameters, it was interesting to elaborate a mathematical tool giving a synthetic view of the different radioactivity exchanges.

The model was built around the 4 biotic units and 2 abiotic units. It was based on a mathematical formulation of these radioactive exchange flows between the different units. It was written in Turbo-Pascal with a separate unit for every trophic level in order to compute the quantity of radionuclide transferred from each possible accumulation vector (water, sediment, food). The radioactive quantities were computed from the equation defining the accumulation and excretion phasis. The ecological parameters were taken in consideration in the computing units. The ecological hypothesis were those defined by seasonal cycles:

- phytoplankton was present only during the plancton bloom in spring,
- daphnids were present in spring and summer,
- both gammarids and midge larvae were present in spring, summer and autumn.

For fish a weight growing curve was defined in order to compute the daily growth rate, taking in account the winter stop for carp, winter and summer stop for trout.

Figure 3a shows an example of a chronic contamination during spring time. The concentration of ^{110m}Ag was fixed to 1 mBq.l^{-1} in water and $10 \text{ Bq.kg}^{-1}\text{WW}$ in sediment (values from the Rhône river). For carp, the model shows large seasonal fluctuations with a clear accumulation phase during spring and summer when all the food species were present, then a slowing down when daphnid consumption stopped. During spring, summer and autumn the trophic way was 92% of total contamination for 0+ year old carps. It was lower for older fish that eat relatively less food according to their own weight. During winter the decrease of radioactivity was in relation with absence of food, and physical and biological decrease of the absorbed silver. The contamination from water and sediment was not able to compensate the decrease. The next year the phenomenon was the same with a lower radioactivity level.

For trout the seasonal impact was less important according to the absence of decontamination phenomenon. The curve was increasing when the fish was eating (spring and summer). The trophic way was 99% of total contamination for 3+ years old fish. There was a decreasing period when consumption was stopped.

The validation of the model with Rhône data was rather good when we measured silver concentrations between 0 and $3 \text{ Bq.kg}^{-1}\text{WW}$ in fish.

Figure 3b shows an example of an acute contamination in spring (which was the Chernobyl accident conditions). The radioactivity was fixed at 50 mBq.l^{-1} in the water. The simulation was done for a two years period. For carp, a rapid contamination occurred from the water during the fallout period then, afterward, from food until the radioactivity of the preys became negligible. The decrease in autumn was due to the disparition of daphnids.

For trouts the accumulation kinetics was slower, coming from water during the fallout period then from food. The radioactive peak was much more shifted on the right than the trophic level was higher.

In both fish, the decrease of radioactivity was in relation with the biologic dilution, the consumption of preys which were less contaminated and the elimination processes when they existed.

The simulation of an accident, like Chernobyl, during the winter time shows that its impact should have been less important for fish in relation with the absence of plancton and 1st order consumers.

In conclusion, we see that such a modelisation brings interesting informations about the exchange flows in an aquatic ecosystem. However, one must be careful when trying to make an extrapolation to natural ecosystems having more living species and more ecological parameters. So, validation with field data is always indispensable to give to the model an explication and predictive quality.

Table 1. Natural radioactivity of different compartments of the Rhône river (1977-1991).

water	0.8 ± 0.2 Bq.l ⁻¹ (124)*
sediment	1990 ± 124 Bq.kg ⁻¹ DW (196)
aquatic vegetation	1832 ± 353 Bq.kg ⁻¹ DW (214)
aquatic moss	2225 ± 602 Bq.kg ⁻¹ DW (75)
fish	115 ± 11 Bq.kg ⁻¹ WW (1524)

* Mean ± 95% confidence intervals obtained from significant values (number of values)

Table 2. Artificial radioactivity of different compartments of the Rhône river, from Creys-Malville to Marcoule, before the Chernobyl accident (1977-1986).

Nuclides	water Bq.l ⁻¹	sediment Bq.kg ⁻¹ DW	aquatic high plants Bq.kg ⁻¹ DW	aquatic moss Bq.kg ⁻¹ DW	fish Bq.kg ⁻¹ WW
^{110m} Ag		3 ± 1.8 (6)*	3.5 (1)		0.1-0.8 (4)
⁵⁷ Co			8.5 ± 19 (6)		0.1-0.4 (2)
⁵⁸ Co	< 0.004 (2)	5.4 ± 4 (5)	165 ± 207 (24)	48-296 (2)	16 ± 15 (35)
⁶⁰ Co	< 0.007 (2)	4.1 ± 2.9 (13)	35.7 ± 41.9 (23)	16-22 (2)	2.3 ± 1.9 (57)
¹³⁴ Cs		1.6 ± 1 (5)	1.7 (1)	8.8 (1)	0.4 ± 0.1 (78)
¹³⁷ Cs	< 0.008 (2)	15.2 ± 6.7 (16)	5.1 ± 2 (25)	5.8 ± 3.7 (6)	1.1 ± 1 (326)
⁵⁴ Mn			42 ± 49 (14)	10-15 (2)	2 ± 2 (19)
¹⁰⁶ Ru + Rh		42-95** (2)	71 (1)		1-8 (3)
⁶⁵ Zn					0.4-20 (13)
⁹⁵ Zr			10-63** (3)		0.1-1 (3)
⁹⁰ Sr	< 0.04 (2)		5.4 ± 5.3 (4)		1.6 ± 0.5 (45)
³ H (Bq.l ⁻¹ in water of combustion)		5960 ± 3400 (11)	85 ± 76 (4)		20-1320 (12)

* Mean ± 95% confidence intervals obtained from significant values (number of values)

** Minimum to maximum observed

Table 3. Artificial radioactivity of different compartments of the Rhône river, downstream from Marcoule, before the Chernobyl accident (1977-1986).

Nuclides	water Bq.l ⁻¹	sediment Bq.kg ⁻¹ DW	aquatic high plants Bq.kg ⁻¹ DW	fish Bq.kg ⁻¹ WW
^{110m} Ag		7.2 ± 2.3 (14)*	5.3 ± 2.9 (9)	0.28 (1)
²⁴¹ Am		14.9 ± 7 (11)	5.1 ± 3 (5)	0.1 (1)
¹⁴⁴ Ce + pr	0.5 ± 1 (12)	139 ± 28 (16)	77 ± 19 (23)	0.3-5.7 (4)
⁵⁷ Co		1 (1)	0.3-14 (6)	
⁵⁸ Co	0.01 ± 0.003 (43)	5.7 ± 1.5 (8)	139 ± 86 (27)	0.06-0.4 (2)
⁶⁰ Co	0.01 ± 0.003 (39)	6.8 ± 1.6 (17)	51 ± 32 (30)	1.9 ± 3.4 (18)
¹³⁴ Cs	0.01 ± 0.003 (63)	58 ± 16 (19)	47 ± 17 (29)	2.3 ± 0.4 (97)
¹³⁷ Cs	0.03 ± 0.06 (100)	403 ± 114 (20)	245 ± 18 (31)	11.5 ± 2.2 (136)
⁵⁴ Mn	0.01 ± 0.003 (43)	34 ± 12 (15)	204 ± 85 (31)	1.9 ± 2.1 (21)
¹⁰⁶ Ru + Rh	0.4 ± 0.09 (100)	368 ± 100 (18)	765 ± 211 (30)	1.5-4.8 (2)
¹²⁵ Sb		13.2 ± 6.1 (12)	13.8 ± 7.6 (16)	
⁶⁵ Zn				4.5 (1)
⁹⁵ Zr		7 (1)	4.2-59** (3)	
⁹⁰ Sr	0.04 ± 0.007 (11)		7.6 ± 1.2 (11) 126 ± 47 (8)	1.5 ± 0.3 (55)
³ H (Bq.l ⁻¹ in water of combustion)	19.3 ± 2.8 (20)	5960 ± 3400 (11)	247 ± 190 (8)	148-24 (21)

* Mean ± 95% confidence intervals obtained from significant values (number of values).

** minimum to maximum observed

Table 4. Artificial radioactivity of different compartments of the Rhône river, downstream from Marcoule, before the Chernobyl accident (1977-1986).

zone	Nuclides	sediment Bq kg ⁻¹ DW	aquatic vegetation Bq.kg ⁻¹ DW	fish Bq.kg ⁻¹ WW
Upstream Creys- Malville	¹³⁴ Cs	122 (1)*	192 (1)	4.2±1.6 (14)
	¹³⁷ Cs	240 (1)	389 (1)	8.8±3.2 (14)
	¹⁰³ Ru	160 (1)	594 (1)	2.1±1.4 (6)
	¹⁰⁶ Ru + Rh	120 (1)	385 (1)	
From Creys to Marcoule	^{110m} Ag	6,1±4.2 (7)	17±11 (7)	1.1±3.4 (3)
	¹³⁴ Cs	90±68 (7)	122±30 (7)	4.2±1.1 (44)
	¹³⁷ Cs	178±132 (7)	363±221 (7)	9.32±2.4 (44)
	¹⁰³ Ru	257±229 (7)	1964±671 (7)	3±1.2 (44)
	¹⁰⁶ Ru + Rh	152±133 (7)	1154±355 (7)	
downstream Marcoule	^{110m} Ag	14 (1)	10 (1)	
	¹³⁴ Cs	195 (1)	179 (1)	3.1±0.8 (6)
	¹³⁷ Cs	520 (1)	386 (1)	21.4±8.1 (6)
	¹⁰³ Ru	610 (1)	983 (1)	6.7 (1)
	¹⁰⁶ Ru + Rh	520 (1)	702 (1)	11.1 (1)

* Mean ± 95% confidence intervals obtained from significant values (number of values).

Table 5. Concentration of ^{110m}Ag in sediment (Bq.kg⁻¹DW) and in fish (Bq.kg⁻¹WW) of the Rhône river between Creys-Malville and Marcoule.

Years	Sediments	Fish
1984	(0/11)*	(0/15)
1985	3.2±1.6 (7/17)	(0/82)
1986	6.2±3.9 (19/22)	0.8±1.6 (5/97)
1987	4.1±2.7 (13/13)	0.9±0.7 (4/178)
1988	9.8±7.9 (16/17)	0.2±0.1 (4/164)
1989	3.3±1.8 (5/14)	0.8±0.8 (9/140)

* Mean ± 95% confidence intervals obtained from significant values (number of significant values/ number of samples).

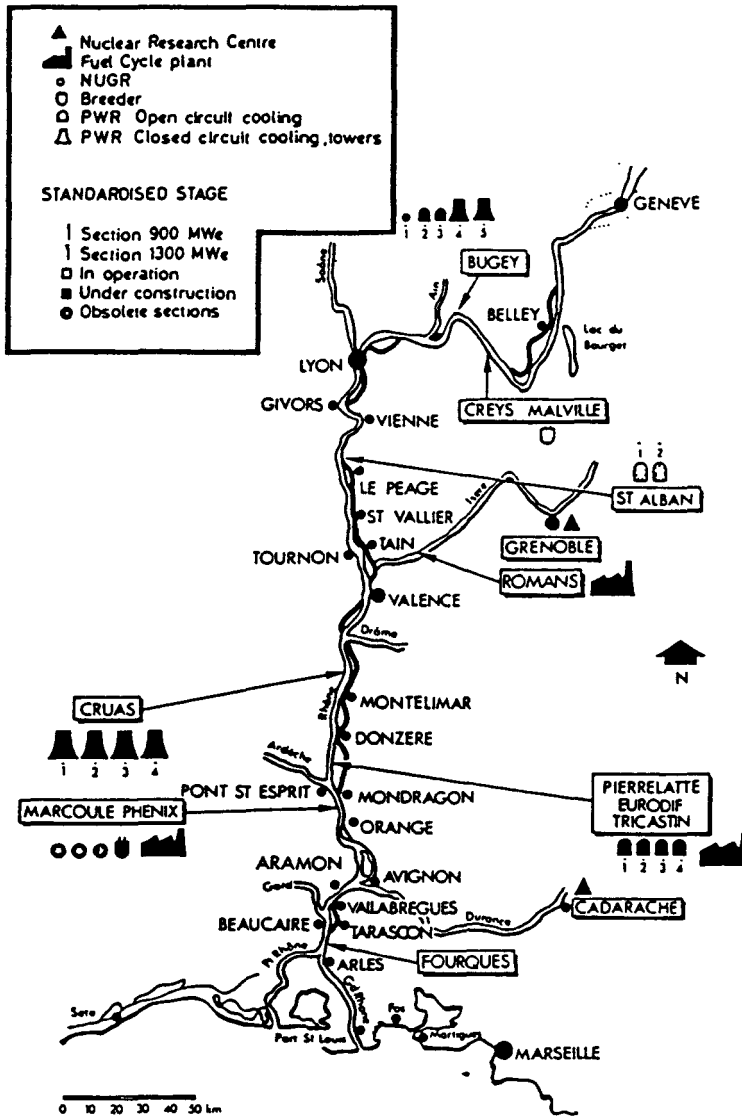
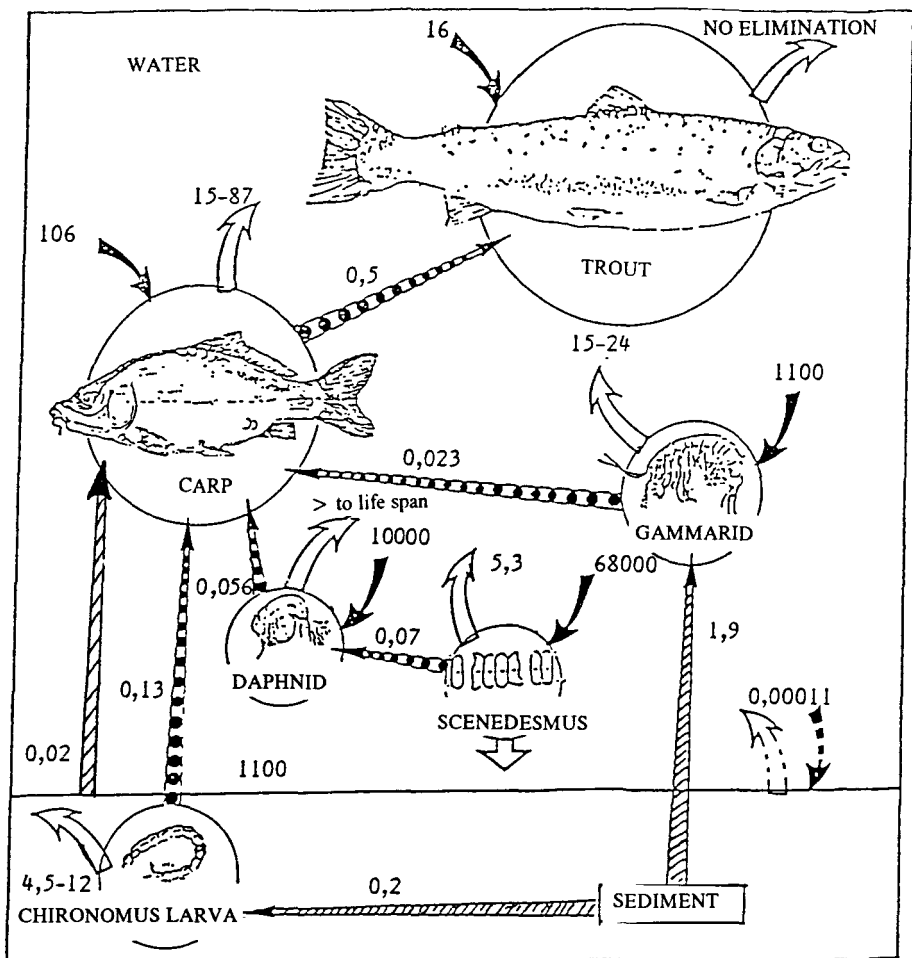


Figure 1: Nuclear reactors on the Rhône.



- 110mAg** Exchange Factor = $[\text{110mAg}]_{\text{water}} (\text{Bq.l}^{-1}) / [\text{110mAg}]_{\text{sediment}} (\text{Bq.kg}^{-1} \text{ W.W.})$
- ↔** Concentration Factor = $[\text{110mAg}]_{\text{organism}} (\text{Bq.kg}^{-1} \text{ W.W.}) / [\text{110mAg}]_{\text{water}} (\text{Bq.l}^{-1})$
- Transfer Factor = $[\text{110mAg}]_{\text{organism}} (\text{Bq.kg}^{-1} \text{ W.W.}) / [\text{110mAg}]_{\text{sediment}} (\text{Bq.kg}^{-1} \text{ W.W.})$
- ↔** Trophic Transfer Factor = $[\text{110mAg}]_{\text{consumer}} (\text{Bq.kg}^{-1} \text{ W.W.}) / [\text{110mAg}]_{\text{prey}} (\text{Bq.kg}^{-1} \text{ W.W.})$
- ↔** long biological period characteristic of the depuration phase (days)

Figure 2: Maximum values of radioecological parameters obtained in the experimental ecosystem (equilibrium value only if it is reached in a time compatible with life span of the organism).

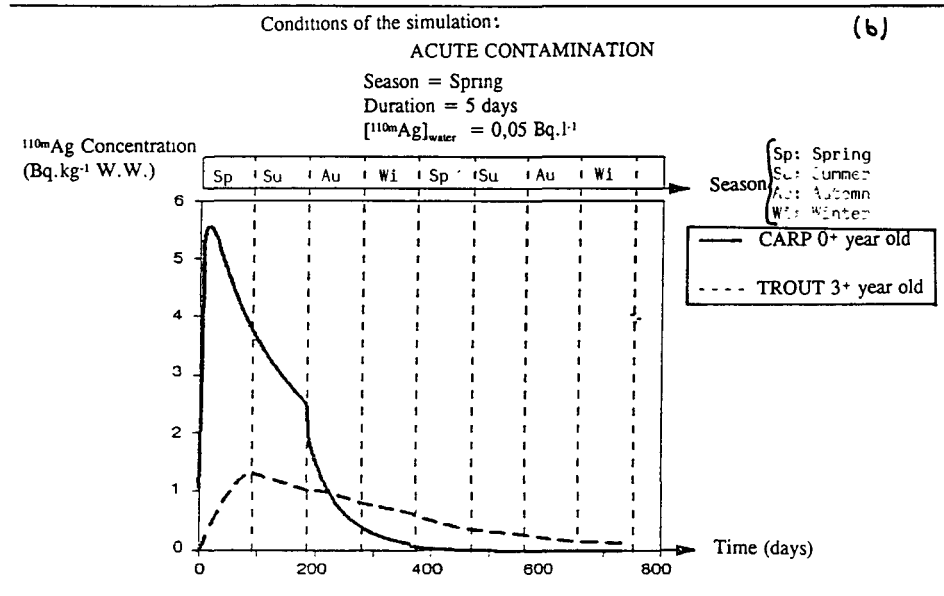
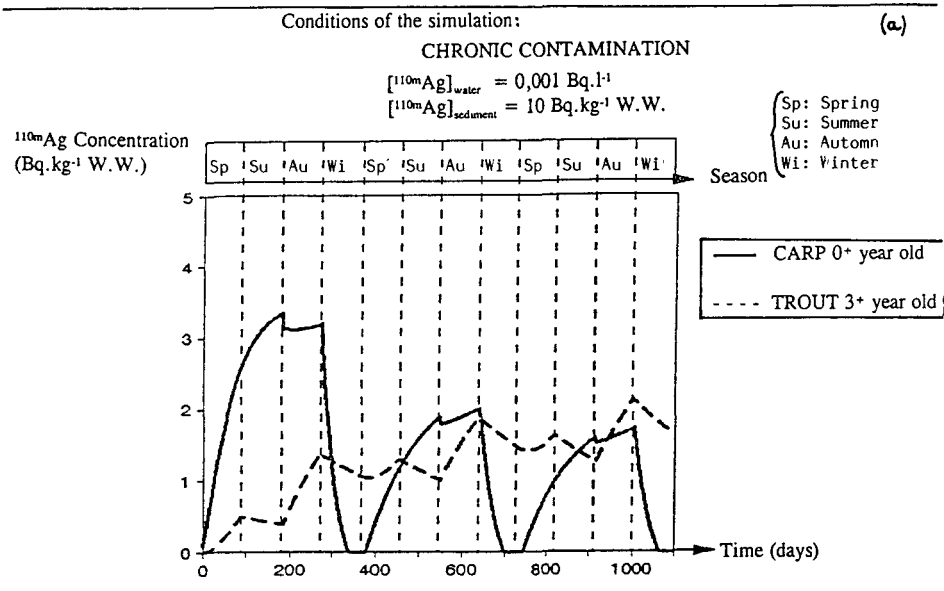


Figure 3: Results of numerical simulations obtained by application of the model under chronic contamination conditions (a) and acute ones (b)

Publications

FOULQUIER L., DESCAMPS B., LAMBRECHTS A. & PALLY M. (1991) Analyse et évolution de l'impact de l'accident de Tchernobyl sur le fleuve Rhône. *Verh. Internat. Limnol.* 24:2352-2355.

FOULQUIER L. & BAUDIN-JAULENT Y. (1990). Impact radioécologique de l'accident de Tchernobyl sur les écosystèmes aquatiques continentaux. *CCE. Radioprotection-50. Rapport XI-3522/90 FR.*

FOULQUIER L., GARNIER-LAPLACE J., DESCAMPS B., LAMBRECHTS A. & PALLY M. (1991). Exemples d'impact radioécologique de centrales nucléaires sur des cours d'eau français. *Hydroecol. Appl. (1991) 3 (2): 3-62.*

GARNIER J. & BAUDIN J.P. (1989). Accumulation and depuration of ^{110m}Ag by a planktonic alga, *Scenedesmus obliquus*. *Water, Air and Soil Pollution*, 45:287-299.

GARNIER J. & BAUDIN J.P. (1990). Retention of ingested ^{110m}Ag by a freshwater fish, *Salmo trutta L.* *Water, Air and Soil Pollution*, 50:409-421.

GARNIER J., BAUDIN J.P. & FOULQUIER. (1990). Accumulation from water and depuration of ^{110m}Ag by a freshwater fish, *salmo trutta L.* *Wat. Res.* 24(11): 1407-1414.

GARNIER-LAPLACE J. (1991) Etude des mécanismes de transfert de l'argent ^{110m}Ag en eau douce. *Thèse de Doctorat Énergétique de l'Université de Montpellier II. Rapport CEA-R-5549* :198 p.

GARNIER-LAPLACE J., BAUDIN J.P. & FOULQUIER. (1991). Experimental study of ^{110m}Ag transfer from sediment to biota in a simplified freshwater ecosystem. *Proceed. of the 5th Internat. Symposium on the interactions between sediments and water. Uppsala, 6-9 August 1990.*

LAMBRECHTS A., FOULQUIER L. & PALLY M. (1990) Méthodes d'évaluation de l'impact radioécologique de l'accident de Tchernobyl sur le fleuve Rhône. in: *Environmental contamination following a major nuclear accident. Proceed. of a symposium, Vienna, 16-20 october 1989, jointly organized by FAO, IAEA, UNEP, WHO. IAEA-SM-306/66* :353-359.

Project 5

Head of project: *Prof. Pieri*

Objectives for the reporting period

Transfer of caesium-137 in eel. This freshwater fish is studied for its economic impact (food). Our goal was to study the chemical behaviour of this radioelement at the molecular level in an edible animal.

Examination of the diffusion of this radionuclide in the edible parts of the animal and connection to the global decontamination time of the animal.

Comparison with the behaviour of other radionuclides (Am-241, Tc-99) in aquatic animals.

Influence of other metals on the behaviour of radionuclide and inhibition if any.

Chemical modifications of the nuclides according to the link with ionic groups at the working pH.

Progress achieved including publications

Towards the understanding of the transfer of radionuclides in to higher food organisms, one step may be of particular interest: the chemical or molecular behaviour of the radionuclides inside the fish to predict its storage or its elimination. This behaviour depends on the speciation of the element and of the chemical environment. A first approach of this problem is the location and identification of radionuclide-protein complexes *in vivo*. this may be followed by kinetics of molecular decontamination and analysis of the nature of the link between the nuclide and its ligand.

One knows now that radiocaesium shows an cationic behaviour in the environment.

The subcellular fractionation has been done on the liver and muscle of the eel according to the method used preceedingly: (Galey et al., 1986; Goudard et al., 1991). the caesium activity is found principally in the cytosol: 87% for the liver and 79% for the muscle.

the chromatographic fractionation of the cytosol is obtained on Sephacryl S300: fig. 5.1 and 5.2.

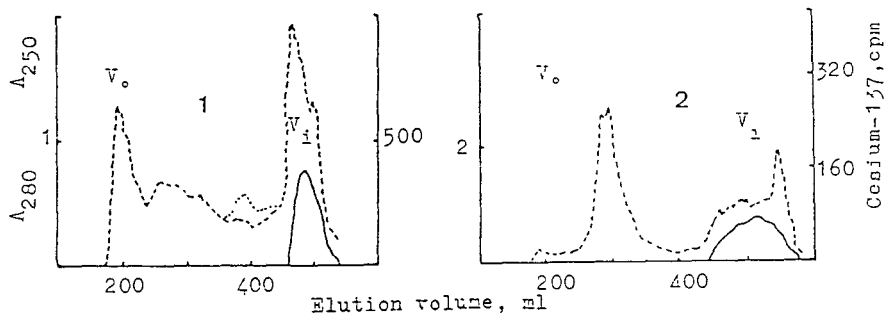
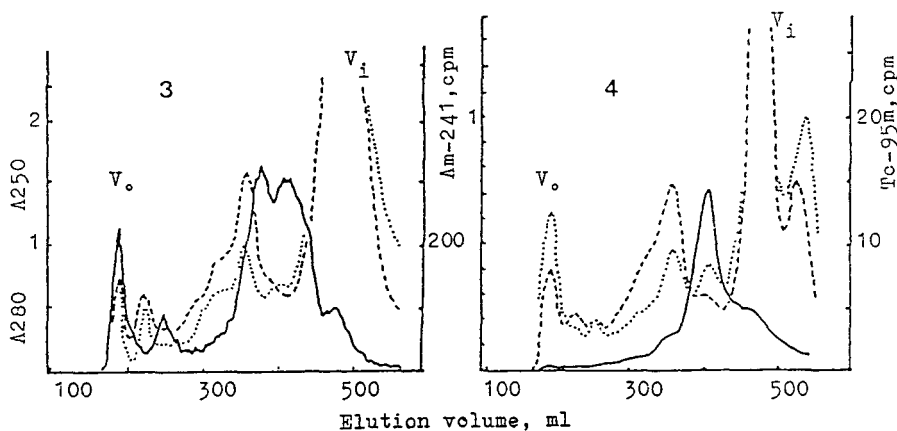


Fig. 5.1 and 5.2 - Gel filtration chromatography (Sephacryl S300) of the cytosol of liver (fig.5.1) and muscle (fig.5.2) cells of the eel contaminated by caesium-137.



Figures 5.3 and 5.4 show cytosol chromatograms contaminated by Am-241 and Tc-95m.

We can see that:

- 1) Caesium is localised with the small molecules in the V_i showing a diffusion of the radionuclide in all the animal organism.
- 2) The activity for the two radioelements (Am and Tc) is situated between the V_0 and the V_i where the molecules show a partition coefficient. Detection of absorption has been done at 280 nm and 250 nm.
- 3) Am-241 is bound in every sample to ferritin. We note a very sharp peak of activity due to Tc-95m in the molecular weight zone of 10000 (metallothionenes). In this zone, the activity curve of Am-241 shows a through enhanced by a metallothionein induction determined by a cadmium-109 injection (fig.5.5, 5.6 and 5.7) (Pieri et al., 1992).

All this shows that americium is in competition at the metabolic level with the inducing metal. A competition is noticed too between Tc and Cu or Cd. The affinity of Tc for the proteins at 10,000 M.W. is 20 times lower with copper injections and 1.5 lower with cadmium injections. On the other hand, no influence of the cadmium prescence is noticed on the chemical or molecular behaviour of caesium.

In a contaminated lobster, after 70 days, 12% of the Americium and 29% of the technecium remains in the muscle. However, after 70 days, 75% of the caesium in the eel remains in the muscle. The biological half life is long, over 300 days. The cytosolic chromatogram for caesium corresponds to the radionuclide diffusion in the organ.

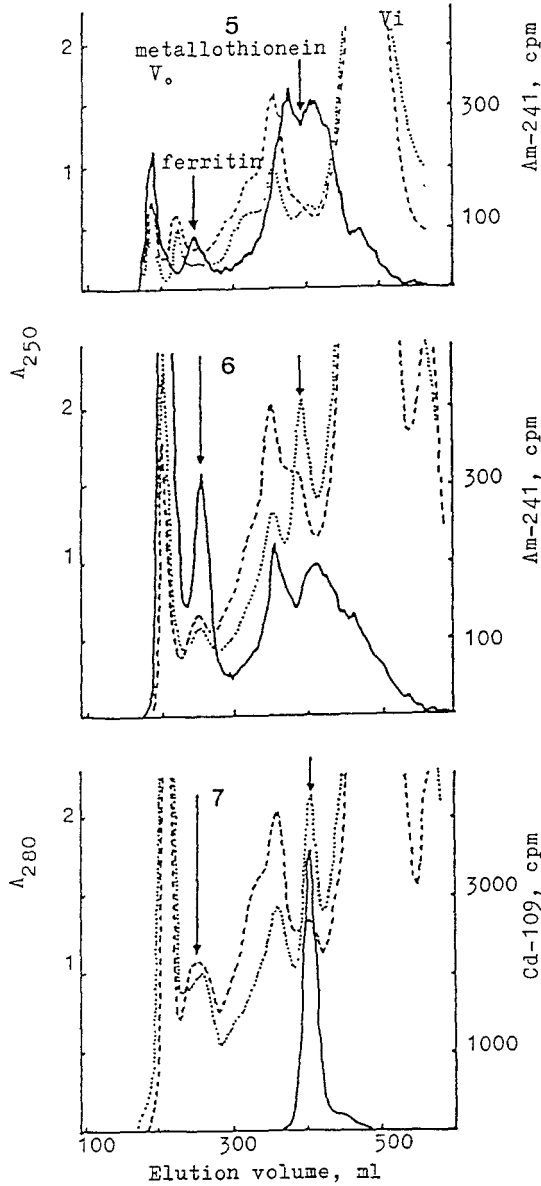


fig. 5.5, 5.6 and 5.7 - Am-241 activity patterns in cytosolic fraction without (fig 5.5) and with (fig. 5.6) cadmium injection. Fig 5.7 shows the localisation of cadmium.

The cytosolic chromatogram for caesium corresponds to the radionuclide diffusion in the organism. Anyway we have noticed the elimination of americium on the chromatographic pattern of the cytosol, 48 hours after contamination in the liver: fig 5.8 and 5.9.

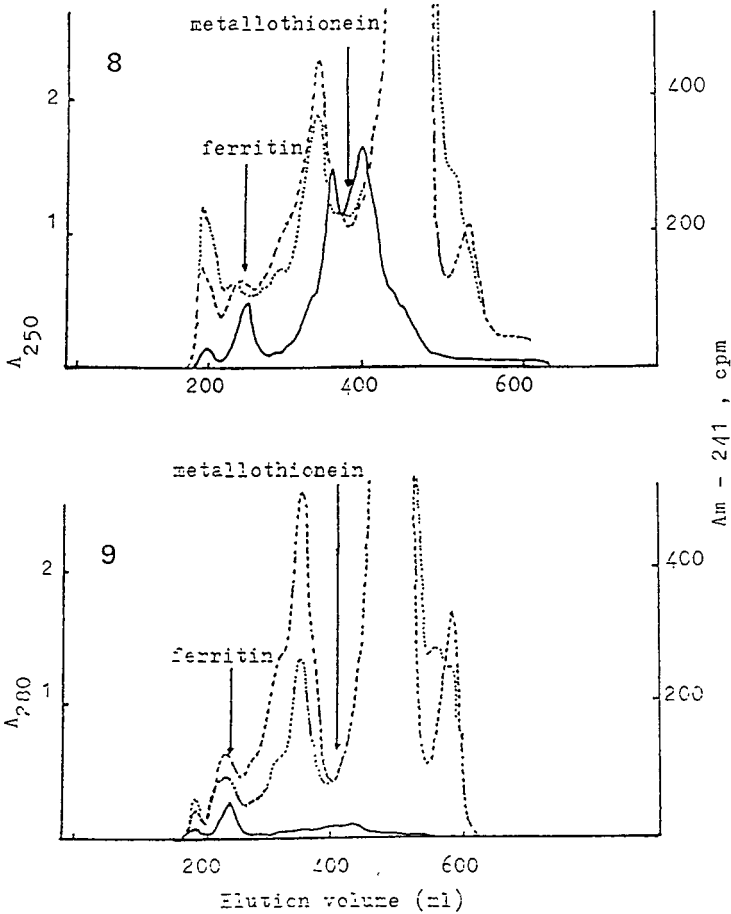


Fig. 5.8 and 5.9 - Chromatographic patterns of Am-241 at 4 hours (fig.5.8) and 48 hours (fig.5.9) after contamination.

It is difficult to know how the chemical form of a radionuclide inside an organism. The case of caesium is relatively simple. Its ionic behaviour exists in the cytosol of the eel.

Concerning americium, we have analysed the primary structure of the 10000 MW proteins which bind this element. The result shows that the aspartic, seric glutamic and histidinic residues represent respectively 10, 14, 15 and 9%. Seric, aspartic and glutamic acids represent 40% of the amino acids entering these protein chains. The pK values for the ionized groups of these residues are respectively 2.09, 2.21 and 2.17. These groups are ionised in the work conditions and probably in the natural conditions (pH 8 and 7). At these pH, we know that americium is on three forms: Am^{+++} , $\text{Am}(\text{OH})^{++}$ and $\text{Am}(\text{OH})_2^+$. These forms could exist in the cytosol.

1 - Finally we can conclude that the contamination by caesium shows an ionic behaviour of the nuclide in the cytosolic fraction of the liver but a diffusion to the muscle.

2 - Although americium is linked to proteins of the cytosol in the liver, it is probably eliminated and diffuse less than caesium; it is not linked to the muscle. Moreover, according to the state of ionisation of the lateral groups of proteins, americium, hydroxolated or not, would be fixed to these anionic groups.

3 - Am uptake by some cytosolic proteins is inhibited by cadmium and probably by metal inductors of metallothioneins. This can increase the importance of the external conditions in the food chains. Models of radionuclide transfer would have to take into account the chemical external environment to explain the accumulation of some radionuclides.

References

Galey J., F.Goudard, J.Pieri, P.Germain and S.G.George Am-241 binding components in the digestive gland cells of the marine prosobranch Littorina littorea. Comparative Biochemistry and Physiology. 85A, 333-340, (1986).

Goudard, F., J.P.Durand, J.Galey, J.Pieri, M.Masson and S.G.George. Subcellular localisation and identification of Tc-95m and Am-241 binding ligands in the hepatopancreas of the lobster Homarus gammarus. Marine Biology. 108, 411-417, (1991).

Pieri, J., F.Goudard and M.C.Milcent. Localisation moleculaire de l'americium, du technecium et du cesium chez des animaux comestible. Leur comportement metobolique et ses consequences. IRPA 8, 1, 751-0754. (1992).

Cheick-Zeyneddine, T. Comparision du transfert du cesium-137, du strontium-90 et du cobalt-60 au niveau moleculaire (these en preparation).

Project 6

Head of project: *Dr. Belli*

Objectives for the reporting period

The main aim of this study was the assessment of the effect of salinity variation of water body, on radiocaesium dissolved in water and that associated with suspended materials.

The research was carried out in the estuary of the Stella river influenced by the salinity variation due to tidal cycle coming from Marano and Grado lagoons (north-eastern part of Italy).

Radiocaesium K_d values for different grain size of suspended material collected along the water column profile have been assessed.

Progress achieved including publications

1. Materials and methods

To define the sampling points in the Stella river, every hour, during the complete tidal cycle (from 8am to 8pm), the water salinity and temperature were measured at different depths along the water profile in four transects located in the terminal part of the river.

The results showed that the saline wedge coming from the lagoons influences the Stella river up to 5 km from the mouth.

In this area, measurements along the water column showed that in the first 2 meters of the superficial layers of the river, there was no influence of the saline wedge during the tidal cycle. The effect of the saline wedge is evident only in the deeper part of the river (from 2 meters to the bottom). On this basis 2 sampling points were selected (near the estuary of the river into the lagoons and outside of the area effected by the saline wedge, 7 km from the mouth of the lagoons).

In these sampling points, water and suspended solids were collected in May and October 1991 along the water column, using two devices capable of performing size fractionation of suspended solids and with a set of columns containing ion-exchange resins to fix Cs-137 dissolved in the water. The sampling system permitted to gather different fractions of suspended particles (from 100 to 20 μm , from 20 to 5 μm and from 5 to 0.1 μm). The system was equipped with resin columns to determine radiocaesium dissolved in the water. During the sampling events the conductivity and pH of the water have been measured.

2. Results and discussions

The following tables report the data collected along the Stella river during the sampling events of May and October 1991.

Table

May 1991	Suspended materials grain size class (μm)											
	1	2	3	1	2	3	1	2	3	1	2	3
Suspended materials (mg/l)	1.7	2.2	0.7	6.4	3.2	0.5	5.9	2.1	0.7	6.6	2.1	0.7
Cs-137 on suspended materials (Bq/g)	0.09	0.10	0.22	0.06	0.09	0.25	0.06	0.11	0.17	0.08	0.07	0.14
Cs-137 dissolved in water (Bq/l)	0.55×10^{-3}			2.57×10^{-3}			0.63×10^{-3}			1.09×10^{-3}		
	Fresh water			Salt water			Fresh water			Fresh water		
	Estuary						7 km from the estuary					

Table

October 1991	Suspended materials grain size class (μm)											
	1	2	3	1	2	3	1	2	3	1	2	3
Suspended materials (mg/l)	2.0	2.2	0.8	4.9	3.8	0.8	3.8	1.2	0.1	3.6	1.7	0.4
Cs-137 on suspended materials (Bq/g)	0.06	0.08	0.11	0.06	0.09	0.09	0.10	0.11	0.52	0.11	0.10	0.22
Cs-137 dissolved in water (Bq/l)	0.81×10^{-3}			3.10×10^{-3}			1.05×10^{-3}			0.85×10^{-3}		
	Fresh water			Salt water			Fresh water			Fresh water		
	Estuary						7 km from the estuary					

- 1 = $100 + 20 \mu\text{m}$
 2 = $20 + 5 \mu\text{m}$
 3 = $5 + 0.1 \mu\text{m}$

During all the tidal cycle, the salinity was about 2 g l^{-1} in the superficial layer of Stella river estuary and 30 g l^{-1} at the depth of 2.5 m, in the period neighborhood of the maximum of the tidal excursion.

The deeper layer is richer of particles with size ranging from 100 to $5 \mu\text{m}$, while fresh water, in the top layer of the river, is characterized by suspended materials with size ranging from 20 to $0.1 \mu\text{m}$.

In the following table are reported the mean values of the distribution coefficient (k_d) measured for the different grain size in fresh and in salt water.

k_d values is defined as the ratio between Cs-137 concentration per gram of suspended material and Cs-137 concentration per milliliter of water.

Table

	Grain size class (μm)	Distribution coefficient (ml g^{-1})
Fresh water (Superficial layer)	100 - 20	$1.00 \cdot 10^5 \pm 3.7 \cdot 10^4$
	20 - 5	$1.12 \cdot 10^5 \pm 4.3 \cdot 10^4$
	5 - 0.1	$2.47 \cdot 10^5 \pm 1.4 \cdot 10^5$
Salt water (Deeper layer)	100 - 20	$2.31 \cdot 10^4 \pm 4.8 \cdot 10^3$
	20 - 5	$2.81 \cdot 10^4 \pm 8.1 \cdot 10^3$
	5 - 0.1	$6.42 \cdot 10^4 \pm 2.8 \cdot 10^4$

These data show that radiocaesium is mainly associated with the finest suspended particles and the dissolved fraction of radiocaesium is lower in fresh water than in salt water.

k_d evaluated from the different grain size of suspended particles show higher values for the grain size ranging from 5 to 0.1 μm and are lower in salt water than in fresh water.

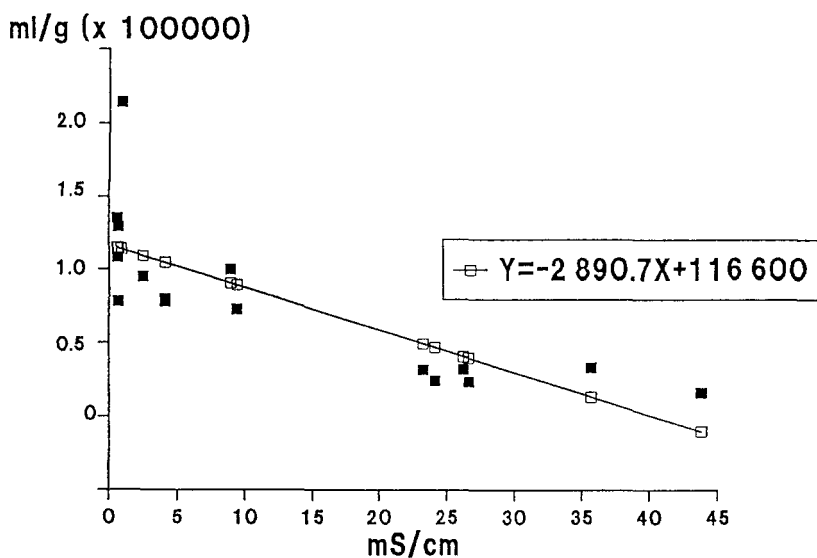
The high standard deviation values found for the distribution coefficient of the finest materials could be attributable to their different composition (organic matter and mineral content) during the different sampling periods.

Total k_d values for fresh and salt water, collected in the sampling points along Stella river, have been assessed considering the Cs-137 concentrations in the different fractions of suspended particles as follows:

$$\text{Total } k_d = \frac{\sum C_i a_i}{C_{\text{water}}}$$

Where C_i is the CS-137 concentration in suspended particles with size class i ; a_i is the concentration of this class of particles in water and C_{water} represents the Cs-137 dissolved in water.

The following figure reports the total k_d values versus conductivity and shows that the salinity of the water body influences highly the distribution of radiocaesium between water and suspended materials.



Figure

References

- Ventura, G., Belli, M., Sansone, U., Nicolai, P., Spezzano, P., Papucci, C., Marinaro, M., Mattassi, G., (1988). "Radioecological research in northern Adriatic lagoons: activities and first results". Proceedings of the international conference on environmental radioactivity in the Mediterranean area, 467-478, Barcellona 10-13 May 1988. September 1989, Elsevier Applied Science, 1989, 382-386.
- Belli, M., Blasi, M., De Guarrini, F., Franchi, M., Giacomelli, R., Marinaro, M., Mattassi, G., Nocente, M., Sansone, U., Spezzano, P., Ventura, G., (1989), "Risultati di due anni di indagini radioecologiche nelle lagune di Marano e Grado"., ENEA, Sicurezza e protezione, 21/89, 77-88.
- Poggi, M., 1989, "Unità modulare per il campionamento delle acque e del particolato in sospensione", Sicurezza e protezione, supp. al Notiziario ENEA, 21, 1989, 77-88.
- Belli, M., Sansone, U., (1992)., Distribution of radiocaesium between dissolved and particulates phases, (in preparation).

Project 7

Head of project: *Prof. Vanderborgh*

Objectives for the reporting period

Theoretical developments:

- 1) Development of a mathematical model for the physical and chemical speciation of radionuclides in salt- and freshwater environments.
- 2) Development of a mathematical model for the biological availability of radionuclides in salt- and freshwater environments.

Experimental developments:

- 1) Uptake of radionuclides in brine shrimp over time in physically and chemically defined conditions with emphasis on the role of biological acclimation processes on radionuclide availability.
- 2) Uptake of radionuclides in brine shrimp over time in physically and chemically defined conditions with emphasis on the role of chemical speciation processes on radionuclide availability.

Progress achieved including publications

The physical and chemical conditions in aquatic environments such as lake, river, estuarine and sea areas are rather different. This does not only influence the speciation of the radionuclides, but also the physiological organisation and condition of the organisms which live in these environments. The most important steps in radionuclide uptake are: 1) the translocation of the radionuclide across the solution-body interface and 2) the transport from the exchange surfaces to the blood. The intracellular environment of the exchange structures has a high metal binding capacity and acts as a free metal ion buffer. Therefore it is anticipated that the effects of changes in the speciation of the radionuclide with changes in the environmental conditions do not extend beyond the solution-body interface. However, changes in environmental conditions such as the hydrogen ion concentration, the salinity and the temperature are likely to influence the uptake of the metal by altering the organisation of the interface and modulating the activity of the transport systems involved. To obtain a basic understanding of the mechanisms controlling radionuclide availability, it is necessary to study the separate and combined effects of changes in the chemical speciation and other environmental factors on the uptake of radionuclides in different types of organisms. To contribute to this goal we have studied the uptake of radioactive cobalt, by a crustacean with a very high capacity to adapt to different conditions, the brine shrimp, *Artemia franciscana*. During these experiments the translocation of the metal across the solution-body interface was followed by measuring uptake over a short period of time in animals exposed and/or acclimated to different conditions (e.g. different hydrogen ion concentrations, salinities and temperatures).

1. Physical and chemical speciation of radionuclides in salt- and freshwater environments

We have developed a model that considers the speciation of an element in a particular aqueous environment as the result of a variety of both physical and chemical processes which act in concert. Acid-base, oxidation-reduction, association-dissociation, adsorption-desorption and precipitation-dissolution processes are the regulatory factors which control the speciation of an element in an aqueous solution. Based upon the concepts of chemical kinetics and equilibrium a theoretical construction has been built that describes the principal physical and chemical processes that take place in such a system.

The model uses the ion-association concept which invokes the existence of molecular species like the free metal ion and metal-ligand complexes. A semi-empirical relation is used to describe the conditional stability of each complex species formed with ionic strength. The major problem in the building of such a speciation model is the compilation of a data base that includes the information needed for a quantitative description of the processes considered. In aqueous systems the number of interactions and species that have to be considered can be considerable depending on the complexity of the system. Although a large number of protonation constants, complex stability constants and solubility products have been measured, independent measurements for the same reaction may vary considerably. Our compilation of the information shows that in the best of all cases, measured values can be considered accurate to about one-tenth of a log unit, but values for constants of the same reaction that differ over an order of magnitude are also found. For many complexes formation constants have not been measured and estimates must be made by comparison with values obtained for other metal ions with the same ligand, or similar ligands with the same metal ion. The selection of the values for the constants that describe the reactions which are considered is the most critical step in the development of a speciation model. Although the methods we have developed for the compilation of a reactions data base has considerably improved the model it is not error free. The most important source of error are the inaccuracies in the values of the constants which describe the reactions. To measure the effect of these errors on the results the model considers these variations in its analysis. The result of the speciation model are the activities or concentration of the different species considered in the model including uncertainty limits determined by the errors in the values of the constants used. The model has been used to model the speciation of radionuclides in defined systems of different composition. It has proved of great value in the design and analysis of experiments concerning the availability and uptake of radionuclides in defined salt-and freshwater systems.

2. Biological availability of radionuclides in salt- and freshwater environments

The process of radionuclide uptake by aquatic organisms is rather complex and involves different steps which up to now have not been integrated into one single model. Briefly, the first step involves the fixation of the element on the cellular surface of the solution-body interface. This initial phase of metal uptake is assumed to be a simple adsorption process, with the cell walls of the living cells perceived as providing surface sites for physical and chemical adsorption. The second step involves the translocation of the metals across the solution-body interface into the cells. This process appears to be a passive facilitated diffusion process driven by the electrochemical gradient existing across the solution-body interface. The third step involves the transfer of the radionuclide to the blood and other body compartments.

The aim of our experimental work concerning the biological availability of radionuclides is to determine the quantitative role of these different steps. Within this framework it is important to know to what extent chemical speciation and biological acclimation processes are important in determining the availability of the radionuclides to the organisms. Studies carried

out with radioactive cobalt have indeed shown that the availability of the radionuclide to the brine shrimp is largely controlled by these two processes.

Cobalt uptake by the brine shrimp from solutions containing different inorganic or organic ligands showed that complexation invariably decreases the availability of the radionuclide to the brine shrimp. Generally, there is reasonable agreement between the free cobalt ion activity in the solution and the availability of the metal to the brine shrimp. The effect of complexation on metal availability is independent of the thermodynamic stability of the metal-complexes formed. However, cobalt uptake is not a sole function of the free cobalt ion activity in the solution.

Cobalt uptake by the brine shrimp increases with decreasing hydrogen ion concentrations. Animals have been acclimated to different hydrogen ion concentrations and exposed to cobalt in solutions of differing pH. Within and among the acclimation groups the uptake of cobalt increases with decreasing hydrogen ion concentration. A simple non-linear model that combines the effect of hydrogen ions on the transport of the metal across the solution-body interface and the effect of hydrogen ions on the speciation of the metal, explained most of the variation observed in the availability of cobalt to the brine shrimp with changes in pH.

Cobalt uptake by the brine shrimp decreases with increasing salinity. Animals have been acclimated to different salinities and exposed to cobalt in solutions of differing salinity and composition. Within each acclimation group the uptake of cobalt decreased with increasing salinity. Among the acclimation groups uptake of cobalt increased with increasing salinity of acclimation. Within each acclimation group uptake increased with increasing activity of the free metal ion. The uptake of cobalt was not altered by changing the concentration of any of the major cations. A simple non-linear model that combines the effects of the salinity of exposure and acclimation on the transport of the metal across the solution-body interface and the effect of the salinity of exposure on changes in the speciation of the metal, explained most of the variation in the availability of cobalt to the brine shrimp with salinity.

Cobalt uptake by the brine shrimp increases with increasing temperature. Temperature exposure and acclimation have different effects on the uptake of cobalt by the brine shrimp. Uptake of cobalt by the brine shrimp increases with the temperature of exposure. The temperature quotient for cobalt uptake is closer to one than to two which indicates that metal uptake is a simple physical process, resembling free diffusion. Cobalt uptake decreases with the temperature of acclimation. This in such a way that exposure to the temperature of acclimation has no effect on metal uptake, but in the lowest temperature where uptake is minimal. This indicates that temperature acclimation invokes a reorganisation of the metal uptake system that compensates for the intrinsic effects of temperature on transport rates. A simple non-linear model that combines the effect of the temperature of exposure and acclimation on the transport of the metal across the solution-body interface and the effect of the temperature of exposure on changes in the diffusion rate of the free metal ion, explained most of the variation in the availability of cobalt to the brine shrimp with salinity.

The results of this study have clearly indicated the importance of both chemical and biological processes in controlling the uptake of radioactive cobalt by the brine shrimp, *Artemia franciscana*. The results obtained for radioactive cobalt have been confirmed by similar experiments on the availability of copper and cadmium to the brine shrimp. Taken into consideration the different effects of the environment on the speciation of the metal and the flux of the metal across the solution-body interface, most of the variation in metal availability

can be explained. The basic understanding concerning the mechanisms controlling metal ion availability to the brine shrimp, provides a preliminary framework for the development of conceptual models. These models can then be used to predict the fate and effects of metals in the aquatic environment.

Publications for the reporting period:

Blust, R. (1990) Modelling the transport of metals across biological interfaces. *Belgian Journal of Zoology*. 120: 8-9.

Blust, R., Fontaine, A. and Declair, W. (1991). Effect of hydrogen ions and inorganic complexing on the uptake of copper by the brine shrimp *Artemia franciscana*. *Marine Ecology Progress Series*. 76: 273-282.

Blust, R., Kockelbergh, E. and Baillieul, M. Effect of salinity on the uptake of cadmium by the brine shrimp, *Artemia franciscana*. *Marine Ecology Progress Series*. In Press.

Blust, R., Baillieul, M. and Declair, W. Metal complex structure-stability relations in metal availability to the brine shrimp. *The Science of the Total Environment*. Submitted.

Blust, R. and M. Baillieul. Modelling the speciation of metals in the aquatic environment. *The Science of the Total Environment*. Submitted.

Project 8

Head of project: *Prof. Serrano*

Objectives for the reporting period

The goal of our Group in the contract was to give a satisfactory interpretation on the degree of variation existing in the present data on radionuclide accumulation by freshwater plants. The data were collected so far for monitoring purposes without a reasonable control of the main variables affecting to the accumulation processes, especially from a physiological point of view. So in order to define which were the main variables influencing the accumulation process, the first step was to build up a conceptual model on the accumulation processes from at least two approaches. Firstly defining the processes at membrane level, and secondly to whole organism level. These approaches are useful because it is possible to restrict the framework in order to deal only with the main variables implied in the transfer of radionuclides between the medium and the plant cell.

Progress achieved including publications

1. Mechanisms of radionuclide transfer and accumulation in plant cells

1.1 Membrane level

There are two mechanisms that account for the accumulation of radionuclides in plant cells: 1-Adsorption, the accumulation of radionuclides to the external part of the cell, including the periplasmic space by binding to the hydroxyl groups of cellulose, and in certain cases by binding to the negatively charged headgroups placed in the outer part of the plasmalemma. 2-Absorption, the accumulation of radionuclides inside the cell. Most of radionuclides go into the cell through channels for other naturally occurring ions. From the point of view of radionuclide accumulation, the more important channels are those existing in the plasmalemma for potassium and for calcium. Channels are pores with only two states: opened and closed. The state of the channel depends mainly on the electrical potential difference across the plasmalemma and internal and external activities of some ions. The best known are the potassium channels, they are permeable to monovalent cations in a permeability order being $K^+ > Rb^+ > NH_4^+ > Na^+ > Li^+ > Cs^+$. This kind of channel is the pore used by Cs^+ radioisotopes to enter the cell. Using "patch clamp" it is possible to define the activity as well as the amount of current that those channels may transport from one side to the another in the plasmalemma, in the figure 1a it is shown the open and close state of K^+ channels in the vacuole of *Chara corallina* (R², 1990). Note that the amount of current passing through the membrane increases as the potential difference across the membrane increases, furthermore the amount of current is zero when the potential difference is zero. So the amount of current (I) is proportional over a certain range to the voltage. This relationship, is usually presented as the classical I/V curves (see figure 1b), often in the bibliography after Neher & Sakman (1976).

Another way to investigate the relative permeability of plant membranes for different ions is with classical electrophysiology. The diffusion potential in most plants is highly dependent on external potassium concentration. Increasing concentrations of potassium in the external medium, produce successive depolarizations of the diffusion potential according with the Nernst equation (Hope, 1971). Under controlled conditions it is possible substitute potassium ions by sodium ions, recording simultaneously the diffusion potential, as we have done for *Riccia fluitans* (figure 2). It is possible to compute the relative permeability of cesium with respect to potassium from the difference between the degree of depolarization with the external ionic concentration for cesium compared with potassium.

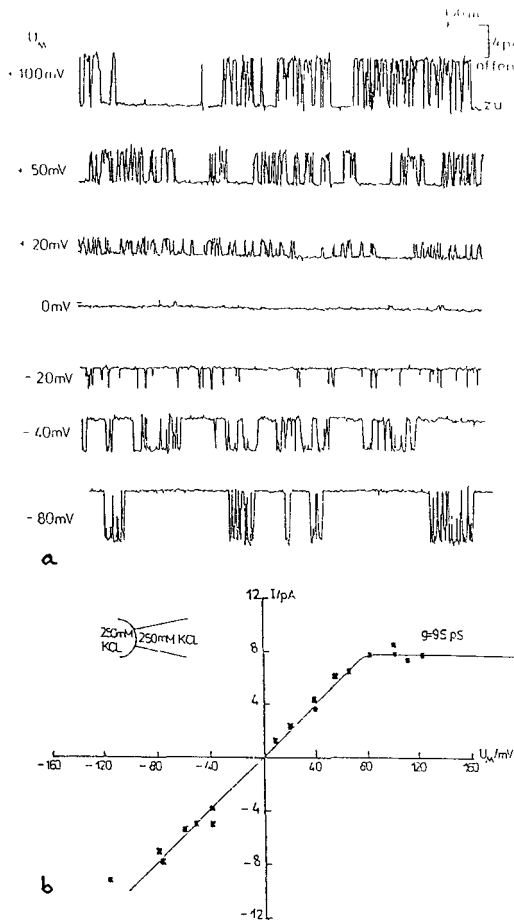


Figure 1: a) Original recording from the current crossing the potassium channels in the vacuole of *Chara corallina*;
 b) amount of current vs voltage in the same organule and the same species.

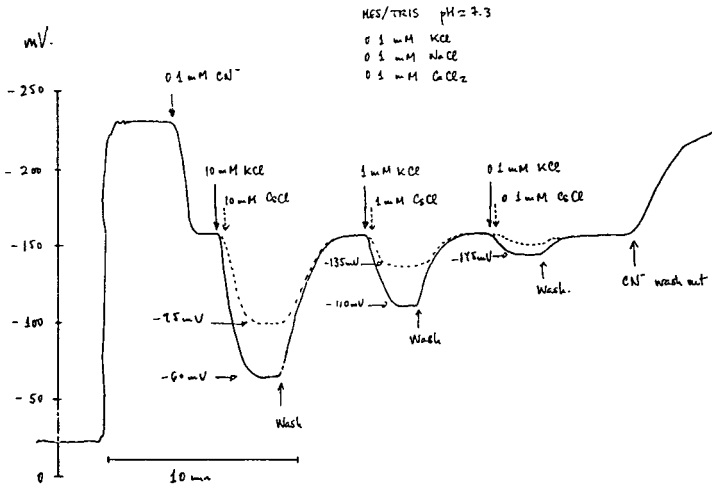


Figure 2: Continuous recording of the membrane potential at the plasmalemma of *Riccia fluitans* under different external potassium and cesium concentrations in the presence of 0.1 mM CN^- .

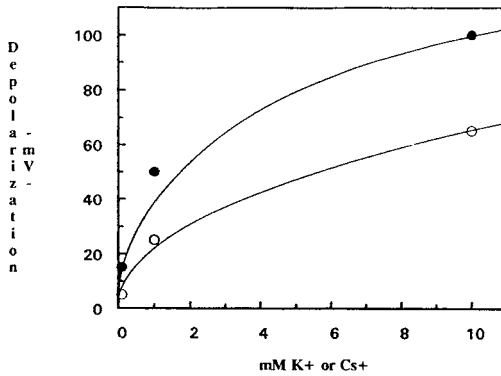


Figure 3: Degree of depolarization of the plasmalemma of *Riccia fluitans* under different external concentrations of potassium (closed circles) and cesium (open circles).

Figure 3 is the plot of the degree of depolarization of the plasmalemma when the external concentration of potassium or cesium are added. The relative permeability of cesium with respect to potassium is accounted for the difference in the initial slope of the curves. This experiment may be performed with others monovalent ions that enter the plant cell through the same channel, and it is also possible to write a permeability sequence as in the first page of this report.

The physical driving force moving the ions into the cell through the channels is the electrochemical gradient for each one, according with the equation,

$$\Delta\mu_i / F = z (E_m - E_N^i) \quad \text{Eqn. 1}$$

where $\Delta\mu_i / F$ is the electrochemical driving force for the "i" ion (being F the Faraday's constant), z the charge of "i", E_m the membrane potential and E_N^i is the Nernst potential for "i". The Nernst potential for "i" is computed by the Nernst equation,

$$E_N^i = RT/zF \ln C_i^o/C_i^i \quad \text{Eqn. 2}$$

where R is the gas constant, T is the absolute temperature, and C_i^o and C_i^i are the amount of radioisotope in equilibrium with its natural existing form, outside and inside the cell respectively. Note that, in the equilibrium C_i^o/C_i^i is an equivalent expression of the inverse of the concentration factor for "i" (1/CF).

After a pulse in the concentration of a radioisotope in the medium, the ion will distribute between both sides of the membrane according with E_m and the external concentration until $\Delta\mu_i / F$ be zero.

Once into the cell, another redistribution will take place between the cytoplasm and the vacuole according with, as in the case of the plasmalemma, the electrochemical gradient and the relative amount in the two cellular compartments.

1.2 Whole organism level

The main assumption made in the model of radionuclide accumulation at membrane level is that adsorption take place several orders of magnitude faster than growth rate.

Growth is the increase of biomass with time, but there is a concomitant increase of water and non-metabolizable elements, i.e. ions involved turgor regulation and coenzymes that are not included in the biomass *sensu stricto*. Most radionuclides are in this category, specially those that are close to potassium (being cesium the most important) and calcium (being strontium the most important). In plants, under constant conditions, growth is dependent of net photosynthesis, that is the difference between gross photosynthesis and respiration.

In fast growing species growth is probably the main variable controlling the radionuclide accumulation processes. Here will be useful some experiments with unicellular algae cultured in chemostats. This culture method permits, by changing the dilution rate, manipulate the growth rate as well.

1.3 Main variables implied in radionuclide accumulation

At membrane level the variables that control the radionuclide accumulation are those controlling the electrochemical gradient and those affecting the operation of the channels.

Variables related to the electrochemical gradient.

1.- pH.

Since freshwater plants have a proton pump as *primary pump*, E_m (the membrane potential) will be in those plants highly dependent on pH.

2.- Temperature.

The membrane potential depends on the amount of cytosolic ATP. It has a respiratory

origin in its most part, so temperature controls the electrochemical gradient by controlling the respiration rate. Furthermore temperature has influence on the Nernst potential for the ion under consideration.

3.- Internal-external ratio of the natural form of the radioisotope.

This ratio determine in part the electrochemical gradient, by affecting to the total Nernst potential of the ion (radioactive part included).

Variables related to the operation of the channels.

1.- External concentration of related ions.

Ions competing for the same pore that the radioisotope. Assuming the permeability order given in the first page, $K^+ > Rb^+ > NH_4^+ > Na^+ > Li^+$ will decrease the accumulation of $^{134}Cs^+$ depending on the external concentration, corrected by the relative permeability with respect to Cs^+ .

2.- External concentration of controlling ions.

In most plants there are channels for potassium controlled by calcium. So the external concentration of calcium may control the degree of accumulation of a certain ion entering the cell through the potassium channels.

At whole organism level the variables that control the radionuclide accumulation, are those related with growth regulation. Assuming that growth is related to net photosynthesis, the variables controlling these processes, probably will exert some kind of influence on radionuclide accumulation.

1.- Light.

Because photosynthesis (that means growth in autotrophic organisms) use light as well as CO_2 as the main substrata.

2.- Temperature.

Because it has influence on both respiration and photosynthesis rates.

3.- Nutrients.

Especially the nutrients known as limiting nutrients, because under a certain limit the concentration of one of those nutrients limits growth.

2. Concluding remarks

From a physiological point of view, according to the model described above, the variables that control the accumulation of a positively charged monovalent radioisotope in plant cells are, in principle: *pH*, *Temperature*, *external concentration of its natural occurring form*, *external concentration of K^+ and Ca^{++}* , *light (daily mean irradiance)* and *nutrients (nitrogen and phosphorus)*. These variables are essentially the same for the rest of radionuclides but considering that the channel used for entering the cell, and the ions competing for the channel are different.

Publications

- Jimenez, C., F.X. Niell & J.A. Fernández. 1990. The photosynthesis of *Dunaliella parva* Lerche as a function of temperature, light and salinity. *Hydrobiologia* 197, 165-172.
- Clavero, V., J.A. Fernández & F.X. Niell. 1990. Influence of salinity on the concentration and rate of interchange of dissolved phosphate between water and sediment in Fuente Piedra Lagoon (S. Spain). *Hydrobiologia* 197, 91-97.
- Clavero, V., F.X. Niell & J.A. Fernández. 1991. Effects of *Nereis diversicolor* O.F. Muller abundance on the dissolved phosphate exchange between sediment and overlying water in Palmones River Estuary (Southern Spain). *Estuarine, Coastal and Shelf Science*. 33, 193-202.
- Flores, A., J.A. Fernández & F.X. Niell. 1992. Influences of light intensity and temperature on the summer disappearance of *Laurencia pinnatifida* (Ceramiales, Rhodophyta). *Cryptogamic Botany*. In press.
- Hernández, I., F.X. Niell & J.A. Fernández. 1992. Alkaline phosphatase activity in *Porphyra umbilicalis* (L.) Kützinger. *Journal of Experimental Marine Biology and Ecology*. 0, 1-13.
- García, M.J., J.A. Fernández & F.X. Niell. 1992. Effect of some metabolic inhibitors on Phosphate uptake in *Ulva rigida* C. Agardh (Ulvales, Chlorophyceae). In press.
- Fernández J.A., W.S. Peters & H. Felle. Submitted. Primary pump and the role of CO₂ for the plasma membrane potential in the marine angiosperm *Zostera marina* L.

Project 9

Head of project: *Dr. Hambuckers - Berhin*

Objectives for the reporting period

- choice of a bacterial population to model the radionuclide transfers in the river ecosystem
- study of ^{60}Co and ^{134}Cs uptake by bacteria in the water column
- study of ^{60}Co and ^{134}Cs desorption by bacteria in relation to environmental parameters such as temperature and hydrogen ion activity

Progress achieved including publications

1. Introduction

In the aquatic environment, bacteria are involved in the radionuclide cycle at two levels. Firstly, they are vectors of radionuclide carriage because they are able to uptake, store and release radionuclides. Secondly, bacteria contribute by biodegradation to the release of radionuclides sequestered in the organic matter. Indeed, it was observed that bacterial yield ranges from 0.1 to 0.3 (Servais et al., 1987), i.e. 90 % to 70 % of the organic matter is hydrolyzed with parallel release of trapped radionuclides.

Living organisms (including bacteria) trap radioelements. When these organisms die, they are transformed into organic particules by the bacteria either in the water column or in the sediment. Then, the radionuclides are released in several ways: (i) the radionuclides are transferred to the aqueous phase (ii) the radiocontaminated organic matter could either remain suspended in the water column or settle to the bottom of the river where bacteria again contribute to hydrolyse the radiocontaminated organic particles. Thus, the radionuclides are transferred to bacteria, to the interstitial water and still to the mineral particules. In addition, the radioactivity could be transferred to the water column. The same transfers could occur in the suspended organic matter of the water column.

Therefore, it is obvious that a whole model of the radionuclide cycling in aquatic environment needs to include the role of bacteria.

2. Results and discussion

1) One of the first questions which arises when studying the role of bacteria in the radionuclide transfer is the choice of the bacterial population. For this purpose, the aerobic bacterial communities colonizing the sediment and the water column of the Meuse river were compared on the ground of the biochemical features of the strains. The strain similarities were estimated by the matching coefficients of Sokal and Michener SM (1958) and of Jaccard SJ (Sneath and Sokal, 1973). Cluster analysis was carried out using the average linkage method (SAS, 1985).

The cluster (Fig.1) shows that all the 50 strains were recovered in two main clusters. Cluster 1 which joined at 70 % of all the strains, is composed of 63 % of water column strains and 37% of sediment strains. Cluster 2, forms at 30% of all the strains with 1

strain of the water column and 14 strains of the sediments. The strains clustered in this group were different from the strains of cluster 1 by the ability to use some carbohydrates as mannitol, sorbitol, rhamnose and saccharose.

The cluster analysis shows that the aerobic bacterial community isolated from the sediment

was constituted of two groups : one group presenting the same biochemical features as the aerobic bacterial community isolated from the water column, and an other group, more extent , composed of strains only present in the sediments.

Thus, in our study on the role of bacteria in the radionuclide transfers in aquatic ecosystem, we use the aerobic bacterial community isolated from the sediment and we consider that we have the responses of all the aerobic bacterial communities of the river.

2) The uptake of ^{60}Co and ^{134}Cs by the bacterial communities collected from the Meuse river was investigated in presence of increasing radiocontamination (up to 2000 Bq ml^{-1}) in a medium-based Meuse water.

The data were plotted according to the reciprocal form of the Michaelis-Menten equation: $1/V = (1/V_{\max}) + (K_m/V_{\max}) \cdot (1/[S])$ where V was the rate of uptake ($\text{Bq} \cdot \text{g}^{-1} \cdot \text{h}^{-1}$), $[S]$ was the activity of medium ($\text{Bq} \cdot \text{ml}^{-1}$), V_{\max} was the maximal rate and K_m was the Michaelis constant.

The uptake of ^{60}Co could be described by two kinetics depending on the range of the water contamination, from 24 to $90 \text{ Bq} \cdot \text{ml}^{-1}$ and from 90 to $2000 \text{ Bq} \cdot \text{ml}^{-1}$. These levels determined respectively the maximal rates $V_{\max 1}$ and $V_{\max 2}$ and the Michaelis constants K_{m1} and K_{m2} (table 1).

The level of radiocontamination respectively explained 58% and 98% of the variation of the contamination rates.

The ^{134}Cs uptake only showed one kinetic. 73% of the variation of the contamination rate were explained by the level of radiocontamination of the water column.

During the radiocontamination, 33% and 24% of the variations of the concentration factor could be explained by the contact duration between the biomass and the radionuclides for the ^{60}Co (from 22 to $2000 \text{ Bq } ^{60}\text{Co} \cdot \text{ml}^{-1}$) and ^{134}Cs (from 16 to $300 \text{ Bq } ^{134}\text{Cs} \cdot \text{ml}^{-1}$) respectively.

At the end of the uptake experiment (24 h; bacterial biomass: 500 mg d.w./l), the activity remaining in the water column ranked between 25% and 40% of the initial activity in the case of ^{60}Co (initial activity: 0 to $2000 \text{ Bq} \cdot \text{ml}^{-1}$) and between 45 and 95% in the case of ^{134}Cs (initial activity: 0 to $300 \text{ Bq} \cdot \text{ml}^{-1}$).

Thus, an important part of ^{60}Co and ^{134}Cs can be kept by the aerobic bacterial communities which constitute therefore, a pool of radionuclides in the river ecosystem.

3) The decontamination of the bacterial community loaded with ^{60}Co and ^{134}Cs was investigated in relation to two environmental parameters, the temperature and the pH.

When the temperature of the water column was maintained at 20°C , the kinetic of the decontamination of the bacterial community was described by a double negative exponential model with four parameters. It was fitted using the procedure NLIN of SAS (1985) following the DUD method of Ralston and Jennrich (1979) :

$y = m e^{-ax} + n e^{-bx}$, where y was the ^{60}Co or ^{134}Cs content of bacteria ($\text{Bq} \cdot \text{g}^{-1} \text{ d.w.}$) and x was the time (h); a and b were parameters depending on the desorption rate and are considered as an estimation of the biological half-lives T_{b1} and T_{b2} respectively.

For both radionuclides, the biological half-lives T_{b1} were found to be extremely low, of the order of few seconds to few minutes whereas the biological half-lives T_{b2} were higher (15h to 461h for ^{60}Co and 39h to 8,976h for ^{134}Cs).

Examples of data with adjusted curve were given for ^{60}Co (Fig.2) and ^{134}Cs (Fig.3).

Except for a high value of T_{b2} observed with ^{134}Cs (367 d) and a very small value observed with ^{60}Co (0.6 d) - both corresponding with the weakest radiocontamination level of the medium during the radiocontamination of the bacteria communities - the values of biological half-lives were of the same magnitude given for *Scenedesmus* (Nucho and Baudin, 1986; Sombré, 1987).

In some cases, the desorption kinetics was not describe by a biphasique process being fitted by a double negative exponential model.

When the temperature of the water column was maintained at 13°C (average temperature of the Meuse river), the results showed that radionuclides fixed by bacteria were not released.

At 20 °C, the decontamination of the bacterial community was followed as the pH increased from 6.5 to 9. The chosen criteria was the increase of radioactivity in the water column. The data were fitted by the following mathematical relation:

$y = m(1 - e^{-ax}) + n(1 - e^{-bx})$, where y was the ^{60}Co or the ^{134}Cs content of the water column ($\text{Bq}\cdot\text{ml}^{-1}$) and x was the time (h); a and b parameters were the biological half-lives. Two values of the water column pH were critical for the release of ^{60}Co and ^{134}Cs by bacterial community; the rate of desorption was the lowest at pH 8.0 and the highest at pH 7.0 (i.e. Fig.4).

These results shown that, when the average temperature and pH of the Meuse river (pH 8.0, 13 °C) were changed, a loss of the radionuclides immobilized by the bacterial biomass occurred and more radioactivity was consequently recovered in the water column.

4) Whole bacterial communities were used in the above experiments because this approach took into account the interspecific links and appeared to be the most ecological. However several practical problems occurred and the reproductibility of the results was sometimes questionable. It's the reason why it was decided to perform the next experiments with a well defined strain, *Alcaligenes eutrophus* CH34. This wild strain was currently investigated in laboratory and it was isolated from an oligotrophic freshwater ecosystem. It was examined for its main morphological and biochemical features and was compared with the aerobic bacterial communities of the Meuse river by cluster analyses. The cluster proves that *Alcaligenes eutrophus* CH34 belongs to the main cluster (cluster1, Fig.1) which joined all the water column strains and a large part of the sediment strains. Therefore it could be concluded that *Alcaligenes eutrophus* CH34 was an appropriate bacterial model of the aerobic bacterial communities of the Meuse river on the basis of its biochemical features.

3. Conclusion

This study dealt with the radionuclide fluxes in aquatic ecosystem between the bacteria and the water (water column and interstitial water).

The comparison of the aerobic bacterial communities colonising the sediment and the water column on the basis of biochemical features yielded results indicating that the aerobic bacterial community isolated from the sediment and the strain *Alcaligenes eutrophus* CH34 constituted an appropriate bacterial model of all aerobic bacterial communities of the river. An important part of ^{60}Co and ^{134}Cs can be immobilized by the bacterial biomass which constitutes therefore a pool of radionuclides capable of being transferred to the water column depending on the environmental conditions.

The uptake of ^{60}Co and ^{134}Cs by bacteria was followed in function of increasing radionuclide levels in the environment and described by a Michaelis - Menten model.

The kinetic of the decontamination of bacteria was described by a double negative exponential relation.

The influence of environmental parameters shows that in the Meuse river, with a mean temperature of 13 °C and a pH of 8, radionuclide elimination rates are very low so that the elements are effectively trapped by bacterial biomass. When the conditions change, the loss of the radionuclides immobilized by the bacterial biomass occurs and radioactivity consequently increases in the water column.

It appears that the environmental parameters play a great role in the radionuclide transfers mediated by bacteria and are to be more deeply investigated in the further.

Other research groups collaborating.

J. Hilton (I. F. E., U. K.):

A. Cremers (K. U. L., Belgium):

A. Lambrechts (C. E. A. Cadarache, France):

Active participation at the meetings of Rome (May 90), Nantes (May 91) and Malaga (January 92).

Publications

Kirchmann R, 1992. La radioécologie des grands fleuves: des données de sites et de l'expérimentation à la modélisation (application à la Meuse et au Rhône) . Rapport BLG 635.

Hambuckers-Berhin F., Hambuckers A and Remacle J.
Characterization and comparison of aerobic bacterial communities colonizing the sediment and the water column in the Meuse river (Belgium). (to be submitted)

Hambuckers-Berhin F, Meurice-Bourdon M. and Remacle J.
Uptake and desorption of ^{60}Co and ^{134}Cs by aerobic bacterial communities isolated from the Meuse river (Belgium). (to be submitted)

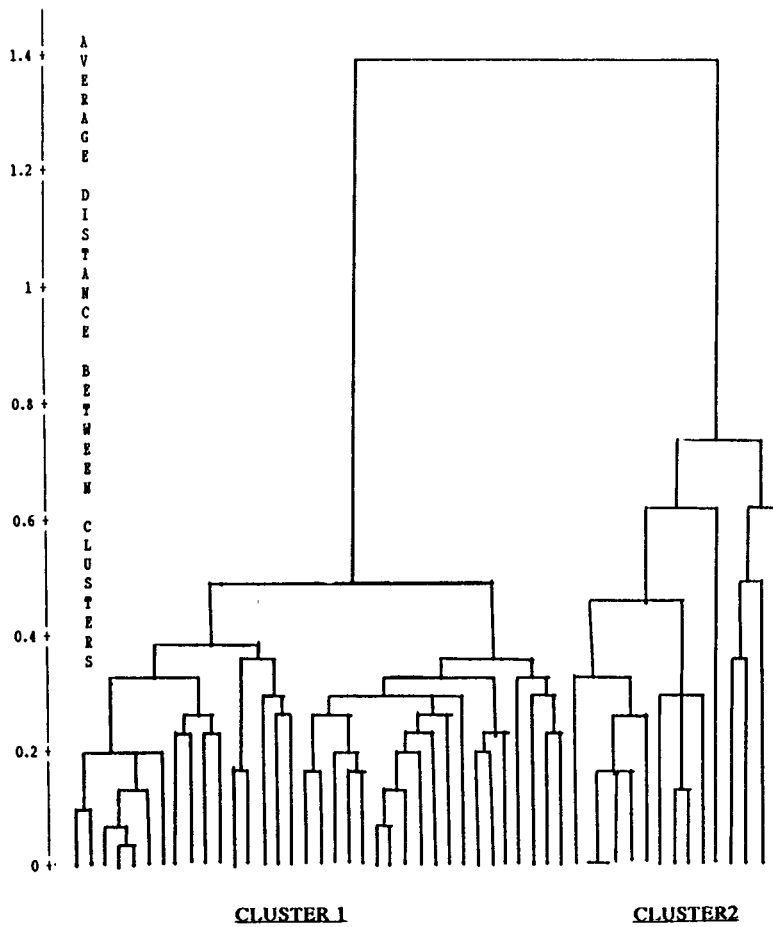


Figure 1: Dendrogram obtained on the basis of the similarity coefficient of Sokal and Michener with the average linkage method.

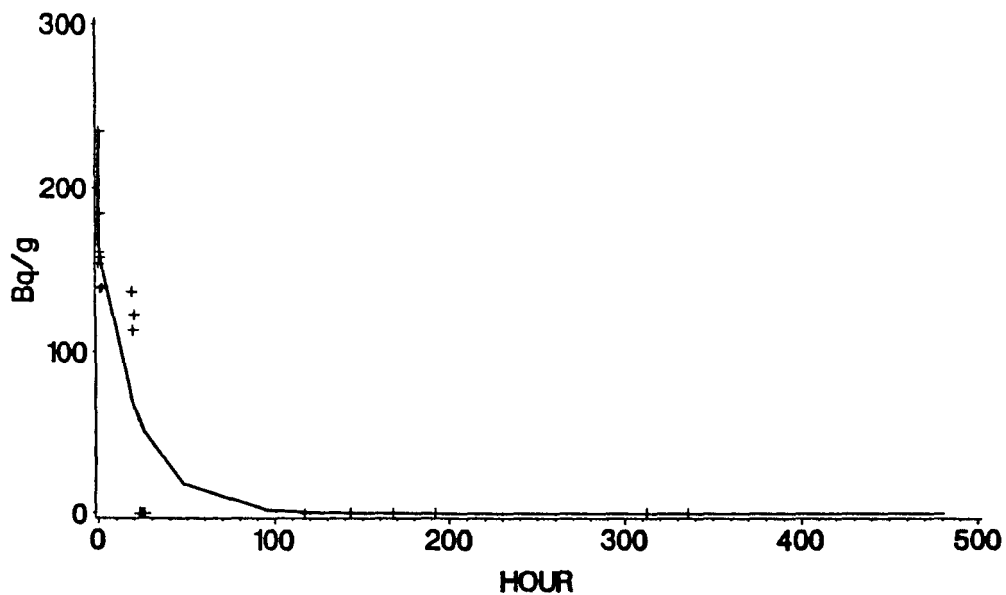


Figure 2: Desorption of ^{60}Co by the bacterial community. Observed and predicted values.

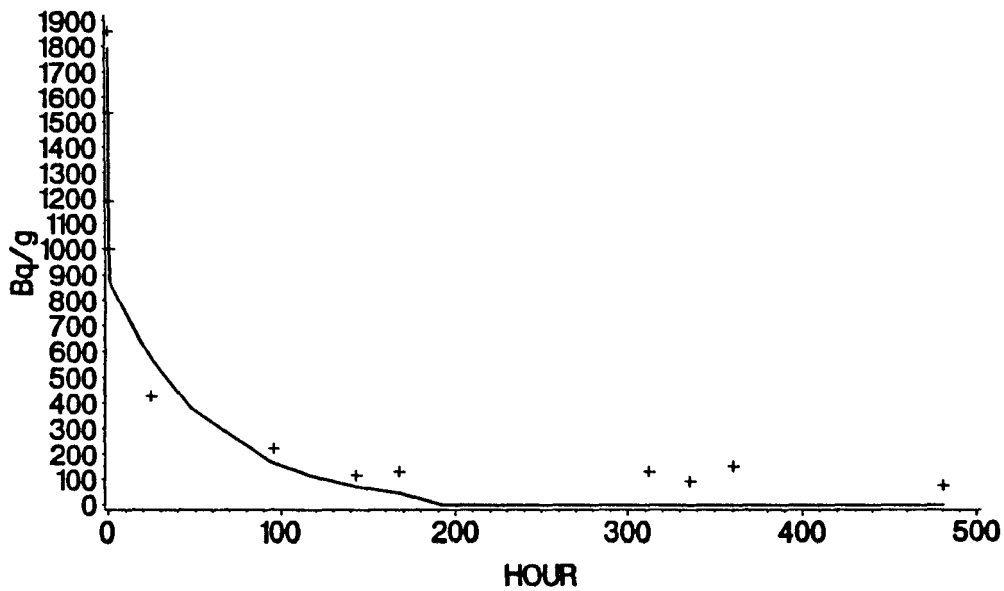


Figure 3: Desorption of ^{134}Cs by the bacterial community. Observed and predicted values.

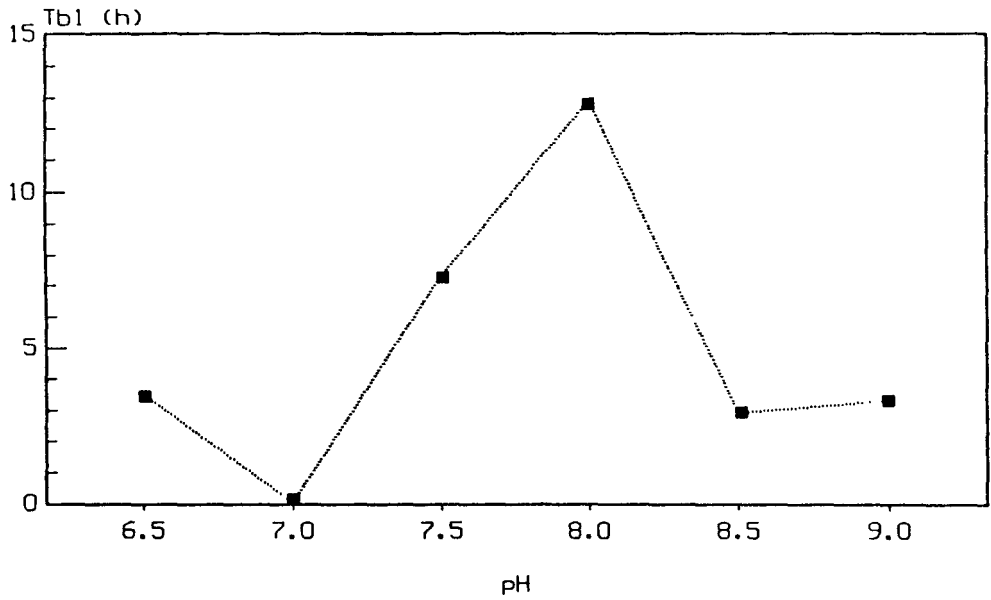


Figure 4: Half-lives (Tb1) for the ^{60}Co desorption of the bacterial community as a function of the water column pH.

Table 1: Kinetics of ^{60}Co and ^{134}Cs uptake by bacterial community. (comments in the text)

	[S]	K_m/V_{max}	$1/V_{max}$	r	V_{max}	K_m
Co^{60}	24->90	$23.8 \cdot 10^{-3}$	$0.4 \cdot 10^{-3}$	0.7595	2500	63.70
	90->2000	$61.3 \cdot 10^{-3}$	$53.5 \cdot 10^{-3}$	0.9924	18692	1145.79
Cs^{134}	22->295	$186.7 \cdot 10^{-3}$	$0.8 \cdot 10^{-3}$	0.8570	1286	240

Project 10

Head of project: *Dr. R.N.J. Comans*

Objectives for the reporting period

The project has the following objectives:

- to study the mechanisms of radiocaesium mobility in freshwater sediments using a combined laboratory and field approach
- to optimize a procedure to measure *in-situ* K_D -values for radiocaesium
- to relate *in-situ* K_D -values for radiocaesium in sediments, and their variation with pore-water concentrations of competing ions, to sorption mechanisms of radiocaesium studied in the laboratory at the microscopic level

Progress achieved including publications

1. Introduction

Since the Chernobyl accident, the interaction of caesium with soils and sediments has been given renewed attention. Although significant progress has been made in laboratory studies of radiocaesium mobility, *in-situ* studies in the environment are hampered by the very low activities in aqueous compartments soon after the accident. Because it is our ultimate goal to predict the transport of radiocaesium through the environment, *in-situ* measurements of this radionuclide and its mobility controlling parameters are necessary to verify our predictions and to indicate additional factors affecting radiocaesium transport that should be considered in our models.

The present study focuses on the solid/liquid distribution coefficient, or K_D , of radiocaesium. This parameter quantifies the interaction of the radionuclide with the solid compartment in sediments and soils and controls, therefore, its mobility. The K_D -value for radiocaesium varies not only between different sediments and soils, which has been attributed by Cremers et al. (1988) to the availability of illitic frayed edges, but is also subject to chemical changes within these environments. Post-depositional changes in the pore water chemistry of freshwater sediments may, therefore, result in a partial remobilization of sediment-bound radiocaesium (Comans et al., 1989). The extent of such a possible remobilization depends on the reversibility of the caesium-sediment interaction and is of great importance for the establishment of the radiological consequences of nuclear accidents. This study includes, therefore, an *in-situ* investigation of radiocaesium mobility in freshwater sediments, as well as an investigation of the mechanisms affecting caesium sorption reversibility.

2. Measurements of *in-situ* K_D 's for radioactive and stable caesium in Esthwaite sediment

In collaboration with the Institute of Freshwater Ecology (Windermere, UK) and the University of Utrecht, Dept. of Geochemistry (The Netherlands), 9 cores of 7 cm diameter were collected from the sediment of lake Esthwaite in the English Lake District. The cores were sliced in a glove box under a nitrogen atmosphere at 1-2 cm intervals over the top 17 cm of the core and at one 4 cm interval from 17-21 cm. The pore water was separated from the individual slices, using a filtration procedure, in a separate glove box under a high purity nitrogen atmosphere ($O_2 < 0.003\%$) to prevent any oxidation of the anaerobic samples. The pore water from each three cores was combined and analyzed for major elements and nutrients. As the pore water chemistry showed no major differences between identical intervals in the three subsets, the remainder of the pore water from each depth-interval was combined to a volume of approximately 200 mL. After preconcentration on ammoniummolybdophosphate (AMP), dissolved ^{137}Cs was measured using an ultra-low-background anti-coincidence γ -counting facility. Counting times varied from three to ten days per sample. Both ^{134}Cs and ^{137}Cs were measured in the sediment. *In-situ* K_D 's for ^{137}Cs were calculated from the activity in the solid and the pore water from each sediment slice.

The sediment profile for ^{134}Cs and ^{137}Cs is shown in Figure 1. The distinct maximum for both isotopes at a depth of 3-4 cm is related to the Chernobyl accident. The $^{134}\text{Cs}/^{137}\text{Cs}$ ratios of approximately 0.5 are characteristic for the Chernobyl fallout (0.5-0.6). A second and broader signature with a maximum around 7-9 cm and $^{134}\text{Cs}/^{137}\text{Cs}$ ratios far below 0.5 is probably related to the nuclear weapons tests in the 1950s and 1960s. The levels of ^{137}Cs in pore water appeared to be extremely low, ~3-30 mBq/L, and could only be measured with a very large uncertainty, despite the counting times of up to 10 days per sample. *In-situ* K_D 's calculated from these values are of the order of 10^4 - 10^5 L/Kg. No significant relationship was observed with sediment depth. Pore-water concentrations of ions competing with caesium for illitic exchange sites were very low ($\text{K}^+ \approx 30$ -50 $\mu\text{moles/L}$; $\text{NH}_4^+ \approx 60$ -190 $\mu\text{moles/L}$) and changed only slightly with depth. These conditions and the relatively high clay mineral content of the sediments (concentration of illitic frayed edge sites ≈ 20 $\mu\text{eq/g}$, as determined by Cremers and coworkers) cause the observed very high K_D -values and, as a result, low dissolved radiocaesium levels.

Figure 2 shows the relationship between the total *in-situ* K_D for radiocaesium and the pore-water ammonium concentrations in sediments from three European freshwater systems; Ketelmeer (Comans et al., 1989), Hollands Diep (Comans, in prep.) and Esthwaite. The concentrations of illitic frayed edge sites in the sediments from these lakes, as measured by Cremers and coworkers, are fairly similar. The negative slope in Fig. 2 reflects the competition of ammonium and caesium for the same exchange sites. The slope of ≈ -1 is consistent with ion-exchange theory, if ammonium controls the radiocaesium K_D in these anoxic sediments.

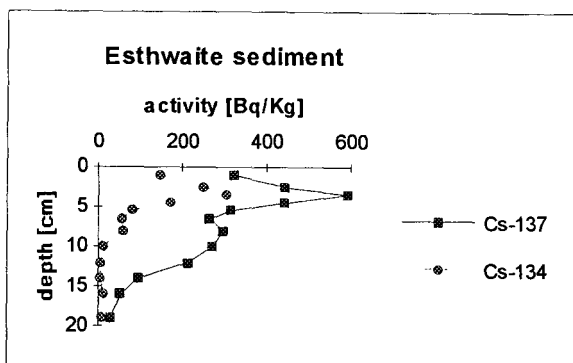


Figure 1. Sediment profiles of ^{137}Cs and ^{134}Cs in Lake Esthwaite (Cumbria, UK). Activities are decay-corrected to April 1986.

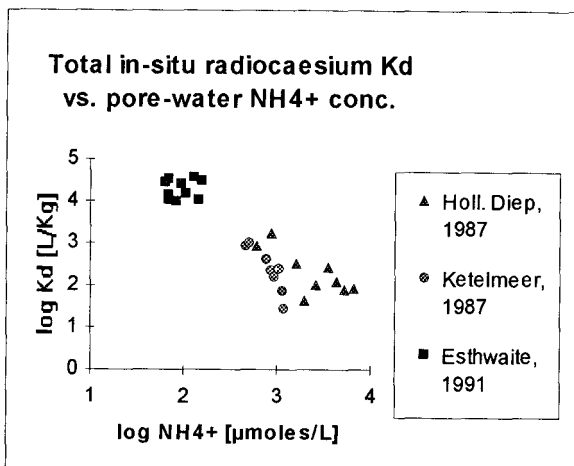


Figure 2. Relationship between ¹³⁷Cs *in-situ* K_D and pore-water NH₄⁺ concentration in sediments from Ketelmeer, Hollands Diep (Comans, in prep.) and Esthwaite.

3. Diffusion-tube experiments

It is well known that K_D-values for trace elements are dependent on the liquid/solid conditions (or particle concentration; see e.g. overview by Honeyman & Santschi, 1988). It is generally observed that K_D's decrease strongly with increasing particle concentration. K_D-values obtained from batch laboratory experiments, using particle concentrations far below those in sediments, are therefore difficult to relate directly to values measured *in-situ*. As an alternative to batch experiments, a radiotracer diffusion-tube procedure is being used and further developed at ECN to study contaminant partitioning under liquid/solid conditions similar to those in sediments or soils. The procedure is briefly outlined in Figure 3. One half of a small tube (typically a few centimetres) is packed with sediment which has been thoroughly mixed with a radiotracer spike. Subsequently, the second half of the tube is carefully packed with the same sediment, but without radiotracer spike. The ends of the tube are sealed and the system is left to equilibrate. For anoxic sediments, all handling is done in a glove box under a nitrogen atmosphere. The radiotracer diffuses slowly from the labelled into the non-labelled segment. After an appropriate equilibration time, the tube is sliced in small segments which are γ or β-counted to construct the diffusion profile. The effective diffusion coefficient of a sorbing trace metal, such as caesium, in sediments or soils is reduced relative to its aqueous diffusion coefficient by a physical (Tortuosity) and a chemical retardation factor. Tortuosity is calculated from a similar diffusion tube experiment with ³H₂O, which shows no chemical interaction with the solids. The K_D is then calculated from the chemical retardation factor.

Figure 4 shows a typical diffusion profile for radiocaesium in Esthwaite sediments. Experiments were done with sediment samples from different depths (i.e. different ammonium concentrations), but the effective diffusion coefficients were not significantly different, probably as a result of the low pore-water NH₄⁺ levels. The K_D-values calculated from the diffusion experiments were about 100 L/Kg, and hence more than two orders of magnitude lower than the values measured *in-situ*. This difference may appear surprising, but will be further discussed below.

Diffusion tube procedure

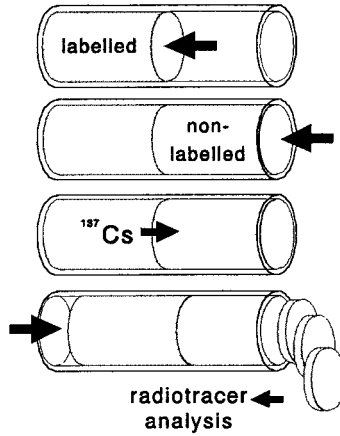


Figure 3. Schematic representation of the radiotracer diffusion-tube procedure. The sediment on the left hand side of the tube is labelled with freshly added ^{137}Cs .

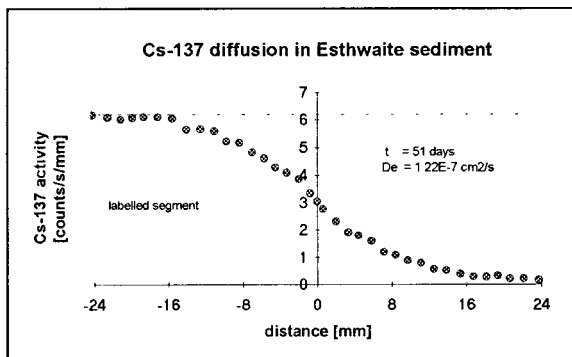


Figure 4. Diffusion profile of freshly added radiocaesium in Esthwaite sediment. The sediment on the left hand side of the tube was labelled with ^{137}Cs .

4. Mechanisms affecting caesium sorption reversibility.

When studying radiocaesium mobility and the potential risk of remobilization from contaminated sediments, knowledge of the underlying mechanisms of caesium sorption on sediments is a prerequisite. Especially the reversibility of the process, which reflects the ability of sediment-bound radiocaesium to be released to the aqueous phase by changing conditions, is pertinent to the question of remobilization.

Since it is now well accepted that interaction with the frayed edges of illitic clay minerals largely controls the mobility of radiocaesium in mineral sediments and soils, it is reasonable to assume that the reversibility of this process largely determines the overall ability of the radioisotope to be released from the solids. Comans et al. (1991) have shown that the reversibility of caesium sorption on illite was strongly affected by slow sorption processes and by the nature of the major competing cation (i.e. calcium or potassium). In a calcium environment, caesium sorption was observed to proceed significantly faster and to reach much higher K_D values than in an environment dominated by potassium. The apparent reversibility of the process was shown to be controlled by the continuing slow sorption processes, but was substantially less in an environment dominated by calcium. Comans et al. (1991) have postulated that a fraction of caesium migrates slowly to highly selective interlayer sites within the clay mineral from it is not easily released. Caesium apparently moves faster through the expanded edge-intelayers in the calcium-dominated system than through the collapsed edges in the potassium system.

The importance of the kinetics of caesium sorption on illite for modelling the mobility and potential remobilization of sediment-bound radiocaesium made it necessary to develop, partly within the framework of the present project, a kinetic model to fully describe caesium sorption and to evaluate the development of reversibly and irreversibly sorbed caesium fractions over time. A three-box model was developed, which includes fast reversible sorption on sites which are partly rapidly accessible and in instantaneous equilibrium, and partly kinetically controlled. The equilibrium condition of the reversible reaction is described by a Freundlich isotherm. Rapid reversible sorption is followed in series by a slow, irreversible first-order process. The model is consistent with the above mechanistic hypothesis and describes the data of Comans et al. (1991) at different caesium concentrations, and a new data set at two different particle concentrations, adequately. The rate constant for the slow irreversible process is 0.0038 d^{-1} for caesium sorption on potassium-saturated illite and 0.020 d^{-1} for calcium-saturated illite. Further details of the kinetic modelling can be found in Comans & Hockley (1992). At the macroscopic level (Fig. 5), the kinetic model predicts that reversible sorption is important over time scales of a few days and less and may, therefore, affect radiocaesium transport in the water column. Irreversible sorption becomes important over time scales of weeks to months and is, therefore, of greatest importance for radiocaesium in sediments. The latter process is especially relevant for estimations of the potential amount of sediment-bound radiocaesium that may be mobilized under anoxic conditions.

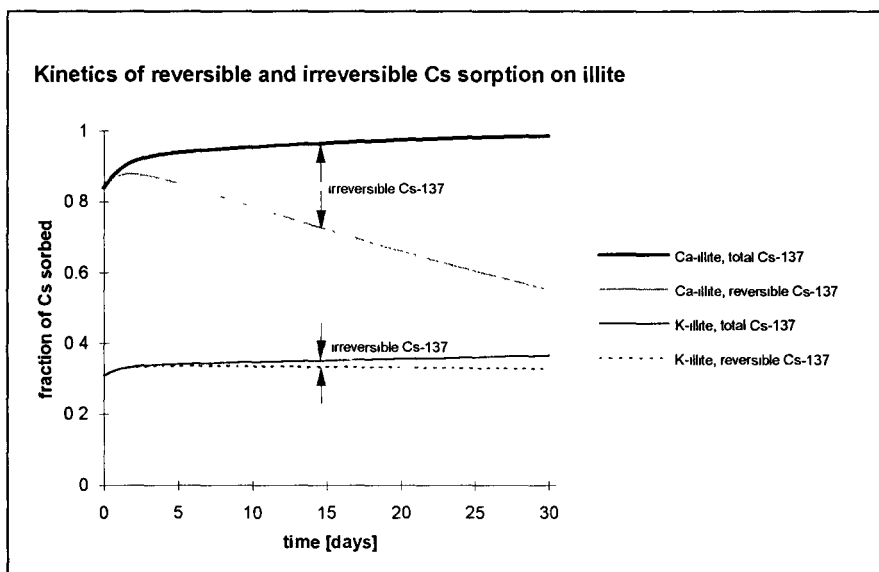


Figure 5. Time evolution of reversibly and irreversibly sorbed Cs, as predicted by the three-box model (Comans & Hockley, 1992), for 5 µg/L total Cs and a particle (illite) concentration of 100 mg/L.

5. Implications of the mechanisms studied in the laboratory for radiocaesium mobility in the field

As Figure 5 clearly indicates, the reversibility of radiocaesium decreases substantially with time. The above laboratory and modelling results suggest that radiocaesium is slowly immobilized by the hypothesized migration into the illitic interlayers. There is, however, evidence that still a few percent of sediment-bound radiocaesium can be remobilized by enhanced NH_4^+ levels in anoxic pore waters, even after many years of contact (Evans et al., 1983; Comans et al., 1989). The necessary backwards reaction is possibly too slow to be noticed in laboratory experiments of a few weeks, but may become important over longer time periods. Combined field work and long-term laboratory sorption experiments are necessary to determine the possible reverse rate.

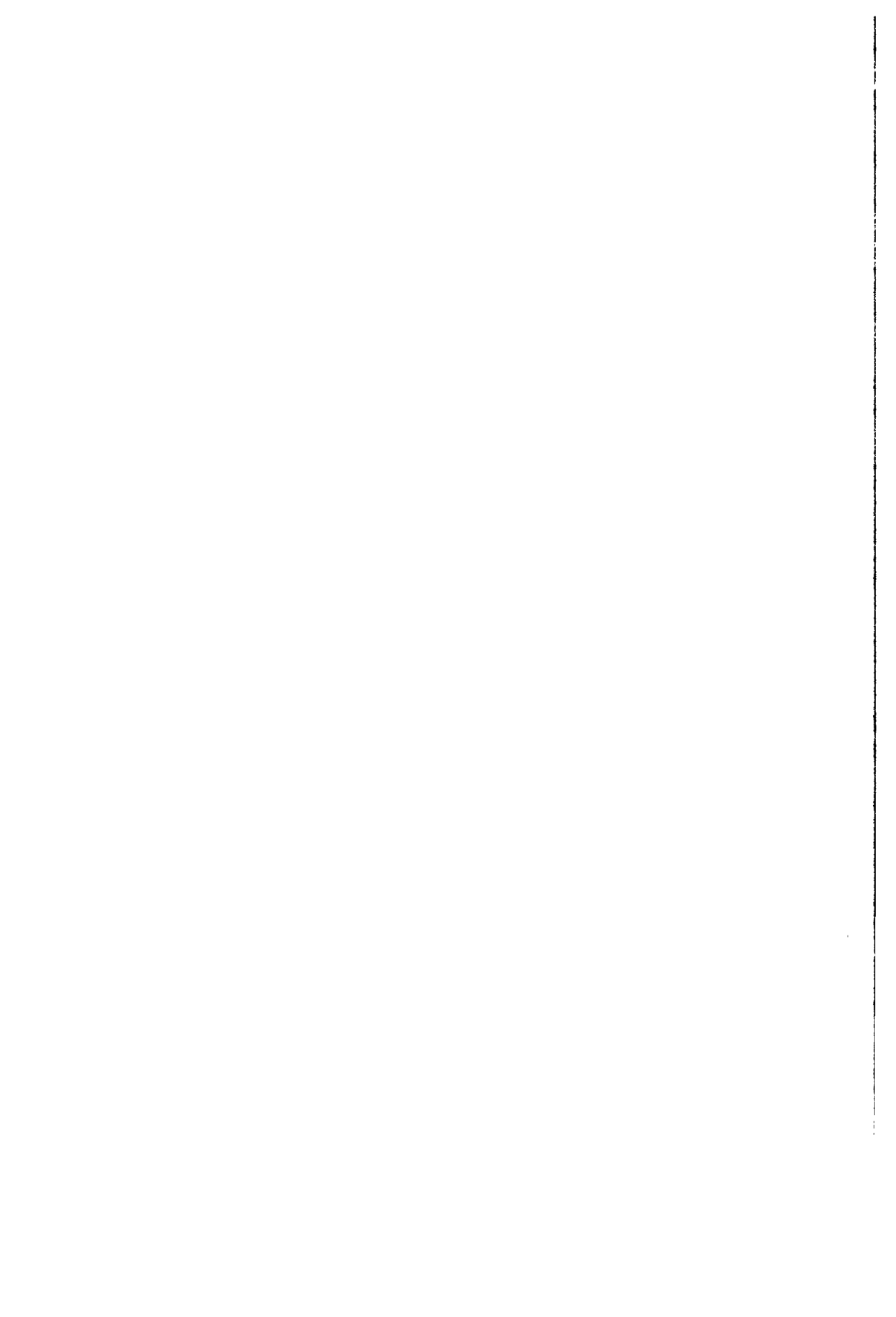
Irreversibly sorbed radiocaesium contributes to the overall (*in-situ*) K_D and may not, or only after long periods of time, respond to high levels of dissolved competing ions. It is, therefore, important to establish the fractions of the overall (*in-situ*) K_D related to the (rapidly) exchangeable and to the apparently non-exchangeable radioisotope. In addition, it is important to know how this relationship changes with caesium/sediment contact time. The two orders of magnitude difference between the overall *in-situ* K_D 's for Esthwaite and the values measured in the diffusion experiments is possibly related to this distinction and would suggest that, five years after the Chernobyl accident, the exchangeable fraction is of the order of a percent. However, considering the large uncertainty in the *in-situ* K_D 's, this needs further study. Obviously, only truly exchangeable radiocaesium can be remobilized and should be considered in transport models. Because the exchangeability is time dependent (Fig. 5), kinetic models are needed for an accurate prediction of radiocaesium transport through the aquatic environment.

References

- Comans, R.N.J., Middelburg, J.J., Zonderhuis, J., Woittiez, J.R.W., De Lange, G.J., Das, H.A. & Van Der Weijden, C.H. (1989) Mobilization of radiocaesium in pore water of lake sediments. *Nature* **339**, 367-369.
- Cremers, A., Elsen, A., De Preter, P., and Maes, A. (1988) Quantitative analysis of radiocaesium retention in soils. *Nature* **335**, 247-249
- Evans, D.W., Alberts, J.J., and Clark, R.A. (1983) Reversible ion-exchange fixation of cesium-137 leading to mobilization from reservoir sediments. *Geochim. Cosmochim. Acta* **47**, 1041-1049.
- Honeyman B.D. and Santschi P. (1988) Metals in aquatic systems. *Environ. Sci. Technol.* **22**, 862-871.

Publications resulting from this work

- Comans, R.N.J., Haller, M., and De Preter, P. (1991) Sorption of cesium on illite: non-equilibrium behaviour and reversibility. *Geochim. Cosmochim. Acta* **55**, 433-440.
- Comans, R.N.J. and Hockley, D.E (1992) Kinetics of cesium sorption on illite *Geochim. Cosmochim. Acta* **56**, 1157-1164.



RADIOECOLOGY OF TRANSURANICS IN THE MARINE ENVIRONMENT

Contract Bi7-042 - Sector A21

1) *Mitchell*, University College Dublin - 2) *Iranzo*, CIEMAT
3) *Guéguéniat*, CEA-Cherbourg - 4) *Damiani*, ENEA

Summary of project global objectives and achievements

The overall objective of the above project was to refine our understanding of the behaviour of plutonium, americium and other long-lived radionuclides such as ^{137}Cs in the marine environment. The study embraced a number of distinct marine zones including the Irish Sea, the Norman-Breton Gulf, the Seine Estuary, the Almanzora Canyon (Palomares) and adjacent Shelf, the Gulf of Taranto - Ionian Sea and the Balearic Sea area. Although these domains differ widely in their physical oceanography (contrast the mega-tidal Norman-Breton Gulf with the weakly tidal Mediterranean), many of the fundamental processes governing the behaviour of transuranics and other long-lived nuclides are common to them all and, accordingly, were the main focus of the work undertaken by the participants.

Specific objectives included:

- (1) An assessment of the distribution of reduced and oxidised plutonium in filtered sea water and suspended particulate matter throughout the Irish Sea and the determination of representative sediment - water distribution coefficients (k_d) for plutonium and americium, particularly in the western Irish Sea (the *so-called* far zone).
- (2) An experimental study of the mechanisms of complexation of americium and its analogues, the rare earths, with organic ligands in zones of high concentration. Also, an evaluation of the well-established principle of analogy between the rare earth elements and the transuranics.
- (3) The measurement of stable rare earths and other elements in a limited selection of bottom sediments from the western Irish Sea in order to complement objectives (1) and (2) above.
- (4) An estimation of the transit time of particles and associated transuranics between Cap de La Hague and Cherbourg Harbour using the $^{137}\text{Cs}/^{241}\text{Am}$ activity ratio.
- (5) The development of an improved technique for the measurement of ^{241}Pu at environmental concentrations in order to use the $^{241}\text{Pu}/^{239,240}\text{Pu}$ activity ratio to determine (a) transuranic residence times in the Irish Sea and (b) the transit time of sediment particles between Cap de la Hague and Cherbourg Harbour.
- (6) The identification and definition of fundamental hydrodynamic processes in megatidal areas such as the Seine estuary and the Norman-Breton Gulf which are important sinks for artificial radionuclides.

- (7) An examination of the mechanisms governing the transfer of transuranics from land to sea *via* the Almanzora River to the continental shelf off Palomares and the Almanzora Canyon system.
- (8) Complementary studies on (a) the transport of radionuclides from the continental shelf to the deep-sea in uncontaminated (Gulf of Taranto - Ionian Sea) and potentially contaminated (Palomares - Balearic Sea) zones and (b) the vertical distribution of natural and artificial radionuclides in the water column and in sediments of Mediterranean deep-sea environments.
- (9) Studies of the bioavailability of transuranics: in particular, (a) the uptake of plutonium by the lobster and (b) the dosimetric implications for a hypothetical Irish critical groups of the uptake of plutonium and americium by fish and shellfish in the western Irish Sea.
- (10) Collaborative research expeditions (with other participants in this programme) in order to (a) complete (7) and (8) above, and (b) initiate a study of the physico-chemical speciation of plutonium and americium in western Mediterranean deep waters and in the Palomares continental shelf zone.
- (11) The development of new techniques for the determination of colloiddally-bound plutonium and americium in marine and estuarine waters.

Although proportionately more of the plutonium and americium in the water column close to the Sellafield outfall was found to be associated with suspended particulate, the percentage of oxidised plutonium, Pu(V,VI), in filtered water sampled throughout the open waters of the Irish Sea showed little variation. No difference between surface and bottom waters was detected, reflecting the shallow nature of much of the Irish Sea and the importance of turbulent mixing in addition to advective transport. Moreover, no distinction was observed between the eastern and western Irish Sea. In fact, the agreement between these two zones was striking with oxidised plutonium predominant ($85 \pm 6\%$) in both. In contrast, the bulk of the plutonium in filtered water from Carlingford Lough was found to be in a reduced form, Pu(III,IV), an observation which is consistent with measured plutonium concentrations being somewhat lower in these waters compared to the open waters outside (plutonium in a reduced form is more particle-reactive and, thus, more readily removed from the water column).

Representative sediment - water distribution coefficients (K_d) for plutonium and americium were determined in the above mentioned zones and systematic differences interpreted in terms of the prevalence of *hot-particles* in the vicinity of the outfall and the presence of a significant colloidal component within the waters of Carlingford Lough.

The complexation of ^{241}Am (and its rare-earth analogues) by organic matter was studied using fresh water from the Vire, Seine, Escaut and Elbe rivers. It was demonstrated that the classical complexing ability of a fresh or marine water based on the addition of a transition metal was not available for the transuranics. Moreover, organically complexed ^{241}Am was shown to be unstable in estuaries with significant americium removal occurring in the pH range 5 to 7. Similar behaviour has been reported for the rare earths and has been attributed to an interaction with iron-organic colloids.

A sediment core, taken from the Irish Sea by University College Dublin, was analysed by CEA-Cherbourg using the technique of neutron activation analysis. Of the various stable elements usually associated with nuclear wastes, only the molybdenum concentrations were found to correlate with the ^{241}Am concentrations.

A novel technique for the determination of β -emitting ^{241}Pu in the presence of α -emitting nuclides was developed in the course of this project which obviates the need for stripping the discs before β -counting and is free from the chemiluminescence and quenching associated with other methods. The technique was used to determine the $^{241}\text{Pu}/^{239,240}\text{Pu}$ activity ratio in a selection of marine samples from the Irish Sea and the Norman-Breton Gulf with a view to determining transuranic residence and transit times in (and through) the respective zones. Details of the technique were presented at an international conference in September 1992 and a paper on the subject has been submitted to *Radiocarbon*. Use was also made of the temporal variation in the $^{137}\text{Cs}/^{241}\text{Am}$ ratio in La Hague effluents by comparing it with the vertical evolution of the same ratio in sediments from the vicinity of Cherbourg, in order to estimate the transit time of particulate-associating nuclides from the source (La Hague) to a zone of continuous sedimentation (Cherbourg).

Suspended particulate matter and sediment collected from the Seine River and its megatidal estuary were subjected to neutron activation and gamma-ray spectrometric analyses. Various geochemical tracers were used to examine riverine and marine inputs and define the fundamental hydrodynamic parameters and processes driving the spatial and temporal variations of particulate pollutants.

The mechanisms and pathways governing the transfer of plutonium, americium and radiocaesium from land to sea *via* the Almanzora River have been investigated in detail. Clear differences were evident between the behaviour of the transuranics on the one hand and radiocaesium on the other. While there was a decrease in the ^{137}Cs inventory in sediments close to the Almanzora River mouth, plutonium concentrations were found to be higher in downstream sediments. In other words, much of the plutonium has migrated downstream in association with river-borne particles and is now found accumulated to higher levels in the sediments near the mouth and the surrounding shelf. Regarding the continental shelf in the Palomares zone, differences in the plutonium/caesium ratio have been used successfully to demarcate the area where there has been a significant terrigenous contribution. It is important to stress that this input, far from being continuous, is the consequence of the rare flash-floods which pass down the Almanzora River, together with a possible land-to-sea transfer *via* airborne translocation due to the resuspension in this arid region of deposited transuranics by the prevailing south-westerly winds. In the Palomares off-shore zone concentrations of plutonium and americium in deep waters were found to be considerably lower than those measured close to Villefrance sur le Mer in 1989. A possible explanation is mediation by Atlantic water *via* the Straits of Gibraltar with a consequent lowering of the salinity and the temperature.

At the outset of this programme, few data were available on transuranic concentrations in Mediterranean slope and deep-sea sediments. For this reason, selected areas having different morphological and sedimentological characteristics were chosen in order to evaluate the transport of such nuclides from the continental shelf to the deep-sea environment. In particular, vertical profiles and inventories of transuranics were measured in sediments from

(a) deep-sea areas characterised by pelagic sedimentation only, (b) areas affected by contributions of terrigenous matter and (c) slope and bottom of complex canyon systems. In addition, a study was initiated on the mechanisms of transport of radionuclides through the different water masses characterising the western Mediterranean Sea.

To this end, sea water and sediment samples were collected in the course of three research cruises in the Ionian and western Mediterranean Sea in 1989, 1991 and 1992. A number of important conclusions have been drawn from the analyses of these samples. For example, in the Taranto canyon (Ionian Sea) plutonium inventories were found to decrease along the canyon from the shelf to the slope and the deepest part of the canyon. This is undoubtedly related to the decrease in sedimentation rates and resuspension processes with depth and is a reaffirmation of an established trend. In general, the plutonium inventories calculated for the Gulf of Taranto were found to be almost twenty times higher than in the open south-western Mediterranean, in an area subject only to pelagic sedimentation. Several factors, the details of which are given below, have been identified which account for this difference.

At the time of the 1991 cruise, the morphology of the Palomares area in the Gulf of Vera was not well known. This has now been rectified, the bathymetry having been carefully determined in the course of research cruises carried out by the participants aboard the research vessels *Bannock* and *Urania* of the Italian National Research Council. The sampling strategy on both occasions was heavily influenced by these new data and interpretation has benefitted accordingly.

The vertical profile of ^{137}Cs in the water column was measured at four stations along the track Cagliari (South Sardinia) - Gulf of Vera (Spain) during the 1991 cruise. Although, in general, concentrations decreased from the surface to the bottom, an exception was the station closest to the coast of Sardinia where a relative maximum was observed in the Levantine Intermediate Water. As this station was the only one, among those studied, situated in the main path of the Levantine Intermediate Water (formed in the eastern Mediterranean), it is likely that the sub-surface maximum observed is related to the transport of Chernobyl-sourced radiocaesium from the eastern to the western basin of the Mediterranean Sea.

The direct radiological protection implications of the presence of transuranics and other long-lived radionuclides in the marine environment have also been addressed in two separate studies. The transfer of plutonium inside an accumulating organ, the hepatopancreas of the lobster, was examined by the CEA-Cherbourg and followed a similar study on the transfer of ^{241}Am in the same species. The dosimetric implications for the critical group consuming fish and shellfish from the western Irish Sea were assessed by University College Dublin (UCD), who concluded that the annual committed effective dose to a member of the critical group was less than 1% of the ICRP-recommended principal dose limit for a member of the general public.

New techniques, based on chemical sorption and ultrafiltration, were developed for the determination of the colloidally-bound fraction of various radionuclides in marine and estuarine waters. Tests were conducted in the field with filtered water from both the Irish Sea and the Mediterranean and some interesting, though preliminary, data were gathered. For example, there appeared to be a strong correlation between the percentage of plutonium in a colloidal form and that in a reduced chemical form. Further refinement and optimization

of these advanced systems will be necessary before fully reliable data can be reported.

A feature of the collaboration outlined herein was the application of compatible and, in some cases, identical analytical techniques to the study of the physical and chemical speciation, dispersion, sediment transport and organic complexation of some of these nuclides under a wide range of environmental conditions. The programmes of the participating laboratories were closely coordinated with the aim of enhancing the value and universality of the results obtained. The Group held four meetings during the reporting period, to discuss the technicalities of coordination and plan research cruises, as well as to review the progress of researches carried out by each participating laboratory. Additional bi-lateral meetings were also held. A number of joint marine research cruises were undertaken in the Irish Sea, the English Channel and the western Mediterranean Sea. Of particular importance were the research cruises aboard the *R.V. Challenger* (1989), the *R.V. Cirolana* (1991, 1992), the *N/O Bannock* (1991) and the *N/O Urania* (1992) in which all four collaborating institutions participated either directly or indirectly. In the course of the Mediterranean cruises, a detailed field study was initiated of the physico-chemical speciation of plutonium and americium in western Mediterranean deep waters and in the Palomares continental shelf zone to determine whether the fundamental mechanisms governing their behaviour in these zones are similar to those elsewhere (Irish Sea).

A significant number of project-related research publications and reports have been published by the participating laboratories or are in press. Further publications relating to the research carried out in the reporting period are in preparation, including a paper reviewing the work carried out in the western Mediterranean in the course of the *N/O Bannock* Cruise (July-August, 1991) by all the participants.

It is the considered opinion of the participants in this project that the specific objectives outlined above have been fulfilled and, in some instances, exceeded. The individual contributions of the participants are summarised below. Further information is available in the publications listed or can be sought directly from the participants themselves.

Project 1

Head of project: *Dr. Mitchell*

Objectives for the reporting period

- (1) To implement in the UCD laboratory dual isotopic tracer techniques to separate the oxidation states of plutonium in filtered sea water and on suspended particulate matter.
- (2) To examine the distributions of plutonium and americium between filtered water and suspended particulate in surface and bottom water throughout the Irish Sea (including Carlingford Lough), and to determine sediment-water distribution coefficients (K_d) for both elements.
- (3) To determine the oxidation state distribution of plutonium in filtered surface and bottom waters in both the eastern and western Irish Sea (including Carlingford Lough).
- (4) To assess the oxidation state distribution of plutonium on suspended particulate near Sellafield and to compare it with the results of similar measurements in the western Irish Sea.
- (5) To develop an improved technique for the determination of ^{241}Pu at environmental concentrations, with a view to using the $^{241}\text{Pu}/^{239,240}\text{Pu}$ isotopic ratio to determine residence and transit times.
- (6) To develop new techniques based on sequential sorption and ultrafiltration for the determination of colloiddally-bound plutonium and americium in marine and estuarine waters, and to conduct preliminary evaluations in the Irish marine environment.
- (7) To examine the dosimetric implications for a hypothetical Irish critical group of the uptake of plutonium and americium by fish and shellfish in the western Irish Sea.
- (8) To carry out collaborative research expeditions (with other participants in this programme) in order to study the physical and chemical speciation of plutonium and americium in (a) western Mediterranean deep waters and (b) the Palomares continental shelf zone.

Progress achieved including publications

A technique to separate the oxidation state groups of plutonium, based on the use of dual isotopic tracers ($^{236}\text{Pu}(\text{VI})$ and $^{242}\text{Pu}(\text{IV})$) and selective coprecipitation on a rare earth fluoride, was successfully implemented in our laboratory at an early stage of the reporting period. The specificity and reproducibility of the technique was confirmed in stringent quality control and quality assurance programmes carried out both in advance of and during the field work.

The physical and chemical speciation of plutonium and americium released from Sellafield were examined at a number of stations throughout the eastern and western Irish Sea and Carlingford Lough, in the course of research cruises carried out in the period 1989-92 aboard *R. V. Lough Beltra*, *R.R.V. Challenger* and *R.V. Cirolana*. In particular, the oxidation states of plutonium (Pu(III+IV) and Pu(V+VI)) were studied in surface and bottom waters in order to determine whether there were differences between the distribution in the vicinity of the Sellafield outfall and that observed in the far field, namely the western Irish Sea. The oxidation state distribution of plutonium on suspended particulate sampled in the Sellafield inshore zone was also examined and compared with similar analyses carried out in the inshore waters of Dublin Bay. In addition, sediment-water distribution coefficients (K_{ds}) were determined for plutonium and americium throughout the Irish Sea and Carlingford Lough. Particular attention was given to the more particle-reactive reduced species in the western Irish Sea zone, where there is evidence (from data collected by this laboratory in the period 1985-92) that plutonium and americium concentrations in both the sea water and surface sediment compartments have been relatively constant. In other words, there appears to be a near equilibrium between the transuranic input and output fluxes to/from the western Irish Sea zone at the present time. Indeed, according to the latest predictive models, this should remain the case for some years to come.

A simple and convenient technique for the determination of β -emitting ^{241}Pu in the presence of α -emitting nuclides was developed in which, following radiochemical separation and solid state α -spectrometry, the electroplated discs are immersed in an appropriate scintillant and counted directly in an actively-shielded liquid scintillation counter. The technique obviates the need for stripping the discs before β -counting and is free from the chemiluminescence and quenching problems associated with certain other methods. Pulse shape discrimination is employed to distinguish α - from β -induced events and corrections are made for the interference in the β -window arising from the presence of α -activity on the disc as well as for self-absorption. The technique was used to measure the ^{241}Pu concentrations and, hence, the $^{241}\text{Pu}/^{239,240}\text{Pu}$ activity ratio in filtered water, suspended particulate and surface sediments sampled in the vicinity of the outfall and the western Irish Sea. The latter enabled us to deduce an effective *hold-up* time for plutonium in the sedimentary deposits close to the Sellafield outfall.

In the latter stage of the programme, complementary techniques to measure the fractions of plutonium and americium in filtered water that are in a colloiddally-bound form were developed and tested both in the laboratory and in the field. The first is based on the principle of sequential sorption onto a set of aluminium oxide beds arranged in series. In this approach, the colloidal fraction is defined as that which can pass through a $0.45\ \mu\text{m}$ filter, but is efficiently sorbed on the first aluminium oxide bed. This fraction can be quantified by the appreciably higher collection efficiency on the first bed compared with the other beds using appropriate sorption isotherms. These latter take account of both reduced and oxidised species and changes in chemical speciation upon passage through the aluminium oxide.

In the second technique, filtered ($<0.45\ \mu\text{m}$) sea water is circulated through a selection of tangential-flow ultrafiltration membranes mounted in acrylic assembly units and operated in concentration (recyclable) mode. The permeates, obtained separately using 100 kD, 10 kD, 3 kD and 1 kD ultrafilters respectively, are then treated using the dual-tracer coprecipitation technique referred to above, in order to establish the oxidation state distribution of plutonium in each size fraction. In addition, samples of permeate are analysed for *colloidal* plutonium

and americium using the aluminium oxide sorption technique. In the course of these operations, strenuous efforts are made to minimize storage time and, thus, preclude the generation of experimental artifacts. In addition, strict precautions must be taken to prevent the samples becoming contaminated during processing. Both techniques have been tested on a number of occasions under field conditions and have already provided some interesting experimental results.

1. Sampling and analysis

Details of the sampling, *in situ* (onboard) sample processing, radiochemical analysis (including plutonium oxidation state separation), and α - and β -spectrometry have been described in the publications given below and will not be dealt with further here.

2. Interpretation of results

The percentages of plutonium and americium on suspended particulate and the percentage of Pu(V,VI) in filtered water from each of the stations analysed are summarised in Table 1. It is evident from the data that proportionately more of the plutonium and americium in the water column close to the outfall is associated with suspended solid. Differences in the suspended load in the eastern and western Irish Sea cannot account for the significant variation in these percentages as one moves away from Sellafield and this suggests that other factors may be involved.

In contrast to the systematic variation with increasing distance from Sellafield in the partition between suspended particulate and filtered water fractions, the percentage of Pu(V,VI) in the latter was essentially constant. No difference between surface and bottom waters was detected, nor was there any distinction between the eastern and western Irish Sea. In fact, the agreement between these zones is remarkable, with little scatter in the data, and demonstrates that throughout the open waters of the Irish Sea the percentage of $^{239,240}\text{Pu(V,VI)}$ in filtered water lies in the range 77-94% with an overall mean of $85 \pm 6\%$. However, in Carlingford Lough, the bulk of the plutonium in filtered water is in a reduced form, which explains why plutonium concentrations within Lough waters are considerably lower than those outside, as reduced plutonium is much more particle-reactive, i.e., adsorbed more readily by sediments.

An examination of the oxidation states of plutonium adsorbed on suspended particulate in the eastern and western Irish Sea confirmed that the plutonium was almost entirely in a reduced form (>97%), in excellent agreement with previous studies.

Measured $^{238}\text{Pu}/^{239,240}\text{Pu}$ activity ratios in filtered sea water, suspended particulate and surface sediment in the western Irish Sea are indicative of releases from Sellafield, being in good accord with those observed throughout the north-eastern Irish Sea. As expected, there is a clear difference between that $^{241}\text{Am}/^{239,240}\text{Pu}$ ratio in filtered sea water and that for the suspended load, reflecting the stronger particle reactivity of americium. The $^{241}\text{Pu}/^{239,240}\text{Pu}$ ratios in filtered sea water, suspended particulate and sediment are observed to diminish with increasing distance from Sellafield, and indicate that the effective transuranic *hold-up* time in the eastern Irish Sea lies in the range 10-15 years.

No systematic variation of K_d with depth at a given location was observed (Table 2).

Table 1. Percentages of plutonium and americium on suspended particulate and percentage of plutonium(V,VI) in filtered ($< 0.45 \mu\text{m}$) sea water sampled throughout the Irish Sea and Carlingford Lough

Location	Fraction	% on suspended particulate			% Pu(V,VI) in filtrate	
		^{238}Pu	$^{239,240}\text{Pu}$	^{241}Am	^{238}Pu	$^{239,240}\text{Pu}$
54°25'N	Bottom	86 ± 3	86 ± 3	-	81 ± 5	81 ± 4
03°34'W	Surface	88 ± 3	88 ± 2	-	77 ± 5	80 ± 4
54°19'N	Bottom	58 ± 4	57 ± 4	-	86 ± 7	85 ± 5
03°42'W	Surface	45 ± 3	48 ± 3	-	85 ± 6	85 ± 6
54°30'N	Bottom	56 ± 4	55 ± 2	93 ± 2	89 ± 5	94 ± 5
04°44'N	Surface	46 ± 3	47 ± 2	90 ± 2	90 ± 6	89 ± 6
53°50'N	Bottom	18 ± 2	21 ± 1	-	70 ± 6	74 ± 4
05°40'N	Surface	12 ± 2	15 ± 1	-	82 ± 7	80 ± 5
53°40'N	Bottom	21 ± 2	25 ± 2	65 ± 3	92 ± 7	90 ± 5
05°50'N	Surface	23 ± 2	26 ± 2	70 ± 2	93 ± 8	92 ± 5
53°30'N	Bottom	36 ± 4	41 ± 3	80 ± 4	85 ± 7	85 ± 5
05°45'N	Surface	14 ± 3	22 ± 3	41 ± 2	80 ± 30	80 ± 20
Dublin Bay	Surface	32 ± 2	32 ± 1	-	69 ± 2	67 ± 2
Eastern Irish Sea	Bottom	70 ± 10	70 ± 10	93 ± 2	85 ± 3	87 ± 5
(mean)	Surface	60 ± 20	60 ± 20	90 ± 2	84 ± 5	85 ± 4
Western Irish Sea	Bottom	25 ± 8	29 ± 9	73 ± 11	82 ± 9	83 ± 7
(mean)	Surface	16 ± 5	21 ± 5	56 ± 21	85 ± 7	83 ± 7
C'ford Lough (mean)	Surface	21 ± 3	19 ± 2	21 ± 4	33 ± 14	30 ± 15

Uncertainties quoted to ± 1 S.D.

Table 2. Total K_d s for plutonium and americium and K_d s for plutonium(III,IV) in filtered (< 0.45 μ m) sea water sampled throughout the Irish Sea and Carlingford Lough

Location	Fraction	Apparent K_d ($l\ kg^{-1}$)		
		Pu (total)	Pu (III,IV)	Am (total)
54°25'N	Bottom	$(6.8 \pm 0.3) \times 10^5$	$(3.5 \pm 0.3) \times 10^6$	-
03°34'W	Surface	$(7.4 \pm 0.3) \times 10^5$	$(3.6 \pm 0.2) \times 10^6$	-
54°19'N	Bottom	$(3.3 \pm 0.3) \times 10^5$	$(2.3 \pm 0.2) \times 10^6$	-
03°42'W	Surface	$(2.6 \pm 0.2) \times 10^5$	$(1.7 \pm 0.2) \times 10^6$	-
54°30'N	Bottom	$(4.0 \pm 0.3) \times 10^5$	$(6.4 \pm 0.8) \times 10^6$	$(4.1 \pm 0.3) \times 10^6$
04°44'N	Surface	$(2.7 \pm 0.2) \times 10^5$	$(2.4 \pm 0.2) \times 10^6$	$(2.7 \pm 0.2) \times 10^6$
53°50'N	Bottom	$(6.7 \pm 0.6) \times 10^4$	$(2.6 \pm 0.3) \times 10^5$	-
05°40'N	Surface	$(1.1 \pm 0.2) \times 10^5$	$(5.4 \pm 0.8) \times 10^5$	-
53°40'N	Bottom	$(6.9 \pm 0.6) \times 10^4$	$(6.9 \pm 0.7) \times 10^5$	$(4.0 \pm 0.3) \times 10^5$
05°50'N	Surface	$(1.1 \pm 0.1) \times 10^5$	$(1.4 \pm 0.2) \times 10^6$	$(7.5 \pm 0.7) \times 10^5$
53°30'N	Bottom	$(6.5 \pm 0.5) \times 10^4$	$(4.5 \pm 0.5) \times 10^5$	$(3.7 \pm 0.3) \times 10^5$
05°45'N	Surface	$(8.7 \pm 1.3) \times 10^4$	$(3.6 \pm 0.4) \times 10^5$	$(2.1 \pm 0.2) \times 10^5$
Dublin Bay	Surface	$(5.4 \pm 0.5) \times 10^4$	$(1.7 \pm 0.2) \times 10^5$	-
Eastern Irish Sea (mean)		$(4 \pm 2) \times 10^5$ (n=6)	$(3 \pm 2) \times 10^6$ (n=6)	$(3 \pm 1) \times 10^6$ (n=2)
Western Irish Sea (mean)		$(8 \pm 2) \times 10^4$ (n=7)	$(6 \pm 4) \times 10^5$ (n=7)	$(4 \pm 2) \times 10^5$ (n=4)
Carlingford Lough (mean)		$(2.1 \pm 0.4) \times 10^5$ (n=3)	$(3 \pm 1) \times 10^5$ (n=3)	$(2.3 \pm 0.6) \times 10^5$ (n=3)

Uncertainties quoted to ± 1 S.D.

Note: Americium is almost exclusively in a reduced chemical form in sea water, i.e., Am(III).

However, a clear difference between the mean K_d values for plutonium and americium in the eastern and western zones was evident from our data. The former are identical to the mean K_d s reported for the north-eastern Irish Sea zone by other workers. Factors which could, conceivably, influence a K_d determination have been summarised in our interim report. Suffice to say that the observed difference in the K_d s between the two zones cannot be accounted for on the basis of differences in chemical speciation, as the oxidation state distribution of plutonium is identical in both the eastern and western Irish Sea. Organic carbon concentrations throughout the open waters of the Irish Sea are known to be much lower than the levels (>10 mg/l) required to alter measured K_d s. Further, although Irish coastal waters are enriched in silicon, while eastern waters are enriched with anthropogenically derived nitrogen and phosphorous, these differences are small and unlikely to give rise to a measurable perturbation in K_d . Moreover, we do not consider that the particle-size distribution or the composition of the suspended load is significantly different in the eastern and western Irish Sea, given the degree of turbulent mixing which takes place in these shallow waters (typically 50-150 metres).

We are forced to conclude that the variation with increasing distance from the source in the percentages of plutonium and americium on suspended particulate, together with the differences between the K_d s for both elements in the eastern and western zones are related to the nature of the discharges themselves. It is known that only about 1% of the plutonium released from Sellafield is in an oxidised form, while all of the americium is in a reduced form. Thus, the preponderance of the particulate fraction in the effluent provides a ready explanation for the elevated percentages on suspended particulate close to the outfall. *Hot* particles have also been identified in the effluent and are known to persist in the environment for months before dissolving. Moreover, it has been established by other workers that about 10% of the plutonium in surface sediments close to Sellafield is in the form of *hot* particles. The presence of these particles in the effluent may be one of the main reasons why K_d s for plutonium and americium in the eastern Irish Sea appear to be significantly higher than in the western Irish Sea, where *hot* particles are less likely to be present and should, indeed, have become fully solubilised before reaching this zone.

An analysis of our data suggests that for the transuranics near-equilibrium conditions may presently prevail in the western Irish Sea, in contrast, for example, to the case of radiocaesium, where the concentrations continue to decline. As transuranic discharges from Sellafield have been reduced to very low levels, it is now clear that the dominant source term for the western Irish Sea has become remobilised plutonium and americium from the sedimentary deposits in the north-eastern Irish Sea close to the outfall, where it has been established that a significant *hold-up* of transuranics occurs.

The fractions of plutonium and americium in colloidal form in sea water have been determined in experiments carried out in Carlingford Lough and the western Irish Sea. Preliminary results indicate that inside the Lough, about 50% of the plutonium and almost all of the americium in the filtered water fraction are in colloidal form. Given that about 70% of the plutonium and (as is well established) almost all of the americium are in a reduced chemical form, it is reasonable to infer that the bulk of both (reduced) fractions is colloidally bound. This may explain why, within the Lough, the concentrations of ^{241}Am in filtered water are higher than those outside and also why the $^{241}\text{Am}/^{239,240}\text{Pu}$ ratios in filtered water and particulate are similar. The similarity between the total K_d s for plutonium and americium in

the Lough is readily explained by the fact that the bulk of the plutonium in filtered water is in a reduced state and, consequently, the oxidised fraction contributes only marginally to the total K_d . Furthermore, competition between suspended solid and other species likely to be present in estuarine waters, such as colloidal organic carbon, will tend to diminish measured K_d s and may explain the lower values (about a factor of two) observed in Lough waters. Outside the Lough, in the western Irish Sea, the plutonium colloidal fraction is much lower, and consistent with the small percentages found to be in a reduced chemical form.

Doses to a hypothetical (Irish) critical group consuming fish and shellfish taken from the western Irish Sea have been estimated in the course of this programme. It has been shown that the annual committed effective dose to a member of the critical group of fish and shellfish consumers (50 kg fish, 10 kg crustaceans and 10 kg molluscs respectively, per annum) in 1989 arose mainly from radiocaesium and the transuranic nuclides and was less than 1% of the ICRP-recommended principal dose limit for a member of the general public. Further, doses incurred by consumers of shellfish taken from the north-east coast of Ireland now arise predominantly from the ingestion of plutonium and americium (> 70%) rather than radiocaesium.

Finally, it should be recorded that two additional, collaborative research expeditions were undertaken in the western Mediterranean Sea in 1991 and 1992 aboard the research vessels *Bannock* and *Urania* at the kind invitation of ENEA. The participation of UCD in both these cruises had not been foreseen in the original proposal, but arose as a natural consequence of the increasingly close collaboration which quickly developed between the participants. The primary purpose of UCD's involvement was to complement the respective programmes of ENEA and CIEMAT by examining the physico-chemical speciation of plutonium and americium in (a) western Mediterranean deep waters (0-3000 m vertical profile) and (b) the Palomares continental shelf zone. The dual isotopic tracer technique referred to above was applied to samples of large volume (270 l) taken with Gerhard-Ewing bottles and the preliminary chemistry completed as quickly as possible onboard ship (essential for the efficient separation of the oxidation states of plutonium). The analysis of the separated reduced and oxidised fractions will be completed within the framework of the Commission's Nuclear Fission Safety Research Programme (1992-93). The results to date are encouraging, being consistent with the general pattern observed throughout the Irish Sea and Carlingford Lough, and lend weight to the importance of focussing on fundamental parameters such as reaction kinetics when attempting to develop a comprehensive understanding of the behaviour of particle-reactive pollutants in the marine environment.

3. Acknowledgement

The support and cooperation afforded the coordinator by the participants in this collaboration and by the Commission throughout the reporting period is gratefully acknowledged. UCD also wishes to acknowledge the generous facilities and technical support provided by ENEA and MAFF in the course of collaborative research cruises in the Mediterranean and the Irish Sea in the period 1989-92.

Publications

Vives i Batlle, J. (1993), 'Speciation and Bioavailability of Plutonium and Americium in the Irish Sea and Other Marine Ecosystems', Ph.D Thesis, National University of Ireland (Spring, 1993).

Mitchell, P.I., Vives i Batlle, J., Leonard, K.S., Ryan, T.P., Sánchez-Cabeza, J.A., Downes, A. and Schell, W.R., 'Chemical speciation and colloidal association of plutonium in the Irish Sea', *J. Radioanal. Nucl. Chem.* (In press).

Ryan, T.P., Mitchell, P.I., Vives i Batlle, J., Sánchez-Cabeza, J.A., McGarry, A. and Schell, W.R., 'Low-level Pu-241 analysis by supported disc liquid scintillation counting', In: *International Conference on Advances in Liquid Scintillation Spectrometry*, 14-18 September, 1992, Vienna (In press).

Mitchell, P.I. and Vives i Batlle, J., 'Studies of the physical and chemical speciation of plutonium and americium in the western Mediterranean Sea zone', In: MED92 Cruise Report, R. Delfanti and C. Papucci (Eds.), ENEA, La Spezia (In press).

Mitchell, P.I., Vives i Batlle, J., Ryan, T.P., McEnri, C., Long, S., O'Colmain, M., Cunningham, J., Caulfield, J.J., Larmour, R.A. and Ledgerwood, F.K. (1992), 'Artificial Radioactivity in Carlingford Lough', Radiological Protection Institute of Ireland Publication, 37 pp.

Mitchell, P.I. and Vives i Batlle, J. (1992), 'The behaviour of plutonium and americium in the western Irish Sea', In: *Proc. AIB Conf. on Environment and Development in Ireland*, 9-13 December, 1992, Dublin, J. Feehan (Ed.), The Environmental Institute, UCD, Dublin, pp. 435-443.

Mitchell, P.I. and Vives i Batlle, J. (1992), 'Plutonium speciation in the western Mediterranean Sea', In: MED91 Cruise Report, R. Delfanti and C. Papucci (Eds.), ENEA, La Spezia, 63 pp.

Mitchell, P.I., Vives Batlle, J., Ryan, T.P., Schell, W.R., Sánchez-Cabeza, J.A. and Vidal-Quadras, A. (1991), 'Studies on the speciation of plutonium and americium in the western Irish Sea', In: *Radionuclides in the Study of Marine Processes*, P.J. Kershaw and D.S. Woodhead (Eds.), Elsevier Applied Science, pp. 37-51.

Mitchell, P.I., Vives Batlle, J., Ryan, T.P., McEnri, C., Long, S., O'Colmain, M., Cunningham, J.D., Caulfield, J.J., Larmour, R.A. and Ledgerwood, F.K. (1991), 'Plutonium, americium and radiocaesium in sea water, sediments and coastal soils in Carlingford Lough', In: *Radionuclides in the Study of Marine Processes*, P.J. Kershaw and D.S. Woodhead (Eds.), Elsevier Applied Science, pp. 265-275.

Mitchell, P.I., Vives Batlle, J. and Ryan, T.P. (1991), 'Factors affecting the mobility and bioavailability in the Irish Sea of plutonium and americium released from Sellafield' (Research abstract), In: *First Irish Environmental Researchers Colloquium*, January 1991, Regional Technical College, Sligo, 2 pp.

Mitchell, P.I., Vives Batlle, J., O'Grady, J., Sánchez-Cabeza, J.A. and Vidal-Quadras, A. (1991), 'Critical group doses arising from the consumption of fish and shellfish from the western Irish Sea', In: *New Developments in Fundamental and Applied Radiobiology*, Proc. 23rd. Annual Meeting of the European Society for Radiation Biology, 23-26 September 1990, Dublin, Taylor and Francis, pp. 380-391.

Crowley, M., Mitchell, P.I., O'Grady, J., Vives, J., Sánchez-Cabeza, J.A., Vidal-Quadras, A. and Ryan, T.P. (1990), 'Radiocaesium and plutonium concentrations in *Mytilus edulis* (L.) and potential dose implications for Irish critical groups', *Ocean and Shoreline Management* 13, 149-161.

Project 2

Head of project: *Dr. Gascó*

Objectives for the reporting period

- (1) Sampling of marine sediments in the continental shelf off Palomares and the Almanzora Canyon
- (2) Sampling of sea water in the same zone
- (3) Sediment pretreatment and analysis
- (4) Analysis of river cores and trenches (sediment sections)
- (5) Interpretation of the first results obtained in the Canyon.

Progress achieved including publications

(Methodology, results and discussion)

1. Sampling

1.1 Sediments

Twelve sampling stations, located in the sea close to the Almanzora River mouth, were selected for study. These stations were chosen in order to assess whether the status of this sensitive environment had changed since the previous study (Gascó *et al.*, 1992a; 1992b) and to determine whether a significant portion of the americium present in this environment is in the form of so-called *hot* particles (Romero *et al.*, 1992; 1991; and Romero, 1991). Additional objectives were to evaluate recent terrigenous river contributions and to investigate the role of submarine canyons in the transport of transuranics. Sampling was carried out at Stations 6, 7, 9, 10, 14, 15 and 16 along the main Almanzora Canyon and Stations 5, 8, 11, 12 and 13 to the south of the river mouth.

Marine sediment samples were collected with a box corer designed by Papucci and Jennings. This corer is designed to slice in sections of 1 cm thickness. Afterwards, the sediments were stored in pre-weighed plastic bottles and preserved in a freezer. They were distributed among three of the participating institutions namely, ENEA, UAB and CIEMAT.

The analyses of plutonium, americium and radiocaesium, as well as sediment dating, were carried out at CIEMAT following standard procedures.

1.2 Sea water and suspended particulate matter

The Palomares area is located in a semi-desert region with frequent winds blowing from the south-west. It is well established that such winds can produce the resuspension of deposited transuranics and may, in fact, give rise to a measurable land-to-sea transfer effect via airborne translocation. This fact could produce a temporary increase in transuranic concentrations in coastal waters close to Palomares and, possibly, further afield.

The water sampling programme (together with that carried out by UCD) is expected to provide the first comprehensive data on transuranic concentrations in suspended particulate matter and filtered sea water in this zone.

Surface and near-bottom water samples were collected from two stations: one close to Palomares in the predominant wind direction and the other near the end of the submarine canyon. Samples of 200 l each were obtained with *Gerhard-Ewing* bottles and transferred to 500 l containers prior to preliminary chemical concentration of the transuranic nuclides. The preconcentration procedure has been described in detail elsewhere. UCD and UAB together carried out the separation of the suspended particulate matter from the sea water and the preconcentration on behalf of CIEMAT.

1.3 Intercomparison analyses

Surface sediment samples were collected at three stations with a *Van Veen* grab sampler. These samples were divided among UAB, ENEA and CIEMAT for the purpose of a radioanalytical intercomparison exercise. The selected stations are expected to exhibit medium to low concentrations of transuranic radioelements.

1.4 Results and discussion

The results of the analysis of river sections are given in Table 1. Some evidence of high plutonium concentrations (an order of magnitude higher than at Stations 1, 2 and 4) is apparent at Station 3 in the 0-10 cm layer. These data were reported at a recent international meeting (Migration 91).¹

A low inventory was previously observed in surface sediments (0-5 cm depth), ranging from 0.4-1.5 Bq(^{239,240}Pu) m⁻² to 1-70 Bq(¹³⁷Cs) m⁻². A change in ratios between these radionuclides close to the beach edge was also detected. This could account for the different ratios observed in the marine sediment from the southern coast compared to the northern (1.2 southwards and 0.3 northwards). These sediments were transported by flash floods from land to sea and the submarine currents, parallel to the coast and southwards, gave rise to the observed distribution. Differences in the Pu/Cs ratio helps to demark the area where there is a terrigenous contribution.

The granulometric distribution at all the stations in the river is indicative of sand, except at Station 4.1 where it is a sandy lime. The clay content, at 2.3%, is very low, the river sediments being depleted of this more chemically reactive component. In Figure 1, the curves of grain size distribution in the surface sediments (0-5 cm) are shown. Curve 1.2 corresponds to a well selected sand while, in the margin of the river (1.1 and 1.3), the curves show more energy and less selective sedimentation capacity. Similar profiles to these were obtained in most of the transects. At Station 6 (beach edge), the grain size is uniform, indicating the predominant influence of the marine media. Distributions such as those at Station 1.1 and Station 1.3, which show significant percentages of very large size particles (gravel), reflect

¹ Data on plutonium and radiocaesium concentrations in surface sediments (0-5 cm), together with a map of the sampling stations, were given in a previous Progress Report to the Commission (1991).

the occasionally high hydrodynamic energy of the system in question, i.e., the flash floods which occur very infrequently.

Table 1. Concentrations and inventories of plutonium and radiocaesium in Almanzora River sediments (1991).

Station	Depth (cm)	Concentration (Bq kg ⁻¹)		Ratios	Inventories (Bq m ⁻²)	
		^{239,240} Pu	¹³⁷ Cs		^{239,240} Pu	¹³⁷ Cs
01	0 - 10	0.047 ± 0.010	0.97 ± 0.17	0.048	6.4	133
	10 - 20	0.027 ± 0.014	0.84 ± 0.08	0.032	7.7	240
	20 - 30	0.043 ± 0.012	†	-	5.2	†
02	0 - 10	0.071 ± 0.020	1.02 ± 0.18	0.069	10.9	157
	10 - 20	0.099 ± 0.010	2.80 ± 0.22	0.035	27.8	787
	20 - 30	0.028 ± 0.008	0.82 ± 0.14	0.034	6.9	203
03	0 - 10	1.880 ± 0.180	1.17 ± 0.10	1.540	243.0	151
	10 - 20	0.108 ± 0.030	2.68 ± 0.18	0.040	13.9	346
	20 - 30	0.080 ± 0.008	2.07 ± 0.16	0.034	7.4	190
04	0 - 10	0.053 ± 0.006	1.07 ± 0.11	0.049	11.3	228
	10 - 20	0.045 ± 0.011	0.54 ± 0.06	0.100	5.3	63
	20 - 30	0.054 ± 0.010	0.41 ± 0.08	0.130	4.9	37

† Insufficient material for ¹³⁷Cs analysis
 Uncertainties are quoted to ± 2 σ.

Another feature of note is the decrease in caesium concentrations close to the Almanzora River mouth. The ratio between plutonium and caesium changes significantly in this area, from 0.03 to 1.2, probably due to the fact that the ¹³⁷Cs penetration through the sediment profile is more extensive in these sediments than in the others, and the influence of saline water close to the beach. Only in a few samples could ²³⁸Pu be determined. In these, the ²³⁸Pu/²³⁹Pu activity ratios were typical of global fallout, indicating that weapons-grade plutonium was not the source. The plutonium inventories to 30 cm depth in the river bed ranged from 19 to 46 Bq m⁻² (with the exception of Station 3).

The decreasing inventory of caesium in the downstream sediments may be due to the salinity differences encountered as one proceeds towards the saline waters of the Mediterranean. A similar difference was noted in the Hudson River Estuary where Simpson *et al.* found that the magnitude of the ^{137}Cs K_d value could be expressed as an inverse function of the chloride ion water concentration. In other words, ^{137}Cs originally associated with fresh water sediments is released back to solution when salt water is encountered. The K_d is larger in a body of fresh water than in a salt water environment. Simpson also noted that there was no difference in the plutonium K_d between fresh and brackish water. In our case, we found similar ^{137}Cs concentrations in the river sediments between Stations 1 to 5, much like Simpson, and a lower concentration at Station 6 near the mouth.

In contrast, the concentration of plutonium is higher at Station 6 than at the upstream stations. Much of the plutonium has migrated downstream (possibly in association with river-borne particles) and is now found accumulated to higher levels in the sediments near the mouth. This is a noteworthy feature and clearly demonstrates the mobility of plutonium in this particular environment.

The analyses of fish, water and selected sediments have been completed and preliminary conclusions have been drawn (the concentrations of plutonium in fish, sea water and particulate matter are summarized in Tables 2-5, inclusive).

Table 2. Concentrations of plutonium in Mediterranean fish flesh samples.

Sample	$^{239,240}\text{Pu}$ (mBq/kg, w.w.)	^{238}Pu (mBq/kg, w.w.)
Small Hake	< LLD	-
Shrimp	1.0 ± 0.5	< LLD
Greater Forkbeard	0.8 ± 0.4	< LLD

Uncertainties are quoted to $\pm 1 \sigma$.

LLD Lower Limit of Detection

The concentrations of plutonium and americium in deep waters from the vicinity of the Palomares offshore zone are considerably lower than in those found at a depth of 2,000 m close to Villefrance sur le Mer in 1989, namely 20 to 32 $\mu\text{Bq/l}$.

Station 10 is influenced by the Atlantic current via the Straits of Gibraltar. For this reason, the salinity and the temperature of the water in its vicinity is lower. This or other factors (such as oxidation state, particulate matter or dissolved organic matter) which have not been considered here, could contribute to increased scavenging of radionuclides and to a decrease in their concentrations.

The concentrations of plutonium in both greater forkbeard (mud-feeder fish) (*Sp. Brótola de fango*) and shrimps (phyto-zooplankton feeders), are close to the detection limit. Until now no evidence of transfer between the different compartments of the food chain has been found.

Table 3. Concentrations of plutonium and americium in filtered sea water.
 St. 10, 37° 09.41'N, 01° 41.952'W; Surface = 33 m, Bottom = 700 m
 St. 15, 37° 12.89'N, 01° 45.70'W; Surface = 3 m, Bottom = 45 m

Station	Depth	^{239,240} Pu (μBq/l)	²³⁸ Pu (μBq/l)	²⁴¹ Am (μBq/l)	²³⁸ Pu/ ^{239,240} Pu	²⁴¹ Am/ ^{239,240} Pu
PASW10	Surface	7 ± 2	0.8 ± 0.6	1.2 ± 0.7	0.12	0.18
	Bottom	5 ± 1	0.1 ± 0.2	1.4 ± 0.7	0.03	0.28
PASW15	Surface	14 ± 3	0.6 ± 0.6	1.9 ± 0.8	0.05	0.14
	Bottom	19 ± 3	0.7 ± 0.6	-	0.04	-

Uncertainties are quoted to ± 2 σ.

Some preliminary data on plutonium and americium concentrations in sediment cores taken during the *Bannock* Cruise (July-August, 1991) are shown in Figure 2. It is clear that very high concentrations of plutonium and americium are found in the southern area of the Almanzora river. The results obtained are being analyzed at the present time.

Figure 2. Plutonium and americium concentrations (Bq/kg, d.w.) in sediment cores (1991).

Table 4. Concentrations of plutonium in particulate matter.

Station	Depth	^{239,240} Pu (μBq/l)	²³⁸ Pu (μBq/l)	²³⁸ Pu/ ^{239,240} Pu
PAPM10	Surface	0.23 ± 0.16	-	-
	Bottom	0.08 ± 0.14	-	-
PAPM15	Surface	0.45 ± 0.16	-	-
	Bottom	1.24 ± 0.27	0.18 ± 0.10	0.14 ± 0.03

Uncertainties are quoted to ± 1 σ

Table 5. Total and relative concentrations of $^{239,240}\text{Pu}$ in filtered water ($< 0.45 \mu\text{m}$) and particulate.

Station	Depth	Suspended particulate (mg/l)	Conc. ($\mu\text{Bq/l}$)	% soluble	% particulate
PASW10	Surface	0.06	7 ± 2	97	3
	Bottom	0.24	5 ± 1	98	2
PASW15	Surface	0.87	14 ± 3	98	2
	Bottom	0.87	20 ± 3	94	6

The characterization of possible *hot* particles, as well as the determination of their size and activity, could form part of a future project.

2. Acknowledgements

The undermentioned wish to thank Dr.V.E. Noshkin for help in the interpretation of results and also ENEA and UCD for technical assistance in the course of the *N/O Bannock* Research Cruise in the western Mediterranean (July-August, 1991).

Publications

Gascó, C., Romero, L., Mingarro, E. and Lobo, M.A. (1992a), 'Geochemical aspects and distribution of long-lived radionuclides in marine sediments from Palomares', *J. Radioanal. Nucl. Chem.* **161**, 389-400.

Gascó, C., Iranzo, E. and Romero, L. (1992b), 'Transuranic transfer in a Spanish marine ecosystem', *J. Radioanal. Nucl. Chem.* **156**, 151-163.

Romero, L., Lobo, A. and Holm, E. (1992), 'New aspects on the transuranics transfer in the Palomares marine environment', *J. Radioanal. Nucl. Chem.* **161**, 489-494.

Romero, L., Lobo, A., Holm, E. and Sánchez, J.A. (1991), 'Transuranics contribution of Palomares coast: tracing history and routes to the marine environment', In: *Radionuclides in the Study of Marine Processes*, P.J. Kershaw and D.S. Woodhead (Eds.), Elsevier Applied Science, pp. 245-254.

Romero, L. (1991), 'Estudio del transporte tierra-mar de elementos transuránicos. Aplicación al accidente de Palomares (Almería) de 1966', PhD Thesis, Universidad Complutense de Madrid.

MED91 Cruise Report (1992), R. Delfanti and C. Papucci (Eds.), ENEA, La Spezia, 63 pp.

Gascó, C., Lobo, A.M., Romero, L. and Antón Mateos, M.P. (1992), 'Transuranics as tracers of land to sea transport' In: *Chemistry and Migration Behaviour of Actinides and Fission Products in the Geosphere*, Jerez de la Frontera, 21-25 October, 1991, Abstracts, CIESM.

Gascó, C., Romero, L. and Antón Mateos, M.P. (1991), 'Informe Sobre el Muestreo de Sedimentos Marinos en la Plataforma Costera Cercana a Palomares', CIEMAT/IMA/UGIA/M5A07/08/ 91.

Leonarte, C.G. and Antón Mateos, M.P. (1992), 'Distribution of Transuranics along the Palomares Submarine Canyon', *Condensés des travaux présentés lors du XXXIle Congrès. Assemblée Plénière*, Trieste (Italy), October, 1992, Vol. 33.

Scientific Staff

Researchers: Gascó Leonarte, Catalina
Antón Mateos, M. Paz
Palomares López, J.
Rivas, P.

Technicians: Meral Carrillo, J.
González Ortiz, A.

Project 3

Head of project: *Dr. Guéguéniat*

Objectives for the reporting period

These were as follows:

- (1) To estimate the transit time of particles and associated transuranics between Cap de La Hague and Cherbourg harbour.
- (2) To understand hydrodynamic processes in megatidal areas such as the Seine estuary and the Norman-Breton Gulf which are important sinks for artificial radionuclides.
- (3) To complete certain studies which have been carried out on the Irish sea, by the measurement of stable rare earths and other elements in bottom sediments.
- (4) To study, experimentally, the mechanisms of complexation of americium and its analogues, the rare earths, with organic ligands in zones of high concentration. Also, to evaluate the well established principle of analogy between rare earth elements/transuranics.
- (5) To study the bioavailability of transuranics.

Progress achieved including publications

(1) To achieve the estimation of *transit time* of particulate and associated radionuclides, variations in the composition of La Hague effluents ($^{137}\text{Cs}/^{241}\text{Am}$) were compared with the evolution of these same radionuclides in sediment cores collected in the vicinity of Cherbourg. The latter is the only site in this region where sedimentation is continuous. The vertical evolution of radioactive elements in the sediments is representative of cumulative (much more than short-term) releases from the La Hague plant and is strongly modulated by pluriannual tidal effects[†]. The sediment banks of both the Norman-Breton and the Seine estuary will be treated in the same way. However, before a study of dynamic hydroprocesses in these megatidal areas can be considered, especially in the case of the Seine estuary, it will be necessary (a) to distinguish the turbidity maximum between marine and fluvial inputs, and (b) to study the residence time of given particles within the estuary.

[†] Publication prévue dans le cadre de réunion spécialisée de la Société Géologique de France. Bordeaux, 2 et 3 mai, 1993.

2. Hydrodynamic processes in the Seine estuary

Samples of suspended particulate matter and sediment, collected from the Seine and its megatidally dominated estuary, were subjected to neutron activation and gamma-ray spectrometric analyses. The study includes results obtained over the period 1978-1992,

making use of various geochemical tracers to monitor the riverine and marine inputs. The memory effect on the turbidity maximum is the main factor to consider in the interpretation of spatial and temporal variation of particulate pollutants. Consequently, it appears that hydrological processes rather than chemical ones are responsible for the variations in the chemical composition of suspended matter in megatidal estuaries. These observations will be developed in a publication which will be submitted to *Marine Chemistry* before the end of 1992, titled 'Application of geochemical tracers (gold, radiocaesium and hafnium) to the study sedimentary processes in the Seine estuary'.

3. Neutronic activation on Irish Sea sediment core

The core was collected by University College, Dublin. The values of ^{241}Am were found to be between 3,000 and 20,000 Bq/kg. Among all the stable elements expected to be associated with nuclear wastes (Cs, Rb, rare earths, Zr and Mo) only molybdenum was detected at a high level (8-17 ppm) with concentrations proportional to the ^{241}Am content. The molybdenum/scandium ratios vary between 1.4 in surface (^{241}Am : 3,000 Bq/kg) to 2.7 in depth (^{241}Am : 19,000 Bq/kg). Comparatively, we have registered only one significant result in the Channel among 40 analyses (Mo/Sc = 0.16 in Brest rade). A publication of all the data obtained in Irish Sea and Channel by neutronic activation will be prepared in 1993. This will help the interpretation of particle movements.

4. Organic complexation of ^{241}Am

The complexing ability of ^{241}Am by organic matter was studied experimentally using fresh water coming from Vire (entering the Seine Bay), Seine, Escaut and Elbe. The first river, the Vire, has shown the strongest complexing ability: about 50 to 70% of the ^{241}Am can be complexed, whereas the same water has the lowest complexing ability for cobalt. This means that the classical complexing ability of a fresh or marine water based on the addition of a transition metal (such as Cu^{++}) is not available for transuranics.

The organic complexes of ^{241}Am in fresh waters are unstable in estuaries: the ^{241}Am removal is about 60-66% at a pH of 5 to 7. This behaviour is similar to the behaviour of rare earths as described by Elderfield (1983). According to this author, the removal occurs via interaction with iron-organic colloids.

5. Uptake of plutonium by the lobster

A study of the transfer of plutonium inside an accumulating organ, the hepato-pancreas of the lobster, has been undertaken. This follows a similar study on the transfer of ^{241}Am in the same animal. Only half an hour after the ingestion of a contaminated mussel, this organ is labelled by ^{241}Am , even at the level of the nucleus. The partition of plutonium in the different sub-cellular fractions depends on the digestive cycle. The cytosol (aqueous solution of the cell containing soluble enzymes intervening in different metabolisms) is the sub-cellular compartment which contains most of the ^{238}Pu . This element appears to be particularly linked to the ferritine and some proteins of molecular weight 10,000 and 20,000.

Publications

Bailly du Bois, P., Guéguéniat, P., Gandon, R. and Léon, R. (1992), 'Percentage contribution of inputs from the Atlantic, Irish Sea, English Channel and Baltic into the North Sea during 1988: a tracer-based evaluation using artificial radionuclides', *Nederland Journal of Sea Research* (Submitted).

Gandon, R., Boust, D. and Bédoué, O. (1992), 'Ruthenium complexes originating from the Purex process: coprecipitation with copper ferrocyanides via ruthenocyanide formation', *Radiochim. Acta* (Accepted in June 1992).

Guéguéniat, P., Bailly du Bois, P., Gandon, R., Salomon, J.C. and Léon, R. (1992), '¹²⁵Sb, an important conservative tracer in the marine environment: application to the study of the penetration of the Channel waters into the North Sea', *Estuar. Coast. and Shelf Sci.* (accepted in May 1992).

Guéguéniat, P., Salomon, J.C., Wartel, M., Cabioch, L. and Fraizier, A., 'Use of artificial radionuclides for the study of dissolved matter transfer mechanism between the Channel and the North Sea', *Estuar. Coast. and Shelf Sci.* (accepted in May 1992).

Fraizier, A., Guéguéniat, P. and Salomon, J.C. (1992), 'Aspects temporels de l'impact de rejets radioactifs, effectués en mer, sur les eaux d'une station littorale de la Manche', *Oceanol. Acta* (In Press).

Gandon, R. and Guéguéniat, P. (1992), 'Preconcentration of ¹²⁵Sb onto MnO₂ in the preparation of seawater samples for gamma-ray spectrometric analysis', *Radiochim. Acta* (In Press).

Guéguéniat, P., Salomon, J.C., Gandon, R., Germain, P. and Baron, Y. (1992), 'Nouvelles données concernant l'utilisation des radionucléides artificiels pour l'observation (1983-1991) des déplacements de masses d'eau en Manche et Pas de Calais', Brest, September 1992.

Salomon, J.C., Breton, M. and Guéguéniat, P. (1992), 'Flux d'eau à travers le détroit du Pas de Calais', Brest, September 1992.

Bailly du Bois, P., Guéguéniat, P., Gandon, R. and Léon, R. (1991), 'Characterizing the mixing of water flowing into the North Sea using artificial gamma-emitters' (Tramanor Cruise, July 1988). Résumé, In: *Radionuclides in the Study of Marine Processes*, P.J. Kershaw and D.S. Woodhead (Eds.), Elsevier Applied Science, p. 363.

Dahlgard, H., Nies, H., Van Weers, A.W., Guéguéniat, P. and Kershaw, P.J. (1991), 'Studies on the transport of coastal water from the English Channel to the Baltic Sea using radioactive tracers' (MAST project). Résumé, In: *Radionuclides in the Study of Marine Processes*, P.J. Kershaw and D.S. Woodhead (Eds.), Elsevier Applied Science, p. 365.

Germain, P. and Salomon, J.C. (1991), 'Transport d'éléments à l'état de traces dans les eaux côtières de la Manche: étude de la distribution spatiale d'un traceur radioactif (¹⁰⁶Ru-Rh) dans les moules et les *Fucus*'. Résumé, In: *Radionuclides in the Study of Marine Processes*, P.J. Kershaw and D.S. Woodhead (Eds.), Elsevier Applied Science, p. 364.

Salomon, J.C., Guéguéniat, P. and Breton, M. (1991), 'Mathematical model of ^{125}Sb transport and dispersion in the Channel', In: *Radionuclides in the Study of Marine Processes*, P.J. Kershaw and D.S. Woodhead (Eds.), Elsevier Applied Science, pp. 74-83.

Guéguéniat, P., Gandon, R., Baron, Y., Salomon, J.C., Pentreath, R.J., Brylinski, J.M. and Cabioch, L. (1988), 'Utilisation de radionucléides artificiels (^{125}Sb , ^{137}Cs , ^{134}Cs) pour l'observation (1983-1986) des déplacements de masses d'eau en Manche', In: *Radionuclides: A Tool for Oceanography*, Cherbourg 1-5 June, 1987, J.C. Guary, P. Guéguéniat and R.J. Pentreath (Eds.), Elsevier, pp. 260-270.

Salomon, J.C., Guéguéniat, P., Orbi, A. and Baron, Y. (1988), 'A lagrangian model for long-term tidally-induced transport and mixing. Verification by artificial radionuclide concentrations', In: *Radionuclides: a Tool for Oceanography*, J. C. Guary, P. Guéguéniat and R. J. Pentreath (Eds.), Elsevier Applied Science, pp. 384-394.

Project 4

Head of project: *Dr. Damiani*

Objectives for the reporting period

- (1) Studies on the vertical distribution of natural and artificial radionuclides in the water column and in sediments of Mediterranean deep-sea environments;
- (2) Transport of radionuclides from the continental shelf to deep-sea in uncontaminated (Gulf of Taranto - Ionian Sea) and potentially contaminated (Palomares - Balearic Sea) areas.

Progress achieved including publications

While a good data set already exists on transuranic levels and inventories in Mediterranean shelf sediments, only few data are presently available for slope and deep-sea areas. For this reason, selected Mediterranean areas, having different morphological and sedimentological characteristics, have been studied and radionuclide background levels have been evaluated. Vertical profiles and inventories of transuranics were determined in sediments from:

- deep-sea areas characterized by pelagic sedimentation only;
- deep-sea areas affected by contributions of terrigenous material (end of river fans);
- slope and bottom of complex canyon systems.

A second topic which at present has not been extensively studied, is the transport of radionuclides through the water masses of the Mediterranean Sea. A study has been initiated on the mechanisms of transport of radionuclides through the different water masses characterizing the western Mediterranean Sea, including transfer of radionuclides from surface to deep waters via dense water formation and transport from the eastern to the western basin through the flux of the Levantine Intermediate Water.

1. Sampling and analysis

Seawater and sediment samples were collected during three different cruises in the Ionian and Western Mediterranean Sea, in 1989, 1991 and 1992. The sampling sites were selected on the basis of the hydrological and sedimentological characteristics of the areas.

Sediment samples were collected in the open Mediterranean Sea, in zones characterized by pelagic sedimentation, in the terminal tract of the Ebro and Rhone fans, in slope and deep-sea areas in the Gulf of Vera (South Balearic Sea) and in the shelf, slope and bottom of the Taranto Canyon (Ionian Sea).

The sediment cores were collected by a modified *Reineck* corer and sectioned on board in slices 1 cm thick. Cs-137 and Pb-210 were analyzed by gamma spectrometry with gamma-X detectors. Pu-239,240 was separated from the matrix by leaching, double anion exchange and

electroplating, and measured by alpha spectrometry. The accuracy of the results was regularly tested by analyzing NIST and IAEA standard reference materials.

Seawater sampling points were selected along the path of the Levantine Intermediate Water in the Western Mediterranean Sea (western coast of Sardinia, Gulf of Lyons, Balearic Sea and open south-western Mediterranean Sea).

Samples of approximately 100 litres were collected in surface, Levantine and bottom waters by *Gerhard-Ewing* or *Go-Flo* bottles. Pre-concentration of caesium was carried out on board by co-precipitation with ammonium molybdophosphate (AMP). The samples were then analysed by gamma spectrometry on land.

2. Results

2.1 Sediments

The study on the distribution and inventories of Pu-239,240 in the Taranto canyon (Ionian Sea) has been completed with the analyses of sediment cores, collected on the bottom of the canyon at depths of 1,500 and 2,000 m. In these cores, the vertical profiles of Cs-137, Pb-210 and Pu-239,240 have been determined. The profiles of Pu-239,240, Cs-137 and Pb-210 show the same trend, with a relative maximum at a depth of 6-8 cm. The inventories of Pu-239,240 ($58 \pm 16 \text{ Bq m}^{-2}$ at 2,000 m and $45 \pm 19 \text{ Bq m}^{-2}$ at 1,500 m) are about 50% of the cumulative fallout deposition at this latitude. In general, there is a decrease in plutonium inventories along the canyon, from the shelf (reported value: 220 Bq m^{-2}) to the slope ($90\text{-}160 \text{ Bq m}^{-2}$) and the deepest part of the canyon (Fig. 1). This trend is well known and is related to the decrease in sedimentation rates and resuspension processes with depth.

To evaluate the influence of morphological and sedimentological factors on the transport of plutonium from the continental shelf to the deep sea, the results obtained for the Taranto Valley have been compared with the vertical profile and inventory of Pu-239,240 in a sediment core collected in the open south-western Mediterranean, in an area where only pelagic sedimentation is active. In the latter case, plutonium is only present in the first 4 cm of the core and the concentration regularly decreases from a surface value of 0.21 Bq kg^{-1} . The inventory is only $3 \pm 2 \text{ Bq m}^{-2}$ and is comparable to those obtained for deep cores from oligotrophic areas, characterized by low productivity, low export production, resulting in low probability, for the particle associated plutonium, of reaching the sea bottom.

The inventories calculated for the Gulf of Taranto are almost twenty times higher than in the open Western Mediterranean and this is due to several factors:

- the continental shelf of the Gulf of Taranto is very narrow, the slope is indented by several small canyons, some of them corresponding to the mouths of rivers. In these conditions, the particulate material exported by rivers and the associated radionuclides may easily be transported to deeper areas preferentially through the small canyons;
- productivity and particle population is very low in the open Mediterranean Sea, but considerably increases in the areas close to land and river mouths;
- slumping processes and hydrodynamic conditions inside the canyons make easier the

resuspension of sediments, thus enhancing the scavenging of particle-associated radionuclides from the water column.

The morphological situation of the Gulf of Taranto is similar to that of the Palomares area in the Gulf of Vera. At the time of the first cruise (1991), the morphology of the area was not well known. The bathymetry has been carefully determined during two sampling cruises carried out on board the research vessels *Bannock* and *Urania* of the Italian National Research Council. The area is characterized by the presence of a complex canyon system, with two main canyons joining in a plain at about 2,000 m depth. The sampling strategy was based on these new data and sediment cores were collected on the shelf, along the main canyons and in the plain. Three of these cores will be analyzed by ENEA. A first screening has been made, by gamma spectrometry on all the 1 cm sections, to evidence high levels of Am-241, that could be related to the presence of *hot* particles in the area.

At present, two cores have been analyzed for these purposes. One of them, collected on the continental shelf south west of Palomares shows, in several layers, high levels of Am-241. These layers will be divided and analyzed again for americium, to determine if this radionuclide is evenly distributed in the layer or the activity is concentrated in a specific part of the sample.

Figure 1. Inventories of Pu-239,240 (Bq m⁻²) in sediments of the Gulf of Taranto

2.2 Radionuclide concentrations in seawater

The Levantine Intermediate Water is formed in the eastern Mediterranean basin, that was heavily contaminated by Chernobyl fallout. This water mass enters the western basin through the Sicily Channel and flows northward, along the Sardinian and Corsican coasts, and then westward along the coasts of Italy, France and Spain at a depth of 300-600 m, forced by buoyancy and constrained by topography.

The aim of the study is to verify if a Chernobyl signal is detectable in this water mass and, if possible, to estimate the transit time of the Levantine Water in the western Mediterranean.

In 1991, the vertical profile of Cs-137 in the water column was determined at four stations along the track Cagliari (South Sardinia) - Gulf of Vera (Spain). At least 4 water samples were collected at each station: surface water, Levantine Intermediate Water and 2 samples of the underlying water, one of which was taken as close as possible to the bottom.

The concentration of Cs-137 generally decreased from the surface to the bottom (from 4 to 2 mBq l⁻¹). In the station closest to the south western coast of Sardinia, a relative maximum (5 mBq l⁻¹) was observed in the Levantine Intermediate Water. Actually, this station is the only one, among those studied, situated along the main path of the Levantine Intermediate Water and the subsurface maximum may be related to the transport of Chernobyl caesium from the eastern to the western basin of the Mediterranean Sea. This maximum is not present in the other stations, located in the Algerian basin, possibly because the Levantine Intermediate Water found in this area is much more diluted with other water masses.

During the second sampling campaign, in August 1992, seawater samples were collected

along the main path of the Levantine Intermediate Water and the resolution of the vertical profiles was increased. The analyses are now in progress.

Publications

MED91 Cruise Report (1992), Delfanti & Papucci (Eds.), ENEA, La Spezia, 63 pp.

Delfanti, R., Fiore, V., Papucci, C., Lorenzelli, R., Salvi, S., Alboni, M., Moretti, L. and Tesini, E. (In Press), 'Monitoraggio della radioattività ambientale nell'Adriatico centro settentrionale', In: *Proc. 5th Convegno Nazionale della Società Italiana di Ecologia*, 1992.

Delfanti, R., Fiore, V., Papucci, C., Moretti, L., Tesini, E., Salvi, S., Bortoluzzi, S., Nocente, M. and Spezzano, P. (1991) 'Chernobyl radionuclides as tracers of sedimentation processes in the Northern Adriatic Sea (Italy)', In: *Radionuclides in the Study of Marine Processes*, P.J. Kershaw and D.S. Woodhead (Eds.), Elsevier Applied Science, London and New York, p. 375.

Queirazza, G., Roveri, M., Delfanti, R. and Papucci, C. (1991), 'Gas exchange at the air-sea interface: a technique for radon measurements in seawater', *Ibid.*, pp. 94-104.



BEHAVIOUR OF POLONIUM-210 AND LEAD-210 IN EUROPEAN MARINE ENVIRONMENTS. APPLICATION OF BIOINDICATORS

Contract Bi7-006 - Sector A22

1) *Köster*, RIVM - 2) *Guéguéniat*, CEA - Cherbourg
3) *Duursma*, NIOZ - 4) *Galvão*, LNETI

Summary of project global objectives and achievements

1. Introduction

The radiation dose of man stemming from the marine environment is dominated by the consumption of fishery products. The radionuclide ^{210}Po ($T_{1/2}$ 138 days), a daughter of ^{210}Pb ($T_{1/2}$ 21 year), causes the major part of this dose (Kö-88). In several estuaries large quantities of ^{210}Po and ^{210}Pb are emitted by local phosphate ore processing industries. A study has been executed with the aim to obtain insight into the effects of these emissions on the activity levels and distribution of ^{210}Po and ^{210}Pb . The study encompassed the Westerscheldt estuary in the Netherlands, the Seine estuary in France and the Tagus estuary in Portugal. A link has been made to the study of the Rhine estuary (Be-92). As yet no techniques exist to distinguish the naturally present from industrially emitted ^{210}Po and ^{210}Pb . Local natural background levels have been studied in Portugal in the Mira estuary, on which no industrial ^{210}Po and ^{210}Pb is discharged.

For each estuary a brief inventory has been made of the geomorphology, hydrology, quantities of industrially emitted ^{210}Po and ^{210}Pb . Levels and characteristics of ^{210}Po and ^{210}Pb have been determined in some industrial effluents. Distribution of ^{210}Po and ^{210}Pb has been determined in field studies of each estuary. For the Westerscheldt a preliminary model has been developed to predict and distinguish the enhancements by different industries.

Results have been published in reports of the respective institutes (Be-92; Ca-92; Ge-92; He-92; Pe-92) and in scientific journals (Ca-91; Ge-i.p.; Kö-i.p.; Pe-i.p.) to which additional articles will be submitted. In the following an overview is given of the work executed, the results and conclusions.

2. Radionuclides emitted by phosphate ore processing industries

2.1 Radionuclide levels in effluents and their characteristics

In the literature so far little or no information can be found on ^{210}Po and ^{210}Pb in phosphogypsum. Analyses of samples from different Dutch and Portuguese industries, showed that the levels of these two radionuclides vary from 500 to 1000 Bq.kg⁻¹ in phosphogypsum in which they are almost in equilibrium. The ^{226}Ra levels found of ca. 1000 Bq.kg⁻¹ are in accordance with values reported in the literature (UNSCEAR-82).

Laboratory studies of phosphogypsum (one grab sample from Vlaardingen) showed the following results:

- At emission the effluent contains approx. 30% m/m solids, about 0,5 % of the activity is dissolved.
- Upon dilution with estuary water (ratio estuary water/effluent = 2300/1) the gypsum component dissolves and an insoluble, finely dispersed residue (8% m/m) remains.
- The insoluble residue contains about 90% of the radioactivity of the ^{210}Po of the phosphogypsum and has an activity of 10.000-15.000 Bq ^{210}Po per kg.

- Very limited desorption of activity from the residue occurs; seawater and 1M CaCl₂ result in a desorption of respectively 0,3 and 3%.

At Vlissingen effluent from wet-filtering of off-gasses of a thermal phosphor plant is emitted into the Westerscheldt. In a grab and a 24 hour proportional sample of the effluent the ²¹⁰Po activities were respectively 7,0 and 3,8 Bq.kg⁻¹, and the ²¹⁰Pb activities approximately 0,3 Bq.kg⁻¹. Laboratory studies of the grab sample showed the following results for the effluent of the thermal plant:

- At emission the effluent contains approximately 1E-5 m/m solids, about 20% of the activity is dissolved.
- The activity of ²¹⁰Po is about 10x as high as that of ²¹⁰Pb.
- Upon dilution with estuary water about 100% of the ²¹⁰Po dissolves. (No info on ²¹⁰Pb).

2.2 Quantities of radionuclides emitted

The radionuclides emitted by the phosphorous industry are generally not monitored. Some rough estimates of these emissions have been made as they lay at the base of the enhancements in the estuaries studied.

The two wet process plants near Rotterdam emit together yearly about 2 Tg phosphogypsum on the Rhine or about 1,5E12 Bq ²¹⁰Po and ²¹⁰Pb. On the Westerscheldt a wet process plant at Zandvliet in Belgium emits roughly 0,3 Tg phosphogypsum or 2,1E11 Bq ²¹⁰Po and ²¹⁰Pb per year, and near Vlissingen a thermal process plant emits annually into this estuary approximately 1,1E11 Bq ²¹⁰Po and 7,5E10 Bq ²¹⁰Pb. The yearly atmospheric emissions from the last plant are roughly 5,5E11 Bq ²¹⁰Po and 2,2E11 Bq ²¹⁰Pb, a certain fraction of this will be deposited on the Westerscheldt.

The wet process plant at Le Havre emits yearly 0,6 Tg phosphogypsum into the Seine estuary, or approximately 4,2E11 Bq ²¹⁰Po and ²¹⁰Pb.

The wet process plant at Barreiro near Lisbon stockpiles its phosphogypsum, ca. 0,1 Tg per year, on the margin of the Tagus estuary. Decantation water and erosion runoff from these stockpiles flow into the estuary. The plant also discharges effluents with ²¹⁰Po and ²¹⁰Pb from wet-filtering of off-gasses. The total emission into the estuary via these different streams is estimated to be maximally 3E10 Bq ²¹⁰Po and ²¹⁰Pb per year.

3. Low and background levels of ²¹⁰Po and ²¹⁰Pb in estuaries

The background levels of natural radioactivity in estuary and coastal waters vary with e.g. geo-mineralogical and hydrological factors. The ²¹⁰Po and ²¹⁰Pb background concentrations dissolved in water, of suspended matter and bottom sediments are generally anthropogenically enhanced and difficult to determine. Some rough indications of low, possibly close to background levels have been obtained.

The levels considered as low in the Netherlands, France and Portugal are the same, for ²¹⁰Po dissolved in water < 1 Bq.m⁻³, and for ²¹⁰Po in suspended matter < 90 Bq.m⁻³. In order to judge the activity levels of bottom sediments their activities have to be normalized. Data on this are limited but indicate that normalized levels up to 60 Bq.kg⁻¹ can be considered as low, while original and normalized levels exceeding 150 Bq.kg⁻¹ are probably enhanced. In mussels ²¹⁰Po levels below 100 Bq.kg⁻¹ can be considered as low.

4. Enhancements of ²¹⁰Po and ²¹⁰Pb in the estuaries studied

4.1 ²¹⁰Po dissolved in water

- The dissolved activities found in the NIOZ sampling trips in 1990 and 1992 are lower (all below 0,6 Bq.m⁻³) than in other Westerscheldt studies, which can not yet be explain-

ned. However the activities exceed those found in the same trips in "close to background locations". So some industrial enhancement is probable, although the activities show no clear relation with the distance to industrial source terms.

- In the Seine estuary at Digue Nord at a distance of 3 km from the phosphate plant outfall dissolved activities were measured on 13 different dates between June 1990 and December 1991. The ^{210}Po levels fluctuate from 0,6-1,6 Bq.m³. In 40% of these samples the activities are probably enhanced, viz. ≥ 1 Bq.m³.
- The ^{210}Po activities dissolved in water in the Tagus estuary are predominantly low (70% between 0,2-0,5 Bq.m³). Within 5 km from the phosphorous plant seven of such low values occur together with the two highest values: 8 and 46 Bq.m³, the last are clearly enhanced by the industry.

4.2 ^{210}Po in suspended matter

- In the Westerscheldt within 5 km distance from outfalls of the phosphorous industries 80% of the suspended matter samples has activities exceeding 150 Bq.kg⁻¹. Beyond this distance 80% of the activities is between 80 and 150 Bq.m³. The enhancement of the suspended matter can only be distinguished near to the industries and is even there somewhat irregular.
- At Digue Nord at a distance of 3 km from the phosphate plant outfall near Le Havre the activities of the suspended matter were measured on 9 different dates between June 1990 and December 1991. The ^{210}Po levels fluctuate from 130-180, in 80% of these samples the activities exceed 150 Bq.kg⁻¹. The activities seem enhanced in all 9 samples compared to samples from Pirou and P. de Moulard, the other locations where suspended matter was studied.
- The ^{210}Po activity concentrations of the suspended matter in the Tagus estuary are relatively high (30% between 65-90, 45% between 90-149 and 25% between 149-265 Bq.kg⁻¹). The different values do not show a clear geographical pattern, the highest value occurs together with low values within 5 km from the phosphorous plant. This is probably caused by the irregular water circulation inside this lagoon type estuary. In 25% of the samples industrial enhancement seems probable.

4.3 ^{210}Po in bottom sediment

- The bottom sediments collected in Antwerp and Vlissingen in the vicinity of outfalls of the phosphorous industry have ^{210}Po levels between 40 and 170 Bq.kg⁻¹, which is lower than found in the suspended matter at those locations. The same is true for the other locations sampled in the Westerscheldt. In an absolute sense no large enhancements of ^{210}Po and ^{210}Pb concentrations occur in the bottom sediments studied.
- Two bottom sediment samples were studied in the Seine estuary taken at different dates at a distance of 0,1 km from the outfall near Le Havre. The ^{210}Po activities are clearly enhanced, viz. 950 and 1050 Bq.kg⁻¹.
- In the Tagus estuary the 4 samples of intertidal bottom sediments, collected within 0,2 km from the phosphate plant, have activities between 240 and 1400 Bq.kg⁻¹ and are clearly enhanced. Elsewhere in the estuary no clear enhancements can be distinguished in bottom sediments.

4.4 Enhancements of ^{210}Po in biota

At sites along the Seine estuary, the coast of Normandy and English Channel mussels were sampled roughly at 6-week intervals during a period of 20 months.

- At Wimereux at 150 km North-East and at Pointe de Moulard 100 km West of the phosphate plant at Le Havre average ^{210}Po activities were respectively 220 (range 140-

290) and 150 (range 90-280) Bq.kg⁻¹.

- In the Seine estuary at Digue Nord at 1 km and at Phare Falaise at 10 km to the East from the phosphate plants average ²¹⁰Po activities were respectively 190 (range 130-310) and 210 (range 120-340) Bq.kg⁻¹.
- At the outfall of the phosphorous plant at Le Havre ²¹⁰Po activities in mussels ranged from 140-700 Bq.kg⁻¹ at times when samples could be collected.
- In the Gulf of St. Malo at Pirou, within 50 km from a phosphate plant at St. Malo and one at Granville, the average ²¹⁰Po activity was 300 (range 170-450) Bq.kg⁻¹. (No data are yet available on actual and past discharges by these two plants).

At some sites the variations in the levels show seasonal trends, lower activities in summer than in winter. However most variations in time and between locations can not yet be explained. The figures indicate that some industrial enhancement of ²¹⁰Po levels in mussels probably occurs.

A preliminary study of ²¹⁰Po activity levels in biota within the Tagus estuary and along the adjacent coast did not yield any conclusive evidence of industrial enhancement effects. Growing conditions in the estuary are poor for some species, which made the study difficult.

5. Modelling levels of radionuclides in the Westerscheldt estuary

OKLSO a steady-state, one-dimensional, model has been developed for the Westerscheldt. The runs made with this model show reasonably good results. In these runs apparent Kd parameter values are used from RIVM/LSO lab experiments and from field surveys; hydrological data from DGW/Middelburg; and effluent emission data from literature and emission permits. The model still requires more thorough validation.

With the OKLSO model estimates have been made of the contribution of the major emission streams to the enhancement of the total ²¹⁰Po activity in the water of the Westerscheldt. The calculations indicate that: the atmospheric emission of the thermal phosphorous plant contributes maximally 10%; the effluent emission of the same plant contributes to the model-compartment at the beginning of the estuary near the Belgian-Dutch border about 10%, and to the compartment at the end of the estuary near Vlissingen about 70%; the contribution of the effluent of the wet phosphorous plant in these compartments is respectively about 80% and 20%.

The OKLSO model is applicable to other similar estuaries, provided all inputs specific for other estuaries are available and provided specific validation.

Test runs made with the dynamic model DELWAQ-IMPAQT indicate that in about 30 years from the start of continuing emissions by the phosphorous industries steady state conditions will have been reached for the total ²¹⁰Po activity in the water of the Westerscheldt.

RADIO a dynamic one-dimensional model is being developed.

6. Conclusions

Phosphogypsum contains approximately 800 Bq.kg⁻¹ dry weight of both ²¹⁰Po and ²¹⁰Pb. When diluted with large amounts of water, as will happen upon emission into estuaries, the gypsum and about 10% of ²¹⁰Po and ²¹⁰Pb dissolve. Thereafter a fine grained insoluble residue remains, which contains ²¹⁰Po and ²¹⁰Pb at levels exceeding 10.000 Bq.kg⁻¹.

In a sample of the effluent of the thermal phosphorous plant at Vlissingen the activity of ²¹⁰Po is about 10 times as high as that of ²¹⁰Pb. At emission about 20% of the activity is dissolved, upon dilution under laboratory conditions 100% of ²¹⁰Po dissolves.

No conclusive information exists with respect to natural background levels of ²¹⁰Po and

^{210}Pb dissolved in water, in suspended matter and in bottom sediments of estuaries. Some tentative ranges have been established which can be considered as low levels, these coincide roughly for the Netherlands, France and Portugal.

Due to the fact that the natural background is not precisely known, it is often not possible to determine if enhancements occur and to quantify these from observed ^{210}Po and ^{210}Pb levels. In many cases levels measured in suspended matter seem a better indicator for industrial enhancements than the levels dissolved in water. The largest enhancements were observed in bottom sediments near outfalls. This is consistent with the chemo-physical characteristics of phosphogypsum and of its insoluble residue as found in the laboratory studies. These characteristics explain the high ^{210}Po levels in the Rhine estuary of ^{210}Po dissolved and in suspended matter near the phosphogypsum outfalls, and in bottom sediments; as found in the former NIOZ project, CEC contract B16-F-328-NL (Be-90).

Modelling the distribution in the water of the Westerscheldt of ^{210}Po and ^{210}Pb after industrial emission shows reasonable first results, further validation is necessary.

In the Seine estuary it was found that *Fucus vesiculosus* is not suited as a ^{210}Po bioindicator, whereas *Mytilus edulis* is. In this estuary and along the adjacent coast of the English Channel ^{210}Po activity levels in *Mytilus* ranged between 100-450 Bq.kg⁻¹, effects of enhancement by phosphorous industries are very probable but could not be distinguished quantitatively. Other factors probably played also a role and no background activities were available for comparison. Along the Portuguese coast *Mytilus galloprovincialis* grows, but can hardly be found in the Tagus estuary, so here its use as a bioindicator is not possible.

Variations in weather conditions, tidal and fluvial fluxes, dredging activities, operational intensity of industrial plants, etc. all affect the activities of ^{210}Po and ^{210}Pb observed in sampling trips in the estuaries, which makes their interpretation complex. Nevertheless in each estuary some clear enhancements occur due to the phosphorous industry, though the extend of the area and the level of enhancement vary. With respect to the differences observed between estuaries the following can be concluded: the widespread and high levels of enhancement in the Rhine estuary coincide with effects of the muddy plug, local high sedimentation rates of fine grained material and the largest emission of ^{210}Po and ^{210}Pb ; the Dutch Westerscheldt is mostly downstream of the muddy plug, has high tidal current velocities in most locations and a large estuary-volume, which all lead to relative low enhancements; roughly the same holds for the Seine estuary; in the Tagus estuary only local enhancements occur, this estuary has the lowest emission of ^{210}Po and ^{210}Pb , and in part of the estuary very high current velocities.

Several items or processes regarding ^{210}Po and ^{210}Pb in estuaries, have not been studied and need future research as e.g.: industrial emissions with concurrent distribution measurements, coupled to model validation; effects of the natural deposition of ^{210}Pb on levels in different geomorphological and hydrological situations; the relation between levels of enhancement in bottom sediments with grain size and other factors; the effects of differences in hydrological conditions within and between estuaries on the distribution of ^{210}Po and ^{210}Pb ; uptake of ^{210}Po by mussels and by other biota from effluents of the phosphorous industry; quantitative environmental distribution balances of ^{210}Po and ^{210}Pb emitted into the environment; the enhancement of the radiation dose of consumers of fish produce. Research proposals focusing on several of these questions have been submitted.

References

Project publications mentioned in paragraph 1 and references, are listed hereafter in the reference paragraphs of the contractor reports.

Project 1

Head of project: *Dr. Köster*

Objectives for the reporting period

1. Studies of effluents from phosphorous producing industries

- a) Physico-chemical and radiological characterization of effluents from phosphorous producing industries in the Netherlands: two wet process plants near Rotterdam at the Nieuwe Waterweg and one thermal phosphate plant near Vlissingen at the Westerscheldt.
- b) Laboratory experiments with mentioned effluents to study: rate of dissolution into surface water; influence of degree of salinity of surface water; adsorption characteristics of ^{210}Po on selected solid matter.

2. Modelling the distribution of ^{210}Po and ^{210}Pb in the Westerscheldt

- a) Expansion of the steady state model OKLSO with $^{210}\text{Po}/^{210}\text{Pb}$ disequilibria and effects of an atmospheric source term.
- b) Calculation of dissolved ^{210}Po and ^{210}Pb and in suspended matter, using in the OKLSO model effluent specific parameter values obtained in the above mentioned effluent studies.
- c) Study of the dynamic model DELWAQ-IMPACT for the Westerscheldt with first try-out runs.

Progress achieved including publications

1. Studies of effluents from phosphorous producing industries

Phosphogypsum effluents collected from a plant at Vlaardingen and one at Vondelingenplaat were studied. After drying both contained about 1000 Bq.kg^{-1} of ^{226}Ra , ^{210}Pb and ^{210}Po . For different definitions used in the literature the respective activity levels have been calculated. Table 1 shows under "Dried effluent" the activities calculated from the activity contents of dry matter and water phase. The results under " $\text{CaSO}_4 \cdot 2\text{H}_2\text{O}$ " were calculated from the "Dried effluent" and the ratio pure gypsum/dry matter. The pure gypsum content was calculated from the calcium content.

Nuclide	Liquid effluent fresh weight basis	Dried effluent dry matter basis	$\text{CaSO}_4 \cdot 2\text{H}_2\text{O}$ pure gypsum basis
$^{226}\text{Ra} \text{ Bq.kg}^{-1}$	232 - 267	980 - 995	882 - 896
$^{210}\text{Pb} \text{ Bq.kg}^{-1}$	230 - 275	970 - 1025	874 - 923
$^{210}\text{Po} \text{ Bq.kg}^{-1}$	175 - 252	739 - 938	666 - 845

In the effluents ^{226}Ra appeared to be in equilibrium with ^{210}Pb . The activity levels of ^{210}Po were 9 to 25% lower than those of ^{210}Pb . This was a small and perhaps not consistent difference, in Portuguese samples the activity of ^{210}Po in phosphogypsum was higher than that of ^{210}Pb (*Ca-91*). The ^{238}U activity level was low compared to that of ^{210}Pb .

After dilution of the Vlaardingen effluent 230 and 2300 times a finely dispersed residue with a weight of respectively 2.3% and 1.6% of the original effluent remained. The particle size distribution of the residue was determined with a laser particle counter in the range between 1.2 and 118.4 μm . Vondelingenplaat appeared to have slightly more fine particles than the Vlaardingen residue. The relative number of small particles decreased upon dilution (Table 2).

Upon dilution with water ^{210}Pb and ^{210}Po of the effluent behaved practically the same. Both nuclides are for 90% contained in the insoluble residue at concentrations of more than 10 kBq.kg^{-1} , and seem nearly desorption proof. In some water samples, collected close to the phosphogypsum outfall into the Nieuwe Waterweg, the suspended matter also had ^{210}Pb and ^{210}Po levels of more than 10 kBq.kg^{-1} (*Be-92*). The peak concentrations of dissolved ^{210}Po in the samples of the Nieuwe Waterweg were about 30 Bq.m^{-3} , which was similar to the 10 and 40 Bq.m^{-3} as observed in the dilution experiments.

Sample	VLA	VLA	VLA	VON
Ratio effluent/water	2.3	230	2300	230
Size of band (μm)	%	%	%	%
1.2 - 2.2	1.0	0.4	0.2	3.9
2.4 - 48.8	98.7	80.8	63.8	82.5
48.8 - 118.4	0.3	18.8	36.0	13.6

The $^{210}\text{Po}/^{210}\text{Pb}$ ratio of the effluent samples and of solutes and particles in the experiments was approximately 1:1. In water samples from the Nieuwe Waterweg this ratio ranged from 0.4 to 1.7 (*Be-88*, *Be-92*). The enhanced levels of ^{210}Po and ^{210}Pb found in bottom sediments in the Nieuwe Waterweg are ascribed to the phosphogypsum emissions (*Be-88*). It is clear that part of the radionuclide containing residue sedimentates, whereas the gypsum dissolves. This has also been observed for ^{226}Ra emitted with phosphogypsum into the Mississippi river (*Kr-i.p.*).

Two samples taken from the effluent of a thermal phosphate plant at Vlissingen (one time proportional and one grab sample) differed clearly in ^{210}Po activity, whereas the ^{210}Pb activities were almost equal (Table 3). Further research is needed to get more information on the activity levels of and the differences between such samples. In the effluent samples the activity levels of ^{210}Po were 10 to 20 times higher than those of ^{210}Pb . In water samples from the Westerscheldt, ^{210}Po and ^{210}Pb levels were enhanced, which has been attributed to the effluents of the phosphate plant (*Be-88*, *Kö-90*). ^{210}Po was present in a soluble form after dilution of the effluent. However the slight enhancement in the bottom sediment in the harbour next to the plant (*Be-91*) indicate that in the Westerscheldt water part of this dissolved ^{210}Po is adsorbed by suspended matter.

Table 3. Activities in effluent from a thermal plant at Vlissingen (VLI)

Nuclide	Total activity (Bq.kg ⁻¹)		Activity in filtrate (Bq.m ⁻³)	
	VLI _{prop}	VLI _{grab}	VLI _{prop}	VLI _{grab}
²²⁶ Ra	<0.05	n.a.	<50	n.a.
²¹⁰ Pb	0.32±0.03	0.30±0.03	92±18	104±35
²¹⁰ Po	3.88±0.10	7.25±0.28	371±19	325±127

Contact experiments of a soluble ²¹⁰Po salt in synthetic estuarine water and sea water with fine-sized Westerscheldt sediment and illite have shown that polonium adsorbed rapidly on suspended matter. In a solution with 1% suspended matter calculated K_d values in m².kg⁻¹ ranged from 20 to 60 and are in the same order of magnitude as found in field studies of the Westerscheldt (*Be-88, He-i.p.*). ²¹⁰Po solutions in synthetic estuarine water and sea water were shown to be unstable. Probably due to fixation on coagulating colloids. In nature different species/forms can show differences in adsorption by suspended matter and sediments or uptake by biota.

The differences found between the phosphogypsum and the thermal process effluents may provide a mean to identify their respective contributions to the increase of the activity levels in the Westerscheldt.

Further research is needed to obtain firm quantitative information, both with regard to the composition of the effluents and the characteristics of the radionuclides.

2. Modelling the distribution of ²¹⁰Po and ²¹⁰Pb in the Westerscheldt

At Rupelmonde in Belgium the river Scheldt flows into the Scheldt estuary, this has an expansion of 94 km to the Northsea. The Dutch part of this estuary is named the Westerscheldt, with a length (measured along specific buoys) of 73 km. Its boundaries are: the Belgian-Dutch border in the East; the line from Vlissingen to Breskens in the West close to the Northsea; and to the North and the South the dikes constructed to reclaim and/or protect land against flooding.

Four different geomorphologic units are distinguished in the estuary: channels, sand flats, mud flats and salt marshes. To maintain the navigability of the Westerscheldt the shallow parts in the channels are dredged frequently.

The total surface area of the Westerscheldt estuary inside the dikes is 3.2E8 m². It contains the sea- or waterway to the Belgian port Antwerp. The width of the Westerscheldt varies between 2 and 10 km, with an average of 5 km. The waterlevel of the Westerscheldt fluctuates with the sea tides, normally from ca. +2 m to -2 m NAP (New Amsterdams Peil). In the Eastern part of the Westerscheldt, between Antwerp and Hansweert, the average depth is 9 m. Whereas in the Western part between Hansweert and Vlissingen the average depth is 11 m.

The fresh water inputs into the Westerscheldt are dominated by the Belgian river the Scheldt with a volumetric flow of 3.8E6 m³.a⁻¹. The relative contribution of Dutch fresh water inputs, outfalls from channels and polders, is approximately 25%.

From the Belgian-Dutch border to the Northsea the percentage of fresh water in the estuary decreases practically linearly. Furthermore hardly any concentration gradients or differences in density occur in a vertical or in a lateral direction in the Westerscheldt.

Consequently the water movement and distribution of compounds in the water can be well approximated by one-dimensional simulation models.

The O'Kane-method offers a tool for simple, steady-state, one-dimensional modelling of estuaries for the calculation of the total concentrations of compounds in water (OK-80). In order to use this method the estuary has to be subdivided in several compartments in a longitudinal direction, over which mass balances are written. In this way the model OKLSO has been developed for the Westerscheldt. Use was made of the hydrological information available from the SAWES project, comprising also the dynamic model DELWAQ-IMPAQT. Compartments 6-14 of this model cover the Westerscheldt and are used in OKLSO.

For the modelling of ^{210}Po and ^{210}Pb enhancements in the estuary the inputs and the boundary conditions of the model (excluding the natural background) had to be defined. In the east, the Belgian-Dutch border gives the boundary condition at compartment 6 of the model. It reflects the emissions into the Scheldt estuary by the wet phosphorous plant at Zandvliet in Belgium. For this boundary an estimate of the average enhancement has been used, which was derived from the measurements carried out at the border during 1987-1990 by RIVM and RWS: for ^{210}Po 18.4 Bq.m^{-3} and for ^{210}Pb 18.1 Bq.m^{-3} . For the western boundary at compartment 14, the sea near Vlissingen, has been taken the average enhancement of the two measurements carried out in 1986 and 1987: for ^{210}Po 2.5 Bq.m^{-3} and for ^{210}Pb 2.4 Bq.m^{-3} . For the input from the thermal phosphorous plant near Vlissingen into compartment 14 the values listed in the emission permit have been taken. For the effluent emission: $1.1\text{E}11 \text{ Bq.a}^{-1}$ ^{210}Po and $7.5\text{E}10 \text{ Bq.a}^{-1}$ ^{210}Pb . For the atmospheric emission: $5.5\text{E}11 \text{ Bq.a}^{-1}$ ^{210}Po and $2.2\text{E}11 \text{ Bq.a}^{-1}$ ^{210}Pb . The deposition from this on the Westerscheldt has been estimated by means of atmospheric distribution model calculations (K6-86): ^{210}Po in $\text{Bq.m}^{-2}.\text{a}^{-1}$ near Vlissingen 110, near the Dutch Belgian border 10; ^{210}Pb in $\text{Bq.m}^{-2}.\text{a}^{-1}$ near Vlissingen 45, near the Dutch-Belgian border 5.

In addition the distribution coefficient K_d has been introduced in the OKLSO model, so that the calculated total concentration can be partitioned over the dissolved and particulate fraction. In studies of the Westerscheldt the observed K_d -values in $\text{m}^3.\text{kg}^{-1}$ range from 20-340 (av. 80) ^{210}Pb and for ^{210}Po from 20-275 (av. 85). This concurs reasonably well with the value of 62 found in the laboratory experiments reported above. The K_d -values of ^{210}Po and ^{210}Pb selected for the modelling are 60 in the eastern part and 50 in the western part of the Westerscheldt.

The calculations with the OKLSO model of the total activity concentrations show an almost linear decrease going seaward from compartment 6 through 11, and from there on a slight increase (Figure 1). The measured concentrations differ to some degree from the calculated ones. This can be due to the uncertainty in the correction of the measurements for the (relatively unknown) natural background in order to estimate the enhancements. Also other factors can cause deviations between the (irregular fluctuating) measured concentrations and the steady state values calculated by the model. E.g. variations in the suspended matter load cause large variations in the total activity concentrations.

Calculations with the OKLSO model indicate with respect to the steady state activity concentrations, that the atmospheric emission of the thermal phosphorous plant contributes maximally 10% in the Westerscheldt. The total contribution of the thermal plant in Vlissingen compared to that of the wet process plant is in compartment 6 roughly a factor 9 lower, and in compartment 14 for ^{210}Po a factor 9 and for ^{210}Pb a factor 4 higher.

Besides the development of and runs with OKLSO a start has been made with dynamic modelling. The dynamic model DELWAQ-IMPAQT has been studied, parameter values specific for ^{210}Po and ^{210}Pb in the Westerscheldt have been selected and test runs were made. Also a simplified version of DELWAQ-IMPAQT is being developed, namely the

dynamic model RADIO.

The test runs made with DELWAQ-IMPACT indicate that about 30 years after the start of continuing emissions by the phosphorous industry, the ^{210}Po and ^{210}Pb concentrations will have been stabilised in the Westerscheldt water (Figure 2). So at that time steady state conditions have been reached for the water.

All conclusions presented above are still preliminary, as at this stage the models have not been validated. For this validation further studies are needed, with a special effort to correlate measured concentrations with concurrent emissions and hydrological conditions.

Köster H.W., Pennders R.M.J., Heling R.H., Eenink R.
Bilthoven 21-07-1992.

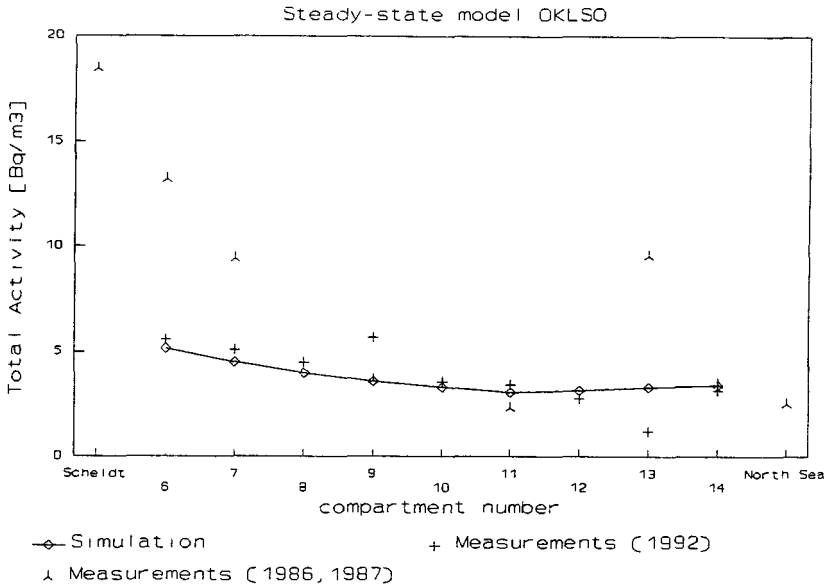


Fig. 1 Simulation results: ^{210}Po in the Westerscheldt. Standard parameter set.

DELWAQ- IMPAQT

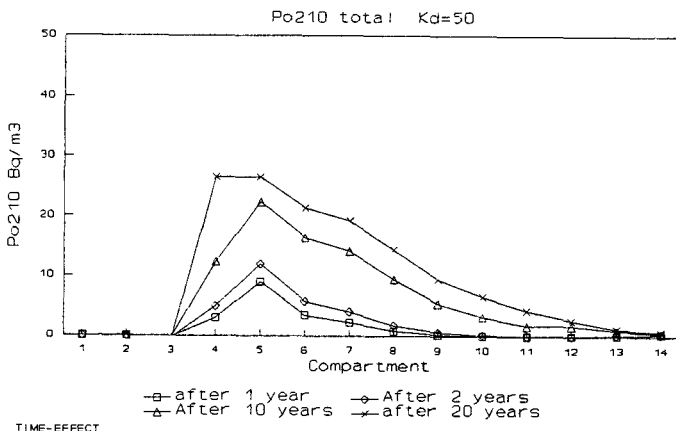


Fig. 2 Time-effect on total ²¹⁰Po activities. $K_d = 50$ (m³/kg)

References

- Be-88 Berger, G.W. and Eisma, D. (In Dutch, Engl. summ.) Survey of ²¹⁰Po and ²¹⁰Pb in Dutch coastal waters, the Nieuwe Waterweg, the Noordzeekanaal and the Westerschelde. pp. 33. Report nr. NIOZ-1988-13, Netherlands Institute for Sea Research, Den Burg, The Netherlands, 1988.
- Be-91 Berger, G.W. NIOZ first year Progress Report. In "Behaviour of ²¹⁰Po and ²¹⁰Pb in European marine environments. Application of bioindicators", Contract Bi7-006. CEC, DGXII, Brussels, 1991.
- Be-92 Berger, G.W. and Köster, H.W. (In Dutch, Engl. summ.) Regional distribution and potential radiological effects of ²¹⁰Po, ²¹⁰Pb, ²²⁶Ra and Th-isotopes in the Nieuwe Waterweg and along the Dutch coast. Series of "Chemical substances, radiation and safety". Ministry of Housing, Physical Planning and Environment (VROM), Leidschendam, The Netherlands. 1992.
- Ca-91 Carvalho, F.P. LNETI first year Progress Report. In "Behaviour of ²¹⁰Po and ²¹⁰Pb in European marine environments. Application of bioindicators", Contract Bi7-006. CEC, DGXII, Brussels, 1991.
- He-i.p. Heling, R., Eenink R.G., Köster, H.W., Berger G.W. Modelling of the distribution of natural radionuclides in the Westerscheldt due to industrial discharges in water. Report, National Institute of Public Health and Environmental Protection, Bilthoven, The Netherlands. In press.
- Kö-i.p. Köster H.W., Marwitz P.A., Berger G.W., Weers A.W. van, Hagel P., Nieuwenhuize J. Po-210, Pb-210 and Ra-226 in aquatic ecosystems and polders, anthropogenic sources, distribution and enhanced radiation doses in the Netherlands. Radiation Protection Dosimetry. In Press.

- Kö-90 Köster, H.W., Marwitz, P.A., Berger, G.W., van Weers, A.W., Hagel, P. and Nieuwenhuize, J. Reconnaissance investigations of ^{210}Po and other radionuclides in Dutch coastal ecosystems. pp.226. Report no. 248476004, National Institute of Public Health and Environmental Protection, Bilthoven, The Netherlands. 1990. (In Dutch).
- Kö-86 Köster H.W., Stoutjesdijk J.F. Should Po-210 and Pb-210 be released into the atmosphere or into surface waters? An aspect of an optimization procedure. pp. 377-387. In: Optimization of radiation protection. Proc. IAEA-SM-285/32. International Atomic Energy Agency. Vienna. Austria. 1986.
- Kr-i.p. Kraemer, T.F. and Curwick, P.B. Radium isotopes in the lower Mississippi River. J. Geophys. Research-Oceans. In press.
- OK-80 O'Kane J.P. 1980. Estuarine Water-Quality Management.
- Pe-i.p. Pennders R.M.J., Köster H.W., Lembrechts J.F. Characteristics of Po-210 and Pb-210 in effluents from phosphate producing industries, a first orientation. Radiation Protection Dosimetry. In Press.

Project 2

Head of project: *Dr. Guéguénat*

Objectives for the reporting period

In the context of this contract, the "Laboratoire d'Etudes Radioécologiques de la Façade Atlantique" (LERFA) at La Hague was specifically asked to test the usefulness of two classic bio-indicators, i.e. the brown algae *Fucus vesiculosus* and the mussel *Mytilus edulis*. In this way, it was decided to measure the activities of ^{210}Po and ^{210}Pb in these species as a function both of space and time. The study area is located in the Seine estuary (figure 1) within a zone affected by industrial releases of phosphatic gypsum.

Progress achieved including publications

The samples were collected at the stations situated in the Seine estuary (Digue Nord, Phare de la Falaise, Tour de Contrôle) ; in addition, samples were taken from control stations located outside the estuary (Wimereux, Pointe de Moulard, Pirou, Agon-Coutainville) (figure 1).

1. Levels of radionuclides

Polonium-210 :

Sea water :

For all the seawater samples filtered at $0.45\ \mu\text{m}$, ^{210}Po activities fall in the range $0.20\text{--}1.6\ \text{mBq.l}^{-1}$. The recorded average values are as follows in mBq.l^{-1} , Digue Nord : 0.90 ± 0.26 ; Pirou : 0.72 ± 0.29 ; Pointe de Moulard : 0.47 ± 0.21 . It would appear that at the Pointe de Moulard station, activity levels are generally lower than at the two other stations. At the Digue Nord, there appears seasonal fluctuations (increasing values in spring and then a drop).

In the unfiltered seawater samples, levels of ^{210}Po are systematically higher ($0.7\text{--}16\ \text{mBq l}^{-1}$) than in the filtered samples. With the unfiltered samples, ^{210}Po activities are a function of turbidity.

^{210}Po levels are relatively homogeneous in the suspended matter samples. The recorded average values are, in Bq kg^{-1} dry weight, Digue Nord : 159 ± 18 ; Pointe de Moulard : 55 ± 22 ; Pirou : 90 ± 16 .

Sediments :

^{210}Po activities were determined in samples taken from the bed of the Seine, near Rouen (at 110 km from Le Havre) at a locality which had been used – up to 1984 – for loading barges with phosphatic gypsum waste ; a small amount of this waste has been carried away by the Seine. Here, the activities are less than $290\ \text{Bq kg}^{-1}$ dry weight, showing a decrease over the past three years.

Near the outlet pipe from the Hydroazote factory into the Seine estuary, activities in the sediments are rather higher (of the order of $1,000\ \text{Bq kg}^{-1}$ dry weight).

Mussels :

During the period of study, the ^{210}Po activity in mussel flesh samples varied – over the complete set of measurements – from $90\ \text{Bq kg}^{-1}$ (dry weight) at Pointe de Moulard to $700\ \text{Bq kg}^{-1}$ (dry weight) at the Hydroazote outfall. The recorded average values are in Bq kg^{-1} dry weight, Digue Nord : 192 ± 60 ; Phare de la Falaise : 212 ± 58 ; Pointe de Moulard : 149 ± 58 ; Pirou : 296 ± 83 ; Wimereux : 221 ± 40 .

A comparison of the activity levels in mussels from these different sites – as well as a comparison of the ranges of variation – enables the recognition of certain trends that may be considered significant, as described by GERMAIN *et al.* (1991).

The ^{210}Po activities in mussel flesh from the Seine estuary are no higher than from other stations along the Channel coast, with the exception – during certain periods – of the outfall zone near the Hydroazote plant. In other respects, some progressive trends are apparent with time in the estuary ; levels are lower in summer and autumn, but higher in late winter and spring.

At Pointe de Moulard, the levels are usually the lowest of all the studied stations, apart from March 1990 and particularly December 1990–April 1991. Here, again, a progressive trend makes its appearance between the periods of summer and winter–spring.

At both Wimereux and Pirou, fluctuations in ^{210}Po do not fit into any regular pattern.

Fucus vesiculosus :

Samples of *F. vesiculosus* display levels of ^{210}Po which are distinctly lower than those observed in the mussels. The activities (in Bq kg^{-1} dry weight) vary from 3 at Pointe de Moulard to 22 in the Seine estuary and at Pirou.

The recorded average values are, in Bq kg^{-1} dry weight, Phare de la Falaise : 13.3 ± 2.4 ; Tour de Contrôle : 14.0 ± 4.2 ; Pointe de Moulard : 4.5 ± 1.0 ; Pirou : 13.7 ± 3.7 ; Wimereux : 8.3 ± 2.1 .

There are significant differences as regards the spatial distribution of ^{210}Po activity in seaweed. Within the estuary (Phare de la Falaise, Tour de contrôle), the ^{210}Po activities are among the highest recorded, along with the values obtained at Pirou. Intermediate values are obtained at Wimereux, whereas the lowest values are seen at Pointe de Moulard.

Lead-210 :

In the mussels, ^{210}Pb activities – when detected – are generally situated between 10 and 20 Bq kg^{-1} dry weight. In the seaweed samples, activities fall in the range 6–23 Bq kg^{-1} dry weight, but ^{210}Pb is often beneath the detection limit.

2. Discussion

A study of the distribution of ^{210}Po in two indicator species has revealed the existence of significant geographical trends in *Fucus vesiculosus* (activities are highest in the Seine estuary and at Pirou) and in *Mytilus edulis* (highest values at Pirou and in the estuary at certain periods).

As regards *F. vesiculosus*, the calculated $^{210}\text{Po}/^{210}\text{Pb}$ ratios are close to unity. Consequently, there is very little exchange of ^{210}Po between the algae and its environment. This means that *F. vesiculosus* is a poor indicator species.

With the mussels, the results are entirely different. The $^{210}\text{Po}/^{210}\text{Pb}$ ratios fall in the range 6–40, indicating that a large part of the ^{210}Po in each individual specimen comes from the environment. Among the studied stations, those located in the Seine estuary – as well as the Pointe de Moulard – exhibit seasonal fluctuations in the exchange between environment and mussel. These fluctuations are linked to parameters which correspond to the source–terms or, otherwise, to various ecological or physicochemical factors,

– Industrial source–term : the lead accumulating in the Seine from phosphate factories in the Rouen area is subsequently remobilized downstream during times of flood. However, these deposits would not appear to constitute an important source since decreasing levels of ^{210}Po and ^{210}Pb are observed in the sediments.

Indeed, a comparison with the results obtained from the control stations – Pte de Moulard, Wimereux, for instance – indicates that there is limited industrial impact in the Seine estuary on the labelling of mussels with ^{210}Pb or ^{210}Po .

- Ecological and physicochemical factors : there is an enrichment of ^{210}Po in mussels with respect to the filtered seawater and suspended matter samples. The ^{210}Po activities in filtered seawater and mussels from Pointe de Moulard are generally less than in samples from Pirou and the Digue Nord taken during the period from June to October.

At the Digue Nord of Le Havre, where seawater sampling started in March 1990, a slight seasonal fluctuation is observed in ^{210}Po levels ; a similar trend can be seen in the mussel flesh samples, with lower activities in summer and autumn and higher activities in late winter and spring.

It is thus possible to conclude that some of the ^{210}Po present in the mussel tissue is derived from polonium dissolved in seawater. Polonium probably follows the metabolic pathways of the digestive system.

But it appears that mussels in the estuary concentrate less ^{210}Po than mussels collected from other stations (comparison levels in mussels and sea water, and suspended particles). It is possible that some physicochemical effect, linked to the estuarine environment, has an influence on radionuclide transfer.

In the estuary, the increasing and decreasing levels of ^{210}Po in mussels are seen to follow the fluctuations in flow-rate of the Seine. The highest flow-rates augment the flux of polonium from geological and agricultural sources, moving the turbidity maximum ("muddy plug") further downstream. However, these processes are not concomitant. And at Pointe de Moulard, it is to be noted that the variations of polonium activity in the mussels follow the rainfall curve, with a time-offset of 2-3 months, and perhaps there is an influence of the Baie des Veys where several rivers enter the sea.

The bio-indicator species studied in the Seine estuary show uptakes of polonium which fall in the same general range as those observed elsewhere by other authors (Germain *et al*, 1991).

Institut de Protection et de Sûreté Nucléaire
Département de Protection de l'Environnement et des Installations - IPSN/CEA
(50444 BEAUMONT-HAGUE CEDEX FRANCE)

P. GERMAIN and G. LECLERC

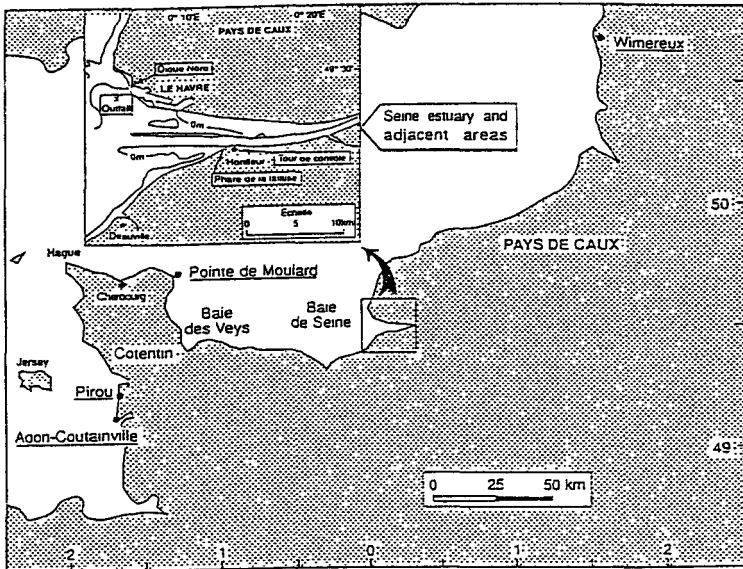


Figure 1 - Sketch map showing location of sampling stations

References

GERMAIN, P., LECLERC, G., SIMON, S. 1991. Distribution of ^{210}Po in *Mytilus edulis* and *Fucus vesiculosus* along the channel french shore : influence of the industrial releases in the Seine : river and estuary. NRE V, Salzburg sept. 22-28, CEC.

Project 3

Head of project: *Prof. Dr. Duursma*

Objectives for the reporting period

The objectives for the reporting period (June 1990-June 1992) were:

- to carry out 2 sampling programs: one in the Westerscheldt estuary and one in the adjacent coastal zone
- to analyse the obtained samples in order to get insight in the sources, pathways, sinks and distribution of ^{210}Po and ^{210}Pb in this area as a logical continuation of work that has been done by the NIOZ in the Nieuwe Waterweg under EC contract B15-0328-NL in previous years.

Based on these data, The RIVM (Bilthoven, the Netherlands) will model the behaviour and transport of ^{210}Po and ^{210}Pb in the estuary.

Progress achieved including publications

The area of interest was seen as to a "box", bordered by the river Schelde on the east and the North Sea on the west side. In this way we hope to be able to describe the sources, sinks, distribution and budgets of the radionuclides involved. During the first week of October 1990 a sampling cruise was undertaken in the Westerschelde. Due to weather conditions sampling in the coastal zone was not possible. Altogether 58 samples were taken: 37 water- and particulate matter samples, 21 sediment samples. Particulate matter concentration, water temperature and salinity were measured. During a second cruise in the last week of March 1992, 20 additional bottom-, water- and suspended matter samples were taken in the North Sea, the Dutch coastal zone and the Westerscheldt.

1. ^{210}Po and ^{210}Pb in sediment samples

The ^{210}Po concentration in the sediment samples collected in the Westerschelde estuary range from 6 to around 400 Bq. kg^{-1} (Fig.1). The highest concentration is found in the Canal van Sas van Gent naar Terneuzen near the former phosphate-ore processing plant "Zoutchemie". Sediment collected near BASF with a concentration of 170 Bq. kg^{-1} seems to be slightly above the natural background, as is the case with a sample, taken in the Sloehaven Vlissingen, with a concentration of 148 Bq. kg^{-1} . With the exception of these three locations, the ^{210}Pb concentration in the sediment is around the natural background or, in areas where fine material settles, not higher than can be expected based on the natural atmospheric ^{210}Pb flux.

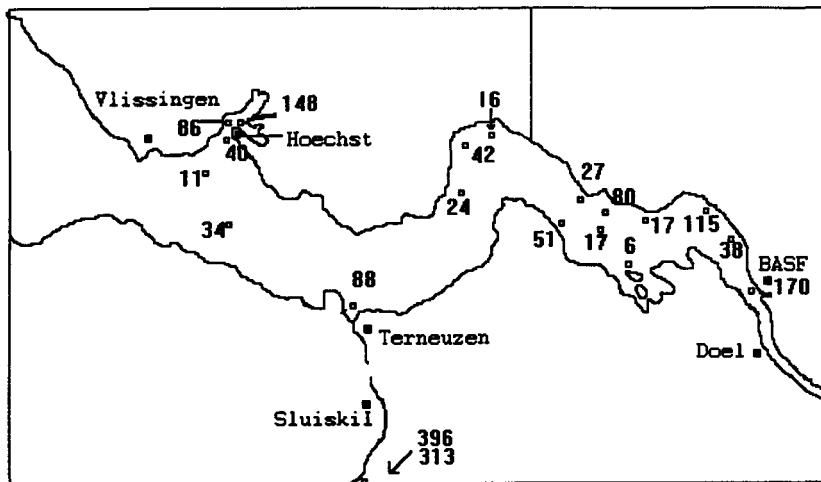


Figure 1. Concentrations of Po^{210} [$Bq.kg^{-1}$] in sediment samples.

This is confirmed by previous ^{210}Pb measurements in sediments in the Westerschelde where relatively fine material settles (Berger, G.W. & D. Eisma, 1988b). Beside ^{210}Po , ^{210}Pb was analyzed in a selection of the sediment samples. The Po/Pb ratio is between 0.75 and 1.56.

2. Thorium isotopes in sediment samples

The ^{230}Th concentration in the sediment samples is between 2.4 and 94 $Bq.kg^{-1}$. the ^{232}Th concentration between 2.6 and 25 $Bq.kg^{-1}$. High ^{230}Th concentrations coincide with high ^{210}Pb and ^{210}Po values, which is not reflected in the ^{232}Th concentration. This indicates an extra source for these isotopes.

3. ^{210}Po and ^{210}Pb in particulate matter

^{210}Po concentrations in particulate material are between 70 $Bq.kg^{-1}$ (coastal water) to 250 $Bq.kg^{-1}$ (Zelzate, Channel of Sas van Gent naar Terneuzen). Relatively high concentrations are found between Doel and BASF in the western part of the estuary near Vlissingen. Fig.2 shows the general distribution pattern of ^{210}Po adsorbed on particulate material.

The $^{210}Po/^{210}Pb$ ratio is between 0.7 and 3.65, the average value being 1.3. Relatively high ratios (3.65 and 1.93) are found near the sluice of the canal from Gent naar Terneuzen and sample W90-15, close to Vlissingen.

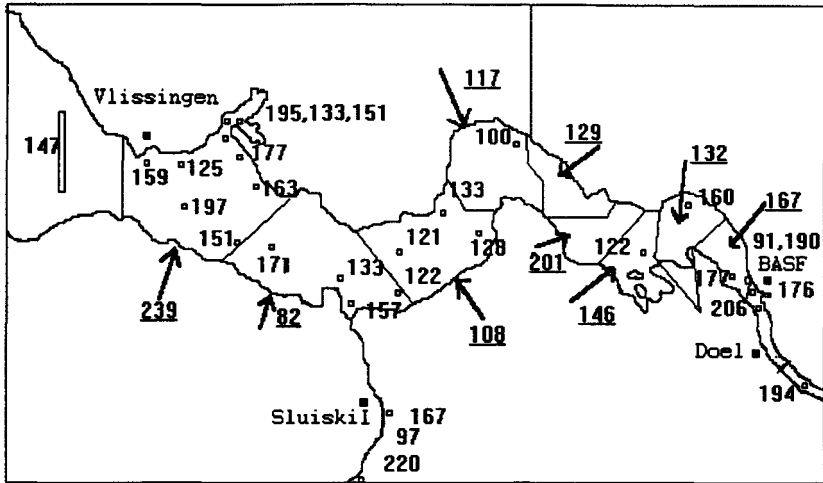


Figure 2. Concentrations of ^{210}Po ($\text{Bq}\cdot\text{kg}^{-1}$) in particulate matter in oct.'90 and average values (underlined) as found in march '92 in the DELWAQ compartments.

4. Thorium concentration in particulate matter

The ^{230}Th concentration in particulate matter samples is between 18 and 83 $\text{Bq}\cdot\text{kg}^{-1}$. The highest value corresponds with the highest ^{210}Po value (sample W90-1, west of Vlissingen).

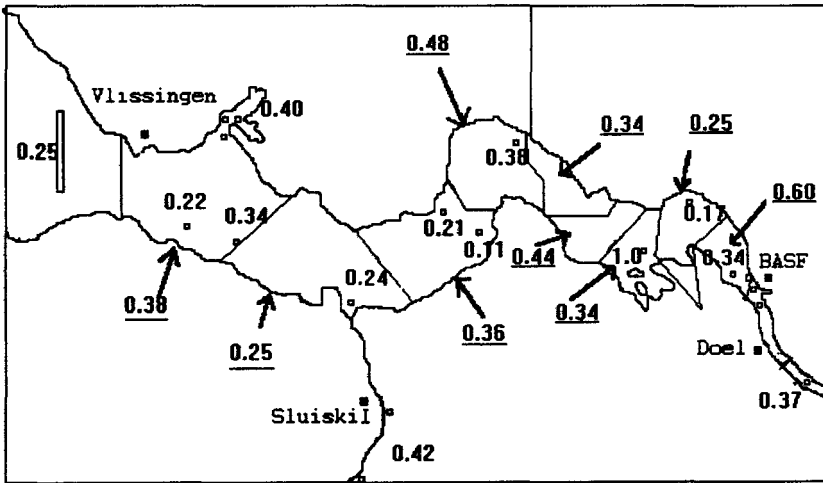


Figure 3. Concentrations of ^{210}Po ($\text{Bq}\cdot\text{kg}^{-1}$) in filtered water in oct.'90 and average values (underlined) as found in march '92 in the DELWAQ compartments.

5. ^{210}Po and ^{210}Pb dissolved in water

Dissolved in water, ^{210}Po concentrations between 0.1 and 0.5

Bq.m^{-3} and ^{210}Pb concentrations between 0.23 and 0.58 Bq.m^{-3} are found. The $^{210}\text{Po}/^{210}\text{Pb}$ ratio is, except one high value of 5.8 between 0.2 and 1.73. The concentration of both isotopes is lower as found in previous surveys (around 2 Bq.m^{-3} , (Berger and Eisma 1988).

Distribution of ^{210}Po along the North Sea coast:

^{210}Po concentrations as measured in particulate matter on the North sea and along the Dutch North Sea coast range from 19 to 171 Bq.kg^{-1} . In the centre of the English Channel the concentration is around 70 Bq.kg^{-1} , along the Dutch coast between 90 and 170 Bq.kg^{-1} . This confirms earlier measurements and conclusions (Berger and Eisma, 1988): ^{210}Po , originating from ore-processing plants in the Westerschelde and the Nieuwe Waterweg are, adsorbed on fine grained particulate matter, transported to the North Sea.

The low concentration of 19 Bq.kg^{-1} was found in a sample that consisted for 95% out of *Phaeocystis*.

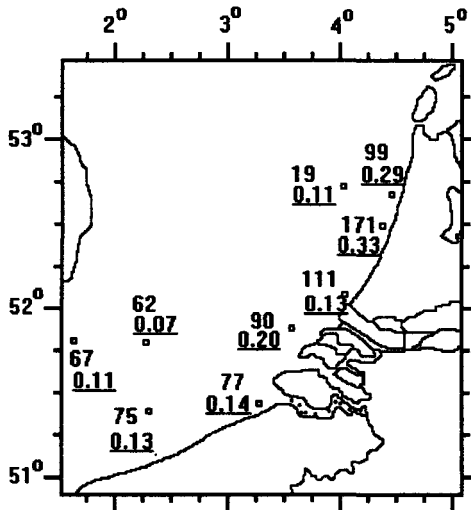


Figure 4. Concentrations of ^{210}Po in part.matter (Bq.kg^{-1}) and in filtered water (underlined, mBq.l^{-1}) in North Sea samples.

6. Conclusion

The ^{210}Po , ^{210}Pb and ^{230}Th isotope concentration in the sediment is more or less around the natural background ($< 100 \text{ Bq.kg}^{-1}$), with the exception of samples taken in the canal van Sas van Gent naar Terneuzen, the Sloehaven near Vlissingen and near BASF. Even in areas where fine material settles, $^{210}\text{Pb}_{\text{excess}}$ concentrations do not exceed the expected values based on the natural atmospheric ^{210}Pb flux.

^{210}Pb concentrations, adsorbed on particulate matter, are between $150\text{-}250\text{ Bq.kg}^{-1}$, which is higher than concentration as found in the North Sea, Oosterschelde and Waddensea in previous studies (Berger, G.W. & D. Eisma, 1988; Köster et al., 1990). ^{210}Pb and ^{210}Po concentrations, dissolved in water, are between 0.2 and 0.6 Bq.m^{-3} . This is lower as found in previous surveys (around 2 Bq.m^{-3}). It is concluded that the Westerschelde and its estuary is not a sink of ^{210}Pb . The extra input of radionuclides, originating from ore-processing plants, have a short residence time in the estuary and are, adsorbed on fine grained particulate matter, transported to the North Sea.

The results of this project were presented at the Radstomp 91 Symposium (Radionuclides in the study of marine processes, 9-14 September 1991, Norwich, UK), title: "Sources, distribution and radiological effects of ^{210}Po , ^{210}Pb , ^{226}Ra and Th isotopes in Dutch rivers and coastal waters related to the discharges of ore processing plants".

Netherlands Institute for Sea Research
PO Box 59
1790 AB Den Burg (Texel)
The Netherlands

G.W. Berger
March 1 1992

Literature

Berger, G.W. & D. Eisma, 1988a, Report of ^{210}Po en ^{210}Pb measurements in the Dutch coastal waters, rivers and Westerschelde estuary (in Dutch, VROM project) NIOZ report 1988-2

Berger, G.W. & D. Eisma, 1988b, Dating of sediments in the Westerschelde with the isotopes $^{134}\text{Cs}/^{137}\text{Cs}$ en ^{210}Pb . NIOZ report 1988-12 (RWS project, in Dutch)

Köster, H.W., P.A. Marwitz, G.W. Berger, A.W. van Weers, P. Hagel, J. Nieuwenhuize. RIVM Report 248476004, august 1990 (in Dutch) ^{210}Po and other natural radionuclides in Dutch aquatic ecosystems; a reconnaissance investigation.

Project 4

Head of project: *Dr. Galvão*

Objectives for the reporting period

Study of ^{210}Po and ^{210}Pb concentrations in the Tagus estuary in relationship with discharges from phosphate industry. Analysis of these radionuclides in water, suspended matter and bottom sediments to characterize enhancement of environmental levels of those radionuclides.

Study of ^{210}Po and ^{210}Pb distribution in the estuary of Mira river, not subjected to any industrial discharges, for comparison purposes.

Additionally, analysis of uranium in both estuaries as well as analysis of ^{210}Po and ^{210}Pb in biota from the Tagus estuary were performed.

Progress achieved including publications

The existence of a phosphate ore processing plant located in the south margin of the Tagus estuary, constitutes a typical scenario in this manufacturing industry. For more than 40 years, most of the phosphogypsum has been piled up on the river margin and waste water has been released into the Tagus estuary. Due to the potential radioecological impact of this industry [1] the present study of enhanced levels of uranium series nuclides in this area was undertaken.

1. Results

1.1 Phosphatic materials

The uranium decay series radionuclides are present in the phosphate ore, mainly imported from Marocco, in activity concentrations of 1 kBq kg^{-1} , in near radioactive equilibrium. In phosphogypsum ^{210}Po is present in concentrations of about 0.6 kBq kg^{-1} in radioactive equilibrium with ^{210}Pb . Concentration of ^{226}Ra is about 1 kBq kg^{-1} , whereas uranium concentration is 0.15 kBq kg^{-1} . At the present, gypsum stock-piles probably contain more than 2×10^6 tons of phosphogypsum. Estimated activities in the stockpiles are in excess of: $3 \times 10^{11} \text{ Bq}$ of ^{238}U , idem for ^{234}U , $2 \times 10^{12} \text{ Bq}$ of ^{226}Ra , and $1.2 \times 10^{12} \text{ Bq}$ of ^{210}Pb in radioactive equilibrium with ^{210}Po .

Analysis of waste water collected in several occasions directly at the pipe outlet, in 1990 and 1991, gave variable results for ^{210}Po : from 29 Bq kg^{-1} up to 465 Bq kg^{-1} (dry weight) in suspended matter. Surface sediment layer ($\sim 0.5 \text{ cm}$) collected during low tide (1990) in the close vicinity of the pipe outlet (0 to 0.2 km), displayed ^{210}Po concentrations ranging from 241 up to 1400 Bq kg^{-1} (dry weight).

1.2 The Tagus estuary

The granulometric composition of the bottom sediments in the Tagus estuary is quite variable, ranging from almost pure sand (98.5% sand) to fine muds (99.2% silt and clay). The organic matter content of sediments, ranging from 0.8% up to 21% of total sediment dry weight, was found to be significantly correlated with the sediment clay

content ($p < 0.01$).

^{210}Po concentrations in sediments analysed in total, range from 1 to 400 Bq kg^{-1} dry weight. The differences in ^{210}Po based in these concentrations are difficult to interpret. However, as ^{210}Po is practically absent in the sandy fraction, the variable percentage of sand in sediments was found to introduce large fluctuations in ^{210}Po concentrations based on total sediment. Measuring ^{210}Po in the $< 63 \mu\text{m}$ size fraction only, the ^{210}Po "dilution" effect produced by sand was largely eliminated. The ^{210}Po concentration in fine sediment particles corresponding to natural (mainly mineralogic) origin is nearly constant and independent of the size of % silt + clay fraction in the sediment. The distribution of ^{210}Po in bottom sediments ($< 63 \mu\text{m}$ size fraction) of the Tagus estuary is given in Fig. 1. ^{210}Po concentrations in the fresh water sediments, upstream in the Tagus, are identical to concentrations measured in the upper estuary and range between 16 and 51 Bq kg^{-1} (dry weight). Sediments in the mid estuary, excluding the south margin area, fall in the same range. Bottom sediments in the inlet channel and in the mouth of the estuary are composed almost exclusively by sand, with one exception, 105 Bq kg^{-1} , and, therefore, only ^{210}Po values for total sediment are available. The highest ^{210}Po concentrations measured are clustered around the Barreiro peninsula, with a maximum value of 1029 Bq kg^{-1} (dry weight).

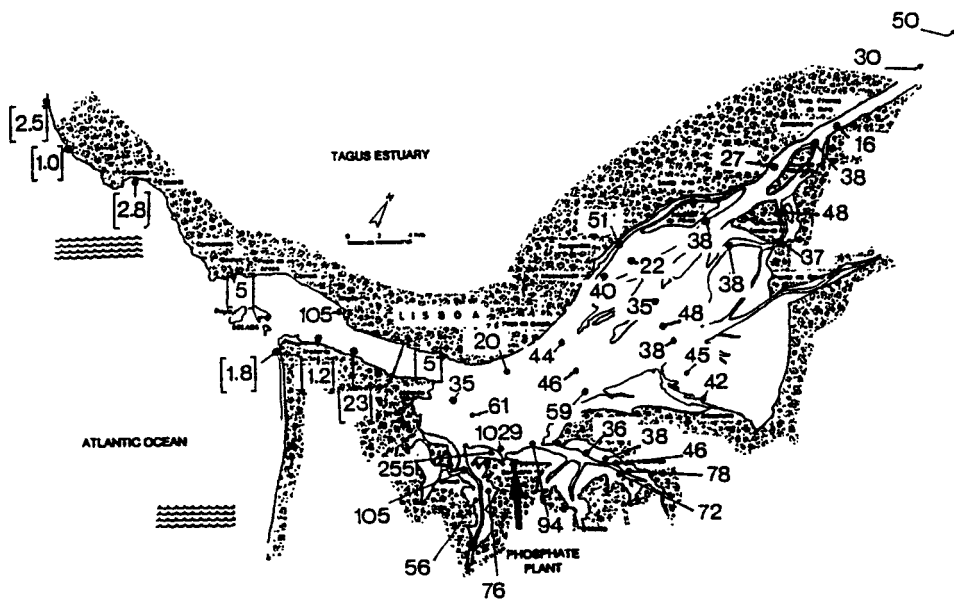


Fig 1. ^{210}Po concentration (Bq kg^{-1} dry weight) in $< 63 \mu\text{m}$ bottom sediment size fraction, collected during February-March 1991. Values in brackets correspond to ^{210}Po in total sediment, in almost pure sandy sediments.

The average concentration of the naturally-occurring ^{210}Po in the bottom sediments ($<63 \mu\text{m}$ fraction) was estimated as $50 \pm 21 \text{ Bq kg}^{-1}$ [3]. Concentration values above 100 Bq kg^{-1} (92 Bq kg^{-1} corresponds to 2σ confidence level) may be considered as enhanced and, likely, have accumulated ^{210}Po from industrial wastes.

^{210}Po concentration in suspended matter carried by the Tagus river into the estuary ranges between 42 and 64 Bq kg^{-1} dry weight. In the upper and mid estuary, ^{210}Po concentration range between 66 and 149 Bq kg^{-1} (excluding south margin), and in the inlet channel they range between 131 and 183 Bq kg^{-1} . Around the Barreiro Peninsula, in the south margin, concentrations were slightly higher ranging between 85 and 262 Bq kg^{-1} . As found for bottom sediments, enhanced ^{210}Po concentration in suspended matter was measured especially around the area with discharges by the phosphate industry.

Concentration of ^{210}Po in $0.45 \mu\text{m}$ -filtered water samples fluctuates between 0.2 and 0.4 Bq m^{-3} throughout the estuary, reaching 1 Bq m^{-3} in sea water at the mouth of the estuary. Unusually high values, of 8 and 46 Bq m^{-3} , were measured in winter (Feb. 91) near the Barreiro peninsula. In summer time (July/Aug. 1991) values in this area fluctuated between 0.46 and 7.3 Bq m^{-3} .

^{210}Po concentration in seaweeds (*Fucus*) collected around the Barreiro peninsula in February 1991, ranged from 10 to 20 Bq kg^{-1} (dry weight). These concentrations are only slightly higher than in samples collected at the mouth of the estuary ($2\text{-}13 \text{ Bq kg}^{-1}$). *Fucus* samples collected during the same season along the atlantic west coast of Portugal, displayed a mean concentrations of $18 \pm 8 \text{ Bq kg}^{-1}$ dry ($n=5$). However, one *Fucus* sample collected near the outlet of phosphate factory, in 1990 during phosphoric acid production, displayed 1348 Bq kg^{-1} .

^{210}Po and ^{210}Pb concentrations in mussels (*Mytilus*), barnacles (*Balanus*), shrimp and fish samples from the Tagus estuary were also measured [3].

1.3 The Mira estuary

Bottom sediments collected in 15 sampling stations display ^{210}Po concentrations with a mean value of $80 \pm 40 \text{ Bq kg}^{-1}$ (dry weight).

^{210}Po concentration in suspended matter in the estuary has maximal values in the vicinity of the maximum turbidity zone, which occurs roughly in the zone between 1 and 6 g L^{-1} salinity. This zone corresponds to the zone of hydroxide precipitation. After this zone, towards the mouth of the estuary, ^{210}Po concentrations in the suspended matter slowly increase again, and show a new drop at the mouth of the estuary. For the entire estuary the average concentration of ^{210}Po in suspended matter was $66 \pm 32 \text{ Bq kg}^{-1}$ (dry weight).

Concentration of dissolved ^{210}Po is very low in fresh water, around 0.1 Bq m^{-3} , increasing tenfold at the entrance of the estuary, before the maximum turbidity zone. Inside the estuary the concentration of dissolved ^{210}Po remains relatively stable at about $0.4\text{-}0.6 \text{ Bq m}^{-3}$ [3]. A similar fluctuation in ^{210}Po concentration, over the the transition zone from fresh water to brackish water, was noted in the Tagus.

2. Conclusions

The analyses of natural radionuclides in phosphorite, phosphate fertilizers and phosphogypsum, provided useful information about the nuclide fractionation during the industrial processing of phosphate rock. A significant proportion of the radioactivity

initially present in the phosphorite is transferred to the superphosphate fertilizers and to the phosphogypsum [4].

In the case of the phosphate plant located close to the Tagus estuary, most of the phosphogypsum has been recovered and stockpiled on the river margin. However, by runoff gypsum piles continue to deliver unknown amounts of resuspended gypsum and dissolved radionuclides into the estuary.

From our measurements it is clear that the Tagus river transports, from sedimentary deposits in the catchment basin, non negligible amounts of uranium series nuclides. The importance of this transport is highlighted through the comparison with Mira river. For instance, the average concentration of the naturally-occurring dissolved uranium in Tagus water entering the estuary is about 17 Bq m^{-3} of ^{238}U , while for the Mira river it is about 1 Bq m^{-3} .

A similar transport into estuaries takes place through the particulate phase, which is especially important for the less soluble ^{210}Po and ^{210}Pb nuclides. In the case of the Mira estuary ^{210}Po concentrations in suspended matter ($66 \pm 32 \text{ Bq kg}^{-1}$, $n=13$) are not higher than ^{210}Po concentrations in the fine fraction ($<63 \mu\text{m}$) of bottom sediments ($80 \pm 40 \text{ Bq kg}^{-1}$). However, in the case of Tagus estuary, where the average ^{210}Po concentration in fine ($<63 \mu\text{m}$) bottom sediments is $50 \pm 21 \text{ Bq kg}^{-1}$ (excluding samples from the vicinity of phosphate plant), the concentrations in suspended matter are generally higher not only around the Barreiro peninsula but also in the upper estuary and towards the mouth of the estuary. These higher concentrations probably originate in the dispersal of phosphogypsum-related radionuclides in this lagoon-type estuary.

At the present, samples from both estuaries under study are still being analysed for ^{210}Pb . Samples collected during summer time, under low river flux conditions, are also being processed for ^{210}Po and for ^{210}Pb . Research will be continued. It is hoped that a better understanding of the geochemical behaviour of these naturally-occurring nuclides can also be obtained.

References

- [1] Koster, H.W., Berger G.W., Weers A.V. van, Hagel P., Nieuwenhuize J., Marwitz P.A. (1991). Po-210, Pb-210, Ra-226, in aquatic ecosystems, anthropogenic sources, distribution and radiation doses in the Netherlands. Vth Int. Symp. on the Natural Radiation Environment, Salzburg (in press).
- [2] Carvalho, F.P.(1991a). Behaviour of ^{210}Po and ^{210}Pb in european marine environments. Application of bioindicators. First-year progress report . CEC Research Contract. Bi7-0006-C (DG XII). LNETI/DPSR, 23 pp.
- [3] Carvalho, F.P. (1992). ^{210}Po , ^{210}Pb and uranium in the estuaries of Tagus and Mira rivers (Portugal). Impact of releases from phosphate industry. Two-year Report.CEC Research Contract BI7-0006-C(DGXII). LNETI/DPSR-A-N^o 4 (III Serie), 34 pp.
- [4] Carvalho, F.P. (1991b). Phosphate fertilizers and natural radioactivity (In portuguese). Proceed. of the XII Nat. Symp. of the Port. Soc. of Chemistry. Coimbra, 10-13 March 1991, pp.451-454).

Contractor:
Laboratorio Nacional de Engenharia e Tecnologia Industrial
Departamento de Proteccao e Seguranca Radiologica
E. N. 10, P-2685 Sacavem, Portugal

Fernando P. Carvalho



BIOGEOCHEMICAL PATHWAYS OF ARTIFICIAL RADIONUCLIDES

Contract Bi6-339 - Sector A23

1) *Plocq*, SCOPE-RADPATH

Summary of project global objectives and achievements

1. Objectives

The RADPATH project has sought to elucidate, in an objective and dispassionate manner, the biogeochemical pathways of artificial radionuclides, following releases from the nuclear fuel cycle, reactor accidents, spillages or from the detonation of nuclear weapons, and to apply these findings to advance knowledge generally of biogeochemical cycling of chemical elements and their compounds. The project aimed to assemble and critically review current knowledge from the interdisciplinary field of environmental radioactivity, focusing upon those radioisotopes considered to be of most importance.

2. Work performed

Through a series of international workshops, which have involved key members of the scientific community, the RADPATH project has reviewed research concerning the present status of knowledge regarding the more abundant and toxic artificial radionuclides, and their environmental pathways. Besides purely physico-chemical processes, pathways involving uptake by biota and transfer through food-chains have been considered. Workshops have permitted both the presentation of latest research findings, combined with visits to sites of importance with regard to the study (e.g. Sellafield, U.K., Chernobyl and its environs, U.S.S.R.) and the opportunity to finalize draft manuscripts for a synthesis volume. Besides the three workshops organized by the Essex Unit (at the University of Essex, U.K., in 1989 and 1991 and the University of Lancaster, U.K. in 1990), RADPATH co-operation has been sought in connection with meetings in Suzdal, U.S.S.R., 1989; Luxembourg, 1990; Gomel, U.S.S.R., 1990; Puschino, U.S.S.R. 1991). RADPATH representatives have also been present at RADPATH-related meetings in Zeleny Mys, U.S.S.R., 1990; Sweden (BIOMOVS), 1990.

As a result of the programme a reference book in the SCOPE (Scientific Committee on Problems of the Environment) series is being published by John Wiley and Sons Ltd., and valuable international contacts have been promoted between researchers. Throughout the duration of the programme a Newsletter, produced on an approximately bi-monthly basis for circulation to about 500 recipients, has reported on the progress of the project and related issues.

As a non-governmental organization which has, nevertheless, permitted participation by scientists with access to official sources of information RADPATH enabled issues concerning man-made radioactivity to be addressed in an authoritative, objective and dispassionate manner, thereby providing impartial views on nuclear issues for both the scientific community and the interested public.

3. Results obtained

The results obtained as a consequence of the RADPATH programme are contained in a book summarizing the project. This volume presents the consensus among leading researchers in the international scientific community concerning the most significant sources and environmental pathways of man-made radionuclides. The magnitude and importance of radionuclide releases from the nuclear fuel cycle, from accidents (e.g. Kyshtym, Windscale and Chernobyl) and other sources are put into perspective and the effects of radioactivity from such sources upon non-human biota are assessed. Knowledge of environmental processes and biogeochemical cycling, which may be gained from the use of radionuclides as tracers, is discussed.

4. Conclusions of the investigator

As a result of the RADPATH programme it is anticipated that an influence on future research in the field of environmental radioactivity will be exerted, since the RADPATH book will identify serious gaps in knowledge and recommend topics requiring further research. It is envisaged that the project findings will be disseminated to a wide audience through translation of the RADPATH volume and summary papers into several languages. Increased awareness of the topic will be further promoted through media approaches.

There are also wider applications of the project's findings e.g. in advancing knowledge generally of biogeochemical cycling of chemical elements and their compounds. In addition, Chernobyl-related research has applications in assisting, for example, with research into the effects of burning oil in Kuwait through models developed for nuclear accident studies.

As a result of the RADPATH programme the value of establishing an independent, non-governmental organization to facilitate international collaboration and promote rapid exchange of information, thereby focusing research effort analyses, has been recognised. Although other organizations, both national and international, have an interest in the field of environmental radioactivity, none has recently attempted such a broadly-based activity as that undertaken by the RADPATH programme. RADPATH has successfully co-ordinated international research efforts in the interdisciplinary field of environmental radioactivity and, in particular, has promoted strong links with Soviet researchers involved in post-Chernobyl investigations. As a result of the RADPATH programme a valuable reference book has been produced and international collaboration has been facilitated. In order to maintain, and promote, co-ordination of international research efforts it is desirable that an independent, non-governmental, framework be established to permit continued collaboration. It has not, however, presently proved possible to secure funding for the establishment of such a programme.

Report on project activities

1. Introduction and overview

This report provides an account of SCOPE-RADPATH activities over the period from January to December 1991.

A major activity during this period was to convene the RADPATH Review and Synthesis Meeting at University of Essex, U.K. RADPATH representatives are also involved with a RADPATH-related meeting being held in Puschino, U.S.S.R., December 1991. Project activities have been directed towards the finalization and editing of draft manuscripts in connection with the final RADPATH report (which will form a volume in the SCOPE series of

publications), and maintaining information dissemination activities. Further details about these activities are provided below.

Invaluable assistance has been provided by the grant received from the Commission of the European Communities (CEC) which has permitted support of investigations into the biogeochemical pathways of artificial radionuclides, through technical workshops to examine and synthesize results from experimental and modelling research studies.

2. Workshops and meetings

2.1 Revisions to 1991 Work Plan

In accordance with the work plan contained in RADPATH's 1990 CEC Report, a Review and Synthesis Meeting was held at University of Essex, U.K. over the period 13-19th April 1991.

An additional meeting, which was not envisaged at the time of summarizing revisions to the 1991 work plan, involving the participation of RADPATH representatives is the "5th All Union Conference on Geochemical Pathways of Chernobyl Radionuclides", Puschino, U.S.S.R., 9-13th December, 1991.

Plans to convene a meeting following the publication of the RADPATH book were not pursued further during 1991, with emphasis instead placed on ensuring adherence to the publication schedule.

2.2 Review and synthesis meeting, April 1991

The RADPATH Review and Synthesis Meeting, held from 13-19th April, 1991, at the Wivenhoe Park Conference Centre, University of Essex, U.K., was organized by the Essex SCOPE Unit. The meeting comprised technical sessions devoted to presenting the findings of latest research, finalization of book manuscripts, and an Open Day to disseminate the findings of the project to a wider audience. In total, thirty-two participants from some ten nations, were present at the meeting, with an additional sixteen participants involved in the Open Day. Sir Frederick Warner (SCOPE-RADPATH Scientific Advisory Committee (SAC) Chairman), who chaired the technical plenary sessions, provided a review of the current status of the RADPATH programme. In the course of the meeting presentations on the latest research findings relating to Chernobyl, and terrestrial, aquatic and urban environment-related studies were given. An additional focus was the inter-connections of Chernobyl-related research and its wider applications (namely in assisting research connected with burning oil in Kuwait), in particular through the Open Day Meeting examining both the Aftermath of Chernobyl and Kuwait Oil Fires. Further discussions within atmospheric, terrestrial and aquatic sub-groups, provided the opportunity to finalize material for inclusion in the RADPATH synthesis volume. A report of this meeting, including summaries of the technical presentations and SAC Meeting Minutes, is provided in Appendix I.

2.3 Puschino Meeting, December 1991

The Puschino meeting, which is being chaired by Dr. L. Khitrov (RADPATH Scientific Advisory Committee Member), is being convened from 9-13th December 1991 in U.S.S.R. A total of 150 Soviet, and 25-30 non-Soviet scientists, including Prof. C. S. Shapiro (Lawrence Livermore National Laboratory/San Francisco State University, U.S.A.) and Dr. E. Voice (Consultant and Lecturer, Thurso, U.K.) as representatives of RADPATH, are expected to be present at the meeting. The main focus of this meeting concerns the problem of landscape-geochemical mapping. A meeting summary is contained in Appendix II.

3. Information dissemination activities

A Newsletter reporting on RADPATH-related topics has continued to be produced at intervals throughout the year by the SCOPE-RADPATH Unit. During 1991 further issues of the Newsletter have been prepared for distribution to some 500 individuals, including members of both the scientific community and the interested public.

Considering presentations given by RADPATH scientists, a number of interviews associated with interconnections of Chernobyl-related research, focusing on Kuwait oil fires, have been given by Sir Frederick Warner.

Various articles about the RADPATH programme and its related findings appeared in both local and national press following the RADPATH Open Day Meeting. These included reports in East Anglian Daily Times, The Evening Gazette and The Times.

As previously noted, in Section 1 above, in order to publicise the findings of the RADPATH programme a volume in the SCOPE series of publications is being finalized. This volume, reviewing the present state of knowledge on the environmental pathways of artificial radionuclides, comprises Chapters on: Sources, Case-studies of Significant Releases, Atmospheric Pathways, Terrestrial Ecosystems, Aquatic Pathways, Urban Environment, Dosimetry and Assessment of Environmental Effects, and Appendices (containing an introduction to radioactive processes, units, methods of analysis and a glossary of terms). Publication of the volume is expected next year. Further details of chapter topics and coordinators are provided in Appendix III.

4. Future workshops

There are presently no plans for any future meetings in connection with the RADPATH programme.

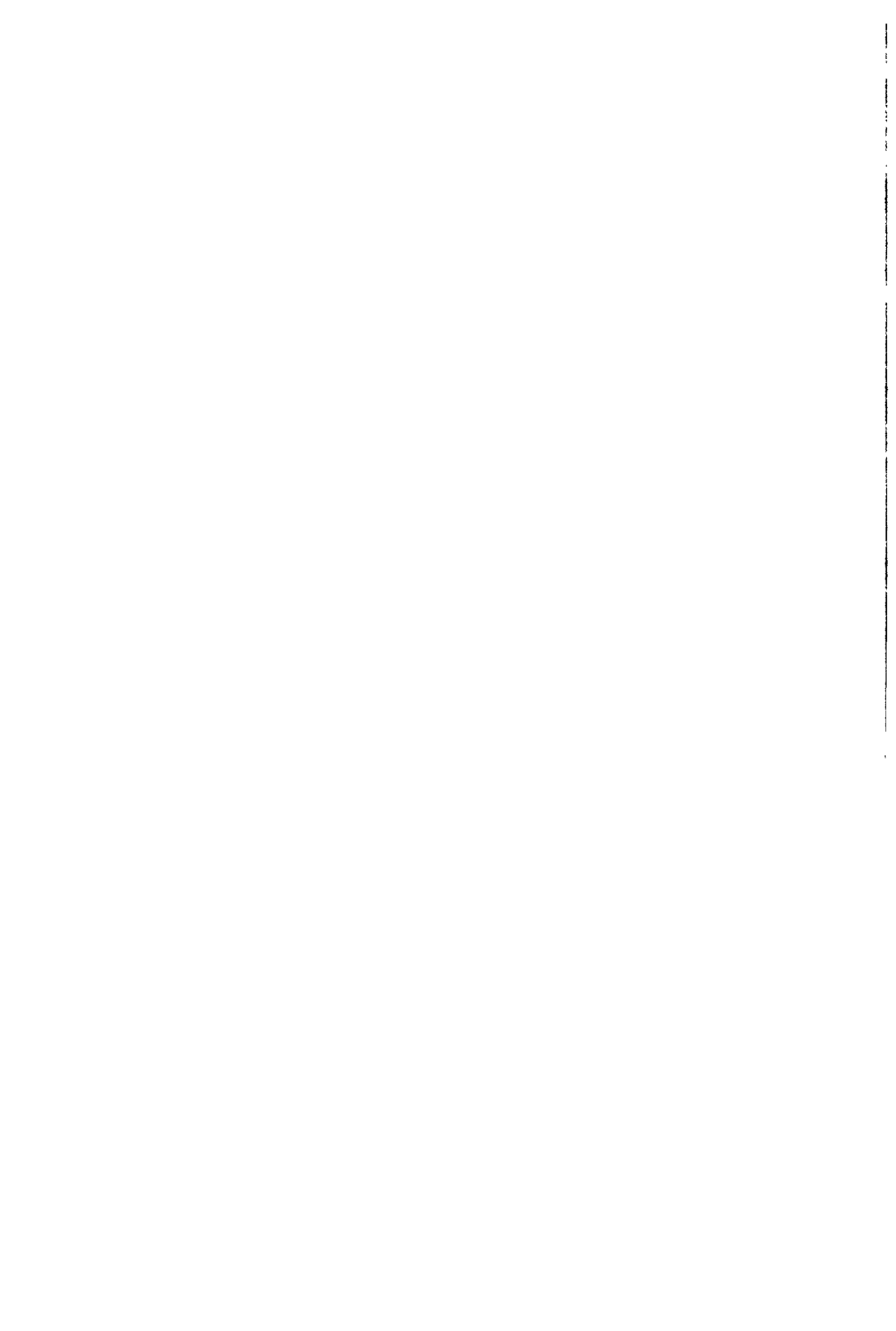
5. Project funding

Besides the financial support provided by the CEC, funding was obtained from The Leverhulme Trust (£ 54,900) to support a postdoctoral research assistant and part-time secretarial assistance in connection with the Essex Unit over the duration of the project. In addition, the University of Essex provided full use of its facilities and office space free of charge, and no charge was made for the time which Sir Frederick Warner and Prof. Roy M. Harrison devoted to the project. To assist with general project activities, grants of £ 1,000 and £ 10,000 were made by The Fellowship of Engineering and The Royal Society (London) respectively, and a grant of £ 2,000 was received from Japan via Dr. Ohkita. The Royal Society also provided supplementary funding, totalling just over £ 1,000, to cover per diem and additional accommodation expenses associated with the presence of five Soviet delegates in the U.K. prior to and following the First Case-study Meeting last year, and is providing the return travel costs required to permit Dr. Voice's participation in the Puschino Meeting. A further grant of £ 17,800 was obtained from The Wolfson Foundation towards case study meeting organization, to examine the pathways of radionuclides, particularly in connection with Sellafield discharges and the Chernobyl accident. The U.S.S.R. Academy of Sciences has also provided financial support covering, for example, expenses within the Soviet Union associated with meetings held there. Another source of support has been through the International Union of Radioecologists (I.U.R.) which has funded the attendance of several representatives to RADPATH meetings.

The application made to UNESCO's (United Nations Educational, Scientific and Cultural Organization) MAB (Man and Biosphere) programme, via Ms. Veronique Plocq (SCOPE Secretariat, Paris), did not prove successful.

6. RADPATH continuation programme: 1992-1994

The need for a continuation programme following the conclusion of the initial phase of the RADPATH programme in December 1991, after the publication of the synthesis volume, has been recognised and is presently under consideration. The value of continued maintenance of the Essex Unit with regard to enabling the promotion of international contacts and collaboration was noted at the RADPATH Review and Synthesis Meeting. The value of the contacts already established with the Soviet Union was acknowledged, the continued operation of the Unit as a rapid response organization considered necessary.



TRANSFER AND CONVERSION MECHANISMS OF H-3 AND C-14 COMPOUNDS IN THE LOCAL ENVIRONMENT

Contract Bi6-345 - Sector A23

1) *Dr. Bunnenberg* , Niedersächsen Inst. Radioökologie

Summary of project global objectives and achievements

Future fusion plants and tritium handling facilities will contain large amounts of tritium, mainly in the highly mobile HT form. Safety analyses and licensing of these facilities require dose calculations. Therefore, models have to be available to describe the environmental behaviour of tritium after chronic or accidental releases. With help of such models it would be possible to incorporate a high degree of passive safety in the design of fusion reactors, if the tritium inventory that could be released accidentally is reduced to a level which would not exceed dose limits.

Because of the higher radiotoxicity of HTO by four orders of magnitude the dose after an HTO release is higher than the dose after an HT release of the same activity amount. However, recent evaluations of environmental experiments have shown that the doses after the release of HT are lower only by a factor of 10 to 100 compared to those after an HTO release. This can be explained by the fact that HT is converted into HTO by soil microbiological processes and a secondary HTO area source is established in the downwind sector of the HT release point as a result of deposition processes to the soil. Therefore, HTO concentrations in the air and the related doses are essentially dependent on the HTO reemission rate of this area source. Furthermore, the reemission efficiency also determines the formation of HTO pools in the soil-plant system and the HTO clearance from the local environment. Reliable predictions of reemission rates of tritiated water from the soil on the basis of general or site-specific parameters are not possible until now, although essential for dose evaluations with help of appropriate models.

To investigate HTO reemission rates in this project experiments were performed with a special wind tunnel in which the air flows across the surface of soil columns under controlled conditions. Thus reemission processes were simulated, to obtain information on the time course of reemission rates under different soil physical and meteorological conditions and to compare the behaviour of HTO with that of H₂O.

These experiments show that the fate of the HTO molecules in the soil and at the interface between soil and atmosphere can be derived to a certain extent from the behaviour of the H₂O molecules. This is valid in case of increasing temperatures and wind speeds when HTO and H₂O emission rates increase correspon-

dingly. It has to be noted that the comparison of these rates requires equivalent calculation bases. The rate of evaporation of H_2O , which usually is expressed in mass of water per unit time, i.e. independent of the water supply, has to be calculated according to the reemission rate of HTO, which is defined as the portion of the momentary content that leaves the soil per unit time (e.g. % per hour).

Except for an isotopic effect, which can be neglected in these investigations, a similar behaviour of HTO and H_2O has to be expected, because all basic physical transport processes in the liquid or gas phase are the same in the soil and the air, whether the water molecules are tritiated or not. It follows that the meteorological and soil physical conditions, which lead to strong evaporation of H_2O , also cause high reemission rates of HTO.

In contrast to the similarity of the behaviour of HTO and H_2O molecules the respective release rates can differ significantly. Wind tunnel experiments with different tritium-free air humidities showed that the reemission rate of HTO exceeded the evaporation rate of H_2O . In principle, the reemission rate is higher than the evaporation rate by the same factor as the saturation pressure exceeds the saturation deficit of the ground level air. E.g. in experiments with an air humidity of 50% the HTO emission rate was about twice as much as the H_2O emission rate. Correspondingly, the specific activity of the emitted water was twice the specific activity of the soil water. This example shows that HTO reemission rates can not be deduced in direct relationship to the H_2O evaporation rates.

Consequently, the specific activity of the air humidity will approach that of the soil water as long as the resupply of activity from deeper soil layers is not limited. However, the adjacent transport processes can not be generalized in a simple manner, as the distributions and the availabilities of tritium and water in the soil and the aerodynamic exchange between the ground level air and the air in breathing height have to be considered.

To be able to predict the radiation dose, e.g. by inhalation, that results from exposure to a definite, contaminated soil surface under natural conditions, more research effort and model developments are necessary going beyond the behaviour of H_2O molecules, which is mainly coupled to the soil matrix and to the availability of energy for evaporation and, therefore, also determines the fate of the HTO molecules. The differences in the behaviour of H_2O and HTO at the soil/air interface are mainly characterized by the fact that the transport rates of each sort of gas are governed by their individual concentration gradients.

Project 1

Head of project: *Dr. Bunnenberg*

Objectives for the reporting period

Improvements of the wind-tunnel equipment by installation of an electronic control and data processing.

Experiments with homogeneously wetted and tritium labeled soil columns and variation of temperature and humidity of air and soil.

Experiments with different wind speeds.

Comparison between reemission and evaporation rates.

Progress achieved including publications

1. Methodology

Reemission processes are simulated with help of the combined device of a wind tunnel and a replaceable soil column. During the reemission phase air samples are collected by drawing the air through washing flasks, which contain a small, tritium free volume of water. After each run the soil columns are disassembled in horizontal layers. The air and soil samples yield time resolved HTO reemission rates and vertical soil profiles of moisture and HTO contents.

2. Results

In order to compare the emission of tritium and water the respective rates are expressed as parts per time unit, which are released of the momentary content of activity and water of the soil. The results presented here refer to experiments with loess soil homogeneously labeled with tritium and with an initial moisture content of 20 wt.%.

The soil and air temperatures were set at 20°C and the air humidity was about 20%. While the wind speed was varied from 0.03 m·s⁻¹ to 0.6 m·s⁻¹ the average evaporation rate of H₂O increased from 0.30(±0.01)%·h⁻¹ to 0.80(±0.03)%·h⁻¹, which is less than proportional to the wind speed. The average reemission rate of HTO increased from 0.37(±0.05)%·h⁻¹ to 1.00(±0.05)%·h⁻¹. Whereas the wind speed was enlarged by a factor of 18 the ratios between the HTO and the H₂O rates remained constant at about 1.2. This value represents also the specific activity ratio of the evaporized water to the soil water.

This ratio rises, if the humidity of the tritium-free air increases. Experiments with air humidities of about 50% yielded ratios of 1.8. While the HTO reemission rate remained at 0.41 (±0.07)%·h⁻¹, which was the same level as in experiments with

lower air humidity, the H_2O evaporation rate decreased to $0.23(\pm 0.03)\% \cdot \text{h}^{-1}$.

While the emission of HTO molecules exceeds that of the H_2O molecules proportionally, the specific activity of the soil water decreases to the same extent. Fig. 1 shows the depth profile of the specific activity normalized to the initial activity of the soil. This profile refers to the group of experiments performed at air humidities of about 50%.

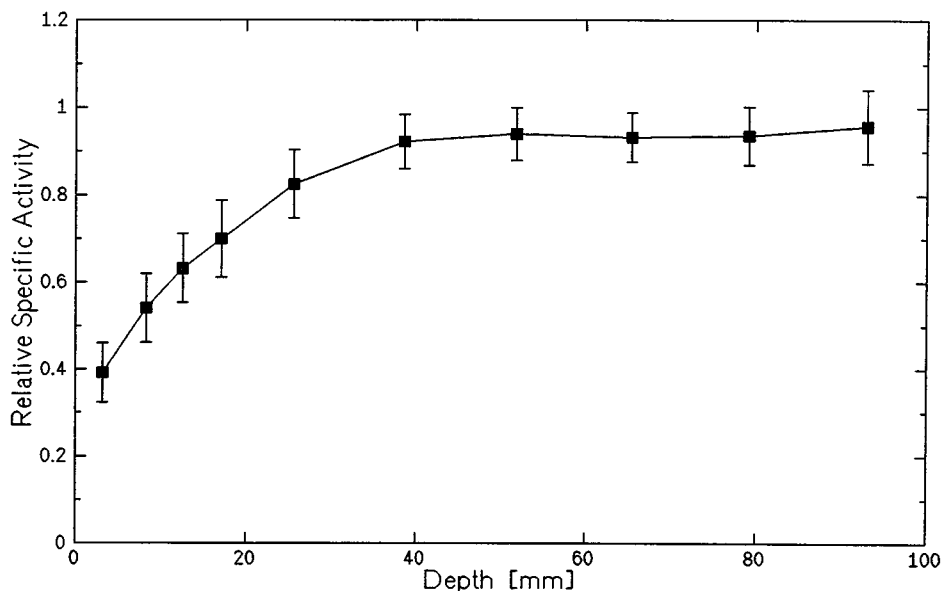


Fig. 1: Depth profile of the relative specific activity of the soil water after a reemission phase of 90 h into a tritium-free atmosphere with an air humidity of 50%.

Below roughly 40 mm the specific activity is not significantly different from the initial value, i.e. the relative specific activity is 1, although all soil layers lost about 20% of the initial moisture. From this it is concluded that tritium moves together with the soil water to the soil surface, where the transformation to the gas phase takes place and the release from the soil compartment happens differentiated at individual rates for each sort of molecules.

The profile of Fig. 1 is the result of a typical diffusion process. The rapid decrease of HTO at the soil surface generates a concentration profile that causes the transport from deeper soil layers. In fact, the diffusion coefficient that can be related to the slope of the profile beneath the soil surface was about $6 \cdot 10^{-10} \text{ m}^2 \cdot \text{s}^{-1}$. This value corresponds to one third

of the diffusion coefficient of HTO in water. The reduction can be attributed to the limited space between the soil grains that is available for the exchange process.

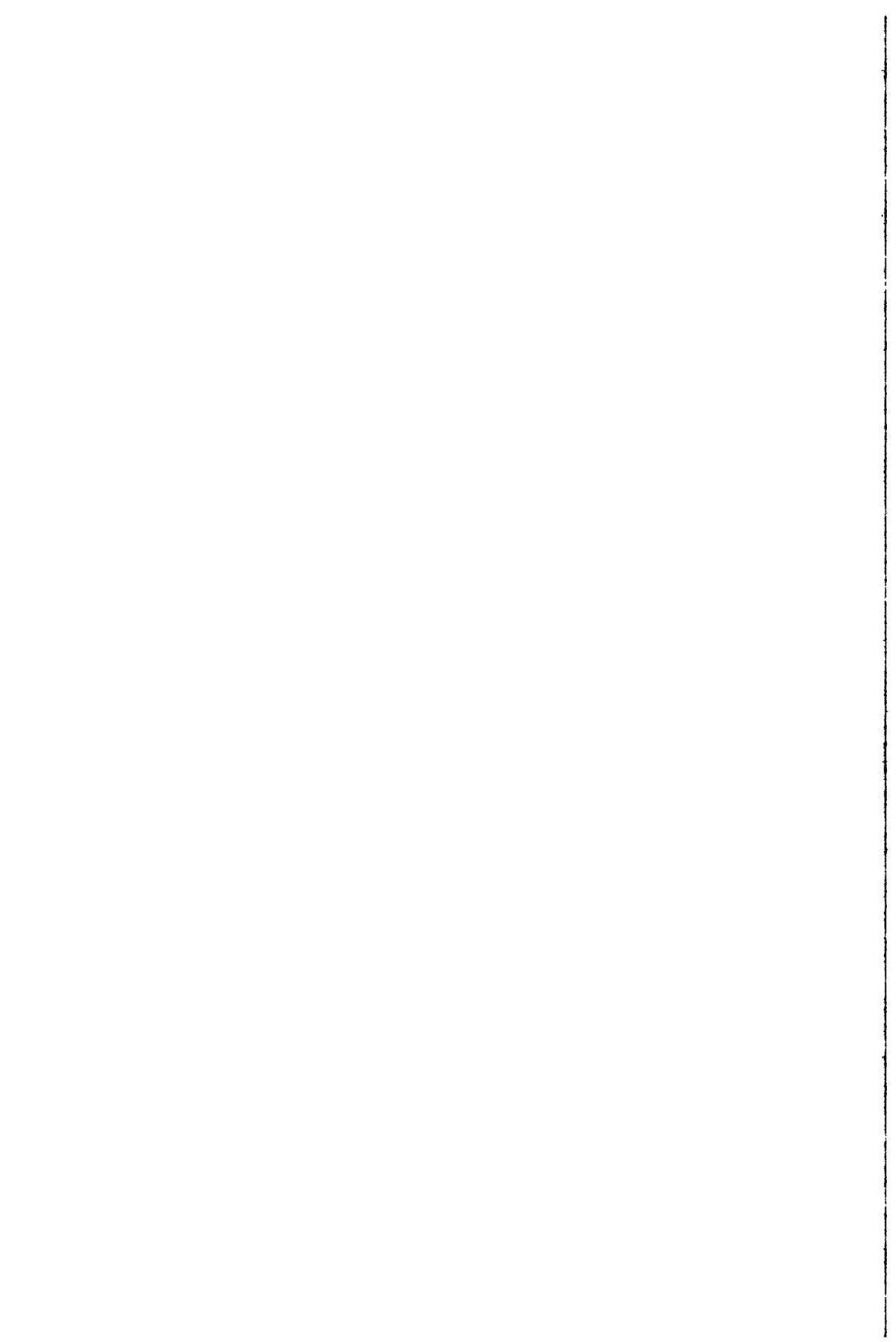
3. Discussion

The exposition of a soil to an atmosphere with lower specific activity yields an increased release rate of HTO compared to H₂O. Therefore, the specific activity of the air approaches that of the soil water. But the question, what burden results from being exposed to a definite, contaminated soil, is not yet answered. Although the conditions have been characterized that lead to different release rates of HTO in contrast to H₂O, namely the individual concentration gradients, the adjacent transport processes can not yet be modeled. These processes are related on the one hand to the distribution and availability of tritium and water in the soil and on the other hand to the aerodynamics of the exchange between the air layers at ground level and at breathing height. Further investigations are planned with non homogeneous soil profiles that are generated by deposition processes and the results will be compared with field experiments.

Publications

Täschner, M., Schubert, K., Bunnenberg, C.:
Tritium Reemission from Soil in a Wind-Tunnel.
NIR-Jahresbericht 1991 (annual report), in press.

Täschner, M., Bunnenberg, C., Gulden, W.:
Maximum Permissible Amounts of Accidentally Released Tritium
Derived from an Environmental Experiment to Meet Dose Limits
for Public Exposure.
Fusion Technology, 20, 58 (1991).



THE BIO-AVAILABILITY OF LONG-LIVED RADIONUCLIDES IN RELATION TO THEIR PHYSICO-CHEMICAL FORM IN SOILS

Contract Bi7-011 - Sector A23

1) *Lembrechts*, RIVM - 2) *Wilkins*, *Nisbet*, NRPB
3) *Sandalls*, AEA Technology Harwell Laboratory - 4) *Cremers*, Univ. Leuven (KUL)

Summary of project global objectives and achievements

1. Global objectives

Two of the major aspects affecting the behaviour of radionuclides in soil/plant systems, were studied : 1) availability in the soil liquid in relation to major characteristics of the soil and 2) the efficiency of the uptake process. The nuclide of main interest is Cs-137, although some experiments on transuranics were done as well.

The speciation study concerned both naturally (well-characterised sites in Cumbria) and artificially labelled soils (eg. lysimeters), and accentuated the quantification of chemical forms in the soil and soil solution and an adequate description of solid-liquid distribution. The soil chemical parameters which regulate the specific interception potential of Cs, were quantitatively characterised in a broad range of soils, with particular attention being given to reversibility aspects and aging effects. Amongst others ultrafiltration techniques were used to investigate the association of radionuclides with different molecular size fractions in solution and to monitor time dependent changes in speciation. By conducting batch equilibrium experiments and by studying soil solution and its associated radiolabelled soil the effects of various treatments on sorption were determined under laboratory conditions. As a result, it will be possible to estimate the effect of amendments on radiocaesium availability in problem soils.

The first part was complemented with experiments on bioaccumulation. Transfer along the soil / soil solution / plant pathway was studied under controlled conditions in phytotrons, and validated with references to field observations on upland soils from Cumbria. The time trend in uptake, im- and remobilization of radiocontaminants was studied throughout the growing period in order to explain changes in transfer and to extend the information derived from the detailed soil studies. Uptake from soils was compared with uptake from nutrient solutions in order to better distinguish between soil-specific and plant-specific phenomena.

2. Achievements

2.1 Sorption/desorption of radiocaesium and radiostrontium

□ A systematic study was carried out on the overall cation exchange capacity (2-106 meq/100g), the clay content (<0.1 to 40%), the organic matter content (<1 to 97%) and the radiocaesium sorption and desorption properties of a variety of soils. The sorption behaviour of strontium was studied for a limited number of soils.

The following techniques were used:

□ In order to study the relation between sorption behaviour and number of specific sites

(micaceous frayed edge sites (FES)), the aspecific sites have been masked with agents like AgTu, followed by Cs-adsorption in a solution with or without KCl or NH_4Cl . (It is hypothesized that the FES are responsible for this long-term immobilization of radio-caesium and that irreversible sorption is proportional to the number of FES).

□ Desorption of radio-caesium was studied by the addition of a resin to a dispersed, contaminated soil, as a result of which a constant gradient was maintained between soil and solution (infinite batch method).

□ A modified batch equilibrium technique was used to evaluate rapidly the effect of various treatments on solid-liquid distribution of radio-caesium and radiostrontium.

Results:

□ The limited variation of the Cs/K selectivity coefficient at 'zero' Cs loadings and the narrow range of the Cs/K selectivity coefficient in comparison with the Cs/ NH_4 selectivity coefficient suggested that soils of widely different texture would have a common Cs binding characteristic, i.e. comparable FES.

□ A determination of the clay content of a soil without analysing the levels of both monovalent (K^+ and NH_4^+) and divalent cations (Ca^{2+} and Mg^{2+}) does not allow the availability of radio-caesium to be estimated. Indeed, although not having an influence on sorption of radio-caesium, Ca and Mg were observed to have a pronounced effect on reversibility of sorption.

□ The affinity of radio-caesium for specific sites (FES) is high as compared with affinity for regular exchange sites (RES). As a result most Cs will be on the FES, unless specific sites are almost absent and CEC is high. Even within one soil class the estimated contribution of RES to Cs interception can, however, easily vary by one order of magnitude. Since desorption of Cs from RES is much faster than from FES and the TF is supposed to mainly depend on readily exchangeable Cs, large differences in TF are to be expected on soils belonging to the same soil class.

□ A comparison of aged and freshly contaminated soil samples demonstrated that the rate of 'irreversible' fixation rapidly decreases with time.

□ Batch-equilibrium experiments on three field moist soils with divergent characteristics showed K_2SO_4 to decrease the Cs/K ratio in the soil liquid; lime did not affect this ratio, whereas ammonium increased it. The treatments studied had no effect on the Sr/Ca ratio in the soil liquid phase of these soils which were already well supplied with calcium.

2.2 Speciation of radio-caesium, radiostrontium and transuranics in soil solution

□ The overall *in situ* solid-liquid distribution of radio-caesium in various Cumbrian soils was comparable to that of the transuranics. The solid-liquid distribution of radiostrontium was about two orders of magnitude lower.

□ Ultrafiltration using Amicon hollow fibre cartridges proved to be a useful technique for determining the association of radionuclides with different molecular size fractions in soil solution.

□ All Cs and Sr were present in the low molecular weight fraction (< 3 kD), whereas large proportions of Pu and Am were associated with the high molecular weight material (> 10 kD).

□ No simple relationship was found between the radionuclides associated with the low molecular mass fraction in soil solution and TF. This was partly due to the importance of other factors such as competition from stable isotopes, and nutrient analogues at the root surface.

2.3 Transfer of radiocaesium to plants grown on hydroponics

- Plants were grown on modified Steiner nutrient solutions for 1 to 4 weeks.
- Within the ranges studied NH_4^+ (0 - 0.89 mM), K^+ (0.06 - 16.7 mM), stable caesium (a background level of some tens of nM - 8 μM) and pH (4.5 - 7.5) had no or very limited effects on the uptake of radiocaesium by lettuce.
- The TF decreased with increasing Ca concentration. When the concentration of all other nutrients was proportionally changed at the same time, no supplementary increase or decrease in TF was observed.
- The TFs to spinach and lettuce, both grown on Steiner nutrient solutions, were of the same order of magnitude. The TF to the roots of spinach was somewhat smaller than the TF to the shoot.
- The data suggested that the effects of changes in mineral nutrition of a crop on transfer of radiocaesium were of secondary importance in comparison with the effects of changes in soil characteristics on availability.

2.4 Transfer from soil to plant

- The range of TFs and of a number of soil solution characteristics as observed in the field (semi-natural peat soils only) and under controlled conditions (sandy, agricultural soils) are given in table 1.

Table 1 TFs and a number of characteristics of the soil liquid for two groups of experiments.

	CUMBRIA: SEMI-NATURAL, FIELD	LABORATORY: AGRICULTURAL SYSTEM
CONDUCTIVITY (mS/cm)	0.04 - 0.23	0.4 - 6.2
K (meq/l)	0.003 - 0.02	0.5 - 42.2
Ca (meq/l)	0.03 - 0.35	2.6 - 30.0
Cs ($\text{Bq.l}^{-1}/\text{Bq.kg}^{-1}$)	$6,5 \cdot 10^{-5}$ - $2,9 \cdot 10^{-5}$	$7 \cdot 10^{-4}$ - $2,7 \cdot 10^{-2}$
pH	3.8 - 5.1	4.4 - 7.3
TF (Bq.g^{-1} pl/ Bq.g^{-1} soil)	0.1 - 0.7	0.028 - 1.24

- The soil solution of the Cumbrian field plots was collected at monthly intervals using porous ceramic cups. The TFs for ^{90}Sr , ^{239}Pu and ^{241}Am were determined together with that for ^{137}Cs .
- The range of TFs on Cumbrian field plots was comparable to that on potted soils. The fraction of radiocaesium dissolved in the soil liquid of the field plots was, however, substantially lower than that of potted soils, as were the levels of K and Ca. Since changes in K-level did correspond with changes in Ca-level, it was impossible to attribute of the resemblance of the TF on both systems to an effect of either of these elements. Differences in ageing time and plant species furthermore limit a straightforward comparison of these data. TFs for ^{137}Cs , ^{90}Sr , ^{239}Pu and ^{241}Am were at the upper end of mean values given by the IUR (1989) for peaty soils, despite extensive sorption of the radionuclides on the solid phase (K_d 10^3 - 10^5).
- The effect of Ca and K on transfer of Cs from soil to lettuce under controlled condi-

tions seemed to be of the same order of magnitude as their effect on transfer from nutrient solutions to lettuce, as long as the soil liquid was not depleted.

Other groups collaborating actively on this project

Although an analysis of the effect of the characteristics of the 'source term on sorption and transfer was not part of this project some attention was given to this problem on two of the progress meetings. They were attended by B. Salbu from the Agricultural University of Norway and/or A. Konoplyev from the Institute of Experimental Meteorology in Obninsk, Russia. They contributed by giving information on time dependent changes in extractability and mobility of radiocaesium and -strontium in a number of soils contaminated by deposits from the Chernobyl accident in comparison with the behaviour of calcium and stable caesium, strontium. The agricultural University furthermore contributed by assisting in the ultrafiltration work done on the lysimeter soils.

Project 1

Head of project: *Dr. J. Lembrechts*

Objectives for the reporting period

Three groups of experiments were planned in order to test whether the availability of radionuclides in soils can be explained and estimated on the basis of the characterization of the soil liquid phase:

- * The TF of caesium from nutrient solution to plant was compared with the TF from soil liquid to plant. The chemical parameters which most pronouncedly affect root uptake of radiocaesium (^{134}Cs) were varied.
- * The effect of changes in solid-liquid distribution of ^{134}Cs on its accumulation by earthworms was monitored.
- * Some illustrative experiments with plants and earthworms had to be done in order to test the relation between soil, soil liquid and organism for another radioelement, i.e. neptunium.
- * In addition, the effect of stable caesium on the transfer of ^{134}Cs was briefly checked.

Progress achieved including publications

Only part of the objectives of this research period could be met, because of 1) the insignificant growth of the crop on one of the soils and 2) the low survival of earthworms in a number of the experiments. As a result the last objective and part of the second one are postponed to the next contract period.

1. Experiments with plants

1.1 Uptake from nutrient solutions (NS)

Because of the very limited possibilities of measuring stable caesium in our samples, its potential, non-linear effect on the TF of radiocaesium was studied by adding different quantities to stable caesium the NS.

Non-linearity of caesium uptake was e.g. suggested by Shaw & Bell (J. Environ. Radioact. 10, 213-231 (1989)). The background level was estimated to be some $\mu\text{g.L}^{-1}$ on the basis of 1) measurements of AEA in the context of this project and 2) data given by Coughtrey & Thorne ("Radionuclide distribution ...", Vol. 1, Balkema, Rotterdam (1983)). No inhibitory effect of an additional 1 mg.L^{-1} could, however, be observed (Figure 1).

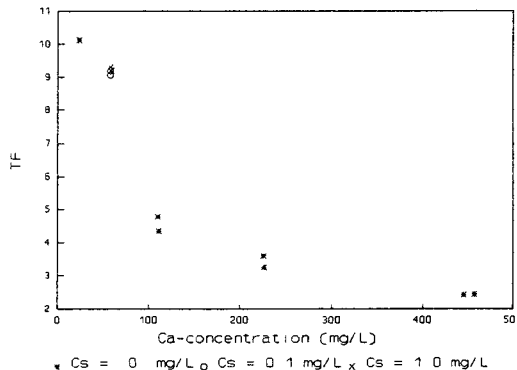


Figure 1: TF of ^{134}Cs as a function of the Ca concentration of the solution for 3 different levels of stable Cs.

1.2 Uptake of Cs from soils

1.2.1 Materials and methods

Experiments complementary to those on NS described in the previous progress report were done. Lettuce seedlings (*Lactuca sativa* L. cv. Ysbergsla) were grown for 3-4 weeks on three different sandy soils, as described elsewhere (Lembrechts et al., Plant and Soil 125, 93-69 (1990)). Variations in soil solution composition were induced by applying various levels of fertilizer (0.1 - 0.75 g.kg⁻¹), Ca(OH)₂ or KOH (0 - 3.0 g.kg⁻¹). Because of the frequently discussed effect of K and Ca on the uptake of Cs and its sorption at the soil exchange complex, most attention was given to these elements. Experiments in which factors such as clay and organic matter content are changed to quantify their effect on solution to plant transfer, are currently under investigation. The soil liquid was removed by centrifugation with an immiscible liquid (chloroform) (Mubarak & Olsen, Soil Sci. Soc. Am. J. 40, 329-331 (1976)).

Transfer data and observed ratios (O.R.) are expressed on the basis of the concentration in the soil liquid phase.

1.2.2 Observations and conclusions

* The observed ranges of pH, conductivity, K- and Ca-concentration in the soil liquid were comparable to those studied on NS (Table 1). Plants grown on soils had a higher Ca content than those grown on NS, their K content was usually lower.

Table 1: Ranges of a number of characteristics of NS, soil liquid and plant for the two groups of experiments (FW=fresh weight, DW=dry weight, * = in meq.L⁻¹, ** = in meq.g⁻¹).

liquid phase	Cond. ms.cm ⁻¹	Bq.mL ⁻¹	K*	Ca*	Mg*	NO ₃ **	pH
soil	0.42-6.3	0.07-2.7	0.53-42	2.6-80	1.7-28	16-47	4.3-7.3
NS	0.34-4.3	5.1-5.5	0.49-17	1.1-33			4.5-7.9

plant	FW (g)	Bq/g	TF	K**	Ca**	O.R.
soil	0.18-7.5	0.23-10	1.3-62	86-260	22-90	0.019-0.70
NS	0.26-13	13-52	2.3-10	150-225	10-24	0.011-0.26

* The unambiguous, inhibitory effect of Ca on Cs uptake as it was observed on NS (N), could not be reproduced on soils (S) (Figure 2). The TFs on soil were comparable to or higher than those on NS. The trend suggested in the previous progress report could not be confirmed; no regular effect of K on transfer could be observed either (within the concentration range studied on NS, K has a minor effect on uptake of caesium).

* At first it seemed improbable that the absence of a relation between the ambient level of Ca and the TF of

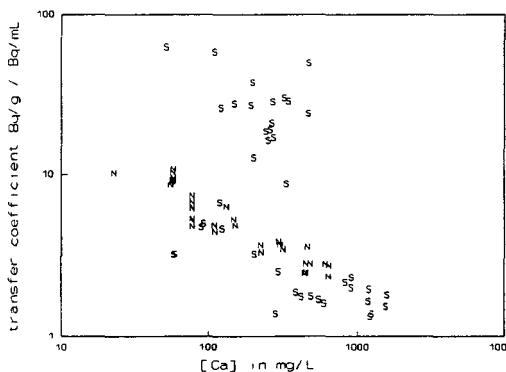


Figure 2: TF of ¹³⁴Cs as a function of the Ca concentration of the nutrient solution or soil liquid.

^{134}Cs was due to the fact that TFs were calculated on the basis of actual levels of ^{134}Cs in the soil liquid without taking replenishment of the liquid phase into account. Indeed, less than 10% of the total quantity of freely dissolved ^{134}Cs was accumulated by the above ground part of the crop. In some cases, however, when soil liquid to plant transfer was high, about 50% of the freely dissolved ^{134}Cs was accumulated. On the basis of literature data (eg. Nishita et al., Plant and Soil 17, 221-242 (1962)) the quantity accumulated by the roots is estimated to be about the same. As a result, desorption of ^{134}Cs from the solid phase must have pronouncedly influenced the soil liquid concentration of ^{134}Cs measured at the end of the experiment. In these cases the TF can not be derived from the actual level of radiocaesium in the soil liquid. In order to correctly quantify the effect of uptake by the roots, their Cs content has to be measured.

2. Experiments with earthworms

2.1 Materials and methods

Earthworms (*Eisenia andrei*) were grown on manure at an ambient temperature of 20-22° C. Adult worms were preincubated in uncontaminated soil for 24hrs. Ten worms were put on containers with 0.4 - 1.0 kg of contaminated soil (moisture content 22%) for a period of 5 - 40 days (temp. 15 - 17° C). Variations in soil liquid concentration of ^{134}Cs were induced by changing the level of fertilization. At the end of the experiments the worms were placed on a wet filter paper for 2x24hrs to allow the gut to empty, frozen at -18° C, dried and digested in HNO_3 . The same characteristics of the soil liquid were analysed as in case of experiments with plants. The desorption yield, using 1M NH_4Ac as desorbing agent, was measured at the beginning and at the end of the experiment. Uptake of ^{134}Cs was studied as a function of the level of ^{134}Cs in the soil liquid phase and of time. Concentration factors are given in $\text{L.g}^{-1}\text{DW}$, i.e. they are based on the soil liquid concentration of ^{134}Cs .

2.2 Results and conclusions

- * The average of recorded concentration factors for freshwater worms is 10 (Coughtrey & Thorne, "Radionuclide distribution...", Vol. 1, Balkema, Rotterdam, 1983). In our experiments the TFs varied between 9 and 30 (70).
- * Activities in worms rose fastly and a balance was achieved within a few days (Figure 3). Changes in the soil liquid concentration of ^{134}Cs resulted in changes in TF (Figure 4). This may be due to effects of other elements on transfer or to the fact that the availability of ^{134}Cs is not reflected by its level in the soil liquid phase. Experiments on soils with different texture are planned to further study this relationship.
- * The presence of earthworms in the soils resulted in an increased conductivity and higher caesium levels in the soil liquid. The extractability, however, decreased in the course of the experiment (Table 2).

Table 2: Ranges of the relative change (result at the end of the experiment / result at the beginning) in extractability of ^{134}Cs and in pH, conductivity and concentration of ^{134}Cs of the soil liquid in the course of a representative experiment with earthworms.

fraction desorbed by 1M NH_4Ac	0.52 - 0.96
fraction in solution	0.79 - 2.01
pH	0.93 - 1.00
Conductivity	0.96 - 2.35

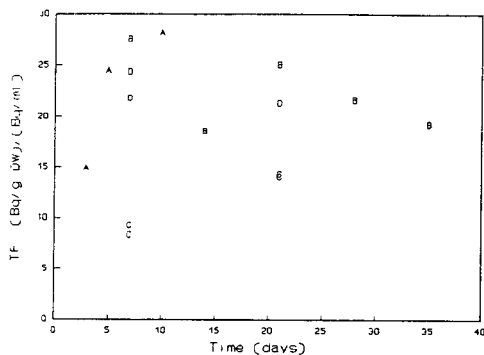


Figure 3: TF of ^{134}Cs to earthworms as a function of time for 4 different experiments.

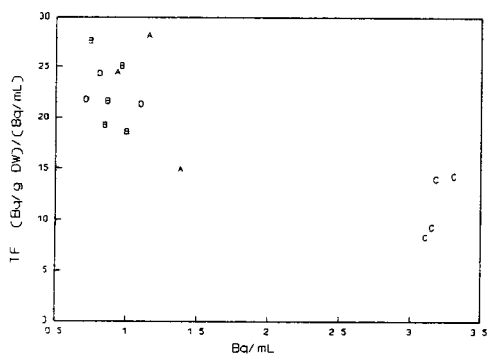


Figure 4: TF of ^{134}Cs to earthworms as a function of its level in the soil liquid, for 4 different experiments.

Publications

Lembrechts J. A review of literature on the effectiveness of chemical amendments in reducing the soil-to-plant transfer of radiocesium and radiocaesium. Science of the Total Environment, in press.

Noordijk H., van Bergeijk K.E., Lembrechts J. & Frissel M.J. Impact of aging and weather conditions on soil-to-plant transfer of radiocesium and -strontium as analyzed by a nonparametric method. J. Environ. Radioactivity 15, 277-286 (1992)

Van Bergeijk K.E., Noordijk H., Lembrechts J. & Frissel M.J. Influence of pH, soil type and soil organic matter content on soil-to-plant transfer of radiocesium and -strontium as analyzed by a nonparametric method. J. Environ. Radioactivity 15, 265-276 (1992)

Project 2

Heads of project: *B.T. Wilkins - A.F. Nisbet*

Objectives for the reporting period (May 1991 - June 1992)

- (i) To complete one full year of sampling and analyses of soil, vegetation and soil solution from Cumbria for ^{137}Cs , ^{90}Sr , ^{239}Pu and ^{241}Am as well as measurements of stable Cs, K, Ca, pH and conductivity on selected samples.
- (ii) To conduct batch equilibrium studies to determine the effect of common agricultural treatments on ^{137}Cs and ^{90}Sr sorption/desorption behaviour in loam, peat and sand soils.
- (iii) To complete ultrafiltration studies on the molecular size distribution of ^{137}Cs , ^{90}Sr , ^{239}Pu and ^{241}Am in soil solution from loam, peat and sand soils, and to finish paper for publication.

Progress achieved including publications

(i) To investigate possible mechanisms for the sustained bioavailability of radiocaesium in upland soils in Cumbria, four soil types (an acid brown earth, deep peat, peat ranker and improved peat ranker) were selected for detailed study involving the measurement of:

- (a) Radiocaesium in soil, soil solution and vegetation;
- (b) Exchangeable K, Ca, and NH_4 in soil;
- (c) Stable Cs in soil and soil solution;
- (d) K, Ca, NH_4 and H in soil solution.

As these Cumbrian soils also contained elevated activity concentrations of ^{90}Sr , ^{239}Pu and ^{241}Am these radionuclides were determined in the same samples collected for radiocaesium analyses. All data are complete for the period July 1990 - December 1991.

Radionuclide uptake by plants depends on the concentration and availability of the radionuclide ion in the soil solution and on the ability of the solid phase to replenish the ion in solution when it becomes depleted. Radionuclide availability to plants depends on the physical and chemical form of the radionuclide as well as on the concentration of other ions that might compete for uptake by plant roots.

Activity concentrations of ^{137}Cs , ^{90}Sr , ^{239}Pu and ^{241}Am in all soil solutions were very low and varied within a small range (Table 1). Those for ^{137}Cs were below the detection limit (ie. $< 15 \text{ mBq l}^{-1}$) for all soils except the peat ranker. In contrast, activity concentrations in the associated soils are much higher (Table 2), suggesting extensive sorption of the radionuclides on the solid phase. The availability of these radionuclides to plants was assessed from their concentrations in pasture, which were determined from samples collected in May and September 1990, and May 1991. Soil-to-plant concentration ratios (dry weight plant:dry weight soil basis) for ^{137}Cs and ^{134}Cs were similar for all three organic soils (ie. {1-8} E-1) and around an order of magnitude higher than for the acid brown earth. The ratios observed in these organic soils were at or above the upper end of the range of mean values given by the IUR (1989) for peat soils of all kinds. Complementary measurement data suggest that this high relative availability may be partly attributable to little or no competition from either potassium or stable caesium ions at the soil water - plant root interface, as indicated by:

- (a) Very low levels of exchangeable K in these organic soils ($0.5\text{-}0.6 \text{ meq } 100\text{g}^{-1}$ dry weight) when compared to agricultural soils ($35\text{-}55 \text{ meq } 100\text{g}^{-1}$ dw);
- (b) Very low concentrations of potassium in soil solution ($< 1 \text{ mg l}^{-1}$ in all samples) when compared to agricultural soils ($> 10 \text{ mg l}^{-1}$);
- (c) Very low levels of total stable Cs in these soils ($0.4\text{-}0.7 \text{ mg kg}^{-1}$ dw) when compared to a "typical" UK soil (6.0 mg kg^{-1} dw);
- (d) Very low levels of stable Cs in soil solutions ($5\text{-}15 \text{ ng l}^{-1}$).

Soil-to-plant concentration ratios for ^{90}Sr were well within the range observed (IUR,1989) for mineral soils ({0.9-3.8} E+0) and organic soils ({0.9-6.0} E-1). Those for ^{239}Pu ({0.6-7} E-2) and ^{241}Am ({0.3-2} E-1) were above the range of mean values given by the IUR (1989). These high values were attributed

to either foliar contamination or to the non-linear uptake of these non-nutrient ions at the low activity concentrations found in these soils

TABLE 1 Activity concentrations of ^{137}Cs , ^{90}Sr , ^{239}Pu and ^{241}Am in Soil Solutions

mBq l⁻¹

	^{137}Cs	^{90}Sr	^{239}Pu	^{241}Am
ABE	< 15	11-48	0.1-3.1	0.1-0.4
DP	< 15	18-45	0.1-1.7	0.1-0.4
PR	15-67	19-64	0.1-1.7	0.2-0.3
IPR	< 15	21-32	0.1-1.0	0.1-0.2

n = 8 samples

TABLE 2 Activity concentrations of ^{137}Cs , ^{90}Sr , ^{239}Pu and ^{241}Am in Soils (0-10 cm)

Bq kg⁻¹ dw

	^{137}Cs	^{90}Sr	^{239}Pu	^{241}Am
ABE	1230	9.6	1.6	1.3
DP	2500	25.3	10.9	3.5
PR	2300	13.7	13.5	5.5
IPR	1410	30.0	2.0	1.8

(ii) A series of batch equilibrium experiments to investigate the effects of sulphate of potash, garden lime and ammonium sulphate on the distribution of ^{137}Cs , ^{90}Sr and their stable nutrient analogues between solid and liquid phases of loam, peat and sand soils has been completed.

Soil-based chemical treatments (inorganic fertilisers and ameliorants) can reduce the transfer of radionuclides to plants by either increasing the fixation of the radionuclide in a non-available or less available form, or by modifying the solid-liquid equilibrium of various ions in soil to increase the concentration of stable nutrient analogues (1,2). Either mechanism decreases the ratio of radionuclide : stable nutrient analogue in the soil solution which should lead to a reduction in radionuclide uptake by the plant. The extent to which this happens depends on the solubility of the applied compound and on the physical and chemical characteristics of the soil itself. Batch equilibrium experiments may be used to study changes in solid-liquid equilibria in response to different chemical treatments.

The batch equilibrium experiments conducted made use of field moist soils, their associated soil solutions and fertiliser treatments corresponding to normal and five times normal application rates i.e. 200 and 1000 kg K ha⁻¹, 100 and 500 kg N ha⁻¹ and 3 and 15 T ha⁻¹ lime. Changes in solid-liquid equilibria induced by applications of potassium, calcium and ammonium-based fertilisers to the soil were reflected in the changes in activity concentrations of ^{137}Cs and ^{90}Sr , and concentrations of potassium, calcium and ammonium ions at the end of equilibration (3). Ratios of $^{137}\text{Cs}^+:\text{K}^+$ and $^{90}\text{Sr}^{2+}:\text{Ca}^{2+}$ concentrations in the liquid phase were determined for each fertiliser treatment. Sulphate of potash decreased $^{137}\text{Cs}^+:\text{K}^+$ ratios in the liquid phase of all soil types and in the peat in particular (Table 3). It has no adverse effects on $^{90}\text{Sr}^{2+}:\text{Ca}^{2+}$ ratios. In contrast, the ammonium treatment increased $^{137}\text{Cs}^+:\text{K}^+$ ratios in the liquid phase of all soil types and in the sand in particular (Table 4). Again, there was no adverse effect on $^{90}\text{Sr}^{2+}:\text{Ca}^{2+}$ ratios. Garden lime was not effective at decreasing $^{90}\text{Sr}^{2+}:\text{Ca}^{2+}$ or $^{137}\text{Cs}^+:\text{K}^+$ ratios in the liquid phase of any of the soil types studied. This was attributed to the low solubility of garden lime and the fact that these soils had previously received large amounts of calcium via irrigation.

The modified batch equilibrium technique used in this investigation proved to be a promising method for evaluating rapidly the immediate effect of different soil treatments and treatment rates on solid-liquid equilibria in soils. This small scale screening procedure enables potentially useful soil-based countermeasures to be identified and selected for use in follow-up soil and plant studies in the field or under controlled conditions

TABLE 3 Effect of sulphate of potash on $^{137}\text{Cs}:\text{K}$ and $^{90}\text{Sr}:\text{Ca}$ ratios in the liquid phase

	K^+	$^{137}\text{Cs}^{++}$	$^{137}\text{Cs}:\text{K}$	Ca^+	$^{90}\text{Sr}^{++}$	$^{90}\text{Sr}:\text{Ca}$
Loam (control)	3.9	0.6	0.15	170	48.8	0.29
Loam (+ K)	77.5	1.4	0.018	190	57.7	0.30
Loam (+ 5K)	440.0	2.3	0.005	250	75.9	0.30
Sand (control)	3.6	0.9	0.25	60	19.3	0.32
Sand (+ K)	72.5	1.4	0.019	90	27.4	0.30
Sand (+ 5K)	420.0	3.2	0.008	90	43.6	0.48
Peat (control)	0.6	1.4	2.3	145	23.6	0.16
Peat (+ K)	37.5	1.9	0.05	125	27.1	0.22
Peat (+ 5K)	215.0	3.3	0.02	205	37.9	0.18

TABLE 4 Effect of sulphate of ammonia on $^{137}\text{Cs}:\text{K}$ and $^{90}\text{Sr}:\text{Ca}$ ratios in the liquid phase

	K^+	$^{137}\text{Cs}^{++}$	$^{137}\text{Cs}:\text{K}$	Ca^+	$^{90}\text{Sr}^{++}$	$^{90}\text{Sr}:\text{Ca}$
Loam (control)	4.3	1.5	0.34	160	49.6	0.31
Loam (+ NH_4)	8.0	2.4	0.30	180	55.3	0.31
Loam (+ 5NH_4)	11.3	5.1	0.45	280	70.6	0.25
Sand (control)	3.4	0.6	0.18	60	18.7	0.31
Sand (+ NH_4)	7.8	2.1	0.27	70	24.9	0.36
Sand (+ 5NH_4)	10.8	6.4	0.59	100	37.2	0.37
Peat (control)	0.5	1.1	2.0	145	22.2	0.15
Peat (+ NH_4)	1.0	3.4	3.3	165	24.0	0.15
Peat (+ 5NH_4)	1.3	5.1	3.3	225	34.6	0.15

$^+ \text{mg l}^{-1}$

$^{++} \text{Bq l}^{-1}$

(iii) The investigation into the molecular size distribution of ^{137}Cs , ^{90}Sr , ^{239}Pu and ^{241}Am in soil solution extracted from loam, peat and sand soils using hollow fibre ultrafiltration has been completed (4). As the soil solution is the intermediary phase in the soil-to-plant transfer of radionuclides, its physical and chemical composition plays a vital role in determining radionuclide uptake by plant roots. For example, it is likely that low molecular mass species would be more mobile and bioavailable than high molecular mass species. A feasibility study carried out in 1990 in collaboration with the Agricultural University of Norway suggested that hollow fibre ultrafiltration could be used to determine the distribution of radionuclides with different molecular mass fractions. A more comprehensive collaborative study making use of three diverse soil types from NRPB's lysimeter facility was carried out in 1991.

Ultrafiltration of soil solution from loam, peat and sand soils was performed using Amicon hollow fibres with a nominal molecular weight cut off of 10 and 3 kilodaltons (kD). The association of ^{137}Cs , ^{90}Sr , ^{239}Pu and ^{241}Am with different molecular size fractions of the soil solution was related to radionuclide uptake by a cabbage crop grown in the same three lysimeter soils but over a different time scale. The results showed that in all the soils studied, ^{137}Cs and ^{90}Sr were present in low molecular weight forms (< 3 kD) and as such were potentially available for uptake by the cabbage. In contrast, a large proportion (61-87%) of the ^{239}Pu and ^{241}Am in the soil solution was associated with colloidal and high molecular weight material. This association of ^{239}Pu and ^{241}Am with higher molecular weight material could be related to their low soil-to-plant transfer in the cabbage crop, particularly for peat soils. However, no simple relationship was found between the proportion of the activity associated with low molecular weight species and the corresponding soil-to-plant transfer factor. This might be expected since not all species with molecular masses of < 3 kD would be equally available for uptake, and factors such as competition from other ions for uptake at the root surface have not been taken into account. In order to improve understanding of the relationship between activity concentrations of radionuclides in soil solution and uptake by plants, further characterisation of the low molecular weight fraction of soil solution is required.

Publications

- (1) Nisbet, A. F. (in press) Effect of soil-based countermeasures on solid-liquid equilibria in agricultural soils contaminated with radiocaesium and radiostrontium. REACT Workshop, 1-4 October 1991. Science of the Total Environment.
- (2) Nisbet, A. F., Konoplev, A.V., Shaw, G., Lembrechts, J.F., Merckx, R., Smolders, E., Vandecasteele, C.M., Lönsjö, H., Carini, F. and Burton, O. (in press). Application of fertilisers and ameliorants to reduce soil to plant transfer of radiocaesium and radiostrontium in the medium to long term - a summary. REACT Workshop, 1-4 October 1991. Science of the Total Environment.
- (3) Nisbet, A. F., Mocanu, N. and Shaw, S. (in preparation). Modified batch equilibrium technique - a rapid laboratory method to predict the effects of agrochemical countermeasures on solid-liquid equilibria in soils contaminated with radiocaesium and radiostrontium.
- (4) Nisbet, A. F., Salbu, B. and Shaw, S. (in press). Association of radionuclides with different molecular size fractions in soil solution: implications for plant uptake. Journal of Environmental Radioactivity.

Project 3

Head of project: *Dr. F.J. Sandalls*

Do plants differentiate between k and cs in root uptake?

Introduction

In the event of a severe nuclear accident resulting in contamination of soils with radiocaesium, it would be advantageous to

- (i) know or be able to test for the sensitivity of the soils with respect to soil-to-plant transfer of radiocaesium
- (ii) to be able to conduct a soil test and thereby determine how much potassium must be added to the soil to give a certain reduction in soil-to-plant transfer of the contaminant radiocaesium.

It is well known that the addition of potassium to soils reduces the soil-to-plant transfer of caesium, but the degree to which plants preferentially take up say K at the expense of Cs has never been established. Recent experiments with excised roots of *Agrostis capillaris* and *Calluna vulgaris* clearly demonstrated that uptake of caesium increased as the supply of potassium decreased (Jones *et al.*, 1991). Handley and Overstreet (1961) demonstrated that excised barley roots took up progressively less ¹³⁷Cs from a solution as the concentration of potassium was increased, so that ¹³⁷Cs uptake in the presence of 40 mg litre⁻¹ K was less than 10% of the uptake when potassium was absent.

In an earlier experiment (as part of this CEC/DEN project), the ratio of potassium to non-radioactive caesium was measured in various parts of tomato plants grown in a commercial hydroponic (NFT) system. The stable K was measured by atomic absorption and the Cs by neutron activation analysis. The results are shown in Table 1.

Table 1 - Potassium and Caesium in Tomato Plants - August 1990

	K (mg/gdw)	Cs* (mg/gdw)	Ratio K/Cs
Fruit	38 ± 2.4	0.14 ± 0.02 x 10 ⁻³	2.7 x 10 ⁵
Shoot	45 ± 2.4	0.17 ± 0.04 x 10 ⁻³	2.6 x 10 ⁵
Calyces	29 ± 1.4	0.012 ± 0.0007 x 10 ⁻³	2.4 x 10 ⁶
	K (mg/ml)	Cs (mg/ml)	
NFT Before	319 ± 20	0.000875 ± 0.0778	3.6x10 ⁵
NFT After	307 ± 20	0.00145 ± 0.212	2.1x10 ⁵

The results, within experimental error, indicated no preferential uptake of either Cs or K by the fruit or shoots since the ratio K/Cs was essentially the same in the tissues as in the NFT solution. The calyces showed an apparent preference for potassium over caesium.

The relative uptake of Cs and K by three different plant species

Experimental

In earlier experiments, we experienced difficulties in measuring the very small amount of non-radioactive caesium in plant tissue. For these experiments therefore, we chose to use ^{134}Cs as a tracer for non-radioactive caesium.

Three different plant species have been grown using a nutrient solution in a fibrous growing medium. The nutrient solution contained ^{134}Cs . The amount of non-radioactive caesium added with the ^{134}Cs was very small and negligible in an experiment designed to show relative updates by the various plant species. In any case, the experimental conditions were the same for all three plant species and the K/Cs ratios would therefore be comparable.

The plant species used were cabbage, spinach and calendula. The plants were all grown from seed on a fibrous medium kept thoroughly wetted with the nutrient solution containing the ^{134}Cs tracer.

The plants were harvested after 5 weeks, dried to constant weight, ground and analysed for ^{134}Cs by gamma ray spectrometry. The dried material was then oxidised in redistilled nitric acid and analysed for potassium by atomic absorption.

Results

The results of the analysis of the plant tissues are shown in Table 2.

Table 2 - Ratio K/Cs in plant tissues grown in nutrient solution

Plant Species	Ratio $\frac{\text{K(ppm)}}{\text{Cs (cpm s}^{-1}\text{)}}$
Cabbage	5.6
Spinach	4.2
Calendula	6.1

Clearly the three different plant species have all shown a similar relative affinity for K and Cs.

References

Jones, H.E., Harrison, A.F., Poskitt, Jan M., Roberts, J.D. and Clint, Gill (1991). The effect of potassium nutrition on ^{137}Cs uptake in two upland species. *J. Environ. Radioactivity*, 14, 279-294.

Handley, R. and Overstreet, R. (1961). Effect of various cations upon absorption of carrier-free caesium. *Plant Physiol.*, 36, 66-9.

Project 4

Head of project: *Dr. A. Cremers*

Objectives for the reporting period

1. A systematic characterization study of soils in terms of specific sorption potentials for radiocaesium
2. The identification of problem soils on the basis of soil chemical characterization
3. Radiocaesium desorption and the effect of aging on radiocaesium fixation
4. Radiocaesium uptake in plants in a controlled environment

Progress achieved including publications

1. Specific radiocaesium sorption potential of soils

A large number of soils (about 60) have been characterized in terms of overall cation exchange capacity (CEC) and specific radiocaesium interception potential, defined as the product of the number of micaceous frayed edge sites (FES) and the trace selectivity coefficient of Cs to K in the FES: $[FES] \cdot K_c(Cs/K)$. This quantity is measured by making use of the silver-thiourea masking technique and is represented by the symbol $[K_{DmK}]$.

The soils studied cover a very wide range in textural properties (sand-clay), CEC values (2-100 meq/100g) and organic matter (OM) content (up to 97%). The series includes a broad set of agricultural soils (including samples from lysimetric studies at NRPB and RIVM), brown earth soils (Cumbria) and peat soils originating from western Cumbria, Ireland (Cavan and Donegal county) and North-East Scotland (Glenshaugh research farm).

Table I shows a summary of characterization data.

Table I. A survey of CEC (meq/100g) and $[K_{DmK}]$ values (in meq/g) for the series of soils studied

Soil Type	CEC (range)	$[K_{DmK}]$ (range)
Agric. (sandy podzolic)	2-18	0.1-0.4
Agric. (loamy sand-clay)	10-35	1-10
Brown earth (20-30% OM)	20-35	1.2-3.5
Forest (10-30% OM)	12-40	0.15-1.5
Peat (80-90% OM)	70-100	0.065-.3
Peat (>95% OM)	100-106	0.01-.02

It is apparent that $[K_{DmK}]$ values may vary by some three order of magnitude and that within each group, quite large differences may occur. For all soils, $[K_{DmN}]$ values were measured as well and it appeared that $[K_{DmK}]/[K_{DmN}]$ ratios systematically varied in the range of 4-7, as was also found in reference micaceous clays. This finding demonstrates the action of the specific sites (sometimes present at very low level) in which the NH_4 ion is 4 to 7 times more Cs-competitive than K. In addition extensive studies have

demonstrated that pH (>4), Ca and Mg have no direct effect on radiocaesium sorption and that the solid/liquid partitioning can be reasonably well predicted on the basis of m_K , m_{NH_4} and $[K_D m_K]$ values.

2. The identification of problem soils

Soil chemical availability of radiocaesium can be expected to be related to the partitioning between the FES and the regular exchange sites (organic, mineral) RES. Such partitioning can be estimated on the basis of $[K_D m_K]$ values and the interception potential of the RES. The latter quantity can be written as the product $\{CEC\} \cdot Z_K \cdot K_c (Cs/K)$ in which Z_K refers to the K-loading in the RES and $K_c (Cs/K)$ to the Cs/K selectivity coefficient in the RES. In the calculations, Z_K was taken 0.05 and $K_c (Cs/K) = 1$, i.e. no discrimination between Cs and K. The results of these calculations are summarized in Table II in terms of (the range of) percentages of radiocaesium, expected to be present in the RES. The lower limit was obtained by combining the upper limit in $[K_D m_K]$ and lower limit in CEC; upper limits in RES interception were obtained by combination of the lower limit in $[K_D m_K]$ with upper limit in CEC.

Table II. Estimate of radiocaesium interception (%) in the regular ion exchange sites in soils

Soil group	% Radiocaesium in RES(range)
Sandy (podzolic)	0.25-8
Loam-clay	0.05-1.7
Brown-earth	0.3-1.5
Forest	0.4-13
Peat (80-90%OM)	10-43
Peat (>95% OM)	70-84

It is apparent that the critical factor is the ratio FES/CEC and that only in cases where combinations occur of very low $[K_D m_K]$ and high CEC values, significant fractions of radiocaesium can be expected to be present in the RES. Experimental evidence in support of these calculations was obtained on the basis of desorption studies using bulky ions (such as bis-quaternary ammonium ions: BTM-6). Such ions displaced very small amount ($\pm 1\%$) of radiocaesium in soils of low OM content whereas in peat soils, significant displacement yields of caesium could be achieved. Additional evidence for radiocaesium with the FES is also apparent on the basis of kinetics. Unlike regular ion exchange reactions, which are characterized by "half-life" values of the order of a minute, radiocaesium desorption is a slow process which may continue for days. It appears that the rate-limiting factor of the process is the built-up of radiocaesium concentration in the liquid phase.

3. Radiocaesium availability: a new methodology

A new procedure has been developed for measuring radiocaesium availability in soils. It is based upon an "infinite bath" scenario and obviates the limitations encountered in the 1M NH_4 -procedure. The radiocaesium-labelled soil is equilibrated with a dispersion of an ion exchanger showing radiocaesium sorption properties strongly exceeding those of the soil studied. Usually such equilibration is carried out in a $10^{-3}M$ solution of either K^+ or NH_4^+ . As a result, the liquid phase radiocaesium is trapped in the ion exchanger, thus leading to a break-up of the soil-solution equilibrium. This generates a desorption flux from the soil into the liquid phase, characterized by "near-zero" levels of radiocaesium (hence the term

"infinite bath"). Usually, such equilibration is carried out for 24 hrs (end-over-end shaking) although in some cases, shorter equilibration times are used. The ion exchanger is then replaced by a fresh sample and the procedure can be repeated any number of times. The process is monitored by counting the activity collected in the ion exchanger. At the termination of the experiment, residual activity in the soil is monitored as well and the result can be expressed in terms of cumulative desorption yield. The number of treatments required to generate reasonably well-defined desorption plateaus can empirically be established. In general, five treatments (usually covering one week) are adequate although in some cases longer desorption periods are required.

Either the ion exchanger or the soil may be enclosed in the dialysis membrane. In some cases where phase separation is easy, such as humic acids, the ion exchanger may be dispersed directly in the solution and the process can be monitored by counting the humic acid solution. The amount of ion exchanger to be used is critical. In order to establish adequate boundary conditions, it is necessary that $K_D^e \cdot m^e > 10K_D^s \cdot m^s$ (e referring to ion exchanger and s to soil; m refers to the mass used in the desorption experiment). In general, we have conditions corresponding to $K_D^e \cdot m^e / K_D^s \cdot m^s = 50$ to 100.

In the early phases, use was made of sulphonic acid resins such as K^+ or NH_4^+ Dowex ($K_D = 5 \cdot 10^3$ ml/g in $10^{-3}M$ K or NH_4). This limits the possibilities to relatively small size laboratory-labelled soil samples. More recently, the methodology has been upscaled by making use of ammonium-copper-hexacyanoferrate (Giese granulate, Fachgebiet Medizinische Physik, Hannover). This material shows exceedingly high K_D values or radiocaesium ($5 \cdot 10^5$ ml/g in $10^{-3}M$). By using this material, it has now become possible to study large size field-contaminated samples.

Figure 1 shows two examples of radiocaesium desorption plots in a commercial humic acid (Fluka) and four forest soils (Belgium). It is apparent that in the humic acid, 100% desorption is accomplished within minutes ($t_{1/2} = 1$ minute), whereas in the forest soils, desorption yields are obtained in the range of 15-30%.

The procedure has been applied to a broad range of agricultural soils which had been thoroughly characterized in terms of specific radiocaesium interception potentials and radiocaesium selectivity pattern in the FES. Such properties were quite similar in every respect. Figure 2 shows the results of a study on the effect of aging (wet conditions) in radiocaesium desorption in 13 agricultural soils. It is seen that desorption yields may vary between rather wide limits (15 to 85%) and that aging effects for periods of up to 9 months have a limited effect on desorption yield. In particular, it appears that very significant fixation processes occur, even for short aging times and in systems characterized by low FES capacity.

A similarly erratic pattern was found for a set of soils (sandy-podzol, loam, clay) samples from RIVM lysimeter experiments (Cs-137 contamination: 1983). Figure 3 shows a comparison of radiocaesium desorption yields in freshly contaminated soils and for the field-radiocaesium (aging time: ± 8 years).

For freshly contaminated soils, the statistical averages of availability are 67% (± 2) for podzols, 34 (± 10)% for loamy soils and 23(± 2)% for clay soils. The aging effects however are quite significant: statistical averages are 24(± 2)% for podzols, 11(± 6)% for loam soils and 10 (± 2)% for clay soils.

In conclusion, it is of interest to make a comparison of desorption yields obtained by the infinite bulk methodology and displacement by 1 M KCl and 1M NH_4Cl . The results are shown in figure 4 for five forest soils. It is apparent that in all cases, significantly higher displacement yields are

obtained in the infinite bath scenario (in spite of a three order of magnitude lower ionic strength) sometimes by a factor of 3. Moreover, it is apparent that significantly higher displacements are obtained in the case of K as compared to NH_4 . The erratic pattern in desorption behaviour is in sharp contrast with the coherence in radiocaesium sorption patterns. Recent evidence obtained in a reference illite clay and sediments have indicated that sorption irreversibility may be promoted by low PAR values (PAR: m_K/m_{Ca+Mg}).

4. Hydroponic experiments

Some preliminary experiments have been performed to test growth rate and reproducibility in transfer factors of radiocaesium in spinach plants. Grow chamber conditions are: 12 hrs/day, day temperature: 18°C; night temperature; 15°C, relative humidity: 75%, light intensity: 65000 lux. So far, four experiments have been performed: two runs on a Steiner growth medium and two on a diluted (1/2) Steiner solution. The relative growth rate of the plants in the exponential phase was quite constant in the four runs: $0.396(\pm 0.006)\text{day}^{-1}$. Table III shows a summary of TF factors as a function of age (expressed w.r. of the day of seeding) for the two growth media. TF values are the averages of five (young plants) to ten (older plants) measurements which were obtained on resp. composite samples or individual plants. Cs-137 concentration was 10 Bq/ml.

Table III. TF values for spinach plants in a Steiner and a Steiner 1/2 growth medium; standard deviations shown in parenthesis

Age days	Steiner		Steiner	
	shoot	root	shoot	root
14	2.45(1.8)	2.20(.08)	3.44(.15)	2.56(.02)
18	2.50(.13)	1.75(.07)	3.03(.17)	2.31(.22)
21	3.09(.27)	1.56(.05)	4.48(.38)	2.15(.10)
24	2.99(.32)	2.26(.43)	4.80(.65)	2.61(.03)
27	3.26(.43)	1.72(.16)	4.60(.78)	2.44(.19)
28	3.23(.50)	1.65(.16)	5.05(.86)	2.48(.34)

It is apparent that TF values for the shoot are higher in the diluted Steiner solutions: the average ratio is 1.50 ± 0.08 . This may be due to the lower K concentration in the Steiner 1/2 solution, or the higher Ca concentration in the Steiner solution or a combination of both. Moreover, it is seen that for the shoot, a slight increase occurs in TF with age the factor amounting to about 1.3 to 1.4 from day 14 to day 28.

Publications

Wauters J., Sweeck L., Valcke E., Elsen A., Cremers A.: Availability of radiocaesium in soils: a new methodology. Sci.Total Environment (in press)

Valcke A., Cremers A.: Sorption-desorption dynamics of radiocaesium in organic matter soils. Sci.Total Environment (in press)

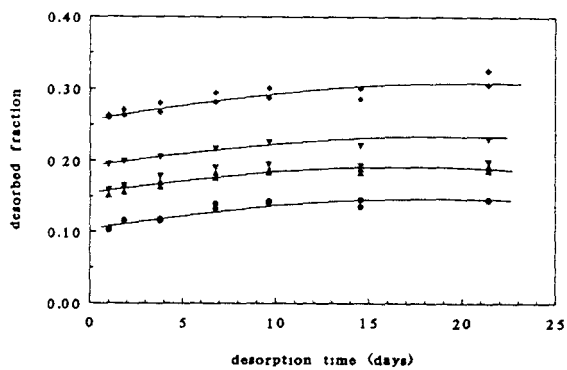
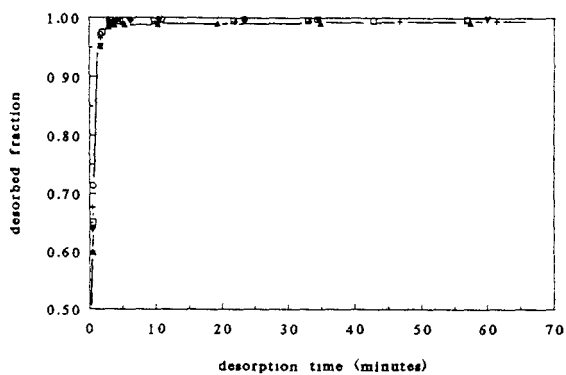


Figure 1. Desorption of radiocaesium in humic acid (top) and four forest soils of OM content in a range of 10 to 20%.

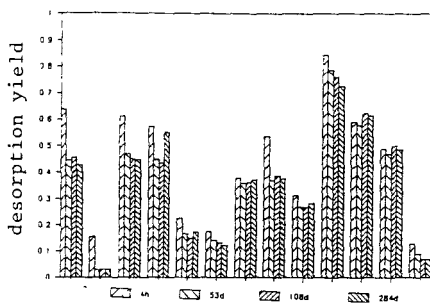


Figure 2. Desorption of radiocaesium and the effect of aging (4 hrs to 284 days) in 13 agricultural soils. The soils are classified according to increasing capacity in FES, covering the range of 0.6 to 2.3 $\mu\text{E/g}$.

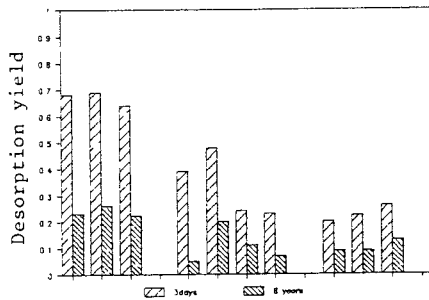


Figure 3. Desorption of radiocaesium and the effect of aging (3 days-8years) in sandy soils (left) loamy (middle) and clay soils (right)

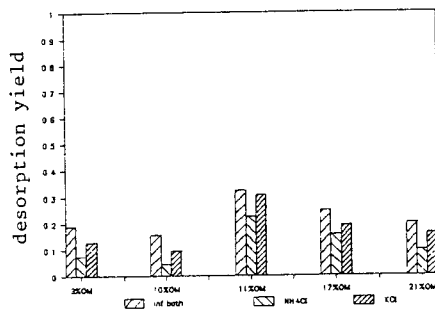


Figure 4. Comparison of desorption yield in five forest soils (OM = 9 to 21%) using the infinite bath methodology, 1M NH₄ and 1M K.

FACTORS AFFECTING RADIOCAESIUM TRANSFER TO RUMINANTS

Contract Bi7-018 - Sector A24

- 1) *Howard*, ITE - 2) *Vandecasteele*, CEN-SCK
- 3) *Mayes*, McAulay Land Use Research. Inst. - 4) *Belli*, ENEA
- 5) *Stakelum*, Agric. and Food Develop. Authority - 6) *Colgan*, NEB
- 7) *Assimakopoulou*, Univ. Ioannina - 8) *Unsworth*, Univ. Nottingham
- 9) *Jones*, Univ. Uppsala Agricult. Sciences

Summary of project global objectives and achievements

1. Introduction

The studies performed in the 2 year research programme described in this report have tried to identify and quantify some of the most important factors influencing the levels of radiocaesium in animal food products. The programme involved 9 laboratories in 6 countries: Belgium, Ireland, Greece, Italy, Sweden and the United Kingdom; scientists from Norway (K. Hove and H.S. Hansen) and Germany (G. Voigt) also participated on an informal basis. The programme has resulted in a number of publications, many in the refereed literature (14 published or in press) and conference proceedings.

Experimental studies have largely been conducted using sheep, although some comparative studies have been performed with dairy cattle. In parallel to the experimental studies a number of research models have been developed by participants in Greece and the UK. Whilst one of these models has primarily been directed at describing the transfer of trace elements to milk and tissues, and has been used to aid experimental studies carried out in Greece, the others have been used interactively with a number of different aspects of the programme.

A summary and discussion of the main findings of each subject area is given below, more detail is given in each participants report. The laboratories involved in each topic area have been identified by participant numbers in parenthesis.

2. Gut absorption

The transfer of a radionuclide to animals has commonly been characterized using the transfer coefficient; defined as the ratio of the equilibrium tissue/milk activity concentration to the daily intake of the radionuclide. Measurements of the transfer coefficient have shown differences in the bioavailability of radiocaesium from various sources, and apparent differences in transfer between ruminants of different species or physiological status. However, the transfer coefficient has the disadvantage that it only applies under equilibrium conditions, which are rarely attained in practice, furthermore it amalgamates a number of different processes including absorption, translocation, deposition and mobilisation in tissues. Therefore, it does not indicate, or quantify, the underlying mechanisms determining the final observed radionuclide levels in tissues.

In this programme a number of the participating laboratories, [01,02,03,05,09], have adopted a more mechanistic approach and conducted experiments to measure the true absorption coefficient (A_t) of radiocaesium, using initially uncontaminated animals. This is a measure of the proportion of a radionuclide which is transferred across the gut wall taking endogenous secretions from blood plasma into the gastrointestinal tract (GIT) into account and can be described by the expressions:

$$A_t = \frac{\text{Radionuclide Intake} - \text{Faecal Output of Radionuclide} + \text{Endogenous Faecal Excretion of Radionuclide}}{\text{Radionuclide Intake}}$$

or

$$A_t = \frac{\text{Plasma Turnover of Radionuclide}}{\text{Radionuclide Intake}}$$

A number of methods can be used to measure A_t although all of those used within this programme involve dual-isotope studies; one isotope is infused intravenously whilst the other is given orally as the dietary source. All methods have the advantage that estimates can be made within a relatively short time period since equilibrium conditions between tissues and diet are not necessary. Probably the most reliable method for calculating A_t was the second approach shown above, where plasma turnover rate was determined from the rate of infusion of ^{134}Cs and ^{137}Cs . ^{134}Cs ratios in urine. The effect on A_t of a number of animal and dietary factors have been assessed; these are summarized below:

a) Effect of age on radiocaesium uptake [01.03]

The absorption of radiocaesium was measured in 7 groups of lambs ranging from 11 to 59 weeks of age. Radiocaesium absorption from milk was complete (ie. $A_t=1$). True absorption of radiocaesium when administered within gelatin capsules (representing solid food) was between 0.80 and 0.85 for all age groups and did not change with age. This value of A_t is similar to that determined for adult sheep in a number of experiments during this programme [01,02,03].

Absorption, when expressed as the apparent absorption coefficient, A_a , (the difference between radiocaesium intake and faecal output expressed as a proportion of intake) appeared to change significantly with age, suggesting an increase in the secretion of radiocaesium from blood plasma into the GIT.

b) The effect of breed and animal species on radiocaesium uptake [03.05.02.09.01]

A range of sheep breeds, used for different purposes, are found throughout Europe and may range in body weight from <30 to >100 kg. Little consideration has been given to the potential effect of breed differences on radiocaesium transfer. A number of different breeds were used by the various participants of this research programme; the A_t of ionic radiocaesium in three breeds of sheep, Texel, Suffolk and Scottish Blackface, was found to be similar.

Sheep were used as 'model ruminants' within the programme. In order to be able to extrapolate some of the results to other ruminants some studies were conducted to compare radiocaesium absorption in cattle and sheep [05,03]. The true absorption coefficients of ionic radiocaesium were measured in Friesian dairy cows and Scottish Blackface ewes. For lactating cows the A_t was 0.71; equivalent values for sheep were slightly higher at 0.84.

Additional experiments have recently been conducted to measure the A_t of radiocaesium in reindeer [09]. Results for this study are still being analyzed.

c) Forage Type [02]

The form of radiocaesium which an animal ingests can influence its transfer to animal tissues, and ruminants may ingest a wide range of radiocaesium sources (see for instance results for free ranging sheep [09])

within this report). However, little consideration has previously been given to potential differences in radiocaesium absorption from different feed types. The harvesting and storage conditions for animal feedstuffs could also influence radiocaesium transfer.

The effect of forage type on radiocaesium transfer was investigated for both ryegrass and clover, prepared in a number of different ways: fresh, hay, silage and frozen [02]. In general A_t values were similar to those determined for ionic radiocaesium and different processing methods did not greatly alter radiocaesium availability from forage. Similarly, differences in the absorption of radiocaesium from various plant species found in this and other studies were not large [01,02,03].

d) Cycling of radiocaesium within the gastro-intestinal tract [03,05]

Studies were conducted on radiocaesium absorption and recycling in various segments of the gastro-intestinal tract in both sheep and cattle using ionic radiocaesium and an organic soil contaminated with ^{134}Cs . Net transfers to and from each gut segment and the blood plasma were determined with most secretion found to occur in the forestomachs and small intestine. Absorption occurred mainly in the small intestine in both ruminant species; very little took place in the hind gut. Ionic radiocaesium was associated largely with the liquid phase of digesta. In contrast most of the ^{134}Cs from the organic soil was associated with the solid phase. Some soil appeared to be retained in the caecum in sheep.

Given an estimation of radiocaesium recycling within the gut the effectiveness of countermeasures under different conditions can be modelled. For instance if a caesium binder such as AFCF were to effectively stop reabsorption of secreted radiocaesium the biological half-life in sheep would be reduced by 25-30% [08].

e) Discussion

These studies have attempted to identify the underlying mechanisms governing radionuclide transfer, rather than using only empirical measurements such as concentration ratios, and have successfully isolated the transfer from feed to blood plasma (ie. by measurement of A_t). A_t did not change with age and similar values were estimated for sheep of differing breeds. The values of A_t for ionic radiocaesium measured in dairy cows were within the observed range, of those measured for sheep. It seems that absorption across the gut wall is not responsible for the observed variations in the transfer coefficient of radiocaesium in ruminants of different ages. Therefore, other processes must be responsible for these differences.

In the next programme the group intends to extend these studies by measuring the effect of various parameters on the transfer from blood plasma and tissues. Models developed during the course of this work [08] suggest that differences in pool size could be the principle cause of observed differences in transfer coefficient and this will be one of the parameters studied in future work.

Results from this programme suggest that variations in the absorption of radiocaesium bio-incorporated into different plant materials is not an important factor in determining radiocaesium levels in tissues. However, other environmental sources of radiocaesium (eg. ingested soil - see also below) may be absorbed to a much lesser extent.

3. Physiological factors affecting radiocaesium levels in meat and milk

a) Radiocaesium metabolism in muscle [08,09]

The transfer of radiocaesium to muscle is higher than that to other tissues, and its biological half-life in the tissue is considerably longer than that in other organs. The rates of radiocaesium uptake and loss in isolated sheep muscle cells have been measured [08] and suggest that long-term binding occurs within cells; the data, in conjunction with *in-vivo* half-life measurements, are currently being incorporated into a physiologically based model.

The transfer of radiocaesium to the different muscles of sheep was also investigated [09]. A two fold difference between the muscle with the highest radiocaesium activity concentrations (*Masseter*) and that with the lowest (*Longissimus dorsi*) was found and appeared to be related to the proportion of Fibre Type 1 in the muscle.

b) Effect of stage of lactation [07,04]

The transfer of radiocaesium to the milk of dairy sheep was measured throughout a complete lactation [07]. The f_m value increased by a factor of three over the 21 week lactating period. A significant correlation was found between f_m and average daily milk yield. Corroborative evidence for such an effect was provided by results from studies in Italy [04], in which f_m increased in late lactation.

4. Soil as a dietary source of radiocaesium

Whilst soil adhesion onto vegetation surfaces is acknowledged as a potential source of radiocaesium intake by grazing animals there is little information on the importance of soil-associated radiocaesium intake and how it varies throughout the year. The importance of soil as a source of radiocaesium will depend upon a) the amount of soil-associated radiocaesium ingested and b) its availability for absorption in the gut. Studies conducted in the programme on both these aspects are summarized below:

a) Soil adhesion [01, 06, 02, 07, 04]

The extent of soil adhesion onto vegetation was measured throughout one year at 17 sites in 5 countries covering a range of different soil types. Previous studies had suggested that determination of the ash content of vegetation samples can be used to determine the amount of radionuclides present in sampled vegetation due to adherent soil. Relationships between Ti (a commonly used soil marker) content and vegetation ash were well correlated [01]. However low levels of soil adhesion were not reliably measured using the ash content approach.

At sites within the UK, Ireland and Belgium soil adhesion onto vegetation was found to be highest in the autumn/winter when it accounted for most of the radiocaesium activity of vegetation samples. In both the UK and Ireland there was a significant correlation between the ^{137}Cs activity and Ti concentrations of vegetation from sites with mineral soils, and adhered soil was the most important factor in determining the ^{137}Cs activity concentration of vegetation samples. However, in both countries on pastures with organic soils, where root uptake of radiocaesium was comparatively high, there were no relationships between ^{137}Cs activity and Ti concentrations of vegetation. Correlations were found between the Ti concentrations in vegetation and those in faeces, showing that animals were ingesting more soil at the times of year when vegetation samples contained more adhered soil.

For many of the sites soil adhesion was estimated to account for >100% of the radiocaesium content of some vegetation samples. This may be because vegetation is contaminated by a sub-fraction of the soil, which is not representative, in terms of Ti and radiocaesium content, of the 0-1 cm soil layer. Furthermore the mechanisms which cause soil adhesion to vegetation vary throughout the year and may result in different sub-fractions of the soil contaminating vegetation samples. Further detailed analyses of the mechanism controlling soil adhesion is needed.

From the samples of winter fodder which were taken it appeared that mechanical harvesting of hay and silage increased soil adhesion onto the crop, especially in dry weather. Soil adhesion onto fodder beet was comparatively high, but declined slightly during harvesting and storage.

b) Radiocaesium availability from ingested soil [04.03.05.07]

The transfer of radiocaesium from a range of soil types was measured in sheep, and in cattle from organic soil. The availability from two mineral soil types was low, with f_m values of $<6.1 \times 10^{-4} \text{ d l}^{-1}$ [04]. This compares to an f_m value of $8.2 \times 10^{-2} \text{ d l}^{-1}$ determined for ionic radiocaesium [09]. Soil was also obtained from an area near to the Chernobyl NPP; radiocaesium from this soil was much more bioavailable ($f_m = 2.6 \times 10^{-2}$), even though its clay content was similar to that of the mineral soils studied [07]. It is possible that the higher transfer is due to the physico-chemical nature of the radiocaesium deposit close to the Chernobyl reactor.

True absorption coefficients determined for radiocaesium from a contaminated organic soil were estimated to be 0.02 ± 0.0003 (mean \pm SE) for sheep and 0.19 ± 0.05 for cattle. The organic soils were therefore about 2% and 28% respectively as available as ionic radiocaesium; estimates of f_m in Norway for an organic litter layer fed to goats gave an equivalent value of 10%. However, from studies on the behaviour of radiocaesium in the sheep gut, outlined above, it appears that soil-bound radiocaesium may have accumulated in the caecum.

c) Discussion

Radiocaesium associated with soil adhered to vegetation surfaces can constitute a considerable proportion of the total radiocaesium activity of sampled vegetation. Therefore soil adhesion should not be ignored when attempting to estimate radiocaesium levels in the tissue or milk of grazing animals from levels in sampled vegetation, since the available radiocaesium intake is likely to be overestimated, particularly in autumn/winter. However in many circumstances reliable site-specific estimates of the comparative importance of radiocaesium associated with adherent soil are difficult to achieve. Therefore since the ultimate aim is usually to estimate the overall, available radiocaesium intake it may be preferable to subject vegetation samples to *in-vitro* availability tests, such as that developed by ITE/MLURI, SCK/CEN and in Norway, which will provide an availability value for use in models.

Using results from this programme the importance of ingested soil in determining radiocaesium levels in grazing animals in the UK has been assessed [08]. In most situations the contribution that radiocaesium from ingested soil makes to levels in tissues is low compared with that from vegetation. However, if gut absorption from ingested soil was high (as measured in this programme for the soil from the Chernobyl area), but root uptake from soil was low, then soil ingestion could be important.

Project 1

Head of project: *Dr. Howard*

Objectives for the reporting period

1. Co-ordination of the programme and preparation of collaborative publications and reports;
2. Carry out a study on the extent of soil adhesion in pastures. Determine Ti and LOI for samples from ITE, CEN/SCK, ENEA and RPII;
3. Carry out an experiment with MLURI to investigate the effect of age on the transfer of radiocaesium to lambs;
4. Development of the true absorption technique (with MLURI);
5. Edit the REACT publication;
6. Prepare and submit publications;
7. Analysis samples from cattle experiments at TEAGASC for radiocaesium (see [05]).

Progress achieved including publications

The summary and publications list for the contract as a whole within this report demonstrates the successful nature of the programme.

1. Soil adhesion study

Previous studies had suggested that determination of the ash content of vegetation samples by loss on ignition can be used to determine the concentration of radionuclides due to adherent soil. Initially we had hoped to use such a method in this study. Two approaches were adopted: i) to calculate the excess ash in sampled vegetation by comparing it to the ash from washed (repeated washing with Teepol) vegetation samples and assuming that this was due to adherent soil, and ii) to conduct a limited number of Ti analysis on vegetation samples and determine the relationship between Ti and ash, thereby allowing Ti concentrations to be estimated in other vegetation samples by determination of their % ash. Relationships between Ti content and vegetation ash were well correlated (eg. Fig. 1). However both approaches did not reliably estimate low levels of soil adhesion. Therefore Ti analysis by HF digest and ICP were conducted on the majority of the samples.

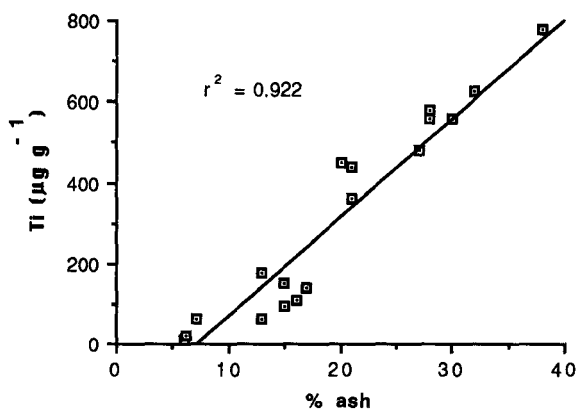


Figure 1. Relationship between Ti concentration ($\mu\text{g g}^{-1}$) and % ash in sampled vegetation.

Vegetation and fresh sheep faeces (when present) were sampled from both an upland and lowland permanent pasture in west Cumbria from May 1990 to April 1991 at the upland site, but only until February 1991 at the lowland site when the pasture was ploughed. Soil samples were also taken from each site on 3 occasions. Soil characteristics at the upland and lowland sites are compared in Table 1.

Table 1. Soil characteristics at the upland and lowland sites.

Soil variable	Upland	Lowland
0-30 cm		
Clay (%)	15.5±1.30	5.0±1.16
Silt (%)	28.1±1.25	15.3±2.65
Coarse Sand (%)	30.5±3.05	25.8±4.44
Fine Sand (%)	25.9±1.07	53.8±1.45
0-1 cm		
Loss on ignition (%)	36±1.5	11.3±0.33
Extractable K ($\text{mg } 100\text{g}^{-1}$)	92±0.6	38±1.2
Ti ($\mu\text{g g}^{-1}$)	3970±186	2070±33
1-30 cm		
Loss on ignition (%)	22±4.7	5.8±0.46
Extractable K ($\text{mg } 100\text{g}^{-1}$)	11.0±3.18	11.1±1.04
Ti ($\mu\text{g g}^{-1}$)	4570±233	2130±186

Radiocaesium activity concentrations of vegetation at the lowland site were considerably higher in the late autumn and winter, whereas no seasonal trend was evident at the upland site. Radiocaesium activity concentrations in faeces were generally higher than those in the vegetation. Soil adhesion at both sites was higher in the autumn and winter months; the magnitude of difference throughout the year was less at the upland site. The Ti concentration in faeces

samples collected from the upland site were correlated with those of vegetation ($r^2 = 0.6$) showing that the animals were ingesting more soil at those times of year when vegetation samples contained more adhered soil.

There was a positive correlation between the radiocaesium activity concentration and Ti concentration of vegetation samples from the lowland site ($r^2 = 0.87$). However at the upland site no relationship was evident. It is likely that at the lowland site, with a mineral soil, root uptake of radiocaesium is low and that seasonal variations in soil adhesion are a dominant factor in determining radiocaesium contents of sampled vegetation. At the upland site greater root uptake of radiocaesium occurs from the organic soils present.

The proportion of radiocaesium measured in sampled vegetation associated with soil followed a similar pattern to that of Ti. However in some cases, at both sites, it was estimated that soil could be responsible for >100% of the radiocaesium activity actually measured in the vegetation samples. This may be because the vegetation is contaminated by one fraction of the soil, therefore by analysing Ti and Cs contents of the total 0-1 cm soil layer we may not be obtaining concentrations representative of the soil adhered to vegetation. Furthermore the mechanisms by which vegetation is contaminated by soil vary throughout the year, and may result in different fractions of the soil becoming adhered onto the plant surfaces.

2. Effect of age on the transfer of radiocaesium to lambs

This study was carried out in collaboration with MLURI and a paper has been accepted for publication (Mayes et al. in press).

The absorption of ionic ^{137}Cs was determined in groups of lambs ranging in age from 11 to 59 weeks fed ewes' milk and/or fresh perennial ryegrass. Radiocaesium was either incorporated into milk or administered within a gelatin capsule. Absorption was measured as either the apparent (A_a) or true absorption coefficient (A_t) (Table 2). Whereas A_a declined with age, A_t did not, but was higher (1.00) when the ^{137}Cs was incorporated in milk, than when administered in a way which simulates incorporation into solid feed (0.80-0.85). Previously observed differences in transfer coefficients for animals of different ages appear not to be due to changes in transfer across the gut.

Table 2. Mean apparent (A_a) or true (A_t) absorption coefficients (\pm SE) determined in groups of Scottish Blackface sheep at various ages.

Age group (weeks)	Diet	Dosing route	A_a	A_t	Lwt* (kg)
11	milk	milk	0.99 \pm 0.004	1.00 \pm 0.001	13 \pm 0.7
16	milk+grass	milk	0.85 \pm 0.037	1.02 \pm 0.007	20 \pm 1.3
16	milk+grass	capsule**	0.75 \pm 0.040	0.85 \pm 0.022	20 \pm 1.5
20	grass	capsule	0.73 \pm 0.018	0.80 \pm 0.016	25 \pm 1.0
30	grass	capsule	0.68 \pm 0.017	0.82 \pm 0.015	31 \pm 0.6
39	grass	capsule	0.69 \pm 0.020	0.84 \pm 0.022	30 \pm 0.8
59	grass	capsule	0.62 \pm 0.026	0.85 \pm 0.016	40 \pm 2.6

* liveweight at the end of the experiment

** Gelatin capsule containing ionic ^{137}Cs on paper filters

3. True absorption and bioavailability

Studies on developing the true absorption technique were carried out in collaboration with MLURI and have been reported in the MLURI part of this report. The bioavailability of radiocaesium from a number of different environmentally sources and ionic radiocaesium has been measured by determining the A_t , by ITE/MLURI as part of a separate UK funded study (Beresford et al. in press). The environmental sources used in this work were selected to complement studies being conducted by other participants within the CEC programme and conducted under the same experimental protocol.

4. Radiocaesium dynamics

An experiment was carried out by MLURI/ITE specifically to provide a data set designed to allow Crout & Galer at Nottingham University to develop a model to describe the dynamic behaviour of radiocaesium in sheep tissues. Single intraruminal administrations of $^{134}\text{CsCl}$ and intravenous administrations of $^{137}\text{CsCl}$ were given to each of 15 Scottish Blackface ewes. The animals were fitted with both indwelling jugular and bladder catheters. Blood, urine and faeces samples were taken at regular intervals throughout the first 1.5 days of the study and 3 animals were slaughtered on each of days 0.5, 1, 4, 12 and 20 after administration. A range of tissue samples and gastrointestinal tract contents were analyzed from these animals. Results of the analysis were provided to Crout & Galer and the resulting model is due for publication (Galer et al. in press).

Experimental data from this study has been used by ITE/MLURI to investigate a potential method of rapidly (<2 days) determining the true absorption of dietary radiocaesium following single administrations of dietary and intravenous radiocaesium. Preliminary analysis suggests that such a technique is possible by measuring the radiocaesium isotopic ratio in red blood cells. The model developed by Crout & Galer confirms the validity of this approach. Further investigations of the technique are planned.

5. React

The co-ordinator (B.J. Howard) together with G.M. Desmet (DGXII) edited the volume of the Science of the Total Environment devoted to papers from the REACT (Relative Effectiveness of Agricultural Countermeasure Techniques) workshop. Other members of the CEC animal group also contributed papers to the workshop. The papers have all been sent to the journal and are awaiting publication.

Publications

Refereed papers

Beresford, N.A. & Howard, B.J. 1991

The importance of soil adhered to vegetation as a source of radionuclides ingested by grazing animals. *Sci. Total Environ.*, 107, 237-254.

Beresford, N.A., Mayes, R.W., Howard, B.J., Eayres, H.F., Lamb, C.S., Barnett, C.L. & Segal, M.G. in press

The bioavailability of different forms of radiocaesium for transfer across the gut of ruminants. *Radiat. Prot. Dosim.*

Crout, N.M.J., Beresford, N.A. & Howard, B.J. in press

Does soil adhesion matter when predicting radiocaesium transfer to animals? *J. Environ. Rad.*

Galer, A.M., Crout, N.M.J., Beresford, N.A., Howard, B.J., Mayes, R.W., Barnett, C.L., Eayres, H.F. & Lamb, C.S. in press

Dynamic radiocaesium distribution in sheep: measurement and modelling.

- J. Environ. Rad.
- Hove, K., Strand, P., Voigt, G., Jones, B.-E.V., Howard, B.J., Segal, M.G., Pollaris, K. & Pearce, J. in press
Countermeasures for reducing radioactive contamination of farm animals and farm animal products. Sci. Total Environ.
- Howard, B.J. in press
Management methods of reducing radionuclide contamination of animal food products in semi-natural ecosystems. Sci. Total Environ.
- Mayes, R.W., Eayres, H.F., Beresford, N.A., Lamb, C.S. & Howard, B.J. in press
Changes with age in the absorption of radiocaesium by sheep. Radiat. Prot. Dosim.
- Wilkins, B.T., Howard, B.J., Desmet, G.M., Alexakhin, R.M. & Maubert, H. in press
Strategies for the deployment of agricultural countermeasures. Sci. Total Environ.
- Mayes, R.W., Lamb, C.S., Beresford, N.A., Barnett, C.L., Howard, B.J., Jones, B.-E.V., Eriksson, O., Hove, K., Pedersen, Ø. & Staines, B.W. submitted
Novel approaches to the estimation of intake and bioavailability of radiocaesium in ruminants grazing forested areas.
- Beresford, N.A., Mayes, R.W., Crout, N.M.J., Howard B.J., Oughton, D.H. & Kanyar, B. in preparation
Dynamic behaviour of ^{110m}Ag in sheep tissues.
- Mayes, R.W., Beresford, N.A. & Howard, B.J. in preparation
The use of the true absorption coefficient as a measure of radiocaesium bioavailability

Conference reports/Other publications

- Galer, A.M., Crout, N.M.J., Beresford, N.A. & Howard, B.J. 1990
Modelling radio-caesium transfer in upland ecosystems. In: 1st Int. Conf on the Atomic Power Plant Accident at Chernobyl, held at Zeleny Mys, p.264.
- Howard, B.J., Beresford, N.A. & Mayes, R.W. 1990
Factors affecting radiocaesium transfer to ruminants. In: Proc. SCOPE RADPATH meeting. RL.13.90. Lancaster March 26-30
- Crout, N.M.J., Galer, A.M., Howard, B.J. & Beresford, N.A. 1991
A comparative assessment of the impact of the Windscale and Chernobyl accidents on Cs-137 levels of upland lambs in west Cumbria using the RUINS model. In: Proc. of a Seminar on Comparative Assessment of the Environmental Impact of Radionuclides Released During Three Major Nuclear Accidents: Kyshtym, Windscale, Chernobyl. Luxembourg, 1-5 Oct 1990. Commission of the European Commission: Luxembourg. pp 1122-1136.
- Howard et al. 1991
Factors affecting radiocaesium transfer to ruminants. Progress Report: April 1990-March 1991 to CEC, DGXII.D.3. Radiation Protection Research Programme. Contract Bi7-018.
- Assimakopoulou, P.A., Ioannides, K.G., Karamanis, D., Pakou, A.A., Stamoulis, K., Mantzios, A.S., Nikolaou, E. & Howard, B.J. 1992
Variation of the transfer coefficient for radiocaesium transport to sheep's milk during a complete lactation period. Report NPL-91-3. Dep. Physics, University of Ioannina, Greece.

Project 2

Head of project: *Dr. Vandecasteele*

Objectives for the reporting period

1. To complete the field sampling and sample analyses to investigate the importance of soil adhesion on the contamination of grazing animals;
2. To compare the radiocaesium uptake in two different Belgian sheep breeds (Suffolk and Texel) by true absorption experiments;
3. To compare the influence of animal foodstuff processing (fresh, drying, ensilaging and freezing) on the absorption of radiocaesium by sheep fed contaminated forage (ryegrass and clover);
4. To produce reports and papers for publication in the open literature.

Progress achieved including publications

1. Breed study

Sheep breeds vary in different regions in Europe and local breeds were intended to be used in each laboratory involved in this co-ordinated research programme. If results obtained in the participating lab's had to be compared, a prerequisite was to check for inter-breed differences in the metabolism of ionic radiocaesium. The breed planned to be used for experimentation at the SCK/CEN was the Suffolk. However, a second breed (Texel), which is widespread in Belgium, was also considered in this comparison.

The availability of ionic radiocaesium was estimated by both Mol and MLURI/ITE with their local breed(s) using the "true absorption coefficient" technique adopted from R.W. Mayes, the collaborator at MLURI. Determining the true absorption has the advantage that equilibrium conditions are not required in the different tissues or in the excreta, so that the experimental period can be comparatively short (eight days). Two methods of calculating true absorption were used: A_{t1} = true absorption coefficient estimated from faeces:urine excretion ratios and A_{t2} = true absorption coefficient estimated from turnover rates through the blood plasma pool.

Six mature non-lactating ewes of each breed, housed in metabolism cages, were used in this experiment. One day before commencing dosing of the animals, they were fitted with a bladder catheter to obtain urine free of faecal contamination and with an intravenous catheter introduced into the jugular vein. On the next day, oral administration of ionic ^{134}Cs and intravenous administration of ^{137}Cs were started simultaneously. The slow perfusion of a sterile physiological serum containing ^{137}Cs was carried out using peristaltic pumps. Ionic ^{134}Cs was dosed twice daily, spiked on rehydrated lucerne pellets. The diet, identical for all animals, also consisted of beet pulp and hay during the night. Total urine and faeces production was collected daily. The faeces samples were dried, ground and homogenised. For each day, duplicate sub-samples were counted with a well-type NaI detector. Some of the samples were also counted on a Ge detector to check the

reliability of the NaI counting technique. On the last day of feeding with ^{134}Cs , blood samples were also collected.

The absorption coefficients were calculated from the integrated excretion activities over the last four days (day 5-8). Grouping the data over four days gives a better estimation since considerable daily fluctuations in the quantity of excreta produced can occur, which can cause variations in the estimation of the absorption coefficients. Days 1-4 were not considered, partly because of the residence of uncontaminated herbage in the gut in the early stages of the experiment.

The results presented in Table 1 show no significant difference between the two Belgian breeds investigated. Moreover the values obtained for Texel and Suffolk are comparable to the value obtained by MLURI/ITE for Scottish Blackface sheep ($A_{11} = 0.84 \pm 0.13$). Therefore the results obtained at the SCK/CEN and in the UK suggest that there is no difference in the true absorption coefficient with breed.

Table 1. Estimations of absorption in two sheep breeds using different techniques (mean \pm SD).

BREED	N	A_a	A_{11}	A_{12}
Texel	4	0.57 \pm 0.15	0.77 \pm 0.10	0.78 \pm 0.06
Suffolk	6	0.59 \pm 0.13	0.79 \pm 0.09	0.84 \pm 0.05

where:

N = number of animals considered in the estimation of the values, some were discarded due to sanitary problems,

A_a = apparent absorption coefficient,

A_{11} = true absorption coefficient estimated from faeces:urine excretion ratios,

A_{12} = true absorption coefficient estimated from turnover rates through the blood plasma pool.

2. Forage type feeding experiments

The composition and physico-chemical characteristics of the diet are thought to be important reasons for observed differences in the availability of radiocaesium ingested by animals. The processing of animal feeding stuffs could also affect bioavailability. Therefore the bioavailability of radiocaesium in three agronomically important types of forage were investigated: fresh vegetation, hay and silage. The effect of deep-freezing plant material was also studied as this is a commonly used method of storing contaminated material, prior to a feeding experiment. Plant species, differing by their fibre or protein content, may also be expected to modify the absorption of radionuclides.

The same method described in the previous section was used in this study. Four mature non-lactating Suffolk ewes per treatment received a small amount of radioactive plant material (ryegrass or clover) once daily which had been grown on ^{134}Cs contaminated nutrient solutions. The rest of the diet consisted of uncontaminated plant material of the same type (*ad-libitum*), together with about 150 g d⁻¹ dw beet pulp. The results are given in Table 2.

Table 2. Estimates of absorption of radiocaesium by sheep from different types of forage (mean±SD).

EXPERIMENT	N	A _a	A _{t1}	A _{t2}
IONIC ¹³⁴ Cs	6	0.59±0.13	0.79±0.09	0.84±0.05
RYEGRASS				
fresh	3	0.79±0.09	0.91±0.04	0.85±0.09
frozen	4	0.75±0.11	0.89±0.06	0.82±0.04
hay	4	0.45±0.17	0.68±0.14	0.73±0.14
silage	4	0.76±0.05	0.89±0.03	0.93±0.09
CLOVER				
fresh	4	0.50±0.04	0.69±0.02	0.67±0.03
frozen	4	0.47±0.04	0.68±0.02	0.71±0.02
hay	3	0.68±0.10	0.83±0.09	0.76±0.05
silage	4	0.70±0.09	0.86±0.04	0.84±0.10

These results are in agreement with values reported by ITE/MLURI for absorption of ionic radiocaesium on filter paper and radiocaesium bioincorporated in grassy vegetation in Scottish Blackface sheep.

The true absorption coefficients estimated using both calculation methods give similar values, suggesting that either method could have been used to measure the degree of absorption in these experiments.

Radiocaesium availability in ryegrass hay appeared to be less than that of the other grassy feed types, although this is not the case for the clover hay. Absorption values for the fresh and frozen clover were low compared with the equivalent grass herbage. Currently we can only speculate on possible reasons for these observed differences such as the length of time between harvest and feeding to the sheep and soil adhesion. The contaminated clover hay was fed a few weeks after harvesting whilst the contaminated ryegrass hay was stored for 6 months prior to feeding. The digestibility of the ryegrass hay may have gone down after storage. Similarly the uncontaminated clover hay used for the "fresh" and "frozen" treatments was harvested in November and December when there was a low biomass compared to the uncontaminated clover used for the "hay" and "silage" treatments. Therefore it is reasonable to expect, from the soil adhesion studies of the CEC group, that soil adhesion would have been greater for the "fresh" and "frozen" treatments. The presence of soil in the uncontaminated vegetation could have reduced the absorption of radiocaesium from the contaminated clover.

The bioavailability of radiocaesium bioaccumulated in fresh grass was the same as that of ionic radiocaesium. Incubating such material in distilled water or in 0.01M HCl at 4°C for 48h extracted more than 90% of the radiocaesium contained within the plant tissues.

There was no difference in absorption between fresh and stored vegetation. This means that fresh vegetation can be harvested and stored frozen for future experiments without invalidating the extrapolation of such results to fresh material. Similarly feeding silage did not alter the absorption of radiocaesium compared with fresh material.

We conclude that the different processing methods tested would not alter, to a large extent, the availability of radiocaesium to ruminants. This may not be true for other radionuclides, such as Tc, since Tc speciation in plant tissues is modified by plant metabolism, and it will probably also not be the case for radiostrontium,

which will be strongly bound to different plant constituents, namely cellulose and other wall constituents.

3. Soil adhesion study

Samples of vegetation, faeces and soil were collected according to the agreed protocol from May 1990 to May 1991. Additional samplings were taken in August and November 1991 in order to test some hypotheses.

Two sites with contrasting soil types (sandy and loamy soils) were selected: i) at experimental farms at SCK/CEN (Mol), and ii) at the University of Louvain (Louvain-La-Neuve (LLN)).

Vegetation and faeces were sampled monthly; soil samples were taken in June and November 1990 and in May 1991. The soil characteristics were determined for both the 0-1cm and the 0-20 cm soil profiles (Table 3). For the two additional samples collected in August and November 1991, only the top layer was sampled and analysed by gamma-spectrometry.

The following winter fodders were collected from local farmers generally at the beginning and the end of the feeding period (the value between brackets is the number of sampling occasions):

MOL : hay (2), hay silage (2), maize silage (2), beet heads (1) and beet roots (2)

LLN : hay harvested in 1989 (2), hay harvested in 1990 (3), hay silage (1), barley (2) and maize silage (1).

Corresponding soil samples were taken from the sites where the fodder was collected for physico-chemical and gamma spectrometry analysis.

Table 3. : Soil characteristics at the two sampling sites.

Soil characteristic	Site			
	Mol		LLN	
	0-1cm	0-20cm	0-1cm	0-20cm
pH	5.49±0.36	5.61±0.18	5.67±0.28	6.51±0.45
OM	15.94±3.65	3.21±0.42	11.60±0.80	3.47±0.36
%Clay	1.3±0.6	1.0±<0.1	9.3±0.6	11.3±0.6
%Sand	90.7±4.5	96.7±0.6	15.0±3.6	11.0±1.7
%Silt	8.0±4.6	2.3±0.6	75.7±3.8	77.7±2.3
Exchangeable K	60.3±21.9	9.5±1.1	93.9±28.3	32.3±5.7

In order to determine the relative importance of soil adhesion and ingested soil as a source of radiocaesium for animals the quantity of adhering soil particles on grassy vegetation was estimated using two methods: loss on ignition (LOI) which measures the intrinsic mineral content of the vegetation, and Ti analysis.

The results obtained with the two methods were in reasonable agreement. However, for the Mol samples (sandy soil), LOI analysis tended generally to give consistently higher values than that obtained using Ti analysis; the two methods gave more similar values for the LLN samples (loamy soil). At both locations, the results showed a significant increase in the contamination of herbage by soil particles in late autumn and winter (periods of the year characterised by a low vegetation biomass and heavy rainfall causing splashing of soil onto vegetation). The contribution of soil to the total vegetation dry weight (dw) reached more than 20% at these times. During the growing season (when herbage biomass was above

150 g m² dw), the soil contributed less than 5% of the total dw and the contribution of soil to the overall radiocaesium contamination of herbage was estimated to be about 8% (Ti) or 20% (LOI) at Mol and to be less than 5% at Louvain-La-Neuve, but was close to 100% in the winter time at both sites using both methods.

At Louvain-La-Neuve, the radiocaesium activity concentration in herbage remained fairly constant all over the year (about 5 Bq kg⁻¹ dw). At Mol, a maximum concentration was observed in the spring (40 Bq kg⁻¹ dw) and a minimum (about 10 Bq kg⁻¹ dw) in the winter period, despite the increased contamination by soil particles.

A high positive correlation was observed for the Ti content in sheep faeces and in the vegetation on which the animals were grazing (Mol $r^2 = 0.55$ and LLN = 0.83).

No significant soil contamination was measured on winter fodders (ie. <5% by weight), except for beet tops (20%) and wilted silage (23%) from Mol. In Belgium the usual practice consists of housing animals for the winter period and feeding them with winter fodders, which are usually less contaminated by soil, if harvested in good growing conditions.

From these results, it appears that for the two Belgian scenario's, the extent to which soil contributes to radiocaesium intake by grazing animals is limited, even in winter.

Publications

Refereed Papers

Hove, K., Strand, P., Voigt, G., Jones, B.-E.V., Howard, B.J., Segal, M.G., Pollaris, K. & Pearce, J. in press

Countermeasures for reducing radioactive contamination of farm animals and farm animal products. Sci. Total Environ.

Conference reports/Other publications

Pollaris, K., Van Hees, M. & Vandecasteele, C.M. 1990

Relative bio-availability of caesium incorporated into plant material to sheep. Communication given at the IUR workshop on Plant-animal transfer-WG, Neuherberg, April 23-25, 1990.

Vandecasteele, C.M., Fagniar, E., Van Hees, M., Hurtgen, C., Burton, O. & Kirchmann, R. 1990

Comparative study of the behaviour of radiocaesium and radiostrontium from different source terms in pasture systems. Communication given at the All Union Conference on the Geochemical Pathways of Artificial Radionuclides Migration in the Biosphere, Gomel, October 13-21, 1990.

Vandenhout, S. 1990

Test de digestibilité in vitro appliqué à des aliments contaminés au Cs-134. Mémoire de Fin d'Etude ISIP Bruxelles, CEN/SCK, Mol, September 1990.

Pollaris, K., Van Hees, M. & Vandecasteele, C.M. 1991

A comparison of the metabolism of radiocaesium in two Belgian sheep breeds. Communication at the IUR workshop on Plant-animal transfer-WG, Uppsala, September 23-25, 1991.

Vandecasteele, C.M., Zeevaert, Th. & Kirchmann, R. 1991.

Factors influencing the transfer of radionuclides in agricultural food chains. In: Anticarcinogenesis and Radiation Protection 2. O.F. Nygaard & A.C. Upton (Eds.), Plenum Press: New York, pp. 181-191.

Vandecasteele, C.M., Van Hees, M., Hurtgen, C. & Kirchmann, R. 1992

Comparative study of the behaviour of radiocaesium and -strontium from different source terms in pasture ecosystems. In: Proc. IRPA-8 Conference held in Montreal, May 17-22, 1992, Vol. 1, pp. 74-77.

Vandecasteele, C.M. in press

Variability of transfer coefficients in terrestrial food chains. In: Workshop on the Effects of Ionizing Radiations at Low Doses. held at Mol, November 10, 1991.

Appendix

1. True absorption coefficients were determined by two different methods:

a) **True absorption (A_{t1})** estimated from the faeces:urine excretion ratio:

$$A_{t1} = \frac{{}^{134}\text{Cs intake (Bq d}^{-1}) - \text{total. faeces. } {}^{134}\text{Cs output (Bq d}^{-1}) + \text{endogenous } {}^{134}\text{Cs faecal output (Bq d}^{-1})}{{}^{134}\text{Cs intake (Bq d}^{-1})}$$

where:

$$\frac{\text{endogenous } {}^{134}\text{Cs faecal output (Bq d}^{-1})}{\text{total faecal } {}^{137}\text{Cs output (Bq d}^{-1})} = \frac{\text{urine } {}^{134}\text{Cs Conc}^n \text{ (Bq l}^{-1})}{\text{urine } {}^{137}\text{Cs Conc}^n \text{ (Bq l}^{-1})} * {}^{137}\text{Cs infusion rate (Bq d}^{-1})$$

b) **True absorption (A_{t2})** estimated from the turnover rates of ${}^{134}\text{Cs}$ through the blood plasma pool:

$$A_{t2} = \frac{\text{plasma } {}^{134}\text{Cs turnover rate (Bq d}^{-1})}{{}^{134}\text{Cs intake (Bq d}^{-1})}$$

where:

$$\frac{\text{plasma } {}^{134}\text{Cs turnover rate (Bq d}^{-1})}{{}^{134}\text{Cs intake (Bq d}^{-1})} = \frac{\text{urine } {}^{134}\text{Cs (Bq l}^{-1})}{\text{urine } {}^{137}\text{Cs (Bq l}^{-1})} * {}^{137}\text{Cs infusion rate (Bq d}^{-1})$$

2. **Apparent absorption (A_a)** estimated from the intake-output balance:

$$(A_a) = \frac{\text{intake} - \text{faecal output}}{\text{intake}}$$

Project 3

Head of project: *Dr. Mayes*

Objectives for the reporting period

1. To conduct studies to quantify the relative rates of absorption and recycling of radiocaesium in different parts of the digestive tract of the sheep;
2. Examination of the effect of age on radiocaesium absorption in sheep (jointly with ITE, Merlewood);
3. To evaluate methods of estimating the true absorption coefficient of radiocaesium in sheep eating different vegetation types.

Progress achieved including publications

1. Radiocaesium absorption from the ruminant gut

The objective of the study was to measure the absorption and resecretion of radiocaesium in different segments of the gut of the sheep (forestomachs, small intestine and hind gut) given two dietary radiocaesium sources (ionic ^{134}Cs and an organic soil, contaminated by injection of ^{134}Cs two years prior to the experiment) and two diets (freeze-stored grass and a maize-based pelleted concentrate).

The sheep, which had been surgically prepared with cannulae in the rumen, proximal duodenum and terminal ileum, were given the ^{134}Cs either as a continuous intraruminal infusion of a solution (as CsCl) or as the soil introduced through the rumen cannula twice daily. The flow rates of digesta passing the duodenum and ileum, and of faecal material were estimated from the analysis of respective samples of duodenal and ileal digesta and of faeces for Cr and Ru which were continuously infused into the rumen as Cr-EDTA and Ru-phenanthroline indigestible markers. Estimates of true absorption and recycling of ^{134}Cs were made possible by the concurrent intravenous infusion of ^{137}Cs (as CsCl in isotonic saline solution). The experiment was carried out in separate periods for each diet type; the animals were rested for two months in order to decontaminate the tissues between periods. In the second period (pelleted diet) ^{51}Cr -EDTA and ^{103}Ru -phenanthroline were used as indigestible markers.

Due to problems in the analysis of non-radioactive Cr and Ru markers, results are given only for the pelleted diet. These are summarised in Table 1.

Table 1. Two-way transfers of ^{134}Cs (% of intake) between various gut segments and the blood for sheep on a pelleted concentrate diet given either ionic or soil-bound radiocaesium (Mean \pm SE).

Pathway		^{134}Cs source	
		Ionic	Soil
Diet	→ Duodenum (dietary*)	72.3 \pm 3.44	102.8 \pm 5.56
Forestomachs	→ Blood (dietary)	27.7 \pm 3.44	-2.8 \pm 5.56
Blood	→ Duodenum (endogenous)	27.7 \pm 1.71	0.5 \pm 0.08
Duodenum	→ Ileum (dietary)	9.0 \pm 2.96	98.4 \pm 7.55
Small intestine	→ Blood (dietary)	63.3 \pm 2.65	4.4 \pm 13.03
Duodenum	→ Ileum (endogenous)	2.5 \pm 0.76	0.1 \pm 0.01
Small intestine	→ Blood (endogenous)	19.1 \pm 2.08	0.5 \pm 0.07
Blood	→ Ileum (endogenous)	13.8 \pm 0.73	0.5 \pm 0.01
Ileum	→ Faeces (dietary)	8.1 \pm 1.53	85.0 \pm 3.83
Hind gut	→ Blood (dietary)	0.9 \pm 1.55	13.3 \pm 4.77
Ileum	→ Faeces (endogenous)	17.4 \pm 3.02	0.5 \pm 0.02
Hind gut	→ Blood (endogenous)	-1.0 \pm 3.37	0.1 \pm <0.01
Blood	→ Faeces (endogenous)	-3.9 \pm 0.73	0.0 \pm 0.02

*Dietary ^{134}Cs represents that which has remained in the gut. Endogenous ^{134}Cs is that which was previously absorbed.

This experiment also provided data enabling the estimation of the true absorption coefficient (A_t) for the two ^{134}Cs sources. Using the faecal balance and plasma turnover methods the respective estimates of A_t for ionic ^{134}Cs (\pm SE) were 0.92 \pm 0.015 and 0.85 \pm 0.017; equivalent values of A_t for soil ^{134}Cs were 0.15 \pm 0.038 and 0.02 \pm 0.003.

The results indicate that although there was little apparent absorption of ionic ^{134}Cs in the forestomachs there was considerable true absorption and resecretion in this segment of the gut. The majority of the true absorption of ionic ^{134}Cs occurred in the small intestine, with little absorption occurring in the hind gut. No absorption of soil-bound ^{134}Cs occurred in the forestomachs. Absorption was poor in the small intestine. The apparently high degree of absorption of soil ^{134}Cs (relative to other parts of the digestive tract) from the hind gut may be an artefact due to retention of soil in the caecum; this would also explain the discrepancy between the two methods of estimating A_t for soil ^{134}Cs . By centrifuging duodenal digesta and analysing for ^{51}Cr and ^{134}Cs it was possible to demonstrate that all of the ionic ^{134}Cs was associated with the liquid phase of digesta (100.7 \pm 5.11%) and very little soil ^{134}Cs was associated with the liquid phase (0.9 \pm 0.86%).

2. Effect of age on the transfer of radiocaesium to lambs

This study was carried out in collaboration with ITE and a paper accepted for publication (Mayes et al. in press). Details of the experimental results are given in ITEs report.

3. Variation in true absorption, estimated by different methods, of different sources of radiocaesium

The purpose of this study, which was carried out in collaboration with ITE Merlewood, was to compare different methods of estimating the true absorption coefficient (A_t). The evaluation was carried out using data from a UK-funded study described below.

Two groups of adult female Scottish Blackface sheep were used, with four animals allocated per treatment from each group. The sheep in one group were lactating; those in the second group were not. With the exception of milk samples being taken from lactating animals, the experimental procedures were similar for both groups. In addition to the two vegetation types under study, the bioavailabilities of four artificial ^{137}Cs sources were also estimated, for the purpose of comparing methods of estimating A_t ; these were: ionic ($^{137}\text{CsCl}$), ^{137}Cs -contaminated bentonite, heat-treated ^{137}Cs -contaminated silica and estuarine silt which had been contaminated with ^{137}Cs from marine discharges from the Sellafield Reprocessing Plant. These sources were placed in gelatin capsules prior to oral administration.

The sheep were housed in metabolism cages and given uncontaminated feed (heather or grass for those sheep intended to receive contaminated vegetation, and pelleted lucerne for remaining treatments) for 10 days. The lactating animals were hand-milked twice each day. All animals were then fitted with bladder and jugular catheters. The oral ^{137}Cs sources were given for seven days. On the same day as beginning ^{137}Cs administration, continuous intravenous infusion of ionic ^{134}Cs solution was commenced. Collections of faeces, urine and (for lactating animals) milk were carried out over the period of radiocaesium administration.

Two methods were used to determine A_t . In Method 1 A_t was estimated from the daily ^{137}Cs intake, and total and endogenous ^{137}Cs outputs in faeces; endogenous faecal output was estimated from the partitioning of ^{134}Cs excretion in faeces and urine. In Method 2, A_t was estimated as the plasma turnover rate of ^{137}Cs expressed as a proportion of daily ^{137}Cs intake. Plasma turnover rate was determined from the rate of infusion of ^{134}Cs and ^{137}Cs : ^{134}Cs ratios in urine or milk. The results are summarised in Table 2.

Table 2. True absorption coefficients (A_t) for ^{137}Cs from contaminated vegetation (heather and hill grass) and from various artificial sources given to adult sheep. Two methods of estimation were used.

Source of ^{137}Cs	Calculation method for A_t (mean \pm SE)		
	Method 1	Method 2 *(urine)	Method 2 *(milk)
Heather	0.73 \pm 0.054	0.67 \pm 0.034	-
Grass	0.82 \pm 0.011	0.88 \pm 0.047	-
Ionic ⁺	0.86 \pm 0.052	0.84 \pm 0.076	0.83 \pm 0.075
Bentonite ⁺	0.56 \pm 0.016	0.79 \pm 0.026	0.81 \pm 0.035
Silt ⁺	0.05 \pm 0.028	0.13 \pm 0.027	0.13 \pm 0.048
Silt	0.14 \pm 0.100	0.12 \pm 0.018	-
Silica	0.54 \pm 0.028	0.40 \pm 0.033	-

* Body fluid used to calculate plasma turnover rate

+ Lactating sheep

Estimates of A_t did not differ significantly between method of calculation, for heather, grass and ionic ^{137}Cs . However, there were larger discrepancies between calculation methods for bentonite, silt (one measurement group) and silica; this may be due to poor mixing of the relatively small quantities of dosed contaminated material in the gut. Similar values of A_t estimated by Method 2 were obtained when either the ^{137}Cs : ^{134}Cs ratio in urine or milk was used.

The different sources of ^{137}Cs exhibited large differences in bioavailability measured as A_t . The ^{137}Cs in the grass had a similar availability to ionic ^{137}Cs . The differences between A_t values for heather and grass were not significant ($0.10 > p > 0.05$).

A paper on the comparison of techniques for estimating A_t is currently in preparation (Mayes et al.).

Publications

Refereed papers

Beresford, N.A., Mayes, R.W., Howard, B.J., Eayres, H.F., Lamb, C.S., Barnett, C.L. & Segal, M.G. in press

The bioavailability of different forms of radiocaesium for transfer across the gut of ruminants. *Radiat. Prot. Dosim.*

Galer, A., Crout, N.M.J., Beresford, N.A., Howard, B.J., Mayes, R.W., Barnett, C.L., Eayres, H.F. & Lamb, C.S. in press

Dynamic radiocaesium distribution in sheep: measurement and modelling. *J. Environ. Rad.*

Mayes, R.W., Eayres, H.F., Beresford, N.A., Lamb, C.S. & Howard, B.J. in press

Changes with age in the absorption of radiocaesium by sheep. *Radiat. Prot. Dosim.*

Mayes, R.W., Beresford, N.A., Barnett, C.L., Howard, B.J., Lamb, C.S., Jones, B.-E.V., Eriksson, O., Hove, K., Pedersen, Ø & Staines, B.W. submitted

Novel approaches to the estimation of intake and bioavailability of radiocaesium in ruminants grazing forested areas.

Beresford, N.A., Mayes, R.W., Crout, N.M.J., Howard, B.J., Oughton, D.H. & Kanyar, B. in preparation

Dynamic behaviour of ^{110m}Ag in sheep tissues.

Mayes, R.W., Beresford, N.A. & Howard, B.J. in preparation

The use of the true absorption coefficient as a measure of radiocaesium bioavailability

Conference reports/Other publications

Howard, B.J., Beresford, N.A. & Mayes, R.W. 1990

Factors affecting radiocaesium transfer to ruminants. In: Proc. SCOPE RADPATH meeting. RL.13.90. Lancaster March 26-30

Howard et al. 1991

Factors affecting radiocaesium transfer to ruminants. Progress Report: April 1990-March 1991 to CEC, DGXII.D.3. Radiation Protection Research Programme. Contract Bi7-018.

Project 4

Head of project: *Dr. Belli*

Objectives for the reporting period

1. Carry out a study to determine the availability of radiocaesium associated with two different soil types for transfer to sheep milk;
2. Conduct a study to determine the extent of soil adhesion onto pastures grasses at 6 Italian sites;
3. Prepare reports and papers for publication.

Progress achieved including publications

1. Availability of soil radiocaesium for transfer to sheep milk

Soil artificially contaminated with radiocaesium was administered orally each day for 33 days to Bergamasca sheep and the transfer to milk measured. Two soil types were used, with a clay content of 11% and 16% respectively. The data presented here gives results of a programme designed to provide appropriate transfer values (f_m) which could be used more realistically to describe the transfer of radiocaesium from ingested soil to grazing animals. The transfer of radiocaesium to sheep milk from 2 different soil types was measured.

1.1 Materials and methods

Two soil types (Soil A and Soil B), artificially contaminated in lysimeters in 1981, were administered to lactating ewes. Table 1. shows the physical and chemical characteristics of the soils administered to the sheep.

Mean ^{137}Cs concentration in soil A and B were 16910 Bq kg^{-1} dry weight (dw) (SD=170) and 17700 Bq kg^{-1} dw (SD=180) respectively. Each soil type was administered to six ewes, housed in individual metabolism cages. The sheep used were an Italian meat breed, called Bergamasca, and are typical of the Alpine region. The ewes that were allocated to each experimental group were selected to be similar on the basis of age, live weight and milk production in the previous lactation periods.

Table 1. Characteristics of the soils fed to the sheep

Soil variable	Soil A	Soil B
Sand (%)	38	6
Silt (%)	51	78
Clay (%)	11	16
Organic Matter (%)	3	1
pH (H ₂ O)	7.7	7.5
CEC (meq 100g ⁻¹)	20	12

During the entire experiment the ewes were fed with lucerne pellets provided "ad libitum", 100 g of barley straw and 20 g of a vitamin supplement. The ewes were given an initial adaptation period in the metabolism cages of 20 to 40 days during which the sheep consumed the same diet (without soil) given during the subsequent 7 week study period. The contaminated soil was administered orally each day for 33 days. Each ewe received 100 g of contaminated soil, suspended in 200 ml of water, using an oesophageal catheter, connected with a syphon to a 500 ml bottle, closed with a non-returnable valve. After day 33 a decontamination phase of 14 days occurred.

Milk was collected from each ewe with the following frequencies:

- daily from day 1 to day 27 after the commencement of soil administration;
- once every 3 days from day 28 until day 33, ie at the end of soil administration;
- daily from day 34 to day 48 during the decontamination period.

^{137}Cs concentrations were determined in all samples.

1.2 Results and discussions

The daily intake of ^{137}Cs for each ewe was 1690 Bq d^{-1} ($\text{SD}=33$) for the ewes with soil A and 1770 Bq d^{-1} ($\text{SD}=35$) for the ewes administered with soil B. The soils used in this experiment are both mineral soils, characterised with a low content of organic matter (<3%). The mean ^{137}Cs activity concentrations and SD in ewes' milk fed with soil A and soil B (Bq l^{-1} ; $n=6$) are shown in Fig. 1.

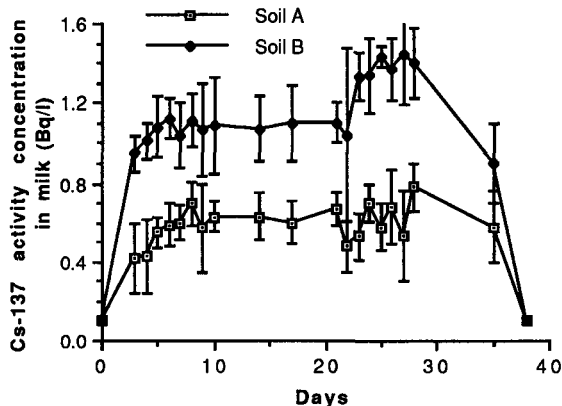


Figure 1 Changes in ^{137}Cs activity concentrations in milk from ewes fed with soil A and soil B (mean \pm SD)

Caesium-137 activity concentrations in milk reached a plateau after only about 7 days. For both soil types, a few days from the end of soil administration (38th day after the start of the experiment) ^{137}Cs levels in milk reached the limits of detection ($<0.2 \text{ Bq l}^{-1}$). The ^{137}Cs transfer coefficients from soil-to-milk calculated at the equilibrium for the 2 soil types were $3.72 \times 10^{-4} \text{ d l}^{-1}$ ($\text{SD}=0.72$) for soil A and $6.11 \times 10^{-4} \text{ d l}^{-1}$ ($\text{SD}=0.91$) for soil B. Student's t-test applied to the f_m values showed that these values are significantly different ($p<0.01$). This result indicates that ^{137}Cs in soil B is more available for uptake in the gut of the sheep than ^{137}Cs contained in soil A. Considering that the clay content in both soils is similar, to explain the observed differences in f_m values, more investigations

would be needed looking at the binding of radiocaesium in these soil types. For the soils used in this study, it is apparent that the availability for uptake of the radiocaesium from the soil is comparatively low. In mineral soils, radiocaesium is largely immobilised by sorption onto clay particles and is therefore unavailable for absorption. Therefore for these 2 soil types soil ingestion would not constitute an important source of radiocaesium to sheep milk or tissues.

An observed increase in f_m in the later stages of the experiment coincided with a dramatic reduction in milk production in the later stages of the lactation period for the particular breed of sheep used in this experiment. This suggests that the f_m is affected by the stage of lactation.

2. Soil adhesion

Samples of vegetation and soil were collected from a range of upland and lowland sites in northern Italy. Soil contamination was low, although in a grazed upland pasture it still on occasions accounted for over 20% of the radiocaesium activity associated with the vegetation samples.

Publications

Refereed papers

Belli, M., Blasi, M., Capra, E., Drigo, A., Menegon, S., Piasentier, E & Sansone, U. in press

Ingested soil as a source of ^{137}Cs to ruminants. *Sci. Total Environ.*

Belli, M., Sansone, U., Piasentier, E., Capra, E., Drigo, A. & Menegon, S. in press

^{137}Cs transfer coefficients from fodder to cow milk. *J. Environ. Rad.*

Conference reports/Other publications

Belli, M., Capra, E., Drigo, A., Marchetti, A., Menegon, S., Menin, A., Piasentier, E & Sansone, U. 1991

Un metodo per la determinazione "*in vivo*" delle concentrazioni del radiocesio nel bestiame. Atti del 4° simposio AIRP sulle Metodologie Radiometriche e Radiochimiche nella Radioprotezione, Alghero, 10-12 Aprile 1991.

Howard et al. 1991

Factors affecting radiocaesium transfer to ruminants. Progress Report: April 1990-March 1991 to CEC, DGXII.D.3. Radiation Protection Research Programme. Contract Bi7-018.

Project 5

Head of project: *Mr. Stakelum*

Objectives for the reporting period

1. To measure the true absorption coefficient (A_t) of both soil-bound and ionic radiocaesium in the gut of the dairy cow;
2. To measure the absorption, secretion and passage of ionic radiocaesium in the forestomach, small intestine and hind gut of the cow as affected by diet composition;
3. To compare the results of these experiments with equivalent experiments carried out with sheep at MLURI;
4. To prepare reports and publications on the experiments.

Progress achieved including publications

1. True absorption of radiocaesium in the gut of the dairy cow

In a UK-funded study the true absorption of ionic and soil-bound radiocaesium was compared in sheep and cattle. This gave us the opportunity, by taking additional samples, to compare different methods of estimating A_t in cattle and sheep in collaboration with Mayes et al. at MLURI.

Eight intact cows in early lactation were used to measure the A_t of both soil-bound and ionic ^{134}Cs (four animals per treatment). Caesium-137 was infused into the jugular vein of all cows. The average milk yield of the cows was 25 l d⁻¹. The average intake was 15 kg d⁻¹ dry matter (dm) and the herbage had an organic matter digestibility coefficient of 0.831.

Two methods were used to determine A_t as described by Mayes in the MLURI report. In Method 1 A_t was estimated from the daily ^{137}Cs intake, and total and endogenous ^{137}Cs outputs in faeces; endogenous faecal output was estimated from the partitioning of ^{134}Cs excretion in faeces and either urine, milk or blood. However, the use of blood to calculate A_t for soil-bound radiocaesium was not possible as the levels of ^{134}Cs in the blood were below detection limits. In Method 2, A_t was estimated as the plasma turnover rate of ^{137}Cs expressed as a proportion of daily ^{137}Cs intake. Plasma turnover rate was determined from the rate of infusion of ^{134}Cs and ^{137}Cs ; ^{134}Cs ratios in urine. The results are summarised in Table 1 and compared with apparent absorption values.

Table 1. Apparent (A_a) and true absorption coefficients (A_t) for ionic and soil-bound ^{137}Cs calculated by using different methods

Source of ^{137}Cs	A_a	Calculation method for A_t (mean)			
		* (urine)	Method 1 * (milk)	* (blood)	Method 2
Ionic	0.54	0.72	0.73	0.71	0.71
Soil-bound	0.16	0.20	0.26	-	0.19

* Body fluid used to calculate plasma turnover rate

2. Sites of absorption and recycling of radiocaesium in the gut of the dairy cow

Eight surgically prepared cows (4 cows cannulated at rumen, proximal duodenum and terminal ileum and 4 cows with rumen and duodenum cannulae) were used. Four cows received a ration of fresh grass in 6 separate feeds daily (Treatment 1) while the four other cows received one feed of 2.7 kg dm of a concentrate ration in addition to the grass (Treatment 2). The grass had an organic matter digestibility coefficient of 0.811 and contained 0.155, 0.222 and 0.420 g g⁻¹ dm of crude protein, acid-detergent fibre and neutral detergent fibre, respectively. The concentrate ration contained 0.151 and 0.137 g g⁻¹ dm of crude protein and crude fibre, respectively. The intakes of grass were 13.4 and 11.1 kg d⁻¹ dm and the milk yields were 21.3 and 20.6 kg d⁻¹ for treatments 1 and 2.

Rumen pH was 6.74 and 6.49 (SE=0.091) and the rumen acetate to propionate ratio was 2.56 and 2.58 (SE=0.042) for treatments 1 and 2. Rumen pH was lowest 4-5 hours after concentrate feeding, when a pH of 6.40 and 5.89 (SE=0.108) was recorded for treatments 1 and 2 respectively.

Six methods of calculating the A_t were used. Methods 1a, 1b and 1c were based on the endogenous faecal excretion rate of the dietary ^{137}Cs using urine, blood or milk ratios of the dosed to the infused ^{134}Cs . Methods 2d, 2e and 2f A_t was estimated as the plasma turnover rate of ^{137}Cs expressed as a proportion of daily ^{137}Cs intake. Plasma turnover rate was determined from the rate of infusion of ^{134}Cs and ^{137}Cs : ^{134}Cs ratios in urine, blood or milk. Table 2 outlines the results for all six methods for both treatments.

Table 2. Estimates of A_a and A_t , based on different calculation methods for both treatment groups.

Treatments	Calculation method						A_a
	1a	1b	1c	A_t			
				2d	2e	2f	
Grass	0.676	0.694	0.650	0.764	0.815	0.682	0.412
Grass+ concentrate	0.645	0.658	0.611	0.701	0.735	0.613	0.362
Mean	0.661	0.676	0.630	0.732	0.775	0.647	0.387
SE	0.0246	0.0243	0.0231	0.0224	0.0233	0.0123	0.0270

The A_t and A_a were slightly higher for treatment 2 in all cases. The difference was significant for method f at the 10% level. The error term was about half that of the others in this case. All methods (1a, 1b, 1c) based on endogenous faecal excretion of the dosed radiocaesium gave good agreement in addition to method 2f. Methods 2d and 1c gave somewhat larger values than the others. Values of A_t for ionic radiocaesium from Experiment 1 were within the range found here while the A_a was lower than Experiment 1.

The behaviour of dietary radiocaesium in different segments of the gut is summarized in Tables 3 and 4. Flow rates of radiocaesium at the duodenum and terminal ileum were estimated using intraruminally infused $^{51}\text{Cr-EDTA}$ and $^{103}\text{Ru-phenanthroline}$ as indigestible markers. The values shown in the tables have been averaged over both treatments as there was no effect of treatment.

Table 3. Two-way transfers of ^{134}Cs (% of intake) between various gut segments and the blood for dairy cattle given ionic radiocaesium (Mean \pm SE).

Pathway		mean \pm SE
Diet	→ Duodenum (dietary*)	93.2 \pm 3.42
Forestomachs	→ Blood (dietary)	6.8 \pm 3.57
Blood	→ Duodenum (endogenous)	26.6 \pm 1.85
Duodenum	→ Ileum (dietary)	39.1 \pm 3.77
Small intestine	→ Blood (dietary)	53.1 \pm 5.50
Duodenum	→ Ileum (endogenous)	10.7 \pm 2.18
Small intestine	→ Blood (endogenous)	14.2 \pm 2.02
Blood	→ Ileum (endogenous)	14.8 \pm 2.48
Ileum	→ Faeces (dietary)	37.7 \pm 3.87
Hind gut	→ Blood (dietary)	1.4 \pm 2.69
Ileum	→ Faeces (endogenous)	23.8 \pm 2.40
Hind gut	→ Blood (endogenous)	1.6 \pm 1.91
Blood	→ Faeces (endogenous)	1.5 \pm 1.20

*Dietary ^{134}Cs represents that which has remained in the gut.
Endogenous ^{134}Cs is that which was previously absorbed.

Table 4. Overall transfer of ^{134}Cs between different gut segments and the blood (% of intake).

	Secretion	True absorption (dietary* +endogenous)	(dietary)	Total flow out of gut segment
Forestomachs	27	7	7	120
Small intestine	15	67	53	64
Hind gut	2	3	1	61

*Dietary ^{134}Cs represents that which has remained in the gut.
Endogenous ^{134}Cs is that which was previously absorbed.

The forestomachs and small intestine were the major sites of recycling of radiocaesium with almost none recycled via the hind gut. The small intestine accounted for 87% of the total truly absorbed radiocaesium; true absorption in the forestomachs was 10% of total absorption. Additionally, endogenous absorption

occurred almost exclusively in the small intestine and forestomachs, with the small intestine accounting for the majority.

Over 120% of the dietary intake of radiocaesium was flowing at the proximal duodenum due to recycling in the rumen. Of this 100% of the dietary radiocaesium and 98% of the endogenous radiocaesium was associated with the liquid fraction of the digesta. Nearly 10% of both the dietary and infused radiocaesium passed through the duodenum in microbial material.

The absence of a major effect of concentrate feeding on radiocaesium behaviour in the gut is not surprising in view of the small effect the concentrate had on rumen fermentation. It was intended to use a concentrate ration which would promote very different digestive conditions to that of the grass ration, but at the very early stages of the experiment the cows were showing subclinical acidosis and were beginning to go off the feed. The concentrate was changed to a more fibrous composition and hence it had very little effect on digestive conditions. The total intake achieved in both groups of cows was identical with the intake of grass substantially reduced (reduction was almost one to one) by the supplementary feed.

Publications

Conference reports/Other publications

Howard et al. 1991

Factors affecting radiocaesium transfer to ruminants. Progress Report: April 1990-March 1991 to CEC, DGXII.D.3. Radiation Protection Research Programme. Contract Bi7-018.

Project 6

Head of project: *Dr. Colgan*

Objectives for the reporting period

1. Carry out soil adhesion study in Ireland as agreed under specified sampling protocol;
2. Calculate soil adhesion based in Ti data supplied by ITE;
3. Compile and analyse all data and produce a final report and publications.

Progress achieved including publications

1. Soil adhesion to vegetation

All samples have been taken and analysed. The data have been compiled and presented for discussion at the groups final meeting. A summary of the methods used and an account of the findings of the study is presented below.

1.1 Summary of methods

Five sites were chosen at working farms. Permanent pasture at each site was sampled monthly for 12 months according to the protocol, from the sites with differing soil types. Fresh sheep faeces were collected from these sites at the time of vegetation sampling. Soils (0-1 cm) were sampled from these sites at three times throughout the year. The winter fodders, hay, silage and fodder beet were sampled from both organic and mineral soils. Fresh fodder samples and soil samples were taken once from the field; stored samples were taken at three intervals throughout the storage period.

Rainfall was determined monthly at the pasture sites and for one week prior to sampling the fresh winter fodders. Biomass was determined for the vegetation samples. All samples were analysed for ^{137}Cs and ^{40}K , titanium (as an indicator of soil contamination) and a range of physico-chemical parameters as outlined in the original protocol.

1.2 Results and conclusions

a) Pasture

The biomass throughout the year fluctuated as would be expected, showing maximum production during the spring and summer months. The difference between the productivity at the three sites reflected the nutrient status of the three soil types and the degree of management. The ^{40}K content of the grass at all three sites showed a seasonal trend which is a typical pattern of uptake and loss of nutrients by many plant species. The magnitude of the ^{40}K values was determined by the soil ^{40}K content at each site but all three sites show similar trends, peaking during peak productivity in summer and declining toward winter and correlated with the biomass data. Calculation of monthly concentration ratios for ^{40}K show that the uptake of ^{40}K is reduced in the winter months

The ^{137}Cs content of the grass throughout the year demonstrated the opposite trend to that of ^{40}K . The concentration of ^{137}Cs in the grass samples increased towards the winter at all sites. Unlike ^{40}K this was inversely related to

biomass. Monthly concentration ratios showed that the apparent uptake of ^{137}Cs by the vegetation increased in winter. This contradicts all established seasonal patterns of uptake of elements by perennial plants and suggests that in the winter months plants are being contaminated by ^{137}Cs by some means other than root uptake (eg. soil adhesion).

The increase in ^{137}Cs activity concentrations observed in the grass was reflected in the faeces results. An example of such increases in the autumn and winter months for the lowland site with organic soil is given in Fig. 1. The results of the rainfall measurement shows that the rainfall increased towards the winter months as expected, but it was highly variable.

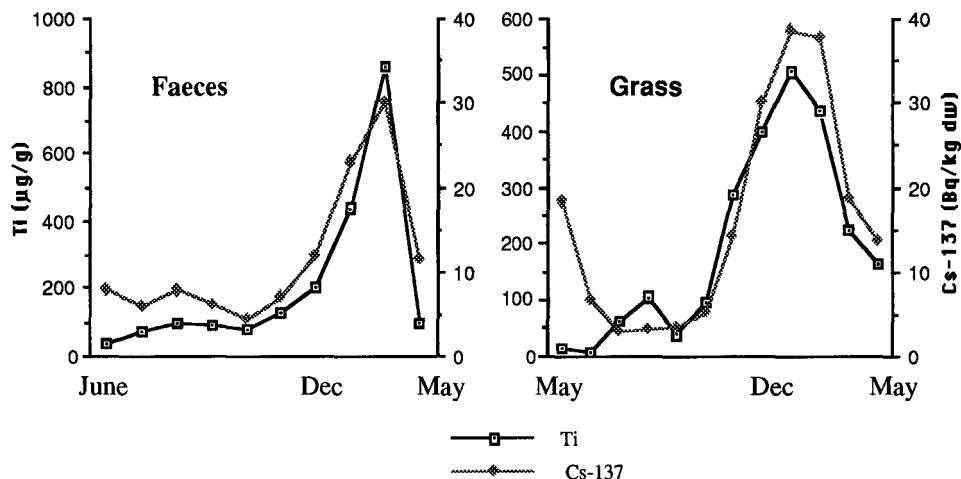


Figure 1. Changes with time in the ^{137}Cs and Ti concentrations in grass and faeces from a lowland site with an organic soil.

The increase in ^{137}Cs and Ti concentrations in the grass and faeces during the period of minimum growth, when the grass was short and had a low biomass, and when rainfall was at its highest, suggested that soil splash and trampling could have been responsible for the ^{137}Cs contamination of the samples.

The same effect was not seen for ^{40}K because the high levels of ^{40}K in the plant, compared to the levels measured in the soil, meant that the contribution to grass ^{40}K levels by soil adhesion was small relative to the concentration in the grass due to root uptake.

Comparison of the levels of Ti in soil with the levels in grass and faeces samples indicated the amount of soil contamination of these samples. In all cases the Ti data appeared to over-estimate the amount of ^{137}Cs on the vegetation which was due to soil adhesion, so the data and the method will need further investigation. However, even if the magnitude of the data is questionable, the seasonal trends should be valid and therefore there is much valuable information in these data.

The Ti content of the grass samples from all three sites increased in the winter months demonstrating that soil adhesion was taking place at this time and confirming the suggestions of the ^{137}Cs data. Just as in the case of ^{137}Cs the Ti concentrations in the vegetation samples showed an inverse relationship with biomass.

Comparison of the sites reveals considerable inter-site differences in the

importance of soil adhesion. There is a close relationship between ^{137}Cs and Ti levels in the grass samples and on the mineral site soil adhesion is the most important means of soil to plant transfer of ^{137}Cs . At the site with organic soil, root uptake of ^{137}Cs is greater so the soil adhesion effect is less pronounced. The third site has a mineral soil, but with a very poor growth of grass under very damp conditions. At this site, soil adhesion is the most important soil to plant transfer route for ^{137}Cs but the situation is complicated by local conditions.

It has already been shown here that there is a good correlation between grass ^{137}Cs levels and that of corresponding faeces samples. The degree of soil contamination of each grass sample is also reflected in the levels of soil contamination of the corresponding faeces samples. As soil is not assimilated by the animals this is to be expected.

b) Winter fodders

The fresh samples of hay and silage had very low levels of ^{137}Cs and Ti, but the first crop of stored samples had, in almost all cases, much higher levels of both these elements (Table 1). Discussions with the farmers revealed that the soil had been very dry and loosely packed during the harvesting period and so the vegetation may have received dust contamination. The exception to this case which showed no difference between mechanical and hand sampling was the hay sampled on mineral soil. This crop was subjected to heavy rainfall at the time of cutting and so the incorporation of dust might in this way have been reduced. In general these data indicate that mechanical harvesting, compared with the careful sampling method, increases the extent of soil adhesion onto the fodder.

Table 1. Summary of ^{137}Cs activity concentrations and Ti concentrations of winter fodder samples (mean \pm SD).

Fodder type	Soil type	^{137}Cs activity conc ⁿ . (Bq kg ⁻¹ dw)				Ti content ($\mu\text{g g}^{-1}$ dw)			
		Fresh	Stored			Fresh	Stored		
			1	2	3		1	2	3
Hay	Org	3.7	14.1	1.8	1.6	4.2	24.6	6.8	-
		± 0.67	± 5.65	± 0.46	± 0.61	± 1.10	± 17.5	± 2.70	-
Hay	Min	1.5	1.2	1.5	3.6	87.7	57.5	13.3	14
		± 0.58	± 0.15	± 1.37	± 0.52	± 66.30	± 20.5	± 1.20	± 2.20
Silage	Org	5.0	51.9	26.4	-	6.0	41.5	18.6	-
		± 0.67	± 5.65	± 0.46	-	± 0.70	± 5.50	± 5.40	-
Silage	Min	1.3	4.2	1.3	1.4	20.0	47.5	32.3	19.3
		± 0.58	± 0.15	± 1.37	± 0.52	± 9.20	± 6.80	± 8.70	± 7.90

With the exception again of the mineral hay values there is a significant decline in the ^{137}Cs content of the fodders throughout their storage period. Similarly the Ti concentrations also declined during storage.

The fodder beet showed the opposite pattern. In this fodder the hand sampled material contained higher levels of ^{137}Cs and Ti than the mechanically sampled material. This was probably due to the loss of adhering soil during the mechanical processing (as the amount of adhering soil is quite significant). The data are limited and variable but there appears, from the Ti data, to be a decline in the extent of soil adhesion onto fodder beet during storage.

1.3 Summary

1. The ^{137}Cs and Ti data for pasture grass samples followed seasonal trends which indicated a winter peak in grass ^{137}Cs levels which was due to soil contamination when the biomass was low and the rainfall high.
2. These Ti and ^{137}Cs data for the vegetation were reflected in the sheep faeces.
3. There was considerable site dependent variability in the extent of soil adhesion onto pasture vegetation.
4. Mechanical harvesting of hay and silage appeared to increase soil contamination of the crop, especially in dry weather.
5. There was high soil contamination of fodder beet and this declined slightly during harvesting and storage.

Publications

Howard et al. 1991

Factors affecting radiocaesium transfer to ruminants. Progress Report: April 1990-March 1991 to CEC, DGXII.D.3. Radiation Protection Research Programme. Contract Bi7-018.

Project 7

Head of project: *Dr. Assimakopoulos*

Objectives for the reporting period

1. Measure the transfer coefficient for radiocaesium transport to various tissues of a sheep (muscle, fat, liver, lungs, etc.);
2. Develop a model for trace element transport to ruminants and their milk;
3. Conduct a study of possible variations in the milk radiocaesium transfer coefficient for sheep during an entire lactation period;
4. Conduct an experiment and analyse samples to measure the transfer coefficient for radiocaesium to ewes' milk from ingested soil;
5. Conduct a study of seasonal variations in soil adhesion on grass in pastures grazed by sheep;
6. Preparation of reports to CEC and papers for publication in the open literature.

Progress achieved including publications

The following is a summary of the activities at the Nuclear Physics Laboratory (NPL), within the research programme covering activities between 1 April 1990 and 31 March 1992. All the above studies were completed with the exception of the soil adhesion study where a few samples remain to be analyzed because of a breakdown in analytical equipment.

1. Modelling

A general multiple-compartment model for the transport of trace elements through animals has been devised and implemented in a computer programme. The model has been calibrated and validated with the help of data obtained in ad-hoc experiments. A feature of this model is that it explicitly takes into account the volume of each compartment of the system, as well as temporal variations in the system's volume compartments. It is thus particularly suited for the description of milk accumulation in the mammary gland. The model has been used to determine transfer coefficient values in the animal studies described below. The model was presented at various Symposia and Workshops. A detailed description of the model has been published in Health Physics.

2. Radiocaesium transfer from a sheep's diet to its tissues

Transfer coefficients for radiocaesium transport from a sheep's diet to its blood, muscle, lung, liver, kidney, spleen, heart, brain, rumen, intestines and fat were measured in a controlled experiment involving fifty adult ewes. The animals were fed dry grass and wheat, both contaminated from the Chernobyl fallout, for a period of 60 d. During this period half of the animals were sacrificed at regular intervals and samples of their blood and tissues were measured to determine their radiocaesium activity concentrations. The rest of the animals were returned to uncontaminated food and were monitored for radiocaesium

concentration through periodic slaughtering for an additional 60 d. Transfer coefficients were calculated from the plateau reached at the end of the contamination phase. The data were also analyzed by means of the model described above and transport rate parameters for each compartment were extracted. Transfer coefficients computed through the model's transport rate parameters show good agreement with the experimentally obtained values. A paper on this experiment will be published in Science of the Total Environment.

3. Effect of stage of lactation on radiocaesium uptake

The transfer of radiocaesium to ewe milk was measured in separate groups of lactating ewes which were at different stages of lactation.

Five groups of animals were studied during the spring of 1990, mainly as a test of the protocol and the model. Systematic measurements were resumed in November 1990. Two hundred ewes, which gave birth between 30 October and 2 November, 1990, were selected for the experiment.

For each treatment a group of five lactating ewes, which were a pre-selected number of weeks into the lactation period, were segregated from the flock for three weeks. During the first "acclimatization phase", the animals were fed uncontaminated wheat for 1 week and both their daily intake and milk production were monitored. During a second week, the "contamination phase", the animals were fed wheat, harvested in northern Greece during the summer of 1986, contaminated with radiocaesium at a level of 1200 Bq kg⁻¹ dw. Daily intake, milk production and Cs activity concentration in the milk were monitored during this phase. The same parameters were also monitored during the third week, the "decontamination phase", during which the animals were returned to an uncontaminated diet. Thus, each stage of the total lactation period was characterised by three weeks of data. Since the animals were milked twice daily, the contamination and decontamination phases yielded 28 data points of radiocaesium activity concentration in milk for each group.

The transfer coefficient for each group was obtained by fitting the data to the milk model, devised by this laboratory (see above).

The results of this analysis showed an increase in the radiocaesium activity concentration in the milk by a factor of three, over the twenty one week lactation period. However, a significant correlation was found between transfer coefficients for radiocaesium and average daily milk yield, providing evidence for a steady radiocaesium transfer to ewe's milk throughout the lactation period.

A paper on this experiment has been submitted for publication.

4. Soil ingestion study

Twenty kilograms of heavily contaminated surface soil were collected from a site near the Chernobyl reactor during a visit of members of the NPL to Zeleny Mys in November 1990. Due to the high activity concentration in the soil, the sample was delivered to the N.R.C. "Demokritos" for processing, where it was dried and sieved. The processed soil, with a measured ¹³⁷Cs activity concentration of 47 kBq kg⁻¹ dw, was encapsulated in gelatin capsules of 8g capacity. Feeding of the capsules (two per day) to animals commenced on 21 March, 1991. The study was carried out according to the protocol followed by ENEA in a similar experiment.

Eight lactating ewes were placed in metabolic cages. The experiment involved a seven day contamination period, followed by a decontamination period of the same duration. Samples of milk, faeces and urine were collected and measured to determine their radiocaesium activity concentrations. Transfer coefficients were obtained through a best fit (minimum χ^2) of the data to predictions of the animal model described above. The values obtained were $f_m = (2.6 \pm 0.7) \times 10^{-2}$ and $f_u = (5 \pm 2) \times 10^{-2} \text{ d kg}^{-1}$ for radiocaesium transport to milk and urine, respectively. These results suggest that soil ingestion can be a major source of radiocontamination for sheep and other free-grazing ruminants. The

availability of soil-associated radiocaesium in this study was three fold higher than that determined by Hansen & Hove and two orders of magnitude higher than that measured by Belli et al., even though in the latter experiment the clay content of the ingested soils was similar. This suggests that there must be some other factor influencing availability and it is possible that the nature of the radiocaesium deposit close to the Chernobyl NPP is responsible for the observed high transfer. Further investigations to investigate the reasons for the differences are in progress.

A paper on this experiment will appear soon in the journal, Science of the Total Environment.

5. Soil adhesion study

Two pastures, with an area of approximately 1.2 hectares each, were selected for this investigation. The soil of Pasture A was predominantly clay and that of Pasture B, near lake Pamvotis, Ioannina, was predominantly a sandy soil. A detailed soil analysis for the pastures was conducted in April, 1990. Both pastures are within 5 km and are owned by the Ioannina Agricultural Research Station. During the spring and summer months they are systematically grazed by the Station's sheep. Daily precipitation data, recorded by the Ioannina Agricultural Research Station, will be used in the analysis of the experiment.

Samples of soil, grass and faeces were collected from both pastures, according to the protocol agreed for this experiment, every 15th of the month, starting on 15 May, 1990. The samples were treated according to the experimental protocol and measured by XRF for Ti concentration. Although appreciable levels of titanium could be detected in the soil samples, Ti concentrations in the grass and faeces samples were found to be below the detection limits of conventional XRF (about 30 to 50 $\mu\text{g g}^{-1}$, depending on background elemental concentrations). All samples of grass and faeces were thus measured through a variation of the XRF method, developed in a different research project of the NPL, at the Nuclear Research Centre "Demokritos" in Athens. This method, usually referred to as XSQR (Karydas, A.G. and Paradellis T. Coal XRF analysis using a proton induced copper x-ray beam, J. of Coal Quality, 9:39-43; 1990), is able to detect concentrations of light elements of the order of 1 $\mu\text{g g}^{-1}$ or better. Using this method Ti concentrations of 20 $\mu\text{g g}^{-1}$ in grass samples and 70 $\mu\text{g g}^{-1}$ in faeces samples were measured. Results obtained with this method and by that used by ITE, for all the other samples in the soil adhesion study, has been compared in an inter-comparison exercise and were in good agreement. Half of the samples collected to date have been processed, but measurements through the method described above were delayed last autumn due to the interruption of operations of the accelerator at the NRC. We expect to complete these measurements during the summer of 1992.

Publications

Refereed papers

Assimakopoulous, P.A., Ioannides, K.G., & Pakou, A.A. 1991

A general compartment multi-compartment model for the transport of trace elements through animals.

Health Phys., 61, 245-253.

Assimakopoulous, P.A., Ioannides, K.G., Pakou, A.A, Mantzios, A.S. & Pappas, C.P. in press

Transport of radiocaesium from a sheep's diet to its tissues. Sci. Total Environ.

Assimakopoulous, P.A., Ioannides, K.G., Karamanis, D., Pakou, A.A., Stamoulis, K., Mantzios, A.G. & Nikolaou, E. in press

Radiocaesium transfer to sheep's milk as a result of soil ingestion. Sci. Total Environ.

Assimakopoulous, P.A., Ioannides, K.G., Karamanis, D., Pakou, A.A, Stamoulis, K., Mantzios, A.S. & Nikolaou, R. submitted

Variation of the Transfer Coefficient for Radiocaesium Transport to Sheep's Milk during a Complete Lactation Period,

Conference reports/Other publications

- Assimakopoulous, P.A., Ioannides, K.G., Pakou, A.A. & Mantzios, A. 1990
Validation of multiple compartment model for the transfer of Cs through animals. Presented at an International Conference on Applications of Nuclear Techniques, Heraklion, Crete, 24-30 June.
- Assimakopoulous, P.A., Ioannides, K.G. & Pakou, A.A. 1990
Validation of a general multiple compartment model for the transport of trace elements through animals. Presented at the Symposium and workshop on the validity of Environmental Transfer Models, Stockholm, 8-12 Oct 1990.
- Assimakopoulous, P.A., Ioannides, K.G. & Pakou, A.A. 1991
Milk: A programme for the analysis of milk contamination and decontamination data. Internal distribution report to CEC group members. Nuclear Physics Lab., Jan 1991. 21pp + discs. University of Ioannina: Ioannina.
- Howard et al. 1991
Factors affecting radiocaesium transfer to ruminants. Progress Report: April 1990-March 1991 to CEC, DGXII.D.3. Radiation Protection Research Programme. Contract Bi7-018.
- Assimakopoulous, P.A. 1991
Environmental Radioactivity Measurements in Northwestern Greece. Symposium on the Long Term Follow up of the Chernobyl Disaster, Hellenic Cancer Society, Athens, 6-8 December, 1991.
- Assimakopoulous, P.A. 1992
Environmental Radioactivity Measurements in Northwestern Greece, 3rd Hellenic Symposium on Nuclear Physics, Technical University of Athens, May 25-26, 1992.
- Assimakopoulous, P.A. 1992
Environmental Radioactivity Measurements in Northwestern Greece, 1st International Symposium on Environment and Development, Metsovo, Greece, May 27-30, 1992.
- Assimakopoulous, P.A., Ioannides, K.G., Karamanis, D., Pakou, A.A., Stamoulis, K., Mantzios, A.S., Nikolaou, E & Howard, B.J. 1992
Variation of the transfer coefficient for radiocesium transport to sheep's milk during a complete lactation period. Report NPL-91-3. Dep. Physics, University of Ioannina, Greece.
- Assimakopoulous, P.A., Aslanoglou, X., Ioannides, K., Pakou, A., Karamanis, D. & Stamoulis, K. 1992
Research Activities of the Nuclear Physics Laboratory, Third Panepirus Congress for Research in Physics, Ioannina, 10-11 April, 1992.

Project 8

Head of project: *Dr. Unsworth*

Objectives for the reporting period

1. Develop the RUINS model for studying the importance of soil adhesion as a source of radiocaesium to animals;
2. Determine the feasibility of using *in-vitro* cell culture techniques for studying the dynamics of radiocaesium in sheep cells;
3. Consider the use of the sheep radiocaesium model for the effect of animal age on radiocaesium metabolism;
4. Develop a physiologically based radiocaesium metabolism model which will have more general applicability;
5. Investigate the sensitivity of the sheep radiocaesium metabolism model to countermeasures such as binders in the gut;
6. Investigate the sensitivity of the RUINS model to environmental factors such as season and grazing.

Progress achieved including publications

1. Modelling studies

Modelling studies have been carried out in two areas, the environmental factors affecting radiocaesium transfer to grazing animals, and the physiological factors affecting the radiocaesium metabolism of ruminants.

1.1 Environmental factors

a. Soil Adhesion Sensitivity

Previous work at Nottingham has led to the development of the RUINS package which is intended to simulate transfer of radiocaesium in the soil-pasture-grazing animal agro-ecosystems. Within this study RUINS has been developed to determine its sensitivity to factors related to the adhesion of contaminated soil to vegetation surfaces. The factors studied were:

1. Availability of radiocaesium in soil relative to plant incorporated material, set by a parameter A_{EX} (which takes a value between 0 and 1).
2. Fraction of vegetation radiocaesium which is attributed to soil adhesion.
3. Importance of soil type and the differing availability from various soil components.

These studies are to be published in a refereed journal (Crout et al. in press) and were discussed in the previous progress report to the CEC (Howard et al. 1991).

b. Effect of Grazing Intensity.

RUINS has also been used to investigate the importance of grazing pressure on radiocaesium uptake by plants and subsequently grazing animals. For reasons of simplicity the model defines grazing pressure as a fractional

utilisation of new sward growth, rather than a specific number of animals per hectare. This means that during a normal prediction run, when climate varies with season resulting in a seasonal pattern of growth, the effective number of animals will vary, but the fraction of growth they remove is always the same. In the case of these calculations the seasonal features have been removed and growth is constant. The prediction was performed for three levels of fractional grazing pressure, 0.05, 0.25, and 0.5, and an assumed A_{EX} of 0.3, and the results shown in Fig. 1. Grazing intensity, as currently modelled in RUINS, exhibits a complex effect on radiocaesium concentrations in the vegetation system and thereby in the animal. Initially a high grazing pressure leads to high animal radiocaesium activity. At later stages the situation is reversed and higher grazing pressure results in lower radiocaesium concentrations.

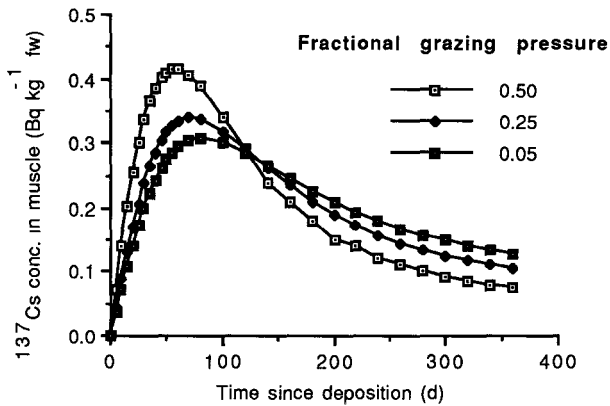


Fig 1. Lamb radiocaesium activity concentration vs time since deposition of 1 Bq m^{-2} ($A_{EX} = 0.3$), for 3 levels of grazing pressure.

A number of factors in the model lead to these interesting results. An intensively grazed sward has a much lower standing biomass than its lightly grazed equivalent. However it will still grow at almost the same rate because both swards will intercept nearly all the available light unless the grazing becomes extreme. The uptake of radiocaesium as modelled in RUINS is driven by growth, and therefore uptake will be similar for a given sward, irrespective of its grazing pressure. Because of the difference in standing biomass this results in a more rapid rise in vegetation activity concentration, and consequently higher initial levels in animals on intensively grazed swards. After the initial 100-150 days the situation is apparently reversed and more intensive grazing of the sward results in lower animal radiocaesium activity concentrations. By this time the radiocaesium in the system will be extensively recycled between the sward and soil and this process is influenced by the level of grazing. This is due to the relative proportions of radiocaesium leaving the sward by grazing compared with senescence and litterfall. During senescence the model assumes that a fraction of the radiocaesium in the senescent tissue is retained. Clearly no such process occurs when plant tissue is removed by grazing. Therefore changes in grazing pressure alter the balance between grazing loss and senescence and thereby radiocaesium concentrations in the sward.

These aspects of RUINS are still under development and should be viewed

with caution, however there is supporting field evidence on the influence of grazing pressure on radiocaesium activity concentrations by Salt & Mayes (1991). They maintained two grass/clover swards at different heights by different intensities of continuous grazing. The more intensively grazed sward consistently had a lower radiocaesium activity concentration, consistent with the predictions presented here for the period after approximately 150 days.

c. Simulation of Countermeasures

By adjusting some of the rate constants in the sheep model it is possible to simulate some of the possible effects of animal countermeasures. For instance radiocaesium binders can reduce the absorption of radiocaesium, and by preventing recycling within the gut of an already contaminated animal may act to reduce the biological half-life of radiocaesium in the muscle of a grazing animal. The potential magnitude of this effect can be simulated using the model by setting the rate constants from gut to extracellular fluid to zero. The predicted reduction for biological half-life of radiocaesium in muscle is 25-30%.

1.2 Physiology

a. Model Validation

A multicompartment model of lamb radiocaesium metabolism has been developed under previous research programmes, and has been further developed and validated in collaboration with CEC partners (Galer et al. in press). As a partial validation the model can be used to calculate various 'macro'-parameters, such as transfer coefficient and true and apparent absorption, for comparison with observed values (Table 1).

Table 1. Predicted values for radiocaesium transfer and absorption

Parameter	Value
Transfer Coefficient ($d \text{ kg}^{-1}$)	0.34
Apparent Absorption (A_a)	0.55
True Absorption (A_t)	0.75

These values are comparable with published literature and data from this CEC group, although the true absorption value is slightly low; experimental measurement of A_t within this CEC group have generally been around 0.8. Calculations of the fluxes of radiocaesium within the gut have also been made (Table 2), these compare favourably with experimental data reported here by Mayes [03] when appropriate gut compartments are grouped together in a manner comparable with the model.

Table 2. Predicted radiocaesium fluxes in the gut.

	Radiocaesium flux (Bq d^{-1})
Rumen -> ECF	0.41
ECF -> Rumen	0.10
Rumen -> GIT	0.69
GIT -> ECF	0.32
ECF -> GIT	0.23

ECF = extracellular fluid; GIT = gastrointestinal tract

b. Effect of Age

There are a number of factors which could alter radiocaesium metabolism and absorption in growing animals. Absorption across the gut wall may be higher in suckling or young animals (Deren 1968) although there appears to be little difference in the absorption of ionic radiocaesium with age in sheep on a diet of fresh ryegrass (Mayes et al. in press). Fractional protein synthesis rates in muscle are higher for young animals (Gill et al. 1989) and this may affect the distribution between tissues although the most obvious effect is that body weight increases significantly. As described above, the model utilises first order rate constants; these represent the fractional turnover of radiocaesium in each compartment per unit time. In order to calculate transfer coefficients the model therefore assumes appropriate tissue masses. Using these assumed masses muscle f_f values for different ages have been calculated from appropriate body weights (Fig 2). This makes the assumption that the fractional rate constants between tissues remain the same in younger animals, which may not be strictly valid. However, a decrease in muscle f_f with age is predicted. Changes predicted by the model are consistent with reported values of f_{fs} for lamb such as 0.63 for animals < 5 months of age (Vandecasteele et al. 1988), 1.61 for animals 4 months of age (Beresford et al. 1989) and the CEC recommendation of 0.6 for lamb (CEC 1987). This illustrates the potential importance of body size on radiocaesium dynamics, indeed the rapid changes in f_f estimated for lambs less than 3 months old may lead to the wide variability reported in the literature.

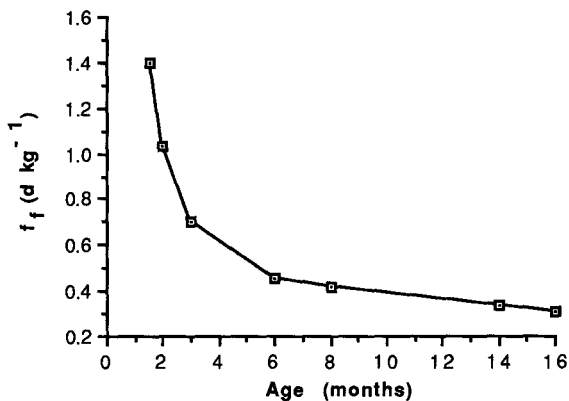


Fig 2. Effect of age on model predicted transfer coefficients.

1.3 Physiological model

In addition to this work the animal model has been extended so that its parameters are based upon the underlying animal physiology, rather than arbitrary 'fits'. This has significant potential benefits.

- i) A model based upon well founded physiological principles can be applied to animals other than sheep, greatly extending the relevance of the overall projects work.
- ii) It will provide a sound theoretical framework, within which countermeasures could be developed and understood.

The principle areas in which this is possible are gut flow and radiocaesium release from muscle. There is a considerable literature describing the rate of

passage of feed through ruminants and this can be used to generate rate constants for the various gut flows described in the animal model. These compare well with the values we have derived previously on the basis of empirical fits to measured data. There is also some evidence from the literature that radiocaesium 'binds' to structural proteins within muscle cells, such as myocin. A simple hypothesis which can then be tested using the model is whether the rate at which radiocaesium is lost from muscle cells is related to the rate of protein turnover within an animal. Again such figures are available from the literature. We have developed a simple model, which combines these ideas and the existing 'empirical' model for sheep and cows. The resulting 'macro'-parameters are presented in Table 3 and compare favourably with published values, although the half-lives for muscle are slightly high.

Table 3. Estimations of Radiocaesium transfer coefficients and half-lives based on a "physiological" approach.

	Lamb	Beef
Transfer Coefficient (d kg ⁻¹)	0.57	0.04
Muscle Half-life (days)	19.8	38.4

2. Experimental studies

In parallel with these modelling studies a limited experimental programme has been conducted in collaboration with the Applied Biochemistry Department at Nottingham (P.J. Buttery). These experiments were of a somewhat speculative nature, the objectives being to characterise the cellular uptake and efflux using standard *in-vivo* culture techniques. The results are intended to relate directly to the modelling studies, described above. Example results from these experiments are shown in Fig. 3 which shows the observed influx and efflux of radiocaesium in sheep muscle cells. Of particular interest in Fig. 3 is the apparent 'tail' to the efflux curve which may suggest that some longer term binding has occurred within the cells. Only a preliminary analysis of this data has taken place, the full incorporation within our models is being done under a separate research project, the principal difficulty lies in 'scaling up' the results to the whole animal.

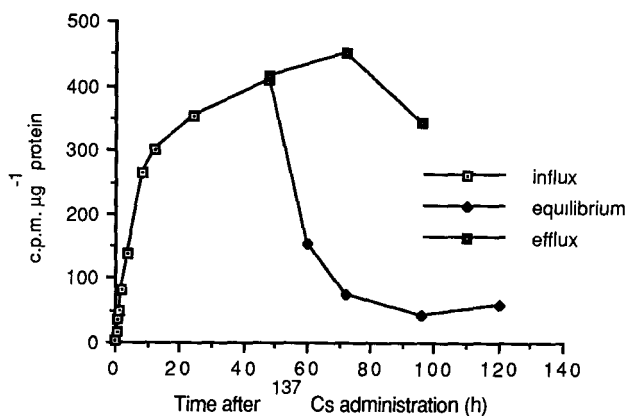


Fig 3. Influx and efflux of radiocaesium from contaminated sheep muscle cells (*in-vitro*) vs time.

Publications

Refered papers

Galer, A.M., Crout, N.M.J., Beresford, N.A., Howard, B.J., Mayes, R.W., Barnett, C.L., Eayres, H.F. & Lamb, C.S. in press

Dynamic radiocaesium distribution in sheep: measurement and modelling. J. Environ. Rad.

Crout, N.M.J., Beresford, N.A. & Howard, B.J. in press

Does soil adhesion matter when predicting radiocaesium transfer to animals? J. Environ. Rad.

Beresford, N.A., Mayes, R.W., Crout, N.M.J., Howard B.J., Oughton, D.H. & Kanyar, B. in preparation

Dynamic behaviour of ^{110m}Ag in sheep tissues.

Conference reports/Other publications

Galer, A.M., Crout, N.M.J., Beresford, N.A. & Howard, B.J. 1990

Modelling radio-caesium transfer in upland ecosystems. In: 1st Int. Conf on the Atomic Power Plant Accident at Chernobyl, held at Zeleny Mys, p.264.

Crout, N.M.J., Galer, A.M., Howard, B.J. & Beresford, N.A. 1991

A comparative assessment of the impact of the Windscale and Chernobyl accidents on Cs-137 levels of upland lambs in west Cumbria using the RUIINS model. In: Proc. of a Seminar on Comparative Assessment of the Environmental Impact of Radionuclides Released During Three Major Nuclear Accidents: Kyshtym, Windscale, Chernobyl. Luxembourg, 1-5 Oct 1990. Commission of the European Commission: Luxembourg. pp 1122-1136.

Howard et al. 1991

Factors affecting radiocaesium transfer to ruminants. Progress Report: April 1990-March 1991 to CEC, DGXII.D.3. Radiation Protection Research Programme. Contract Bi7-018.

Project 9

Head of project: *Prof. Jones*

Objectives for the reporting period

1. To study the transfer of radiocaesium from grazing plants to free ranging sheep
2. To study the correlation between radiocaesium content and muscle fibre composition in different muscles of the sheep. This study was initiated to try and understand the reasons for the observed 20% variation in radiocaesium contents in different muscles.
3. To study the transfer of radiocaesium to ewes milk.
4. To estimate the true absorption of radiocaesium in reindeer. This study was performed to provide data for inter-species comparisons.

Progress achieved including publications

1. Studies of free ranging sheep

The uptake of radiocaesium from pasture to lambs meat was studied in the mountainous area around Klimpfjäll, County of Västerbotten (latitude 65 N; longitude 15 E). The deposition of ^{137}Cs in this area from the Chernobyl accident was 20-30 kBq m². The animals have been followed for three years, two within this project, and their forage intake and radiocaesium uptake estimated at slaughter in early October each year.

The results show that the radiocaesium content of muscular tissue varied considerably in these lambs from year to year. The mean ^{137}Cs activity concentration in muscular tissue was 860 Bq kg⁻¹ (range 677-1258) in 1989, 1660 Bq kg⁻¹ (range 1370-2084) in 1990 and 415 Bq kg⁻¹ (range 279-563) in 1991. One important reason for this variation is the presence of fungal fruit bodies in the grazing area, but differences in green plant intake also accounted for some of the observed differences. For instance, in 1990 a substantial intake (6% of ruminal content) of ferns, with high radiocaesium levels was seen compared with only 0.2% in 1989. Although the ruminal content at slaughter only reflects a short preceeding period these figures show that the animals had been grazing plants with a high radiocaesium content.

2. Studies of radiocaesium accumulation in muscles with different fibre composition

Four male 8 month old lambs were fed a standard pelleted lucerne diet and given 1200 Bq ionic ^{137}Cs in a gelatine capsule daily. After 28 days the animals were slaughtered and seven different muscles taken for determination of ^{137}Cs content and fibre composition using conventional histo-chemical methods. The results show that there is a correlation between radiocaesium concentration and muscle fibre composition (see Table 1). It was also found that although the animals have received the same diet and the same amount of ^{137}Cs , the mean ^{137}Cs activity concentration varies between the animals from 239 to 361 Bq kg⁻¹. But

perhaps more important, especially from a theoretical point of view is the variation between the different muscles in the same animal. Such differences have been reported previously, but are often not considered when transfer from feed to meat (ie. muscular tissue) is calculated. In this study there was a two-fold difference between the muscle with the lowest mean ^{137}Cs activity concentration, the *Longissimus dorsi*, and that with the highest, the *Masseter*, which is a greater variation than seen in most studies (generally a 20% difference). The reason for the larger difference in this study is not known.

The f_f values calculated in this study vary between 0.15 to 0.46 d kg^{-1} depending on the lowest or highest ^{137}Cs activity concentration of the different muscles. The mean value was calculated to be 0.23 d kg^{-1} which is similar to values obtained earlier in our laboratory as well as by other authors.

Table 1. The concentration of ^{137}Cs Bq kg^{-1} fresh weight in different muscles of lambs and the histo-chemical fibre composition of these muscles.

Muscle	Radiocaesium activity concentration (Bq kg^{-1} fw)		Fibre type 1 (%)	
	mean	range	mean	range
<i>Masseter</i>	408	317-582	100	
<i>Ext. carpi radialis</i>	266	196-348	39	35-46
<i>Sterno-mandibularis</i>	334	274-369	39	32-55
<i>Supraspinatus</i>	286	223-336	28	26-67
<i>Longissimus dorsi</i>	209	192-275	33	5-60
<i>Biceps femoris</i>	283	245-345	24	21-27
<i>Semimembranosus</i>	254	228-275	14	12-14

3. Transfer of radiocaesium to ewes milk

Radiocaesium transfer to the milk of a typical Swedish sheep, Swedish Landrace, was studied in six ewes in their third week of lactation. The ewes received a standardized feed of pelleted lucerne. The radiocaesium was given as ionic ^{137}Cs in gelatin capsules at a rate of 12,000 Bq d^{-1} for 5 days. Milk samples were taken during the period of ^{137}Cs administration, and for the 5 days after ^{137}Cs administration was stopped. The mean transfer coefficient was calculated to be 0.082 d l^{-1} (range 0.06 - 0.11 d l^{-1}) by model predictions based on the experimental data, using a similar approach to that outlined by the Greek participants in this programme.

4. Determination of true absorption of radiocaesium in reindeer

Two groups of three, male 20 months old reindeer were used to study the true absorption of radiocaesium comparing ionic ^{137}Cs and ^{137}Cs in lichens contaminated by the Chernobyl accident. Continuous infusion of ^{134}Cs was used and blood samples taken at the end of a ten day experimental period to determine the ^{137}Cs dietary turnover rate through the blood plasma and hence true absorption.

The results from the experiment are still under evaluation.

Publications

Refereed Papers

Hove, K., Strand, P., Voigt, G., Jones, B.-E.V., Howard, B.J., Segal, M.G., Pollaris, K. & Pearce, J. in press

Countermeasures for reducing radioactive contamination of farm animals and farm animal products. *Sci. Total Environ.*

Jones, B.-E.V. in press

Management methods of reducing radionuclide contamination of animal food products. *Sci. Total Environ.*

Mayes, R.W., Lamb, C.S., Beresford, N.A., Barnett, C.L., Howard, B.J., Jones, B.-E.V., Eriksson, O., Hove, K., Pedersen, Ø. & Staines, B.W. submitted

Novel approaches to the estimation of intake and bioavailability of radiocaesium in ruminants grazing forested areas. *Sci. Total Environ.*

Jones, B.-E.V. in preparation

Transfer of ionic radiocaesium to ewes milk.

Jones, B.-E.V., Eriksson, O. & Raunistola, T. in preparation

Transfer of radiocaesium from pasture to free ranging sheep.

Jones, B.-E.V. & Essen-Gustavsson, B. in preparation

Radiocaesium uptake and muscle fibre composition in lambs.

DEPOSITION OF RADIONUCLIDES ON TREE CANOPIES AND THEIR SUBSEQUENT FATE

Contract Bi7-009 - Sector A25

- 1) *Minski* , ICSTM - 2) *Belot* , CEA - FAR
- 3) *Rauret* , Univ. Barcelona - 4) *Ronneau* , Univ. Cathol. Louvain-la-Neuve

Summary of project and global objectives

It is known from studies of the deposition of conventional pollutants to forest canopies that trees are highly efficient in their interception and retention of airborne particulate materials. This has also proved to be the case for radioactive aerosols following the Chernobyl accident and as a consequence large areas of forest throughout Europe are still contaminated to some extent by ^{137}Cs . Following initial capture of radioactive fallout nuclides such as ^{137}Cs may then become incorporated into foodchains with the possibility of their ultimate transfer to man, especially *via* wild food products.

While much is known about the deposition processes involved in the initial contamination of grassland areas with radioactive fallout very little knowledge exists which relates directly to the mechanisms of deposition, accumulation, transfer and recycling of radionuclides within forest ecosystems. It seems likely that these processes will be considerably more complex within the latter ecosystems which comprise canopies of considerable architectural complexity and morphological variety, often underlain by herbaceous understories. The overall objective of this project is to provide an insight into the physical processes operative in such complex ecosystems which result in aerosol capture, recycling and loss. This is being approached at various levels within the project by each member group.

Dr Belot's group is performing detailed studies of the effects of wind speed and particle size on the deposition of aerosols onto individual leaves and twigs of Pine, Spruce and Holm Oak. These experiments make use of a relatively narrow cross section wind tunnel into which dye-laden aerosols are released. The data so derived, and that from the other groups, will be used to assist in the validation of a multi-layered model currently being developed by this group.

Professor Ronneau's group is carrying out similar wind tunnel studies of deposition onto isolated trees and twigs with the novel use of thermo-generated generated $\text{UO}_2\text{-Cs}$ aerosols, considered to be representative of the particulates which emerge from reactors undergoing catastrophic failure. The data resulting from these studies is being interpreted in the light of deposition data collected from a forest site contaminated by the Chernobyl accident (Donon in the French Vosges).

Miss Minski's group is studying the deposition processes of labelled silica aerosols in a wind tunnel of sufficient size to allow the construction of 'model' canopies of Norway spruce, and Holm oak saplings above which a well characterised turbulent boundary can be established. This allows the effects of canopy architecture and morphology to be taken into account when deriving deposition parameters for the validation of the model being developed at CEA-FAR.

Dr Rauret's group is deriving data on the deposition and recycling of aerosols within instrumented catchments situated in the Prades mountains of NE Spain, a site which provides conditions typical of southern European forest ecosystems. As well as characterising the properties of aerosols falling into these catchments this group is also investigating the environmental behaviour of ^{134}Cs , ^{85}Sr and $^{110\text{m}}\text{Ag}$ within forest soils.

Project 1

Heads of project: *Dr. G. Shaw, Miss M.J. Minski*

Objectives for the reporting period

The two year programme of work at Imperial College has been centred around the environmental wind tunnel facility at CARE, Silwood Park, Ascot, UK. The tunnel is large enough to accommodate small tree saplings (2 - 3 year old) while still retaining sufficient head space for the development of a representative turbulent boundary layer above the canopy. The main objective has been to investigate and quantify dry deposition of labelled silica aerosols to 'model' canopies of Norway spruce (*Picea abies*) and Holm oak (*Quercus ilex*) saplings situated within this wind tunnel, as well as rates of resuspension of aerosol after deposition to tree surfaces. Spatial patterns of deposition velocities have been determined throughout the canopy, as well as interception fractions. Initial results obtained with spruce canopies suggested a complex interaction between deposition rates, leaf and needle biomass distributions and micrometeorological parameters. For this reason the deposition experiments described in the current report were supplemented by detailed determinations of wind speed and turbulence profiles throughout the canopies, as well as measurements of friction velocities within the boundary layer.

<u>Notation</u>	u', v'	horizontal and vertical velocity fluctuations	($m s^{-1}$)
	U	free stream wind velocity	($m s^{-1}$)
	U^*	friction velocity	($cm s^{-1}$)
	z	height above soil surface	(m)
	z_0	roughness length	(m)
	d	zero plane displacement	(m)
	K	Von Karman's constant (= 0.41)	(dimensionless)
	V_g	deposition velocity	($cm s^{-1}$)
	f	interception fraction	(dimensionless)
	Λ	resuspension rate	(s^{-1})
	F	cumulative resuspended fraction	(dimensionless)

Progress achieved including publications

1. Methods

'Model' canopies of both Norway spruce and Holm oak were established by spacing 2 - 3 year old saplings in a regular pattern on the floor of the wind tunnel. In the case of Norway spruce, trees were spaced 3 abreast (wind tunnel width = 0.8m) in 24 rows (wind tunnel length = 6m) giving a total of 72 trees within the tunnel. A total of 175 trees were used in the case of Holm oak, which were arranged seven abreast in 25 rows. The trees were planted in plastic troughs which were arranged across the tunnel's width; the gaps between these troughs were filled in with the same compost in which the trees were planted in order to create a continuous ground surface beneath the canopy itself. The average height of the spruce canopy was ~45cm whereas the Holm oak canopy was ~25cm high.

Having established model spruce or oak canopies in this fashion a bank of six 450W sodium lamps, operating on a 16h day 8h night diurnal cycle, allowed the trees to be maintained in a healthy condition for up to two months while measurements of micrometeorological parameters were made. A traversing hot wire anemometry rig within the tunnel enables vertical profiles of mean wind speed **above** the canopy to be determined. High resolution measurements of mean wind speed in the region of the boundary layer just above the canopy are necessary for reliable calculations of friction velocity. This characterises the rate of momentum transfer into the canopy from the air just above, where $U^* = (u'v')^{0.5}$. A more robust omnidirectional hot film probe can be used to make measurements of wind speed and turbulence **within** the canopy. In addition to these variables within and above canopy determinations of temperature and relative humidity were made. All determinations were made at the free stream wind speed (5 m s^{-1}) at which deposition experiments were carried out.

A monodisperse silica aerosol with mass median aerodynamic diameter of $1 \mu\text{m}$ was used in all experiments. This was labelled with $^{151}\text{Eu}(\text{NO}_3)_3$ and liberated above the canopy for a duration of 108 minutes. The mean air concentration of the aerosol during the experiment was determined using an array of isokinetic air samplers arranged downwind from the tunnel working section within the boundary layer. Deposition onto the canopy itself was determined by destructively harvesting all of the trees within the last 2m of the tunnel, the region in which a fully developed turbulent boundary layer exists above the canopy. Randomly interspersed beneath the trees were 20 filter papers placed on the soil surface either between stems or directly next to stems. These were analysed to assess the extent to which the depositing aerosol was able to penetrate the canopy to the ground surface.

In addition to deposition experiments, pre-contaminated canopies were used to determine resuspension rates from both spruce and oak when subject to 5 m s^{-1} free stream wind velocities - aerosol liberated from the canopies was sampled isokinetically using the same arrangement as above.

All analyses were by instrumental neutron activation analysis (INAA) which made use of the $^{151}\text{Eu}(n,\gamma)^{152}\text{Eu}$ reaction to allow the determination of deposited europium. Checks on uncontaminated saplings revealed a negligible 'background' concentration of stable europium within both Spruce and Holm oak tissues (the existence of stable Cs at substantial and variable concentrations within spruce tissues had previously resulted in serious interferences when ^{133}Cs had been used as an aerosol label). Sampling of the trees for analysis was carried out such that 14 categories of tissue were defined for spruce, and 6 categories for Holm oak (Table 2). These were dried to constant weight at 80°C , homogenised, ashed at 450°C and irradiated within the Imperial College reactor before the determination of ^{152}Eu by high resolution gamma ray spectrometry. Specific activities of ^{152}Eu were converted to μg of ^{151}Eu per gram of sample using standards made up in a cellulose matrix. Isokinetic air filter samples were analysed in an identical manner and time averaged air concentrations of ^{151}Eu calculated. From these data deposition velocities were calculated as

$$V_g = \frac{\text{aerosol flux to tree surface}}{\text{time averaged air concentration in air}}$$

Deposition velocities were calculated for each canopy component and for soil surfaces within and directly beneath trees. From these two sets of values it was possible to calculate the interception fraction, f , a parameter which indicates the scavenging efficiency of the canopy for depositing aerosol. Results were subject to a series of 2-way analyses of variance.

2. Results and discussion

Temperature profile measurements showed that there was no significant variation of temperature with height for either canopy. Under these neutral conditions the wind speed profile in the region near to the canopy top is described by the expression

$$U = \frac{U^*}{K} \ln \left\{ \frac{z-d}{z_0} \right\}$$

Friction velocity can be calculated from the gradient of plots of U versus $\ln(z-d)$; estimates of U^* are given in Table 1 for both tree canopies and a rye grass canopy examined in the same wind tunnel.

Table 1: Friction velocity, total deposition velocity and total interception fraction estimates for Norway spruce, Holm oak and Rye grass canopies under similar conditions of aerosol particle size and free stream wind velocity.

Canopy	U^*	V_g	f
Norway Spruce	128.0	7.77	0.98
Holm oak	104.0	16.5	0.99
Rye grass	31.6	1.0	0.86

This table also includes total V_g and f estimates, indicating that the tree canopies received a much higher flux of aerosol and exhibited a higher filtration efficiency than did the grass.

Table 2 shows the manner in which total canopy V_g partitioned throughout the tissues within the tree canopies indicating, in both cases, a significant ($p < 0.001$) decrease in deposition flux with downwards vertical penetration of the aerosol into the canopy. In the case of spruce, deposition to outer and inner canopy components was also significantly different ($p < 0.05$); for outer and inner canopy regions V_g and f attenuated in an approximately exponential fashion with respect to depth of penetration from the boundary layer.

Table 2: Deposition velocity and interception fraction values obtained for canopy components within 'model' Norway spruce and Holm oak canopies. Canopy components were as follows:

F	Flag	(Layer I)
UC	Upper Canopy	(Layer II)
MC	Middle Canopy	(Layer III)
LC	Lower Canopy	(Layer IV)
L	Leaf (ie. needle in the case of spruce)	
S	Stem	
NG	Current year's growth (ie. 'outer' canopy)	
OG	Previous years' growth (ie. 'inner' canopy)	

Canopy Component	Norway Spruce		Holm oak	
	V_g	f	V_g	f
FL	4.220	0.530	-	-
FS	0.269	0.034	-	-
UC NG L	1.294	0.163	5.394	0.324
UC NG S	0.225	0.028	6.982	0.420
UC OG L	0.799	0.100	-	-
UC OG S	0.126	0.016	-	-
MC NG L	0.243	0.031	1.409	0.085
MC NG S	0.083	0.010	1.459	0.088
MC OG L	0.228	0.029	-	-
MC OG S	0.027	0.003	-	-
LC NG L	0.089	0.011	0.713	0.043
LC NG S	0.029	0.004	0.540	0.032
LC OG L	0.109	0.014	-	-
LC OG S	0.028	0.004	-	-
Soil Beneath Trees	0.091	0.011	0.066	0.004
Soil Between Trees	0.098	0.012	0.058	0.003

Table 3 shows resuspension rates (Λ) determined for Norway spruce, Holm oak and Rye grass as well as estimates of the fraction of initially deposited material resuspended within the experimental period (F). Resuspension rates exhibited a significant decrease with time ($p < 0.001$) in all cases. Λ values were initially similar for all canopies but decreased in the order spruce > oak > grass towards the end of the experiment. F values decreased in the same fashion; the loss of initially deposited material was much the highest for the spruce canopy which experienced resuspension of 37% of its initial aerosol burden within 3.8 hours.

Table 3: Resuspension rates determined for Norway spruce, Holm oak and Rye grass canopies (aerosol particle size = $1\mu\text{m}$ MMAD, free stream wind velocity = 5ms^{-1}).

Canopy	t (s)					
	90	1000	2800	6400	13600	
Norway Spruce	2.3E-3	7.8E-5	7.7E-5	2.8E-5	1.6E-5	F = 0.37
Holm oak	1.4E-4	2.8E-5	1.3E-5	4.0E-6	2.9E-6	F = 0.05
Rye grass	1.3E-3	2.6E-5	5.3E-6	2.3E-6	1.5E-7	F = 0.09

The results indicate a potential for relatively high rates of deposition to both Norway spruce and Holm oak canopies. Furthermore, resuspension of aerosols from spruce canopies appears to be considerable, suggesting that this process may be of considerable significance when considering the behaviour of aerosols within boreal forests shortly after a deposition event.

Publications

1. *G. Shaw, J. G. Farrington-Smith, R. Kinnersley and M. J. Minski.* Dry Deposition of Aerosol Particles within Model Spruce Canopies. Paper presented at a Seminar on the Dynamic Behaviour of Radionuclides in Forest, Stockholm, May 1992. To be published in *Science of the Total Environment*.
2. *R. Kinnersley, J. G. Farrington-Smith, G. Shaw and M. J. Minski.* Aerodynamic characteristics of Model Tree Canopies in a Wind Tunnel. Paper presented at a Seminar on the Dynamic Behaviour of Radionuclides in Forest, Stockholm, May 1992. To be published in *Science of the Total Environment*.
3. *G. Shaw, R. Kinnersley, J. G. Farrington-Smith and M. J. Minski.* Wind Tunnel Simulations of Aerosol Dry Deposition and Resuspension in Tree Canopies. To be submitted to *Atmospheric Environment*.

Project 2

Head of project: *Dr. Belot*

Objectives for the reporting period

An understanding of particle deposition to vegetated surfaces of forest trees is important in predicting the input of detrimental compounds to forest ecosystems. Many studies have been carried out on the deposition of particles to low-growing herbaceous vegetation. In contrast, very few studies have been performed on the deposition of particles to forested areas, due to the difficulties encountered in sampling tree canopies. The rare data obtained suggest that the deposition of particles to forest canopies is particularly favoured by the large projected surface areas of the trees and the relatively high ventilation rate that characterize them.

The strategy used in the present work for studying the deposition of particles to stands of trees, was similar to the one already used by several investigators. It consists in measuring the deposition of well-characterized particles to isolated leaf-bearing twigs placed in a wind-tunnel under realistic conditions of particle size and wind velocity, and to extrapolate the data to a complete canopy of leaves in a forest, by means of a model that simulates the uptake of particles and the cleansing of the atmosphere.

We put emphasis on particles in the submicrometer size range whose deposition is poorly known in spite of their importance in the long-range transport of products from accidental releases. The canopy elements chosen were taken from the evergreen species : Norway spruce (*Picea abies*), Scots pine (*Pinus sylvestris*) and Holm oak trees (*Quercus ilex*) that can be found in extended areas and keep leaves during several consecutive years.

Progress achieved including publications

The experiments were performed in a wind tunnel allowing canopy components to be exposed to a flow of suspended fluorescent particles of almost uniform size. Emphasis was put on particles in the 0.3-1.2 μm subrange, since most of the radioactive particles sampled at long distance from sources are comprised in this size interval. The leaf deposition rates were determined for leaf-bearing twigs of several evergreen species, as a function of wind speed and particle size. Care was taken to avoid the build-up of electrical charges on the leaf-bearing twigs, since it was felt that an increase in charges could enhance the rate of particle deposition onto the leaves. The rates obtained were used as input to a model that describes the uptake of particles by a large-scale canopy under specified conditions of weather and canopy structure. Simulations carried out for a typical spruce canopy indicate that the deposition is limited by the strong decrease of wind speed with height in the canopy. The deposition rate to this typical forested horizontal surface (canopy deposition rate) was estimated to be comprised between 10^{-4} and 10^{-3} $\text{m}\cdot\text{s}^{-1}$ depending on wind friction velocity. This rate is practically independent of particle size in the size subrange of interest.

1. Experimental methods

A closed-circulation wind tunnel was used with an internal test section 130 cm long and 30 cm by 30 cm in cross section perpendicular to the flow. The tunnel produced wind speeds from 0.5 to 10 $\text{m}\cdot\text{s}^{-1}$. The tunnel could be filled with air taken from the outside and freed from any particle by passage through a filter.

Particles of sodium fluorescein with a narrow dispersion of diameters were produced by an ultrasonic generator, such as used in inhalation therapy. The generator was fed with solutions of sodium fluorescein at different concentrations between 0.1 and 25 $\text{g}\cdot\text{l}^{-1}$. After evaporation of water, particles of a fixed mass median diameter comprised between 0.2 and 1.4 μm were obtained. At the outlet of the generator inside the wind-tunnel, two radioactive

sources of Thallium 204 were placed: they were designed to produce positive and negative small ions and neutralize the excess of electrical charge present on the generated particles.

In each determination, a leaf-bearing twig was placed in the center of the test section and exposed to the fluorescent aerosol at a fixed windspeed and particle size. During the exposure time (5-15 minutes) the particles present in the tunnel were sampled through an eight-stage Andersen cascade impactor and a total filter to determine the size characteristics and total concentration of particles. After exposure, the twig, impactor plates and filters were washed in 100 ml of a pH 9 buffer solution. The fluorescence of the rinse water was measured with a Perkin-Elmer fluorometer. The completeness of the particle washoff was provided by sequential rinsing of sample material, which showed no additional fluorescence removed after the first rinse.

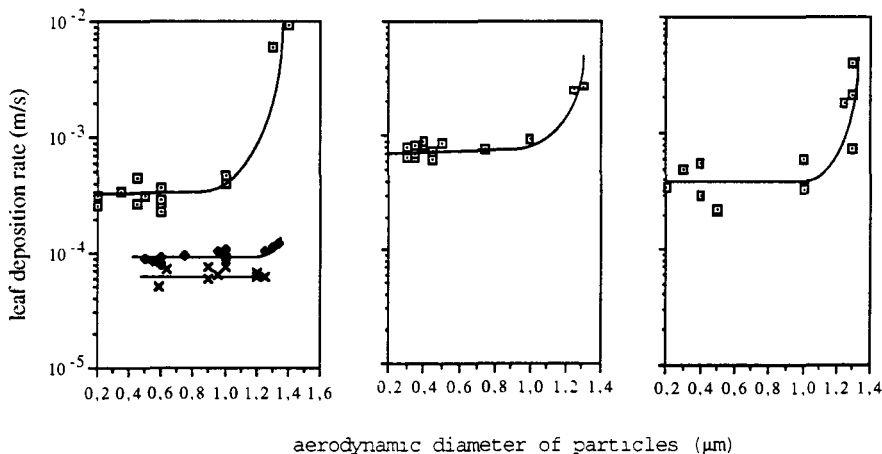


Figure 1 Leaf deposition rate vs particle diameter for Norway spruce (left), Holm oak (middle) and Scots pine (right); wind speed $u = 5 \text{ m.s}^{-1}$ (white dots), $u = 1 \text{ m.s}^{-1}$ (black dots) and $u = 0.5 \text{ m.s}^{-1}$ (crosses)

2. Results

A total of 70 separate determinations of particle uptake were made in the wind tunnel with a variety of target specimens, particle sizes and wind speeds. The total developed surface area of each of the leaf-bearing twigs used in the experiments was of 200-300 cm². The twigs were exposed to particles of a fixed aerodynamic mass median diameter (MMD) comprised between 0.2 and 1.4 μm with geometric standard deviations (GSD) between 1.3 and 1.5. The deposition of particles on the target was characterized by a leaf deposition rate defined as the flux of particles to the leaves (per unit area of leaf surface) divided by the air concentration of particles in the surrounding air. The leaf deposition rate was plotted against the size of particles for each of the three species.

It can be seen on the graphs of Fig. 1 that the values of leaf deposition rate obtained for each species do not depend very much on MMD in the subrange 0.3 - 1.0 μm. The influence of wind speed was studied for the Norway spruce. Average leaf deposition rates of 3.3×10^{-4} , 9.4×10^{-5} and $6.5 \times 10^{-5} \text{ m.s}^{-1}$ were obtained at wind speeds of 5, 1 and 0.5 m.s⁻¹ respectively. This shows that, at least in the explored range of windspeed, the deposition rate is proportional to the wind speed raised to the power 0.7 ± 0.1 .

For particles larger than 1 μm the deposition rate increases rapidly with the size of particles and the wind speed.

3. Extrapolation to a canopy

The model used for extrapolation of wind-tunnel data to a real canopy is adapted from Waggoner and Lovett. It considers an uniform concentration of particles over a forest extending uniformly on all sides. The forest is arbitrarily divided into N strata of known surface area index (surface area of leaves per unit area of ground surface). The values of turbulent diffusivity and wind speed at the top of the canopy are calculated from the friction velocity and the geometrical characteristics of the canopy. These parameters are considered to decrease exponentially within the canopy as a function of the cumulative surface area index. The turbulent transfer of particles from the surrounding air to the canopy is modeled by direct analogy to Ohm's law for electrical circuits. The resistances represent either the resistances of the air among foliage or the resistances of the boundary layers near the foliage. The currents (or fluxes) are the amounts of particles deposited to each stratum per unit time and per unit of horizontal surface area.

Using electrical analogy, N algebraic equations between the fluxes and the resistances can be written and then solved for the fluxes of particles deposited in each stratum: the detail of equations is given in Waggoner and Lovett. Finally, the fluxes so obtained are used to determine the average concentration of particles in the air of each stratum.

4. Example of calculation

The model was applied to a typical stand of Norway spruces (*Picea abies*) aged 21 years and situated in the East of France. The average height of the trees is 11.4 m, their number per unit area of ground surface 4286 trees per ha. The canopy is segmented into 7 horizontal strata of known surface area index (see Table 1). These data are taken from a field study by Granier and Claustres.

The calculation of particle transfer to the canopy is made for particles of diameter 0.4 - 1 μm , using the wind-tunnel data and our observation that the deposition rate of such particles is proportional to the wind speed raised to the power 0.7. The turbulent diffusivity and wind speed are assumed to decrease exponentially from the top to the bottom of the canopy as a function of the cumulative surface area index. Extinction coefficients of -0.14 and -0.27 respectively are taken for the exponential functions, the value -0.27 having been measured in a fir canopy that was probably very similar to the spruce canopy considered in the present work. The data given as entry to the model are the height of the midpoint of each stratum, the leaf surface area index of each stratum, the average height of the trees, the displacement height and the roughness length of the canopy, and the wind friction velocity. The program calculates the turbulent diffusivity, wind speed, concentration of particles and deposition rate for each stratum of the canopy (stratum deposition rate). This rate is defined as the flux of particles deposited in the stratum (per unit area of horizontal surface) divided by the air concentration of particles at the top of the canopy.

The data obtained in the case of a friction velocity of 0.5 m.s^{-1} are given in Table 1. It appears that both wind speed and deposition rate decrease rapidly with the height of the stratum in the canopy. The depletion of the particle concentration in air within the canopy is rather small: only a few per mil of the concentration at the top of the canopy. Finally, by summing the deposition rates in the different strata, one obtains $1.07 \times 10^{-3} \text{ m.s}^{-1}$ which represents the total deposition rate of particles on the canopy (canopy deposition rate). In the present case, the canopy deposition rate varies between 5.6×10^{-4} and $1.7 \times 10^{-3} \text{ m.s}^{-1}$ for friction velocities between 0.2 and 1 m.s^{-1} .

Table 1 · Leaf area index, wind speed, particle air concentration and deposition rate in the different strata of a typical spruce canopy. Average height of trees : 11.4 m, displacement height : 9 m, roughness length : 0.3 m, friction velocity : 0.5 m.s⁻¹. The deposition rate per stratum is defined as the flux of particles to the stratum (per unit area of ground surface) divided by the air concentration of particles at the top of the canopy

height of each stratum midpoint (m)	leaf surface area index per stratum	wind speed in the stratum (m.s ⁻¹)	particle air concentration in each stratum*	deposit. rate per stratum (10 ⁻⁴ m.s ⁻¹)
10.64	2.56	1.94	0.998	4.35
9.23	2.44	0.99	0.995	2.58
8.42	3.42	0.45	0.994	2.08
7.58	3.33	0.18	0.993	1.07
6.82	3.38	0.07	0.993	0.57
6.04	0.77	0.04	0.992	0.09
3.02	0.00	0.04	0.992	0.00

* The air concentration of particles at the top of the canopy is equal to unity

5. Discussion and conclusions

The leaf deposition rates obtained in the experimental part of this work, for particles in the subrange 0.2-1 μm , are situated between 10⁻⁵ and about 10⁻³ m.s⁻¹. The values obtained are nearly independent of particle size, and are particularly related to leaf morphology and wind speed. The non influence of particle size can be explained by the common observation that the deposition rate is generally minimal for particles in this size range and increases for particles outside that range. The influence of morphology and wind speed is not surprising, since these two factors are recognized to have a pronounced influence on the thickness of the boundary layers near the leaves and consequently on the deposition rate onto the leaf-bearing twigs. The relationship found between the leaf deposition rate and the wind speed agrees with the theoretical relationship established for the diffusion of particles through laminar and turbulent boundary layers near individual small obstacles. It would be advisable to supplement the present set of data by further systematic experiments on the uptake of small particles by leaves under conditions where electrical charges can accumulate on the leaves.

The model used for extrapolation of data to a canopy is useful for identifying the main factors that control the deposition of particles inside a canopy. In a dense homogeneous forest of extended area, the wind speed and hence the deposition rate of particles are strongly reduced, particularly in the low-level strata. As a consequence, in that type of forest, the canopy deposition rate of small particles is not very high in spite of the large surface area index of the trees: generally it amounts only to a few 10⁻⁴ m.s⁻¹. Nevertheless, it should be noticed that the model used in this work is a one-dimension model which assumes that the transfer of momentum and mass is primarily in the vertical direction, with net horizontal advection being negligible. This model does not apply when the forest in question has not sufficient upwind fetch to allow equilibrium to be reached between the airflow and the surface. In particular, the deposition rate is probably greatly enhanced at the border of a forest or wooded strip where the trees are fully exposed to the wind.

Publication

Belot Y., H. Camus, D. Gauthier and C. Caput, "Uptake of Small Particles by Tree Canopies" Seminar on the Dynamic Behaviour of Radionuclides in Forests, Stockholm, Sweden, May 18-22, 1992, to be published in *the Science of the Total Environment*.

Project 3

Head of project: *Dr. Rauret*

Objectives for the reporting period

1. Study of the properties of the aerosols collected in the experimental forest and their interactions with leaves. In order to ascertain the role played by the holm oak canopy in the retention of aerosols, we have studied several aspects:
 - quantification of the dry deposition into holm oak forest,
 - leaf anatomy and morphology and the distribution of the aerosol on holm oak leaves, and
 - incorporation into the leaves of a radioactive aerosol released in an accidental situation.
2. Study of ^{134}Cs , ^{85}Sr and $^{110\text{m}}\text{Ag}$ migration in Mediterranean forest soils according to organic matter decomposition in the soil:
 - design and evaluation of methodology,
 - study of litter decomposition processes,
 - role of soil fauna activity in radionuclide migration.

Progress achieved including publications

1. Study of the interaction of aerosols and leaves

1.1 Quantification of the dry deposition

The retention of the aerosols by the canopy of holm oak trees in a typical Mediterranean forest is studied. Dry deposition is measured both under and outside the canopy. No clear differences are observed either between the amount of particles collected under and outside the canopy or in the chemical composition of the aerosol. The deposition of aerosols on leaf surfaces is greater in young leaves than in old ones.

1.2 Leaf anatomy and morphology

The leaf morphology and anatomy as well as the amount of aerosol deposited onto the leaf surfaces are studied by scanning electron microscopy. Cuticle thickness is measured and differences are observed between young and old leaves. Cuticle thickness increases during leaf ontogeny mainly on the adaxial epidermis of the leaf whereas there are no changes at the leaf base. The cuticle of the abaxial epidermis is thinner than that of the adaxial epidermis. The distribution of aerosol particles over leaf surface is also established.

1.3 Incorporation into the leaves of a radioactive aerosol released in an accidental situation

The last studied aspect is the possible incorporation into leaves of a radioactive aerosol released in an accidental situation. This aspect has been studied in more detail in order to know the percentage of the radionuclides rapidly incorporated into the plant, the percentage retained by the cuticle and the percentage which could be washed by the rain of resuspended. A two step procedure, based on successive extractions, has been established, using distilled water, to evaluate the fraction possibly removed by rain, and organic solvent

(chloroform: hexane 1:2), to differentiate between the fraction bound to the cuticle and the one which has penetrated into the leaves. From this procedure five fractions are obtained:

- 1st soluble in water,
- 2nd particulate leached with water,
- 3rd soluble in the organic solvent,
- 4th particulate leached with the organic solvent and
- 5th residual in leaves.

From the results obtained, it can be deduced that nor the abiotic layer neither the cuticle of the leaves do not play any important role in the retention of caesium. Approximately 45% of caesium and 20% of silver remain on the leaf surface but are leached by water, while 55% of caesium and 80% of silver are retained by the leaves (Fig. 1). Sequential extraction of leaves seems to be a good methodology to ascertain the incorporation into the leaves of radionuclides from deposited aerosols.

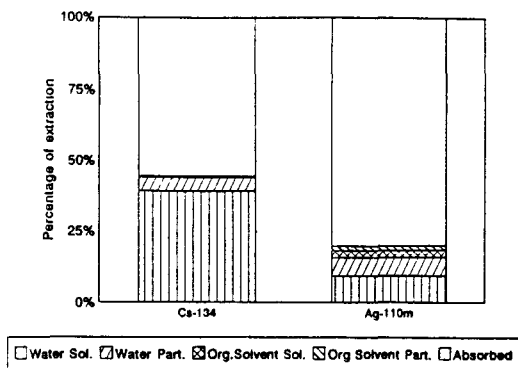


Figure 1 - Distribution of ¹³⁴Cs and ^{110m}Ag using the proposed sequential extraction procedure.

2. Radionuclide migration in forest soil

2.1 Design of the methodology

Field experimentation has been designed to describe the key role of litter decomposition and faunal activity in the radionuclides migration in the forest floor and mineral layers: *In situ* incubation of contaminated green leaves in plastic cylinders. The contaminated green leaves replace the original litter layer and then the decomposition processes was studied in field conditions. At the same time, another cylinder with an exchange cationic resin bag between the contaminated green leaves and the F layer allow to discriminated the soluble and the particulate radionuclides migration. Incubation of classical litter bags was used for the calibration of this new field method. Periodical sampling of the remaining polluted leaves, the different underlying forest floor layers and the first 5 cm of mineral soil will allow to model the radionuclides migration. Seasonally, during two years four points are sampled. Each point is composed of:

- a. one cylinder with polluted green leaves,
- b. one cylinder with polluted green leaves and exchange cationic resin,
- c. one cylinder with non-polluted green leaves,
- d. one litter bag with green leaves, and
- e. one litter bag with brown leaves.

2.2 Evaluation of the methodology

Weight loss shown no significant differences between litter layer collected from cylinder with resin bag, open cylinder (without resin) and standards litter bags (Fig.2).

Litter quality dynamics as expressed by the C/N ratio was significant different between the two types of cylinders, lower C/N ratio and carbon content began to appear for the open cylinder (Fig. 3).

In the open cylinder and litter bag fecal pellets began to be present after 76 days and were relatively abundant after 132 days.

No signs of animals activity were observed in the contaminated litter from the resin bag cylinder, fact which corroborates the effectiveness of the bag to prevent the pass of burrowing macrofauna.

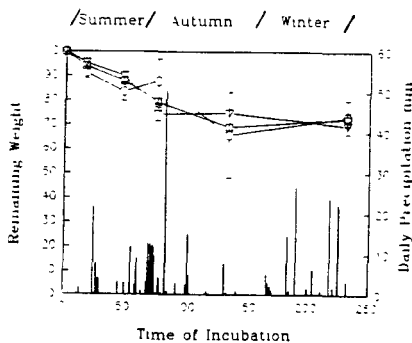


Figure 2 - Green leaves weight loss for the three methods used: ○ Open cylinder, □ The resin cylinder and 7 Litter bags. Mean values with standard errors. Bars represent daily precipitation.

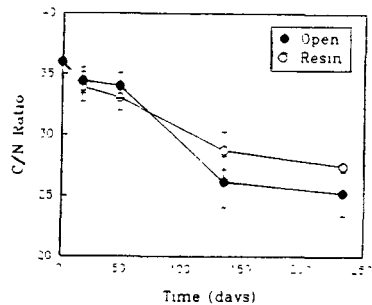


Figure 3 - Contaminated green leaves C/N ratio dynamics for the two cylinder types tested.

2.3 Radionuclide migration

The results for a 232 days period of incubation shown that Cs and Sr behaved similarly, with an initial rapid leaching period which corresponded to the soluble fraction extracted from the contaminated leaves, and further release related to litter decomposition (Fig. 4). No significant differences were observed between open and resin cylinders, indicating that all migration was insoluble form for both radionuclides (Fig. 5). After 3 months of incubation, around 70% of the initial radiocesium was transferred to the underlying layers, mainly to the F layer.

Cs absorbed into the leaves was released at the same rate than K, whereas Sr shown different behaviour than Ca (Fig. 6, 7).

^{110m}Ag shown different migration pattern, with total activity loss from the contaminated litter amounting around 45% in the open cylinders (Fig. 4), from which 15 to 20% was attributed to particulate form migration. Significant differences between open and resin cylinders were found (Fig. 7).

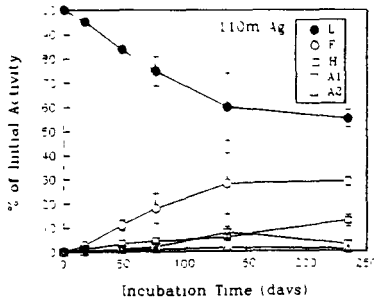
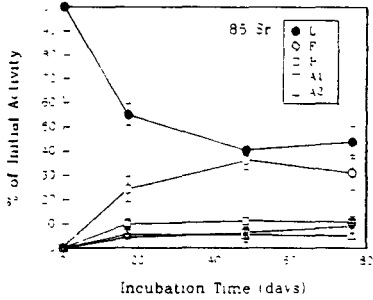
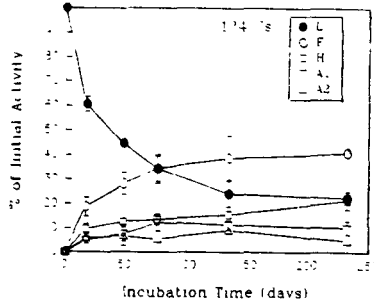


Figure 4 - Distribution of radionuclides among the forest floor and top soil layers during the incubation period. Samples from the open cylinder.
 a) ^{134}Cs b) ^{85}Sr c) $^{110\text{m}}\text{Ag}$

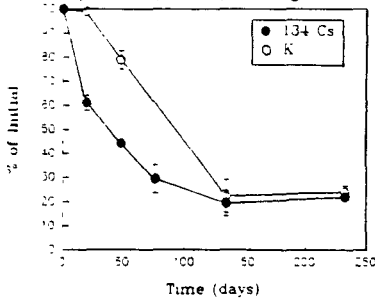


Figure 6 - Comparative dynamics of ^{134}Cs vs. K release from contaminated leaves incubated in open cylinders.

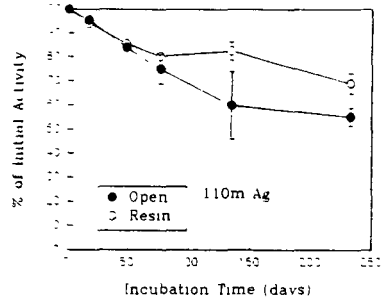
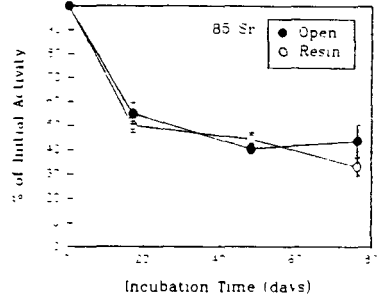
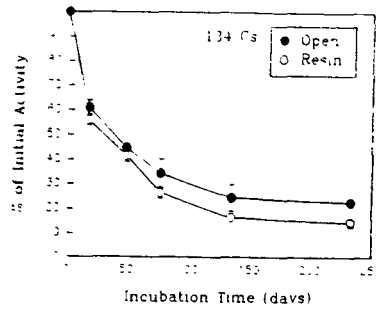


Figure 5 - Dynamic of radionuclides release from open and resin cylinders.
 a) ^{134}Cs b) ^{85}Sr c) $^{110\text{m}}\text{Ag}$

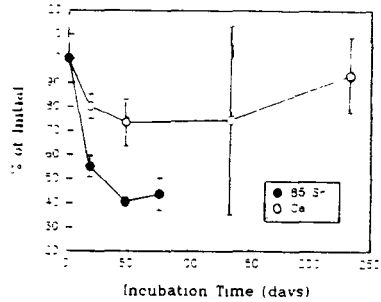


Figure 7 - Comparative dynamics of ^{85}Sr vs. Ca release from contaminated leaves incubated in open cylinders.

2.4 Conclusions

The field methodology proposed proved to be useful to describe radionuclide migration in the forest floor profile and the mechanisms involved.

Migration in solution was the dominant process for the three radionuclides studied, but evidences of particulate transfer began to appear for ^{110m}Ag coinciding with the signs of macrofaunal activity. Water extractable ^{134}Cs from leaf surfaces was leached with the first rainfall events. Afterwards, ^{134}Cs , ^{85}Sr and K released closely correlated with litter mass loss, making evident that radionuclide release during this period was dependent on litter decomposition.

3. Publications

1. Rauret, G., Llauradó, M., Tent, J., Rigol, A., Alegre, L.H. and Utrillas, M.J.: *Deposition on holm oak surfaces of accidentally released radionuclides*. Seminar on the dynamic behaviour of radionuclides in forest, Stockholm, Sweden, May 18-22, 1992.
2. Sauras, T., Roca, M.C., Vallejo, R.V., Tent, J., Llauradó, M., Vidal, M. and Rauret, G.: *Field migration study of radionuclides in Mediterranean forest soils using synthetic aerosols*. Seminar on the dynamic behaviour of radionuclides in forest, Stockholm, Sweden, May 18-22, 1992.
3. Llauradó, M., Vidal, M., Rauret, G., C. Roca, Fons, J. and V.R. Vallejo, V.R.: *Radiocaesium behaviours in Mediterranean conditions*. Journal of Environmental Radioactivity (submitted).

Project 4

Head of project: *Dr. C. Ronneau*

Objectives for the reporting period

The research aimed at defining the fate of radionuclides in forest ecosystems and, more precisely, of radiocesium which is very disquieting because of its similarities with potassium and sodium. There were four aspects in this study:

- I. Study of the physico-chemical nature of "fuel particles" emitted by a damaged reactor: indeed such particles efficiently confine radionuclides (radiocesium) and delay their dissolution.
- II. Study of the interaction of canopies with aerosols and precipitations which are the main vectors of airborne radioactivity to the forest ecosystem.
- III. Study of the mechanisms of retention of soluble cesium in forest soils. The interactions of Cs with clay and organic matter is very strong and result in a immobilisation of cesium in the very first centimeters of the soil profile.
- IV. Study of the transfer and cycling of radiocesium in the forest environment which may constitute a long-term radiation hazard.

Progress achieved including publications

1. The physico-chemical nature of Cs in thermo-generated UO₂ aerosols

The relative mobility of cesium in flooded soils observed after the deposition from Chernobyl led us to suggest that a fraction of the radionuclide was trapped into insoluble, vitrified UO₂ particles which prevented Cs from being adsorbed by clay. In western countries, such particles, are much too thin to be collected and analysed. It was then necessary to produce such particles in the laboratory in order to get enough samples for physico-chemical analyses.

Aerosols are produced from UO₂ pellets contaminated by small quantities of ¹³⁴Cs and heated in an inert atmosphere up to temperatures of the order of 2300°C. This thermal shock on UO₂ pellets is followed by a maturation of the aerosols in different atmospheres likely to simulate the stay in the plume of the reactor. The aerosols (0.4 - 0.6 µm aerodynamic diameter) are then collected and analysed by various non-destructive physico-chemical methods which allow to determine some chemical forms of cesium and uranium: X-Ray Photoelectron Spectrometry (XPS or ESCA), X-Ray Diffraction (XRD), Mössbauer Spectroscopy (MS) for the analysis of a limited range of elements such as Fe, Ru, Eu, ... and Electron microprobe.

Solubility tests were conducted in parallel with these analyses in order to ascertain the chemical forms responsible for the immobilisation of cesium. The main conclusions drawn from these experiments may be summarized as follows:

- When emitted in an inert atmosphere (argon), the aerosols are composed of a UO₂ nucleus onto which cesium vapours have recondensed to form a layer of highly soluble Cs (95% of solubility).

- When matured in an oxidizing atmosphere, U (IV) in the aerosols is oxidized into U(VI) and is then able to react with Cs to give different uranates which are highly insoluble: almost 50% of the cesium remains insoluble after 500 hours of contact with pure water. We think that the presence of Cs uranates in small, vitrified UO₂ particles from Chernobyl could explain the mobility of Cs in clay soils.
- When brought in contact with iron from the reactor structures, Cs is able to react and form ferrites. Although Cs ferrites are soluble when in pure form, they could partially insolubilise Cs by catching it into Fe oxides matrices.

1.1 Publications

A.H. Al Rayyes, C. Ronneau, W. Stone, J. Ladrière and C. Cara, "Radiocesium in hot particles: solubility vs. chemical speciation", submitted for publication in "Journal of Environmental Radioactivity".

A.H. Al Rayyes, J. Ladrière, C. Ronneau and D. Apers, "Chemical characterization of UO₂/Fe and Fe/Cs aerosols generated at high temperature", *Radiochimica Acta*, 56, 47-50, (1992).

A.H. Al Rayyes and C. Ronneau, "X-Ray photoelectron spectroscopy of cesium uranates", *Radiochimica Acta*, 54, 189-191 (1991).

2. The interaction of canopies with aerosols and precipitations

2.1 Interception of aerosols: laboratory experiments

Preliminary studies have been made on the interception of radioactive and inert aerosols by spruce canopies. A first series of experiments aimed at contaminating small trees by means of aerosols, thermo-generated in the laboratory as described here above; these aerosols (0.4-0.6 µm aerodynamic diameter) were deposited in non turbulent conditions and, in that case, diffusion was the main transport mechanism toward needle surfaces. Deposition was found to be very homogeneous throughout the canopy.

A second series of experiments were performed in a wind-tunnel where wind speed could be varied from very low values (of the order of a fraction of m/s) up to about 3 m/s. Such a low speed was preferred in order to have a closer look to the micro-scale mechanisms of deposition onto the needles and the twigs. Indeed, single twigs were used in this kind of experiments. The main observations made during these experiments may be summarized as follows:

- The global yield of capture of aerosols by twigs is low: in our experiments, a maximum of about 0.01% of the particles penetrating into the volume defined by the twig and its needles are deposited onto plant material (needles + twig).
- Deposition onto single twigs increases as wind speed is reduced; note that this behaviour is in contrast with the wind effect observed in medium-scale experiments where turbulence is the main transfer factor through the atmosphere. In our micro-scale experiments, diffusion is the parameter to be taken into account and its yields are enhanced at low wind speed (see graph n. 1: results of a typical set of experiments).
- Twigs accumulate more aerosols than needles and this could be tentatively explained by: (i) a reduced wind speed in the core of the twigs favouring deposition by diffusion (ii) the roughness of the wood which favours the retention of the aerosols.

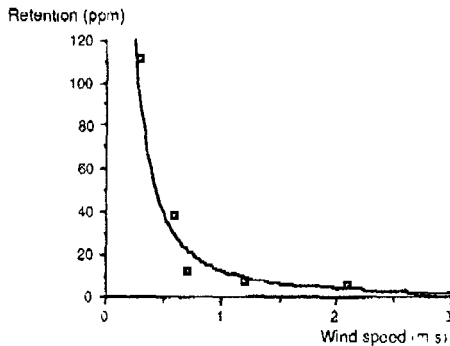


Figure 1 - Retention ($10^{-4}\%$) of aerosols by single twigs, as a function of wind speed: typical experiment

2.2 Interception of aerosols: on-field experiments

During a two-year period, sampling operations have been performed at the tower of the "Station du DONAN" (47 m, Vosges, France) where impactors, air filters and rain gauges have been placed into and above the canopy of a spruce stand. The collected samples were submitted to different analytical techniques, in order to determine their elemental and ionic content (by Instrumental Neutron Activation Analysis, Atomic Absorption Spectrometry and Ion Chromatography). These determinations aimed at observing a possible effect of aerosol interaction with the canopy by detecting slight differences of concentrations between the two sampling altitudes (in and above the trees). Sampling was also made with impactors in order to try detecting a possible effect of aerosol granulometry.

Despite a huge material of analytical determinations on about 30 substances (elements and ions and cations), during the two-year period, it has not been possible to observe systematic, significant differences between elemental or ionic concentrations in the air at the two altitudes. As a consequence, there is no demonstration of a clear-cut effect of the canopy on the interception of aerosols. This result has to be put in parallel with the very low capture yields observed in the wind-tunnel experiments.

It is probable that medium-scale wind turbulences homogenize the concentration of aerosols between the two observation levels. In our sense, such experiments could lead to more conclusive results if realised inside much more dense canopies.

2.3 Interaction of canopies with precipitations

Rain water was sampled at different sites in Belgium (Vielsalm and Louvain-la-Neuve) and at the Donon station. At the Donon, sampling was made above and under the canopy while at the other sites, samples were collected under trees and in clearings. Note that a few samples were taken in the same way in the vicinity of Chernobyl (Novoshepelichy). Here again, it was hoped that differences in concentrations between samples leached from the canopy and samples collected in clearings would give indications on the accumulating power of canopies as a function of granulometries. Indeed, the elements detected by us are vehicled by aerosols of different, characteristic granulometries.

Such differences were not systematically observed and, as a consequence, it is not possible to deduce the role of granulometry in the capture of aerosols by trees.

During the same campaign, ^{137}Cs was also determined in rain water samples. The results of these determinations relate to part 4 of this report.

3. The retention of soluble Cs in forest soils

In the present research, we tried to make a closer approach towards the identification of the mechanisms of retention of Cs^+ by forest soils where the situation is rather complex because of their stratification and of the synergisms between organic and inorganic matter.

Undisturbed forest soils were contaminated by ^{134}Cs -labelled CsCl . The distribution profile of radioactivity between the different horizons (Of, OAh, Ah, and B) was measured after a 8-month period of daily washing with 30 ml of pure water. The kind of absorption was studied by means of sequential extractions with different salts:



which are known to attack characteristic adsorption sites. The extraction yields of potassium were determined together with Cs in order to observe a possible parallel behaviour of both alkaline ions.

Finally young trees were grown in four reconstituted forest soils where the different horizons were specifically contaminated by ^{134}Cs . The transfer to plants from the root system was determined by making a global balance of the activity present in the different plant tissues. This experiment aimed at examining the disponibility of Cs toward plants via the root system.

The conclusions drawn from these studies may be summarized as follows:

- Cs is most intensively retained in the OAh organic layer: even NH_4Ac does not succeed in desorbing more than 1-2% of its content;
- Extraction is somewhat more important from the mineral layer where ammonium acetate displaces up to 25% of the Cs;
- Cs and K evolve in opposite directions: the more Cs is retained into the solid phase, the more K is exchangeable;
- Transfer factors toward young spruce from the different substrates pertain to the same logic: transfers are very low when Cs is contaminating the OAh horizon.

All the observations lead to suggesting that there is a synergism between organic matter and mineral (clay) structures. Given the importance of the retention in the surface organic layer, it should be useful to identify the mechanisms of retention as well as the factors likely to perturbate this retention. This should be done in order to prevent unfavourable counter-measures which could disrupt the retention equilibria which have been established in the forest. Examples of such counter-measures are: slight thinning, clearing, litter removal, ...

3.1 Publications

C. Ronneau, K. Fonsny and C. Myttenaere, "Production of ^{134}Cs thermo-generated aerosols. Study of their behaviour after deposition on spruce trees", Published in "Biological Trace Element Research" Ed. G.N. Schrauzer (1990), Humana Press Inc.

Y. Thiry, S. De Brouwer and C. Myttenaere, "Status of radiocesium in complex forest soils" Conference delivered at the International Meeting: "Geochemical Pathways of Artificial Radionuclide Migration in the Biosphere", 9-13 Dec. 1991, Puschino, Russia.

Y. Thiry and C. Myttenaere, "Behaviour of radiocesium in forest multilayered soils" submitted for publication to the Journal of Environmental Radioactivity.

4. The transfer and cycling of radiocesium in the forest environment

A first series of experiments have been performed in order to determine, under natural conditions, the leaching of Cs from the foliage of spruce contaminated, either artificially by the deposition of thermo-generated, Cs-containing aerosols, either by the deposition from Chernobyl. Other observations were made in order to determine the distribution of residual ^{134}Cs in trees after field leaching of (i) one growth period in the case of artificial contamination, (ii) five years in the case of the contamination from Chernobyl.

4.1 Leaching of the radio-Cs from Chernobyl

Rain gauges have been installed under trees in three different forests. Rain water was collected during two meteorological cycles. Cs was concentrated by extraction with copper hexacyanoferrate and determined in each sample. Potassium was analysed too (by ion chromatography) in order to detect a possible parallel behaviour of these two related cations. The main conclusions to be drawn from these experiments may be expressed as follows:

- Soluble radiocesium was translocated very rapidly directly into plant foliage after the reactor accident, as young needles sampled in October 1986 already showed a significant level of contamination.
- Seasonal cycles are important in translocation phenomena: ^{137}Cs is systematically enhanced in new shoots.
- Three years after the accident, trees which act as a radioactivity reservoir seem to have attained a mid-term equilibrium in which radioactivity is now washed away at a rate determined by the physiological activity of the tree.
- The rate of leaching is less important under caduc trees (for example, oaks) than under spruce, because at the time of the accident buds were not yet open.
- There is a strong parallelism between the leaching of ^{137}Cs and K suggesting a close physiology. Potassium could be used as an indicator of the behaviour of radiocesium in plant and this could greatly enhance our knowledge of contamination pathways in forest ecosystems.

4.2 Leaching of radio-Cs in controlled conditions

In springtime, before budding, the canopy of two young spruces were dry contaminated by thermo-generated aerosols. The global contamination was measured in a total-body counter. It appears that contamination is related to the mass of the surface of the foliage. The trees were then put in field conditions, under natural rain. Water leaching from the trees was collected and the loss of ^{134}Cs is followed as a function of time and of rainfall. In a first period, the washing-off of the Cs can be modeled as an exponential evolution.

If one considers each single rain period, we found no correlation between rain quantity and the amount of Cs which was washed off. During this first phase, the number of episodes is of importance. This first period of relatively rapid decontamination is followed by a second period during which a correlation is observed between wash-off and rainfall. The first period

involves a decontamination of the trees of the order of 60% while the second period, as already mentioned, closely depends on rainfall.

At the end of the washing-off experiment, the distribution of radio-caesium was determined in the different parts of the trees: distinction was made between surface and internal contamination by washing the surfaces of the organs by chloroform. Needles and twigs are more contaminated.

Measurements were also made as a function of time to determine the activity in young needles as compared with 1 year-old needles. The activity reaches a maximum in mid-July in younger needles; a slight decrease is observed thereafter and this is the result of translocation to perennial organs. Cs is easily transferred to active new tissues.

4.3 Publication

C. Ronneau, L. Sombé, C. Myttenaere, P. André, M. Vanhouche and C. Cara, "Radiocesium and potassium behaviour in forest trees", Journal of Environmental Radioactivity, 14, 259-268 (1991).

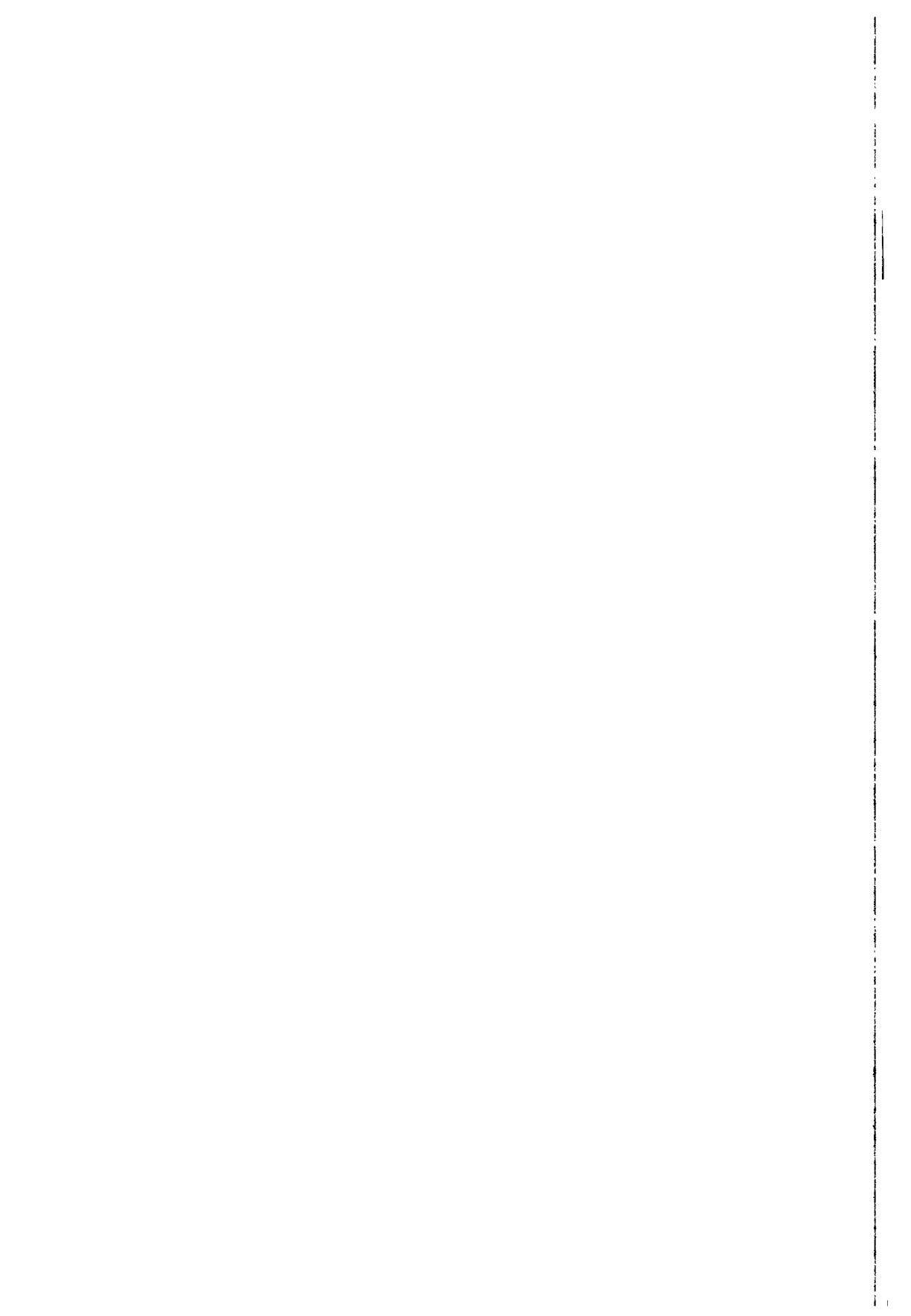
5. Conclusions

These different studies have demonstrated that modelling the transfer of radiocesium in the environment and, more particularly in a forest environment, is not a simple task because of the complexity of its physical, chemical and biological behaviour.

We think that conclusions about the observations should be considered with great care and we suggest that the paper referred to hereunder which has been accepted for publication in "Total Environment" be taken as the general conclusion of this work. It was written in collaboration with Professor W.R. SCHELL of the Pittsburgh University in the framework of a convention with the US Nuclear Regulatory Commission.

6. Publication

C. Myttenaere, W.R., Schell, Y., Thiry, L., Sombré, C., Ronneau and J. Van der Stegen de Schriek, "Radiological Safety: Evaluation of Contamination in Forest and Natural Ecosystems", to be published in "Total Environment".



BEHAVIOUR OF Cs AND Sr IN NATURAL ECOSYSTEMS AND THE POTENTIAL RADIATION EXPOSURE OF THEIR EXTENSIVE USE

Contract Bi7-016 - Sector A25

- 1) *Wirth* , Bundesgesundheitsamt - 2) *Guillitte* , Univ. Liège
- 3) *Palo* , Univ. Umeå Agricultural Sciences - 4) *Nimis* , Univ. degli Studi di Trieste
- 5) *Bergman* , Swedish Defense Res. Establ. - 6) *Wickman* , Univ. Umeå
- 7) *Melin* , Nat. Inst. of Rad. Protection (SSI)

Summary of project global objectives and achievements

1. Introduction

Radionuclides behave differently in natural ecosystems than in agricultural areas which is expressed by the significantly higher activities in forest's, plants and animals, compared to agricultural ones at same deposition rates. As forest ecosystems are important to man since they provide wood, paper, wild berries, mushrooms, game and recreation it is of interest to analyse the behaviour of radionuclides and estimate the potential radiation exposure from their extensive use by the population. In this research project, the behaviour of radiocesium has been studied in different natural forests in Belgium, Germany, Italy and Sweden. In these investigations the emphasis was put on the behaviour of radiocesium in soil, its migration rates, uptake and distribution within plants, transfer to animals, and its cycling within and loss from forest systems. Cycling and transfer mechanisms are analyzed and discussed. Finally doses to critical groups are estimated. The joint project with the European Community started in April 1990, but most of the selected sites have been investigated since 1986. To complete the overview and to better understand the radiocesium behaviour after the Chernobyl fallout, the former results are integrated in this report.

2. Selected investigation sites

The selected investigation sites represent different types of forests. In Italy, a mixed beech fir stand developed on undulating ground on calcareous parent material was chosen in the Carnic Alps, 1417 m above sea level. Additionally, 36 subsidiary stations have been used for sampling plants and fungus which are scattered throughout the province of "Udine".

The investigations in Germany were concentrated on three coniferous sites in South-Bavaria: a 120 year old mixed Scots pine (*Pinus sylvestris*, 30% of the stand on Norway spruce (*Picea abies* 70% of the stand) on pararendzina. The second site is a pure about 100 year old Norway spruce stand on cambisol on calcareous moraine, and the third site is characterized by 90% Scots pine and Norway spruce on nutrient poor dune sand. The forest is about 120 years old.

The investigations in Belgium were carried out in the Lorrain phytogeographical district. Two main stations were chosen: An old beech stand on an eutric cambisol with a silty sand texture (plant association: Melico-Fagetum luzuletosum) and an old spruce stand on a dystric cambisol with a eumodeth humus type (plant association: Luzulo-Fagetum typicum).

The Swedish sites cover coniferous and deciduous forests in central and northern Sweden: Pine (*Pinus sylvestris*), spruce (*Picea abies*), beech (*Fagus sylvatica*), larch (*Larix*) and birch (*Betula* spp) on different soils: Podsol, cambiozol, fluvisol.

The contamination of these stands range from about 2 -300 kBq Cs 134 + 137/m².

3. Direct deposition

The interception of radioactive material in the tree crowns and in the understory vegetation is one of the major pathways to retain the radionuclides in the forest environment. Some of the intercepted radionuclides will be assimilated by the aerial parts of the plants and retained in the plants by translocation and redistribution for a substantial period of time. The intercepted or assimilated radionuclides will sooner or later be transferred to the forest floor by wash off, litter fall or by herbivory. Factors which will effect the initial distribution of radionuclides between the different compartments in the forest environment are determined by the type of forest, stand density, stage of development, season of deposition, etc.

An investigation into direct deposition was not part of this project. Nevertheless, some studies carried out in 1986 are of interest in understanding the cesium cycling.

The interception of dry deposited cesium released after the Chernobyl accident was studied by direct measurements in different ecosystems in Sweden. The content of cesium in soil and understory vegetation was measured within three weeks after the accident. The amount not recovered compared to that found in the open field was assigned to the amount intercepted by the above-named parts of the stand (Table 1).

Table 1: Relative initial interception (tree areas with dry deposition of Cs 137 in different types of forests after the Chernobyl accident. Time of sampling: May 1986.

Stand	Stand Age (Year)	Stem Density Stems/ha	Relative Interception (/m ²)
Spruce	84	1336	1
Pine	139	1622	0.8
Beech	87	687	0.4
Birch	68	573	0.4
Alder	116	605	0.1

A rough estimate indicates that the spruce stand will intercept about 90% of the deposited radionuclides while the defoliated deciduous stands of beech, birch and alder will intercept less than 35% of the dry deposited radionuclides.

At Svartberget, Sweden, most of the fallout originates from wet deposition during a rainfall of 14 hours on April 29, 1986, yielding a precipitation between 3 and 6 mm, depending on local variations in the area. The protracted input, mediated by a particularly light rainfall most likely made the initial distribution within the forest relatively homogeneous in comparison to the possible result from a more intense rainfall. In support of this assumption is the fact that no significant difference in the concentration of radioactive cesium occurred in needles at different height in trees or between the average values from different sampling sites in a pine stand in contrast to results from studies of other sites.

Due to interception, forest soils are not contaminated homogeneously. Higher activities have been measured near the trunk under the beech canopy (stem - flow effect) and in small gaps below the spruce canopy (funnel effect). For example at the Mersch-site, radiocesium deposits vary between 3.4 kBq/m² far off the trunk and 24 kBq/m² near the trunk around the same beech tree. These spatial micro-patterns must be considered when discussing mean activities in forest soils or transfer parameters.

4. Measuring deposition patterns by bioindicator

In case of a sudden radiodeposition, it is important to have a rapid, efficient and inexpensive method to assess main deposition patterns within large areas. Particu-

larly in mountain areas, the deposition patterns may be very complicated due to the rugged geomorphology and the unequal distribution of precipitation. Detailed maps of mountain areas are often difficult to draw, because they require a high density of sampling points. To facilitate this task it is possible to use different organisms as monitors of radioactive deposition. An organism is here defined as "bioindicator" if the concentration of given pollutants measured within the organism are used to reconstruct the deposition patterns of the pollutants.

A good bioindicator should have the following main characteristics:

- 1) High tolerance for given pollutants, and thus:
- 2) capacity of accumulating the pollutants indefinitely
- 3) wide distribution in the survey area
- 3) scarce mobility
- 4) long life-cycle

Since mosses are devoid of vascular tissues, roots and of a cuticle, and are highly water absorbing, most nutrients and elements are acquired from liquid deposition; therefore, mosses can be profitably used as bioaccumulators of radiocontamination, when liquid deposition plays an important role.

In several ecosystems, as in the eastern Alps with a more pronounced oceanic climate, bryophytes are an important part of the total biomass. The thick carpets of bryophytes covering large parts of the forest floor can intercept a great quantity of total deposition, slowing down the transfer to soil.

A preliminary study has been carried out in the main research station of Passo Pura, in the Carnic Alps. 110 samples of bryophytes belonging to different species have been collected on different substrates (bark, rock, soil) at different exposures and inclinations in respect to the tree canopy. The data were submitted for statistical analysis. The highest and more constant contamination values were recorded on compact mats of *Ctenidium molluscum* collected on horizontal surfaces and growing directly on calcareous rocks; thickness varied between 0.5 and 2 cm. The samples collected just below a trunk showed higher contamination values, probably because of secondary enrichment from stem flow. Otherwise, no statistically significant difference was observed among samples collected in different positions in respect to the tree canopy. The study was then extended to 21 stations characterized by different deposition values due to the Chernobyl accident: 112 bryophyte samples and 53 soil samples were collected in the 21 stations and their radiocesium content was measured. There is a very good correlation between radiocontamination in the bryophytes growing on rock and soil. The results per-

mitted the set up of a standard sampling protocol to use this type of bryophytes as indicators of radioactive deposition. The main recommendations are:

- a) The samples should belong to epilithic species.
- b) The samples must grow on horizontal surfaces.
- c) The samples must belong to species forming carpets with a lower part consisting of organic soil and an upper part consisting of the living gametophyte.

- d) The thickness of the samples should range between 1 and 2 cm.

5. Behaviour of radiocesium in soils

The investigated forest soils are generally characterized by widely undisturbed profiles with superficial organic L- and O- horizons, a transition A - organic matter enriched mineral horizon above the parent mineral B- and C-horizons can be subdivided by the degree of disintegration of the organic materials in O_f (original form of the litter still detectable, strong microbial decomposing activities) and O_h (strongly decomposed organic materials without detectable texture) horizons. The thickness of the soil horizons varies.

The organic and intermixed organic - mineral horizons are densely rooted by the fine root systems of the trees and undergrowth plants and visibly penetrated by hyphae and rhizomorphs of soil fungi. Generally, these layers are characterized by a high physiological activity of soil organisms.

The concentrations of essential nutrients as phosphorous, nitrogen, potassium etc. in the O-horizons are by one order of magnitude higher than in the deeper mineral B-horizons.

After the radioactive material has reached the soil as a direct deposition, litter fall or wash-off from the plant material, begins as an interaction between the components of the soil and the radioactive material. Several processes are involved in the interaction between the radioactive material and the constituents of the soil. It must, however, be stressed that measured values of radionuclide concentrations in the soil profile are a result of the vertical movement mechanisms of radionuclides in soil and of the retention mechanisms by the soil media. The radionuclide and its chemical form will influence the processes involved in the interaction. According to the general concept of soil science, factors as: cation exchange capacity, clay, pH, litter quality, climate, will influence the retention of radionuclides in the soil. In addition, the activity of the soil micro-flora, soil micro-fauna and digging animals will influence the rate of decomposition and thus the release of immobilized radionuclides from organic matter.

6. Sorption of cesium in soils

The K_d value indicates the plant availability of an element in soil. It is defined as activity per gram soil divided by the activity per ml solution. High K_d values means a strong adsorption of a radionuclide in soil and, consequently, low uptake rates. Reversely, low K_d values indicate a higher plant availability and higher uptake rates. In arable soils, cesium is strongly immobile if this element is fixed in clay minerals. In contrast to cesium, strontium is more easily available in agricultural soils. K_d values of about 9000 ml/g have been measured for cesium and of about 30 ml/g for strontium in mineral soil. According to these K_d values, strontium is about 10 times more easily available for plant uptake than cesium. This is reflected by the transfer factors soil-plant which in agricultural soils are roughly 10 times higher for strontium than for cesium.

The K_d measurements show diversified results for the different horizons in undisturbed soils of coniferous forests in South Germany. The K_d values for cesium are low in L-horizons ranging between 20 ml/g and 40 ml/g. The corresponding K_d values for strontium vary between 50 ml/g and 170 ml/g. The K_d value of an element in an organic horizon is basically dependent on its valence. Elements with higher valences are more strongly adsorbed possibly explaining the higher K_d values for strontium in L-horizons in comparison to cesium. This trend continues in O_f and O_h -horizons in Siegenburg and Hochstadt/Germany. On both of these sites, K_d values for cesium and strontium increase slightly, which could be explained by the decomposition of the organic material resulting in an enhanced exchange capacity. Different results were seen in Garching/Alz, Germany. On this site, the K_d value for cesium was significantly increased in O_f - and O_h -horizons, but not that for strontium. This site is characterized by a high earthworm activity causing a mixing of the mineral and organic fractions. Accordingly, the amount of the mineral soil in the O_f horizon is significantly higher in Hochstadt than in Siegenburg. Therefore, these high cesium K_d values may be explained by the cesium adsorption in clay minerals.

Similar to arable soils, cesium is very strongly adsorbed in the A- and B-horizons. Extremely high K_d values of 10 000 ml/g and more have been measured at Garching/Alz and Hochstadt, where the soil is of a texture from silty to clayey. In Siegenburg, the K_d values are comparatively low and range between 480 ml/g and 830 ml/g, typical for sandy soils.

The K_d values for strontium are similar in the organic and mineral soil layers at each site (20 - 100) and can be compared with K_d values from agricultural soils.

The results indicate that cesium is much more mobile in organic than in mineral layers, meaning a higher plant availability in organic soils. Considering the Cs uptake on arable soil, the transfer of cesium from the mineral layers should be very insignificant in comparison to the uptake from the organic layers particularly if they are of clayey texture.

7. Migration of cesium in soil

Highest activities of up to 100% were measured in the L-horizon in 1986. The total activities generally decreased in this horizon within the next 2 years to below 20% on Belgian, Swedish and German sites. In later years, the Cs-concentration in the litter was nearly constant or slightly decreases. In the O_F and O_h - horizons of the German sites the maximum was reached in 1988. In 1990 and 1991, about 65% of the total Cs-activity was found in these two organic layers of the coniferous sites in Belgium, Sweden and Germany.

This enhancement of Cs 137-activity in the O-horizons might not be alone due to radionuclide migration. The organic substance of L-horizons is transferred into O-horizons by litter decomposition. Therefore, it appears to be more likely that this transfer is also due to the process of decomposition rather than physico-chemical migration of the Cs 137 nuclide. The migration of the radionuclide from the organic into the mineral horizons is relatively low. The amount of the Cs-activity migrated into the mineral horizons at coniferous sites increased to about 30% in 1991.

The migration rates in the mineral layers are probably dependent on the clay content of the soil. The capacity for Cs remaining in the mineral fraction is poor in sandy soils.

A more rapid migration was observed in a beech stand on a cambisol. On this site mineral layers mixed with organic matter follow the litter layer (L). Under favourable conditions, the litter will be decomposed within one year. Most of Chernobyl radiocesium passed the A-horizon in 1990 and is found in the B-horizons (7-17 and 17-27 cm).

For further prognosis the migration rates of the Chernobyl cesium and that from weapons fallout have been investigated on the two Swedish soils. The cesium distribution pattern from the weapon's fallout is very similar to the Chernobyl one on the Beech-Cambisol stand. In 1980 the highest activities (about 40%) were found in the A-horizons.

On a Spruce-Podsol stand, more than 90% of the Chernobyl Cs 137 was detected

in the O-horizons, the rest of the total deposition in the litter in 1990. On this stand, about 40% of the weapons fallout migrated into the mineral soil layers and is measured to a depth of 33 cm in the B-horizon 27 years later.

The results indicate that even though cesium is weakly bound to the organic horizons, its migration rate is low. This discrepancy cannot be explained by chemico-physical processes alone. This low migration rate must be due to additional parameters. It can be assumed that the strong sorption of cesium on clay minerals prevent the migration of cesium in agricultural soils. This is not the case in organic horizons. Heavy rainfalls in some areas in South-Bavaria caused a significant amount of Cs 137 to be directly washed down to the mineral horizons penetrating the organic horizons. If cesium would behave like a cation in the organic horizons, it should only be washed out into the mineral soils by later rainfalls. However, this was not observed. From our measurements we conclude that most of the cesium is very quickly incorporated into soil organisms and plants. This biological fixing prevents the migration of cesium.

This conclusion was confirmed by an experiment on undisturbed upper parts of forest soils in controlled chambers of the Belgian group. Half of the samples were irradiated to kill living organisms in the soil. After two weeks of artificial rain, the radiocesium concentration levels of the irradiated samples were 62% from those of the non-irradiated samples. This percentage agrees quite well with the theoretical percentage of cesium, which might be fixed by the fungal biomass of the soil.

8. Macrofungi

According to their living habits three different groups of macro-fungi can be distinguished:

- The saprophytes live on organic substrate which they decompose by excreting extracellular enzymes.
- The parasites take their nutrients, proteins and carbohydrates exclusively from their host plants.
- The symbiotic fungi form a mutual association with the fine root system of trees. This symbiosis is called mycorrhiza and is essential for both partners in forest ecosystems. From a fungal sheath covering the fine roots, intercellular hyphae penetrate the root cortex cells up to the endodermis. From the surface of the fungal sheath, hyphae or rhizomorphs grow into the soil forming a high nutrient absorbing network of hyphae which supplies the host plant very efficiently with water and nutrients. On the other hand, the host plant supplies

the heterotrophic fungus with carbohydrates, proteins and several other essential organic compounds. Besides uptake of nutrients and direct transport from soil to host plants these fungi are able to accumulate excess nutrients in the fungal sheath in the rhizomorphs or hyphae. This living fungal biomass is a very effective biological sink for available plant nutrients like phosphorus, potassium etc.

The most important mycorrhiza forming fungi are basidiomycetes species. Besides strict host specification (e. g. *Suillus greillei* only in association with *Larix decidua*), several species are more or less host specific and form mycorrhizas with different tree species (e. g. *Amanita muscaria* with deciduous as well as coniferous trees). A third group of fungi is able to change the living habit, forming facultatively mycorrhizas or live as saprophytes. This is due to the strong competition for host plants among mycorrhizal fungi in the soil.

For further radioecological considerations the fact is important that the bulk of mycorrhizal roots, vegetative hyphae and rhizomorphs can be visibly detected in the organic horizons. The Cs 134/137 ratios of fruitbodies of these fungi are identical with those of the organic soil layers in most cases, indicating that the vegetative mycelium takes up radionuclides mainly from these organic soil compartments.

Differences in the Cs 137-activities might be dependent on the depth of the mycelium. In the first year saprophytic species which have a superficial mycelium in the L-horizon were the highest contaminated in the Carnic Alps and in the Lorrain district. Lowest activities were measured in fungi which are in symbiosis with deep rooting deciduous trees. Nimis et al (1986) were able to subdivide the macrofungi in four ecological categories (parasites, symbionts with deciduous plants, symbionts with coniferous trees and saprophytes) which indicated different levels of Cs 137-activities. Similar results were obtained in the Belgium forests.

Only a year after the Chernobyl deposition, the pattern changed. Now, the mycorrhiza fungi showed significantly higher Cs 137 activities than the saprophytes. Their Cs 137-activities were comparable to the activities of parasites (fig. 1)

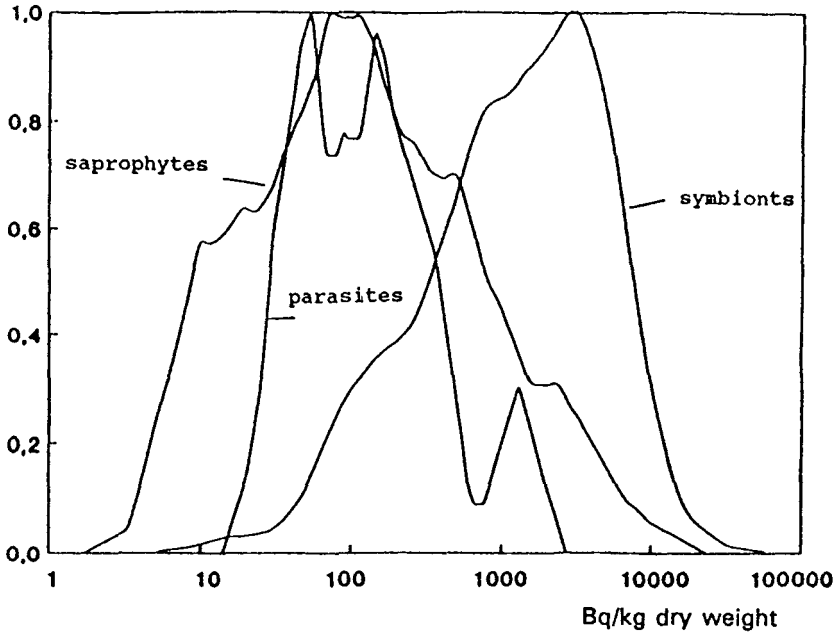


Figure 1: Frequency distribution of the radiocesium activities in saprophytes, symbionts and parasites from 1987 - 1989 on three sites in South-Bavaria (Römmelt, 1991)

To analyze whether the relatively wide distribution of the Cs 134 + 137-activities in fungi are at random or an expression of species-specific accumulation of cesium, the ratio between the cesium activity of each species and the activity of *Xerocomus badius* was calculated for each site and each year.

The *Xerocomus badius* was found in Siegenburg and Hochstadt, Germany from 1987 - 1990 each year and at Garching/Alz, Germany only in 1987 and 1990.

The quotient species *Xerocomus badius* indicates that *Hydnum repandum* accumulates about three times and *Paxillus involutus* about two times more cesium in comparison to *Xerocomus badius*. The results for the *Paxillus involutus* could be verified only for one site, but for *Hydnum repandum* on two sites. Most of the species accumulate significantly less cesium in comparison to *Xerocomus badius*. Relatively constant values for the ratio species/*Xerocomus badius* were found for *Russula emetica* (0.64 - 0.87), *Amanita rubescens* (0.14 - 0.47), and *Russula cyanoxantha* (0.35 - 0.52). There are only a few species which indicate no systematic values like *Laccaria amethystystina* (0.3 - 2.0) or *Cantharellus tubaeformis* (0.39 - 1.44). This is remarkable in so far as the samples were taken on natural

sites, where the activity concentration in soil may vary as well as the growing conditions between the years. Comparing the activities in edible mushrooms, it has to be stated that most species accumulate significantly less cesium than *Xerocomus badius*. According to our results *Amanita rubescens* accumulates between 19 and 39%, *Cantharellus cibarius* between 6 and 36%, and the *Boletus edulis* between 8 and 14% in comparison to *Xerocomus badius*. *Macrolepiota procera* (2 - 6%), *Agaricus silvaticus* and *Agaricus silvicola* (0.3 - 1%) show only a small ability for accumulation of cesium. These three species however belong to the group of saprophytes.

9. Transfer factor soil/fungi

For calculating the transfer factors soil/plant, the concentrations of radionuclides in the rooted zone should be respected. Therefore, the mean concentrations at plough depth are recommended for arable soils. The forest soils differ from agricultural soils by more or less distinct horization. Mushrooms are heterotrophic organisms which live on organic substrate, therefore their myceliums are preferably found in the organic horizons. As shown before, the radiocesium activities vary significantly in the different horizons of forest soils. Highest activities are measured in the organic L- and O-horizons. Respecting the high cesium activity especially in symbionts and the ratio Cs 137 : Cs 134, it can be assumed that fungi take up most of radiocesium from these layers. This is indicated by the very similar ratio of Cs 134/ Cs 137 in O-horizons and mushrooms. If cesium should migrate into the mineral horizons, it is expected to be adsorbed strongly, so that it is hardly plant available; in this case lower transfer rates might be expected. Therefore, it is proposed to calculate the transfer factor soil-fungi by taking the cesium activity in the organic horizons into account. There are some practical aspects for this proposal since samples of the L- and O-horizons can be taken relatively easy. A mixing of the organic and mineral horizons of soil is not recommended as their properties are too different. Consequently, constant transfer factors are not to be expected when the activity of a radionuclide varies in the different layers of a soil.

As described before, each species seems to have an individual ability for cesium accumulation. It is therefore suggested to calculate transfer factors for the different species separately. For the public, the values for edible mushrooms are of special interest. Therefore mean transfer factors soil/fungi defined as Bq/g fungi (fresh weight)/Bq/g O-horizon (DW) are suggested for some edible mushrooms. Transfer factors between 0.7 and 5 have been calculated for *Xerocomus badius*. A mean value of 2.2 is suggested. The transfer factors for *Amanita rubescens* range between 0.15 and 0.8, for *Cantharellus cibarius* between 0.6 and 0.75, and for *Boletus edulis* between 0.12 and 0.36. Lower transfer factors are calculated

for saprophytic fungi, e. g. *Macrolepiota procera* (0.01-0.012), *Agaricus silvaticus* and *Agaricus abruptibulbus* (0.01 and 0.02).

10. Vascular Plants

10.1 On the expression of radiocontamination in vascular plants

The reliability of radioecological parameters is dependent on their statistical distribution. To improve a parameter means at to least minimize its distribution. The radionuclide activities in plants are generally expressed in Bq/kg dry weight. However, the expression of radiocontamination on a dry weight basis does not take into account that potassium and cesium are mostly related to the liquid phase of a cell. Furthermore, the dry weight of different plant species or different parts of the same species may differ considerably in their cellulose and lignine content. If the concentration of potassium and cesium in the liquid phase is fairly constant, the results expressed in Bq/l should be rather independent from the organic matter content of a plant and the distribution of the data should therefore be less wide.

A study was devoted specifically to this problem. The radiocesium and potassium 40 contamination of 47 vascular plant species collected at the Passo Pura station was expressed in two ways: Bq/kg dry weight, and Bq/l (Fig. 2). Expressed in Bq/kg especially the K 40, shows a relatively wide distribution which is reduced significantly when potassium is related to the liquid-phase of the plants. In radioecological considerations this narrower distribution provides a greater degree of accuracy. Therefore, this type of expression was adopted by the Italian group in their considerations.

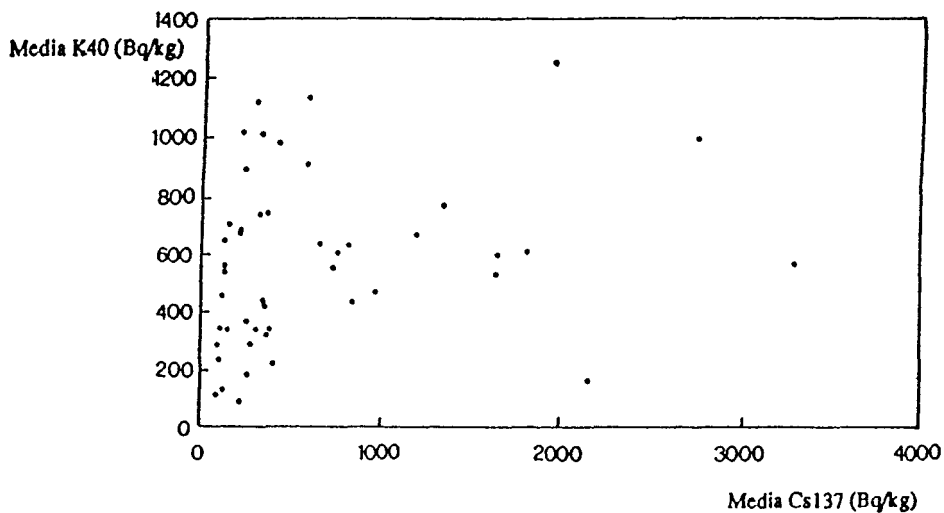
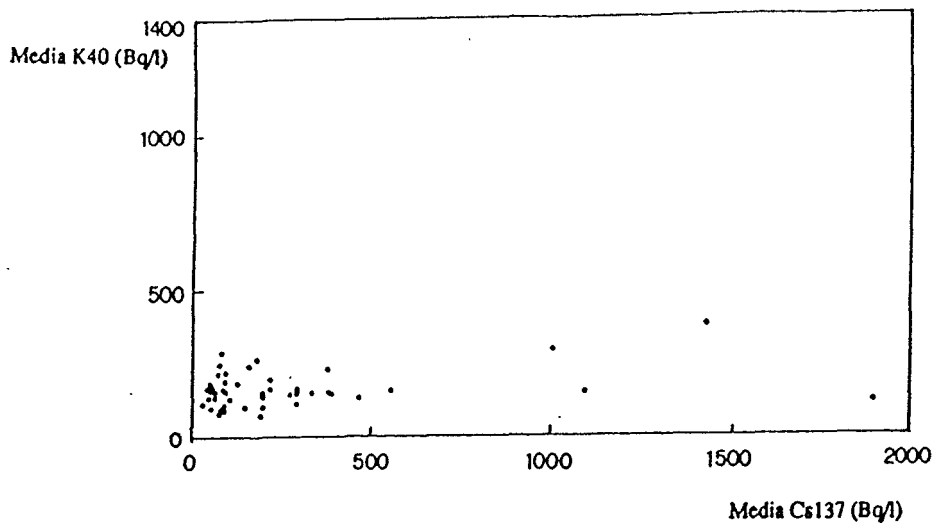


Figure 2: Relations between concentrations of radiocesium and K 40 in 47 vascular plant species collected at the Passo Pura station, expressed in Bq/l (a) and Bq/kg (b). The data for each species are averages of leaves, stems, and roots. (Nimis)

10.2 Groupings of plants according to their ability to accumulate cesium

The contamination of 42 species of vascular plants, collected in an area of 0.3 km² was studied in a mixed *Fagus-Abies* forest in Passo Pura.

Leaves, stems and hypogeal organs were separately sampled from each species. A sample is a mixture of at least 20 individual plants collected at random points within the sampling plot. For each sample, radiocesium and K 40-content have been measured. The data analysis was based on the multivariate analysis (classification and ordination) of a matrix of the 42 species and of 6 radioecological variables.

The main results may be summarized as follows:

- 1) The correlation between classification of species on the basis of radionuclide data and their ecological behaviour allowed to subdivide the species into 4 groups; each group was characterized by a different ecology within the forest (shallow rooting forest species, deep-rooting forest species, plants of forest clearings); thus with the radiological data it is possible to distinguish between at least three main microniches of direct radioecological relevance: two microniches depend on the vertical variation of soil features, one on the horizontal patterning of the forest soils.
- 2) The content of radiocesium is highest in plants where root systems occupy the upper soil layer of acidic humus, and lowest in the deep rooting megaphorbs of the wood clearings. This is due to the unequal distribution and the different plant availability of radiocesium in the organic and mineral soil horizons.
- 3) The K 40-concentration is much less subject to variation than radiocesium concentrations. This is probably related to the regulation of this essential element by plants.
- 4) The megaphorbs growing in beech forest clearings tend to retain radiocesium in their root systems. It appears that the plants discriminate between Cs versus K during translocation, as the ratio Cs 137/ K 40 between roots and leaves is greater than 1 in the majority of species, but is particularly pronounced in the plants of the clearings.
- 5) Trees and shrubs of the beech forest tend to have a higher Cs 137/Cs 134 ratio than understory vegetation, probably on account of the greater depth of their root systems. These plants might take up relatively more pre-Chernobyl

cesium having already migrated into deeper soil horizons. These plants may also have the tendency to store old, pre-Chernobyl radiocesium in their roots. The latter may be due to the fact that several of these plants have hypogeal organs transformed into storage organs.

The results of the analysis may permit a simplification of the ecosystem for modelling purposes: 47 species can be reduced to 4 groups, each being characterized by a peculiar ecology and by different contamination patterns.

11. Long-term contamination

The Cs 137-activities in different perennial vascular plants have been investigated in Sweden since 1986.

Most perennial "key"-plants (except *Epilobium angustifolium*) (milkweed) were directly exposed to the Chernobyl fallout. The activity concentration of radioactive cesium in these species decreased rapidly during the early summer of 1986, according to results from sampling with a fourteen-day interval. This very fast decline seems to be caused by a combination of removal during rainfall, translocation within the plant and "dilution" in growing parts of the plants. The changes in concentration of Cs 137 are generally much smaller after this initial phase during the spring and summer in 1986. The step towards a much lower rate of change appears already in late summer, which is the first sampling period for the data illustration in fig. 3.

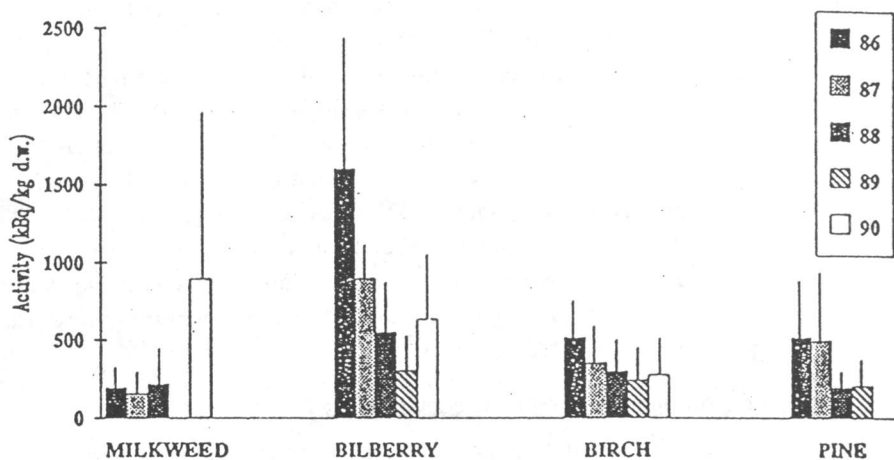


Fig. 3: The concentration of cesium 137 during 1986-1990 in "key"-plants based on pooled data from samples in July (bilberry twigs, birch twigs and milkweed) and October (bilberry twigs, birch twigs and pine). Bergman et al 1991)

The trend toward decreasing levels from the autumn 1986 and onwards is in many cases not significant (see birch and milkweed in fig. I). There are, however, some exceptions to that general trend:

- The relative change in concentration of Cs 137 found in bilberry twigs from the first sampling occasion (6th of June 1986) till mid-July 1986 is about 50% based on the single sampling site used in this early phase. After this initial decrease a further significant decline of about 85% occurred for bilberry over the period from July 1986 to October 1990.
- Pine needles born in 1985 were directly exposed to the fallout and exhibit a fast decrease of 50% in Cs 137-activity concentration from the first week in June 1986 to November 1986. These one-year-old needles do not change their biomass considerably during 1986, so that the pattern for needles "current 85" cannot be explained by dilution of the cesium concentration due to growth of this year's class. The conditions are quite different for the needles current in 1986. These were not directly exposed to the deposition of Chernobyl cesium, but contain early in June 1986 (probably as a consequence of surface contamination and translocation) about 1/4 of the activity concentration of the older year classes. The rapid decline in these needles current in 1986 during summer results from the combined effects of dilution in the increasing biomass, due to a very high growth-rate, counteracting the contributions by internal translocation and contamination from older needles. When the change in the level of Cs 137 is calculated per branch for the whole compartment of needles current in 1986 (based on sampling with a two weeks interval from early June to October 1986), a significant increase is obtained during late June to mid July, due to the input by internal translocation and/or contamination from earlier year classes. For all directly exposed needles remaining in the pine, a further significant decrease of about 80% has occurred till June 1989, as compared to the level in November 1986. Each year, the class of needles directly exposed to Chernobyl cesium has in turn, after its typical four years lifetime, transferred about 0.5 - 1 kBq/m² of Cs 137 to the forest floor by litter fall during autumn 1986-1989.

12. Translocation of cesium within vascular plants

In literature it has been shown that in agricultural plants cesium behaves similar to potassium, an essential element with characteristic concentrations in different tissues, due to regulation processes.

Analyzing the distribution of potassium within the stem, leaves and berries of a plant shows that significantly lower concentrations are measured in stems than in

leaves. If cesium behaves similar to potassium, higher cesium activities must be expected in organs that are rich in potassium and vice versa. In other words, the ratio of Cs 137/K should be the same in each organ of the same plant. Table 2 shows that within the range of standard deviation the ratio of Cs 137/K is nearly constant in leaves and stems of a plant. In some plant species, both Cs and K were measured in stems, leaves and fruits. Blueberries show the lowest C 137-activities, but the ratio Cs/K corresponds with the values in stems and leaves. This means that cesium behaves physiologically very similar to potassium. Therefore, it will be examined whether the prognosis of cesium uptake can be improved by transfer equations taking the potassium concentrations in plant and soil into consideration.

Table 2: Mean Cs 137/K 40 Ratio and Standard Deviation in Different Tissues of Plants in Hochstadt and Garching/Alz, Germany, Sampled in 1991

Plant Type	Location	Number of Samples	Leaves	Stems
Vaccinium myrtillus	Hochstadt	3	22.9 ± 8.6	21.8 ± 1.4
	Garching/Alz	5	4.7 ± 2.2	5.0 ± 2.2
Rubus fruticosus	Hochstadt	4	8.1 ± 1.5	8.2 ± 3.1
	Garching/Alz	4	1.3 ± 1.9	0.6 ± 0.4
Rubus idaeus	Garching/Alz	6	1.2 ± 0.5	0.8 ± 0.3

13. Transfer of radiocesium from soil into autotrophic plants

When analyzing the transfer of radiocesium from soil into autotrophic plants, only understory vegetation were taken into consideration, as these plants take up their nutrients mainly from the O-horizons. This is indicated by the ratio of Cs 137/Cs 134 being 8.9 ± 0.8 in plants and 8.6 ± 0.8 in the O-horizons.

Fourteen different species of autotrophic plants were sampled in Hochstadt and Garching/Alz during the vegetation period in 1991. The radiocesium activity in these plants varied between 10 (berries) and 10000 Bq/kg DW (ferns), and the potassium concentration between 1 (berries) and 29 g/kg DW (wood-sorrel). The potassium concentration in soil is calculated from K 40-activity measurements in soil: it varies between 1 and 6 g/kg. The mean cesium activities in soil in Hochstadt and Garching/Alz were about the same. However, the activities in some plant species are significantly higher in the samples from Hochstadt. This might be due to the relative high amount of clay in the O-horizon in Garching which is

strongly Cs absorbent making it less available for plant-uptake. Accordingly the K_d -values are significantly higher in the O_f -horizon in Garching compared to those in Hochstadt.

14. Transfer factor soil/plant

As the understory vegetation takes up most of the nutrients from the O-horizons, the transfer factor is defined, according to fungi, as cesium activity in plants (Bq/kg DW) to the cesium activity in the O-horizon (Bq/kg DW). Assuming a linear approximation the correlation for the transfer factor was estimated to be $r = 0.39$ for all plant samples taken in Hochstadt and Garching/Alz. This corresponds with the determination coefficient of $r^2 = 0.15$, meaning that 15% of the variation of radiocesium activity in plants can be explained by the cesium concentration in the organic horizon. Analyzing the results from Hochstadt and Garching/Alz separately, the correlations do not improve ($r = 0.36$ for Hochstadt, $r = 0.32$ for Garching/Alz).

Considering grass species separately, there is no correlation at all between the activity in soil and in plants ($r = < 0$). If grass species are not taken into account, the correlation coefficient increases to $r = 0.51$ for the remaining plants. As the consumption of berries is of interest for the radiation exposure to man, the transfer factor of cesium for bilberries (*Vaccinium myrtillus*), blackberries (*Rubus*) strawberries (*Fragaria vesca*) and raspberries (*Rubus idaeus*) was analysed separately. The correlation coefficient of $r = 0.63$ is acceptable.

15. Transfer equations

In a first approach for improving the reliability of prognostic estimation, the potassium concentration in the organic horizon was considered in the transfer equation:

$$Cs\ 137_{Plant} = a + b\ Cs\ 137_{Soil}/K_{Soil} \quad (\text{equation 1})$$

Taking all plants at both sampling sites into account, the correlation ($r = 0.35$) is nearly the same as that for the transfer factor ($r = 0.39$). In Garching/Alz the correlation is $r = 0.42$ when taking all plants into consideration. The corresponding value for Hochstadt only is $r = 0.19$. Also, the prognosis for the Cs 137-activities is not improved by equation 1 for grasses ($r = -0.05$) as well as for dictyledons plus ferns ($r = 0.47$) and for the leaves of berry plants ($r = 0.59$) in comparison to the corresponding correlation calculated for the transfer factor.

The potassium concentrations in plants have been additionally considered in the next equation:

$$Cs\ 137/K_{Plant} = a + b \times Cs\ 137/K_{Soil} \quad (\text{equation 2})$$

Although it was found that Cs is similarly translocated within a plant as K, the correlation for equation 2 decreases slightly for all groups of plants considered. The correlation for all plants at both sites was $r = 0.20$, for the dicotyledons $r = 0.38$, and for the berry plant leaves $r = 0.53$. This means that the prognosis of the cesium concentration in plants could not be improved by taking potassium into account. These results are in opposition to the results received from agricultural plants grown on ploughed soils. In these studies the correlation is $r = 0.3$ for the transfer factor, and $r = 0.7$ for equation 2 taking into account 107 plant samples from 20 different species grown on 60 different soils.

16. Discussion of the transfer soil/plant

The summary of results from Cs-uptake by plant and fungi represents a puzzling picture.

In comparison to agricultural plants, a relatively good correlation was found to exist for the transfer factor for dicotyledons ($r = 0.51$), however, there was no correlation at all for monocotyledons ($r = -0.15$). These correlations could not be improved by taking the potassium concentrations in soil and plants additionally into consideration. Fungi seem to have a species-specific accumulation rate of Cs 137. Especially the activities in symbionts vary in a wide range at one site. This gives rise to the question as to what might be the reason for this puzzling picture.

From literature it is known that Cs behaves similarly as potassium, as was shown with agricultural plants. In a literature survey C. Leising (1986) came to the result that cesium behaves similarly as potassium, whereas during plant uptake cesium is always discriminated versus potassium. For root uptake, the OR-ratio varies between 0.2 and 0.5 in hydroculture and between 0.001 and 0.03 in soils. Accordingly, it can be assumed that fungi discriminate Cs against K during uptake from soil. Symbionts support their host with nutrients, meaning they take up more nutrients from soil than they need. It is not unlikely that Cs is discriminated a second time during the transfer from the mycelium into the root cells of the host. In this case fungi would accumulate the more Cs the more intensive they supply their hosts with nutrients. The amount of Cs 137 in the fruitbody of a fungus might then be an indicator of the intensity of the symbiotic relationship.

Thus saprophytic fungi have generally lower activities than symbiotic fungi, which was demonstrated. But there is an overlapping of the specific activities. This might express the ability of some fungi to live saprophytic as well as symbiotic, but it might also be that the degree of discrimination effects varies in different mushroom rooms.

Discussing the measurement results of autotrophic plants one has to be aware that most plants live in symbiosis with fungi. This means that a more or less high amount of their nutrients is not only taken up directly from the soil but via fungi. Besides soil and plant characteristics, symbiotic fungi are therefore another important parameter for the amount of radionuclide uptake. Currently, not enough background is available to quantify the influence of symbiotic transfer mechanisms on the amount of Cs 137-activity in autotrophic plants.

17. Mammals

17.1 Mooses and roedeers

During the project, material from moose collected during the years 1986-1991 in the county of Västerbotten were analyzed. The main results from this animal study showed a considerable variation in radiocesium activities between the years. During the hunting seasons of September 1987, 1989 and 1991, the Cs 137-activity in meat was about the same as the mean concentration of about 300 Bq/kg (Median = 253, SD = 250) in adult moose in 1986. The years 1988 and 1990 showed dramatically higher levels than other years. The average activity concentration in 1988 was 640 Bq/kg in adults and 1300 Bq/kg in calves. In 1990, the mean was 514 Bq/kg in adults and 1120 Bq/kg in calves. Generally, calves showed about 40% higher radiocesium activities than adults. A multivariable linear estimation indicates that the Cs 137-concentration in moose meat is independent of sex and year, but can be largely explained by the amount of deposition at collection site. Age showed a negative relationship which supports the higher levels found in calves.

The diet of moose in northern Sweden in early September might be composed of at least 36 plant species, as is indicated by the rumen content analysis. The major part of the diet is composed of only three plants e. g. *Vaccinium myrtillus*, *Betula* spp. and *Salix* spp. The proportion of a single plant species in the diet has a highly skewed distribution function in the moose population. Few animals have a large proportion of single plant species diet, whereas most of them have quite a mixed diet. No relationship was found between the proportion of specific plant species in the moose rumen and the activity concentration in flesh. This is probably dependent on a time lag between actual diet and manifestation of the Cs-level in the flesh.

The Belgium group observed significant differences of Cs 137 activities in kidneys of roedeer killed on four different soil types. Furthermore, on two sites the mean activities were significantly higher during the autumn-winter season than during spring and summer. Highest activities were found on podsolic soils, lowest on eutric cambisol. The activities in roedeer correspond well with the activities of the

indicator plants *Rubus sp* and *Deschampsia flexuosa*. (Table 3, Fig. 4).

Table 3: Comparison between Roedeer Kidney Contamination (Cs 137-activities in Bq/kg-1 DM) in Spring-Summer period and in Autumn-Winter Period on Different Soil Types within the Lorrain District (A: Sandy soils with dysmoder, B: Silty-sandy soils with eumoder, C: Silty-clayey soils with meso trophic mull, D: Clayey soils with eutrophic mull)

Soil Type	Spring-Summer			Autumn-Winter		
	n	mean	± std	n	mean	± std
A	7	1060	± 170	7	3530	± 930
B	13	520	± 180	14	1150	± 430
C	4	290	± 90	4	330	± 50
D	6	120	± 50	17	140	± 50

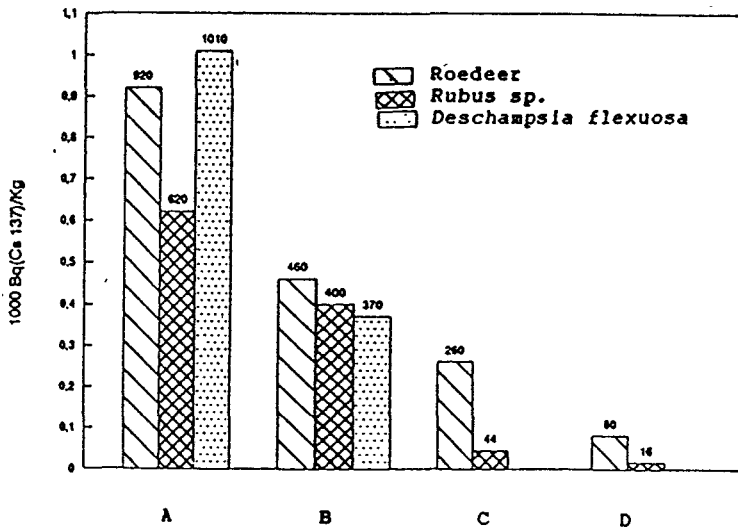


Figure 4: Comparison between Roedeer Kidney Contamination and Plant Contamination (Cs 137-activities in Bq/kg DW) in different Soil Types within the Lorrain District.

17.2 Voles

Bank voles (*Clethrionomys glareolus*) and grey-sided voles (*C. rufocanus*) are small rodents common in the boreal forest. These mammals show pronounced periodic fluctuations in numbers with a peak population density about every fourth year. At the time of the Chernobyl accident, the bank vole population was about to increase and peaked in 1987. The grey-sided vole peaked in 1988. However, the number of trapped animals of the latter species was much lower than that of bank voles, irrespective of the year of collection. The yearly variation of activity concentration in the bank vole is shown in fig. 5.

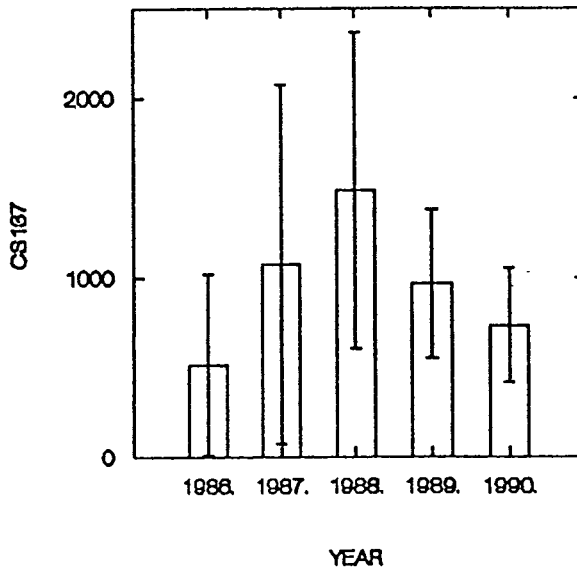


Figure 5: Yearly Variations in Cs 137-Activity Bq/kg) in Bank Vole. Mean and SD. (Palo 1992)

The grey-sided vole did not show such trend, the mean activity concentration of Cs 137 was 877 Bq/kg (SD = 847) and for Cs 134 259 Bq/kg (SD = 257) during the period. No significant differences in Cs 137-activity were found between species, age or sex, irrespective of the year of collection. The body mass of bank voles was not significantly different between the years, and no relationship between body mass and activity concentration was apparent. From 1986 to 1988 the grey-sided vole showed a significant increase in body mass. A too low number of animals of this species were trapped in 1989 and 1990 for analysis. A stepwise linear regression eliminated age, sex, and body mass from an explanatory model for Cs 137 concentration in voles. In these small mammals the year of collection and amount of deposition explained most of the variation in Cs 137 concentration (Figure 6).

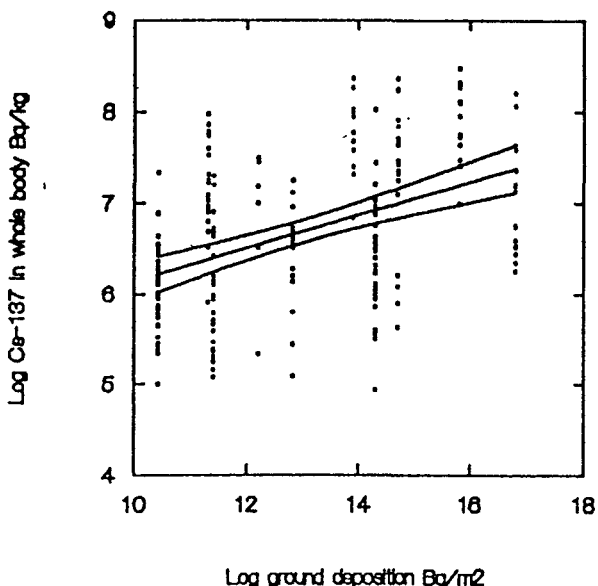


Figure 6: Correlation between the natural logarithm of Cs 137 concentrations in whole body of Bank Vole and Ground Deposition at Site of Collection. In $Y = 0.858 + 2.396 \ln x$, $r = 0.443$, $p < 0.001$, $N = 106$. (Palo 1992)

18. Modelling

The results obtained so far permit modelling of the ecosystem with respect to radionuclide turnover. Two approaches have been used to model the system with the focus being on the role of herbivores in the transfer of radionuclides. The first is an attempt to analyze the effect of different diet compositions on the population distribution of Cs 137 in moose. The other is to model the importance of herbivores on voles and moose in relation to the annual litter fall. The basic algorithm is extended to take the population density of herbivores into account.

Two important processes for the transfer of matter in ecosystems are herbivores and litter fall with associated decomposition of organic material in soil. The relative significance of the different processes in ecosystem dynamics are controversial. Herbivores are estimated to remove about 10 percent of annual net primary productivity on the average, while 90 percent is removed by decomposers in most systems. These figures are by necessity crude estimates and neglect variations between different systems. For example, individual plant species could lose less than 2 percent to herbivores in one situation but up to 100 percent of the annual production in other situations, depending on type and interaction. We analyzed herbivory by bank vole (*Clethrionomys glareolus*) and moose (*Alces alces*) by a

simple model in relation to litter fall in a typical forest. This analysis was based on mass balance calculations of Cs 137 in annual litter fall and periodic-oscillations in vole numbers. Moose population density was kept constant in the analysis. At peak density of bank vole, the effect on Cs 137 turnover by total herbivores was almost equal to that by litter fall. The largest influence by herbivores on Cs 137 turnover was caused by fluctuations in the vole population. This is because voles have a mass specific energy metabolism that is one order of magnitude higher than that of moose, resulting in an increased effect on the vegetation at peak density. It is also possible that the bio-availability of Cs 137 from herbivores is larger, compared to the rather slow decomposition rate of plant litter. It is argued that the transfer processes of Cs 137 into soil are more effectively mediated by herbivores, than is apparent from the ratio of organic matter in the food to that in the litter fall.

19. Long-term distribution of radiocesium in forest systems

The retention and distribution of cesium on a long-term schedule have been studied in a mixed pine/spruce stand on podzol in central Sweden. The stand was established in 1930 and the sampling was carried out in 1980. This implies that the stand was exposed to the nuclear weapon fallout in the fifties and sixties but not to the fallout from the Chernobyl accident.

About 85% of the recovered deposition was found in soil. About 50% has migrated into the mineral horizons of the soil, but 50% remained in the organic layer.

About 10% of cesium recovered in the stand was found in tissues generated during the year of sampling (Table 7, 8). This clearly demonstrates the high mobility of cesium as long as 20 years after the time of deposition. Whether the cesium recovered in the recently formed tissues is the result of root uptake or is the outcome of a redistribution within the tree cannot be concluded from this experiment.

The concentration of cesium in understory vegetation species is high compared to the plant tissues of the trees on the site (Table 10). The low biomass of herbs, grass etc. will result in only 1% recovery of the gross amount of cesium in the understory vegetation.

Table 4: Distribution of Cs 137, Bq/tree in different fractions of Scots pine and Norway spruce. Mean of six trees. Site A, Reference Date 1990. Type of Deposition: Nuclear Explosions 2100 Bq/m². Sampling Date: 1980 (Melin)

Fraction	part in the canopy	<u>1981</u>	<u>older</u>	<u>total</u>	<u>1981</u>	<u>older</u>	<u>total</u>
Needles							
	upper 1/3	18	17		83	59	
	middle 1/3	38	33		74	105	
	lower 1/3	25	9		36	89	
	S U M:	81	59	140	193	253	446
Branches							
	upper 1/3	9	12		25	151	
	middle 1/3	8	61		14	97	
	lower 1/3	8	88		7	99	
	S U M:	25	161	186	46	347	393
Crown total		106	220	326	239	600	839
Stem							
	bark			163			145
	wood			332			312
	S U M:			495			457
Stump and roots < 20 mm				271			180
Total in Tree				1092			1476

Table 5: Concentration of Cs 137 in Understory Vegetation.

Mean of four replicates of 1/4 m²

Site A

Reference Date: 1990

Type of Deposition: Nuclear Weapon Fallout: 2100 Bq/m²

Sampling Date: 1980

	Cs 137 Bq/kg	biomass kg/ha	Cs 137 Bq/m ²
Vaccinum myrtillus	25	111	0.28
Bushes	28	8	0.02
Deschampsia flexuosa	39	112	0.44
Pteridium aquilinum	52	27	0.14
Herbs	90	26	0.23
TOTAL			1.11

Table 6 shows the distribution of Cs 137 between soil, trees and understory vegetation 17 years after the stop of nuclear weapons test

Table 6: Distribution of Cesium 137 (% of total recovered) in different compartments of a mixed pine/spruce forest stand.

Site A

Type of deposition: Nuclear Eapon Fallout: 21 Cs 137/m²

Date of Sampling: Sept 1980

Ref. date: 1990

	% of total recovered (areal)
Trees	14
Understory vegetation	1
Soil (depth 50cm)	85
T o t a l:	100 (1260 Bq/m²)

From the estimated figures of cesium deposited in the area and the amount recovered in the system, about 35% of the deposited cesium has left the part of the ecosystem included in this study.

The amount of cesium not recovered has, to some extent, been removed from the

ecosystem by forest treatment (thinning the stand). In addition, cesium might have moved through the soil profile and leached out from the rooting zone. The surface run-off of cesium on this site can be largely excluded as the topography of the studied area is flat.

20. Loss of Cs 137 from forest systems

20.1 Waterborne transport

To estimate the loss of Cs 137 from forest systems, the content of radioactive cesium in water has been studied with regard to run-off from a catchment area in northern Sweden. Based mainly on waterflow and radioactive concentration in 1986, 1989 and 1990, the amount of radioactive cesium leaving the terrestrial compartment by water has been estimated.

The time when the main deposition of Chernobyl cesium occurred (April 29th), snow-melting and run-off reached their maximum intensity. The amount of Cs 137 discharged from the studied 0.5 km² catchment was about 600 MBq during this period. In the following years, only low levels of radioactive cesium were detected in the stream. The values are summarized in table 7.

Table 7: The Activity concentration of Cs 137 in Run-Off Water from the Forest Catchment at Svartberget over the Period from 1986 to October 1991

Year	Season	Concentration of Cs 137 (Bq/l)
1986	29.4. - 31.5. - spring	1 - 21
1986	01.6. - 17.8. - summer	0.2 - 5
1986	18.8. - 1.11 - autumn	0.1 - 1
1986	02.11.- 31.12.-winter	0.08 - 0.1
1989	14.4. - 07.5. -spring	0.1 - 0.4
1990	11.4. - 02.5 -spring	0.06 - 0.2
1990	10.9. - 01.10 -autumn	0.06 - - 0.12
1991	14.04. - 15.05.- spring	0.12 - 0.15
1991	13.10. - 17.10.-autumn	0.08 - 0.10

21. The loss of Cs 137 from different parts of the catchment

The remaining deposition in the catchment is inhomogeneously distributed, and the average level of radioactive cesium decreases in the following order: ridge and plateau areas at the water dividers; slopes; valleys; open peat bogs. This supports the interpretation that snow-melting plays an important factor in the distribution pattern obtained in the catchment. Furthermore, the low levels in the valley and the bog (partly water-covered during the most intense phase of run-off) indicates that initially, at least, discharge areas have been the main source for Cs 137 in the stream.

Table 8: The distribution of Cs 137 (kBq/m²) remaining in a 0.5 km² catchment, derived from soil sampling (n=330, 66 groups) and a classification of biotopes

Site Description	Cs 137-activity concentration (kBq/m ²) Mean; σ
Hylocomnium and Plevorizm rich forests on podzols	23; $\sigma = 7$
Peat moss on peat partly covered by Calluna, Betula, Pinus and Picea	13; $\sigma = 7$
Open peat bog covered by peat moss (Sphagnum)	5; $\sigma = 3$

The integral ground deposition in the 0.5 km² catchment, determined by soil and water sampling after the Chernobyl event, is 8.6 GBq (17.2 Bq/m²). The leakage by run-off from the catchment was thus about 7% or 1.2 kBq/m² in 1986. During the subsequent years this leakage decreased to about 0.2% per year. On the assumption that only peat areas are responsible for the release of activity to the stream, their total loss of Cs 137 during 1986 was 6 kBq/m². This corresponds to an early fractional loss of about 30% from such sites under the "Chernobyl" conditions. On the same assumption, the fractional loss per year during 1987-1990 was 1 - 2%. This estimate constitutes an upper limit for the loss from the whole open and forest covered peat bog, since any distribution from other parts of the catchment is neglected. Furthermore, the ratio between the activity concentration in the open peat bog and the average whole podzol area provides another measure of the loss from peat and shows that only about 1/3 of the Cs 137 remains deposited on the open peat bog.

The possible differences between nuclear weapons- and Chernobyl-cesium with regard to such factors should result in a different behaviour or distribution in the environment and is not evident from our studies.

22. Dose to man

Lapps who breed reindeers traditionally base their food consumption on reindeer, moose and game meat, lake fish and wild berries. These foodstuffs can also be found in many of the food baskets of people who live in the north of Sweden. The cesium activity in such food can be comparatively high. Typical activities and their seasonal variation in man have been measured by whole body measurements and analysis of tissue available from autopsy or surgical procedure.

The measured persons have been divided into 4 groups, according to their eating habits and the Cs 137 deposition in the area where they gather their food:

- 1 Moose, lake fish and reindeer less than once a month in all areas.
- 2 Moose and lake fish more than once a month, but reindeer less than once a week in all fallout-areas.
- 3 Moose and/or lake fish more than once a month and reindeer more than once a week, living in fallout-areas with less than 10 kBq/m².
- 4 Moose and/or lake fish more than once a month and reindeer more than once a week, living in areas with a deposition of 10-40 kBq/m² of Cs 137.

In Figure 7, the Cs 137-activity divided by the total body mass as a function of time, is shown for the four groups. Group 1 and 2 had an activity concentration slowly varying with time, while in group 3 the time variation is very uncertain. In group 4 (mainly reindeer breeding Lapps) a sharp rise was observed in March 1987, probably mainly due to the fact that people became less concerned about the activity in food after the first year. An explanation could also be that the reindeer slaughtered in the spring 1987 had a higher Cs 137-concentration because reindeer eat more lichen in winter. In June 1987, a more constant value was reached, which decreased slightly till 1991. It has to be emphasized, that activity levels of 100 Bq/kg muscle and more are only measured in a minority of the Swedish population. (Fig. 8).

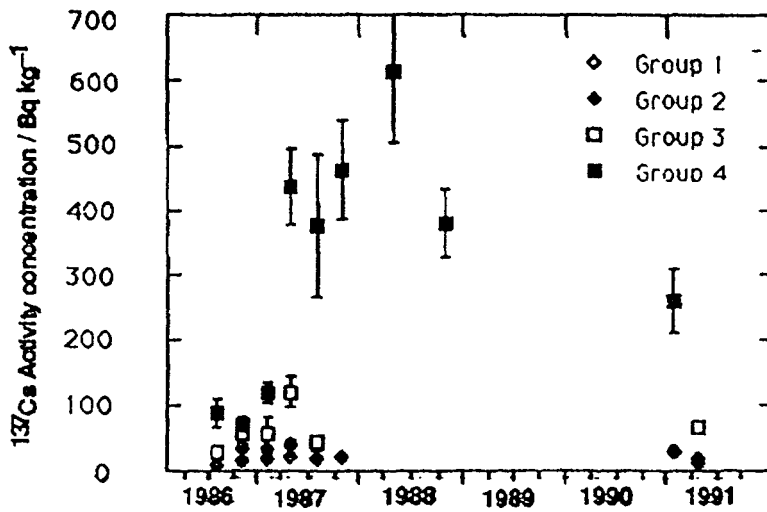


Figure 7: Mean Activity Concentration for Man. The different groups are defined in the test. The standard errors indicated.

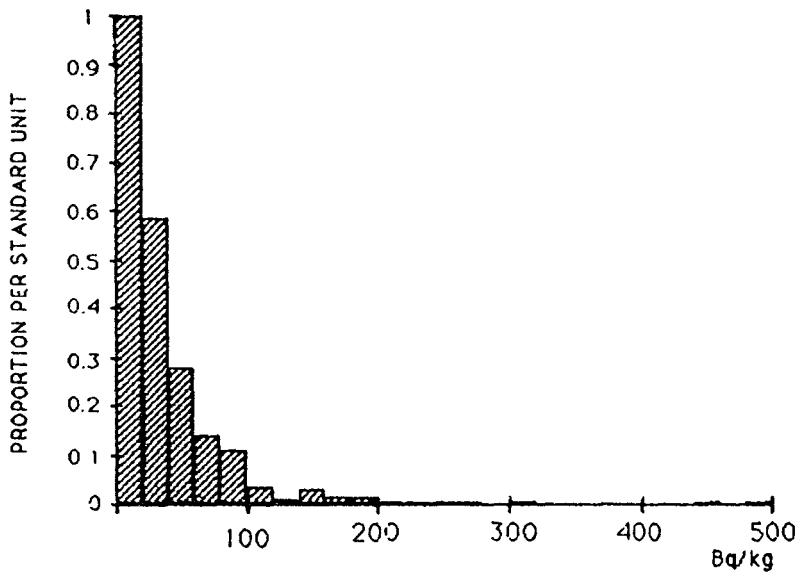
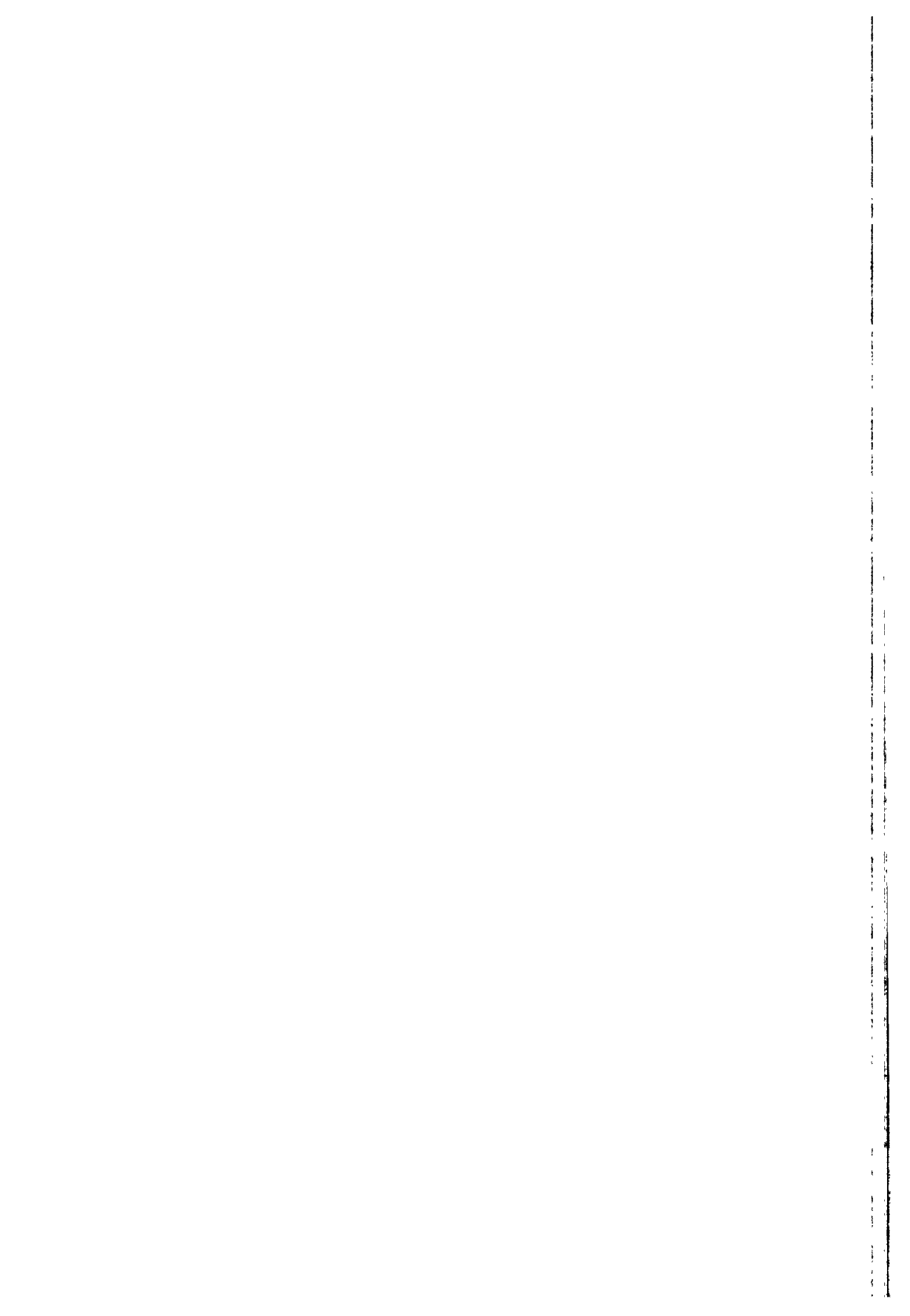


Figure 8: Frequency distribution of Cs 137 concentration in muscle tissue in a Northern Swedish population 1988-1990.



RADIOECOLOGY OF SEMI-NATURAL ECOSYSTEMS

Contract Bi7-044 - Sector A25

- 1) *Colgan*, RPII - 2) *Horrill*, NERC
- 3) *Aarkrog*, Risø National Laboratory - 4) *Johanson*, Univ. Agricult. Sciences, Uppsala
- 5) *Veresoglou*, Univ. Thessaloniki

Summary of project global objectives and achievements

1. Introduction

Member States of the European Community have suffered fallout from nuclear weapons testing and following the Chernobyl accident. Radionuclides from both these sources are present in soils in varying amounts and may be in a form available for uptake by vegetation. This can result in radiation doses being received by man, primarily due to consumption of contaminated products from agricultural and semi-natural ecosystems.

Deposition of nuclear weapons fallout took place primarily in the years 1954-1965 and the radionuclides still present in the environment in measurable amounts include caesium-137, strontium-90 and isotopes of plutonium. Following the Chernobyl accident the insignificant deposition of actinides and of strontium-90 in western and southern Europe leaves caesium-137 (and to a lesser extent caesium-134) as the radionuclide of greatest long term radiological significance.

Meteorological conditions in the days immediately following the Chernobyl accident led to widespread fallout across European semi-natural ecosystems with predominantly organic soils. Unfortunately models in use at the time of the Chernobyl accident were almost exclusively based on radionuclide behaviour in mineral soils and consideration of organic soils typical of upland and forest ecosystems was largely disregarded. Uplands include acidic grasslands, heaths, natural meadows and bogs and, because of the limited interference by man, are often referred to as semi-natural ecosystems. They differ from agricultural ecosystems in that they are often characterised by soils with a high organic matter and moisture content, a pH in the range 3-5 and low nutrient content. When compared with mineral agricultural soils they are usually deficient in potassium, nitrogen and phosphorus. Radiocaesium deposited onto such organic soils has been found to be more readily available for plant uptake than radiocaesium incorporated into mineral lowland soils. In addition, these areas are often subject to extreme environmental conditions of rainfall, temperature and altitude and the absence of ploughing has allowed the litter layer to remain intact. The vegetation typical of semi-natural environments shows a greater species diversity than that observed in areas used for agricultural production and the main plant communities include dwarf shrubs, grasses, sedges, mosses and lichens.

The behaviour of radionuclides in semi-natural ecosystems is important because they are the natural habitat of wild animals and are also grazed by domestic stock. Animals such as moose, roe-deer, sheep and goats are the most important herbivores of semi-natural systems in Northern Europe. Indigenous populations and even some hunters may source a large percentage of their diet from semi-natural environments. As well as giving rise to radiation doses to these critical groups, food products from semi-natural ecosystems can also reach the marketplace, thereby giving rise to radiation exposure of the general population. Because of the long ecological half-life of radiocaesium in vegetation and in animal species which characterise semi-natural environments, this dose can be delivered over a timescale of several decades.

The programme of work undertaken as part of this contract was formulated with a view to obtaining a better understanding of the cycling of radiocaesium in semi-natural ecosystems. This in turn will allow a more accurate calculation of ecological half-life to be made, thereby improving calculations of collective and critical group radiation doses. Preliminary estimates have been made of radiation doses arising from the consumption of foodstuffs produced in semi-natural ecosystems.

In comparative studies similar techniques have been used to evaluate the distribution of caesium-137 in different ecological compartments of blanket bogs (Ireland), upland heaths (UK), Northern Boreal forests (Sweden) and grassland habitats in the Faeroe Islands. Laboratory studies have been undertaken to identify the mechanisms controlling the uptake and movement of caesium and strontium in Greek soils containing different quantities of organic matter. The importance of other soil parameters including pH, clay mineral type, bulk density and moisture regime, have also been assessed.

The ability to predict radiocaesium levels in vegetation and in grazing animals has received some attention. The use of plant-to-plant ratios, with Calluna vulgaris as the bioindicator species, has been compared with the classical approach of calculating transfer factors or concentration ratios. Prediction of mean and maximum activities in a flock of free-ranging mountain sheep by measuring radiocaesium levels in faeces has also been investigated.

2. Intercalibration studies

In order to ensure uniformity of measurement and comparability of results, a number of intercalibration studies was undertaken. Three aspects of the work programme were identified where direct comparison of results produced by all participants would be necessary. These were the determination of the radionuclide content of environmental samples, the estimation of total radionuclide deposition to soils and laboratory measurement of physical and chemical soil characteristics.

2.1 Laboratory measurement of radionuclides

Four of the participant laboratories took part in an intercomparison exercise to assess precision in the measurement of radionuclides. Samples of soil and vegetation collected from semi-natural ecosystems were chosen to give a range of activities typical of those found in the participating countries, following the Chernobyl accident. Following testing for homogeneity, aliquots were distributed and each laboratory was requested to report results for ^{137}Cs , ^{134}Cs and ^{40}K in accordance with their usual procedures. A normal probability plot of the pooled data showed ten of the 161 readings to be obvious outliers and seven of these were attributed to one of the laboratories. One laboratory consistently overestimated relative to the global mean, another laboratory consistently underestimated while the other two showed positive and negative bias dependant on isotope. Both bias and measurement errors were found to increase in the order ^{137}Cs , ^{134}Cs , ^{40}K . A need for greater standardisation of analytical techniques is identified. The participants have agreed to participate on an annual basis in similar intercomparisons co-ordinated by international organisations as a means of ensuring in-house accuracy of measurement and comparability of results.

2.2 Laboratory measurement of soil physical and chemical characteristics

Sub-samples of the homogenised organic and inorganic soils for radionuclide analysis distributed to all participants were also analysed for a range of physical and chemical parameters. Each participating group used their own analytical techniques. Reported results were very variable, particularly for K_{ex} , cation exchange capacity and total nitrogen. This highlights the need for caution when looking for correlations between soil nutrient and soil radionuclide status and the dangers of assuming that nutrient results in the published literature are directly comparable.

2.3 Estimates of radionuclide deposition

Calculations of total deposition usually involve the sampling of both soil and bulk vegetation. One of the variables which may give rise to divergence of results is the sampling techniques used. Soils typical of semi-natural ecosystems often have a high moisture content and a heterogenous vegetation cover that can lead to significant small-scale variations in cover. Both of these characteristics suggest that sampling methodologies used routinely for lowland agricultural soils may be inappropriate for semi-natural ecosystems.

In order to evaluate the importance of sampling methodologies, each of the five

participating laboratories used their own sampling techniques to collect samples of vegetation and of soil (sub-divided into 0-5 cm, 5-10 cm and 10-20 cm sections) at two upland sites in the UK. Four of the laboratories used techniques of cutting horizontal slices of soil blocks to obtain the desired sections while one laboratory used a coring method. Three of the five participants undertook multiple sampling as part of their normal procedures.

Analysis of variance was used to test the hypothesis that there were no systematic differences between the results from the different laboratories. For the determination of total ^{137}Cs deposition, the results give no indication of differences between laboratories compared to the observed stochastic variability, which correspond to standard deviations of 33% and 26% at the two sampling sites. Comparing the results for ^{137}Cs distribution within the vertical soil profile indicates significant differences between laboratories and this has been attributed to the different sampling techniques employed. Analysis of the results for vegetation showed good agreement between all participants.

3. Distribution of ^{137}Cs within ecosystems

The relative activity concentrations of ^{137}Cs within different compartments of semi-natural ecosystems have been investigated by the group. Across the range of sites studied there are considerable differences in climate, soil-type, vegetation and herbivore species. The main characteristics of each site are summarised in the accompanying table.

Comparison of the ecosystems shows that up to 95% of the deposited ^{137}Cs still remains in the soil compartment. It is not clear how much of this is associated with plant roots and the mycelium of fungi - this aspect of the ecosystems should be investigated. Between 5% and 27% of the deposition is contained in the above-ground vegetation and seasonal variations in the percentage of total ^{137}Cs retained in the above-ground vegetation compartment have been observed. The animal compartment represents, in most cases, less than 1% of the ^{137}Cs within the ecosystem. Returns to and losses from the system via animal export are low. With the exception of the Greek soils, plant uptake within the systems is high and there is no evidence of progressive fixation of ^{137}Cs .

Although vertical migration in soils does take place, the rate of movement down the soil profile is slow so that most of the ^{137}Cs is still retained within the plant rooting zone. It is estimated that up to 90% of the Chernobyl ^{137}Cs is still retained with the top 10cm in each of the ecosystems studied. Different vertical distribution patterns of both the nuclear weapons and Chernobyl components have been observed and, through comparison, these data can assist in an evaluation of the long-term fate of ^{137}Cs in these ecosystems.

Within the vegetation compartment, among vascular plants the highest concentrations are usually found in C. vulgaris. Activity levels are normally an order of magnitude lower in other ericoid and in the graminoid species. The grasses tend to show a seasonal variability in ^{137}Cs content similar to that observed for other nutrients. Deer grass (Scirpus caespitosus) is one of the few species that shows very marked seasonal variability and the exceptionally high levels in late spring is of particular relevance for sheep in the UK and Ireland transferred to upland grazing at this time. Where present, fungi normally show the highest levels of ^{137}Cs and their consumption can result in large increases in the ^{137}Cs content of the animal compartment.

It is more useful for comparative purposes to calculate the radiocaesium content of vegetation in terms of deposition ($\text{Bq}\cdot\text{m}^{-2}$) rather than activity ($\text{Bq}\cdot\text{kg}^{-1}$) since deposition accounts for differences in species composition and biomass. Biomass estimates to facilitate calculation of deposition to vegetation are currently underway in each country.

There is also clear evidence that plant to animal transfer shows considerable variability. For example, soil deposition in the Swedish forest research site is of the order of $30,000 \text{ Bq m}^{-2}$, and roe-deer grazing these forests show concentrations of up to $12,000 \text{ Bq kg}^{-1}$ in August and September. On the other hand, moose show a mean activity of $750 \text{ Bq}\cdot\text{kg}^{-1}$ in an area where the ground deposition is up to $40,000 \text{ Bq}\cdot\text{m}^{-2}$. In contrast Irish peat soils received relatively low mean deposition (approximately $5,000 \text{ Bq m}^{-2}$) yet sheep grazing these areas contain up to $3,000 \text{ Bq kg}^{-1}$. Dietary selectivity and animal metabolism of different species account for differences in plant animal transfer, and dietary data from rumen content analysis of Swedish roe-deer in comparison to diet of sheep in Ireland (based on epidermal plant fragments in faecal samples) has shown the divergence in dietary habits of the two species.

During the period of the study considerable seasonal and year-to-year variability in the ^{137}Cs content of the different compartments has been observed. There is no clear statistical evidence of reductions in activity. An ecological half-life similar to the physical half-life of 30y for ^{137}Cs should therefore be assumed. A programme of work of many years will be necessary if these annual trends are to be properly evaluated against a background of large site and seasonal variability. A more accurate estimation of ecological half-life is necessary if the contribution of semi-natural ecosystems to radiation doses is to be properly assessed.

4. Laboratory studies

4.1 Soil factors affecting movement and uptake of ^{137}Cs in Greek soils

Six soils with different contents of organic matter (2-55%) clay materials (9-33%) and pH

(6-7) were packed in 25 cm tubes and wetted to field capacity prior to the addition of 130 kBq m⁻² ¹³⁷Cs. The columns were sown with alfalfa seeds and the effects of the addition of potassium (in the form 100kg K₂O per hectare) on ¹³⁷Cs uptake with depth over an 8-month period was investigated. The results indicate that the addition of K does not affect the depth distribution of ¹³⁷Cs. In soils with a high clay content, all of the activity was retained within the top 3 cm. Even in the soil with the highest organic content, all of the ¹³⁷Cs was retained in the top 4 cm.

4.2 Uptake of Cs and Sr by different plant species

Experimental pots containing soils of different physical and chemical characteristics were sown with several different plant species, including Lolium perenne and Trifolium repens. Stable Cs and Sr were added to the soils up to 2 months prior to sowing. The effects of added potassium and calcium on the uptake rates of caesium and strontium respectively were investigated.

The highest concentration of Cs in above ground biomass was in L. perenne grown on organic soils. Sr concentration in the above ground biomass was higher in T. repens and higher in the mineral than the organic soil. This suggests that Sr is immobilised more effectively than Cs in organic soil. The addition of Cs to the soil was found to increase the Cs concentration in the vegetation but did not affect Sr uptake.

4.3 Effects of biological activity on ¹³⁷Cs migration

A preliminary investigation into the relationship between biological activity (as measured by CO₂ evolution) and radiocaesium concentrations has been undertaken by ITE Merlewood. Soil monoliths of 20 cm depth were collected from 4 upland sites in the UK and samples of C. vulgaris were also taken. Microbial respiration was determined by infrared gas analysis.

Both ¹³⁷Cs and CO₂ respiration were found to decrease with depth and hence were strongly correlated with each other. A multiple regression technique was used to separate the effects of depth and respiration. For all four sites microbial respiration rates were found to be a more consistent and better estimator of radiocaesium levels than depth. If radiocaesium entering peats has become incorporated into soil organic matter it will be affected by microbial decomposition processes and microbial activity may be a key process in the slow release of ¹³⁷Cs for plant uptake. Further investigations are needed to determine the importance of this process.

Main Characteristics of Research Sites

Country	Ecosystem	Soil Description	Dominant Vegetation	Animal Species
Sweden	Nemo-Boreal Forest	Shallow Peat pH 3.1-3.4 omc ~ 75%	Pinus sylvestris Picea abies Betula spp.	Moose Roe-Deer
Denmark	Cultivated Peatland	Shallow Peat omc > 80% pH 4-5	Mixed Grasses	Sheep and Cattle also used for crop production
Ireland	Montane Peatland	Deep Peat pH 3-5 omc ~ 90% 3-6 kBq m ² , ¹³⁷ Cs	Calluna vulgaris Cyperaceae and Mosses in ground layer	Sheep
UK	Upland Acidic Grassland and upland heath	Pure or Podzolic Peat pH 3-5 omc(0-10cm) ~ 90% 15-20 kBq m ² , ¹³⁷ Cs	Mixed grasses or Calluna vulgaris with hydnaceous mosses in ground layer	Sheep, Deer and Grouse
Greece	Upland Pasture	Peaty Podzol pH 6-7 omc ~ 3-15% ~ 25 kBq m ² , ¹³⁷ Cs	Mixed Grasses Fagus sylvestris stands	Sheep and Goats

5. Dietary studies

Investigations into the grazing habits of animals populating semi-natural ecosystems have been undertaken in both Ireland and Sweden. The Irish study has concentrated on sheep grazing upland pastures dominated by C. vulgaris while in Sweden the diets of both roe-deer and moose populating forestry areas have been studied.

The vegetation composition of the diet of mountain sheep was determined by faecal fragment analysis. A comparison of diet composition with available vegetation revealed selection of grasses in preference to the more abundant ericoid vegetation. During the summer months the Ericoid species, which represent over 60% of the biomass composition and almost 80% of the ^{137}Cs in the vegetation component of the ecosystem, accounted for less than 30% of the ^{137}Cs intake by sheep. In contrast, the graminoid species represent less than 10% of the available biomass but account for over 75% of the diet, even in October when many of these species have already senesced and died back. Herbs (Potentilla erecta and Galium saxatile) account for less than 2% of the biomass yet contribute between 5% and 7% of the diet and of the ^{137}Cs intake throughout the period of mountain grazing. While certain drawbacks with the fragment analysis technique are acknowledged, the results clearly indicate the need to consider ^{137}Cs concentrations in individual species rather than in samples of bulk vegetation if the transfer to sheep is to be properly quantified.

In Sweden, dietary habits of both moose and roe-deer grazing forestry areas have been studied by botanical analysis of the rumen content of animals. For moose Epilobium angustifolium is the dominating plant species in July and August (55% and 34% respectively) while birch Betula spp. (48%) and V. myrtillus (38%) are the most important dietary components in September and October respectively. A mean aggregated transfer factor for moose of $0.02 \text{ m}^2 \text{ kg}^{-1}$ was calculated for the most contaminated area, and typical contamination levels in the test area were 750 Bq kg^{-1} . In contrast to moose, roe-deer can show large seasonal as well as year-to-year variations in their ^{137}Cs content and this has been attributed to the production and consumption of fungi. Peak concentrations are found in either August, September or October, depending on the period of peak fungi production. A change in the hunting season to May has been introduced and this simple countermeasure has resulted in a 5-fold reduction in mean ^{137}Cs levels in the flesh.

6. Radiation doses

The concentrations of ^{137}Cs in products from semi-natural ecosystems are in general higher than those taken from agricultural ecosystems. Hence individual doses to consumers of food taken mainly from semi-natural ecosystems are expected to be relatively high. The production of food from such environments is, however, low compared to that obtained

Project 1

Head of project: *Dr. Colgan*

Objectives for the reporting period

1. To assess, on a compartment basis, the distribution of radiocaesium within Irish peatland ecosystems.
2. To describe the vertical distribution of radiocaesium in soils and identify seasonal variability in the radiocaesium content of upland vegetation and mountain sheep.
3. To evaluate the diet selectivity of mountain sheep and assess the relative contribution of individual species to the radionuclide burden of the animals.
4. Preliminary investigation of the potential use of bioindicators for radiocaesium contamination of semi-natural ecosystems.
5. Co-ordination of the research group by means of regular meetings and intercomparison exercises.

Progress achieved including publications

More than 17% of the land surface in Ireland consists of peatlands. These soils, with very low pH, high organic matter content and low clay content provide extreme conditions under which high rates of uptake of radiocaesium by plants have been observed. These soils are relatively unproductive, but are exploited for low grade solid fuel extraction (turf) and are often used for low intensity grazing by sheep, and less frequently by deer or cattle.

Because of the mobility of radiocaesium in these ecosystems, peatlands have become an important focus of research over recent years. In Ireland, research sites on which sheep show radiocaesium concentrations in excess of 1500 Bq kg⁻¹ during the months of summer grazing were chosen for detailed investigation.

The distribution of caesium-137 within the ecosystem as a whole has been evaluated and each of the compartments separately assessed (see Figures 1-3). The largest percentage of the deposition is associated with the soil/root compartment, and the radiocaesium content of sheep is less than 1% of that retained within the entire ecosystem.

Seasonal fluctuations in radiocaesium content of sheep flesh in relation to management practices and flock movement have been demonstrated. Lambs were shown to initially contain lower concentrations than ewes, but tended to accumulate greater concentrations

later in the season (*Reference 1*). Even where the flock grazes upland pasture throughout the year, measurable concentrations are present in the flesh during the winter months.

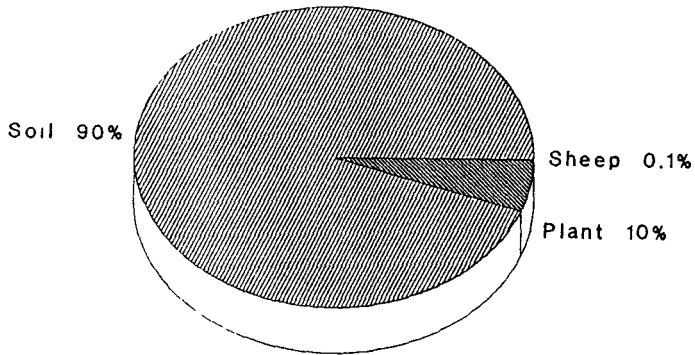


Figure 1

Distribution of Caesium-137 (Bq m^{-2}) within Peatland Ecosystem

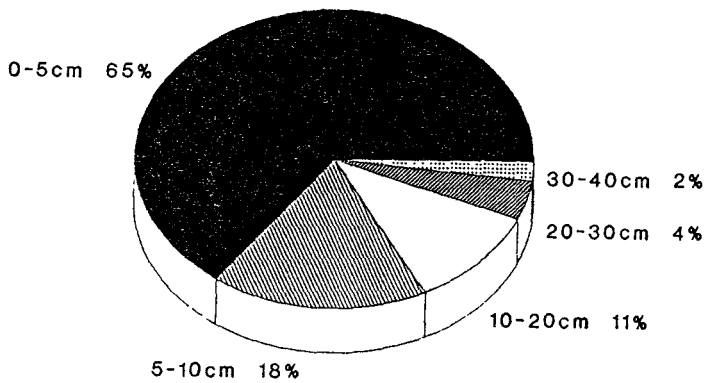


Figure 2

Distribution of Caesium-137 (Bq m^{-2}) in Soils

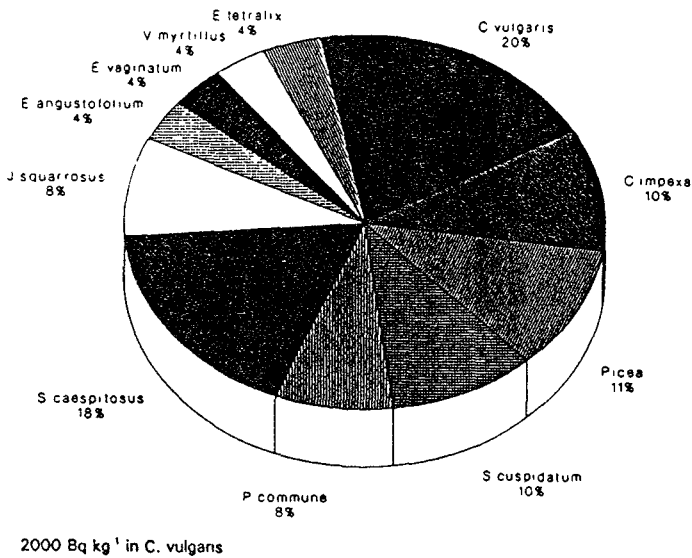


Figure 3

Caesium-137 (Bq kg⁻¹) in Vegetation

Further studies on sheep flocks have led to the development of a new alternative to *in-vivo* monitoring based on the use of faecal droppings from sheep as a means of predicting flesh radiocaesium concentrations (Reference 2). By following *in-vivo* activity in a single sheep flock between 1989 and 1991 it was possible to prove the hypothesis that radiocaesium in faecal samples could be used to predict flesh concentrations using an independent data set (Reference 3). Findings of this work also illustrate how concentrations in flocks can fluctuate considerably from one year to the next. One flock showed a 4% increase in radiocaesium in flesh between 1989 and 1990, and an overall decrease of 35% between 1990 and 1991 (see Figure 4).

In order to investigate the contribution made by different plant species to the diet of animals grazing peatland pastures, epidermal fragments of vegetation were identified and quantified in sheep faeces. Data revealed that sheep were highly selective in their grazing habits. The sheep tended to exclude the high activity Ericoid species and select the Graminoid species when available - these on average have lower radiocaesium levels. Dietary analysis is shown to provide a better approximation of radiocaesium intake than estimations based on field availability of plant species. Data clearly shows that a minor dietary component may provide a major contribution to radiocaesium intake (Reference 4).

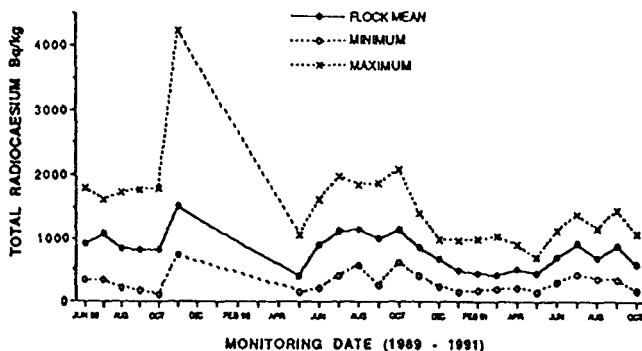


Figure 4

Seasonal variation in radiocaesium levels in mountain sheep grazing upland pastures throughout the year

One such minor constituent of sheep diet has been the subject of detailed investigations. Samples of sheep faeces from animals grazing a forestry area showed higher radiocaesium concentrations than those recorded in animals grazing an adjacent open hillside. This peak coincided with the fungal production season. A study was carried out which identified fungal species from spores contained in faecal samples, and relative percentage spore counts in samples from forest and hillside were compared (*Reference 5*). This work provides new evidence that measurement of fungal spores in faecal samples can be useful in determining the availability of fungi to grazing animals.

Red deer also graze many peatland areas in Ireland, and have also been the subject of some research by our group in the past two years (*Reference 6*). Radiocaesium activity in rumen contents of red deer were compared with corresponding concentrations in vegetation that constituted part of the animals' diet - concentrations in rumen contents were found to approximate to concentrations in Graminoid species favoured by the animals. This study also identified an altitude related effect whereby greater soil radiocaesium concentrations were found at higher elevations. This altitude effect was further substantiated by a more detailed follow-up investigation (*Reference 7*) which showed a highly significant positive correlation between altitude and deposition of Chernobyl ^{137}Cs across two adjacent valleys.

Initial studies into plant:soil uptake of radiocaesium provided an overall picture of the relative concentrations in plant species which colonise Irish peatlands. Data showed that species within the same Genus can show very large differences in radiocaesium concentrations. This underlined the necessity for identification of vegetation to species level, and makes clear the danger of analysing samples of mixed species (*Reference 8*). The seasonality of certain plant species has been clearly defined: it has been shown that some species exhibit a marked seasonal effect (e.g. *Scirpus caespitosus*) while others maintain a constant radiocaesium concentration throughout the year (e.g. *Juncus squarrosus*).

Biomass determinations for these areas were carried out facilitating calculation of deposition values for vegetation (as opposed to activity per unit dry weight). Biomass data have also shown the differences between field availability and dietary composition of vegetation species. Under conditions of overgrazing there is reduced availability of palatable species (Graminoids) and animals consume greater quantities of species containing higher concentrations of radiocaesium - overgrazing should be avoided if radiocaesium ingestion is to be minimised (*Reference 9*).

Plant:soil concentration parameters have also been evaluated. The inadequacies and inconsistencies in the traditional plant:soil transfer parameters led the group to investigate the possibility of developing an alternative prediction system. Radiocaesium concentrations in plants may be predicted based on measured concentrations in appropriate indicator species. Calluna vulgaris has been identified as one such bioindicator (*Reference 10*). An experiment which replicated traditional plant:soil concentration ratios and plant-plant ratios (based on C. vulgaris as an indicator species) at three different sites has further confirmed the potential of using bioindicators in predictive systems (*Reference 11*).

More recent work shows that there is less variability associated with radiocaesium in vegetation than in soil samples taken from the same locations. The co-efficient of variation for ¹³⁷Cs deposition, integrated to 40 cm at sixteen sites was 24%. Samples of C. vulgaris and J. squarrosus, collected at the same sampling location, showed less variability - coefficients of variation were 12% and 20% respectively. These findings provide support for the use of plant-to-plant ratios which show less variability than do soil-to-plant concentration ratios or transfer factors. The data also provide estimates of the numbers of soil and vegetation samples which must be taken in order to achieve an estimate of the true mean deposition value within a given confidence interval.

Some problems associated with soil sampling have been identified. Soil radiocaesium levels show large spatial variability over a distance of a few metres. There are also problems with interpretation of peat soil data; the normal expression of deposition per unit area can be greatly influenced by the moisture content of the peat which expands and contracts dramatically with wetting and drying. These fluctuations may result in considerable discrepancies in bulk density estimations between one sampling occasion and another, and this in turn leads to problems with the calculation of soil deposition values (*Reference 12*).

As co-ordinators, the RPII arranged and participated in three separate intercomparison exercises (*References 13 and 14*). These covered aspects of radiological investigations of direct relevance to the group: laboratory measurement of radionuclides, analysis of soils for physical and chemical parameters, and sampling strategies for upland soils and vegetation. Responsibility for implementation of the agreed programmes and analysis of results was assigned to individual participants. The group met on three occasions during the course of the project and regular contact was maintained through participation in relevant scientific meetings.

Publications

1. Pearce, J., Colgan, P.A., Scully, B.J. & Moss, B.W. Radiocaesium activity in sheep: Variation within flocks and with time. In: Transfer of Radionuclides in Natural & Semi-natural Environments. (G. Desmet, P. Nassimbeni & M. Belli, Eds.) *Elsevier Applied Science*.
2. McGee, E.J., Colgan, P.A. & Synnott, M. A rapid method of predicting of radiocaesium concentration in mountain sheep from activity levels in faeces. (accepted for publication, 1992, *Journal of Environmental Radioactivity*).
3. McGee, E.J., Synnott, H.J., Keatinge, M. & Colgan, P.A. Persistence and prediction of radiocaesium concentrations in animals grazing semi-natural environments. (accepted for publication, 1992, *Science of the Total Environment*.)
4. Rafferty, B., McGee, E.J., Colgan, P.A., & Synnott, H.J. Dietary intake of radiocaesium by free ranging mountain sheep. (accepted for publication, 1992, *Journal of Environmental Radioactivity*).
5. Rafferty, B., Dowding, P. & McGee, E.J. Fungal spores in faeces as evidence of fungus ingestion by sheep. *Science of the Total Environment* (submitted for publication).
6. McGee, E.J., Colgan, P.A. & O'Keefe, C. (1991) Radiocaesium activity in soils, plants and red deer (*Cervus elaphus*) in Glenveagh National Park, Co. Donegal, Ireland. In: *New Development in Fundamental and Applied Radiobiology*. (C.B. Seymour & C. Mothersill, Eds). Taylor and Francis.
7. McGee, E.J., Colgan, P.A., Dawson, D.E., Rafferty, B & O'Keefe, C. The effects of topography on the fallout of radiocaesium to montane peat soils in Ireland. (*The Analyst*. 117(3) 461-464 1992).
8. Colgan, P.A., McGee, E.J., Pearce, J., Cruickshank, J.M., Moss, B. & McAdam, J. (1991) Behaviour of radiocaesium in organic soils - some preliminary results on soil-plant transfers from a semi-natural ecosystem in Ireland. In: *Transfer of Radionuclides in Natural and Semi-Natural Environments*. (G. Desmet, P. Nassimbeni & M. Belli, Eds) *Elsevier Applied Science*.
9. Pearce, J., McGee, E.J., McAdam, J.H., Colgan, P.A. & Synnott, H.J., Radiocaesium cycling in upland pasture. *Proceedings of Royal Irish Academy*. (In press)
10. McGee, E.J., Colgan, P.A. & Synnott, H.J. (1991) Prediction of radiocaesium levels in vegetation and herbivores using bioindicators. In: *Bioindicators and Environmental Management* (D.J. Jeffrey & B. Madden, Eds). *Academic Press Limited*.

11. McGee, E.J., Colgan, P.A. & Synnott, H.J. A new method for prediction of radiocaesium in vegetation: evidence from Irish uplands. (accepted for publication, 1992, *Journal of Environmental Radioactivity*).
12. McGee, E.J., Colgan, P.A. & Synnott, H.J. Measurement of radiocaesium in Irish peatland soils. (*Journal of Radioanalytical and Nuclear Chemistry*. 165(2) 79-93 1992)
13. McGee, E.J., Colgan, P.A., Keatinge, M., Horrill, A.D., Kennedy, V.H., Johanson, K.J., Aarkrog, A & Nielsen, S.P. Bias and measurement errors in radioactivity data from four European radiation research laboratories. (*The Analyst* 117(6) 941-945 1992).
14. Nielsen, S.P., Aarkrog, A., Colgan, P.A., McGee, E., Synnott, H.J., Johanson, K.J., Horrill, A.D., Kennedy, V.H. and Barbayiannis, N. An intercomparison of sampling techniques among five European laboratories for measurements of radiocaesium in upland pasture and soil. (*Risø-R-620 (EN)* 1992).
15. Colgan, P.A., Safeguarding the quality of Irish lamb. (*Irish Farmers' Journal* August 1991)
16. Colgan, P.A., Chernobyl radioactivity in Irish mountain sheep. (*Journal of the Institute of Food Science and Technology of Ireland* January 1992 p5-9).

Project 2

Main Researchers: *A.D. Horril, V.H. Kennedy*

Objectives for the reporting period

1. To identify the chemical and physical characteristics of soils from UK upland ecosystems affected by the Chernobyl fallout and assess the distribution of the radiocaesium systems. Data sets to be produced in a format that can be used in an overall northern european ecosystem study.
2. To participate in four inter-laboratory comparison studies concerned with field sampling, radioanalytical measurement, radiocaesium uptake by a range of plant species and chemical analysis of soil samples.
3. To conduct a preliminary study on the measurement of biological activity in a range of upland soils and to investigate any correlation with radiocaesium concentrations in the soils.
4. To supply the Risø National Laboratory with a summary of radionuclide concentrations found in wild animal populations in the UK food chain. These data will be used in dose assessment calculations.
5. To assist the Greek participants with radiochemical analyses.

Progress achieved including publications

Most research topics covered by this report were designed so that data produced would form part of an overall intercomparison study of the fate of radiocaesium in European semi-natural ecosystems.

1. Upland ecosystems

Upland heaths selected for this study were chosen from areas of known high Chernobyl inputs. Three main study sites have been used:-

Sillathwaite, Ennerdale, (Nat grid ref NY065128) north west England. Altitude 275m, acidic grassland over podzolic soil, grazed by sheep.

Corney Fell, (Nat grid ref SD150897) north west England. Altitude 400m, acidic grassland over peat, grazed by sheep.

Ardverikie, (Nat grid ref NN533902) central north Scotland. Altitude 320m, heather

(*Calluna vulgaris*) dominated vegetation over deep wet peat, grazed at low density by sheep and red deer.

Three to six replicate soil and vegetation samples were collected from each site. Soil cores were divided into 2.5cm sections. These samples were then used for radiocaesium determinations. All data has been supplied to the group co-ordinator for collation with data from other groups.

1.1 Results

Total deposition at Ennerdale, Corney Fell and Ardverikie has been estimated as 12,200, 16,000 and 14,000 Bqm⁻² of ¹³⁷Cs respectively. These represent minimum values as they are calculated only to 20cm depth in the soil.

In order to make a meaningful comparison of distribution within the three sites radiocaesium in all components of each ecosystem have been measured. The data from the three sites are presented in Figure 1.

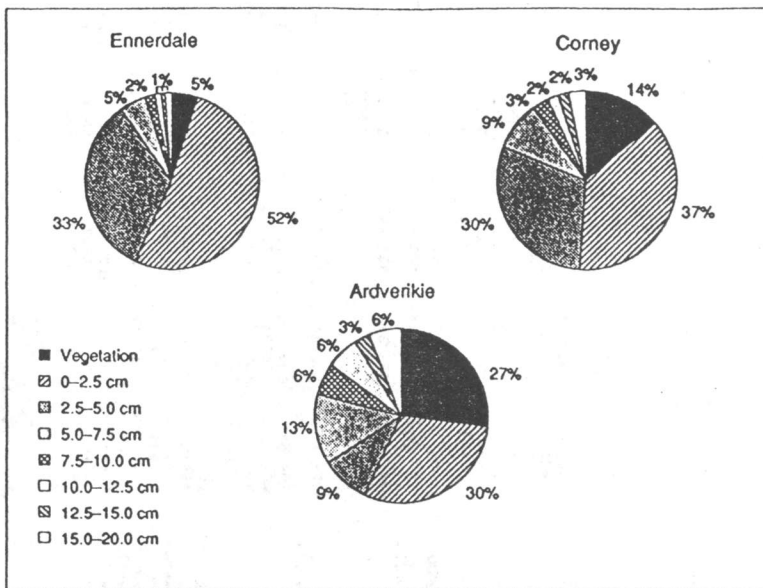


Figure 1: Percentage contribution of ¹³⁷Cs to 3 ecosystems in the United Kingdom.

Table 1 Ecosystem intercomparison samples

Sample type	134Cs		R3	137Cs		R5	40K	
	R1	R2		R1	R2		R1	R2
1. ANOVERLAKK (NWS33902)								
Mollisic	161± 2.6%	126±2.7%	118± 3%	121±3.6%	988±3.5%	901±3.6%	340±15%	316±13%
Associated soils	208± 2.6%			1561±3.5%			108±30%	
0-5 cm	66± 3%			594±3.6%			199±16%	
5-10 cm	5±11%			62±4%			529± 6.5%	
10-20 cm								
Calluna	346± 1.8%	316±1.8%	304± 2%	271±3.5%	2438±3.4%	2364±3.5%	202±13.5%	197±13%
P. commune	132± 2.4%	102±3%	164± 2.5%	999±3.5%	777±3.6%	1255±3.5%	338±12.5%	219±25%
Associated soil	160± 2.8%	138±2.6%	165± 3%	1047±3.6%	969±3.5%	1144±3%	983±54%	590± 5.6%
0-2.5 cm	32± 3.6%	37±4%	98± 4.9%	478±3.6%	288±3.7%	363±4%	593±57%	494± 6%
2.5-5 cm	31± 4.7%	14±4.4%	60± 9%	259±3.9%	126±3.7%	391±5%	487± 4.3%	<80
5-7.5 cm	12± 5.7%	7±9%	37±11%	136±3.9%	56±4.3%	261±5%	<80	<80
7.5-10 cm	12± 9%	5±9.5%	22±12%	112±4.4%	58±4.2%	190±5%	<80	<80
10-12.5 cm	6±17%	ND	20±15%	70±4.8%	32±3%	142±6%	<80	<80
12.5-15 cm	4±14%	ND	13±14%	7±5%	186±4%	125±5%	<80	<80
15-20 cm							<80	<80
2. DEVOOR VALLEI (SD160975)								
E. angust.	54± 3.7%	32± 4.9%	15± 7%	438±3.7%	263±3.9%	121±4.5%	234±18%	189±21%
Associated soils	84± 4.5%	93± 3%	87± 4%	689±3.8%	724±3.6%	685±3.8%	1570± 6%	322±28%
0-5 cm	34±14%			325±5%			<80	
5-10 cm	22±10%			231±4.7%			<80	
10-20 cm								
P. commune	309± 2%	57± 4%	136± 2.7%	2447±3.5%	459±3%	1033±35%	140±28%	250±20%
Associated soils	20± 5%	19± 4.5%	19± 5%	181±3.9%	180±3.7%	176± 3.9%	117±36%	123±29%
0-5 cm	ND	3±17%	3±17%	39±5%	37±5%	39± 5%	553± 5.5%	484± 5.6%
5-10 cm	ND	ND	ND	24±5%	23±5%	23± 6%	128±28%	<80
10-20 cm								
3. KEMERDALE (NT132138)								
Calluna ag	159±2%	72±2%	179±2%	1426±3%	636±3.5%	1543±3.5%	184±25%	<80
Vaccinium leaves	75±3%	90±3.5%	95±3.5%	823±3.6%	775±3.6%	744±3.7%	327±17%	280±21%
Vaccinium ovy	75±3%	86±3%	50±3.5%	621±3.6%	754±3.6%	754±3.6%	157±23%	797± 5%
Vaccinium ovy	68±3.1%	56±2.5%	50±3.5%	561±3.6%	477±3.5%	388±3.7%	145±23%	156±17%
Associated soils	108±3.1%	104±3.1%	103±3.3%	875±3.6%	851±3.6%	839±3.7%	<80	85±50%
0-2.5 cm	10±8%	9±7%	10±7%	155±4%	149±3.8%	176±3.8%	261±14%	236±11%
2.5-10 cm	ND	ND	ND	33±5%	33±5%	33±5%	101±2.4%	88
10-15 cm								

Calluna vulgaris
 Vaccinium myrtillus
 Polytrichum commune
 Eriophorum angustifolium

Calluna vulgaris
 Vaccinium myrtillus
 Polytrichum commune
 Eriophorum angustifolium

±± confidence limits of counting
 R replicate samples
 ND not detected
 SS sample too stoney for analysis
 ag arial growth
 ovy current year's growth
 ovy other years' growth

Previous work indicates that the percentage radiocaesium in vegetation falls as the amount of organic matter in the rooting zone decreases. Data from this study confirms the trend. Ardverkie (27%) > Corney (14%) > Ennerdale (5%). The range of radiocaesium concentrations within species growing on the same site is also known to vary greatly. Ericaceous plants have been found to take up radiocaesium more readily than many other species. The presence of *Calluna vulgaris*, combined with the highly organic nature of the soil at Ardverkie, probably accounts for the relatively high percentage of radiocaesium in the standing vegetation at that site. Data presented shows that c.80-95% of the total radiocaesium for the three sites is still present in the vegetation and rooting zone (0-7.5cm) 5 to 6 years after the Chernobyl deposition. These data imply that radiocaesium will remain in the rooting zone of UK upland ecosystems for many years to come and may continue to be available for plant uptake during that time.

Estimates of removal by animals have been carried out for the Corney Fell site and, ignoring return in faeces and urine, each sheep would remove of the order of $50 \text{ Bq m}^{-2} \text{ y}^{-1} \text{ }^{137}\text{Cs}$. The grazing intensity at this site was about one animal per hectare.

2. Inter-laboratory comparison studies

2.1 Field sampling

One day of a group meeting in Cumbria UK, organised by Merlewood, was used to carry out an intercomparison study of field sampling techniques. Sites at Corney Fell and Ennerdale (see previous section) were used and five laboratories participated. Results for plant biomass, soil bulk density, radionuclide and nutrient elements, were obtained from three replicate locations at each site. After analysis the radiochemical data set was passed to the Risø National Laboratory for collation with results from the other groups. A joint publication has been produced and the data show that the Merlewood sampling methodology does not produce results which differ significantly from the overall mean values.

2.2 Radioanalytical measurements

Merlewood participated in this exercise by analysing both soil and vegetation samples for caesium isotopes. Our laboratory also provided the vegetation samples for the exercise. These samples were of two activity levels. The low level activity sample (c. $80 \text{ Bq kg}^{-1} \text{ }^{137}\text{Cs}$) was bracken (*Pteridium aquilinum*) obtained from near Sellafield, UK and the high activity sample (c. $3800 \text{ Bq kg}^{-1} \text{ }^{137}\text{Cs}$) was a heather litter from Scotland. Results have been collated by the co-ordinating organisation. A joint publication has resulted from this study. This has shown that Merlewood's quality control procedures and results are consistent with international standards.

2.3 Radiocaesium uptake by a range of plant species

It was agreed by all participants that a number of species, common to the ecosystems studied, would be collected. These samples have been analysed for radiocaesium isotopes and nutrient elements. The aim of this exercise was to measure radiocaesium concentrations in the same species over a spectrum of upland ecosystems and to determine the overall range of plant/soil transfer factors. In all, 27 vegetation samples of *Calluna vulgaris*, *Vaccinium myrtillus*, *Eriophorum angustifolium* and *Polytrichum commune* together with 56 soils samples have been collected and analysed from sites in the UK (Table 1). All soils have been analysed for pH, loss on ignition, cation exchange capacity, extractable potassium and phosphate and total nitrogen and phosphorus. These results have been passed to the co-ordinator with the aim of producing a joint account.

2.4 Chemical analysis of soil samples

The organic and inorganic soils distributed to all group members for radiochemical analysis were also analysed for a range of physical and chemical parameters. Each participating group made their own arrangements for analysis and no analytical technique was specified.

Table 2 Showing the main chemical and physical characteristics of intercalibration soils as measured by four analytical services regularly used by group members.

Organic Soil				
Parameter	Lab 1	Lab 2	Lab 3	Lab 4
pH	3.5	4.1	3.5	4.1
% Organic matter	76	81	67	76
Extractable K mg 100g ⁻¹	11	11	20	4.5
Extractable PO ₄ -P mg 100g ⁻¹	1.8	-	-	1.7
Cation exchange capacity meq 100g ⁻¹	40	45	367	84
% P	0.05	0.05	0.07	0.01
% N	1.68	1.56	0.03	0.45
Inorganic Soil				
pH	3.6	4.0	4.0	4.1
% Organic matter	39	40	27	36
Extractable K mg 100g ⁻¹	22	23	6.3	24
Extractable PO ₄ -P mg 100g ⁻¹	7.4	-	-	23
Cation exchange capacity meq 100g ⁻¹	22	37	113	46
% P	0.16	0.20	0.15	0.11
% N	1.51	1.25	1.5	1.23

Results supplied to group members by their analytical services are very variable, particularly for extractable potassium, cation exchange capacity and total nitrogen. (Table 2). This

highlights the need for recommended European methods for the analysis of extractable and exchangeable soil nutrients and the dangers of assuming that nutrient results in the published literature are directly comparable. A paper is in preparation but is awaiting details of analytical/methodological errors from two of the service laboratories before submission for publication.

3. Biological activity and radiocaesium concentrations in upland soils

Many upland areas affected by Chernobyl deposition have been found to retain radiocaesium in the rooting zone for relatively long periods. The mobility of this radiocaesium may be affected by the activity of microbial decomposers within the surface layer of the peat. A pilot study was therefore established to assess whether or not biological activity (as measured by CO₂ evolution from the soils) could be linked with radiocaesium concentrations found in UK upland sites. Four field sites were used - Ennerdale Fell (Nat grid ref NY131128), the Summit, New Galloway (Nat grid ref NY384939), Ardverikie 1 (Nat grid ref NN533902), Ardverikie 2 (Nat grid ref NN528915). All sites are predominately heather moorlands on peat with a ground layer of hypnaceous mosses.

For each field site 20cm soil monoliths were extracted at three random locations. Prior to extraction the vegetation and litter layers were removed. Each monolith was then divided into 5cm sections which were prepared for respiration determinations. Microbial respiration from the fresh sections was determined by infra-red gas analysis at 12°C and 2°C. The release of CO₂ was monitored by an ADC model 225 MK3 plant physiology infra-red gas analyser. All samples were also analysed for soil moisture, organic matter content and radiocaesium concentrations.

3.1 Results

The results for ¹³⁷Cs determinations and respiration rate at 12°C are presented in Figure 2. Both variables are obviously highly correlated with depth and hence with each other. An attempt has been made to separate the effects with a multiple regression technique using respiration rate and depth individually and combined as estimators of the radiocaesium concentrations. The R² values from these calculations (Table 3) are taken as representing the variability accounted for by the two parameters.

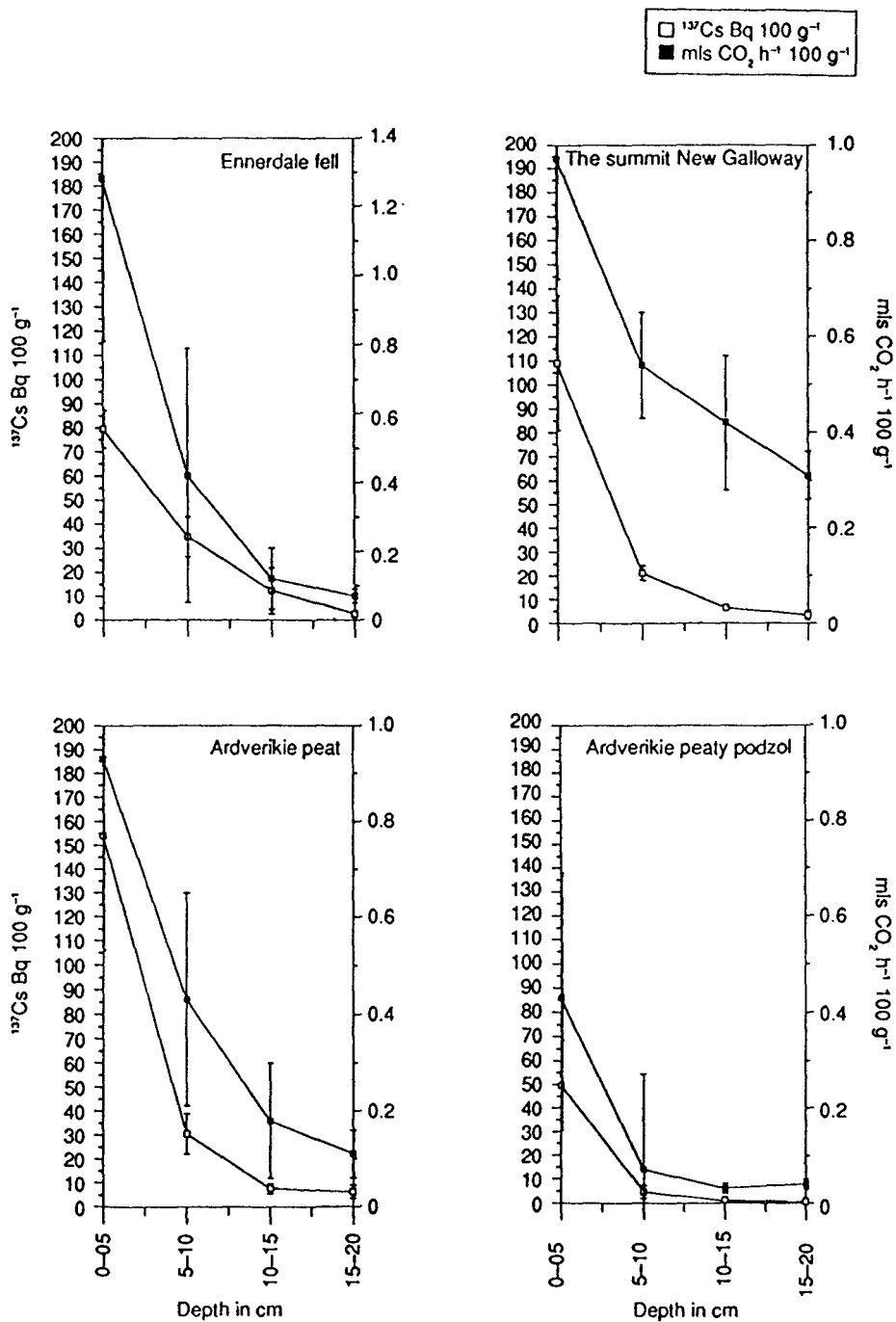


Figure 2: Showing the variation with depth of ^{137}Cs and CO_2 respiration (at 12°C) for four UK upland sites.

Table 3 R² Values obtained for four upland sites.

	Ennerdale	New Galloway	Ardverikie 1 Peat	Ardverikie 2 Peaty Podzol
Depth	87.3	68.5	65.7	58.3
Res. Rate	86.9	87.1	84.2	89.5
Both	96.1	87.6	84.4	91.2

In all cases the respiration rate is a more consistent and better estimator of the radiocaesium levels. The added effect of depth on the estimates is minimal with perhaps the exception of the Ennerdale site. Decomposition processes in peat are slow, with the more readily degradable compounds being broken down by microbial activity. If radiocaesium entering peats has become incorporated into soil organic matter it will be affected by microbial decomposition processes. Therefore microbial activity could be a key process in the slow release of radiocaesium for plant uptake.

This preliminary study has established that microbial activity and radiocaesium levels are linked. Further investigations are needed to determine the nature and extent of this link. A paper is in preparation.

4. Radionuclide concentrations in wildlife

Since Chernobyl the Merlewood laboratory has determined radiocaesium levels in a number of wild animal species. These species include red deer (Cervus elaphus), red grouse (Lagopus lagopus) and rabbits (Oxyctolagus cuniculus) all of which pass directly into the food chain to man. Samples have been collected from over 56 different sites covering a wide range of Chernobyl fallout values and these data have been passed to the Risø National Laboratory to help in dose assessment calculations from natural communities.

Radiocaesium concentrations in fresh tissues are variable but rabbits always had the lowest values rarely exceeding 100 Bq kg⁻¹ fresh weight of ¹³⁷Cs. Animals feeding on heather for all or part of their diet produced relatively high levels of radiocaesium with red deer stags producing c. 1500 Bq kg⁻¹ and red grouse up to 2000 Bq kg⁻¹ fresh weight in muscle tissue.

5. Analysis of materials from Greece

Over 50 soil and vegetation samples have been counted for the group at Thessalonika University. Full details will be found in their contribution to this report. In no instances

were the concentrations in vegetation in excess of a few hundred becquerels per kilogramme dry weight. It would appear from the soil samples that much of the material has become bound into the inorganic matrix and become immobilised.

Publication list

1. McGee E.J., Colgan P.A., Keatinge, M., Horrill, A.D., Kennedy, V.H., Johanson, K.J., Aarkrog, A. & Nielsen, S.P. 1992. Bias and measurement errors in radioactivity data from four european radiation research laboratories, *Analyst* 117, 941-945.
2. Nielsen, S.P., Aarkrog, A., Colgan, P.A., McGee, E., Synnott, H.J., Johanson, K.J., Horrill, A.D., Kennedy, V.H., & Barbayiannis, N. 1992. An intercomparison of sampling techniques among five european laboratories for measurements of radiocaesium in upland pasture and soil Riso-R-620 (EN), Roskilde, Denmark.
3. Horrill, A.D., & Howard, D.M., 1991. Chernobyl fallout in three areas of upland pasture in West Cumbria. *J. Radiol. Prot.* 11(4), 249-257
4. Kennedy, V.H., Horrill, A.D., McGee, E.J., Colgan P.A., Johanson, K.J., Nielsen, S.P. & Aarkrog, A (in prep). Pitfalls associated with the use of soil characterisation data when looking for possible correlations with radionuclide concentrations.
5. Kennedy, V.H. & Horrill, A.D. (in prep) A preliminary investigation into the relationship between soil respiration rate and radiocaesium concentrations in upland ecosystems.

Project 3

Head of project: *Dr. Aarkrog*

Objectives for the reporting period

1. The comparative study of radiocaesium in a number of selected vegetation species from Ireland, United Kingdom, the Faeroe Islands, Sweden and Greece will be completed in 1991.
2. An estimate of doses received from radiocaesium in foodchain in semi-natural ecosystems will be carried out. The doses (individual and collective) will be compared with those received by the general population in the EC.

Progress achieved including publications

1. The comparative study

In the summer of 1991, six selected plant species were collected at 10 sites in the Faeroe Islands. The samples were analysed for ^{137}Cs , ^{134}Cs and ^{40}K and an analysis of variance were carried out on the data. The following conclusions were drawn:

- (a) The ^{40}K content differed significantly between species: *Calluna vulgaris* ~ *Polytrichum commune*, \leq *Vaccinium myrtillus* \leq *Deschampsia flexuosa* \leq *Eriophorum angustifolium* ~ *Molinia caerulea*.
- (b) There was no significant local variation with respect to ^{40}K in the vegetation.
- (c) The ^{137}Cs concentrations (Bq kg^{-1}) did not differ significantly neither between species nor between sites, but $\text{Bq }^{137}\text{Cs} (\text{gK})^{-1}$ differed between species: *Molinia caerulea* ~ *Deschampsia flexuosa* ~ *Eriophorum angustifolium* $<$ *Vaccinium myrtillus* ~ *Polytrichum commune* $<$ *Calluna vulgaris*.
- (d) The $^{134}\text{Cs}/^{137}\text{Cs}$ ratio did not differ significantly neither between species nor between sampling sites.

The large local variation and in homogeneities of semi-natural ecosystems make a detection of significant interspecific differences for radiocaesium difficult; this was demonstrated in the Faroese sampling. Table 1 shows the mean values of ^{137}Cs obtained from the analysis of variance. The $^{134}\text{Cs}/^{137}\text{Cs}$ ratio indicates that about 50-75% of the ^{137}Cs in Faroese vegetation in 1991 was of Chernobyl origin. This study should be seen in the context of those performed by the other participants in this project.

Table 1
Faroesee Vegetation 31st July - 1st Aug. 1991

Species	Bq Cs-137 kg ⁻¹ d.m.	Bq Cs-137 (gK) ⁻¹	Cs-134/Cs-237
Polytrichum commune	47	11.3	0.054
Eriophorum angustifolium	58	3.8	0.056
Deschampsia flexuosa	33	2.5	0.076
Calluna vulgaris	104	17.4	0.070
Vaccinium myrtillus	46	8.7	0.055
Molinia caerulea	24	1.9	0.079

Chernobyl ¹³⁴Cs/¹³⁷Cs = 0.106 (1 August 1991)

2. Intake of ¹³⁷Cs from products of semi-natural ecosystems

The concentrations of radiocaesium in products from semi-natural ecosystems are in general higher than those seen in agricultural ecosystems. Hence individual doses to consumers of food mainly from semi-natural ecosystems are expected to be relatively high. The production of food from such environments is, however, low compared to that obtained from agricultural ecosystems. The question is whether the collective doses to the population of a country is influenced significantly by the radioactive contamination of its semi-natural ecosystems.

We have considered the situation in Denmark, Ireland, Sweden and UK, and estimated the mean individual intake of ¹³⁷Cs only. We assumed that all foods obtained from natural and semi-natural ecosystems are consumed nationally, i.e. no export. We have considered three main contributors only in this context: game (deer and moose), freshwater fish and mushrooms.

We have applied a common transfer-factor (Bq¹³⁷Cs kg⁻¹y (Bq¹³⁷Cs m⁻²)⁻¹) for the calculations. A first estimate obtained from Swedish, Finnish and Danish observations after Chernobyl is:

$$0.5 \text{ m}^2 \text{ y kg}^{-1}$$

This figure seems with reasonable approximation (probably within a factor of 3) to be valid for mean values of game, freshwater fish and wild mushrooms.

By multiplying 0.5 m² y kg⁻¹, the mean deposition of ¹³⁷Cs in Bq m⁻² from the Chernobyl accident for each country and the annual per capita consumption of the various products from semi-natural ecosystems (kg y⁻¹ cap⁻¹), we obtain the total individual mean intake of ¹³⁷Cs in Bq from such ecosystems. The data for this calculation are shown in Table 2.

Table 2

Deposition and consumption data.

Country	Mean deposition Bq ¹³⁷ Cs m ⁻²	Consumption Rate (Kg y ⁻¹ cap ⁻¹)		
		Game	Freshwater Fish	Mushrooms
Denmark	1290	0.2	0.1	0.05
Ireland	3400	0.05	0.01	0
Sweden	9500	2.0	0.2	0.5
UK	900	0.02	0.01	0

In Table 3, the total ¹³⁷Cs intakes from semi-natural ecosystems in the four countries is shown.

Table 3

Individual mean intake with diet of ¹³⁷Cs from Chernobyl (global fallout excluded)
from semi-natural ecosystems compared with total intake

Country	Intake for semi-natural ecosystems Bq ¹³⁷ Cs	Intake from agricultural ecosystems Bq ¹³⁷ Cs	% of ¹³⁷ Cs from semi-natural ecosystems of total ¹³⁷ Cs intake
Denmark	226	2000	10 %
Ireland	102	5500	2 %
Sweden	12825	14500	47 %
UK	14	1500	1 %

3. Conclusion

The present estimate of the relative importance of semi-natural ecosystems as a dose contributor of ^{137}Cs after Chernobyl from diet intake should be considered as a first trial. Large uncertainties are connected to the transfer factor as well as to the individual mean consumptions applied to this estimate. We will, however, consider this an iterative process, where this first approach should be refined when more solid information become available.

The preliminary conclusion is that semi-natural ecosystems may contribute with half of the total dietary intake of Chernobyl ^{137}Cs in Sweden, 10% in Denmark, but only about 1% in Ireland and the UK. Furthermore it should be noted that the relative contribution from semi-natural ecosystems is anticipated to be higher in the Chernobyl case than for global fallout. This is because the ^{137}Cs contribution from agricultural ecosystems in Northern Europe was relatively low for Chernobyl compared to global fallout due to seasonality, which did not influence the semi-natural ecosystems to the same extent .

Publication list

1. Aarkrog, A., Botter-Jensen, J., Chen, Q.J., Dahlgaard, H., Hansen, H., Holm, E., Lauridsen, B., Nielsen, S.P. and Sogaard-Hansen, J., (1991). Environmental Radioactivity in Denmark in 1988 and in 1989. RISO-R-570, pp212.
2. Aarkrog, A., Buch, E., Chen, Q.J., Christensen, G.C., Dahlgaard, H., Hansen, H., Holm, E & Nielsen S.P., (1992). Environmental radioactivity in the North Atlantic Region. including the Faroe Islands and Greeland, 1988 and 1989. RISO-R-571 (EN) pp98.
3. Aarkrog, A., Dahlgaard, H., Frissel, M., Foulquick, L., Kulikov, N.V., Molshanova, I.V., Myttenaere, C., Nielsen, S.P., Polikarpov, G.G. & Yushkov, P.I., (1992). Sources of anthropogenic radionuclides in the Southern Urals. J. Environ. Radioactivity 15, 69-80.
4. Nielsen, S.P., Aarkrog, A., Colgan, P.A., McGee, E.J., Synnott, H.J., Johanson, K.J., Horrill, A.D., Kennedy, V.H., Barbayiannis N. (1992). An intercomparison of sampling technique among five European laboratories for measurements of radiocaesium in upland pasture and soil RISO-R-620 (EN)
5. McGee, E.J., Colgan, P.A., Keatinge, M., Horrill, A.D., Kennedy, V.H., Johanson, K.J., Aarkrog, A & Nielsen, S.P., Bias and measurement errors in radioactivity data from four European radiation research laboratories (The Analyst 117,(6) 941-945)

Project 4

Head of project: *Prof. Johanson*

Objectives for the reporting period

The aim of this study has been to obtain an understanding of the behaviour of ^{137}Cs in forest ecosystem in the central part of Sweden. The study has included soil-plant and plant-animal studies as well as an estimation of the transfer of ^{137}Cs to man. Studies with the aim to find methods to reduce the ^{137}Cs activity concentrations in moose and roe-deer and thereby also reduce the collective dose to man have been included.

Progress achieved including publications

1. Soil-plant studies

The transfer factor (Bq per kg dry weight of plant/Bq per m^2) for ^{137}Cs from soil to plant has been studied in the most common berries in Sweden. Transfer factors of 0.13 for cloudberry *Rubus chamaemorus*, 0.041 for bilberry *Vaccinium myrtillus* and 0.032 $\text{m}^2 \text{kg}^{-1}$ for lingonberry *Vaccinium vitis-idaea* were found. For all species of edible fungi fruitbodies picked within four plots over two years a mean transfer factor of 1.2 was found. In Swedish forests the pathway by fungi is very important since the ^{137}Cs activity concentrations in fungi is often 10 times higher than in the most common vascular plants. The mean levels of edible fungi in our study area, where the ^{137}Cs deposition is about 35,000 Bq m^{-2} , have been around 50,000 Bq kg^{-1} with some annual variation. The mean levels for heather have been 10,000 Bq kg^{-1} , for bilberry 3,000 Bq kg^{-1} and for lingonberry 4,000 Bq kg^{-1} . In bilberry and lingonberry a significant decrease has been observed. By using potassium fertilization of forest area (KCL, 50 or 200 kg per ha) a decrease up to 50% of the ^{137}Cs activity concentration in heather was obtained.

2. Plant-animal studies

The transfer from fodder plants to moose harvested during July to October in mid-Sweden has been studied using our ^{137}Cs activity determination and botanical analysis of rumen content of moose. In July and August fire-weed *Epilobium angustifolium* represented 55% and 34% respectively of the diet, while in September birch *Betula sp.* and in October bilberry *V. myrtillus* were the dominating plants, representing 48% and 38% respectively of the diet. Using the measured ^{137}Cs activity concentrations determined in the fodder plants (Bq per day) and the observed botanical composition of rumen content a mean transfer coefficient (Bq per kg muscle mass/Bq daily intake) of 0.16 day kg^{-1} was calculated. A mean aggregated transfer factor of 0.013 $\text{m}^2 \text{kg}^{-1}$ was also calculated.

The annual mean ^{137}Cs activity concentrations for about 200 to 250 moose harvested each year within our research area in the central part of Sweden has been 750 kg^{-1} and no decreasing trend has been observed. The conclusion is that the ecological half-life of ^{137}Cs is very long and probably similar to the physical half-life of ^{137}Cs . Since the mean ^{137}Cs deposition in our research area is between 35,000 and 40,000 Bq m^{-2} an aggregated transfer factor of $0.02 \text{ m}^2 \text{ kg}^{-1}$ for moose was found. The seasonal variation of ^{137}Cs activity concentrations in roe-deer have been studied and a peak level appeared in either August, September or October depending on the mushroom peak of the year. A hunting season in May has been introduced in the most contaminated counties in Sweden and this rather simple countermeasure reduces the ^{137}Cs levels in harvested roe-deer from a mean level of about 5,000 to 1,000 Bq kg^{-1} or a reduction with 20% of the autumn level. The mean ^{137}Cs activity concentration for the years 1989 to 1991 has been 1,850 Bq kg^{-1} and the aggregated transfer factor will be $0.05 \text{ m}^2 \text{ kg}^{-1}$.

The use of salt licks with giesesalt for moose has been studied and the results indicate a reduction of 20 to 25% in areas where salt licks with giesesalt have been used. There were, however, rather large variations from area to area indicating suboptimal conditions for placing the salt licks.

3. Animal-man studies

The annual transfer of ^{137}Cs to man by moose meat is about 2.5 GBq per year corresponding to an annual collective dose in Sweden of about 30 man Sv. Since the ecological half-life for the forest-moose and forest roe-deer systems seems to be very long the dose commitment over 50 years will be high or 1000 manSv due to intake of moose meat and more than 300 due to roe-deer meat.

Publication list

1. Johanson, K.J., Bergstrom, R. Radiocaesium from Chernobyl in Swedish moose. *Environmental Pollution* 61 (1989) 249-260.
2. von Bothmer, S., Johanson, K.J., & Bergstrom, R. Caesium-137 in moose diet; consideration of intake and accumulation. *Sci. Total Environment* 91 (1990) 87-96.
3. Karlen, G., Johanson, K.J. & Bergstrom R. Seasonal variation in the activity concentration of ^{137}Cs in Swedish roe-deer and in their daily intake. *J. Environmental Radioactivity* 14 (1991) 91-103.
4. Johanson, K.J., Bergstrom, R., von Bothmer, S. & Karlen G. Radiocaesium in wildlife of a forest ecosystem in central Sweden. In "Transfer of radionuclides in natural and semi-natural environments" (G. Desmet, P. Nassimbeni and M. Belli. Eds.) Elsevier Applied Science 1990.

5. Johanson, K.J., Bergstrom, R., von Bothmer, S. & Kardell, L. Radiocaesium in Swedish forest ecosystems. In "The Chernobyl fallout in Sweden" Edited by L. Moberg, *The Swedish Radiation Protection Institute* 1991, pp 477-486.
6. Johanson, K.J. & Bergstrom, R. Radiocaesium transfer to man from Swedish forests. Presented at the seminar "*The dynamic behaviour of radionuclides in forests*" held in *Stockholm 18-22 May 1992*.
7. Fawaris, B. & Johanson, K.J. Radiocaesium in soil and plants in a forest in central Sweden. Presented at the seminar "*The dynamic behaviour of radionuclides in forest*" held in *Stockholm 18-22 May 1992*.
8. Johanson, K.J., Bergstrom, R., Eriksson, O. & Erixon, A. Activity concentration of ¹³⁷Cs in moose and their forage plants in Mid-Sweden. *submitted to J. Environ. Radioactivity*.
9. Johanson, K.J. Countermeasure in forest ecosystems - is there a need and is it possible? Presented at the *Nordic Radioecology Meeting in Torshavn 15-18 June 1992*.
10. Johanson, K.J. von Bothmer, S. The uptake of radiocaesium in heather in the central part of Sweden. *manuscript 1992*.

Project 5

Head of project: *Dr. Veresoglou*

Objectives for the reporting period

1. Field surveys: Measurements of Cs-137 in soil and vegetation samples taken by a site of North Western Greece which is grazed by sheep and goats.
2. Laboratory experiments by using Cs-137 in columns filled with six soils, with and without K addition, and sown with Medicago sativa.
3. Laboratory experiments using stable isotopes of Cs and Sr.

Progress achieved

1. Field surveys

The upland pasture site selected had climatic, topographic and vegetation composition and soil characteristics similar to pastures on organic soils of north Europe, and received high inputs of Chernobyl radiocaesium.

Soils were collected once, on 15 May 1991, but vegetation samples were taken on 15 May, 15 June, 15 July and 15 September. A summary of the values of Cs-137 measured on these samples is shown in Table 1. Although the input of radiocaesium was very high, radiocaesium content of vegetation samples has been very low. The bulk vegetation of some areas, which were very difficult to approach on 15 May, have shown relatively higher amounts of radiocaesium, possibly because of the higher organic matter content of the soil.

2. Laboratory experiment using Cs-137

The experiment was aimed at the identification of those soil factors that affect the movement and uptake of Cs-137 under laboratory conditions using soils that differ mainly in organic matter content.

Six soils (0-25 cm) were sampled with organic matter content ranging between 2-55%, clay content 9-33%, and pH 6,6-7, 6. PVC columns 25 cm long, 6,7 diameter were filled with the <2mm fraction of the soils using a specially constructed device in order to achieve a uniform packing as possible. There were two treatments: i) K added, at a rate of 100 kg K₂O/ha a rate usually used in practice ii) no K added. Each treatment was replicated twice.

The soil columns were wetted to field capacity and Cs-137 was added in a solution form, at a rate corresponding to 130 kBq/m², almost ten times higher than the fallout from

Chernobyl. After Cs-137 addition the columns were sown with four alfalfa seeds. Four harvests were taken at 2 month intervals. Each harvest was followed by sectioning of a pair of columns (slices 2 cm thick). The soil samples were air-dried and Cs-137 was measured using a NaI detector. However in one of the soils plants failed completely due to nematodes infection.

The results obtained are summarised as follows. i) For all soils the addition of potassium does not affect the depth distribution of Cs-137. ii) As expected for one of the soils with micas prevailing in the clay fraction all Cs-137 added remained at the top 3 cm. iii) For the most organic soil (55% org. matter) it was found that Cs-137 remained at the top 4 cm in contradiction to what is believed, that Cs-137 in organic soils or peats moves relatively deeper. iv) For the other three soils approximately 50% of the Cs-137 was found at the top 4 cm and the rest was rather uniformly distributed with depth (Fig.1).

3. Laboratory experiments by using stable isotopes of Cs and Sr

The aim of the experiments was to find out if the uptake of Cs or Sr is species specific and if it is affected by the physiochemical characteristics of the soil, the timing of Cs or Sr application and the addition of K or Ca, respectively. In all experiments pots of 1 dm³ in volume were used. In the first experiment the pots were filled with either inorganic (pH: 5.4, Organic matter: 1.8%, C.E.C.: 15.0 meq/100g, and 59.8-26.0-14.2 sand-silt-clay %, respectively) or organic (pH: 7.3, Organic matter: 30%, C.E.C.: 103.6 meq/100g and 66-25-9% sand-silt-clay respectively) and sown with either Lolium perenne or Trifolium repens, 300 or 190 mg per pot of Cs or Sr respectively were applied 2, 1 and 0 months before sowing. For the inorganic soil only and for the case of Cs or Sr application at the time of sowing, potassium or calcium were added at the rates of 0, 100 and 200 mg per pot of K₂O) or Ca in the pots received Cs or Sr, respectively. In the second experiment two soils again, an inorganic (pH: 7.3, Organic matter: 3%, and 67-18-15% sand-silt-clay respectively) and an organic (pH: 5.2, Organic matter: 50% and 71-24-5% sand-silt-clay, respectively) were used. For the inorganic soil only, Ca was added in the rates of 0 and 1.65 g CaO per pot. Sr was applied at the rate of 67 mg per pot. The pots were sown in monocultures with the species: Lolium perenne, Dactylis glomerata, Medicago sativa, Lotus corniculatus, Trifolium repens, Plantago major, Plantago lanceolata and Rumex crispus. The first and second experiments were harvested 2 and 4 months, respectively, after sowing. The results of the two experiments are as follows:

4. First experiment

Cs concentration in the above ground biomass was higher in Trifolium and in the organic soil in comparison to Lolium and to the inorganic soil, respectively, and was reduced with the addition of K (Fig. 2A). Extractable Cs in the soil at the end of the experiment was generally higher when Cs was applied 1 and 2 months before sowing in comparison to addition at sowing and was higher in the organic soil in comparison to the inorganic. The proportion of immobilised Cs is higher in the inorganic soil (Fig. 2B). Sr concentration in the above ground biomass was higher in Trifolium in comparison to Lolium but lower in the organic soil in comparison to inorganic and increased with the addition of Ca (Fig. 3A).

Values of extractable Sr were about similar in both soils (Fig. 3B), but higher when Sr was applied 1 and 2 months before sowing in comparison to addition at sowing. The similar values of extractable Sr in both inorganic and organic soil and the fact that Sr application per weight of the soil was about 2 times higher in the organic soil, because of the differences in bulk density, show that Sr is immobilised more effectively in organic soils.

5. Second experiment

In all three treatments Sr concentration in the above ground biomass is correlated very closely with that of Ca concentration. The simple linear correlation coefficient (r) between the means of the 24 treatments (3 soils X 8 species) of Sr and Ca concentration was 0.836. Both Sr and Ca concentrations were lower in the organic soil in comparison to the inorganic one. The addition of Ca increased the Ca concentration but did not affect Sr concentration. In all three soil treatments the ranking of plant species in both Ca and Sr concentrations seems to be the same. The slopes of regression lines between Sr and Ca concentrations in the above ground biomass seems to differ in the two soils i.e. organic and inorganic (Fig. 4).

Table 1

A summary of values of Cs-137 content (Bq.kg^{-1}) of soil and vegetation samples taken from the Florina area during the period May to September

	Range of Values	n
Soil (0-5cm)	960	1
Bulk Vegetation	8.56 - 308	1
Leaves of Fagus	25.3 - 30.2	3
Agrostis stolonifera	12.5 - 95.1	3
Dactylis glomerata	22.8 - 31.6	3
Trifolium spp.	31.6	1
Vicia villosa	21.0 - 44.8	3
Origanum spp.	22.9 - 34.9	3
Pteridium aquilinum	10.7	1
Lotus corniculatus	8.32 - 14.34	2

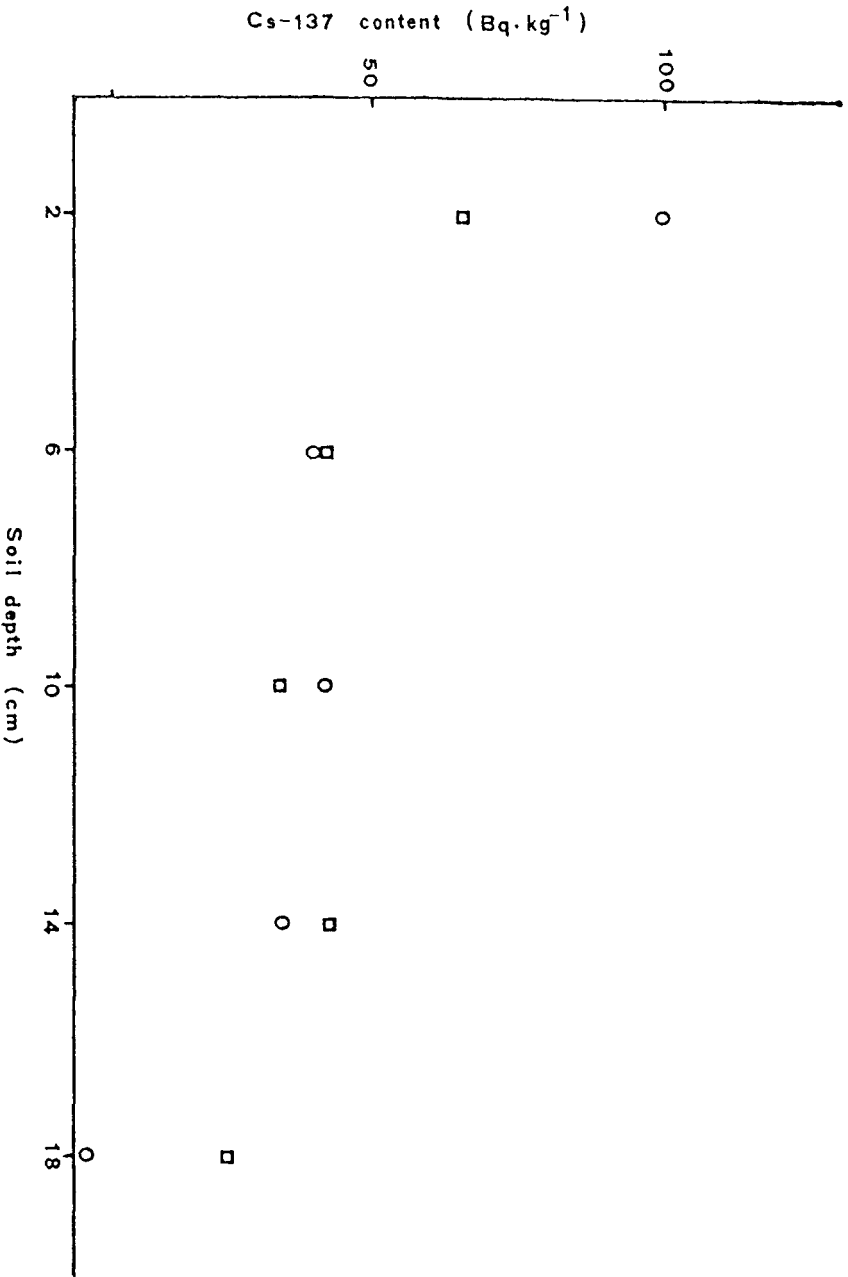


Figure 1 Caesium-137 distribution with soil depth after 8 months for two of the soils used. (O, Soil with 8% organic matter; □, Soil with 2% organic matter content).

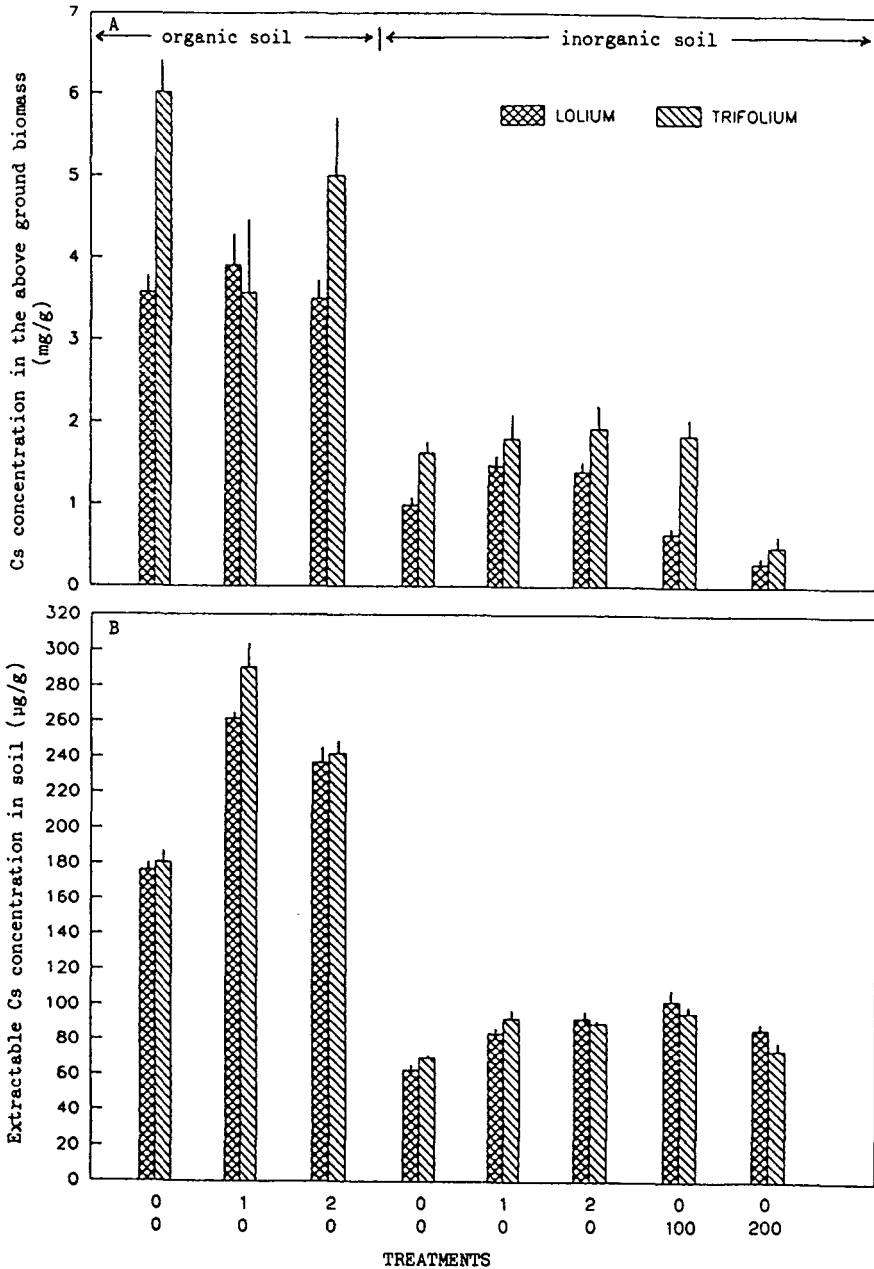


Figure 2

Caesium concentrations (mean values + standard errors) of the above ground biomass (A) and of the soil (B) for the different treatments used in the first experiment with stable isotopes. Figures in the first row on the x axis refer to the months of Cs application before sowing while those in the second row to the rates of potassium application in mg K₂O per pot.

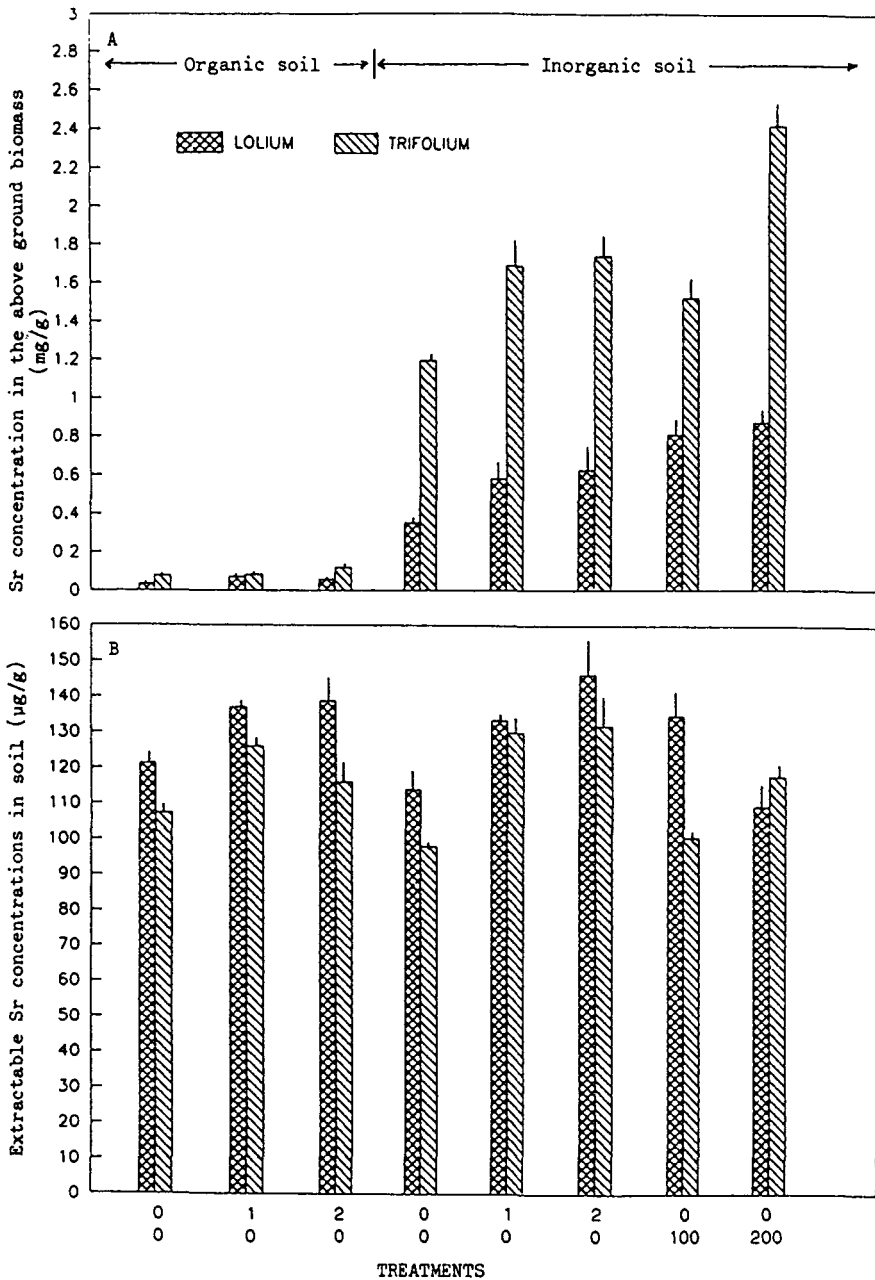


Figure 3

Strontium concentration (mean values + standard errors) of the above ground biomass (A) and of the soil (B) for the different treatments used in the first experiment with stable isotopes. Figures in the first row on the x axis refer to the months of Sr application before sowing while those in the second row to the rates of calcium application in mg Ca per pot.

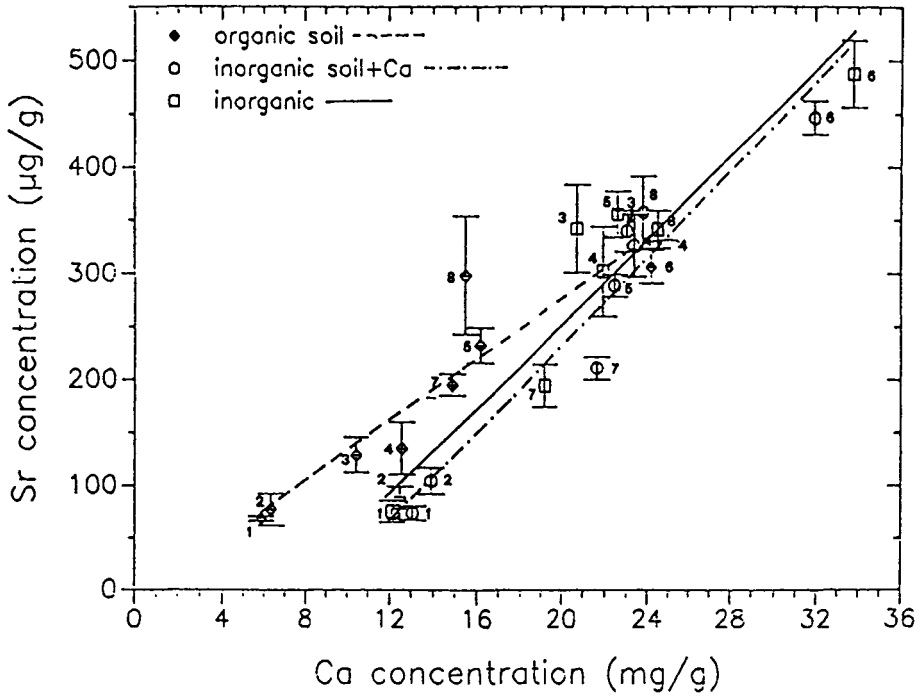


Figure 4

Relationships between the means of Sr concentrations and Ca concentrations in the above ground biomass for the eight species used in the second experiment with stable isotopes. For the means of Sr concentrations standard deviations are also shown with bars. Standard deviations for the means of Ca concentrations are not shown. They were generally lower than those of Sr concentrations. The species are referred to as numbers as follows: 1, *Lolium perenne*; 2, *Dactylis glomerata*; 3, *Medicago sativa*; 4, *Lotus corniculatus*; 5, *Trifolium repens*; 6, *Plantago major*; 7, *Rumex crispus*; 8, *Plantago lanceolata*.

TRANSFER OF ACCIDENTALLY RELEASED RADIONUCLIDES IN AGRICULTURAL SYSTEMS (TARRAS)

Contract Bi7-046 - Sector A26

- 1) *Cancio*, CIEMAT - 2) *Maubert*, CEA-Cadarache
- 3) *Rauret*, Univ. Barcelona - 4) *Colle*, CEA-Cadarache
- 5) *Cawse*, AEA Technology Harwell Lab. - 6) *Grandison*, Univ. Reading
- 7) *Gutierrez*, CIEMAT

Summary of project global objectives and achievements

The assessment of the radiological consequences of a severe accident in a nuclear plant relies on the quantification of several processes. The experience accumulated following the Chernobyl accident has emphasized the need to improve the knowledge of the processes and parameters relevant in the transfer of radionuclides along the food chain.

Some of the most important aspects have been identified in the conclusions and recommendations on further research needs in the "Post Chernobyl Actions" (i.e. EUR12550 EN, 12553 EN and 12554 EN). This project answers very precisely the need for new experimental evidence that has been identified as necessary for certain topics.

One of the important aspects considered in this project has been the utilization of an aerosol source term as similar as possible to accidental conditions. The physico-chemical characteristics of aerosols have a great influence on the radionuclide deposit and its behaviour in soil and plants.

The speciation of radionuclides in soils and the behaviour of radioactivity deposited to foliage are important to understand the transport mechanisms in soils and the availability for plants.

The factors modifying the radionuclide content in food during food processing have not received the attention they deserve and it was evidenced by the handling of products after the Chernobyl accident. The amount of radionuclides present in processed food is of great interest both for ingestion dose assessment and to select the most efficient procedures to reduce contamination in foodstuffs.

The need to acquire more information about the relevance for dose calculations of the agricultural practices and dietary habits of Mediterranean countries has also been identified.

All these different aspects have been included in the project with the aim of contributing to the reliability of the radiological assessment methods and to establish a scientific basis to be used in the design of post-accident countermeasures.

The global or overall objectives that have been attained may be summarized as follows:

- Simulated PWR accident source term has been used and the behaviour of aerosol deposits containing Sr, Cs, and Ag isotopes have been followed in a soil/vegetable system.
- The extent of radionuclide transfer as modified by well established food processing techniques have been studied for Sr, Ru, Co and Cs nuclides in several products.
- Some relevant characteristics for dose calculation in a specific Mediterranean region, representative of Southern European countries, have been studied.

The principal achievements during the two years of work have been:

1. Aerosol transfer experiments

Two different types of soil were selected, a French one and a Spanish one. Both soils were selected taking into account that they will be used in the RESSAC-EUROSOIL Project. The main crop that has been selected is lettuce (*Lactuca sativa*) one of the most universal plants in vegetable gardens. An experiment was carried out with wheat, one of the most important cereals in Europe, in order to study the soil-plant dynamics and the activity transfer to mature grain. Unfortunately the wheat cultivation was not completely successful and therefore results were obtained only for young plants.

Ten experimental contaminations were performed in CEA - Cadarache, five of them with each type of soil. Four of them use lettuce as vegetation and the other one uses wheat. Four growing stages were considered for lettuce: mature, young, seedling and sowed plant.

The main physical and chemical characteristics of the aerosol generation are included in the participant #2 report. The fraction intercepted by plants, the dynamics of leaf washout, root uptake, migration in soil and speciation of radionuclides have been studied at different growth stages of the lettuce plants. Treatment and analysis of samples were performed at Barcelona University. Some radioactive measurements and evaluation of results were performed at CIEMAT in Madrid.

Valuable results have been obtained on soil migration, leaf retention and soil speciation of radionuclides and consequently some conclusions on radionuclide migration and mobility, the influence of soil type and growth stage on it, and the soil-plant transfer factors. All these aspects are included in the reports of participants #1 and #3.

2. The influence of food processing on the radionuclide content of foodstuffs

The factors that modify the radionuclide content using well established food processing techniques have been studied in several food products.

Agricultural produce including potatoes, carrots, peas, beetroot, brussel sprouts, wheat and mushroom were obtained by Harwell (UK) in a region having relatively high concentration of radionuclides in soil. The food processing of these raw materials has been performed at the pilot plant in Reading University (UK).

Analyses for K-40, Co-60, Sr-90, Ru-106 and Cs-137 were performed together with their stable isotopes. The effects of freezing, canning, drying, milling of wheat and culinary preparation have been studied. Dairy products have also been produced and samples of raw material and products were also obtained from factories for stable element analysis.

Processing methods and retention factors for several food products as well as other complementary studies are presented in participants #5 and #6 reports.

Vegetable product have been collected in French factories and studied by CEA-Cadarache. Stable elements or/and radionuclides were measured for wheat, rice, potatoes, peaches, peas, tomatoes, peas, olive and sunflower oils.

Some complementary studies have been performed in the laboratory for juices, canning and wines. The retention factors and residual activity measured in food products before and after processing are presented in the participant #4 report.

Results from the British and French studies show that food processing in most cases decreases significantly the content of radionuclides in agricultural products.

3. Specific characteristics of the Mediterranean diet and agricultural production

The main characteristics of a typical Mediterranean diet have been studied and the major agricultural crops produced as well as the consumption habits have been identified. The potential influence of diet on dose assessment after accidental contamination has also been analysed.

The study has been performed at CIEMAT for the Spanish region and compared with similar data for all the EC countries.

The results are presented in the participant #7 report. The data obtained show that when comparing Mediterranean and EC countries differences are less significant for diets than for agricultural production. Consequently the exportation of food may be important for collective doses in the event of an accidental contamination.

Project 1

Head of project: *Dr. Cancio*

Objectives for the reporting period

- Overall coordination of the whole project
- Evaluation of results for the aerosol transfer experiments. Collaboration in experimental work.
- Determination of some parameters which control the transfer of radionuclides in the foodchain from the aerosol deposit experimental data: interception factor, translocation inside the leaves, washout, radionuclide migration in soil, soil to plant transfer factors, etc.

Progress achieved including publications

The activities measured in soils and plants have been normalized to the soil deposition in order to be able to compare the contamination. In all cases, those values out of the range of twice the standard deviation have been neglected.

Ten experiments were designed to study the behaviour of soil and plant systems. Contaminations by pairs, one for each soil type, have been carried out with plants at different growth stages (sowed, seedling, young and mature plant). Except for the sowed plants, the samples were taken some hours after the deposition and later at each of the plants growth stages. A scheme of the experiences is shown in Table 1.

Table 1.

	SandyLoam Soil	Sandy Soil
Contamination of Mature lettuce	Experiment 1	Experiment 2
Contamination of Bare soil and Sowed wheat	Experiment 3	Experiment 4
Contamination of Bare soil and Sowed lettuce	Experiment 5	Experiment 6
Contamination of Seedling lettuce	Experiment 7	Experiment 8
Contamination of Young lettuce	Experiment 9	Experiment 10

1. Analysis of plant deposition

1.1 Interception factor

The interception factor by dry deposition on the plant is defined as the fraction of the deposited activity retained by crops on the surface.

The results measured of interception factor (R), yield factor (Y) and the rate R/Y for mature and young plants are shown in Table 2. The experimental crops were grown under high density in order to obtain enough matter for sampling. It does not reflect the usual field agricultural practice. Nevertheless, a R/Y factor ranging between 0.20 to 0.26 is obtained for mature lettuces, and this is similar to the values observed in natural conditions and generally used in models. The results for young plants are clearly higher, this shows that the foliar effective surface for deposition on leaves in a young stage of the plant is larger than in latter stages.

Table 2.

	Yield Factor Y(Kg(fw)/m ²) avg	Interception Factor						Cs-134	R/Y Ag-110m	Sr-85
		Cs-134		R Ag-110m		Sr-85				
		avg	sdv	avg	sdv	avg	sdv			
Sandy Soil(Exp2) Mature lettuce	4.08	0.80	0.01	0.80	0.01	0.79	0.01	0.20	0.20	0.19
SandyLoam Soil(Exp1) Mature lettuce	3.52	0.91	0.03					0.26		
Sandy Soil(Exp10) Young lettuce	0.1	0.5	0.2	0.80	0.04	0.76	0.07	5	8	7.6
SandyLoam Soil(Exp9) Young lettuce	0.06	0.4	0.2	0.5	0.2	0.5	0.2	6.7	8.3	8.3

1.2 Translocation inside the plant

From the analysis of sequential extraction with water and chloroform applied to the plants, it is seen that Caesium is readily incorporated by the lettuce and stays in water soluble form; Strontium penetrates less than Cs-134 and it also remains in water soluble form. Ag-110m is more actively fixed to the fraction adhered to the waxes of lettuce cuticle (extractable with chloroform). So, it can be concluded that the rank of translocation of these radionuclides inside the plant is Cs >> Sr > Ag, and the rate of absorption depends on the plant growth stage and the irrigation period. After 9 days of irrigation, the water extractable fraction decreases for the three radionuclides and the fraction absorbed by the plant increases. The washout process, beside the translocation inside the plant, causes the decrease of the water and chloroform phases. The experiences designed do not allow to quantify the relative importance of both processes, washout and translocation.

1.3 Washout

The measure of contamination in three growth stages of the plants was carried out to determine the leafy irrigation washout. In the experience with mature lettuces the washout factor has been calculated from the increment of activity in soil during the experimental period of time. On the other hand, the calculations for seedling and young plants are done with the decrease of activity on plant surface.

The values obtained for irrigation washout decrease when the plant grows, probably due to the larger biomass in latter stages. The results range from 0.021 for seedling plant to 0.001 for mature lettuce in days⁻¹. In the literature, the weathering parameter includes other factors than irrigation, such as wind, rain, and translocation. The values given for weathering range from 3.4E-2 to 9.5E-2 d⁻¹; these larger values probably reflect the effect of including all these processes.

2. Analysis of soil deposition

2.1 Soil migration

Soil profiles were sampled at the end of each experiment. Three soil samples were taken in layers of 2cm with depths from 0cm to 6 cm and another sample from 6 to 10 cm was taken. In sandy soil 97% Cs-134 and 91% Ag-110m remain in the first layer; after three months with irrigation this distribution does not change. However, Sr-85 migrates to deeper soil layers, remaining most of all in the layers 0-4cm. In sandy-loam soil, Sr-85 is retained mostly in the first layer, in contradistinction to sandy soil (See participant 3 report). These results are in accordance with the values in post-Chernobyl Caesium measurements.

2.2 Soil speciation

Two schemes for soil speciation have been proposed in this phase of the project, presented by participant 3.

Caesium is strongly associated with the soil components, and less than 10% of the total extracted activity in sandy soil or 4% in the sandy-loam is released in the first extraction, and therefore this is the fraction that has been considered as very movable in the short term. Similar values were observed in field studies after the Chernobyl accident. Between 90 to 100% of Sr-85 in soil is extracted in the first extraction of the scheme; these values also agree with the literature.

After an initial irrigation period, the radionuclide mobility decreases, and the remaining activity is retained in the soil.

A mobility factor for each radionuclide is defined as the rate between the easily extracted soil activity and the total activity (MF). For Cs-134, the fraction extracted with Cl_2Mg is considered as the easily movable fraction; for Ag-110m, the addition of $HAcO$ and $NH_2OH - HCl$ is used to extract the easily movable fraction. Sr-85 activity is always removed in the first fraction. The mobility of Caesium is lower compared to Strontium or Silver. The rank of fixing in these soils is $Cs > Ag > Sr$. (Table 3).

Table 3.

	Mobility Factor		
	Cs-134	Ag-110m	Sr-85
Sandy Soil (Exp2)			
Mature lettuce			
Before Irrigation (0-2 cm depth)	0.29	0.07	1.0
9 days irrigation (10 cm depth)	0.16	0.07	1.0
Sandy Loam Soil (Exp5)			
Sowed lettuce			
Before Irrigation (0-2 cm depth)	0.10	0.03	0.87
3 months irrigation (10 cm depth)	0.06	-	0.84
Sandy Soil (Exp6)			
Sowed lettuce			
Before Irrigation (0-2 cm depth)	0.18	0.16	0.95
3 months irrigation (10 cm depth)	0.10	0.05	1.0

3. Soil to plant transfer factors

The Soil-Plant Transfer Factor is the most usual parameter to describe the transport between the soil and plant compartments. It is defined as the rate of plant activity (fresh weight) to soil activity (dry weight) TF_{sp} . The soil depth is generally taken as 10 cm. It is necessary to point out that the activity in soil is mainly present in the first 4 cm depth layer. If only that layer would have been considered, the transfer factor would be lower. Nevertheless, in normal agriculture practice after each recollection, the soil is mixed. For this reason, the 10 cm soil depth is more adequate to calculate the TF_{sp} . Results are shown in Table 4.

Table 4

Growth Stage		Soil-Plant Transfer Factor (Bq/Kg(fw plant)) / (Bq/Kg(dw soil)) 10 cm Soil Depth					
		Cs-134		Ag-110m		Sr-85	
		avg	sdv	avg	sdv	avg	sdv
Sandy Loam Soil (Exp5)	Seedling lettuce	0.04	0.01	0.18	0.07	0.67	0.07
	Young lettuce	0.016	0.001	0.031	0.008	0.4	0.1
	Mature lettuce	0.011	0.005	0.015	0.007	0.5	0.1
Sandy Soil (Exp6)	Seedling lettuce	0.20	0.07	0.7	0.1	2.0	0.5
	Young lettuce	0.035	0.009	0.050	0.006	1.49	0.06
	Mature lettuce	0.09	0.06	0.047	0.001	1.2	0.5

The transfer in both compartments decreases as plants grow (Figs. 1 and 2). In sandy soil the transfer factors are larger than in sandy-loam soil, as radionuclides are more available in the former. For the same reason Sr-85 uptake is much greater than for the other radionuclides.

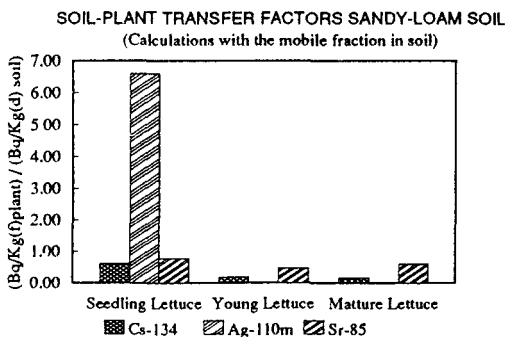


Fig.1.

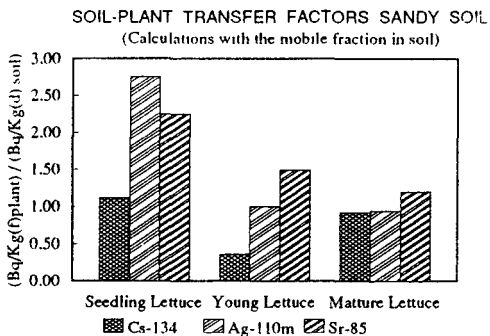


Fig. 2.

In the previous chapter, mobility factors were defined. These have been used to calculate the transfer factors considering the movable activity fraction in soil. Larger values are obtained for Cs-134 transfer factors due to its larger retention rate and the available activity for plants is very small. This effect is clearly seen for sandy-loam soil. For Sr-85 it is less obvious because its fixation in soils is lower (Table 5).

Table 5

		Soil-Plant Transfer Factor (Movable fraction) (Bq/Kg(dw plant)) / (Bq/Kg(dw soil)) 10 cm Soil Depth		
	Growth Stage	Cs-134 avg	Ag-110m avg	Sr-85 avg
Sandy Loam Soil (Exp5)	Seedling lettuce	0.62	6.59	0.76
	Young lettuce	0.178	-	0.5
	Mature lettuce	0.175	-	0.6
Sandy Soil (Exp6)	Seedling lettuce	1.1	2.75	2.3
	Young lettuce	0.363	1.0	1.49
	Mature lettuce	0.92	0.94	1.2

Another way to represent the transfer factors is to consider the soil deposition activity (Bq/m^2) (3rd chapter, participant 3 report). In this case, the transfer factors do not take into account the radionuclide concentration distribution in soil depth which has some influence in the radionuclide availability for plant uptake.

Project 2

Head of project: *Dr. Maubert*

Objectives for the reporting period

The aim of these tests is to study the transfer of radioactive aerosols onto two types of plants in relation to two types of soil and to the degree of maturity of the plants. In order to do so, we had to adapt our system of radioactive aerosol release to the types of experiment that were planned, and to carry out contamination on the crops to be studied.

In collaboration with our partners, we determined the plant species to be studied, that is to say lettuce and wheat; the radioelements to be used: Cs134, Sr85, Ag110m; the two types of soil. We set up a schedule for the different releases to be performed as well as for the measurements to be made. The various experiments have been carried out as planned and all the parameters considered have been studied.

Progress achieved

In the frame of the TARRAS project, the "Service d'Etudes et de Recherches en Environnement" of Cadarache is responsible for:

1. The generation of heat generated polymetallic aerosols that are representative of a real accidental release: This involves a mixture of 16 elements representing fuel and cladding, structural materials, control rods and of course, fission products. The mixture is heated to 2750° in the graphite tube of an electrically heated furnace. The aerosols thus produced are then scattered into a tight containment in which we can set up cultivation. We can also introduce radioactive elements into such a mixture; their measurement can later be made by means of gamma spectrometry.

Figure 1 below gives us the chemical composition of the mixture that is used.

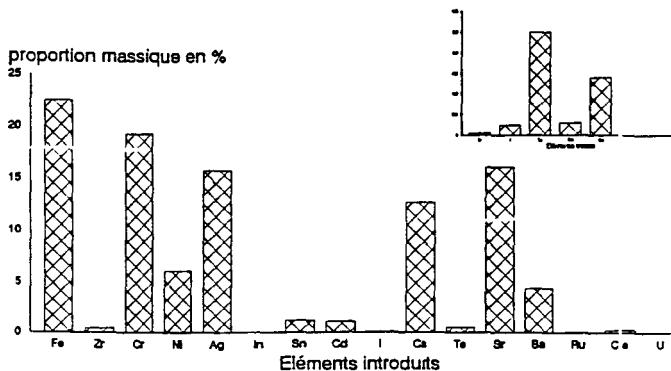


Figure 1 CHEMICAL COMPOSITION OF THE MIXTURE OBTAINED BY ICP/MS

2. Characterization of aerosols thus produced

2.1 Physical characteristics

We established the particle size curve of the aerosols which gives us particle size distribution. The measurements were made with Andersen impactors. Figure 2 below represents the distribution frequency in percentage in relation to the diameter of the particles in microns, for two tests. The mean geometrical diameter is obtained from the experimental particle size distribution; we can see that it is 0.75 μ in the first test and 0.4 μ in the second. The D25 to D75 diameter range is of 0.35 to 3 μ for the first test and of 0.26 to 1.1 μ for the second.

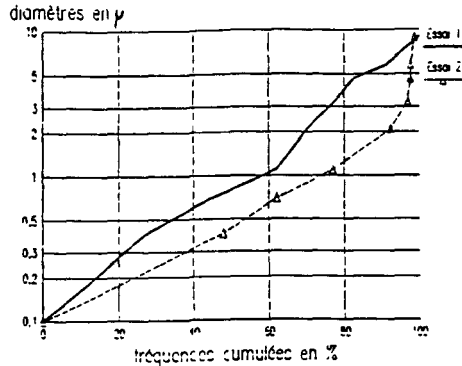


Figure 2: PARTICLE SIZE DISTRIBUTION CURVES

2.2 Chemical characteristics

In order to globally analyse the chemical composition of the aerosols, we used the same method as for the composition of the mixture, that is to say ICP/MS mass spectrometry. Figure 3 below shows the chemical composition of the aerosols during the two tests. It is to be noted that all the elements were released, and if these results are compared with the calculated theoretical values, we can see that certain elements are released in greater quantity, such as iron, chrome, nickel, strontium and barium. On the other hand, others are released in smaller quantities or found in the aerosols, such as zirconium, indium, tin, cadmium, iodine, tellurium and ruthenium. The proportions of silver, cesium and cerium found in the aerosols are, however, close to the theoretical values.

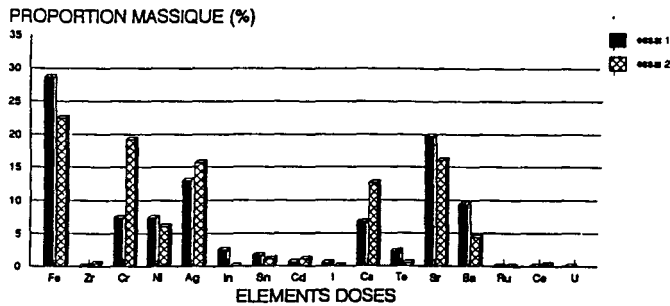


Figure 3: CHEMICAL COMPOSITION OF THE AEROSOLS

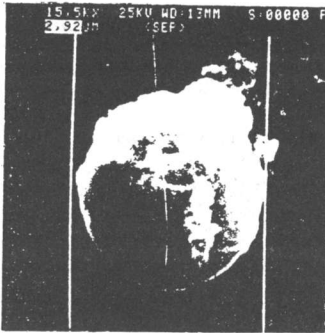
The determination of the chemical species was obtained by X diffraction, a method that only enables crystalline phases to be distinguished. These measurements allowed, in particular, the identification of non oxidized metal Ag, of metal Sr that rapidly changes into $\text{Sr}(\text{OH})_2$ in the air, and metal Cs that also rapidly changes into cesium hydroxide.

The aerosols then underwent observation through an electronic scanning microscope coupled to a retrodiffusion probe. These two methods enable a visual evaluation of the samples to be made, in particular of their geometrical form. Retrodiffusion enables the elementary composition of a particle to be determined. We were thus able to observe Ag particles in the form of spherical globules of 1 to 4μ , Sr alone or more often associated with other elements, as well as other associations.

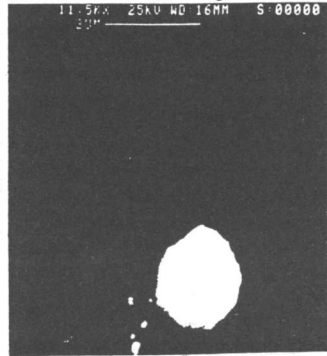
Figure 4 shows several of the photos of the aerosols produced by our facilities.

All these measurements and analyses thus enabled us to characterize the aerosols produced by our facilities and to clearly show the similitude between them and the modelling.

Ag (C₁)



Sr (C₅)



Fe,Cr,Ni,Sr,Zr,Ru (C₅)



Zr,Ag

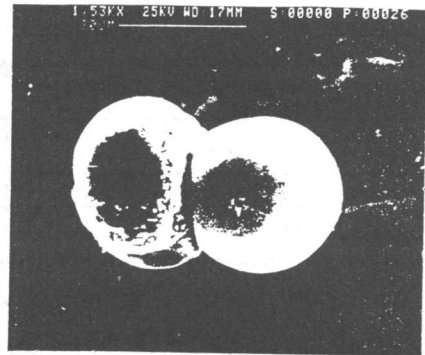


Figure 4 PHOTOS OF THE AEROSOLS

3. The contamination of chosen plant species

Different contaminations or "shoots" have already been carried out in collaboration with partners. We have performed "shoots" over the two chosen soils on fully grown lettuces, on bare soil just sown with wheat on one hand and lettuce on the other hand. We are soon to contaminate lettuce seedlings and half-grown lettuce plants, so as to cover the different vegetative stages. Table 1 below shows the characteristics of the radioelements that were present in the source term of each "shoot".

Solubilization tests of the radioactive aerosols deposited on filters during the shoots were performed. The filters were at first coated raw, then washed with demineralized water and counted again; on the other hand, the washing water itself was measured. The results obtained show that, in these experimenting conditions, Strontium is 90% soluble, Silver 20% and Cesium 100%.

Table 1 Characteristics of the various "shoots": activity in Bq per shoot

	SPANISH SOIL			FRENCH SOIL		
	85 Sr	110m Ag	134 Cs	85 Sr	110m Ag	134 Cs
Contamination of fully grown lettuces	132219	341030	468258	175152	447545	867790
Contamination bare soil sown with wheat	49586	327092	799661	65770	448000	1021000
Contamination bare soil sown with lettuces	470400	724000	2515000	872400	1349500	5033000
Contamination of seedlings	115300	794200	2162500	161000	1071000	2624000
Contamination of half-grown lettuces	84110	816280	2984000	94130	941380	4071000

Our objectives have been reached, all tests have been carried out. Difficulties appeared about the radioactivity of the source term on the one hand and in particular of Sr85. Because of its period, the difference of the radioactivity of Sr85 was too big from one shoot to the other. On the other hand, we had difficulties in growing the wheat in the conditions imposed by radioprotection. We expect to be able to solve this problem shortly.

Project 3

Head of project: *Dr. G. Rauret*

Objectives for the reporting period

1. Characterization of the soils;
2. Study of the radionuclide migration during irrigation;
3. Study of root uptake;
4. Influence of plant growth stages at the contamination time in final radionuclides level in plant;
5. Study of foliar uptake by sequential extraction;
6. Soil speciation by sequential extraction.

Progress achieved including publications

1. Experimental design

The experimental design has been explained in the general explanation of the project.

2. Results

2.1 Characterization of the soils

Two soils have been selected to carry out the plot experiments with contrasted properties to compare radionuclides behaviour. Main characteristics are summarised in Table I.

Table I - Soil characteristics

	Soil 1	Soil 2		Soil 1	Soil 2
pH H ₂ O	7.5	6.7	Exchangeable cations (cmol kg ⁻¹)		
pH KCl	7.1	6.0	Ca	9.15	1.56
% M.O.	2.40	0.22	Mg	1.85	0.19
% CaCO ₃	5.86	0.00	Na	0.35	0.11
Bulk density (g cm ⁻³)	1.29	1.39	K	1.54	0.10
Texture	Sandy-loam	Sandy	NH ₄	1.65	1.86
Cs	36.8	86.2	Exchan. acidity	1.90	2.72
FS	16.4	4.1	C.E.C. (cmol kg ⁻¹)	16.44	6.54
CSi	15.6	0.2			
FSi	13.6	1.7	Clay types (%)		
Cl	17.6	7.8	Kaolinite	12	35
Water soluble cations (cmol kg ⁻¹)			Illite	79	65
Ca	0.41	0.11	Vermiculite	9	-
MG	0.18	0.04			
Na	0.08	0.05	K fixed (cmol kg ⁻¹)	1.25	0.27
K	0.22	0.05			

2.2 Study of the radionuclide migration in soil

The study of radionuclides migration is carried out in the three following experiences: a) intensive irrigation during two weeks (experience 2): no differences between radionuclides studied (^{134}Cs , $^{110\text{m}}\text{Ag}$ and ^{85}Sr) were detected and about 90% remains in the two first cm. b) Radionuclides migration during the growing period: b.1) After three months growing period (experience 5 and 6, lettuce), for the sandy-loam soil no differences between radionuclides were detected. In sandy soil Cs and Ag have similar behaviour than in sandy-loam soil. For the Sr the migration was higher in sandy soil (figure 1).

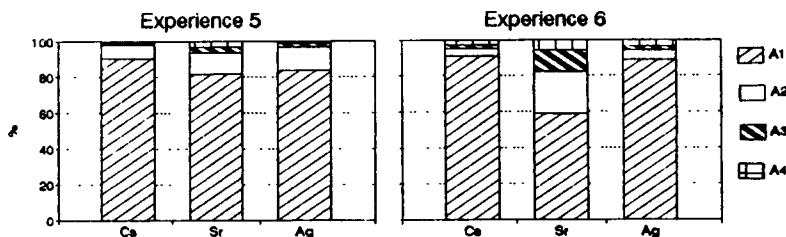


Figure 1. Soil migration taken 100% equal to total activity in profile (A1 = 0-2 cm, A2 = 2-4 cm, A3 = 4-6 cm and A4 = 6-end of profile).

b.2) Six months growing period (experience 3 and 4, wheat), no differences between the radionuclides studied (Cs and Ag) were observed. In general the migration was low in both soils (around 85% remains in the two first cm), but in sandy soil it was slightly higher than in the sandy-loam soil.

3. Study of root uptake

In table II the transfer factor (experience 5 and 6) for the three radionuclides are given. TF for Sr is one order higher than for Cs and Ag in both soils. TFs for Cs and Ag decrease with the plant growth whereas for Sr it remains in the same order. For sandy soil the TFs observed were always higher for the three radionuclides studied. TFs have large variability due to the experimental conditions.

Table II - Transfer factors ($\text{m}^2 \text{kg}^{-1} (\text{dw})$). $X \pm 2 \sigma$

Experience	^{134}Cs	^{85}Sr	$^{110\text{m}}\text{Ag}$
5, seedling lettuce	0.006 ± 0.003	0.065 ± 0.026	0.015 ± 0.006
5, mature lettuce	0.002 ± 0.001	0.061 ± 0.015	0.002 ± 0.002
6, seedling lettuce	0.026 ± 0.020	0.288 ± 0.202	0.056 ± 0.038
6, mature lettuce	0.010 ± 0.009	0.204 ± 0.160	0.007 ± 0.004

In Table III show the mean values of Cs/Sr, Cs/Ag and Ag/Sr ratios present in seedling, young and mature lettuce. It can be noticed that this ratios increased in the following order

Sr > Cs > Ag. For sandy soil constant values were obtained more quickly than for sandy-loam soil.

Table III - Mean values of Cs/Sr, Cs/Ag and Ag/Sr ratios present in seedling, young and mature lettuce.

	Sandy soil			Sandy-loam soil		
	Cs/Sr	Cs/Ag	Ag/Sr	Cs/Sr	Cs/Ag	Ag/Sr
Seedling	0.29±0.12	1.72±0.35	0.17±0.04	0.55±0.34	1.59±0.57	0.37±0.20
Young	0.12±0.01	2.73±0.56	0.05±0.01	0.29±0.14	2.92±1.34	0.11±0.05
Mature	0.12±0.02	2.96±1.64	0.04±0.02	0.16±0.07	3.22±0.47	0.05±0.02

4. Influence of plant growth stages at the contamination time in final radionuclides level in plant

The % of Cs and Ag in mature plant v.s. total deposition decreased in the following order referred to contamination time: mature lettuce >> young lettuce > sowed lettuce > seedling lettuce (Fig. 2). For Sr no significant differences were observed and the % of Sr is always higher than the other two radionuclides, it seems to be correlated with the high solubility of this radionuclide.

Comparing the two types of soils, the contamination level in the sandy soil is higher due to the low soil fixation that can increase the root uptake. The differences between the two types of soil increased when the time elapsed between contamination and the harvesting increased too. For contamination in mature lettuce, % remaining in plant was 90% in soil 2 and 100% in soil 1. For the other studied growth stages the % of activity in mature lettuce was very low as it is shown in Figure 2.

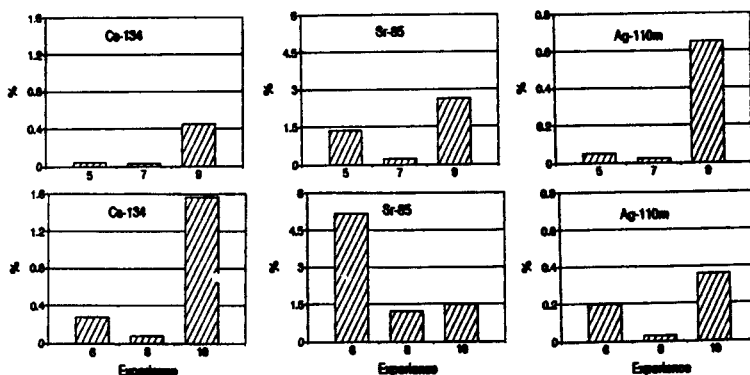


Figure 2. % of different radionuclides in mature plant v.s. total deposition (Experience 5, 7 and 9: soil 1; Experience 6, 8 and 10: soil 2)

5. Study of foliar uptake by sequential extraction

An experiment based on successive extraction has been designed to study the foliar uptake after deposition on leaves surface. The applied procedure use as extractant reagents distilled water, in order to wash not adhered aerosol and chloroform, in order to solubilize the waxes of plant cuticle and to release adhered aerosol. Both extracts were filtered (0.45 μm) to distinguish between soluble and particulate fractions. This experiment was carried out with seedling lettuce, young lettuce and mature lettuce (1, 2, 7, 8, 9 and 10 experiences) in order to study the influence of plant growth stages on deposition. Moreover the successive extraction procedure was carried out on mature lettuce before and after irrigation (1 and 2 experiences).

a. Influence of plant growth stages.

In figure 3 percentages of each fraction has been represented for three plant growth stages cultivated in sandy soil. It can be noticed that:

1. The percentages of radionuclide absorbed by the plant are 60-80% for ^{134}Cs , 40-50% for ^{85}Sr and 30-40% for $^{110\text{m}}\text{Ag}$.
2. The cesium absorbed by the plant decreased in the following order: mature > young > seedling. No difference is noticed in Ag and Sr behaviour.
3. From percentages of water soluble fraction and absorbed fraction, the solubility of aerosol deposited on leaves surfaces is 93% for ^{134}Cs , 84% for ^{85}Sr and 47% for $^{110\text{m}}\text{Ag}$.
4. Solubility in water and in chloroform decreased in the following order: Sr > Ag > Cs and Ag >> Sr > Cs, respectively.
5. The % Ag present as particulate phase is very high.

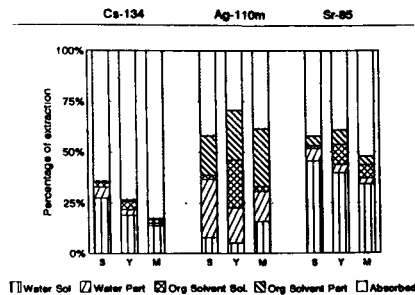


Figure 3. Percentages of each fraction for three plant growth stages cultivated in sandy soil

b. Influence of irrigation.

In sandy soil experience with mature lettuce the water extractable fraction decreases after irrigation as it was expected. In sandy-loam soil, on the contrary, this fraction increases for the radionuclides determined, Cs and Ag (Figure 4). For Cs this different behaviour could be related with the different K contents in soils.

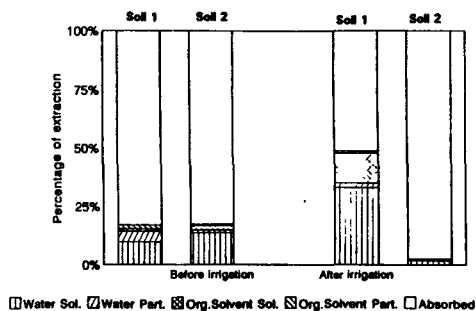


Figure 4. Cs % of each fraction before and after irrigation for two types of soils

Finally, the mean value Cs/Sr, Cs/Ag and Ag/Sr ratios present in the lettuce before and after irrigation and before and after applying the sequential extraction procedure have been calculated (Table IV). It must be pointed out a notable variation of all the radionuclides ratios before and after successive extraction for the recently polluted lettuces whereas for similar samples after irrigation no variation is observed.

Table IV - Radionuclides ratios in leaves before and after sequential extraction and before and after irrigation for sandy soil.

		Before extraction	After extraction
Before irrigation	Cs/Sr	4.96 ± 0.08	7.86 ± 0.08
	Cs/Ag	2.02 ± 0.04	5.18 ± 2.18
	Ag/Sr	2.45 ± 0.01	1.67 ± 0.05
After irrigation	Cs/Sr	5.55 ± 0.29	5.51 ± 1.02
	Cs/Ag	3.35 ± 1.52	3.19 ± 1.44
	Ag/Sr	1.92 ± 0.83	1.90 ± 0.50

The increase of the Cs/Sr and Cs/Ag ratios after successive extractions before irrigation would show that Cs is selectively absorbed by the plant. However after irrigation radionuclides ratios after successive extraction do not change significantly, probably due to a possible selective incorporation of Sr and Ag in the leaves and/or a selective leaching of Cs from the leaves.

6. Soil speciation by sequential extraction

In order to study the soil phases where radionuclides may be bound and the evolution of their distributions along the time, two sequential extraction schemes have been applied to both types of soil. One scheme points out organic matter role in radionuclide retention, and uses $MgCl_2$, $Na_4P_2O_7$, $NaOH$ and $H_2O_2-HNO_3-NH_4AcO$ as extractant reagents (1).

The second scheme, which has been used in BCR's working group (2) in solid speciation of heavy metals, has HAcO, NH₂OH.HCl and H₂O₂-NH₄AcO as extractant reagents.

Radionuclide distribution were studied at different stages from deposition time using both schemes. From the results the following behaviour can be concluded for the studied radionuclides:

a. Initial stage.

Sr is mainly extracted in the first fraction. Cs and Ag have similar behaviour, but residual fraction being higher in the former and exchangeable fraction higher in the latter. In general, soluble fractions are higher in sandy soil, residual fractions being higher in sandy-loam soil.

b. Stage after irrigation.

In this case the successive extraction has been carried out 15 days after the aerosol deposition. During these days the soil have received a similar amount of soluble Cs from the irrigation water. No difference is noticed in Sr distribution which keeps being mainly extracted in soluble fractions. For Cs and Ag soluble fraction practically keeps constant, with a slight decrease of residual fraction, may be due to input of soluble radionuclide coming from plant washings.

c. Stage after plant growth (3 months since deposition day).

A general decrease of soluble fraction and an increase of residual fraction are observed for Cs and Ag, showing an evolution from the original distribution. After three months Sr is completely soluble. The Figure 5 shows in bar diagram the obtained distribution for the three radionuclides at the initial stage and after plant growth using the BCR scheme for sandy-loam soil.

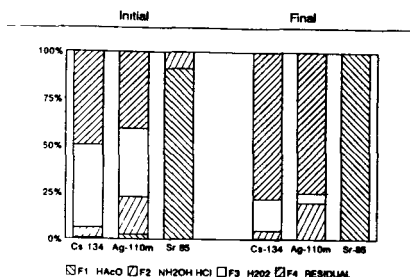


Figure 5. The distribution obtained for the three radionuclides at the initial stage and after plant growth using the BCR scheme for sandy-loam soil.

Publications

- (1) Rauret, G., Llauradó, M., Vidal, M., Vallejo, V.R., *Solid speciation of radiocesium in soils, Transfer of Radionuclides in Natural and Semi-natural Environments*, Ed. by Desmet, G., Nassimbeni, P., Belli, M.; Elsevier Applied Science, 538-545, 1990.
- (2) Vidal, M., Rauret, G., *Two approaches for sequential extraction of radionuclides in soils: batch and column methods*, Intern. J. Environ. Anal. Chem. (submitted).
- (3) Rauret, G., Llauradó, M., Tent, J., Rigol, A., Alegre, L.H., Utrillas, M.J., *Deposition on holm oak surfaces of accidentally released radionuclides*, Seminar on the dynamic behaviour of radionuclides in forest. Stockholm, Sweden. May 18-22, 1992

- (4) Sauras, T., Roca, M.C., Vallejo, R.V., Tent, J., Llauradó, M., Vidal M., Rauret, G., *Field migration study of radionuclides in Mediterranean forest soils using synthetic aerosol*, Seminar on the dynamic behaviour of radionuclides in forest. Stockholm, Sweden. May 18-22, 1992.
- (5) Llauradó, M., Vidal, M., Rauret, G., Roca, C., Fons, J., Vallejo, V.R., *Radiocaesium behaviour in Mediterranean conditions.*, Journal of Environmental Radioactivity (Submitted).
- (6) Vidal, M., Tent, J., Llauradó M., Rauret, G., *Study if the evaluation of radionuclides distribution in soils using sequential extraction schemes*, International Symposium on Radioecology. Znojmo, Czechoslovakia, October 1992.
- (7) Tent, J., Vidal, M., Llauradó, M., Rauret, G., Real J., Mischler, P., *Sequential extraction as a tool to study foliar uptake of radionuclides*, International Symposium on Radioecology. Znojmo, Czechoslovakia, October 1992.

Project 4

Head of project: *Dr. Colle*

Objectives for the reporting period

The knowledge of residual radioactivity in processed foods allows improvement in the estimations of ingested radioactivity for dose assessments and reveals the most efficient manufacturing processes for reducing the contamination of foodstuffs. Within this scope, the objectives of the programme are to quantify losses of potassium, strontium, caesium, cobalt and ruthenium during industrial processing of vegetable products.

Progress achieved

The artificial radioactivity of vegetables processed in French industry is under or near detection limits. This fact led us to measure stable isotopes, making the hypothesis that they behave in the same way as radioactive isotopes. This work was done through radioactivity measurements (gamma Ge spectrometry) and stable isotope measurements ((K by ICP/AES, Co, Cs, Sr and Ru, by ICP/MS), of samples collected in factories before and after processing. In parallel, we did complementary experimentations on contaminated vegetables which were processed in the laboratory.

Conventionally, results are relative to fresh weights and are presented as follows:

Rw Retention factor: Bq (μ g)/kg of processed food by Bq (μ g)/kg of raw food,

Rmw Mass retention factor: kg of processed food / kg of raw food,

Rt Residual activité in percent: total Bq (μ g) of processed food / total Bq (μ g) of raw food
 $Rt = Rw \times Rmw \times 100$.

1. Industrial products measurements (cf. table 1)

Vegetable Oils:

It was impossible to mineralize oils, and so to measure stable elements. During the process olive \rightarrow olive oil, ^{40}K is totally eliminated (60 % in water and 40 % in oil cake); ^{137}Cs residual activity is less than 13% .

Cereals:

Generally, cereals processing causes a noticeable decrease of the mineral content in commercialized cereal products. The retention factors *Rw* from whole raw grains are respectively in the order of 0,4 to 0,6 for durum wheat semolina, of 0,2 to 0,3 for soft wheat flour and of 0,1 to 0,4 for milled rice, depending on the element. The mass retention factor *Rmw* being 0,70 to 0,75, this leads to residual activities from 10 to 40 % .

Potatoes:

More than 99 % of potassium is retained in crisps, whereas for cobalt and caesium, respectively 50% and 20% of the initial content in potatoes remains in crisps. There is no evident explanation for the observed increase of strontium.

Canned fruits and vegetables:

After industrial canning, the dry matter loss varies from 20% (green beans, peas), to 50% (tomatoes), although the fresh mass retention factor is only about 0,90 for vegetables. Retention factors are variable depending on the product and the element; highest values are observed for fruits in syrup, lowest values for tomatoes. The apparent increase of strontium in canned fruits seems to be due to syrup strontium content.

Tableau 1. : Industrial foodstuffs data: retention of elements by processed crops

Product	R _{mw}	Retention factor R _w					Residual activity R _t			
		⁴⁰ K	K	Sr	Co	Cs	⁴⁰ K	Sr	Co	Cs
Sunflower seed oil raw -> refined	0,95	<0,25	-	-	-	-	< 24	-	-	-
Olives -> oil cake	0,52	0,75	-	-	-	0,84*	39	-	-	43*
Olives -> olive oil	0,19	<0,001	-	-	-	<0,7*	0	-	-	<13*
Durum wheat -> semolina	0,75	0,45	0,57	0,48	0,57	0,47	34	36	43	36
Durum wheat -> by-products	0,23	2,86	3,15	3,50	-	1,39	66	81	-	32
Soft wheat -> flour	0,75	0,31	0,29	0,27	0,19	0,28	20	20	14	21
Soft wheat -> by-products	0,23	3,68	3,00	3,17	2,62	1,53	80	73	60	35
Round paddy rice -> husked	0,80	0,9	-	0,5	0,6	0,8	72	40	48	64
Round husked rice -> milled	0,88	0,4	-	0,3	0,6	0,3	35	26	53	26
Round paddy rice -> milled	0,70	0,4	-	0,15	0,36	0,24 0,14*	28	11	25	17 10*
Long paddy rice -> husked	0,80	0,63	-	-	-	-	50	-	-	-
Long husked rice -> milled	0,88	0,42	0,28	0,20	0,16	0,27	37	18	14	25
Long paddy rice -> milled	0,70	0,26	0,20	0,17	0,37	0,14*	18	12	26	10*
Long husked rice -> flour	0,13	6,17	4,54	6,7	6,3	7,4	74	84	78	57
Long paddy rice -> by-products	0,20	1,78	1,72	-	-	-	36	-	-	-
Long paddy rice -> flour	0,10	3,87	-	-	-	-	39	-	-	-
Potato -> cripsa	0,75	-	-	4,6	0,7	0,3	-	350	50	19
Cherry -> canned in syrup	0,90	0,60	0,47	0,5**	0,5	0,9	54	54**	44	85
Peach -> canned in syrup	0,88	0,50	0,58	-	0,4	0,7	44	-	37	57
Pear -> canned in syrup	0,88	0,53	0,53	0,6**	0,8	0,8	47	63**	67	73
Peas -> canned	0,97	0,42	0,36	1,6	0,2	-	45	175	23	-
Green bean -> canned	1,03	0,45	0,53	0,9	0,4	0,5	47	87	44	51
Tomato -> canned	1,07	0,25	0,41	0,3	0,3	0,3	25	25	27	30

* values from ¹³⁷Cs

** values after correction including strontium content of syrup

2. Laboratory food processing

Some processing was done in laboratory: namely, making apple juice, canning vegetables, and making wines.

Apple juice (made with samples from Chernobyl)

Apples collected in Bielorusia, near Chernobyl, in September 1991, were used to make apple juice. The ¹³⁷Cs residual activity, relative to the whole raw apple is 56% for juice, 19% for squeezed pulp, 26% for peel and core, which corresponds exactly to the mass distribution in fruit. The activity reduction in juice reflects only the mass decrease due to processing.

Canned vegetables (cf table 2 and figure 1):

Green beans and peas grown on soils contaminated by radioactivity, were treated in laboratory: vegetables were washed, peeled or stalked, washed, blanched and then canned in water with 2% salt. One month later, vegetables were drained and rinsed. Various parts before and after processing were measured by gamma Ge spectrometry. Relative to raw vegetables, the recovery in canned beans was 24 % of ¹³⁴Cs, 31 % of ⁵⁷Co and 50 % of ⁸⁵Sr. Concerning canned carrots, only 3 % of ¹³⁴Cs, 4 % of ⁵⁷Co et 13 % of ¹⁰⁶Ru remained.

Table 2. : Experimental data: root contaminated vegetables canned in the laboratory.

	R _{mw}	Retention factor R _w			
		⁵⁷ Co	¹³⁴ Cs	⁹⁰ Sr	¹⁰⁶ Ru
R _w bean pods -> tinned	1,0	0,31	0,24	0,46	-
R _w raw carrots -> tinned	0,5	0,1	0,1	-	0,2

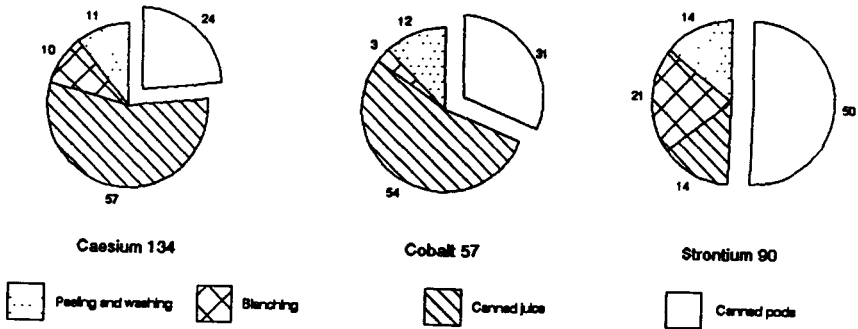


Figure 1 - Green bean radioactivity distribution during canning (%)

Wine making (Cf table 3 and figure 2)

Measurements (gamma Ge and ICP/MS) were done on two batches of grapes used for making red and rosé wine. The wines residual activity is about 20 % for strontium, 5 to 30 % for caesium, 10 à 30 % for cobalt, and 20 to 40% for potassium.

Table 3. : Data concerning experimental wine making.

	R _{mw}	Retention factor R _w				R _{mw} ⁹⁰ Sr	
		⁴⁰ K	Co	Cs	Sr		
Rosé wine	46	0,48	0,50	0,58	0,38	42	0,37
Red wine from whole bunch	54	0,92	0,62	0,42	0,62	46	0,49
Red wine from grapes	43	0,87	0,32	0,13	0,61	52	0,37

R_{mw} : l wine/ kg (fresh weight) of grappes

R_w : Bq (or µg) /l of wine per Bq (or µg) per kg (fresh weight) of grappes

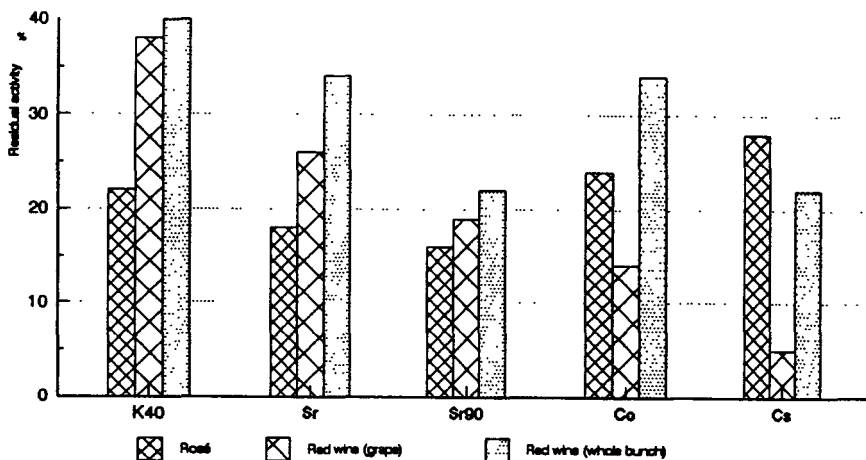


Figure 2 - Retention of radioactive and stable elements in wine (% of grapes activity)

3. Conclusions

The analogy between stable and radioactive isotopes seems rather coherent; nevertheless, the use of stable measurements data in industrial French products appears to be a disappointing option:

- getting samples is very difficult,
- raw and processed foods might come from different batches,
- samples preparing is long and critical due to the kind and quantities (up to 3 kg) of samples,
- some ICP/MS data are unusable (ruthénium: data below detection limits) or uncertain (caesium or cobalt: data near detection thresholds),
- stable element addition during the industrial process itself makes extrapolation of data for contaminated vegetables quite difficult.

On the other hand, a study of experimentally processed vegetables may not give full satisfaction if the studied processes are the simplest ones (such as canning) and use few raw products. Technically, it is rather impracticable to grow large amounts of contaminated foods and to use several different pilot processing installations with contaminated materials. Nevertheless, experimental data from radioisotopes are more reliable than stable element results, because experimental parameters are more controlled and radioactivity levels high enough for reliable detection. Moreover, these kind of experiments may give a better knowledge of the relative efficiency of different processes by studying radionuclides distribution in vegetables.

In spite of difficulties inherent in the present project, useful data were obtained. The results show that food processing is an interesting means of decreasing the radioisotope contamination of agricultural products. The reduction is more often very superior to the mass decrease (due to the processing itself), and this is obviously expressed by retention factors mainly below unity. In the case of crops contaminated by radioactivity, as food processing allows long storage of foodstuffs, this decrease should be amplified with physical decay of radioactive nuclides.

Project 5

Head of project: *Dr. Cawse*

Objectives for the reporting period

The objectives in 1990/91 were to (i) cultivate and/or obtain food products from a region having relatively high concentrations of radionuclides in soil, for processing in the pilot plant facilities at Reading University Department of Food Science and Technology, (ii) prepare raw and processed foods for analysis of radionuclides and stable elements, and (iii) analyse the samples for K-40, Co-60, Sr-90, Ru-106 and Cs-137 together with their stable isotopes. Analysis of some factory processed vegetables would be started.

In 1991/92 an equal balance was required between measurements of radionuclides and stable elements in foods processed by the pilot plant facilities and by factories. Products to be examined were potatoes, carrots, peas, beetroot, fruit juices (apple and blackcurrant), mushrooms and rape seed oil. In addition, some dairy products would be analysed. Ruthenium-103 tracer would be applied to leafy vegetables to assess the removal by normal culinary practice. Discussion of results was required with CEN Cadarache (Dr C Colle and Dr S Roussel-Debet) who have studied crops specific to France. (See Project 4).

Progress achieved including publications

1. Processing in the pilot plant facilities

The Sellafield region of Cumbria, North West England, was chosen for cultivation by Harwell of beetroot, peas, potatoes, brussels sprouts, carrots, wheat and for collection of field mushrooms. This region has a relatively high concentration of Cs-137 in soil owing to fallout from the Chernobyl accident in 1986 and historical releases of radionuclides from Sellafield Works. Concentrations of Sr-90 are ~10 Bq/kg dry soil, and ~60 Bq/kg for Cs-137. Dairy products were also prepared from milk obtained in this region. Varieties of vegetables were selected according to their use by the food processing industry in Gt. Britain. For example, four varieties of peas and six varieties of potatoes were grown to include freezing, canning and dehydration processes, and domestic uses. Details of processing methods used for vegetables in the pilot plant studies are described in Project 6, by Reading University.

The processed samples were oven-dried and ashed for analysis of radionuclides. A sub-sample of 50 g of dry material was ground in an agate ball-mill for measurement of stable elements: 0.5 g of the ground sample was then wet-ashed in nitric/perchloric acid and diluted to 10 ml for analysis by ICP-MS. Cs-137 was present in raw crops at a maximum concentration of 2.2 Bq/kg dry weight, except for 44 Bq/kg in field mushroom in 1990 and 13.5 Bq/kg in 1991. For Sr-90 and K-40, maximum values were 12 Bq/kg and 2340 Bq/kg dry weight (for details see project 6). All raw samples contained <1 Bq Co-60 and <1 Bq Ru-106/kg dry weight. Ag-110 m was detected in mushroom in the course of γ -spectrometry, at 28 Bq/kg dry weight in 1990. It is known from measurements by other workers that fungi accumulate this radionuclide.

Food processing retention factors for radionuclides and stable cobalt in vegetables and wheat in vegetables and what were derived as defined in Table 1, with examples. Retention factors on a wet weight basis (R_w), as in food prepared for human consumption, are shown in Figs. 1 and 2 for Sr-90 and Cs-137 and Fig. 3 for Co (radioactive Co not measurable). Retention factors varied according to processing treatments, with R_d in the range 0.1 - 2.4 for Cs-137, 0.2 - 3.2 for K-40, 0.2 - 2.7 for stable Co, and 0.1 - 1.3 for Sr-90. Increased concentrations of radionuclides in some products were more pronounced for retention factors derived on a fresh weight basis (R_w) where the range was increased in dehydrated products and potato crisps (Figs. 1 to 3). Measurements of Cs-137 in dairy samples are described in Project 6.

Table 1. Comparison of Some Processing Retention Factors for Sr-90 and Cs-137 Derived on a Dry weight, Fresh Weight and Total Recovery Basis (Pilot Plant)

Crop	Variety	Processing Method	Rd	Rw	Rt	Rd	Rw	Rt
			Sr-90	Sr-90	Sr-90	Cs-137	Cs-137	Cs-137
Beetroot	Boltardy	Canning	1.0	0.76	0.75	1.4	0.96	1.11
		Boiled	0.25	0.26	0.26	0.46	0.46	0.37
Pea	Maro	Canning	0.93	0.76	0.76	<0.2	<0.1	<0.2
		Dehydrated	0.93	3.9	0.75	1.1	2.5	0.85
Potato	Record	Crisps	1.3	3.0	0.78	0.71	1.8	0.43
Potato	Maris Peer	Canning	0.67	0.50	0.51	0.55	0.41	0.42
Potato	Romano	Dehydrated	0.98	4.5	0.54	1.1	4.9	0.61
B.Sprouts	Beford	Boiled	0.53	0.44	0.47	1.0	0.78	0.88
Carrot	Narman	Boiled	0.81	0.52	0.47	0.14	0.06	0.08
Wheat	Tonic	Milled Flour	0.10	0.10	0.06	0.36	0.36	0.22
Mushroom (1991)	Agaricus campestris	Dehydrated	0.84	10.0	0.60	0.96	12.2	0.68

Notes: RETENTION FACTORS

$$R_d = \frac{\text{Activity/g in dry processed food}}{\text{Activity/g in dry raw food}}$$

$$R_w = \frac{\text{Activity/g in fresh raw food}}{\text{Activity/g in fresh raw food}}$$

$$R_m = \frac{\text{total dry wt processed food}}{\text{total dry wt raw food}}$$

$$R_t = R_d \times \text{dry matter retention factor (R}_m\text{)}$$

Retention of Cs-137 and K-40 by processed foods showed a highly significant correlation whereas no correlations existed between Sr-90 and Cs-137 retention or between Sr-90 and K-40. This is attributed to the association of strontium, like calcium, with cell wall structures unlike potassium which is essentially a constituent of the cell sap and cytoplasm and provides a useful indicator for Cs-137 behaviour during processing.

The parameter R_t for the total recovery of radioactivity (Table 1) is more appropriate to process stream analysis with potential releases of activity in waste rather than assessment of food chain transfer, unless by-products containing radionuclides are used for animal feed. Losses of dry matter during food processing were recorded and retention factors (R_m) were derived. In some canned crops considerable amounts of dry matter were lost, and retention factors (R_m) were in the region 0.5 - 0.6. However, factors of 0.8 - 0.9 were evident for many of the boiled and dehydrated crops.

Stable R_u was <0.02 $\mu\text{g/g}$ dry weight in all samples except raw carrot (0.065 $\mu\text{g/g}$): soil to plant transfer of this element is known to be low. Therefore a foliar application of Ru-103 tracer was made to spinach, cauliflower and brussels sprouts at maturity, and removal by boiling was recorded after 24 hours (Table 2). The R_w 0.63 for Ru-103 applied to spinach was similar to factors for internal tracers K-40 and Cs-137 ie. from soil to plant transfer. For cauliflower, R_w for Ru-103 and K-40 were comparable, but in the case of sprouts Ru-103 showed less retention than the other crops but there was higher retention of K-40.

2. Factory processing

Retention factors for stable Sr, Cs and K in processed vegetables and wheat are listed in Table 3. The parameters R_m and R_t cannot be derived from factory studies, where processing is continuous. Very low retention factors (R_w) for Sr, Cs and K were found for oilseed rape, as anticipated from the extraction process. In contrast, elevated factors occurred for blackcurrant and apple juice concentrates. As in the pilot plant measurements, increased R_w factors were evident for crisps, dehydrated potato and mushrooms.

Results from both the pilot plant and factory studies show that elimination by food processing of radioactive material from the food chain can be considerable, according to the crop and processing method used, although potato crisps and other dehydrated products show increased concentrations of radioactivity, and fruit juices are

expected to be similar, based on results from analysis of stable Sr, Cs, K and Co. Further, from our knowledge of soil to plant transfer factors for crops grown in the W. Cumbria area, the influence of food processing on removal or concentration of radionuclides taken up by crops from contaminated soils following an accidental release may be assessed. The project was jointly supported by the CEC and Ministry of Agriculture, Fisheries and Food, London.

Publications

- (i) Cawse, P.A., Baker, S.J., Grandison, A.S., Lewis, M.J. and Patel, S. (1991). The influence of processing on the radionuclide content of food. CEC Seminar on Intervention Levels and Countermeasures for Nuclear Accidents, Cadarache, 7-11 October, 1991.
- (ii) Patel, S., Grandison, A.S., Cawse, P.A. and Lewis, M.J. (1991). A poster entitled 'Influence of Processing on the Radionuclide Content of Food', was presented at the 8th World Congress of Food Science and Technology, Toronto, 29 September - 4 October 1991.

Table 2. Retention Factors for Ru-103, K-40 and Cs-137 after Boiling Vegetables

Crop		Rd	Rw	Rt	Rm
Spinach	Ru-103	0.69	0.63	0.60	0.88
	K-40	(0.68)	(0.63)	(0.60)	
	Cs-137	(0.78)	(0.68)	(0.69)	
Cauliflower	Ru-103	0.81	0.55	0.53	0.65
	K-40	(0.88)	(0.59)	(0.57)	
Brussels Sprouts	Ru-103	0.54	0.49	0.52	0.96
	K-40	(0.85)	(0.77)	(0.82)	

Notes: (i) For retention factor definitions see Table 1. K-40 and Cs-137 data is in parentheses to indicate activity in vegetables by soil-to-plant transfer (internal tracer).

(ii) Ru-103 was applied as a spray to mature vegetables (external tracer). The activity was present as chloro-complexes of ruthenium.

Table 3. Retention Factors for Stable Sr and Cs Derived on a Dry Weight and Fresh Weight Basis for Factory Processed Crops

Crop	Processing Method	Rd Sr	Rw Sr	Rd Cs	Rw Cs	Rd K	Rw K
Pea	Canning	0.88	0.78	0.43	0.40	0.51	0.48
	Freezing	0.98	1.1	0.44	0.67	0.82	0.93
Potato	Crisps	4.2	15.7	<0.5	<2	0.61	2.4
Potato	Canning	1.3	0.80	4.0	2.5	1.1	0.68
Potato	Dehydrated	0.79	3.0	4.0	15.7	1.4	5.0
B. Sprouts.	Freezing	1.1	0.91	0.86	0.75	0.87	0.73
Carrot	Canning	0.63	0.56	2.0	1.5	0.84	0.71
Wheat (flour)	Milled	0.42	0.43	0.48	0.52	0.37	0.36
Mushrooms	Dehydrated	0.61	11.0	0.94	13.9	0.93	13.9
Blackcurrant	Juice Conc.	1.8	96.7 ⁺	1.7	75.0 ⁺	1.4	86.1 ⁺
Apple	Juice Conc.	0.25	13.7 ⁺	0.56	26.7 ⁺	1.4	2450 ⁺
Oilseed Rape	Solvent Extn.	-	0.002	-	<0.03	-	<0.0005

Note: $^+Rw = \frac{\mu\text{g/ml fresh juice}}{\mu\text{g/g fresh fruit}}$. The fruit juices are concentrates.

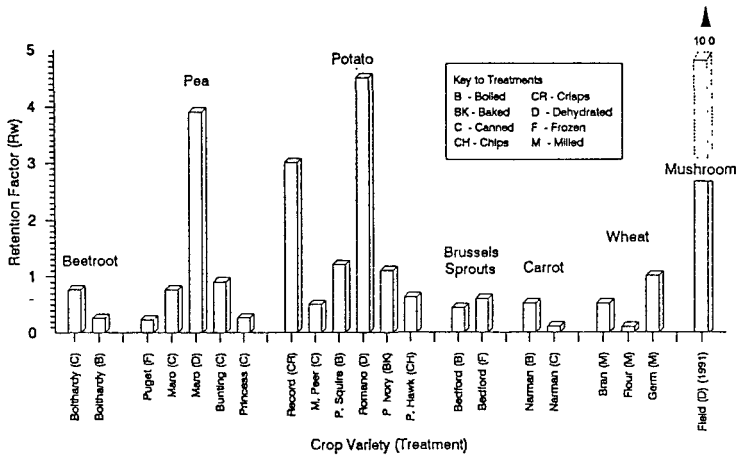


Figure 1: Food processing retention factors for Sr-90 derived from fresh weight concentrations, for pilot plant processed crops.

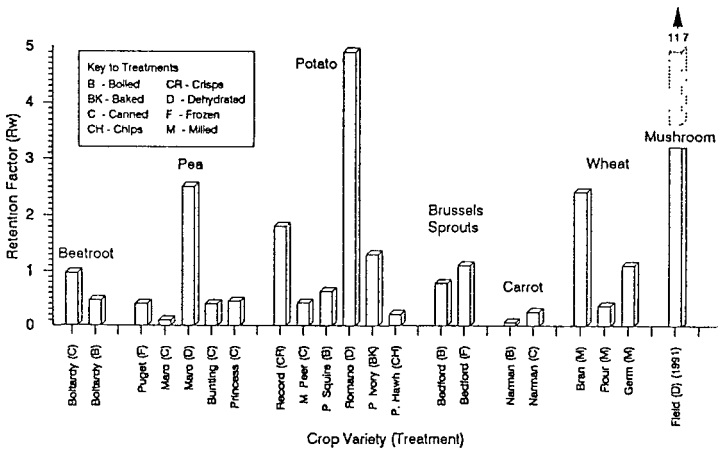


Figure 2: Food processing retention factors for Cs-137 derived from fresh weight concentrations, for pilot plant processed crops.

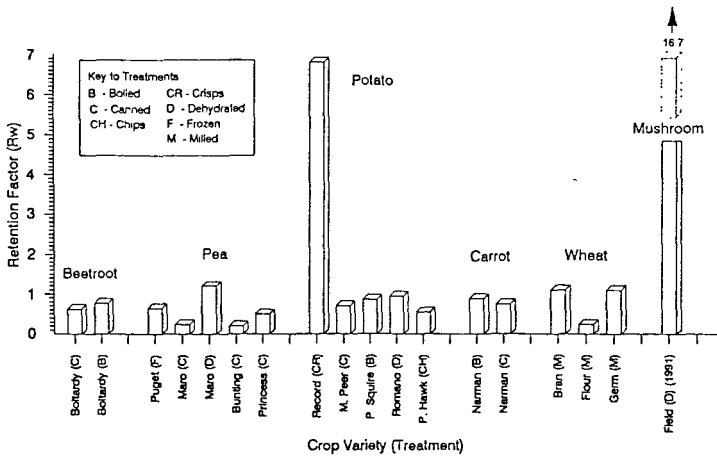


Figure 3: Food processing retention factors for stable cobalt derived from fresh weight concentrations, for pot plant processed crops.

Project 6

Head of project: *Dr. Grandison*

Objectives for the reporting period

To determine the extent of radionuclide transfer through the food chain to man as modified by food processing, and thus to improve the reliability of radiological assessment. The study includes assessment of radionuclides Sr-90, Cs-137, Co-60 and Ru-106 following pilot plant processing at Reading University of raw materials produced in the Sellafield region of Cumbria as directed by Harwell Laboratory. Additionally, assessment of stable isotopes of Cs, Sr, Ru and Co in raw materials and products would be made. Natural radioactivity due to K-40 and stable K will also be measured.

In the first year effort will be concentrated on measurements using pilot plant to help identify the most important processes that modify the concentrations of radionuclides in food. The effects of freezing, canning, drying and culinary preparation on vegetables and milling of wheat will be studied. Measurements are required on some dairy products such as cream, skimmed milk, hard and soft cheeses and whey.

In the second year a comparison between pilot plant and factory studies is required. Therefore, samples from the processing of vegetables and wheat, and the production of fruit juices, rapeseed oil and dairy products obtained from United Kingdom factories would be examined.

This programme of measurements complements the studies of French samples carried out by CEN Cadarache (Project 4).

Progress achieved including publications

1. Crops for food processing

Crops were produced in the Sellafield region of West Cumbria which received significant fallout of radioactive caesium following the Chernobyl accident in April 1986. This region has a relatively high concentration of Cs-137 owing to fallout from Chernobyl and historical releases of radionuclides from Sellafield works. The crops examined were beetroot, peas (4 varieties), potatoes (6 varieties), Brussels sprouts, carrots, mushrooms and wheat.

2. Pilot plant studies

A list of crops and varieties grown is given in Table 1, together with the type of processing carried out. Varieties were selected according to their use by the food processing industry in Great Britain. Processes were established to simulate commercial production of a range of products. All foods were processed using pilot plant facilities available at the University of Reading. Methods used for processing are summarised in Table 2.

Total dry matter recovery from prepared foods after processing was recorded (Table 1). This was expressed as R_m , which is the food processing retention factor for dry matter. Princess and Bunting peas (both varieties used for canning) showed a marked difference in the R_m factor (0.5 and 0.98 respectively), suggesting factors such as state of maturity and variety are of importance. The low R_m value for Romano potatoes may be accounted for by processing loss. Raw and processed samples were sent to Harwell for radionuclide and stable element analysis. The concentrations of Sr-90, Cs-137 and K-40 in the washed raw crops are listed in Table 1. For the vegetable and wheat crops, the concentrations of radionuclides were in the range of 0.023 - 12.0 Bq/kg for Sr-90, 0.42 - 2.2 Bq/kg for Cs-137 and 178 - 2340 Bq/kg for K-40.

In addition, milk from an area to the North-West of Sellafield was obtained to make dairy products using established methods. Cheddar and soft cheese were both made using rennet for coagulation. Cs-137 concentrations and retention factors are shown in Table 5.

3. Factory samples

Samples of raw materials and products were obtained from commercial producers for analysis of stable elements by Inductively Coupled Plasma Mass Spectrometry (ICP-MS) at AEA Harwell Laboratories. These results are summarised in Table 3. Wheat bran and germ showed concentration of all stable elements and radionuclides suggesting that they are associated with these fractions of the wheat (Table 4). Fruits are commercially processed to produce concentrates which are then diluted to produce juice (blackcurrant concentrate would be diluted approximately 20 times and apple concentrate about 10 times). The samples analysed were concentrates, therefore concentrations of Sr, Cs and K in blackcurrant and apple concentrate showed Retention factors on a wet weight basis (Rw) that far exceeded the corresponding factors for other products (see Project 5, Dr Cawse). Preparation of dehydrated products such as potato powder causes an increase in concentrations of radioactivity, although rehydration before human consumption will reverse this effect. Oil recovery from rape seed is approximately 40%, the extraction being achieved by pressing followed by solvent extraction.

This project was jointly funded by the CEC and Ministry of Agriculture, Fisheries and Foods, London.

Table 1 Food processing retention factors (Rm) for dry matter.

Crop	Variety	Processing	Moisture content in raw crop (%)	Rm for products	Radionuclide concentration in raw crops (Bq/kg dry weight)		
					Sr-90	Cs-137	K-40
Beetroot	Boltardy	Canning	86.9	0.75	3.8	2	391
		Domestic		0.8			
Pea	Puget	Freezing	78.3	0.87	1.8	0.7	430
Pea	Maro	Canning	67.7	0.82	1.4	0.64	450
		Dehydration		0.81			
Pea	Bunting	Canning	66.4	0.98	1.5	0.75	499
Pea	Princess	Canning	71	0.5	1.4	0.85	629
Potato	Record	Crisps	75.2	0.6	0.023	2.1	730
Potato	Maris Peer	Canning	73.6	0.76	1.2	2.2	454
Potato	Pentland Squire	Domestic boiled	77.1	0.82	0.17	2.1	660
Potato	Romano	Dehydration	78.4	0.55	0.61	0.67	370
Potato	Pentland Ivory	Domestic baked	78.2	1.0	0.26	0.89	680
Potato	Pentland Hawk	Chips	78.6	0.77	0.55	0.52	827
Brussels sprouts	Bedford	Domestic boiled	88.1	0.88	3.6	0.75	1710
		Canning		0.93			
Carrot	Narman	Domestic boiled	90.7	0.58	12	1.7	324
		Canning		0.53			
Wheat	Tonic	Flour milled	15	0.61	2.5	0.42	178
Mushroom (1990) (1991)	Agaricus campestris	Dehydration	93.7	0.86	N.A.	44.0	1630
			92.5	0.71	1.90	13.5	2340

Notes.

1. $R_m = \frac{\text{total dry weight of processed food}}{\text{total dry weight of raw food}} = \text{food processing retention factor for dry matter}$
2. Concentrations of Co-60 and Ru-106 in all samples were < 1 Bq/kg dry weight.
3. All crops were grown in the Sellafeld area and were sampled in autumn 1990, except beetroot in 1991 and mushrooms which were resampled in autumn 1991 to provide data for Sr-90.
4. Root crops were peeled before analysis.
5. All processing was carried out in the pilot plant.
6. N.A. - not available.

Table 2 Summary of processing methods in the pilot plant.

Crop	Processing method	Treatment
Beetroot	Canning	Canned in a solution of 2% NaCl and 2% sugar Cans were processed for 30 minutes at 121° C.
	Domestic	Boiled for 30 minutes.
Pea	Freezing	Blanched for 1.5 minutes, cooled and frozen.
	Canning	Blanched for 2 minutes, cooled and canned in a solution of 2% NaCl and 3% sugar Cans were processed for 45 minutes at 115° C.
Potato	Canning	As for peas except cans were processed for 32 minutes at 121° C
	Dehydration	Sliced to ~12 mm thickness and pre-cooked for 120 minutes in atmospheric steam, then mashed and placed in a drum drier.
	Baking	In aluminium foil for 60 minutes at 230° C.
	Domestic	Boiled for 25 minutes.
Brussels sprouts	Domestic	Boiled for 10 minutes
	Freezing	Blanched for 5 minutes, cooled and frozen.
Carrot	Domestic	Sliced and boiled for 15 minutes.
	Canning	Whole carrots were blanched for 3 minutes, cooled and canned in 2% NaCl solution. Cans were processed for 25 minutes at 121° C.
Mushroom	Dehydrated	Blanched for 5 minutes, cooled and freeze-dried for 24 hours.

Table 3 Stable element concentration on dry weight basis, during food processing (factory operations).

Crop	Stable element concentration in crop (µg/g dry weight)									
	Raw					Prepared				
	Sr	Cs	K (mg/g)	Co	Treatment	Sr	Cs	K (mg/g)	Co	
Pea	12.2	0.016	14.0	0.061	Frozen	11.9	0.007	11.5	<0.02	
	10.9	0.007	14.0	0.081	Canned	9.6	0.003	7.2	<0.02	
Potato	0.31	0.0098	15.7	0.078	Crisps	1.3	<0.005	9.6	0.030	
	2.1	0.002	14.1	<0.02	Canned	2.7	0.008	15.6	<0.02	
	4.2	0.003	16.1	<0.02	Dehydrated	3.3	0.012	22.2	0.058	
B sprouts	6.8	0.049	31.5	0.060	Frozen	7.5	0.042	27.4	<0.02	
Carrot	19.5	0.004	15.2	<0.02	Canned	12.2	0.008	12.7	<0.02	
Wheat (milled)	2.6	0.012	3.8	0.053	Bran	7.8	0.021	11.8	0.082	
	2.6	0.012	3.8	0.053	Flour	1.1	0.0058	1.4	0.055	
	2.6	0.012	3.8	0.053	Germ	6.5	0.0092	7.5	0.079	
Mushroom	1.8	0.054	37.1	0.097	Dehydrated	1.1	0.051	34.4	0.028	
Blackcurrant	7.1	0.010	15.8	0.16	Concentrate	13.0	0.017	21.5	0.15	
Apple	1.9	0.052	7.1	<0.02	Concentrate	0.48	0.029	9.6	<0.05	
Rape Seed	15.1	0.033	6.4	0.054	Oil	0.030	<0.001	<0.003	<0.02	

Note Rape seed oil concentrations are expressed as µg/g fresh weight basis

Table 4 Concentrations of radionuclides and retention factors derived on fresh weight basis (Rw) from wheat processed in the pilot plant and in factory operations.

Variety	Product	Radionuclide Concentration (Bq/kg dry weight)			Retention factor (Rw)		
		Sr-90	Cs-137	K-40	Sr-90	Cs-137	K-40
Pilot plant processed							
Tonic	Raw	2.5	0.42	178			
	Bran	1.3	1.0	573	0.52	2.4	3.2
	Flour	0.25	0.15	63	0.10	0.36	0.35
	Germ	2.4	0.47	220	0.96	1.1	1.2
Factory processed							
Mercia/ Avalon	Raw	0.11	<0.05	145			
	Bran	0.41	0.16	510	4.0	>3.0	3.7
	Flour	0.04	0.029	59	0.38	>0.5	0.42
	Germ	0.24	0.10	360	2.3	>2	2.6

Note: 1. All products resulted from milling of the raw wheat.
 2. $Rw = \text{retention factor on fresh weight basis} = \frac{\text{activity/g in fresh processed food}}{\text{activity/g in fresh raw food}}$

Table 5 Cs-137 concentrations and retention factors for dairy products.

	Milk	Skim milk	Cream	Cheddar	Cheddar whey	Soft Cheese	Soft Cheese Whey
Cs-137 (Bq/kg fresh weight)	0.24	0.25	0.11	0.21	<0.8	0.30	0.27
Ft	--	0.92	0.04	<0.3	0.66	0.20	0.82
Fe	--	0.90	0.08	0.10	0.74	0.18	0.64

Note: $Ft = \text{Processing retention factor} = \frac{\text{total Bq product}}{\text{total Bq raw milk}}$

$Fe = \text{Processing efficiency factor} = \frac{\text{kg prepared product}}{\text{kg raw milk}}$

Publications

4.1 Cawse, P.A., Baker, S.J., Grandison, A.S., Lewis, M.J. and Patel, S. (1991). The influence of processing on the radionuclide content of food. CEC Seminar on Intervention Levels and Countermeasures for Nuclear Accidents, Cadarache, 7-11 October, 1991.

4.2 Patel, S., Grandison, A.S., Lewis, M.J. and Cawse, P.A. (1991). 'The influence of processing on the radionuclide content of food' was presented at the 8th World Congress of Food Science and Technology held in Toronto from 30 September-4 October, 1991.

Project 7

Head of project: *Dr. Gutiérrez*

Objectives for the reporting period

In the first year of the project (1990-91) the objectives dealt with the establishment of the main characteristics of Spanish Mediterranean diet, identification of the major agricultural cultures produced and consumed and a comparison of the differences in relation with other EC areas.

For the 1991-92 period a further analysis at a national level was envisaged keeping as the main objective to establish the potential influence of diets in dose estimation by ingestion as a consequence of an accidental radiological contamination.

As a secondary objective an attempt to obtain soil-plant transfer factors (Cs and Sr) for selected crops (experimental work) was envisaged.

Progress achieved

1. Food consumption and agricultural production

A characterization of Spanish Mediterranean food consumption and agricultural production (including cattle) has been made from statistical information based on national official sources. Five regions have been considered as specific Mediterranean areas. For comparison purposes, information of the whole country and data of EC countries have also been taken into account. In a first step, the comparison focusses on the differences between Spanish Mediterranean area and other EC areas and the whole EC. In relation with food consumption Table 1 present a summary analysis showing ratios between different diets.

Table 1.- Food consumption ratios

FOOD	1	2	3	4	5
Cereals	1.07	1.40	1.30	1.66	1.27
Milk & product	0.83	1.04	1.15	0.96	0.83
Eggs	0.86	1.19	1.17	1.21	1.04
Oil(l)	1.01	2.43	1.75	3.73	2.12
Potatoes	0.97	1.06	1.25	0.93	0.75
Vegetables & pulses	1.10	0.95	0.79	1.20	1.51
Fruit	1.00	1.12	0.94	1.38	1.47
Meat	0.99	0.95	0.83	0.88	1.06
Fish	0.95	1.98	1.86	2.15	1.16
Wine(l)	0.88	2.03	1.11	3.64	3.28
Beer(l)	1.24	1.32	2.62	0.89	0.34

1. Ratio Spanish Mediterranean to total Spanish diet

2. Ratio Spanish Mediterranean to CE diet

3. Ratio Spanish Mediterranean to CE Mediterranean countries diet

4. Ratio Spanish Mediterranean to CE no Mediterranean countries diet

5. Ratio CE Mediterranean countries to CE no Mediterranean countries diet

Table 2 summarizes the important role of Mediterranean contributions to some global EC agricultural productions. From this comparison it seems that even if some differences in consumption of oil, vegetable, fruit and wine clearly appear for different EC areas, diets are, in general, more similar than agricultural productions, which keep more significant variations. It gives to some Mediterranean foods a potentially growing influence in dose estimations following an accidental radiological contamination.

Table 2. Percentages of Mediterranean contribution to some representative agricultural productions

	RICE	TOMATOES	ONIONS	CITRICS	OTHER FRUITS	OLIVE	WINE
SP.MEDIT/SP	88	55	53	100	55	84	29
EC.MEDIT/EC	100	86	66	100	--	100	90
SP/EC	26	19	38	50	--	42	18

The limited scope of the project does not allow further analysis at an European level. However Spain, even considered as a Mediterranean country, has a wide diversity of climates involving significant regional differences on agricultural productions and practices. A deeper study at a national level has been made in a second step of the project.

Agricultural cultures are grouped in eight major blocks: cereals (rice excluded), rice, potatoes, dry pulses, roots, vegetables, fruits (citrics excluded) and citrics.

Table 3 and Fig. 1 show average food consumption for the Spanish Mediterranean areas, the rest of the country and the whole country. In Table 3, where specific data for each of the five Spanish Mediterranean region considered and other groups of foods are included, the values are corrected to take into account outside home contribution to diet. Fig. 2 and 3 summarize data concerning agricultural production and cattle (production and consumption) respectively. More detailed information on specific crops consumption and production is shown in figs. 4 to 10. In order to take into account the differences concerning the size of agricultural lands in the regions considered, all production data are normalized to the total cultivated area (Ha) and for cattle to the total area.

Table 3. Food Consumption by person and year (Kg)

FOOD	CATALUÑA	BALEARES	C.VALENC	R.MURCIANA	ANDALC	MEDIT.R	SPAIN	%(MED.R/SP)
A-CEREALS								
RICE	11.2	17.8	15.4	13.8	9.1	13.5	9.0	150
OTHER	108.6	106.1	101.9	115.8	116.0	109.6	105.1	104
B-MILK	127.5	117.8	112.2	133.6	152.1	128.6	154.4	83
L.IQUID MILK(l)	112.4	103.9	90.8	110.3	133.8	110.2	137.5	
MILK PRODUC	3.1	1.8	8.0	6.8	4.2	4.8	4.3	
OTHER	12.0	12.1	13.4	16.5	14.1	13.6	12.6	
C-EGGS	18.3	14.2	15.8	15.7	18.9	16.6	19.1	87
D-OIL(l)	31.4	34.7	28.8	33.1	36.2	32.8	32.2	102
E-DRY PULSES	8.3	5.1	4.6	12.0	12.0	8.4	9.7	87
F-VEGETABLES								
POTATOES	77.0	86.5	59.6	118.5	86.4	85.6	88.0	97
OTHER	101.8	92.5	87.8	96.4	79.3	91.6	82.9	110
G-FRUIT	72.2	70.0	82.5	76.3	85.1	77.6	76.3	102
CITRIC	38.7	33.7	23.2	33.8	33.0	32.5	34.5	94
GRAPES	4.4	6.5	6.7	5.2	6.1	5.8	5.2	
OLIVES	2.8	1.8	3.9	5.6	2.4	3.3	2.4	
OTHER	65.0	63.7	71.9	65.5	76.6	68.5	68.7	
H-MEAT	83.7	76.7	80.1	72.9	65.7	75.8	76.3	99
I-FISH	27.1	22.8	22.4	25.1	31.7	25.8	30.7	84
J-WINE(l)	104.5	74.3	63.2	72.3	36.9	70.2	79.2	89
K-BEER(l)	69.9	48.5	104.5	159.3	125.7	103.6	83.5	124

From the analysis of the obtained information the following points can be remarked:

- Spanish Mediterranean and all Spanish diets are very similar, showing differences lower than 20% excepting rice and beer consumption
- regional differences are larger in agricultural and cattle productions than consumptions
- rice, fruits, vegetables and pork meat appear as typical Mediterranean products. Potatoes and cereals other than rice are more produced in non Mediterranean areas

- citrics are practically only produced in the Mediterranean areas but they show an uniform pattern of consumption
- rice production and consumption have a good correlation in Mediterranean regions, excepting Baleares and Murcia, where consumption is much higher than production
- taking into account the slight differences observed for diets, important variations on individual dose due to ingestion of accidentally contaminated food cannot be expected. Moreover, since productions have more specific distributions, they will have more repercussion on the collective dose from the accidental contaminations of foods

2. Dose estimations

In order to investigate the influence of the diet on the individual committed dose an hypothetical accidental situation was analyzed. For this analysis some assumptions were taken as follows:

- a uniform deposition of 10^3 Bq.km⁻² of Cs-137 on agricultural and grass land of Spain was supposed.
- the individual dose is referred to an adult population.
- the dose is limited to the only pathway of ingestion of contaminated foods.
- it is assumed that the 100% of the foods ingested are contaminated foods; it results the maximum individual committed dose (average man of the critical group).

From the Cs-137 deposition supposed, the evolution on activity during the first year after the accident in each group of involved foods was calculated using transfer models for terrestrial foods from NRPB publications excepting the model for pork meat that was developed by the CIEMAT group. pig diet was made without inclusion of industrial subproducts, (figs. 11 to 13 show it for six of food groups). Then the averaged annual activity (Bq.kg⁻¹) was calculated.

Using ICRP ingestion model and caesium parameters together with food consumption data obtained in the project, the committed dose for the first year ingestion was evaluated.

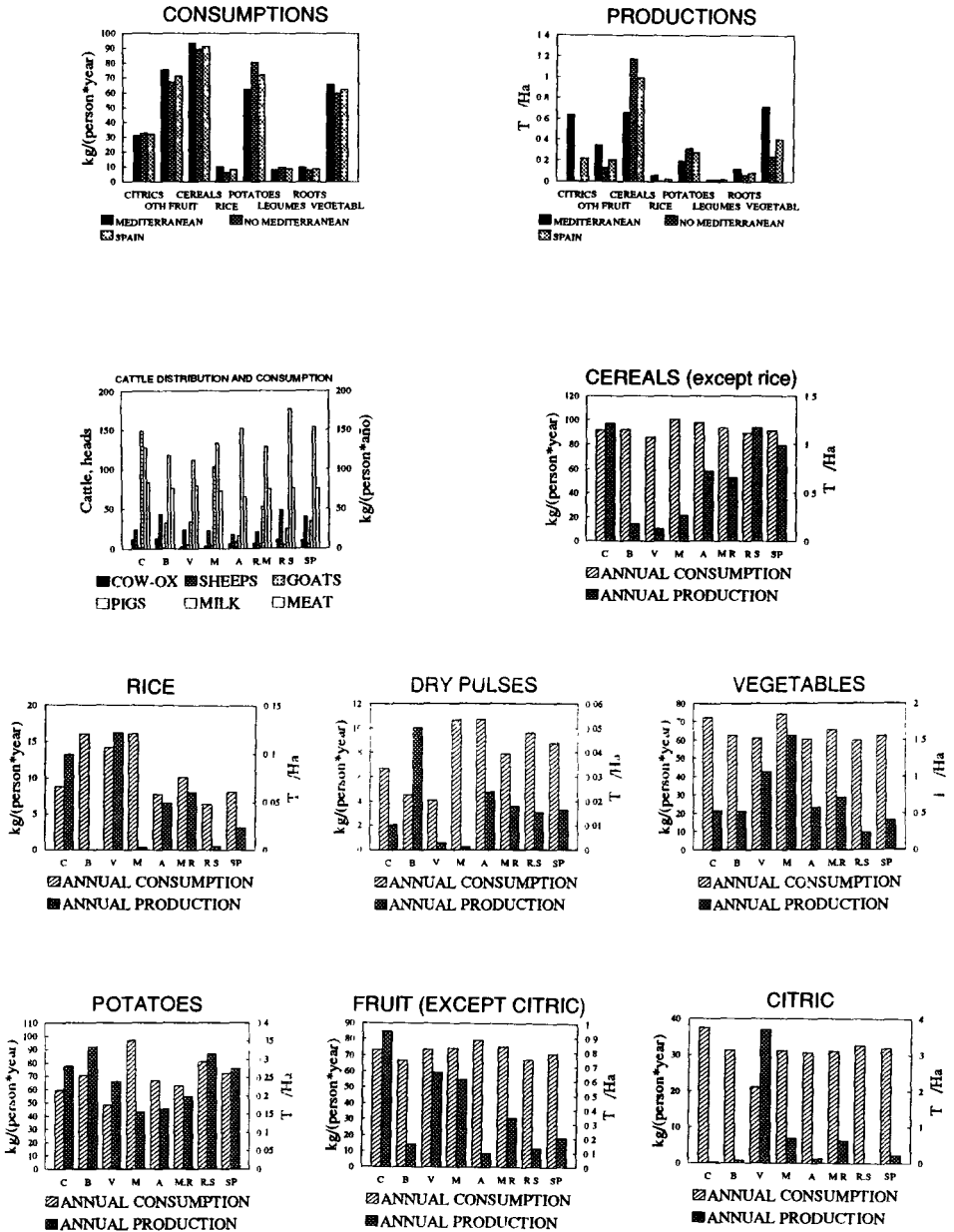
Since the repercussion of the deposition may be highly conditioned by seasonality, the analysis was made for three different dates of accident (January 1st, May 1st and July 1st). Concerning cereals and potatoes, one or two harvesting dates were considered respectively; for vegetables, continuous collection through the year was assumed.

Figure 14 shows a summary of the dose estimations obtained for each of the five Mediterranean regions, the averaged Mediterranean area and the whole country. The importance of both consumption habits and seasonality of Cs-137 deposition is reflected. It can be seen that seasonality has a larger influence on the dose than diet.

3. Soil to plant transfer factors

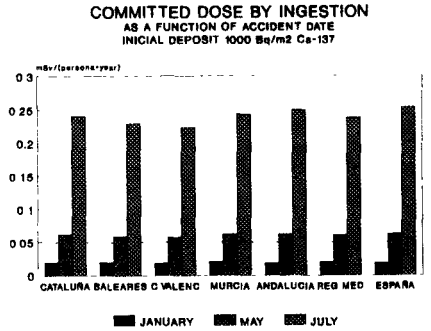
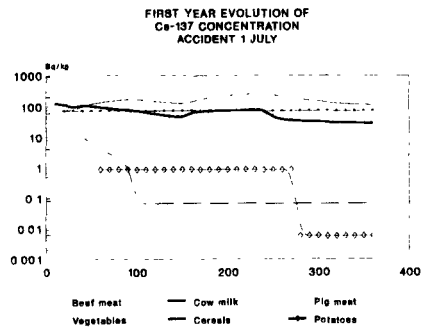
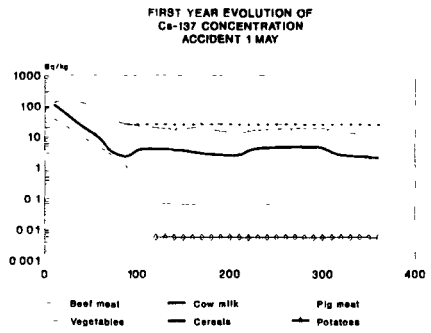
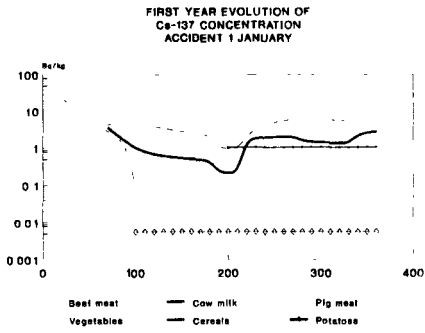
An attempt to obtain data on soil to plant transfer factors was envisaged by sampling and analysis of soils and selected crops from spanish Mediterranean regions. Expected levels of Cs activities being very low (fallout from past nuclear weapons), a great sample size is needed in order to achieve detection of activity. In a first step only a few crop samples shown activity results above the instrument detection limit. Cs in soil was measured in almost all collected soil samples.

A mechanical system allowing the reduction of volume of larger sample sizes is presently being used in order to reach detection of lower Cs activity levels. The preliminary results obtained until now show data in the order of $2 - 4 \cdot 10^{-3}$ (Bq.kg⁻¹ f.w. of plant per Bq.kg⁻¹ d.w. of soil) for potatoes, lettuces, and beans) and lower (10^{-4}) for tomatoes. The experimental work is still running and the complete information will be enclosed as soon it becomes available.

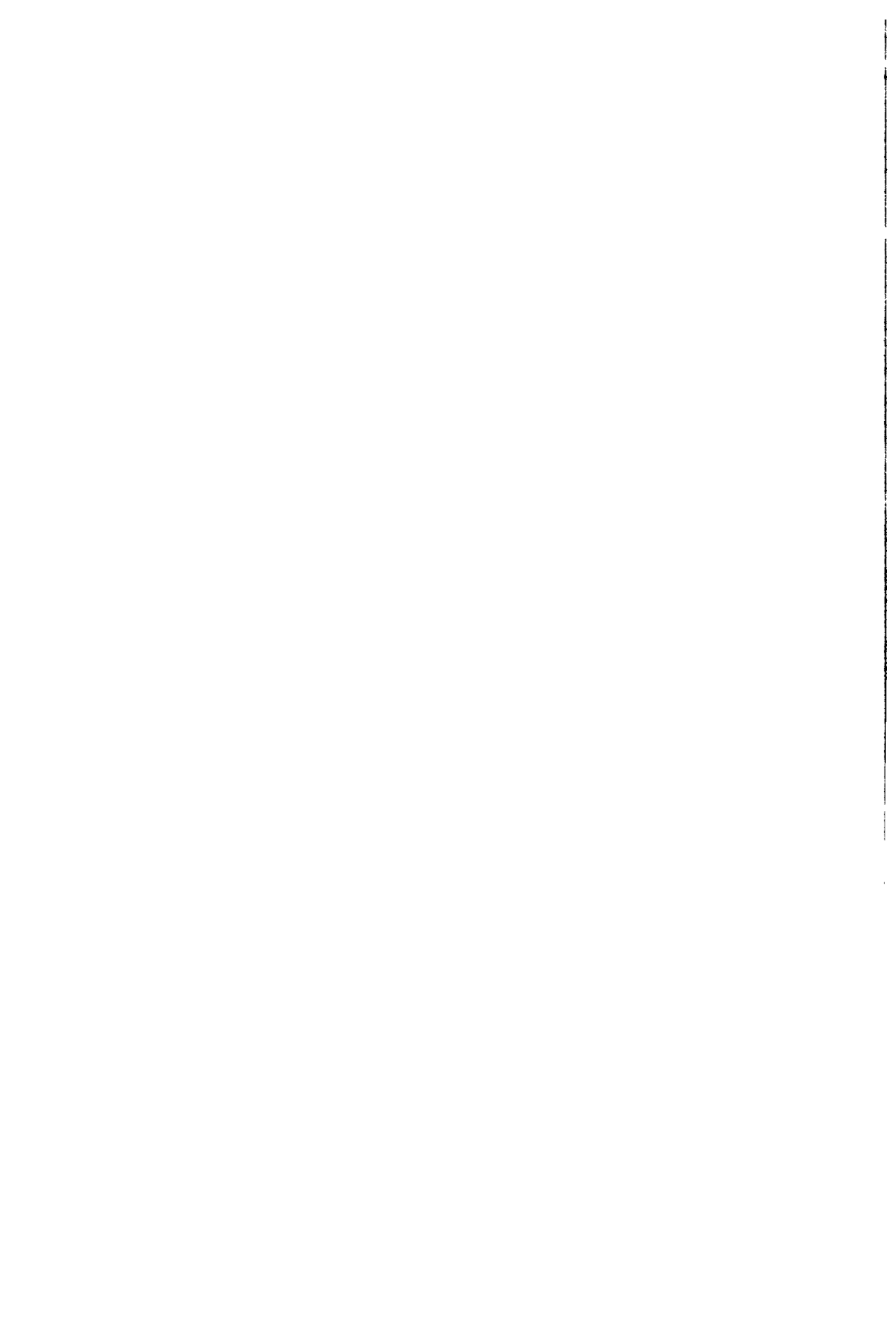


Figures 1 to 10

Keys for figs (Autonomous Communities): C: Catalana - V: Valenciana - B: Balear - M: Murciana - A: Andaluza - M.R: Mediterranean Region - Sp: Spain - R.S: Rest of Spain

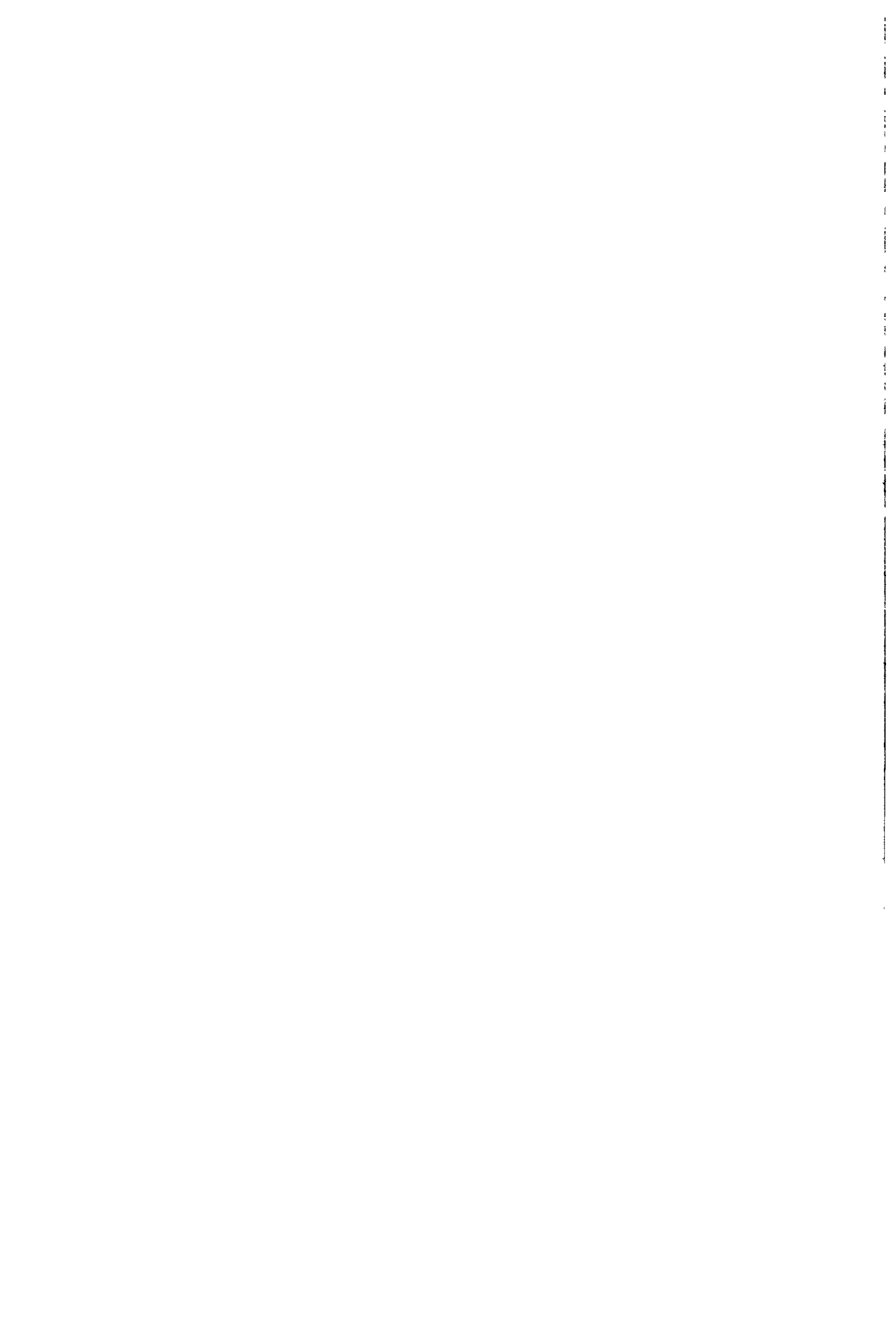


Figures 11 to 14



II

CONSEQUENCES OF RADIATION EXPOSURE TO MAN; THEIR ASSESSMENT, PREVENTION AND TREATMENT



Stochastic effects of radiation



BIOPHYSICAL MODELS FOR THE EFFECTIVENESS OF DIFFERENT RADIATIONS

Contract Bi7-032 - Sector B11

- 1) *Paretzke*, GSF Neuherberg - 2) *Goodhead*, MRC Radiobiological Unit
3) *Terrissol*, ADPA - 4) *Leenhouts* - RIVM

Summary of project global objectives and achievements

The global objectives of this project are to carry out experimental and theoretical research with the aim of achieving a better understanding of the biological effects of different radiation fields with particular emphasis on low doses and low dose rates. The results of this project should improve our present knowledge of somatic and genetic radiation risks in man, and help to develop radiation protection instrumentation which measures the characteristic properties with regard to these endpoints in mixed radiation fields.

In addition, the combined action of ionizing radiation and chemicals (also of those prevalent in the environment) will be investigated on a mechanistic level.

- This goal should be reached by the development of new models based on:
- the improvement of biophysical track structure calculations for relevant radiation fields (photons, neutrons, electrons, ions) in particular by introducing structured cell geometry, condensed state cross sections, time dependency, and chemical and biological reactions;
 - the analysis of such physical-chemical-biological track structures by new cluster algorithms and by testing biophysical models developed by participants 3 and 4.
 - selective radiation biological experiments with soft X-rays and UV-photons, as well as with alpha-particles and gamma-rays; the biological systems include appropriate transformational and inactivation assays, etc.

The need of a better understanding of radiation effects on members of the public has often been emphasized as being highly desirable. This understanding is necessary also to improve the protection of workers and the public in the ALARA-sense of the ICRP, where overestimates of radiation risks might lead e.g. to a not optimum allocation of large resources.

Partner 1 (GSF) improved mainly the physical track structure code for fast electrons, photons and protons by introducing complex geometry describing structured targets and by working on condensed state cross sections for water, carbon and DNA.

Partner 2 (CPA) improved the cross sections for slow electrons and applied a different approach to condensed state cross sections as compared to GSF, he was the leading partner in the intercomparison of results from various other track structure codes in a benchmark and validation study, and he was responsible for the introduction of the simulation of chemical reactions in the code.

Partner 3 (MRC) analysed dedicated track structure calculations to test and improve his biophysical model for radiation actions of different fields, he accumulated for the comparison the theory and experiment selected radiobiological data from the literature and performed own experiments with soft X-rays, alpha particles, etc. using appropriate combinations of genetic, chromosomal, transformational and inactivation assays.

Partner 4 (RIVM) analysed results from dedicated track structure calculations in the framework of his DNA damage model, tried to make a sensitivity analysis of model parameters in order to understand their significance and the influence of different irradiation conditions. He investigated the interaction of radiation with other DNA damaging agents to better understand the influence of such agents on the effects of low radiation doses. He studied experimentally effects of UV radiation of different wavelengths and the interaction with damage from gamma irradiation.

Project 1

Head of project: *Dr. Paretzke*

Objectives for the reporting period

1. Measurement of double differential secondary electron emission induced by MeV-protons in solid targets for the analysis of phase (gas-solid) effects on track structures.
2. Calculation of inelastic scattering cross sections for a) fast protons, b) photons from 10 eV to 100 MeV, and c) for electrons up to 100 MeV in condensed low-Z targets.
3. Intercomparison of electron track structures as calculated by MOCA8B (GSF) for water vapour and by ORETC (ORNL) for liquid water.
4. Auxiliary work for code transport on new fast parallel computer (random number generator, multi-user system software, tools for solution of linear differential equations).
5. Simulation of chemical reactions in tracks in structured biological targets.
6. Simulation of geometric and material structure of lymphocytes and of TEPC.
7. Simulation of photon transport in sub-nanometer (atomic) to centimeter (tissue) dimensions.
8. Absolute calculation of biological radiation effects of photons on DNA and on chromosomes and comparison with experiments.
9. Analysis of somatic radiation effects on man by Radon daughter products in homes and by cosmic rays in airplanes.

Progress achieved including publications

The work carried out in the areas of this project mentioned above was as follows :

1. Measurement of electron emission : In cooperation with L.H. Toburen et al. of the Radiological Physics Group of Battelle Pacific Northwest Laboratory, Richland, USA, a time-of-flight electron spectrometer for slow electrons (i.e. for ca. 0.1 to 100 eV) was build at the medium energy ion accelerator of that group which had to be pulsed for this purpose. The proper functioning of the apparatus was successfully tested by reproducing previously measured double differential secondary electron spectra ejected by MeV protons from Xe gas. Then measurements of electron spectra ejected from solid DNA were foreseen. However, because of problems of the supplier (University of Stockholm) with the preparation of sufficiently thin, vacuum-proof DNA-foils, until now only spectra from thin Carbon foils could be measured instead (1). These measured spectra indicate the influence of a time dependent surface layer from adsorbed residual gases (as shown by Rutherford backscatter analysis) even at gas pressures as low as 10^{-9} mbar which complicate the subsequent data analysis. It is unexpected that such layers alter the electron spectra even at energies above 100 eV. It is planned to improve the vacuum conditions to avoid these surface layers and to manufacture finally biologically relevant solid targets for future electron emission measurements.

2. Calculation of electron cross sections : a) In order to study also theoretically the magnitude of the influence of phase on the important electron emission and scattering cross section calculations based on the density-functional theory were performed for the single and double differential emission of electrons (at 50 electron energies and 16 angles) by proton impact (at 0.15, 0.3, 0.5, 1.0, 1.5, 3.0, 4.2, and 10 MeV) from a single water molecule (gas) and a 5 water molecule cluster (considered here as a model for condensed water). The results were compared to the measurements in water vapor of Toburen and Wilson and to the empirical model for the single differential cross section of Rudd. In general good agreement was

found for forward angles, whereas the experimental data show a significantly higher emission in the backward hemisphere due to reflection at the molecular Coulomb potential wall. Rudd's model can be shown to agree better with experimental data at low proton energies than at high energies. Within the validity of the theoretical model used and in the energy range considered no significant phase related difference in these electron ejection cross section was found.

b) For the more atomic constituents of biological cells and of tissue equivalent proportional counters (TEPC) H, C, N, O, P, S, Na, Cl, Fe, and Al the total and differential photoelectric, Compton, coherent scattering and pair-production cross sections were estimated from various literature sources for photons in the energy range from 10 eV to 100 MeV (3). These cross sections were then used in the track structure calculations described below.

c) For input in high energy charged particle track calculations an empirical analytical model was developed for the computation of single differential and total ionization cross sections for electron impact up to relativistic energies of 100 MeV (4). The model is applicable to various multi-shell atoms and molecules and compares well to experimental data were these are available. The results suggest that in addition to the use of Platzman plots one should also use plots in which the cross sections are normalized to the Mott cross section, and in which one plots against the secondary electron energy (instead of the inverse energy).

3. Intercomparison of tracks in gaseous and liquid water : In cooperation with the group of J.E. Turner et al. in Oak Ridge National Laboratory, USA, a study was performed of the phase difference of spatial distributions of ionizations and other inelastic events in charged particle tracks that influence the final outcome of radiation interaction. This was done for electrons in the energy range from 0.1 to 10 keV (5). The distributions calculated include the frequency of nearest-neighbor distances for all inelastic events and that for ionizations only, the frequency of all distances between inelastic events and the farthest distances between all inelastic events in electron tracks. The differences found are discussed in terms of the inverse mean free paths for inelastic events in liquid water and water vapor, the collision spectra, and the nonlocalization of energy losses that are likely to occur in the liquid. These differences are found to have pronounced effects in separating neighboring events in the liquid out to distances of several nanometers compared to the vapor. In addition, the liquid is characterized by a larger cross section for ionization. These effects in the condensed phase can be expected to play an important role in subsequent intratrack chemistry and in producing different types of indirect and direct biological damage. However, it should be pointed out that no direct evidence exists hitherto as to the actual existence of plasmon excitations in water, and there exist also no measurements of ionization cross sections in the liquid water case.

4. Auxiliary code development : The progress planned for this work period depended strongly on an optimum use of a new computational tool, i.e. an INTEL-Hypercube Parallel Computer of 32 risc processors of the type 860. Since the system software delivered was still at an early stage significant own informatics developments were required. A software tool permitting a multi-user operation and batch scheduling was designed and implemented in cooperation with Prof. A. Bode, Inst. f. Informatik, TU München (6). In the frame work of the same cooperation several numerical methods were tested for solving stiff linear differential equations in complex compartment models (as they are used in simulations of chemical reactions) on such a multi-processor computer (7). In addition several test routines were developed and successfully applied for testing the performance of the random number generator used in the track structure calculations on this new fast computer (8).

5. Simulation of chemical reactions : For consideration in the simulation calculations of the dissociative break up of irradiated molecules, their subsequent diffusion and chemical reactions several subroutines for the new particle track simulation code PARTAC were designed, implemented and tested against experimental radiation chemical data (3,9). Using appropriate diffusion and reaction constants acceptable agreement could be obtained in particular for the action of OH radicals on the bases and backbone of the DNA molecule.

6. Simulation of target structures : Previously track structure calculations could be performed for homogeneous targets only. During this project period complex geometry algorithms (boolean operations for various regions (e.g. spheres, boxes, ellipsoids, parallel epipeds, cylinders) the surfaces of which were described with mathematical equations) and voxel methods were used to permit simulation in PARTRAC of structured targets made up by regions of different molecular constitutions and different densities. One particular problem in this context is the balance to be made between speed of computation and accuracy of the numerical approximations to be made to the mathematical description of the intersection of a vector with a surface; in addition the wide range of spatial dimensions to be considered here (from sub-nanometer molecules to centimeter tissues) posed additional numerical problems. These program modules were tested and then applied to simulate in a first step the DNA structure in chromosomes of a human lymphocyte (since many experimental radiation biological data for this target await quantitative theoretical interpretation) (3,10) and to the KFA low pressure proportional counter with which experimental pulse height spectra were taken for a variety of incident photon fields. A direct comparison of absolute calculations of these spectra with these measurements showed excellent agreement (3).

To facilitate microdosimetric calculations for neutron or proton irradiations an analytical approximation for the frequency distributions of energy deposition and of ionizations in small sites produced by energetic protons (energy range from 0.3 to 20 MeV) passing through or near an absorber site of submicron dimensions (from 2 to 100 nm diameter) was developed (11). The frequency density distributions for ion paths which intersect the site are approximated by a lognormal function. For ions which pass outside the site but deposit energy within the site via delta ray transport, it was found that the density distributions can well be described by an exponential function that depends on site size but is independent of radial distance from the ion path.

7. Photon transport : Using the photon reaction cross sections mentioned above and the complex geometry routines described in (3), many photon transport calculations were performed e.g. for different shapes of irradiated lymphocytes for a variety of different photon fields as they were actually used in experimental radiobiological work. Hereby e.g. the significant influence of the shape of a lymphocyte for the effects regarding the induction of dicentric chromosomes of an irradiation with low energy C_K -photons could be quantified.

8. Calculations of biological radiation effects : To simulate the production of a single strand break of DNA via direct effects a minimum energy deposition of 17.5 eV (as proposed by Charlton and Humm) in a sugar-phosphate volume was assumed (a sensitivity study of this assumption was also performed) to lead to a SSB. Furthermore strand breaks are induced by reactions of OH radicals with the sugar molecules. Double strand breaks were computed by assuming that two single strand breaks on opposite strands separated by less than a certain number of base pairs (e.g. 10) lead to DSB (also here a sensitivity study was made). Such calculations were performed for a wide variety of photon fields from 288 eV up to more than 100 kV X-rays (10); the calculated data appear to be in acceptable agreement with measured data for SSB and DSB. Under certain assumptions regarding the molecular movement and repair of DSB in a chromosome tentative calculations of the linear and quadratic component of the dose - effect relationship for the formation of dicentric chromosomes for these radiation fields were done. Whereas good relative agreement was found for the higher photon energies significant differences are seen for the 288 eV photons. However, here the actual experimental data permit also the conclusion that these photons might have only a smaller linear term than claimed in the interpretation of these data by the authors.

9. Analysis of somatic radiation effects : Since epidemiological data alone are not to be expected to resolve finally the important question of the form of the dose-effect relationship for somatic late effects in man integrated models (regarding the physical, chemical, biological, and medical aspects of radiation action) must be developed to aid in the solution

of this problem. Preliminary considerations along these lines show the great potential of track structure calculations as an important physico-chemical contribution to such an integral model (12,13). However, there is still a long way to go until such a model will be quantitative and reliable enough for radiation risk assessments. Therefore, risk estimates for the important exposure situation for the public through radon and radon daughter isotopes (14,15) and through moderated cosmic rays in civil aircrafts (16) were based on human epidemiological results only

Publications

1. Chr. Drexler, "Messung doppelt differentieller protoneninduzierter Sekundärelektronenausbeuten von Xenon-Gas und einer dünnen Kohlenstoffolie", Diplom-Thesis, TU-München, 1992.
2. K.A. Long, H.G. Paretzke, "Comparison of calculated cross sections for secondary electron emission from a water molecule and clusters of water molecules by protons", *J.Chem.Phys.* 95(2) (1991) 1049-1056.
3. S. Henß, "Biophysikalisches Modell zur Induktion dizentrischer Chromosomen durch ionisierende Strahlung", PhD-Thesis, TU München, 1992.
4. K.A. Long, H.G. Paretzke, "An analytical model for single differential and total ionization cross sections and the energy loss for electron impact on water, helium and nitrogen from 20 eV up to 100 MeV", submitted to *J.Chem.Phys.* (1992).
5. H.G. Paretzke, J.E. Turner, R.N. Hamm, R.H. Ritchie, and H.A. Wright, "Spatial distributions of inelastic events produced by electrons in gaseous and liquid water", *Rad.Res.* 127 (1991) 121-129.
6. S. Bressler, "Werkzeuge für den Mehrbenutzerbetrieb von Parallelrechnern in einer Netzwerkumgebung", Diplom-Thesis, TU München, 1990.
7. M. Perzl, "Implementierung eines numerischen Algorithmus zur Lösung steifer gewöhnlicher Differentialgleichungen - zur Anwendung auf komplexe Kompartiment-Modelle - für Multiprozessoren unter verschiedenen Programmiermodellen", Diplom-Thesis, TU München, 1992.
8. M. Reck, H.G. Paretzke, "Test programs for pseudo-random number generators", GSF-Report, in preparation, 1992.
9. I. Rivals, "Modelisation des effets directs et indirects de radiations ionisantes sur l'ADN cellulaire", Rapport Technique, Ecole Supérieure de Physique et Chimie Industrielles, Paris, 1991.
10. S. Henß, H.G. Paretzke, "Biophysical modelling of radiation induced damages in chromosomes", in : *Biophysical Modelling of Radiation Effects*, K.H. Chadwick, G. Moschini, and M.N. Varma, Eds., Adam Hilger, Bristol, p.69 - 76, 1992.
11. W. Wilson, H.G. Paretzke, "A stochastic model of ion track structure", to be published in the proceedings of the 11th Symp. on Microdosimetry, Gatlinburg, 1992.
12. H.G. Paretzke, "Biophysical models of radiation action - development of simulation codes", in : *Early Effects of Radiation on DNA*, M. Fielden, P.O'Neill, Eds., Springer Verlag, Heidelberg, p.17-32, 1991.
13. H.G. Paretzke, "Potentials and limitations of empirical models", loc. cit. 10, p.335-337.
14. H.G. Paretzke, "Strahlenexposition und Strahlenwirkung bei der Energieumwandlung", in : *Schadstoffemissionen bei der Energieumwandlung*, Inforum-Verlag, p. 143-156, Bonn, 1991.
15. H.G. Paretzke, "Strahlenexposition und -Risiko durch Radon", in : *Strahlenrisiko durch Radon*, Eds. Chr. Reinert, Chr. Streffer, O. Messerschmidt, *Strahlenschutz in Forschung und Praxis*, Band 33, p.81-90, G. Fischer Verlag, Stuttgart, 1992.
16. H.G. Paretzke, W. Heinrich, "Radiation exposure and radiation risk in civil aircrafts", *Proceed. CEC Workshop on Radiation Exposure of Civil Aircrews*, Luxembourg, 1992.

Project 2

Head of project: *Dr. Goodhead*

Objectives for the reporting period

1. Simulation and scoring of monoenergetic electron tracks from code MOCA8b, to generate frequency distributions of energy deposition in microscopic volumes and compilation of these into a monograph of electron-scoring tabulations..
2. Initiate a comparison of track-scoring results obtained by using tracks simulated with other Monte-Carlo codes developed in the world to allow testing of the stability of the results and conclusions.
3. Develop methods and obtain experimental data on biological effects of radiations with well-defined track structures, including induction by α -particles of HPRT-mutations in haemopoietic cells and V79 cells including the effect of reducing dose rate.
4. Compare theoretical and experiment data to seek track properties of biological relevance and evaluate implications especially for low-level effects.

Progress achieved including publications

The work carried out in three related parts of our component of the contract was as follows:

1. Track structure analysis

We have used the Monte-Carlo track structure code MOCA8b of Paretzke to compute distributions of the absolute frequencies of energy deposition by electrons in small cylindrical targets in water. For this purpose statistically representative numbers of full slowing down tracks, in water, of initially monoenergetic electrons were generated for initial electron energies at intervals from 0.1 to 100 keV. These were randomly sampled with cylindrical volumes (diameters 1 to 100 nm; lengths 0.5 to 64 times diameter) to obtain statistically stable frequency distributions of energy deposited within the cylinders, per Gy of absorbed dose to the macroscopic medium. A summary and discussion of these extensive data was published [1], including some comparisons with high-LET α -particles (4 MeV). The complete set of results has been prepared in tabular form for publication as a monograph [11], to accompany our previously published monographs on energy deposition in similar volumes by protons and α -particles of diverse energies and ultrasoft X-rays of selected characteristic energies. Together these monographs provide an extensive and consistent data base for comparison of the energy-deposition properties of different radiations in cylindrical target volumes including those of dimensions similar to subcellular biological structures such as DNA, nucleosomes and chromatin fibre. These data and their applications to understanding DNA damage and cellular effects were reviewed last year [12].

The track structure code has also been used to compare the abilities of different low-LET radiations to deposit their energy in the form of low-energy secondary electrons.

The results indicate that low-energy electrons of 0.1-5 keV account for about 30-50% of the total dose imparted to a medium irradiated by any conventional low-LET radiation [2] and hence that these electrons may play a dominant role in the biological consequences.

Our existing data base on frequencies of energy deposition by different radiations has been derived exclusively from the codes MOCA8b (for electrons and photons) and MOCA14 (for protons and α -particles) of Paretzke and Wilson, which are based on water vapour cross sections with adjustment to the density of liquid water. We have initiated studies to test the generality of our data, and conclusions drawn from them, by carrying out identical scoring computations on tracks from alternative codes currently in existence or under advanced development. Representative numbers of electron tracks of a few selected initial energies have been obtained from the water codes of Terrissol (Toulouse; liquid), Turner *et al.* (Oak Ridge; liquid) and Michalik *et al.* (Prague; vapour) and prepared for scoring. In addition, Terrissol has installed his code on our computers and prepared for its extension to initial energies up to 100 keV. This should now allow comparative scoring to investigate code differences from the point of view of the user interested in energy-deposition distributions and detailed modelling of damage to DNA.

The track structure codes are also being used to develop models of the initial stages of damage to DNA [3] with a view to incorporating chemical processes, starting from the initial stochastics of the tracks. With a different approach, sensitization of DNA and chromatids has also been modelled for comparison with experimental data [13,14].

2. Biological experiments on radiation-quality

To complement our theoretical studies of radiation track structure we are investigating their biological consequences in a number of ways. Alpha particles of about 3 MeV have LET in the region of maximum relative biological effectiveness for most cellular effects. We have previously constructed, and now extensively characterised and described, a versatile irradiator for radiobiological studies with α -particles of about this energy [4]. It is based on a disc of plutonium-238 and allows irradiation, of thin biological samples, with an approximately parallel beam of monoenergetic α -particles in the track-segment mode. We have developed methods for irradiation both of attached monolayers of cells and of thin volumes of cells in suspension. Dose rates can be varied over wide limits, with the sample dishes being maintained under gassed and incubated conditions.

This irradiation has been applied to a variety of cell types including rodent fibroblasts, rodent and human haemopoietic progenitor cells and human peripheral lymphocytes. Studies include assessment of the abilities of different cell types to survive the passage of a single α -particle and hence their inherent mutability as well as their ability for expression as viable cells. This survival factor varies considerably with cell types and geometry, being almost zero for some pre-B haemopoietic cells, ~ 10-20% for CFU-S and CFU-A haemopoietic stem cells and up to more than 80% for fibroblasts. Induction of HPR^T mutations is being investigated in V79 hamster

cells, murine haemopoietic progenitor cells and human lymphocytes, the latter two including external collaborations with M. Greaves and S. Griffiths (London) and B. Bridges *et al.* (Brighton). In accordance with our previous results for chromosome aberrations and cell inactivation, we have found little or no dose-rate dependence for HPRT⁻ mutations in plateau-phase V79 cells, irradiated at 0.2 and 0.0001 Gy min⁻¹ under optimal culture conditions in Hostaphan/glass dishes. Curiously, however, there was an apparent enhancement of effect by 2-3 times at low dose-rate in experiments with Hostaphan/titanium dishes, possibly associated with sub-optimal conditions. The α -source is being used also for investigation of dose-rate dependence of transformation of C3H 10T $\frac{1}{2}$ mouse cells, in collaboration with A. Mill *et al.* (Berkeley).

Mechanistic interpretation of the effects of ultrasoft X-rays or α -particles, in terms of their individual tracks, requires accurate measurement of the dimensions of the cells, or their nuclei, under the exact conditions of irradiation. For this purpose we have developed methods of confocal microscopy to make measurements of thicknesses [5] and areas [6,15] on living individual cells in the monolayer cultures as irradiated. The thicknesses were compared with measurements on the same cell populations obtained by the more conventional methods of electron microscopy after fixation and sectioning [5]. Confocal methods have now also been developed for measurement of cells in thin suspensions as irradiated.

The track structure analyses have revealed the clear expectation that slow α -particles can produce grossly clustered damage at the level of DNA and its structures, some of which damage can never be produced by relevant doses of low-LET radiations. This raises the possibility not only of reduced reparability of classes of α -particle induced DNA damage, as appears to be confirmed by our collaborative measurements of repair of double-strand breaks, but also of some unique final cellular effects. We have previously found such apparently unique effects for induction of sister chromatid exchanges in human lymphocytes irradiated before stimulation, but now collaborative studies have revealed a new effect in murine haemopoietic stem cells that lies well outside of usual radiobiological expectations and may be unique to high-LET radiations. This is the appearance of new, non-clonal chromosome aberrations many cell cycles (~ 10-13) after a cell has been traversed by a single α -particle [17]. Thus, it appears that the α -particles have induced long-term chromosomal instability in the progeny of the irradiated stem cells.

3. Comparative analysis of track properties with biological effectiveness

In the publications quoted above we have drawn a variety of inferences on the biologically critical features of radiation tracks from low- and high-LET radiations. The implications have been considered further in relation to potential classes of initial DNA damage and quantitative models of radiation action [16]. We have suggested that a particularly important feature of tracks may be the very locally clustered ionisations/excitations that can produce complex damage to DNA and associated structures, even for low-LET radiations, and especially for high-LET radiations [7,8]. We have also discussed the reparability of different types of measurable DNA damage and their possible relationship to cluster size and explored the consequences for low level radiation effects that are due to single tracks alone [9,10,18-20].

Publications

- [1] H. Nikjoo, D.T. Goodhead, D.E. Charlton and H.G. Paretzke. "Energy deposition in small cylindrical targets by monoenergetic electrons." *International Journal of Radiation Biology*, 60, 739-756 (1991).
- [2] H. Nikjoo and D.T. Goodhead. "Track structure analysis illustrating the prominent role of low-energy electrons in radiobiological effects of low-LET radiations." *Phys. Med. Biol.*, 36, 229-238 (1991).
- [3] H. Nikjoo. "What basis for the development of radiation-induced DNA damage." In: *The Early Effects of Radiation on DNA*. Eds. E.M. Fielden and P. O'Neill (Springer-Verlag, Heidelberg), pp.211-212 (1991).
- [4] D.T. Goodhead, D.A. Bance, A. Stretch and R.E. Wilkinson. "A versatile plutonium-238 irradiator for radiobiological studies with α -particles." *International Journal of Radiation Biology*, 59, 195-210 (1991).
- [5] K.M.S. Townsend, A. Stretch, D.L. Stevens and D.T. Goodhead. "Thickness measurements on V79-4 cells. A comparison between laser scanning confocal microscopy and electron microscopy." *International Journal of Radiation Biology*, 58, 499-508 (1990).
- [6] S. Marsden. "Non-invasive nuclear area measurements using confocal laser scanning fluorescence microscopy for the assessment of alpha particle inactivation of plateau phase V79-4 Chinese hamster cells." M.Sc. Thesis, University of St. Andrews (1990).
- [7] D.T. Goodhead. "Models to link DNA damage to RBEs for final cellular effects." In: *The Early Effects of Radiation on DNA*. Eds. E.M. Fielden and P. O'Neill. (Springer-Verlag, Heidelberg), pp.271-286 (1991).
- [8] D.T. Goodhead. "Summary comments from a physicist." *ibid.* pp.413-416 (1991).
- [9] D.T. Goodhead. "Biophysical features of radiations at low doses and low dose rates." In: *New Developments in Fundamental and Applied Radiobiology*. Eds. C.B. Seymour and C. Mothersill (Taylor and Francis, London), pp.4-11 (1991).
- [10] D.T. Goodhead. "Radiation tracks in biological materials: initial damage in cells, DNA and associated structures." In: *Genes, Cancer and Radiation Protection*. (NCRP, Bethesda) (in press).
- [11] H. Nikjoo, D.T. Goodhead, D.E. Charlton and H.G. Paretzke. "Energy deposition in cylindrical targets by monoenergetic electrons, 10 eV to 100 keV." MRC Radiobiology Unit Monograph (Didcot, U.K.) (in press).
- [12] D.E. Charlton, H. Nikjoo and D.T. Goodhead. "Energy deposition in sub-microscopic volumes." In: *Radiation Research - A Twentieth-Century Perspective, Vol.II*. Eds. W.C. Dewey *et al.* (Academic Press, San Diego), pp.421-426 (1992).

- [13] H. Nikjoo, J.R.K. Savage, D.E. Charlton, A. Harvey and S.Z. Aghamohammadi. "Test of radiation damage enhancement due to incorporation of BrdU into DNA using chromatid aberrations." In: *Biophysical Aspects of Auger Processes*. Eds. R.W. Howell *et al.* (American Assoc. of Physicists in Medicine) (in press).
- [14] D.E. Charlton and H. Nikjoo. "An attempt to model the increase of radiation sensitivity due to incorporation of cold IUdR or BrdU into DNA of irradiated cells." *ibid.* (in press).
- [15] S. Townsend and S. Marsden. "Nuclear area measurement on viable cells, using confocal microscopy." *International Journal of Radiation Biology*, 61, 549-551 (1992).
- [16] D.T. Goodhead. "Biophysical modelling in radiation protection." In: *Biophysical Modelling of Radiation Effects*. Eds. K.H. Chadwick, G. Moschini and M.N. Varma (Adam Hilger, Bristol), pp.113-124 (1992).
- [17] M.A. Kadim, D.A. Macdonald, D.T. Goodhead, S.A. Lorimore, S.J. Marsden and E.G. Wright. *Nature*, 355, 738-740 (1992).
- [18] D.T. Goodhead. "Track structure considerations in low dose and low dose rate effects of ionizing radiation." In: *Advances in Radiation Biology: Low Level Radiation Effects*. Eds. O.F. Nygaard and W.K. Sinclair (Academic Press, Orlando) (in press).
- [19] D.T. Goodhead. "Biological effects of high energy radiations." In: *Proc. CEC Workshop on Radiation Exposure of Civil Aircrew, Luxembourg, July 1991* (in press).
- [20] D.T. Goodhead. "Consequences of radiation track structure for low level radiation effects." In: *Proc. Int. Conf. on Radiation Effects and Protection, Mito, Japan, 18-20 March 1992* (in press).

Project 3

Head of project: *Dr. Terrissol*

Objectives for the reporting period

Our main objective is to set up a biophysical model able to simulate what happens in an irradiated cell : the more realistic possible description of the physical and chemical steps at early times and up to 10^{-6} second, and then give the data to the radiobiologist. In a cell there are several different centers of interest, and we have tried to adapt our model.

Progress achieved

Our biophysical model able to compute as a function of space and time physical and chemical events in liquid water irradiated by low energy electrons has been enriched with the possibility to add various finite volumes containing solutes like scavengers (Tris, formate ions,) chemically active with water radicals, or volumes containing set of biological molecules (DNA or other) also chemically active with water radicals or scavengers. All the chemical reactions between these species are taken into account.

At present, due to computer time consuming and memory limitation, these finite volumes are limited about hundreds of cubic nanometers, sufficient to contain a DNA helix of 14 nm length with 2 nm radius and a surrounding media of liquid water with a concentration of scavengers not exceeding 2M.

As a first exemple, before future developments, we took an infinite media of liquid water (see figure 1). Inside there is a first little volume of interest supposed containing DNA molecules, taken as a cylinder of 2 nm radius and 14 nm length, and a second scavenger volume (no matter the shape) large enough to contain evolutions of all the involved species around the volume of interest until 10^{-8} second. An electron with 278 eV energy is supposed created as indicated by the little arrow on the figure 1, at a distance of 3 nm of the axis of the volume of interest.

At early times, saying between 10^{-18} and 10^{-15} second, the slowing down of the electron is done, elastic and inelastic (ionizations and excitations) collisions take place, and every ionization localized in the volume of interest is counted as "direct". Then thermalization of solvated electrons and creation of water radicals arise and a data set in a four coordinates system (t, x, y, z) is obtained for each species : e^-_{aq} , OH^\cdot , H^\cdot , H_3O^+ , H_2O_2 , OH^- , H_2 , HO_2 , starting at 10^{-15} second. In the volume containing the volume of interest,

molecules of Tris are added. As a function of time, all water species and Tris can diffuse and react together. When $\text{OH}\cdot$ or $\text{H}\cdot$ radical enter the volume of interest, there are counted as "indirect".

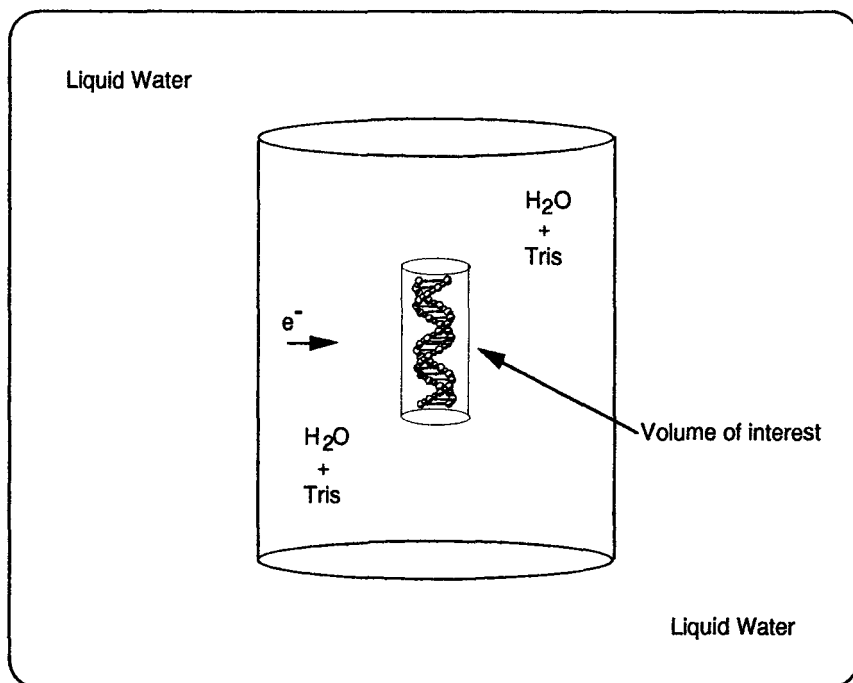


Figure 1 : Schema of the model used. Monoenergetic 278 eV electrons are emitted in the direction of the volume of interest, as indicated by e^- and the little arrow.

For 278 eV electron (like C_K Auger electrons), and in the case represented in figure 1, we found a "direct" yield of 0.242 per electron and a value of 0.192 for the "indirect" yield at 10^{-12} second. The variations of "indirect" yields as a function of time and concentration of Tris, are represented on figure 2.

We have begun to introduce interactions of water radicals with DNA units : sugar, phosphates adenine, guanine, cytosine and thymine. If there is no major problem for the chemical phase (10^{-12} to 10^{-6} second), we are looking for the initial interaction cross-sections of electron with DNA molecules (atoms) to do a more realistic simulation.

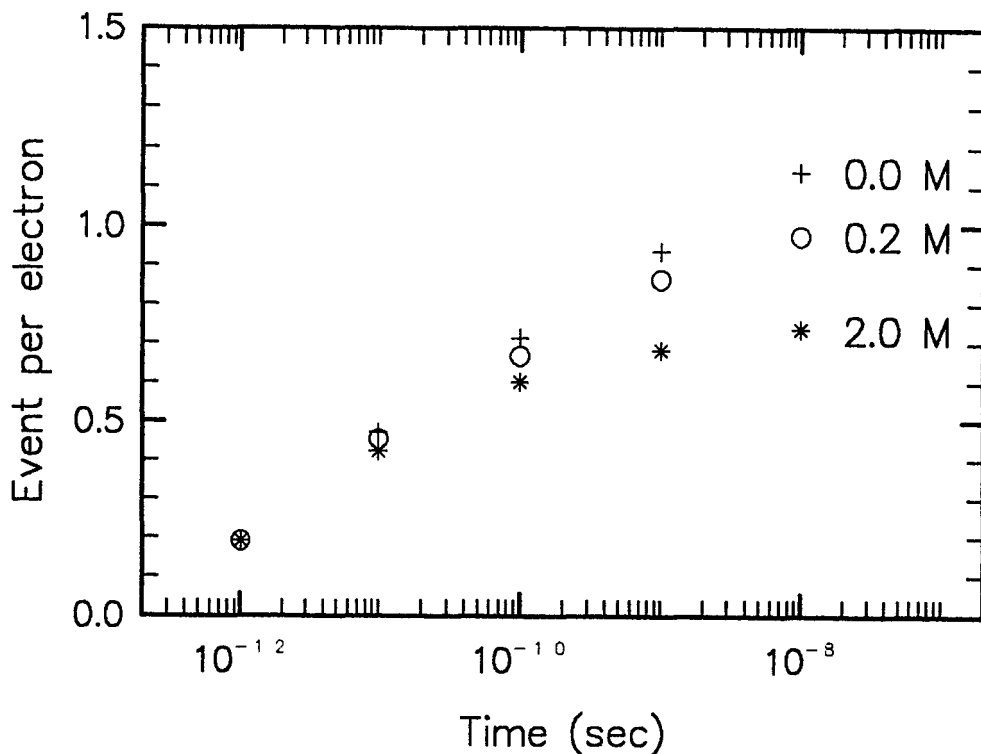


Figure 2 : Variations of "indirect" yield, the number of OH and H radicals entering the volume of interest per electron, as a function of time. The concentration of Tris is expressed in mole per litre.

A. SAIFI, M. ROCH, M. TERRISSOL : " Application de l'approche déterministe à l'étude sur ordinateur des processus radiolytiques induits dans l'eau par des électrons". Compte rendus du XXXème Congrès de la SFPH, CHU de Rennes, juin 1991, pp 305-316.

A. SAIFI : "Approche déterministe à l'étude sur ordinateur des processus radiolytiques induits dans l'eau par des électrons". Doctorat de l'Université Paul Sabatier, Toulouse, n° 915 (1991).

E. POMPLUN, M. ROCH, M. TERRISSOL : " Simulation of strand break induction by DNA-incorporated 125 Iodine". Biophysical aspects of Auger Processes, AAPM Symposium series N° 8 (1992), pp 137-152, Eds RW Howell, VR Narra, KSR Sastry, DV Rao.

M. ROCH : "Simulation des effets des rayonnements au niveau de l'ADN". Doctorat de l'Université Paul Sabatier, Toulouse, (1992).

Project 4

Head of project: *Dr. Leenhouts*

Objectives of the reporting period

1. Track structure: application of the track structure model to the analysis of the initial slope of the dose-effect relationship of chromosomal aberrations in human lymphocytes for different radiations; sensitivity analysis to investigate the influence of the various components of the model.
2. Comparison of UV effects: interactions of UV of different wavelengths with gamma rays; influence on dose relationships.
3. Fractionation effects: continue the work on the effect of fractionated irradiation of gamma rays with different time intervals.
4. Application of models to low-dose risk assessment; continue the investigation of the application of the Knudson-Moolgavkar model for radiation to study the implications for the absolute and relative risk models.

Progress achieved including publications

1. Track structure

The track structure model (TRAX) has been modified and is now operational on a personal computer using Turbo-Pascal. Different sets of data of DNA double-strand breaks (Ritter et al) and the linear dose term of cellular effects (V79, humal cells) with LET have been used to test the model and it is possible, in general, with reasonable choises of the radiation interaction distance and the effectivity factor to achieve a satisfactory description of the data. It turns out that a cut-off energy of 25 eV for secondary electrons, below which the contribution of events from secondary particles is considered to belong to the original track, leads to the optimum solution of the fits. The case of chromosomal aberrations in lymphocytes is still not satisfactorily solved and will be reported in the next period.

2. Comparison of UV effects

The experiments on stationary CHO cells have concentrated on the interaction of the effect of 300 nm UV with gamma radiation. Although the interaction is not large and the interpretation of the experimental results, therefore, laborious, as yet all experiments are in line with a two-hit character of the interaction term, with one hit induced by gamma radiation and the other by UV. These results indicate and confirm that the quadratic term with dose for ionizing radiation and for UV are of different nature, because of the different lesions involved: DNA breaks in the case of gamma rays and dimers in the case of UV. Nevertheless, these lesions can

interact to form a sort of compound double-strand lesion which is cytotoxic.

3. Fractionation effects

The experiments of interaction of fractions of gamma radiation have been continued with different time intervals between fractions. The results are compatible with the expected repair of sublethal damage, confirming the two-hit character of the quadratic term. For the interpretation of the magnitude of the quadratic term in comparison with the linear term a survey was made of literature on the specific nature of DNA during synthesis. It appears that the DNA has to unwind and open the well known double helix structure in order to allow synthesis to take place. This implies that DNA single-strand breaks many base pairs apart may disturb the integrity of the DNA and have an effect equivalent with a double-strand break. Preliminary calculations indicate that this effect may contribute significantly to the quadratic dose term and could explain the discrepancy found with conventional calculations for the comparability of the contributions of the linear and quadratic terms in the radiobiological effect.

4. Applications of models to low-dose risk assessment

The two-stage model of carcinogenesis of Knudson-Moolgavkar combined with the molecular radiation model for cellular radiobiological effects is investigated and applied to animal and human data sets for tumour incidence. The results are very promising, but more time is needed to make coherent interpretations of different sets of data and to attach significance to the parameters used.

Up till now, data on lung, skin and bone tumours have been investigated for a number of data sets. Age dependence and dose-effect relationships could, in general, satisfactorily be described. In particular, the model can have serious implications for the influence of irradiation time and natural incidence of the tumour on the extrapolation of data to the risk at low doses and continuous irradiations. The preliminary results also can influence the interpretation of quality factors for radiation protection purposes.

Publications

[1] K.H. Chadwick and H.P. Leenhouts. "Animal models in radiation carcinogenesis - biophysical considerations". *Radiat. Environ. Biophys.* 30: 169 - 171 (1991)

[2] H.P. Leenhouts and K.H. Chadwick. "A molecular model for the cytotoxic action of UV and ionizing radiation". In: *Photobiology*. (E. Riklis, ed.; Plenum Press, New York), pp 71 - 81 (1991).

[3] H.P. Leenhouts and K.H. Chadwick. "Analysis of the interaction of different radiations on the basis of DNA damage". In: *Biophysical Modelling of Radiation Effects*. (K.H. Chadwick, G. Moschini and M.N. Varma, eds; Adam Hilger, Bristol), pp. 29 - 36 (1992).

SPECIFICATION OF RADIATION QUALITY AT THE NANOMETRE LEVEL

Contract Bi7-040 - Sector B11

- 1) *Colautti* , INFN-Frascati - 2) *Watt* , St. Andrew Univ.
- 3) *Harder* , Georg-August Univ. - Göttingen - 4) *Leuthold*, GSF
- 5) *Izzo* , Univ. degli Studi di Roma

Summary of project and global objectives

Research concerning the best way of specifying radiation quality for radiobiology and radiation protection by physical parameter expressing the track structure-target structure relation remains a central task of microdosimetry. Since both molecular biology and radiobiological analysis (track segment method) suggest for cellular radiation effects, critical target sizes of few nanometre, the imperfection of present microdosimetric simulation of volumes in the micrometer range have become evident. For all ionizing particles or particle configuration (e.g. Auger cascade) which produce a high concentration of deposited energy on the nanometre scale, but having ranges much smaller than the micrometer dimensions, the spatial resolution of present microdosimetric detectors is inadequate. The project has four main aims.

1. Track structure studies for nanometer targets

AIM

To establish the approximated constancy of the delta-ray contribution to the energy deposition fluctuation in a nanometer target. To establish the constancy of the ratio of restricted LET to linear primary ionisation.

Track structure studies, based on computer simulation, recent cross section updates and adequate statistical concepts such as distribution parameters, pattern recognition and target modelling, will provide the physical basis for the validation of the proposed quantities linear primary ionisation or restricted LET. The phenomenon of d-ray cutoff at nanometre target boundaries will need further study and the proposed close correlation of these quantities with lineal energy in simulated nanometre volumes will have to be substantiated. The work will include updated cross-sections and genomic target structure.

2. Biological validation of the best suited parameter

AIM

To select bench-mark sets of survival, chromosome aberration and molecular lesion data to test and confirm the ability of linear primary ionisation and restricted LET to determine their variation with radiation quality.

The ultimate decision concerning the suitability of the new radiation quality parameters must be provided by their ability to predict the dependence of radiobiological yields on radiation quality. This work, already started by the cooperating groups in promoting linear primary ionisation or restricted LET, needs further effort in broadening the biological data base and stepping forward from retrospective analysis to predictive approach.

3. Experimental studies of associate detector systems

AIM

Measurements of the ionisation pattern around charged particles tracks and study of a portable device able to simulate T.E. volumes of few tens of nanometres in size.

The actual experimental studies, which aim to determine the lowest simulation limit of a TEPC, will continue with the use of slow ions as probes to explore the avalanche characteristics of single-wire and field-grid TEPC. A tissue-equivalent multistep parallel plate avalanche chamber will be manufactured to measure single ionisations in order to study the correlation between primary ionisation and restricted LET. The possibility to manufacture a small cylindrical avalanche chamber will be studied. In parallel with the gas-filled detectors, a feasibility study will be carried out with the object of simulating the biological response to radiations in nanometre dimensions in condensed phase detectors. The optimum method will be selected, guided by the biological analysis, and work will begin on a device.

4. Quantification of indirect action from single tracks.

AIM

To conduct an experimental study of the yield and spatial distribution of paramagnetic free radicals formed in the wake of individual tracks by measurement of relaxation time and using ESR technique. To compare the experimental results with the predictions of a simplified theoretical model of biological effectiveness.

ESR measurements will be used to explore the spatial distribution, mean life times and reaction rates of free radicals generated by charged particle tracks in nucleic acids, proteins, aminoacids from cell cultures and possibly whole tissues. Measurement of radical density is based upon the dependence of the saturation value of microwave magnetic fields upon the spin-spin relaxation time. The possibility of adapting simplified theoretical methods, developed for enzyme inactivation by indirect action, will be explored in an attempt to obtain a more meaningful model of radiation action for radiation protection purposes.

Project 1

Head of project: *Dr. Colautti*

Objectives for the reporting period

To measure the ionisation distributions near the track of a charged particle in the range from few nanometres to few tens of nanometres from the particle track.

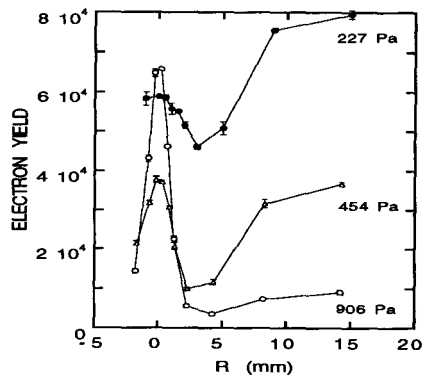
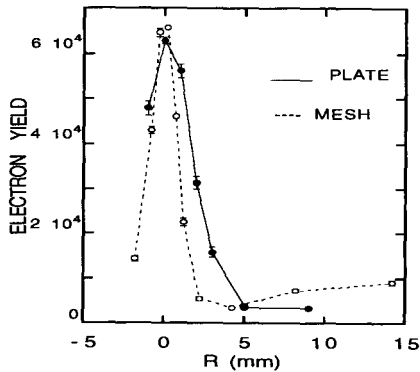
Progress achieved including publications

We have manufactured the first track detector prototype. The detector is made up of two parts: a small drift region to obtain a good tracking and a relative large multiplication region to get a gain high enough at low pressure. In figure 1 the track detector is shown. A stainless steel block has been drilled to obtain a cylindrical cavity of 20.4 mm in diameter, two cylindrical guard tubes (10 by 1.8 mm) define the 25 mm long proportional counter; in these measurements we have used a 10 μm anode wire. The proportional counter is almost tangent to the lower side of the block in which a 25 mm long, 1 mm large and 0.5 mm thick slit has been milled. Through the slit the multiplication region communicates with the drift region which is 4 mm deep, behind this there is a well 10 mm deep to trap the scattered electron, an electroformed mesh of copper with 45 wires per inch and 88% of transperance closes the well and defines the lower side of the diffusion region; an identical mesh is attached on the upper side in order to prevent the electrical field distortions due to slit. The mesh in the lower side of the diffusion region can be removed and substitutes with a stainless steel plate to evaluate the influence of the boundaries on the electron backscattering.

The particle beam travels at the centre of the drift region parallel to the slit and strikes a solid state detector the signal of which opens a coincidence gate for the proportional counter, the pulses are then produced by the electrons which are in the region defined by the projection of the slit into the drift region. These electrons are produced by the d-rays emerging from the track of the charged particle opening the coincidence gate. All the track detector can be moved in the direction perpendicular to the beam by means of a micrometric screw, so the distance between the particle track and the slit can be determined with a precision better than 0.01 mm.

Three sets of measurements have been taken at three different pressures of 227 Pa, 454 Pa and 906 Pa in the propane-based tissue-equivalent gas mixture by using as an α -particle source of ^{244}Cm . The radial track profiles have showed a relevant background, at all the pressures, at the increasing distances from the track.

The background, likely due to secondary electron emission from walls of drift region, has been reduced replacing the anode wall with a grid (left side of the figure), but in spite of that the background remained so high to destroy the track profile at distances bigger than four millimetres from the centre of the track. Nevertheless the remaining meaningful data collected at three different pressures were sufficient to get the ionization profile from 5 to 40 equivalent nanometres from the track core.



The results shows a maximum of ionization yield between 10 and 15 nanometres.

The results are encouraging, but a relevant backscattering or secondary emission component has forced to use only the data collected very close to the beam which are in turn dirty because of the PC "insider ionizations" which are important just at small R. In order to improve the detector we are going to increase the transparence of the drift region replacing the cathode wall with a grid. Although the experimental findings suggest interesting features of the ionization pattern at nanometre level, they have to be still confirmed in different experimental conditions before to be sure they are really related to the track structure rather than to radiation field distortions due to the detector itself.

Publications

P.Colautti, G.Leuthold, G.Talpo and G.Tornielli
Parallel-to-Anode Ion Probe in a Cylindrical TEPC at Simulated Lengths Less Than 1 μm
 Radiation Protection Dosimetry 31, 129 - 135 (1990)

E.B.Saion, D.E.Watt, B.W.East and P.Colautti
A Co-Axial Double Cylindrical TEPC for the Microdosimetry of Selected Neutron Energy Bands in Mixed Fields of Faster Neutrons
 Radiation Protection Dosimetry 31, 149 - 153 (1990).

P.Colautti, G.Talpo and G.Tornielli
Measurements of Ionization Distributions at Nanometre Level
 Biophysical Modelling of Radiation effects, ed by K.H.Chadwick, G.Moschini and M.N.Varma, Adam Hilger Bristol, Philadelphia and New York, pp. 269-276 (1992).

P.Colautti, G.Talpo and G.Tornielli
Microdosimetry as Specification of the Radiation Quality
 Topics on Biomedical Physics. ed by L.Andreucci, Word Scientific Publ. Singapore, New York and London, (1992).

P.Colautti, V.Conte, G.Talpo, G.Tornielli and M.Bouchefer
A Method to Investigate the Working Characteristics of New Microdosimetric Detectors which Use Low Gas Pressure
 Nuclear Instruments and Methods, in press in NIM A (1992).

Project 2

Head of project: *Dr. D.E. Watt*

Objectives for the reporting period

(i) to pursue detailed analyses of the validity of the proposed new quality parameters, dose restricted LET and linear primary ionisation, for correlation of radiobiological data in a manner which is independent of radiation type. This involves development of a model for radiation action and its comparison with other proposed models with the intention of obtaining improved methods for extrapolation of effects to low doses near environmental levels.

(ii) On the basis of (i), to define the desired response function for design of a new generation of detectors which will be capable of providing an absolute measure of radiation effectiveness.

(iii) to appraise the feasibility of making suitable detectors.

Progress achieved including publications

1. Interpretation of radiation effects and model development

1.1 Calculation of basic quantities for interpretation of biological effect

To facilitate interpretation of radiation effects in terms of physical parameters of special interest to those in our collaborative group, and to provide formal information to other interested parties, a publication has been prepared which contains calculations performed in the csda approximation for a wide range of electron and photon energies and for some commonly used radioisotopes. Quantities calculated are: track and dose average LET, restricted LET ($=100\text{eV}$), relative variances, the mean linear primary ionisation and the corresponding mean free path, csda ranges, the mean energies required to produce a *primary* ion pair and kerma factors for electrons and photon radiations interacting in water. The minimum cut-off energy is 30eV . Results are tabulated for monoenergetic electrons (50eV to 30MeV), characteristic K_{α} X-ray line spectra (carbon to uranium), some commonly used bremsstrahlung (50kV to 300kV) and gamma-spectra (^{241}Am , ^{137}Cs , ^{60}Co , ^{125}I and ^{131}I) and for some typical radionuclides that decay by β -emission or electron capture accompanied by Auger electron cascades (^3H , ^{14}C , ^{32}P , ^{125}I and ^{131}I). Each set of tables is divided into four parts, viz. data for the instantaneous electron energies; averages over the whole primary electron tracks (track averages); averages for the secondary charged particle equilibrium spectrum; information on the build-up factors, spatial concentration of primary and secondary source electrons, fluence of primary and secondary electrons and a quality modified fluence. For photon irradiation there is additional information on the weighted mean free paths for electron production, the weighted mass energy transfer coefficients, the mean photoelectron and Compton electron energies and their net mean range. Wherever relevant, graphical displays are given to facilitate interpolation. Work on part 2 (neutrons) and Part 3 (protons and accelerated ions from protons to uranium ions) is near completion.

1.2 Radiobiological data for analysis

An extensive data base is being compiled of published results for a wide range of relevant biological endpoints and radiation types. Endpoints included are chromosome aberrations, inactivation, mutations, transformations, DNA strand breaks and inactivation of mammalian cells for external irradiation and for radionuclides incorporated into cell nuclei. Initial results show that all of these end-points have a common causal mechanism attributed to double-strand breaks in the DNA. The

radiosensitive target size is demonstrated unambiguously to have a mean chord thickness of about 2 nm and not larger as is sometimes claimed by others. The maximum effect cross-section of about 45 μm^2 for heavy particles, observed and reported by many in the past, is interpreted as the product of the projected cross-sectional area of the DNA in the cell nucleus ($3\mu\text{m}^2$) and the number of DNA segments penetrated on average by a particle traversal of the mean chord through the cell (15 segments). Electrons in equilibrium, at their most damaging energies of about 100eV, cannot penetrate more than one segment and hence for these the maximum effect cross-section is about 3 μm^2 . The ratio of the maxima cross-sections for high and low LET radiations, about 15, gives a biophysical explanation for the magnitude of the allocated quality factors for these radiations. These results have led to a simple model of direct radiation action which has led to novel interpretations of the mechanism for the inverse dose-rate effect for neutrons and heavy particles and the conclusion that the linear-quadratic model is meaningless for extrapolation of effects to low doses. Studies of the component of damage due to indirect action have been pursued with the object of improving the model for application to electron and photon radiations as described below.

1.3 Indirect action by radicals

Preliminary results have been published on the analysis of indirect effects and a full publication is in preparation. The philosophy applied is based on the assumption that since DNA strand breaks are the dominant lesion then if inactivation of single hit targets (e.g. enzymes) can be adequately well quantified for model purposes, it will be a simple process to apply statistical arguments to determine the probability for induction of double strand breaks by indirect action in mammalian cells. Towards this objective experimental measurements have been carried out in this laboratory to investigate the biophysical mechanisms of direct and indirect radiation action using the metallo-enzyme Dihydro-orotic dehydrogenase (Di-Dnase). By measuring the inactivation of the enzyme in solution and in the dry state, with Cu K_{α} X-rays at different dose-rates, it is possible to isolate the respective contributions to damage from direct and indirect (radical) action. Also, the diffusion length can be estimated for the radicals that cause the major damage. The results are consistent with this being the OH^{\cdot} radical. A simplified model has been constructed to take account of direct and indirect action at different concentrations and dose-rates. From this the probability of damage to the DNA in cellular material can be deduced, assuming Poisson statistics apply, and an appropriate model formed. It remains to explore the reliability of the model for a wider range of photon energies. Experimental data (unpublished) for inactivation of ribonuclease in solution is available from earlier studies in this laboratory and is currently being analysed with the object of testing the ability of the model to correlate the data in a unified way.

As the model, in effect, predicts the number of double-strand breaks in cellular material, comparison with data on dsb production in the DNA in cells is seen as a crucial test. Such information is now appearing in the literature and is being compiled on a data base. The model is reasonably sophisticated in the sense that it allows for direct and indirect action, repair, rate effects, irradiation times, varied concentration etc.

1.4 Interpretation of damage to cells by inner shell photoionisation

An important test of the validity of our conceptual notions on radiation action is that the derived model should have the capability of describing apparently anomalous damage situations e.g. the inverse dose-rate effect and the large damage enhancement observed for inner shell excitation accompanied by Auger electron cascades. The model discussed above has been applied to the results for prolonged irradiations of mammalian cells, E-coli and bacteriophages with incorporated radionuclides and the physical mechanism accounting for the high radiation quality is attributed to the total fluence of secondary electrons in the slowing down equilibrium spectrum which, of course, is enhanced by the Auger electron cascades. The action is consistent with that deduced for external photon irradiations. Very recently, in collaboration with colleagues in China (Jin) and Japan (Kobayashi) further confirmation of the validity of the concepts has been using experimental results

performed with monoenergetic synchrotron radiation used to selectively excite the K shell of phosphorus atoms in the DNA of yeast cells and for yeast cells labelled with ⁷⁷ Br.

Plans are in progress to examine the overall significance of the biophysical parameters of the model in a new system of radiation protection against risk.

2. Progress in novel detectors for absolute dosimetry

2.1 MOSFET - type devices

If it is accepted that a double strand break in the DNA of mammalian cells constitutes the fundamental lesion responsible for biological effectiveness then, in principle, a physical detector having a response made to simulate that of the DNA will provide a reading which is directly proportional to biological effectiveness. Exploratory studies are being made on various novel types of detector which it is thought offer good prospects of simulating the response of the cellular DNA.

No knowledge of the type, intensity or quality of the radiation field is required. Research is being carried out in solid phase materials and is intended to complement the studies in gaseous and liquid phase detectors being pursued by our collaborative partners at INFN, Legnaro.

Initial experiments have been performed with MOSFET devices but which are operated in completely novel configurations. In the first instance measurements have been made of the five characteristic modes of operation of various semiconductor devices having different doping materials (p- and n-type), obtained from commercial suppliers. It was found that the n-type MOSFET responded encouragingly well to alpha, X- and gamma- radiation exposures. An exciting feature of the new system used is that it has the ability to distinguish between different radiation types! The source-drain current was found to be a linear function with respect to the drain voltage and corresponded to the dose-rate delivered. A method has been developed to ensure that the signal can be accurately reproduced in successive measurements. In these exploratory experiments, the intrinsic efficiency of the commercially obtained devices is close to 100% . So far experiments have been performed only in the integrated mode. Single particle, and single electron, counting have yet to be investigated. There are no theoretical reasons preventing single particle detection, and indeed, single *charge* sensitivity, if appropriate design modifications are made and if the device is coupled to apparatus with a higher specification. These detectors are expected to offer a variety of possibilities: detector arrays; position sensitive counters with high spatial resolution; particle type identification (they are already capable of distinguishing between high and low LET radiations), in addition to the main objectives of applying the devices to measurement of biological effectiveness. Future progress will depend on gaining access to specialist National nano-electronic facilities, and appropriate funding, so that custom designed devices may be fabricated.

2.2 Thin film scintillators

Although commercially available plastic scintillators can be prepared in nanometre layers they are unsuitable for use for the present dosimetry purposes because of their limiting threshold energy of 1 keV for a useable light output. Nevertheless it is quite possible that more efficient scintillants can be developed. Meantime some preliminary research has been started on the design of the required response for an absolute dosimeter. Towards this objective small spheres of scintillant of micron dimensions were suspended in a matrix of non-scintillating plastic at a concentration selected to give the desired mean spacing between spheres. Studies of light output were analysed in terms of proximity function theory and mean chord distributions to try to relate the light pulse to the mean number of spheres penetrated at the appropriate spacing. In this way it is hoped to be able to scale to nanometre dimensions and to simulate the number of double strand breaks produced simultaneously by individual tracks. Then the signal can be related to biological effectiveness. Much further work remains to be done in this area as present theory is unsatisfactory. However, ideas on a new theory of the scintillation yield for particles of different LET are being developed and will be tested as a guide to improving scintillation yield.

2.3 Langmuir Blodgett films, lipid membranes and other devices

Contact has been made with specialists in the application of LB organic films with a view to applying these to detection of single electrons. Initial discussions have been arranged and will take place soon to explore the feasibility of their application to dosimetry at the nano-metre level. There is the possibility of construction of a solid phase proportional counter and the feasibility is being investigated. Other approaches to be investigated are : superconducting particle detectors; low-dimensional quantum well structures and molecular electronics. It is expected to complete the survey in the next year.

Publications

- (1) Track Structure Data for Ionizing Radiation in Liquid Water: Part 1: Electrons and Photons. D.E.Watt. University report for International distribution. October, 1989.
- (2) Announcement: Track Structure Data for Ionizing Radiations in Liquid Water. Part 1: Electrons and Photons. D.E.Watt. Int. J.Radiat. Biol. 58, (5), 917, 1990. [S]
- (3) Biophysical Calculations of the Initial Yield of DNA Double Strand Breaks in Irradiated Mammalian Cells. Kadiri, L.A., Watt D.E. and Al-Affan I.A.M. Abstract published in Int. J. Radiat. Biol. 57, 1253, 1990. [S]
- (4) Common Mechanism in the Induction of Various Biological Effects by Ionising Radiations. Kadiri L.A. and Watt D.E., 1990. Presented at the Association for Radiation Research Meeting, St. Andrews, April 1990. Abstract published in Int. J.Radiat. Biol. 57, 1259, 1990. [S]
- (5) Interpretation of Damage to Mammalian Cells, E-coli and Bacteriophages by Incorporated Radionuclides for Prolonged Irradiation. A-R.S.Younis and D.E.Watt. Radiat. Protect. Dosim. 31, (1/4), 339-342, 1990. [RCP]
- (6) The quality of ionising radiations emitted by radionuclides incorporated into mammalian cells. Younis A-R.S. and Watt D.E. Phys.Med Biol. 34, (7), 821-834, 1990.
- (7) Physical Quantification of the Biological Effectiveness of Ionizing Radiations. D.E.Watt and L.A.Kadiri. International Journal of Quantum Chemistry. Vol. XXXVIII, 501-520, 1990. [P]
- (8) Physical Specification of Charged Particle Fields for Optimisation of Therapy. Watt D.E. Presented at the Second European Particle Accelerator Conference, Nice June 12-16, 1990. Proceedings edited by P. Marin and P. Mandrillon and published by Editions Frontieres B.P. 33, Gif-sur-Yvette Cedex, France. [S]
- (9) A Co-axial Double Cylindrical TEPC for the Microdosimetry of Selected Neutron Energy Bands in Mixed Fields of Faster Neutrons. E.B.Saion, D.E.Watt, B.W.East and P.Colautti. Radiat. Protect. Dosim. 31, (1/4), 149-153, 1990. [RCP]
- (10) Microdosimetry Concepts in Radiation Protection. Saion E. and Watt D.E. Review Paper in JSNM 8 (1) 1-13, 1990 (Malaysia). [P]
- (11) Biophysical Quantification of Radiation Effectiveness. Watt D.E. and Glodic S. Presented at the Ninth International Congress of Radiation Research. 7th 12th July, 1991. Toronto, Canada. Volume 1, Eds: Dewey, Edington, Fry, Hall, Whitmore. Academic Press. [S]
- (12) Intrinsic Quality of Heavy Particle Beams for Therapy. Watt D.E. Presented at the Fourth Workshop on Heavy Charged Particles in Biology and Medicine. September 23-25, 1991. GSI Darmstadt, Germany. [UCP]
- (13) Observed Cellular Effects Lead to a Track 'Core' Model of Radiation Action. Workshop on 'Biophysical Modelling of Radiation Effects', Watt D.E. Padua, Italy. September 2-7, 1991. Chapter 7, Adam Hilger, 1992. [RCP]
- (14) Comment on Radiation Effects with Special Reference to Transformations. D.E.Watt. Letter to the Editor. Int. J. Radiat. Biol. Vol 61, No.2, 263-267, 1992. [L]

A list of theses for MSc and PhD may be obtained on request.

Project 3 - Theoretical foundations for the specification of radiation quality at the nanometre level

Head of project: *Prof. Dr. Dietrich Harder*

Objectives for the reporting period

It is accepted that the effect of "radiation quality" is caused by the track structure of the ionizing particle. The degree of proximity between radiation-induced chemical radicals or molecular lesions along the track determines the efficiency with which these species can interact with each other in a bimolecular mode during the chemical and biochemical stages of radiation action. For radiation protection it is therefore of primary importance that a powerful descriptive parameter of track structure should be available to make these changes of biological efficiency predictable.

Kellerer and Chmelevsky (Rad. Res. **63**, 226 - 234) clarified that the yield of second-order reactions between radiation-induced species depends on the width of their statistical distribution in an "interaction region" traversed by the ionizing particle, and they proved that unrestricted LET is unable to represent this fluctuation because it leaves the statistical contribution of the delta rays undetermined. However, this fundamental criticism of unrestricted LET was carrying an imperfection in itself, since the geometrical region considered in Kellerer's and Chmelevsky's quantitative estimates was of cellular (0,1 - 10 μm) rather than molecular dimensions, so that most delta rays originating in it were reabsorbed in the same region. Already Kellerer and Chmelevsky predicted that this topologic situation could be essentially changed in smaller regions. When turning to Monte Carlo studies of regions with nanometer dimensions resembling, e. g., the DNA molecule, the nucleosome or the chromatin fibre, our group recognized that long-range delta rays escaped through the region's surface. Only small-range delta rays are reabsorbed in a nanometer region, and their initial spectrum is practically invariant against changes in type and energy of the primary particle as they are generated by "glancing collisions". This "invariance theorem" means that only the statistical distribution of the interactions of the primary particle remains as a fluctuation determinant which depends on type and energy of the primary particle, needing to be characterized by a variable parameter of track structure. Since the number of primary ionizations in a given target region is Poisson distributed, a simple arithmetic mean such as the mean linear primary ionization, I_p , or a quantity proportional to it such as restricted linear energy transfer, L_{Δ} , is sufficient as a measure of the variance.

This insight into the role of L_{Δ} means a breakthrough in view of the old attempt of sufficiently representing track structure (and therefore "radiation quality") by a single physical parameter, at least for all biological and chemical radiation actions whose efficiency depends upon the proximity between radiation-induced species or lesions on the molecular scale.

Progress achieved including publications

In the first two years the Göttingen group has been able to study, by Monte Carlo methods, the fluctuation of energy deposition in targets of nanometer dimensions traversed by electrons, protons, alpha particles and secondary electrons produced by X-rays. The results unambiguously confirmed the "invariance theorem", meaning that the restricted LET of the primary ionizing particle determines the magnitude of the energy deposition fluctuation, since the low-energy delta ray contribution to this fluctuation remains invariant. Calculations by Dr. Michalik (Inst. Nucl. Res. Dubna, E 19-91-63, 1991) and by Dr. Leuthold (unpubl.) independently confirmed our observations. The appro-

appropriate mean values of restricted LET were calculated for various radiations, and cut-off energy $\Delta = 100$ eV was chosen as a standard, providing proportionality between L_{Δ} and I_D . Delta rays with initial energies exceeding 100 eV were treated as independently contributing to the mean values of L_{Δ} . Plots of radiobiological yield values, such as coefficient α for exchange-type chromosome aberrations, showed a unique dependence upon dose-mean restricted LET.

We are in the process of incorporating the description of track structure, simplified by the "invariance theorem", into a biophysical model of intra-track lesion interaction. The continuation of this project will comprise further proofs of the significance of quality parameter L_{Δ} both under the aspects of track structure and from the view of radiation bioeffects.

Publications

- [1] E. R. Bartels and D. Harder: The microdosimetric regularities of nanometre regions. *Radiation Protection Dosimetry* 31 (1990) 211 - 215.
- [2] E. R. Bartels und D. Harder: Mikrodosimetrische Untersuchungen zur Eignung des beschränkten LET als Parameter der Strahlenqualität. *Gemeinsame Jahrestagung 1990. Strahlenschutz im medizinischen Bereich und an Beschleunigern*; Hrsg. D. Harder; Verlag TÜV Rheinland, Köln, S. 44 - 45 (1990).
- [3] D. Harder and E. R. Bartels: Statistical theory of the LET dependence of cellular cross sections for heavy ions. *Fourth workshop on heavy charged particles in biology and medicine*, Darmstadt 1991.
- [4] M. Abou Mandour and D. Harder: Improved representation of scattering and straggling in Monte Carlo simulations of electron beam absorption. *Nuc. Instr. and Meth. in Phys. Res. A* 300 (1991), 403 - 408
- [5] D. Harder, P. Virsik-Peuckert and E. Bartels: Theory of pairwise lesion interaction. In: *Biophysical modelling of radiation effects*. Ed. by K. H. Chadwick, G. Moschini, M. N. Varma. Adam Hilger, Bristol, Philadelphia and New York, 1992, p. 179 - 184.
- [6] E. R. Bartels und D. Harder: Mikrodosimetrische Untersuchungen zur Eignung des beschränkten LET als Parameter der Strahlenqualität. *Strahlenschutz in Forschung und Praxis*, Band 32, S. 275 - 282. Gustav Fischer Verlag (1992).
- [7] D. Harder and E. R. Bartels: Restricted LET determines the yield of intratrack pairwise lesion interaction. In: *Radiation Research - A Twentieth Century Perspective*. Ed. by W. C. Dewey, M. Edington, R. J. M. Fry, E. J. Hall and G. F. Whitemore, Academic Press, 1992, p. 427 - 432.
- [8] D. Harder, R. P. Virsik-Peuckert and E. R. Bartels: Theory of intra-track pairwise lesion interaction. *11th Symp. on Microdosimetry, Gatlinburg, Tennessee (USA), 1992 (accepted)*
- [9] D. Harder and E. R. Bartels: Specification of radiation quality by microdosimetric parameters appropriate at the nanometer level. *11th Symp. on Microdosimetry, Gatlinburg, Tennessee (USA), 1992 (accepted)*

Project 4

Head of project: *Dr. Leuthold*

Objectives for the reporting period

1. Calculation of distribution functions of ionizing events during the random passage of protons through small spherical volumes in order to study the "invariant straggling contribution" of secondary electrons postulated by the Goettingen group.
2. Calculation of proximity functions and dose mean lineal energy for protons below 100 keV.

Progress achieved

1. The distribution of the number of ionizing events by secondary electrons during the random passage of protons through nanometer spheres was calculated by the Monte Carlo method in the energy range from 10 keV to 10 MeV.

The protons started uniformly distributed from a circular area of the same diameter as the sphere. 1000 tracks were produced for each proton energy.

From the distribution the first and second moment were calculated. Especially the ratio of the second to the first moment is of interest, as it is predicted to show nearly no dependence on the primary proton energy for small nanometer targets.

Fig. 1 shows this ratio as function of proton energy in the energy range from 10 keV to 10 MeV. For 2 nm sphere diameter there is only a small variation over the whole energy range. For 5 nm diameter this is no longer valid below 1 MeV, but above 1 MeV the ratio remains constant.

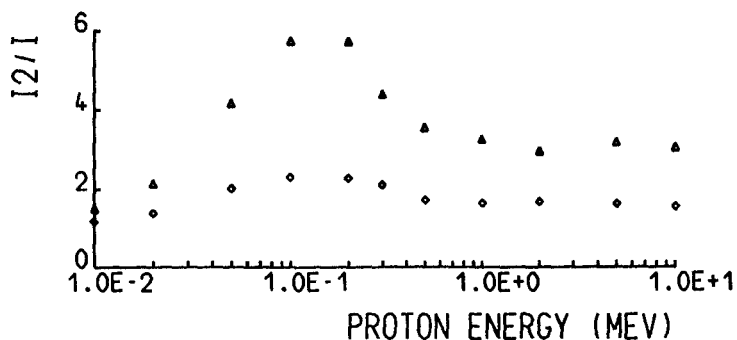


Figure 1 - Ratio of second to first moment of the number distribution of ionization as function of proton energy for spheres of 2 nm (diamonds) and 5 nm (triangles) diameter.

2. The analysis of track structure by means of the proximity functions gives the possibility of distinguishing different track components (G. Leuthold, G. Burger, Rad. Environ. Biophys. 27, (1987)) which contribute to the energy deposition.

The calculation was extended to proton tracks in the energy range from 10 keV to 100 keV. The particle tracks were produced by Monte Carlo simulation. From the proximity function the dose mean lineal energy \bar{y}_D was calculated for spherical targets.

Fig. 2 shows the ion (i.e. proton interaction events only) and the electron (i.e. interactions by secondary electrons within the same electron track) component of \bar{y}_D for 10, 50 and 100 keV protons as function of the sphere diameter.

With decreasing proton energy the ion component becomes dominant and remains nearly constant for higher sphere diameters. The electron component decreases because of the decreasing kinetic energy of the secondary electrons.

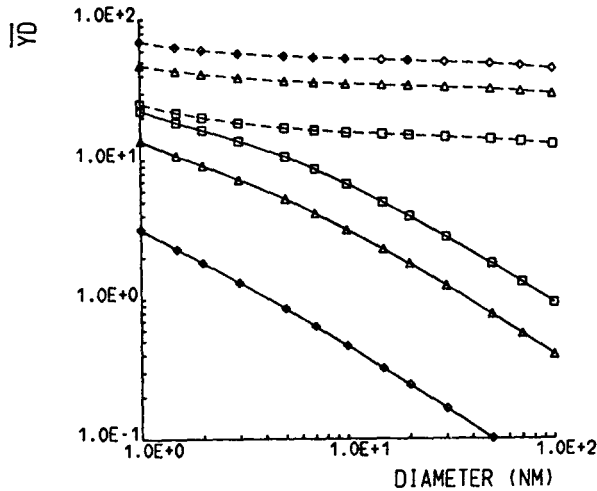


Figure 2 - Dose mean lineal energy \bar{y}_D (eV/nm) of ion (dashed lines) and electron (solid lines) track component as function of sphere diameter for 10 keV (diamonds), 50 keV (triangles) and 100 keV protons (squares).

Project 5

Head of project: *Dr. Izzo*

Objectives for the reporting period

1. Determination of local radical densities in γ -ray irradiated samples of solid biochemicals as a function of imparted dose.
2. Measurements of local radical densities in the irradiated frozen tissues and cell samples
3. study of the effect of dose rate on the local radical densities.
4. In order to make possible the measurements listed above the following modifications and additions to the basic ESR instrument were necessary :
 - a. Adaptation of an existing ESR spectrometer to precise measurements of the spin-spin relaxation times, by means of the determination of field intensity in the cavity.
 - b. Development of software for absolute measurement of local radical density.
 - c. Installation of a refrigeration system and other modifications of the spectrometer for the ESR measurements on tissue and cell samples down to the temperature of liquid nitrogen.
 - d. Incorporation of digitizers for digital data acquisition, storage and manipulation, in order to improve the performance in respect of sensitivity and resolution. These improvements are necessary for completion of the project.

Progress achieved including publications

The work of the group in Rome centers around the use of electron spin resonance measurements on radicals created by ionizing radiation. While the average radical density produced by ionizing radiation in condensed state is a measure of absorbed dose, the discrete character of deposition of energy results in formation of regions (spurs, columns, clusters) with local densities much higher than the average value. The distance between the nearest radicals are of an order of tens and hundreds of nanometers. With an increase in restricted LET the ratio of local to average density increases.

The method used for evaluation of the local spin densities was that of continuous saturation, performed with an X-band spectrometer fitted with additional components to assure a precise measure of power level in microwave cavity. Furthermore, the magnetic field in the cavity was calibrated using the Slater perturbation method. In that way the absolute values of local spin densities were obtained, unlike the

relative values (comparison with some substance taken as a standard or the same substance irradiated with radiation of different quality). Some measurements were also done with another technique based on line broadening. This last method promises to be suitable for a broad range of samples, but requires to install a digital readout and processing of spectra to utilize its superior potential. The results found so far were obtained with an analog read out. Further information obtainable from ESR spectra are the mean size of clusters and the distribution of their sizes, both obtainable from the build-up kinetics. The materials studied (water, bovine muscle, aminoacids, some polymers) were irradiated with 12 MeV bremsstrahlung, and cobalt-60 γ -rays. The samples from irradiation to readout were kept at liquid nitrogen temperature to avoid radical changes, slow cluster diffusion and drift etc.

An ionizing particle passing through the medium leaves behind ion-radicals, neutral radicals and electrons. All those can be trapped in the solid in a sufficiently low temperature.

While the average radical (spin) density produced by ionizing radiation in solids is proportional to the absorbed dose, the discrete character of deposition of energy results in formation of regions (spurs, columns, clusters) with local densities much higher than the average value. These local densities are related to the LET of radiation (Wyand, in "Charged Particle Tracks in Solids and Liquids" eds. G.E. Adams, D.K. Bewley and J.W. Boag, publ. Inst. of Physics, Bristol, 1970 ; Katsumura et al., Radiat. Phys. Chem. 16.255.1980; Ogawa et al., Radiat. Phys. Chem. 16.15.1980; Ettinger et al. in "Neutron Dosimetry", eds. M. Schraube, G. Burger and J. Booz, publ. EEC-Euratom, Brussels 1985). The determination of local radical densities in irradiated materials complements microdosimetry in describing the effects of irradiation and may lead to the development of a practical method of simultaneous evaluation of the absorbed dose and the LET.

Determination of the radical densities is accomplished e.g. through the observation of the broadening of ESR spectral lines. If all radicals (spins) are identical and stay in the same magnetic environment the system is regarded as homogeneous. Few spins can group together forming a spin packet which also will be homogeneous; its line shape is Lorentzian. However, ensembles of spin packets are as a whole inhomogeneous and are described by a Gaussian envelope. In experiments we often encounter line shapes inhomogeneously broadened with diverse contributions of the homogeneous broadening (e.g. from dipole-dipole interactions) and there exist mathematical techniques for unfolding such distributions. The contribution of neighbouring spins to the line width can be found from a relation $\Delta H_L = kC$ where k depends

on the substrate in which radicals are formed and C is the local spin concentration (cm^{-3}). For a polycrystalline sample $k = 9.3 \times 10^{-24}$ Tesla cm^3 (Wyard, op. cit.). The local radical density is thus $C = \Delta H_L/k$. In order to find the line width of the Lorentzian component only, one needs to unfold the line shape or to use indirect methods, e.g. the progressive saturation method. To use this method it is necessary to construct the power saturation curve which is a plot of ESR signal amplitude as a function of microwave magnetic field intensity inside the cavity, in a point corresponding to the position of the sample. From the study of saturation behaviour one can find relaxation times T_1 , (spin-lattice) and T_2 (spin-spin). The Lorentzian line width is linked to T_2 by relation $\Delta H_L = (\gamma T_2)^{-1}$, where γ is the gyromagnetic ratio of electron (1.76×10^{11} Tesla $^{-1}$ sec $^{-1}$). For a homogeneous saturation behaviour $T_1 T_2 = (\gamma H_{1/2})^{-2}$, $H_{1/2}$ is the value of RF magnetic field at which the ESR signal amplitude is a half of what it would have been in the absence of signal saturation. This RF field must be found from an experiment. For an inhomogeneous case $T_1 T_2 = 3(\gamma H_{1/2})^{-2}$. For an intermediate case one needs to know α , the ratio of Lorentzian spin packet width to observed Gaussian line width, which is found from the saturation curve (Katsumura et al., op. cit.). Once α is determined, the spin-spin relaxation time can be found from $T_2 = 1.70(\alpha \gamma H_{1/2}^G)^{-1}$ where $H_{1/2}^G$ is the measured line width at the maximum slope of the experimental Gaussian line (Zimbrick et al., J. Phys. Chem 16.15.1968). The radical density follows from $C = (k \gamma T_2)^{-1}$.

There are several ways of trapping electrons in irradiated molecular crystals and amorphous substances : formation of a negative ion as a result of the capture of a slow electron by a molecule of the medium, capture of an electron by trapped radical, stabilization of an electron in an intermolecular trap. The first process is very likely in irradiation of substances with positive electron affinity (e.g. proteins). The capture of electrons by radicals is probable only within a particle track. In many compounds (water, alcohols, aliphatic hydrocarbons, ethers, amines, aminoacids) electrons are trapped predominantly in intermolecular traps at low doses. With an increase in temperature the electrons are released from traps. This gives rise to a thermostimulated current (TC). If a movement of electron ends in recombination with a radical the effect is organic thermoluminescence (TL) (e.g. Weinberg C.J., Nelson D.R., Carter J.G. and Augenstein L.G., J. Chem Phys. 36.2869.1962). The ratio of TC/TL is depending upon the

product of trapped electron density and trapped radical density.

The density of trapped electrons can be found by electron spin resonance, the shape of electron spectral line being very narrow (E.L. Frankevich, *Uspekhi Khimii* 365.1161.1966; Ekstrom A. *Radiat. Res Rev.* 2.381.1970). With an increased polarity of the medium the trapping efficiency increases, which makes the conditions favourable for the study of DNA. The trapped electrons are formed in the local regions, just like radicals. The local concentrations of trapped electrons can be found by a continuous saturation method, in a way analogous to that used for radicals. The results of determination of local density of both electrons and radicals can be checked also by observation of the kinetics of trapped electron decay.

Table 1 - Some local densities of radicals created by low let radiations in solids

Substance	Local Density	Average Density	Ratio of densities
Pure water ice (77 K)	5.5×10^{19}	3.2×10^{18}	17.2
Tap water ice (77 K)	5.6×10^{19}	3.2×10^{18}	17.5
Bovine muscle (77 K)	5.7×10^{19}	3.0×10^{18}	19.0
L- α -Alanine	4.3×10^{19}	3.0×10^{18}	1.4
Perspex	1.1×10^{20}	3.1×10^{17}	350.0
PTE	3.1×10^{20}	3.2×10^{17}	970.0

Publications

1. Spatial Distribution of Free Radicals Produced By Neutrons (K.V. Ettinger, U.J. Miola, A.R. Forrester and A. Ghosh) in "Neutron Dosimetry" , Proc. Int. Symp. eds. M. Schraube, G. Burger and J. Booz, publ. EEC-Euratom, 1988).
2. Free radical dosimetry Techniques and their suitability for precise and accurate measurements of radiation (K.V. Ettinger) *Appl. Radiat. Isotopes*, 40, 865, 1989.
3. A precise S-band ESR reader for free radical routine dosimetry (C. Franconi, J. Holowacz, E.M. Staderini, M. Bonori, K.V. Ettinger and R.F. Laitano) *Appl. Radiat. Isotopes*, 40, 835, 1989.
4. On the magnetic RF Fields in some resonant systems used in the radical local density determination by saturation method. (K.V. Ettinger and J. Holowacz) Proc. 3rd Int. ESR Symposium gaithersburg USA, 1991. Ed. M. Desrosiers and W.L. McLaughlin.
5. Investigation of specialized S-band spectrometer for ESR dosimetry. (C. Franconi, J. Holowacz, M. Bonori, K.V. Ettinger and R.F. Laitano) Proc. 3rd Int. ESR Symposium gaithersburg USA, 1991. Ed. M. Desrosiers and W.L. McLaughlin.
6. ESR windows onto the nanometer Landscape. (G. Izzo, K.V. Ettinger and J. Holowacz) Accepted for the Int. Microdosimetry Symp., Oak Ridge, Tenn. USA, 1992
7. Features of radiation field measurement by ESR (K.V. Ettinger and J. Holowacz) Submitted for the congress of Italian Society for Radiation Research, Capri 1992.

LATE SOMATIC EFFECTS OF IONIZING RADIATION ON THE MAMMALIAN ORGANISM

Contract Bi6-099 - Sector B12

1) *Maisin* , Univ. Cathol. Louvain à Woluwe

Summary of project global objectives and achievements

The objective of the European Late Effects Project Group (EULEP) is to improve the understanding of late biological effects of exposure to ionising radiation. Its work consists of the standardization and development of methodology in the member institutions, the co-ordination and promotion of co-operative research by means of task groups, and the organisation of training activities, workshops and symposia. Twenty-three laboratories have participated in this work.

1. Standardisation and Development of Methodology

This aspect of the work was carried out by the standardisation committees:

- Committee of External Radiation Dosimetry and Techniques
- Committee of Internal Radiation Dosimetry and Techniques
- Committee on Pathology
- Committee of Cell and Molecular Biology
- Expert Group on Physiological Methodology

2. Co-ordination and Promotion of Co-operative Research

The co-ordination of collaborative research work between the member institutions has been organised by means of a number of problem-orientated task groups and special task group actions. In addition work has commenced to establish an archive of long-term radiobiological studies.

3. Training Activities

EULEP has been concerned to promote the training of young radiobiologists. High priority continued to be attached to the support of scientific exchange visits between laboratories for the purpose of acquiring technical expertise. EULEP has also organised special training courses, in order to promote the introduction of new methodologies into member laboratories.

Project 1

Head of project: *Dr. Maisin*

Objectives for the reporting period

- (a) to continue to develop the programme of standardisation and development of methodology through the committees;
- (b) to promote the co-ordination of research by the task groups and special task group actions, including the review of existing work and the establishment of new task groups and actions as opportunities presented themselves; to plan and commence work on the radiobiology archive;
- (c) to plan training activities as outlined in (I) above and to review the teaching of radiobiology in the different countries of the EC, with a view to preparing standardised course material for lectures on the subject.

Progress achieved including publications

1. Standardisation and development of methodology

1.1 Committee of external radiation dosimetry and techniques

High dose total body irradiation (TBI) in combination with intensive chemotherapy followed by bone marrow transplantation (BMT) has shown to be of increasing benefit for the treatment of acute leukaemia and some other disseminated diseases. The long-term surviving patients constitute a very interesting group in which stochastic and deterministic effects of total body irradiation can be studied. Under the auspices of EULEP, the European Society for Therapeutic Radiology and Oncology (ESTRO) and the European Bone Marrow Transplant Group (EBMT), a meeting was organised on the physical, biological and clinical aspects of total body irradiation (Broerse *et al.*, 1990).

The results of the sixth EULEP X-ray dosimetry intercomparison have been analysed by the Standardisation Laboratory of the Dutch National Institute of Public Health and Environmental Hygiene (Aalbers and Bader, 1991). Concerning dose values in the centre of the mouse phantom it appeared that ten out of fifteen participants had deviations of 5 per cent or less from the reference value which is considered to be adequate. For three participants the dose deviations in the centre of the mouse phantom were between 5 and 10 per cent. These deviations are somewhat too large and it was recommended that these participants should check their dosimetry procedures including calibration of the dosimeters used. The dose deviations of two participants were 12 and 14 per cent. For these participants a check of their dosimetry procedures was recommended including a recalibration of the dosimeters; in addition a site visit was offered to resolve the dosimetry problems.

With regard to dose distribution in the mouse phantom, it is recommended in the EULEP code of practice for X-irradiation of small animals that the irradiation of an animal should be uniform, i.e., a maximum ratio of 1.10 in the absorbed dose for different positions in the

subject but preferably less than 1.05. Nine participants fulfilled the criterion of a maximum dose ratio of less than 1.10 and five of them reached a dose ratio of less than 1.05. Five participants had dose ratios in excess of 1.10, whereas one participant did not aim for a uniform irradiation. The situation is considerably improved compared to the fifth intercomparison in which only four out of ten participants achieved a ratio of 1.10 at maximum.

It is concluded from the results that there is obviously a continued need for such intercomparisons.

1.2 Committee of internal radiation dosimetry and techniques

The scientific activities of the committee have included detailed discussions of the new Recommendations of the ICRP (Publication 60). Through a number of its members the Committee has been involved with ICRP and other international groups in the work of developing age-dependent dosimetry and new biokinetic models for workers and for the general public. The new biokinetic models are needed for the revision of dose coefficients, radiation dose per unit intake of radionuclide in Sv/Bq, which are necessitated by the new ICRP Recommendations. In another area the committee discussed the role of chelation therapy in the reduction of the risks of late effects from radionuclide incorporation. It has drawn attention to areas in which the methods of chelation therapy could be used to provide information which could assist in the elucidation of some fundamental problems in the radiobiology of internal irradiation; these relate especially to changes in dose rate and to the determination of the importance of the early and late periods of irradiation in relation to the induction of cancer or other late effects.

A workshop on *Age-Dependent Factors in the Biokinetics and Dosimetry of Radionuclides* was held at Schloß Elmau, Germany, in November 1991. This very successful four-day meeting, which was organised jointly with the CEC and the United States Department of Energy, attracted 53 scientists from many countries ranging from Brazil to Russia. Some 40 invited or contributed papers were presented in nine sessions covering many topics from gastrointestinal physiology, through embryo and fetal physiology and dosimetry, bone, lung and other tissues to the difficult problem of how to extrapolate animal data to human situations. Numerous areas were identified in which further research is urgently needed. The proceedings of the workshop will be published in *Radiation Protection Dosimetry* in the autumn of 1992.

The Committee has continued to advise and assist the task groups working in the field of radionuclide metabolism, dosimetry and effects, especially by encouraging multidisciplinary approaches to problems and the introduction of the latest molecular biological techniques into the investigation of radionuclide effects.

1.3 Committee of pathology

The main goals of this committee are (i) to standardise further and to update diagnostic terminology as used by pathologists of the EULEP member laboratories, and (ii) to increase the expertise of members in various morphological aspects of late effect studies in laboratory animals, including the application of new techniques.

The Committee organised a half-day symposium on 'Molecular-Biological Methods in Pathology' at Reisenburg in 1991. The topics covered included a description of the principles, practice and applications of PCR, the principles and applications of *in situ* hybridization, and immunocytochemical methods for the location of DNA adducts in sections.

The annual slide seminar for 1990 was on 'Exocrine Pancreas and Salivary Glands'. Three lectures on lesions in human tissue provided background information on current classification practice, special stains and immunohistochemistry. Experimental reports included detailed descriptions of preneoplastic and neoplastic lesions in the pancreas of rats, mice and hamsters, illustrations of retrovirus- and radiation-induced lesions in experimental animals, and presentation of some controversial results derived from a rat pancreatic carcinoma model.

In 1991 a slide seminar was held on the Central Nervous System. This included an overview of the classification of neoplasms of the nervous system. The classification was illustrated by slides of characteristic experimentally-induced tumours in rats. Additional cases in different rat strains were discussed. Peculiar neoplasms originating at the brain base/skull base border of the TXHT/F₁ mouse were presented. The classification of tumours of the central nervous system in humans seems to be applicable to tumours in experimental animals. Modern immuno-histochemical methods for the characterization of the glial cell lineage was demonstrated using glial cells cultured *in vitro*.

Three new fascicles of the EULEP Pathology Atlas were published (see list of publications below). The committee is arranging for a new version of the Atlas with colour pictures to be published by F K Schattauer (Stuttgart). The first volume, covering liver, kidney, pancreas, mammary gland, urinary bladder, lymphoid system, central nervous system and bone, will be prepared in 1992.

1.4 Committee of cell and molecular biology

The Committee's main aim has been to intensify efforts to provide a valuable technical and scientific background for EULEP laboratories involved in molecular and cellular projects.

As a major step in this direction a chemical synthesis project for oligonucleotide probes has been established in the Department of Molecular Biology, Aarhus. The project started with the production of a stock of oligonucleotides from sequences of endogenous murine retroviruses. A database for these sequences has been established and made accessible to EULEP laboratories; it has been extended considerably over the reporting period. The project was later expanded to offer EULEP members free synthesis of oligonucleotides and consultation on their design e.g. as primers for PCR. The demand for this service increased markedly over the two-year period.

To introduce molecular methods further into the framework of EULEP activities, the Committee organised a course in PCR techniques at GSF Neuherberg in 1991. The 3-day course included a theoretical introduction to the field with practical examples of application as well as the different possibilities of technical instrumentation and a discussion of detailed problems. The course was given by experts from different EULEP laboratories; it was attended by 12 participants.

1.5 Expert group on physiological methodology

There have been consultations concerned with two projects:

(i) Late effects after total body irradiation for bone marrow transplantation (see also below). Consideration has been given to questions relating to the standardisation of functional tests in patient follow-up. The EULEP/EBMT review of patients surviving over 5 years has prompted consideration of liver and brain function. Whatever the origin of hepatitis (viral, toxic, radioinduced), the consequence is a destruction of the hepatocyte population. The ^{14}C -aminopyrine breath test of hepatocyte viability would be suitable for detecting a reduction of liver functional volume after conditioning. As far as the brain is concerned, children and adult patients are to be considered separately. The mental evolution of BMT children should be scaled (Wechsler Intelligence Scale, Burt Reading Tests) and correlated with endocrinological and growth changes. These latter changes are planned for suitable extensive investigations under the control of specific task groups. Both children and adult patients should be checked for brain atrophy by MRI and for cerebrovascular disease by perfusion mapping. For possible effects of conditioning on the lungs, functional investigations of BMT patients have been proposed. The diffusion capacity of the lungs, as measured by DL_{CO} , has been recommended.

(ii) Late effects after local irradiation of the heart. The group has contributed to the work of the task group on radiation effects on the heart (see below). Essentially three types of technique have been used. These were validated and radiation-induced variations in cardiac output correlated.

2. Co-ordination and promotion of co-operative research

(Note: The EULEP task groups have all held regular meetings, typically once or twice per year, often in addition to interlaboratory consultations including exchange visits by members.)

Some of the more significant aspects of progress achieved by the task groups and special task group actions are as follows:

2.1 Molecular approach to the study of radiation-induced osteosarcoma

The goals of this task group are aimed at studying molecular mechanisms underlying radiation-induced osteosarcomagenesis. This task represents more specific and in-depth studies operating in and serving research activities carried out in the programmes of the two participating institutes and of the EC Radiation Protection Research Action. Particular emphasis is put on rapidly disseminating current advances in molecular and cellular biology, developing new methods, and training young colleagues from these and other EULEP laboratories.

Based on the model of radiation-induced osteosarcomagenesis in mice, the mode of action of radiation-activated endogenous retroviruses has been studied, and their role in bone tumour development. Retroviruses, activated dose-dependently by α -irradiation, provide a powerful model system to study the induction of early genetic effects and the development of late somatic effects in the skeleton, to elucidate additional factors required for the development of

neoplastic bone disease, and to identify and isolate critical cellular targets of presumed relevance for radiation-induced osteosarcomagenesis.

The following have been task accomplished: (i) isolation of radiation-activated endogenous retroviruses, newly integrated in radiation-induced osteosarcomas; (ii) molecular characterization and analysis of the bone disease-inducing potential of radiation-activated retroviruses; (iii) molecular cloning and analysis of a prototype bone disease-inducing retrovirus, RFB; (iv) molecular and biological characterization of the prototype endogenous, ecotropic murine retrovirus Akv with emphasis on bone disease-inducing properties; (v) establishing the sensitivity of different mouse strains for bone disease induction of viruses of the Akv family; (vi) studies on the co-operation of activated endogenous retroviruses with the *fos* oncogene in the development of malignant bone tumours in *c-fos* transgenic mice: expression of endogenous retroviral sequences in transgenic tumours suggested an interaction of activated proviruses with the transgene in osteosarcomagenesis.

Present research activities include: (i) altering the disease-inducing specificity by introducing point mutations into the regulatory region of a prototype T-lymphoma-inducing retrovirus, SL3-3; and (ii) effect on gene expression by retrovirus infection of primary target cells in culture.

The support of EULEP has successfully fostered the transfer and complementation of the methodologies of the two partners by enabling interlaboratory consultations and training visits to take place each year.

2.2 Cell and molecular studies on radiation-induced haemopoietic neoplasias

Acute Myeloid Leukaemia (AML) Studies on the nature of chromosome (ch)2 deletions and rearrangements in radiation-induced murine CBA/H AMLs have centred on the nature of the radiation-sensitive fragile sites that appear to be involved in AML-initiating ch2 breakage and gene loss. Previous cytogenetic evidence suggested that these interstitial chromosomal sites might have some structural relationship with the telomeric (TTAGGG)_n DNA repeat arrays that are found at chromosome ends. Accordingly, using synthetic telomere sequence probes (provided by EULEP), genomic sequences encoding interstitial telomere-like repeat (TLR) sequences were cloned from gel-purified mouse DNA restriction fragments and microdissected ch2 DNA libraries. One such TLR clone had a characteristic inverted repeat structure and, in fluorescence *in situ* hybridization (FISH) studies, revealed multiple sites of TLR sequences at interstitial locations on all murine and human metaphase chromosomes.

The specific location of TLR arrays on murine ch2 were mapped by FISH; five sites were identified, two of which corresponded with two principal radiation-sensitive fragile sites (2B and 2F) seen in AMLs and irradiated normal marrow cells. In addition, a ch2 F region TLR array was mapped by pulsed field gel techniques to within 250 kb of the *IL-1* haemopoietic gene cluster. These data add weight to the argument that AML initiation by radiation is driven by gene loss from ch2 resulting from misrepair at specific fragile sites containing recombinogenic TLR sequence arrays.

It seems likely that certain classes of ch2 rearrangements may be an initiating event for AML, but insufficient for the development of overt leukaemia. Activation of a *ras* oncogene is considered with a few exceptions as a late carcinogenic event and studies have addressed

the question as to whether such mutations are present in radiation-induced mouse AMLs.

Male CBA/H mice were irradiated at the age of 3 months with a single X-ray dose of 3 Gy. AML was diagnosed on the basis of haematological and pathological examination. The search for mutations was performed by oligodeoxyribonucleotide mismatch hybridization with *ras* gene segments (exons 1 and 2) that had been amplified by the polymerase chain reaction (PCR). Only one mutation was detected among the 26 AML samples examined. This was detected in both the spleen and the bone marrow, where at least 50 and 25 per cent of the cells were involved respectively. It appears therefore that classical oncogenic *ras* mutations are much less frequent in mouse radiation AMLs than in human AMLs. Moreover, it should be noted that an overwhelming majority of the mutations in human AMLs involve *N-ras*, while the only mutation found in murine AMLs was located in *K-ras*.

Thymic lymphoblastic lymphomas Studies on the role of cytokines such as interferon gamma (IFN- γ) or tumour necrosis factor alpha (TNF- α) in the protection of lymphoma development after bone marrow grafting have been extended. At the molecular level, *in situ* hybridization has been used to localize the production of TNF- α in the thymus of marrow-grafted irradiated animals. It was shown that TNF- α positive cells were more frequent in these thymuses than in those of irradiated animals. In parallel, studies have been performed to define the ontogeny of cytokine (TNF- α , IL-2, IL-4, IL-1, IFN- γ)-producing cells in the normal thymus; the normal differentiation of thymocytes is closely regulated by these cytokines.

2.3 Cell biology of haemopoietic tissues

The objectives of the task group are (i) to characterise radiation-induced leukaemias in the NFS strain of mice; (ii) to identify factors produced by the bone marrow that prevent the development of leukaemia.

Radiation-induced leukaemias in NFS and CBA mice The NFS strain of mice has been chosen because it is free of endogenous ecotropic retroviruses. Since viruses do not seem to be implicated in most human leukaemias, the NFS mouse model may be more relevant for human pathology. Split-dose irradiation (4 x 1.75 Gy) yielded 32 thymic lymphomas and 16 non-thymic leukaemias or lymphomas. The characterization of the latter form has recently been completed and is being published.

Nine cell lines have been established from primary leukaemias induced by X-rays in intact or thymectomized NFS mice. Mercaptoethanol was essential for their growth. The cells were found to be cortisone-resistant, but sensitive to irradiation. Apoptosis was induced in all lines by as little as 2 Gy. Cytochemical markers (eg chloroacetate esterase) suggested a myeloid nature for all cell lines. Further analysis revealed expression of receptors for the calcitonin gene-related peptide (CGRP), previously identified on cells of the myeloid (and not of the lymphoid) lineage. By immunophenotyping, all cell lines were negative for pre-T and T-cell specific markers. In contrast, pre-B or B markers were consistently present (6C3-HSA-B220). Some of the lines also expressed CD5 molecules. Analysis of the IgH locus in these cell lines demonstrated rearrangement of the J region, indicative of a B-cell origin. Furthermore, using PCR, expression of the *v* pre-B surrogate light chain component was documented. The lines were tested for the expression of different cytokines at the mRNA

level: they did not express IL-2, IL-4 or INF- γ ; some expressed IL-1 α , IL-7, TNF- α , TNF- β in various combinations, eight lines expressed IL-6, and one line expressed IL-3.

Factors preventing the development of leukaemia Previous data indicated that in mice irradiated at a leukaemogenic dose, alterations of the thymic epithelium and of thymic lymphopoiesis are strictly correlated to the leukaemogenic process. A bone marrow graft prevents the development of radio-induced thymic lymphomas. It does not inhibit the emergence of preleukaemic cells, but induced their disappearance after a few weeks. Simultaneously, intrathymic differentiation and the functions of the thymic epithelial cells are restored.

A working hypothesis to explain how the preleukaemic cells disappear after a bone marrow graft is that cytokines produced by bone marrow precursors interfere with the development of leukaemias by acting on the functions of the thymic microenvironment. Attempts have been made to inhibit the development of lymphomas by administering cytokines. IL-1 did not reduce the incidence of lymphomas, whereas repeated injections of TNF- α and/or γ -IFN did inhibit the development of lymphomas. These cytokines restored intrathymic lymphopoiesis and the functions of thymic epithelial cells. Moreover, the bone marrow graft induced a wave of intrathymic TNF- α production.

2.4 Cellular basis of late vascular changes in the areas at risk in the irradiated brain

The current objectives are (i) to study the pathophysiology of late radionecrosis in the CNS to determine its causes, and (ii) to identify possible methods of prevention.

It is hoped that the first goal can be achieved by identifying the morphological and physiological changes preceding the development of necrosis in the brain. To investigate this question, 200 rats have been irradiated with doses of 17.5, 20, 22.5 and 25 Gy and groups of 6 to 8 rats sacrificed at three month intervals. One hemisphere was prepared for histological study using the routine as well as special methods. The other hemisphere was prepared for electro-microscopic studies using selected brain sections. Several papers have already been published in international journals and others will be prepared based on observations not yet completely evaluated.

Physiological studies of blood circulation and water content in the brain of rats after 20 Gy have already been published. Recent studies on the brain of rats irradiated with a dose of 25 Gy showed an important decrease in regional cerebral blood flow, particularly in the white matter of the fimbria, 6 months after irradiation.

Observations on dose-limiting factors in radiotherapy of the brain, pathogenesis of brain radionecrosis as a late effect of CNS irradiation, and radiation damage to the microcirculation of the brain have been reported in two papers at the International Symposium on Acute and Long-Term Side Effects of Radiotherapy in October 1991. A paper based on the electron microscopic findings is also being prepared.

The second line of research of the group includes the special task group action entitled 'Amelioration of the Development of Late Radiation Damage'. The objective of this project is to prevent, reduce, or delay the appearance of late radiation damage to the CNS. Such an effect might be achieved by means of drugs which are able to ameliorate microcirculatory

conditions impaired by irradiation. Several drugs are currently available to protect the vessel walls. Pentoxifylline exhibits characteristics which are important for maintaining the microcirculation flow in ischemic conditions, e.g. by increasing ATP control, furthering the deformability of erythrocytes, inhibiting the aggregation of thrombocytes, decreasing the fibrinogen concentration and increasing prostacyclin release from the vascular endothelium. The consequence of such effects should be a decrease in the tendency for thrombus formation and an improvement in blood flow.

Based on the above considerations a research program was established involving five European laboratories. The aim is to keep the microcirculation of the brain intact as long as possible after irradiation. Female rats receive local X-irradiation to the brain with a single dose of 25 Gy. It is expected that the vessels will be protected by Pentoxifylline at a dose of 50 mg/kg per day in the food. Animals have been irradiated for morphological studies and also to study the brain circulation. Preliminary results have been presented at a task group meeting in November 1991. Animals treated with Pentoxifylline showed a reduction in the damaging effects of irradiation as observed in the fimbria of the brain in the 39th week. The protecting effect of Pentoxifylline was not observed in animals in the 52nd week after irradiation.

2.5 Radiation effects on the heart

Three techniques were used to assess changes in cardiac function in the rat after irradiation. These were: an *in vitro* isolated heart preparation; a non-invasive *in vivo* method using a single crystal detector for external radioactivity measurements; and a γ -camera method as used clinically which allows the evaluation of the left ventricle ejection fraction. These techniques are complementary to each other; measurement of cardiac output was standardised between them. The criteria for radiation-induced heart disease were explicitly defined for use by the participating laboratories. Functional changes were compared with histological studies in the rat heart. There was generally good agreement between experimental findings in the rat and clinical observations.

This task group has been closed: it achieved its original objectives for the standardisation of experimental techniques, and the results were published.

2.6 Effects of radiation of pre-implantation mouse embryos

Previous experiments have shown that Heiligenberger mouse strain responds with a higher frequency of malformations (mostly gastroschisis) after radiation exposure of the preimplantation stages. The studies have been extended to radiation exposure of various stages of oogenesis and spermatogenesis. The problem with the high dose rates (1 Gy/min) used initially is that immature mouse oocytes are very sensitive with regard to lethal effects under such conditions. Therefore experiments with a lower dose rate (0.4 Gy/h) using a ^{137}Cs source were carried out. The most obvious effect was a markedly reduced frequency of lethal effects on embryos originating from oocytes up to an age of four weeks before ovulation. The number of malformed fetuses was also somewhat lower than in the high dose rate experiments. However, despite the much lower dose rate, it was not possible to obtain living embryos from oocytes older than five weeks after radiation exposure. Therefore experiments have commenced with an even lower dose rate (0.016 Gy/h).

An experiment has been completed on the radiation response of various stages of spermatogenesis. After a gamma-dose of 4 Gy (dose rate: 0.4 Gy/h), 32 out of 508 living fetuses (= 6.3%) showed a gastroschisis compared to 16 out of 686 (= 2.3%) in the controls ($p < 0.01$). For resorptions and dead foetuses, lethality was most pronounced in those stages shortly after meiosis, whereas premeiotic stages did not show an increased frequency of these lethal effects. However, if preimplantation death is included, then premeiotic stages were clearly affected.

Results obtained on the relation between gastroschisis and protein patterns confirmed the conclusions drawn from previous experiments: those fetuses with a radiation-induced gastroschisis showed the highest numbers of changes in the protein pattern of liver proteins. There were no specific changes that could be related to the occurrence of gastroschises. The results support the hypothesis that the mechanism of the induction of malformations after radiation exposure during oogenesis or preimplantation stages (in particular, the 1-cell stage) is related to a general labilization of the genome.

A comparison has been made of the radiosensitivities of the resting oocyte of the guinea-pig in its two different states, the 'large' resting oocyte and the 'contracted' one, also extending the investigations to the radiosensitivity of the immature oocyte at earlier stages during intrauterine life. The aim was mainly the verification of the extreme radioresistance of the guinea-pig oocyte and the consequent suitability of this species for further detailed studies in relation to genetic hazards in man.

The radiosensitivity of the guinea-pig oocytes was evaluated by testing the fertility of the animals 6 months and one year after irradiation of the ovaries with high doses (2 or 4 Gy) of X-rays. Animals had been treated *in utero* (target cells: oogonia and oocytes at leptotene), at birth (target cells: resting oocytes of the 'large' type) or as adults (target cells: resting oocytes of the 'contracted' type). No loss of fertility appeared, even one year after treatment, whatever the stage or dose. These investigations were completed by histological studies of the ovaries from treated and control animals. Irradiation induced a dose-dependent decrease in the total number of oocytes, and this effect was more pronounced in animals irradiated as adults (target cells: 'contracted' resting oocytes). A preliminary cytogenetic study was also performed on resting oocytes of the two different types. It appears that irradiation can induce chromosomal aberrations in the resting oocyte, a stage which had always been thought to be refractory to such effects.

2.7 Effects of radiation on the development of the central nervous system

The end-points studied comprised acute and delayed types of neuronal damage, neuro-structural damage and growth retardation, and neuro-functional disorders.

(i) *Neuronal damage* Preliminary results have been obtained for gamma irradiation of nerve cells in culture. Isolated rat mesencephalic and striatal nerves cells were irradiated with 0.25-3.0 Gy and cultured during 3 days in serum-free medium. The number of living cells decreased significantly with even 0.25 Gy. More mesencephalic cells were killed by the same dose of irradiation than striatal cells. Dopamine and Gamma Amino Butyric Acid (GABA) uptake by mesencephalic cells and GABA uptake in cells of both types were decreased after 0.25 Gy irradiation. All these effects were dose-dependent.

The role of nerve growth factor (NGF) has been studied in the effects of low-dose X-irradiation on the development of mouse brain. NGF plays an important role for the maintenance of cholinergic neurons in the basal forebrain during development and adulthood. After 20-30 days in culture, 0.5 Gy doubled the amount of NGF produced.

X-irradiation has also been shown to enhance naturally occurring cell death in the cerebral cortex and subcortical white matter of developing rats. In the telencephalic mantle cell death occurs in two separate compartments, the subcortical plate plus future subcortical white matter, and the cortical plate which progressively transforms into the cerebral cortex. In rats aged 0-15 days, 2 Gy X-rays greatly increased naturally occurring cell death in the cerebral cortex and subcortical white matter.

(ii) *Neurostructural damage and growth retardation* Studies have continued on structural damage and growth retardation in the developing brain in mice and rats. Permanent brain atrophy has been induced after only 0.01 Gy of neutrons on day 15 post-conception. Growth responses to irradiation were not dependent on dose rate for X-rays or neutrons in the rat, in contrast to previous studies on the mouse.

Studies have continued on the alignment of the Va layer cortex neurons and the diminution of the diameter of the cortex and brain commissures, as determined by computerised image analysis. Exposures to acute 250 kV X-rays (dose-range 3-200 cGy) were performed on each day between days 12-18 p.c. Brains were examined on day 50 p.c. For all the parameters which have been studied, the curves showed a progressive shift towards decreasing inclination with increasing fetal age at the time of exposure. The lowest doses for detectable effects ranged from 12 cGy for exposure day 12 p.c. to 25 cGy for exposure day 13 p.c. and to 50 cGy for the later exposure days.

(iii) *Neurofunctional disorders* Continued concern about the effects of prenatal exposure to ionising radiation on mental function in adults prompted an investigation into the effects of exposure to X-rays on learning and memory in mice: the effects on spatial memory function in adult CD1 mice following irradiation during the few days before or after birth have been examined using a radial arm maze. Exposure to 1 Gy of X-rays between day 18 p.c. and postnatal day 1 caused severe deficits in the acquisition of the task. 0.5 Gy caused a significant but less severe impairment; 0.25 Gy did not result in a significant deficit in performance compared to control animals.

2.8 Radiation-induced carcinogenesis in the liver

The goals of this study are (i) to study the combined effects of diethylnitrosamine (DEN) with a dose of 250 kV X-rays or of neutrons (6.3 MeV) on the induction of hepatic tumours in C57BL male mice; and (ii) to determine the RBE of neutrons against X-rays for the induction of liver tumours and the other types of cancers in C57BL/Cnb mice.

Quantitative results have been obtained for the combined effects of DEN and X-ray dose on the induction of tumours in the liver of C57BL/Cnb mice. Infant mice were distributed in four treated groups: mice treated with DEN alone; with X-rays alone; with DEN + X-rays; with X-rays + DEN. Mice from each group were killed at 10-week intervals during 70 weeks. The following parameters were measured: body weight, liver weight, the number and the size of macroscopic and microscopic liver lesions, and the surface of the different

types of the liver lesions. The number of induced liver foci and carcinomas depended essentially on the dose of DEN. No combined effect could be demonstrated between an exposure to X-rays 7 days before or after DEN administration on foci and carcinoma induction.

2.9 Interspecies comparison of lung clearance

Studies have continued, the aim of which is to explain important interspecies differences in the rate of translocation to blood of dissolved cobalt oxide particles. The extent of retention in lung tissue of ionic cobalt has been investigated in the rat, guinea pig, dog and baboon: all the species studied showed a long-term retained fraction but whose kinetics differed significantly among the species. These data also show that Co is specifically taken up into collagen of cartilagenous structures such as the tracheal rings.

The rate of dissolution of cobalt oxide particles in alveolar macrophages has also been compared in short-term culture *in vitro*. Measurements of intracellular dissolution (IPD) in alveolar macrophages (AM) of dogs and F-344 rats using monodisperse porous $^{57}\text{Co}_3\text{O}_4$ particles yielded IPD rates which confirmed the difference between the *in vivo* absorption rates; however the first results obtained from baboon AM were not conclusive. It is intended to measure IPD in AM of the other species studied *in vivo*. First results of IPD in dog AM using monodisperse MnO_2 particles (which are insoluble extracellularly) indicate fast IPD and similar kinetics as observed for $^{57}\text{Co}_3\text{O}_4$ particles. Comparing IPD and the intraphagolysosomal pH (PLpH) in AM of baboon, dog and rat, it was found that in those species (baboon, dog) where IPD rate was high (0.013 d^{-1}) the PLpH was about 4.5 whereas in rat AM where IPD was low (0.005 d^{-1}) PLpH was 5.1. This indicates that PLpH is an important co-factor for IPD but cannot explain the mechanism of IPD. From the first results of immunochemical studies it is hypothesised that the metal-chelating protein metallothionein (MT) could well maintain the mechanism of IPD. Differences in the content and/or affinity of MT in AM of the different species could then explain the differences in absorption found *in vivo*.

In order to study the lung clearance of another particle material the task group has designed a multi-step investigation using e.g. monodisperse uranium oxide particles at about $0.5 \mu\text{m}$ diameter which could be produced by a spinning top aerosol generator with a heat degradation unit. This study will again include man, baboon, dog, guinea pig, rat (HMT, F-344, Sprague-Dawley) and mouse.

2.10 Deposition and clearance of inhaled particles in the human respiratory tract

The objective of this task group, formed in conjunction with EURADOS, is to develop improved respiratory tract models to relate intakes of radionuclides by workers to organ doses and bioassay measurements, and to calculate the distribution of doses to the general population for any given exposure. The approach adopted is to identify important areas of uncertainty, and to conduct experimental studies to address them.

Several members of this task group are also members of the ICRP task group in Respiratory Tract Models for Radiological Protection, and considerable effort went towards finalising its revised model and on developing PC software to implement it. A related project initiated and co-ordinated by the task group is to conduct a sensitivity and uncertainty analysis on the

proposed ICRP model. The objectives are to assess overall uncertainty in dose coefficients and identify key areas of future research to reduce uncertainties.

Experimental studies were carried out by the group to quantify human respiratory tract deposition and clearance. Deposition measurements focused on areas where data are sparse. Measurements of regional deposition in humans were made for ultrafine ($< 0.1 \mu\text{m}$) and hygroscopic particles; total deposition was compared between adults and children, and nasal deposition between subjects with rhinitis and healthy subjects.

Clearance studies have continued to focus on particle clearance and retention in the bronchi and bronchioles, because of the high radiosensitivity attributed to the bronchial epithelium. Human studies following the retention of radiolabelled particles administered as a small aerosol bolus were extended to ultrafine particles, and to gamma camera imaging to determine the initial distribution. The human studies are complemented by experiments on rats and dogs. Among other matters, these are addressing the key issue of whether material initially deposited in the alveoli is subject to retention when cleared through the tracheobronchial tree. In addition, a two-year study of particle retention in the human alveolar region was started.

2.11 The reduction of risk of late effects from incorporated radionuclides

The data obtained after the administration of the siderophore analogues supports the long-held view of the task group about the potential usefulness of these substances. Preliminary studies on the efficacy of 3,4,3-LIHOPO for enhancing the excretion of ^{238}Pu from the rat after inhalation as nitrate or the TBP complex, or after intravenous injection as citrate, show that it is substantially more effective than in the current agent of choice, DTPA. The ligand is also active orally and causes a substantial decrease in the systemic content of ^{238}Pu when administered by this route. These observations could represent a most significant development in the reduction of risk from plutonium exposure but more work is required to optimise the treatment regimen and assess whether there are any contra-indications to its use. The substance is also at least as effective as DTPA for the decorporation of ^{241}Am . It is also noteworthy that a pilot experiment has shown that 3,4,3-LIHOPO is much more effective for thorium than DTPA. However, more work is required to assess its full potential for thorium. Studies with DTPA-DX and DFO-HOPO have shown that the former was more effective than DTPA for removing ^{241}Am from the liver of experimental animals, while the latter was as effective as 3,4,3-LIHOPO for inhibiting skeletal deposition of ^{238}Pu after its intravenous injection.

Studies using orally administered DTPA have shown that at intakes of $100 \mu\text{mol kg}^{-1}\text{d}^{-1}$ it is as effective as repeated injections of $30 \mu\text{mol kg}^{-1}$ for enhancing the excretion of ^{238}Pu after its inhalation as nitrate. However, the continuous administration of DTPA resulted in slight damage to the gut. This effect may be species-dependent and further work is required to optimise the oral treatment regimen and to assess its toxicity under these conditions.

Studies with some polyaminophosphonic acids, bisphosphonates and phosphonoalkylphosphinates have shown that after intraperitoneal injection they are only partially successful for enhancing uranium excretion. However, because of the importance of reducing the risk from uranium incorporation, other phosphonates and clathrate-type compounds named calixarenes have been synthesised for testing, and alternative methods of administration will be considered.

2.12 Stem cell studies after contamination with alpha-emitters

Co-ordinated studies have continued on stem cell responses in murine bone marrow after *in vivo* alpha contamination at early stages of development. Preliminary results were obtained on paternal contamination of DBA-2 mice with ^{239}Pu and of Balb/c mice with ^{241}Am . Data were collected in the offspring up to 160 days and one year after birth respectively. The offspring showed changes in the microenvironment of the bone marrow (CFU-f assay, capacity to maintain haemopoiesis in long-term bone marrow cultures, osteogenic capacity as measured by renal ossicle development). Haemopoietic precursor cells (*in vitro* CFC and bone marrow CFU-S) showed somewhat unstable changes but normal overall cell production was maintained. The cause and significance of the observed changes need further investigation.

Comparative studies have been initiated where effects on stroma and haemopoietic stem cells are studied after external irradiation with X-rays. This should allow a comparison between X-rays and α -particles for similar effects, and estimates to be made of the RBE.

In vitro assays have been developed which allow bone marrow cells belonging to the stromal microenvironment to express osteogenic characteristics. The assay applies to human bone marrow as well as to murine bone marrow. The *in vitro* assay has been found useful for the study of changes induced by α -particle irradiation. Up to one year after injection of male Balb/c mice with an osteosarcomogenic dose of ^{241}Am , changes in the osteogenic capacity of the bone marrow stroma could be detected.

2.13 Metabolism, dosimetry and effects of bone-seeking radionuclides

A number of co-ordinated studies have continued on the spatial distribution of radionuclides in bone. The dose rate from incorporated ^{239}Pu to the endosteum of rat bone varied considerably in different parts of the skeleton. The distribution also depended on the amount of ^{239}Pu injected. A large investigation has continued into the distribution and consequent effects of different actinides, where the dose distribution in bone varied but the average dose was approximately the same. The dose to bone marrow increased with time for ^{239}Pu but very little ^{233}U was seen in marrow. Both myeloid leukaemia and osteosarcoma have been observed in the animals.

Radionuclide distribution in bone has also been measured for certain accident cases and patients. In the case of thorotrast, the material was found principally in the cellular bone marrow and hardly at all in yellow marrow. Useful data predicting the long-term retention of radium in bone has been gained from volunteer studies with ^{133}Ba . Studies have also continued on natural levels of α -particle emitters in human tissues, including measurements on fetal tissues. The hypothesis has also been explored that environmental levels of radon can result in significant α -particle irradiation of bone marrow, as a result of radon solubility in fat droplets in the marrow.

Ongoing studies of late effects in mice have questioned the assumption that the effects of two radionuclides administered at the same time are the sum of the effects of each radionuclide given separately. In the CBA mouse it is now very clear that there is a level of administered ^{224}Ra where the incidence of myeloid leukaemia is considerably greater than that of osteosarcoma. Experiments are continuing with multiple and continuous administration for

studying the effect of a reduced dose rate. Finally, it now appears that patients treated with ^{224}Ra for ankylosing spondylitis have shown a significant increase in the incidence of leukaemia.

2.14 Fetal dosimetry and effects of incorporated radionuclides

Several large studies are being co-ordinated, in the light of considerable interest (e.g. by ICRP) in fetal dosimetry and effects *in utero*, particularly from alpha-emitters.

Measurements have been made of the concentration of alpha-emitters in human fetal tissues. Naturally-occurring ^{210}Po is readily measurable with the highest concentrations in developing bone. Levels of fallout plutonium are around the limits of detection by alpha spectrometry but the measurements made provide valuable information on the relatively low concentrations of Pu in the fetus compared with fetal Po and maternal Pu concentrations.

Animal studies on radionuclide transfer to the embryo/fetus and associated tissues have been undertaken in a number of laboratories using different animal species: mouse, rat, guinea pig, baboon. Radionuclides studied were ^{210}Po , ^{224}Ra , ^{237}Np , ^{238}Pu , ^{239}Pu and ^{241}Am . In general there was an increasing transfer with increasing gestational age and a concentration of the actinides in fetal liver and bone late in gestation, but with important differences between elements e.g., transfer of Am was lower than that of Pu or Po. Measurements have included the accumulation of nuclides in the yolk sac membrane, the first site of haemopoiesis in mammals and the origin of the germ cells.

Studies of the effects of radionuclide incorporation into the fetus have centred on damage to the developing CNS by ^{125}I , comparing sodium iodide with iododeoxyuridine. Measuring changes in mice including reductions in the diameter of the cortical plate and neuron alignment disorders. In both cases, damage to the cerebral cortex was much less than expected in comparison with exposure to external irradiation.

2.15 Retention and absorption of ingested radionuclides and irradiation of the gastrointestinal tract

The aim of this task group was to provide experimental data for use in radioprotection and to define specific risks associated with radionuclide ingestion.

A human volunteer study to measure the absorption of ^{239}Np and ^{242}Cm was completed. Administration of the citrate complexes to five subjects resulted in f1 values of about 2×10^{-4} for both nuclides.

Factors affecting the absorption of ^{210}Po were studied using rats and guinea-pigs. Results obtained for the fractional absorption of polonium after administration as the nitrate, citrate or incorporated into liver were in the range 0.06 - 0.13. Experiments with primates have shown that ingestion of plutonium with soya-bean increased absorption by about a factor three compared with values for plutonium nitrate but no increase was observed for plutonium incorporated into winkles. The tissue distribution of plutonium after administration in biologically incorporated forms was different from that observed after ingestion of the nitrate or the citrate: most plutonium was retained in the skeleton with less than 20% in the liver.

In neonatal baboons, absorption of plutonium administered as the citrate was as high as 2% in some individuals. Increased absorption appeared to be due to uptake in distal epithelial cells which contained an apical canalicular system connected to transport vacuoles. The number of these cells, characteristic of fetal intestinal epithelium, varied considerably between individual animals and was related to the observed differences in absorption of about an order of magnitude.

The original objectives of the task group have been realised and the results published; the group was closed in 1991.

2.16 Effects of radon and radon daughters *in vitro* and *in vivo*

This task group was established in 1991. The most important initial aims were (i) to organise interlaboratory comparisons of radon and radon daughter metrology in the exposure chambers operated by the three participating laboratories and (ii) to relate the concentration and aerosol characteristics of radon daughters to their deposition in different regions of the rodent respiratory tract. When the programme of intercomparisons is complete, it is hoped that information on the effects of radon exposure derived by one laboratory can be compared directly with results obtained by another.

At its inaugural meeting the task group held a one-day symposium on 'Radon exposure systems, radon metrology and the effects of exposure to radon and its daughters'.

The first interlaboratory comparison has been carried out. Samples were taken in the exposure chamber during the exposure of rats to radon/radon daughters using a variety of standard and newly-developed techniques. Although reasonable agreement was obtained between two of the laboratories using the standard Thomas three-count technique, the results of the third laboratory were much more variable.

In a collaborative study groups of rats were exposed to radon/radon daughters at levels ranging from 150 to 1000 WLM. Measurements are being carried out on nuclear aberrations in alveolar macrophages, and cell proliferation indices in epithelial cells from different regions of the respiratory tract.

2.17 Radiation late effects in bone marrow transplant patients

This special task group action is a co-operative study of EULEP and the European Bone Marrow Transplant Group. Its objectives are (i) retrospective analysis of risk factors for the development of neoplastic and non-neoplastic late effects of radiation; and (ii) definition of parameters for prospective analysis and prophylactic intervention. One specific role for EULEP is to promote interactions between clinicians and radiobiologists with expertise in late effects.

Total body irradiation followed by bone marrow transplantation is a form of curative treatment for severe neoplastic and non-neoplastic disorders of the lymphohematopoietic system. As more patients survive for prolonged periods of time, late effects become a matter of concern. Whole body exposure has been extensively studied in animal experiments, but late sequelae of whole body exposure of human beings to between 5 and 15 Gy of radiation are largely unknown.

Presently the number of patients surviving more than 10 years is still limited, but many patients are expected to enter the second decade after transplantation in the next few years, since marrow transplantation became more common as a treatment of leukaemia about 10 years ago. Therefore retrospective analyses on the few long-term survivors are urgently needed for a prospective study on the greater number of patients that can be expected in the future.

Almost 200 reports have been received from 22 co-operating centers and have been evaluated. The great majority of patients are back to work or school full-time. However there is a minority of patients with significant problems that deserve more studies in detail. Task groups have been formed of clinicians and scientists who are interested in studying these problems in more detail. Specific proposals have been returned for dosimetry, ophthalmological examinations, measurements for growth and development, and study of lung function. Information on new malignancies is being collected from all patients surviving more than 5 years.

2.18 Radiobiology archive

It has been decided to establish an archive of long-term animal experiments in Europe. This was timely because the number of such studies on the effects of external radiation or internal radionuclide exposure has decreased substantially in recent years. Furthermore, except for some studies from Eastern Europe which could be included, all the long-term animal experiments which have been set up in the past 10-15 years have been in EULEP member laboratories.

The aim is to prevent data and material from such studies from being lost, and to preserve it for analysis and for later use with new methodologies. The EULEP archive will consist of a centralised database with standardised terminology, e.g. in pathology; and a decentralised specimen archive including microscope slides and embedded tissues. To establish the database, questionnaires were sent to EULEP laboratories and the collection of relevant information has already begun.

3. Symposia and training activities

The external EULEP symposium in 1990 was held in Oxford on "The Role of the Alveolar Macrophage in the Clearance of Inhaled Particles". In addition, a symposium was organised at Reims on "Molecular-Biological Methods in Pathology".

In 1991, at the ICRR in Toronto, EULEP contributed to an international symposium on Mutation and Cancer; also to a joint EULEP/DOE workshop on Radiobiology of Bone. The symposium at Reims was on "Molecular Markers for Differentiation". Also in 1991 there was a EULEP/CEC/DOE workshop at Schloss Elmau on Age-Dependent Factors in the Biokinetics and Dosimetry of Radionuclides. A symposium was held at Reims in 1992 on Transgenic Mice.

Training activities in 1990 included numerous inter-laboratory exchange visits for communicating expertise from one laboratory to another; other activities with a training component organised by the standardisation committees are outlined above.

Finally, EULEP has initiated an investigation into the possibility of providing course material for the teaching of radiation biology. It is aimed to produce material based on approx. 100 slides which could be made available for teachers of medical students including radiologists.

Publications

(This list is not exhaustive, but includes some papers reporting collaborative studies as well as publications by or on behalf of EULEP itself.)

EULEP Newsletter: 14 issues were published during the reporting period (Nos. 55-68).

EULEP Pathology Atlas: 3 new chapters were published:

- (i) Preneoplastic and neoplastic lesions of the kidney of the rat, by P. Bannasch and H. Zerban;
- (ii) Neoplastic lesions of the mouse lymphoid system, by P.K. Pattengale;
- (iii) Haematopoietic neoplasms in the mouse and rat including LGL lymphoma and non-lymphoid neoplasms, by C.H. Frith.

Proceedings of EULEP symposium on Skin - Its Relevance in Radiation Accidents and Radiological Protection, organised by J.W. Hopewell, *International Journal of Radiation Biology* 57, 737-896, 1990.

Aalbers, A.H.L. and Bader, F.J.M., The sixth EULEP X-ray dosimetry intercomparison. Report No.249108001, RIVM Bilthoven, 1991.

Broerse, J.J., Dutreix, A., and Noordijk, E.M., Proceedings an international meeting on Physical, Biological and Clinical Aspects of Total Body Irradiation, *Radiotherapy and Oncology* 18, supp.1, 1-162, 1990.

Hallberg, B., Schmidt, J., Luz, A., Pedersen, F.S. and Grundström, T., SL3-3 Enhancer factor 1 transcriptional activators are required for tumour formation by SL3-3 murine leukaemia virus. *J. Virol.* 65, 4177-4181, 1991.

Kreyling, W.K., André, S., Collier, C.G., Ferron, G.A., Métivier, H. and Schuman, G., Interspecies comparison of lung clearance after inhalation of monodisperse solid cobalt oxide aerosol particles. *J. Aerosol Sci.* 22, 509-535, 1991.

Kreyling, W.K., Nyberg, K., Nolibé, D., Collier, C.G., Camner, P., Heilmann, P., Lirsac, P.N., Lundborg, M. and Matejkova, E., Interspecies comparison of phagolysosomal pH in alveolar macrophages. *Inhalation Toxicology* 3, 91-100, 1991.

Pedersen, F.S., Paludan, K., Dai, H.Y., Duch, M., Jorgensen, P., Kjeldgaard, N.O., Hallberg, B., Gundström, T., Schmidt, J. and Luz, A., The murine leukaemia virus LTR in oncogenesis: effect of point mutations and chromosomal integration. *Radiat. Environ. Biophys.* 30, 195-197, 1991.

Pedersen, L., Strauss, P.G., Schmidt, J., Luz, A., Erfle, V., Jorgensen, P., Kjeldgaard, N.O. and Pedersen, F.S., Pathogenicity of BALB/c derived N-tropic murine leukaemia viruses. *Virology* 179, 931-935, 1990.

Reinhold, H.S., Calvo, W., Hopewell, J.W. and van den Berg, A.P., Development of blood vessel-related damage in the fimbria of the central nervous system. *Int. J. Radiat. Oncol. Biol. Phys.* 18, 37-42, 1990.

Reinhold, H.S., Hopewell, J.W., Calvo, W., Keyeux, A. and Reyners, H., Connective tissue of the vascular system, *in* Radiotherapy of Organs and Tissues, eds Streffer, C. and Trott, K.R., pp.243-268, Springer, Heidelberg, 1991.

Van den Aardweg, G.J.M.J., Arnold, M. and Hopewell, J.W., A comparison of the radiation response of the epidermis in two strains of pig. *Radiat. Res.* 124, 283-287, 1990.

Weinsheimer, W., Kolb, B.J., Duell, T. and Fleidner, T.M., Late effects in bone marrow transplanted patients - a multicenter study supported by EBMT and EULEP. *Bone Marrow Transplantation* 8, Suppl 1: 25, 1991.

Yeung, T.K., Lauk, S., Simmonds, R.H., Hopewell, J.W. and Trott, K.R., Morphological and functional changes in the rat heart after X-irradiation: strain differences. *Radiation Research* 119, 489-499, 1989.



INDIVIDUAL RADIOSENSITIVITY AND ITS RELATION TO COLO-RECTAL CANCER

Contract Bi7-022 - Sector B12

- 1) *Dutrillaux* , Institut Curie - 2) *Léonard* , Univ. Cathol. Louvain à Woluwe
- 3) *Rueff* , New University of Lisbon

Summary of project global objectives and achievements

Colorectal cancer is a major cause of mortality, treatments remaining largely insufficient. Epidemiological and now molecular data point out that some individuals are predisposed to develop such cancer. The best known predisposing condition is the familial adenomatosis polyposis coli (APC), determined by a gene mapped on the long arm of chromosome 5, but other predispositions exist, as mutation of p53 gene.

However, the process of carcinogenesis is not simple, the genetic and cytogenetic analysis of tumor samples demonstrating the existence of many other genomic alterations. This is why a susceptibility to mutagenes of APC gene carriers is suspected. A study was developed to characterize APC patients, to look for their eventual chromosomal instability by analysis of lymphocytes and tumor cells. In addition, studies on radiation sensitivity of the lymphocytes were conducted by comparing, in the same families, affected and non affected relatives using cytogenetic and molecular techniques.

Patients were first ascertained on clinical criterial, in various specialized consultations and clinics of Paris region. When an APC syndrome was suspected, a familial analysis was performed, and a pedigree established. Then, blood samples of members of the family were obtained. Aliquots of these samples were used for DNA extraction. DNA was cut by different restriction enzymes permitting the detection of polymorphisms, with tested markers located on both sides of the APC gene. Then, using Southern's technique, the haplotype of the chromosomal segment 5q21-q22 was established for each individual. The 2 haplotypes of each individual were compared with those of their relatives to determine which one is associated with the disease and to localize the mutant gene. This part of the work was performed by the group of Gilles THOMAS, at Institut Curie (Paris).

The cytogenetic analysis was developed in several directions :

1) Characterization of "spontaneous" chromosomal anomalies in blood lymphocytes. After molecular confirmation of the status of the patients, heterozygote carriers were selected. Short term cultures were developed and 100 R-banded metaphases are analysed per patient. Each suspected anomaly led to the establishment of the karyotype. Metaphases from synchronized cultured were also analysed to detect eventual constitutional microdeletion of chromosome 5.

The same study was developed on patients ascertained for colorectal cancer, but without FAP syndrome, to obtain a control group.

2) Cytogenetic study of benign and malignant tumors. Polyps and adenocarcinomas were dissected and cell suspensions were cultured for a short term to obtain metaphases. The karyotypes of polyps and adenocarcinomas from APC and non APC patients were compared.

3) Effect of radiations on blood lymphocytes. An aliquot of the blood from APC patients and relatives was irradiated by X-rays very soon after sampling, in Paris. The blood samples were sent to Brussels, where short term cultures were developed. Cell kinetics were studied using a BrdU incorporation technique, and the chromosomal lesions of cells exposed to 0.02 and 2 Gy irradiations were scored, and compared in APC patients and relatives, and in cancer patients without APC syndrome.

Points 1 and 2 were developed in Paris (URA 620 CNRS, Institut Curie), coordinating the researches. Point 3 was developed in Brussels by the TEMU Laboratory.

DNA breakage analysis was performed on blood samples from APC patients irradiated by X-rays at doses of 0.2, 1 and 2 Gy. DNA breaks were analysed using fluorimetric analysis of DNA unwinding (FADN) method. The role of DNA repair systems, and in particular the activity of poly (ADP-ribose) polymerase was studied in relation with the production of DNA breaks and the kinetics of DNA repair.

The part played by active oxygen species, through modulation of endogenous levels of catalase activity and usage of OH scavengers was also studied. This part of the work, performed on blood samples obtained locally, was developed by the department of Genetics of UNL (Lisboa).

Project 1

Head of project: *Dr. Dutrillaux*

Objectives for the reporting period

A first objective was to ascertain families affected by APC, to obtain an estimate of the incidence of the disease, to characterize the region of chromosome 5 carrying the APC gene, by the presence of polymorphic locus on either side of the gene, and obtain a risk estimate to develop APC for young relatives.

A second objective was to look for an eventual chromosome instability in APC patients, which would explain the multiple genomic changes occurring in carcinogenesis. This was performed by comparing the "spontaneous" chromosome breakages and aneuploidies in the lymphocytes of APC and non APC patients, and also by comparing chromosome alterations in colorectal cancer cells from APC and non APC patients.

Progress achieved including publications

1. Ascertainment of cases

Since 1990, 271 unrelated FAP patients have been identified. Extensive genealogical investigations performed on each patient did not disclose any common ancestor in the last two centuries of their family history. Three-generation pedigrees have been drawn for 132 patients.

- Linkage analysis has been performed on DNA from peripheral blood of 76 families (717 individuals). The use of probes detecting polymorphisms at intragenic loci and at loci on either side of the APC gene, allowed :

1 - to estimate the risk of carrying the mutated APC gene for 200 young first-degree relatives.

2 - to determine the parental of mutation in 13 new-mutation families (submitted).

3 - to characterize two constitutional deletions involving the APC gene in two unrelated FAP families (submitted).

- Germ line mutations have been searched in the first fourteen exons of the APC gene among a total of 160 unrelated FAP patients and 26 different allelic variants have been detected (submitted). One of the consequences has been to determine the genetic status by direct diagnosis for 14 at-risk children.

2. Analysis of lymphocytes

Control studies were performed on a small series of 8 individuals, 0 to 77 year old, for whom 1000 metaphases at least were karyotyped using R-banding. Analyses of breakages and rearrangements were developed in the course of a previous contract of the Communities.

Analysis of aneuploidy was developed for this contract. It is shown that :

- aneuploidy, principally chromosome losses, affects the late replicating X in the females preferentially.
- this loss increases with aging : from 1 in newborns to 5 per 100 metaphases in 75 year old adults.
- autosome losses are as frequent in newborns as in old adults.
- autosome losses are inversely related to their size in adults, but not in newborns.

In non APC colorectal cancer patients, 100 metaphases per individual were studied in a series of 15 patients.

- For 11 of them, no other predisposition to cancer was suspected. By comparison to age matched controls, the rate of aneuploidies involving autosomes was similar, but the rate of X chromosome loss was 3 fold higher (about 14 % of metaphases are 45, X, in patients more than 70 year old). The rate of chromosome breakage was similar to that of controls for old but increased for young patients (table I).

No difference was observed between the 11 non familial and the 4 familial, non APC, cancer patients.

For the 9 APC patients studied, aneuploidies were not different from age matched controls. Chromosome breakage was comparable in old (> 50 years) controls and FAP patients. However, in young FAP patients, it was much increased (5 fold increase) by comparison to controls.

The comparative cytogenetics of primary colorectal cancers from APC and non APC patients demonstrated that the same types of chromosome aberrations exist. Interestingly, deletions of 5q arm, where the APC gene is mapped, seem to have a similar incidence in the 2 groups, and the rate of chromosome aberration was similar.

The study of constitutional karyotype was performed on 3 series of cancer patients, affected by breast, colorectal or endometrial adenocarcinoma. A significant excess of translocation carriers was observed : 4 cases among 329 patients, which is a 6 fold increase by comparison to general population. Thus, translocation carriers

may have an increased risk to develop a solid tumor.

In conclusion, an increased rate of X chromosome losses was observed in old colorectal cancer patients, and chromosome breakage was found significantly increased in young APC patients. Thus, the hypothesis of a genome instability, occurring early in APC patients, appears likely. However, our results are too limited to be proposed as a predictive test. Data on chromosome breakage may however constitute an interesting information as a complement of other methods.

Publications

- Olschwang S., Weiffenbach B., Laurent-Puig P., Melot T., Vassal A., Falls K., Parc R., Strong L., Nakamura Y., Herrera L., Thomas G.
Genetic characterization of APC locus involved in familial adenomatous polyposis.
Gastroenterology, 101, 154-160 (1991).
- Olschwang S., Laurent-Puig P., Thomas G.
Reliability of presymptomatic test for adenomatous polyposis coli.
The Lancet, 337, 1171-1172 (1991).
- Olschwang S., Fabre R., Laurent-Puig P., Vassal A., Hamelin B., Nakamura Y., Thomas G.
Detection by DGGE of a new polymorphism in the APC region.
Hum.Genet., 88, 658-660 (1992).
- Olschwang S., Laurent-Puig P., Thuille B., Thomas G.
Frequent polymorphism in the 13th exon of the APC gene.
Hum.Genet. (In press).
- Richard F., Muleris M., Couturier J., Gerbault-Seureau M., Lombard M., Dutrillaux B.
Constitutional balanced translocations in patients with solid tumors.
Cancer Genet.Cytogenet. (In press).

Table I : Rate of rearrangements and aneuploidies observed in lymphocytes from controls and APC and non APC colorectal cancer patients. Samples indicate the number of individuals X number of metaphases studied.
 ct = chromatid, cs = chromosome, b = break, g = gap, del = deletions. Numbers in columns give the rate per 100 metaphases.

Sample category	8 x 1000 controls		11 x 100 non familial colorectal cancer		4 x 100 non APC familial colorectal cancer		9 x 100 APC patients	
	Total	age (year) < 50 > 50	Total	age (year) < 70 > 70			Total	age (year) < 50 > 50
ctb, cs	10.89	6.13 20.41	13.18	14.72 11.33	7.85		17.9	18.52 16.67
csb, del	1.93	1.78 2.23	3.41	3.13 3.75	2.71		2.05	1.41 3.33
Other rearrangements	12.94	7.98 22.84	16.77	18.01 15.28	11.18		19.95	19.93 20
Autosomes	0.84	0.82 0.88	0.5	0.63 0.27	0.28		0.19	0.1 0.3
-X	2.51	1.32 4.3	9.8	5.30 13.12	0.54		4.6	3.3 5.8
+X	1.17	0.89 1.59	3.12	5.0 1.7	0.81		0.8	1.17 0.45

Project 2

Head of project: *Prof. Léonard*

Objectives for the reporting period

The activities of the TEMU laboratory of the Catholic University of Louvain were devoted to the comparison of the cytological and cytogenetical radiosensitivity of CPA carriers and normal individuals from the same family.

Progress achieved including publications

Blood samples from 6 CPA carriers and 6 normal individuals were exposed to 0, 1, 2 or 4 Gy of γ -radiation within 2-3 hr after collection. The cells were set up in culture at 37°C in 5 ml Ham's F-10 medium supplemented with foetal calf serum (15 %), phytohemagglutinin and antibiotics. The cells were cultured for 48 h or 72 h and preparations were made according to the method routinely used in our laboratory. The slides coded for blind analysis were examined for structural chromosome aberrations, (200 cells per individual and per treatment), cell kinetics (100 cells per individual and per treatment) and mitotic index (on 1000 stimulated cells per individual and per treatment).

The results of the observations are summarized in tables II - IV. In both groups the distribution of dicentrics and centric rings followed Poisson distribution and the dose-response relationships for those aberrations were linear - quadratic. In controls as well as in APC patients very large interindividual variation was observed with respect to cell kinetics, mitotic index, and yield of radiation-induced structural aberrations. Those interindividual variations largely exceeded the differences between the groups of APC patients and controls.

In conclusion, our results demonstrate that the spontaneous genome instability occurring early in APC patients is not linked to an increased sensitivity of somatic cells to the induction of structural chromosome aberrations by ionizing radiations.

Publications

- A.Hilali, E.D.Léonard, A.Léonard (1992).
Does irradiation of human blood causes a production or activation of clastogenic factors ? (In preparation).

- A.Hilali, E.D.Léonard, G.B.Gerber, A.Léonard (1992).
Etude de l'influence possible d'une réaction mixte lymphocytaire sur les modèles expérimentaux utilisés en dosimétrie biologique.
C.R.Soc.Biologie (In press).

- A.Hilali, E.D.Léonard, G.B.Gerber, A.Léonard (1992)
A comparative study of radiosensitivity of peripheral blood lymphocytes from controls and APC patients (In preparation).

- A.Hilali, E.D.Léonard, G.B.Gerber, A.Léonard (1992).
Effect of caffeine on radiation-induced G2 delay in peripheral blood lymphocytes (In preparation).

Table II - Cell kinetics and mitotic index in controls and APC patients

	Dose (Gy)	M1 %	M2 %	M3 %	I.P	MI%
C O N T R O L S	0	86.4±9.4	13.6±9.4	-	1.14±0.09	70.5±23.5
	1	91.8±5.9	8.2±5.9	-	1.08±0.06	46.8±19.2
	2	95.0±4.3	5.0±4.3	-	1.05±0.04	48.0±15.3
	4	97.0±4.7	3.0±4.5	-	1.03±0.04	26.3±12.04
A P C	0	91.0±6.0	9.0±6.0	-	1.09±0.06	75.3±11.6
	1	94.6±4.6	5.4±4.6	-	1.05±0.04	57.0±19.6
	2	97.4±2.8	2.6±2.8	-	1.03±0.02	59.3±29.7
	4	97.6±3.7	2.4±3.7	-	1.02±0.03	39.3±19.8

Table III - Structural aberrations in controls and APC patients

	Dose (Gy)	% of cells with aberrations	Chromatid aberrations (per 100 cells)		Chromosome aberrations (per 100 cells)				
			Gaps	Fragments	Translocations	Fragments	Centric rings	Dicentrics	Tricentrics
C O N T R O L S	0	0.4±0.5	0.1±0.2	0.1±0.2	-	0.1±0.2	-	-	-
	1	16.0±1.4	0.5±0.3	0.5±0.5	0.5±0.5	4.6±3.0	0.5±0.3	10.5±1.5	-
	2	42.6±5.6	0.6±0.8	1.2±1.0	2.3±1.4	14.2±5.2	2.5±1.3	33.3±1.5	0.1±0.2
	4	81.1±5.0	0.8±0.5	2.7±2.8	5.5±1.4	30.9±7.6	8.1±3.0	94.1±9.1	1.2±1.1
A P C	0	1.3±0.6	0.5±0.4	0.4±0.5	0.1±0.2	0.6±0.5	-	-	-
	1	15.0±4.3	0.7±0.9	0.8±0.7	1.3±1.1	4.7±4.3	0.4±0.4	8.9±1.6	-
	2	39.2±4.7	0.3±0.5	1.3±1.3	2.1±1.7	10.7±3.9	1.9±1.7	33.6±3.0	0.2±0.2
	4	80.6±15.7	0.8±0.8	1.2±1.2	3.7±1.9	29.2±8.2	5.9±2.7	101.7±6.9	1.5±1.2

Table IV - Distribution of dicentrics and centric rings

	Dose (Gy)	Dicentrics and centric rings per 100 cells	Distribution of dicentrics and centric rings (%)					
			0	1	2	3	4	5
C O N T R O L S	0	0	-	-	-	-	-	-
	1	10.8±1.3	89.6±1.5	10.2±1.9	0.3±0.4	-	-	-
	2	35.8±5.8	68.4±3.8	27.5±3.3	3.9±2.5	0.2±0.2	-	-
	4	104.6±10.2	28.7±6.4	42.3±3.8	23.4±1.6	4.7±2.4	0.6±0.4	0.1±0.2
A P C	0	0	-	-	-	-	-	-
	1	9.4±1.5	90.9±1.3	9.7±1.2	0.4±0.3	-	-	-
	2	35.8±2.2	68.2±3.3	26.5±1.7	4.6±0.9	-	-	-
	4	112.2±11.0	24.4±1.7	45.6±7.6	24.2±4.0	4.3±1.9	1.3±1.2	0.2±0.3

Project 3

Head of project: *Dr. Rueff*

Objectives for the reporting period

Work concentrated in :

- establishing the doses for normal subjects with induced DNA breakage
- studying DNA breakage in normal and familial adenomatous polyposis (FAP) patients.

Progress achieved including publications

1. Materials and methods

The study groups were composed of normals and Familial Adenomatous Polyposis (FAP) patients belonging to 6 different families and diagnosed in several hospitals of Lisbon.

Cells of normals and FAP patients were studied for two genetic end-points, namely DNA breakage and chromosomal aberrations.

DNA breakage was assessed through the Fluorometric Analysis of DNA Unwinding (FADU method) as developed by Birnboim and Jevcak (1981). For detection of chromosomal aberrations, the cells were cultured for 48 h in Ham's F-10 medium and the preparations were obtained by standard techniques. The scoring of chromosomal aberrations was made by two independent observers in 200 cells per individual and per treatment.

Doses of 1 Gy and 2 Gy ^{60}Co gamma radiation and 0.5 mM H_2O_2 were used throughout the study after the establishment of effective doses.

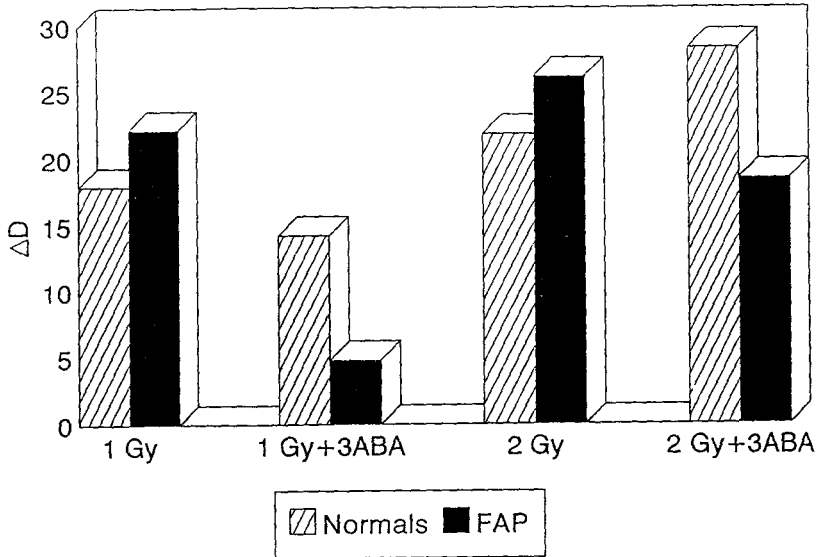
2. Results

DNA strand breakage analysis

Our results for the induction of DNA strand breaks by gamma radiation show that there is no statistically significant difference between normals and FAP patients in presence and in absence of 3-minobenzamide (3ABA) as an inhibitor of poly(ADP-Ribose) polimerase (Figure 1).

As a consequence of water radiolysis, ionizing radiation produces H_2O_2 . Both ionizing radiation and H_2O_2 can give rise to the highly reactive $\text{OH}\cdot$.

DNA STRAND BREAKS Normals/FAP



$\Delta D = \%D$ (control samples) - $\%D$ (treated samples)

FIGURE 1 - Comparison of the effect of ^{60}Co gamma radiation in presence and absence of 5 mM, 3ABA in human leukocytes of normals and FAP patients.

A comparison of the percentage of DNA strand breaks produced by these two agents show that 0.5 mM H_2O_2 and 2 Gy ^{60}Co gamma-radiation produced similar results 17.41 % and 17.14 % respectively. Also, the difference between DNA strand breaks by two agents in presence and absence of 3ABA is not statistically significant (Figure 2).

The increase of the percentage of DNA strand breaks by 0.5 mM H_2O_2 for 10 minutes at room temperature was statistically significant ($P < 0.001$) as estimated by Student's t test.

The effect of presence of sodium azide (NaN_3), an inhibitor of catalase or dimethylsulfoxide (DMSO), a scavenger of OH^\cdot radical in human leukocytes exposed to 0.5 mM H_2O_2 for 10 minutes is show in Figure 3.

DNA STRAND BREAKS Ionizing Radiation/H₂O₂

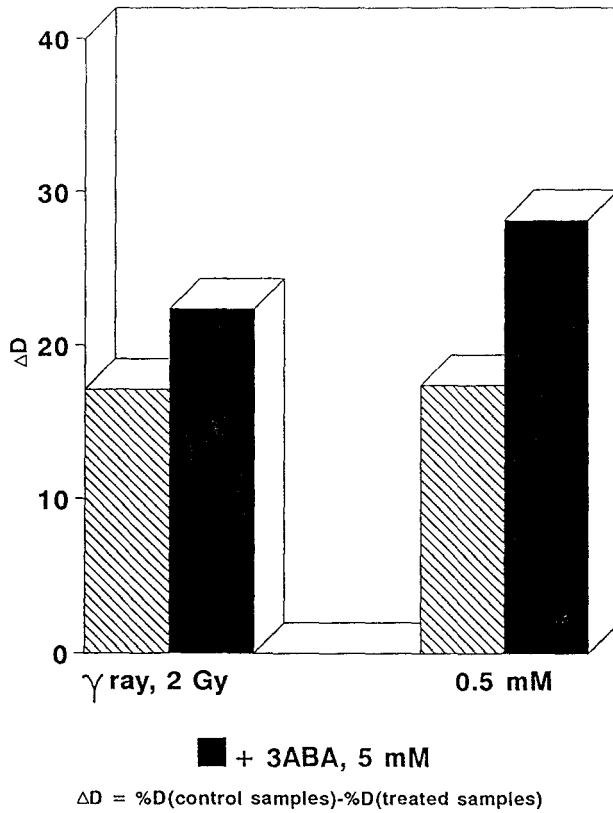
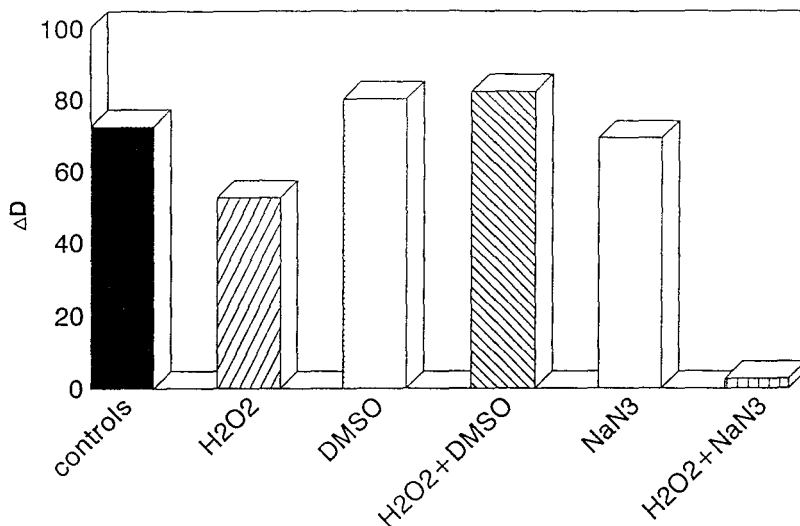


FIGURE 2 - Induction of DNA strand breaks by ⁶⁰Co gamma radiation and hydrogen peroxide (H₂O₂) in the presence and absence of 5 mM, 3ABA.

DNA STRAND BREAKS Effect of H₂O₂/DMSO/NaN₃



$\Delta D = \%D \text{ (control samples)} - \%D \text{ (treated samples)}$

FIGURE 3 - Effect of hydrogen peroxide (0.5 mM, H₂O₂) in presence and absence of dimethylsulfoxide (150 mM, DMSO) and sodium azide (3.96 mM, NaN₃) in human leukocytes. Controls with DMSO and NaN₃ were used. The Student t-test revealed a statistically significant difference between non exposed and exposed cells to H₂O₂ (P < 0.001) and to H₂O₂ + NaN₃ (P < 0.001).

The production of DNA strand breaks is markedly increased when cells are incubated in the presence of 3.96 mM NaN₃ (P < 0.001). When cells were exposed to 0.5 mM H₂O₂ in the presence 150 mM DMSO there was no statistically significant difference between non-exposed and exposed cells.

2.1 Cytogenetic analysis

Our results show that 1Gy and 2 Gy ⁶⁰Co gamma radiation produce a significance increase of chromosomal aberrations (P < 0.05) as estimated by the F test.

In contrast with H₂O₂, which produces more chromatid aberrations than chromosome aberrations and no dicentrics or rings (data not shown), these latter aberrations are the major findings in radiation exposed cells. The frequency/100 cells of dicentrics was 11.95 and 31.70 when we used 1 Gy and 2Gy, respectively.

Table V presents the results of the cytogenetic observations in normals and FAP patients.

Table V - Results of the cytogenetic observations in normals and fap patients

		Chromosomal Aberrations (per 100 cells)							
Treatment	Dose	ctg	ctb	csg	csb	dic+r	others	CA/100 cells	
N	—	0	2.0	1.0	0	0.5	0	0	3.5
O	γ ray	1 Gy	0.7	0	0	0.4	12.0	0	13.0
R	γ ray	2 Gy	1.0	0	0	14.1	31.7	1.0(t)	47.8
M	3ABA	5 mM	1.0	0	0	0	1.0	0	1.8
A	γ ray+	1 Gy							
L	3ABA	5 mM	1.5	1.0	0	10.0	11.0	1.5(t)	25.0
S	γ ray+	2 Gy							
	3ABA	5 mM	3.0	1.7	0	14.3	37.0	0.9(t)	57.0
	—	0	1.6	0.9	0	0	0	0	2.5
F	γ ray	1 Gy	4.3	1.0	0	4.3	8.2	0.5(tr)	18.4
A	γ ray	2 Gy	0.3	1.5	0.3	19.2	39.5	1.2(t)	62.0
P	3ABA	5 mM	1.0	0	0	0	0	0	1.0
	γ ray+	1 Gy							
	3ABA	5 mM	1.0	1.0	0.5	7.0	12.9	0	20.4
	γ ray+	2 Gy							
	3ABA	5 mM	0	0.9	0	22.5	40.1	0.5(t)	64.0

In agreement with the observations performed in Brussels (Project 2) we could not find any statistically significant difference between the frequency of chromosomal aberrations in normals and FAP patients. However, a greater radiosensitivity of FAP cells when irradiated in presence of 3-aminobenzamide was detected ($P < 0.05$) as revealed by F test (Figure 4).

DISTRIBUTION OF DICENTRICS IN NORMALS AND FAP PATIENTS

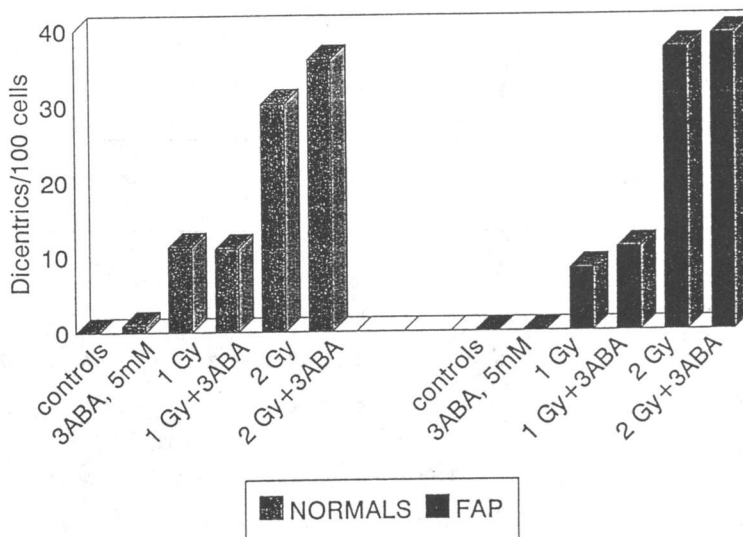


FIGURE 4 - Frequency of dicentrics in peripheral lymphocytes exposed to 1 Gy and 2 Gy ^{60}Co gamma radiation in the presence and absence of 5mM, 3ABA. ^{60}Co gamma radiation in the presence of 3ABA significantly increased this frequency in cells from FAP patients as analyzed by F test ($P < 0.05$).

Publications

J.A.Rueff, A.L.Bras, L.M.F.Cristovao, J.T.Mexia, M.S.da Costa (1992) Damage to human DNA and chromatin by H_2O_2 and ^{60}Co gamma irradiation (In preparation).

THE GENETIC AND BIOCHEMICAL BASIS OF HUMAN DNA REPAIR AND RADIOSENSITIVITY

Contract Bi7-026 - Sector B12

- 1) *Lohman*, Univ. Leiden, Sylvius Labor. - 2) *Bridges*, MRC Cell Mutation Unit
3) *Bootsma*, Erasmus University Rotterdam - 4) *Moustacchi*, Institut Curie
5) *Thacker*, MRC Radiobiological Unit - 6) *Backendorf*, Gorlaeus Laborat.

Summary of project global objectives and achievements

Objectives

1. To devise sensitive methodologies to identify radiosensitive individuals both in the normal population and in individuals with known radiosensitive genetic disorders.
2. To employ different and complementary strategies to understand the molecular basis of radiation sensitivity in humans.

Achievements

1. Determination of radiosensitivity

The ability to clone T-lymphocytes with high plating efficiencies has made it possible to measure the radiosensitivity of T-lymphocytes. T-lymphocytes from cord blood are more radiosensitive than those from adult blood. When compared to normal donors, T-lymphocytes from A-T patients are more sensitive. In addition the single cell microgel or 'comet' assay has been employed to measure DNA breaks at doses of gamma-radiation down to 0.25 Gy. Cellular radiosensitivity has also been measured by a delayed plating/micronucleus assay. In this assay A-T heterozygotes appear to be unable to repair potentially clastogenic damage.

Recovery from low-dose-rate irradiation has been employed to distinguish the radiosensitive hamster *irs* mutants, with mutant *irs 2* responding similarly to A-T cells.

2. Analysis of the cellular responses to radiation

2.1 Cloning and characterization of DNA repair genes and proteins

To study the mechanism of nucleotide excision repair and the repair defect in human disorders, major research efforts have been focussed on the isolation and characterization of DNA repair genes and proteins. Four new human repair genes have been isolated: ERCC6 (encoding a putative DNA helicase), HHR6A and 6B (ubiquitin-conjugating enzymes, homologous to the yeast repair protein RAD6), HHR23 (homologous to the yeast gene RAD23). The ERCC6 gene turned out to be responsible for the UV-sensitive human disorder Cockayne's syndrome (CS) complementation group B which is defective in preferential repair of

active genes. The very rare xeroderma pigmentosum complementation group B has been found to be caused by mutations in the ERCC3 gene. The ERCC1 and 3 genes have been inactivated in pluripotent mouse embryonal stem cells by homologous recombination. Several chimaeric mice were obtained after injection of ERCC3 homologous recombinants. These and ERCC1 chimaeras will be used to try to generate ERCC1 and 3 deficient mouse strains that may be valuable models for human repair disorders.

By chromosome transfer it was shown that the human gene XRCC5 which corrects the radiosensitive hamster xrs mutants was located on chromosome 2. Using radiation reduction hybrids the gene has been located subchromosomally to a small fragment containing region 2q34-36. Transfer of human chromosome 11 to hamster mutants phenotypically resembling ataxia telangiectasia (A-T), has shown that these mutants were not defective in the gene homologous to A-T cells (A-T complementation groups A,C and D located on chromosome 11). It remains to be established whether the A-T like hamster mutants are defective in a gene homologous to AT group E.

To identify the nature of the defect in the human repair disorder Fanconi anemia (FA), sensitive to crosslinking agents, complementation has been performed with mouse DNA. Only FA group D could be complemented. Sequence data obtained from a 4kb transcript, indicate that the c-DNA encodes for a protein sharing common motifs with the family of 'motor' proteins. The anomalies detected in the production of IL6 and TNF in FA cells account for the defect in differentiation and genomic instability. A testable model implying a control by a protein mutated in FA of the expression of a network of genes including those coding for these cytokines has been proposed.

A large number of genes from the fission yeast *S. pombe* which are involved in the response to radiation damage, have been cloned and analysed. Several genes involved in excision repair have homologues in the distantly related budding yeast *S. cerevisiae*. Comparison of sequences provides information on structure/functional relationships of the gene products as well as providing the starting point for cloning the homologous *Drosophila* and human genes.

Several yeast genes which acts in a G2 checkpoint pathway following DNA damage, have been identified. Four radiation-sensitive mutants fail to show the G2-arrest observed in normal cells after DNA damage, and these are being used to understand the mechanisms of the G2 checkpoint.

2.2 Topography of DNA repair

Analysis of repair at the gene level has revealed distinct differences in the rate and extent of repair of UV-induced cyclobutane dimers (CPD) between transcriptionally active and inactive sequences. Normal human cells exhibit more rapid repair of CPD from active housekeeping genes when compared to inactive X-chromosomal genes. Even within active genes repair of CPD turns out to be heterogenous: the transcribed strand is more quick repaired than the nontranscribed strand. This accelerated rate of repair of the transcribed strand depends on active transcription; however differences in the extent of repair

between active and inactive genes are not influenced by transcription.

Xeroderma pigmentosum group C cells only possess the capability to remove CPD from active transcribed sequences: the defect in these cells confers to inability to remove CPD from nontranscribed sequences including the nontranscribed strand of active genes. In Cockayne's syndrome cells no preferential repair of active genes was observed: active genes are repaired with the slow rate of inactive X-chromosomal genes and without faster repair of the transcribed strand. The CPD repair phenotypes suggest various hierarchies of DNA repair: (i) a slow and inefficient repair of inactive genes, (ii) the fast and efficient repair of (potentially) active genes, and (iii) the accelerated rate of repair of the transcribed strand of active genes (transcription coupled repair).

Sequential digestion of DNA with photolyase and UvrABC exci-nuclease has been used to determine the frequency of another important UV-induced photolesion in specific DNA sequences i.e. the pyrimidine 6-4 pyrimidone photoproduct (6-4PP). The rate and extent of repair of 6-4PP in the active HPRT and inactive c-mos protooncogene in UV-irradiated hamster cells was similar, suggesting that at least at high UV-doses, repair of 6-4PP is homogenous within the genome.

2.3 *In vitro* repair assays

Novel methods have been employed to analyse the rejoining of site specific breaks using human cell free extracts. Under defined conditions, double strand breaks could be rejoined with high efficiency. The rejoin process was found to require multiple components, one of which was purified 500 fold and stimulates the rejoin activity of the extracts and of purified DNA ligase 1. Correct repair of double strand breaks was found to vary with the DNA site, but the relative rejoin efficiency is constant for extracts of different cell types including those from the human radiosensitive disorder ataxia-telangiectasia. However misrejoining of breaks was elevated in A-T lines and molecular analysis showed that a defined type of deletion was formed, with the involvement of short direct sequence repeats. Extracted cells encapsulated in agarose beads, have been employed to measure UV-induced DNA repair in intact chromatin by *in vitro* reactions. Cells are lysed and extracted with buffers that mimic the physiological conditions of the cell as much as possible. With this protocol 80% of the cellular proteins are extracted, but the remaining nuclei are able to replicate, to transcribe and to carry out DNA repair. Incorporation of radioactive dNTP (in the presence of ATP, Mg²⁺, dNTP's and NTP's) is inhibited in UV-irradiated growing cells, but stimulated in UV-irradiated confluent normal fibroblasts. No such incorporation was found in XP-A cells, nor in CS cells. The latter is surprising since CS cells have a normal genome overall repair capacity. An explanation would be that in encapsulated and extensively extracted cells only nuclear skeleton centered repair enzymes are retained. Such compartmentalization has been observed for enzymes involved in replication and transcription.

2.4 Analysis of radiation induced mutations

UV-induced mutations in the HPRT gene were analysed in repair proficient and (partly) deficient mammalian cell lines. Rodent cells selectively remove CPD from the transcribed strand of active genes. In wild type hamster cells (CHO and V79) all types of point mutations have been observed, the majority of which were generated by photolesions at the poorly repaired non-transcribed strand of the HPRT gene. Repair deficient hypermutable cells belonging to rodent complementation group 2 (V-H1, UV-5), or complementation group 3 (UV24) exhibit predominantly GC → AT transitions almost exclusively arising from photolesions in the transcribed strand. In a revertant cell line derived from V-H1, with normal frequencies of UV-induced mutations and intermediate level of UV-resistance, the types and distribution of mutations were similar to wild-type cells in spite of the fact that these cells have a poor capacity to remove CPD from the transcribed strand. From these experiments it is concluded that fidelity of DNA synthesis on damaged DNA templates might be different for leading and lagging strand synthesis and that under repair deficient conditions, 6-4PP are the most mutagenic lesions.

X-ray induced and spontaneous HPRT mutants in primary human cells were isolated and characterized at the molecular level. Mutants carrying deletions and rearrangements were identified and deletion breakpoints were mapped using PCR methods. The breakpoint junctions of 4 large deletions were sequenced. The primary mechanism for deletion formation appears to be illegitimate recombination and one radiation-induced mutant revealed a novel junction suggesting a mechanism of templated repair of a break site. Some large deletions were visible by chromosome banding. Additionally a rapid PCR-based method was devised for assessing the presence of large genetic changes in the HPRT gene; using this method the mutation spectra for X-rays and alpha-particles in hamster cells were not found to differ.

A complementary genetic and physiological characterisation of FA showed that the hypomutability at the HPRT gene is associated with a high frequency of deletions and to a tendency towards spontaneous loss of heterozygosity as seen in the glycophorin A assay.

2.5 Effects of radiation on cell proliferation and differentiation

The effects of radiation on the process of proliferation and differentiation have been investigated in human skin cells (keratinocytes). In order to measure such effects, the expression of a new class of keratinocyte differentiation markers (spr genes), which code for cornified envelope precursor proteins has been followed. The expression of these genes is repressed in proliferating cells and strongly induced in differentiating cells. Consequently, radiation induced changes in spr expression enable changes in the normal balance between keratinocyte proliferation and differentiation to be monitored. The results obtained so far are very promising as both UV and X-rays can interfere with keratinocyte maturation. Interestingly,

this interference depends on the differentiation state of the cell at the moment of irradiation. Furthermore, UV and X-rays appear to affect keratinocyte maturation differently. Whereas UV has an inhibiting effect on differentiation when proliferating cells are irradiated, no such inhibition is found with X-rays, but rather a slight potentiating effect is observed. When cells, which are committed to differentiation are irradiated, both kinds of radiation appear to act similarly by speeding up the differentiation process. A number of regulatory factors, involved in these processes have been identified (FOS, JUN, OCT-1). An important finding is the observation that long-term exposure of human skin to sunlight results in induced changes in tissue homeostasis (epigenetic changes), which can be recognized in skin biopsies (in collaboration with the group of B. Gilchrest, Boston, MA). As ionizing radiation and UV affect keratinocyte maturation differently, one might expect that the induced epigenetic changes will also be different and recognizable as such.

Project 1

Head of project: *Prof. Lohman*

Objectives for the reporting period

1. To study intragenomic heterogeneity of DNA repair we have investigated the repair of UV-induced photolesions at the gene level. Moreover we developed a method to measure DNA breaks induced by ionizing radiation in defined genomic fragments.
2. For detailed analysis of DNA repair we have established an in vitro repair system to study repair of DNA lesions in intact chromatin.
3. To investigate the mutagenic consequences of different repair phenotypes, we have made UV-induced mutation spectra in normal and UV-sensitive mammalian cells.
4. Novel hamster cell lines sensitive to UV-light and ionizing radiation have been isolated.
5. We have started to clone human DNA repair genes using repair deficient hamster cells. *Drosophila* repair genes involved in repair of X-ray damage, are in the process of being cloned by using cloned yeast genes as heterologous probes.

Progress achieved including publications

1. Topography of DNA repair

Analysis of repair at the gene level has revealed distinct differences in the rate and extent of repair of UV-induced cyclobutane dimers (CPD) between transcriptionally active and inactive sequences. Normal human cells exhibit preferentially repair of CPD from active housekeeping genes when compared to inactive X-chromosomal genes. Even within active genes repair of CPD turns out to be heterogeneous: the transcribed strand is faster repaired than the nontranscribed strand. This accelerated rate of repair of the transcribed strand of active genes depends on active transcription; however differences in the extent of repair between active and inactive genes are not influenced by transcription.

Xeroderma pigmentosum group C cells only possess the capability to remove CPD from active transcribed sequences: the defect in these cells confers to inability to remove CPD from nontranscribed sequences including the nontranscribed strand of active genes. In Cockayne's syndrome cells no preferential repair of active genes was observed: active genes are repaired with the slow rate of inactive X-chromosomal genes and without faster repair of the transcribed strand. The CPD repair phenotypes observed in normal and UV-sensitive human cells, suggest various hierarchies of DNA repair: (i) a slow and inefficient repair of inactive genes, (ii) the fast and efficient repair of (potentially) active genes, and (iii) the accelerated rate of repair of the transcribed strand of active genes (transcription coupled repair).

We have developed the methodology to determine the frequency of another important UV-induced photolesion in specific DNA sequences i.e. the pyrimidine 6-4 pyrimidone photoproduct (6-4PP).

The method is based on sequential incubation of purified DNA obtained from UV-irradiated cells with photolyase and E.coli UvrABC excinuclease complex. With this technique we measured an induction of one 6-4PP per 4 CPD both in active and inactive sequences. The rate and extent of repair of 6-4PP in the active HPRT and inactive c-mos protooncogene in 30 J/m² UV-irradiated hamster cells was similar, suggesting that at least at high UV-dose repair of 6-4PP is homogenous within the genome.

Pulsefield electrophoresis has been employed to study DNA breaks in defined DNA sequences. In these experiments cells were encapsulated in agarose plugs, lysed, restricted and single strand DNA breaks were converted into double strand breaks using nuclease S1. We have established conditions which minimize nonspecific cutting by nuclease S1 and determination of DNA breaks in defined genomic fragments should now be feasible.

We have used cells encapsulated in agarose beads to measure DNA repair in intact chromatin by in vitro reactions. Cells are lysed and extracted with buffers that mimic the physiological conditions of the cell as much as possible. With this protocol 80% of the cellular proteins are extracted, but the remaining nuclei are able to replicate, to transcribe and to carry out DNA repair. Incorporation of radioactive dNTP (in the presence of ATP, Mg²⁺, dNTP's and NTP's) is inhibited in UV-irradiated rapidly growing immortalized human cells, but stimulated in UV-irradiated confluent normal fibroblasts. No such stimulated incorporation was found in XP-A cells, nor in CS cells. The latter is surprising since CS cells have a normal genome overall repair capacity. Also in vitro repair studies using cell free extract and UV-irradiated plasmids, have shown normal repair levels when extracts were prepared from CS cells. An interesting explanation would be that in encapsulated and extensively extracted cells only nuclear skeleton centered repair enzymes are retained. Such compartmentalization has been observed for enzymes involved in replication and transcription.

2. DNA repair and mutagenesis

We have extended our studies to analyse UV-induced mutations in the HPRT gene in repair proficient and (partly) deficient mammalian cell lines. Rodent cells selectively remove CPD from the transcribed strand of active genes. In wild type hamster cells (CHO and V79) all types of point mutations have been observed the majority of which were generated by photolesions in the poorly repaired non-transcribed strand of the HPRT gene. Repair deficient hypermutable cells belonging to rodent complementation groups 2 (V-H1, UV-5), and 3 (UV24) exhibit predominantly GC -> AT transitions which almost exclusively arise from photolesions in the transcribed strand. In a revertant cell line derived from V-H1, with normal frequencies

of UV-induced mutations and intermediate level of UV-sensitivity, the types and distribution of mutations was similar to wild-type cells in spite of the fact that these cells have a poor capacity to remove CPD from the transcribed strand. From these experiments it is concluded that fidelity of DNA synthesis on damaged DNA templates might be different for leading and lagging strand synthesis and that under repair deficient conditions, 6-4PP are the most mutagenic lesions.

3. Isolation and characterization of repair deficient mutants

Some ionizing radiation sensitive mutants (V-C4,V-E5,V-G8) isolated from Chinese hamster V79 cells, show typical features of the human radiosensitive disorder Ataxia Telangiectasia (AT). To determine whether the AT-like hamster mutants were defective in the gene homologous to the gene defective in AT cells (AT complementation groups A,C and D located on chromosome 11) the human chromosome 11 was introduced into the hamster mutants by microcell-mediated chromosome transfer to check complementation. Despite the presence of an intact chromosome 11 all hybrid clones showed a lack of complementation of the X-ray sensitivity. It remains to be established whether the AT-like hamster mutants are defective in a gene homologous to AT group E.

A V79 Chinese hamster mutant V-B11 has been assigned to a new complementation group (group 7) and characterized with regard to repair defects and mutability.

4. Cloning of DNA repair genes

In order to clone Drosophila genes involved in repair of ionizing radiation induced DNA damage, repair genes from *S. cerevisiae* were used as heterologous probes. To overcome the great evolutionary distance between *S. cerevisiae* and *Drosophila*, the homologue genes from *S. pombe* were cloned first. In this way RAD 51 and 54 were cloned and the genes from both yeast strains will be used to identify homologues in *Drosophila*.

A V79 mutant cell line defective in the rodent gene homologous to the Fanconi's anemia (group A) gene, has been transfected with human genomic DNA to clone the gene. Secondary transfectants resistant to several crosslinking agents, have been obtained and are currently used to isolate human sequences.

Publications

Natarajan A.T. and L.H.F.Mullenders. Chromosomal aberrations from radiation induced DNA lesions. In Recent trends in Radiobiological Research (Ed.P.Emi Devi) Scientific Publisher, Jodhpur (1990) 33-41

Venema J., A.van Hoffen, A.T.Natarajan, A.A.van Zeeland and L.H.F.Mullenders. The residual repair capacity of xeroderma pigmentosum complementation group C fibroblasts is highly specific for transcriptionally active DNA. Nucleic Acids

Research (1990) 18,443-448.

Venema J., L.H.F.Mullenders, A.T.Natarajan, A.A van Zeeland and L.V.Mayne. The genetic defect in Cockayne syndrome is associated with a defect in repair of UV-induced damage in transcriptionally active DNA. Proc. Natl. Acad. Sci. USA (1990) 87,4707-4711.

Vaughn J.P., P.A.Dijkwel, L.H.F.Mullenders and J.L.Hamlin. Replication forks are associated with the nuclear matrix. Nucleic Acids Research (1990) 18,1965-1969.

Mullenders L.H.F., J.Venema, A.van Hoffen, L.V. Mayne, A.T.Natarajan, and A.A.van Zeeland. The role of the nuclear matrix in DNA repair. Mutation and the environment, part A (Eds. M.L.Mendelsohn and R.J.Albertini) (1990) 223-232.

Zeeland van A.A., H.Vrieling, M.L.van Rooyen, J.Venema, M.Z.Zdzienicka, J.W.I.M.Simons, L.H.F.Mullenders, and P.H.M.Lohman. Influence of DNA excision repair on UV-induced mutation spectra in chinese hamster cells. Mutation and the environment, part A (Eds. M.L.Mendelsohn and R.J.Albertini) (1990) 249-254.

Mullenders L.H.F., J.Venema, A.van Hoffen, A.T.Natarajan, A.A.van Zeeland, and L.V.Mayne. Heterogeneity of DNA repair in relation to chromatin structure. In Chromosomal Aberrations (Eds.G Obe and A.T.Natarajan) (1990) 13-21.

Zdzienicka M.Z., F.Arwert, I.Neuteboom, R.Rooymans and J.W.-I.M.Simons. The V79 Chinese hamster cell mutant V-H4 is phenotypically like Fanconi anaemia cells. Som. Cell Mol. Genet. (1990) 16,575-581

Venema J.A., A.van Hoffen, V. Karcagi, A.T.Natarajan, A.A.van Zeeland, and L.H.F.Mullenders. Xeroderma pigmentosum complementation group C cells remove pyrimidine dimers selectively from the transcribed strand of active genes. Mol.Cell.Biol. (1991) 11,4128-4134

Vrieling H., J.A. Venema , M.L.van Rooyen, A. van Hoffen, P.Menichini, M.Z.Zdzienicka, J.W.I.M. Simons, L.H.F.Mullenders and A.A.van Zeeland. Strand specificity for UV-induced DNA repair and mutations in the Chinese hamster hprt gene. Nucleic Acids Research (1991) 19,2411-2415

Mullenders L.H.F., H.Vrieling, J.A.Venema and A.A.van Zeeland. Hierarchies of DNA repair in mammalian cells: biological consequences. Mutation Research (1991) 250,223-228.

L.H.F.Mullenders, J.A.Venema, A van Hoffen, R.J.Sakkers, A.T.Natarajan, and A.A.van Zeeland. Genomic heterogeneity of UV-induced repair: relationship to higher order chromatin structure and transcriptional activity. in press

M.Z.Zdzienicka, D.L.Mitchell, J.Venema, A.van Hoffen, A.A.van Zeeland, L.H.F.Mullenders, J.de Wit, and J.W.I.M.Simons. DNA repair characteristics and mutability of the UV-sensitive V79 Chinese hamster cell mutant V-B11 (complementation group 7). *Mutagenesis* (1991) 6, 179-183.

P.P.W.van Buul, F.Darroudi, A.A.W.M.van Loon, L.H.F.Mullenders, A.T.Natarajan, H.Vrieling, M.Z.Zdzienicka, and P.H.M.Lohman. Genetic and biochemical basis of radiation sensitivity in cultured human and other mammalian cells. In: *Frontiers in Radiation Biology*. (Ed. E. Riklis) (1991) 427-435. Balaban Publisher New York.

Venema J. Gene specific repair of UV-induced DNA damage in mammalian cells. (1991) Thesis, University of Leiden

Venema J., Z.Bartosova, A.T.Natarajan, A.A.van Zeeland and L.H.F.Mullenders. Transcription affects the rate but not the extent of repair of cyclobutane pyrimidine dimers in the human adenosine deaminase gene. *J.Biol.Chem.* (1992) 267, 8852-8856

Zdzienicka M.Z., J.Venema, D.L.Mitchell, A.van Hoffen, A.A.van Zeeland, H.Vrieling, L.H.F.Mullenders, P.H.M.Lohman, and J.W.I.-M.Simons. (6-4) Photoproducts and not cyclobutane pyrimidine dimers are the main UV-induced mutagenic lesions in Chinese hamster cells. *Mutation Res.* (1992) 273, 73-83

Menichini P., H.Vrieling and A.A. van Zeeland. Strand specific mutation spectra in repair proficient and deficient hamster cells. *Mutation Res.* (1992) 251, 143-155.

Lehman A.R., J.H.J.Hoeijmakers, A.A.van Zeeland, C.M.P. Backendorf, B.A.Bridges, A.Collins, R.P.D.Fuchs, G.P.Margison, R.Montesano, E.Moustacchi, A.T.Natarajan, M.Radman, A.Sarassin, E.Seeberg, C.A.Smith, M.Stefanini, L.H.Thompson, G.P.van der Schans, C.A.Weber, and M.Z.Zdzienicka. workshop on DNA repair. *Mutation Res.* (1992) 273, 1-28

Vrieling H., Li-H. Zang, A.A.van Zeeland and M.Z.Zdzienicka. UV-induced HPRT mutations in a UV-sensitive hamster cell line from complementation group 3 are biased towards the transcribed strand. *Mutation Res.* (1992) 274, 147-155

Project 2

Head of project: *Prof. Bridges*

Objectives for the reporting period

1. To establish reliable laboratory procedures for measuring human cellular radiosensitivity based on (a) clonal assays with T-lymphocytes, (b) the single cell microgel assay and (c) a delayed plating clastogenicity assay with fibroblasts.
2. (a) To localise the human gene (XRCC5) which corrects the defects in *xrs* mutants; (b) to clone and characterize DNA repair genes from *Schizosaccharomyces pombe*, as a model for human DNA repair.

Progress achieved including publications

Sub-project 1

(a) Clonal assays with human T-lymphocytes

Our ability to clone circulating T-lymphocytes with reproducibly high plating efficiencies has made it possible to utilize this readily available material in assays of cellular radiosensitivity. We have established that an estimate of radiosensitivity can be achieved rapidly (within 2-3 weeks of taking a blood sample). No period of *in vitro* cellular multiplication is required between biopsy and test. Thus any observations closely reflect the *in vivo* situation, in contrast to studies based upon other cell types such as fibroblasts or keratinocytes. Our results show: (i) although the range of sensitivity between T-lymphocytes ($\bar{D} = 1.26 - 2.15$ Gy) and fibroblasts ($\bar{D} = 0.90 - 1.68$ Gy) from 34 normal donors is similar, there is little evidence for a correlation in individual radiosensitivities between the two cell types. (ii) T-lymphocytes from ataxia-telangiectasia (A-T) donors are significantly more radiosensitive than cells from normal donors. (iii) Neonatal cord blood derived T-lymphocytes (18 samples) are significantly more radiosensitive ($\bar{D} = 1.54$ Gy) than T-lymphocytes derived from normal adult blood ($\bar{D} = 1.90$ Gy, $p = <0.001$). Overall, these results indicate that T-lymphocytes are a convenient source to estimate cellular radiosensitivity. They may not necessarily however reflect the responses of other cell types. The hypersensitivity of neonatal cells may be of relevance to radiation protection of the unborn child.

(b) The Single Cell Microgel (Comet) Assay

We have established this assay as a reliable laboratory procedure for measuring single strand breaks. This has required the procurement of image intensification and computerised scoring facilities in addition to defining critical experimental parameters. We have trained visiting workers from a number of other laboratories in the use of this assay.

(i) The procedure is rapid (results within 1 day) and can be used with any tissue from which a single cell suspension can be obtained, it is economical in requiring a minimal number of cells (20 μ l of blood provides sufficient material).

(ii) We have shown that the assay can detect breaks produced indirectly during the excision repair of UV-C damage in human T-lymphocytes thus providing an efficient

procedure of minimal invasiveness for the detection of excision-defective xeroderma pigmentosum patients.

(iii) We have been able to detect breaks induced directly by gamma-irradiation at doses down to 0.25 Gy. There do not appear to be any differences in initial damage between cells from normal donors or ataxia-telangiectasia patients.

(iv) We have shown that diet can significantly modify the spontaneous frequency and inducibility by ionising radiation of single strand breaks in circulating mononuclear cells from a panel of six donors. This observation has implications both for radiotherapy and for the assessment of the radiosensitivity of individuals.

(c) The delayed plating-micronucleus assay

Ataxia-telangiectasia (A-T) fibroblasts are defective in the repair of potentially lethal and potentially clastogenic damage which is revealed by a procedure whereby cells are held out of cycle to permit repair. We have shown that while A-T heterozygotes as a population are defective in the repair of potentially lethal damage the extent of the defect is not sufficient to permit identification of individual heterozygotes. Preliminary investigations suggest that the defect in repair of potentially clastogenic damage is more discriminatory. We have, therefore, undertaken a substantial highly replicated study of a coded series of normal, A-T and heterozygote samples to determine (i) the reliability and (ii) potential application of the assay, to assess the frequency of heterozygotes amongst at risk populations, such as breast cancer populations. The results show that while A-T patients are unambiguously detectable in the assay its intrinsic variability precludes its application (at this time) for the detection of heterozygotes.

Sub-Project 2

(a) Localisation of the XRCC5 gene

Chinese hamster *xrs* mutants are sensitive to the lethal effects of ionising radiation as a consequence of a genetic deficiency in the ability to rejoin double-strand breaks. As a first stage in cloning the gene defective in *xrs* mutants we have localised the human gene correcting these mutants using the procedure of microcell-mediated chromosome transfer. The starting material for this project was a panel of mouse/human hybrids each containing a single human chromosome tagged with a selectable marker (*gpt*). Microcells derived from this panel were fused to *xrs* mutants, and hybrids containing the donor human chromosome were obtained by selecting for the *gpt* marker. Resulting hybrids were analysed for their radiation sensitivity. Hybrids containing human chromosome 2 were considerably more resistant than the recipient cells, whereas those containing other chromosomes did not show any increased resistance. This suggested that the human functional homologue of the *xrs* gene, which has been designated XRCC5 is located on chromosome 2.

In order to further localise the XRCC5 gene to a subchromosomal region of chromosome 2, the radioresistant *xrs* hybrids containing human chromosome 2 were lethally gamma-irradiated and then fused once again to the *xrs* parents, in order to rescue fragments of chromosome 2. This resulted in a panel of *xrs* hybrids containing different fragments of chromosome 2. These hybrids were analysed (a) for radioresistance, (b) for a series of different markers mapping to different regions of chromosome 2. The latter analysis used PCR to identify the presence or absence of the markers. Using these procedures we found that radioresistance segregated with a small region of chromosome 2 locating in the region 2q34-36. We have thus isolated, in this procedure, an *xrs* line containing a small fragment of human chromosome 2 on which the correcting XRCC5 gene is located. This cell line will form the starting material for cloning the XRCC5 gene.

(b) Cloning and analysis of DNA repair genes from the model eukaryotic organism *Schizosaccharomyces pombe*

Fundamental metabolic processes, such as cell cycle control, DNA replication and repair are known to be tightly conserved across the eukaryotic kingdom. Thus lower eukaryotes provide excellent model systems for understanding these processes in human cells, as well as offering new procedures for cloning human genes. We have used radiation-sensitive mutants of the fission yeast, *S. pombe* to clone DNA repair genes from this organism. The general procedure involves transforming the mutants with a genomic DNA library, selecting for radiation-resistance and recovering and analysing the correcting plasmids. We have also studied properties of some of the mutants in relation to cell cycle control.

(1) Excision-repair. We have cloned 3 genes involved in the excision-repair processes. The *rad16*, *rad13* and *rad15* genes of *S.pombe* are the homologues of the *RAD1*, *RAD2* and *RAD3* genes of the distantly related budding yeast, *Saccharomyces cerevisiae*. Comparison of the sequences shows interesting differences in the type of homology between the gene pairs. *rad16* and *RAD1* have 35-40% amino acid sequence identity throughout the predicted protein, whereas *rad13* and *RAD2* have regions of very high sequence similarity at either end of the protein, with very little similarity in between. This points to important functional domains close to both termini. *rad15* and *RAD3* have 55% sequence identity, but the sequence identity is much higher in seven domains conserved in DNA helicases. The products of these genes are known to have ATP-dependent DNA helicase activity.

(2) G2 checkpoints. Radiation results in a delay in the G2 phase of the cell cycle, presumably to allow the cell to repair DNA damage prior to mitosis. We have shown that mutants at the *rad1*, *rad3*, *rad9* and *rad17* loci fail to arrest the cells in G2 following irradiation. Instead they enter a catastrophic mitosis with their DNA unrepaired. The products of these genes not only monitor the DNA for damage but also for completion of DNA replication. Hydroxyurea, an inhibitor of DNA synthesis, normally blocks cell cycle progression, but in these checkpoint *rad* mutants, cycle progression continues and again a catastrophic mitosis results. These mutants therefore delineate a new pathway involved in the response of cells to DNA damage. We have isolated new mutants involved in this pathway and we have cloned the *rad9* and *rad17* genes. The sequence of the genes has not provided any evidence of homology with previously cloned genes from other organisms.

(3) Other genes. We have also cloned and sequenced the *rad4* and *rad18* genes. The former is an essential gene. The functions of these two genes are not yet known.

Publications

1. Plowman, P. N., B. A. Bridges, C. F. Arlett, A. Hinney, and J. E. Kingston (1990) An instance of clinical radiation morbidity and cellular radiosensitivity, not associated with ataxia-telangiectasia. *Brit. J. Radiol.*, 63, 624-628.
2. Newton, J. A., A. K. Black, C. F. Arlett, and J. Cole (1990) Radiobiological studies in the naevoid basal cell carcinoma syndrome. *Brit. J. Dermatol.*, 123, 573-580.
3. Green, M. H. L., C. F. Arlett, J. Cole, S. A. Harcourt, A. Priestley, A. Waugh, G. Stephens, D. Beare, N. A. P. Brown, and G. A. Shun-Shin (1991) Comparative human cellular radiosensitivity III. gamma-radiation survival of cultured skin fibroblasts and resting T-lymphocytes from the peripheral blood of the same individual. *Int. J. Radiation Biol.*, 59, 749-765.

4. Waugh, A., D. Beare, J. Cole, C. F. Arlett, and M. H. L. Green (1991) Increased radiosensitivity in a clonal survival assay of T-lymphocytes isolated from neonatal cord blood samples. Proceedings of the European Society for Radiation Biology meeting, Dublin, In press.
5. Parris, C. N., J. R. W. Masters, and M. H. L. Green (1990) pSV3neo transfection and radiosensitivity of human cancer cell lines. *Cancer Letters*, 55, 171-175.
6. Broughton, B. C., N. Barbet, J. Murray, F. Z. Watts, M. H. M. Koken, A. R. Lehmann, and A. M. Carr (1991) Assignment of ten DNA repair genes from *Schizosaccharomyces pombe* to the chromosomal *NotI* restriction fragments. *Mol. Gen. Genet.*, 228, 470-472.
7. Murray, J. M., A. M. Carr, A. R. Lehmann, and F. Z. Watts (1991) Cloning and characterization of the DNA repair gene, *rad9*, from *Schizosaccharomyces pombe*. *Nuc. Acids Res.*, 19, 3525-3531.
8. Lehmann, A. R., A. M. Carr, F. Z. Watts, and J. M. Murray (1991) DNA repair in the fission yeast, *Schizosaccharomyces pombe*. *Mutation Res.*, 250, 205-210.
9. Barbet, N. C., W. J. Muriel, and A. M. Carr (1992) A versatile series of shuttle vectors and genomic libraries for use in the fission yeast, *Schizosaccharomyces pombe*. *Gene*, 114, 59-66.
10. Fenech, M., A. M. Carr, J. M. Murray, F. Z. Watts, and A. R. Lehmann (1991) Cloning and characterisation of the *rad4* gene of *Schizosaccharomyces pombe*. *Nuc. Acids Res.*, 19, 6737-6741.
11. Bridges, B. A., J. Cole, C. F. Arlett, M. H. L. Green, A. P. W. Waugh, D. Beare, D. L. Henshaw, and R. D. Last (1991) Possible association between mutant frequency in peripheral lymphocytes and domestic radon concentrations. *Lancet*, 337, 1187-1189.
12. Green, M. H. L., J. E. Lowe, S. A. Harcourt, P. Akinluyi, T. Rowe, J. Cole, A. V. Anstey, and C. F. Arlett (1992) UV-C sensitivity of unstimulated and stimulated human lymphocytes from normal and xeroderma pigmentosum donors in the Comet Assay: A potential diagnostic technique. *Mutation Res.*, 273, 137-144.
13. Arlett, C. F., S. A. Harcourt, J. Cole, M. H. L. Green, and A. V. Anstey (1992) A comparison of the response of unstimulated and stimulated T-lymphocytes and fibroblasts from normal, xeroderma pigmentosum and trichothiodystrophy donors to the lethal action of UV-C. *Mutation Res.*, 273, 127-135.
14. Lehmann, A. R., J. H. J. Hoeijmakers, A. A. Van Zeeland, C. M. P. Backendorf, B. A. Bridges, A. Collins, R. P. D. Fuchs, G. P. Margison, R. Montesano, E. Moustacchi, A. T. Natarajan, M. Radman, A. Sarasin, E. Seeberg, C. A. Smith, M. Stefanini, L. H. Thompson, G. P. Van Der Schans, C. A. Weber, and M. Z. Zdzienicka (1992) Workshop on DNA repair. *Mutation Res.*, 273, 1-28.
15. Barnes, D. E., A. E. Tomkinson, A. R. Lehmann, A. D. B. Webster, and Lindahl T. (1992) Mutations in the DNA ligase 1 gene of an individual with immunodeficiencies and cellular hypersensitivity to DNA damaging agents. *Cell*, 69, 495-503.
16. Al-Khodairy, F., and A. M. Carr (1992) DNA repair mutants defining G2 checkpoint pathways in *Schizosaccharomyces pombe*. *EMBO J.*, 11, 1343-1350.
17. Bridges, B. A., and C. F. Arlett (1992) Risk of breast cancer in Ataxia-Telangiectasia. *New Eng. J. Med.*, 326, p1357.
18. Murray, J. M., C. Doe, P. Schenk, A. M. Carr, A. R. Lehmann, and F. Z. Watts (1992) Cloning and characterisation of the *S. pombe rad15* gene, a homologue to the *S. cerevisiae RAD3* and human *ERCC2* genes. *Nuc. Acids Res.*, 20, 2673-2678.

Project 3

Head of project: *Prof. Bootsma*

Objectives for the reporting period

In order to elucidate the molecular mechanism of mammalian DNA repair processes, to unravel the molecular basis of human repair syndromes and to understand the relationship between DNA repair and carcinogenesis we have focused on:

1. Isolation and functional characterization of human genes involved in DNA repair (nucleotide excision repair and post replication repair) notably the genes: *ERCC1*, *XPBC/ERCC3*, *CSBC/ERCC6*, *HHR6A*, *HHR6B* and *HHR23*.
2. Generation of mouse models for human repair disorders, utilizing cloned genes and targeted gene inactivation in embryonal stem cells.

Progress achieved including publications

1. Isolation and characterization of human genes involved in DNA repair

We have followed 2 strategies for the cloning of human repair genes.

- a. DNA transfection to repair-deficient rodent and human cells followed by selection of UV-resistant transformants and 'rescue' of the correcting gene. This has resulted in the cloning of *ERCC1*, *XPBC/ERCC3* and *CSBC/ERCC6*
- b. Sequence homology to cloned repair genes of lower eukaryotes, particularly yeast (*S.cerevisiae*). This approach has yielded *HHR6A*, *HHR6B* and *HHR23*.

The main results on the isolation and analysis of these genes are summarized below.

ERCC1

The *ERCC1* gene, which corrects the repair defect of rodent group 1 mutants, was cloned prior to the start of this project and was further characterized. Mutation analysis revealed that the strongly conserved C-terminal 2/3 of the encoded 297 amino acid protein is essential for its role in nucleotide excision repair (NER) and showed that the protein has a distinct other function in the cellular response to cross-linking agents. It may be that this second property of the *ERCC1* gene product is identical to the role of its yeast homolog, the repair protein RAD10, in mitotic recombination, and that the repair of some cross links requires this ERCC1-dependent recombination pathway. A ubiquitin-ERCC1 fusion protein was overproduced in *E.coli* and is now being characterized using the *in vitro* NER assay developed by R. Wood (ICRF).

XPBC/ERCC3

The *ERCC3* gene, which corrects UV-sensitive rodent mutants of group 3, was cloned just prior to the start of this project. It specifies a protein of 782 amino acids. The deduced amino acid sequence suggests it to be a chromatin binding helicase. No homologous (repair) proteins in any organism were identified in data bases. However, the gene appeared very strongly conserved, which permitted isolation of the *Drosophila* and yeast (*S.cerevisiae* and *S.pombe*) homologs. Gene disruption in yeast indicated that *ERCC3*^{sc} participates in a process essential for viability in addition to its role in NER (results in collaboration with L. and S. Prakash, Rochester). Transfection

and microinjection experiments demonstrated that mutations in *ERCC3* are responsible for xeroderma pigmentosum (XP) complementation group B, a very rare form of XP that is simultaneously associated with Cockayne's syndrome (CS). Determination of the causative mutation in the *XPBC/ERCC3* gene presented the first elucidation of the molecular defect in a human repair syndrome. Using microinjection of the gene, 2 new patients were assigned to this group. In spite of the severe NER deficiency, both patients have not developed skin cancer (in striking contrast to the sole known XP-B case) even at relative advanced age. This points to the involvement of additional factors required for cancer proneness.

CSBC/ERCC6

The *ERCC6* gene, was cloned after extensive genomic DNA transfections to a member of the moderately UV-sensitive rodent group 6. The -for transfection cloning-very large gene (≥ 85 kb) encodes a protein of 1493 amino acids. The central part harbours all "signatures" of a recently discovered, highly homologous helicase subfamily, consisting of proteins involved in transcription regulation and in all major repair pathways of yeast. This suggests that *ERCC6* after *ERCC2* and 3 is the third DNA helicase in mammalian NER. No equivalent of *ERCC6* is known in any species. The chromosomal localization of *ERCC6* to a region deleted in a CS patient, pointed to a possible involvement of this gene in one of the forms of CS. Transfection experiments revealed that the gene specifically corrects the repair defect in cells of CS complementation group B. Subsequent sequence analysis of DNA and RNA of a CS-B patient disclosed severe mutations in both *ERCC6* alleles. This established that *ERCC6* is not a vital gene and resolves the molecular defect in the most common form of CS, that has been shown by Venema et al. (SGL) to be impaired in the preferential repair of (the transcribed strand of) active genes. The *CSBC/ERCC6* gene is the first cloned gene specifically implicated in this subpathway of NER.

HHR6A and *B*

The strong evolutionary conservation of most of the repair genes analyzed until now has prompted us to see whether isolated yeast genes could be recruited to identify and clone homologous human genes. This approach was applied to the *S.cerevisiae RAD6* gene, which plays a central role in postreplication repair, damage induced mutagenesis and sporulation. The 172 amino acids *RAD6* protein is a ubiquitin-conjugating enzyme (E2) that *in vitro* (poly)ubiquitinates histones. By evolutionary walking based on nucleotide sequence homology we have cloned two human *RAD6* homologs (designated *HHR6A* and *HHR6B*) using the *Schizosaccharomyces pombe* and *Drosophila melanogaster* genes as "intermediates". The two 152 amino acids human proteins, share 95% sequence identity with each other and approximately 70% and 85% overall identity with the yeasts (*S.cerevisiae* and *S.pombe*) and *D.melanogaster* homologs respectively. Intriguingly, none of the *RAD6* homologs possesses the acidic C-terminal sequence present in the *S.cerevisiae RAD6* protein, which is required for sporulation. The central part, harbouring the cysteine residue involved in thiolester formation with ubiquitin, displays significant homology with other ubiquitin-conjugating and- activating enzymes. Genetic complementation experiments reveal that *HHR6A* as well as *HHR6B* can carry out the repair and mutagenesis functions of *RAD6* in *S.cerevisiae rad6Δ* mutants but not its role in sporulation (in collaboration with S. and L. Prakash, Rochester). The striking conservation of *RAD6* structure and function throughout eukaryotic evolution suggests that the essential components of the repair- and mutagenesis-machinery with which *RAD6* interacts have also been conserved. Both proteins are expressed in all cells and tissues analyzed. Elevated

levels of RNA and protein are registered in Sertoli cells and round spermatids in a stage, prior to the substitution of histones by protamines. The latter observation is consistent with the idea, that HHR6A and B function in chromatin remodelling. Immuno-electronmicroscopy suggests that both proteins are associated with euchromatin.

HHR23

Very recently, the human homolog of the yeast *NER* gene *RAD23* was identified. Sequence analysis indicates that the ubiquitin-like N-terminus as well as the remainder of the protein are clearly conserved. Characterization of this gene, that in yeast is involved only in part of the *NER* pathway, is in progress.

Other human repair genes, gene products and mutants.

We have also attempted to clone the human *NER* genes *ERCC7* and *ERCC13*, but no promising transfectants were obtained. Therefore, these projects were -at least for the time being- stopped.

Furthermore, the XP-A correcting (XPAC) protein was purified from calf thymus using correction of repair synthesis of living XP-A fibroblasts after microinjection as assay system. The surprisingly heat-stable protein was partially characterized and found to have a high affinity for (UV-irradiated) ds and ss DNA.

In collaboration with Dr. A. Lehmann (Sussex) and Dr. M. Stefanini (Pavia) we have identified a trichothiodystrophy (TTD) patient with a *NER* defect which does not fall into XP group D, to which thus far, all known UV-sensitive TTD individuals are assigned, nor does the patient belong to any of the other XP complementation groups. This case, therefore, defines a new complementation group and reveals the existence of a second previously unknown *NER* gene, that shows the striking and unexplained overlap with the clinical manifestations of TTD. Furthermore, two severe patients with mainly CS symptoms (identified by Dr. Jaeken, Leuven) were by complementation analysis assigned to the rare XP group G, previously not associated with CS. This identifies the third XP group with XP and XP/CS patients, and further extends the overlap between these repair disorders.

2. Generation of mouse models for human repair-disorders

Using the recently developed technology of gene targeting in totipotent embryo-derived mouse stem cells (ES-cells) we have inactivated one of the alleles of *ERCC1* and 3. Because of the possible vital role of both genes also constructs were made which induce more subtle mutations and -in the case of *XPBC/ERCC3*- mimic one of the mutations found in an XP-B patient. For each gene and type of mutation several homologous ES recombinants were obtained and have been injected into mouse blastocysts. After implantation into pseudo-pregnant foster mothers a number of *ERCC3* chimeric mice were born, that are now being tested for germline chimerism. The eventual aim is to generate by interbreeding mouse mutants with the same biochemical defect as in human repair syndromes and patients. Such experimental mouse models are extremely valuable for studying the relationship between repair deficiency and cancer, risk assessment, genotoxicity and carcinogenicity testing etc.

Thesis

Weeda G.

Molecular characterization of a DNA repair defect in xeroderma pigmentosum and Cockayne's syndrome. State University Leiden. 1990.

Roza L.

Processing of UV-induced DNA damage in human skin cells.
Erasmus University Rotterdam. 1990.

Publications

Weeda G, van Ham RCA, Mazurel R, Westerveld A, Odijk H, de Wit J, Bootsma D, van der Eb AJ, Hoeijmakers JHJ.

Molecular cloning and biological characterization of the human excision repair gene *ERCC-3*.

Molec.Cell.Biol. 1990; 10: 2570-2581.

Hoeijmakers JHJ, Eker APM, Wood RD, Robins P.

Use of *in vivo* and *in vitro* assays for the characterization of mammalian excision repair and isolation of repair proteins.

Mutat Res 1990; 236: 223-228.

Hoeijmakers JHJ.

Cryptic initiation sequence revealed. Nature 1990; 343:417-418

Weeda G, van Ham RCA, Vermeulen W, Bootsma D, van der Eb AJ, Hoeijmakers JHJ.

A presumed DNA helicase, encoded by the excision repair gene *ERCC-3* is involved in the human repair disorders xeroderma pigmentosum and Cockayne's syndrome.

Cell 1990; 63: 777-791.

Troelstra C, Odijk H, de Wit J, Westerveld A, Thompson LH, Bootsma D, Hoeijmakers JHJ.

Molecular cloning of the human excision repair gene *ERCC-6*.

Molec Cell Biol 1990; 10: 5806-5813.

Hoeijmakers JHJ, Bootsma D.

Molecular genetics of eukaryotic DNA excision repair.

Cancer Cells 1990; 2: 311-320.

Jaspers NGJ, van der Kraan M, Linssen PCML, Macek M, Seemanova, Kleijer WJ.

First-trimester prenatal diagnosis of the Nijmegen breakage syndrome and ataxia telangiectasia using an assay of radioresistant DNA synthesis. Prenatal Diagnosis 1990; 10: 667-674.

Gradwohl G, de Murcia JM, Molinete M, Simonin F, Koken MHM, Hoeijmakers JHJ, de Murcia G.

The second Zinc finger domain of poly(ADPribose) polymerase targets single strand break specificity.

Proc Natl Acad Sci USA 1990; 87: 2990-2994.

Reynolds P, Koken MHM, Hoeijmakers JHJ, Prakash S, Prakash L.
The *rhp6+* gene of *Schizosaccharomyces pombe*: a structural and functional homolog of the *RAD6* gene from the distantly related yeast *Saccharomyces cerevisiae*. EMBO J 1990; 9: 1423-1430.

Roza L, Vermeulen W, Bergen Henegouwen JBA, Eker APM, Jaspers NGJ, Lohman PHM, Hoeijmakers JHJ.
Effects of microinjected photoreactivating enzyme on thymine dimer removal and DNA repair synthesis in normal and xeroderma pigmentosum fibroblasts. Cancer Res 1990; 50: 1905-1910.

Smeets H, Bachinski L, Coerwinkel M, Schepens J, Hoeijmakers J, van Duin M, Grzeschik KH, Weber CA, de Jong P, Siciliano MJ, Wieringa B.
A long-range restriction map of the human chromosome 10q13 region: close physical linkage between *CKMM* and the *ERCC-1* and *ERCC-2* genes. Am J Hum Genet 1990; 46: 492-501.

Klein B, Pastink A, Odijk H, Westerveld A, van der Eb A.
Transformation and immortalization of diploid xeroderma pigmentosum fibroblasts. Exp Cell Res. 1990; 191:256-262.

Thesis

Belt P. Development of an Epstein-Barr virus derived cDNA expression vector system. State University Leiden. 1991.

Publications

Bootsma D, Hoeijmakers JHJ.
The genetic basis of xeroderma pigmentosum.
Ann Genet (Paris) 1991; 34:143-150.

Eker APM, Formenoy L, De Wit LEA.
Photoreactivation in the extreme halophilic archaeobacterium *Halobacterium cutirubrum*.
Photochemistry and Photobiology 1991; 53/5: 643-651.

Hoeijmakers JHJ.
How relevant is the *Escherichia coli* Uvr ABC model for excision repair in eukaryotes?
J Cell Sci 1991; 100: 687-691.

Koken M, Reynolds P, Bootsma D, Hoeijmakers J, Prakash S, Prakash L.
DHR6, a Drosophila homolog of the yeast DNA repair gene *RAD6*.
Proc Natl Acad Sci USA 1991; 88: 3832-3836.

Koken MHM, Reynolds P, Jaspers-Dekker I, Prakash L, Prakash S, Bootsma D, Hoeijmakers JHJ.
Structural and functional conservation of two human homologs of the yeast DNA repair gene *RAD6*.
Proc Natl Acad Sci 1991; 88: 8865-8869.

Vermeulen W, Stefanini M, Giliani S, Hoeijmakers JHJ, Bootsma D.
Xeroderma pigmentosum complementation group H falls into complementation group D.

Mutat Res 1991; 255: 201-208.

Weeda G, Ma L, van Ham RCA, Bootsma D, van der Eb AJ, Hoeijmakers JHJ.
Characterization of the mouse homolog of the *XPBC/ERCC-3* gene implicated in xeroderma pigmentosum and Cockayne's syndrome.
Carcinogenesis 1991; 12: 2361-2368.

Weeda G, Ma L, van Ham RCA, van der Eb AJ, Hoeijmakers JHJ.
Structure and expression of the human *XPBC/ERCC-3* gene involved in DNA repair disorders xeroderma pigmentosum and Cockayne's Syndrome.
Nucl Acids Res 1991; 19: 6301-6308.

Weeda G, Wiegant J, van der Ploeg M, Geurts van Kessel AHM, van der Eb AJ, Hoeijmakers JHJ.
Localization of the xeroderma pigmentosum group B-correcting gene *ERCC-3* to human chromosome 2q21.
Genomics 1991; 10: 1035-1040.

Belt PBGM, Oostenrijk van MF, Odijk H, Hoeijmakers JHJ, Backendorf C.
Induction of a mutant phenotype in human repair proficient cells after overexpression of a mutated DNA repair gene.
Nucl Acids Res 1991; 19: 5633-5637.

Belt PBGM, Jongmans W, de Wit J, Hoeijmakers JHJ, Putte van de P, Backendorf C.
Efficient cDNA cloning by direct phenotypic correction of a mutant human cell line (*HPRT*) using an Epstein-Barr virus derived cDNA expression vector.
Nucl Acids Res 1991; 19: 4861-4866.

Broughton BC, Barbet N, Murray J, Watts FZ, Koken MHM, Lehmann AR, Carr AM.
Assignment of ten DNA repair genes from *Schizosaccharomyces pombe* to chromosomal *NotI* restriction fragments.
Mol Gen Genet 1991; 228: 470-472.

Zdzienicka MZ, Mitchell DL, Venema J, van Hoffen A, van Zeeland AA, Mullenders LHF, de Wit J, Simons JWIM.
DNA repair characteristics and mutability of the UV-sensitive V79 Chinese hamster cell mutant V-B11 (complementation group 7).
Mutagenesis 1991; 6/3: 179-183.

Lehmann AR, Hoeijmakers JHJ et al.
Workshop on DNA repair. Mutat. Res. 1991; 273: 1-28.

Koken MHM, Smit EME, Jaspers-Dekker I, Oostra BA, Hagemeyer A, Bootsma D and Hoeijmakers JHJ.
Localization of two human homologs, *HHR6A* and *HHR6B*, of the yeast DNA repair gene *RAD6* to chromosome Xq24-25 and 5q23-31.
Genomics 1992; 12: 447-453.

Troelstra C, Landsvater RM, Wiegant J, van der Ploeg M, Viel G, Buys CHCM and Hoeijmakers JHJ.

Localization of the nucleotide excision repair gene *ERCC-6* to human chromosome 10q11-21.

Genomics 1992; 12: 745-749.

Eker APM, Vermeulen W, Miura N, Tanaka K, Jaspers NGJ, Hoeijmakers JHJ and Bootsma D.

Xeroderma pigmentosum group A correcting protein from Calf Thymus. Mutat Res. 1992; 274: 221-224.

Weeda G, Hoeijmakers JHJ, Bootsma D.

Genes controlling nucleotide excision repair in eukaryotic cells.

Bioassays 1992 (in press).

Hoeijmakers JHJ and Bootsma D.

DNA repair: two pieces of the puzzle.

Nature Genetics 1992; 1: 313-314.

Hoeijmakers JHJ, Troelstra C and Weeda G.

DNA repair and syndromes: from man to yeast. Alfred Benzon Symposium Vol. 35. V.A. Bohr, K. Wassermann, K.H. Kraemer and J.H. Thaysen, eds. Munksgaard, Copenhagen. 1992 (in press).

Troelstra C, van Gool A, de Wit J, Vermeulen W, Bootsma D, Hoeijmakers JHJ.

ERCC6, a member of a subfamily of putative helicases, is involved in Cockayne's syndrome and preferential repair of active gene. Cell 1992 (in press).

Yasui A, Yajima H, Kobayashi T, Eker APM, Oikawa A.

Mitochondrial DNA repair by photolyase. Mutat Res. 1992; 273: 231-236.

Ziv Y, Frydman M, Lange E, Zelnik N, Rotman G, Julier C, Jaspers NGJ, Dagan Y, Abeliovicz D, Dar H, Borochowitz Z, Lathrop M, Gatti RA and Shiloh Y.

Ataxia-telangiectasia: linkage analysis in highly inbred Arab and Druze families and differentiation from an ataxia-microcephaly-cataract syndrome. Hum Genet. 1992; 88: 619-626.

Project 4

Head of project: *Dr. Moustacchi*

Objectives for the reporting period

A variety of biochemical pathways ranging from the control of cellular growth to the fidelity of DNA repair and replication appear to be involved in the maintenance of genomic integrity. The "chromosomal instability disorders", including Fanconi anemia (FA), due to human mutations may allow to elucidate these pathways and shed light on their role in individual variations in sensitivity to radiations and chemicals and cancer-predisposition. FA is genetically heterogeneous; 4 genetic complementation groups have been recently identified and one of such genes, FA group C, has been cloned and characterized (Strathdee et al., *Nature*, 356, 763, 1992 and Strathdee et al., *Nature Genetics*, 1, 196, 1992). During the last three years using a different strategy, our group has been involved in the cloning and characterization of a DNA sequence which corrects the defect of FA group D. On the other hand, the mutations spontaneously arising in patients or induced *in vitro* have been analysed in relation with the cancer proneness characteristic of the disease. Finally, the anomalies in the production of cytokines that we discovered while studying some of the DNA repair features of FA have been analysed at the molecular level.

Progress achieved including publications

1) FA group D cells transfected with mouse DNA showed an almost normal response to mitomycin C (MMC) (*Human Genet.*, 1990). After screening a genomic library of the corrected FA(D) cells DNA in a lambda phage vector, with mouse repeated DNA, recombinant DNA phages were isolated. One out of these recombinants showed an almost complete restoration of resistance to MMC following transfection of the FA(D) cells. Transfection of this DNA in FA(D) cells gave negative results, indicating specificity. Transfection of the FA(D) correcting DNA fragments in the newly defined FA complementation groups B and C is in progress.

Molecular characterization of the FA(D) correcting DNA fragment have been achieved by restriction mapping and partial sequencing. Maps in normal human, FA and mouse genomic DNA were established. Comparison of these maps indicate that the structure is conserved among human and mouse, with an insertion of mouse repeated DNA. At the genomic level, no gross structural alterations of this DNA region were observed neither in FA cells nor in mouse "FA like mutants". The gene is conserved in man, monkey, rat, mouse, hamster, bovin, dog and drosophila. The chromosomal localisation is now established and does not correspond to chromosomes 9 and 20.

A unique DNA sequence in FA(D) correcting fragment DNA is used as a probe to detect a transcript of 3.5-4 kb in polyadenylated RNA from normal and FA cells by Northern blot. The detected transcript is identical in size and abundance in normal and different FA cells polyA⁺ RNAs. This indicates that a point mutation or a deletion < 200 kb is likely to be involved. The expression of this gene is not inducible by DNA damaging agents.

The unique DNA probe allowing to detect a transcript has been used to screen cDNA libraries to isolate the corresponding cDNA. Yet, three cDNA libraries have been screened to obtain the complete cDNA (3.10⁶ clones of the Okayama and Berg cDNA library in the pCDV vector, 10⁶ clones of the Ragi cDNA library in lambda GT10 vector from Clontech and 10⁶ clones of a random cDNA library from HBL 100 cells in lambda GT10 vector).

Sequences data analysis indicate that the cDNA isolated encodes a protein which contains motifs common with the super family of motor proteins (Kinesin, Dynein, Dynamin) including a GTP site. These proteins are known to be involved in protein sorting, organisation of intracellular membranes, establishment of cell polarity, spindle pole-body separation of chromosome segregation during mitosis and a number of developmental processes. These properties could be relevant to the FA phenotype.

2) We have shown that the frequencies of *HPRT*⁻ mutants as well as mutants in the Na⁺/K⁺ ATPase gene (ouabain resistance) were significantly lower in FA than in normal human lymphoblasts following treatments which induce DNA monoadducts or interstrand cross-links (*Cancer Res.*, 1990). The hypomutability in FA cells was then shown to be associated with an increased deletion frequency at the *HPRT* gene level (*Proc. Natl. Acad. Sci. USA*, 1990). Characterization of 70 unrearranged mutants demonstrate considerable differences in mRNA phenotyping between normal and FA cells. Indeed, in contrast to normal cells, the *HPRT* gene expression is affected in FA cells; a large proportion of either spontaneous or induced mutants did not produce in FA mutants detectable amounts of mRNA (*Som. Cell. Molec. Genet.*, 1991).

More recently, we have shown that the frequency of *HPRT*⁻ mutants is not significantly different in lymphocytes of 23 FA patients compared to age matched healthy donors. In contrast, in an assay which detects allele-loss and recombinational events in erythroïd progenitor cells, the mean frequency of glycophorin A (GPA) variants was very significantly elevated in FA patients erythrocytes compared to FA heterozygotes and normal donors (submitted, 1992).

Knowing that the cellular events allowing detection at the *HPRT* and the *GPA* loci differ, our results emphasize the correlation between events of spontaneous loss of heterozygosity, increased sensitivity to DNA damaging agents and predisposition to myelogenous leukemia as seen in FA.

3) The correction in FA of chromosomal and cellular hypersensitivity to DNA cross-linking damage to an almost normal level can be achieved by addition of interleukin-6 (IL-6) to the growth medium. The other cytokines tested (IL-1, IL-2, etc.) do not have this effect. Both lymphoblasts and fibroblasts derived from FA patients (groups A and non-A) demonstrate a reduction in IL-6 production. In contrast to normal cells, this lymphokine is not induced in FA by usual inducers (TNF α and β , etc.). This deficiency may account for the defect in differentiation of the hematopoïetic system characteristic of FA (*Human Genet.*, 1992). An increased level of tumor necrosis factor α (TNF α) is observed both *in vitro* and *in vivo* in FA and a similar observation holds for Ataxia telangiectasia. This may account for the chromosomal fragility observed in FA and AT cells. Southern and Northern blot analysis do not demonstrate major alterations at the genes and at the transcription level for IL-6 and TNF α in FA (submitted, 1992). We propose that the wild type gene product, mutated in FA, controls at the translational level a network of genes including those coding for IL-6 and TNF α and error-prone repair.

- Is the induction of pyrimidine dimers relevant for the phototoxicity of 7-methyl(3-4c)pyridopsoralen ? S. NOCENTINI. *Mutation Res.*, **235**, 203-208 (1990).
- Removal of psoralen photo-induced DNA cross-links in normal and Fanconi's anemia fibroblasts : a molecular analysis by electron microscopy. S. ROUSSET, S. NOCENTINI, B. REVET & E. MOUSTACCHI. *Cancer Res.*, **50**, 2443-2448 (1990).
- Cocultivation of Fanconi's anemia cells and of mouse lymphoma mutants leads to complementation of chromosomal hypersensitivity to DNA cross-linking agents. E. ROSSELLI & E. MOUSTACCHI. *Human Genet.*, **84**, 517-521 (1990).
- The mutagenic response of Fanconi's anemia cells from a defined complementation group after treatment with photoactivated bifunctional psoralens. D. PAPADOPOULOU, B. PORFIRIO & E. MOUSTACCHI. *Cancer Res.*, **50**, 3289-3294 (1990).
- Hypomutability in Fanconi anemia cells is associated with increased deletion frequency at the *HPRT* locus. D. PAPADOPOULOU, C. GUILLOUE, H. MOHRENWEISER & E. MOUSTACCHI. *Proc. Natl. Acad. Sci. USA*, **87**, 8383-8387 (1990).

- Partial complementation of the Fanconi's anemia defect upon transfection by heterologous DNA. Phenotypic dissociation of chromosomal and cellular hypersensitivity to DNA cross-linking agents. C. DIATLOFF-ZITO, F. ROSSELLI, J. HEDDLE & E. MOUSTACCHI. *Human Genet.*, **86**, 151-161 (1990).
- Mutagenic effects photoinduced in normal human lymphoblasts by a monofunctional pyridopsoralen in comparison to 8-methoxypsoralen. D. PAPADOPOULO & E. MOUSTACCHI. *Mutation Res.*, **245**, 259-266 (1990).
- Genotoxic effects of radiotherapy and chemotherapy on the circulating lymphocytes of breast cancer. III : Measurement of mutant frequency to 6-thioguanine resistance. M. SALA-TREPAT, J. COLE, M.H.L. GREEN, Q. RIGAUD, J.R. VILCOQ & E. MOUSTACCHI. *Mutagenesis*, **5**, 593-598 (1990).
- Fanconi anemia : Genetic and molecular aspects of the defect. E. MOUSTACCHI, C. GUILLOUF, D. FRASER, F. ROSSELLI, C. DIATLOFF-ZITO & D. PAPADOPOULO. *Nouv. Rev. Fr. Hematol.*, **32**, 387-389 (1990).
- DNA ligase activity in human cells from normal donors and from patients with Bloom's syndrome and Fanconi's anemia. M. MEZZINA, S. NOCENTINI, J. NARDELLI, I. SCOVASSI, U. BERTAZZONI & A. SARASIN. In : "*DNA repair mechanisms and their biological implications in mammalian cells*". Eds. : M.W. Lambert & J. Laval, pp. 461-469 (1990).
- Processing of photoinduced cross-links and monoadducts in human cells DNA : genetic and molecular features. E. MOUSTACCHI, D. PAPADOPOULO, D. AVERBECK, D. FRASER & C. DIATLOFF-ZITO. In : "*DNA repair mechanisms and their biological implications in mammalian cells*". Eds. : M.W. Lambert & J. Laval, pp. 471-482 (1990).
- Decreased mutagenicity in Fanconi's anemia lymphoblasts following treatment with photoactivated psoralens. D. PAPADOPOULO, C. GUILLOUF, B. PORFIRIO & E. MOUSTACCHI. In : "*Mutation and the Environment*", Part A : *Basic Mechanisms*". Eds. : M.L. Mendelshon & R.J. Albertini, Wiley-Liss Inc., pp. 241-248 (1990).
- Studies on the influence of the presence of an activated *ras* oncogene on the *in vitro* radiosensitivity of human mammary epithelial cells. C. ALAPETITE, C. BAROCHE, Y. REMVIKOS, G. GOUBIN & E. MOUSTACCHI. *Int. J. Radiat. Biol.*, **59**, 385-396 (1991).
- Transfection of wild type and "Fanconi anemia like" mouse lymphoma mutant cells by electroporation. D. FRASER, C. DIATLOFF-ZITO & E. MOUSTACCHI. *Mutation Res.*, **263**, 165-171 (1991).
- Formation of cyclobutane thymine dimers photosensitized by pyridopsoralens : Quantitative and qualitative distribution within DNA. A. MOYSAN, A. VIARI, P. VIGNY, L. VOITURIEZ, J. CADET, E. MOUSTACCHI & E. SAGE. *Biochemistry*, **30**, 7080-7088 (1991).
- Damage distribution and mutation spectrum : the case of 8-methoxypsoralen plus UVA in mammalian cells. E. SAGE & A. BREDBERG. *Mutation Res.*, **263**, 217-222 (1991).
- *HPRT* gene expression differs in mutants derived from normal and Fanconi anemia cells : analysis of spontaneous and psoralen photoinduced mutants. C. GUILLOUF, E. MOUSTACCHI & D. PAPADOPOULO. *Somatic Cell Mol. Genet.*, **17**, 591-599 (1991).

- Mammalian DNA repair mutants : recent progress in the genetic and molecular biology of the processing of DNA lesions induced by UV and by DNA cross-linking agents. E. MOUSTACCHI. In : "*Light in Biology and Medicine*", vol. 2. Eds. : R. Douglas, J. Moan & G. Ronto. Plenum Press, London, pp. 463-475 (1991).
- Repair control of photoinduced cross-links and monoadducts in DNA : Genetic, molecular and evolutionary features. E. MOUSTACCHI. In : "*Photobiology*". Ed. : E. Rikklis, Plenum Press, New York, pp. 223-233 (1991).
- Abnormal lymphokine production : A novel feature of the genetic disease Fanconi anemia. I: Involvement of interleukin-6. F. ROSSELLI, J. SANCEAU, J. WIETZERBIN & E. MOUSTACCHI. *Human Genet.*, **89**, 42-48 (1992).
- Maladies génétiques associées à une hypersensibilité cellulaire, à des agents génotoxiques et à une forte prédisposition aux cancers. A. SARASIN & E. MOUSTACCHI. Dans : "*Cancers Cutanés*". Ed. : L. Dubertret, Collection Encyclopédie des Cancers dirigée par B. Hoerni et M. Tubiana, Flammarion Médecine Sciences, Paris, chapitre 2, pp. 16-40 (1992).
- *In vitro* DNA synthesis by DNA polymerase I and DNA polymerase α on single-stranded DNA containing either purine or pyrimidine monoadducts. J.S. HOFFMANN, E. MOUSTACCHI, G. VILLANI and E. SAGE. *Biochem. Pharmacol.*, **41** (in press).
- UV damage distribution of the *LacI* gene of *Escherichia coli* analysed with various probes on an automated DNA sequencer : correlation with mutation spectrum. E. SAGE, E. CRAMB & B.W. GLICKMAN. *Mutation Res.* (in press).
- Decreased deletion mutation in radioadapted human lymphoblasts. O. RIGAUD, D. PAPADOPOULOU and E. MOUSTACCHI. *Radiation Res.* (in press).
- Distribution and repair of photolesions in DNA : Genetic consequences and the role of sequence context. E. SAGE. *Photochem. Photobiol.* (in press).
- 8-methoxypsoralen induced mutations are highly targeted at cross-linkable sites of photoaddition on the non-transcribed strand of a mammalian gene. E. SAGE, E.A. DROBETSKY and E. MOUSTACCHI. *EMBO J.* (in press).

Project 5

Head of project: *Dr. Thacker*

Objectives for the reporting period

To exploit a novel cell-free method for assessing the repair and misrepair of DNA double-strand breaks, to help understand the molecular nature of certain radiosensitive disorders and the enzymatic basis of break-rejoining. To characterize the molecular basis of deletion formation by human cell extracts.

To characterize spontaneous and radiation-induced mutations of primary human fibroblasts. To identify those mutations with large deletions and to map their breakpoints using a polymerase-chain-reaction (PCR) strategy. To map the extent of the deletions using flanking marker sequences (DXS probes) and high-resolution cytogenetic methods. To isolate deletion breakpoint junctions and sequence these to determine mechanisms of deletion formation.

To examine the radiosensitive *irs* mutants derived in this laboratory for their response to irradiation conditions that reveal altered cellular repair capacity (e.g. low dose rate irradiations). To assess the feasibility of gene mapping/cloning strategies for the human genes complementing specific radiosensitive mutants based on the use of somatic cell hybrids.

Progress achieved including publications

A number of studies implicate the DNA double-strand break as an important and serious type of damage following exposure of cells to ionising radiation. Several radiosensitive mutants are now known to have impaired break-rejoin abilities; however in some mutants, such as the human disorder ataxia-telangiectasia (A-T), the evidence of a break-rejoin defect is equivocal.

To follow the ability of the cell to repair double-strand breaks (DSB) with precision it is necessary to produce site-specific DSB that can be relocated and examined following exposure to a cellular environment. We have achieved this using an endonuclease to produce the initial break at a unique site in a simple sequenced molecule, followed by exposure of this broken DNA to human nuclear extracts. We have compared the rejoin activities of extracts from both normal cells and cells derived from A-T patients. Additionally extracts from transformed cell lines and primary cultures have been used to consolidate the data.

Our initial studies compared rejoin activity on a number of different DNA break sites in the same molecule, showing that: (a) different sites were rejoined with different efficiencies by human extracts, reflecting both the location of the site and the type of termini involved, and (b) extracts from different cell lines, whether radiosensitive or not and from transformed or primary lines, all had the same relative efficiency of rejoining at different sites. However, the fidelity of rejoining by extracts varied with the cell line used: in particular extracts from 2 A-T lines showed high levels of mis-rejoining at certain

initial break sites. These data support our previous findings with broken DNA molecules transferred into cells.

We have examined the correct rejoining of breaks further using cell free extracts derived from human 293 cells. We have developed a highly efficient system for the rejoining of double strand breaks and, using this as an assay, we have separated the nuclear extract into multiple components. The unfractionated extract will rejoin 100% of the input DNA template, linearized with a restriction enzyme, to high molecular weight material at low temperatures (17°C). We have also demonstrated that the reaction is active (80% conversion of monomer units) at the physiological temperature of 37°C. At this temperature however, the profile produced is different to that observed at 17°C, with the products forming a characteristic pattern of dimer, trimer and higher species. We have shown that this distribution is due to a nuclease or phosphatase in the extract, which is active at 37°C, and makes a proportion of the DNA ends refractory to ligation. We have succeeded in the biochemical fractionation of the nuclear extract into multiple components which, when assayed in different combinations, reveal properties not observed with the crude extract (e.g. the rejoining of blunt DNA termini). One of these fractions has been purified 500-fold (designated REP 1) and has been shown to stimulate the break-joining activity observed in the nuclear extracts. In addition, REP 1 increases the activity of purified DNA ligase I, which on its own is inactive under these conditions. The further purification of the various factors involved in the rejoining of double-stranded breaks is in progress.

The fidelity of rejoining has also been pursued by molecular analysis of mis-rejoined molecules. It was found that mis-rejoining exclusively followed a mechanism which gave deletions of varying size (up to 600 bp) with short direct sequence repeats at each breakpoint. One copy of the repeat remained in the deleted molecule. Approx. 50 mis-rejoined molecules were sequenced, mostly after treatment with A-T extracts, showing that a variety of short repeats were used in the process but that about half the molecules had a common 25 bp deletion. Additionally, a small number (about 1%) of the mis-rejoined molecules had insertions of DNA; one such molecule when sequenced revealed that the alteration was complex, with both a deletion (121 bp) and an insertion (320 bp) at the same site. A model of these processes was put forward based on a simple scheme of excision, polymerization and ligation to give illegitimate recombination leading to deletion at specific sites. This model, with refinements based on the action of certain other DNA-modifying enzymes, is being tested at present.

The major mutation type induced by ionising radiations is the large deletion or rearrangement. To help understand the mechanism(s) of deletion formation in a relevant cell type, we have established conditions for the isolation and analysis of mutations of the *hprt* gene in primary human fibroblasts. This choice has both advantages and disadvantages: the advantages are that the complete human gene (56 kb) has been sequenced and that flanking marker sequences are available to map the extent of deletions in the genomic region containing *hprt* (Xq26). A disadvantage is that these cells have a limited lifespan so that loss of some mutants before analysis is completed is inevitable. We have established a mutation system with early-passage male

cells (HF12 or HF10); mutants have been isolated after no treatment (spontaneous) or after X-ray treatment. A total of 75 mutants (41 independent mutations) were characterized, initially using Southern blots, but latterly using a battery of PCR primers covering most of the gene. Approximately 42% of X-ray induced mutants were large deletions, of which many had both breakpoints falling outside the gene. Of those with at least one breakpoint within the gene, these were localized to within 2 kb using presence or absence of PCR products for defined parts of the gene. Four of these deletions were localized further using PCR techniques, followed by isolation and sequencing of their breakpoint junctions. There were several interesting features of these junctions: although the common human *alu* repeat was found at one end of several deletion breakpoints the deletions did not seem to occur through homologous recombination between these repeats. Rather, illegitimate recombination processes were implicated in the deletions, and in one radiation-induced mutant a unique deletion-duplication junction was formed. This type of junction may occur in response to heavily-damaged sites. Flanking (DXS) sequences in the Xq26 region, covering more than 1.5 Mb, were also used to show that many of the breakpoints were localized to within 1 Mb of the gene. However, four of the mutants had more extensive deletions especially distal to the gene. Cytogenetic analysis of these large deletions showed that several could be visualized using high-resolution banding; one mutant carried an X/11 translocation in addition to the molecular deletion.

In addition to these studies with primary cells, we have devised a method for the rapid analysis of the mutation spectrum using hamster V79 cells. DNA was extracted directly from mutant colonies and used in a multiplex PCR reaction to yield a spectrum from very few cells. We have checked the mutation type in a total of 138 independent mutants, comprising approximately equal numbers induced by X-rays, α -particles or spontaneously-occurring. While the proportion of deletion mutations was low for the spontaneous set (13%), those for both the X-ray and α -particle set were very similar at 55 and 57% respectively. This result suggests that despite the differences in energy deposition expected for these two types of ionising radiation, they may induce mutants in the *hprt* gene by similar mechanisms.

The characterization of radiosensitive (repair-defective) mutants is an important way to understand the repair pathways used by the cell to combat radiation damage. We have previously isolated three new radiosensitive mutants, the *irs* mutants, and have characterized these extensively. An important cellular indication of repair capacity is ability to recover from the lethal effects of radiation when the dose is given at a low dose rate. Normal cells in plateau phase growth show a large recovery factor when irradiated under these conditions compared to acute irradiation. We have shown previously that A-T cells and the DSB-repair defective *xrs* mutants have little or no recovery factor under low dose rate conditions. Experiments have recently been completed to analyse the response to low dose rate of the mutants *irs1*, *irs2*, and *irs3*. We found that *irs2* showed little or no recovery factor under these conditions; taken with our previous data on DNA synthesis inhibition and hypersensitivity to camptothecin, this response strengthens the similarity of *irs2* to A-T cells. Both *irs1* and *irs3* respond like the parental cells,

providing for the first time a clear separation of these mutants from the A-T/*irs2* type and suggesting that despite their similar sensitivity levels they may be part of different repair pathways.

Mapping and cloning the genes complementing radiosensitive mutants is a challenging but worthwhile remaining task. Attempts to complement the radiosensitive *irs* mutants using cell fusion to human lymphocytes or fibroblasts yielded insufficient hybrids for useful studies. Plans to use microcell-mediated transfer of chromosome 11 into the A-T-like *irs2* line were abandoned, despite obtaining a suitable donor cell line, because of parallel efforts within this CEC group. We have however used an *irs1*-human lymphocyte hybrid (kindly donated by Dr. L.H. Thompson, Lawrence Livermore Laboratories) containing a small part of human chromosome 7 as a source of human DNA carrying the gene complementing the *irs1* radiosensitivity. These studies are yielding promising data and are still in progress.

Publications

THACKER, J., E.W. FLECK, T. MORRIS, B.J.F. ROSSITER and T.L. MORGAN. Localization of deletion breakpoints in radiation-induced mutants of the hprt gene in hamster cells. Mutation Research, 232 (1990) 163-170.

THACKER, J. Molecular nature of ionising radiation-induced mutations of native and introduced genes in mammalian cells. In Ionising Radiation Damage to DNA: Molecular Aspects, (Eds. S. Wallace & R.B. Painter), Wiley/Liss: New York. 1990, pp.221-229.

NORTH, P., A. GANESH and J. THACKER The rejoining of double-strand breaks in DNA by human cell extracts. Nucleic Acids Research, 18 (1990) 6205-6210.

THACKER, J., and R.E. WILKINSON The genetic basis of resistance to ionising radiation damage in cultured mammalian cells. Mutation Research, 254. (1991) 135-142.

THACKER, J. The measurement of radiation-induced mutation in mammalian cells at low doses and dose rates. Advances in Radiation Biology, 16 (1992)

AGHAMOHAMMADI, S.Z., T. MORRIS, D.L. STEVENS and J. THACKER Rapid screening for deletion mutations in the hprt gene using the polymerase chain reaction: X-ray and α -particle mutant spectra. Mutation Research, in press.

COSTA, N.D., and J. THACKER The efficiency of restriction endonuclease digests determined by PCR. Biotechniques, 13, 190.

GANESH, A., P. NORTH and J. THACKER Repair and misrepair of site-specific DNA double-strand breaks by human cell extracts. Mutation Research, in press.

FAIRMAN, M.P., A.P. JOHNSON and J. THACKER Multiple components are involved in the efficient rejoining of double stranded DNA breaks in human cell extracts. Nucleic Acids Research, in press.

Project 6

Head of project: *Dr. Backendorf*

Objectives for the reporting period

It has now been firmly established that exposure of living cells to radiation results in rapid changes in gene expression. However, the physiological significance of these changes is still poorly understood. Recently, we have obtained evidence that UV induced changes in gene expression can affect the normal balance between proliferation and differentiation of human skin cells (keratinocytes). The finding that the same genes are deregulated in cancer cells, suggests that these induced changes are very likely to contribute to the process of carcinogenesis (tumor promotion). The objectives for the reporting period (12 months) were to determine whether ionizing radiation can also interfere with the normal balance between keratinocyte proliferation and differentiation and whether the induced changes are different or similar to the ones observed with UV light.

Progress achieved including publications

1. SPR genes: a new class of keratinocyte differentiation markers

SPR (small proline rich) genes constitute a new family of related genes (*spr1*, *spr2*, *spr3*), which have recently been isolated in our department. These genes are strongly induced during the normal process of keratinocyte differentiation, but respond aswell to the treatment with UV light, X-rays and chemical tumor promoters. In keratinocytes, which have undergone cancerous transformation, the expression of these genes is strongly repressed and deregulated. Very recently we found, by sequence comparison, that SPR genes are related to loricrin and involucrin, two precursors of the cornified cell envelope (CE). Synthesis of the CE represents one of the most characteristic features of keratinocyte differentiation. The sequence homology suggests that SPR genes constitute a new class of CE precursors. Very recently, evidence has been obtained that SPR proteins are indeed incorporated into the cornified envelope by the action of transglutaminase I. As such *spr* genes are excellent markers for keratinocyte differentiation. Consequently, the expression and the regulatory elements of these genes constitute an ideal tool to analyse the molecular mechanisms which underlie both normal gene regulation during keratinocyte differentiation and its deregulation following the action of UV light or X-ray irradiation.

2. Interference of UV light and X-rays with gene regulation in human keratinocytes depends on the differentiation state of the irradiated cell

During the initial stages of this work, the effects of UV irradiation on gene regulation in human keratinocytes were performed on cells cultured under standard calcium concentrations. Such cultures contain a mixture of prolifera-

ting and differentiating keratinocytes. In these experiments we found reproducibly that the expression of *spr2* was significantly increased after UV irradiation. An identical pattern was found, when instead of UV light, X-rays (300 cGy) were used. However, when "stripped" cells (= monolayer of undifferentiated basal cells) were irradiated and subsequently allowed to differentiate by the addition of high calcium medium, a clear difference between UV light and X-rays was observed. Whereas in control cells induction of *spr* genes is readily observed (= normal induction during differentiation), this process is clearly inhibited by UV light, but slightly potentiated by X-ray irradiation. Apparently, UV light inhibits and X-ray enhances terminal differentiation if basal (proliferating) cells are irradiated. In contrast both agents enhance the differentiation process if cells, which have already committed to differentiation, are irradiated. These unexpected results are interesting as they show that cells of the same lineage (but in a different state of differentiation), can respond completely differently to radiation and that these differences are depending on the sort of radiation which is used. The effects of radiation on basal or differentiating cells are described separately:

- *) molecular mechanisms of UV and X-ray induced expression of *spr2* in differentiating cells: deletion mapping of the *spr2-1* promoter resulted in the identification of a UV responsive element (URE) situated 300 bp. ahead of the transcriptional initiation site. Until now the URE has been cut down to a sequence of 60 bp. An interesting feature is the presence of 2 adjacent NF- κ B sites in this region. Theoretically, NF- κ B would be an interesting candidate, as it has been shown by others that this transcription factor is activated by direct interaction with radicals. It remains, however, to be established whether NF- κ B is involved both in UV and X-ray induced expression of *spr* genes.
- ***) modification of *spr2* expression during keratinocyte differentiation after irradiation of undifferentiated cells: we have previously shown that the OCT-1 transcription factor, which binds to an octamer site (-100) in the *spr2-1* promoter, plays an essential role in *spr2* induction during keratinocyte differentiation. If undifferentiated cells are exposed to UV light this process is repressed, whereas when cells are exposed to X-rays the same process appears to get slightly induced. The induction of *spr* genes by X-rays is accompanied by an increased binding of OCT-1 to its target sequence. No such increase is observed with UV light. Here, however, in contrast to X-rays, a very strong induction of AP-1 (FOS/JUN) is observed. We have convincingly shown, by transfection of FOS and JUN expression plasmids, that increased AP-1 expression is responsible for the inhibition of keratinocyte differentiation after UV irradiation. Although, the molecular mechanisms of these regulations are not yet known, we do find these results very exciting as they clearly show that two different types of radiation do interfere with gene regulation during keratinocyte maturation, but that the factors which are affected are completely different in both cases. More work will be needed to explain these differences at a molecular level.

3. Identification of longterm changes in tissue homeostasis in sun-exposed areas of human skin

This part of the project has been performed in collaboration with Drs. M. Garmyn and B. Gilchrest at the Boston University School of Medicine. SPR expression was monitored in a large panel of primary keratinocytes from many different donors of different age classes. Aging comparisons were made between keratinocytes from sun protected sites in newborn, young adult and old adult donors; photoaging comparisons were made between keratinocytes from the inner (sun protected) and outer (sun exposed) aspects of the upper arm of old adults. These experiments showed that baseline expression of *spr2* is clearly increasing with age (50 fold when comparing 70 year old to newborn keratinocytes). However, when sun exposed and sun protected sites from the same donor (old adult) were compared, a significant reduction (50%) was found at sun exposed sites. These results indicate that UV exposure of human skin results in long-lasting changes in the balance between proliferation and differentiation, and that in this case the balance is shifted to a more proliferative (high FOS) and a less differentiated (lower *spr*) state. The interest of these findings, as far as the present project is concerned, relies in the fact that radiation exposure can be recognized by a long-lasting change in the expression of specific genes. From the results described above (part B), it is likely that the signature, left after radiation injury, might be different for different kinds of radiation.

Publications

1. Gibbs, S., Lohman, F., Teubel, W., van de Putte, P. and Backendorf, C. (1990). Characterization of the human *spr2* promoter: induction after UV irradiation or TPA treatment and regulation during differentiation of cultured primary keratinocytes. *Nucleic Acids Research* 18: 4401-4407
2. Backendorf, C., Gibbs, S., Lohman, F. and van de Putte, P. (1990). UV and TPA inducible genes in human keratinocytes. *Mutagenesis* 5: 77a
3. The *spr* gene family: involvement in UV response and carcinogenesis. *Int. J. Radiat. Res.* 57: 1251a
4. Gibbs, S., Fijneman, R., Wiegant, J., Geurts van Kessel, A., van de Putte, P. and Backendorf, C. (1992). Molecular characterization of a human gene family encoding small proline rich proteins. Submitted for publication
5. Gibbs, S., Borgstein, A-M., van de Putte, P. and Backendorf, C. (1992). Identification of the promoter sequence of a novel gene regulated during keratinocyte differentiation: differential responsiveness to UV irradiation and TPA treatment. Submitted for publication
6. Garmyn, M., Yaar, M., Boileau, N., Backendorf, C. and Gilchrest, B. (1992). Effect of aging and habitual sun exposure on the genetic response of cultured human keratinocytes to solar-simulated irradiation. Submitted for publication
7. Gibbs, S. (1992) Interference of UV light with gene regulation in epidermal keratinocytes. PhD thesis. University of Leiden.
8. Backendorf, C. and Hohl, D. (1992) A common origin for cornified envelope precursor proteins. *Nature Genetics* (accepted for publication)

EVALUATION OF THE FREQUENCIES OF CHROMOSOMAL ABERRATIONS INDUCED IN HUMAN BLOOD LYMPHOCYTES BY LOW DOSES OF NEUTRONS

Contract Bi6-0225 - Sector B13

- 1) *Lloyd* , NRPB (Bi6-225) - 2) *Natarajan* , Univ. Leiden Sylvius Lab. (Bi6-166)
- 3) *Obe* , Univ. Essen (Bi6-223) - 4) *Verschaeve* , Cen-SCK (Bi6-146)
- 5) *Palitti* , Univ. degli Studi della Tuscia (Bi6-171)

Summary of project global objectives and achievements

The project forms an extension of work that was funded by CEC to investigate the low dose response for chromosomal aberrations in human lymphocytes exposed in vitro to x-rays (Int. J. Radiat. Biol. 61: 335 (1992)). This study showed that, over the dose range 0-50 mGy, the data fitted well to a linear regression. However, below 20 mGy, despite 200,000 cells being scored from 24 donors, the uncertainties on the data were such that one could not discount the possibility of a threshold. Therefore, below 20 mGy, the data were unable to support or reject the Pohl-Rüling hypothesis (Mutation Res. 110: 71, 1983) that such low doses to G₀ lymphocytes could induce repair and indeed result in aberration yields below those for zero dose controls.

The purpose of the present project is essentially to repeat that work but to use low doses of fission spectrum neutrons. Five collaborating laboratories, listed above, were supported by the CEC and this report has been written to cover them jointly. Dr. E.J. Tawn of BNF plc Sellafield, UK, also collaborated in the work. The main part of the work was completed. However, towards the end of the contract period it became apparent that a further experiment should be carried out to provide some data at a higher dose, and also to enable inter-laboratory variations in scoring to be examined more critically. The irradiations for this have been completed but the results of the microscope analysis are not yet available.

Project 1

Head of project: *Dr. Lloyd*

Objectives for the reporting period

- 1) To irradiate blood with eight doses in the range 0-65 mGy of fission spectrum neutrons of incident mean energy 1.0 MeV. This was to be replicated with blood from four donors.
- 2) To culture the lymphocytes, make coded metaphase preparations and to distribute them to the collaborating laboratories.
- 3) The collaborators should analyse chromosomal damage in 500 metaphases per donor per dose.
- 4) To collate and decode the data, analyse it for donor and laboratory variability in aberration yield, and to deduce a dose response relationship.
- 5) In a separate study added later: To supplement the data with studies of blood from the same donors irradiated at higher doses; 0, 0.1 and 1.0 Gy and to circulate the same slides for each laboratory to score.

Progress achieved

Objectives 1 to 4 have been achieved and the data are presented in this report. Objective 5 is partially completed in that the irradiations have been carried out and the circulation of slides has commenced. The microscope scoring is not yet completed. It is intended that the work will be written up fully for publication in the open literature.

Methods

Blood samples from four healthy male donors, with unremarkable histories of exposure to clastogenic agents, were irradiated with the eight doses shown in Table 1 of fission spectrum neutrons of mean energy 1.0 MeV. The exposures were performed at the Reactor Centre Petten; the gamma-ray contribution to dose was low, about 7%. Lymphocytes were cultured at the University of Leiden where an initial check was also made with fluorescence plus Giemsa staining to ensure that the cultures contained a low (<5%) frequency of second division metaphases. Giemsa stained slides were scored by six collaborating laboratories; 1) Chilton, 2) Essen, 3) Leiden, 4) Mol, 5) Rome, 6) Sellafeld.

Results and Discussion

Table 1 shows the scoring results for dicentrics plus centric rings (D+R) and for excess acentric fragments (AF) noted by each laboratory for the four donors. In addition to the aberrations shown, seven rogue cells were also observed. These are metaphases which contain an exceptionally large number of aberrant chromosomes; these are considered to be unrelated to the irradiation. It may be seen from the asterisks in Table 1 that all rogue cells were derived from one donor. Thus, analysis of data presented in this report has not included the rogue cells.

Table 1 Aberrations scored in 500 cells by 6 laboratories at 8 doses. Dicentrics and rings are shown on the left and excess acentrics on the right. At each dose the totals for all laboratories and donors are given

Dose (mGy)	Donor	Laboratory						Total
		1	2	3	4	5	6	
0	1	0/0	0/7	0/0	0/2	0/2	1/1	1/12
	2	1/1*	0/9	1/1	0/0	1/6	0/0	3/17
	3	0/1	0/1	0/1	0/9	1/10	1/0	2/22
	4	0/0	0/0	0/0	0/10	2/3	0/0	2/13
	Total	1/2	0/17	1/2	0/21	4/21	2/1	8/64
0.26	1	0/1	1/1	0/1	0/4	0/6	0/0	1/13
	2	0/2*	0/6	1/0	5/5	0/0	0/0*	6/13
	3	1/1	0/0	1/2	1/5	0/5	0/1	3/14
	4	0/1	0/0	0/1	0/0	1/6	0/1	1/9
	Total	1/5	1/7	2/4	6/14	1/17	0/2	11/48
0.48	1	0/2	0/4	0/1	0/4	0/2	1/0	1/13
	2	0/2	0/5	1/1	1/1	1/9	0/0*	3/18
	3	0/1	0/0	0/2	3/3	1/1	0/3	4/10
	4	0/0	0/1	0/1	0/2	0/4	0/0	0/8
	Total	0/5	0/10	1/5	4/10	2/16	1/3	8/49
0.84	1	3/1	0/9	1/1	5/20	0/7	0/2	9/40
	2	0/1	0/3	0/2	0/0	0/11	0/0	0/17
	3	0/0	0/1	0/3	0/7	1/6	0/0	1/17
	4	1/0	0/5	1/0	0/2	1/3	0/0	3/10
	Total	4/2	0/18	2/6	5/29	2/27	0/2	13/84
1.20	1	0/2	1/8	2/0	0/9	1/2	0/1	4/22
	2	†2/0*	0/13	1/0	0/0	0/5	2/1	5/19
	3	0/2	0/3	1/5	0/3	1/3	0/2	2/18
	4	0/1	1/7	0/2	0/5	1/1	0/0	2/16
	Total	2/5	2/31	4/7	0/17	3/11	2/4	13/75
2.50	1	2/2	1/8	2/1	0/12	1/19	0/2	6/44
	2	2/3	3/11	2/2	0/5	1/5	0/0*	8/26
	3	0/0	0/0	1/3	0/3	2/5	1/0	4/11
	4	0/0	2/5	2/4	0/5	0/1	0/0	4/15
	Total	4/5	6/24	7/10	0/25	4/30	1/2	22/96
12	1	2/2	1/6	3/3	8/12	3/10	3/5	20/38
	2	4/6*	4/7	9/7	3/10	0/6	2/2	22/38
	3	2/1	3/1	8/12	7/5	0/8	6/3	26/30
	4	3/6	1/10	5/11	8/17	1/2	2/5	20/51
	Total	11/15	9/24	25/33	26/44	4/26	13/15	88/157
64	1	†12/6	†10/12	9/12	9/15	15/17	†10/5	65/67
	2	†15/13	††17/29	20/23	†14/26	14/11	22/26	102/128
	3	13/13	†7/21	17/20	†14/16	5/16	17/7	73/93
	4	17/21	†10/13	††16/23	†17/30	25/25	†17/12	102/124
	Total	57/53	44/75	62/78	54/87	59/69	66/50	342/412

* Rogue cell seen but not included in 500 cells scored

† Centric ring scored

Table 2 includes the results of an analysis of variability between the six laboratories in scoring replicate slides using the chi-squared method. For this analysis the data for the four donors have been pooled. The analysis shows that for D+R a laboratory variation is evident. At two doses (0.26 and 12 mGy) this is significant ($p > 0.05$) and four other doses show variability close to significance. With reference to Table 1 it may be seen that at 0.26 mGy, laboratory number 4 observed 5 dicentrics in donor 2; this is exceptionally high and the dicentrics were each present in separate cells. Conversely at 12 mGy fewer than expected D + R were recorded by laboratory 5 for donors 2-4. For AF, Table 2 shows that there was considerably more variability between laboratories. For example, at zero dose three laboratories have observed very few AF whilst three reported many. Moreover, this distinction between the same groups of laboratories is evident throughout the doses zero to 2.5 mGy, but for the two highest doses the difference is not as obvious. This raises the possibility of some systematic difference in scoring criteria. Laboratory variation, especially in the yields of AF, was not unexpected; it is usually evident in reports of interlaboratory comparisons. The general view is therefore reinforced that AF scoring is less certain and quantitative analysis of data is more reliable if restricted to yields of exchange type aberrations.

Table 3 shows an analysis of variability in aberration yields based on the four donors and for this the data from the six laboratories have been pooled at each dose. Here, for D+R, there is some evidence for donor variability. At 64 mGy Table 1 shows that all laboratories generally scored low D+R values for donor 1, as compared with donors 2 and 4, whilst the low yield for donor 3 is mainly due to the values recorded by laboratories 2 and 5. At 0.84 mGy reference to Table 1 shows that variability is considerably influenced by 5 dicentrics scored by laboratory 4 in donor 1. These 5 dicentrics include one cell that contained a dicentric and a trivalent. This is not a rogue cell and the possibility arises that it could be due to the high LET radiation in this study. Rare events such as a knock-on oxygen ion might occur in such neutron irradiations and if so could deliver up to about 1.4 Gy to a lymphocyte nucleus. Donor variability in AF yield is more evident than for D+R, notably at 0.84, 2.5 mGy and 64 mGy.

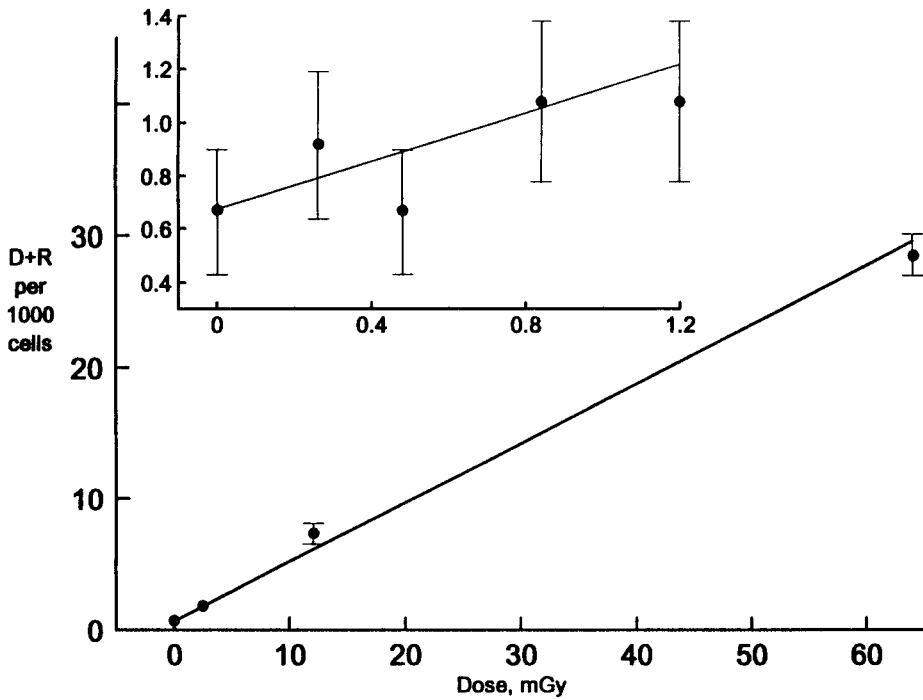
The D+R data have been pooled for examination of the dose response relationship. A linear regression has been fitted with a slope of $(4.5 \pm 0.2) \times 10^{-4}$ per mGy (Figure). The fit to a straight line was good (chi-square = 4.6, DF = 6, P = .60). The uncertainties on the data points, as shown in the Figure, are such that there is only clear evidence for a yield of D+R above background at doses of 2.5 mGy and above. The corresponding value from our previous work with x-rays was 20 mGy which is consistent with an RBE of about 10. Previous dose response work, albeit with higher doses, has shown RBE values of about 20 for fission spectrum neutrons with respect to x-rays. We note that the linear slope in the present study is lower by a factor of about 2 from that generally reported for fission spectrum neutrons. With the present data the slope of the dose response is essentially dependent on the highest dose (64 mGy). In view of this, it was resolved (section 2, objective 5) to extend the data to higher doses, and at the same time to use this material to investigate further the extent of inter-laboratory variability in aberration scoring.

Table 2. Chi² analysis for homogeneity between the 6 laboratories. The data in Table 1 for each donor have been pooled.

Dose (mGy)	Laboratory						Dicentric + Rings (DF = 5)		Acentrics (DF = 5)	
	1	2	3	4	5	6	χ^2	P	χ^2	P
0	1/2	0/17	1/2	0/21	4/21	2/1	8.5	.13	46.6	<.0001
.26	1/5	1/7	2/4	6/14	1/17	0/2	12.5	.03	21.9	.0005
.48	0/5	0/10	1/5	4/10	2/16	1/3	8.5	.13	14.1	.015
.84	4/2	0/18	2/6	5/29	2/27	0/2	9.6	.09	54.5	<.0001
1.20	2/5	2/31	4/7	0/17	3/11	2/4	4.1	.54	41.9	<.0001
2.50	4/5	6/24	7/0	0/25	4/30	1/2	10.2	.07	62.6	<.0001
12	11/15	9/24	25/33	26/44	4/26	13/15	27.1	.0001	23.7	.0002
64	57/53	44/75	62/78	54/87	59/69	66/50	5.1	.40	15.4	.0008

Table 3. Chi² analysis for homogeneity between donors. The data in Table 1 for each laboratory have been pooled.

Dose (mGy)	Donors				Dicentrics (DF = 3)		Acentrics (DF = 3)	
	1	2	3	4	χ^2	P	χ^2	P
0	1/12	3/17	2/22	2/13	1.0	0.80	3.0	.39
.26	1/13	6/13	3/14	1/9	6.1	0.11	1.2	.75
.48	1/13	3/18	4/10	0/8	5.0	0.17	4.6	.20
.84	9/40	0/17	1/17	3/10	15.0	0.01	24.5	<.0001
1.20	4/22	5/19	2/18	2/16	2.1	0.55	1.0	.80
2.5	6/44	8/26	4/11	4/15	2.0	0.57	27.3	<.0001
12	20/38	22/38	26/30	20/51	1.1	0.78	5.8	.12
64	65/67	102/128	73/93	102/124	13.1	.0044	23.9	<.0001



Yields of dicentrics plus rings plotted against neutron dose. Inset is expansion of the lower dose portion. Also shown is the best fit linear regression.

Project 2

Head of project: *Prof. Natarajan*

This is a multilaboratory project. For a common report on the project see the report of Contract No. Bi6-0225 (NRPB).

Project 3

Head of project: *Prof. Obe*

This is a multilaboratory project. For a common report on the project see the report of Contract No. Bi6-0225 (NRPB).

Project 4

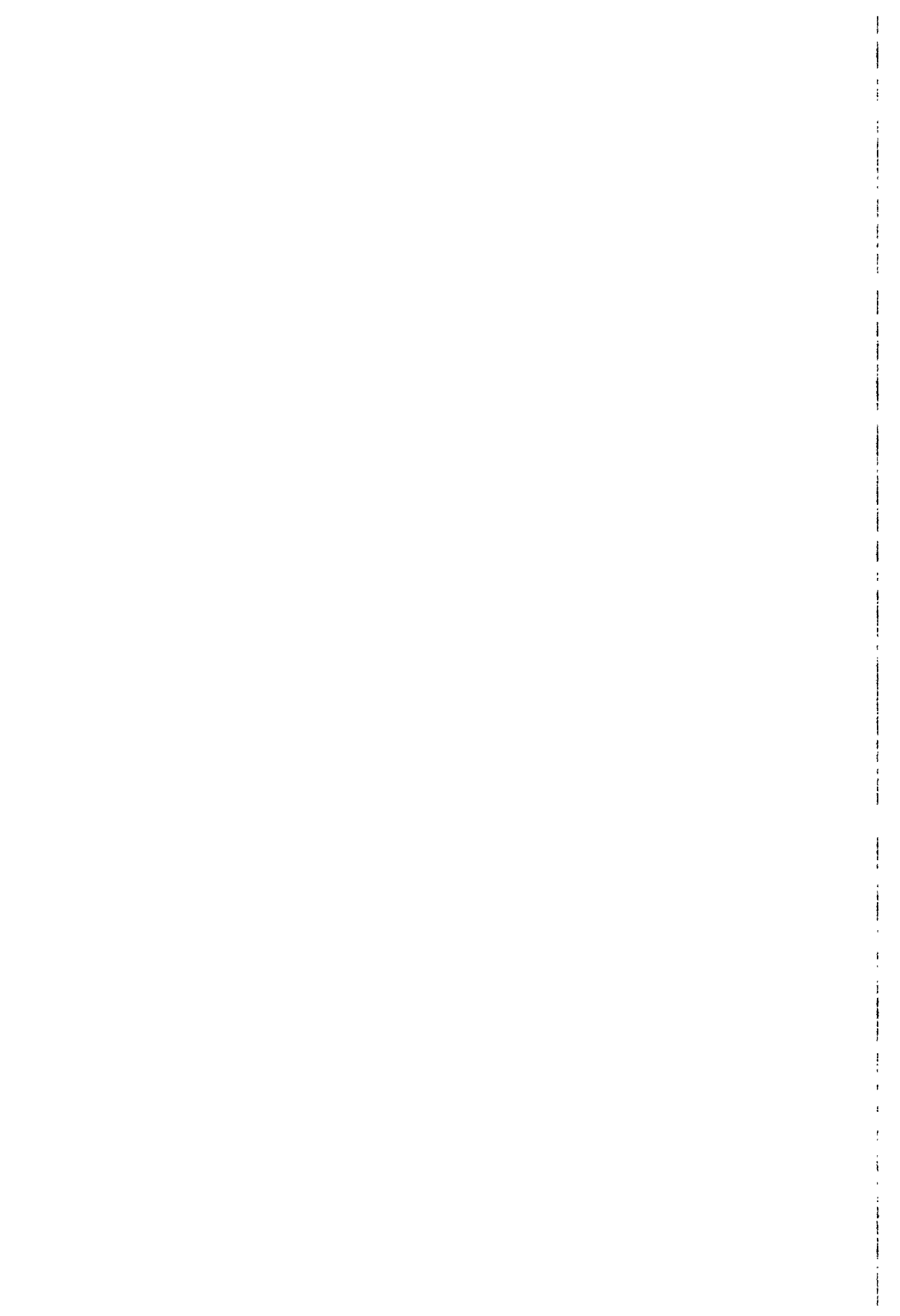
Head of project: *Dr. Verschaeve*

This is a multilaboratory project. For a common report on the project see the report of Contract No. Bi6-0225 (NRPB).

Project 5

Head of project: *Dr. Palitti*

This is a multilaboratory project. For a common report on the project see the report of Contract No. Bi6-0225 (NRPB).



EVALUATION OF EXISTING AND DEVELOPMENT OF NEW EPITHELIAL CELL TRANSFORMATION SYSTEMS AND DETERMINATION OF THEIR POTENTIAL IN RADIATION PROTECTION STUDIES

Contract Bi70-023 - Sector B13

- 1) *Seymour*, NEB - 2) *Riches*, St Andrews University
- 3) *Pertusa*, Univ. Valencia

Summary of project global objectives

There is a need for a relevant in vitro assay for studying cell transformation of human cells. In this way the molecular mechanisms and dose response relationships of carcinogenesis in humans can be studied. As about 85-90% of human tumours are of epithelial origin, it is important to utilise cultures of normal human diploid epithelial cells in transformation studies.

Studies on human epithelial systems, reviewed at the Dublin workshop on Cell Transformation, revealed that a promising approach to the investigation of oncogenic transformation in human systems was to utilise lines that had been developed from different tissues. The most promising of these are the SV40 immortalised human urothelial cell line, SV-HUC-1, developed by Reznikoff and the HPV 16 or 18 immortalised lines which can be developed routinely using the technique developed by DiPaolo from the transformation zone of the human cervix or from human skin keratinocytes. This system has the advantage of being immortalised by a human virus rather than SV40, although there is considerable variation from line to line, and the system is technically more difficult. A third promising human system is the immortalised keratinocyte line (HaCaT) developed by Boukamp et al. This line arose spontaneously in normal keratinocyte cultures from a subject with skin carcinoma.

The overall aims of the project were to collaborate on a systematic study of radiation induced oncogenic transformation using different human epithelial cell lines and to study initiation of carcinogenesis by radiation by examining changes which occur in molecular, genetic and morphological features of normal human cells after exposure to radiation. This more long term aim is at present being approached at a mainly qualitative level. It has proved extremely difficult to transform primary cultures of normal human epithelial cells and thus this approach provides the next logical step in developing a full understanding of radiation-induced transformation of human epithelial cells.

The specific objectives for this contract were:

- (1) To compare available human transformation systems in terms of their ability to address radiation protection problems, particularly radiation quality and low dose and low dose rate effects.
- (2) To attempt to develop new human epithelial systems capable of looking at initiation of carcinogenic damage, particularly by target specific radionuclides on the target organ in culture.

Summary of global achievements

- (1) HPV-G, SV HUC-1, CGL1 and HaCaT lines were established and a feasibility study undertaken to assess the technical difficulty, reproducibility and possibility of performing quantitative transformation assays using irradiation. It was found that both HPV-G and SV-HUC-1 were suitable but HaCaT had an unstable plating efficiency at low cloning density and results were very dependent on serum batch. CGL1 which is the HeLa X Fibroblast line developed by Stanbridge was rejected because of the large amount of American work being done and because the system appears to be a mutation assay and not strictly a transformation assay.
- (2) Work with the HPV line in Dublin and St Andrews showed that following irradiation (1-6Gy single dose) and serial passaging, tumours could be produced in nude mice. Tumours derived from injected irradiated progenitor populations were squamous carcinoma - like and were positive for ras protein product (p21). Considerable melanisation was noted in the tumours. The size of these tumours was monitored to estimate growth rate and detailed results are presented in the report from St Andrews. A problem with the results was that tumour nodules formed in some controls. These were presumably due to proliferation of the immortalised but untransformed cells. This problem arises when the HPV G cells are used at passages ≥ 80 . The line is available from DiPaolo at passage 54, therefore care has to be taken with the number of passages used between irradiation and testing.
- (3) The SV HUC-1 line was also used successfully in St Andrews and using the same protocol, tumours could be produced in nude mice. The frequency of tumour production with this line was very low indeed. Foci of small cells were detected following 4gy and these had a high cloning efficiency in soft agar.
- (4) The problem with transformation systems which separate the irradiated population in time from their progeny, which are eventually injected in high numbers into animals, is quantification of the frequency of tumour production. In an attempt to study this Dublin and St Andrews did cumulative growth curves so that the expansion of the irradiated survivors could be determined. The results can then be related back to the number of survivors. It is still not possible to overcome the need to inject approximately 10^6 cells to produce a single tumour. With systems such as HPV-G which can have a high background level and where many tumours occur in irradiated samples it is very difficult to see how meaningful quantitative data can be obtained.
- (5) A major finding with the HPV-G system was that considerable numbers of lethal mutations occur at each passage in populations which received radiation only. This cell loss reduces the population which derive from the irradiated progenitor cells and which are available for malignant progression. Significantly, where cells were treated with a chemical carcinogen in addition to radiation, this cell loss factor was reduced, allowing many more cells to progress to the next passage.
- (6) Because of the problems of quantification of the nude mouse end point, a major part of the project concerned the identification of cell based changes which could indicate that a transformation event had taken place. The end points included morphological

changes, proliferation rate changes, oncoprotein expression and oncosuppressor protein mutation or loss. The frequency of these end points is being measured with respect to radiation dose in Primary cultures of normal human urothelium or human oesophageal epithelium, in HPV and SV HUC 1 cell lines and in tumours produced by these cells in nude mice.

- (7) The following changes were detected in primary cultures of human oesophagus and ureter -
- a. Increased proliferation
 - b. Decreased nuclear size
 - c. Dose dependent focus formation with the following characteristics:
 - (i) foci are cmyc positive
 - (ii) Focal cells express endothelial and epithelial cell markers
 - (iii) Some foci express mutant p53 protein
 - (iv) Focal cell ultrastructure resembles squamous carcinoma and shows reduced interaction with neighbours
 - d. Increased numbers and organisation of endothelial cells.

Detailed quantification of some of these features are presented in the Dublin and Valencia reports.

8. Current ideas on radiation induced cancer risk assessment suggest that (a) several steps are necessary to produce a cancer and (b) certain individuals have a genetic predisposition to cancer and are therefore more susceptible to radiation than others.

A preliminary survey of 8 patients from which ureter samples were obtained revealed considerable differences in p53 mutant protein expression. Some patient cultures were positive even without irradiation. Others were negative unless treated with radiation or other carcinogen. One patients tissue was negative even when exposed to radiation and chemical carcinogen. This illustrates the importance of a) studying the human genome and b) studying individual patient response if risk is to be adequately and meaningfully quantified.

Project 1

Head of project: *Dr. Seymour*

Objectives for the reporting period

1. To establish and test the radiosensitivity of HPV-G, HaCaT and CGL1 cells and to determine their suitability for transformation assay.
2. To test tumorigenicity of these cell lines in nude mice.
3. To establish human normal epithelial cells and to quantify the appearance of certain changes in irradiated cells populations.
4. To isolate and culture foci appearing in cultures of irradiated cells.
5. To assess the importance of lethal mutations occurring in distance progeny of irradiated cells.

Progress achieved including publications

1. Survival curves for each cell line revealed little difference in radiation response. However examination of control data revealed that the C.E. of HaCaT cells was dependent on the number of cells plated. This makes it difficult to obtain accurate survival data. HPV-G and CGL1 cells presented no practical problems but the end point CGL1 cells is expression of a specific protein (p75) which is due to a specific single mutation. It is likely that the system measures mutation rather than transformation frequency. The project therefore focused on HPV-G cells. Figure 1a shows the initial survival curve and the cumulative survival curve for the passage which was injected into nude mice. It is clear that there is a very considerable loss of cells which initially survive irradiation by the time these cells are injected into mice.

Figure 1b shows that when a chemical carcinogen is added to the cells at the time of irradiation it reduces the level of lethal mutations at each passage. This is seen as an increased plating efficiency of the treated cells and means that more potentially transformed progeny survive. This result is important for two reasons (i) it shows that it is necessary to monitor the surviving population of cells during complex transformation protocols where several population doublings separate the initial exposure of the cells and the testing of their progeny and (ii) it highlights the fact that interactions may occur between radiation and other environmental carcinogens.

2. Cells at passage 7 of the transformation protocol were sent to St Andrews for injection into nude mice. The results are presented in the St Andrews report. Because of the high background and the occurrence of tumours at all doses of radiation, sections of tumours are being examined in Dublin for expression of markers. This work is not yet complete but initial histological evaluation shows ras

expression in tumours from irradiated cells. Other morphological differences are obvious but difficult to quantify.

3. **Analysis of Marker expression in Primary Cultures:** Data are summarised on table 1. Data for p53 expression revealed great variation in individual patient response. This is shown on Table 2. This highlights the importance of trying to develop transformation assays for risk assessment using primary cultures from individuals rather than specialised cells which may not represent the true heterogeneous situation in the human. Further analysis of p53 expression in tissues, cultures and cell lines is planned.
4. **Morphological Analysis:** Cultures were sent to Valencia for morphological analysis and data are presented in their report and in appendix 1. There was a decrease in nuclear size in the ureter specimens following irradiation. This is consistent with the increased numbers of focal cells which are very small. Technical problems prevented a more comprehensive analysis.
5. **Ultrastructure:** Analysis of the number of desmosomes and microvilli shows that in foci of irradiated cells, the normal cell interactions break down and cells are more isolated than in controls.

Summary:

1. Work with the established HPV G line allows some quantification of the population at risk for transformation to be determined. Tumours were obtained in nude mice following injection of irradiated cells but the high background creates problems.
2. Work with the primary system suggests p53-240 (oncosuppressor gene mutant protein) expression occurs following radiation exposure in sensitive individuals. Further work is necessary to evaluate this. Other markers are unlikely to be indicators but they support the p53 data and provide mechanistic information.

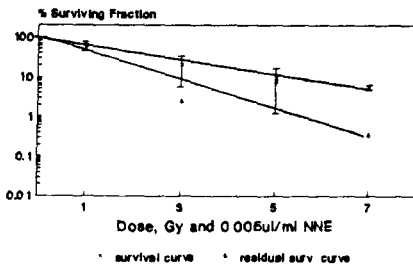


Figure 1a - HPV-G radiation and/or NNE
Radiation and NNE

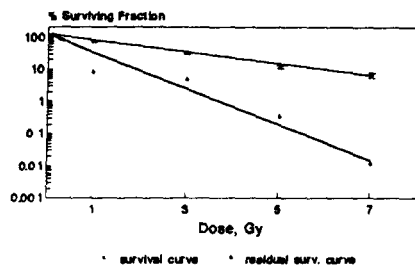


Figure 1b - HPV-G radiation and/or NNE
Radiation only

Table 1

Analysis of Marker Expression
 Results expressed as % cells in sample at day 21 after exposure
 except where indicated. Mean of 8 ureter cultures

Marker	Control	Irradiation		Nitrosamine	
		3 Gy	10 Gy	No Radiation	+ Irradiation
1. Proliferation (K _i 67 antigen)	0.2%	15%	70%	91%	95%
2. Total proliferating cells X 10 ⁶	10.3 ± 4.2	4.6 ± 3.3	2.2 ± 3.1	18.9 ± 1.2	21.2 ± 10.5
3. No. of Foci per culture	2 ± 1	5 ± 3	20 ± 7	25 ± 4	57 ± 7
4. cmyc (Whole Population)	0.02 % ± 0.005	2.1 % ± 14.0	23.2% ± 14.0	22.4 ± 7	60.2 ± 20.1
5. cmyc (Foci Only)	0	70% ± 3	90% ± 3.2	92% ± 3.4	95% ± 3.4
p53 mutant protein	*12.1 ± 24	25.2 ± 27.1	40.3 ± 22.3	92.1 ± 12.4	93.2 ± 7.1
Endothelial Cell Antigen (Factor VIII)	0.25 ± 0.25	6.5 ± 5.8	52.4 ± 12.2	54.3 ± 13.2	55.1 ± 14.2

Table 2

Analysis of p53 - 240 expression in Ureter tissue cultures
 from 8 patients

Patient No.	p53 expression		
	Control	Irradiation (3gy)	Irradiation + Nitrosamine
1	-	+	+
2	-	+	+
3	-	-	+
4	-	-	+
5	+	+	+
6	-	-	+
7	-	-	-
8	-	-	+

Publications

Full papers:

- 1 **Mothersill, C., O'Brien, A. and Seymour, C.B.** The effect of radiation in combination with carcinogens on the growth of normal urothelium in explant culture. Radiat Environ Biophys (1990) 29: 213-223.
- 2 **Mothersill, C., Seymour, C.B. and Bonnar, J.** Effect of radiation and other cytotoxic agents on the growth of cells cultured from normal and tumour tissues from the female genital tract. Gynaecologic Oncology, (1990) 37, 210-218.
- 3 **Mothersill, C.** Cell transformation systems relevant to radiation-induced cancer in man. Int. J. Radiat. Biol, 1990, vol. 57, No.2, 443-447.
- 4 **Mothersill, C. Seymour, C.B., Cusack, A., O'Brien, A. & Butler, M.** The effect of radiation and cytotoxic platinum compounds on the growth of normal and tumour bladder explant cultures. Acta Oncologica 29 (1990) Fasc. 2.
- 5 **Mothersill, C., Seymour, C.B., O'Brien, A. and Hennessy, T.P.** (1991). Proliferation of Normal & Malignant Human Epithelial Cells Post Irradiation. Acta Oncologica 30 (7) 851-858.
- 6 **Seymour, C.B. and Mothersill, C.** (1991). Chemotherapy agents and the Induction of Late Lethal Defects. Anticancer Research II 1605-1608.
- 7 **Mothersill, C., Seymour, C.B. and O'Brien, A.** (1991). Induction of Cmyc Oncoprotein and of Cellular Proliferation by radiation in Normal Human Urothelial Cultures. Anticancer Research. II 1609-1612.
- 8 **Seymour, C.B. & Mothersill C** (1992) All colonies from cells which survive ionising radiation contain non viable progeny. Mutation research (in Press).
- 9 **Seymour, C.B. & Mothersill C** (1991) Induction of late expressed Lethal Mutations by radiation in synchronised CHO-K1 cells as a function of cellular multiplicity and time post plating. In Seymour and Mothersill (eds) New Developments in Fundamental and Applied Radiobiology. Taylor & Francis London & New York pp 132-138.
- 10 **Mothersill, C., Seymour, C.B. & O'Brien A** (1991) changes induced in primary human urothelial cells by radiation. In Seymour and Mothersill (New Developments in Fundamental and Applied Radiobiology. Taylor & Francis London & New York) pp 195-202.
- 11 **Mothersill, C.,** (1992). Food Irradiation and Health - Research Gaps. Irish Journal of Biomedical Science 2 (2) in press.

- 12 **Mothersill, C., Seymour C.B., Mulvin D and Hennessy T.P.** Endothelial cell Proliferation is induced by radiation in cultured explants of Human Urothelium and oesophageal mucosa. In *Angiogenesis: Key Principles - Science - Technology - Medicine.* eds Steuier, Weisz & Langen Burkhauser Verlag Basel/Switzerland.

Book Published

Seymour, C.B. & Mothersill, C. (1991)

New Developments in Fundamental and Applied Radiobiology. Taylor & Francis, London & New York.

Project 2

Head of project: *Dr. Riches*

Objectives for the reporting period

1. To establish immortalised human urothelial cell lines (SV-HUC-1; NT11; BC16) in our laboratory and define their radiation sensitivity.
2. To characterise these lines using monoclonal antibodies to cytokeratins and SV40 large T protein.
3. To assess the genetic stability of these lines using the micronucleus assay.
4. To define whether the human urothelial cell lines (SV-HUC-1, BC16, and NT11) and the human keratinocyte cell line (HPV-G) are tumorigenic following transplantation to nude mice.
5. To define whether the cell lines SV-HUC-1, BC16 and NT11 can be transformed by radiation.
6. To investigate suitable end-points for transformation following radiation.
7. To investigate the dose effect relationship for transformation by radiation.

Progress achieved including publications

1. Characterisation of human urothelial cell lines

A number of human urothelial cell lines which have been immortalised by transfection with SV40 or SV40 origin-minus were kindly supplied by Dr. Catherine Reznikoff and have been established in our laboratory. These lines, designated SV-HUC-1, NT11, BC16 and CK2 grow as epithelial sheets. The growth rates of these lines are rather slow with doubling times typically of about 40 hours. Using immunocytochemical methods, the lines have been shown to express human cytokeratins in the cytoplasm (including keratins 10,17 and 18) and the SV40 large T protein in the nucleus. Immunocytochemical staining with antibodies to p53 indicated expression of p53. As mutant p53 has a longer half-life than the wild-type p53, immunocytochemical detection usually suggests the presence of mutant p53. However wild-type p53 associates with large T antigen and stabilises the molecule. Thus with these cell lines it is not possible to ascribe these findings to mutant p53 expression using immunocytochemical methods.

2. Radiation responses of human urothelial cell lines

The responses to ionising radiation of the cell lines were measured using the cytokinesis-block micronucleus assay. Following irradiation, cells were exposed to cytochalasin B and micronuclei counted in binucleate cells. Optimal sampling times were defined using the binucleate index and the frequency of micronuclei. Similarly the optimal cytochalasin B concentration was evaluated by comparing the binucleate index and the number of spontaneously arising micronuclei. A concentration of 3 µg/ml with a harvest time of 48 hours were found to be optimal for the SV-HUC-1, BC16 and NT11 cell lines. There were found to be differences in the spontaneous micronucleus frequency between the different cell lines which correlated with their ability to transform following chemical treatment and thus might reflect varying degrees of intrinsic genetic instability. The cell lines exhibited a

linear response to micronucleus induction with both X-rays and ^{137}Cs gamma irradiation.

3. Phenotypic changes in irradiated human urothelial cell lines

Human urothelial cell cultures were exposed to doses of 2, 4 or 6 Gy of gamma irradiation and following regrowth exposed to a second dose of equal magnitude. Cells were then passaged once more and then held without passaging for a further 4 weeks. Control (untreated) and methylcholanthrene treated cultures were passaged similarly. Opaque foci were observed in some culture flasks. These consisted of papillary like processes made up of numerous small round cells. The foci were only observed in the 4 Gy treated groups and the methylcholanthrene treated groups. Cells from the cultures exhibiting these foci were cloned in soft agar and an increased cloning efficiency was observed in the irradiated and methylcholanthrene treated groups relative to the control untreated cultures (Fig.1). The nature of the changed phenotype is being investigated by passaging cells into nude mice and immunocytochemical staining.

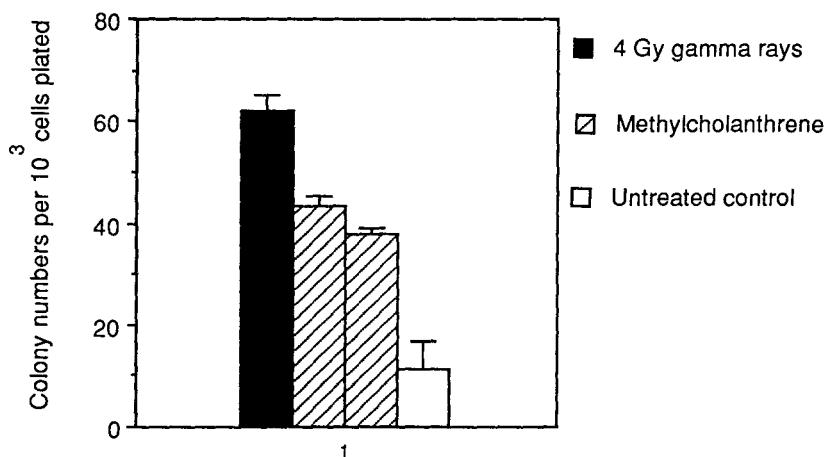


Fig. 1. Colony numbers in soft agar of SV-HUC-1 human urothelial cells following treatment with 4 Gy irradiation or methylcholanthrene.

4. Screening of irradiated human epithelial cells in nude mice

Human urothelial cell cultures were irradiated in 75 cm² flasks and then passaged at least five times to allow the possibility of expression and expansion of any transformed clones. Cells were then injected subcutaneously into nude mice and screened for tumour development for at least 3 months. The control untreated human urothelial cell lines (SV-HUC-1, BC16, NT11) were all non-tumorigenic following this passaging regime. A small nodule develops within the first 3-7 days after injection but has disappeared by 14 days. In the irradiated groups, one tumour was observed following 2 Gy and no tumours were observed after 0, 4 or 6 Gy treatments. The tumour did not form a cell line on *in vitro* transfer but the cells were positive for human cytokeratins and SV40 large T antigen.

An HPV16 transfected human keratinocyte cell line (HPV-G) was also investigated. The *in vitro* studies were carried out in Dublin and flasks sent to St. Andrews for passage of the cells into nude mice. Cells were irradiated or treated

with a combination of irradiation and nitrosoethanolamine (NNE), passaged at least 5 times before expansion of the cell numbers and injection into nude mice. Progressively growing tumours were observed in virtually all recipients. Latent periods ranged from 20 to 50 days with a doubling time of the order of 10 days (Fig.2). Tumours, in general, exhibited a high degree of differentiation. Secondary tumours could be produced following passage of the primary tumours. Untreated cells were also tumorigenic and a more detailed analysis of the characteristics of the tumours produced from the irradiated cells compared to the untreated cells is in progress.

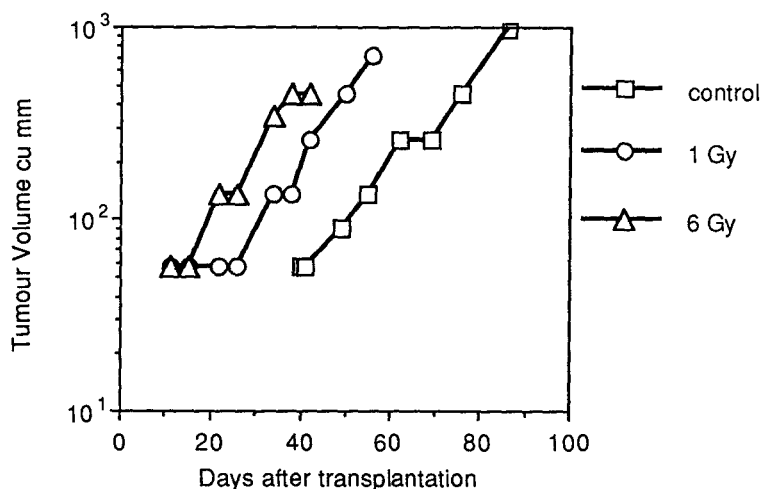


Fig. 2. Volume growth curve of HPV-G human keratinocytes irradiated in vitro and transplanted to nude mice.

Publications

Armitage, M.P., Bryant, P.E. & Riches, A.C. (1990)
Response of human bladder epithelial cell lines to X-irradiation monitored using the cytochalasin B micronucleus assay.
International Journal of Radiation Biology 57 : 1271

Armitage, M.P., Bryant, P.E. & Riches, A.C. (1991)
Radiation-induced transformation of human urothelial cells.
In *Radiation Research : a Twentieth-Century Perspective*. W.C. Dewey et al (eds.)
Academic Press p341.

Armitage, M.P., Bryant, P.E. & Riches, A.C. (1991)
Cytogenetic responses of human urothelial cell lines and a malignant bladder carcinoma cell line to X-rays.
Mutagenesis 6 : 515-518

O'Reilly, S., Riches, A.C., Bryant, P.E., Mothersill, C. & Seymour, C. (in press)
Quantification of survival and transformation of progeny of irradiated HPV transfected human keratinocytes.
International Journal of Radiation Biology

Project 3

Head of project: *Prof. Pertusa*

Objectives for the reporting period

The main objective of this project has been the morphometric and densitometric quantification of the experiments carried out by the other laboratories participating in the contract, by using advanced image analysis techniques. The purpose of this work was the search of a set of morphodensitometric parameters useful to evaluate the cellular variation induced by irradiation.

Progress achieved

1. Image analysis

Morphologic and densitometric image analysis techniques have been applied in transformed and non-transformed cells treated with several ionizing doses to obtain the morphodensitometric characteristics. The system of image analysis building was a Kontron IBAS2000 (Munich) with a multiple device of image capture.

The biological samples were stained by Feulgen technique; a random microscopic field was selected and automatically digitized; after the segmentation of the cellular nuclei the result was a binary image in which each pixel has one of two states and then, pixels were quantified.

It has been studied:

- a. Morphometric parameters: area, perimeter and maximum diameter.
- b. Shape factors:
 - b.1 Circular shape factor (FFC), defined as
$$FFC = 4\pi A/P^2$$
where A is the area and P is the perimeter.
 - b.2 Convolutness (Convol), defined as
$$CONVOL = P/SQR(A)$$
where P is the perimeter and SQR(A) is the square root of the area
- c. Densitometric parameters:
 - c.1 Optical density (DO), defined as
$$DO = -\log_{10} T$$
where $T = I/I_0$, the proportion of incident light which passes through the specimen.
 - c.2 Integrated optical density (DOI), defined as
$$DOI = DO * A$$
where DO is the optical density and A is the area.

2. Selected parameters

Area, perimeter and maximum diameter were selected because they are the immediate parameters that characterize any nuclear variation involved with induced poblational changes.

The most commonly used dimensionless, orientation - independent shape factor must surely be FFC. This has a maximum value of unity for a circle and decreases with increasing departure from circularity. CONVOL is another compactness (roundness) parameter; for a circle, $CONVOL=2*\sqrt{\pi}$ and it increases with decreasing departure from circularity.

The most direct densitometric parameter is Grey Value expressed as the average grey value of each pixel of specimen. The amount of light (of a given wavelength) which is absorbed is directly proportional to the mass or concentration of the absorbing substance. Transmission (T) or absorption (1/T), as densitometric parameters, take into account the incident light; because absorption is multiplicative rather than additive, a logarithmic scale for absorption is useful to allow values of two or more absorbing items to be added simply (OD).

Specimens of interest often do not have the same DO over their whole area; DOI can be defined as the sum of individual DOs of each pixel in the area being measured.

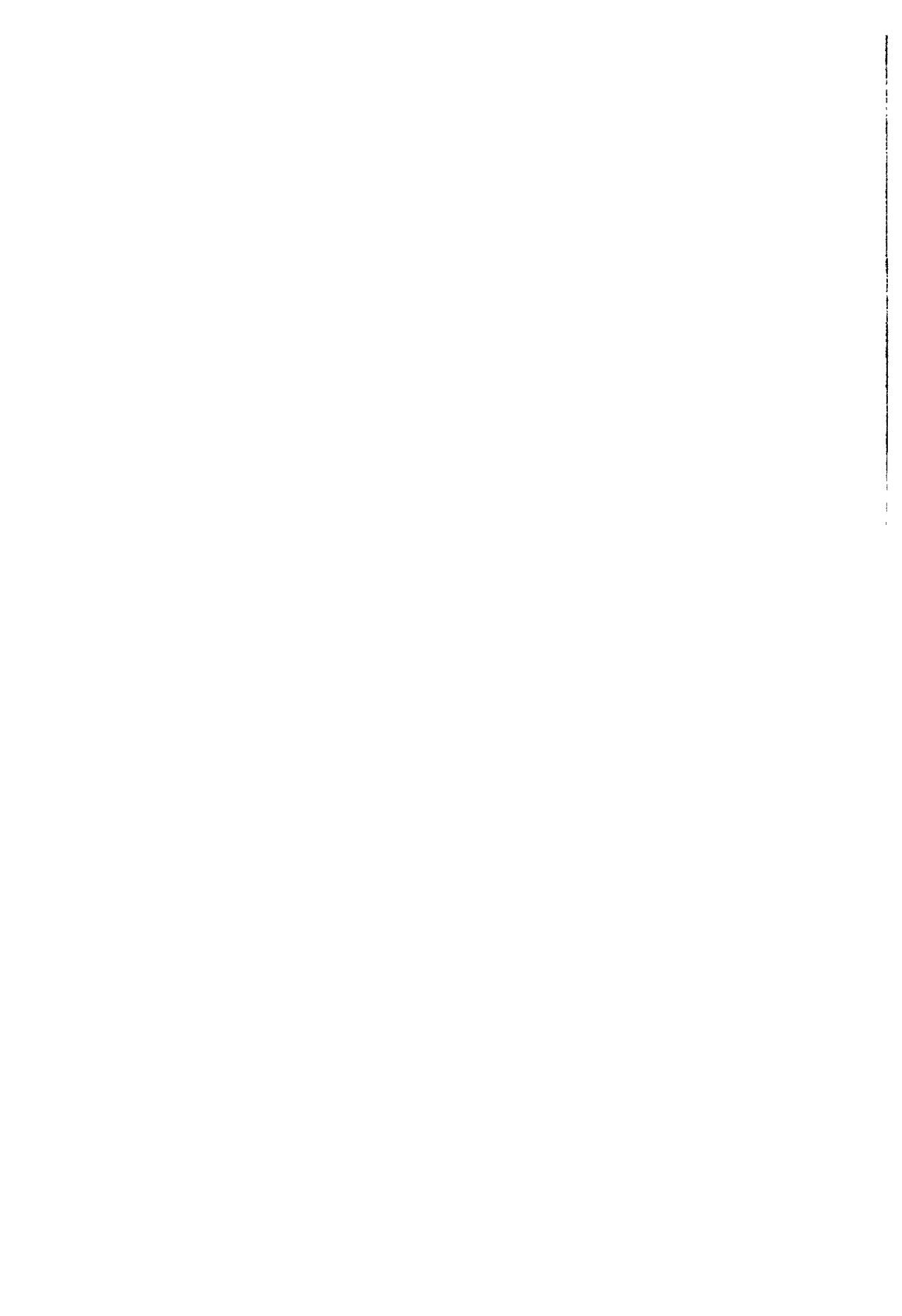
3. Results

The highest difficulty to make measurement was found in primary explants, because in the growth border they are some cells with variable morphology that have an influence, in our opinion, in the variability of nuclear area obtained. The cellular population with small nuclei has been interpreted as non-adherent cell or as the result of a recent division.

The cellular cultures growing on flasks which contained coverslips were easy to evaluate and the results were coherent.

It is possible to observe the homogeneity of cellular populations of non transformed cultures, especially in the area an DO, in contrast to the dispersion of these parameters of transformed cellular cultures. No significant differences can be observed in the shape factors between transformed and non transformed cell cultures, but CONVOL has shown more variability than FFC.

Radiation exposure allows to observe some alterations in densitometric parameters in relation to the dose. Lower doses have shown bimodal distributions while higher doses have shown unimodal distributions in DO, accordingly with the presumed mitotic delay.



CELLULAR AND MOLECULAR STUDIES ON RADIATION QUALITY: A COMPARISON BETWEEN GENETICALLY RELEVANT DAMAGE AND CELL INACTIVATION

Contract B17-033 - Sector B13

1) Kraft, GSI - 2) Sideris, NCSR "Demokritos" -
3) Lloyd, NRPB - 4) Natarajan, Univ. Leiden Sylvius Lab.

Summary of project global objectives and achievements

The influence of radiation quality has been measured for different biological endpoints like induction of DNA double strand breaks, the incidence of chromosome aberrations and the changes in radiosensitivity for mitotic inactivation during the course of cell cycle progression. In addition, changes in thermodynamical parameters following the exposure of mammalian DNA to alpha particles and their relationship to double strand breaks were studied.

In radiobiology, the quality of the radiation is classified according to its linear energy transfer LET although it is wellknown that LET is not a good parameter for the description of the radiation response. Microdosimetric quantities which indicate differences in high LET radiation fields mostly produced by neutrons explained the fact of differences observed in the biological reactions but they could not explain quantitatively the observed effects.

Measurements using heavy particles over a large range of energies and atomic numbers revealed some general pattern for the radiation response as function of LET (for review see Kraft, Nucl. Science Application 3: 1-28, 1987). Action cross sections of biological effects which can be related to DNA double strand breaks exhibit an increase more than proportional to LET corresponding to elevated values of the relative biological efficiencies up to LET values at 100 keV/ μ m. Then the common curve for all atomic numbers split into separate curves for each atomic number forming σ -LET hooks. These hooks have not been predicted by microdosimetry. But the track structure model of Katz and co-workers, Radiat. Protect. Dos. 13: 281-284, 1985, yielded a very similar pattern for the dependence of the action cross section from the LET with the working hypothesis that at the very end of the particle track more damage is produced than it can be expressed biologically (overkill effect). Other mechanisms than the overkill effect for the waste of deposited energy have been postulated too like the physical or chemical recombination processes. The only possibility to differentiate between these processes are measurements at subcellular level like chromosomal damage or DNA breaks in order to verify these assumptions or not.

However, up to now measurements of intracellular DNA damage produced by particle radiations are scarce and problematic because conventional methods of DSB detection require high radiation doses. They might allow to determine to some extent the induction probability but are not accurate for the determination of the long term remaining damage. Therefore the development of low dose techniques and their use is essential for the determination of the genetically relevant DNA lesions.

Similar problems arise with the measurement of chromosome damage where the changes in cell cycle progression interfere strongly with the expression of the chromosomal damage in mitosis. There, techniques had to be developed to qualify the state of the cells during exposure and to measure the time needed to reach the first or second mitosis.

In parallel the initial chromosome damage has to be determined using PCC techniques for instance. Finally high LET specific effects like the potentiation in fractionated or protracted exposure have to be understood.

In the experiments of the reporting period the following achievements have been made: For the measurement of DNA breaks sensitive methods using pulsed field gel electrophoresis have been established and first experiments have been performed. In the chromosome experiments synchronized cells have been used which determine the state at exposure time and the Giemsa/Hoechst technique has been introduced to distinguish between the cells in different cell cycles. This combination allows to determine the fate of the primarily induced damage with high accuracy.

The changes in radiosensitivity during cell cycle measured for particle radiation showed the opposite dependence from cell cycle then after x-ray exposure. This behavior could be explained by geometrical arguments, i.e. changes in the hit probability rather than by the changes in the repair efficiency. The corresponding calculation allowed also to explain with this geometrical arguments the frequently observed potentiation effects for fractionated particle exposure.

Finally, the measurements of the thermodynamical parameters yielded new insights in the radiation induced structural alterations of the DNA molecules.

Project 1

Head of project: *Dr. Kraft*

Objectives for the reporting period

Measurements of the induction of DNA double strand breaks, chromosome aberrations and cell inactivation in mammalian cells with x-rays and particles (C to U ions) in the energy range between 5 and 500 MeV/u.

Development of an experimental procedure for the DNA measurements for low particle fluences normally used for chromosome and inactivation measurements.

Progress achieved including publications

1. DNA measurements

The study of double strandbreaks in DNA of high molecular weight without further degradation became feasible with the introduction of pulse field electrophoresis (PFGE). This technique circumvents problems which arise when conventional methods of neutral filter elution or sedimentation were used. Artificially shearing of DNA caused by experimental handling is avoided by embedding cells in agarose. For experiments at the UNILAC, cells (CHO-K1; American Type Culture Collection CCL 61) were exposed to the heavy ion beams as monolayers in 35mm petridishes (this is necessary due to the limited range of particles of energies < 15 MeV/u). They were harvested with cell scratchers at 0° C and sealed in 0.5% LMP-agarose before subsequent preparation. For experiments with x-rays or particles at SIS-energies, cells were irradiated already embedded in plugs. After cell lysis and equilibration, electrophoresis was performed under standard conditions [Blöcher, D. et al.; *Int.J.Radiat.Biol.*, 56/4, 437-448 (1989)] (40V -22h with 75min intervals). Gels were stained with ethidiumbromide, photographed and the negatives analysed with a PC connected scanning device coupled to a CCD-camera [Stanton, J. et al.; *Rad.Prot.Dosim.*, 31, 253-256 (1990)]. The calculation of DNA double strandbreaks is based on the amount of DNA which enters the gel; intact genomic DNA remains in the slots due to its target size. The estimated exclusion size is about 9-10Mbp [Blöcher]. Dose effect curves are calculated by integration of the migrated DNA. The digitalized density of scans was normalized to approximately equivalent amounts in non-irradiated controls to obtain consistent values. Typical dose response curves show a linear behaviour up to a saturation effect for higher doses [Schneider, M. et al.; *GSI Scientific Report*, 210 (1990)]. Depending to radiation type, different initial slopes for DNA double strandbreak induction were observed (fig.1). The dependance of double strandbreak induction on LET is comparable to the intracellular SV40 data. In contrast to SV40 DNA exper-

iments, the application of PFGE shows the advantage to study double strandbreaks in eukaryotic DNA at low doses. This method is sensitive enough to detect DNA damage within a dose range which corresponds to cell inactivation studies. For radiotherapeutical applications the repair of cellular DNA is of interest. Cells were allowed to recover after irradiation and the rejoining of DNA was measured according reduction of DNA released into the gels (fig.2). The time course of rejoining depends significantly on the radiation quality (fig.3). For X-rays we found a fast component of rejoining with a halftime of $t_{1/2} \approx 25$ -30 minutes following 40 Gy irradiation. At 20 Gy X-rays the $t_{1/2}$ is diminished to about 15 minutes. The rejoining of lesions introduced by high LET radiation is substantially delayed. For a 13 MeV/u Ne beam we estimate a $t_{1/2}$ greater than one hour. The dose given here corresponds to less than the 20 Gy of X-rays but the surviving fraction of cells is in that case comparable to the 40 Gy of X-rays. After irradiation with particles at SIS energies the time course of rejoining is similar to that for x-rays.

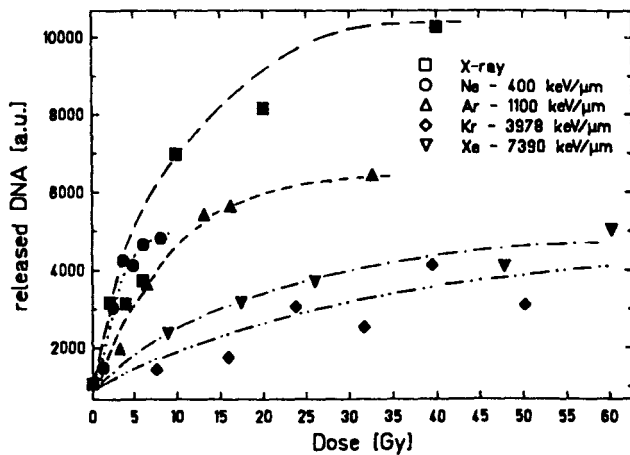


Fig. 1: Amount of extracted DNA as a function of dose.

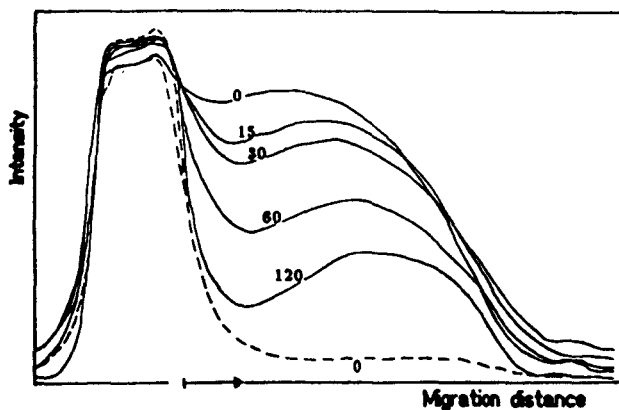


Fig. 2: Electrophoretic pattern of DNA entering the gel under PFGE (40V/22h,75min pulse time); densitometric scans after ethidiumbromide staining. X-ray (40 Gy) with different subsequent incubation times [min] at 37° C; scattered line (0 Gy).

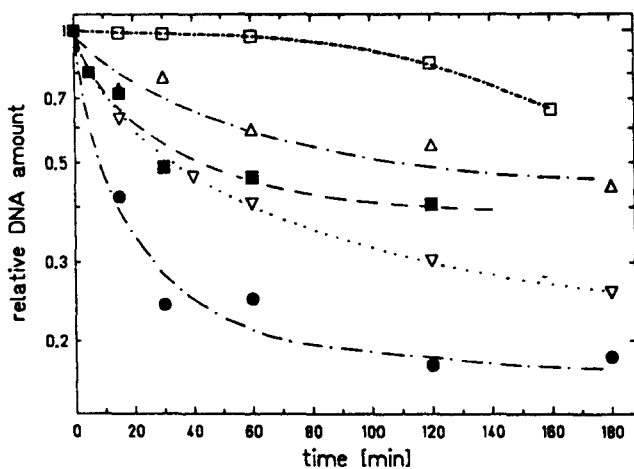


Fig. 3: DNA out of slots after irradiation with subsequent incubation times; DNA amount is normalized to 1.0 for the beginning of incubation times.

- X-ray - 20 Gy
- X-ray - 40 Gy
- △ Ne 10 MeV/u - 2·10⁷p/cm²
- ▽ Ne 400 MeV/u - 2·10⁸p/cm²
- Ar 6 MeV/u - 2·10⁷p/cm²

2. Chromosome experiments

The interpretation of heavy ion induced chromosome aberrations is especially complicated due to the inhomogeneous energy deposition of particle irradiation and the delay in cell proliferation, which depends on the amount of cellular damage. The number of particle hits per cell is determined by the poisson statistics. Therefore, cells with different numbers of hits are present in the same sample. After exposure to low particle fluences a large fraction of cells is not hit at all and proliferates like the unirradiated control cells. The cell cycle progression of cells, which are hit, however, is significantly slowed down according to the amount of lesions induced. In consequence, several hours after exposure a mixture of 1st, 2nd and 3rd generations of cells are found. With conventional methods it is impossible to distinguish these subpopulations. In addition, with an increasing number of cell divisions, damaged cells are lost from the population. To overcome these problems

1. synchronous cells of a well defined cell cycle stage were irradiated and
2. the Fluorescence-Plus-Giemsa Technique was used to determine the number of cell divisions after exposure.

In the experiments V79 Chinese hamster cells with a cell cycle time of 12 hours were used. Cells were synchronized by centrifugal elutriation and irradiated in G₁-phase with 4.6 MeV/u Ar ions (LET 1840 keV/μm) as well as with 250 kV x-rays. After different time intervals cells were harvested, preceded by a 2-hours colcemid treatment. Chromosome preparations were made according to standard protocols. Slides were stained with the Fluorescence-Plus-Giemsa Technique (Perry P. and S. Wolff, Nature 251, 156, 1974). First and second generation metaphases were scored separately.

These experiments revealed remarkable differences in the response of cells to densely and sparsely ionizing radiation:

After x-ray irradiation an proportional increase in the number of damaged cells with dose is observed. After heavy ion irradiation the amount of aberrant cells does not increase proportional to dose or particle fluence (fig.4). Especially that fraction of cells which reaches the 1st postirradiation mitosis in a time comparable to control cells (within 12 to 14 hours) is characterized by a very low amount of damaged cells. In addition, in this sample the rate of aberrations per damaged cell is very low. This indicates that only cells are enabled to reach mitosis in time, if they are not or only slightly damaged. Several hours later up to 100% of damaged cells are found. The same tendency was observed for 2nd generation cells.

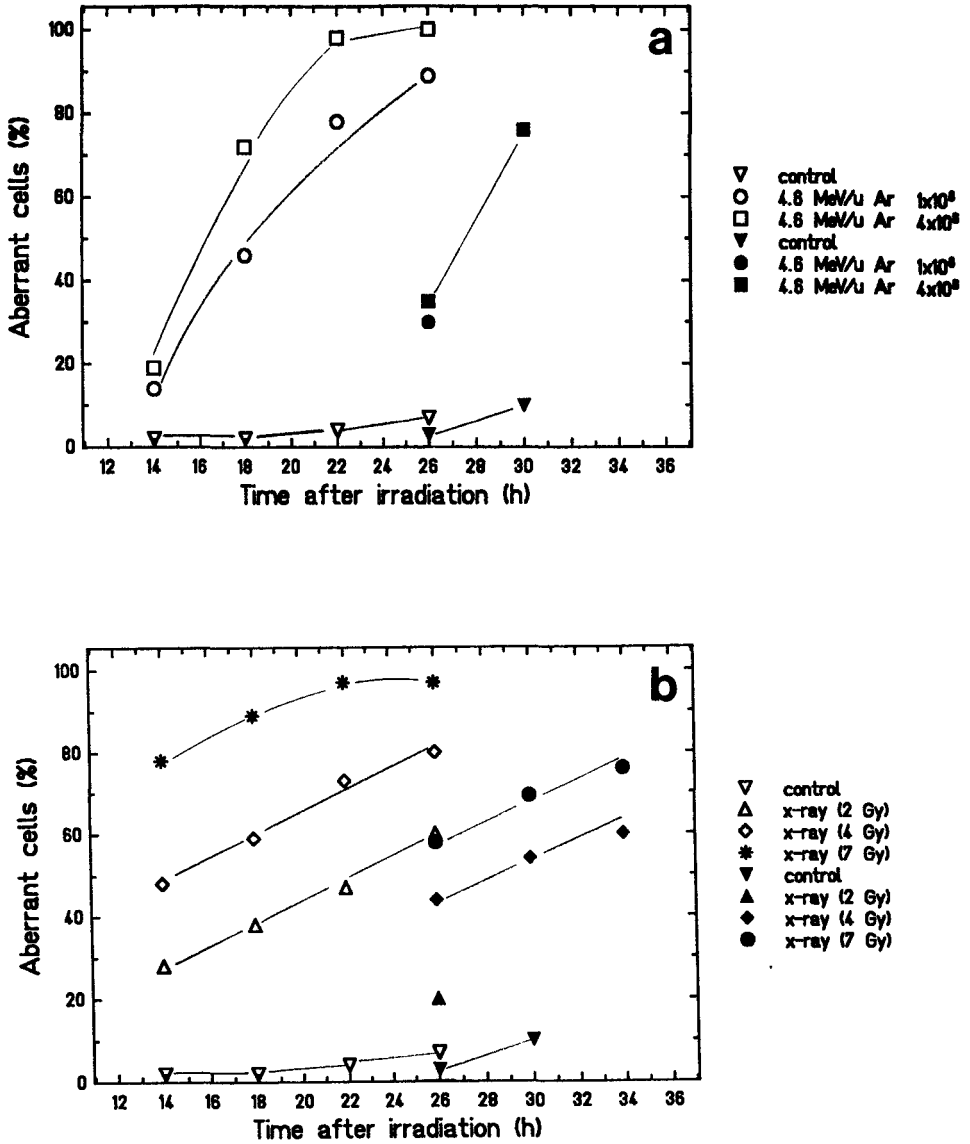


Fig. 4

The percentage of aberrant 1st and 2nd cycle metaphases observed after heavy ion irradiation (a) and x-ray irradiation (b). open symbols - 1st cycle metaphases; solid symbols - 2nd cycle metaphases.

Particles are more effective in the production of aberrations if the efficiency is compared to x-rays on the basis of equal doses. For both irradiation types a clear relationship between the number of aberrations per cell and the mitotic delay was measured, but this delay is more pronounced after particle radiation.

Finally, the distribution of aberration types is different for densely and sparsely ionizing radiation. After heavy ion exposure a high rate of chromosome- and chromatid-breaks is observed, whereas after x-ray exposure the formation of exchange-type aberrations is favoured. Similar results were obtained previously with asynchronous V79 cells (Ritter S. et al., Rad. Prot. Dosimetry 31, 257, 1990).

In summary, chromosome damage induced by radiation of different quality cannot be compared on the basis of dose introducing a single quality factor like RBE. The analysis is complicated by the statistical nature of the energy deposition of particle irradiation and the delay in the cell cycle progression (Scholz M. et al., Adv. in Space Research 9, 91, 1989) which depends on the type of the lesions. However, decisive results can be obtained, when the cell cycle stage is known at exposure time using synchronous cells. In addition, the cell progression after irradiation has to be measured in order to correlate the observed damage to the appropriate cell generation.

3. Inactivation measurements

The influence of the phases of the cell cycle on the radiosensitivity of mammalian cells has been measured for different radiation qualities (Terasima, T. and L.J.Tolmach, Biophys. J. 3, 11-32 (1963), Sinclair, W.K. and R.A.Morton, Rad. Res. 29, 450-474 (1966)). The highest variation of sensitivity throughout the cell cycle has been found for x-rays. Measurements using light ions with high energies (Blakely, E.A. et al., LBL Report 11220 125-135 (1980)) show a diminished cell cycle response. However, the maxima and minima of the radiosensitivity are approximately located at the same position in the cell cycle.

In the experiments with low energetic heavy ions, cells were synchronized by centrifugal elutriation and irradiated after different incubation times. At each time the progression of the cells in their cycle was controlled by cytofluorometric measurements of the DNA content. Complete survival curves were measured for each time interval and the cross sections were calculated as function of the time after synchronisation.

In all experiments the sensitivity increases from G1 to S phase whereas for x-irradiation a maximum for resistance is found at the end of S phase (fig 5). The

change in radiosensitivity observed after x-ray exposure has been frequently attributed to the variation in repair capacity and velocity during cell progression. After the exposure to particle radiation repair is drastically diminished and the probability to hit the cell nucleus governs to a great extent the radiation response. Therefore the variation of the cross section of the cell nucleus as the critical target has been correlated with the measured inactivation cross section. Good agreement was found in the position of the general time course also when cells of different cell-cycle times were compared. The model of the calculation of geometrical hit probabilities and their correlation to the radiosensitivity after particle irradiation was also used to describe the observed potentiation effect after fractionated particle exposure.

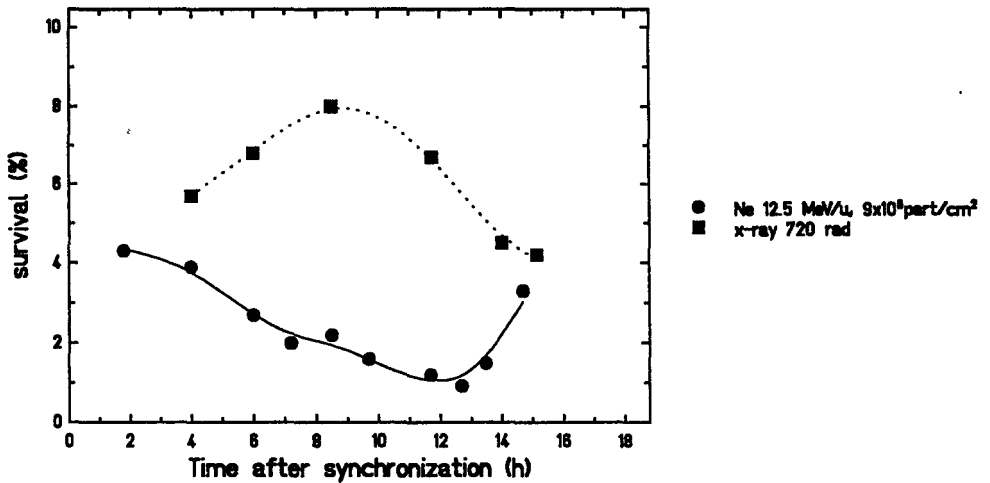


Fig.5

Survival of V79 chinese hamster cells irradiated with Ne 12.5 MeV/u particles (9×10^9 part/cm²) ●, or with 720 rad x-rays ■ .

S. Ritter, W. Kraft-Weyrather, M. Scholz and G. Kraft

Influence of radiation quality on heavy ion induced chromosome aberrations in V79 cells

Radiat. Protect. Dos. 31 257-260 (1990)

F. Kraske, S. Ritter, M. Scholz, M. Schneider, G. Kraft, U. Weisbrod and E. Kankeleit
Directed irradiation of mammalian cells by single charged particles with a given impact parameter

Radiat. Protect. Dos. 31 315-318 (1990)

J. Stanton, G. Taucher-Scholz, M. Schneider and G. Kraft

Comparison between indirect and direct effects for high and low LET radiations in SV 40 DNA strand break induction

Radiat. Protect. Dos. 31 253-256 (1990)

M. Schneider, G. Taucher-Scholz, J.A. Stanton, H. Penninger and G. Kraft

Evaluation of DNA double strandbreaks by pulsed field gel-electrophoresis
GSI Scientific report 91-1 p.210

S. Ritter, E. Kehr, W. Kraft-Weyrather, H. Penninger, M.Scholz and G. Kraft

Induction of chromosomal disintegrations in V79 Chinese hamster cells af.br heavy ion irradiation

ibid, p. 224

W. Kraft-Weyrather, E. Kehr, G. Kraft, S. Ritter and M. Scholz

Fractionated irradiation with heavy ions at low energy

ibid, p.225

M. Scholz (Strahlenklinik der Universitaet Heidelberg, M. Wannemacher),S. Ritter, W. Kraft-Weyrather, G. Kraft(GSI Darmstadt)

Investigation of heavy induced cell cycle delays by means of the BrdU-Hoechst-Quenching method

ibid, p.226

M. Schneider, G. Taucher-Scholz, J. Heilmann and G. Kraft

Evaluation of DNA double strand breaks after heavy ion irradiation in mammalian cells

GSI scientific report 92-1, p. 291

S. Ritter, E. Nasonova, W. Kraft-Weyrather, M.Scholz and G. Kraft

Induction of chromosome aberrations in first and second generation cells after heavy ion and x-ray irradiation

ibid, p. 296

G. Taucher-Scholz, J.A. Stanton, M.Schneider and G. Kraft

Induction of DNA breaks in SV40 by heavy ions

Adv.Space Res. 12 No.2-3 73-80 (1992)

S. Ritter, W. Kraft-Weyrather, M.Scholz and G. Kraft

Induction of chromosome aberrations in mammalian cells after heavy ion exposure

Adv. Space Res. 12 No. 2-3 119-125 (1992)

U. Weisbrod, H. Buecker, G. Horneck and G. Kraft

Heavy ion effects on bacteria spores: the impact parameter dependence of the inactivation

Radiat. Res. 129 250-257 (1992)

M. Schneider, G. Taucher-Scholz, C. Wiese, J. A. Stanton, J. Heilmann and G. Kraft

Detection of radiation induced DNA double strand breaks in mammalian cells using PFGE

Fourth Workshop on Heavy Charged Particles in biology and medicine

GSI report 91-29, B9

Project 2

Head of project: *Dr. Sideris*

Objectives for the reporting period

Study of thermodynamic parameters following exposure of mammalian DNA to α -particles and gamma rays and their relationship to biological parameters. Theoretical analysis of the results towards the development of a model describing the evolution of primary lesions induced on the DNA molecule.

Progress achieved including publications

The presented work was designed under the assumption that most of radiation damage effected in vitro on DNA molecule is due to the induced water free radicals unless the DNA samples had been subjected to extremely low vacuum. Dielectric studies on mammalian DNA, conducted by our research group, have shown that there are 18-20 water molecules per nucleotide pair irrotationally bound to the DNA molecule forming a first hydration layer around the macromolecule (Anagnostopoulou-Konsta et al 1991a). These water molecules can be removed only if the DNA samples will be subjected to low vacuum of the order of 10^{-5} to 10^{-6} Torr (Pilakouta et al in press).

The energy and radiation fluency in the samples were obtained from measurements taken with a silicon surface detector. The interactions with the water molecules were investigated using a semi-empirical model based on an asymptotic expansion of the first Born approximation and the radiation tracks were simulated with a Monte-Carlo code (Sideris et al 1992). The primary chemical species, from which the water free radicals evolve are presented on Figure 1, where the relative contribution of the different species is given.

Our work with Inverse Gas Chromatography (IGC) shows that the negative values of the Enthalpy of the reactions of the DNA macromolecule with non-polar injected probes are increasing as the irradiation dose increases. This indicates that exposure in vitro of DNA samples to ionizing radiation results on disruption of the Van der Waals stacking forces of the DNA double helix. These conclusion is supported by our work with Thermal Transition Spectrophotometry and preliminary work on the conductivity of DNA aqueous solutions, which are discussed later on. This apparent disruption of the stacking forces is not related at the higher doses, at least, with a decrease of the Gibb's Free Energy values, indicating that the observed changes at the Entropy of the system leads to less spontaneous reactivity (Loukakis et al 1991).

Our results from the work with Thermal Transition Spectrophotometry indicate that, contrary to what has been reported earlier, neither the temperature of the DNA helix-to-coil transition, T_M , nor the number of disrupted DNA base pairs,

i.e. the radiation induced loss in hyperchromicity, is related to the gamma irradiation dose by a simple function, though both are severely effected by the the exposure to ionizing radiation.

For the interpretation of these results a model had to be developed since existing models for thermal-to-coil transition of the DNA molecules have been developed and tested for either simple polynucleotide molecules, or low molecular weight viral or plasmid DNA. The most recently advanced modified consistent phonon theory for DNA thermal denaturation stops short of the transition region. The proposed model leads finally to the expression:

$$\ln[A_{st} + A_u - A(\theta)] = \ln A_u - \frac{c(\theta - \theta_0)^{N+1}}{N+1}$$

where $A(\theta)$ is the A_{266} at a given temperature θ ; A_{st} is the A_{266} of the tight DNA helix at the threshold temperature θ_0 for the helix-to-coil transition; A_u is the increase of A_{266} corresponding to denatured DNA, i.e, the hyperchromic effect; N is an exponent related to the possible paths of energy propagation along the DNA macromolecule; and c is a proportionality constant. under the assumption that, during melting transitions of DNA, changes in A_{266} are directly proportional to the changes of the DNA base pairs the equation takes the form:

$$y = g + h \cdot (1 - e^{-\frac{c(\theta - \theta_0)^{N+1}}{N+1}})$$

where g is the available number of stacked base pairs at the threshold temperature, capable of A_{266} absorption, h is the maximum number of disrupted base pairs during thermal denaturation, and c , θ , θ_0 and N as above.

On the basis of this model the sigmoid melting curves of the expected $A(\theta)$ values were fitted to the original data through the use of the MINUIT code giving an excellent agreement between the expected according to the model and the observed values of $A(\theta)$ in the non irradiated and irradiated DNA samples.

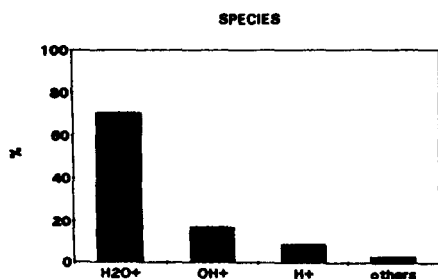


Figure 1

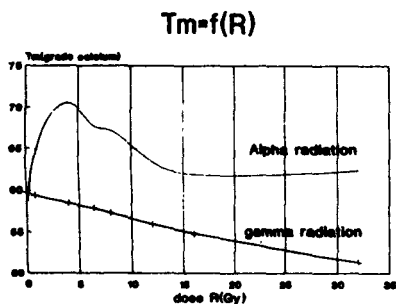


Figure 2

At the asymptotic region of the helix-to-coil transition curves, at the lower temperature range, a variation was observed among the A_{st} values of the irradiated samples in relation to those of the non irradiated samples. Not all the A_{st} values of the irradiated samples are higher than those of the control as it has been observed earlier. This variation could be attributed to early severance of stacking DNA forces, as it has been indicated also from the Enthalpy changes of the work with Inverse Gas Chromatography, coupled with the presence, due to the exposure to ionizing radiation, of DNA segments of various sizes.

The induction, in vitro, of early alterations on the DNA molecules, proceeding the disruption of hydrogen bonds and the helix-to-coil transition, is being supported by the observed changes on the conductivity of irradiated DNA samples, which proceed the changes on A_{266} related to the helix-to-coil transition (Anagnostopoulou-Konsta et al 1991b).

From the first derivatives of the fitted curves the T_M values of the non irradiated and irradiated DNA were estimated. A sharp deference was observed between the effect of α -particles and that of the gamma rays as it can be seen on Figure 2.

When the N values, that is according to the proposed model the values related to the number of possible paths of energy propagation along the DNA molecule, were calculated, it was found that at the region of irradiation doses where sharp decrease of the excess enthalpy values (ΔH_e) were observed (Loukakis et al 1991) a sharp increase of the N values corresponds, indicating a high efficiency of induction at this region of extensive structural alterations of the DNA molecule.

Publications

1. ANAGNOSTOPOULOU-KONSTA A, D DAOUKAKI, P PISSIS, G LOUKAKIS, E G SIDERIS. 1991a. Dielectric study of DNA-water systems by the thermally stimulated currents method. *Journal of Non-Crystalline Solids* 131-133:1182-1185.
2. ANAGNOSTOPOULOU-KONSTA A, H DAMASKOPOULOU, C A KALFAS, G LOUKAKIS, P PISSIS, E G SIDERIS. 1991b. Dielectric and physicochemical studies of γ -irradiated DNA-water systems. 7th International Symposium on Electrets. Berlin.
3. LOUKAKIS G, E G SIDERIS, C A KALFAS, B MAZOMENOS, A ANAGNOSTOPOULOU-KONSTA. 1991. Measurements of structural characteristics of damaged DNA, through the use of Inverse Gas Chromatography. In *Chemistry and Properties of Biomolecular Systems* Kluwer Academic Publishers:45-53.

4. PIALOGLOU P, E G SIDERIS, A PERRIS. 1990. Enhancement of cellular damage induced by gamma rays after inhibition of poly-(ADP)-ribose polymerase by 3-aminobenzamide. In **Frontiers in Radiation Biology** VCH Verlagsgesellschaft, Weinheim:459-464.

5. PIALOGLOU P, E G SIDERIS, A PERRIS. 1990. Cell survival and chromosomal aberration frequency in V79 Chinese hamster cells exposed to low energy protons. In **Frontiers in Radiation Biology** VCH Verlagsgesellschaft, Weinheim: 296-300.

6. PILAKOUTA M, X ASLANOGLU, A SAVIDOU, T PARADELLIS, E G SIDERIS (in press). A study of the effects of ^{15}N ion beam on organic compounds. **Nuclear Instrument. Meth.**

7. SIDERIS E G, G ZARRIS, A ANAGNOSTOPOULOU-KONSTA, C A KALFAS. 1992. DNA-water free radicals interaction and the thermostability of the DNA molecule. **European Biophysical Societies Association Workshop. Palermo.**

Project 3

Head of project: *Dr. Lloyd*

Objectives for the reporting period

The objective of this experiment was to provide data on the production of chromosomal aberrations in human lymphocytes in order that models of biological effect can be tested. This part of the experiment utilized accelerated charged particles to expose blood lymphocytes to radiations of nearly constant LET. The main objectives were:

- a. To produce sample holders so that sufficient volumes of blood held as a thin layer could be irradiated with accelerated particles at G.S.I. Darmstadt.
- b. To undertake at least two visits to Darmstadt to irradiate blood specimens and culture the lymphocytes so that dose response curves for induced chromosomal damage can be constructed for carbon-12 ions or ions of similar LET. It was hoped to complete work for at least two different ion/energy combinations.
- c. To complete the microscope evaluation of the mitotic preparations and to collate and analyse the results.

Progress achieved including publications

The specimen holders have been constructed and tested to ensure that good yields of metaphases may be obtained.

One visit to Darmstadt was made to irradiate human lymphocytes with neon-20 ions with a mean energy in the sample of about 180 MeV. The LET of such ions was in the region of 460 KeV μm^{-1} , which was a little higher than we required. Microscope scoring of the mitotic preparations has been completed and results analysed.

Staff at G.S.I. provided measurements of the fluence of charged particles for each exposure. For each dose point six samples were irradiated successively and the samples combined. By this means lymphocytes from about 0.4 ml of blood could be cultured. Nine different doses covering the range from .06 to 4.5 Gy were used and the whole experiment was repeated. Some data at each of the nine dose points was obtained although in some instances cultures were not of high quality. The results obtained are shown in Table 1. All the dicentric and centric rings scored were in separate cells but some cells contained multiple acentrics or excess acentrics with a dicentric. This multiple damage is a feature expected from high LET radiation. Despite the low number of aberrations scored it was still possible to fit a linear dose-response relationship to the data. The linear coefficient for dicentric induction was $.0042 \pm .0016 \text{ Gy}^{-1}$. With the same system the linear coefficient for cobalt-60 gamma irradiation was $.0142 \pm .0044 \text{ Gy}^{-1}$ leading to a value for RBE at low doses (RBE_m) of about 0.3. This value may be compared with a quality factor of 14 and a radiation weighting factor of 20 as recommended by ICRP (1991) for the same ion.

This low value for RBE_m is in very good agreement with prediction from neutron data from the same cell system (Edwards *et al*, 1985). These suggested that the linear coefficient α should increase with increasing LET up to about 70 keV μm^{-1} and then fall more rapidly than LET^{-1} . The predicted curve showed that α reduced to a value equivalent to that of

gamma rays at an LET value between 300 and 400 keV μm^{-1} and a further increase in LET would decrease the linear coefficient further. The explanation for the low value of RBE_m lies in the competition between aberration production and interphase death. A single neon ion of 460 keV μm^{-1} crossing the diameter of a human lymphocyte nucleus, assumed to be 6 μm , will deliver a dose to that nucleus of nearly 4 Gy. The average dose per particle passage is in excess of 2 Gy. These doses are sufficiently high to give a high probability of interphase death. The only cells which are likely to survive to be seen at metaphase are those that are missed by the neon ions or those where the cell nucleus is intersected by a small length of ion track, that is a grazing collision. In the former case no radiation induced aberrations will be seen and in the latter case the yield of aberrations will be low. It is clear that interphase death plays an overwhelming part in the failure to see many aberrations following irradiation by 180 MeV neon-20 ions.

Because G.S.I. have no immediate plans to provide accelerated light in the LET range 10 to 200 keV/ μm approaches have been made to GANIL at Caen in France to provide such ions. They are able to supply ion beams of particles from carbon to neon in the energy range 20 to 50 MeV/u. Permission to use these facilities has been obtained and it is intended to apply for an extension of time until December 31st 1992 to irradiate with one more ion to complete the contract.

Table 1 - Results of scoring chromosome aberrations in human lymphocytes following irradiation with 180 MeV neon-20 ions

Dose Gy	Cells scored	Dicentric	Centric rings	Excess acentrics	Damaged cells
.066	1984	2	1	6	7
.147	321	0	0	1	1
.289	128	1	0	2	1
.525	66	0	0	0	0
.687	18	0	0	0	0
1.34	350	1	0	2	2
2.35	220	3	0	4	6
2.95	30	0	1	0	1
4.41	181	4	0	16	13

References

ICRP (1991). The 1990 Recommendations of ICRP. Annals of the ICRP 21, 1-3

Edwards, A.A., Lloyd, D.C. and Prosser, J.S., Radiation Protection Dosimetry 13, 205-209 (1985).

Publications

Edwards, A.A., Loyd, D.C., Finnon, P., Moquet, J.E., Darroudi, F. and Natarajan, A.T. Chromosomal aberrations in human lymphocytes induced by 10 MeV/u ^{20}Ne ions. In Annual Report of G.S.I. (1992).

Project 4

Head of project: *Prof. Natarajan*

Objectives for the reporting period

The aim of the project was to use the heavy ions accelerator at GSI Darmstadt to irradiate specimens of human blood lymphocytes with ions of nearly constant LET and assess the induction of chromosomal damage using premature chromosome condensation (PCC) technique.

Progress achieved

Human lymphocytes were isolated by Ficoll-Hypaque and were irradiated with neon-20 ions with a mean energy of about 180 MeV in the sample. The LET of such ions was in the region of 460 keV/μm. The lymphocytes were injected into sample holders (1x10⁶ cells/sample holder). For each dose point 3-4 samples were irradiated successively. Following irradiation lymphocytes were pooled and fused immediately with mitotic Chinese hamster ovary (CHO) cells. The CHO cells were obtained by mitotic shake off and were prelabelled with 5-Bromodeoxyuridine for at least 2 cell cycles. With this method mitotic cells could be differentiated from interphase cells based on the Giemsa staining property of BrdUrd substituted chromosomes. Following fusion of lymphocytes and mitotic CHO cells in the presence of polyethylene glycol (MW = 1450), cells were allowed to grow for one hour in complete growth medium in the presence of Colcemid. Routine air-dried preparations were made and stained according to fluorescence plus Giemsa technique. The lymphocytes were irradiated with 3 doses of 1.4, 2.2 and 4.4 Gy neon-20 ions. 35-60 cells were scored for each dose point. The data are presented in Table 1 and Fig. 1. The number of elements in each metaphase was scored and excess of PCC fragments was determined. Since it can be assumed that cells in irradiated samples with no excess PCC fragments were not traversed by particles and those that hit visible damage, the frequency of breaks was calculated on the basis of excess of elements per damaged cell (Table 1). A linear dose response curve was obtained (Fig. 1). One interesting observation was the distribution of PCC fragments following irradiation with different doses of neon-20 ions (Table 1). There was no overlapping of the number of PCC fragments for different doses, for 1.2 Gy excess PCCs was between 4 and 8, for 2.2 Gy between 11 and 14 and for 4.4 Gy between 17 and 22 breaks/cell. These cells with such a high frequency of aberrations obviously will die and may never reach mitosis in routine mitotic chromosome analysis. This observation indicates high interphase death and mitotic delay specially at higher doses (i.e. 2.2 and 4.4 Gy) operating with this type of irradiation, as the frequencies of aberrations observed at mitotic metaphases are very low.

Table 1

Dose Gy	cells scored	Distribution of PCCs (Number of elements/cell)														Excess PCCs	% cells damaged	Mean PCC/ damaged cell
		46	50	51	53	54	57	58	59	60	63	64	66	68				
0	60	60														0	0	0
1.3	55	25	5	20	4	1										156	55	5.2
2.2	48	28					1	9	8	2						251	42	12.6
4.4	35	20									1	2	10	2		297	43	19.8

PCCs in HPBL induced by Neon-20 ions

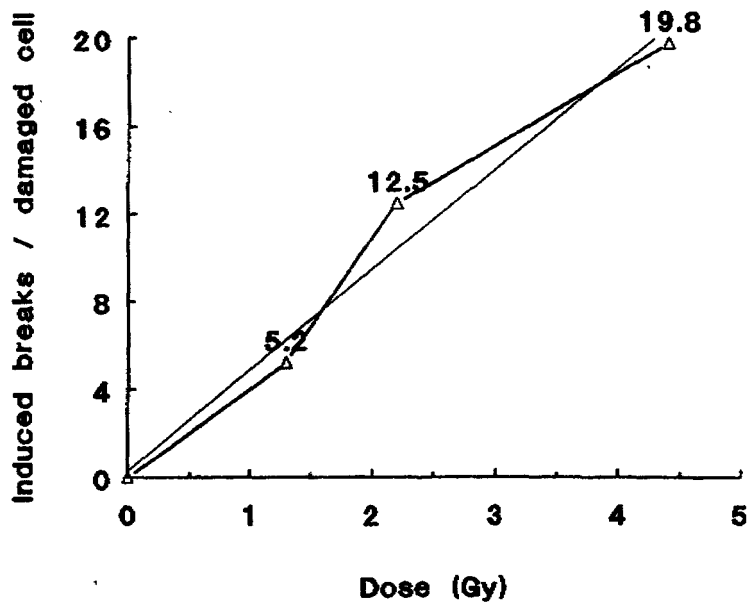
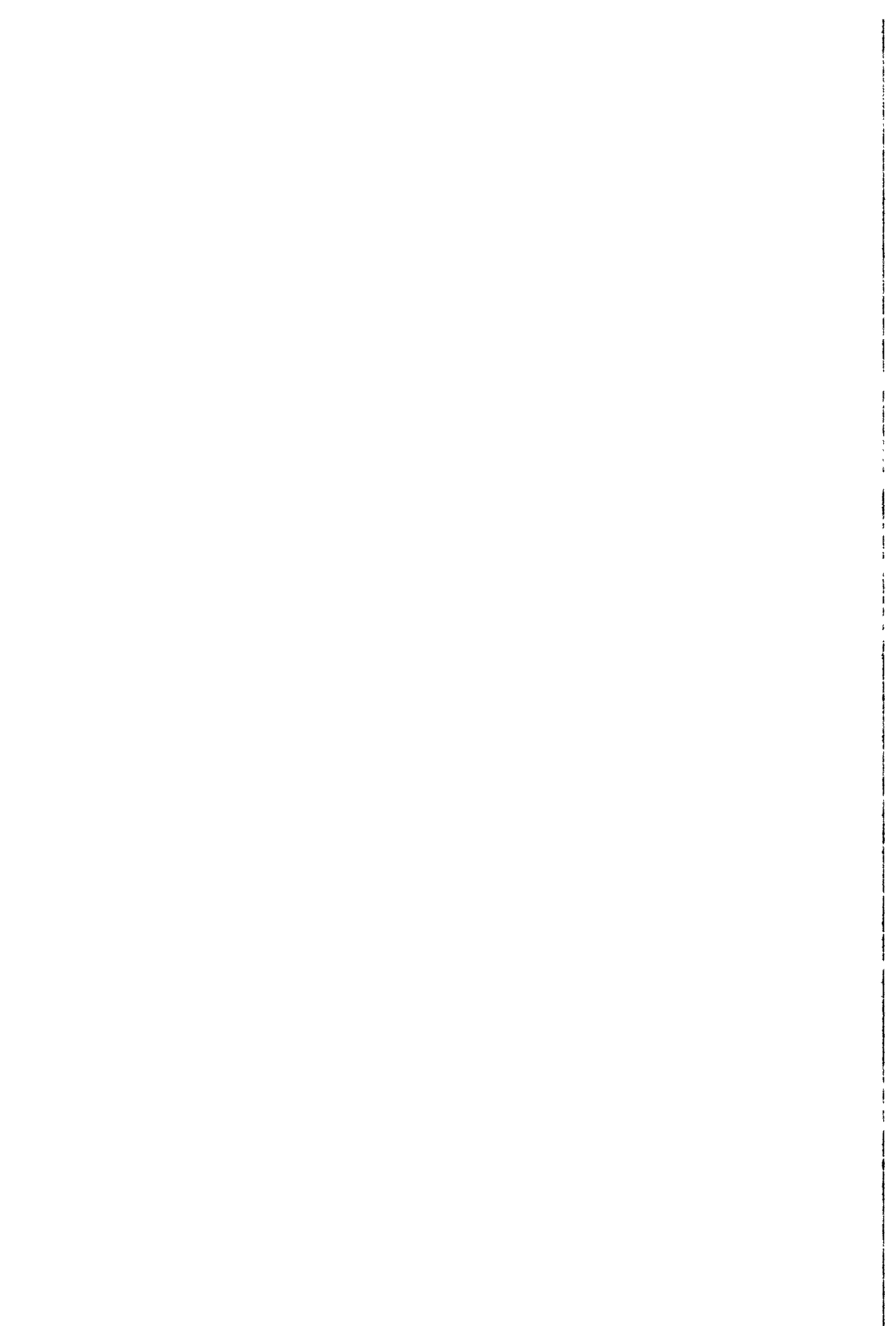


Figure 1 - PCCs in HPBL induced by Neon-20 ions



RADIATION INDUCED PROCESSES IN MAMMALIAN CELLS: PRINCIPLES OF RESPONSE MODIFICATION AND INVOLVEMENT IN CARCINOGENESIS

Contract Bi7-034 - Sector B13

- 1) *Van der Eb* , Univ. Leiden Sylvius Lab. - 2) *Sarasin* , CNRS
- 3) *Devoret* , CNRS - 4) *Rommelaere* , Université Libre de Bruxelles
- 5) *Bertazzoni* , Consiglio Nazionale delle Ricerche
- 6) *Thomou-Politi* , Greek Atomic Energy Commission

Summary of project global objectives and achievements

In the expired research contract 6 different laboratories have collaborated on a theme involving the induction of stress responses in mammalian cells. Stress responses are defined as the phenomena occurring after exposure of cells to DNA damaging agents, including UV- and ionizing radiation. These responses influence the subsequent fate of the cells, giving rise to mutation, recombination, DNA amplification and cancer.

The laboratory of Devoret focuses on the identification of RecA-like genes in mammalian cells. In *E.coli* the RecA gene plays a central role in a variety of processes that protect the cells from the deleterious effects of radiation. The group has identified in mammalian cells a cDNA from a gene (*KINI7*) which exhibits partial homology with the *E.coli* recA gene. Further work is concentrated on the identification of the functions of this gene.

The relationship between DNA repair, mutagenesis and cancer is most clearly illustrated in the human DNA repair-deficient syndrome xeroderma pigmentosum (XP). Such patients show a high incidence of skin tumors in sunlight-exposed areas of the body. The group of Sarasin has found that an unusually high percentage of skin tumors in these patients contain mutated *ras* oncogenes. This shows that unrepaired lesions in DNA can give rise to point-mutations. A small proportion of XP patients, however, does not develop skin tumors, a phenomenon which was found to be correlated with abnormal expression of the stress response. Enhanced Reactivation (Van der Eb) Elucidation of the molecular events occurring during induction and expression of several ("SOS-like") stress responses is the subject of research of the groups of Rommelaere, Sarasin, Bertazzoni and Van der Eb. The following phenomena are investigated: Enhanced Reactivation, the mechanisms of induction by UV of UV-inducible genes, gene amplification, induction of mutations (in particular at a-basic sites) and the role of poly (ADP-ribose) polymerase during recovery following radiation damage. Furthermore, biochemical and genetic analysis of repair-deficient cell lines is carried out by Bertazzoni. Finally, the group of Thomou-Politi investigates the effect of radiation on cell surface expression of the transfected human CD2 gene (coding for a cell surface antigen that binds sheep erythrocytes).

Project 1

Head of project: *Prof. Van der Eb*

Objectives for the reporting period

1. Search for suitable *in vitro* cell culture systems to assay the carcinogenic effects of radiation (ionizing and UV-irradiation).
2. Characterization of UV-inducible phenomena in human cells: a) from normal humans and XP-patients; b) from "non-cancer-prone" XP- and TTD-patients; c) from cancer-prone genetic syndromes.

Progress achieved including publications

1. Induction of *in vitro* cell transformation by radiation

The objective of this study is to develop *in vitro* assay systems for the assessment of the contribution of ionizing and UV-irradiation to the process of radiation-induced carcinogenesis. The aim is to derive an assay system consisting of primary or secondary cell cultures from mice transgenic for an activated oncogene. Such cells will be non-oncogenic, since conversion to a fully oncogenic phenotype requires activation of at least 2 complementing oncogenes, and possibly inactivation of tumor suppressor genes. However, since the cells have already made 1 step in the process of carcinogenesis, it should be possible to convert them to a (more fully) oncogenic phenotype with lower doses of radiation than when the cells are completely unchanged. In the latter case very high doses of radiation would be required to bring about in the same cell the 2 or 3 genetic events necessary for complete transformation. The following types of transgenic mice were available: mice transgenic for the pim-1 oncogene (regulated by the H2 promoter) showing pim-1 expression in the kidney; mice transgenic for the polyoma large-T antigen; and mice transgenic for the polyoma middle-T antigen, the latter genes regulated by the polyoma promoter/enhancer.

None of the primary or secondary embryo cultures nor the cultures of baby mouse kidney cells from these transgenic animals developed any sign of morphological transformation upon irradiation with UV-light or X-rays. The possible cause of this negative result is that expression of the transgene in the cells was very low or absent. It was decided, therefore, to discontinue these attempts and to try and create suitable tester cells from established swiss mouse 3T3 cells which, in contrast to NIH 3T3 cells, are completely non-oncogenic in nude mice. If introduction of a single activated oncogene does not yet render the cells tumorigenic, they might be suitable for our screening test. This approach will be continued as part of a new project (funded elsewhere) which aims at creating transgenic mice expressing selected oncogenes. These mice will be used as a model for UV-induced carcinogenesis.

2. Inducible repair processes in human cancer-prone syndromes

Exposure of human cells to UV-light or ionizing radiation results in induction of a number of stress or SOS-like phenomena, including Enhanced Reactivation (ER) of UV-treated virus and Enhanced Mutagenesis (EM) of untreated virus. We have recently noted that the ER phenomenon was absent in xeroderma pigmentosum patients which, for

unknown reasons, lacked tumors in sunlight-exposed areas of the skin, in contrast to most other XP-patients. This suggests that the ER phenomenon might be co-regulated with events that give rise to oncogene activation, or activation of certain types of oncogenes. Since EM was unchanged in these ER⁻ XP patients, it seems likely that the ability to induce point mutations in response of DNA damage, and hence the ability to activate oncogenes by point mutations, is not affected.

Recently it was demonstrated that two XP patients (brothers, cancer free) had inherited the ER⁻-phenotype from the father, whereas the mother and the daughter are normal. All individuals of this family showed normal induction of EM.

Further work showed that cells from various UV-sensitive trichothiodystrophy (TTD) patients, which are also "non-cancer-prone", show no ER-response, and that cells from hereditary cancer-prone syndromes (e.g. Polyposis coli, Dysplastic naevus syndrome, Wilm's tumor, etc.) respond to UV irradiation with super-induction of ER. This confirms the notion that cancer induction is somehow correlated with super-induction of ER. High levels of ER have also been observed in cells from the Li-Fraumeni cancer-prone syndrome (LF). Moreover LF cells exhibited a lower survival of UV-treated cells and HSV-1, whereas the kinetics of the removal of thymidine dimers is slower in LF cells than in normal cells.

Work in the reporting period has concentrated on identification of molecular "defects" in ER⁻ cells or in ER^{super+} cells. So far it was found that induction by UV-irradiation of UV-inducible genes (*c-jun*, *c-fos*, metallothionein, HSP70, collagenase) is not affected in ER⁻ and ER^{super+} cells. However, induction of RNA transcription upon UV irradiation could be shown for the ornithine carboxylase gene, albeit at a low level, in ER⁺ and ER^{super+} cells but not in ER⁻ cells. This finding will be further investigated. Moreover an abnormality was found for UV-induced stabilization of the tumor-associated protein p53. In ER⁻ cells, no UV-induced stabilization of p53 was found. However, it turned out that p53 was already constitutively stabilized in such cells. The phenomenon is investigated in more detail.

Publications

G. Weeda, R.C.A. van Ham, R. Masurel, A. Westerveld, H. Odijk, J. de Wit, D. Bootsma, A.J. van der Eb and J.J. Hoeijmakers. Molecular cloning and biological characterization of the human excision repair gene ERCC-3. *Mol.Cell.Biol.* 10(1990) 2570-2581.

G. Weeda, R.C.A. van Ham, W. Vermeulen, D. Bootsma, A.J. van der Eb and J.J. Hoeijmakers. A presumed DNA helicase encoded by the excision repair gene ERCC-3 is involved in the human repair disorders Xeroderma pigmentosum and Cockayne's syndrome. *Cell* 62(1990) 777-791.

G. Weeda. Molecular characterization of a DNA repair defect in Xeroderma pigmentosum and Cockayne's syndrome. Thesis, September 1990.

B. Klein, A. Pastink, H. Odijk, A. Westerveld and A.J. van der Eb. Transformation and immortalization of diploid Xeroderma pigmentosum fibroblasts. *Exp.Cell Res.* 191(1990) 256-262.

G. Weeda, J. Wiegant, M. van der Ploeg, A.H.M. Geurts van Kessel, A.J. van der Eb and J.J. Hoeijmakers. Localization of the Xeroderma pigmentosum group B-correcting gene ERCC-3 to human chromosome 2q21. *Genomics* 10(1991) 1035-1040.

G. Weeda, L. Ma, R.C. van Ham, A.J. van der Eb and J.H.J. Hoeijmakers. Structure and expression of the human XPBC/ERCC-3 gene involved in DNA repair disorders xeroderma pigmentosum and Cockayne's syndrome. Nucl.Acids Res. 19(1991)6301-6308.

G. Weeda, L. Ma, R.C.A. van Ham, D. Bootsma, A.J. van der Eb and J.H.J. Hoeijmakers. Characterization of the mouse homolog of the XPBC/ERCC-3 gene implicated in xeroderma pigmentosum and Cockayne's syndrome. Carcinogenesis 12(1991) 2361-2368.

P.J. Abrahams, A. Houweling and A.J. van der Eb. High levels of Enhanced Reactivation of HSV-1 in UV-treated skin fibroblasts from various hereditary cancer-prone syndromes. Cancer Research 52(1992) 53-57.

L. Ma, G. Weeda, A.G. Jochemsen, D. Bootsma, J.H.J. Hoeijmakers and A.J. van der Eb. Molecular and functional analysis of the XPBC/ERCC-3 promoter: transcription activity is dependent on the integrity of an Sp1-binding site. Nucl.Acids Res. 20(1992)217-224.

Abstracts

P.J. Abrahams, A. Houweling, R. Schouten and A.J. van der Eb. The induction of SOS-like responses and the stabilization of p53 oncoprotein in UV-exposed skin fibroblasts derived from Xeroderma pigmentosum, Trichothiodystrophy and various hereditary cancer-prone syndromes. Workshop on DNA repair, Noordwijkerhout, April 14-19 1991.

Libin Ma, G. Weeda, A.G. Jochemsen, J.J. Hoeijmakers and A.J. van der Eb. Characterization of a promoter of the human XPBC/ERCC-3 gene. Workshop on DNA repair, Noordwijkerhout, April 14-19-1991.

Project 2

Head of project: *Dr. Sarasin*

Objectives for the reporting period

- 1 - Mutagenic properties of abasic sites produced on double-stranded and single-stranded shuttle vectors.
- 2 - Construction of EBV-shuttle vectors and human cell systems for analysing mutagenesis, recombination and viral amplification.
- 3 - UV-induced mutagenicity in human cells isolated from the DNA repair deficient disease : xeroderma pigmentosum.

Progress achieved including publications

1) Abasic sites have been proposed as cryptic DNA lesions to explain most of the "spontaneous" mutagenesis and also as intermediates due to depurination of bases modified by chemicals. Their mutagenic characteristics are relatively well known in bacteria but nothing has been done in cultured mammalian cells. In order to approach this question, we have used the shuttle vector technology developed in our laboratory since several years. We have specifically constructed shuttle vectors containing unique lesions (abasic sites here) at a given position and shuttle vectors produced in their single-stranded genome state in order to better localize the damaged template.

The mutagenic properties of a true unique abasic site located opposite the four possible bases were studied. An oligonucleotide containing a chemically-produced abasic site was inserted into a shuttle vector able to replicate both in simian cells and in bacteria. Plasmid DNA was rescued from simian cells and screened in bacteria by differential hybridization with a labelled oligonucleotide probe. Using this technique, mutations were easily detected without genetic selection and then sequenced. Results showed that the abasic site was error free repaired or replicated by mammalian cells with an efficiency of about 99 %. Point mutations occurred at a frequency of approximately 1 % in control host cells and at more than 3 % in UV-pre-irradiated host cells. No preferential insertion of a particular base was observed in contrast to that reported in bacteria. However, less Gs seem to be incorporated as compared to the 3 other bases.

The effect of local sequence on the type of bases inserted opposite a true Ap site is probably important to explain mutational hot spots. We have therefore developed a shuttle vector system which will allow us to look at mutation specificities on mutational hot spots of the Ha-ras oncogene. A 25-mer oligonucleotide corresponding to the Ha-ras gene sequence around codons 12-13 has been inserted in our shuttle vectors. In collaboration with J.L. Imbach we have incorporated unique abasic sites at either the 1st or 2nd positions of codons 12 and 13 which are hot-spots of mutagenesis during oncogene activation of Ha-ras in human tumors. Our results have shown that abasic sites on these codons are also mutagenic (around 1 to 2 %) and no preferential insertion of adenine was found.

The single-stranded shuttle vector (pCF3A) has been treated by heat at pH 4.5 in order to produce random abasic sites along the genome. This vector contains the supF tRNA gene as mutagenesis target. Abasic sites on single-stranded DNA are mutagenic giving rise to point mutations. They are exclusively produced at guanine and at adenine. The use of a single-stranded genome allowed us to determine the exact position of the lesions.

These two classes of shuttle vectors can be used in human cells to detect and analyze

mutagenesis with almost any type of DNA lesion.

2) The EBV-based shuttle vectors can be maintained stably and episomally for a long period of time in cultured human cells. We have used this system in order to determine if such vectors can be amplified *in vitro* as a response to stress. These vectors carry a target gene for mutagenesis studies (lac Z') which has enabled us to determine the fidelity of the amplification process in mammalian cells, this amplification being a characteristic of some tumour cells. The accuracy of the amplification process can be monitored by studying restriction maps of individual plasmid molecules or more precisely the integrity of the lac Z' sequence, carried by our vectors. Preliminary experiments showed us that indirect amplification after fusion of treated cells (by UV or MNNG) with untreated host cells harboring the vectors, was associated with a slight, but detectable increase in mutation frequency. All analyzed mutations were due to point substitution.

We also constructed hybrid plasmids (p205-GTI) containing both the EBV and the SV40 replication origins. These molecules are able to replicate episomally either like an EBV vector or like SV40 if the SV40 large T antigen is provided at the same time. UV irradiation of both human adenovirus transformed 293 or SV40-transformed MRC5 host cells leads to vector amplification whatever the type of replication origin used for the episomal maintenance. Our results clearly show that the EBV latent replication origin (OriP), in the presence of the Epstein-Barr Nuclear Antigen-1 (EBNA-1) and the SV40 large T antigen, is sensitive to overreplication in UV-irradiated human cells. Since the UV doses were small enough to induce very little damage, if any, on the plasmid sequences, this amplification may be mediated through a cellular factor acting *in trans*.

We also demonstrated that the p205-GTI plasmid could be rearranged in cultured human cells. Studies on plasmids rearranged by illegitimate recombination were carried out in various human cell lines containing the p205-GTI after several weeks in culture. In 293 cells, the recombined vectors exhibited a heterogeneous size pattern and contained a duplication of the early promoter region of SV40. One of the recombination junctions implicated two GC boxes which constitute the essential components of the promoter sequences. The analysis of rearranged plasmids in the human Hela cell line allowed us to understand the recombination process leading to their formation. These recombined vectors originated from the excision of a unique copy of the p205-GTI plasmid integrated into the cellular genome. The plasmid and cellular sequences implicated in this integration and the chromosomal localization have been determined. The excised molecules produced from an SV40 T-antigen dependent replication were circularized by illegitimate recombination. Extensive analysis of numerous recombination junctions demonstrated that no specific nucleotide sequence is required at the joining points but there exist regions preferentially implicated in the circularization.

These results showed the existence of a DNA region more prone to be involved in rearrangement by illegitimate recombination in human cells. Several classes of sequence implicated in this type of recombination process have been reported. The episomal EBV vectors we have developed are very well adapted for this type of study in human cells.

3) Xeroderma pigmentosum is one of the best examples of the relationship between unrepaired DNA lesions, mutations and carcinogenesis in man. This rare, autosomal recessive hereditary disorder is deficient in excision repair of DNA lesions after UV irradiation. This results in a high incidence of cancers of the skin, particularly in sun-exposed parts of the body. Using the 3T3 transfection assay we have detected an activated N-ras gene in two XP tumours due to a T to A transversion in codon 61 and a transforming Ki-ras gene in a third XP tumour by mutation at codon 12 resulting in the substitution of a C to A. Screening for ras mutations in skin tumours from XP and normal patients by PCR followed by differential hybridization, we detected ras mutations in 55 % of XP tumours (in 30 XP tumours) compared to 20 % in controls (in 50 tumours). Parallel experiments have been carried out on XP skin tumours for analysing

UV-induced mutations on the P53 tumor suppressor gene. Initial results indicate that a high level of point mutations are observed for XP samples with a particular hot-spot leading to a C-C to T-T tandem transition. This class of mutation is characteristic of UV-induced lesions. Similar results have been published on non-XP skin tumours by Brash et al. Hence unrepaired DNA lesions persisting in XP skin results in higher levels of mutations compared to the same type of carcinomas from individuals with normal repair capacities.

Southern analysis of genomic DNA from XP tumours has shown high levels of Ha-ras gene amplification and rearrangement not found in skin tumours from normal individuals. Oncogene amplification of the c-myc protooncogene was also found in XP tumours.

This result indicates clearly that XP cells are hypermutagenized by UV-light in patients as they are in vitro. The high level of oncogene amplification found in XP cells agrees with the model of overreplication due to blockage of DNA polymerase at unrepaired lesions. The presence in the same cell of amplified and mutated oncogenes can easily explain the higher cancer frequency in XP patients compared to normal individuals.

Publications

M.R. James, A. Sarasin, M. Perricaudet and I. Joab. Constitutive and inducible expression of Epstein-Barr virus nuclear antigen 3 carried on stable episomal vectors in human cells.

Gene, 1990, 86, 233-239.

C.F.M. Menck, M. James, A. Benoit and A. Sarasin. Constraints in SV40 encapsidation as determined by SV40-based shuttle viruses. *J. Gen. Virol.*, 1990, 71, 143-150.

A. Sarasin, F. Bourre, L. Daya-Grosjean, A. Gentil, C. Madzak and A. Stary. Mechanisms and consequences of mutation induction in mammalian cells. *Int. J. Radiat. Biol.*, 1990, 57, 665.

B.C. Broughton, A.R. Lehmann, S.A. Harcourt, C.F. Arlett, A. Sarasin, W. Kleizer, F. A. Beemer, R. Nairn and D.L. Mitchell. Relationship between pyrimidine dimers, 6-4 photoproducts, repair synthesis and cell survival : studies using cells from patients with Trichothiodystrophy. *Mutation Res.*, 1990, 235, 33-40.

A. Gentil, G. Renault, A. Margot, R. Teoule and A. Sarasin. Mammalian cell processing of a uracil-containing mismatch in SV40 DNA. *Nucl. Acids Res.*, 1990, 18/21:6361-6367.

P. Di mascio, C.F.M. Menck, R.G. Nigro, A. Sarasin and H. Sies. Singlet molecular oxygen induced mutagenicity in a mammalian SV40-based shuttle vector. *Photochem. Photobiol.*, 1990, 51, 293-298.

C. Madzak and A. Sarasin. Single-stranded DNA shuttle vectors for analyzing DNA-damage processing, in "Anticarcinogenesis and radiation protection", O. Nygaard and A.C. Upton, Eds, Plenum Press. New York, 1991, 79-84.

A. Stary and A. Sarasin. Ultraviolet-light induces a copy number increase of epstein-barr virus-based shuttle vectors. in "New Horizons in Biological Dosimetry", B.L. Gledhill and F. Mauro, Eds, J. Wiley & Sons Inc., New-York, 1991, pp. 291-299.

C. Madzak and A. Sarasin. Mutation spectrum following transfection of ultraviolet-irradiated single-stranded or double-stranded shuttle vector DNA into monkey cells. *J. Mol. Biol.*, 1991, 218:667-673.

A. Stary and A. Sarasin. Amplification of Epstein-Barr virus-based shuttle vectors by UV light in human cells. *Biochimie*, 1991, 73:509-514.

A. Sarasin. The paradox of DNA repair-deficient diseases. *The Cancer Journal*, 1991, 4:233-237.

L. Daya-Grosjean, C. Robert-Knebelman, C. Drougard, M.F. Avril and A. Sarasin. Modified oncogenes in skin tumors from repair deficient xeroderma pigmentosum patients and normal individuals. In "Environment and Genome", S.B. Bhattacharjee Ed., New R.K. Printa, Calcutta, 1991, pp. 103-114.

M. Mezzina and A. Sarasin. Modifications in DNA ligase activity during DNA repair in mammalian cells. *Molecul. Toxicol.*, 1991, In press.

F. Bourre, A. Lichtenberger and A. Sarasin. Comparison of spontaneous and ultraviolet-induced mutagenesis on naked SV40 DNA and SV40 virus. *Mutation Res.*, 1991, 250:49-53.

C. Madzak and A. Sarasin. Conversion of a single-stranded SV40-based shuttle vector to its double-stranded form does not require SV40 large T antigen in monkey cells. *J. Gen. Virol.*, 1991, 72, 3091-3093.

S. Michelin, I. Varlet, C. Martinerie, B. Perbal, A. Sarasin and H.G. Suarez. V-myc transformation of Xeroderma Pigmentosum human fibroblasts : overexpression of the c-Ha-ras oncogene in the transformed cells. *Exptl. Cell Res.*, 1991, 196, 314-322.

A. Sarasin, C. Robert-Knebelmann, A. Margulis, M. Zghal and L. Daya-Grosjean. Oncogene activation in ultraviolet-induced skin tumors from normal individuals and xeroderma pigmentosum patients. *Radiation Research*, 1992, 2, 386-391.

C. Madzak and A. Sarasin. Ultraviolet mutational spectrum of a single-stranded shuttle vector comprises frameshifts and multiple mutations. *Mutation Res.*, 1992, In press.

A. Sarasin, C. Blanchet-Bardon, G. Renault, A. Lehmann, C. Arlett and Y. Dumez. Prenatal diagnosis in a subset of trichothiodystrophy patients defective in DNA repair. *Br. J. Dermatol*, 1992, submitted.

A. Stary and A. Sarasin. Illegitimate recombination following amplification of an EBV.SV40 hybrid shuttle vector integrated into the human Hela cell genome. *J. Gen. Virol.* in press, 1992.

D.T. Ribeiro, C. Madzak, A. Sarasin, P. Di mascio, H. Sies and C.F. Menck. Singlet oxygen induced DNA damage and mutagenicity in a single-stranded SV40-based shuttle vector. *Photochem. and Photobiol.* 1992, 55:39-45.

M. Vuillaume, L. Daya-Grosjean, P. Vincens, J.L. Pennetier, P. Tarroux, A. Baret, R. Calvayrac and A. Sarasin. Striking differences in cellular catalase activity between two DNA repair-deficient diseases: xeroderma pigmentosum and trichothiodystrophy. *Carcinogenesis*, 1992, 13: 321-328.

A. Stary and A. Sarasin. Description of a new amplifiable shuttle vector for mutagenesis studies in human cells: Application to N-methyl-N' nitro-N-nitrosoguanidine-induced mutation spectrum. *Mutation Res.*, 1992, 73, in press.

J. Cabral Neto, A. Gentil, R.E. Casiera Cabral and A. Sarasin. Mutation spectrum of heat-induced abasic sites on a single-stranded shuttle vector replicated in mammalian cells. *J. Biol. Chemistry*, 1992, in press.

A. Gentil, J. Cabral Neto, R. Mariage-Samson, A. Margot, J.L. Imbach, B. Rayner and A. Sarasin. Mutagenicity of a unique apurinic/aprimidinic site in mammalian cells. *J. Mol. Biol.*, 1992, in press.

D.T. Ribeiro, F. Bourre, A. Sarasin, P. Di mascio and C.F.M. Menck. DNA synthesis blocking lesions induced by singlet oxygen are targeted to deoxyguanosines. *Nucl. Acids Res.*, 1992, 20:2465-2469.

Project 3

Head of project: *Dr. Devoret*

Objectives for the reporting period

In a search for repair enzymes induced by radiations in mammalian cells, we have identified a new mouse gene called KIN17. Our objective were:

- 1) to clone into a convenient vector the KIN17 cDNA in order to express kin17 protein in *E.coli*.
- 2) to purify kin17 protein
- 3) to determine *in vitro* if kin17 protein is a protein involved in DNA transactions.
- 4) to establish kin17 functions *in vivo*, and in collaboration with Van der Eb's and Sarasin's groups, to determine its effect on SOS in mammalian cells.
- 5) to clone the mouse or the human KIN17 gene.

Progress achieved including publications

We answered the first 3 questions raised:

1) We were able to produce kin17 protein in *E.coli* by using a new plasmid construction.

2) Using the new vector, we have purified kin17 protein produced in *E.coli*.

3) We have demonstrated that kin17 protein binds to zinc ions and to double-stranded (ds) or heat denatured (hd) DNA in a zinc dependent manner. When we deleted the zinc finger carried by the protein, no longer did kin17 bind to zinc ions. Nevertheless, it could still bind to DNA albeit with a decreased efficiency.

The results we have obtained show that there are at least two domains of the protein involved in DNA-binding. One domain is the zinc finger whose properties were just described above. The other domain might be the domain homologous to RecA.

We have succeeded in showing that kin17 protein is involved in DNA metabolism.

We have demonstrated that kin17 is a nuclear protein. The bipartite nuclear localization signal present in the amino acid sequence has been shown to direct *b*-galactosidase to the nucleus of HeLa cells.

4) We were recently able to show *in vitro* the functions of kin17. The protein binds preferentially to DNA containing bent DNA. This function was demonstrated using the pBR322 tn3 region cut off by restriction enzymes. The same region has been previously shown to be bound by the IHF (Integration Host Factor).

This factor raises interesting questions. Such bent DNA has been shown to be a substrate for some site specific recombinases. Kin17 might be one of those recombinases.

5) The KIN17 mouse genomic DNA has just been cloned. The human gene is still not yet cloned.

Publications

Loh, S., Skurray R., Celerier J., Bagdasarian M., Bailone A., Devoret R. Nucleotide sequence of the psiA (plasmid SOS inhibition) gene located on the leading region of plasmids F and R6-5. *Nucleic Acids Res.* 18(1990)4597.

Sommer S., Leitao A., Bernardi A., Ballone A., Devoret R. Introduction of a UV-damaged replicon into a recipient cell is not a sufficient condition to produce an SOS-inducing signal. *Mutation Res., DNA repair* 254(1991)107-117.

Angulo J.F., Rouer, E., Benarous, R., Devoret, R. Identification of a mouse cDNA fragment whose expressed polypeptide reacts with anti-recA antibodies. *Biochimie* 73(1991)251-256.

Rao B.J., Jwang, B., Dutreix M. Production of triple-stranded recombination intermediates by RecA protein, in vitro. *Biochimie* 73(1991)363-370.

Bailone A., Sommer S., Knezevic J., Devoret R. Substitution of UmuD' for UmuD does not affect SOS mutagenesis. *Biochimie* 73(1991)471-478.

Bailone A., Sommer S., Knezevic J., Dutreix M., Devoret R. A RecA protein mutant deficient in its interaction with the UmuDC complex. *Biochimie* 73(1991)479-484.

Angula J.F., Rouer E., Mazin A., Mattei M.G., Tissier A., Horrellou P., Benarous R., Devoret R. Identification and expression of the cDNA of KIN17, a zinc finger gene located on mouse chromosome 2, encoding a new DNA-binding protein. *Nucleic Acids Res.*19(1991)5117-5123.

Devoret R. Les fonctions SOS ou comment les bactéries survivent aux lésions de leur ADN. *Anales de l'Inst. Pasteur Actualités* 1(1992)11-22.

Bagdasarian M.M., Bailone A., Angulo J., Scholtz P., Bagdasarian M., Devoret R. PsiB an anti-SOS protein, is transiently expressed by the F sec factor during its transmission to an Escherichia coli K12 recipient. *Molecular Microbiology* 6(1992)885-893.

Dutreix M., Burnett B., Bailone A., Radding C.M., Devoret R. A partially deficient mutant, recA1730, that fails to form normal nucleoprotein filaments. *Molec.Gen.Genet.* 232(1992)489-497.

Project 4

Head of project: *Prof. Rommelaere*

Objectives for the reporting period

- a) The modulation of gene expression in irradiated cells has been investigated. Exposure of eucaryotic cells to genotoxic agents disturbs gene expression in these cells. We have analyzed the effect of UV-light and X-rays on the level of specific RNAs in human kidney cells and in mutant TTD and XP-D cells.
- b) The transforming action of ionizing radiation has been investigated on normal human keratinocytes *in vitro*.

Progress achieved including publications

1. Control of gene expression in irradiated cells

1.1 Introduction

It is well known that physical and chemical genotoxic agents disturb gene expression in mammalian cells. Elongation of nascent RNA molecules is impeded by the presence of ultraviolet-light-induced lesions in DNA templates, resulting in a reduction of the overall rate of transcription in irradiated cells. In addition to this inhibitory effects, subtoxic UV-doses also stimulate the expression of a set of genes whose products appear to be involved in the cell cycle or the various protective, degradative and inflammatory processes. Although this stimulation occurs at the level of initiation of transcription it is not excluded that stabilization of mRNAs is increased, as it has been demonstrated in cells exposed to peptide and non-peptide signalling molecules.

We have thus examined whether modulation of gene expression by genotoxic agents also includes a post-transcriptional component. We have compared the fate of specific RNAs in control, UV and X-ray-irradiated human cells. Our results clearly show a dose-dependent UV-light stabilization of performed mRNAs while a stimulation of transcription rather than stabilization of the transcripts is observed in X ray-irradiated cells.

1.2 Results

1.2.1 Effects of UV-light-irradiation on the abundance of IFN-a, IL-1a and poly(I).poly(C) induced mRNAs

In order to distinguish between transcriptional and post-transcriptional effects, we have focused on six genes whose transcription is conditionally induced by interferon-1a (IFN-1a) interleukin-1a (IL-1a) or the double-stranded RNA, poly(I).poly(C). We have analyzed six transcripts that are induced by IFN-a [2',5'-oligoadenylate synthetase, 6-16, 1-8, interferon-induced 15 kDa protein (IFI-15K)], IL-1a (IL-1b) or poly(I).poly(C) [interferon-induced 54-kDa protein (IFI-54K)]. NB-E human kidney cells were treated (or not) with IFN-a, IL-1a or poly(I).poly(C) for either 6 (IFN-a) or 4 hours (IL-a or poly(I)poly(C)) prior to exposure (or not) to 5 J/m² (IFN-a) or 30 J/m² (IFN-a, IL-1a,

poly(I).poly(C) UV light and incubated in the absence of inducers for different periods of time. Total RNA was extracted and the abundance of the induced transcripts (see above) measured by Northern blotting.

The level of cytokine- and poly(I).poly(C)-induced transcripts was significantly higher in UV-irradiated than in control cultures. We have shown by pulse/chase experiments and run-on assays that this differential accumulation of induced mRNAs in control and in irradiated cells is the consequence of an increased stability of these transcripts in irradiated cells rather than a stimulation of the transcription.

1.2.2 Effects of UV-light and X-rays irradiation on the level of IL-a-induced mRNAs

We have investigated whether the accumulation of IL-1a induced IL-1b mRNA after UV light irradiation also occurs after X-ray irradiation and whether the same phenomenon could be obtained with other IL-1a induced cytokine mRNAs. The transcripts analyzed were respectively: IL-1b, IL2, IL6 and TNF (Tumor Necrosis Factor). NB-E cells were treated (or not) with IL-1a for 6 hours irradiated (or not) with UV light (30 J/m^2) or X-rays (1000,2000,3000 and 5000 Rads) and incubated in the absence of the inducer for different periods of time. Total RNA was extracted and the abundance of the induced transcripts measured by Northern blotting. We observed accumulation of induced mRNAs in all UV or X-rays-irradiated cells except in two cases:
a) no accumulation of TNF was observed after UV-irradiation
b) no accumulation of IL-2 after X-rays.

In order to determine whether the accumulation of mRNAs after X-ray irradiation was due to either stabilization of preformed mRNAs or stimulation of transcription, cells were irradiated without pretreatment with the inducer and the mRNAs analyzed by Northern blotting as described above. By contrast to the results obtained with UV-irradiation, the mRNA accumulation after X-ray irradiation is likely due to a transcriptional stimulation rather than a stabilization of the transcripts.

1.2.3 Effects of UV-light irradiation on the level of induced cytokine mRNAs in mutant TTD and XP-D cells

We have measured by Northern blotting the level of IL-1 β and IL-6 induced mRNAs after UV-light irradiation (5 J/m^2 and 30 J/m^2) in TTD1B1 (class 3) and in XP-D cells respectively. XP-D cells are characterized by an hypersensitivity to UV-light and a reduced UV-induced DNA repair synthesis (UDS). On the contrary to XP-D cells, the TDD1B1 cells (class 3) survival is normal after UV irradiation although UDS is also reduced in these cells.

An accumulation of these mRNAs is observed in both cell types after UV irradiation. However, this accumulation is much higher in TDD1 cells than in normal and XP-D cells. Whether this accumulation in these cells is the consequence of either stimulation of transcription, stabilization of preformed mRNAs or both remains to be elucidated.

1.2.4 Conclusion

This work uncovers a new facet of the cellular response to genotoxic stresses, i.e. extension of the life-span of transcription products after UV irradiation. This phenomenon

could be a putative adaptive response that may compensate for at least part of the inhibition of gene expression in cells exposed to genotoxic stresses.

2. Induction of cells resistant to terminal differentiation in cultures of normal human keratinocytes exposed to X-rays

Long term effects of ionising radiation was sought by studying the process of cells transformation. Cell lines established from human and murine squamous cell carcinomas as well as keratinocytes transformed by viral transforming genes can be grown under restrictive conditions and are more resistant than their normal counterparts to terminal differentiation stimuli. These alterations have been exploited to study the proneness of normal human foreskin keratinocytes to transformation by X-rays.

Keratinocytes were grown in the low Ca^{++} (0.1 mM) medium MCDB153 supplemented with 10 ng/ml EGF, hydrocortisone and bovine pituitary extract which allows their clonal growth but limits differentiation. After irradiation (2 or 4 Gy X-rays), cultures were incubated in MCDB153 medium until subconfluent and split in 3 parts. 2 dishes were incubated in the MCDB153 medium until subconfluent and split in 3 parts. 2 dishes were incubated in supplemented MCDB153 medium, the third in selective medium. One of the subcultures grown in MCDB153 medium was used to measure plating efficiency, the other was further irradiated at subconfluency, and processed as above. The selective medium consisted of complete MCDB153 medium as described, but contained a lowered EGF concentration (0.1 ng/ml) and an elevated (1.2 mM) concentration of Ca^{++} . This selective medium caused growth arrest and terminal differentiation of normal keratinocytes but allowed *in vitro* immortalized (HaCaT cells) and tumour-derived keratinocytes (SCC-25, A431) to proliferate. Clones able to develop in selective medium appeared in a dose-dependent fashion after repeated irradiations. Two transformed clones were further characterized. They exhibited an extended life-span, were aneuploid and stained positive and mostly negative for markers of proliferating basal and differentiating skin keratinocytes, respectively. One of the clones survived more than 50 subcultures and may be considered immortalized. However, it failed to form tumours in nude mice. Thus both transformants appeared to be arrested in an early stage of differentiation and to exhibit growth properties and differentiation profiles similar to those of virally-transformed keratinocytes and cells established from skin carcinomas.

This procedure may be useful to study early events in the process of malignant transformation.

Publications

J.J. Cornelis and J. Rommelaere. Parvoviral probes for cellular responses to DNA damage. In: Handbook of Parvoviruses" Ed. P. Tijssen, CRC Press, Boca Raton, vol.II, pp. 231-246 (1990).

M. Tuynder, S. Godfrine, J.J. Cornelis and J. Rommelaere
Dose-dependent induction of resistance to terminal differentiation in X-irradiated cultures of normal human keratinocytes. Proc.Natl.Acad.Sci.USA 88(1991)2638-2642.

G. Hilgers, I. Clauss, G. Huez and J. Rommelaere
Post-transcription effect of UV-light on gene expression in human gels. Eur.J.Biochem. 201(1991)483-488.

S. Plaza, A. Boullard, D. Pele, J.J. Cornelis, J. Rommelaere, P.U. Giacomoni and M. Prunieras. Unscheduled DNA synthesis: a quantitative indicator of residual immunodetectable pyrimidine dimers in human fibroblasts after ultraviolet-B irradiation. Photochem.Photobiol. 53(1991)217-227.

Project 5

Head of project: *Dr. Bertazzoni*

Objectives for the reporting period

Cellular and genetic characterization of trichothiodystrophy (TTD) and xeroderma pigmentosum (XP) patients. Study of the TTD/XP association. Chromosomal instability of homozygous and heterozygous carriers of XP mutations. Cellular and genetic characterization of mutagen-sensitive rodent mutants (F. Nuzzo and M. Stefanini).

Study of the poly(ADP-ribose)polymerase (ADPRP) during proliferating activity of mammalian cells occurring in rat liver regeneration. Identification of inhibitors of poly(ADP-ribose)polymerase with low toxicity (U. Bertazzoni and A.I. Scovassi).

Progress achieved including publications

1. Cellular and genetic characterization of DNA repair mutants

Chromosome analysis in cultured fibroblasts from unaffected skin of XP patients and their relatives demonstrated the presence of structural chromosome changes in all the individuals. Furthermore multiple unrelated clonal chromosome rearrangements were observed in four subjects carrying the XP-C mutation (two homozygotes and two heterozygotes) and in one XP-D patients. The anomalies were apparently balanced translocations, deletions, and inversions. These results suggest that the occurrence of cytogenetic abnormal clones represents an initial step in the process leading to neoplastic transformation.

Consanguinity studies in three Italian families with members showing the complex phenotype due to the association of XP-D with TTD, demonstrate the presence of multiple remote inbreeding within and among the families. These observations suggest that the mutations responsible for TTD and XP-D should be at loci closely linked or affect the same gene. DNA repair investigations extended to TTD patients from different countries (referred to us by Dr. Lehmann, MRC Cell Mutation Unit, Falmer, U.K. and by Dr. A. Sarasin, IRCS, Villejuif, France) confirmed the association with TTD with XP-D in unrelated patients.

Two new complementation groups of UV-sensitive (UV^S) excision repair-defective rodent mutants were identified among the mutants isolated in our lab. These mutants are hypersensitive to a broad spectrum of mutagens, partially unable to perform UV-induced DNA repair synthesis, and partially defective in the incision step of the DNA excision repair pathway and in the removal of cyclobutane pyrimidine dimers and (6-4) photoproducts, the main lesions caused by UV. The characterization for the UV sensitivity and the human chromosome content of hybrids obtained by fusing the mutant CHO7PV (representative of the group 9 of UV^S rodent mutants) with normal human lymphocytes indicates the human chromosome 7 as the best candidate for the localization of the human gene able to correct the repair defect in CHO7PV cells.

2. Study of the role of poly (ADP-ribose) polymerase in mammalian cells

The nuclear enzyme poly(ADP-ribose)polymerase (ADPRP), which is activated in response to DNA damage, modifies chromosomal proteins and plays a key role in DNA repair. The involvement of ADP-ribosylation in rat liver carcinogenesis has been suggested by earlier studies in which we observed that ADPRP activity was depleted and catalytic protein was lost during treatment with 2-acetylaminofluorene (2AAF). To verify the specificity of this compound in inducing ADPRP loss during initial steps of malignant transformation, we have determined the ADPRP activity and its mRNA level in the livers of rats treated according to three different carcinogenesis models (Teebor and Becker, Solt and Farber, Druckrey). The evaluation of the activity of the enzyme indicated that 2AAF exerts a specific effect on ADPRP. The levels of ADPRP mRNA, measured by northern blot, did not show a significant variation and therefore could not be responsible for the loss in enzyme activation.

To further clarify the function of ADPRP in the regulation of different cellular processes of DNA metabolism, and in particular during proliferation, ADPRP activity was determined in total liver extracts during the early and late phases of rat liver regeneration and evaluated also in liver nuclei and nuclear extracts by differential assays, allowing the measurement of the active fraction of the enzyme with respect to the total ADPRP level. In isolated nuclei, two different phases were observed: an early wave occurring before the onset of DNA synthesis, and a second one, starting several hours after the peak of DNA synthesis. In nuclear extracts, a more gradual increase was noted, starting in concomitance with DNA synthesis. These data suggest that the early increase is resulting from the activation of pre-existing ADPRP molecules, whereas the second phase can be associated to the *de novo* synthesis.

To further explore the possible correlation between variations of ADPRP activity and cell proliferation, we have extended this study by determining the level of ADPRP mRNA during rat liver regeneration and found that the level of specific mRNA showed an enhancement before the onset of DNA synthesis.

The inhibitors of ADPRP potentiate the effect of DNA-damaging agents. We have studied the relationship between chemical structure and biological activity of a series of compounds substituted in different ways at the ring of benzamide (the most used inhibitor) or modified at the amidic residue of the benzene ring. The results of a set of experiments performed *in vivo* and *in vitro* indicated that the substitution at the position 3 of the NH₂ function increased the specificity of the compound and decreased its cellular toxicity.

In order to characterize the non-histone proteins ADP-ribosylated in human and mouse cells, we have followed different experimental procedures which allowed specific labelling of modified proteins and their immunological recognition. The experiments were essentially based on the isolation of ADP-ribosylated proteins from intact or permeabilized cells or isolated of ADP-ribosylated proteins from intact or permeabilized cells or isolated nuclei. Using various approaches (microinjection of ³²P-NAD in mouse embryos, incubation of intact HeLa cells with ³H-adenosine, incubation of HeLa cell nuclei or permeabilized cells with ³²P-NAD and isolation of ADP-ribosylated proteins on boronate column) the same non-histone proteins were found to be ADP-ribosylated, showing sizes of 170, 115, 85 and 65 kDa. We have focused our attention on the 170kDa peptide, possibly corresponding to DNA topoisomerase II. To obtain direct evidence for this hypothesis, we have immunoprecipitated the enzyme from HeLa cell nuclei incubated with ³²P-NAD. Our results demonstrated that topoisomerase II is ADP-ribosylated in physiological conditions. In order to verify if this post-translational modification is

dependent on DNA repair, we have treated HeLa cells with dimethylsulfate and the results obtained indicated that the modification of topoisomerase II is not affected by the damage to DNA.

Publications

Cesarone C.F., Scarabelli L., Scovassi A.I., Izzo R, Menegazzi M, Carcereri De Prati A., Oruneso M. and Bertazzoni U. Changes in activity and mRNA levels of poly(ADP-ribose)polymerase during rat liver regeneration. *Biochem.Biophys.Acta.* 1087(1990) 241-246.

Nuzzo F., Zei, G., Stefanini M., Colognola R., Santachiara A.S., Lagomarsini P., Marinoni S. and Salvaneschi L. Search for consanguinity within and among families of patients with trichothiodystrophy associated with xeroderma pigmentosum. *J.Med.Genet.* 27(1990)21-25.

Sestili P., Spadoni G, Balsamini C., Scovassi I, Cattabeni F., Duranti E., Cantoni O, Higgins D. and Thomson C. Structure requirements for inhibitors of poly(ADP-ribose)polymerase. *J.Cancer Res. and Clin.Incol.* 116(1990)615-622.

Stefanini M., Lagomarsini P., Gilliani S., Marinoni S., Borrone C., Trevisan G and Nuzzo F. Association of xeroderma pigmentosum with trichothiodystrophy. *Clinical Dermatol.* 3(1990)823-826.

Stefanini M., Collins A., Riboni R., Klaude M., Botta E., Mitchel D.L. and Nuzzo F. Novel Chinese hamster UV-sensitive mutants for excision repair form complementation groups 9 and 10. *Cancer Res.* 51(1991)3965-3971.

Cesarone C.F., Suzuki H., Scovassi A.I., Scarabelli L., Izzo R., Giannoni P., Mariani C., Miwa M., Oruneso M. and Bertazzoni U. Influence of poly(ADP-ribose)polymerase depletion on promotion of rat liver carcinogenesis. *Molecular Carcinogenesis* 5(1992)111-117.

Short communications

Botta E., Riboni R., Mondello, C., Nuzzo F. and Staffani M. Mapping of the human gene complementing the DNA repair defect in a UV sensitive Chinese hamster mutant. *Ass. for Radiation research - DNA repair network Joint meeting, 3-5 jan.St.Andrews 1990*

Marioni S., Trevisan G., Not T., Lagomarsini P. and Stefanini M. Trichothiodystrophy with photosensitivity: overlook of six Italian cases. *Congress on Clinical Dermatology in the Year 2000. May 22-25 London, 1990.*

Marioni S., Trevisan G., Gaeta G., Not, T., Lagomarsini P., Stefanini M. Nazzaro V. and Ermacola E. Trichothiodystrophy associated with group D xeroderma pigmentosum in seven italian patients. *Third Congress of the European Society for Paediatric Dermatology. Sept. 21-23, Bordeaux, Arachon (France). 1990.*

Betta E., Riboni R., Pellegata N.S. Mondello C., Nuzzo F. and Stefanini M. Mapping on human chromosomes of the gene complementing the DNA repair defect in the group 9 of UV sensitive rodent mutants. Workshop on DNA repair with emphasis on eukaryotic systems. Noordwijkerhout, ND April 14-19, Abstr. 1A2, 1991.

Lehmann A.R., Stefanini M. and Vermeulen W. Relationships between xeroderma pigmentosum, Cockayne's syndrome and trichothiodystrophy. An AACR special conference on "Cellular responses to environmental DNA damage", Banff, Alberta, Canada December 1-6, 1991.

Scovassi A.I., Negroni M., Mariani C., Negri C. and Bertazzoni U. ADP-ribosylation of topoisomerase II in intact HeLa cells. N.Y. A.S. Conference on Aging and cellular defence mechanisms, Modena, Italy, September 22-26, abstr. PIII-18, 1991.

Scovassi A.I., Scarabelli L., Giannoni P., Mariani C., Suzuki H., Orunesu M., Bertazzoni U. and Cesarone C.F. Poly(ADP-ribose)polymerase is involved in promotion of rat liver carcinogenesis N.Y.A.S. Conference on aging and cellular defence mechanisms. Modena Italy, Sept. 22-26, abstr. PIII-17, 1991.

Scovassi A.I., Izzo, R., Mariani C., Negroni M., Negri C. and Bertazzoni U. ADP-ribosylation of human DNA topoisomerase II in physiological conditions. Paul Mandel International Meeting on poly(ADP-ribosylation)reactions. May 30-June 3, Quebec, Canada, (1991).

Stefanini M., Casati A., Girogi R. and Nuzzo F. Cytogenetic abnormal clones in fibroblasts from xeroderma pigmentosum mutation carriers. Keystone Symp. on genomic instability and cancer. Tamarron (USA) Febr. 4-10, J.Cel.Biochem., S 15D:145, 1991.

Stefanini M., Lagomarsini P., Gilliani S., Nardo T. and Nuzzo F. Genetic analysis in xeroderma pigmentosum, trichothiodystrophy and Cockayne's syndrome. Workshop on: A new look at excision repair disorders. Eastbourne (UK) February 27th, March 1st. Abstr. p.10, 1991.

Stefanini M., Vermeulen W., Gilliani S., Nardo T., Sarasin A., Lehmann A.R. and Hoeijmakers J.H.J. Identification of patients affected by trichothiodystrophy showing DNA repair defects different from that present in xeroderma pigmentosum complementation group D. UKEMS/DNA REPAIR NETWORK Joint meeting, Swinsea, U.K. March 23-27, 1992.

Project 6

Head of project: *Dr. Thomou-Politi*

Objectives for the reporting period

1. Construction of stably transformed CHO cells deficient in HPRT (HAT sensitive) and cotransfection, using the calcium phosphate coprecipitation technique, with pSV2-gpt vector and π H3-CD2 vector which carries the human CD2-cDNA.
2. The stably cotransfected CHO cells express the cell surface CD2 antigen as was verified by using rosette assay, flow cytometric analysis and Southern blotting.

Our aim was the titration of the bioresponse of these cells to very low doses of radiation affecting the quantitative expression of the CD2 gene. Especially, we have studied the increase or decrease of the cell surface antigen CD2, responsible for binding sheep erythrocytes and rosette formation. This antigen is implicated mainly in the immune response of the human T lymphocytes and recently there seems to be a shift of interest toward the effect of low-dose radiation (<0.5 Gy) on the immune response.

Progress achieved including publications

The objective of this study is to develop indicator cell lines that would respond to low levels of radiation, not affecting cell survival, by producing quantitative signals indicative of new defined phenotypes.

Therefore, thioguanine resistant CHO cells were stably cotransfected with π H3-CD2 and pSV2-gpt vectors. The resulted cotransfected CHO clones are HAT resistant and constitutively express the human cell surface CD2 antigen. A number of independent clones (more than 20) were then isolated from this bulk population by cylinders. A further isolation, by limiting dilution, of a series of clones derived from cotransfection experiments expressing human CD2 receptor, was based on their ability to sustain rosette formation. One representative clone, namely CL13 was chosen for further study. This clone had only one copy of π H3-CD2 plasmid as revealed from Southern blot analysis (Fig. 1).

As the CD2 antigen on human T cells mediates rosetting with sheep red blood cells (SRBC) (Howard et al. 1981) it was important to know whether the transfected cells shared this characteristic property. After incubation at 37°C with SRBC all the transfected cells but not untransfected CHO cells, strongly bound sheep erythrocytes. This result indicates that the transfected CD2 antigen on CHO cells can, like its human T cell counterpart, interact with its specific ligand T11TS (Huning 1985). Moreover, previous treatment of CL13 clone with CD2 mAb (OKT11) resulted in the inability of clone cells to bind sheep erythrocytes. These observations may suggest that this clone encodes the entire CD2 antigen and that the transfected gene product expressed in CL13 clone may have adopted a conformation similar to that present on human T lymphocytes.

The CL13 clone was subjected to CD2mAb (OKT11) and stained with FITC labeled goat anti-mouse IgG and subsequently analysed by FACS (Becton Dickinson). The FACS profiles given by CL13 with the OKT11mAb are presented in Figure 2 with those for purified peripheral blood human T lymphocytes. The level of CD2 expression of CL13 cells as judged from the transposition of fluorescence intensity, was similar to that of peripheral T lymphocytes.

The results of hybridization of restriction endonuclease cleaved cell DNA from cotransformed clone CL13 that were probed with digoxigenin-labelled CD2-cDNA are shown in Figure 1. So, BamHI cleaved the π H3-CD2 cDNA only once and the cleavage site is outside

of the CD2-cDNA. Consequently, with genomic DNA from the transfected clone, each hybridizing band represents one copy of all or part of a transfecting DNA sequence embedded in the genomic DNA. The molecular size of this hybridizing band is 5.0 Kb. Moreover, EcoRI cleaves π H3-CD2 vector only once. The cleavage site is in the CD2-cDNA. Therefore, a single integrated uninterrupted vector should yield two bands. As it can be seen two bands are revealed with molecular sizes 5.8 Kb and 4.8 Kb. BglII and PvuII restriction enzymes have both two restriction sites in π H3-CD2 vector. One is in the CD2 insert while the other is outside it. Consequently, a single integrated uninterrupted vector should yield two hybridizing bands. As it can be seen (Fig. 1) two bands are revealed for BglII and PvuII with molecular sizes 6.4 Kb, 4.3 Kb and 4.1 Kb, 3.7 Kb respectively.

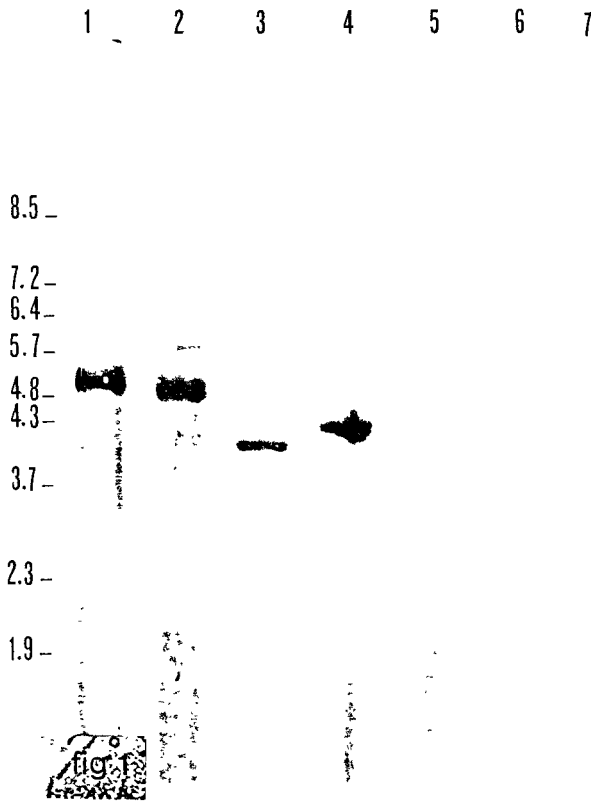


Figure 1 - Transformed clone CL13 DNA hybridization analysis. Ten micrograms of DNA was electroforesed, transferred and hybridized with dig-labelled CD2-cDNA. DNAs were digested with the following endonucleases 1, BamHI; 2, EcoRI; 3, PvuII; 4, BglII; 5, KpnI; 6, PstI; 7, CHO/BamHI. BstEII digested λ DNA was used as standard and sizes (in Kbs) are indicated.

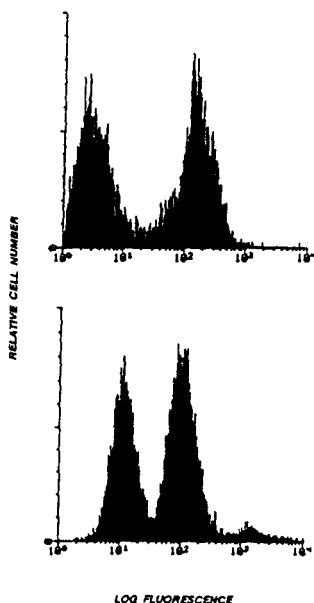


Figure 2 - Expression of CD2 antigen by the CHO transformed clone CL13 defined by the OKT11 mAb. Human T lymphocytes, upper panel; CL13 clone, lower panel. Each profile is overlaid with the negative control profile, derived by staining cells with the fluorescein-labeled goat anti-mouse IgG reagent alone.

These results support the aspect that only one copy has been integrated in the CHO genome given that no other hybridizing bands were detected. Furthermore, the molecular size of hybridizing bands excludes the presence of the vector as an episome. Moreover, KpnI does not cleave π H3-CD2 vector. Consequently, the absence of hybridizing band comparable to the molecular size of the plasmid (4.4 Kb) strongly support the aspect that π C3-CD2 vector is integrated in the CHO genome (Fig. 1). The results from this Southern blot suggest that the co-transformed clone CL13 contains only one copy of π H3-CD2 vector integrated in the CHO genome.

The transfected cells were further tested by titrating their bioresponse to low doses of radiation affecting the quantitative expression of the CD2 gene. The use of these transfectants as biological markers in response to low doses of X-irradiation and their ability to express the CD2 antigen on their surface in relation to dose level has been studied. It was found that very low doses of X-ray did not affect the level of CD2 antigen compared to unirradiated CL13 cells. As a tool of CD2⁺ phenotype we used a rosette assay (Politis et al. 1975) 24h after irradiation. It is of interest to note that the radioresistance of CD2⁺CL13 cells is demonstrable only within a narrow radiation dose range (Fig. 3). In contrast, the irradiated transfectants CL13 seem to be very sensitive and show a dramatic decrease by 50% of the CD2 antigen at 10 cGy (rads). Higher doses do not further affect the percentage of rosette forming cells. These results strongly suggest that the CD2 antigen is a very sensitive radiation marker. Support for this aspect comes also from preliminary results with human T lymphocytes. The influence of radiation effects on CD2 expression may be used as a very sensitive indicator of very low doses in conjunction with problems associated with the immune response of human T lymphocytes (Tuschl et al. 1990; Makinodan and James 1990).

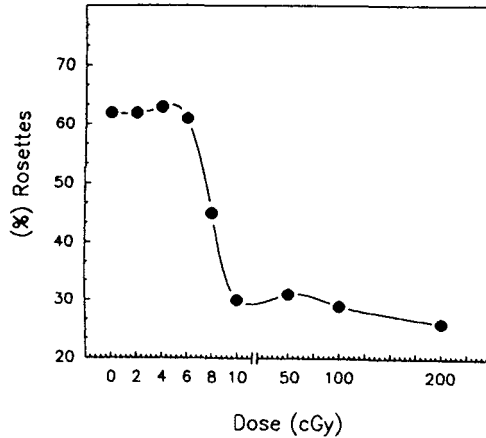


Figure 3 - Effect of X-ray radiation dose on the ability of transformed clone CL13 to form rosettes with SRBC.

In conclusion all the results presented support the aspect that the π H3-CD2 vector has been integrated into the CHO genome. The results from Figure 1 strongly suggest that π H3-CD2 vector is unable to replicate as an episome that allows the continuous replication and expression of the cloned foreign gene independently from chromosomal control. Moreover, it is indicated that the transfected CD2 antigen in CHO cells can, like its human T cell counterpart, interact with its specific ligand T11TS. This observation, taken together with the FACS data and the fact that CD2⁺CL13 cells preincubated with OKT11 Mab did not form rosettes with SRBC, provide strong evidence that the CL13 clone encodes the entire CD2 antigen, an aspect that is also supported by Chipstone and Crumpton (1988). So, the transfected gene product expressed on CL13 is quite comparable to that of CD2 antigen present on human T lymphocytes.

The results of X-irradiated transfectants suggest that this CD2⁺ clone might be a very sensitive indicator for doses as low as 2-10 cGy. The radioresistance of CD2⁺ clone in a narrow dose range (2-6 cGy) depicted in Fig. 3 may suggest that the CD2-cDNA remains intact. In contrast, the alteration of CD2⁺ cells to CD2⁻ at 10 cGy suggests that radiation affects either the CD2-cDNA and/or the gene(s) regulating its expression. Experiments towards this direction are in progress.

References

- Clipstone, N.A. and Crumpton, M.J., (1988) *Eur. J. Immunol.* 18:1541.
 Howard F.D., Ledbetter, J.A., Wong, J., Bieber, C.D., Stinson, E.B. and Herzenberg, L.A. (1981) *J. Immunol.* 126:2117.
 Huning, T. (1985) *J. Exp. Med.* 162:890.
 Makimodan, T., and James, S.J. (1990) *Health Phys.* 59:29.
 Politis, G., Plassara, M. and Thomou, H., (1975) *Nature*, 257:485.
 Tuschl, H., Kovac, R. and Wottawa, A., (1990) *Int. J. Radiat. Biol.* 58:651.

Publications

Thomou, H., Sambani, C., Kitsiou, P., Spanakos, G. and Politis, G. (1991) "Human Chromosome 19 Confers the CD2/E Rosette Receptor Phenotype in Interspecific Cell Hybrids", *Anticancer Res.* 11:1571.

Kitsiou, P., "Study of gene expression in stimulated human T lymphocytes: regulation of CD2 gene expression during the cell cycle", Ph.D. Thesis, University of Athens, 1991.

METHODOLOGY FOR THE ANALYSIS OF RADIATION CARCINOGENESIS STUDIES AND APPLICATION TO ONGOING EXPERIMENTS

Contract Bi7-035 - Sector B13

- 1) *Broerse* - Academisch Ziekenhuis Leiden - 2) *Chmelevsky* - GSF Neuherberg
3) *Masse* - CEA - FAR - 4) *Morin* - CEA - FAR
5) *Zurcher* - TNO - 6) *van Bekkum* - TNO-ITRI

Summary of project global objectives and achievements

Large scale animal experiments at various European institutes have been undertaken in the past decade. The information from different laboratories can be meaningfully combined if the experimental procedures and the pathology are closely coordinated to the methods of statistical analysis. Analysis of the tumour induction data reveals differences, which may be partly explained by a diversion of the cohorts under study, but are also believed to result from the employed analysis methods. In particular the different mathematical models, e.g. the parametric Weibull model versus the non parametric proportional hazards model have been under discussion. A unified approach to the analysis of experimental data of animal carcinogenic studies is the aim of this contract. To this aim a framework has been laid down for the analysis of dose-effect relationships in a concorded way for the existing data in Europe. A number of studies in experimental animals is included in the contract, to provide a database on stochastic effects after low dose irradiation.

- Within project 1 (Academic Hospital Leiden) the computer codes for LifePrep and LifeStat have been developed.
- In project 2 (GSF Neuherberg) new mathematical methods have been implemented with emphasis on estimations of the time-dependent tumour incidence rate.
- In projects 3 and 4 (CEA Fontenay-aux-Roses) detailed information has been collected on the dosimetry for neutron irradiations and observed tumours of various histological types.
- Within project 5 (IVVO-TNO Leiden) histological examinations of lesions induced after low dose gamma irradiations has been performed.
- In project 6 (ITRI-TNO Rijswijk) a new set of experiments has been analyzed indicating very small risks after fractionated exposure to low LET radiation.

Project 1

Head of project: *Dr. Ir. J. Davelaar, Prof. J.J. Broerse*

Objectives for the reporting period

Within the framework of the contract two computer programs have been developed: LifePrep connected with the creation of a database and LifeStat connected with the statistical analysis of the incidence data. The latest version of the computer program LifePrep with a program users guide was circulated to the participants of the contract in the beginning of 1992, whereas the final LifeStat version and its program users guide can be made available upon request. The LifeStat users guide includes a proposed structure on the data format, which permits efficient comparison of results between laboratories.

Progress achieved including publications

Animal experiments can provide information on the carcinogenic risk of exposure under different experimental conditions. The interpretation of tumour incidence data involves a sequence of procedures, including observation of lesions in the course of time, corrections for competing risks, histological classification of the induced tumours and mathematical analysis of the tumour incidence data. This sequence of procedures in order to derive dose effect relations is illustrated in figure 1.

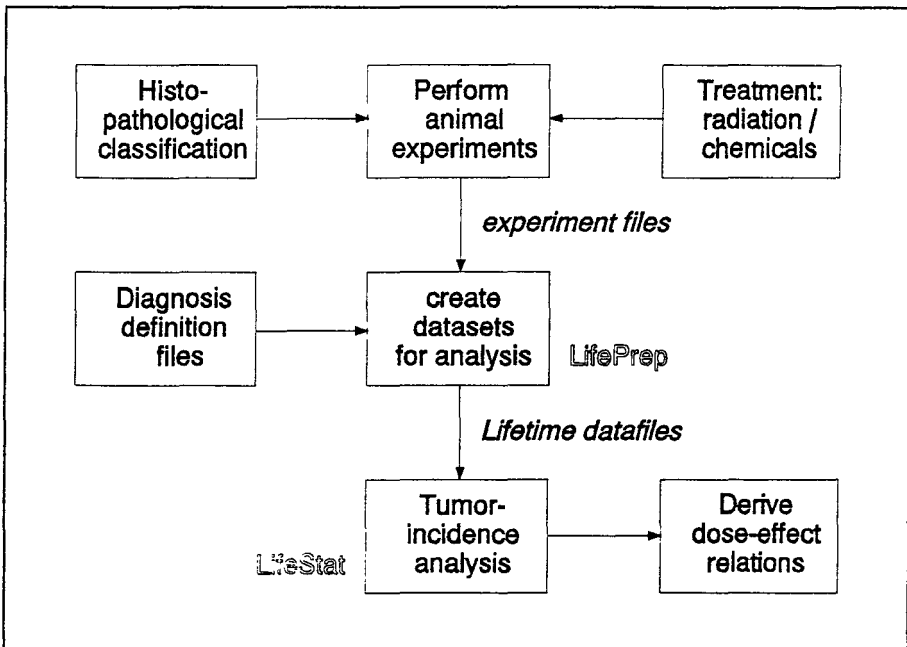


Figure 1

The interaction within the sequence of the programs LifePrep [1] and LifeStat [2] is also indicated in figure 1. The program LifePrep is designed to handle the following information for each animal:

- an animal identification,
- the age at death,
- a list of histological codes of the tumour types found by means of either palpation f.i. in the case of mammary tumours or a histo-pathological examination at obduction.

The above information in the format of a particular laboratory is rearranged by LifePrep to serve as input to the analysis program LifeStat. A structure for the obtained general input file to LifeStat is described in detail in the LifeStat program users guide. Animal experiment data given in this structure can be analyzed with LifeStat, which will permit a comparison of results on carcinogenesis from different laboratories with the same set of mathematical methods.

The LifeStat program is designed for analysis of tumour incidence data. Two types of observations are considered in LifeStat 3.00 for one animal: a time-to-failure or simply a failure, occurring at the incidence of a lethal or palpable tumour type. Right-censoring appears when no failures could be observed before the end of the follow-up period i.e. usually at the death of the animal. Each individual animal contributes to the group list of event times of failures and right-censors. LifeStat data will analyze several groups of animal data, each group consisting of event times that are linked to treatment parameters. The program permits separate and joined analysis of groups.

The following analysis tools are available in LifeStat:

Inventory of rough data:	list of treatment parameters and incidence data.
Kaplan-Meier:	actuarial analysis (product or sum limit).
Parametric:	Weibull functions, maximum likelihood or chi-square optimization, single dose or fractionated. Fitting parameters can be fixed or optimized as individual or common values. The relative hazard of the studied groups to the control group is calculated.
Non-Parametric:	The Cox' proportional hazards model assumes the cumulative tumour rate from one group to be proportional to another group. The cumulative tumour rate $H_i(t)$ for group i is proportional to $H_0(t)$, the base-line function of the reference group. The relative hazard and baseline function are calculated.
Miscellaneous:	directory for input and output files, time unit for display, printer type.
Graphics:	output device (screen, printer, plotfile), attributes for graphics setup.

The analysis methods described above have been applied to mammary tumour induction data from experiments on the WAG-Rij rats at ITRI-TNO to test the analysis tools and to make a comparison between parametric and non-parametric methods. For each cohort the control group has been taken in the same year of the experiment, since a statistically significant variation in the survivor function of the control groups of various years was observed. For both these control groups and the cohorts exposed to radiation the survivor time distribution $S(t)$ was best described by a Weibull function:

$$S(t) = \exp(-(t-\gamma)/\alpha)^b,$$

which is also found by the linear time dependence of $\log[H(t)]$, where the cumulative hazard $H(t) = -\log[S(t)]$. The parameters α , β and γ represent the time-scale, shape and time-offset in $S(t)$. A common β is usually assumed, whereas the time-offset is mostly taken zero. The forward shift in the exposed group is parametrized by $\alpha(t,D)$. The relative hazard $\eta(t,D)$ for the cohort exposed to dose D with respect to the control group is defined as:

$$\eta(t,D) = \alpha(t,0)/\alpha(t,D),$$

Figure 2 shows the relative hazard as a function of dose for the parametric Weibull analysis of three different cohorts of rats, exposed to total body gamma radiation: single dose at an age of 8 and 17 weeks respectively and 120 fractions given between 8 and 17 weeks. The relative hazard for the same cohorts from a non-parametric proportional hazards analysis is shown in figure 3. An excellent agreement is demonstrated between the parametric and non-parametric analysis methods.

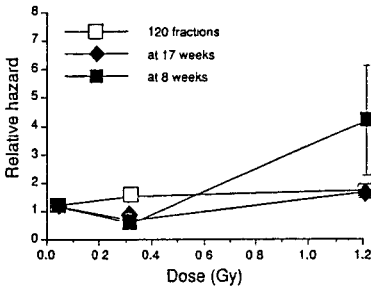


Figure 2

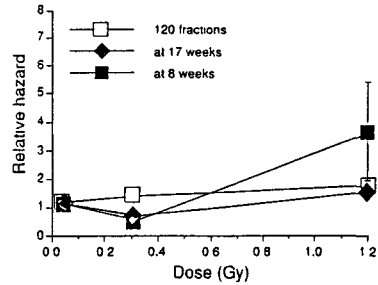


Figure 3

The analysis methods, developed under this contract, have also been applied to data from the long-lasting monkey experiment performed at TNO-Rijswijk since 1961. The monkeys were subjected to total body irradiation up to relatively high doses of both X-rays and neutrons, followed by a bone marrow transplantation. The late effects observed in the animals surviving more than 3 years include a number of neoplasms. Up to now the prevalence of animals with these induced tumours was quoted to be nine out of twenty over an observation period of 227 monkey-years for X-ray irradiated monkeys (average dose 6.7 Gy) and seven of the nine monkeys exposed to fission neutrons (average dose 3.4 Gy) during 87 monkey-years. In a control group of 21 animals two animals were observed with lethal neoplasms.

A detailed analysis with Lifestat serves a dual purpose: (i) a correction for the animals dying intercurrently from causes unrelated to the endpoint, being the induction of a tumour, (ii) the analysis of the distribution of tumour induction times will provide the most information on carcinogenicity for the two cohorts of monkeys. Figure 4 shows the cumulative hazard of the X-ray and neutron irradiated monkeys, corrected with the Kaplan-Meier product limit for intercurrent deaths, as a function of the follow-up time of the monkeys in years. The full

drawn lines represent maximum likelihood fits to the data on the basis of a Weibull function, which proves to be a good model for both the neutron and X-ray data. No common slope of the Weibull fits is observed however and the cumulative hazard has a steeper increase for X-rays with ultimately a crossover point at around twenty years. The derived RBE will vary markedly depending on the time of follow-up: close to 17 at ten years follow-up, decreasing to 5 at fifteen years and around 2 at twenty years.

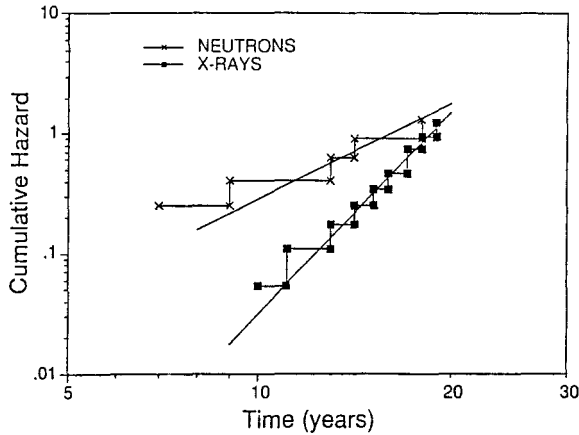


Figure 4

- (1) Weeda, J., Davelaar, J., Broerse, J.J., LifePrep 1.00 users guide, AZL January 1992.
- (2) Weeda, J., Davelaar, J., Broerse, J.J., LifeStat 3.00 users guide, AZL July 1992.
- (3) Davelaar, J., Weeda, J., Broerse, J.J., "Analysis of animal carcinogenesis data by various mathematical methods", Rad.Env.Biophys. 30, 249-252, 1991.
- (4) Broerse, J.J., Davelaar, J., Zurcher, C., "Tumour induction in animals and the radiation risk in man", Proceedings of the Symposium on Biological Effects and Physics of Solar and Galactic Cosmic Radiation, in press, 1992.

Project 2

Head of project: *Dr. Chmelevsky*

Objectives for the reporting period

Objectives of the reporting period have been the development and application of methods for the analysis of animal data.

Progress achieved including publications

We have together with the University of Leyden specified in the evaluation of animal experiments the conditions for performing data analyses which are properly corrected for competing risks. This includes to adequately characterize the nature of the data.

Tumors may be lethal or observable. This is in radiation carcinogenesis the most common situation.

The other type of data arises for tumors which are neither lethal nor observable. This is the situation for lung cancer in the rats. The tumors when observed i.e. at death for unrelated reason release the information that at the time of observation an animal had already a tumor. This is to be compared with the preceding situation where, at observation, the tumor is starting; before this time there was no tumor.

Although this distinction between two types of tumors may be too clear cut, it has to be considered, in an analysis, as guide line.

Independently of the nature of the tumors, the carcinogenic effect of radiation is quantified by estimating the rate of a given type of tumors as a function of time or age $r(t)$. Alternatively to the rate of a tumor, functions which are derived from $r(t)$ can be used. These are the integral tumor rate $R(t)$ or the tumor incidence $I(t)$.

According to the nature of the data, the basic functions will be estimated with quite different methods. We have, up to now, essentially defined and developed the methods appropriate for observable or lethal tumors. A software package has been developed in Leyden which includes a non-parametric estimation of $R(t)$ and $Z(t)$. This is the Kaplan-Meier or product limit estimate.

For a joint analysis of an experiment with several groups of animals, the Cox proportional hazards model has been adapted to the following simplified model:

$$r(D,t) = \alpha(D) r_0(t)$$

where α is a parameter, depending on D , which characterizes the increase on the rates due to irradiation. $r_0(t)$ is the rate of the reference group, i.e. a control group or an irradiated group which is assigned the parameter $\alpha = 1$. The parameter α is then a hazard factor which is estimated non parametrically, i.e. with no explicit dependence on dose (D).

As a special case of the proportional hazards model, the package allows an analysis on terms of the Weibull function i.e.:

$$r(D,t) = \alpha(D) t^\beta$$

then the base-line rates are assumed to be a power function of time (or of age).

As an alternative to proportional hazards models, and therefore for data which do not appear to follow the basic assumption of such models, the package includes the possibility of an analyse with log normal functions. These functions belong to the general class of accelerated time models. Unfortunately there is not, as with the proportional hazards model, a non parametric estimate of the accelerated time model.

Relevant Publications.

Mathematical methods in the analysis of animal experiments:

D. Chmelevsky, M. Morin: *Radiat. Environ. Biophys.* (1991) 30: 253 - 257.

Project 3

Head of project: *Dr. R. Masse*

Objectives for the reporting period

To propose standardization exposure to carcinogens and for autopsy protocols; to select histologic criteria accounting for classification of fatal and incidental tumors.

Progress achieved

Attention has been focussed on experiments carried out in controls and in animals exposed at low doses, for which no intercurrent cause of mortality due to irradiation would bias the conclusions. Additionally an attempt has been made to have a complete autopsy protocol carried out in rats exposed for a short time to a carcinogen (beryllium dust), with serial sacrifices and complete histopathology starting 18 months after exposure including 10 animals each month. This later experiment, launched in late 89, is still in progress; 300 rats were included. From the first observation we have obtained, this relatively neglected protocol seems to be promising in animals in which it is really difficult to decide whether the tumors are fatal or incidental in this respect that latency period can be determined with some accuracy. This was especially the case for lung and pituitary tumors. Complete results will be obtained in the next 6 months. At least a first conclusion to be drawn is that side groups, killed at chosen dates, should be included in life span studies to get information on this parameter and on early precancerous lesions. This was included in the last experiments performed at Battelle by F. Cross in the series exposed to radon and tobacco smoke.

Conventional lifetime experiments, with standardized protocols similar to those utilized by industry or NTP are suitable in most cases. We have noted the following unspecified requirements: there is a need for a sub total serial sectioning of the brain to have a precise idea of CNS system tumors. This makes a problem of archiving and of quality insurance since it may well be that no CNS tissue remain in formalin or in paraffin blocks. We have the same difficulties with thyroid whose tumors are mostly tiny. There is also some advantage (in terms of total tumors recovered) to proceed to serial sectioning of the lungs. All these points are to be taken in consideration for risk assessment schedules.

Table 1 provides the histological basic classification of spontaneous tumors in our strain. We did not notice significant differences all along the 10 years that made up our observation time. It does not mean that there is no individual sensitivity to tumor formation, but it suggests that we have only little influence of this parameter in this strain. It should be noted that metastases are rare in cancers, accounting for about 10%. A special case is the case of so called angiosarcomas all sites. It is possible that these tumors are misdiagnosed with angioblastic hamartomas with abnormalities, despite the low percentage of metastases however these tumors were often found hemorrhagic and the lifespan of animals bearing such tumors was relatively short (table 3 which summarizes controls and animals exposed to neutrons). Pituitary tumors are puzzling: histologically characterized tumors are found at later time than benign adenomas. This suggests that malignancy of pituitary tumors is not the cause of the death. In contrast central nervous malignancies are associated with shorter life span than benign tumors in the same tissue.

Table 2 which provides the total number of tumors in controls and exposed rats. A general conclusion to be drawn is the very narrow range of doses which can be explored without reaching exceedingly high number of tumors in the groups. Designing an experiment should therefore be done within one order of magnitude at most. Table 4 provides an answer as to whether life shortening due to tumor formation is to be corrected for in the range of low doses for occurrence of site specific cancers in the rat. In fact as a matter of simplification it appears that all tumors as a whole may be considered as incidental. At higher doses life shortening occurs in benign tumors and in malignancies. We have observed one group with a large excess of metastases due to irradiation: the low dose rate 1 Gy gamma group (Table 4), it was associated with some decreased lifespan suggesting that metastases are the real parameter to take in account for deciding incidental or fatal tumors.

Table 1 - Spontaneous tumors in Sprague-Dawley male rats.

	cancers	metastases	benign tumors
thyroid	88	4	41
skin and annexes	22	3	0
lymphosarcomas, leukemias	19	1	1
soft tissue sarcomas	18	3	68
adrenals	17	4	10
pituitary	13	0	16
central nervous system	11	1	5
angiosarcomas (all sites)	8	1	4
urinary (including bladder)	6	4	0
GI tract	6	2	1
lung	5	0	9
pancreas	5	0	2
salivary glands	3	0	0
genital system	2	0	0
mammary gland	2	0	11
bone	2	1	0
liver	1	0	2
others	3	0	0
total	231	24	170

Table 2 - Tumor number as a function of dose

	n rats	Dose	Tumors	
			benign	malignant
Controls	754	0	231	170
Neutron	300	0.016	158	57
(Triton)	158	0.08	109	22
	150	0.4	140	30
	101	1.5	102	30
	120	2.4	142	31
	80	3.5	87	17
	40	4.4	43	6
	40	5.6	37	9
	20	8.0	11	0
(Silene)	116	0.4	102	37
	80	1.15	116	73
	40	1.73	54	32
	104	2.0	176	23
	40	2.86	46	18
Gamma (Co 60)				
(1.34 mGy/h)	304	2.83	165	146
(78 à 100 mGy/h)	505	1.0	359	294
	120	3.0	87	41
	48	6.0	37	21
	30	10.0	27	6
	40	12.0	38	9
	20	13.0	12	6
	36	16.5	37	10
	40	18.0	27	11
	20	20.0	7	6
	20	26.0	11	1
	30	28.0	25	3
	20	31.0	1	0
	20	39.0	0	1

Table 3 - Time to tumor discovery (days) - Neutron (Triton).

Dose (Gy)	0.0	0.016	0.08	0.4	1.5	2.4	3.5	4.4	5.6	8.0
1- Carcinomas										
lungs	992	870	839	735	628	590	566	534	467	357
salivary glands	605	-	920	700	551	408	-	-	454	-
GIT	796	888	884	-	587	610	302	-	385	-
liver	901	708	488	644	674	639	-	-	269	-
pancreas	921	990	891	702	568	664	499	512	-	293
skin and annexes	778	863	822	596	596	550	532	534	449	314
mammary glands	810	984	-	638	555	469	547	532	494	-
genital system	801	835	755	655	637	620	494	-	303	-
urinary system	922	943	812	616	627	570	526	510	491	-
adrenals	857	867	854	757	692	615	595	479	-	-
teratocarcinomas	783	904	-	594	275	-	-	-	447	-
pituitary	960	1095	-	851	-	-	-	-	-	-
thyroid	900	942	825	723	627	590	583	565	-	-
2- Sarcomas and others										
central nervous system	735	845	-	427	-	466	473	-	-	-
bone	943	904	726	631	529	511	481	518	479	360
leukemia-lymphosarc	778	745	824	532	452	393	391	461	479	285
sarcomas (NOS)	782	832	667	735	681	528	500	508	549	-
angiosarcomas	817	798	640	607	495	552	499	460	431	-
soft tissue sarcomas	743	813	795	586	547	531	511	423	497	349
mesotheliomas	-	541	826	-	533	425	340	-	-	-
3- Benign Tumors										
lungs	936	931	745	702	651	563	503	462	457	-
salivary glands	-	-	-	619	-	-	-	-	-	-
GIT	1043	-	-	-	-	-	-	-	-	-
liver	903	-	-	-	-	-	-	-	-	-
pancreas	-	-	-	830	-	641	-	-	-	-
skin & annexes	884	986	-	673	537	568	-	-	-	-
mammary glands	852	1023	826	548	634	552	545	-	-	-
genital system	-	-	-	-	341	-	-	-	-	-
urinary system	-	-	-	-	-	470	-	-	-	-
adrenals	786	370	-	782	-	-	-	-	-	-
pituitary	845	-	-	-	-	-	-	-	-	-
thyroid	834	948	-	650	531	-	-	-	-	-
CNS	819	920	-	715	-	485	590	-	-	-
angioma	776	741	-	684	-	397	464	-	-	-
soft tissues	884	888	763	698	636	595	562	526	488	-

Table 4 - Lifespan and time to tumor discovery, and metastases in function of dose.

	Dose (Gy)	Lifespan (days)	Time to tumor onset		n metastases	% / all types
			malignant	benign		
Controls	0	837	813	868	23	10.5
Neutron (Triton)	0.016	838	848	882	15	9.5
	0.08	755	770	768	12	11.0
	0.4	642	648	697	19	13.6
	1.5	565	576	626	9	8.8
	2.4	536	552	581	7	4.9
	3.5	491	518	540	10	11.5
	4.4	471	490	483	8	18.6
	5.6	446	454	480	4	10.8
	8.0	329	328	-	4	36.4
(Silene)	0.4	638	635	678	11	10.8
	1.15	575	630	661	12	10.3
	1.73	536	563	609	8	14.8
	2.0	506	534	510	17	9.7
	2.86	541	579	573	4	8.7
Gamma (Co 60) (1.34 mGy/h)	2.83	726	740	774	47	28.5
(78 à 100 mGy/h)	1.0	789	839	831	28	7.5
	3.0	738	774	784	7	7.9
	6.0	657	668	723	2	5.3
	10.0	621	589	659	6	22.2
	12.0	591	596	710	1	2.6
	13.0	581	630	615	0	0
	16.5	548	581	604	7	18.9
	18.0	480	549	557	3	11.1
	20.0	425	474	499	3	42.9
	26.0	288	430	427	0	0
	28.0	480	551	589	3	12.0
	31.0	126	296	-	0	0

Project 4

Head of project: *Dr. M. Morin*

Objectives for the reporting period

- The first objective was to select appropriate exposure levels, to design the exposure facility and to decide on the protocol of exposure. Review had to be made on the spectrum of cancers and benign tumours found in the strain, with consideration to time to tumour onset, criteria for malignancy and for lethality.

Four series of rats were exposed to neutrons according to the following schedule.

Neutron exposure

	Number of rats	Start	Total Dose (cGy)	Dose Rate at beginning	Exposure Period	Age at beginning of exposure	Age at end of exposure
1 st series	150	6.91	2.5	950 μ Gy/h	26 hours	3 month	3 month
2 nd series	250	5.92	2.5	760 μ Gy/h	33 hours	14 month	14 month
3 rd series	250	2.91	2.5	3.58 μ Gy/h	1 year	3 month	15 month
4 th series	50	2.91	5.3	7.72 μ Gy/h	1 year	3 month	15 month

All irradiations were completed by July 1992.

Progress achieved including publications

1 - Methods

- Dosimetry

Series 1 and 2 were exposed at Arcueil ETCA, the californium 252 source was located at a distance of 2 meters and neutrons and gamma kerma (as of May 1992) appear in Figure 1.

Series 3 and 4 were exposed at Bruyères le Châtel according to the following protocol:

A californium source has been sealed up and installed at the top of a well pole at 2 meters above the basement in a circular room of 12 m in diameter. Animals are being continuously exposed with a daily interruption for cleaning and feeding of about 1 h per day, 6 days per week.

Dosimetric measurements performed by Dr Nguyen van Dat provided the following results in air.

Dosimetry Dose rate (μ Gy/h - January 1991)

Distance from the source (meter)	Total dose (CIRCE)	Neutron (Bubble dosimeter)	Gamma (Panasonic)
2.4	5.49	3.58	1.66
1.4	11.21	7.72	3.46

Rats were housed 5 in each aluminium cage, rotated once a week, at a given distance of the source in order to reach the following neutron doses.

- Animals

All animals were male Sprague Dawley rats. According to our previous experiments a significant reduction of cancer induction was observed in 1 year old rats as compared to 3 month old rats. Exposures protracted over a significant fraction of the life span call therefore for

checking the effect of aging.

In these series of experiments, age effect will appear by comparing the ratio for cancer induction in series 1 and series 2. Comparing series 1 and series 3 and 4 will provide an overall estimate of the dose protraction including dose rate and aging.

- Pathology

Up to now it is not possible to conclude since only a little fraction of the animals died during the 1991-1992 period of time.

	Dead rats	Start exposure
1 st series	9	19.6.1991
2 nd series	16	12.5.1992
3 rd series	51	15.2.1991
4 th series	10	15.2.1991

No dominant intercurrent disease occurred in the colony.

2 - A side experiment carried out on rats chronically exposed to alpha-emitting radon daughters is now achieved.

Lung cancers were checked for and results appear in the following table :

	<u>Radon exposure</u>			
	Number of rats	Total Dose (WLM)	Dose Rate (WL)	Incidence of lung carcinomas (%)
Controls	800	0	0	0.6
1 st series	500	25	2	0.6
2 nd series	500	25	100	2.2
3 rd series	500	25	150	2.4
4 th series	500	50	100	3.8

We observed a dose-effect relationship for lung tumour induction, but also a decreased effect at the lower dose rate. With a dose rate of 2 WL the lung carcinomas incidence was equal to the incidence of control rats.

Publication of these results is in preparation .

We may expect to have the whole study completed by the end of 1993.

From our experiments in rats exposed to radon we can exclude that inverse dose rate effect for cancer induction is a valid hypothesis in animals exposed to high LET radiations at low dose and low dose-rate.

Publications

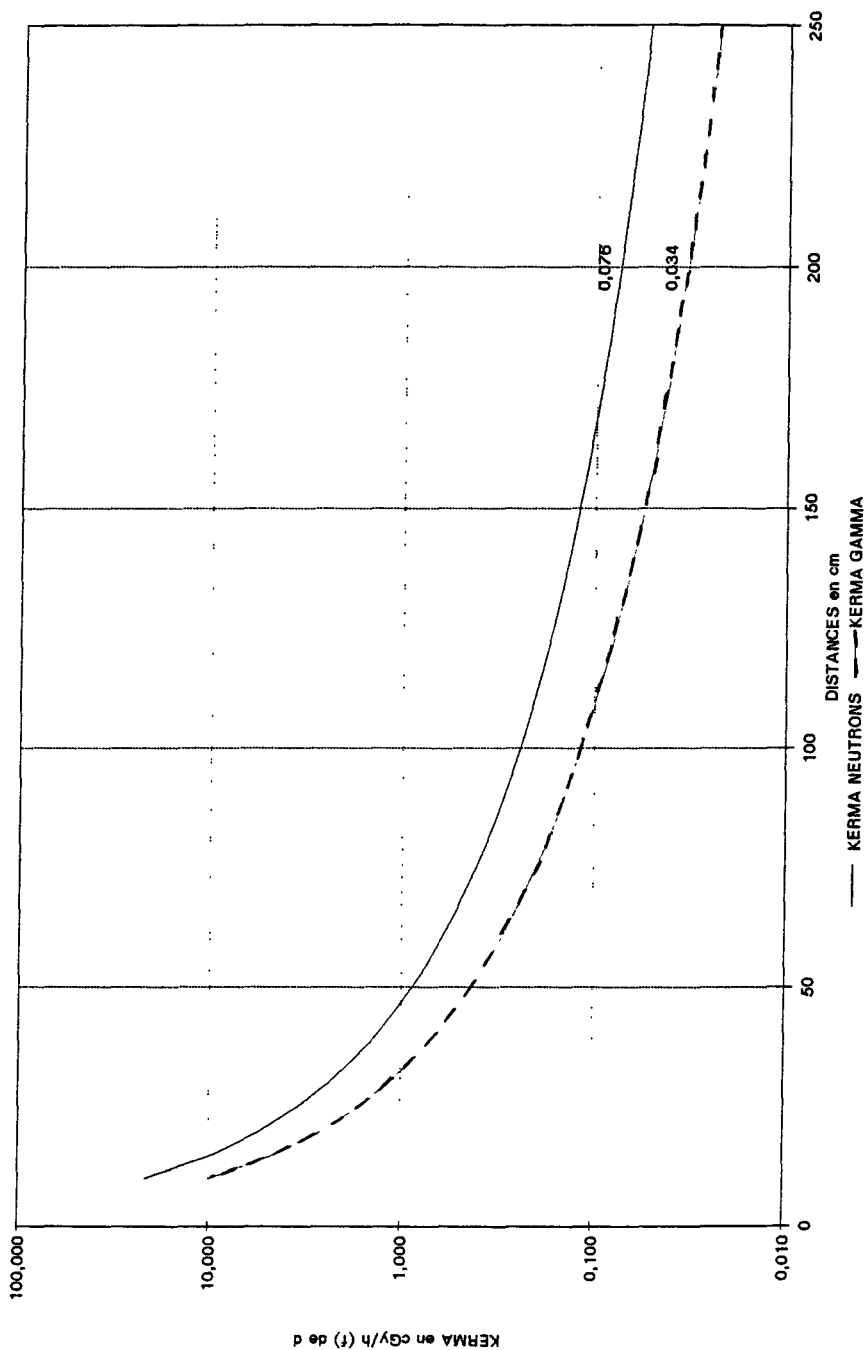
Chmielewsky D., Morin M., Mathematical models in the analysis of animal experiments, Radiation and Environmental Biophysics, 1991, 30, 253-257.

Masse R., Lung cancer in laboratory animals, Radiation and Environmental Biophysics, 1991, 30, 233-237.

Morin M., Masse R., Lafuma J., Rôle de l'âge au moment de l'irradiation sur l'induction des tumeurs, CR. Acad. Sc., t. 312, série III, p. 629-634, 1991.

Masse R., Morlier J.P., Morin M., Chameaud J., Lafuma J., Animals exposed to radon, 5th International symposium on the natural radiation environment radiation protection dosimetry, CEC, Salzburg-Autriche, 1991.

CAS N°8 CF252 RATS MAI 1992
 COURBES FIT NEUTRONS/GAMMA



Project 5

Head of project: *Dr. C. Zurcher*

Objectives for the reporting period

The main goal of this combined project was to make experimental data, gathered during late effects studies within several EC countries, intercomparable.

This could lead to a database of experiments performed within the EC and limit duplication of experiments.

A prerequisite for such a database is that the endpoints of late effect studies within the collaborating laboratories are standardized with respect to methodology and terminology. In carcinogenicity studies the endpoints are mostly reported in the form of pathology diagnoses. However diagnostic criteria and terminology are not always unambiguously defined making interlaboratory comparison of experimental data hazardous. Several nomenclature proposals and guidelines have been published, presenting either a structured system of names and codes for organs and lesions or defining diagnostic criteria to be used in animal pathology. Meanwhile, a generally accepted standardized nomenclature system for experimental animal pathology which is also suitable for use in electronic data processing is still lacking.

Two international endeavours have to be mentioned in this respect: one by the American Society of Toxicologic Pathologists (STP) and another by the Fraunhofer Gesellschaft sponsored by ILSI and WHO. Both systems of standardized diagnostic criteria for neoplastic disease in toxicologic pathology are not yet complete. They are to a large extent intercomparable due to a wide distribution of drafts all over the world and by the international representation of members of review committees.

During the present contract we used diagnostic terminology and criteria which were in accordance with drafts of STP if available.

Another aspect of standardization is related to the fact that the statistical evaluation of life time experiments requires an estimation of whether a certain lesion might have caused the premature death of the animal. The determination of the cause of death of aged animals dying at the end of their lifespan is a hazardous task. In many toxicologic laboratories a cause of death is determined by the judgement of the pathologist in charge and not formalized in defined criteria. Furthermore often no subdivision of probably fatal or contributing to the death of the animal is mentioned.

During the contract period we tried to define criteria used for distinguishing lesions in 4 categories relating to the cause of death as: nonfatal, probably nonfatal, probably fatal and fatal.

These criteria were applied when evaluating clinical condition, gross morphology and microscopic examination of completely necropsied rats from life long radiation carcinogenicity studies.

Progress achieved

Ascertaining the relationship between the death of an animal and the presence of individual lesions is of paramount importance for the statistical evaluation of lifelong carcinogenicity studies. Determining the cause(s) of death in laboratory rodents differs in many respects from

that in man. Apart from sacrifice of animals in a relatively good condition because of ethical reasons (e.g. painful or large tumors, skin ulcers etc.) and "spontaneous" death, the most frequent cause of death of rodents in lifespan experiments is the decision of the investigator to sacrifice the animal because he is considered to be "moribund". This conclusion is reached mainly because of a deteriorating general condition and the fear of the investigator that spontaneous death is imminent with ensuing loss of information because of rapidly progressive autolysis. Therefore, any lesion severe enough to lead to a decreasing general condition is associated with an increased risk of being sacrificed "moribund" and because of this, probably fatal. Another difference with the situation in man is the frequently insufficient clinical chemistry data. This means that determining the cause(s) of death heavily relies on postmortem gross and microscopic examination. A relationship between a specific lesion and cause of death cannot simply be deduced from the histological diagnosis. Knowledge about location, size and biological behavior are equally important. For instance, malignant tumors especially in rodents often are non metastasizing and do not necessarily lead to the death of the animal. Benign tumors on the other hand, e.g., large pituitary adenomas because of their intracranial localization, may represent lethal lesions.

The decision whether or not a lesion is fatal or contributing to the death of the animal (probably fatal) is to some degree always subjective and very much dependent on the judgement of the individual pathologist. The uncertainties involved make many pathologists reluctant to make such a decision unless the case is without any doubt. Therefore, attitudinal differences may have a great influence on intercomparability of studies performed in different institutes. This can be prevented by employing a set of well defined guidelines acceptable for most pathologists in making a decision between nonfatal, probably nonfatal, probably fatal and fatal lesions. By using clinical, gross necropsy and histological data we developed a protocol which allowed us to decide to what measure lesions contributed to the death of the animal (see table 1 and 2). Those lesions which were judged to have affected the general condition of the animal only to a minor extent were indicated as probably nonfatal. Lesions without any implication for the clinical condition (e.g. microtumors) were scored as nonfatal (incidental). The distinction between probably fatal and probably nonfatal is most important as it severely affects statistical evaluation.

This protocol was tested in about 200 rats from lifespan radiation carcinogenicity studies for its applicability. Two groups of irradiated rats each comprising 40 rats (1.2 Gy Single Dose (SD) and 1.2 Gy Fractionated Dose (FD) at 8 weeks) were evaluated in greater detail. In these groups in total 270 tumors (136 SD, 134 FD) were observed. Scoring of the cause of death was consistent between 3 pathologists for > 95%. For both experimental groups one third of these tumors were scored as fatal or probably fatal. Sixty percent of these fatal or probably fatal tumors appeared to be benign tumors. Within this group of benign tumors pituitary adenoma was the most frequent diagnosis (40%). Mammary gland tumors were the next most common in the fatal or probably fatal category. The majority (60%) of these mammary gland tumors were benign. These and other causes of death expressed as a percentage of neoplastic and nonneoplastic lesions together are presented in table 3. In lifespan studies multiple pathological changes are to be expected. In both groups mentioned before 270 tumors were observed in 80 rats (i.e. 3.5 tumor/rat). It appeared that often not a single lesion could be incriminated as being the cause of death. In the category probably fatal, multiple candidates were often present (ranging from 1-3, mean 1.5/rat). In the category fatal this was maximally 1 (range 0-1, mean 0,25).

In conclusion:

- * A protocol for estimating certain neoplastic and non neoplastic lesions as fatal or probably fatal was developed.
- * Scoring was reproducible between different pathologists in a series of 200 rats.
- * Preliminary results obtained in lifespan radiation carcinogenicity studies revealed:
 - a. one third of all tumors belonged to the category fatal or probably fatal.
 - b. 60% of the tumors from this category were benign.
 - c. pituitary adenomas and mammary tumors were the most common tumors contributing to the death of the animal.
 - d. 98-99% of the rats necropsied at the end of their lifespan exhibited lesions in the category fatal or probably fatal. Clearcut fatal lesions were observed in 26% of the rats.
 - e. nonneoplastic lesions did not feature as important fatal or probably fatal lesions. They were present amongst other (neoplastic) lesions in 22% of all rats.
- * The data obtained in the 200 rats examined thus far and of those from the extended contract (920040) will be evaluated statistically, using the software developed by the AZL group (Davelaar, cs).

Table 1

Protocol for determining lesions as fatal or probably fatal

Parameters	Determinants for categorization as fatal or probably fatal		
clinical condition	good	signs of clinical disease (deteriorating general condition/ moribund)	
reason for sacrifice	↓ painfull or large (≥5cm) tumors skin ulcers	↓ bad general condition	
gross and microscopic findings:	[large benign or malignant tumor skin ulcer]	↙ lesions which could explain specific clinical condition, e.g., pituitary tumors ≥0,5cm causing head tilt	↘ lesions which most probably compromised the general condition, e.g., pituitary tumors ≥0,5cm, without clearcut neurological symptoms
<u>Categorization</u>	↓ fatal	↓ fatal	↓ probably fatal

Table 2

Criteria used for the classification of lesions as fatal or probably fatal, according to clinical -, gross necropsy -, and histological findings

LESIONS	CAUSE OF DEATH CATEGORY	
Neoplastic (T)	Fatal	Probably fatal/ contributory to death
pituitary T	≥0.5cm + clin.sympt	≥0,5cm without neurol.dis.
medullary thyroid T	-	large, and inhibiting air passage
adrenal T	-	large tumor with extensive necrosis/hemorrhage/metastasis
mammary T	≥5cm <5cm, ulcerating	tumors with extensive necrosis/hemorrh./metastasis
brain/meningeal T	with neurological symptoms	compression/invasion/ destruction of brain tissue without overt neurol. sympt.
other tumors	painful, inhibiting vital functions, as evident from clinical condition	extensive necrosis/hemorrhage/ metastasis
Nonneoplastic		
reactive/ inflammatory/ degenerative/ lesions	inhibiting vital functions, as evident from clinical condition [eg, severe pneumonia, abdominal hemorrhage, enteritis with diarrhea, meningo-encephalitis with neurol. sympt.	severe inflammatory lesions, abscessation, necrosis, hemorrhage, etc, without directly related clinical symptoms

Table 3

Frequency of fatal and probably fatal neoplastic and nonneoplastic lesions in lifelong studies in female WAG/Rij rats

	%*
<u>Neoplastic (T)</u>	
- pituitary T	34
- mammary gland T	24
- uterine T	10
- hemolymphoreticular T	7
- brain/meningeal T	4
<u>Nonneoplastic</u>	
- degenerative/necrotic liver lesions	6
- clitoral gland abscessation	6

* percentage of all (neoplastic as well as nonneoplastic) fatal or probably fatal lesions

Project 6

Head of project: *Prof. D.W. van Bekkum*

Objectives for the reporting period

Many uncertainties remain concerning the carcinogenic effects of very low doses of gamma-radiation and the effects of fractionation. The problem is that tumour incidence following exposure to total doses below 0.5 Gy can not be measured accurately, because the number of animals required is prohibitive. We attempt to solve this dilemma by investigating the induction of mammary tumours after exposure to a large number of very low dose fractions (fraction dose 2.5 and 10 mGy) with intervals of 12 hrs to a total dose of 1 and 2 Gy. This study offers a unique opportunity to collect data on the carcinogenic effects of very low dose fractionation as compared to a single high dose. It is envisaged that the results will provide experimental evidence concerning the question of the existence of a threshold for radiation carcinogenesis.

Progress achieved including publications

As reported previously, the radiation exposures of all groups of rats have been completed by the end of 1990. Observation and analysis have continued during the report period. By the end of 1991 a significant proportion of all groups was still surviving as expected. Autopsies of animals found dead and of animals sacrificed because of poor general conditions was performed according to the protocol and histological analysis of detected tumours is made as the preparations become available. It is expected that most if not all the experimental groups will die out during 1992 and that the processed results will be available in 1993.

Data from a similar study which involved treatment of the rats with estradiol-17 beta (E_2) have now become available and have been partly analyzed.

In this study fractionated irradiations were performed with doses of 2.5, 10 and 30 mGy per fraction administered with 12 hours intervals. The exposures were continued to accrue total doses of 1 and 2 Gy. The maximum period for the protracted irradiations was 400 days. Singled dose irradiations with 0.3 and 1.2 Gy gamma radiation were included as reference points. In general, the animals were introduced to the total body exposure regimen at the age of eight weeks, except for two additional groups receiving single doses at the age of 17 weeks to investigate the age factor in the groups exposed to the fractionated irradiation over a period of 60 days. Increased hormone levels were achieved by subcutaneous implantation of a estradiol-17 beta pellet containing 2 mg of E_2 in a paraffin-cholesterol base at the age of six weeks.

Identical sets of tumour induction data have been analyzed with a parametric Weibull function optimized via the maximum likelihood method, as well as with the non-parametric proportional hazards model. The results using the two methods were similar within the statistical uncertainties, indicating the appropriateness of both models.

The relative hazard for total doses of 1 and 2 Gy delivered in the three different fractionation regimens are shown in Figure 1. With fraction sizes of 2.5, 10 and 40 mGy administered with intervals of 12 hours the total dose of 2 Gy was reached after time periods of 400, 100 and 25 days, respectively. For reasons of comparison the results of the single dose irradiations with 1.2 Gy of hormone treated animals are included. For the fractionated irradiations with 25 and 10 mGy per fraction no increase in the relative hazard had been observed at a total dose of 1 Gy.

From these and previous studies the following conclusions can be drawn:

1. For fractionated irradiation with fraction sizes of 2.5 and 10 mGy the values for increased hazards are too small to be of statistical significance.

2. The susceptibility for tumour induction is considerably reduced when the irradiation is performed at an older age.
3. The relative hazards for radiation-induced mammary carcinomas are higher in the hormone treated animals than in the normal animals.
4. For mammary carcinogenesis in the rat approximately quadratic dose response curves are observed for the single dose and fractionated irradiations, indicating appreciably smaller risks per unit dose in the low region in comparison with the higher dose results that are generally used as a basis for extrapolation.

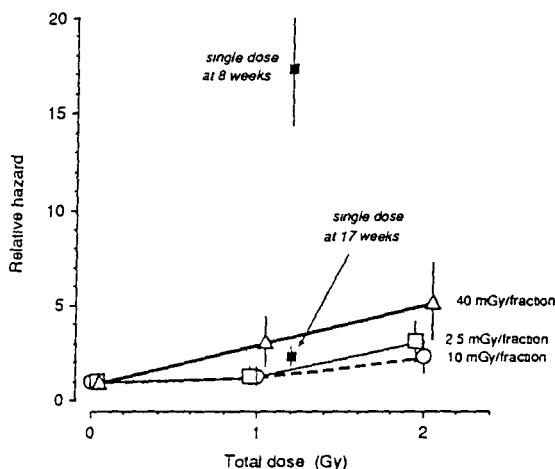


Figure 1: Relative hazard for mammary carcinomas in WAG/Rij rats treated with E_2 and fractionated doses of 2.5, 10 and 40 mGy gamma irradiation. For reasons of comparison the results for single dose irradiations at an age of 8 and 17 weeks are included.

Publications

1. Broerse, J.J. and Van Bakkum, D.W. Animal models of radiation carcinogenesis and developments in molecular biology. *Radiat. Environ. Biophys.* 30, 161-163, 1991.
2. Van Bakkum, D.W. and Broerse J.J. Induction of mammary tumours by ionizing radiation. *Radiat. Environ. Biophys.* 30, 217-220, 1991.
3. Broerse, J.J., Van Bakkum, D.W., Zoetelief, J. and Zurcher, C. Relative biological effectiveness for neutron carcinogenesis in monkeys and rats. *Radiat. Res.* 128, S128-S135, 1991.
4. Broerse, J.J., Davelaar, J., Weeda, J., Bartstra, R.W. and Van Bakkum, D.W. Mammary carcinogenesis in the rat after low-dose irradiation. *Proc. Int. Conf. on Effects of Low Dose Irradiation and Biological Defense Mechanisms*. Kyoto, 1992, in press.

STUDY OF RADIOBIOLOGICAL EFFECTS AT LOW DOSES

Contract Bi6-004 - Sector B13

1) Coppola, ENEA-CRE Casaccia

Summary of project global objectives and achievements

The aim of the contract was to gain knowledge and understanding of the biological action of radiation and to tackle specialized problems relevant, in the context of radiological protection, to the assessment of radiological risks at low doses. In general terms, the contractual activity included the study of the biological effectiveness of low radiation doses *in vivo* and *in vitro*, also with respect to interaction mechanisms. This represents part of an extended programme that the ENEA has in progress aiming at studying the dose-effect relationships at low level exposures to various noxious agents, and in particular to different radiation qualities for various modes of irradiation, using appropriate experimental model systems for well identified endpoints, including life-shortening and tumour induction in experimental animals as well as neoplastic transformation of immortalized cell lines.

In this respect, the late biological effects of fast neutron irradiation were considered a particularly interesting problem to investigate experimentally, as no suitable estimate of neutron RBE for cancer mortality can be derived from the available human data. Differences in susceptibility to tumour induction by radiation of various organs and tissues, together with the observation of the shapes of the dose-response relationships at low doses, also called for careful consideration. Furthermore the variation of carcinogenic effectiveness consequent to dose fractionation deserved particular attention. Study of the influence of exogenous or host factors, able to modify the neutron RBE, was also considered a qualifying aspect of this project.

To these aims, irradiation of BC3F₁ and CBA/Cne mice, with low to intermediate doses of fission spectrum neutrons and X rays, was planned, and is partially completed, using various irradiation protocols, including acute and fractionated dose exposures. Experimental data are still being collected and analyzed both with respect to after-irradiation survival and induction of a number of selected tumour types. The results collected up to now show a striking age dependence for neutron-induced liver tumours in BC3F₁ mice. In addition, a preliminar evaluation of the available data for these hybrids suggests no marked dose-rate effect on tumour induction, apart from myeloid leukaemia. This calls for further investigation using CBA/Cne animals, as they show higher susceptibility to induction of myeloid leukaemia.

Since transformation of normal into malignant cells is a prerequisite for the induction of cancer, the understanding of the mechanisms governing this process may shed much light on the problem of radiation carcinogenesis. Therefore, we have investigated *in vitro* some aspects of the radiation induced neoplastic transformation of mouse embryo fibroblast C3H10T1/2 cell system, also in a cooperative effort with a group of European laboratories aiming at the standardization of experimental methods and protocols. This system allows a closely quantitative determination of the dose-effect relationship for this endpoint. Our attention was mainly focused on the effect on transformation of dose fractionation of various radiation qualities, including fission spectrum

and monoenergetic neutrons. This interest was triggered by the possibility that fractionated doses or low dose rates would enhance the transforming potential of neutron in the dose range of 0 to 1 Gy, compared to acute exposures. The results indicate that with the experimental protocols adopted and within the experimental uncertainties neither direct nor inverse dose-rate effect is seen, regardless of the number of fraction or time between fractions, and independently of neutron quality.

For the interpretation of radiobiological experiments the knowledge of the microscopic distribution of energy deposition remains of a primary importance. Therefore studies have been pursued on the complete microdosimetric characterization of the radiation fields used in our work.

Because of the long lasting experience of the ENEA group in the field of late somatic effects of radiation, and the existence at Casaccia Centre of adequate irradiation facilities and animal housing, as well as well equipped laboratories for cell cultures, collaboration with other European groups interested in the study of radiation carcinogenesis is actively running.

It is also worth mentioning that, since animal experiments require long planning times and have very long duration, the research lines cited in this programme extend of necessity beyond the limits of time covered by a single contractual term.

Project 1

Head of project: *Prof. Coppola*

Objectives for the reporting period

- Age dependence of liver tumour induction in mice after acute whole-body irradiation.
- Effect of dose fractionation of neutrons of various radiation qualities on the neoplastic transformation of C3H10T1/2 cells irradiated *in vitro*.
- Carcinogenic effect of fractionated low doses of fission neutrons in irradiated BC3F₁ mice from the observation of various induced tumour types.
- Acute irradiation of CBA/Cne mice for studies of myeloid leukaemia induction at low doses.
- Ovarian tumour induction, in respect to hormonal imbalance, by partial body irradiation of BC3F₁ mice.
- Experimental and theoretical studies of the microdosimetric characteristics of the neutron radiation field of the fast research reactor RSV-TAPIRO at ENEA Casaccia Research Centre in different irradiation geometries.

Progress achieved including publications

The present programme was mainly based on the use of low doses of different radiation qualities and various modalities of irradiation on different experimental model systems, for suitable endpoints, including life-shortening and tumour induction in experimental animals.

We had already shown that liver tumours can be induced in mice exhibiting either a high or a low spontaneous incidence, namely 67% in CBA/Cne, and 11% in BC3F₁. Based on these findings, we have then investigated the influence of radiation quality and age-at-irradiation (17.5 days *post coitum*, 3 months, 19 months) on the induction of liver tumours by radiation preferably in BC3F₁ male mice. Irradiations were performed with fission spectrum neutrons from the RSV-TAPIRO reactor (mean energy 0.4 MeV in terms of kerma, γ -ray contamination 13%, $\bar{y}_D=51$ keV/ μ m measured at $d=2$ μ m for the total radiation field, dose rate 0.4 cGy/min), and with 250 kVp X rays (HVL=1.5 mm Cu).

A marked age-dependence of the frequency of induced tumours was found with a much higher susceptibility in young than in old mice. In the dose range where the risk appears to increase as a function of the dose, the experimental points after fission neutron irradiation were well fitted assuming a linear dependence of the incidence on the dose, with the values of the linear term coefficient ranging from a maximum of 1.18 per Gy for prenatal irradiation to a minimum of 0.03 per Gy for mice irradiated at 19 months of age, with an intermediate value of 0.35 per Gy for young-adult mice (Fig. 1). In the case of X-ray irradiation the dose-response data were adequately described assuming a quadratic dose dependence. Here the values of the coefficient of the quadratic term are fairly close to each other for the *in utero* and 3-month-old irradiated animals (1.7 and 1.2 per Gy², respectively), and not significantly different from zero for old mice.

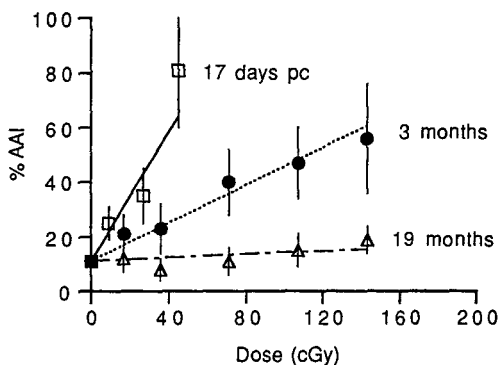


Fig. 1. Percentage age-adjusted incidence (AAI) of liver tumours in mice irradiated with fission neutrons at various ages. Bars are standard errors.

Age-dependence also appears to affect neutron RBE relative to X rays for the induction of liver neoplasms. In fact, the RBE value for prenatal irradiation (28 at 0.09 Gy) is about two times higher than for young adult animals irradiated at comparable low doses (13 at 0.17 Gy).

In order to obtain experimental evidence on the influence of exposure prolongation (low dose-rate or fractionation) on the effectiveness of low neutron doses, an *in vivo* study of the carcinogenic effect of fractionated doses of fission neutrons was undertaken. About 1200 BC3F₁ male mice, subdivided in 9 groups, were given each five equal daily dose fractions, corresponding to cumulative doses of 2.5 to 70 cGy of fission neutrons from the RSV-TAPIRO reactor. Irradiated and control animals were followed-up for their entire life span. Soon after spontaneous death a complete autopsy was performed. The necropsy included a complete external and internal gross examination. Tissue masses as well as sections of the major organs were taken and processed for histological analysis. Experimental data analysis is now complete with respect to life-span shortening, while it is still in progress for the induction of a number of selected tumour types, including malignant lymphoma and myeloid leukaemia. Data treatment includes the correction for competitive risks and the analysis in terms of cumulative mortality, death-rates for specific causes, and trend. A comparison is being carried out with data for acute exposure of BC3F₁ mice at comparable doses of fission spectrum neutrons, for critical endpoints.

The analysis of the decrease in mean survival time in animals irradiated with neutrons indicates that the life shortening is reasonably correlated linearly with increasing dose in the interval from 0 to 71 cGy (Fig. 2). From the Figure it is evident that there is no consistent increase in the magnitude of the life-span shortening if neutron doses are fractionated. Assuming as the baseline the effect of acute X rays, neutron RBE values result to be 5.6 ± 0.9 and 5.2 ± 1.2 for acute and fractionated doses, respectively. Cumulative mortality data have been fitted by the Weibull model, and the mortality patterns compared after fractionated or acute irradiation at each dose level. The modality of treatment had only a scarce and erratic influence on the mortality curve shape in all cases.

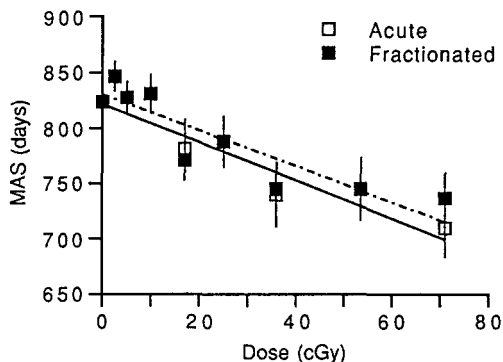


Fig. 2. Mean aftersurvival time (MAS) of animals irradiated with acute (solid line) and fractionated (broken line) fission neutrons.

Pathology data are still preliminary and incomplete. From those available we do not observe any marked influence of the time mode of irradiation on tumour induction. Only in the case of myeloid leukaemia the initial slope of the dose-response curve for multi-fractionated neutron doses appears consistently higher than for acute doses up to about 30 cGy. However, this lesion is absent in the controls and a very rare event in irradiated BC3F₁ mice. Under these circumstances it is unlikely that a conclusion about an enhanced leukaemogenic effect of neutron dose fractionation can be drawn. For these reasons further investigation using CBA/Cne mice have been initiated, as these animals show higher susceptibility to induction of myeloid leukaemia.

Research on *in vitro* effects of ionizing radiation carried out at ENEA Casaccia has been supported up to now by contract Bi6-004. However, during 1990 it was decided to establish a cooperation with the group of five European laboratories which had received a CEC Contract for "Measurement of transformation of C3H10T1/2 cells by low doses of ionizing radiation", in order to exchange more readily results and information, and to collaborate to the attempt of standardizing experimental methods and protocols. This participation did not require any extra financial support to our team by the CEC during the period 1990-92. However, since for the sake of coherence of presentation it has been decided to describe the details of the progress achieved in this cooperation under contract Bi7-043, project 6, the same will not be repeated here, and the reader is invited to refer to the final report of that contract for information. Here we only summarize the main results of our investigations carried out with reactor fission spectrum neutrons and monoenergetic neutron beams. They show that a) the survival curves after neutron irradiation are very nearly exponential for both acute and fractionated exposures and there is no appreciable effect of dose fractionation; b) dose fractionation does not modify significantly the transformation rate compared to acute irradiation; c) in the low-dose region, cell transformation frequency is very nearly linear with the dose for exposure either to neutrons or X rays; d) maximum values of fission neutron RBE relative to X rays determined from survival and transformation data are in the region of 14 to 16, in close agreement with those obtained by other laboratories.

Since the RSV-TAPIRO reactor is routinely employed by ENEA laboratories and associated research groups for radiobiological experiments using fission neutrons, the characterization of the radiation fields at the biological

facilities was carried on in collaboration with the University of Saarland. In this work, microdosimetric measurements were performed in the different field configurations by means of a 1/2" Rossi counter and the characteristics of the facilities described in terms of distribution of the lineal energy and the related average quantities for the total field and the neutron component.

Finally, further investigation was conducted on the dependence of the frequency ratio of acentrics to dicentrics produced in human lymphocytes on treatment with radiation, misonidazole (a cell sensitizing chemical compound) and the combination of the two agents. This confirmed the previous finding that this ratio is markedly influenced by the presence of the chemical substance, especially at low radiation doses.

Publications

- 1) V. Di Majo, M. Coppola, S. Rebessi, V. Covelli. Age-related susceptibility of mouse liver to induction of tumors by neutrons. *Radiat. Res.* 124, 227-234, 1990.
- 2) V. Covelli, M. Coppola, V. Di Majo, S. Rebessi. The dose-response relationships for tumor induction after high-LET radiation. Proceedings of the International Symposium on Radiation Carcinogenesis in the Whole-Body System, Tokyo, December 4-7, 1990. In Press.
- 3) A. Saran, S. Pazzaglia, M. Coppola, S. Rebessi, V. Di Majo, and V. Covelli. Neoplastic transformation of C3H10T1/2 cells following single or fractionated doses of fission spectrum neutrons and X rays. 38th Annual Meeting of Radiation Research Society, New Orleans, April 1990 (Book of Abstracts, Abstract Eo-3, p. 183).
- 4) S. Pazzaglia, A. Saran, M. Garavini, M. Coppola, S. Rebessi, V. Di Majo, and V. Covelli. Absence of a dose-fractionation effect in the transformation of C3H10T1/2 cells by fission spectrum neutrons. III Italian-Yugoslav Symposium, Plitvice, June 1990.
- 5) V. Di Majo, S. Rebessi, M. Coppola, V. Covelli. Induction of liver tumors by X rays and fission neutrons in hybrid mice (BC3F₁). 38th Annual Meeting of Radiation Research Society, New Orleans, April 1990 (Book of Abstracts, Abstract Cw-3, p. 102).
- 6) A. Saran, S. Pazzaglia, M. Coppola, S. Rebessi, V. Di Majo, M. Garavini, V. Covelli. Neutron dose-fractionation does not enhance neoplastic transformation of C3H10T1/2 cells. 23rd Annual Meeting of the ESRB, Dublin, September 1990.
- 7) V. Covelli, V. Di Majo, M. Coppola, and S. Rebessi. Dose Response Relationships for Lymphoma and Skin Cancer in Mice after Total Lymphoid Irradiation (TLI). 23rd Annual Meeting of the ESRB, Dublin, September 1990.
- 8) N. Vulpis, and M. Coppola. Ratio of acentrics to dicentrics in human lymphocytes exposed to X rays and misonidazole. *Mutation Research* 245, 107-110, 1990.

- 9) A. Saran, S. Pazzaglia, M. Coppola, S. Rebessi, V. Di Majo, M. Garavini and V. Covelli. Absence of a dose-fractionation effect on neoplastic transformation induced by fission spectrum neutrons in C3H10T1/2 cells. *Radiat. Res.*, 126, 343-348, 1991.
- 10) A. Saran, S. Pazzaglia, M. Coppola, S. Rebessi, V. Di Majo, J.J. Broerse, J. Zoetelief, and V. Covelli. Neoplastic transformation of C3H10T1/2 cells by single and fractionated doses of monoenergetic neutrons. In: Proc. of Workshop on Oncogenic Mechanisms in Radiation-Induced Cancer. Fort Collins, USA, January 1991.
- 11) M. Coppola and N. Vulpis. Chromosome aberrations and radiosensitizers. In: *New Horizons in Biological Dosimetry* (B.L. Gledhill and F. Mauro eds.), pp 413-421. Wiley-Liss, Inc., New York, 1991.
- 12) V. Di Majo, M. Coppola, S. Rebessi, A. Saran, S. Pazzaglia and V. Covelli. Do multifractionated neutron doses enhance mortality in mice? Proc. of 9th International Congress of Radiation Research, Vol. I, p. 437, Academic Press, San Diego, 1991.
- 13) A. Saran, S. Pazzaglia, M. Coppola, S. Rebessi, V. Di Majo, J.J. Broerse, J. Zoetelief, and V. Covelli. Neoplastic transformation of C3H10T1/2 cells by fractionated doses of monoenergetic neutrons. Proc. of 9th International Congress of Radiation Research, Vol. I, p. 345, Academic Press, San Diego, 1991.
- 14) M. Coppola, V. Di Majo, S. Rebessi and V. Covelli. RBE modifying factors. Proc. of 7th Symposium on Neutron Dosimetry, Berlin, 14-18 Oct., 1991. In Press.
- 15) V. Covelli, V. Di Majo, M. Coppola and S. Rebessi, S. Neutron carcinogenesis in mice: a study of the dose-response curves. *Radiat. Res.* 128, 114-116, 1991.
- 16) M. Coppola. How to model radiation carcinogenesis? In: *Biophysical Modelling of Radiation Effects*, pp 339-342. Adam Hilger, Bristol, 1992.
- 17) M. Coppola and V. Covelli. Experimental models for ionizing radiation carcinogenesis. Proc. of International Workshop on Recent Advances in Human Radiobiology. Ferrara, Sept. 1991. In Press.
- 18) M. Coppola. Modelli matematici in radiobiologia. Scuola Superiore dell'Associazione italiana di Fisica Biomedica: Effetti biologici in radioterapia. Como, Novembre 1991. In Press.
- 19) V. Di Majo, S. Rebessi, M. Coppola, A. Saran, S. Pazzaglia and V. Covelli. Are somatic effects of low neutron doses detectable *in vivo*? The International Conference on Low Dose Irradiation and Biological Defense Mechanisms. Kyoto, July 1992. Accepted for presentation.
- 20) V. Di Majo, S. Rebessi, M. Coppola and V. Covelli. Induction of tumors in hybrid mice (BC3F₁) after multifractionated neutron doses. Radiation Research Society, 40th Annual Meeting. Salt Lake City, 1992.
- 21) A. Saran, S. Pazzaglia, L. Pariset, M. Coppola, V. Di Majo, S. Rebessi and V. Covelli. Dose fractionation dependence of C3H10T1/2 cell transformation by fission spectrum neutrons. Radiation Research Society, 40th Annual Meeting. Salt Lake City, 1992.

- 22) P. Pihet, M. Coppola, T. Loncol, V. Di Majo and H.G. Menzel. Microdosimetry study of radiobiological facilities at the RSV-TAPIRO reactor. Seventh Symposium on Microdosimetry. Gatlinburg, Sept. 1992. Accepted for presentation.

LATE EFFECTS IN RHESUS MONKEYS AFTER WHOLE-BODY IRRADIATION WITH X-RAYS AND FISSION NEUTRONS

Contract Bi6-075 - Sector B13

1) *Broerse* , TNO-ITRI

Summary of project global objectives and achievements

The experience on late effects in man after accidental exposure to high doses of total body irradiations is only based on a limited number of cases. In the medical area total body irradiation (TBI) followed by bone marrow transplantation is the treatment of choice today for many patients with haematological malignancies and severe congenital or acquired disorders of the haemopoietic system. However, specific information related to the risk of radiation induced tumours and other late effects in man is limited. Studies on acute and late effects in non-human primates are relevant for man since the radiation effects in both species do not seem to show significant differences. This type of studies with larger animals are valuable for risk assessment in man and for estimation of the relative biological effectiveness (RBE) for tumour induction by neutron irradiation of human patients. In addition, the induction of deterministic effects in various tissues and the RBE of neutrons for these effects are of increasing importance for radiation protection problems. The response of rhesus monkeys after exposure to relative high doses of X-rays and fission neutrons has been investigated. The protective effect of autologous bone marrow transplantation was initially demonstrated, however, new research has shown an increasing importance of the application of haemopoietic growth factors. The study on longevity, tumour induction and other late effects of total body irradiation of rhesus monkeys with fission neutrons and X-rays was initiated in the time period 1963-1973. In the irradiated groups 4 out of 29 animals are still alive, whereas the group of untreated controls still comprises 11 out of 21 monkeys.

A middle aged cohort consisting of 9 monkeys (irradiated in the period 1978-1981) and a young cohort consisting of 21 monkeys (irradiated in the period 1988-1990) are also kept under observation. It is too early to expect already radiation induced neoplasms in the last group. It has to be realized, however, that all three cohorts are also of interest for the study of deterministic effects. During the final phase of the contract, provisional studies have been performed on the occurrence of radiation cataract.

Project 1

Head of project: *Dr. Broerse*

Objectives for the reporting period

The study of deterministic and stochastic effects in three groups of long-term surviving rhesus monkeys, exposed to relatively high doses of total body irradiation, is performed to assess the possible risks for man. In the oldest cohort approximately 90 per cent of the irradiated monkeys have died compared with 50 per cent of the control group. All remaining monkeys received a physical examination each month by a veterinarian with extensive experience with non-human primates for the clinical presence of tumours, cataract formation and changes in general condition.

The necropsy results over the total contract period are summarized (Broerse et al., 1991) and the diagrams for malignant tumour development are updated. Risk factors and RBE values are derived from the tumour incidence results. Cataract data obtained in the United States after proton-irradiation are compared with those observed in the rhesus monkeys irradiated with photons and neutrons at TNO.

Progress achieved including publications

The long-term surviving irradiated monkeys are part of a study on the effectiveness of bone marrow transplantation to prevent death due to the haemopoietic syndrome (Broerse et al., 1978). One group of long-term survivors consisted of nine macaques irradiated with fission neutrons with doses ranging from 2.3 to 4.4 Gy (average dose 3.4 Gy) and another of 20 X-irradiated macaques which received doses between 3.0 and 8.6 Gy (average dose 6.7 Gy). A group of 21 untreated rhesus monkeys of comparable age distribution was maintained under identical husbandry conditions to serve as a control group.

The tumour incidence and post-irradiation observation periods for rhesus monkeys are shown in Figures 1 and 2. Time of irradiation and time of occurrence of tumours are indicated. Lines ending in cross bars signify death and arrow heads denote that the monkeys are still alive.

In the groups of rhesus monkeys irradiated with high doses of X-rays (average dose 6.7 Gy) and fission neutrons (average dose 3.4 Gy) an appreciable number of malignancies have been observed. In a number of cases the animals died with multiple tumours of mutually different types. The tumours observed include glomus tumours, osteosarcomas, renal adenocarcinomas, thyroid follicular carcinomas and central nervous system tumours (astrocytoma and glioblastoma). In the group of 21 control monkeys, two monkeys died with malignant tumours. The latency periods for induction of neoplastic diseases varied between 7.5 and 16 years for X-irradiated animals and between 4 and 18 years after neutron irradiation. As a consequence of this study, it is recognized that there is a strong need to screen regularly for secondary tumours, which may arise in patients who have previously received high-dose whole-body irradiation.

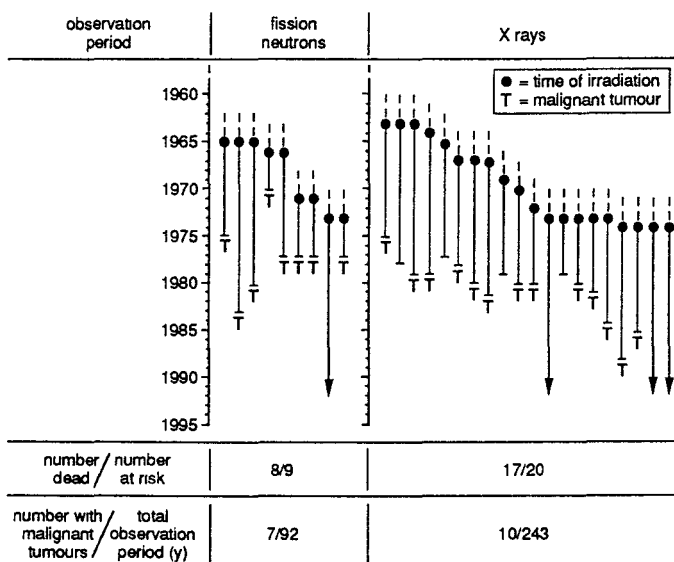


Figure 1 Tumour incidence in long-term surviving rhesus monkeys after irradiation and bone marrow transplantation.

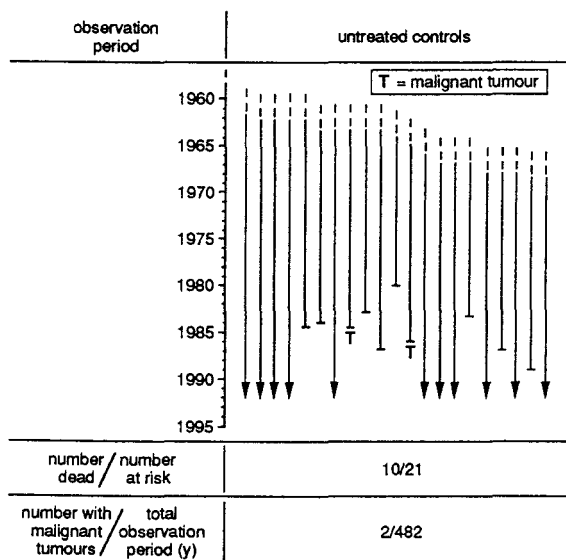


Figure 2. Long-term surviving monkeys in the control group.

The results can be analyzed in terms of the number of animals developing tumours per group as a function of the total observation period for the entire group. In the total observation period of 92 monkey-years, seven neutron-irradiated monkeys developed malignant tumours.

For the X-irradiated monkeys, ten have died with malignant neoplasms during the observation period of 243 monkey-years, while two animals died with malignant neoplasms in the control group during 482 monkey-years. The simplest way to obtain a quantitative assessment of the risk for tumour induction is to divide the number of observed tumours by the years at risk and the average absorbed dose. In this way, risk factors of $10 \times 243^{-1} \times 6.7^{-1} = 61 \times 10^{-4} \text{ Gy}^{-1} \text{ year}^{-1}$ for X-rays and $7 \times 92^{-1} \times 3.4^{-1} = 224 \times 10^{-4} \text{ Gy}^{-1} \text{ year}^{-1}$ for fission neutrons and an RBE of approximately 4 can be derived. It should be realized that these risk factors are derived from tumour incidence data obtained at relatively high doses and that they pertain to risk factors per monkey-year. Furthermore, this approach does not take into account the time-dependence of the tumour appearance.

These drawbacks can partly be overcome by assessing the cumulative tumour rate from data for survival without evidence of tumour in course of time (see Figure 3). The cumulative hazard $H(t)$ is related to the survival function $S(t)$ as follows:

$$H(t) = -\ln S(t) = [(t-\gamma)/\alpha(D)]^\beta$$

where α is the time-scale parameter, β the shape parameter and γ the time offset parameter, which indicates the time prior to which tumours have not been observed.

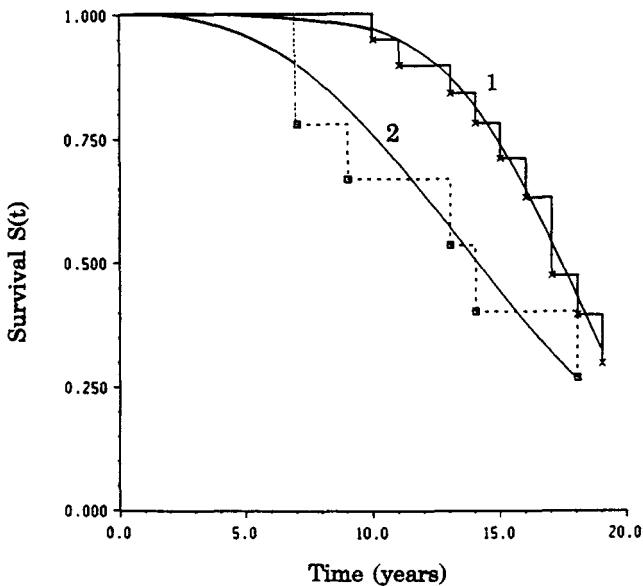


Figure 3. The survival without evidence of tumour as a function of time for two groups of rhesus monkeys, irradiated with average doses of 6.7 Gy (curve 1) and 3.4 Gy fission neutrons (curve 2).

The cumulative hazards at 15 years past irradiation amount to 0.84 and 0.31 for the neutron and X-ray experiments, respectively, leading to an RBE of $(0.84 \times 3.4^{-1}) / (0.31 \times 6.7^{-1}) = 5$. This RBE value is similar to the one derived from the total observation period for the groups under consideration. Due to difference in the time dependence of tumour induction in the X-ray and neutron irradiated monkeys, the RBE will, however, vary from 15 at 10 years to a lower value of 2 at the maximum follow-up time of 20 years. It is clear that the different approaches

can produce some ambiguities in the assessment of risks resulting from different types of irradiation.

For a comparison of the risk factors for induction of fatal malignancies in sub-human primates, it should be realized that the life span of monkeys is approximately one third of that in man. On the basis of recent epidemiological studies risk coefficients have been derived for occurrence of fatal malignancies after exposure of man to high doses of low-LET radiation (Broerse and Dennis, 1990). With the additive risk projection model the lifetime risks of mortality vary between 4 and $5 \times 10^{-2} \text{ Gy}^{-1}$, whereas the multiplicative model results in a lifetime risk between 7 and $11 \times 10^{-2} \text{ Gy}^{-1}$ for the whole population. These risk estimates apply to a dose range of 0.5-6 Gy and they are strongly influenced by the finding that children are considerably more sensitive to radiation effects than are adults. Assuming a mean latency period of 20 years for the manifestation of malignancies the yearly risks would vary between 20 and $55 \times 10^{-4} \text{ year}^{-1}$. It is interesting that the risk factor of $61 \times 10^{-4} \text{ Gy}^{-1}$ for X-rays derived from the monkey experiments is resembling the human experience.

Among the radiation effects monitored as the animals aged, were cataracts (Sonneveld et al., 1979) but it was not until 1991 that cataracts were graded with a new scoring system (Cox et al., 1992). In Figure 4 selected data from monkeys which were exposed to 55 MeV protons in the USA are compared to the results from macaques exposed to 300 kV or 6 MV X-rays at TNO. It can be concluded that the results for cataract formation in the control animals belonging to the American Delayed Effects Colony (DEC) and to the Dutch cohort are closely similar. For the irradiations with X-rays the cataract index increases substantially with dose at a fixed time post irradiation. Furthermore, the latency period for cataract formation is reduced with increasing dose.

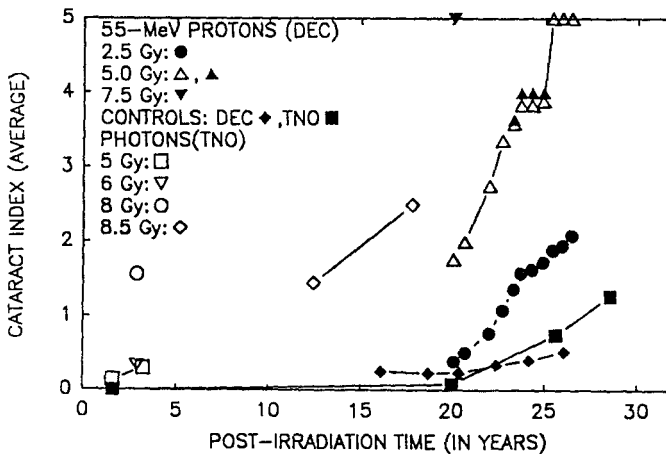


Figure 4. Temporal development of cataracts in rhesus monkeys following whole-body exposure to protons (55 MeV) or X-rays (300 kV or 6 MV) at about 2 years of age. The proton-irradiated animals are being followed in the USA (DEC), and the photon-irradiated subjects are being followed in The Netherlands (TNO). Symbols for each dose group studied appear in the figure.

Publications

- Broerse, J.J., Van Bekkum, D.W., Hollander, C.F. and Davids, J.A.G. Mortality of monkeys after exposure to fission neutrons and the effect of autologous bone marrow transplantation. *Int. J. Radiat. Biol.* 34, 253-264, 1978.
- Broerse, J.J., Hollander, C.F. and Van Zwieten, M.J. Tumour induction in rhesus monkeys after total body irradiation with X-rays and fission neutrons *Int. J. Radiat. Biol.* 40, 671-676, 1981.
- Broerse, J.J. and Dennis, J.A. Dosimetric aspects of exposure of the population to ionizing radiation. *Int. J. Radiat. Biol.* 57, 633-645, 1990.
- Broerse, J.J., Van Bekkum, D.W., Zoetelief, J. and Zurcher, C. Relative biological effectiveness for neutron carcinogenesis in monkeys and rats. *Radiat. Res.* 128, S-128-S135, 1991.
- Broerse, J.J., Davelaar, J. and Zurcher, C. Tumour induction in animals and the radiation risk for man. In: *Proceedings of NATO Advanced Study Institute on Biological Effects and Physics of Solar and Galactic Cosmic Radiation*. Plenum Press (C.E. Swenberg, G. Horneck, and E.F. Stassinopoulos, eds.). In Press, 1992.
- Cox, A.B., Salmon, Y.L., Lee, A.C., Lett, J.T., Williams, G.R., Broerse, J.J., Wagemaker, G. and Leavitt, D.D. Progress in the extrapolation of radiation cataractogenesis data across longer-lived mammalian species. In: *Proceedings of NATO Advanced Study Institute on Biological Effects and Physics of Solar and Galactic Cosmic Radiation*. Plenum Press (C.E. Swenberg, G. Horneck, and E.F. Stassinopoulos, eds.). In Press, 1992.
- Sonneveld, P., Peperkamp, E. and Van Bekkum, D.W. Incidence of cataracts in rhesus monkeys treated with whole-body irradiation. *Radiology* 117, 227-229, 1979.
- Wielenga, J.J. Hemopoietic stem cells in rhesus monkeys - surface antigens, radiosensitivity and responses to GM-CSF. Thesis, Rotterdam, 1990.
- Zurcher, C., Van Zwieten, M.J., Hollander, C.F. and Broerse, J.J. Radiation carcinogenesis in large animals. *Radiat. Environm. Biophys.* 30, 243-247, 1991.

MOLECULAR AND CELLULAR EFFECTS OF PROTONS, DEUTERONS AND ALPHAPARTICLES

Contract Bi7-0036 - Sector B13

- 1) *Moschini* , Istituto Nazionale di Fisica Nucleare
- 2) *Goodhead* , MRC Radiobiological Unit - 3) *Belli* , Istituto Superiore di Sanità
- 4) *Michael* , CRC-Gray Laboratory

Summary of project global objectives and achievements

Objectives

Since the first systematic study on RBE-LET relationship reported by Barendsen (1968), who analyzed the inactivation of cultured human cells by different types of radiation, LET was assumed as the general index of radiation quality. However in recent years it has been showed by several laboratories that, at low doses, protons result considerably more effective in inducing cell inactivation than other light charged particles in the LET region 10-30 keV/μm.

The present project was intended:

- (i) to extend the existing data on the effectiveness of low energy protons by measuring genetic (HPRT mutation) and molecular (DNA dsb) damage;
- (ii) to investigate the biological effectiveness of other light charged particles, such as deuterons and alpha particles of the same and higher LET,
- (iii) to search possible correlation and causes in terms of dose rate and microscopic track structure with the investigated biological effects.

Achievements

1. Effectiveness of low energy protons in inducing HPRT mutations in V79 cells

In the course of the present contract activities, during the upgrading of the radiobiological facility at the Laboratori Nazionali di Legnaro (LNL) necessary to perform deuterons irradiations, some numerical inconsistencies in evaluating energy in air for protons were found. This circumstance prompted us to perform a complete re-evaluation (accepted for publication in Int. J. Rad. Biol.) of the physical parameters for all the proton beams used previously.

Hereafter all the correct parameter values will be used, justifying in this way the discrepancies with the numerical values appearing in the previous progress report.

V79-753B Chinese hamster cells have been irradiated with protons having energies of 6.0, 4.5, 3.3 and 3.0 MeV, corresponding to LET values, evaluated at the cell midplane, of 7.7, 11, 20 and 30.5 keV/μm respectively, in the dose range 0.5 - 3.0 Gy, at a dose rate of 1 Gy/min.

The mutation curve obtained with 200 kV X-rays was used for comparison. The mutation frequency induced by all the proton beams is considerably higher than that induced at the same dose by X-rays and it is linearly related to the dose. As it is shown in fig.1, in the LET range we have

considered, low energy protons appear to have a higher effectiveness than other charged particles of comparable LET, as available in the literature, confirming the same results found for cell inactivation and implying that also for mutation induction the RBE-LET relationship may depend on the type of radiation.

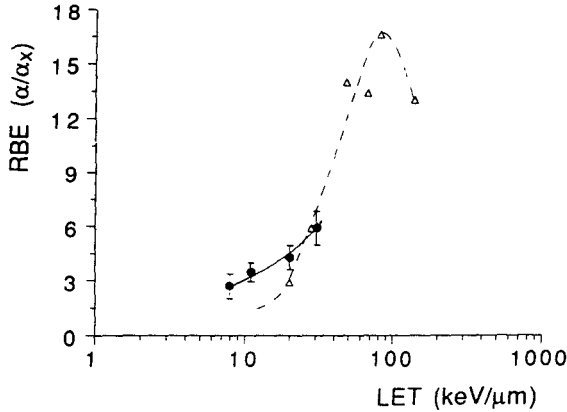


Fig.1 RBE-LET relationship for mutation induction. (○) Protons (present results); (Δ) ⁴He.

2. Biological effectiveness of protons compared to α-particles of the same LET

A more direct comparison between the biological effectiveness of different light charged particles of the same LET have been performed with the Variable Energy Cyclotron at Harwell, in the framework of a collaboration between ISS and MRC groups. Experiments had been carried out to measure inactivation of V79-4, HeLa, HeLa S3 and C3H 10T1/2 cells, HPRT⁻ mutations in V79-4 cells and double-strand breakage of DNA, by protons and α-particles each of 20 and 23 keV/μm. During this contract the raw data were analysed and prepared for publication.

From cell inactivation studies, protons resulted more effective than α-particles for all cell lines used, by ratios of the linear terms of protons to α-particles ranging from 1.75 to 1.35 for 20 keV/μm LET and from 1.45 to 1.32 for 23 keV/μm LET.

For mutations at the HPRT locus in V79-4 cells it was found that protons were more effective than α-particles of the same LET by ratios 1.85 (at 20 keV/μm) and 2.07 (at 23 keV/μm).

3. Effectiveness of low energy protons in causing DNA double strand breaks (initial) in V79 cells, as a function of LET

The initial yields of DNA dsb in V79-753B cells irradiated with protons of 4.5, 3.3 and 3.0 MeV at the LNL 7 MV CN Van de Graaff accelerator have been evaluated in the dose range 10-120 Gy. The sucrose gradient sedimentation technique was used for such determinations and irradiation with X-rays was used for comparison. Linear dose-response curves were obtained in all cases and only little differences among radiations were found, so that the RBE's for protons result very close to 1 for all the conditions studied. This finding is consistent with the results obtained at Harwell on direct comparison between protons and α -particles. Since the variations with LET observed for other end-points are not reproduced for the initial yield of DNA dsb, it would appear that if this kind of damage is related to cell inactivation or mutation, different types of radiation produce dsb that differ in their nature and/or spatial distribution leading to different reparability.

4. Development of an irradiation facility for deuteron beams

To perform cell irradiations in air with deuteron beams, that have virtually the same track structure but twice the range of protons with the same LET, the existing facility at the Van de Graaff CN accelerator of the LNL have been improved with a remote controlled multisample holder housing up to 20 Petri dishes that can be irradiated at a prefixed temperature. The basic components of the multisample holder are:

- external parallelepiped aluminium box
- internal cylindrical copper container
- rotating table supporting 20 holders for housing samples
- automatic Peltier cooling system
- remote controlled multistepper electric motor
- aluminium plate as cover.

The aluminium box is provided on a lateral wall with a circular port serving as entrance for the beam. The cylindrical copper container is centered in the aluminium box frame and supported by thermally insulated material with respect to the aluminium walls. The bottom of both of the aluminium and copper containers is provided with a hole, in which a bearing shaft mechanism, driven by the multistepper motor, passes through. The cylindrical copper container is thermally connected to the Peltier cooling system, which permits to maintain constant a chosen temperature during the irradiation (in the range 20-0 °C). This whole unit, with its accessories, rests on a thick sliding aluminium table, which is anchored to the beam-line support.

5. Effectiveness of deuteron beams in inducing inactivation in V79 cells

V79-753B Chinese hamster cells have been irradiated with deuterons having energies of 6.5, 5.2, 4.4, 4.2, 4.0 and 3.9 MeV, corresponding to LET values, evaluated at the cell midplane, of 13.4, 18.4, 26.3, 30.8, 39.4 and 48.0 keV/ μ m respectively, in the dose range 0.5 - 4.0 Gy, at a dose rate of 1

Gy/min. The inactivation curve obtained with 200 kV X-rays was used for comparison. The RBE values, calculated in terms of the linear coefficient ratios, range from 1.9 to 6.5, as listed in Tab.1 of the LNL group final report. The relationships between RBE and LET appear considerably different for protons and deuterons. Since protons and deuterons with the same LET, having the same charge and velocity, are expected to have similar energy deposition pattern, their different effectiveness must originate from some features until now overlooked in the track structure. These results, quite unexpected, support once more that the RBE-LET relationship depend on the type of radiation, as already stated for other findings in this study, and suggest that a better understanding of the general features of track structure, in particular those that depend on the highest spatial and energy resolution, is needed.

6. Design and construction of small size systems for cell irradiation with alpha sources during incubation

Two prototypes of small size irradiators have been designed and constructed. They consist of a plexiglass cylindrical body with a trapezoidal internal section, designed to fit the source geometry. At the bottom it is housed an α -emitter source (^{241}Am or ^{244}Cm) while the upper side is closed by a thin Mylar foil kept tight in side by an aluminium ring fixed by screws. A lateral valve permit to fill the irradiator with Helium gas, after evacuation of the air. The path of the particles, from the source to the cells, is designed in order to achieve acceptable uniformity of dose to the cell monolayer attached to the Mylar foil forming the bottom of especially designed Petri dish located on the top of the irradiator. Preliminary test and dosimetric measurements have been carried out revealing performances adequate to the foreseen use.

7. Effectiveness of deuteron for mutation at the HPRT locus in V79 cells as a function of LET

Due to the extension of the study on cell inactivation, we performed only two independent experiments for determining the effectiveness of 31 keV/ μm deuterons in inducing HPRT mutation. Deuterons resulted slightly less effective than protons of the same LET. More experiments are in progress at this LET in order to achieve a number of determination useful for a significant statistical analysis. An extension of the study to a more wide range of LET values will be included in the objectives of the next contract.

8. Analysis of microscopic track structure of the radiations

Differences in biological effectiveness of protons, alphas and deuterons of the same LET must, in some way, originate from their differences in track structure. To quantify differences between the tracks over dimensions similar to DNA, nucleosomes and chromatin fibre, statistically representative tracks of protons, α -particles and deuterons have been

simulated by the Monte Carlo code MOCA14 of Wilson and Paretzke. These were then scored for energy deposition in small cylindrical volumes positioned randomly with respect to the tracks and absolute frequency distributions of energy deposition in the target volumes have been generated for several different conditions. Analyses were then performed to seek microscopic properties of the tracks that may correlate with the biological effectiveness. Track scorings showed negligible differences between protons and deuterons of the same velocity (and therefore the same LET) as expected on the basis of the existing Monte-Carlo track simulation codes that generate essentially identical tracks, including delta-rays, for primary particles of identical velocity and charge. Therefore real differences in biological effectiveness between protons and deuterons could arise only from some unknown primary processes of relevance that are not included in the current track codes. On the contrary significant differences between the scored distributions of protons and α -particles of the same LET were found, as expected from their different charges and velocities. In spite of this the parameters investigated prove themselves unsuitable to indicate the biological effectiveness and lead to the underlying mechanisms. (For more details see MRC group final report).

Project 1

Head of project: *Prof. Moschini*

Objectives for the reporting period

1. Extension of the studies on effectiveness of deuterons for inactivation of V79 cells as a function of LET.
2. Measure the effectiveness of deuterons for V79 cell mutation at the HPRT locus as a function of LET.
3. Start comparative experiments with low energy α -particle radionuclide sources at different dose-rate.
4. Determination of the RBE-LET relationship for the initial yield of DNA dsb in V79 cells irradiated with proton beams.

Progress achieved including publications (In collaboration with ISS group)

1. One of the more relevant purposes of the first period of the present project activities was to compare the biological effectiveness of protons and deuterons in inducing cell inactivation. Deuterons with the same LET of protons have been used to extend the inactivation study to higher LET values than those used with protons, that have a limited range with respect to cell thickness. Since protons and deuterons with the same LET should have an identical track structure, a radiobiological equivalence was expected. Preliminary results showed, on the contrary, that deuteron effectiveness resulted similar to that of protons only at 31 keV/ μ m, while at lower LET, deuterons appeared to be less effective. For this reason to obtain a more complete set of data and to extend RBE-LET relationship over a wider region of LET, an extension of the study was decided for LET values ranging from 13 to 48 keV/ μ m. Survival curves for V79 cells irradiated with deuterons at various LET are showed in the ISS group report together with best-fit parameters.

Table 1 lists the RBE values for protons and deuterons calculated in terms of the linear coefficient ratio.

Table 1.

deuterons		protons	
LET (keV/ μ m)	$\alpha/\alpha_x \pm$ s.e.	LET (keV/ μ m)	$\alpha/\alpha_x \pm$ s.e.
13.4	1.87 \pm 0.34	7.7	2.37 \pm 0.28
18.4	2.23 \pm 0.42	10.9	2.88 \pm 0.36
26.3	4.09 \pm 0.39	20.0	3.65 \pm 0.43
30.8	5.08 \pm 0.47	30.5	5.77 \pm 0.55
39.5	5.81 \pm 0.59	34.6	5.06 \pm 0.15
48.0	6.43 \pm 0.67	37.8	4.37 \pm 0.42

Figure 2 shows the RBE-LET relationships for cell inactivation induced by protons and deuterons with different energies. In the LET range we have studied, such relationships result considerably different; in particular deuterons appear less effective than protons up to 31 keV/μm and more effective for higher LET values, without reaching a maximum. Since protons and deuterons with the same LET are expected to produce the same δ-rays pattern, these results could imply that relevant interaction processes, other than the continuous δ-electron emission, considered determinant for the track structure, have been overlooked till now or that further information may be required on the physics of their interactions with biological targets.

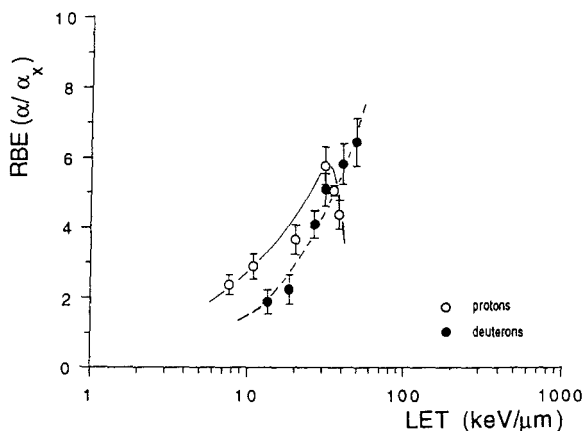


Fig. 2 RBE-LET relationship for V79 cell inactivation.

2. Due to the extension of the study on cell inactivation induced by deuterons, we could perform only a limited number of experiments to evaluate the effectiveness of deuterons in inducing mutation at the HPRT locus in V79 cells. Fig. 3 shows the results of two independent experiments on mutation induction obtained with 31 keV/μm deuterons compared with those obtained, for the same end-point, with protons of the same LET. From these preliminary data it appears that deuterons are less effective than protons.

Completion of the analysis of the mutation induction in a more wide range of LET values will be included in the objectives of the next contract.

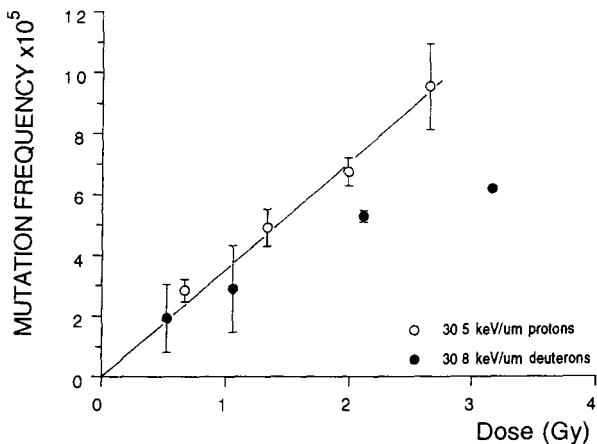


Fig.3 Dose-response relationship for the induction of HGPRT⁻ mutants by protons and deuterons of 30.5 and 30.8 keV/μm LET respectively.

3. In order to perform comparative experiments with low energy alpha particles radionuclide sources at different dose-rates, two prototypes of small size irradiators have been designed and constructed. They consist of a plexiglass cylindrical body, 10.3 cm. in diameter and 6 cm high, with a trapezoidal internal section, designed to fit the source geometry. At the bottom it is housed an α-emitter source (241 Am or 244 Cm) while the upper side is closed by a thin Mylar foil kept tight in side by an aluminium ring fixed by screws. A lateral valve permit to fill the irradiator with Helium gas, after evacuation of the air. The path of the particles from the source to the cells is designed in order to achieve acceptable uniformity of dose to the cells which are attached as a monolayer on the Mylar foil forming the bottom of especially designed Petri dish of 19.6 cm² area, located on the top of the irradiator. The small size dimensions of the irradiators permit continous irradiation during cell growth inside incubator, in order to study the effects of low dose rates, such as 0.005-0.01 Gy/min. The close adhesion between the upper mylar foil of the irradiator and the Petri dish one provide cells uniform irradiation.

Preliminary test and dosimetric measurements have been carried out revealing performances adequate to the foreseen use. Due to the reasons already described in 2. and to the delay in arrival of the special (in geometry) α-source ordered to an USA supplier, radiobiological experiments are planned to start within the present year.

4. The initial yield of dsb induced by protons of 10.9, 20.0 and 30.5 keV/μm LET has been determinate. RBE values have been found very close to unity for all proton beams used showing the independency of the amount of induced damage on LET (see project 3 report for a more detailed discussion).

Publications

M. Belli, F. Cera, R. Cherubini, F. Ianzini, G. Moschini, O. Sapora, G. Simone, M.A. Tabocchini and P. Tiveron. "*LET dependence for cell inactivation, mutation induction and DNA DSB on V79 cells irradiated with high LET protons*", Thirty-Eight Annual Meeting of the Radiation Research Society, Tenth Annual Meeting of the North American Hyperthermia Group, New Orleans, Louisiana, April 7-12, 1990, Abstract Book: Ek-7, p. 164.

M. Belli, F. Cera, R. Cherubini, F. Ianzini, G. Moschini, O. Sapora, G. Simone, M.A. Tabocchini and P. Tiveron. "*RBE-LET relationship for V79 cells irradiated with low energy protons*", Radiation Protection Dosimetry, vol. 31, n. 1/4, 309-310, (1990).

F. Barone, M. Belli, F. Cera, R. Cherubini, F. Ianzini, G. Moschini, O. Sapora, G. Simone, M.A. Tabocchini and P. Tiveron. "*Initial yield of DNA DSB in V79 cells irradiated with low energy protons and X-rays*", 23rd Annual Meeting ESRB, Dublin, Ireland, September 23-26, 1990.

G. Simone, M. Belli, F. Ianzini, O. Sapora, M.A. Tabocchini, F. Cera, R. Cherubini, P. Tiveron and G. Moschini. "*Lethal and mutagenic effects of 7.6 keV/ μ m protons on V79 cells*", 9th International Congress of Radiation Research, Toronto, Canada, July 7-12, 1991,; Vol. I, Congress Abstract, Eds. J.D. Chapman, W.C. Dewey and G.F. Whitmore, Academic Press, Inc.

R. Cherubini, F. Cera, A.M.I. Haque, P. Tiveron, G. Moschini, G. Galeazzi, G. Simone, M. Belli, F. Ianzini, O. Sapora and M.A. Tabocchini. "*The biological effectiveness of deuterons: description of the facility at LNL and preliminary results on V79 cells*", 9th International Congress of Radiation Research, Toronto, Canada, July 7-12, 1991; Vol. I, Congress Abstract, Eds. J.D. Chapman, W.C. Dewey and G.F. Whitmore, Academic Press, Inc.

F. Cera, R. Cherubini, A.M.I. Haque, G. Moschini, P. Tiveron, M. Belli, F. Ianzini, O. Sapora, M.A. Tabocchini and G. Simone. "*Radiobiology and radiotherapy projects with accelerated charged particles at the INFN-Laboratori Nazionali di Legnaro: present status and future perspectives*", VII Congresso Nazionale dell'Associazione Italiana di Fisica Biomedica, Ancona, Italy, June 8-12, 1992; to be published in Physica Medica

M. Belli, F. Cera, R. Cherubini, D.T. Goodhead, F. Ianzini, T.J. Jenner, G. Moschini, O. Sapora, G. Simone, D.L. Stevens, A. Stretch, M.A. Tabocchini and P. Tiveron. "*Relevance of experiments with different charged particles having the same LET for biophysical modelling of radiation effects*", In: Biophysical Modelling of Radiation Effects. Eds. K.H. Chadwick, G. Moschini and M.N. Varma (Adam Hilger, Bristol), pp. 285-292 (1992)

M. Belli, F. Cera, R. Cherubini, F. Ianzini, G. Moschini, O. Sapora, G. Simone, M.A. Tabocchini and P. Tiveron. "*RBE-LET relationship for survival and mutation induction of V79 cells irradiated with low-energy protons: re-evaluation of the LET values at the LNL facility*", Int. J. Rad. Biol., 61, no. 1, 145-146, (1992).

M. Belli, F. Cera, R. Cherubini, D.T. Goodhead, A.M.I. Haque, F. Ianzini, G. Moschini, O. Sapora, G. Simone, M.A. Tabocchini and P. Tiveron "*The importance of the track structure of different charged particles having the same LET for biophysical modelling*", The International Conference on Low Dose Irradiation and Biological Defense Mechanisms, Kyoto, Japan, July 12-16, 1992.

M. Belli, F. Cera, R. Cherubini, D.T. Goodhead, A.M.I. Haque, F. Ianzini, G. Moschini, H. Nikjoo, O. Sapora, G. Simone, D.L. Stevens, M.A. Tabocchini and P. Tiveron. "*Inactivation induced by deuterons of various LET in V79 cells*", Eleven Symposium on Microdosimetry, Gatlinburg, TN, USA, September 13-18, 1992. To be published in Radiat. Prot. Dosim.

M. Belli, F. Cera, R. Cherubini, A.M.I. Haque, F. Ianzini, G. Moschini, O. Sapora, G. Simone, M.A. Tabocchini and P. Tiveron. "*Cell inactivation induced by light ions in V79 cells: RBE-LET relationship for low energy deuterons*", 24th ESRB Meeting, Erfurt, Germany, October 4-8, 1992.

M. Belli, F. Cera, R. Cherubini, A.M.I. Haque, F. Ianzini, G. Moschini, O. Sapora, G. Simone, M.A. Tabocchini and P. Tiveron. "*Comparison between cross section of deuterons and protons for cell inactivation and mutation induction*", Presented at the B.A.R.N., Biological applications of relativistic nuclei, Clermont-Ferrand, France, October 14-15, 1992.

M. Belli, F. Cera, R. Cherubini, A.M.I. Haque, F. Ianzini, G. Moschini, O. Sapora, G. Simone, M.A. Tabocchini and P. Tiveron "*Inactivation and mutation induction in V79 cells by low energy protons: re-evaluation of the results at the LNL facility*", Accepted for publication in Int. J. Rad. Biol., oct. (1992).

Project 2

Head of project: *Dr. Goodhead*

Objectives for the reporting period

Jointly, with partners, analyse experimental data on biological effectiveness of protons (p) compared to α -particles (α) of the same LET. Generation, by Monte Carlo methods, of simulated tracks of p, α and deuterons (d), covering energies for which the LETs of the particles are the same and for which radiobiological data are available on their effectiveness; randomly sample these to obtain absolute frequency distributions of energy depositions in microscopic target volumes including those corresponding approximately to dimensions of DNA, nucleosomes and chromatin fibre, and also to compute their frequency- and dose-mean specific energies (\bar{Z}_F and \bar{Z}_D). Compare the frequency distributions of energy deposition in microscopic volumes by particles of the same LET and compare these with their relative effectiveness as observed in biological experiments.

Progress achieved including publications

1. Analysis of experimental data

Together with others in this coordinated contract, we have analysed raw experimental data obtained previously in a direct comparison of the biological effectiveness of p and α of the same LET. Experiments had previously been carried out on the Variable Energy Cyclotron at Harwell to measure inactivation of V79, HeLa and C3H 10T $\frac{1}{2}$ cells, HPRT⁻ mutations in V79 cells and double-strand breakage of DNA, by p and α each of 20 and 23 keV μm^{-1} . In this contract the data were analysed and prepared for publication [1,2,3].

For cell inactivation it was found that the ratio of the linear (low dose) terms of p to α , for 20 and 23 keV μm^{-1} , respectively, were as follows: for V79-4 cells 1.75 ± 0.38 and 1.45 ± 0.32 ; for HeLa cells 1.32 ± 0.40 and 1.33 ± 0.20 ; for HeLa S3 cells 1.35 ± 0.28 and 1.32 ± 0.18 ; and for C3H 10T $\frac{1}{2}$ cells 1.08 ± 0.25 (both LETs combined) [1]. The probability that these seven ratios, taken together, are greater than unity by statistical chance alone is $< 1\%$. Hence it may be concluded that, overall, p are more effective at cell inactivation than α of the same LET. The largest ratios were obtained for V79-4 cells. In a different line of V79 cells Belli *et al.* (1989) had previously reported a high effectiveness of p, apparently larger than the relative effectiveness of α as available in the literature and these results have subsequently been extended [4].

For mutations at the hprt locus in V79-4 cells it was found that p were more effective than α of the same LET by ratios 1.85 ± 0.31 (at 20 keV μm^{-1}) and 2.07 ± 0.19 (at 23 keV μm^{-1}) [2].

By contrast, the initial yield of DNA double-strand breaks (dsb) in V79-4 cells, as measured by neutral sucrose sedimentation was smaller for p than α (ratios 0.73 ± 0.11 at 20 keV μm^{-1} and 0.86 ± 0.11 at 23 keV μm^{-1}). By the Olive method of DNA precipitation the relative yield of breaks was only slightly higher with p than with α (ratios 1.08 ± 0.13 at 20 keV μm^{-1} and 1.23 ± 0.17 at 23 keV μm^{-1}). Hence, it would appear that the residual damage that leads to cell inactivation or mutation is not a random sample from the initial dsb [3].

2. Track scoring: frequency distributions of energy deposition

The above differences in biological effectiveness of p and α of the same LET must, in some way, originate from their differences in track structure. Thus, the experimental data provide a useful new constraint on the biologically critical microscopic properties of radiations. In addition, recent results obtained at Legnaro (see Projects 1 and 3), indicate also differences in effectiveness between p and d of the same velocity (and hence the same LET).

To quantify differences between the tracks over dimensions similar to DNA, nucleosomes and chromatin fibre, representative segments of tracks of p and α have been simulated by the Monte-Carlo code MOCA14 of Wilson and Paretzke. These were then scored for energy deposition in small cylindrical volumes positioned randomly with respect to the tracks. In this way, absolute frequency distributions of energy deposition in the target volumes have now been generated for the conditions listed in the Table.

Particle	Energy (MeV)	Energy (MeV/ μ)	LET (keV/ μ m)	diameter (nm)	Particle	Energy (MeV)	Energy (MeV/ μ)	LET (keV/ μ m)	diameter (nm)
alpha	35.56	8.89	21.9	2	alpha	21.84	5.46	29.8	2
"	35.56	8.89	21.9	10	"	21.84	5.46	29.8	10
"	35.56	8.89	21.9	25	"	21.84	5.46	29.8	25
proton	1.38	1.38	20.7	2	proton	0.79	0.79	31.0	2
"	1.38	1.38	20.8	10	"	0.79	0.79	32.3	10
"	1.38	1.38	21.3	25	"	0.79	0.79	32.3	25
deuteron	2.76	1.38	21.3	2	deuteron	1.58	0.79	31.6	2
"	2.76	1.38	20.7	10	"	1.58	0.79	31.6	10
"	2.76	1.38	20.7	25	"	1.58	0.79	31.2	25
alpha	30.48	7.62	24.4	2	proton	0.63	0.63	36.0	2
"	30.48	7.62	24.4	10	"	0.63	0.63	36.0	10
"	30.48	7.62	24.4	25	"	0.63	0.63	36.0	25
proton	1.16	1.16	23.9	2	proton	0.53	0.53	40.3	2
"	1.16	1.16	23.6	10	"	0.53	0.53	40.3	10
"	1.16	1.16	23.6	25	"	0.53	0.53	40.3	25
deuteron	2.30	1.15	23.6	2					
"	2.30	1.15	24.2	10					
"	2.30	1.15	24.2	25					

The last column indicates the diameters of the target cylinders. For each diameter (D), the cylinder length was varied from 0.5D to 8D. In all cases a total track length of at least 10 μ m was scored, as shorter 'monoenergetic' segments.

3. Comparison of track scoring with biological effectiveness

General features of the biological results to date for V79 cells (see Projects 1 and 3) indicate that: at ~ 20 keV μ m⁻¹, p are more effective than α at cell killing and particularly at mutation induction; the p effectiveness then rises steeply with increased LET to ~ 30 keV μ m⁻¹ while the α effectiveness does not; d are less effective than p at the lower end of this LET range but rise later and more rapidly to reach the p effectiveness at the upper end; for initial yield of DNA dsb p are no more effective than α of the same LET, suggesting that the differences in final biological effectiveness may lie in differences of complexity (and hence reparability) of the dsb.

Analyses have commenced to seek microscopic properties of the tracks, from the scored frequency distributions for small targets, that may correlate with the biological effectiveness and therefore provide mechanistic insight into the biologically critical features. Firstly, it should be noted that the track scorings show negligible differences between p and d of the same velocity (and therefore the same LET). This is as expected on the basis of the existing Monte-Carlo

track simulation codes that generate essentially identical tracks, including delta-rays, for primary particles of identical velocity and charge. Thus the very close similarities in our scored distributions show only that the scoring has been efficiently carried out with good statistics. Real differences in biological effectiveness between p and d could arise only from some unknown primary processes of relevance that are not included in the current track codes.

There are significant differences between the scored distributions of p and α of the same LET, as expected from their different charges and velocities (and hence delta rays). From the above distributions, and those that we have previously published for p and α of other energies, it is seen that the α values of \bar{Z}_F and \bar{Z}_D for α generally lie below those for p, although this is least for the smallest targets (2 nm). The values all rise as LET increases from 20 to 30 keV μm^{-1} but only slightly (~ 10%) for the smallest targets and insufficient to correlate with cell killing and mutation even for the largest targets, \bar{Z}_F showing the largest increases. Also, contrary to the results for biological effectiveness, the values for α rise proportionately about as much over this LET range as do those for p. Thus these parameters seem unsuitable to indicate the biological effectiveness or lead to the underlying mechanisms.

We have commenced comparisons of the distributions also in terms of absolute frequencies of deposition of threshold energy in the targets, on the underlying assumption that this may reflect the yield of damage of sufficient severity to have reduced repairability in the cell. This work is still in progress but the generalizations to date include that for small threshold energies in any of the targets there is little or no rise in frequency from 20 to 30 keV μm^{-1} for any of the particles. As the selected threshold energy is increased, the rise becomes steeper, with rises of 100% or more being readily obtainable with the larger targets. However, in most cases considered to date the α frequencies also rise by a comparable amount. But comparisons at some of the more interesting threshold energies have been inhibited by insufficient track sampling to date. The analyses have revealed that 10 μm of total track length of the faster α is insufficient to represent their true stochastics, no matter how thoroughly they are sampled and scored.

Our interim conclusions, therefore, are that the yields of dsb (little dependence on radiation type) could be associated with fairly small threshold energies in targets of approximately DNA dimensions, but that the cellular consequences, after repair, require consideration of larger thresholds in larger targets. The experimentally observed biological difference between p and d also raises questions about the completeness of the physical processes included in the current Monte-Carlo track-simulation codes themselves.

4. Comparison of experimental methods

In the collaborative experiments with p and α on the VEC at Harwell, our dosimetry was based on ionization chambers, with CR39 track-etch plastic (plus Si surface-barrier detector energy measurements) as an independent comparator [1]. The p and d experiments at Legnaro use Si detectors (for both fluence and energy) for primary dosimetry. We have therefore commenced a comparison by applying our methods on the Legnaro beam. The CR39 exposures have the additional advantage of allowing also assessment of beam uniformity and particle scatter as well as comparisons of Harwell and Legnaro beams in these respects. One working visit to Legnaro has been carried out to date and the data are undergoing analysis. The overall interim assessment is that our dosimetric results do not differ much from those of Legnaro and that we observe no significant differences between the Legnaro p and d beams including in their very small component of scattered, reduced-energy or otherwise abnormal etched pits in CR39.

Publications

- [1] D.T. Goodhead, M. Belli, A.J. Mill, D.A. Bance, L.A. Allen, S.C. Hall, F. Ianzini, G. Simone, D.L. Stevens, A. Stretch, M.A. Tabocchini and R.E. Wilkinson. "Direct comparison between protons and α -particles of the same LET: I. Irradiation methods and inactivation of asynchronous V79, HeLa and C3H 10T $\frac{1}{2}$ cells." *International Journal of Radiation Biology*, 61, 611-624 (1992).
- [2] M. Belli, D.T. Goodhead, F. Ianzini, G. Simone and M.A. Tabocchini. "Direct comparison between protons and α -particles of the same LET: II. Mutation induction at the HPRT locus in V79 cells." *International Journal of Radiation Biology*, 61, 625-629 (1992).
- [3] T.J. Jenner, M. Belli, D.T. Goodhead, F. Ianzini, G. Simone and M.A. Tabocchini. "Direct comparison between protons and α -particles of the same LET: III. Initial yield of DNA double-strand breaks in V79 cells." *International Journal of Radiation Biology*, 61, 631-637 (1992).
- [4] M. Belli, F. Cera, R. Cherubini, D.T. Goodhead, F. Ianzini, T.J. Jenner, G. Moschini, O. Sabora, G. Simone, D.L. Stevens, A. Stretch, M.A. Tabocchini and P. Tiveron. "Relevance of experiments with different charged particles having the same LET for biophysical modelling of radiation effects." In: *Biophysical Modelling of Radiation Effects*. Eds. K.H. Chadwick, G. Moschini and M.N. Varma (Adam Hilger, Bristol), pp.285-292 (1992).

Project 3

Head of project: Dr. M. Belli

Objectives for the reporting period

1. Extension of the studies on effectiveness of deuterons for inactivation of V79 cells as a function of LET.
2. Measure the effectiveness of deuterons for V79 cell mutation at the HPRT locus, as a function of LET.
3. Start comparative experiments with low energy α -particle radionuclide sources at different dose-rate.
4. Determination of the RBE-LET relationship for the initial yield of DNA dsb in V79 cells irradiated with proton beams.

Progress achieved including publications (in collaboration with the LNL)

1. The unexpected results obtained near the end of the preceding period prompted us to extend the experiments on cell inactivation produced by deuterons. Our previous studies with protons gave the first evidence that the RBE-LET relationships obtained with charged particles may depend on the particle type, at least in the LET range 7-38 keV/ μ m. Since it was impossible to explore higher LET due to the limited proton range, experiments with deuterons were undertaken as these particles have twice the range of protons with the same LET but still the same charge and velocity. An identical track structure and consequently a radiobiological equivalence were therefore expected. However, the analysis of the data obtained with deuterons having LET of 18, 26 and 31 keV/ μ m showed that at 31 keV/ μ m cell inactivation is similar for protons and deuterons while, at lower LET deuterons seemed to be less effective than protons in inducing lethality. After this finding we decided to extend our study to lower and higher LET values in order to allow a more detailed comparison with the proton data. Also, we repeated a number of experiments in order to have at least 7 independent determinations for each LET value improving data precision and reliability.

The results we obtained in the LET range 13-48 keV/ μ m are shown in Figure 1 and Table 1. A comparison with the proton data shows that the RBE-LET relationships (with the RBE expressed in terms of linear coefficient ratio) are not the same for the two kinds of particles, deuterons being less effective than protons for cell inactivation at LET < 30 keV/ μ m and more effective at higher LET (see LNL report Fig.1).

It can be concluded that, although protons and deuterons at the same LET are expected to produce the same δ -ray pattern since they have the same charge and velocity, their different effectiveness must originate from some differences in their track structure.

These results have a potential impact on biophysical modelling of radiation action. In effect, they could imply that relevant interaction processes, other than the continuous δ -electron emission, have been overlooked in the existing track structure simulation codes for such particles, or that further information may be required on the physics of their interactions.

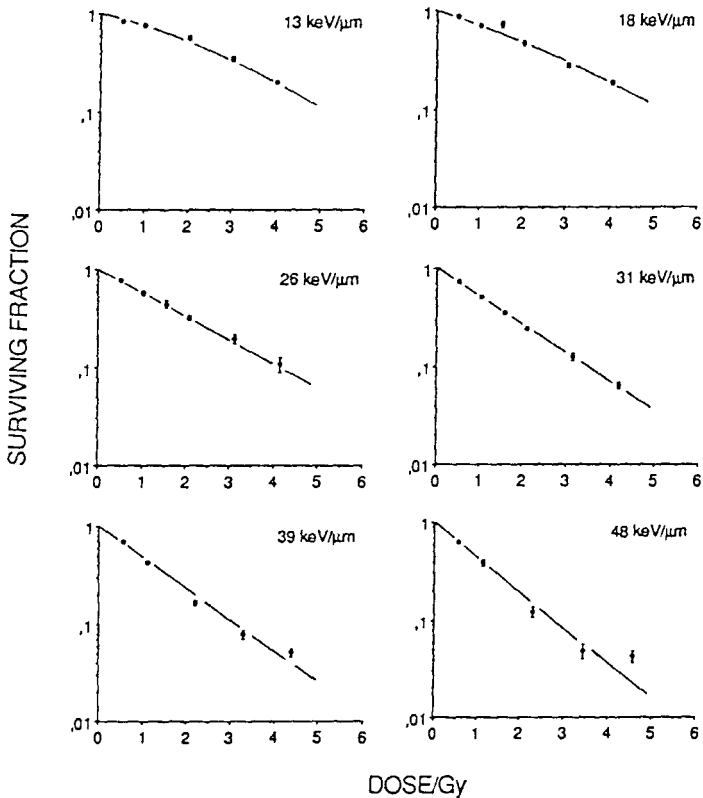


Figure 1. Survival curves for V79 cells irradiated with deuterons at various LET.

Table 1. Best-fit parameters for inactivation of V79 cells irradiated with deuterons at various LET. Fits were performed by linear or linear-quadratic, when appropriate, expressions. The α/α_x ratios are representative of the RBE at low doses.

LET (keV/ μ m)	$\alpha \pm \text{s.e.} (\text{Gy}^{-1})$	$\beta \pm \text{s.e.} (\text{Gy}^{-2})$	$\alpha/\alpha_x \pm \text{s.e.}$
13.4	0.24 ± 0.04	0.04 ± 0.01	1.87 ± 0.34
18.4	0.29 ± 0.05	0.03 ± 0.01	2.23 ± 0.42
26.3	0.53 ± 0.01		4.09 ± 0.39
30.8	0.66 ± 0.01		5.08 ± 0.47
39.5	0.75 ± 0.03		5.81 ± 0.59
48.0	0.83 ± 0.04		6.43 ± 0.67

2. Due to the extension of the study reported for the objective 1, we performed experiments for determining the effectiveness of deuterons in inducing mutation at the HPRT locus in V79 cells only at 31 keV/ μ m.

The results obtained from two independent experiments show that deuterons are somewhat less effective in mutation induction than protons of the same LET (see LNL report for further details).

More experiments are in progress at this LET in order to achieve a number of independent determinations useful for a significant statistical analysis. Completion of the analysis of the mutation induction in a range of LET similar to that used for inactivation studies will be included in the objectives of the next contract.

3. Two prototypes of small size irradiators have been designed and constructed for performing comparative experiments, at LNL and ISS, with low energy alpha particles from ^{241}Am or ^{244}Cm sources (see present LNL report for a detailed description of the irradiators).

Such devices permit continuous irradiations at low dose rates (0.005-0.01 Gy/min) during cell growth.

Preliminary tests and dosimetric measurements have been already carried out and the first radiobiological experiments are planned to start within the present year.

4. Data analysis relative to the initial yield of dsb induced by protons of 4.5, 3.3 and 3.0 MeV (corresponding to LET values, evaluated at the cell midplane, of 10.9, 20.0 and 30.5 keV/ μ m) has been completed. The RBEs,

evaluated from the ratio of the slopes of the dose-response curves for protons respect to X-rays, have been found very close to unity for all the proton beams used.

These results, are consistent with those obtained at Harwell with protons and alpha particles of 20 and 23 keV/ μ m (Jenner *et al.* 1992). In Fig. 2 the two sets of data are compared in terms of RBE versus LET.

In the considered range of LET, the results relative to the initial yield of dsb show the independency of the amount of induced damage on the LET as well as on the particle type. These findings do not parallel what found for cell inactivation and mutation induction and indicate that, if dsb are the critical lesions for cellular effects, different types of radiation may produce dsb with different biological consequences.

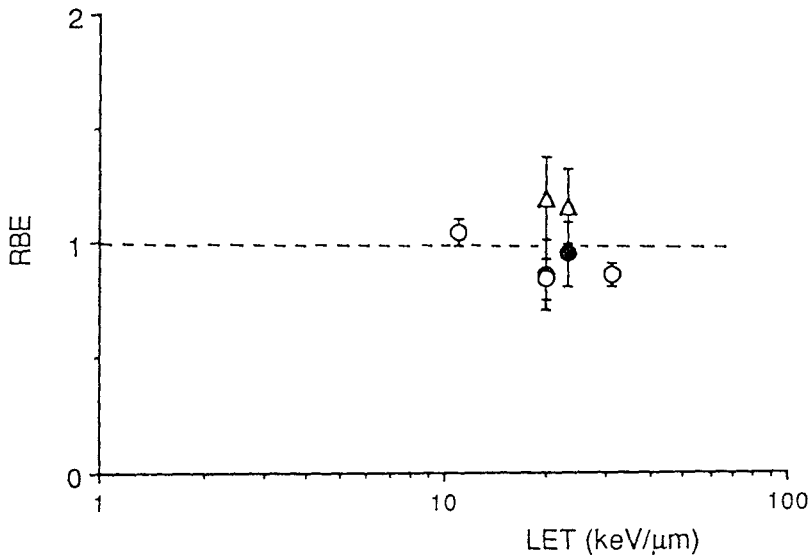


Fig. 2 RBE-LET relationship for V79 cell dsb production: (\circ) proton results obtained at LNL; (\bullet) proton and (\triangle) alpha particle results obtained at Harwell.

Publications

M. Belli, F. Cera, R. Cherubini, F. Ianzini, G. Moschini, O. Sapura, G. Simone, M.A. Tabocchini and P. Tiveron. "*LET dependence for cell inactivation, mutation induction and DNA DSB on V79 cells irradiated with high LET protons*", Thirty-Eight Annual Meeting of the Radiation Research Society, Tenth Annual Meeting of the North American Hyperthermia Group, New Orleans, Louisiana, April 7-12, 1990, Abstract Book: Ek-7, p. 164.

M. Belli, F. Cera, R. Cherubini, F. Ianzini, G. Moschini, O. Sapura, G. Simone, M.A. Tabocchini and P. Tiveron. "*RBE-LET relationship for V79 cells irradiated with low energy protons*", Radiation Protection Dosimetry, vol. 31, n. 1/4, 309-310, (1990).

F. Barone, M. Belli, F. Cera, R. Cherubini, F. Ianzini, G. Moschini, O. Sapura, G. Simone, M.A. Tabocchini and P. Tiveron. "*Initial yield of DNA DSB in V79 cells irradiated with low energy protons and X-rays*", 23rd Annual Meeting ESRB, Dublin, Ireland, September 23-26, 1990.

G. Simone, M. Belli, F. Ianzini, O. Sapura, M.A. Tabocchini, F. Cera, R. Cherubini, P. Tiveron and G. Moschini. "*Lethal and mutagenic effects of 7.6 keV/ μ m protons on V79 cells*", 9th International Congress of Radiation Research, Toronto, Canada, July 7-12, 1991; Vol. I, Congress Abstract, Eds. J.D. Chapman, W.C. Dewey and G.F. Whitmore, Academic Press, Inc.

R. Cherubini, F. Cera, A.M.I. Haque, P. Tiveron, G. Moschini, G. Galeazzi, G. Simone, M. Belli, F. Ianzini, O. Sapura and M.A. Tabocchini. "*The biological effectiveness of deuterons: description of the facility at LNL and preliminary results on V79 cells*", 9th International Congress of Radiation Research, Toronto, Canada, July 7-12, 1991; Vol. I, Congress Abstract, Eds. J.D. Chapman, W.C. Dewey and G.F. Whitmore, Academic Press, Inc.

F. Cera, R. Cherubini, A.M.I. Haque, G. Moschini, P. Tiveron, M. Belli, F. Ianzini, O. Sapura, M.A. Tabocchini and G. Simone. "*Radiobiology and radiotherapy projects with accelerated charged particles at the INFN-Laboratori Nazionali di Legnaro: present status and future perspectives*", VII Congresso Nazionale dell'Associazione Italiana di Fisica Biomedica, Ancona, Italy, June 8-12, 1992; to be published in *Physica Medica*

M. Belli, F. Cera, R. Cherubini, D.T. Goodhead, F. Ianzini, T.J. Jenner, G. Moschini, O. Sapura, G. Simone, D.L. Stevens, A. Stretch, M.A. Tabocchini and P. Tiveron. "*Relevance of experiments with different charged particles having the same LET for biophysical modelling of radiation effects*", In: *Biophysical Modelling of Radiation Effects*. Eds. K.H. Chadwick, G. Moschini and M.N. Varma (Adam Hilger, Bristol), pp. 285-292 (1992)

M. Belli, F. Cera, R. Cherubini, A.M.I. Haque, F. Ianzini, G. Moschini, O. Sapura, G. Simone, M.A. Tabocchini and P. Tiveron "*Inactivation and mutation induction in V79 cells by low energy protons: re-evaluation of the results at the LNL facility*", Accepted for publication in *Int. J. Rad. Biol.*, oct. (1992).

Project 4

Head of project: *Dr. B.D. Michael*

Objectives for the reporting period

Earlier work by ourselves and the partners we joined during the term of the contract had indicated that at matched LETs the effectiveness of singly-charged particles was appreciably higher than that of doubly-charged particles. The objectives during the reporting period were to study, jointly with partners, the biological effectiveness of singly- and doubly-charged particles in respect of cell kill, DNA damage and its repair, extending the range of LET beyond that covered previously. This included the use of deuterons in place of protons, exploiting their more favourable range-energy properties to enable us to examine the RBE-LET relationship closer to the track end and in the region of peak effectiveness. Also, to make a direct comparison of singly- and doubly-charged particles at near-matched LETs close to peak-effectiveness, we aimed to explore the feasibility of using helium-3 ions in our experimental system, these being preferable to α -particles to enable a match to be achieved in the important 50-60 keV/ μ m region, near to the expected RBE peak for protons/deuterons. In common with other partners, this work was in part directed at providing useful constraints for the studies modelling microscopic properties of radiation in relation to biological effect. We also aimed to commence development of a charged-particle microbeam irradiation facility to enable our studies to be extended into the extreme low-dose region. One of the objectives of the microbeam system is to set up *in vitro* models of low-dose exposures, with no more than one particle traversal per cell, as occurs in most environmental and occupational exposures involving α -particles or neutrons. A further project proposed by our group was to develop a novel approach to the study of the chemical stage of radiation effect to enable the induction and subsequent reactions of clustered damage to DNA to be determined.

Progress achieved, including publications

1. Biological effectiveness of singly- and doubly-charged particles for molecular and cellular endpoints

For this contract period, we initiated an experimental programme in three phases; first, to determine whether the properties of protons and deuterons of matched LET are indeed similar, second, to measure the effectiveness of deuterons at LETs beyond those possible using protons, and finally, to make a direct comparison of the RBEs of singly- and doubly-charged particles (specifically, deuterons and helium-3 ions) at near-matched LETs, using the same experimental arrangement. This programme required modifications to the existing experimental set-up to reduce as much as possible, the energy lost by the particles before reaching the cells. Additional modifications are required, to reduce the energy losses even further, before phase three can commence. The new arrangement has been characterised in terms of dose (using an extrapolation chamber), dose distribution (using CR39 etchable plastic) and energy (using a calibrated silicon surface-barrier detector). Data have been obtained using protons with mean incident energies of 0.74

and 1.07 MeV (41 and 27 keV/ μ m mean LET) and deuterons between 0.89 and 2.14 MeV (58 - 25 keV/ μ m). The mean LETs were determined by calculating the energy distribution within a typical cell nucleus, using stopping power tabulations and incorporating the measured incident energy spectrum. Our results so far are summarised below.

1.1 Cell survival

Preliminary studies have used cell survival as an end-point in Chinese hamster V79 cells. Cells have been irradiated on membrane filters with protons between 0.74 and 1.07 MeV (41-27 keV/ μ m) and deuterons between 0.89 and 2.14 MeV (58-25 keV/ μ m). The RBEs for these radiations relative to 240 kVp X-rays are shown in figure 1.

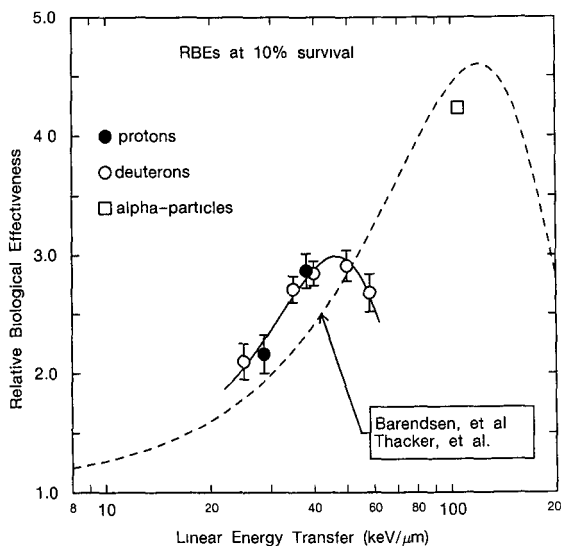


Figure 1 RBE (relative to 250 kVp X-rays) versus LET for V79 cells, measured at the 10 percent survival level.

This indicates that there is no significant difference between protons and deuterons within the LET range we have covered, as would be predicted from their identical net charge, and that the maximum effectiveness of deuterons and protons is in the range 40-50 keV/ μ m. We are liaising with the other groups in the consortium in connection with the differences they have detected between protons and deuterons at lower LETs.

1.2 DNA damage and repair

Parallel studies have also been carried out using these radiations to determine their effectiveness at inducing DNA damage in cells. In particular the induction and rejoining of DNA dsb have been measured using the neutral filter elution assay. Initial results indicate that protons and deuterons are about equally as effective as X-rays at inducing DNA dsb after doses of 2 - 20 Gy. This is in line with our previous studies where we have shown that the relative biological effectiveness for dsb induction is around 1.0 for a range of radiations with LETs of up to 100 keV/ μ m. This work indicated that, if dsb are the critical lesion, there is up to a 20-fold range of probabilities of an

initial dsb leading to cell kill, dependent on the type of radiation or chemical agent used to induce the damage. This we have postulated is due to undetected differences in the complexity of the initial lesions scored simply as dsb in this type of assay and, for various types of radiation, may reflect different frequency distributions of energy deposition in nanometer target volumes. We are developing several experimental methods to detect and quantify these complex lesions, and a chemical approach is described below. One possible consequence of differences in the complexity of dsbs is that there may be corresponding differences in their rejoining kinetics. Our data indicate that the rejoining of dsb after irradiation with protons or deuterons is reduced in comparison with X-rays. Figure 2 shows the rejoining of DNA dsb induced by 20 Gy of X-rays,

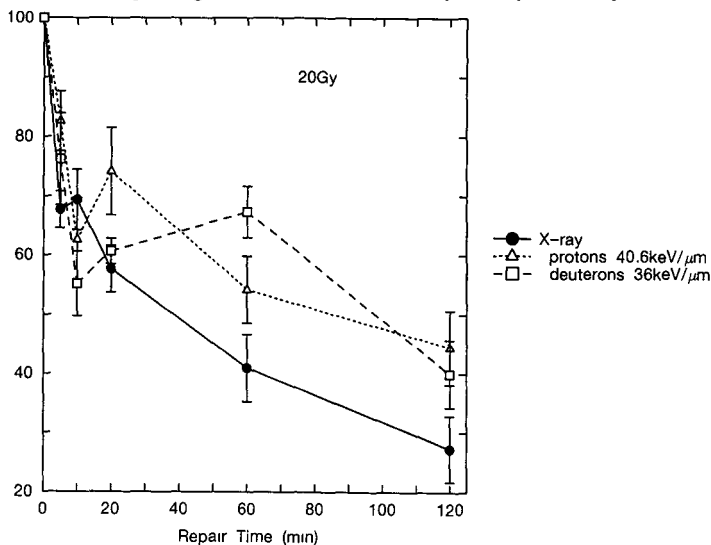


Figure 2 Rejoining of DNA dsb in V79 cells after 20 Gy of protons, deuterons or X-rays.

0.74 MeV protons or 1.46 MeV deuterons. Both the proton and deuteron data show reduced repair, relative to X-rays, in the form of an overall increase in the number of unrejoined dsb at the end of the 2-hour repair time studied in these experiments. We conclude that the increased effectiveness of protons and deuterons over X-rays is explainable not in terms of the initial yield of dsb but by a decrease in their reparability. The observed decreased rate of dsb rejoining for protons and deuterons may reflect clustering of damage associated with elevated frequencies of higher energy depositions in nanometer regions by these particles.

2. The chemical stage of radiation effect

We and others have made extensive studies of the chemical stage of radiation effect and this will contribute to the current aim of developing an integrated model linking the physical, chemical and biological stages. In common with others, our own work on the chemical stage has mainly employed low-LET radiation and, as a consequence, has tended to be dominated by single-radical chemistry, by default overlooking the multiple-radical chemistry that takes place at the important clustered

damage sites referred to above. During the present contract period, we have begun studies to enable us to follow the fast free-radical chemistry of clustered lesions in DNA. The methods we are developing are based on our work using fast-response techniques to measure reactions of thiols and oxygen with DNA radicals, but have now been adapted to the use of pulsed proton irradiation, rather than the pulsed electrons used before. Initial results show substantial differences from the reaction kinetics of low-LET-induced radical sites, consistent with the reactions expected of clustered lesions. Ongoing work aims to use this system as a means of quantifying damage clustering in terms of reaction kinetics and relating it to effects observed at the cellular level, including the LET dependences of the oxygen effect and of biological effectiveness.

3. Charged particle microbeam development

The first phase of the charged particle microbeam development was completed towards the end of the contract period and comprised the installation of a new beamline and the associated beam-bending and focussing elements. Also complete are the installation of a pneumatically-operated radiation beam-stop and a radiation interlock system. The new arrangements deliver the beam to a purpose-built experimental area equipped with cell culture facilities.

For this project, we have acquired a solid-state microscope recently developed by Killion Technologies Corp., based at the BC Cancer Research Center, Vancouver. This state-of-the-art instrument will have a key role in the microbeam project as it will be used for recognition and alignment of the cells and the targets therein, also subsequently to follow and score radiation damage to individual cells. Preliminary evaluation of the microscope's capabilities has been completed. The microscope and various micropositioning elements have been assembled. The section of beamline beneath the optical table contains the first stage of collimation. Two pairs of manual micropositioning linear motion drives serve as X-Y slits. These slits will pre-collimate the beam, to a width of a few tens of microns. The pre-collimator is designed to ensure that the particles are reasonably co-linear with the final collimator, and to minimise to number of particles striking other parts of the beamline (which causes unwanted characteristic X-ray production). Three independent micropositioning elements have been assembled to position and manoeuvre accurately the various components that make up the irradiation stage (i.e. the solid-state microscope, the dish of cells and the 1 m collimator/detector - see below). The microscope has been modified so that it can be secured to a manual X-Y micropositioning stage which is, in turn, bolted to the optical table. The microscope supports a computer-controlled X-Y-Z positioning stage for aligning and focussing the sample. The positioning arrangement for the collimator/detector assembly is largely complete. This unit enables the collimator to be positioned to within a few microns of each cell. After each cell irradiation, the collimator can be lowered about a millimetre (and subsequently raised) to facilitate location and focussing of the next cell. Progress has been made with the development of a final microcollimator for the beam, the objective being to deliver charged particles with 1 μ m precision to individual cell nuclei. Also, progress has been made with the development of a transmission type of particle detector using a thin scintillator and coincidence detection. This will enable the exact number of particle traversals to be pre-programmed on a cell-by-cell basis. Preliminary tests of the system have been carried out including irradiation of cells.

Several other centres from the EC (this consortium), the USA and Japan are

active or interested in charged particle microbeam developments, with objectives similar to our own in setting up *in vitro* models of extreme low-dose exposures. We are organizing a Gray Workshop on this topic with representation from all of the centres involved, taking place at the Gray Laboratory 8-10 July 1993.

Publications

- HARROP, H.A., HELD, K.D. AND MICHAEL, B.D. (1991). The oxygen effect; Variation of the K-value and lifetimes of O₂-dependent damage in some glutathione-deficient mutants of *Escherichia coli*. *Int. J. Radiat. Biol.*, **59**, 1237-1251.
- KYSELA, B.P., MICHAEL, B.D. AND ARRAND, J.E. Field-inversion gel electrophoresis analysis of the induction and rejoining of DNA double-strand breaks in cells embedded in agarose -technical note. *Radiat. Res.* (accepted).
- KYSELA, B.P., MICHAEL, B.D. AND ARRAND, J.E. The relative contributions of levels of initial DNA damage and repair of double-strand breaks to the ionizing radiation-sensitive phenotype of the Chinese hamster cell mutant, XR-V15B. *Int. J. Radiat. Biol.* (accepted).
- MICHAEL, B.D. (1991). Will DNA damage measurements ever be sensitive enough to validate models? In: '*Biophysical Modelling of Radiation Effects*', K.M. Chadwick, G. Moschini, M.N. Varma (eds) (Adam Hilger, Philadelphia).
- MICHAEL, B.D., PRISE, K.M., FAHEY, R.C. AND FOLKARD, M. (1991). Radical multiplicity in radiation-induced DNA strand breaks: implications for their chemical modification. *Early Effects of Radiation on DNA*, E.M. Fielden and P. O'Neill (eds) (Springer-Verlag, Berlin-Heidelberg), *NATO ASI Series Vol. H 54*, 332-346.
- PRISE, K.M., DAVIES, S. AND MICHAEL, B.D. (1992). A comparison of the chemical repair rates of free radical precursors of DNA damage and cell killing in Chinese hamster V79 cells. *Int. J. Radiat. Biol.*, **61**, 721-728.
- PRISE, K.M., DAVIES, S. AND MICHAEL, B.D. Evidence for DNA double-strand break induction at paired radical sites. *Radiat. Res.* (accepted).
- PRISE, K.M., FOLKARD, M., DAVIES, S. and MICHAEL, B.D. (1991). The lethality of radiation-induced DNA double-strand breaks for radiations of differing LET. *NATO Advanced Research Workshop on Cell Biology: Early Effects of Radiation on DNA*. E.M. Fielden and P. O'Neill, (Springer-Verlag, Berlin), 103-104.
- PRISE, K.M., STRATFORD, M.R.L., DAVIES, S. AND MICHAEL, B.D. (1992). The role of non-protein sulphhydryls in determining the chemical repair rates of free-radical precursors of DNA damage and cell killing in Chinese hamster V79 cells. *Int. J. Radiat. Biol.*, **62**, 297-306.

I Partner: Cancer Research Campaign Gray Laboratory

(Please note: this partner joined the contract part way through its term)

CELLULAR AND MOLECULAR MECHANISMS OF RADIATION-INDUCED MYELOID LEUKAEMIA IN THE MOUSE

Contract Bi7-037 - Sector B13

1) Janowski, CEN-SCK - 2) Cox, NRPB

Summary of project global objectives and achievements

Animal models of induced neoplasias have an important role to play in the elucidation of the mechanisms of radiation tumorigenesis. An understanding of these mechanisms for a range of radiogenic tumour types will allow the more confident extrapolation of human epidemiological data obtained at high doses and dose rates to the low doses and dose rates that are of principal importance in radiological protection. In addition, there is increasing awareness of the influence that genetic factors can exert on the incidence of some human tumours and, for induced neoplasia, animal models may provide the most important experimental approach to this problem.

Leukaemia is a major radiogenic neoplasm in man and a number of mouse strains, including CBA/H, provide an excellent non-viral model of induced acute myeloid leukaemia (AML). While there is a wealth of quantitative data relating to the induction of murine AML by radiation, our understanding of the mechanisms through which initial damage to haemopoietic target cells leads to the multi-step development of malignancy remains rudimentary.

In a previous CEC-supported study on radiation induced AML in the CBA/H mouse it has been established that: (a) chromosome (ch)2 rearrangements and/or deletions was a consistent feature of murine AML; (b) these ch2 events were induced directly by radiation in target haemopoietic cells and probably represent an initiating event for AML; (c) the expression of interstitial fragile sites (c-fra) on ch2 appear to underly region-specific damage to this chromosome; (d) these ch2-c-fra show a recombinational affinity for the terminal (telomeric) regions of other chromosomes; (e) some AMLs exhibit DNA sequence loss and/or modification in the interleukin (IL)-1 haemopoietic gene cluster region that was mapped to 2F; (f) there was cytogenetic evidence that genetic or epigenetic factors affect the expression of c-fra. The principal objective of this current research programme was to extend knowledge of the cellular, cytogenetic and molecular events that drive radiation myeloid leukaemogenesis. The main emphasis was placed on characterising the early ch2 events that are believed to initiate murine AML but consideration was also given to genetic factors influencing leukaemogenic predisposition and other cellular and molecular events involved in the malignant process.

Following indications that the region-specific breakage of ch2 involved interstitial telomere-like repeat (TLR) sequences at c-fra, cloned TLR sequences were used as probes for fluorescence in situ hybridisation mapping of ch2. These studies strongly suggest that AML-associated ch2 breakage occurs preferentially at c-fra containing TLR arrays having an inverted repeat DNA structure. One such array was mapped close (ca. 270 kb) to the IL-1 haemopoietic gene cluster which is known to be altered in some AMLs. In genetic studies, CBA/H mice were unexpectedly found to be heterogeneous for a particular sequence TLR locus; it was subsequently established that this locus was associated with AML-predisposition such

that the vast majority of induced AMLs derive from a sub-population of animals in the colony that constitute only 20-25 % of the total. Further studies showed that the informative TLR sequence polymorphism was of germ line origin and was often inherited in an irregular fashion but, unfortunately, the inherent instability of this sequence has created great problems for molecular cloning.

A possible role of recombinant retroviruses (of which the proviral genome might provoke chromosomal rearrangements) in radiation leukaemogenesis remains a debated question. A few whole body irradiated patients were reported to have developed leukaemia from healthy, transplanted bone marrow. The fact that we succeeded in inducing radiation non-T leukaemias in NFS mice (which do not carry endogenous ecotropic proviruses susceptible to generate leukaemogenic recombinants) pleads against a viral etiology. However, the interesting point in these experiments is that the induced NFS neoplasms appeared as a new murine model for the rather common human bi-phenotypic myeloid/pre-B leukaemias.

Besides the early ch2 deletions and/or rearrangements in radiation murine AMLs, additional events must take place for the completion of the multi-step leukaemogenic process. A literature survey revealed that activation of a ras oncogene, considered with few exceptions as a late carcinogenic event, was observed in 113 out of 412 (27 per cent) human AMLs. This certainly is a minimal estimate, the reported studies having rarely dealt with all the possible oncogenic mutations at codon 12, 13 or 61 of all three H-, K- and N-ras genes. An exhaustive screening of radiation murine AMLs showed that they are much less frequent than in human AMLs.

Disturbed expression of haemopoietic growth and/or differentiation factors might play an important role in the multi-step leukaemogenesis. Their production pattern was investigated in a variety of radiation leukaemias (T, myeloid and bi-phenotypic myeloid/pre-B) and the NFS radiation leukaemias and in the N122 cell line, derived from a radiation murine AML. Testing also for the expression pituitary hormones (growth hormone and prolactin), we confirmed literature data reporting their expression in haemopoietic tissues. Interestingly, their transcription factor pit-1 (of which the gene contains a homeobox domain) was not expressed in radiation leukaemias.

Finally, the lack of monoclonal antibodies for the murine myeloid lineage justifies the search for other biochemical markers. Membrane receptors for neurotransmitters could be useful in this regard. Receptors for the calcitonin gene related peptide (CGRP-R), which are not commonly encountered on blood cells, were identified on myeloid and bi-phenotypic (myeloid, pre-B) leukaemic cells, but in no single instance on T-cell leukaemias. CGRP-R thus appears as a promising potential marker for non-T radiation leukaemias.

Project 1

Head of project: *Dr. Janowski*

Objectives for the reporting period

- Screening mouse radiation AMLs for all possible oncogenic point mutations in codons 12, 13 and 61 of the H-, K- and N-ras genes.
- Characterising the NFS X-ray induced neoplasms, a new mouse model for the rather common biphenotypic human leukaemias.
- Determining the expression pattern of growth and differentiation factors in a radiation leukaemias and in the N122 AML cell line.
- Testing for the expression of receptors for neurotransmitters coupled to adenylate cyclase (potential markers for differentiation and for leukaemic transformation) on various radiation leukaemia types.

Progress achieved including publications

1. Search for ras mutation in radiation AMLs of the CBA/H mouse

The polymerase chain reaction (PCR) products of the H-, K- and N-ras genes from 25 radiation-induced acute myeloid leukaemias (AML) of various origins (11 tumours from X-irradiated CBA/H mice, 5 transplanted tumours from X-irradiated SJL/J mice, 4 cell lines established from tumours of X ray-induced NFS mice, and the virally transformed N122 cell line from a 229-Ra treated mouse) were screened by oligonucleotide mismatch hybridisation with probes for all the known oncogenic ras mutations in codons 12, 13 and 61.

Only one mutation was found, consisting in a gly to cys transition in codon 13 of the K-ras gene of a X-ray induced CBA/H AML. It thus appears that classical oncogenic ras mutations are much less frequent in mouse radiation AMLs than in human AMLs, of which 27 per cent were reported to display such a mutation.

2. A mouse model for the bi-phenotypic human leukaemias

At the cellular level, we have characterised X-ray induced neoplasms in the NFS mouse. Eight non-thymic leukaemias were adapted to tissue culture and subsequently cloned. Mercaptoethanol was essential for their growth. The cells were found to be cortisone-resistant, but sensitive to X-irradiation. Apoptosis was induced in all the lines by as little as 2 Gy.

Cytochemical markers (e.g. chloroacetate esterase) suggested a myeloid nature for all cell lines. Further analysis revealed the expression of receptors for the calcitonin gene related peptide (CGRP), previously identified on cells of the myeloid (and not of the lymphoid) lineage. By immunophenotyping, all cell lines were negative for pre-T and T markers. In contrast, pre-B or B markers were consistently present (6C3-HSA-B220). Some of the lines also expressed CD5 molecules. Analysis of the IgH locus in

these cell lines revealed clonal rearrangement of the G region. Furthermore, the expression of the v pre-B surrogate light chain component, a hallmark of pre-B cells, was documented by PCR and molecular hybridisation. The lines were tested for the expression of various cytokines at the mRNA level. They did not express IL-2, IL-4 and IFN- Γ , some expressed IL-1 α , IL-7, TNF- α , TNF- β in various combinations. The eight lines expressed IL-6, and one line IL-3. These radiation-induced neoplasms of the NFS mouse thus represent murine models for the rather common bi-phenotypic human leukaemias.

3. Expression of cytokines in the radiation AML N122 cell line

The expression of various cytokines (GM-CSF, IFN- α 1, IFN- α 2, IFN- β , IFN- Γ , IL-1 α , IL-2, IL-3, IL-4, IL-5, IL-6, IL-7, IL-10, LIF, N-CSF, TGF β , and TNF α) was analysed in the N122 cell line, synthesising cDNA from the cellular RNA and using adequate probes for molecular hybridisation with the PCR products. The expression of these cytokines was studied without and after activation of the cells with polyclonal activators such as PMA, Ca-ionophores (A23187), and lipopolysaccharide which activate preferentially macrophages. The expression of actin was used as a control.

The studies revealed that IL-6, IL-7, LIF and TGF β were expressed constitutively, while the expression of most of the other cytokines (GM-CSF, IFN α -1, IFN- α 2, IFN- β , IFN- Γ , IL-1 α , IL-3, IL-5, IL-10, TNF- α) showed to be inducible after stimulation.

Bri and Peter: please check for the exactness of the origin of N122 described above (in 1.). Also, a short conclusion about the implications of the results (Macrophage nature? myelomonocytic?)

4. Membrane receptors for neurotransmitters on radiation leukaemias

Since receptors for neurotransmitters coupled to adenylate cyclase represent potential markers for differentiation and for leukaemic transformation, their expression in the radiation neoplasms of the NFS mouse was investigated. Most promising in this respect are receptors for CGRP (CGRP-R). They are not commonly encountered on blood cells. In collaboration with P. Robberecht (Medical School, Free University of Brussels ULB), we have identified CGRP-R on myeloid and bi-phenotypic (myeloid, pre-B) leukaemic cells, but in no single instance on T-cell leukaemias. CGRP-R positive lines included 14-259 (SJL, radiation induced, myeloid) and N122. The human HL60 line expressed CGRP-R only after treatment with inducers of differentiation such as retinoic acid. Constitutive expression of CGRP-R thus appears as a most promising potential marker for non-T radiation leukaemias.

5. Growth and differentiation factors in radiation leukaemia cells

Several cell types in the haemopoietic system express receptors for growth hormone (GH) and prolactin (PRL). These pituitary hormones have occasionally been detected in haemopoietic tissues. In collaboration with E. Peters (Medical School, Free University of Brussels VUB), we have investigated the expression of GH, PRL and pit-1 (a transcription factor which controls GH and PRL expression) using both PCR (combined with molecular hybridisation when necessary), by in situ molecular hybridisation and immunochemistry.

Most important, expression of pit-1 was, for the first time, detected in adult non-pituitary tissues. A panel of leukaemic cell lines was also investigated. Surprisingly, no subgroup of leukaemias was identified that expressed pit-1. Rather, pit-1 expression was found in cell lines comprising one myeloid (HL60, out of 4 tested), one B (RAJI, out of 4 tested), one myeloma (SP 2/0) and one T leukaemia (JURKAT, out of 6 tested). So far, none of 10 radiation-induced leukaemias (T, myeloid, or bi-phenotypic) expressed pit-1.

These, together with literature data, support the idea that PRL (and its transcription factor pit-1) are involved in some human and murine leukaemia types. It should be noted that the pit-1 gene contains a homeobox domain and that rearrangements and/or altered expression of homeobox genes have already been implicated in leukaemia.

Publications

1990

M. Janowski, R. Cox and P.G. Strauss: The molecular biology of radiation-induced carcinogenesis: thymic lymphoma, myeloid leukaemia and osteosarcoma. *Int. J. Rad. Biol.* 57, 677-691, 1990.

E.A. Bruyneel, M. De Smets, C.H. Dragonetti, R.J. Hooghe, S. Di Virgilio and M.M. Mareel: Effect of glycosylation inhibitors on N-glycosylpeptides and on invasion of malignant mouse MO4 cells in vitro. *J. Cell Sci.* 95, 279-286, 1990.

1991

F. Bollengier, R. Hooghe, B. Velkeniers, A. Mahler, L. Vanhaelst and E. Hooghe-Peters: Further characterisation of rat 26,000 prolactin as a glycoprotein with essentially O-linked carbohydrate chains. *J. Neuroendocrin.* 3, 375-381, 1991.

S. Di Virgilio, K.P. Hellman, P. Robberecht, E.A. Bruyneel, G. Van Dessel, M. Rampelberg, M. Marcel, R. Hooghe & H.J. Gabius: Multiple differences between wild-type B16 melanoma cells and a wheat germ agglutinin resistant clone. *Anticancer Res.* 11, 1815-1822, 1991.

E. Hooghe-Peters, B. Velkeniers, L. Vanhaelst & R. Hooghe: Interleukin-1, Interleukin-6: Messengers in the neuroendocrine immune system? *Path. Res. Pract.* 187, 622-625, 1991.

R. Hooghe, M. Rampelberg, S. Di Virgilio : Cell surface glycans influence the fate of circulating white blood cells. *Lectins and Cancer*, H.J. Gabius & S. Gabius eds., pp. 283-292, 1991.

M. Janowski: The ras proteins and the ras-related signal transduction pathway. *Radiat. Env. Biophys.* 30, 185-189, 1991.

Submitted

M.P. Defresne, B. Borremans, C. Verhofstede, A. Peled, A. Thiry, R. Greimers, P. Robberecht, B. Nabarra, L. Verschaeve and R. Hooghe: Bi-phenotypic murine leukaemias.

Project 2

Head of project: *Dr. Cox*

Objectives for the reporting period

The principal objectives in this project were:

- 1) To use various molecular cloning strategies to isolate interstitial TLR sequences from the CBA/H mouse.
- 2) To use cytogenetic and molecular techniques to establish a relationship between TLR sequences, c-fra and ch2 breakage.
- 3) To initiate work on the construction of a ch2-specific DNA library.
- 4) To investigate the possibility that CBA/H mice carry an AML-predisposing mutation.

Progress achieved including publications

1) The molecular cloning of telomere-like repeat sequences

As well as being present at chromosome termini, telomere-like repeat (TLR) sequence arrays containing the motif (TTAGGG)_n are also represented at interstitial sites where they may be highly recombinogenic. Accordingly, it was proposed that such arrays may be represented at c-fra breakpoints on murine ch2. A polymerase chain reaction (PCR) methodology was developed to obtain molecular clones representing interstitial TLR sequences in the CBA/H mouse and, subsequently, TLR-containing plasmid clones were isolated from a) size-fractionated Bal31 exonuclease-insensitive DNA restriction fragments from whole genomic DNA and b) ch2 DNA microdissected from metaphase preparations (see 3).

Some of these TLR clones were fully or partially sequenced and of particular interest was ptel300 (from size fractionated DNA) that contained an inverted repeat of the (TTAGGG)_n motif. In contrast, ptel1800 (from microdissected ch2 DNA) contained a simple linear repeat of this motif, ie. (TTAGGG)₃.

2) The relationship between TLR arrays and chromosome 2 breakage

It was argued that if radiation sensitive c-fra are represented by TLR sequences then in situ fluorescence hybridization (FISH) techniques should reveal concordance between the patterns of induced ch2 breakage and TLR hybridization. This question was addressed in extensive studies using ptel300 and the appropriate sub-clone of ptel1800.

The ptel1800 sub-clone, while showing specific hybridization to the termini of mouse chromosomes, exhibited minimal affinity to interstitial sites suggesting that extensive linear repeats of TTAGGG are not well represented outside the terminal regions. In contrast, ptel300 hybridized very strongly at multiple interstitial sites on all chromosomes but less efficiently at chromosome termini. The ptel300 FISH signals in ch2 G-bands were subsequently mapped and compared with the pattern of induced breakage using Monte Carlo statistical procedures. This analyses revealed concordance for all but the terminal regions with the B, C and F regions showing particularly strong associations. Overall, at the cytogenetic level, the ptel300 FISH pattern was highly predictive of chromosome 2 breakage suggesting that the putative c-fra involved in AML initiation may contain TLR sequence arrays of the inverted repeat form.

3) Chromosome 2 microdissection and microcloning

The further characterisation of AMLs and their early progenitor clones would be facilitated by the availability of a ch2-specific DNA library for the FISH 'painting' of this chromosome. This problem was approached by the use of a novel technique whereby ch2 DNA was scraped from metaphase chromosome preparations using micromanipulated glass needles. Multiple scrapes provided sufficient target DNA for PCR which was used to generate DNA products for plasmid cloning. Using this technique a composite ch2 DNA library currently containing ~3000 clones of ~0.2-2.0 kb has been generated. Whilst yet of sufficient complexity to allow routine identification of ch2 by FISH painting, this library shows preferential labelling of the chromosome and has also acted as a resource for the isolation of TLR sequences (see 1). Preliminary studies on the capacity of this technique to produce region specific ch2 libraries have been initiated and a sub-library of ~500 clones representing the distal region of ch2 has been generated.

4) Molecular studies on telomere-sequence involvement in myeloid leukaemogenesis

Pulsed field gel electrophoresis studies had previously established that some ch2-rearranged AMLs exhibit DNA losses and/or modification in a 800 kb, 2F-encoded segment that includes the IL-1 α and β haemopoietic genes. The FISH mapping of a TLR sequence array to 2F (see 2) prompted a reanalysis of this 800 kb region for the presence of such arrays. These studies revealed a strongly hybridizing TLR sequence within 270 kb of the IL-1 gene cluster raising the possibility that some 2F region breakpoints occur close to these genes. Conclusive evidence for this proposal is currently being sought.

Telomeric DNA probes were used in parallel in order to screen DNA from AMLs for evidence of informative restriction fragment length polymorphisms (RFLPs) that might be associated with ch2 breakage. During these studies it became necessary to also screen DNA from normal animals that make up the CBA/H colony from which these AMLs had been derived. This latter study revealed that, although highly inbred and by implication genetically homogeneous, the colony contained four genotypic sub-groups of animals that were distinguished by RFLPs for a specific TLR sequence array. These RFLPs were shown not to be determined by any obvious tissue-specific mosaicism in the mice nor by differences in the methylation status of the informative DNA restriction sites. Rather, it seems, DNA events occurring during germ line development and/or very early in embryogenesis are creating specific TLR sequence heterogeneity in the offspring leading to a stable contribution from four genotypic variants, ie. TLRpA, ~40%; TLRpB, ~30%; TLRpC, ~5-10% and TLRpD, ~20-25%. Of greatest importance however was the subsequent observation that 23/25 AMLs derive from variant D mice, a result that strongly implies that AML-predisposition within the colony is genetically determined by a locus that is either represented by or physically linked to the TLR sequence array of interest. Although as yet incomplete, TLR locus analysis of offspring from variant mouse crosses has indicated a degree of non-Mendelian inheritance of these RFLPs and the possibility that genotypic variation in the colony and the associated AML-predisposition is maintained by high frequency TLR sequence-directed recombination.

Equal importance was attached to the molecular cloning of the informative TLR locus. Using size-fractionated DNA highly enriched for the polymorphic TLR restriction fragment, λ bacteriophage libraries totalling ~10⁷ recombinants were constructed and screened for telomeric sequences. No TLR-positive clones were found, a result that is explained by the known instability of these arrays in conventional cloning vectors. In response to this problem, current molecular cloning strategies include the use of cosmid vectors designed for use with unstable DNA repeat sequences.

During the reporting period collaborations were established with other European, North American and Japanese laboratories in order to determine whether the unexpected genetic inhomogeneity of CBA/H and the associated AML predisposition is a feature of other mouse strains. Collaboration has also been sought in order to initiate studies on the role of TLR sequence arrays in human leukaemogenesis.

Publications

Breckon G, Papworth D and Cox R. Murine radiation myeloid leukaemogenesis: A possible role for radiation-sensitive sites on chromosome 2. *Genes, Chrom. Cancer* 3: 367-375 (1991).

Silver A, George A, Masson W, Breckon G, Adam J and Cox R. DNA methylation changes in the II-1 (2F) chromosomal region of some radiation-induced acute myeloid leukaemias carrying chromosome 2 rearrangements. *Genes. Chrom. Cancer* 3: 376-381 (1991).

Cox R, Breckon G, Silver A, Masson W and George A. Radiation-sensitive sites on chromosome 2 and their role in radiation myeloid leukaemogenesis in the mouse. *Radiat. Environ. Biophys.* 30: 177-179 (1991).

Breckon G, Silver A and Cox R. Radiation-induced chromosome 2 breakage and the initiation of murine radiation acute myeloid leukaemogenesis. *Japanese J. Radiat. Res.* (in press).

Bouffler S, Silver A, Papworth D, Coates J and Cox R. Murine radiation myeloid leukaemogenesis: The relationship between interstitial telomere-like sequences, chromosome 2 fragile sites and leukaemogenic initiation (submitted for publication).

Silver A and Cox R. Germ line telomere-like DNA repeat polymorphisms associated with pre-disposition to radiation-induced acute myeloid leukaemia in CBA mice (submitted for publication).

AUTOMATED DETECTION OF RADIATION INDUCED CHROMOSOME ABERRATIONS BY SLIT-SCAN FLOW CYTOMETRY

Contract Bi7-038 - Sector B13

- 1) *Barendsen*, Univ. Amsterdam - 2) *Green*, MRC Human Genetics Unit
- 3) *Nüsse*, GSF Neuherberg - 4) *Bauchinger*, GSF Neuherberg
- 5) *Aubele*, GSF Neuherberg

Summary of project global objectives and achievements

The development of techniques which will allow rapid assessment of chromosome aberrations will enable the determination of doses which human individuals or groups have received as a result of occupational or accidental exposures. Protection and intervention measures require dose assessments which, in most cases, cannot be based on physical dosimetry alone, but require also a biological method to be applied to individuals. In this project studies were carried out aimed at the automation of techniques for detecting karyotype abnormalities in large numbers of cells. Methods were developed for the preparation and staining of metaphase chromosomes and radiation induced micronuclei, suitable for application in automated analysis procedures. Chromosome aberrations and micro nuclei were analyzed by transmission and fluorescence microscopy and by flow cytometry. To evaluate the data, various techniques were developed for the analysis of the digitally recorded microscopic images and for the quantitative evaluation of the flow cytometry data. The investigations were carried out jointly by Dr. D. K. Green (MRC, Edinburgh), Dr M. Nüsse (GSF, Neuherberg), Prof. Dr. M. Bauchinger (GSF, Neuherberg), Dr. M. Aubele (GSF, Neuherberg), and Prof. Dr. G.W. Barendsen and Dr. J.A. Aten (UvA, Amsterdam).

Barendsen and Aten (UvA, Amsterdam).

We have developed a slit-scanning flow cytometer for the analysis of chromosome aberrations. In our slit-scanning flow cytometer, stained chromosomes are injected into the liquid flow and are aligned in the flow channel as they pass the laser beam, with their long axis parallel to the flow direction. In this manner the silhouette of the chromosome is recorded as a fluorescence profile. These chromosome profiles are characterized by the centromeres that appear as dips in the silhouette.

We tested the effectivity of the method for the morphological analysis of human chromosomes by simultaneously evaluating their centromeric index (CI) and their DNA content. In these experiments the resolution of the resulting DNA vs CI flow karyogram was considerably higher than the resolution obtained in the DNA based monovariate flow karyogram. Dicentric chromosomes were identified on the basis of their two centromeres. This was achieved by counting the number of centromere dips in the slit-scan profiles. Normal chromosomes were expected to produce bimodal profiles and dicentric chromosomes would generate trimodal profiles. To detect and

sort chromosomes associated with trimodal profiles, we developed an analog pulse shape analysis module that can be used for sorting chromosomes with respect to the number of centromere dips. We showed that these sorted chromosomes can be identified using fluorescence in situ hybridization techniques. As dips in the slit-scan profiles are not caused by centromeres only, we investigated which quantifiable profile features can be used to distinguish dicentric chromosomes from artefacts.

Green (MRC, Edinburgh)

The objectives of the Edinburgh team were to explore several fluorescence in-situ hybridisation labelling techniques for labelling human metaphase chromosomes and to assess the efficiency of each approach in terms of highlighting random chromosome damage. Priority has been given to chromosome painting techniques and the work began with an investigation into generating chromosome painting libraries using sorted chromosomes followed by Alu-PCR amplification. These gave disappointing results. Commercially available chromosome painting libraries performed more efficiently and with the addition of specific centromeric probes gave rise to near complete coverage of the chosen chromosome DNA. Attention has been focussed on painting the large human chromosomes, usually chromosomes 1 and 2, to ultimately test the hypothesis that counting painted chromosome fragments (translocations or dicentrics) which must be smaller than the whole painted chromosomes, would lead to a routine and sensitive radiation dosimetry method. The feasibility of manually counting painted chromosome fragments was tested with hybridisation of a chromosome 12 DNA library to metaphase chromosomes following in vitro X-irradiation. The results largely agreed with the theoretical predictions.

Image processing techniques will ultimately be required for routine analysis of microscope slides containing counterstained and painted metaphase chromosomes. Without automation the advantages over traditional dicentric chromosome scoring would be minimal. A fluorescence imaging platform was constructed and a high resolution CCD camera was installed to capture metaphase chromosomes stoichiometrically stained with DAPI and painted with FITC. Algorithms were assembled to segment the DAPI image into whole chromosome boundaries, to bring the FITC image into registration with the DAPI image and to quantitate the FITC fluorescence corresponding to whole or translocated chromosomes. Damaged chromosomes either dicentric or translocated were clearly recognised. A similar image processing system for recognising centromeric and telomeric probes is in place. With the addition of an automatic metaphase finder for fluorescently labelled metaphase spreads the automation of painted chromosome fragment counting now seems possible.

Work has also commenced on in-situ hybridisation of DNA probes to chromosomes in suspension. The technique of capturing suspended chromosomes in agarose beads prior to hybridisation has shown some promising results.

Nüsse (GSF, Neuherberg)

The primary goal of our investigations was the development and application of a new automated flow cytometric method to measure induced micronuclei in human lymphocytes for a possible detection of low doses in irradiated humans. The dose sensitivity of this new assay was studied using human lymphocytes irradiated in vitro, factors that influence the sensitivity of this new assay were identified. A second objective was the identification and analysis of several factors that influence the DNA distribution of radiation-induced micronuclei using flow cytometry in combination with several immunofluorescence techniques as for example anti-kinetochore antibodies and in situ hybridization with DNA probes against centromeric and telomeric regions of chromosomes.

A new flow cytometric method was developed that quantifies the frequency of radiation-induced micronuclei (MN) in mammalian cell cultures and human lymphocytes with high precision. Nonspecific debris hampering the measurement of MN was discriminated from MN using several flow cytometric parameters simultaneously. For human lymphocytes the fraction of cells in the second cell cycle was measured additionally using flow cytometry. Eight individual linear-quadratic dose response curves derived from five donors revealed inter- and intraindividual variabilities of all curve parameters. Since also an age-dependence was found for spontaneous MN-frequencies and for the linear curve parameter, a combined linear-quadratic age-dose-effect-model was used to fit the data. The 90% prediction interval showed that a reliable individual dose estimation cannot be achieved for exposures of humans below about 1 Gy.

Fluorescence in situ hybridization (FISH) with a combination of telomeric and centromeric DNA probes was used to analyse the nature of radiation-induced MN in mouse fibroblasts. The frequency of MN derived from whole chromosomes and from one or multiple acentric fragments could be measured with the technique. These data were used for a quantitative analysis of the DNA distribution of radiation-induced MN. The DNA content of MN was found to be influenced by several factors: The DNA distribution and the centromeric index of the chromosomes, the cell cycle phase at time of MN measurement due to DNA synthesis in MN, the presence of chromosome fragments in MN and the presence of whole chromosomes in MN.

Bauchinger (GSF, Neuherberg)

The response relationships of radiation-induced (X-, ^{60}Co gamma-rays, fission neutrons), and micronuclei (MN) were analyzed in a cytokinesis block (CB) MN assay in human lymphocytes. In serial examinations of 4 donors during a period of one year, intra and interindividual variations of background and induced MN (^{137}Cs gamma-rays) were analyzed and described by a variance component model. The content of MN was analyzed in mouse liver cells, exposed to ^{137}Cs gamma-rays or Vinblastine. We have shown that in situ hybridization with a biotinylated degenerate DNA probe of mouse gamma (major) satellite DNA can be reliably used in a CB MN assay to discriminate between MN containing centromeres, i.e.

chromosomes or acentric fragments.

Aubele (GSF, Neuherberg)

The objectives of our project are the establishment of dose-effect-curves for Chromatin Texture Assay in in vitro exposed human lymphocytes. The experiment shall also elucidate the role of varying chromatin texture during the cell cycle on damage expression.

In the reporting period we have firstly concentrated on preparatory protocols and the investigation of conceptual relations of chromatin texture features on size and staining density of nuclei. Using features independent of those parameters we have then defined chromatin pattern differences of nonirradiated human lymphocytes in different functional states of the cell cycle.

For evaluation of the role of chromatin pattern features in cell nuclei for monitoring radiation exposure we have then investigated the expression of radiation effects on chromatin texture within the different cell cycle groups G1, S, G2.

Finally with the group of most expression of these effects (G1-phase) discriminant analysis was performed between the different dose-groups with textural parameters to establish dose effect curves.

Human PHA-stimulated lymphocytes show changes in growth kinetics and in the occurrence of highly aneuploid cell components.

By high resolution image cytometry we could define a clearly distinct chromatin pattern in unirradiated cells in different functional states of the cell cycle using DNA-independent textural parameters. Also significant differences in the chromatin texture as a function of radiation dose were quantitatively measured. The latter we found more expressed in G1-cells than in S- or G2-phase cells. Dose-effect-curves derived from linear discriminant analysis and from regression analysis were established.

Variations between the donors concerning chromatin pattern in different cell cycle phases are subtle, whereas variations concerning radiation induced changes in chromatin texture do clearly exist.

Project 1

Head of project 1: *Prof. Barendsen*

Objectives for the reporting period

This part of the project was aimed at the automation of techniques for detecting karyotype abnormalities in large numbers of cells using slit-scanning flow karyotyping of fluorescent chromosomes in suspension. To achieve this goal we carried out the following studies:

- Investigation of the suitability of the slit-scanning system for recognizing human chromosomes.
- Investigation of the advantages of state of the art chromosome isolation and chromosome labelling techniques for the analysis procedure.
- Testing of the method for the detection of radiation-induced chromosome aberrations and incorporation of additional selection criteria to increase the sensitivity and to reduce the number of false positive signals.

Progress achieved including publications

Flow cytometry provides a fast method for the analysis of metaphase chromosomes. Using mono-disperse suspensions of chromosomes stained with one or more fluorescent dyes, the DNA content and base-pair composition of large numbers of chromosomes can be measured. Attempts have been made to apply flow karyotyping for the analysis of chromosome aberrations induced by radiation. These chromosome aberrations, however, are characterized by morphological changes which cannot be analyzed by conventional flow cytometry that provides information on the DNA content of chromosomes only but not on their morphology. To overcome this limitation we have developed a slit scanning method that combines the quantitative aspects of flow karyotyping with morphological analysis.

In our slit-scanning flow cytometer, stained chromosomes are injected into the liquid flow and are aligned in the flow channel as they pass the laser beam, with their long axis parallel to the flow direction. The fluorescence of the chromosome is detected as a function of time as it passes the laser beam that is focussed to a diameter of 2.7 μm . In this way the silhouette of the chromosome is recorded as a fluorescence intensity profile. These chromosome profiles are characterized by the centromeres that appear as dips in the silhouettes. From the fluorescence profiles, the number and positions of centromeres can be determined, which provide information on morphological changes of chromosomes. Our slit-scanning chromosome sorter is constructed on the basis of a commercially available cell sorter. This facilitated the construction of the instrument and makes the method available for wider application. With our slit-scanning method, profiles can be acquired at a rate of 500 per second.

Analysis of the profiles is performed on-line, allowing chromosomes with characteristics corresponding to specific morphological criteria, to be sorted and deposited on slides for subsequent visual inspection.

1. Human chromosomes

During the development phase, the system was tested on chinese hamster chromosomes. For radiation protection purposes the method has to be applied to human chromosomes. We, therefore, extended the method to analyse the shapes of human chromosomes as expressed by their centromeric index (CI) and their DNA content. These two variables were used as parameters in bivariate flow karyotyping analysis, Fig.1. The resolution of the DNA vs CI flow karyogram of the larger chromosomes, #1 to #13, is much higher than the resolution obtained in the DNA based monovariate flow karyogram. Several of these chromosomes cannot be distinguished or are difficult to discriminate in the DNA-based human karyogram. With slit scanning flow cytometry of these chromosomes can now be distinguished as individual peaks, e.g. chromosomes #1 and #2. The peak representing the chromosomes #9-#12 can be separated into two peaks formed by chromosomes #9 and #11, and #10 and #12, respectively.

2. Chromosome isolation and labelling

The length of the isolated chromosomes appears to be an important factor in the detection of the centromeres. For the isolation and staining of the chromosomes we used propidium iodide because its intercalating action results in long chromosomes. After isolation the length of the chromosomes was increased by incubating the unfixed chromosome suspension with trypsin. Pulse length and pulse shape analysis with the slit scanning flow cytometer was used to determine changes in morphology and mean length of the isolated chromosomes. By trypsin treatment the chromosomes could be stretched effectively in a controlled way. The treatment resulted in an increase in the average length of up to 40%. An additional advantage is that the centromeres are stretched more effectively than the arms of the chromosomes. The effect of the stretching is reflected in a 50% increase in efficiency for the registration of centromere dips which allows a more efficient detection of dicentric chromosomes isolated from irradiated cells. In our study chromosome morphology should be optimally preserved after the slit-scanning analysis and sorting procedures. The fragility of the stretched chromosomes, therefore, could pose a problem. To overcome this difficulty we investigated which procedure for sorting and collecting chromosomes on slides yields the best results. We found that the chromosomes could be sorted intact and could be stored on slides for up to 4 months at 4° C, if they were fixated with glutaraldehyde before flow karyotyping.

Our aim is not only to detect chromosome aberrations but also to study the process of their formation. For the investigation of mechanisms involved in the generation of chromosome aberration more detailed analysis techniques are required. In situ hybridization with chromosome specific DNA probes is useful in this respect as it offers an efficient

method for the analysis of the chromosomal composition of slit-scan sorted aberrations. The concept behind these experiments is that the chromosomal composition of dicentrics should depend, among other things, on the organization of the chromosomal material and on the interaction of the chromosomes in the interphase nucleus at the time of irradiation. We developed a method for fixating chromosomes individually slit-scan sorted on slides and showed that these sorted chromosomes could be identified using multi-color fluorescence in situ hybridization and chromosome painting techniques.

3. Testing the method for detecting chromosome aberrations

Dicentric chromosomes are assumed to be random aberrations that are variable in size and DNA content. They, therefore, cannot be detected by conventional flow karyotyping methods, but, using slit-scanning flow karyotyping, they can be identified on the basis of their two centromeres. This was achieved by counting the number of centromere dips in the slit-scan profiles. Normal chromosomes were expected to produce bimodal profiles and dicentric chromosomes would generate trimodal profiles.

To detect and sort chromosomes associated with trimodal profiles we developed an analog pulse shape analysis module for the on-line counting of dips in slit-scan fluorescence profiles. This module is very fast and it can be interfaced easily with commercial flow cytometers. In combination with cell sorters, the module provides an output signal that can be used for sorting chromosomes with respect to the number of detected dips. The module first generates a time derivative of the electrical signal corresponding to the fluorescence pulse shape. It then detects the zero-crossings of this derivative. Each zero-crossing is considered as a pulse maximum or a pulse dip. The module then determines whether the signal corresponds to a bimodal or to trimodal profile by counting the number of zero-crossings.

Dips in the slit-scan profile, however, are not caused by centromeres only. Aggregates of chromosomes or irregularly stretched chromosome arms can also result in trimodal profiles. To investigate the relation between the morphology of a chromosome and the shape of its slit-scan profile, we sorted chromosomes yielding trimodal profiles, one by one on separate slides, Fig.2. After sorting, these chromosomes were photographed, and for further analysis the negatives were digitized with a micro-densitometer for the construction of DNA-density profiles. This type of analysis provides valuable clues that can help to distinguish between true dicentrics and artefacts. Profiles with deep dips for example are always generated by chromosome aggregates. We also found that the edges of profiles corresponding to artefact profiles usually were less steep than the edges of profiles corresponding to dicentric profiles.

In order to determine which quantifiable profile features can be used to distinguish dicentric chromosomes from artefacts, the shapes of 136 profiles were analysed in relation to the type of particle, i.e. dicentric or artefact, that they represented. In these experiments chromosomes were

sorted on separate slides and the corresponding slit-scan profiles were tagged and stored. When we applied various tests to these profiles we could find no criteria with which dicentric chromosomes could be identified unambiguously. We, however, did find that for the analysis of tri-modal profiles: (1) the relative difference between the nadir values of the two dips, $\Delta D/\Sigma D$, and (2) the value of the largest relative difference between the heights of the three fluorescence maxima, $\Delta H/\Sigma H$, cf Fig.3, were useful parameters. Their effectiveness for the analysis of slit scan profiles was evaluated by determining the fraction of dicentric profiles, i.e., the ratio of the number of dicentric chromosomes relative to the total number of profiles, as a function of the values of these parameters. Depending on the parameter values we found fractions of dicentrics varying between 0 and 0.7. Based on these results we have started the construction of a module for implementation in our sorter system that uses these criteria in on-line evaluation of slit-scan profiles. The high analysis rate and the sorter facility, in combination with the visual inspection of the sorted chromosomes, will provide a method that can cope effectively with the remaining false positives.

Another factor reducing the effectiveness of the analysis of chromosome morphology by slit scanning flow cytometry is the photon counting noise present in the fluorescence profiles. To overcome this problem we also have started the development of a highly sensitive slit scanning detector for implementation in commercial flow cytometers and cell sorters.

In the next phase of the project, the techniques for chromosome enrichment by slit scan sorting and for chromosome staining with DNA probes discussed above and the techniques under development, will be applied for the analysis of the frequency and chromosomal composition of radiation induced dicentrics.

Publications

- Boschman G.A., Rens W., Manders E.M.M., van Oven C.H., Barendsen G.W., Aten J.A. (1990). On-line sorting of human chromosomes by centromeric index and identification of sorted populations by GTG-banding and fluorescent in situ hybridization. *Hum.Genet.* 85: 41-48.
- Van Oven C., Aten J.A. (1990). Instrument for real-time pulse-shape analysis of slit-scan flow cytometry signals. *Cytometry* 11: 630-635.
- Hausmann M., Dudin G., Aten J.A., Diaz E., Cremer C. (1991). Slit-scan flow cytometry of isolated chromosomes following fluorescence hybridization. An approach of on-line screening for specific chromosomes and chromosome translocations. *Z.Naturf.* 46c: 433-441.
- Hausmann M., Zuse P., Aten J.A., Rens W., Männer R., Cremer C. (1991) High speed analysis of slit-scan profiles of normal and aberrant metaphase chromosomes. In: *Advances in Analytical Cellular Pathology*. Eds. Burger G, Oberholzer M and Vooijs GP. Elsevier Publ., Amsterdam, pp. 67-68.

- Boschman G.A., Rens W., Manders E.M.M., Slater R.M., Aten J.A. (1992). Flow cytometric detection of chromosome abnormalities by measurement the DNA base composition, DNA content and centromeric index. (submitted).
- Heilig R., Hausmann M., Rens W., Aten J.A., Cremer C. (1992) Time optimized analysis of slit-scan profiles on a general purpose personal computer. Comp. Appl. Biosc. (submitted).
- Rens W., van Oven C.H., Stap J., Aten J.A. (1992). Effective of pulse shape criteria for the selection of dicentric chromosomes by slit scan flow cytometry and sorting. Anal. Cell. Pathol. (submitted).

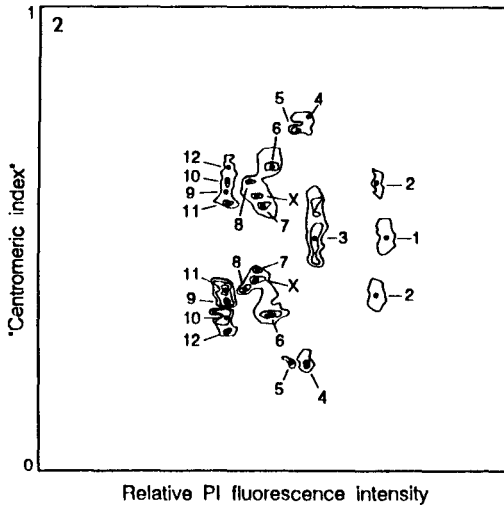


Fig. 1. Bivariate slit scanning analysis of metaphase chromosomes isolated from human skin fibroblasts. The relative fluorescence intensity (DNA content) and the "centromeric index" were used simultaneously as parameters; 100.000 particles were analyzed in 10 min. The dark spots represent the tops of the peaks and are used to indicate the peak positions.

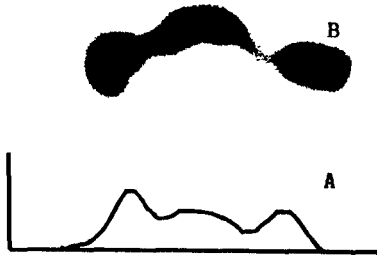


Fig. 2.
 A. Tri-modal slit-scan fluorescence profile detected on-line by the "pulse dip counter" module.
 B. Corresponding dicentric chromosome, sorted by the cell sorter system.

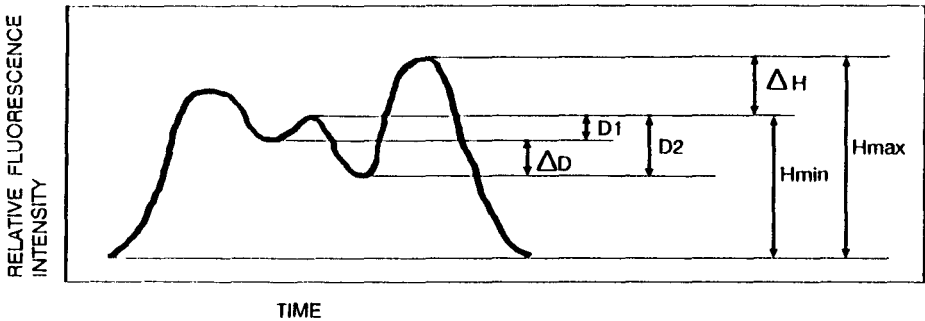


Fig. 3. The two pulse-shape parameters that were used to characterize the slit-scan profiles. The first parameter is $\Delta H / \Sigma H$ with $\Delta H = H_{max} - H_{min}$ and $\Sigma H = H_{max} + H_{min}$. H_{max} is the largest top height and H_{min} is the smallest top height of the profile. The second parameter is $\Delta D / \Sigma D$ with $\Delta D = D_1 - D_2$ and $\Sigma D = D_1 + D_2$. D_1 and D_2 are the depths of the first and the second dip respectively.

Project 2

Head of project: *Dr. Green*

Objectives for the reporting period

Our main objective was chromosome painting by in-situ hybridisation of chromosome specific DNA probes to detect abnormal chromosomes caused by randomly induced breaks. The subjects for investigation were as follows:-

- a) Extensive use of commercially available chromosome painting libraries with a view to their routine use for painting large metaphase chromosomes.
- b) Testing the theory that abnormal chromosomes can be recognised unambiguously where a "less than normal size" painted area is observed.
- c) Development of image processing algorithms to detect abnormal painted chromosome fragments from digitised counterstained metaphase chromosomes.
- d) Comparison of the efficiency of manual and image processing methods for detecting chromosome damage.

Progress achieved including publications

Specific chromosome painting libraries were initially constructed using the Alu-PCR technique applied to somatic cell hybrids containing a single human chromosome and to 'in house' flow sorted human chromosomes. These libraries, although useful for identifying chromosomes in complex rearrangements, were found to have several disadvantages for this project. Significant non-specific labelling of other chromosomes and background was often present. In addition the clustering of Alu sequences in R-bands produced a slight R banding pattern on the chromosome arms, and this, combined with the lack of signal at the centromeres could easily lead to false interpretation of the painted area by image processing approaches. Several commercial libraries (Imagenetics; Cambio) were tested: both gave less background especially the directly labelled Imagenetics libraries and both gave a more even coverage of the chromosome arms. However neither of the chromosome 1 libraries painted the heterochromatic region at the centromere and we have had to add a labelled probe for the this region to ensure complete coverage of chromosome 1. Directly labelled chromosome 1 and 2 libraries from Imagenetics were used individually and in combination to paint normal and irradiated metaphase preparations and this material is being used to build up a data set for testing algorithms.

A trial experiment was set up at an early stage to see if damaged chromosomes could be detected by chromosome painting. A chromosome 12 Alu-PCR library was hybridised to metaphase preparations from peripheral blood lymphocytes previously irradiated with 2 and 4 Gy X-rays. The slides were scored using the confocal microscope.

Two significant observations can be drawn from these results. Firstly the loss of chromosome morphology after in situ hybridisation made dicentrics as a class difficult to detect, and some were obviously missed. Secondly both dicentrics and translocations involving chromosome 12 were readily detectable; more translocations than dicentrics were found in the 4Gy data set. When the results for 2 and 4Gy are pooled the numbers of dicentrics and translocations are approximately equal, as current theory would predict.

Result 1

Sample - 50 metaphase cells, Radiation dose - 4Gy

Painting library - No. 12 chromosome (4.5% of genome)

	No Dicentrics	No. Dicentrics involving Ch.12	No. Translocations involving Ch.12
EXPECTED	60	2.7	2.7
OBSERVED	33	4	7

Result 2.

Combined counts from 4Gy and 2Gy experiments where Chromosome 12 painting library was used.

Sample - 100 metaphase cells.

DICENTRICS INVOLVING Ch.12	7
TRANSLOCATIONS INVOLVING Ch.12	8

Until recently the detection of radiation damage to chromosomes by image processing approaches has been concentrated on the detection and counting of dicentric metaphase chromosomes [Bayley et al, 1991]. This has involved creating sophisticated image processing software which was required to produce a complete description of each metaphase cell in terms of the segregation of each chromosome, including those which were overlapping or touching, and detailed pattern information which was sufficient to give a high confidence count of chromosome centromeres.

We investigated the proposed simpler method of recording random chromosome damage using chromosome painting and similar microscope image processing and computing equipment to that used in the dicentric scoring approach. Here fluorescence images were produced by standard epi-illumination microscopy and captured with a sensitive CCD array camera. The first image was generated by the fluorescence emission of a DNA counterstain and following a highly developed image segmentation process [Ji, 1989] gave rise to defined metaphase chromosome regions. Fluorescence emission from the chromosome painting probes falling inside these regions was considered to be a positive painting signal. Software was generated to properly register and superimpose the painted and counterstained images.

Events which involve two random chromosome breaks (leading to stable, balanced translocations or unstable dicentric chromosomes), where one break occurs in the 'painted region' appear as partially painted chromosomes. The painted region will be smaller than a completely painted chromosome. Figure 1, which is constructed from a superimposition of a counterstained image (light) and a chromosome paint image (dark), shows a damaged chromosome involving part of No 1 chromosome. The remaining part of the damaged chromosome appears to have been lost in this particular cell. A simplified image processing approach need only identify painted chromosome regions and then search for regions which are less than the expected size.

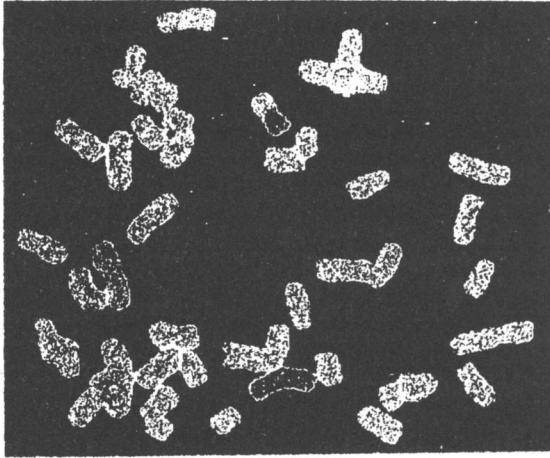


Figure 1

Counterstained human metaphase chromosomes, reconstructed from CCD camera images of DAPI and FITC fluorescence. Whole and translocated chromosome 1 painted regions are highlighted as dark areas on the light counterstain image.

Figure 2 shows the predicted radiation damage detection performance where increasing proportions of the genome are painted with a single colour. The proportion of the total amount of damage which becomes 'visible' is shown as a function of the percentage of painted genome, which naturally subdivides into whole chromosomes. The experiment described earlier, where only 4.5% of the genome was exposed to painting, which gives a maximum damage visibility of 5.2%, provide strong evidence for the feasibility of the painted fragment approach. One of the main advantages of recording random chromosome damage by analysing the fragmentation of selected painted chromosomes is that stable chromosome damage is detected with equal sensitivity to unstable damage. An accumulation of radiation exposure to an individual is detectable for many decades through measurement of the stable chromosome damage.

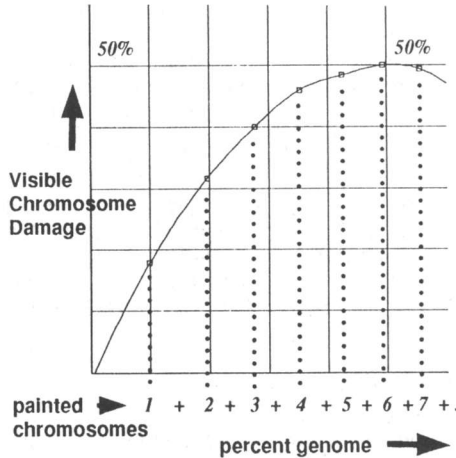
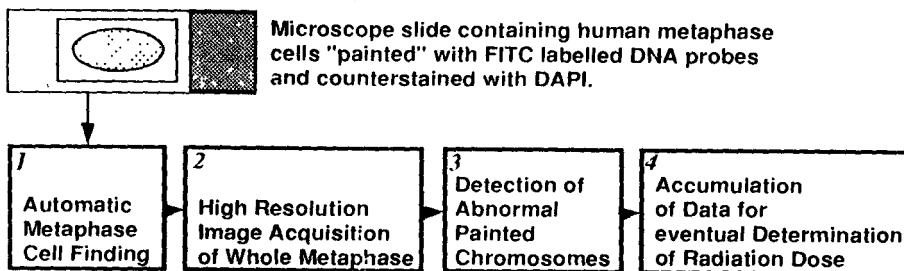


Figure 2

The approach also lends itself to a simpler pattern recognition task to that associated with detecting dicentric chromosomes from shape alone. Automation of the chromosome painting approach, which is essential for routine dosimetry requires several modules. These are illustrated below:-



1. Metaphase finding for homogeneously stained chromosomes imaged with transmission microscopy is available in a choice of high performance imaging systems. Translating this function to fluorescence imaging, where light levels are several orders of magnitude lower than the transmission case, has a high priority.

2. High resolution image acquisition has received the greatest attention. It has been demonstrated that DAPI counterstained metaphase chromosomes serving as a primary image can be accurately registered with FITC labelled painted regions and that the painted regions can be quantitatively compared with the expected 'normal' size [Piper et al. 1992].

3. Fragmented painted chromosomes have been shown to be detectable in a small data set. A larger data set will be required to attach statistical significance to these promising results.

4. The relation between a dicentric chromosome count and radiation dose has received a great deal of attention and has been applied to a great many data sets. Experiments will be designed in the context of the chromosome painting approach to establish similar relationships between fragmented chromosomes and radiation dose.

We have developed a pan-centromeric probe which labels every human chromosome centromere except the Y. This probe will allow us to improve our detection of dicentric chromosomes, either in conjunction with chromosome painting probes or with the telomere probes previously developed at this institute.

The detection of painted, damaged chromosomes by flow cytometry may offer significant advantages of speed and multicolour analysis. Preliminary experiments have shown that isolated metaphase chromosomes can be encapsulated in agarose beads preserving chromosome structure and integrity during repeated manipulations. This could provide the ideal starting material for in situ hybridisation of isolated chromosomes.

Publications

Fantes JA, Green DK and Sharkey A. (1992) Chromosome sorting by flow cytometry: Production of DNA libraries and gene mapping. IN *Methods in Molecular Biology*, Vol 6 (Ed. Pollard JW and Walker JM) Humana Press (in press).

Piper J, Bayley R, Boyle S, Fantes J, Green D, Hill W, Ji L, Rutovitz D and Whale D, (1992) Automatic aberration scoring using painting probes. *Anal. Cell Pathology* 4, 211 (abstract to poster).

References

Van Dilla MA et al. (1986) Human chromosome specific DNA libraries: Construction and availability. *Biotechnology* 4, 537-552.

Bayley R et al. (1991) Radiation dosimetry by automatic image analysis of dicentric chromosomes. *Mutation Res.* 253, 223-235

Ji L. (1989) Intelligent splitting in the chromosome domain. *Pattern Recognition* 22, 519-532.

Project 3

Head of project: *Dr. Nüsse*

Objectives for the reporting period

The primary goal of our investigations was the development and application of a new automated flow cytometric method to measure radiation induced micronuclei (MN) in human lymphocytes for a possible detection of low doses in irradiated humans. For this purpose a new flow cytometric technique had to be developed especially for the discrimination of MN from debris. The dose sensitivity of the new MN assay was investigated using human lymphocytes from various donors with different ages. Lymphocytes were irradiated in vitro to induce MN. parameters that could influence the sensitivity of this new MN assay were studied in detail.

A second objective was the analysis of factors that influence the DNA distribution of radiation-induced MN using flow cytometry in combination with several immunofluorescence techniques as for example anti-kinetochore antibodies and anti-BrdUrd antibodies and in situ hybridization with DNA probes against centromeric and telomeric regions of chromosomes. With the results obtained by these combined techniques it was possible to understand quantitatively the shape of the DNA distribution of radiation-induced MN.

Progress achieved including publications

The induction of MN in cells exposed to ionizing radiation is used as a measure for both structural and numerical chromosome aberrations. MN represent genetic material that is lost from the genome during mitosis. Scoring of MN provides therefore a quantitative measurement for the degree of cytogenetic damage in cells and is therefore increasingly used for a dose estimation of humans exposed to ionizing radiation. However, although scoring of MN should be faster than the established chromosome analysis, it cannot yet provide the capacity needed to screen larger human populations. We have therefore developed a new flow cytometric technique for scoring of MN in human lymphocytes using multiparametric flow cytometry, because the high measuring rates of flow cytometers could supply the capacities to screen larger groups of persons exposed to ionizing radiation.

The primary objective of our investigations was the development and application of a new flow cytometric technique to measure the frequency of radiation-induced MN in cell cultures and human lymphocytes. This new technique deals especially with the discrimination of debris from MN so that frequency and DNA distribution of MN could be measured precisely by flow cytometry.

A careful and easy preparation of a suspension of MN and main nuclei needed for flow cytometric measurements of MN was developed using a modification of a method published earlier (Nüsse and Kramer, 1984). The DNA containing particles (nuclei and micronuclei) were stained with the two fluorescent dyes ethidium bromide and Hoechst 33258. The two dyes were excited with two lasers (488 nm and UV) and forward scatter intensity, ethidium bromide fluorescence, Hoechst 33258 fluorescence and ethidium bromide fluorescence excited by the Hoechst 33258 fluorescence via energy transfer were measured

simultaneously in MN, main nuclei and debris. By gating on the respective particles and calculating fluorescence ratios MN could be discriminated from debris still present in the suspension of nuclei and MN (Schreiber et al., 1992). Using this new technique the frequency of MN as well as the DNA content distribution of MN could be measured.

Using this new technique dose effect relationships for radiation-induced MN were measured for various mammalian cell lines growing in vitro. The results agree well with independent measurements by microscopic scoring (Schreiber et al., 1992). In the cell lines studied here, the frequency of MN has reached a plateau when nearly all cells have divided once. It was therefore not necessary to correct the data for the presence of undivided cells. This correction is, however, especially necessary, if MN in irradiated human lymphocytes have to be analysed. With the flow cytometric BrdUrd/Hoechst quenching technique this problem could, however, also be solved for the flow cytometric analysis of radiation-induced MN in human lymphocytes. With this technique, the fraction of cells in the second cell cycle can be determined easily. By correcting the frequency of MN in all irradiated human lymphocytes by the fraction of divided cells it was also possible to measure the frequency of MN in irradiated human lymphocytes with high precision (Schreiber et al., 1993). All flow cytometric data were automatically analysed by the DAS software developed in our laboratory to increase the speed and reliability of the results.

The two main factors influencing the sensitivity of the MN assay were found to be interindividual differences in spontaneous MN frequencies and intraindividual variations of spontaneous and induced MN frequencies during subsequent, independent analyses. Eight individual linear-quadratic dose response curves derived from 5 donors of different ages revealed inter- and intraindividual variabilities of all curve parameters. Fig. 1 shows as an example dose response curves for radiation-induced MN in lymphocytes of three donors with different ages (23, 36 and 54 years) irradiated in vitro. A linear fit of the data derived from three analyses is included (straight lines). Fig. 2 shows the age dependence of spontaneous MN frequencies of 12 donors. An age-dependent trend is recognizable for the spontaneous MN frequencies. Based on these results a linear-quadratic age-dose-effect model for the frequency of MN was derived and its parameters calculated from the data. The model combines two separate fits for spontaneous and induced MN frequencies. Considering the range of variability of the parameters it could be concluded that the lower limit for an individual dose estimation of a donor aged between 23 and 54 years is about 1 Gy. This lower limit of dose estimation in irradiated humans using the MN assay is mainly caused by the inter- and intraindividual variabilities in addition to the influence of age.

In addition to the analysis of the frequency of radiation-induced MN in human lymphocytes the distribution of the DNA content of MN measured by the flow cytometric technique was studied in detail using mouse, Chinese hamster and Syrian hamster cell lines (Nüsse et al., 1992). The DNA content of MN was found to be influenced by several factors:

1. The DNA content and the centromeric index of the chromosomes in the various cell lines. Fig. 3 b shows the DNA distributions of MN induced in Chinese and Syrian hamster cells. Syrian hamster cells have smaller chromosomes compared to Chinese hamster cells, MN induced in Syrian hamster cells, therefore, are smaller compared to MN induced in Chinese hamster cells. These results were confirmed by computerized random breakage of chromosomes in these two cell

lines (Fig. 3 a). For these calculations it was assumed that radiation-induced MN were produced by single acentric fragments. The model could also be used to calculate random combinations of fragments as well as whole chromosomes (see below).

2. The cell cycle phase at time of MN measurement due to DNA synthesis in MN (Kramer et al., 1990). DNA synthesis in MN was studied using pulsed incorporation of bromodeoxyuridine (BrdUrd) during S-phase and anti-BrdUrd antibodies. With synchronized cells irradiated during G1-phase and analysed during the 1. and 2. G1-phase after division DNA synthesis in MN could also be observed in the DNA content distribution of radiation-induced MN measured by flow cytometry (Fig. 4).

3. The presence of chromosome fragments and whole chromosomes in MN. With the in situ hybridization technique using centromeric and telomeric DNA probes simultaneously the chromosomal composition of radiation-induced micronuclei in mouse NIH 3T3 cells was studied in detail (Miller et al., 1992). It could be shown with this technique that about 22% of the MN did not reveal any hybridization signal suggesting their origin from interstitial fragments, and approximately 17% showed one centromeric hybridization signal and 4 telomeric signals suggesting their origin from whole chromosomes. Almost 60% of radiation-induced MN had telomeric signals only, suggesting their origin from acentric fragments. A fraction of MN were found to contain two (21%) or more (4%) acentric fragments probably derived from acentric fragments produced during exchange aberrations. Using anti-kinetochore antibodies (CREST-antibodies) similar results were obtained for the fraction of MN containing whole chromosomes.

With the results from the in situ hybridization experiments the distribution of the DNA content of radiation-induced MN was calculated using random breakage of chromosomes and random combination of chromosome fragments and including also the presence of some MN containing whole chromosomes. A good agreement with the MN distribution measured by flow cytometry was obtained (Nüsse et al., 1992).

Publications

Kramer, J., Schaich-Walch, G., Nüsse, M.: DNA synthesis in radiation induced micronuclei studied by bromodeoxyuridine (BrdUrd) labelling and anti-BrdUrd antibodies. *Mutagenesis* 5, 1990, 491-495.

Miller, B.M., Werner, T., Weier, H.-U., Nüsse, M.: Analysis of radiation-induced micronuclei by fluorescence in situ hybridization (FISH) simultaneously using telomeric and centromeric DNA probes. *Radiat. Res.* 130, 1992, in press.

Nüsse, M., Kramer, J., Miller, B.M.: Factors influencing the DNA content of radiation-induced micronuclei. *Int. J. Radiation Biol.*, 1992 (in press).

Schreiber, G.A., Beisker, W., Bauchinger, M., Nüsse, M.: Multiparametric flow cytometric analysis of radiation induced micronuclei in mammalian cell cultures. *Cytometry*, 13, 1992, 90-102.

Schreiber, G.A., Beisker, W., Braselmann, H., Bauchinger, M., Bögl, K.W., Nüsse, M.: An automated flow cytometric micronucleus assay for human lymphocytes. *Int. J. Radiat. Biol.*, 1992 (in press).

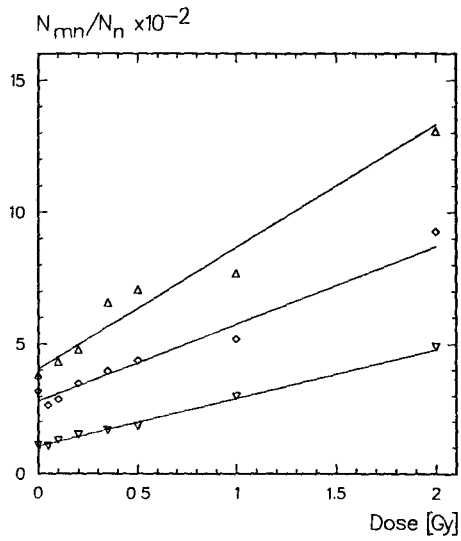


Figure 1 - Frequency of MN, N_{mn}/N_n , in irradiated lymphocytes as a function of dose. Age of the three donors: 54, 36 and 23 years.

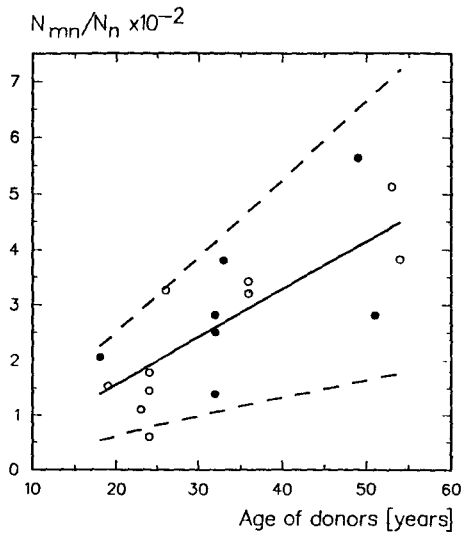


Figure 2 - Age dependence of spontaneous MN-frequency of 12 donors. Full circles: smokers. Open circles: nonsmokers.

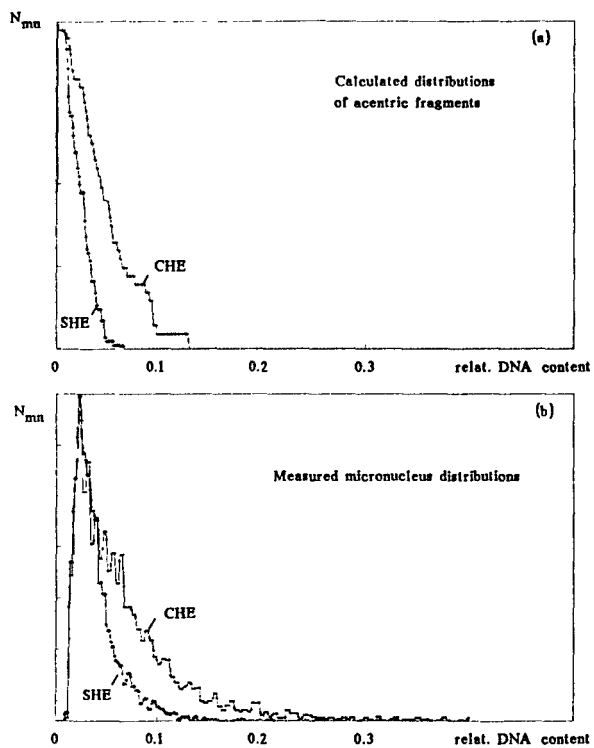


Figure 3 -Distributions of DNA content of radiation-induced MN in Chinese hamster (CHE) and Syrian hamster (SHE) cells.

- a: Distributions of acentric fragments calculated with a random breakage model.
- b: Distributions of MN measured by flow cytometry.

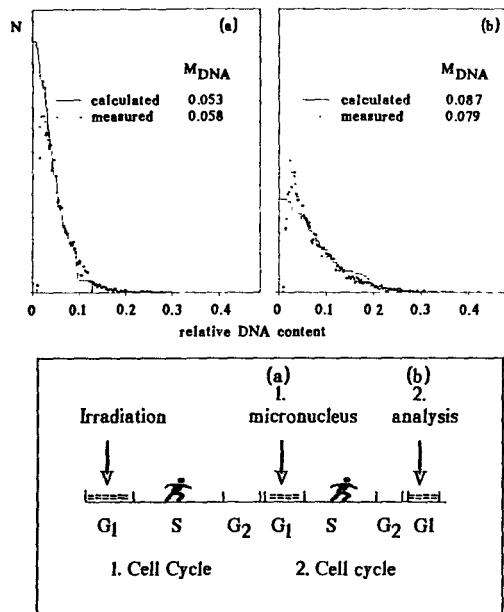


Figure 4 -Distributions of DNA content of radiation-induced MN in synchronized CHE cells irradiated during G1-phase and measured during 1. G1-phase (a) and 2. G1-phase (b) after division. Comparison with calculations M_{DNA} : mean DNA content of MN.

Project 4

Head of project: *Prof. Bauchinger*

Objectives for the reporting period

1. Analysis of the dose response relationships for micronuclei (MN) induced by sparsely and densely ionizing radiations in cytokinesis blocked (CB) human lymphocytes.
2. Analysis of intra- and inter-individual variations of background and induced MN frequencies in human CB lymphocytes.
3. Analysis of the content of MN by means of fluorescence in situ hybridization (FISH) with a satellite DNA probe.

Progress achieved including publications

1. Compared to dicentric analysis, scoring of micronuclei (MN) is a faster and easier approach of measuring radiation-induced chromosome damage in human lymphocytes. It has therefore been suggested as an alternative biological dosimeter system. For comparison of data sets derived by flow cytometric MN analysis experiments were carried out to establish in vitro dose effect curves for MN induced by different radiation qualities. Lymphocyte suspensions obtained from freshly drawn whole blood from either of three donors were exposed to ^{60}Co γ -rays or fission neutrons (converter neutron beam) and from two donors to 220kV X-rays. To account for cell proliferation kinetics a cytokinesis block (CB) MN assay was applied (Fenech and Morley 1985, Huber et al. 1989). 19.000 CB cells were analyzed for the experiments with ^{60}Co γ -rays, 10.000 CB cells for X-irradiation, and 18.000 CB cells for the experiments with fission neutrons. An iteratively weighted least squares method was applied for curve fitting. Each observation was weighted by the number of analyzed cells and the inverse yield Y , assuming that the inter-cellular variance σ^2 of the number of MN is proportional to Y , i.e. $\sigma^2 = d \cdot Y$ with a mean dispersion index d slightly greater than 1. No specific dose-dependence of the dispersion index d was recognizable. The resulting dose response curves were linear-quadratic for ^{60}Co γ -rays and X-rays, whereas for fission neutrons a clear tendency for saturation became apparent with increasing dose (fig.1). As compared to data from conventional scoring of neutron-induced acentrics, an increasing number of MN observed at higher doses must contain more than one acentric fragment leading to the decreasing slope of the curve.

2. In serial blood samples from four healthy donors the intra- and interindividual variations of background and radiation-induced MN frequencies were analyzed in three-monthly intervals during 1 year. Leukocyte suspensions were prepared and exposed to 3Gy of ^{137}Cs γ -rays or left unirradiated as controls. 800-1000 CB cells per donor were analyzed at each examination stage from control (fig. 2) and irradiated samples (fig. 3). Significant inter- and intra-donor variations of background and radiation-induced MN incidences became apparent. The two

different sources of variation lead to an extra variance σ_i , in addition to the sample variance σ_e of MN incidences. The contributions of the different components to the total variance were estimated by means of a variance component model. The deviation σ_i for the mean background MN level of 1.53×10^{-2} MN/CB cell was $\pm 0.67 \times 10^{-2}$ and for the mean radiation-induced MN level of 0.53 MN/CB cell it was ± 0.10 . The contribution of the intraindividual variance to σ_i was about 50% for background MN levels and 75% for radiation-induced MN frequencies. To account for the observed intra- and interindividual variations of MN frequencies, a standard calibration curve should be based upon data of 3 to 5 donors with about 500 cells to be scored at a particular dose point. Due to the considerable variation of background MN frequencies observed in samples from a single donor at different examination stages, it seems difficult to derive a reliable individual low-dose estimate below 0.2 Gy. A statistical analysis of the data shows that such an estimate cannot be substantially improved by scoring of more than 500 CB cells.

3. Since MN may contain *acentric fragments* or *whole chromosomes*, a MN assay should be able to discriminate between clastogenic or aneuploidogenic agents. Up to now, mostly antikinetochores antibodies, e.g. from patients with the CREST syndrome, are used to identify MN with kinetochores. A modern alternative is the application of centromere-specific DNA probes in fluorescence in situ hybridization (FISH) for classification of MN.

In the present experiments mouse liver cells were treated with the reference spindle poison Vinblastine sulfate (VBL), or exposed to ^{137}Cs gamma rays used as reference clastogen (Salassidis et al. 1991). For FISH of CB cell preparations a biotin-labeled degenerate DNA probe homologous to part of the 234 bp repeated mouse gamma (major) satellite DNA was used. MN were examined in 500 CB cells per dose (154 for 0.06 μM VBL) from exposed cultures and in 1000 CB cells from unexposed control cultures.

A clear dose response was observed for the number of micronucleated CB cells and MN per cell induced by both agents. VBL-induced MN were centromere-positive in an order of magnitude of 70-90%, but radiation-induced MN only in an order of magnitude of 10-20% (Fig.4). In controls, 29% of MN were centromere-positive.

Our results show that FISH with a mouse gamma satellite DNA probe can be a reliable alternative to the use of antikinetochores antibodies for the discrimination between MN containing *centromeres*, i.e. chromosomes, or *acentric fragments*, respectively. Relevant gamma satellite DNA probes can be generated repeatedly in stable quality by PCR. More than CREST staining the centromere detection by FISH is reproducible and exact since the gamma satellite DNA probe directly identifies centromeric sequences. FISH can thus be applied in a CB MN assay to distinguish between an agent's clastogenic or aneuploidogenic capacity.

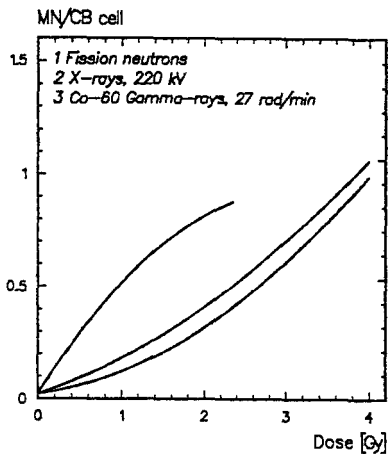


Figure 1 - Dose effect curves for different radiation qualities (1)-(3) fitted by the linear-quadratic model $Y = c + aD + \beta D^2$. Curve parameters for:
 (1) $a = 0.616 \pm 0.026$; $\beta = -0.085 \pm 0.019$;
 (2) $a = 0.128 \pm 0.049$; $\beta = 0.033 \pm 0.004$;
 (3) $a = 0.054 \pm 0.010$; $\beta = 0.047 \pm 0.007$.
 One background level for all is calculated from 16.000 cells of 15 donors;
 $c = 0.021 \pm 0.010$.

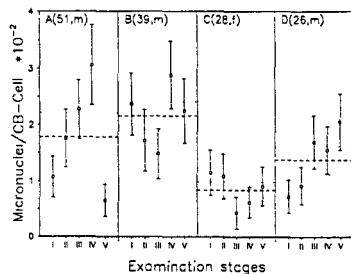


Figure 2 - Diagram of micronucleus frequencies in control samples from four donors A-D (age and sex are given in parentheses) analysed at examination stages I-V (time interval between successive stages 3 months). Data arranged by donors. Error bars represent SD of micronucleus frequency per CB cell, broken lines are individual means and dotted lines are SE of individual means.

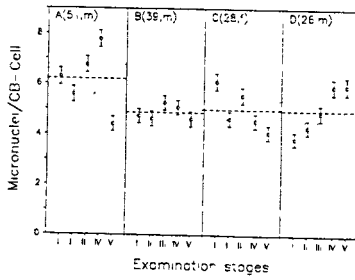


Figure 3 - Diagram of micronucleus frequencies in irradiated samples from four donors A-D. Data arranged by donors. For explanation see legend to Fig. 2.

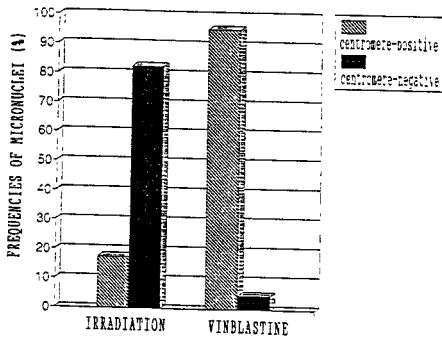


Figure 4 - Percentages of centromere-positive and of centromere-negative MN from the total of all irradiated cells (0.5-3 Gy) and of all VBL-treated cells (0.01-0.06 μ M).

Publications

Salassidis K., Huber R., Zitzelsberger H., and Bauchinger M. (1992): Centromere detection in Vinblastine- and radiation-induced micronuclei of cytokinesis-blocked mouse cells by using In situ hybridization with a mouse gamma (major) satellite DNA probe. Environ Molec Mutagenesis 19:1-6.

Huber R., Braselmann H., and Bauchinger M. (1992): Intra- and inter-individual variation of background and radiation-induced micronucleus frequencies in human lymphocytes. Int J Radiat Biol: 61/5:655-661.

Project 5

Heads of project: *M. Aubele, G. Burger*

Objectives for the reporting period

The objectives of the project are the establishment of dose-effect-curves for CTA in in vitro exposed human lymphocytes. The experiment shall also elucidate the role of varying chromatin texture during the cell cycle on damage expression.

In the reporting period we have firstly concentrated on preparatory protocols /12/14/16/ and the investigation of conceptual relations of chromatin texture features on size and staining density of nuclei /10/18/. Using features independent of those parameters we have then defined chromatin pattern differences of nonirradiated human lymphocytes in different functional states of the cell cycle /15/.

For evaluation of the role of chromatin pattern features in cell nuclei for monitoring radiation exposure we have then investigated the expression of radiation effects on chromatin texture within the different cell cycle groups G_1 , S, G_2 . Finally with the group of most expression of these effects (G_1 -phase)/15/ discriminant analysis was performed between the different dose-groups with textural parameters to establish dose effect curves.

Progress achieved including publications

1. Introduction

In the reporting period we have developed methods of high resolution image analysis for the featuring of subtle chromatin texture changes /1/2/4/7/8/15/. The investigation concentrated on parameters describing chromatin pattern of growing lymphocytes in different cell cycle phases and on measurement of specific radiation induced genomic defects in interphase nuclei by those parameters /3/.

2. Material and methods

From human blood samples mononuclear cells were separated by density gradient centrifugation and resuspended in culture medium containing PHA. After 30 min. they were irradiated by Cs-137 gamma rays with 0, 0.25, 0.5, 0.75 and 1.0 Gy (3 experiments, 3 donors), and with 1.0, 2.5, 5.0, 7.5, and 10.0 Gy (3 experiments, 3 different donors). Cytological specimens from irradiated and nonirradiated lymphocytes were prepared after 5, 24, 48, 72, 96, 120 and 144 hours by cyto-centrifugation, fixation and DNA-specific Feulgen staining /16/. The measurements were performed by high resolution image cytome-

try, 100x objective with oil immersion (digital pixel size 0.25 micron). 200 well preserved cells were randomly selected and measured on each specimen /11/.

3. Results

3.1 Cellular growth

The rationale is that stimulation into proliferation as well as cell cycling may be influenced by the exposure. To investigate the first effect we have pooled all cells after 5 h and 24 h, when we do not yet expect G_1 -cells and also all 'diploids' after 120 and 144 hours, when the vast majority should be in the G_1 -phase, reclassified them by multivariate discriminant analysis and used the such trained classifier for all the diploid cells of the remaining time intervals. From this the $G_0/(G_0+G_1)$ ratios were derived as a function of time and dose. Fig.1 shows the results for all culturing times for cells from one donor as an example. There seems to be a somehow enhanced G_0 - G_1 transfer at intermediate times (48 h) and a retardation of the G_0 -depletion at higher times. After cleaning the histograms from G_0 -cells we assessed G_1 , S-phase, G_2 and $> 5c$ cellular contributions by conventional Gauss-fitting of G_1 and G_2 -peaks. At higher doses and after more than 100 hours also lymphocytes with DNA $>5c$ occur. However all dose effects on the proliferation behaviour of lymphocytes are not very distinct.

3.2 Chromatin texture assay

3.2.1 Cell cycle analysis

Different genomic activity causes variations in the chromatin pattern of proliferating cell nuclei during the cycle /15/. We have therefore investigated numerous cytometric features with respect to their invariance of mean optical density and size variations of cell nuclei /13/. Only features proved to be independent from these parameters were used for all texture investigations by means of linear discriminant analysis (LDA).

G_0/G_1 cells were identified by the above mentioned trained classifier. The results of the discriminant analysis were between 94% and 99% correct classification ($p < 0.001$). Cells from G_1 -, S-, and G_2 -phases were classified in the same manner. Fig.2 shows as an example a plot of the multidimensional feature space with the cells from one donor splitted into five different cell cycle phases (G_1, S_1, S_2, S_3, G_2) with a correct classification of 57% ($p < 0.001$). The correct classification rates for the different donors are between 70% and 80% ($p < 0.001$) for three-class-cases (G_1 -, S-, G_2 -phase). Even after pooling the cells from several donors the cell classification into the three cycle phases is highly significant by using textural parameters (72%, $p < 0.001$) (table 1).

3.2.2 Dose effect on chromatin texture

Multivariate discriminant analysis /9/5/ between the different dose-groups was performed within the G₁-, the S-, and the G₂-phase cells for each experiment. As a result, radiation effects concerning chromatin pattern seem to be more expressed in G₁-cells /15/. Therefore only G₁-cells have then been compared as a function of time and dose by multivariate discriminant analysis. Fig.3 shows plots of the multidimensional feature space for two examples: A- pooled G₁-lymphocytes irradiated with doses from 0.0 to 1.0 Gy; B- lymphocytes irradiated with doses from 0.0 to 10.0 Gy. In both the cases G₁-cells 48 and 72 hours after irradiation are pooled. The classification results for G₁-cells were for these examples 32% and 31%, respectively, (p<0.001)(table 2). Fig.3B shows also as an example three multivariate measures derived from the five-class-LDA and from regression analysis for the dose dependence 48 and 72 hours.

As textural features correlating with dose vary between the different donors, these results could only be achieved within each single donor and not after pooling the cells from all donors. It seems that there is a high biological variance between the different donors concerning textural changes after exposure.

4. Summary

Human PHA-stimulated lymphocytes show changes in growth kinetics, in the occurrence of highly aneuploid cell components and in the chromatin texture (CT) as a function of radiation dose. The latter was found more expressed in G₁-cells than in S- or G₂-phase cells. Variations between the donors concerning chromatin pattern in different cell cycle phases are subtle, whereas variations concerning radiation induced changes in chromatin texture are clearly expressed. Further methodological work is necessary to validate the findings, to increase the sensitivity of the CT assay, and to clarify the degree of individual variances in expressing chromatin pattern changes after exposure.

Table 1: Cell classification matrix for LDA of pooled lymphocytes from three different experiments:

	G ₁	S	G ₂	total	
G ₁	941	217	39	1197	
S	90	203	132	425	
G ₂	8	72	228	<u>308</u>	
			correct	71.2%	p<0.001

Table 2: Cell classification matrix for LDA of G₁-lymphocytes irradiated from 0.0 to 10.0 Gy 48 and 72 hpr:

GY	0	2.5	5.0	7.5	10.0	total	
0	61	12	5	25	17	120	
2.5	56	14	13	30	37	150	
5.0	59	22	33	47	64	225	
7.5	42	13	18	59	62	194	
10.0	27	14	24	64	133	<u>262</u>	
					correct	31.6%	p<0.001

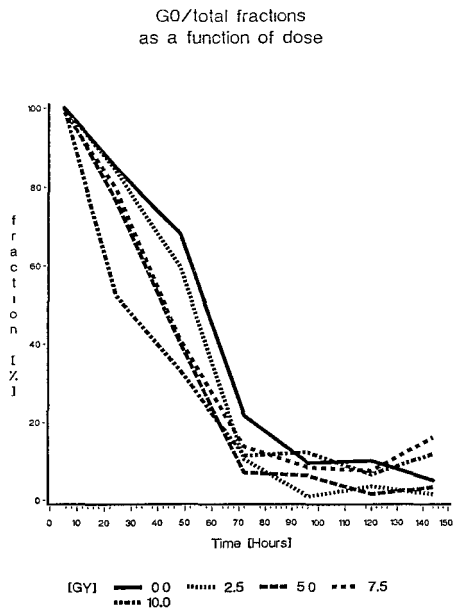


Fig.1: G₀/G₁-transition as a function of dose for all culturing times.

Discriminant analysis of G₁-S₁-, S₂-, S₃-, and G₂-phase-cells
from experiment B (0 Gy)

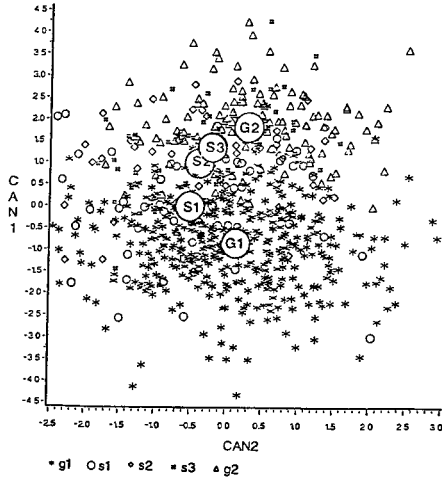
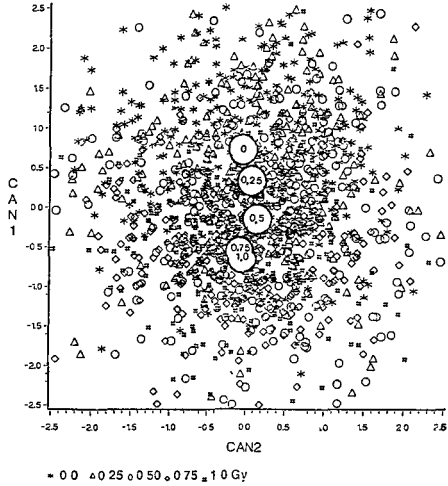


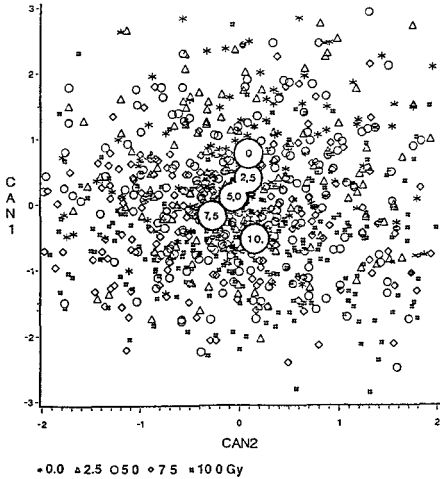
Fig.2: Distribution of nonirradiated G₁-, S₁-, S₂-, S₃-, and G₂-cells in the multidimensional feature space for one experiment.

3 A

Discriminant analysis of the G1-cells from
experiment E (0 to 1.0 Gy)



Discriminant analysis of the G1-cells from
experiment B (0 to 10 Gy)



3 B

Dose response relationship for the G1-cells
from experiment B

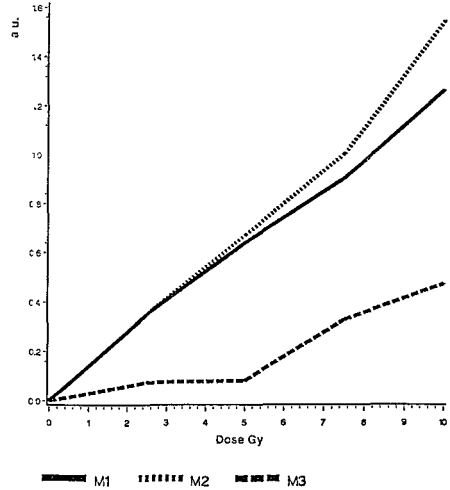


Fig.3: Discriminant analysis of G₁-lymphocytes irradiated
with different doses (48 and 72 hpr):

A- Distribution of cells in the multidimensional feature
space, irradiated from 0.0 to 1.0 Gy.

B- Distribution of cells in the multidimensional feature
space, irradiated from 0.0 to 10.0 Gy. Additionally
three different multivariate measures derived from
the five class LDA and from multiple regression
analysis as a function of dose are shown

- M₁ First canonical variable (A.U.)
- M₂ Sum of Mahalanobis distances in between
classes in the feature space (A.U)
- M₃ Multiple correlation (A.U.)

Publications in scientific journals, monographs etc.

- 1) Schmidt, J., Aubele, M., Jütting, U., Rodenacker, K., Luz, A., Erfle, V., Burger, G.: Computer-assisted imaging cytometry of nuclear chromatin reveals bone tumor virus infection and neoplastic transformation of adherent osteoblast-like cells. *Biochem. and Biophys. Res. Communications.* 164, 728-735 (1989).
- 2) Aubele, M., Guttenberger, R., Gais, P.: Morphological changes in murine lymphocytes and vaginal cells during experimental tumorigenesis. In: *Advances in Analytical Cellular Pathology* (Eds.: G. Burger et al.) Amsterdam: Elsevier Science Publishers, Excerpta Medica, Internat. Congress Series 911, 87-88 (1990).
- 3) Aubele, M., Jütting, U., Rodenacker, K., Gais, P., Burger, G., Hacker-Klom, U.: Quantitative evaluation of radiation-induced changes in sperm morphology and chromatin distribution. *Cytometry*, 11, 586-594 (1990).
- 4) Burger, G., Jütting, U., Aubele, M.: Malignancy associated changes and their cytometric evidence. In: *Advances in Analytical Cellular Pathology* (Eds.: G. Burger et al.) Amsterdam: Elsevier Science Publishers, Excerpta Medica, Internat. Congress Series 911, 153-154 (1990).
- 5) Burger, G., Jütting, U., Aubele, M., Auer, G.: The role of high resolution cytometry in the prognosis of breast cancer. In: *Advances in Analytical Cellular Pathology* (Eds.: G. Burger et al.) Amsterdam: Elsevier Science Publishers, Excerpta Medica, Internat. Congress Series 911, 179-180 (1990).
- 7) Reith, A., Reichborn-Kjennerud, S., Aubele, M., Jütting, U., Burger, G.: The detection of unspecific cellular changes in normal epithelial cells of nasal smears for monitoring workplace hazards of nickel workers. In: *Advances in Analytical Cellular Pathology* (Eds.: G. Burger et al.) Amsterdam: Elsevier Science Publishers, Excerpta Medica, Internat. Congress Series 911, 261-262 (1990).
- 8) Schmidt, J., Aubele, M., Jütting, U., Rodenacker, K., Luz, A., Erfle, V., Burger, G.: Differentiation of spontaneous and virus-transformed osteoblast-like cells by computer-assisted imaging cytometry. In: *Advances in Analytical Cellular Pathology* (Eds.: G. Burger et al.) Amsterdam: Elsevier Science Publishers, Excerpta Medica, Internat. Congress Series 911, 85-86 (1990).
- 9) Parui, S.K., Jütting, U., Burger, G.: Methods for classification of two thyroid follicular tumor classes, *Int. J. of System Science*, 10, 1985-1991, (1991).
- 10) Burger, G., Rodenacker, K., Aubele, M., Jütting, U.: Stability and normalization of chromatin features in imaging cytometry. *Cytometry S 5*: 62-63, 1991.

11) Burger, G., Aubele, M., Jütting, U., Auer, G.: Interactive breast cancer cytometry, chance or evil of bias?. Pathology, research and practice (M. Oberholzer et al., eds.), in print, 1992.

Short communications, internal reports etc.

12) Aubele, M., Burger, G., Leuthold, G.: Problems of DNA-standardization in imaging cytometry: influence of preparation. CAAC-meeting, Brüssel, 18.10.-19.10.1990.

13) Rodenacker, K., Aubele, M., Gais, P., Jütting, U. Burger, G., Gössner, W., Oberholzer, M.: Cytometric measurements in histological sections improving prognosis of colorectal cancer. CAAC-meeting, Brüssel, 18.10.-19.10.1990.

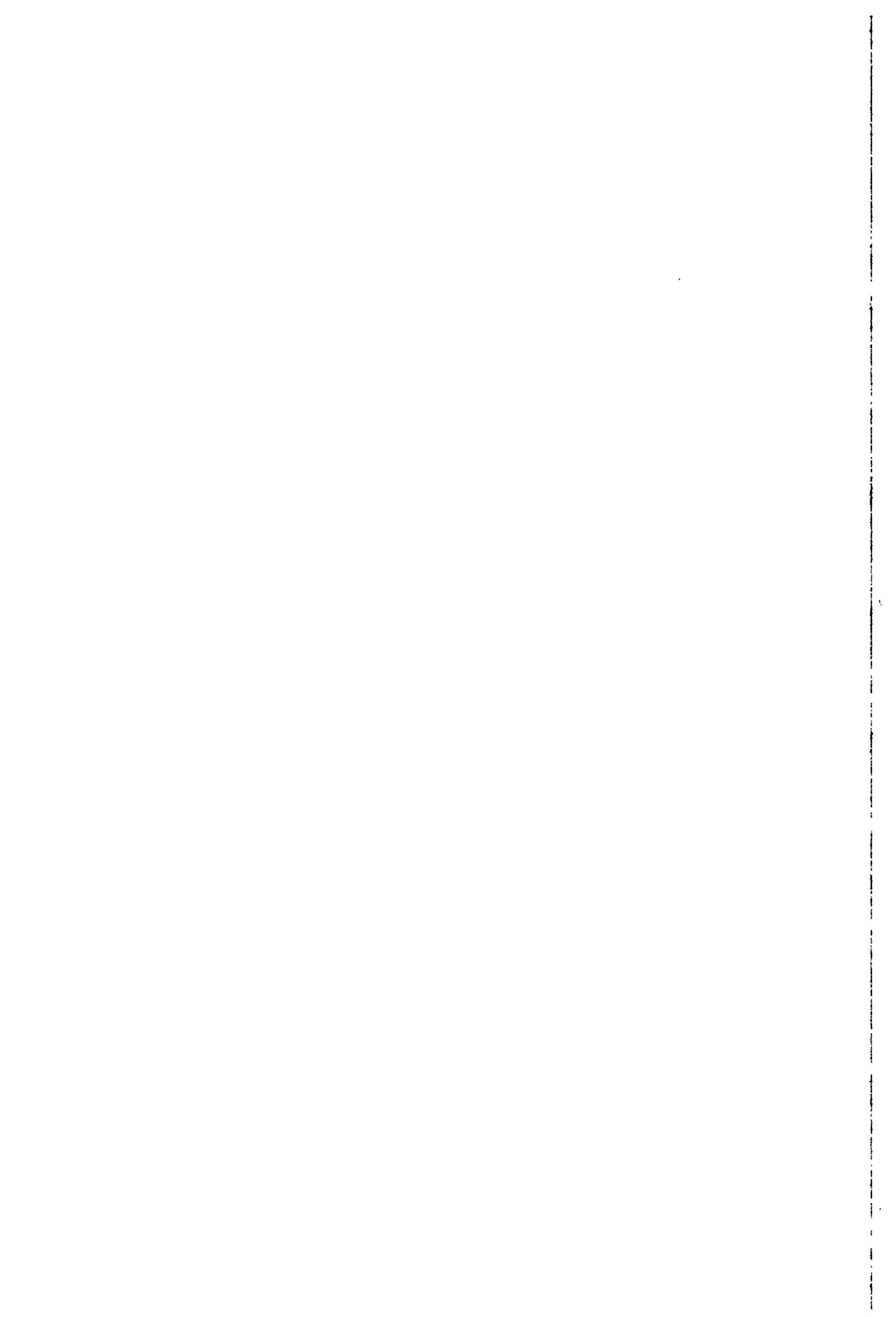
14) Aubele, M., Burger, G.: Problems of DNA-standardization in imaging cytometry. XVII.Symposium on Quantitative Morphology in Pathology, Dresden, 25.3.-27.3.1991.

15) Burger, G., Aubele, M., Clasen, B., Jütting, U., Gais, P., Rodenacker, K.: Malignancy associated changes in intermediate cells of oral smears. Analytical Cellular Pathology 4/3: p.139, 1992.

16) Aubele, M., Burger, G.: Quality assessment of DNA-image cytometry. Analytical Cellular Pathology 4/3, 1992.

17) Aubele, M., Burger, G., Rodenacker, K.: Chromatin pattern changes during cell proliferation, a potential assay for monitoring genotoxic effects. Analytical Cellular Pathology 4/3: p.127, 1992.

18) Rodenacker, K., Aubele, M., Jütting, U., Gais, P., Burger, G.: Textural features of cell nuclei: standardization and perception. Analytical Cellular Pathology 4/3: p.219, 1992.



STUDIES ON BASIC AND APPLIED ASPECTS OF RADIATION-INDUCED CHROMOSOMAL ABERRATIONS IN HUMAN CELLS

Contract Bi7-0039 - Sector B13

- 1) *Natarajan*, Univ. Leiden Sylvius Lab. - 2) *Savage*, MRC Radiobiological Unit.
- 3) *Olivieri*, Università di Roma "La Sapienza" - 4) *Cortés-Benavides*, Univ. Sevilla
- 5) *Bryant*, Univ. St. Andrews - 6) *Ahnström*, Univ. Stockholm
- 7) *Baverstam*, Nat. Inst. of Rad. Protection - 8) *Feinendegen*, KFA Jülich GmbH
- 9) *Johanson*, Univ. Uppsala Agricult. Sciences - 10) *Ehrenberg* - Univ. Stockholm
- 11) *Palitti*, Univ. degli Studi della Tuscia - 12) *Laurent*, Univ. Liège Sart Tilman
- 13) *Pantelias* - NCSR "Demokritos" 14) *Jorge*, Inst. Portug. Oncol. Francisco Gentil
- 15) *Pereira-Luis*, LNETI

Summary of project global objectives and achievements

Chromosomal aberration is considered to be as one of the most important biological effects arising as the consequence of exposure to ionizing radiation in man. The project aims at clarifying the mechanisms of chromosome aberrations formation at different cell cycle stages following irradiation at different conditions in mammalian cells including man. Though DNA double strand breaks (DSBs) are considered to be the probable DNA lesion leading to radiation induced chromosomal aberrations, the factors such as the exact repair mechanisms that operate and the influence of cell cycle on the type and frequency of aberrations are not well understood. techniques such as premature chromosome condensation (PCC) and chromosome painting (in situ hybridization with chromosome specific DNA libraries) are used in this project to study the kinetics of formation and frequencies of exchanges respectively. The mechanisms behind the phenomenon of adaptive response (the resistance of cells which have been adapted with a low dose of radiation to a further challenging dose) have to be clarified. Attempts will be made to do this using diverse biochemical and cytological approaches. The formation of radiation induced chromosomal aberrations in G₂ stage of cell cycle is being studied in mammalian cells using different classes of DNA repair inhibitors in order to understand the influence of various repair enzymes on the induced frequency of aberrations. Attention is also paid to the problem of low dose and dose rate effects by choosing appropriate in vivo and in vitro models.

1. Detection of translocations using chromosome specific probes: possible use in biological dosimetry

Chromosome specific DNA libraries and fluorescent in situ hybridization (FISH) technique were used to detect radiation induced translocations in human lymphocytes irradiated with different doses of X-rays and Fission neutrons (1 MeV) (Leiden). Composite probes of chromosomes 1,3,X and 2,4,8 were used as two different cocktails for painting the chromosomes. In view of the high resolution of FISH technique, in addition to obvious reciprocal translocations, terminal translocations and interstitial translocations were found. The frequencies of translocations were found to be 1.5 to 2 times higher than the frequencies of dicentrics following X-ray treatment. These observations are contrary to expected similar induction of

dicentric and translocations found by using G banding techniques. The possibility to score translocations and dicentric in the same cell will greatly improve the sensitivity of the technique using the frequencies of exchange aberration for estimating absorbed radiation doses in radiation accidents. The increase in translocation frequency was less evident following neutron irradiation especially at low doses (0.1 to 0.25 Gy). Studies using three different fluorochromes to detect exchanges in individual chromosomes indicated that chromosome 1 participates in exchange aberrations more frequently than other chromosomes (Leiden). It is of interest to note that in the both the atom bomb victims of Hiroshima-Nagasaki and Goiania radiation accident excess of translocations involving chromosome 1 has been found.

2. Premature chromosome condensation (PCC) to detect fragments and dicentric induced by ionizing radiation

When interphase cells are fused with mitotic cells in the presence of polyethylene glycol (PEG), in the ensuing hybrids due to precocious condensation, interphase chromosomes can be visualized. PCC technique can be used with great advantage because one can evaluate radiation induced chromosome aberrations (fragments or dicentric) without waiting for cells to undergo mitosis. This technique has been used for biological dosimetry (Athens, Leiden) as well as to study the mechanisms of radiation induced chromosome aberrations (Athens, Leiden).

3. Mechanisms of formation of radiation induced chromosome aberrations

3.1 Utilization of radiation sensitive mutant cell lines

There are several radiation sensitive human and rodent cell lines available which yield increased frequencies of aberrations following X-irradiation in comparison to parental wild type cells. Chinese hamster mutant cells (xrs 5) are defective in DNA double strand break repair and respond with several fold increased frequency of aberrations following X-rays (St. Andrews, Leiden). In spite of the increased frequency in xrs cells, the kinetics of repair of chromosome breaks in G_2 appears to be similar to wild type cells indicating that these cells may be proficient in repairing DSBs at G_2 stage (St. Andrews) and that efficiency of repair may vary at different cell cycle stages. In another radiosensitive Chinese hamster mutant cells VC4, which are competent in repairing DSBs efficiently, the frequency of X-ray induced aberrations is high in comparison to wild type V79 cells. However, these mutant cells respond with similar frequencies of aberrations following neutron irradiation or treatment with restriction endonucleases. These results indicate that DNA lesions other than DSBs can play a role in induction of aberrations (Leiden).

An efficient method to porate cells by streptolysin O to introduce enzymes has been standardized (St. Andrews) which opens up several possibilities of unravelling different steps involved in chromosome repair. Treatment of gamma irradiated streptolysin porated AT lymphoblastoid cells with crude nuclear extracts from normal human cells has led to reduced frequency of aberrations indicating a partial correction of radiosensitivity (St. Andrews).

3.2 Alteration of chromatin structure during irradiation of the yield of chromosome aberrations

When human lymphocytes are UV irradiated first and then post-treated with X-rays the frequency of dicentric chromosomes increases by a factor of two (Stockholm). This increase could be due to interaction between the strand breaks generated during repair of UV damage and those induced by X-rays or due to excision repair of UV damage the chromatin is decondensed leading to increased damage. By measurement of DNA strand breaks under appropriate experimental conditions, the hypothesis of interaction between UV and DNA lesions has been ruled out (Stockholm). Decondensation of chromatin may be responsible for increased sensitivity as it is known that condensation of chromatin (by salt treatment) leads to radioresistance (Leiden).

3.3 Adaptive response studies

When human lymphocytes are irradiated with a low radiation dose (adaptive) and challenged later with a higher dose, the frequency of chromosomal aberrations is lower than expected indicating an adaptive response (Rome). Lymphocytes from most of the individuals studied, show an adaptive response (AR) and some individuals are AR. A detailed analysis has shown that pH of the culture medium is an important factor in mediating adaptive response (Rome). Cells do not progress at the same speed during cell division and it is important that one is examining similar cohort of cells for studying AR. An elegant method to label cells at different stages of S phase by pulse BrdU treatment has been standardized (Harwel). AR experiments using this technique indicate that AR is cell cycle dependent and cells challenged 6h after adaptation show an AR+ effect, whereas challenging dose at 9h does not show any AR effect (Harwel). To overcome the cell cycle effects in AR experiments, a micronucleus method using cytochalasin B has been standardized for this type of experiments (Sevilla). One can analyze micronuclei in binucleated cells accumulated over a long period of time by this technique, which avoids the bias of scoring only cells irradiated at a particular stage in cell cycle. Using this technique it has been shown that one can adapt cells with low concentrations of hydrogen peroxide for a further challenging dose of X-rays (Sevilla). In vivo experiments using rats using micronuclei and HPRT mutations in lymphocytes as end points have shown that one can demonstrate an AR for the clastogenic effect but not for mutagenic effect (Leiden, Stockholm). A detailed statistical method to analyze data from such experiments has been developed (Stockholm). Induction of several important enzymes such as thymidine kinase following very low dose irradiation of mice has been detected which may have bearing in the AR phenomenon (Jülich).

3.4 Influence of DNA repair inhibitors and radio-protectors on the yield of radiation induced chromosome alterations

When X-irradiated cells are post-treated with inhibitors of DNA synthesis/repair such as araC, aphidicolin, hydroxyurea etc., the yield of induced aberrations increases upto a factor of two. When G₂ lymphocytes were irradiated with high LET radiation (neutrons) and post treated with hydroxyurea (HU) or caffeine or araC, the potentiating effect was found for HU and caffeine, but not for araC indicating that the repair of neutron induced lesions

leading to chromosomal aberrations are not inhibited by araC (Viterbo).

It has been demonstrated earlier that pretreatment of mice with cysteine prior to X-irradiation reduces the frequencies of radiation induced sister chromatid exchanges. Since this would be an interesting in vivo model to study the effects of radioprotectors, these experiments were repeated, but without success (Leiden, Stockholm).

Project 1

Head of project: *Prof. Natarajan*

Objectives for the reporting period

(1) Detection of chromosomal translocations induced by low and high LET radiation in human lymphocytes, using chromosome specific DNA libraries and in situ hybridization.

(2) Utilization of DNA repair deficient radiosensitive rodent cell lines to establish correlations between radiation induced DNA lesions and chromosomal aberrations.

Progress achieved including publications

(1) Irradiation of human lymphocytes in G₀ stage leads to stable (translocations) and unstable (dicentrics, rings and fragments) chromosome aberrations. Unstable aberrations are easy to detect using conventional Giemsa staining whereas for detection of stable aberrations special techniques such as G or R banding have to be used. Recently human chromosome specific DNA libraries have become available which has made it possible by in situ hybridization with biotinylated probes and immunological detection ("chromosome painting") to specifically stain individual chromosomes. This allows detection of translocations involving painted chromosomes easily and accurately. In this technique under standard conditions 1 µg of biotin labelled DNA representing library was combined with competitive DNA followed by denaturation then hybridized in situ (over night) with chromosome preparations. After hybridization, the slides are washed carefully (50% formamide in 2X SSC and 4X SSC/0.05% Tween 20) and then incubated in 5% natural non-fat dry milk for 15 min. Detection of biotinylated probes was achieved by using Avidin.FITC. Amplification of signals was made by reincubation with 5 µg/ml biotin conjugated anti-avidin antibody for 30 min. If necessary further amplifications were carried out. For detection of translocations we used cocktails of libraries from 3 chromosomes, namely 1,3, and X or 2,4 and 8. Each cocktail represents about 20% of the whole genome.

Chromosome painting technique, in view of its high resolution, allows one to detect in addition to reciprocal translocations, also small terminal and interstitial translocations. Dose response curves for induction of dicentrics (detected in Giemsa stained preparations) and translocations (by chromosome painting) following irradiation of lymphocytes with X-rays (0.25 to 4.0 Gy) and 1 MeV neutrons (0.1 to 1.0 Gy) are presented in Figure 1. Acentric fragments associated with dicentrics were occasional translocated to another chromosome terminally. Assuming that translocations occur at random among the chromosomes depending on their DNA content one can calculate the expected frequencies for the whole genome. In the case of X-rays the translocation frequencies were about 1.5 to 2.0 times higher than the frequencies of dicentrics for a given dose. Following neutron irradiation, the frequencies and translocations

were similar up to 0.25 Gy and at higher doses, they were 1.3 to 1.5 times higher than the frequencies of dicentric. The increased induction of translocations after X-rays in contrast to neutrons can be interpreted on the basis of the way these two types of radiation induce lesions in a nucleus, sparsely ionizing X-rays providing more opportunities for interaction of lesions. Since it is possible, with some improvements in the technique, to detect both dicentric and translocations simultaneously in the same cell, in future it will be possible to make absorbed radiation dose estimates in case of accidents even at very low exposures (around 0.1 Gy).

Since the use of the same fluorochrome (FITC) for staining all three chromosomes does not allow detection of translocations between the stained chromosomes, three different triphosphates during nick translation (biotin 11-dUTP, digoxigenin 11 dUTP and fluorescein dUTP) and three fluorochromes (FITC, AMCA, TRITC) were used to distinguish them. The chromosomes appear green, red and blue following this staining procedure. This technique allows one to estimate the participation of different chromosomes in exchanges. Using chromosome 1 as standard, the relative frequencies of observed aberrations involving other chromosomes (corrected for their DNA content) were calculated. The results are presented in Table 1, which indicate that chromosome 1 participates more often in exchanges than other chromosomes. This interesting finding has a parallel in both Hiroshima and Nagasaki atom bomb victims as well as victims of Goiania (Brasil) radiation accident, in whom higher frequencies of translocations involving chromosome 1 than expected have been observed.

(2) In our earlier studies, using different biochemical and cytological approaches, we have provided convincing evidence that among the ionizing radiation induced DNA lesions, double strand break (DSB) is mainly responsible for induction of chromosomal aberrations. We have used several radiation sensitive Chinese hamster mutant cell lines to gain further insight into this problem. Different radiation sensitive xrs mutant cell lines are defective in repairing DNA DSBs to different degrees and there is a good correlation between the extent of this defect and the increase in the frequencies of radiation induced chromosomal aberrations for a given dose, giving further support for the involvement of DSB in chromosome aberrations. Recently, another radiosensitive mutant (VC4) from Chinese hamster V79 cells has been isolated. These cells are sensitive to X-rays and have no defect in DSB repair. When VC4 cells are X-irradiated, they respond with higher frequencies of aberrations in comparison to the wild type cells, in spite of their efficient capacity to repair DSBs. When VC4 cells were irradiated with different doses of 1 MeV neutrons (which induce high proportion of DSBs), the yields of aberrations were very similar to those obtained with wild type V79 cells (Fig.2). When these mutant cells were treated with restriction endonucleases (which induce exclusively DSBs) the yield of aberrations were very similar to that of the wild type cells. These observations provide additional evidence for efficient DSB repair capacity of VC4 cells. The increased frequencies of aberrations in these cells may be due to a defect in the repair of lesions other than DSBs. When VC4 cells were irradiated with short wave UV, the yield of aberrations was 4 to 5 times more than the wild type cells (Fig.3). These results

indicate that VC4 mutant cells are defective in some type of excision repair and in repair defective cells, lesions other than radiation induced DSB can lead to chromosome aberrations.

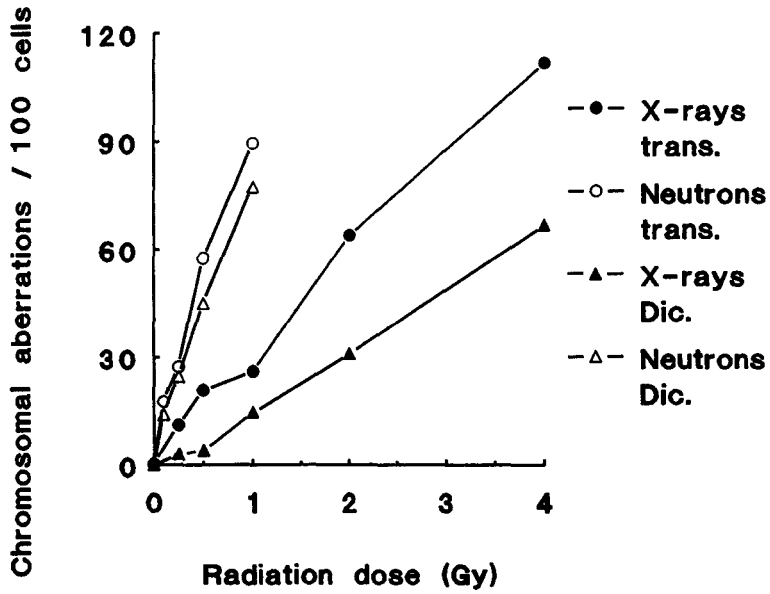


Figure 1 - Low and high-LET-radiation-induced chromosomal aberrations.

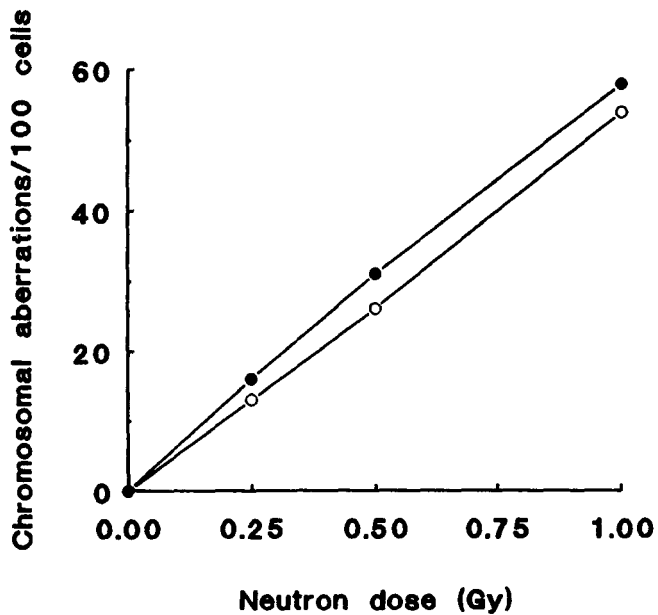


Figure 2 - Frequency of cromosomal aberrations in V79 (o) and VC 4 (•) cell lines following G_1 neutron irradiation.

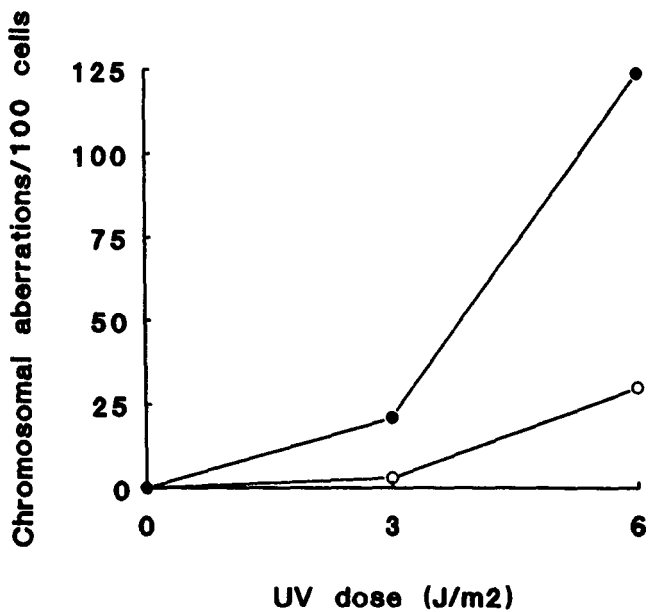


Figure 3 - Frequency of cromosomal aberrations in V79 (o) and VC 4 (•) cell lines following UV irradiation.

Publications

- Darroudi, F., A.T. Natarajan, G.P. van der Schans and A.A.W.M. van Loon (1990) Biochemical and cytogenetical characterization of X-ray-sensitive Chinese hamster ovary mutant cells xrs 5 and xrs 6. V. The correlation between DNA strand breaks and base damage to chromosomal aberrations and sister-chromatid exchanges induced by X-irradiation, *Mutation Res.*, 235, 119-127.
- Darroudi, F., A.T. Natarajan and G.P. van der Schans (1990) Biochemical and cytogenetical characterization of Chinese hamster oary X-ray-sensitive mutant cells xrs 5 and xrs 6. VI. Correlation between UV-induced DNA lesions and induction of chromosomal aberrations, and their modulations with inhibitors of DNA repair synthesis, *Mutation Res.*, 235, 129-135.
- Darroudi, F., Z. Farooqi, D. Benova, and A.T. Natarajan (1992) The mouse splenocyte assay, an in vivo/in vitro system for biological monitoring: studies with X-rays, fission neutrons and bleomycin, *Mutation Res.*, 272, 237-248.
- Lloyd, D.C., A.A. Edwards, A. Leonard, G.L. Deknudt, L. Verschaeve, A.T. Natarajan, F. Darroudi, G. Obe, F. Palitti, C. Tanzarella and E.J. Tawn (1992) Chromosomal aberrations in human lymphocytes induced in vitro by very low doses of X-rays, *Int. J. Radiat. Biol.*, 61, 335-343.
- Natarajan, A.T., R.C. Vyas, F. Darroudi and L.H.F. Mullenders (1990) The relation between DNA damage and chromosome aberrations, *Proceedings of Brezelius Symposium, UMEA Sweden, 1988*, 117-121.
- Natarajan, A.T., R.C. Vyas, F. Darroudi, L.H.F. Mullenders and M.Z. Zdzienicka (1990) DNA lesions, DNA repair and chromosomal aberrations, in: *Chromosomal alterations*, G. Obe and A.T. Natarajan (Eds.), Springer Verlag, pp. 31-40.
- Natarajan, A.T., R.C. Vyas, J. Wiegant and M.P. Curado (1991) A cytogenetic follow-up study of the victims of a radiation accident in Goiania (Brazil), *Mutation Res.*, 247, 103-111.
- Natarajan, A.T., F. Darroudi, S. Vermeulen and J. Wiegant (1992) Frequencies of X-ray and fast neutron induced chromosome translocations in human peripheral blood lymphocytes as detected by in situ hybridization using chromosome specific DNA libraries, in: *Sugahara, T., I.A. Sagan and T. Aoyama (Eds.), Low dose irradiation and biological defense mechanisms, Excerpta Medica, Tokyo*, pp. 343-346.
- Natarajan, A.T., R.C. Vyas, F. Darroudi and S. Vermeulen (1992) Frequencies of X-ray induced chromosome translocations in human peripheral lymphocytes as detected by in situ hybridization using chromosome specific DNA libraries, *Int. J. of Radiat. Biol.*, 61, 199-203.
- Natarajan, A.T., F. Darroudi, A.N. Jha, M. Meijers and M.Z. Zdzienicka (1993) Ionizing radiation induced DNA lesions which lead to chromosomal aberrations, *Mutation Res.* (in press).
- Vyas, R.C., F. Darroudi and A.T. Natarajan (1991) Radiation-induced chromosomal breakage and rejoining in interphase-metaphase chromosomes of human lymphocytes, *Mutation Res.*, 249, 29-35.

Project 2

Head of project: *Dr. Savage*

Objectives for the reporting period

Because no known target cell population has a uniform sensitivity for the production of chromatid-type aberrations, the observed frequency of such changes fluctuates with sample time after treatment and is subject to additional modification by mitotic perturbation. This introduces considerable uncertainties for quantitative work.

Our objectives have been to apply BrdU cell-marking/cohort analysis (a technique developed under previous contracts) to some areas where chromatid aberration frequencies are used to demonstrate effects. In particular, we have concentrated on the "adaptive response" and also begun to investigate the effects of mitotic delay on observed aberration yield.

Progress achieved including publications

1. Adaptive Response.

If a very small (0.01-0.02 Gy) "*priming*" or "*adapting*" dose of radiation is given to actively dividing lymphocytes, the observed frequency of chromatid-type aberrations produced by a higher (0.75-1.5 Gy) "*challenge*" dose given some hours later is often less than that observed in the absence of primer. One explanation is that the adapting dose initiates or "primes" a repair system so that it is up and running when the heavier damage arrives and hence, the cell copes more efficiently.

The stimulated lymphocyte population is very complex with regard to its kinetic properties, and a very heterogeneous mixture of cycle stages is present at the time of irradiation. The observed yield of aberrations will depend upon the mixture of cells present at the time of sampling and any differential delay or perturbation is likely to change that mixture, and thus the yield.

If we are to make valid comparisons after different treatments, then it is necessary to ensure that sample cell mixtures are similar, i.e. that the frequencies being compared were produced in cells at the same developmental stage at the time of exposure.

Ideally, for adaptive response studies, we would like to know where any metaphase was at the time of the primer dose and at the time of the challenge dose. Then we could adjust the composition of the samples for legitimate comparisons.

We have done just that [1], by adapting a pulse-BrdU protocol and following it with replication-band staining.

The adaptive response regime used was based on that first employed by Olivieri (1984, *Science*, 223:594-597.). PHA-stimulated lymphocytes at 50h were irradiated with a primer dose of 0.01 Gy. These, and sham-irradiated controls, were then given 10µg/ml BrdU which remained in the culture for 6h. At this time, a challenge dose of 1.5 Gy was given to some primed and some control cultures, the BrdU was removed, the cultures rinsed, and normal medium replaced. Samples of the resulting four treatments (unirradiated, primer only, challenge only, primer+challenge) were taken at 3, 6 and 9h after challenge, and air-dried metaphases stained for

replication banding.

The staining reactions obtained allow one to assign the interphase position of each metaphase at the time of primer and at the time of challenge (Table 1), so that we can indeed make valid comparisons of defined cell mixtures.

Table 1: Staining Patterns after a 6h BrdU pulse and their interpretation.

Observed Staining Pattern	Position at Primer	Position at Challenge
Merging G-zone *	Pre-S	Early-S
Incomplete G-zone *	Pre-S	Mid to Late-S
Uniform Pale, Unbanded	Pre-S	Post-S (BrdU pulse > S duration)
Mixed pattern, R + G zones	Early-S	Late-S (BrdU pulse < S duration)
Incomplete R-zone *	Early-S	Post-S
Merging R-zone *	Mid to Late-S	Post-S
Uniform Dark, sometimes with granular/coiled structure	Post-S	Post-S (or whole pulse lies Pre-S)

* The patterns can be objectively defined to delimit precise sub-phases of S (Savage et al., 1984, *J.Theor.Biol.*, 111;355-367.)

Briefly, when scored cells remained unclassified (equivalent to a conventional experiment with solid staining), a depression in total aberration yield in the primer+challenge (ie. an adaptive response) was seen at 6h but not at 9h. However, when defined cohorts were summed for both sample times, no depression was observed. There was no measurable effect of the primer on mitotic delay with or without the challenge, so the explanation of our observations does not appear to lie here. We cannot, however, rule out more subtle cell mixing.

Our results serve to emphasise the complexities of the lymphocyte system, and the care needed in interpreting results obtained from it.

2. Mitotic delay and perturbation.

Many years ago, we showed (Savage & Papworth, 1973, *J.Theor.Biol.*, 38;17-38.) that when the target-cell population has a heterogeneous sensitivity to aberration production, then not only does the aberration yield fluctuate with sample time (ie. no unique yield to set against dose) but that any observed frequency is markedly influenced by changes in the kinetics of the cell population. Whilst we were aware that treatment-induced mitotic delay would exacerbate this problem, we did not have available sufficient computer power to investigate it.

All that has now changed, and today's enormous computer sophistication makes it possible to model cell populations to a high degree

of accuracy. We have therefore begun to look at the effects of delay upon observed chromatid aberration frequency [3]. A cell cycle model has been developed, into the G_2 of which we can insert any pattern of intrinsic sensitivity, and from which we can generate a yield-time curve of chromatid aberrations. Upon this population we can superimpose any of the various models of mitotic delay found in the literature, and study the effects on the yield-time profile.

The results so far indicate that even very simple models of delay can introduce into the profile peaks and troughs which are not found in the given G_2 sensitivity pattern.

Since different doses will confer different degrees of delay on the population, it is obvious that the various modifications of the observed aberration yields that will occur will seriously warp dose response curves, and complicate experimental interpretation.

A more detailed investigation of these phenomena forms part of the next (approved) CEC contract.

3. Cohort analysis and delay.

Theoretical work needs experimental back-up, and here, again, our various methods of cohort analysis [3, 4] are proving of value.

Because we can mark cells with BrdU at precise positions in interphase at the time of irradiation and identify those positions in metaphase cells later at the time of scoring, irrespective of any delay or perturbation they have experienced, we have the ideal system for unscrambling a perturbed population.

We have just completed a pilot experiment in stimulated human lymphocytes, irradiated with 1.5 Gy X-rays [4]. BrdU was added immediately after irradiation and sequential sampling performed at intervals up to 14h. Fluctuations in yield with sampling time were found for all chromatid aberration categories, but these could not be related simply to either the developmental stage of the cell at the time of exposure or to the time-to-run to metaphase. Mitotic delay at this dose extends to all sub-phases of S and was found to be as great, if not greater, in the earliest S cells as it is in G_2 . This work is also continuing into the next CEC contract.

Publications

[1] Aghamohammadi S Z and Savage J R K (1991). A BrdU pulse double-labelling method for studying adaptive response. *Mutation Res.*, 251;133-141.

[2] Aghamohammadi S Z and Savage J R K (1992). The effect of X-irradiation on cell cycle progression and chromatid aberrations in stimulated human lymphocytes using cohort analysis studies. *Mutation Res.* (in press).

[3] Savage J R K and Papworth D G (1991). Excogitations about the quantification of structural chromosomal aberrations. p 162-189 in "*Advances in Mutagenesis Research; 3*", (ed. G Obe), Springer-Verlag.

[4] Savage J R K (1990). Bromodeoxyuridine and chromosome "banding". *Clin.Cytogenet.Bull.*, 4;63-67.

Project 3

Head of project: *Prof. Olivieri*

Objectives for the reporting period

During 1991 the objectives of our research with human lymphocytes were to study the growth conditions that can effect: a) the radiosensitivity of cells irradiated in the G₂ stage; b) the expression of the "adaptive response".

Progress achieved including publications

- A) Experiments were carried out using human lymphocytes in order to test the effect of pH shifts on radiosensitivity of cells irradiated in the G₂ stage.

Whole blood (0.5 ml) was added to 4.5 ml of RPMI 1640 medium (Gibco) without fetal calf serum (Wolff et al., 1984), 2 mM glutamine, 100 units/ml penicillin, 100 µg/ml streptomycin and 2% phytohemagglutinin M (Wellcome). The cultures were incubated at 37°C in sealed vials in air.

Blood withdrawal and seeding were performed between 8 and 9 a.m. Irradiation was carried out with 250 kVp X-rays (Gilar-doni MLG 300/6D, 0.3 mm Cu added filtration, 6 mA, 0.20 Gy/min). 90 min. before fixation was performed according to standard cytological procedures; for each point examined 2 parallel cultures were set up.

The pH of the medium was adjusted with NaOH or HCl and was measured using a pH meter.

In our culture conditions constant variations in medium pH over the range of 7.4-6.8 were observed as a function of incubation time after PHA stimulation; in addition the pH of the medium was adjusted in parallel cultures over the range of 5.9-8.2. Then we exposed the cultures with different pH to a treatment of X-rays delivered 2 h before fixation.

Our results show that, as pH varies, the frequency of the breaks depends on the pH of the cultures at the time of irradiation; moreover our experiments indicate that variations in pH per se in the range tested by us do not cause chromatid aberrations.

- B) Eleven experiments were carried out using cultures of blood from donors which, in previous experiments, had not displayed an adaptive response. The experiments consisted first of exposing cultured human lymphocytes to adapting treatment and subsequently challenging the cells with high doses of X-rays. The cells were scored to see whether the prior exposure reduced the number of chromatid and isochromatid breaks induced by the challenging doses. Few chromatid exchanges (less than 10%) and gaps were recorded but not included in the analysis.

In all experiments the conditioning pretreatment consisted of 0.02 Gy of X-rays administered 26 h after stimulation with

PHA. The cells were subsequently challenged with 0.30 Gy of X-rays and fixed 2 h later. The challenge treatment was given after 50.78 h. Irradiation was carried out with 200 kVp X-rays (Gilardoni MGL 200/8D, 0.2 mm Cu added filtration, 8 mA, 0.60 Gy/min). 90 minutes before fixation 0.1 ml of colcemid (final concentration 2×10^{-7} M) was added to each culture.

The pooled data of 7 experiments indicate at 52 h fixation time a synergistic interaction between the adapting and the challenging dose of ionizing radiations; on the contrary at 78 h fixation time a significant adaptive response has been observed.

We considered these variations to be dependent on possible differences in the culture medium on days 2 and 3 after PHA stimulation. We therefore performed a number of experiments to investigate the effect of variations in one of the main characteristics of the medium itself, i.e., pH, since it has been observed that, in our culture conditions, on day 3 the pH of the extracellular medium was always lower than on day 2.

The pooled results of 6 experiments show that the pH of the medium affects the yield of induced chromatid aberrations and the type of interaction between the adapting and the challenging dose of ionizing radiations. With standard growth conditions we observe a pH shift as a function of incubation time after PHA stimulation and a synergistic interaction at 52 h fixation time, followed by an adaptive response at 80 h fixation time. Moreover the adjustment of pH with NaOH or HCl shows that variations in pH modify the interaction between the adapting and the challenging dose. At pH higher than 7.2 both the synergistic response and the adaptive response in the standard growth conditions at 52 h and 80 h are not observed. At pH lower than 6.4 we found an adaptive response at 80 h and the same trend (even if not statistically significant) at 52 h. Together these results seem to indicate that by lowering the pH of extracellular medium it is possible to obtain an adaptive response even in those donors who displayed no adaptive response or a synergistic response at high pH.

Publications

Bosi A., Micheli A., Pietrosanti S., Olivieri G. - Effect of pH shifts on radiosensitivity of human lymphocytes irradiated in the G₂ stage, *Mut. Res.* 250 (1991), 325-329.

Olivieri G., Bosi A., Grillo R., Salone B. - Interaction of low dose irradiation with subsequent mutagenic treatment. Studies with human lymphocytes. In: *Low Dose Irradiation and Biological Defence Mechanisms*. Eds. T. Sugahara et al., Elsevier, 1992, 279-282.

Project 4

Head of project 4: *Dr. Cortés-Benavides*

Objectives for the reporting period

Regarding adaptive response (AR), interindividual differences have been reported which pose serious doubts as to whether this is or not a general feature in human population. In order to further characterizing this phenomenon, we proposed the use of the binucleate cell micronucleus test (Fenech and Morley, 1985) in human lymphocytes from different donors conditioned with hydrogen peroxide (H_2O_2) and challenged with two doses of X rays (1.5 or 3.0 Gy).

As compared to the classical chromatid aberrations (CA) analysis at metaphase using a single fixation time, the study of chromosome damage in binucleated cells blocked at cytokinesis by an exposure to cytochalasin B (Cyt B) offers the advantage of allowing many cells which underwent the conditioning and challenge treatment to be collected for the analysis of AR. Moreover, by using this protocol, it is possible to quantify not only chromosome damage induced in G2 but also earlier in the cell cycle, as well as detecting any protective effect of the conditioning treatment with H_2O_2 .

Progress achieved including publications

Fig. 1 shows the experimental procedure followed to study adaptive response (AR).

Human lymphocytes from two healthy donors were conditioned by a single 30 min pulse with different doses of H_2O_2 given 24 h after setting up the cultures. Preliminary experiments carried out to score chromosomal aberrations at metaphase demonstrated that the most suitable concentrations for the conditioning treatment were 25, 75 and 250 μM H_2O_2 (Cortés et al., 1990). Challenge treatment was given 24 h later by exposing the cells to 1.5 Gy or 3.0 Gy of X-rays, and Cyt B, at a final concentration of 6.0 $\mu g/ml$ was added immediately after the X-ray exposure. The recovery period in Cyt B was for either 12 or 20 h (1.5 Gy) or for 12, 20 or 30 h (3.0 Gy) after exposure to ionizing radiation.

Fixation was performed by the standard cytological procedure and two thousand binucleated cells were scored blind for micronuclei in each treatment by two different observers. To determine if the number of micronuclei observed in conditioned cells was significantly lower than expected, a one-tailed t-test was used. The frequencies of micronuclei in binucleate cells observed in cells irradiated with 1.5 Gy or 3.0 Gy of X-rays was compared with that found in cells which underwent the combined treatment as shown in Table I and II for the two donors. As can be seen, the difference between the expected and observed frequencies of

MN was, in general, statistically significant, i.e., they showed the AR. Another interesting observation was that the longer the recovery in Cyt B, the higher the frequency of micronuclei observed (Table I and II), as expected if cells damaged earlier in the cell cycle are allowed to reach mitosis when given a longer recovery time (20 h versus 12 h, or 30 h versus 20 h) in Cyt B. On the other hand, in order to make an overall assessment for AR, the frequencies of micronuclei at both fixation times (Table I) or three fixation times (Table II) were pooled and compared with the expected values. The statistical analysis showed that, in all cases, there was a significant AR effect (Table I and II).

In our opinion, these results lend further support to the induction of AR to ionizing radiation by non toxic doses of hydrogen peroxide, in agreement with that previously reported in human lymphocytes.

One of the most questionable points in the AR to ionizing radiation using the Ca test, has been the possibility of the AR being an artefact caused by radiation-induced mitotic delays. Nevertheless, experiments with human lymphocytes conditioned with [³H]dThd to high doses of ionizing radiation have shown that AR is not the result of such an artefact nor of selection against a radiosensitive population of cells that have incorporated [³H]dThd.

The use of the cytokinesis-block method to analyze the AR after different recovery times in Cyt B has given us the additional advantage of being able to collect the cells exposed to X-rays not only in G₂, but also earlier in the cell cycle and allow them to undergo any delay needed to repair damage before entering mitosis and showing up as binucleated cells.

Publications

Dominguez, I., Panneerselvam, N., Escalza, P., Natarajan, A.T. and Cortes, F. - Adaptive response to radiation damage in human lymphocytes conditioned with hydrogen peroxide as measured by the cytokinesis-block micronucleus technique, *Mutation Res.*, 301 (1993), 135-141.

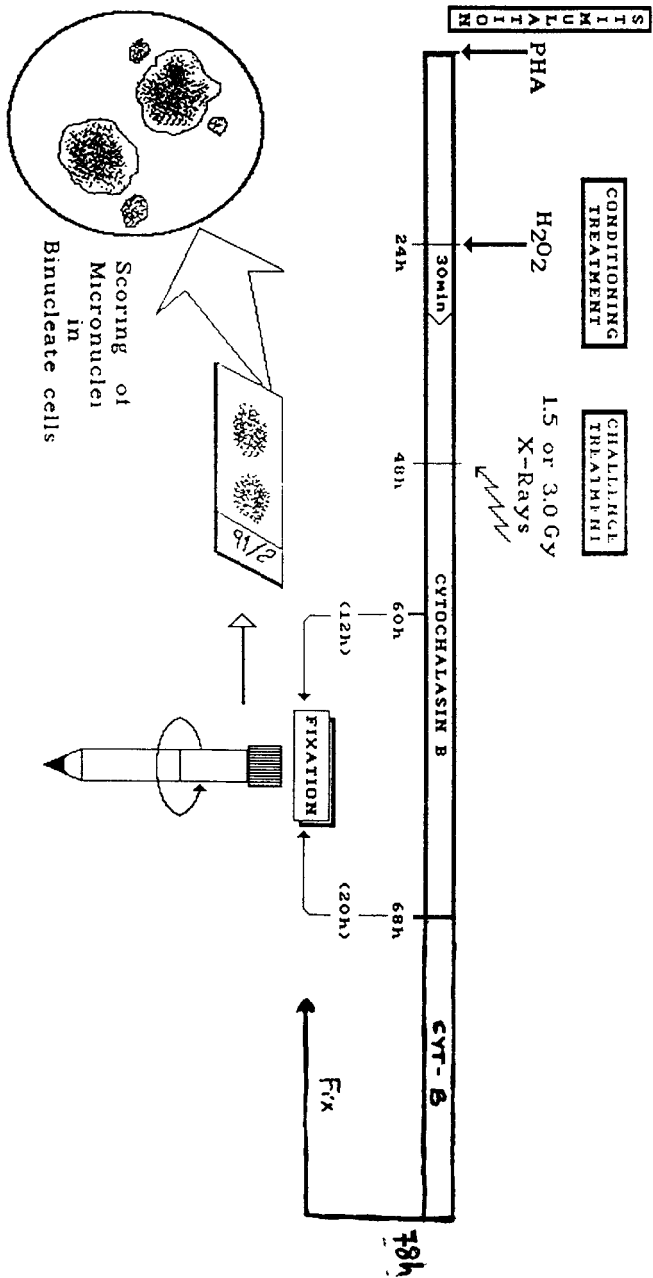


Figure 1

Table I - Effects of a single pulse with different concentrations of H₂O₂ on the frequency of micronuclei observed in human lymphocytes challenged with 1.5 Gy of x-rays at 12 or 20 h recovery times in cytochalasin B.

Donor	Conditioning pretreatment H ₂ O ₂ (M)	Challenge treatment X-rays	12 h cyt B			20 h cyt B			Total of micronuclei observed		
			Number observed	%	micronuclei expected(a)	Number observed	%	micronuclei expected(a)	N°	%	
A	None	None	14	7	-	5	2.5	-	19	4.75	
	2.5x10 ⁻⁵	None	13	6.5	-	32	16	-	45	11.25	
	7.5x10 ⁻⁵	None	13	6.5	-	20	10	-	33	8.25	
	2.5x10 ⁻⁴	None	20	10	-	29	14.5	-	49	12.25	
	None	1.5 Gy	151	75.5	-	178	89	-	329	82.25	
	2.5x10 ⁻⁵	1.5 Gy	122	61	75(b)	184	92	102.5(d)	306	76.5	
	7.5x10 ⁻⁵	1.5 Gy	104	52	75(b)	160	80	96.5(b)	264	66	
	2.5x10 ⁻⁴	1.5 Gy	96	48	78.5(b)	178	89	101(d)	274	68.5	
	B	None	None	15	7.5	-	20	10	-	35	8.75
		2.5x10 ⁻⁵	None	18	9	-	22	11	-	40	10
7.5x10 ⁻⁵		None	17	8.5	-	11	5.5	-	28	7	
2.5x10 ⁻⁴		None	9	4.5	-	16	8	-	25	6.25	
None		1.5 Gy	145	72.5	-	230	115	-	375	93.75	
2.5x10 ⁻⁵		1.5 Gy	144	72	74(ns)	171	85.5	116(b)	315	78.75	
7.5x10 ⁻⁵		1.5 Gy	114	57	73.5(b)	169	84.5	110.5(b)	283	70.75	
2.5x10 ⁻⁴		1.5 Gy	113	56.5	69.5(c)	186	93	113(b)	299	74.75	

a. Sum of the two individual treatments minus the control.
 b. Observed frequency significantly lower than expected (P<0.01)(one-tailed t-test)
 c. Observed frequency significantly lower than expected (P<0.05).
 d. Observed frequency significantly lower than expected (P<0.1).
 ns. Observed frequency not significantly lower than expected.
 2000 binucleated cells were scored in all cases.

Table II - Effects of a single pulse with different concentrations of H₂O₂ on the frequency of micronuclei observed in human lymphocytes challenged with 3.0 Gy of x-rays before 12, 20 or 30 h recovery in Cyt B.

Donor	Conditioning pretreatment H ₂ O ₂ (M)	Challenge treatment X-rays	12 h Cyt B			20 h Cyt B			30 h Cyt B						
			Number of observed N°	%	micronuclei expected(a) %	Number of observed N°	%	micronuclei expected(a) %	Number of observed N°	%	micronuclei expected(a) %	Total of observed N°	%	micronuclei expected %	
A	None	None	14	7	-	17	8.5	-	8	4	-	39	6.5	-	
	2.5x10 ⁻⁵	None	13	6.5	-	17	11.5	-	14	7	-	61	10.16	-	
	7.5x10 ⁻⁵	None	13	6.5	-	23	11.5	-	20	10	-	56	9.33	-	
	2.5x10 ⁻⁴	None	20	10	-	22	11	-	9	4.5	-	51	8.5	-	
	None	3 Gy	**126	81.8	-	383	191.5	-	627	313.5	-	1136	205.09	-	
	2.5x10 ⁻⁵	3 Gy	212	106	81.3(ns)	323	161.5	200(b)	632	316	316.5(ns)	1167	194.5	208.75(b)	
	7.5x10 ⁻⁵	3 Gy	164	82	81.3(ns)	353	176.5	194.5(c)	457	228.5	319.5(b)	974	162.3	203.43(b)	
	2.5x10 ⁻⁴	3 Gy	143	71.5	84.8(c)	324	162	194(b)	435	217.5	314(b)	902	150.3	207.09(b)	
	B	None	None	22	11	-	17	8.5	-	14	7	-	53	8.8	-
		2.5x10 ⁻⁵	None	12	6	-	23	11.5	-	15	7.5	-	50	8.3	-
7.5x10 ⁻⁵		None	12	6	-	24	12	-	13	6.5	-	49	8.1	-	
2.5x10 ⁻⁴		None	21	10.5	-	19	9.5	-	20	10	-	60	10	-	
None		3 Gy	225	112.5	-	335	167.5	-	710	355	-	1270	211.6	-	
2.5x10 ⁻⁵		3 Gy	200	100	107.5(ns)	318	159	170.5(d)	609	304.5	355.5(b)	1127	187.8	211.11(b)	
7.5x10 ⁻⁵		3 Gy	253	126.5	107.5(ns)	*236	162.4	171(ns)	540	270	354.5(b)	1029	188.7	210.9(b)	
2.5x10 ⁻⁴		3 Gy	***222	117.2	112(ns)	297	148.5	168.5(b)	539	269.5	358(b)	1058	179.5	211.8(b)	

a. Sum of the two individual treatments minus the control.
b. Observed frequency significantly lower than expected (P<0.01)(one-tailed t-test)
c. Observed frequency significantly lower than expected (P<0.05)
d. Observed frequency significantly lower than expected (P<0.1)
ns. Observed frequency not significantly lower than expected.
2000 binucleated cells here scored in all cases, except:
^Δ 1453 binucleated cells scored
**1359 binucleated cells scored
***1814 binucleated cells scored

Project 5

Head of project: *Dr. Bryant*

Objectives for the reporting period

- 1) Manipulation of the G2 phase of Chinese hamster ovary cells by lowering temperature to lengthen the time window during which the kinetics of disappearance of chromatid breaks can be studied.
- 2) To measure the kinetics of G2 chromatid aberrations in radiation sensitive mutant rodent and human lines and their normal counterparts under various conditions.
- 3) To use cell and nuclear extracts of normal cells (CHO and human cells) together with poration techniques to correct (complement) defects in radiosensitive mutant cell lines (*xrs 5* and AT cells) that show high frequencies of X-ray induced chromatid breaks, and in the case of *xrs 5* a reduced ability to rejoin DNA double-strand breaks.
- 4) To carry out parallel studies of repair of DNA double-strand break repair using neutral filter elution.

Progress achieved including publications

- 1) We have shown in Chinese hamster ovary cells (MacLeod et al 1990) that when cells are incubated at lowered temperatures (33°C or 29°C) for short periods prior to, during and after irradiation (transient hypothermia) the G2 phase is lengthened, up to more than twofold, thereby extending the range of time over which the kinetics of chromatid breaks can be observed. This allows the establishment of more accurate kinetics of chromatid breaks than was previously possible. Using this system we showed that the rate of disappearance of chromatid breaks with time in CHO cells (Fig 1) was similar at 37°C and 33°C and only very slightly altered at 29°C (MacLeod and Bryant 1990).

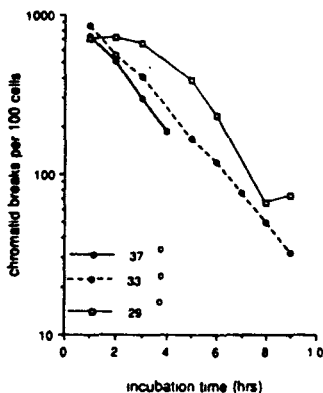


Figure 1. Frequencies of chromatid breaks in CHO cells incubated at various temperatures after X-irradiation (1.5 Gy).

We also found that the rate of disappearance with time of chromatid breaks in xrs 5 cells (a radiosensitive dsb repair defective mutant derived by Jeggo et al, (1982, Biochemie, 64, 713-715) was similar to that for its WT parental CHO K1 cell line. These results were obtained when equiclastogenic doses of X-rays were employed to damage cells. We have repeated these experiments using the same X-ray dose (0.75 Gy) in both cell lines. Again our results (Bryant et al, 1991) show a similar rate of disappearance of chromatid breaks occurs in both lines (xrs and CHO) following X-irradiation. This result seems paradoxical in view of the fact the the overall rate of rejoining of DNA double-strand breaks (as measured by neutral elution) is known to be severely reduced in xrs 5 cells as compared to the WT CHO cell line. The result may thus indicate that G2 xrs 5 cells are proficient in the repair of DNA dsb. Measurements of repair of dsb in synchronized G2 cells will be made in these cell lines using the neutral filter elution technique.

2) We have studied the effects of the DNA double-strand break inhibitor 9- β -D-arabinofuranosyladenine (ara A) on the frequency and kinetics of chromatid breaks and exchanges in both CHO (Singh, Slijepcevic and Bryant, in preparation) and human lymphocytes (MacLeod and Bryant 1992). In both types of cell, following radiation exposure, chromatid breaks disappear with exponential kinetics although the $t_{1/2}$ for disappearance of breaks is different for different cell lines: 0.87h in human lymphocytes, 2.7h for human fibroblasts (Mozdarani and Bryant, 1987, Mutagenesis 2, 371-374) and 1.5h for CHO cells (MacLeod et al 1990). The reasons for these differences in disappearance of breaks is not yet understood.

Treatment of CHO cells with ara A at 100 μ M led to the abolishment of disappearance of breaks, and a level response was obtained (Singh et al, in preparation). However, in human lymphocytes, ara A alone even at 200 μ M was found to be ineffective in inhibiting of disappearance of breaks. This was thought to be due to the presence of high levels of adenine deaminase, leading to the breakdown of ara A to arabinofuranosyl-hypoxanthine. Treatment of lymphocytes with the adenine deaminase inhibitor cofomycin confirmed this hypothesis and led to strong inhibition of disappearance of breaks following irradiation. Since ara A is a known inhibitor of DNA synthesis and DNA double-strand break repair (Bryant and Blöcher, 1982 Int. J. Radiat. Biol., 42, 385-394) we deduce that the level response in chromatid break experiments indicates inhibition fo the rejoining of a class of dsb which are converted into chromosome breaks.

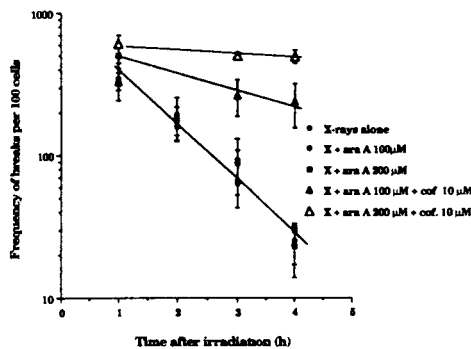


Figure 2. Kinetics of chromatid breaks as a function of time after X-irradiation of human lymphocytes treated with ara A and cofomycin.

3) We also examined the kinetics of exchanges in irradiated G2 CHO cells and human lymphocytes (MacLeod et al 1990; MacLeod and Bryant 1992). Few exchanges were found when cells were sampled immediately following irradiation (as was found also for breaks), presumably as a result of lack of time for expression of damage as visible aberrations. At later times (>30min) after exposure cells showed a level frequency of exchanges, the kinetics of which thus did not parallel the disappearance of breaks (Fig 4). The frequency of exchanges in human lymphocytes was found to be about 7 fold lower than that in CHO cells, although the frequencies of breaks induced was similar.

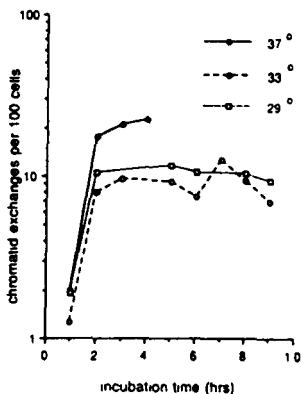


Figure 3. Frequency of chromatid exchanges in G2 CHO cells at various times after X-irradiation.

Two deductions can be made from our results so far: firstly, that the change in frequency of breaks through G2 following irradiation is not a result of differences in radiosensitivity at different times during the G2 phase, since frequency of exchanges remain constant, and the ara A results together with the results obtained by holding cells after X-irradiation at reduced temperature where the frequencies of breaks at 33°C decrease by almost an order of magnitude below those at 37°C indicate a rejoining process, probably reflecting the underlying repair of a class of dsb; secondly, that the mechanisms of rejoining (of chromatid breaks) and misjoining (to give exchanges) must be different, as we postulated previously from data with human fibroblasts (Mozdarani and Bryant, 1987, *Mutagenesis* 2, 371-374).

Although we recognize that further work needs to be done, taken together the results of our experiments with rodent and human cells indicate that the disappearance of breaks in G2 cells represents a manifestation of underlying repair of a lesion, and from other previous and current work in our laboratories (Bryant 1984, *Int. J. Radiat. Biol.*, 46, 57-65; Bryant 1992) we deduce that these lesions are probably a specific type of dsb, possibly those with blunt ends. Current experiments are aimed at testing this notion by examining the responses of G2 cells also to various restriction endonucleases.

2) Protein extracts (whole cell and nuclear extracts) have been prepared from both CHO and xrs 5 cells. These extracts are being assayed in various ways. Using Southwestern blots we have found differences in the DNA binding properties of proteins present in the extracts. These proteins have been separated on polyacrylamide gels by electrophoresis and are currently being further characterized. A protein with altered ssDNA binding has been identified in xrs 5 extracts. Assay of CHO cell extracts in gamma irradiated, streptolysin 0 porated (Bryant 1992) xrs 5 cells is currently being carried out. As a control, T4 ligase was used to treat porated and Pvu II treated CHO and xrs 5 cells. This ligase treatment led to a marked dose dependent decrease in

frequencies of micronuclei induced by Pvu II in both lines (Bryant and Johnston, 1992). However, experiments suggest that it leads to little or no change in the frequencies of X-ray induced micronuclei, indicating that although T4 ligase can join restriction-endonuclease cuts in cellular DNA, dsb induced by X-rays are not strongly subject to 3' hydroxyl-5' phosphoryl end ligation.

Treatment of gamma-irradiated, streptolysin-porated (Bryant 1992) AT lymphoblastoid cells with crude nuclear extracts from normal human cells has led to reduced frequencies of chromatid aberrations, indicating a partial correction of the chromosomal radiosensitivity defect, but increased frequencies in normal cells indicating the possible presence of nucleases. Extracts are currently being further purified using affinity chromatography and other means.

Publications

- Bryant, P.E.** (1990) Restriction endonuclease- and radiation-induced DNA double-strand breaks and chromosomal aberrations; similarities and differences. In 'Chromosome aberrations: Basic and applied aspects'. G. Obe and A.T. Natarajan Eds., Springer Verlag, Berlin. pp 61-69.
- Bryant, P.E.** (1991) Relationships between DNA double-strand breaks and chromosomal aberrations. In 'New Developments in Fundamental and Applied Radiobiology', Proceedings of the European Society of Radiation Biology, Eds. C. Mothersill and C. Seymour, Taylor and Francis, London. pp 84-94.
- Bryant, P.E.** (1992) Induction of chromosomal damage by restriction endonuclease in CHO cells porated with streptolysin O. *Mutation Research*, **268**, 27-34.
- Bryant, P.E. and Johnston, P.J.** (1992) Restriction endonuclease induced DNA double-strand breaks and chromosomal aberrations in mammalian cells. *Mutation Research*, in the press.
- Macleod, R.A.F., and Bryant, P.E.** (1990c) Similar kinetics of chromatid aberrations in X-irradiated xrs 5 and wild-type Chinese hamster cells. *Mutagenesis*, **5**, 407-410.
- Macleod, R.A.F. and Bryant, P.E.** (1992) Effects of adenine arabinoside and cofomycin of the kinetics of G2 chromatid aberrations in X-irradiated human lymphocytes. *Mutagenesis* **7**, 285-290.
- Macleod, R.A.F., A.F.Christie, Costa, N.A., and Bryant, P.E.** (1990) Repair kinetics in CHO cells of X-ray induced DNA damage and chromatid aberrations during a cell cycle extended by transient hypothermia. *Mutagenesis*, **5**, 279-283.
- chromatid aberrations in X-irradiated xrs 5 and wild-type Chinese hamster ovary cells. *Mutagenesis*, **5**, 407-410.

Project 6

Head of project: *Prof. Gunnar Ahnström*

Objectives for the reporting period

Introduction

X-rays induce dicentric chromosomal aberrations in the first division after irradiation of human lymphocytes. Most other agents, including UV, induces only chromatid aberrations. However, UV given simultaneously with X-rays, doubled the number of dicentrics, although the doses of UV alone hardly gave any aberrations at all. If UV and X-rays were separated in time allowing repair between the two agents, the number of dicentrics decreased with time if X-rays were given first. In contrast to this the aberrations initially increased if UV was given as the first treatment to reach a maximum after about half an hour of incubation before X-rays were given. After this time the dicentrics decreased slowly down to the level given by X-rays alone. This last observation showed that the UV-stimulated increase of dicentric aberrations was not due to interaction between primary lesions.

There are several possible mechanisms for this effect.

1. UV-induced open excision repair sites interacts with X-ray induced double strand breaks.
2. UV induces condensation of the chromatin which might increase the probabilities for X-ray induced DSBs to interact and form dicentric aberrations. In addition chromatin decondensation may also increase the initial number of DSBs. UV act as a modifying agent.
3. UV induces only few dicentric aberrations. Post treatment with DNA-polymerase inhibitors increases the yield of dicentrics in lymphocytes dramatically. The question is if ionising radiation can act as modifying agent in the same way as the inhibitors.

The objective of this project is to design experiments to discriminate between these.

Progress achieved

For the experimental part of the project it was planned that Holmberg and his group should be responsible for the cytological part and Ahnström for the work on molecular level. This involved DNA lesions and their repair and chromatin studies. However after the death of Mats Holmberg the working plan had to be changed and the cytology as well had to be done at the Department of Radiobiology, Stockholm University. This required that a new person was hired and trained to take care of the cytological part.

1. Cytological observations

UV gamma rays: The observation that UV interacts with X-rays was made in human lymphocytes. In order to be able to use the numerous mutant lines in cultured cells we have repeated

Holmbergs lymphocyte experiments in a human fibroblast line. Cells grown to confluence were exposed to UV (6 J/m²) and gamma rays (1.5 Gy) alone, respectively, and combined treatments with UV and gamma rays. For the combined treatments we selected one treatment where gamma rays and UV followed each other without any repair incubation in between (gamma + UV) and one treatment starting with UV followed by 30 minutes incubation in medium at 37° and then gamma irradiation (UV - 30 - gamma). Dicentric aberrations were scored in the first division after treatment.

Results: One pilot experiment and 2 larger scale experiments have been performed. All three experiments indicated an increase in dicentric aberration frequencies in the combined treatment (gamma + UV) compared to gamma irradiation alone. In contrast to this no effect in the (UV - 30 - gamma) treatment, which gave maximal response in the lymphocyte system, was observed.

UV DNA polymerase inhibitor: Confluent cells were irradiated with UV (6 J/m²) and treated with aphidicolin (10 µM) for one hour.

Results: The aphidicolin treatment resulted in a large increase of dicentric aberrations compared to UV alone, 0.06 dicentrics/cell after UV, 0.28 dicentrics/cell after UV + aphidicolin.

2. DNA-lesions and chromatin

We have earlier shown that the yield of X-ray induced single strand breaks changes drastically as the chromatin configuration is modulated by variation in Mg²⁺ (Ljungman 1991, Ljungman et al. 1991). Pretreatment with UV also increased the single strand breaks which indicated that such a process could to some extent be responsible for the UV-induced increase in dicentric aberrations. A similar investigation has shown that induction of double strand breaks also are strongly dependent on chromatin structure (Nygren et al., manuscript submitted to I.J.R.B.).

Addition of aphidicolin to UV-irradiated cells increase the life times of open repair sites considerably.

Combined treatments with gamma rays and UV did not influence the life times of breaks.

3. Conclusions

About the models discussed above it seems that number 3 can be ruled out, since gamma rays do not have the same effects as aphidicolin to modify the life time of UV induced repair sites.

The (gamma + UV) treatment showed a synergistic reaction similar to that observed in lymphocytes although not of the same magnitude. The unexpected result was that (UV - 30 - gamma) which gave maximal response in the lymphocyte system did not show any significant synergism between UV and gamma rays. Therefore there is also some doubt about model number 1 since one would not expect that the damage from 6 J/m² could be repaired in half an hour, i.e. there should be as many repair sites open to interact with gamma-ray damage as if the two agents were given simultaneously.

This leaves model 2 as the most attractive hypothesis.

It is possible that the lower degree of synergism obtained in fibroblast compared to lymphocytes reflects the degree of condensation in the two cell types, respectively. The chromatin in G1 fibroblasts may already be decondensed to such an extent that the UV-treatment plays a little role. We are presently running an experiment where the fibroblast cells are kept on low serum to increase the degree of condensation.

Project 7

Head of project: *Dr. M. Harms-Ringdahl*

Objectives for the reporting period

This joint research program between Holmberg and Ahnström deals with the dose response curves of chromosome exchange aberrations at very low doses of X-rays, and how they are influenced by other agents such as UV-radiation and DNA-repair inhibitors. Experimental evidence has been produced showing that these factors affect the radiation induced yield of chromosome exchange aberrations. To obtain correct estimates of radiation exposure, based on cytogenetical studies of exposed subjects, the mechanisms as well as the level of variation induced by this type of agents has to be studied. The role of Holmbergs group was to conduct cytogenetical experiments on the interactions between ionizing radiation and UV-radiation or various DNA-repair inhibitors in order to elucidate the mechanisms for the formation of chromosome aberrations.

Progress achieved

Due to the unexpected and tragic death of M. Holmberg in May 1990, the formal responsibility was temporarily taken by U. Bäverstam. From August 1991, M. Holmbergs position was given to M. Harms-Ringdahl, and together with Ahnström the cytogenetical part of the project could, to a limited extent, be performed. Initially the work also involved training of new personnel for the cytogenetical studies. The progress of this part of the project has been summarized in the report of Ahnström.

In order to progress with the major goal of the project under the new situation and with new persons involved, experimental techniques based on molecular biology has been established. The program has been extended to include the effects of low dose rates on the mutational spectrum of ionizing radiation, and will continue with M. Harm-Ringdahl as project leader, within the 1992 CEC-program for radiation protection.

Project 8

Head of project: *Prof. L.E. Feinendegen*

Objectives for the reporting period

In radiation protection, the conservative assumption is being made that detrimental radiation effects such as radiation induced carcinogenesis are proportional to absorbed dose at low radiation doses. However, the natural incidence of cancer is high and hence the direct observation of radiation carcinogenesis at low doses virtually impossible. Therefore new sensitive methods must be developed and applied to better understand radiation mechanisms at and biological responses to low dose radiation at cellular, tissue and animal levels.

In this project it is proposed to investigate the correlation between biological responses at two different biological end points: a) adaptive response of cells in vivo and b) formation of unrepaired strand breaks of cells in vivo.

Both effects will be investigated for different radiation qualities. Adaptive response is understood as a cellular defense mechanism against radicals. Unrepaired strand-break formation is taken as a radiation induced biological end point at the origin of carcinogenic point mutations.

It is the aim of the project to get information on the correlation between end points a) and b) for different radiation qualities in order to better understand the "vertical risk", meaning the propagation of radiation detriment and resistance from lower to higher levels of biological organization. This also includes new information on the question as to the proportionality between risk and dose and the possible existence of threshold doses and threshold dose rates.

The studies will also address the question as to the existence of beneficial radiation effects at low doses and their radiation quality dependence.

Progress achieved including publications

1. Correlation of adaptive cellular response and unrepaired strand break formation at low doses and dose rates

1.1 Effect of low radiation doses on the "Salvage Pathway"

In mammalian organisms rapidly proliferating cell populations reutilize the molecular building stones liberated as a result of cell death for the synthesis of new DNA molecules. In this process the "Salvage Pathway" of thymidine has a special role. The effect of radiation on this metabolic pathway can be investigated with the aid of ^3H -thymidine (^3H -TdR) or ^{125}I -iododeoxyuridin (^{125}I -UdR).

Total-body irradiation of mice with 0.005 - 1 Gy temporarily gamma-radiation inhibits the incorporation of ^3H -TdR or ^{125}I -UdR into proliferating bone marrow cells. This inhibition is maximally expressed at 4 hours after gamma or neutron irradiation. Nonspecific metabolic substrate such as ^3H -

deoxyuridine and ^3H -cytidine as precursors of DNA and RNA, ^3H -leucine as precursor of proteins, ^{125}I -heptadecanoic acid as a precursor of lipids and ^3H -methylglucose as a substrate for measuring carbohydrate - specific transport processes show no changes in their respective metabolic kinetics after acute total - body irradiation.

The diminished tracer incorporation into DNA following low dose irradiation is the result of a decreased thymidine kinase activity (TdR-K). This decreased enzyme activity involves all 4 isoenzymes of TdR-K and cannot be explained on the basis of impairment of transcription or inhibition of translocation.

1.2 Effect of low radiation doses on hemopoietic stem cells

The number of blood-forming stem cells (spleen colony test according to Till and McCulloch, 1960) is diminished nearly concurrently with the temporary enzyme inhibition after whole -body irradiation of donor animals with 0.01 - 0.10 Gy gamma-irradiation. This effect is maximally expressed 0.25 - 4 hours after irradiation.

1.3 Simulation of the radiation effect by vitamin-E-deficiency

Experimentally induced vitamin-E-deficiency (to 15% of the normal value) reduces the activity of TdR-K in bone marrow cells and, correspondingly, decreases the incorporation of ^3H -TdR and ^{125}I -UdR into DNA. The hemopoietic stem cells are also sensitive to a reduction of Vitamin E levels. The effect of an induced vitamin-E-deficiency mimicked in all respects a whole-body irradiation with low doses.

1.4 Reaction of cells to multiple irradiations

Irradiation of animals with a low dose of gamma-radiation alters the reaction of their bone marrow cells to subsequent low dose irradiations.

1.4.1 Temporary resistance of TdR-K

If a whole body gamma-irradiation of mice with 0.01 or 0.10 Gy is followed 30 mins later by another irradiation of the same quality, the inhibition of TdR-K in bone marrow cells and the subsequent recovery are accelerated; the maximal radiation effect was observed as early as 2 hours after the last irradiation and control levels were attained again within 4 hours. - If the second dose of radiation was given 4 hours after the first, i.e., at the time of maximal inhibition of enzyme activity, the TdR-K activity reached control levels with 0.5 hours and remained there for at least another 4 hours. - If the temporal interval between the two successive exposures was prolonged to 12 hours, bone marrow cells behaved as if they had not been irradiated earlier.-

The induced resistance at 4 hours after a first irradiation depended on the magnitude of the conditioning dose and was expressed more intensely after conditioning dose of 0.1 Gy than 0.01 Gy.

In the case of three irradiations with 0.01 or 0.10 Gy at intervals of 4 hours each, the last radiation exposure again elicited an enzyme inhibition, although less intense and of a more rapid recovery as compared to a single irradiation. This suggests that the cellular defense has been exhausted after repeated irradiation.

1.4.2 Radiation sensitization of hemopoietic stem cells

In contrast to the reaction of thymidine kinase two irradiations of hemopoietic stem cells at intervals of 0.5 of 4 hours resulted in a potentiation of the effect of a single dose. The effect of two irradiations with 0.1 Gy exceeded that of a single irradiation with 0.2 Gy.

1.5 Increase of the free, non-protein bound concentration of glutathione (GSH)

Whole-body gamma-irradiation with 0.01, 0.10 and 1.0 Gy resulted in a small, temporary increase of the free, non-protein bound GSH in bone marrow cells, in parallel with the reaction of TdR-K. The elevation of the concentration of GSH in bone marrow cells of vitamin-E-deficient mice was similar to that observed after low radiation doses.

Since GSH is not only an essential constituent of the cellular radical detoxification system, but also involved in various enzyme-catalyzed reactions, it was investigated whether a casual relationship exists between alterations in GSH concentration, inhibition of TdR-K and decrease of stem cells.

1.6 The relation of the glutathione concentration to the activity of thymidine kinase and the reaction of blood-forming stem cells

In these investigations GSH synthesis was inhibited by buthionine sulfoximine (BSO) or free GSH was bound to diethyl maleate (DEM), or GSH synthesis was stimulated by 1-2-oxothiazolidine-4-carboxylate (OTC). In addition, bone marrow cells were incubated with GSH-ester or isolated TdR-K with GSH.

Increased GSH concentration in bone marrow cells was accompanied by a decreased enzyme activity as well as a decrease of ^{125}I -UdR into DNA. Both parameters returned to control levels when the GSH concentration decreased. This action of GSH was shown not to affect the enzyme directly, but requires the intact structure of the cell.

Hemopoietic stem cells are more sensitive than the aforementioned parameters to a change in GSH concentration. A decrease in stem cells was observed either after a rise or a decline in GSH concentration.

Thus, the elevation of GSH concentration after a single low dose gamma-irradiation, demonstrated in these investigations, is sufficient to explain the observed radiation effect. A second irradiation at the time of elevated GSH concentration, i.e., at the time of GSH consumption, apparently raises the TdR-K activity to its normal level, whereas the number of CFU-S is further reduced.

1.7 Evaluation

These investigations show that murine bone marrow cells can react to low radiation doses by activation of the radical detoxification system so that their sensitivity is altered with respects to a following irradiation. This radiation induced resistance may well operate also against radicals that we produce in the course of normal oxidative metabolism. The observed changes cannot be viewed as damage, even if only temporary, but require further analysis. Independent of this it seems clear that the usually applied linear extrapolation for risk assessment is questionable.

Publications

Feinendegen, L.E. - The cell dose concept; a potential tool for analyzing the net effect of radiation in multicellular systems. Z. Phys. Med. Baln. Med. Klim. 19 (1990) 8-11.

Feinendegen, L.E., Booz, J. - Radiation-induced cancer from low doses of ionizing radiation: risk analysis using the cell dose concept. Def. Sci. J. 40 (1990) 383-388.

Feinendegen, L.E. - Radiation risk of tissue late effects, a net consequence of probabilities of various cellular responses. Europ. J. Nucl. Med. 18 (1991) 199-212

Mühlensiepen, H., Hennesen, U., Feinendegen, L.E. - Bedeutung der intrazellulären Glutathionkonzentration für die Reaktion der Thymidinkinase auf kleine Strahlendosen. in: Strahlenschutz für Mensch und Umwelt - 25 Jahre Fachverband für Strahlenschutz, Hrsg. H. Jacobs, H. Bonka, Verlag TÜV Rheinland 1040-1043 (1991)

Peterson, H.-P., Wangenheim, K.-H. v, Feinendegen, L.E. - Sensitivity of CFU-S 7d to 0.1 Gy gamma-irradiation after a pre-irradiation with the same dose. in: New developments in fundamental and applied radiobiology, Ed. C.B. Seymour & C. Mothersill (1991) pp. 12-17 Taylor & Francis Inc.

Peterson, H.-P., Wangenheim, K.-H. v, Feinendegen, L.E. - Magnetic field exposure of marrow donor mice can increase the number of spleen colonies (CFU-S 7d) in marrow recipient mice. Radiat. Environ. Biophys. 31 (1992) 31-38

Project 9

Head of project: *Prof. Johanson*

Objectives for the reporting period

Unlike x-rays or other forms of long-range radiation, Auger emitters in general and ^{125}I in particular, cause differential deposition of energy in a range of nanometers, highly and selectively irradiating the volume immediately surrounding the place of decay. The submolecular range of energy deposition cause that ^{125}I when incorporated into DNA induces high LET-like character of damage with RBE values of 10 - 40, whereas ^{125}I placed in cytoplasm or extracellularly has biological effect comparable to x-rays.

Iodine atoms are necessary components of thyroid hormone molecules which in turn play an important role in development and metabolism of vertebrates. Thyroid hormones (T_3 and T_4) regulate gene transcription by receptor mediated interaction with DNA. The question and the aim of this study was if thyroid hormones can transport iodine radioisotopes to the nanometer neighbourhood of DNA. Two cell lines, thyroid hormone responsive (GC) and thyroid hormone non-responsive cells, were cultured with a single $^{125}\text{I}\text{-T}_3$ activity concentration for one doubling time (t_d) or up to 6 t_d . The kinetics of uptake and retention was studied by measuring ^{125}I activity concentrations every t_d as well as the frequency of micronucleated cells were estimated every t_d in both labelling modes using the cytochalasin B micronucleus test.

The second aim was to study the possible effect (measured as the micronucleus frequency in peripheral blood) of low doses of radiation from ^{137}Cs in wild populations of bank voles (*Clethrionomys glareolus* Schreb.).

Progress achieved including publications

1. Toxicity of $^{125}\text{I}\text{-T}_3$

Increased frequency of micronucleated cells was observed in GC cells in both labellings. $^{125}\text{I}\text{-T}_3$ did not induce micronucleated CHO cells. Thus the first conclusion was that in the responsive cells thyroid hormone brings ^{125}I close to DNA.

Since the frequency of micronuclei is correlated with dose and the dose delivered to DNA by $^{125}\text{I}\text{-T}_3$ is related to the number of T_3 receptors, we tried to deduce the fluctuations in dose delivery to DNA (due to the

fluctuation of receptor density) from the kinetics of micronuclei obtained in both labelling modes. In a simple model of the dose delivery to DNA by $^{125}\text{I-T}_3$, we found, in agreement with the biochemical observations, that after administration of $^{125}\text{I-T}_3$ to T_3 -depleted cells, the dose first decreased (due to the down-regulation of receptors by its ligand) and then increased (due to utilization of the ligand and reappearance of T_3 receptors).

2. Effectiveness of $^{125}\text{I-T}_3$

The relationship of micronuclei frequency with ^{125}I activity concentrations accumulated to nuclei of the target cells was linear indicating a high LET-like character of damage. However, in comparison with induction of micronuclei by $^{125}\text{IUdR}$ the effectiveness of $^{125}\text{I-T}_3$ was about 10 times lower. The measurements of the activity concentrations/nucleus is, however, an inadequate dosimetric approach for Auger emitting nuclides since, whereas $^{125}\text{IUdR}$ is incorporated into DNA, the proximity of $^{125}\text{I-T}_3$ to DNA vary during the cell cycle and is probably associated with DNA only during 2 - 4 hours of the 30-hour cell cycle of GC cells. This means, that the toxicity of $^{125}\text{I-T}_3$ during association with DNA could quantitatively be comparable with $^{125}\text{IUdR}$.

3. Effect of low doses of radiation from ^{137}Cs on wild population

Bank voles (*Clethrionomys glareolus* Schreb.) captured on ^{137}Cs contaminated areas of central Sweden had been studied on the presence of micronuclei in their peripheral blood erythrocytes. Both erythrocyte subpopulations, poly- and normochromatic erythrocytes manifested micronuclei. The population mean frequency of micronuclei was significantly lower in area III (90 kBq m⁻²) compared to the control, area I (1.8 kBq m⁻²). Animals from the most contaminated area IV (145 kBq m⁻²) showed frequency of micronuclei in PCE significantly higher than in the control and area III, however, the mean micronucleus frequency in NCE was lower than in the control but higher than in area III. The population mean frequency of micronuclei of area II (22 kBq m⁻²) was similar as in the control. (The data concerning the levels of ^{137}Cs ground deposition are taken from Cristaldi, M., L.A. Ieradi, D. Mascanzoni and T. Mattei; *Int. J. Radiat. Biol.*, 1991, **59**, 31-40).

Publications

1. Ludwikow, G., F. Ludwikow and K.J. Johanson, 1992. Kinetics of micronucleus induction by ^{125}I -labelled thyroid hormone in hormone-responsive cells. *Int. J. Radiat. Biol.* **61**, 639-653

2. Ludwikow, G., 1992. Application of the micronucleus test based on peripheral blood erythrocytes to environmental studies, Submitted to *Int. J. Radiat. Biol.*
3. Ludwikow, G., 1992. Radiotoxicity of ^{125}I bound to the thyroid hormone. The micronucleus test in assessments of radiation induced damage. Ph.D. Thesis.

Project 10

Head of project: *Prof. L. Ehrenberg*

Objectives for the reporting period

1 To establish an *in vivo* mouse model to study the mechanism of radiation protection using induced frequencies of sister chromatid exchanges (SCEs) as the biological end point (in collaboration with A.T. Natarajan, Leiden).

2 Adaptive responses of radiation-induced mutation and chromosomal aberrations *in vivo* in the rat (in collaboration with A.D. Bates and A.T. Natarajan, Leiden)

In preliminary studies, pre-irradiation of rats with a low dose (8 cGy) affected the response to a challenge dose (2 and 4 Gy of 6 MeV photon) differently for different end points. The frequency of micronuclei (MN) in binucleated splenocytes being decreased (75 and 22.5% respectively) whereas the HPRT mutant frequencies (MF) the opposite effect (2.2 and 7.5 fold increase) of adaptation was observed. Although these effects were different at the two dose, with a clear effect on MN at 2 Gy and a stronger effect on MF at 4 Gy, they are concluded to be significant.

Data of HPRT mutant frequencies show a poor reproducibility considering the individual MF estimates and their confidence intervals as calculated by the commonly used formula. A major cause of this is the varying cloning efficiency (CE) that leads to a poor correlation between the number of mutants scored and CE.

In this situation the procedure for significance testing was based on the observed number of mutants (X), i.e., number of positive wells, under the assumption that X is an overdispersed Poisson variable:

$$\text{Var}(X) = k \cdot E(X)$$

where $E(X) \approx n \cdot N \cdot \text{CE} \cdot \text{MF}(\text{dose})$; n is the number of wells scored and N is the mean number of cells/well.

The overdispersion index k includes errors introduced by experimental procedures (steps of growth and dilution as well as determination of CE). The CE values used for correction are the mean values within the respective challenge dose group. The mutant frequency, MF(dose), and the over-dispersion index, k, are estimated by reweighted least-square technique, and significance testing conducted by t-test assuming the above error structure.

Progress achieved

1 Morales-Ramaires et al. (Radiation Res. 1989) reported an induction of SCEs by X-rays in bone-marrow cells of mice. They also found that a pretreatment with cysteamine reduced the frequencies of radiation induced SCEs. We wanted to use this model to study the mechanisms of radiation protection in vivo. As a first step, we repeated the experiments of Morales-Ramaires.

In order to determine the base line frequencies of SCEs in bone marrow of Balb C mice, BrdUrd tablets were implanted subcutaneously and 22 hrs. after which colcemid was injected (intraperitoneally) for 2 hrs., then the animals were sacrificed and bone marrow was isolated from both femurs, treated with hypotonic and fixed in acetic methanol (1:3). Air-dried preparations were differentially stained by fluorochrome plus Giemsa technique. In X-ray experiments, BrdUrd tablets were implanted immediately following irradiation (2 Gy) and frequency of SCEs determined by the above procedure. Radioprotector B-mercaptothylamine (cysteamine), 150µg/g body weight was injected 30 mins. before irradiation with 2.0 Gy of X-rays. The results are presented in the following tables. There was no evidence for induction of SCEs by X-rays in bone marrow cells of mice in these experiments.

Frequencies of SCEs in bone marrow cells in control and irradiated mice.

No.	controls	2.0 Gy	Cyst+2Gy	Cyst.
1	4.72	5.90	3.7	2.90
2	3.54	5.10	4.5	4.06
3	2.96	4.80	3.4	
4	2.74	3.50		
5	3.36	3.10		
6	4.06	4.06		
7	4.06	3.70		
8	4.06	3.50		
9	3.54	3.10		
10.	5.10	3.80		
Average	3.81	4.06	4.20	3.48

Project 11

Head of project: *Dr. Palitti*

Objectives for the reporting period

1. To irradiate in G2 phase with 10,15 and 20 cGy of fission neutrons (0.4 MeV average energy) and 30 and 45 cGy of x-rays lymphoblastoid cells derived from normal, AT heterozigotes (GM02781A)(HzAT) and AT patients(GM01525C) and post-treat them with aphidicolin (APC) and arabinfuranosilcytosine (ARA-C)
2. To analyze the data for:
Effect of different DNA repair inhibitors on the yield of radiation induced chromosomal aberrations (Ch.Ab's)

Progress achieved including publications

The cell cultures were irradiated at 3 hrs and post treated with the inhibitors 2 and 1/2 hrs before fixation.

Fig.1a shows the yield of Ch.Ab's induced by different doses of fission neutrons on normal, HzAT and AT lymphoblastoid cell type.

Fig.1b shows the yield of Ch.Ab's induced by different doses of x-rays on the same cell lines.
A higher radiosensitivity to both types of radiation was found in AT as expected.

Fig.2 shows the potentiating factor(PF)(*) on radiation induced Ch.Ab's by ARA-C or APC G2-post-treatment in the tested cell lines.

In both normal and HzAT cell lines there is a strong potentiation by both inhibitors. On the contrary there is a lack of potentiation by both inhibitors in the AT cells.

These results suggest that the enzymes which can be inhibited by these agents are not directly involved in repair of radiation damage induced in G2 cells derived from AT patients, suggesting that probably that AT cells lack the capability to transform the radiation induced primary DNA lesions into repairable products.

$$(*) \text{ PF} = \frac{E(i+p) - E_c}{(E_i + E_p) - 2E_c}$$

E_i: effect of neutrons or x-rays
E_p: effect of the inhibitor.
E_c: frequency of chr.ab's in the untreated control.

It should be noted a clear difference in response to ara-C post-incubation between neutron-treated lymphocytes (previous report) and lymphoblastoid cells from a normal individual. No potentiating effect, except at the highest dose of neutrons, was observed when irradiated lymphocytes were subsequently treated with ara-C. The reason for this discrepancy is not understood; it may be related to the cell type. It should also be noted that ara-C alone did not lead itself to a significant level of aberrations in lymphoblastoid cells. On the contrary about 13-14 aberrations per 100 cells were induced by ara-C alone in human lymphocytes.

Publications

A. Antocchia, F. Palitti, T. Raggi, C. Catena and C. Tanzarella. The yield of fission neutron-induced chromatid aberrations in G2-stage of human lymphocytes: effect of caffeine, hydroxyurea and cytosine arabinoside post-treatments. International Journal of Radiation Biology in press 1992.

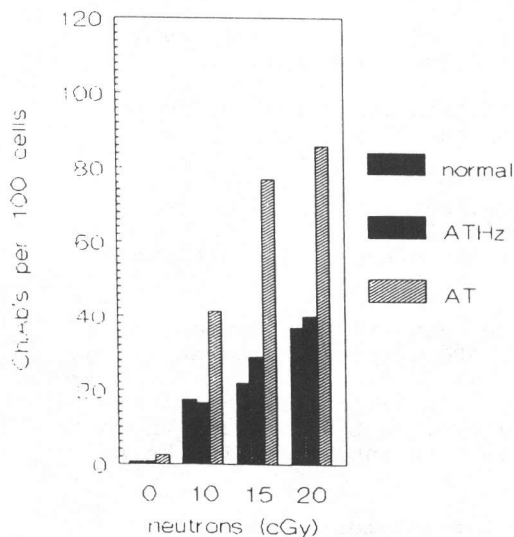


Fig. 1a

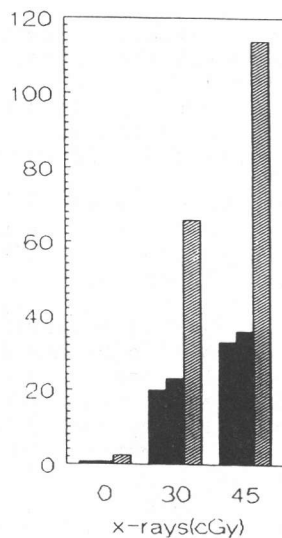


Fig. 1b

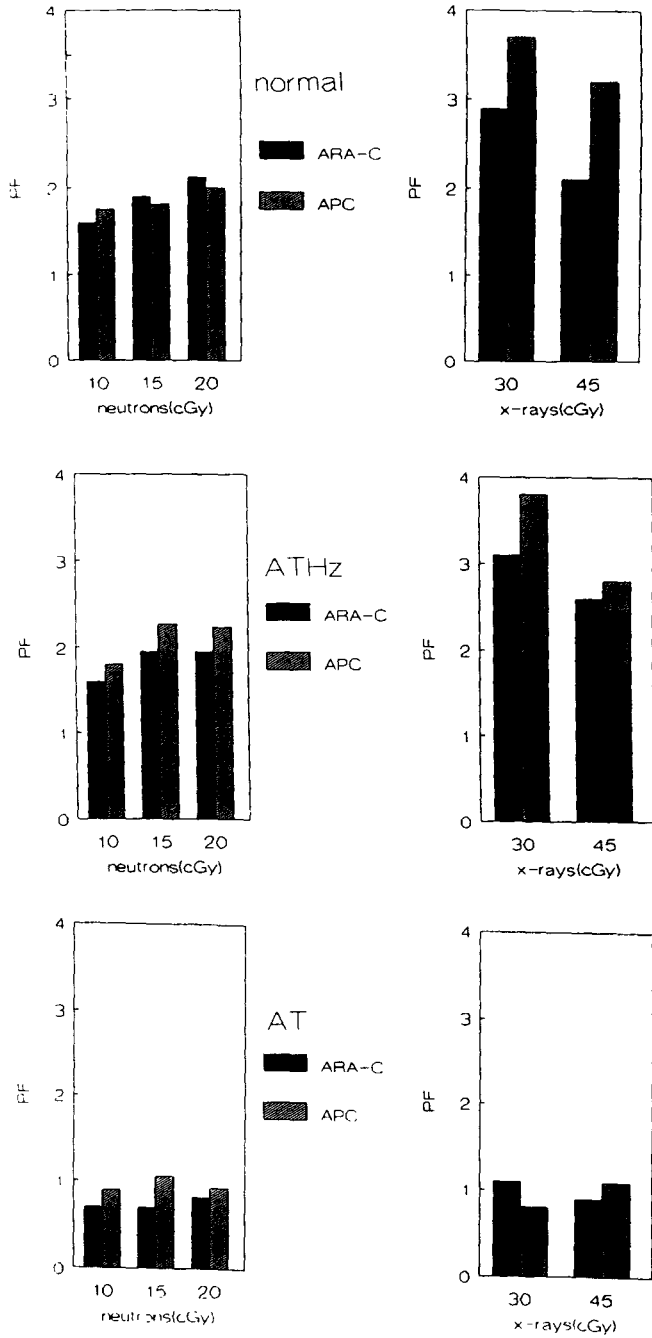


Fig.2

Project 12

Head of project: *Dr. Laurent*

Objectives for the reporting period (01 - 92 to 09 - 92)

- 1) Finalize the setting up of the HPRT- clonal assay
- 2) study of potential confounding factors which might affect the baseline mutant frequency in controls ;
- 3) Study of the HPRT Mutant Frequency (MF) at different time intervals (before therapy ; $T_0 \pm 24$, end of therapy ; ± 3 weeks after T_0) in patients under Curietherapy for uterine cervix carcinoma or endometrial carcinoma.
- 4) set up an **alternative** method to the clonal technique of Albertini using incorporation of BrdU in PHA stimulated T lymphocytes and scoring mutant frequencies on labelled lymphocytes nuclei. In case of interesting results, the study could be extended to patients injected with radioactive isotopes(Tc, 132).
- 5) study on a molecular level, the genomic structural rearrangement of more than 100 base-pairs in the HPRT gene.

Progress achieved

1. Study of mutant frequency in healthy non-exposed people

Using the clonal assay on PHA-stimulated cryopreserved lymphocytes in normal health female individuals (n=7) without any known exposure to genotoxic chemicals, the Thioguanine resistant mutant frequency (TG^rMF) has been shown to fall at $9.14 \pm 8.07 / 10^6$ cells (Mean \pm SD). Our TG^rMF data are in accordance with Branda *et al.* (1992) who describes a Mutant Frequency of $9.2 \pm 1.8 / 10^6$ cells (n=26) under the same conditions but for a human population comprising men and women, Tate and coworkers (1991) have obtained TG^rMF of $10.40 \pm 12.60 / 10^6$ cells with extreme value ranging from 1.1 to $81.7 / 10^6$ cells (n=55). The large variations observed TG^rMF between normal donors, could be, to a large extent, related with variation in the donor's cloning efficiency - the capacity of an individual's T lymphocytes to form clones (Albertini, 1985; Cole *et al.*, 1988; Messing *et al.*, 1989).

2. Potential role of a technical factor: cryopreservation on the mutant frequency in healthy non-exposed people

TG^rMF were measured in fresh and cryopreserved lymphocytes from the same samples obtained in women. A value of $9.14 \pm 8.07 / 10^6$ cells (cf 1) has been found in

cryopreserved cells whereas mutant frequency was of $6.83 \pm 5.85 / 10^6$ cells in *fresh* cells. Our results are in agreement with the findings of *Tates et al. (1991)*; *O'Neill et al. (1987)* and *Branda et al. (1992)*, these authors having shown a similarity in the yield obtained by the 2 methodologies.

Davies et al. (1992) having performed the assay on fresh cells on a mixed human population (men & women) have obtained TG^fMF ranging from 0.48 to 11.53 / 10⁶ cells (n=48).for a similar population we have obtained a TG^fMF = $7.15 \pm 5.08 / 10^6$ cells (n=8).

Cryopreservation have been used in other cytogenetic studies and similar response in the endpoint have been described (*Littlefield et al.,1987* ; *Murli et al ,1987*). In addition to the practical advantages - such as facilitate blood sample settings, same external technical conditions when multiple samples are set-up, *Albertini et al. (1982)* - isolation and cryopreservation of T-lymphocytes contribute to synchronize the lymphocyte population helping to solve the false positive results and the problem of phenocopies.

3. Study of the HPRT Mutant Frequency (TG^fMF) in patients under Curietherapy for uterine cervix carcinoma or endometrial carcinoma.

Under the same technical conditions, samples of 4 patients have been set-up for the study of the Mutant Frequency. (before therapy ; T0 ± 24, end of therapy ; ± 3 weeks after T0).

Patient code	Age	Endometrial Carcinoma	Mutant frequency / 10 ⁶ cells			
			T0	T0± 24H	T end	T + 2/3 weeks
PI	78	yes	18.40	31.70	32.30	42.19
DU	65	yes	79.83	123.61	181.85	70.80
MO	?	yes	13.26	21.17	ND	ND
DE	71	yes	81.77	ND	60.04	ND
Mean			48.31	58.82	91.40	56.50

Up to now, we do not have enough data for a valid discussion because of several patients have been rejected because of previous chemotherapy and or radiotherapy. therefore, we decide to collaborate with the University of Leuven and we plan to investigate 20 patients without previous treatment. For now, we already have cryopreserved bloods samples of 6 patients; once the selection will end, they will be analyzed. Nevertheless, at the T0 time (prior any treatment) 2 patients are characterized by an very high mutant frequency (79 ; 81) whereas 2 display a rather small increase (18 ; 13). Our preliminary results are not in concordance with those of *Tates et al (1991)* who did not see difference between similar human populations. Moreover, a similarity in TG^fMF of untreated cancer patients and healthy adults has earlier been reported by several investigators in pre-therapy cancer patients

(Albertini 1982, 1985, 1988; Dempsey *et al.*, 1985, Sala-Trepat *et al.*, 1990). For Branda *et al.* (1992), patients with breast cancer did not differ significantly in T cell HPRT mutant frequencies compared to normal women.

The mean age of the population under study (ctrl = ± 30 ; cancer patients = ± 70) could only partially explain that difference. In fact, an effect of age has been well established with a variety of point mutation detection systems for lymphocytes in human blood (Soper *et al.*, 1984, ; Trainor *et al.*, 1984; Vijayalaxmi and Evans, 1984; Albertini *et al.*, 1988; Cole *et al.*, 1988; Turner and Morley, 1990; Albertini *et al.*, 1990; Davies *et al.*, 1992). The percental increase of mutations/mutants per year fluctuates between 1 and 5 %. In any case, we need to wait until our cancer group will have a confident size (± 3 months) before being able to discuss the results.

4. Alternative method to the clonal technique of Albertini using incorporation of BrdU

We have modified the technique of Ostrovsky (1987) who identify the mutant nuclei after incorporation of BrdU. Nuclei having incorporated the BrdU are those from mutant cells allowed to growth in presence of thioguanine. BrdU react with an antibody (antiBrdU) coupled with alkaline phosphatase itself revealed by its substrate (Boeringer). The double staining Alkaline phosphatase -Giemsa allows an easy detection between mutant cells (brown) and non mutant cells (blue).

For now, we plan experiments to have a mutant frequency in a control population before doing this method on the 20 patients samples.

5. Molecular level

This approach necessitates many technical set-up. They were realized on DNA from human lymphoma cells (CEM) cultivated *in vitro*.

In a first step, HPRT probe has been amplified, isolated and purified (cDNA of the HPRT inserted at the site Pst 1 of the plasmid pUC8 from E. coli pHPT31).

DNA (25 μ g) of CEM cells was then digested by 5 restriction enzymes during 48 h : Bam H1, Bgl II, Eco R1, Hind III et Pst 1; we tried to reveal fragments by Southern Blotting. Labeling of the P32 is already done.

Actually, the digestion step is still under study. It seems that we need to use very high enzymes concentrations (20000 to 40000 U/ml instead of 2000 à 5000 U/ml). This digestion step appears to be essential and critical because only very few amount of DNA will be available from a mutant clone. Once the technical step solved, structural rearrangement of more than 100 base-pairs in the HPRT gene will be studied..

Project 13

Head of project: Dr. Pantelias

Objectives for the reporting period

1. To develop a biological dosimetry method, based on the C-banding of interphase chromosomes in peripheral blood lymphocytes, for the early assessment of radiation injury and the establishment of absorbed dose estimates in accidental overexposure.
2. To better the understanding of the mechanisms of radiation action at the DNA, chromosomal and cellular levels by means of the study of:
 - 1) the effects of thymidine substitution in the DNA by BrdU on the repair of DNA breaks, interphase chromatin breaks and potentially lethal damage in plateau-phase Chinese Hamster Ovary (CHO) cells.
 - 2) DNA and interphase chromosome damage induction by hydrogen peroxide in plateau-phase CHO cells.

Progress achieved including publications

1. **Biological dosimetry for the early assessment of radiation injury and the establishment of absorbed doses.**

Conventional biological dosimetry following exposure to ionizing radiation usually involves the analysis of dicentric and centric ring chromosomes in peripheral blood lymphocytes, as visualized at metaphase after their stimulation with the mitogen phytohaemagglutinin (PHA). In order to develop a quick methodology for biological dosimetry that could be used as an alternative to this conventional metaphase technique, in this project the analysis of radiation-induced dicentric and centric ring chromosomes was carried out directly in G₀ peripheral blood C-banded lymphocyte prematurely condensed chromosomes (PCCs). The C-banding procedure used, refined to avoid swelling and chromosome distortion of freshly prepared PCCs spreads, allowed the identification of such aberrations in non-stimulated human lymphocytes. The method enables visualization and scoring of dicentric and ring chromosomes within 3-4 h after blood sample withdrawal, which represents only a fraction of the time normally required when cells stimulated to proliferate are analyzed at metaphase.

Dicentric, ring and acentric fragments analysis in C-banded PCCs provides not only early confirmatory evidence of an exposure but also quantitative estimates in terms of equivalent whole-body doses, if representative calibration curves for different kind of radiations could be established. Towards this goal, experiments complementary to those carried out in the previous funding period (BI6-E-206-GR) were conducted. The frequency of dicentric plus centric rings as well as of acentric fragments increased with dose according to a linear-quadratic relationship. Similar yields were obtained with cells analyzed in interphase using the PCC method or with cells analyzed at metaphase. In order to determine whether other human cell systems, besides lymphocytes, could be used for the standardization of this

cytogenetic approach for biological dosimetry, normal WI-38 human embryo fibroblasts were employed. Similar yields for dicentric plus centric ring chromosomes and acentric fragments were obtained again in interphase and in metaphase but the overall yields were slightly lower than those obtained with human lymphocytes. This similarity indicates that the formation of ring and dicentric chromosomes does not require DNA replication. Moreover, it suggests that the analysis of chromosomal damage at their first mitosis does not underestimate the radiation-induced residual cytogenetic damage.

Several are the advantages that the introduction of this method for biological dosimetry provides compared to the conventional chromosome analysis at metaphase:

- a) It reduces the time interval between withdrawal of the blood sample and estimation of the absorbed dose, especially because the mitotic cells required for PCC induction can be readily obtained from frozen stocks.
- b) It reduces the risks of sample deterioration due to contamination or other causes.
- c) It eliminates possible complications arising from variations in the stimulation and cell cycle progression of lymphocytes in different donors blood samples.
- d) It expands the range of doses where analysis can be carried out since the complications arising from radiation induced delays in cell cycle progression and interphase cell death are not present.

2. Mechanisms of radiation action

a) Effects of BrdU incorporation on radiation-induced damage.

Experiments designed to study the mechanisms of radiosensitization induced in mammalian cells by substitution in the DNA of thymidine with BrdU were carried out, and cell capability to repair radiation-induced damage was examined at the DNA, chromosomal and cellular levels. Induction and rejoining of DNA DSBs were assayed by pulsed-field gel electrophoresis and induction and rejoining of DNA SSBs by DNA unwinding. Induction and rejoining of interphase chromosome breaks was assayed by means of premature chromosome condensation and repair of potentially lethal damage (PLD), as measured by delayed plating of plateau-phase cells, was used to assay cellular repair capacity.

A decrease was observed in the rate of repair of PLD in cells grown in the presence of BrdU, the magnitude of which depended upon the degree of thymidine replacement. The relative increase in survival caused by PLD repair was larger in cells substituted with BrdU and led to a partial loss of the radiosensitizing effect compared to cells tested immediately after irradiation. A decrease was also observed in the rate of rejoining of interphase chromosome breaks as well as in the rate of rejoining of the slow component of DNA DSBs in cells substituted with BrdU. The time constants measured for rejoining of the slow component of DNA DSBs and of interphase chromosome breaks were similar both in the presence and in the absence of BrdU, suggesting a correlation between this subset of DNA lesions and

interphase chromosome breaks. It is proposed that a larger proportion of radiation-induced potentially lethal lesions becomes lethal in cells grown in the presence of BrdU. Potentially lethal lesions are fixed via interaction with processes associated with cell cycle progression in cells plated immediately after irradiation, but can be partly repaired in cells kept in the plateau-phase. It is hypothesized that fixation of PLD is caused by alterations in chromatin conformation that occur during normal progression of cells throughout the cell cycle. Results on the quantitation of DNA DSBs and SSBs in cells substituted with BrdU suggest that quantitative measurements of alterations in the induction by radiation of damage in BrdU-substituted DNA may be hampered by changes induced in the physicochemical properties of the molecule that affect the behaviour of DNA molecules during the assays and complicate the interpretation of the results obtained.

b) Induction of DNA and interphase chromosome damage by hydrogen peroxide

DNA DSBs and interphase chromatin damage induced by H_2O_2 and their relationship to cytotoxicity were studied in plateau-phase CHO cells. Damage in interphase chromatin was assayed by means of PCC. DNA DSBs were assayed by non-denaturing filter elution (pH 9.6), and DNA breaks by hydroxyapatite chromatography. Cells were treated with H_2O_2 in suspension at $0^\circ C$ for 30 min and treatment was terminated by the addition of catalase. Concentrations of H_2O_2 lower than $1mM$ were not cytotoxic, whereas concentrations of 40 and 60 mM reduced cell survival to 0.1 and 0.004, respectively. An induction of DNA breaks that was dependent on H_2O_2 concentration was observed at low H_2O_2 concentrations that reached a maximum at approximately $1mM$; at higher H_2O_2 concentrations induction of DNA breaks either remained unchanged or decreased. Damage at the chromosome level was not evenly distributed among the cells, when compared to that expected based on a Poisson distribution. Three categories of cells were identified after exposure to H_2O_2 : cells with intact, control-like chromosomes, cells showing chromosome fragmentation similar to that observed in cells exposed to ionizing radiation, and cells showing a loss in the ability of their chromatin to condense into chromosomes under the PCC reaction. The fraction of cells with fragmented chromosomes as well as the number of excess chromosomes per cell, showed a dose response similar to that of DNA DSBs, reaching a maximum at $1mM$ and decreasing at higher concentrations. The results indicate that induction of DNA and chromosome damage by H_2O_2 follows a complex dependence probably resulting from a depletion of reducing equivalents in the vicinity of the DNA. Reducing equivalents are required to recycle the transition metal ions that are needed to maintain a Fenton-type reaction. The absence of cell killing at H_2O_2 concentrations that yielded the maximum amount of DNA and chromosome damage suggests that this damage is nonlethal and repairable. It is suggested that lethal DNA and chromosome damage is induced by an unidentified mechanism at higher concentrations of H_2O_2 where cell killing is observed.

PUBLICATIONS

1. Iliakis, G., D. Blocher, L. Metzger, and G.E. Pantelias (1991). Comparison of DNA double strand break rejoining as measured by pulsed field electrophoresis, neutral sucrose gradient centrifugation, and non-unwinding filter elution in irradiated plateau phase CHO cells. *International Journal of Radiation Biology*, 59, 927-939.
2. Iliakis, G., Y. Wang, G.E. Pantelias, and L. Metzger (1992). Mechanisms of radiosensitization by halogenated pyrimidines: Effect of BrdU on repair of DNA breaks, interphase chromatin breaks and potentially lethal damage in plateau-phase CHO cells. *Radiation Research*, 129, 202-211.
3. Iliakis, G., G.E. Pantelias, R. Okayasu, and W.F. Blakely (1992). Induction by H₂O₂ of DNA and interphase chromosome damage in plateau phase CHO cells.² *Radiation Research*, accepted for publication.
4. Iliakis, G., D. Blocher, L. Metzger, R. Okayasu, G.E. Pantelias, and O. Cicilioni (1991). Measurement of DNA double strand breaks in mammalian cells: Comparison between pulsed field gel electrophoresis and non-unwinding filter elution. *NATO ASI Series*, vol. H54, 55-69.

Projects 14-15

Heads of projects: *Dr. Jorge, Dr. Pereira-Luis*

Objectives for the reporting period

Evaluation of the sensitivity of lymphocytes from new-born babies and adults to gamma radiation as a function of dose and donor age.

For this evaluation we analysed chromosomal and chromatidic aberrations induced *in vitro* in G0 and G2 lymphocytes by gamma radiation respectively of 100, 200 and 50, 100 cGy at a dose rate of 5 cGy/s.

On these two populations we also studied the frequency of cells in first and second divisions using the BrdU incorporation in G0 cells.

Progress achieved

1. Introduction

The existence of a differential radiosensitivity between adults and new-born babies must be taken in account when measures of radiologic protection, in case of accidents or incidents with ionizing radiation, are taken.

In the literature we found some works that refer a greater radiosensitivity of the newborns while others refer a marginally higher sensitivity yield.

Our work was undertaken in order to give some more insights to this important problem.

We present dose-response curves (dicentric and fragments in G0 irradiated cells) and chromatidic aberrations (in G2 irradiated cells).

2. Methods

For this study of the radiosensitivity two different protocols were followed (Exp. 1 and Exp. 2).

In the first one, we studied the radiation effects in cells exposed in G0 with 100 and 200 cGy doses. In the second one, we studied the same effect in cells irradiated in G2 with 50 and 100 cGy doses.

Exp. 1:

Cord blood of 20 new-born babies and peripheral blood of 9 adults were used as controls as well as irradiated with 100 and 200 cGy from a gamma radiation font at a dose rate of 5 cGy/s.

The new-born babies had healthy non-smoker mothers, (except one who was a smoker). The control adults were all females, aged between 25 and 50 years old, 6 of them being smokers and 3 non-smokers (Table I).

The blood samples were set up as three whole blood cultures (0.25 ml) in 5 ml Ham's F10 medium containing Welcome PHA 15 and antibiotics. The cultures were incubated for 48 h at 37°C.

The control of first and second division cells was done through the BrdU incorporation.

Colcemid was added at 45 h (0.1 ml of a stock solution of 25µg/ml) and the cultures allowed to grow till 48 h.

The cells were harvested and processed for chromosomal preparations according to the standard process.

The slides were stained with 2% aqueous Giemsa for 10 minutes, mounted and scored for chromosomal aberrations.

The cells in first and second division were detected by the Fluorescence plus Giemsa technique.

Exp.2:

The donors used in Exp. 2 were the same used in Exp. 1 but the cells were irradiated in G2 with 50 and 100 cGy from a gamma radiation font at a dose rate of 5 cGy/s.

The blood samples were set up as three whole blood cultures (0.25 ml) in 5 ml Ham's F10 medium containing Welcome PHA 15 and antibiotics. The cultures were incubated for 72 h at 37°C.

Colcemid was added at 69 h (0.1 ml of a stock solution of 25µg/ml) and the cultures allowed to grow till 72 h.

The cells were harvested and processed for chromosomal preparations according to the standard process.

The slides were stained with 2% aqueous Giemsa for 10 minutes, mounted and scored for chromatidic aberrations.

Microscope slides were coded and scored at two different laboratories (IPOFG and LNETI).

In the scoring process only the metaphases with 46 centromeres were considered.

3. Irradiation

The irradiations were done by Radiotherapy Department of Centro de Lisboa do Instituto Portugues de Oncologia.

Groups of three or four blood samples in test-tubes, placed up-right, were irradiated simultaneously. The test-tubes were lined on a suitable acrylic stand. This stand was designed in order to ensure the electronic balance in the interior of the liquid volumes to be irradiated.

The photon beam of 25 MV, an Electron Linear Accelerator, type Sagittaire, was directed horizontally so that its central axis struck perpendicularly the plane defined by the axes of the above-mentioned tubes. The intersection point of this plane with the central axis was made to coincide with the geometric centre of the area of irradiation, the dimensions of which were 20 x 18 cm, and became the reference point for the dosimetry.

The area limited by the isodose of 85%, where the samples were fitted in, was thoroughly studied through radiological pellicules, read on a high powered resolution photo-densimeter, and it was concluded that the homogeneity of the dose was perfect in the area under consideration.

A correlation was established between the doses measured in the ideal conditions of full-scattering and the measurements in the interior of the samples, so that it was possible to introduce the necessary correlative factors.

4. Results

We scored a total of 9265 cells in experiment 1.

Table III shows the number of cells, dicentrics and fragments observed per donor and per studied dose, in G0 irradiated cells. The frequency of dicentrics and fragments per cell are also shown.

In experiment 2, we scored 6881 cells. Table IV shows the number of cells and fragments observed per donor and per studied dose, in G2 irradiated cells.

Table II shows the results of a study to determinate the contamination of metaphases with cells on second division at 48 h of culture for adults and newborns at different doses.

Although we had sampled 20 new-born donors and 9 adults, some of them were not available for study because of culture failures or problems with irradiation.

5. Discussion

Figures 1 and 2 show the dicentric and fragments frequencies distribution as a function of dose in adults and newborns.

The mean frequencies of dicentric and fragments observed for the 100 cGy dose from the newborns are analogous to those of the adults and show a small dispersion, as we can see in figure 2, where the mean frequencies of newborns and adults are compared. The mean frequencies of dicentric and fragments observed for the 200 cGy dose from the newborns show a greater dispersion than the one found for 100 cGy even though the differences between the mean frequencies are not significantly different in the two studied groups.

Comparing chromosomal aberrations on adults and new-borns irradiated in G0 we found that adults have a lower radiosensitivity than new-borns. However, statistically regarding their responses to radiation, we can not consider new-borns and adults as two different populations, as we can see in figure 2, where the error bars represent the standard deviation.

Figures 3 and 4 show respectively the distribution of chromatidic aberrations and the mean frequencies the respective errors (SD) on new-borns and adults irradiated in G2. Also in this case, the values we found were not significantly different between these two populations.

The results found do not permit us to conclude that the lymphocytes of new-born babies are more radiosensitive than adults. What we found was a great variability related to the radiosensitivity in newborns as well as in adults, both in G0 and in G2. We however note that although we had restricted the scoring to the cells with 46 chromosomes, as we can see in Table II, in the 48 h cultures of the new-born, there is a high percentage of cells in second division in the 0 and 100 cGy cultures. So we must consider that 37.2% of the cells from new-born cultures were in second division. Our results show clearly that the new-born cells, in these experimental conditions, enter into second division sooner than those of the adults.

Table I - Adults' data

Adult	Smoking habits	Age
A1	Y	35
A2	Y	50
A3	Y	42
A4	Y	29
A5	Y	29
A6	Y	42
A7	N	50
A8	N	50
A9	N	25

Y - Smoker

N - Non-smoker

Table II - Percentage of new-born and adult cells on first division at 48 H of culture

DOSE (cGy)	ADULTS	NEW-BORNS
0	95.0* (2)	48.1* (7)
100	96.5* (5)	62.8* (6)
200	97.5* (4)	71.3* (8)

* - Mean

() - Number of studied cases

Table III - Frequency of chromosomal aberrations of new-born babies and adults' peripheral blood after *in vitro* irradiation of G0 lymphocytes with 100 and 200 cGy

	DOSE												
	0 cGy			100 cGy					200 cGy				
	C	D	F	C	D	D/C	F	F/C	C	D	D/C	F	F/C
N1	200	0	0	209	4	.019	7	.033	205	36	.175	31	.151
N2	204	0	0	213	14	.065	16	.075	221	46	.208	19	.085
N6	-	-	-	200	20	.100	20	.100	200	70	.350	49	.245
N7	200	0	0	199	18	.090	8	.040	140	28	.200	11	.078
N8	200	0	0	180	8	.044	14	.077	100	13	.130	13	.130
N9	158	0	0	200	6	.030	8	.040	200	28	.140	34	.170
N10	200	0	0	161	10	.062	0	.000	180	41	.227	26	.144
N14	200	0	0	200	12	.060	11	.055	200	31	.155	26	.130
N15	100	0	0	100	4	.040	1	.010	100	18	.180	24	.240
N16	100	0	0	100	2	.020	8	.080	100	20	.200	10	.100
N18	100	0	0	100	6	.060	5	.050	100	18	.180	29	.290
N19	200	0	0	200	13	.065	23	.115	200	61	.305	58	.290
N20	150	0	0	200	15	.075	17	.080	200	68	.340	62	.310
A1	200	0	0	200	6	.030	6	.030	179	44	.245	24	.134
A2	94	0	0	122	7	.057	7	.057	29	2	.068	4	.137
A3	-	-	-	55	1	.018	0	.000	164	28	.170	44	.268
A4	200	0	0	200	9	.045	14	.070	-	-	-	-	-
A5	200	0	0	200	11	.055	11	.055	200	33	.165	14	.070
A7	-	-	-	50	5	.100	0	.000	89	10	.112	12	.134
A8	75	0	0	50	3	.060	1	.020	39	8	.205	1	.020
A9	100	0	0	200	15	.075	13	.065	199	38	.190	16	.080

N - NEW-BORN BABIES

A - ADULTS

C - NUMBER OF SCORED CELLS

D - DICENTRICS

F - FRAGMENTS

Table IV - Frequency of chromatidic aberrations of new-born babies and adults' peripheral blood after *in vitro* irradiation of G2 lymphocytes with 50 and 100 cGy

	DOSE							
	0 cGy		50 cGy			100 cGy		
	C	F	C	F	F/C	C	F	F/C
N1	200	0	203	201	.990	201	452	2.240
N2	211	0	211	64	.303	164	197	1.201
N6	-	-	150	209	1.390	200	451	2.250
N7	200	0	168	125	.744	200	571	2.850
N8	200	0	200	376	1.880	200	595	2.970
N9	194	0	200	59	.295	200	72	.360
N10	200	0	200	93	.465	200	176	.880
N14	200	0	162	240	1.480	62	349	5.620
N15	100	0	100	170	1.700	100	319	3.190
N16	100	0	100	209	2.090	100	409	4.090
A1	200	0	200	188	.940	200	320	1.600
A3	-	-	115	162	1.400	177	398	2.840
A4	200	0	163	179	1.098	200	640	3.200
A5	200	0	200	103	.515	-	-	-
A7	150	0	-	-	-	50	222	4.440

N - NEW-BORN BABIES

A - ADULTS

C - NUMBER OF SCORED CELLS

F - FRAGMENTS

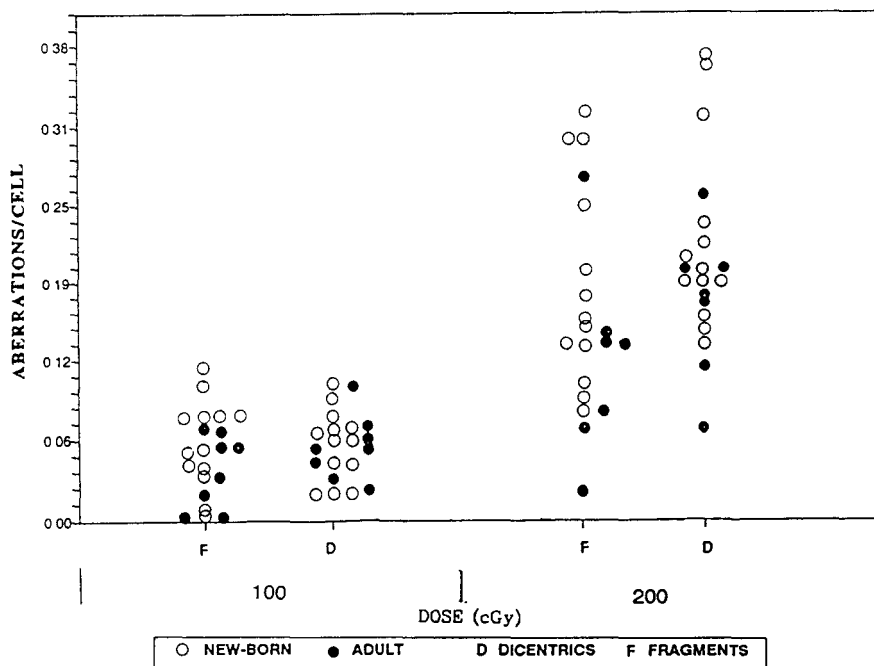


Figure 1 - Frequency of chromosomal aberrations on lymphocytes irradiated in G0

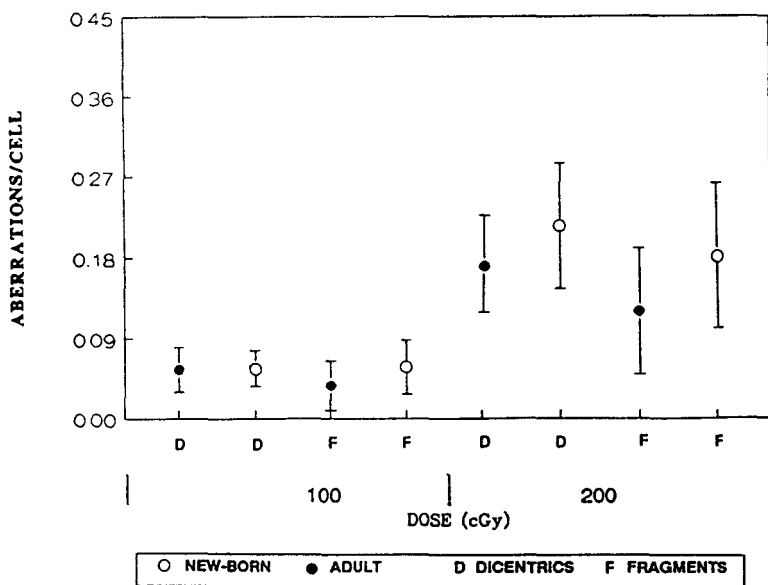


Figure 2 - Comparison of chromosomal aberrations on adults and new-borns irradiated in G0

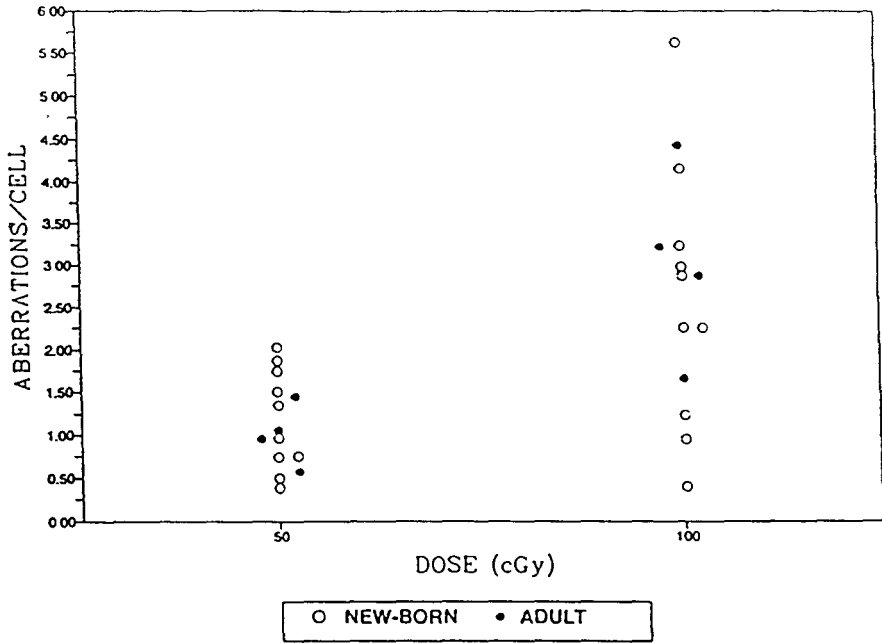


Figure 3 - Frequency of chromatidic aberrations on lymphocytes irradiated in G2

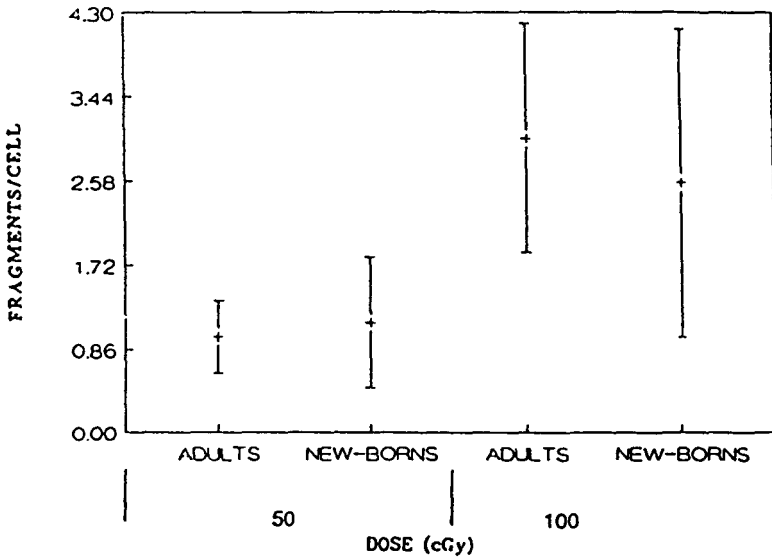


Figure 4 - Comparison of chromatidic aberrations on adults and new-borns irradiated in G2

MEASUREMENT OF TRANSFORMATION OF C3H 10T^{1/2} CELLS BY LOW DOSES OF IONIZING RADIATION

Contract: Bi7-043 - Sector: B13

- 1) *Morgan* , AEA Technology Harwell Laboratory - 2) *Mill* , Nuclear Electric
3) *Kellerer* , GSF Neuherberg - 4) *Frankenberg* , GSF Frankfurt
5) *Tallone Lombardi* , Università degli Studi di Milano - 6) *Saran* , ENEA Casaccia Roma*

Summary of Project Global Objectives

The global objectives of this project are two fold:-

- (1) To establish a standardised experimental protocol for C3H 10T^{1/2} cell transformation assay between European laboratories to ensure compatibility of results.
- (2) Using the standardised assay, to establish the shape of the dose-response relationship for survival and transformation of C3H 10T^{1/2} cells exposed to a range of radiation doses.

Summary of Project Global Achievements

1. Introduction

The principal risk from low doses of radiation is the induction of cancer. Currently the risks of developing cancer are predicted by various methods but these have not been validated at low radiation doses as routinely received during the operation of nuclear facilities and other sources of occupational exposure. Dose-response relationships for tumour induction can be studied using animal models but at low doses these become prohibitively expensive and anyway, may not be morally justifiable. An alternative is to use cell transformation *in vitro* for which a variety of systems are available. However only one, the C3H 10T^{1/2} mouse fibroblast system, provides the relatively high precision needed for work at low doses and dose-rates. This system is used in a number of laboratories in Europe and the USA.

It is clear that, if reliable data at low doses are to be obtained, a large number of transformants must be scored to reduce the statistical variation. For one laboratory this may put a large strain on resources. For such an internationally important topic, this seems an ideal area for collaboration between laboratories. With this in mind six European laboratories have spent some time during the past two years on a collaborative project with the following objectives.

- (1) To standardise the C3H 10T^{1/2} assay between participating laboratories.
- (2) To produce a standard code of practice for cell transformation in C3H 10T^{1/2} cells; so that other laboratories may have a standard for the comparison of results.
- (3) Ultimately, to establish the shape of the dose-response curve for cell transformation at low doses and dose-rates.
- (4) To extend these studies to more relevant cell transformation systems (eg. human epithelial systems) as and when they become available.

* Although not funded by CEC contract No. B17-043, the ENEA Casaccia Laboratory, Rome, has contributed fully to this programme and therefore has been included as project 6.

These objectives were formalised during a meeting of five of the participating laboratories held at the AEA Technology laboratories at Harwell in January 1990.

The intercomparison experiments carried out between November 1990 and June 1992 and involving all six participating laboratories are described in sections 2 and 3 below. This is followed by individual reports from each participating laboratory.

2. Investigation of factors likely to affect transformation frequency

The transformation assay, like many other biological assays, is susceptible to perturbations from a variety of influences. These perturbations do not normally hinder the comparison of results when made internally within each laboratory but often preclude the direct comparison of results between laboratories. Hence intercomparison of results between laboratories is difficult unless steps are taken to minimise the effects of these factors. Probably the most important factors for transformation are the criteria used for scoring transformed foci, the growth conditions (particularly serum batch) used for the assay and the source of cells used for experimentation. The initial phase of this project thus entailed the determination of the effect of the various factors on plating efficiency, cell inactivation and transformation frequency.

2.1 Transportation of cells

The C3H 10T½ transformation assay was first detailed by Reznickoff *et al.* (Cancer Research 33, 3239-3249) in 1973, thus the cell-line has been around for a number of years. The histories of some sources of 10T½ cells are dubious, therefore it was essential for these experiments to select a good low passage source of cells. It was also important to irradiate the cells at a single facility to eliminate differences in dosimetry and radiation quality. For these reasons a decision to use only one source of cells from the Berkeley laboratories was made. The choice of one laboratory to supply irradiated cells meant that it was necessary to study the effect of transportation. Some initial experiments showed that plating efficiency of 10T½ cells ranged from 0.52 to 0.15 for cells stored on melting ice over a time period of 48 hours, indicating that the decrease in plating efficiency was strongly dependent on the time on ice. One question which arises from this finding is whether any decrease in plating efficiency concomitantly changes the shape of the survival curves. To study this possible problem cells were irradiated and then either plated immediately or placed on melting ice for 24, 48 or 72 hours, to mimic transportation, after irradiation. Although the plating efficiency decreased with time on ice from 0.51 at zero time down to 0.09 after 72 hours, the surviving fractions of the cells held on ice for different time intervals did not differ significantly from cells plated immediately. In later experiments, using more concentrated suspensions of cells, high plating efficiencies were maintained for cells kept on melting ice for up to 72 hours. The protocol subsequently adopted (see section 3.0) regularly results in plating efficiencies in the range 0.35 to 0.60 when each laboratory processes samples 48 hours after trypsinisation.

2.2 Serum effects

In a series of transformation experiments, parallel studies were carried out using both local serum and serum supplied by Berkeley. Figure 1 shows data for the plating efficiency of 10T½ cells in all six participating laboratories. It can be seen that the plating efficiency varies by a

factor of 2 between laboratories, when using serum supplied by Berkeley. When local serum is used results are similar with the possible exception of Frankfurt.

Figure 2 shows for each laboratory the ratio between local and reference (Berkeley) serum for both survival and transformation frequency after an absorbed dose of 5 Gy. These results, and those reported in section 2.1 suggest that, providing account is taken of variations in plating efficiency, there are no significant differences in surviving fraction and transformation frequency for different sera.

2.3 Effect of trypsin on plating efficiency

There is some evidence that trypsin concentration or batch may affect the plating efficiency of C3H 10T½ cells. Since all participating laboratories obtain trypsin from different companies it was felt important to clarify this situation. It was found that trypsin is not a critical parameter for plating efficiency.

2.4 Antibiotic effects

Bertram (Cancer Letters, 7, 289-298, 1979) reported that penicillin could suppress the transformation frequency of C3H 10T½ cells after chemical or radiation insult. However, his data suggested little effect on plating efficiency or saturation density, and the mechanism by which suppression worked was unknown. However, plating efficiency can be affected by choice of antibiotic and this may reflect on the transformation frequency. When cells are grown and replated with 100 units ml⁻¹ penicillin and 100 µg ml⁻¹ streptomycin, (P&S), in the culture media, the plating efficiency is variable with the highest value approximately 30%, in agreement with data from other laboratories. When cultures of 10T½ cells are grown in culture medium containing gentamicin (0.5 µg ml⁻¹) and plated into culture medium containing P&S, the plating efficiency is also low. However, when cells grown in medium containing P&S are replated into medium containing gentamicin then the plating efficiency increases to 50%. For cells both cultured and replated in medium containing gentamicin the plating efficiency is reliably 70%. Thus, gentamicin should be used on a routine basis to achieve reproducible plating efficiencies and stabilise the transformation frequencies for intercomparison purposes.

2.5 Scoring of Foci

One of the critical factors for cell transformation is the convention used for scoring transformed foci, hence one of the first exercises carried out by the six collaborating groups was a focus-scoring intercomparison. For this purpose each group circulated a number of flasks or petri dishes for scoring by the other groups. This was followed up by a joint scoring exercise during which a consensus score for each flask or dish was determined. Altogether four such exercises have now been completed. Initially, there was a relatively large discrepancy between some laboratories (up to a factor of 2), but the disagreement following the third scoring exercise was reduced to a maximum of about 20%. In Table 1 are shown the results of the statistical analysis after three intercomparison and consensus scoring sessions (the fourth consensus scoring exercise was carried out in June 1992 and analysis of the results is not yet complete).

TABLE 1: Ratios and Standard Deviations of Individual Score to Consensus Score for Transformed Foci

Laboratory	Date of Focus Scoring Intercomparison		
	July 1990	May 1991	October 1991
BERKELEY	1.8 ± 0.6	0.7 ± 0.2	1.0 ± 0.2
FRANKFURT	1.3 ± 0.3	0.8 ± 0.3	0.8 ± 0.2
HARWELL	1.4 ± 0.2	1.3 ± 0.7	0.8 ± 0.3
MILAN	0.8 ± 0.1	1.1 ± 0.3	1.0 ± 0.1
MUNICH	1.0 ± 0.3	1.1 ± 0.3	0.9 ± 0.1
ROME	-	1.2 ± 0.6	1.1 ± 0.2
OVERALL	1.13 ± 0.19	1.05 ± 0.49	0.95 ± 0.24

As a basis for the consensus scoring, the criteria of Reznickoff *et. al.* (Cancer Research, **33**, 3239-3249, 1973) were used. Type I foci (foci containing tightly packed cells) are not scored as malignantly transformed. Type II (massive piling up into opaque multilayers; cells only moderately polar; criss-crossing not pronounced) and Type III (highly polar, fibroblastic; multilayered criss-crossed arrays of densely stained cells) are scored as malignantly transformed. The diameter of the foci is not considered as a relevant parameter. For the intercomparison of scoring no distinctions between type II and type III foci are made and the most important criterium is the presence of criss-crossing. In addition there is one other class of focus, designated type X (this type was originally identified during a meeting of the group held in Frankfurt in July 1990). Type X foci are characterised by long fibrous sheaths of cells. There is sometimes heavy piling-up along the strands but criss-crossing is absent. Evidence from other work reported recently (Hei *et. al.*, Proceedings of the Joint Meeting of the Association for Radiation Research, the Netherlands Radiobiology Society and the Swedish Radiobiology Society, St Andrews University, April 1-4 1992) suggests that foci with similar morphology to type X foci are not malignantly transformed.

It is clear that scoring is an influential parameter in the 10T½ transformation assay and regular joint scoring intercomparisons are necessary in order to maintain consistency between participating laboratories. An important goal is the production of a catalogue depicting various classes of foci and the score assigned to these foci (a draft has already been produced). This will be a unique reference for scoring foci and will be an aid to other laboratories using the C3H 10T½ cell transformation assay to whom it will be made readily available.

3. Survival and transformation intercomparison experiments

Direct intercomparison transformation experiments have been carried out in order to determine the influence of medium type and other parameters on the transformation frequency. Cells from one participating laboratory (Berkeley) were irradiated and immediately placed on melting ice at 0 C along with a sample of unirradiated cells. These cells were then despatched to the other laboratories for subsequent culture. Samples kept at Berkeley were processed immediately after irradiation with a second set of samples kept on ice for about 48 hours before processing. A common protocol was adhered to within the limits of each laboratory. This involved the culture of cells in both local medium and in medium as supplied by Berkeley (see figure 3 where the basic protocol is outlined). Since it was impractical to despatch large amounts of complete growth medium to cover all the subsequent changes needed for the transformation assay the medium changes at weeks 2, 3, 4 and 5 were carried out using local

medium supplemented with Berkeley serum. As discussed above in section 2.2 the use of locally purchased serum, provided it is of comparable quality, does not drastically affect the transformation frequency.

It was decided initially that these experiments should be of limited size and hence an absorbed dose of 5 Gy was chosen such that an adequate number of foci would be obtained. Altogether four experiments at 5 Gy have been carried out. The results of the first three of these experiments have been presented above in section 2.2; in Figure 4 the results from intercomparison experiments two and three carried out under similar experimental conditions (i.e. same time on ice and same serum) are shown. The results from the fourth experiment, designed specifically to address the question of cell-seeding densities in the range 1-3 cells/cm⁻², are shown in Figure 5.

The main conclusions from these experiments are:

- (i) the viability of cells up to 72 h on ice is not a problem for the intercomparison experiments;
- (ii) the choice of medium (local or Berkeley) has no significant effect on the results; and
- (iii) for transformation, the seeding density interval between 1 and 3 viable cells per square centimetre is a region of small variation in transformation values; transformation frequency decreases rapidly at values higher than 4 to 5 viable cells per square centimetre.

As a result of these intercomparisons the six laboratories have now established standard protocols for the culture and scoring of transformation in C3H 10T^{1/2} cells.

More recently four further intercomparison experiments at doses of 1, 2 and 3 Gy have been completed. Survival data from these, and earlier intercomparisons, are shown in Figure 6; transformation data are in the process of analysis and will be available after the six groups meet in Rome in September 1992.



Figure 1. The Effect of Serum (local or Berkeley) on Plating efficiency

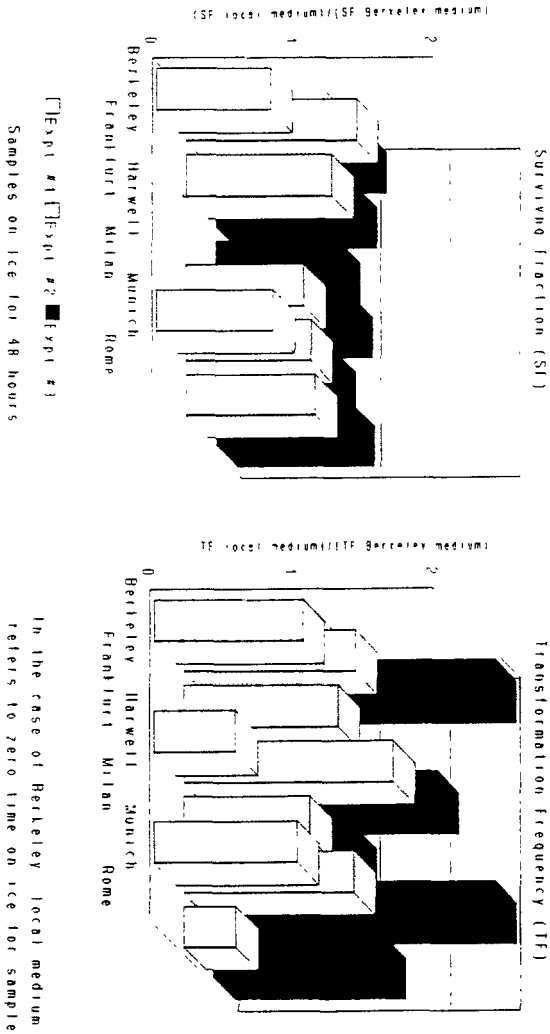


Figure 2. The Effect of Serum on Surviving Fraction and Transformation Frequency.

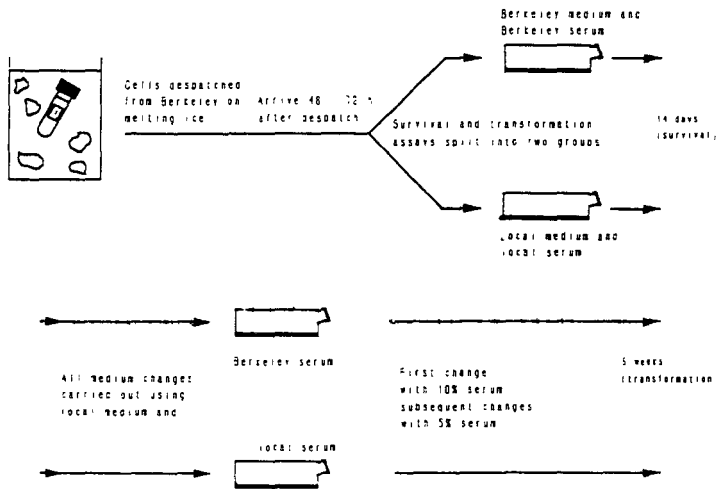


Figure 3. Protocol for Cell Transformation Intercomparison Experiments.

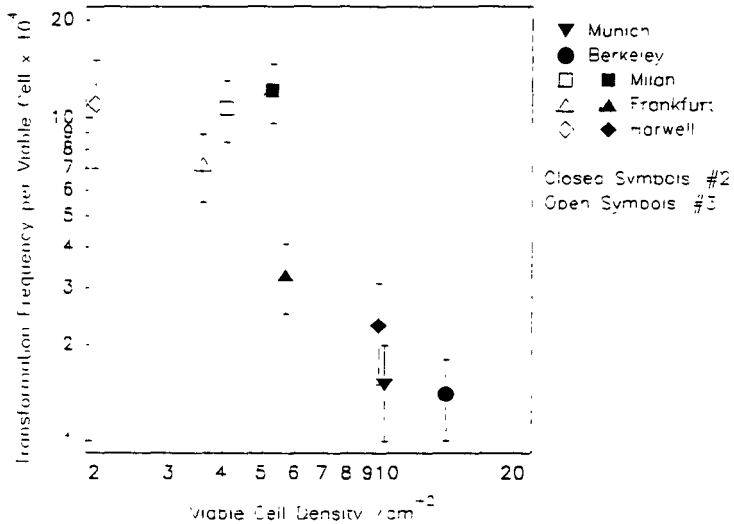


Figure 4. Transformation Frequency and Seeded Cell Density: 5 Gy X-rays: Expt. 2 & 3.

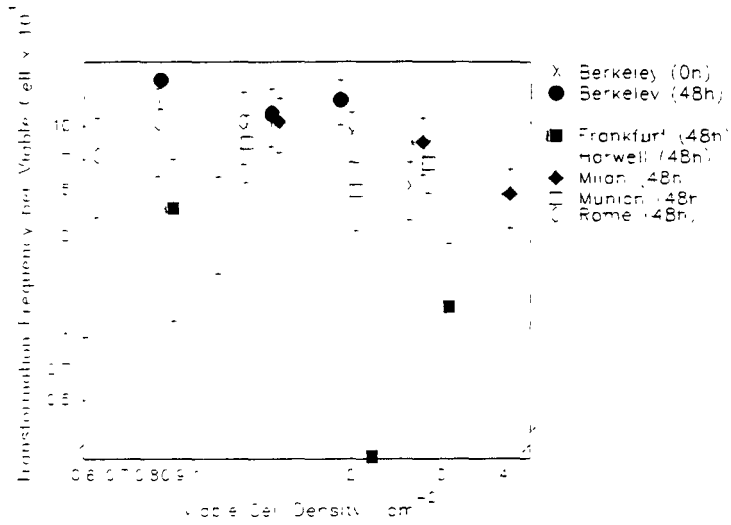


Figure 5. Transformation Frequency and Seeded Cell Density: 5 Gy X-rays: Expt. 4 .

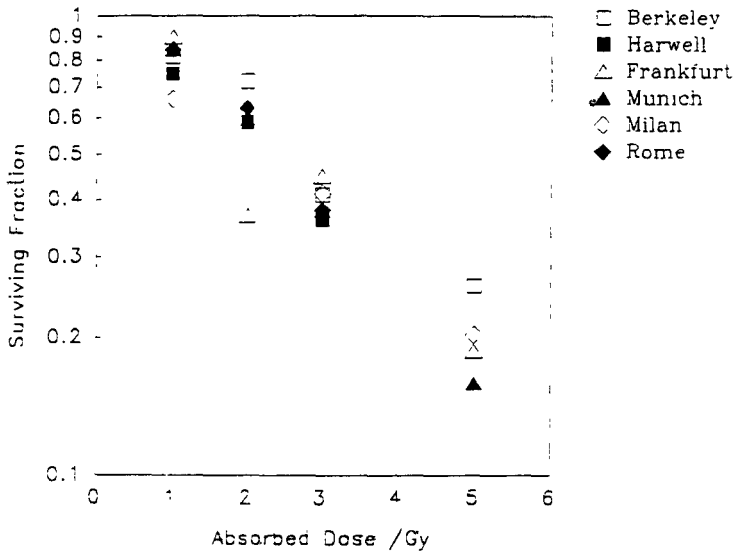


Figure 6. Intercomparison of Survival Fraction: Experiments 1-8.

Project 1

Heads of project: *Dr. Morgan, Mr. Roberts*

Objectives for the reporting period

- (a) To participate in the standardisation and intercomparison exercises for the C3H 10T $\frac{1}{2}$ cell transformation assay.
- (b) To characterise cell surface markers for transformed and non-transformed C3H 10T $\frac{1}{2}$ cells *in vitro*.

Progress achieved including publications

The characterization of C3H 10T $\frac{1}{2}$ cell surface markers and their exploitation to enable single transformed cells to be detected with immunological probes

As part of a large 5 year project funded by the UK Department of Health (DH), the cell surface proteins of normal and transformed C3H 10T $\frac{1}{2}$ cells were investigated to try to identify differences in protein expression between them. It was hoped to exploit such differences by raising monoclonal antibodies to the proteins of interest to generate a new immunological assay, offering greater speed, sensitivity and objectivity for detecting transformation of C3H 10T $\frac{1}{2}$ cells by low doses of radiation.

The major part of this work involved a comparison between cell surface proteins from normal C3H 10T $\frac{1}{2}$ cells and those transformed by either ^{60}Co γ rays or the chemical carcinogen 3-methylcholanthrene (MCA). This involved growing the cells in large scale microcarrier cultures to provide sufficient material for biochemical analysis and then extracting the membrane components with non-ionic detergent. Membrane proteins from both normal and transformed cells were then analysed and compared by sodium dodecyl sulphate polyacrylamide gel electrophoresis (SDS PAGE). This led to the detection of consistent differences in membrane protein expression between the normal and transformed cells and, in particular, the identification of four proteins of special interest. These were of approximate molecular weight: 66, 49, 44 and 37 kD; the first of which showed greatest expression in the normal cells and was reduced in the transformed cells. The reverse was true of the other three, i.e. they showed increased expression in the transformed cells.

During 1990 - 92, CEC funding contributed to continued DH work to generate monoclonal antibodies against the four proteins of interest, using two separate approaches, each with their relative merits, as outlined below.

A *In vitro* immunization/isolated proteins

The initial approach involved raising the antibodies to isolated membrane proteins using *in vitro* immunization techniques. This method was adopted as it was reported to give a good response with small amounts of antigen, the immunization procedure is rapid, and normal

regulation of the immune response does not occur *in vitro*, allowing antibodies to be raised against the C3H 10T $\frac{1}{2}$ mouse proteins using a convenient mouse fusion system. By this approach, the four proteins of interest were isolated from the SDS PAGE gels by electroelution and coupled to octyl sepharose beads, firstly to avoid problems of keeping them in solution on removal of detergent, and secondly to attempt to maintain their antigenic orientation during immunization procedures. Monoclonal antibodies were then raised against a mixture of the four proteins using *in vitro* immunization techniques in which isolated mouse spleen cells were cultured with the protein-coated beads in the presence of lymphokines and growth factors to promote an immune response *in vitro*. Monoclonal antibody-secreting hybrid cells were selected for by standard hybridoma technology and tested for relevant antibody activity. This was achieved by screening against a mixed population of normal and gamma-transformed C3H 10T $\frac{1}{2}$ cells by both enzyme linked immunosorbent (ELISA) or immunofluorescence (IFA) assays.

By this approach, 15 positive clones were identified, all of which were IgM immunoglobulin isotype. The fine specificity of these fifteen was then investigated by (i) screening against separate populations of normal and transformed cells, (ii) quantifying fluorescent staining in a flow cytometer and (iii) Western blot analysis to determine which proteins bound which antibody. Only slight differences in antibody reactivity could be detected between normal and transformed cells, whilst the Western blotting indicated that the binding was non-specific as the antibodies bound to multiple protein bands.

These combined results suggested that the antibodies were reacting with epitopes common to a variety of cell surface proteins rather than to those which were transformation-related, and this lack of specificity was attributed to epitope denaturation during the protein isolation/coupling steps.

B *In vivo* immunization/intact cells

To try to overcome the problems of specificity, an alternative approach was adopted in which antibodies were raised by the more conventional route of immunizing an animal, and isolating the spleen cells just prior to fusion. As the antibodies were to be raised against murine C3H 10T $\frac{1}{2}$ cells *in vivo*, a rat fusion system was adopted to obtain the necessary cross-species reactivity. Additionally, intact normal/gamma-transformed C3H 10T $\frac{1}{2}$ cells were used as the immunogen instead of isolated proteins, in order to maintain the native antigenic form of the membrane proteins as far as possible. To avoid degradation of the proteins by trypsin during cell harvesting procedures, the cells were grown on microcarrier beads and these were injected straight into the animals.

By this method, seven different clones with antibody activity against C3H 10T $\frac{1}{2}$ cells were isolated from three separate fusion experiments. Two of these were found to be of IgG2a isotype, whilst the remainder were IgM. Fine screening by IFA and ELISA against separate populations of normal and transformed C3H 10T $\frac{1}{2}$ cells, again failed to reveal any significant difference in antibody reactivity between the normal and transformed cells. Western blot analysis yielded a more positive result in that one of the antibodies (clone 3.1) appeared to be specific for the 66kD protein which is prevalent in normal cells and lost in both radiation and chemically transformed cells. However, in view of continued doubts over the specificity of the antibodies, it was decided not to pursue this work on the C3H 10T $\frac{1}{2}$ transformation assay.

Instead the problems will be further addressed using a human epithelial cell system as part of a separate research programme.

Acknowledgement The major part of this work was funded by the UK Department of Health, as part of their Radiological Protection Research Programme.

Publications

Brown, V.A. and Davison, W. (1989) Development of an improved C3H 10T½ assay. In: 'Cell Transformation and Radiation-Induced Cancer' (Chadwick, K.H., Seymour, C. and Barnhart, B., editors) pp127-134, Adam Hilger, Bristol and New York.

Brown, V.A. and Davidson, W. (1990) Development of an improved C3H 10T½ assay for use in radiobiology research. *International Journal of Radiation Biology*, 57, 608.

Roberts, C.J., Briden, P.E. and Mill, A.J. (1990) Effects of Cell Density on the Plating Efficiency of C3H 10T½. *International Journal of Radiation Biology*, 57, 608.

In Vitro Cell Transformation at Low Doses of Ionising Radiation: A Collaborative European Project. A.J. Mill, S.C. Hall, D. Frankenberg, C.J. Roberts, D. Bettega, P. Calzolari, L. Hieber and A. Saran. (Abstract: Joint Meeting of the Association for Radiation Research, Netherlands Radiobiology Society and Swedish Radiobiology Society, St Andrews University, 1-4 April 1992) To be published. *International Journal of Radiation Biology*, 1992.

Project 2

Heads of project: *Dr. Mill, Dr. Hall*

Objectives for the reporting period

(a) Participation in the standardisation of the C3H 10T½ cell transformation assay. Our particular role was to prepare and despatch samples of irradiated cells to the other five participants.

(b) A study of dose-rate effects using 3.3 MeV α -particles from plutonium-238.

Progress achieved including publications

The study of the effects of high-linear energy transfer (LET) α -particles is of importance for radiation protection as the human population is exposed to both natural and artificial alpha-emitting radionuclides in the environment. Of special relevance were the findings of Hill *et al.* (International Journal of Radiation Biology, 46, 11-16, 1984) on the greatly enhanced transformation frequencies at very low dose-rates of fission neutrons. Data from our laboratory with neutrons and from elsewhere (Balcer-Kubiczek, *et al.*, International Journal of Radiation Biology, 59, 1477-1482, 1991.) have not confirmed these initial findings. However, the controversy still exists as to whether irradiation by neutrons and α -particles at very low dose-rates can be more effective than at high dose-rates. In particular, it has been suggested (Elkind, International Journal of Radiation Biology, 59, 1467-1475, 1991) that experimental artefacts could explain why many laboratories do not observe enhanced transformation rates at low doses of high-LET radiation. We report here the results of experiments using α -particles provided by the MRC Radiobiology Unit at Harwell. Exponentially growing (log phase) and plateau phase C3H 10T½ cells cultured on Hostaphan based dishes (2.5µm thick) were irradiated with a ²³⁸Pu source. The α -particle energy was 3.3 MeV and the LET 121 keV μm^{-1} . A dose of 0.36 Gy was chosen for the dose-rate comparison. The dose rates used were 0.18 Gy min^{-1} and 0.12 mGy min^{-1} , the lower dose rate extending over an irradiation period of 45 hours. Samples for irradiation were transported by car in a battery-operated portable incubator and the temperatures of the samples were maintained at 37 C throughout the irradiation period. Three different irradiation/processing schemes were used for the acute dose-rate irradiations: (i) irradiation and processing at the start of the chronic irradiation period; (ii) irradiation and processing at the end of the chronic irradiation period; and (iii) irradiation at the start and processing at the end of the chronic irradiation period (see Figure 1.2). No significant differences in the transformation frequencies were observed between these acute dose-rate regimes for log-phase cells (Figure 2.2). A summary of the results obtained to date are also shown in table 1.2. The relative biological effectiveness of ²³⁸Pu α -particles compared with X-rays at the dose chosen for the dose-rate comparisons is 9 (Figure 3.2).

Table 1.2: Summary of the Data

Irradiation Regime	Surviving Fraction	Viable Cell Density /cm ²	Number of 162 cm ² Flasks		Mean Number of Foci per Flask	Transformation Frequency x 10 ⁴
			Total	With Foci		
Control	1	2.7	58	1	0.017 ± 0.017	0.4 ± 0.4
Acute/ Log-Phase	0.70 ± 0.05	3.4	159	39	0.28 ± 0.04	5.1 ± 0.7
Chronic/ Log-Phase	0.61 ± 0.04	2.9	157	25	0.17 ± 0.03	3.7 ± 0.7
Acute/ Plateau-Phase	0.65 ± 0.06	2.4	231	18	0.081 ± 0.019	2.1 ± 0.5
Chronic/ Plateau-Phase	0.69 ± 0.12	1.8	174	15	0.090 ± 0.023	3.0 ± 0.7

These data clearly show no enhanced dose-rate effect by irradiation with α -particles at low dose-rates (on the contrary, there is the possibility of the existence of a small sparing effect for log-phase cells). Moreover, because of the long irradiation times used and the experimental protocol adopted, the results do not support Elkind's proposal that the lack of an inverse dose-rate effect is due to the removal of mitotic cells. They do, however, suggest that plateau phase-cells may be more resistant to transformation (but not to cell killing) than are log-phase cells. This is interesting since measurements on log- and plateau-phase cultures imply no significant differences in nuclear area (230 μm^2) and thickness (1.5 - 2.5 μm) exist for these two types of cultures. The general conclusion to be made from these and our earlier data is that, since there exist no significant dose-rate effects for cell transformation in vitro after irradiation with both fast neutrons and α -particles, any pressure to increase quality factors for high-LET radiations on the basis of an inverse dose-rate effect is unfounded.

Acknowledgement

This project was carried out in collaboration with the MRC Radiobiology Unit at Harwell. The MRC personnel involved in this work are: Dudley Goodhead, David Stevens and Samantha Marsden.

Publications

Direct comparison between protons and alpha-particles of the same LET: I. irradiation methods and inactivation of asynchronous V79, HeLa and C3H 10T $\frac{1}{2}$ cells. D.T. Goodhead, M. Belli, A.J. Mill, D.A. Bance, L.A. Allen, S.C. Hall, F. Ianzini, G. Simone, D.L. Stevens, A. Stretch, M.A. Tabocchini and R.E. Wilkinson. International Journal of Radiation Biology, 61, 611-624, 1992.

Oncogenic Transformation of C3H 10T½ Cells with ²³⁸Pu α-Particles at Low and High Dose-Rates. S.C. Hall, A.J. Mill, L.A. Allen, A. Butler and D.L. Stevens. (Abstract: Joint Meeting of the Association for Radiation Research, Netherlands Radiobiology Society and Swedish Radiobiology Society, St Andrews University, 1-4 April 1992) To be published. International Journal of Radiation Biology, 1992.

In Vitro Cell Transformation at Low Doses of Ionising Radiation: A Collaborative European Project. A.J. Mill, S.C. Hall, D. Frankenberg, C.J. Roberts, D. Bettega. P. Calzolari, L. Hieber and A. Saran. (Abstract: Joint Meeting of the Association for Radiation Research, Netherlands Radiobiology Society and Swedish Radiobiology Society, St Andrews University, 1-4 April 1992) To be published. International Journal of Radiation Biology, 1992.

Radiological-protection-related neutron studies using the C3H 10T½ cell transformation system: I the RBE of 24 keV neutrons; II an investigation into the inverse dose-rate effect using 2.5 MeV neutrons. S.C. Hall, A.J. Mill, L.A. Allen, A. Butler, M.H. Crowe and C.D. Hart. New Developments in Fundamental and Applied Radiobiology, 202-207 (Editors C.B. Seymour & C. Mothersill), Taylor and Francis, 1991.

The relative biological effectiveness of 24 keV neutrons; cell survival and micronucleus induction in mammalian cells. A.J. Mill, S.C. Hall, J. Wells and D.P. Ransome. In: Frontiers in Radiation Biology (editor, E. Riklis), pages 279 - 285 (VCH Verlagsgesellschaft mbH, Weinheim) 1990.

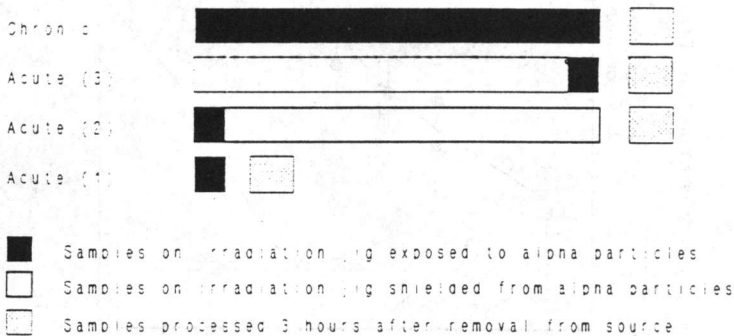


Figure 1.2 Irradiation scheme for 3.3 MeV α-particles

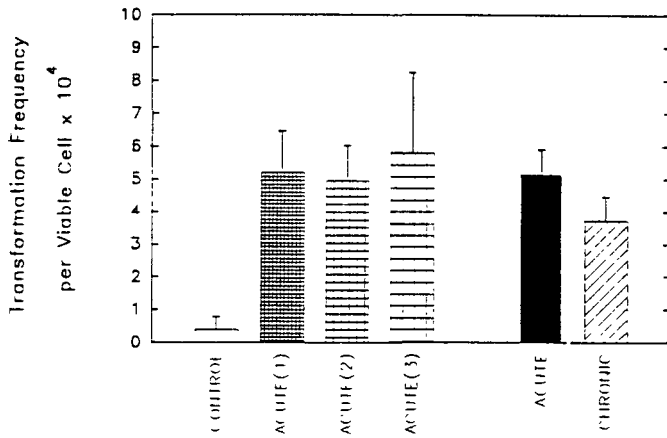


Figure 2.2 The effects of dose-rate for log-phase cells: the acute dose-rate regime adopted has no significant effect

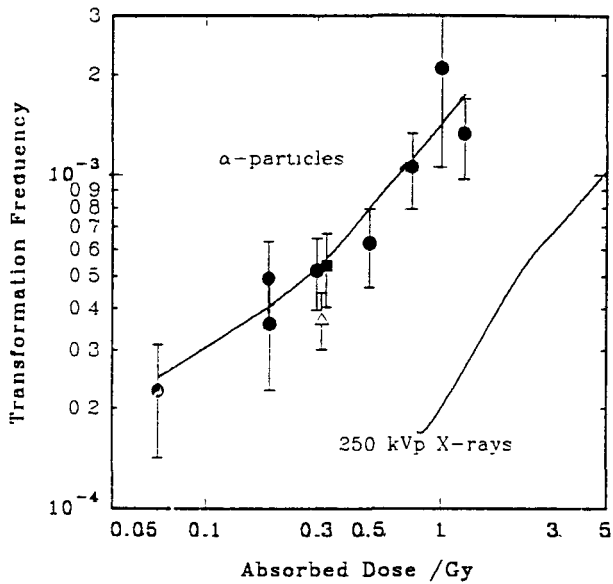


Figure 3.2 Dose-response relationship for 3.3 MeV α -particles and 250 kVp X-rays

Project 3

Heads of project: *Prof. Dr. Kellerer, Dr. Hieber*

Objectives for the reporting period

- (a) Participation in the standardization of the C3H 10T½ transformation assay to measure the transformation frequencies at low doses of sparsely ionizing radiation
- (b) Determination of the RBE of 5.4 keV Cr K_α soft x-rays
- (c) Study of the inverse dose-rate effect for cell transformation by different kinds of ionizing radiations.
- (d) Investigation of cellular, cytogenetic, and molecular mechanisms underlying radiation-induced cell transformation.

Progress achieved including publications

1. Standardization of transformation assay

Progress in the standardization of the transformation assay and the relevance of influence of certain parameters for different results in various laboratories are described in part I of this report. Increased agreement in transformation frequencies at moderate doses has been achieved between the participating laboratories mainly due to standardization of foci scoring. A catalogue of transformed and non-transformed foci has been developed.

2. Neoplastic transformation by soft x-rays

As described in a previous report, soft x-rays have been shown to be more effective than conventional x-rays or γ-rays in the inactivation of mammalian cells, in the production of chromosomal aberrations and in the induction of mutations; transformation data were missing.

In a comparative study with soft x-rays and γ-rays the transformation efficiency of Cr K_α soft x-rays has been determined. The relative biological effectiveness (RBE) value for soft x-rays versus γ-rays was approximately 1.3 in the range of soft x-ray doses from 2 Gy to 5 Gy; the same value as was found for cell inactivation. The RBE was independent of dose. The essential result of this study is that electrons of low energy and with ranges less than 1 μm are more effective than fast electrons not only for cell inactivation but also for cell transformation. An energy dependence of the RBE has been investigated in project 4.

3. Inverse dose-rate effect for cell transformation by different ionizing radiations

Increased transformation frequencies have been found by Hill *et al.* (1984) when 10T½ cells were exposed to fission neutrons at low instead of high dose rate. This effect has been termed

inverse dose-rate effect. Hieber *et al.* (1987) failed to see a similar effect for high-LET α -particles. There were, in addition, a series of studies with different kinds of ionizing radiations of different laboratories that were contradictory in whether an inverse dose-rate effects exists or not. In order to study a possible LET dependence of the inverse dose-rate effect induction of transformation incidence was examined in C3H 10T $\frac{1}{2}$ cells after exposure to fractionated doses of intermediate and high-LET particles.

Accelerated particles with LET values of 12.5, 25, 40, 75, 90 and 120 keV/ μ m produced by the RARAF (Columbia University, New York) have been used to expose the cells to doses divided in 3 fractions with different time intervals (0.3, 1.5, 15, 45 and 150 min) between the fractions. Doses were chosen leading to surviving fractions of 0.6 to 0.7.

Enhancement of transformation by a factor of about 2 was evident for 40 to 120 keV/ μ m but not for 12.5 and 25 keV/ μ m (see Figure 1.3). Increased frequencies were only seen if the time intervals between the fractions were greater than 15 min. In further experiments with helium ions of 150 and 200 keV/ μ m and α -particles of 147 keV/ μ m no such enhancement has been found. Thus an inverse dose-rate effect does only appear at intermediate ionisation density.

The finding that transformation frequency is increased only when exponentially growing cells but not plateau-based cells were exposed in several fractions or at low dose rate supports the proposed mechanism in which a period of extra sensitivity exists in the cell cycle (Rossi and Kellerer, 1986).

Sensitive periods may be in G2-phase and mitosis as well as at the G1/S border of the cell cycle as found for radiation-induced G2 delay (Hieber *et al.*, 1981).

4. Cytogenetic and molecular mechanisms in radiation-induced cell transformation

Syrian Hamster embryo (SHE) cells were used as a model system to study mechanisms of radiation-induced cell transformation. Several transformed cell lines have been established and tumour-cell lines were derived from tumours of nude mice that have been injected with transformed cells. Transformed and tumour cells grow faster and exhibit an increased cloning efficiency than non-transformed SHE cells.

Most of the cell lines investigated exhibit numerical and structural chromosome aberrations. About 75% of the cell lines have lower chromosome numbers per cell than normal diploid SHE cells with 44 chromosomes. There are certain translocations, some cell lines have additional marker chromosomes. Spontaneously transformed SHE cell lines exhibit a common deletion in the short arm of chromosome 2; at present, there is preliminary evidence that radiation-transformed cells do also show the same deletion.

Investigations of the expression of cellular oncogenes such as ras and myc lead to the result of increased expression of these genes by factors of 2 to 4 in transformed and tumour cells. There was no evidence for any RFLP or amplification of the oncogenes. A sequence analysis of the Ha-ras gene did not indicate any oncogene activation by specific point mutation.

Alterations in gene expression indicate basic processes in tumorigenesis. In order to identify genes that are involved in cell transformation either by increased expression (up-regulation) or

by repression (down-regulation or deletion) a differential hybridization analysis with cDNA libraries has been carried out. Clones that hybridize preferentially to cDNA probes of normal or transformed cells were further analysed. The DNA inserts of these phage clones were partially sequenced after amplification by PCR, and the sequences were then compared with known mammalian DNA sequences recorded in the EMBL gene bank.

Up to now, 20 genes have been identified (see Table 1.3). The genes can be divided into 4 groups, i.e. (i) energy housekeeping genes, (ii) translation genes, (iii) cytoskeleton genes and (iv) genes that are involved in the formation of extracellular matrix. The most interesting gene from the last group seems to be the laminin receptor gene. It is known that laminin and laminin receptor is involved in cell adhesion and especially in tumor metastasis (Liotta *et al.*, 1986).

Energie Housekeeping	Translation	Cytoskeleton	Extracellular Matrix
51c(+) GAPD	107c(+) rib.prot.S19	7c(-) β -actin	14c(+) laminin receptor
55c(+) cytochrome a	39c(-) rib.prot. r	41c(+) thymosin β 4	43c(+) collagenase IV
	66c(-) EF1	54c(-) γ -actin	
	69c(-) EF1	44c(-) vimentin	
	76c(-) rib.prot.pho.	63c(-) vimentin	
	21c(+) rib.prot.L5	82c(-) gelsolin	
3c(+) and 65c(-) unknown sequences			
64c(+) tumor transplantation antigen (mouse)			

References

Hill, C.K., Han, A., and Elkind, M.M. Fission-spectrum neutrons at low dose rate enhance neoplastic transformation in the linear, low dose region (0-10 cGy). *Int. J. Radiat. Biol.*, 46, 11-15 (1984)

Hieber, L., Ponsel, G., Fenn, S., Fromke, E and Kellerer, A.M. Absence of a dose-rate effect in the transformation of C3H 120T1/2 cells by α -particles. *Int. J. Radiat. Biol.*, 52, 859-869. (1987)

Rossi, H.H., and Kellerer, A.M. The dose rate dependence of oncogenic transformation by neutrons may be due to variation of response during the cell cycle. *Int. J. Radiat. Biol.*, 50, 353-361 (1986).

Hieber, L., Beck, H.P. and Lucke-Huhle, C., G2-delay after irradiation with α -particles as studied with synchronized cultures and by the BudR-33258H technique. *Cytometry* 2, 175-178 (1981).

Liotta, L.A., Rao, C.N. and Wewer U.M. Biochemical interactions of tumour cells with the basement membrane. *Annu. Rev. Biochem.* 55, 1037-1057 (1986).

Induced Transformation Frequency per 10^4 Survivors

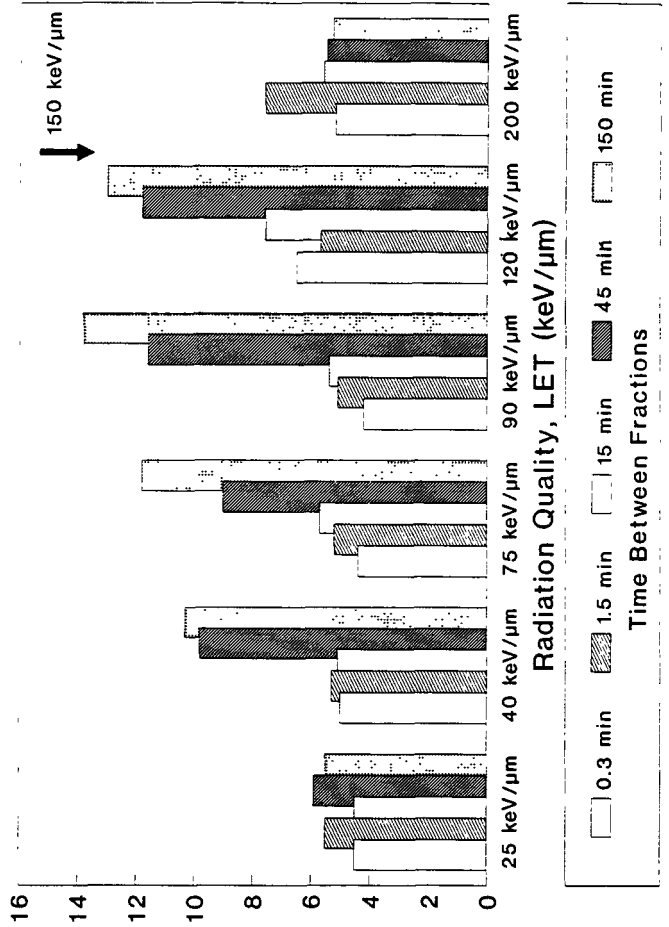


Figure 1.3 Effect of radiation quality and fractionation on the transformation frequency of C3H 10T1/2

Project 4

Head of project: *Dr. Frankenberg*

Objectives for the reporting period

- (a) Participation in the standardisation and intercomparison exercises for transformation in C3H 10T½ cells.
- (b) The measurement of the RBE for carbon K ultra-soft x-rays.

Progress achieved including publications

A characteristic carbon K photon produces a single photoelectron of about 260 eV with a range of about 5 nm which is comparable to the diameter of the DNA double helix. 10 to 15 ionisations are generated in a volume with a mean cord length of about 5 nm. Therefore, carbon K characteristic ultrasoft x-rays are an excellent tool to investigate the role of energy deposition patterns responsible for induction of DNA double strand breaks (DSB) which are considered to be DNA lesions involved in chromosomal aberration formation which in turn may lead to oncogenic cell transformation.

Carbon K photons are produced by bombarding an extremely pure graphite target with 520 keV protons at a beam current of 600 mA. The photon beam is of high purity with a small ($\ll 1$ per cent) contamination of bremsstrahlung. Primary dosimetry was carried out with a small (0.17 cm^3) fixed volume and an extrapolation chamber which agree to each other within 5 per cent. The cell nucleus of the C3H10T½ cells is very flat and has a mean thickness of about 2 μm . The ratio of average dose D within the cell nucleus to the dose at the entrance of the cell nucleus is 0.55. The entrance dose rate was 6 Gy min^{-1} .

For the evaluation of oncogenic transformation, cell survival as a function of the average dose D was determined as shown in Figure 1.4. The RBE-value of the carbon K photons relative to ^{60}Co gamma-rays is dose dependent and decreases from 4 to 2 when the surviving fraction decreases from 0.9 down to 0.1. This dose dependency of the RBE value for carbon K photons is mainly due to the much less pronounced shoulder in the survival curve after carbon K photon exposure compared to ^{60}Co gamma-rays. The transformation frequencies per 104 viable cells after exposure to carbon K photons and ^{60}Co gamma-rays as a reference radiation are presented in Figure 2.4. The RBE-value is found to be dose independent and amounts to about 3. Apart from the dose dependency of the RBE value for cell inactivation, the RBE values for cell transformation and cell inactivation are comparable. These RBE values are in good agreement with the RBE value of 3.8 observed for DSB induction and also with those found for the formation of chromosomal aberrations which are around 3. This agreement of RBE values suggests that a highly localized (5 nm) small energy deposition event (278 eV) can efficiently induce DSBs and chromosomal aberrations which in turn may lead to oncogenic cell transformation. Furthermore, the RBE value of about 3 corresponds with the small fraction of absorbed dose of ^{60}Co gamma-rays which is generated by electron track ends. In contrast, carbon K characteristic ultrasoft x-rays deposit all their energy by such electron track ends.

Publications

D.Frankenberg, H.Kühn, M.Frankenberg-Schwager, Dosimetric and biological studies with the facility for the production of characteristic ultrasoft x-rays at Frankfurt. Abstract, 2nd Ultrasoft X-ray Workshop, Toronto/Canada, 12/13.7.1991.

D.Frankenberg, M.Frankenberg-Schwager, B.Bourdeaux, S.Beckonert, Effectiveness of 0.28 keV carbon K characteristic X-rays at inducing transformation of C3H 10T1/2 cells. Abstract. Int.J.Radiat.Biol., in press.

O.Vetter, Spektrometrie und Dosimetrie ultraweicher charakteristischer Röntgenstrahlen im Hinblick auf eine biologische Anwendung. Diplomarbeit, Frankfurt/M., 1989.

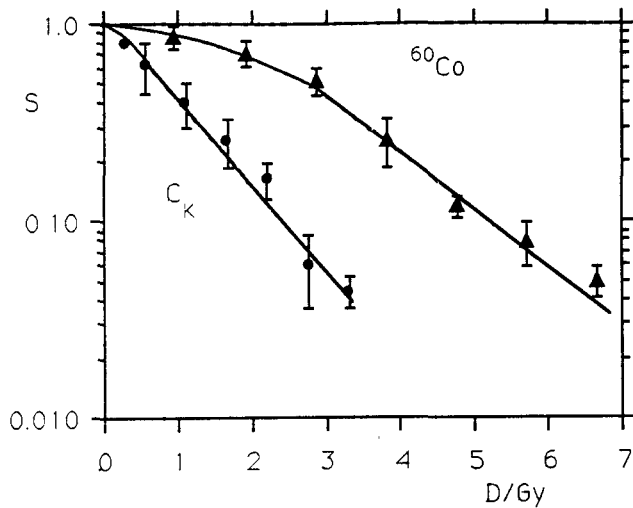


Fig.1.4: Inactivation of C3H10T½ cells by carbon K characteristic ultrasoft x-rays and ⁶⁰Co gamma rays (reference radiation). S: cell survival; D: average dose.

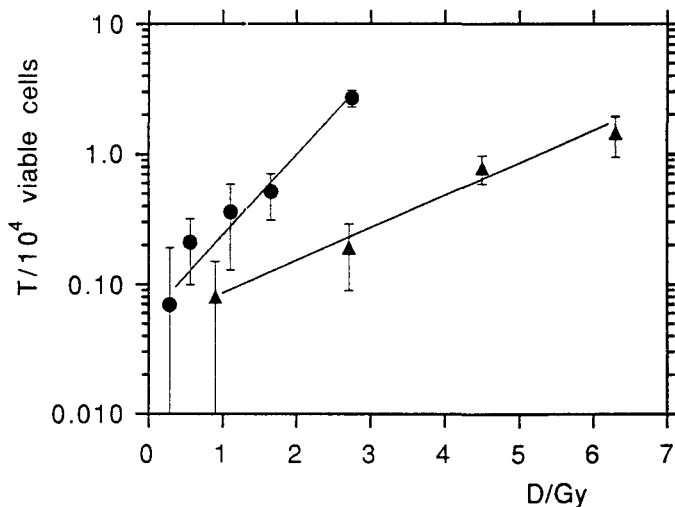


Fig.2.4: Oncogenic transformation of C3H 10T½ cells by carbon K characteristic ultrasoft x-rays. T: transformation frequency; D: average dose

Project 5

Heads of project: *Prof. Talloni Lombardi, Dr. Bettega*

Objectives for the reporting period

- 1) Participation in the standardisation of the C3H 10T $\frac{1}{2}$ transformation assay and intercomparison experiments on survival and transformation after graded X-ray doses.
- 2) Oncogenic transformation induced by α -particles of 4.3 MeV, LET=101 keV/ μ m in 10T1/2 cells: study of low doses and fractionation effects.
- 3) Study of the mitotic delay at various time after irradiation and its influence on the inverse dose-fractionation effect. Preliminary results on synchronized cell populations.

Progress achieved including publications

1. Low doses and inverse dose-rate effect

Transformation and inactivation frequencies induced in 10T $\frac{1}{2}$ cells exposed to α -particles were determined in the range interval between 0.2 and 300 cGy with special emphasis on the low dose region. Three experiments were performed involving the use of about 6,000 samples. Seven points were determined in the interval between 0.2 and 10 cGy. Transformation frequency increased linearly with dose up to 2 cGy; it seems to flatten at doses between 2 and 20 cGy but increases again at higher doses. This behaviour is predicted by a model based on the assumption that there is a brief period of high sensitivity to radiation in the cell cycle as originally proposed by Rossi and Kellerer. The entire dose-effect curve has been fully discussed in the interim report. A total of 21 cGy was delivered in a single dose or three equal fractions at time intervals of 1.5, 3 and 6 h between the fractions or ten equal fractions or ten equal fractions at intervals of 1.5 h. In each experiment single and fractionated doses were delivered in parallel and under the same experimental conditions. Results are reported in Figure 1.5. The values are the results of five independent experiments involving the use of about 3,600 samples. Transformation frequencies after fractionated exposure are always higher than after single doses. The enhancement factor with the various schemes is equal within the error and has a mean value of 1.5 ± 0.1 .

2. Mitotic delay and cell synchronization

Mitotic indices were determined at various times after the first dose fraction by counting the number of mitosis on fixed samples. Figure 2.5 shows mitotic index value relative to the control as a function of time interval after the first 7 cGy fraction. As can be seen, relative mitotic index decreases down to 0.5 within the first 3 h and then it increases again reaching a value of about 0.9 after an interval of 4.5 and 6 h. Cells in mitosis at 1.5 and 3 h after irradiation were probably in G₂. Figure 3.5 shows the measured values of the relative mitotic index at the time of the second and third fraction with the two fractionation schemes at time interval of 1.5 and 6 h respectively. The resulting percentages of cells in mitosis was quite

different in the two cases. Nevertheless, as shown before, the enhancement in the transformation frequency is the same. This result seems to indicate that the period of high sensitivity to transformation, proposed in the literature to explain the inverse dose-rate effect, is not the mitosis. The same conclusion seems to be suggested by the results of one experiment in which samples were incubated 24 h before irradiation with Colcemid at a concentration of 2×10^{-2} $\mu\text{g/ml}$ and then irradiated with a 21 cGy of α -particles. The percentage of mitosis at the time of irradiation was as high as 10.5%. Spontaneous transformation frequency increased up to $(28 \pm 12) \times 10^{-5}$ transformants/survivor. If this background is subtracted, transformation frequency induced by 21 cGy is the same as that of the asynchronous normal population.

We are now studying 10T $\frac{1}{2}$ progression through the cell cycle after low doses of α -particles and cell cycle phase dependence of radiation induced transformation. Preliminary results obtained with cells released from confluence and replated at low density have shown that within the first 16 h about 90% of the cells are in G1. The percentage of cells in S increases from about 6% to 30% at 28 h. Samples at various times after replating were exposed to low doses of α -particles and will be scored for transformation and mortality.

Publications

D Bettega, P Calzolari, A Ottolenghi and L Tallone Lombardi. Oncogenic transformation induced *in vitro* by radiation of varying LET. *Radiation Protection Dosimetry*, **31**, 279-283 (1990)

D Bettega, P Calzolari, A Ottolenghi and L Tallone Lombardi. The effects of 4.3 MeV α -particles on C3H 10T1/2 cells. RBE for survival and transformation. In *Recent Developments in Radiation Biology*, C. Seymour and C. Mothersill Eds., Taylor and Francis Ltd., London (1991).

A Ottolenghi, D Bettega, P Calzolari, and L Tallone Lombardi. Cell survival: how to characterize cell response to radiation. *ibidem*

A Ottolenghi, C K Hill, D Bettega, P Calzolari, and L Tallone Lombardi. Transformation of C3H 10T1/2 cells exposed to radiations of different LETs.. *ibidem*

D Bettega, P Calzolari, A Ottolenghi and L Tallone Lombardi. Criteria and techniques for analysing cell survival data. *Radiation and Environmental Biophysics* **30**, 53-70, (1991)

D Bettega, P Calzolari, A Ottolenghi and L Tallone Lombardi. Neoplastic transformation *in vitro* induced by high LET radiation: the "inverse dose-rate effect". *Relazione su invito. Atti del Congresso Nazionale Associazione di Fisica Biomedica*. Genova (guigno 1991).

A Ottolenghi and L Tallone Lombardi. Radiation induced transformation in C3H 10T1/2 cells: dose-effect curve models. *Proceedings of the Workshop on Biophysical Modelling of Radiation Effects*. Padua (K H Chadwick, G Moschini, M N Varma Eds.) 91-98 (1991)

D Bettega, P Calzolari, A Ottolenghi and L Tallone Lombardi. Transformation of C3H 10T1/2 cells exposed to single and fractionated doses of α -particles. Radiation Research. A Twentieth-Century Perspective. Vol. I: Abstracts of the 9th International Congress of Radiation Research, Toronto (J D Chapman, W C Dewey, G F Withmore Eds). p. 346 (1991) Academic Press, Inc.

D Bettega, P Calzolari, G Noris Chiorda and L Tallone Lombardi. Transformation of C3H10T1/2 cells with 4.3 MeV α -particles at low doses: single and fractionated dose effects. Radiation Research, in press (1992).

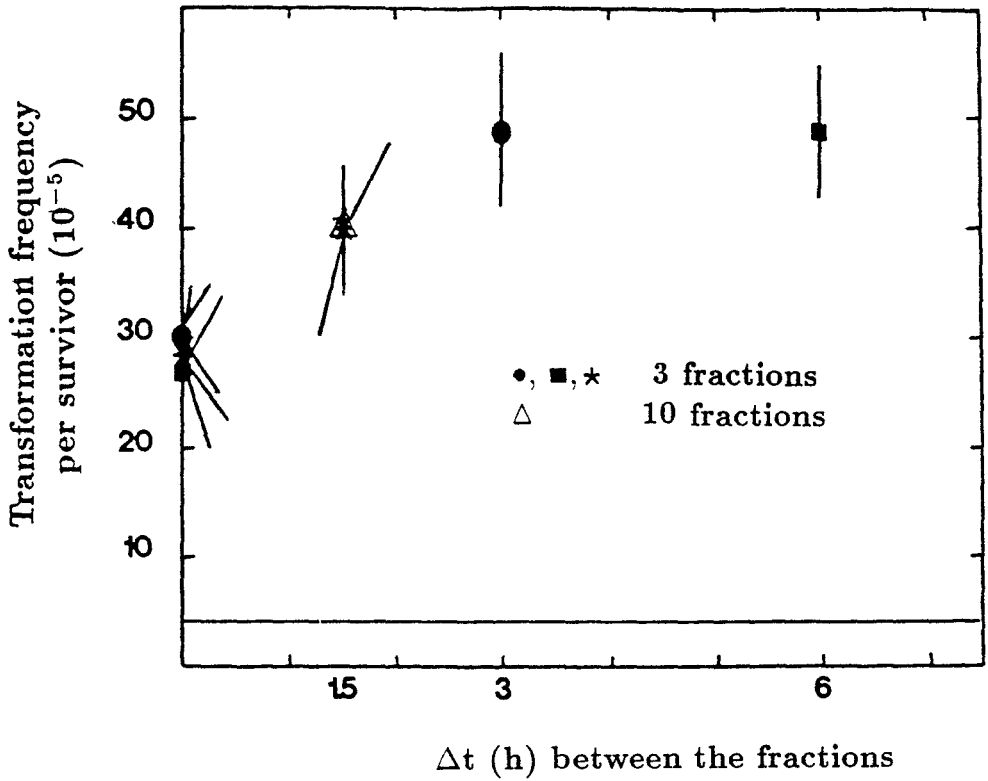


Figure 1.5 The effect of fractionation on transformation frequency in C3H 10T1/2.

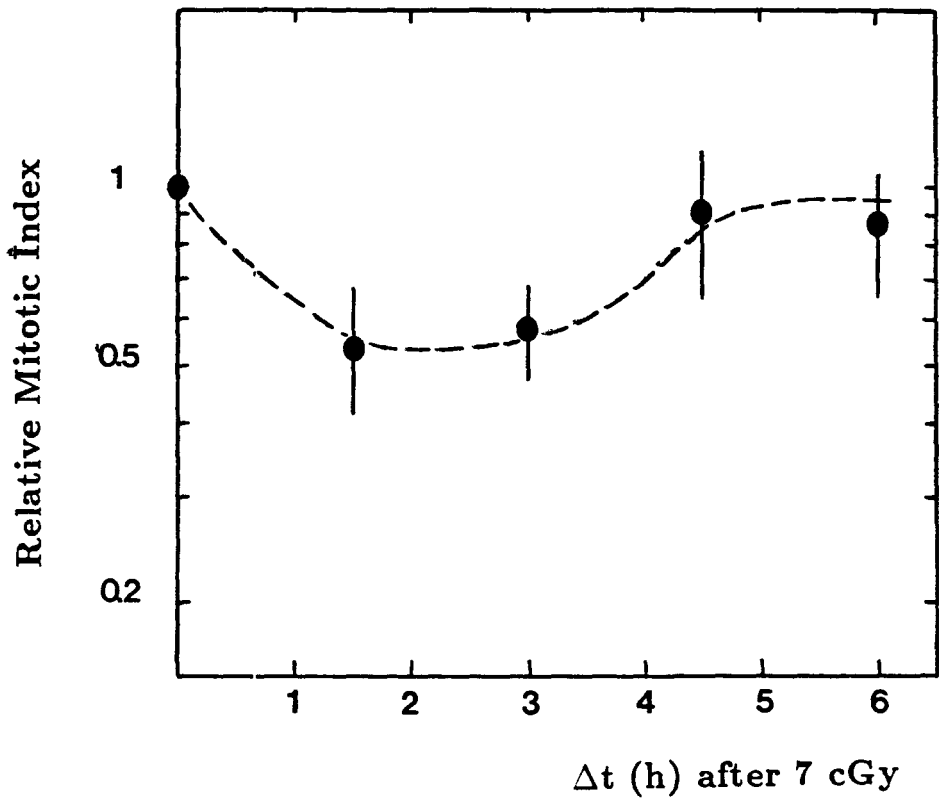


Figure 2.5 Mitotic index value relative to the control as a function of time interval after the first 7 cGy fraction

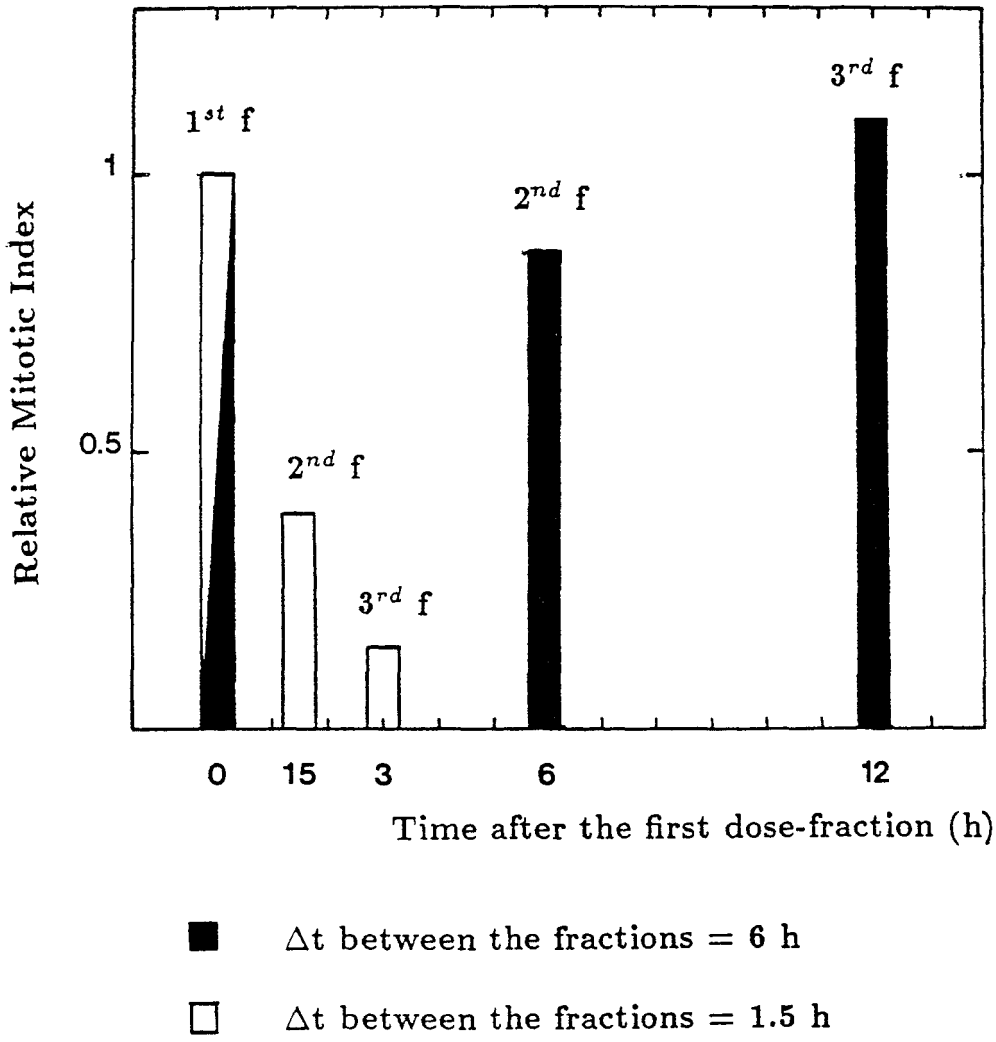


Figure 3.5 Measured values of the relative mitotic index at the time of the second and third fraction with the two fractionation schemes at time interval of 1.5 and 6 h respectively

Project 6

Head of project: *Dr. Saran*

Scientific staff: *Prof. Coppola, Dr. Covelli, Dr. Di Majo, Dr. Rebessi, Dr. Pazzaglia*

Objectives for the reporting period

- (a) Participation in the intercomparison of cell survival and transformation frequencies of C3H 10T½ cells exposed to X rays. This includes the study of the effect of trypsin on plating efficiency, and the study of the influence of seeding density on the transformation frequency of C3H 10T½ cells.
- (b) Study of the inverse dose-rate effect of fission neutrons and monoenergetic neutrons of different energies.
- (c) Study of the effect of a freeze-thaw technique on the plating efficiency and neoplastic transformation of C3H 10T½ cells.

Progress achieved including publications

Research on *in vitro* effects of ionizing radiation carried out at the ENEA Casaccia Laboratories has been supported up to now by contract Bi6-004 with the CEC. During 1990 it was decided to join the group of the five European Laboratories, which had received a CEC Contract for "Measurement of transformation of C3H10T½ cells by low doses of ionizing radiation", in order to exchange more readily results and information, and to collaborate to the attempt of standardizing experimental methods and protocols. This participation did not require any extra financial support to our team by the CEC during the period 1990-92. The common aspects and activities of the project are described in the general part of this report, and therefore will not be considered here.

Recent *in vivo* and *in vitro* studies of carcinogenesis, life shortening, and oncogenic transformation induced by high-LET radiation indicated either increased effectiveness or no change in effectiveness after dose protraction. As most occupational exposures are at low dose rates or by small dose fractions, risk assessment requires the evaluation of the dose-rate effect. In addition, recent studies by Miller and collaborators (*Radiat. Res.* 114, 1988) on a wide range of neutron energies indicate that the inverse dose-rate effect may be radiation-quality dependent. Therefore, we have investigated the effect on the neoplastic transformation of C3H 10T½ cells of dose fractionation of various neutron radiation qualities, in particular monoenergetic and fission spectrum neutrons. The cells used were obtained from the stock of M.M.Elkind in 1987, and maintained in Eagle's basal medium supplemented with 10% heat-inactivated fetal calf serum. They were inoculated at low density 48 to 72 hours before irradiation, trypsinized immediately after, then either (a) diluted and replated into 90-mm Petri dishes for survival and transformation assay in the case of fission spectrum neutrons, or (b) frozen into liquid nitrogen for transportation and later use in the case of monoenergetic neutrons. Neutrons of 0.5, 1.0 and 6.0 MeV from the Van de Graaff accelerator at TNO Rijswijk were used for irradiations at doses of 25 and 50 cGy (dose-rate: 0.6 cGy/min for 0.5 MeV, 2.0 cGy/min for 1.0 and 6.0 MeV; γ -ray contamination: 2% - 6%). Fission neutrons

were obtained from the RSV-TAPIRO reactor at Casaccia (average neutron energy 0.4 MeV in terms of Kerma, $\bar{y}_D=51.5 \text{ keV}/\mu\text{m}$, dose rate 1.8 cGy/min). The dose range examined was between 10.8 and 108 cGy. Four different fractionation schemes were adopted: for monoenergetic neutrons cells received 5 fractions at 2 h intervals, while for fission neutrons they were irradiated with 10 fractions at 2 h intervals, 5 fractions at 4.5 h intervals, and 5 fractions at 24 h intervals. Transformed foci were identified following an incubation period of 6 weeks, with weekly refeedings. Details of the experimental results are presented in Table 1.6. It is clear that within the experimental errors there is no difference in transformation frequency between acute and fractionated irradiation, regardless of the number of fractions or time between fractions, and independently from neutron quality. Transformation data were analyzed using a linear dose-effect relationship, which proved to be adequate to fit the experimental results.

We have also investigated the effects of freezing on the plating efficiency, survival and neoplastic transformation of the C3H 10T $\frac{1}{2}$ cells. After irradiation with fission neutrons cells were centrifuged and resuspended in 10% dimethyl sulfoxide (DMSO) in culture medium. Aliquots of this cell suspension were added to vials which were stored into liquid nitrogen. One week after freezing, cells were thawed at 37 C and centrifuged to discard the freezing medium; they were then resuspended in complete medium, counted, diluted and plated into 90-mm Petri dishes at concentrations estimated to result in either 300 and 60 surviving cells per dish for transformation and survival assay, respectively. As a general feature, no significant difference between the values determined after freeze-thawing and those obtained with unfrozen cells was detected.

As far as the studies of the effect of trypsin on the plating efficiency and the influence of the seeding density on the transformation frequency are concerned, the results of our experiments have already been made available to the other participating groups and included in the report prepared for CEC in 1991.

Since the main perspective of this project is to gain more understanding of the complex mechanisms that underly the initial stage in radiation carcinogenesis, future efforts will be directed towards the investigation of the cytogenetic and molecular nature of early radiation-induced events.

Publications

1) A. Saran, S. Pazzaglia, M. Coppola, S. Rebessi, V. Di Majo, and V. Covelli. Neoplastic transformation of C3H 10T $\frac{1}{2}$ cells following single or fractionated doses of fission spectrum neutrons and X rays. 38th Annual Meeting of Radiation Research Society, New Orleans, April 1990 (Book of Abstracts, Abstract Eo-3, p. 183).

2) S. Pazzaglia, A. Saran, M. Garavini, M. Coppola, S. Rebessi, V. Di Majo, and V. Covelli. Absence of a dose-fractionation effect in the transformation of C3H 10T $\frac{1}{2}$ cells by fission spectrum neutrons. III Italian-Yugoslav Symposium, Plitvice, June 1990.

3) A. Saran, S. Pazzaglia, M. Coppola, S. Rebessi, V. Di Majo, M. Garavini, V. Covelli. Neutron dose-fractionation does not enhance neoplastic transformation of C3H 10T $\frac{1}{2}$ cells. 23rd Annual Meeting of the ESRB, Dublin, September 1990.

- 4) A. Saran, S. Pazzaglia, M. Coppola, S. Rebessi, V. Di Majo, M. Garavini, and V. Covelli. Absence of a dose-fractionation effect on neoplastic transformation induced by fission spectrum neutrons in C3H 10T1/2 cells, *Radiat. Res.* 126, 34-348, 1991.
- 5) Saran, A., Pazzaglia, S., Coppola, M., Rebessi, S., Di Majo, V., Broerse, J.J., Zoetelief, J., Covelli, V. Neoplastic transformation of C3H 10T1/2 cells by single and fractionated doses of monoenergetic neutrons. In: *Proc. of Workshop on Oncogenic Mechanisms in Radiation Induced Cancer*. Fort Collins, USA, January 1991.
- 6) Saran, A., Pazzaglia, S., Coppola, M., Rebessi, S., Di Majo, V., Broerse, J.J., Zoetelief, J., Covelli, V. Neoplastic transformation of C3H 10T1/2 cells by fractionated doses of monoenergetic neutrons. *Proc. of 9th International Congress of Radiation Research*, Toronto, 1991.
- 7) Saran, A., Pazzaglia, S., Pariset, L., Coppola, M., Di Majo, V., Rebessi, S. and Covelli V. Dose fractionation dependence of C3H 10T1/2 cell transformation by fission spectrum neutrons. In: *Proceedings of the 40th Annual Meeting of the Radiation Research Society* (Salt Lake City, 1992). In press.
- 8) Saran, A., Pazzaglia, S., Rebessi, S., Pariset, L. A freezing technique applicable to transformation studies of C3H 10T1/2 cells. *Int. J. Radiat. Biol.*, in press.

Table I.6 Survival and Transformation of C3H10T1/2 Cells Irradiated with Monoenergetic Neutrons

No. fractions and dose per fraction (cGy)	Total dose (cGy)	Surviving fraction	No. of dishes	Total No. foci	No. of dishes without foci	Avg. No. of foci per dish (λ) ^a	Transformation frequency per 10 ⁴ surviving cells (\pm SE)
Monoenergetic Neutrons							
Controls	0	1	1125	6	1119	0.0054	0.181 (\pm 0.074)
0.5 MeV							
1 x 25	25	0.536	447	8	441	0.0135	0.917 (\pm 0.373)
5 x 5	25	0.618	445	8	437	0.0181	0.780 (\pm 0.275)
1 x 50	50	0.422	368	15	356	0.0332	1.827 (\pm 0.523)
5 x 10	50	0.388	278	9	269	0.0329	1.710 (\pm 0.564)
1 MeV							
1 x 25	25	0.680	583	16	570	0.0226	0.794 (\pm 0.219)
5 x 5	25	0.761	589	17	578	0.0189	1.060 (\pm 0.318)
1 x 50	50	0.551	425	19	406	0.0457	1.162 (\pm 0.263)
5 x 10	50	0.593	462	24	443	0.0420	1.262 (\pm 0.286)
6 MeV							
1 x 25	25	0.801	634	9	625	0.0143	0.363 (\pm 0.121)
5 x 5	25	0.753	643	8	651	0.0124	0.393 (\pm 0.138)
1 x 50	50	0.663	677	16	661	0.0239	0.694 (\pm 0.172)
5 x 10	50	0.674	551	13	538	0.0239	0.707 (\pm 0.195)
Fission Neutrons							
Controls	0	1	1063	4	1059	0.0038	0.156 (\pm 0.078)
1 x 25	25	0.462	879	10	869	0.0114	0.640 (\pm 0.202)
5 x 5	25	0.544	665	9	656	0.0136	0.602 (\pm 0.199)
10 x 2.5	25	0.591	674	7	667	0.0104	0.504 (\pm 0.190)
1 x 10.8	10.8	0.849	261	3	258	0.0115	0.483 (\pm 0.278)
1 x 27	27	0.655	371	11	363	0.0296	0.913 (\pm 0.321)
1 x 54	54	0.410	651	29	623	0.0445	1.570 (\pm 0.294)
1 x 108	108	0.139	478	48	433	0.1004	3.523 (\pm 0.512)
5 x 2.16	10.8	0.843	178	2	176	0.0113	0.534 (\pm 0.376)
5 x 5.4	27	0.646	146	3	143	0.0207	1.140 (\pm 0.652)
5 x 10.8	54	0.402	244	11	233	0.0461	1.510 (\pm 0.451)
5 x 21.6	108	0.140	173	26	149	0.1490	3.930 (\pm 0.774)

^a $\lambda = -\ln$ (Number of dishes without foci/Number of dishes).

RADIATION-INDUCED MUTATIONS IN MAMMALS

Contract Bi6-156 - Sector B14

1) Ehling, GSF Neuherberg

Summary of project global objectives and achievements

An estimation of the genetic risk resulting from an increased mutation rate due to radiation exposure in man must be based on experimental results in animals. As in any extrapolation, that estimate will have a higher likelihood of accuracy which is based on an experimental system most closely reflecting the situation to be estimated. For an estimate of the genetic risk in man, a number of *in vivo* mammalian germ cell mutation tests have been developed, including methods to screen for recessive coat color mutations at specific loci, dominant cataract mutations, enzyme charge or activity mutations at selected loci and chromosome aberrations.

Two methods have been developed and used to estimate the human radiation genetic risk based upon experimental animal data: The direct approach estimates the frequency of induced dominant deleterious mutations in man based on experimental results in the mouse for induced dominant mutations. The second approach, the indirect method, estimates the frequency of dominant deleterious mutations in man based on the estimated doubling dose determined in the mouse for recessive specific locus mutations. Both extrapolation procedures require the assumption that there are no species differences in the sensitivity to radiation mutation induction. The indirect approach requires the additional assumption that the doubling dose estimated in the mouse for induced specific locus mutations is representative for other genetic endpoints. To test these assumptions required for extrapolation, we have developed a multiple genetic endpoint mutation test protocol to determine the induced mutation rate for recessive specific locus alleles, dominant cataract alleles and enzyme charge or activity alleles in the same experimental animals. Results provide a systematic comparison of the induced mutation rate for different genetic endpoints in the mouse. Further, we have established an experimental procedure to screen for dominant cataract and enzyme activity mutations in the two mammalian species, *Mus musculus* and *Mesocricetus auratus*. Experiments were designed to estimate the effects of various factors which influence the sensitivity to radiation mutation induction in germ cells of mammals.

Project 1

Head of project: *Dr. Ehling*

Objectives for the reporting period

During the last contract period, the dominant cataract and enzyme activity control groups were extended in both *Mus musculus* and *Mesocricetus auratus* to provide a more accurate estimation of the spontaneous mutation rate in both species. These data are critical in estimating the doubling dose for these endpoints in germ cell of mammals. Experiments to determine the mutation rate following 2 + 2 Gy spermatogonial exposure for dominant cataract and enzyme activity alleles in mouse and hamster were carried out as well as experiments to measure the radiation induced mutation rate in oocytes for both genetic endpoints in both species.

Progress achieved including publications

A comparison of the mutation frequencies in germ cells of the mouse and hamster for both dominant cataract and enzyme activity mutational endpoints is given in Table 1. These results represent the first systematic comparison of transmissible mutational events in different species of mammals and are relevant to the consideration of extrapolation procedures. The dominant cataract spermatogonial results are comparable in both the mouse and the hamster, which would support the assumption required for extrapolation of a similarity of sensitivity to induction of mutations by radiation among mammalian species. The dominant cataract oocyte data as well as the data for enzyme activity mutations are still too preliminary to allow species comparisons. These experiments will be continued in the next contract period.

Table 1. Comparison of the mutation frequency following 2+2 Gy irradiation in germ cells of the mouse (*Mus musculus*) and the golden hamster (*Mesocricetus auratus*)*

	MOUSE			HAMSTER		
	Mutant	Offspring	Freq	Mutant	Offspring	Freq
<u>Dominant cataract</u>						
pg	0	1949	-	0	808	-
g	6	18521	3.2	3	8780	3.4
o	2	6155	3.2	1	1055	9.5
<u>Enzyme activity</u>						
pg	1	1098	9.1	0	281	-
g	1	9370	1.6	0	938	-
o	6	5868	10.2	1	743	13.4

* Freq = mutation frequency x 10⁴; pg = post-spermatogonial stages; g = spermatogonia; o = oocytes

The first enzyme activity mutation has been recovered in the mouse control group, which allows an estimate of the spontaneous mutation rate for this endpoint (0.4×10^{-5} per locus per gamete) as well as a calculation of the radiation doubling dose based upon enzyme activity mutation rate data. These estimates are presented in Table 2 based on radiation experimental results from Neuherberg. It should be noted that the estimation of the doubling dose ranged from 0.3 Gy to 13.3 Gy with a weighted average of 6.6 Gy. These comparisons must be interpreted with caution since the control and most experimental group results consisted of a single mutational event. However, if these results should be supported by more extensive data, they will confirm our previous observations for dominant cataract mutations indicating a higher radiation doubling dose for these endpoints than the doubling dose estimated from specific locus mutation rate data. These observations are at variance with the assumption necessary for the indirect method of genetic risk estimation, i.e. the radiation doubling dose for all genetic endpoints is equal to the doubling dose estimated from specific locus mutation rate data.

Table 2. Estimation of the radiation doubling dose (DD) for induced enzyme activity mutations in spermatogonia of mice

<u>Dose (Gy)</u>	<u>Mutants</u>	<u>Offspring</u>	<u>DD</u>
0	1	10775	-
1.5	0	6467	-
3	1	7048	2.8
6	1	7539	7.0
2+2	1	9370	13.3
3+3	1	3388	1.4
5+5	5	3187	0.3

We will extend these results to make the comparisons more meaningful and begin to genetically and molecularly analyze recovered mutations to determine the radiation induced DNA alterations which result in mutations in germ cells of mammals.

Publications

Ehling, U.H.: Quantification of the radiation induced genetic risk. In: Chauhan, P.S. (Ed.) Environmental Mutagenesis and Carcinogenesis. EMSI, BARC, Bombay, 1990, pp. 57-70.

Ehling, U.H.: Genetic risk assessment. Ann. Rev. Genet. 25, 225-280, 1991.

Favor, J.: Risk estimation based on germ-cell mutations in animals. Genome 31, 844-852, 1990.

Favor, J.: Multiple endpoint mutational analysis in the mouse. Prog. Clin. Biol. Res. 340C, 115-124, 1990.

Favor, J., and W. Pretsch: Genetic localization and phenotypic expression of X-linked cataract (*Xcat*) in *Mus musculus*. Genet. Res., Camb. 56, 157-162, 1990.

Kratochvilova, J., and J. Favor.: Allelism tests of 15 dominant cataract mutations in mice. *Genet. Res., Camb.* 199-203, 1992.

Merkle, S. and W. Pretsch: A glucosephosphate isomerase (Gpi) null mutation in *Mus musculus*: Evidence that anaerobic glycolysis is the predominant energy delivering pathway in early post-implantation embryos. *Comp. Biochem. Physiol.* 101B, 309-314, 1992.

Merkle, S. and W. Pretsch: Characterization of two electrophoretic lactate dehydrogenase-A mutants in *Mus musculus*. *Biochem. Genet.* 30, 49-59, 1992.

Pretsch, W., and S. Merkle: Glucose phosphate isomerase enzyme-activity mutants in *Mus musculus*: Genetical and biochemical characterization. *Biochem. Genet.* 28, 97-110, 1990.

MUTATION STUDIES UPON SPERMATOGONIAL STEM CELLS OF MAMMALS AND GENETIC TESTS FOR NON-DISJUNCTION IN THE MOUSE

Contract Bi6-143 - Sector B14

1) *Cattanach*, MRC Radiobiological Unit

Summary of project global objectives and achievements

1. Factors affecting the yield of mutation from spermatogonial stem cells in mammals (Cattanach)

Assessment of the genetic risk to man of exposure to radiation is largely dependent upon experimental work in the mouse. It is based on the assumption that man and mouse have similar sensitivities to mutation-induction and that factors that modify the mutation responses in the two species are the same. Work in a number of laboratories has established that the spermatogonial stem cells of several rodent and monkey species vary in their sensitivity to translocation-induction by radiation and we have more recently shown that male mice of the 101/H inbred strain give lower translocation yields, but higher levels of stem cell killing, than the standard C3H/HeH x 101/H hybrid (3H1) following a range of X-ray doses. Other strains showing even greater sensitivities to stem cell killing, and therefore likely to have yet lower sensitivities to genetic damage, have also been identified. For the 101/H strain the basis of the difference is suggested to lie with a higher proportion of radio-sensitive cells in the heterogeneous stem cell population.

We have now utilised a different genetic end-point, specific locus mutation, to investigate the radiation-sensitivity of 101/H male spermatogonial stem cells. Following a 24h fractionated 3 + 3 Gy X-ray dose, as used at Neuherberg to screen for strain differences, the yield differed little from the standard 3H1 control. This result was in accord with the Neuherberg findings but was unremarkable in that because the fractionation reduces the heterogeneity of the stem cells little reduction in yield might have been expected. However, with a single 6 Gy dose, in contrast to expectation, the 101/H specific locus mutation response significantly exceeded that of the 3H1 control. Such a qualitative difference in genetic response with different genetic end-points has been found previously with fractionated treatments but have not been demonstrated before with a single acute dose. The finding further complicates the difficulties of extrapolating mouse data to man.

A number of other factors which influence the genetic response of mouse spermatogonial stem cells to radiation have also been distinguished. Thus, both translocation and specific locus mutation yields are enhanced when the radiation follows 24h after population depletion (by triethylenemelamine for example) when the surviving cells appear to be 'triggered' into a radio-sensitive phase prior to repopulating the germinal epithelium. And, at greater times after population depletion when repopulation is under way, sub-normal mutational responses to radiation are obtained. Pretreatments of previously undamaged stem cell populations with high doses of hydroxyurea (HU) which kill cells in the S phase, have also indicated that most genetic damage recoverable from spermatogonial stem cells following radiation derives from those cells which are in the G₁ phase of their cell cycle at the time of radiation exposure.

We have now used the HU system to search for a residual heterogeneity among stem cells present in the germinal epithelium 24h after population depletion translocations being the end-point screened. Although interpretation of the results was complicated by a curiously high control radiation response. The HU pretreatments enhanced both the translocation yield and stem cell killing indices. It is therefore likely that some dividing cells are present in the stem cell population 24h after depopulation and this may help to explain the differences in responses with

differing genetic end-points. The same approach has also provided evidence to support the view that re-establishment of a heterogeneous population has occurred 4 days after population depletion when recovery of the germinal epithelium is underway.

The genetic and cytogenetic analyses of a new class of mutations recovered from the specific locus experiments has revealed that most are associated with large deletions comprising up to 30% of individual chromosomes or other gross forms of chromosome damage. This may constitute a major new finding of significance for risk assessment, and potentially also for investigation of gene dosage effects, genome organisation, oncogene expression and the development of cancers.

2. Experimental studies on non-disjunction in the mouse (Cattanach)

Numerous cytogenetic tests for non-disjunction in the mouse have been devised but are handicapped by the need for skilled expertise, by the low spontaneous non-disjunction frequency in the mouse and the problems of distinguishing the consequences of primary and tertiary non-disjunction. We have recently developed two systems of genetic (complementation) tests using Robertsonian translocations in tester animals to detect gain or loss events in normal mice. Several chromosomes have been studied using this approach.

Recent work has evaluated the two systems for chromosome 11; as previously found with chr 1, the MBH method was more effective than the Rb method although more difficult to operate but neither system worked as well with chromosome 11 as with chromosome 1. The difference seems to be attributable to differences between the sensitivities of the different chromosomes to damage, and this may indicate the best use for these test systems.

3. Radiation effects in mouse oocytes (Tease)

These studies were undertaken to provide information on radiation-induced genetic damage in mouse oocytes which would be of use for extrapolating human genetic risks from experimental data from female germ cells.

An experiment was initiated to investigate the possibility of inter-strain variation in oocyte radiosensitivity, comparable to that described for spermatogonial stem cells of some strains. The incidences of structural chromosome anomalies after X-irradiation were compared in oocytes from two inbred mouse strains; the strains chosen were the parental ones of the F₁ hybrid type generally used for mutation studies in the laboratory.

The data obtained showed that oocyte radiosensitivity varied between the inbred strains C3H/HeH and 101/H. At the 2 Gy dose, the ratio of aberration induction for C3H/HeH to 101/H was 1.2 : 1 and at the 4 Gy dose, 1.4 : 1. The magnitude of the inter-strain variation in oocyte radiosensitivity is not large and appears to be significant only after large doses of radiation. Previously published information from an identical experiment using the F₁ hybrid females of these 2 strains showed a comparable rate of aberration induction at the 4 Gy dose to the 101/H strain, although at the lower dose the hybrid females yielded a rate in excess of both inbred strains. A degree of heterogeneity in response therefore appears to occur; this precludes reaching a general conclusion at this time on the influence of inter-strain oocyte variation in radiosensitivity on the use of experimental data for extrapolations of genetic risk.

Cytogenetic analyses of unfertilized eggs, pre- and post-implantation embryos have been used in previous studies to investigate radiation-induced aneuploidy in mouse oocytes. This approach has provided information on the frequency of aneuploidy after irradiation, the possible mechanisms involved, and has allowed those factors that influence the response of oocytes to induced numerical anomalies to be identified and evaluated. Further experiments have been initiated that are complementary to the cytogenetic studies already carried out but which use a genetic method to

detect induced chromosome loss. The information generated from these studies should provide further insight into the mechanisms of induced nondisjunction and chromosome loss and be of value in assessing the relative abilities of the cytogenetic and genetic assays to detect and quantify the effects of ionizing radiation on mouse oocytes.

The present study estimated that 1.68% of oocytes had induced loss of chromosome 19 following 1 Gy of X-rays at the immediately preovulatory stage. An earlier experiment (Tease and Fisher, unpublished) produced an estimate of induced chromosome loss after 4 Gy of X-rays to dicytate stage oocytes of 1.18 % (95% confidence limits: 0.40% - 2.59%). Comparison of these 2 estimates shows the expected increased sensitivity of the diakinesis stage oocyte compared with that of dictyate cells. The difference in sensitivity as adjudged by this method is in the same direction as that found by other experimental approaches, such as cytogenetic analysis of chromosome anomalies. Tease and Fisher (unpublished observations), for example, found that 30.6% and 58% of metaphase I cells had 1 or more chromosome anomalies respectively after 4 Gy of X-rays to 2 different dictyate oocyte stages, whereas after 1 Gy to diakinesis cells, the corresponding figure was 59%. The cytogenetic data indicate diakinesis cells to be approximately 4 to 8 times as sensitive to chromosome aberration induction as dicytate cells. The induced chromosome loss data indicate a similar difference in oocyte sensitivity at different cell stages.

4. Analysis of chromosome anomalies by in situ hybridisation (Tease)

The improvements in nonisotopic in situ hybridisation have developed this technology to the point where it should be of considerable value to the analysis of radiation effects on chromosomes in germ line cells. The initial part of this project was to establish the methodology within the laboratory. This having been accomplished to a sufficient extent, a small-scale experiment was undertaken to analyse the breakpoints of 3 X chromosome rearrangements in relation to the position of a locus defined by a repeat sequence X chromosome probe.

Project 1

Head of project: *Dr. Cattnach*

Objectives for the reporting period

- 1a. To compare the specific locus mutation responses of the spermatogonial stem cells of inbred 101/H and 'standard' hybrid C3H/HeH x 101/H (3H1) male mice to fractionated and single acute X-ray doses, the study to include analyses of mutations induced. 1b. To investigate the bases of the modified genetic response of spermatogonial stem cells to X-radiation at different intervals following population depletion.
2. To compare the effectiveness of the Rb and MBH tester methods for detecting chromosomal loss in chromosomally normal mice.
- 3a. To compare the oocyte sensitivity of two inbred mouse strains. 3b. To determine the rate of induced chromosome loss in mouse oocytes following irradiation of immediately preovulatory eggs.
4. To analyse chromosome aberrations by nonisotopic *in situ* hybridisation.

Progress achieved including publications

1. Factors affecting the yields of mutations from spermatogonial stem cells

a) 101/H males gave longer sterile periods than control 3H1 males following 24 h 3+3 Gy X-radiation (median day of return to fertility 119 cf 76) but the specific locus mutation frequency did not differ significantly (24.91×10^{-5} /locus/gamete, $n = 7,457$, cf 28.19×10^{-5} , $n = 15,202$; $P = 0.42$). With a single 6 Gy dose, the sterile period was again longer than the control (116 cf 72 days) but rather than giving a low specific locus frequency, as expected from previous translocation studies, an elevated response was obtained (22.35×10^{-5} , $n = 10,226$, cf 7.75×10^{-5} , $n = 18,441$, $P = 0.11$, or 13.29×10^{-5} , $n = 119,326$, $P = 0.059$ for the historical control of Russell, 1958).

Genetic and cytogenetic analyses of dominant mutations causing growth retardation have shown that most are associated with large deletions or other major chromosome changes.

b) Evidence has been obtained that pretreatments with hydroxyurea, which kill cells in S phase to enrich the proportion of cells in G_1 , increase the extent of cell killing by X-rays and probably enhance the translocation response from spermatogonial stem cells surviving 24h after population depletion (induced by triethylenemelamine). A similar effect was obtained from stem cells repopulating the germinal epithelium 4 days after depopulation (Table 1). Both findings suggest the existence of heterogenities in radio sensitivity among the cells present at these times.

Table 1

Group	Treatments, interval	Recovered testis weight (mg)	% cells with translocations	Translocations/cell
1	X-ray	101.44	12.82 ± 1.84	.148
2	TEM + X-ray 24h	78.95	23.08*± 2.04	.285
3	TEM + (HU + HU, 3h + X-ray), 24h	52.20	25.23 ± 2.15	.297
4	TEM + X-ray, 3h	85.90	9.33 ± 1.45	.103
5	TEM + X-ray, 4d	88.94	9.60 ± 1.62	.110
6	TEM + (HU + HU, 3h + X-ray) 4d	41.10	14.78 ± 1.78	.170
7	X-ray + (HU + HU, 3h), 4d	92.5	10.56 ± 1.57	.119
8	X-ray + (HU + HU, 3h), 24h	97.20	14.24 ± 1.84	.178
9	HU + X-ray, ½h	73.65	10.9 ± 1.51	.130

* Response exceptionally high compared with previous published findings.

2. Experimental studies on non-disjunction

The Rb tester method, used to detect chromosome 11 and 13 loss following X-irradiation of chromosomally normal males or females, employed the Rb(11.13)Bnr translocation carried heterozygously in the tester animals. The chromosome 11 and 13 markers were vestigial tail (*vt*) and satin (*sa*), respectively. Following irradiation with 4 Gy X-rays the normal wild type animals were mated for one week to the tester mice and the progeny screened for the *vt* and *sa* young, these indicated chromosome 11 and 13 loss events. The same mating regime and X-ray dose was used with monobrachial homology (MBH) tester method but here the tester animals carried both the Rb(11.13)4Bnr and RB(10.11)8Bnr translocations heterozygously. Chromosome 11 loss again was detected using *vt* as the marker.

In females, at least, the MBH system appeared to be the more effective for detecting chromosome 11 loss (0.22% marked young in 916 scored 916, calculated chromosome 11 loss = 0.90%, cf 0.08% in 3925, calculated chromosome 11 loss = 0.66%, for the Rb method) but not so in males (0.11% in 1750, calculated chromosome 11 loss = 0.48%, cf 0.18%, in 1082, calculated chromosome 11 loss = 0.80% for the Rb method). Only one chromosome 13 loss event was found with the Rb method among 1897 progeny recovered following female X-irradiation; none were recovered among only 292 progeny from irradiated males. The incidence of chromosome 11 and 13 losses have yet to be calculated.

3. Radiation effects in mouse oocytes

a) The frequencies of chromosome anomalies in metaphase I oocytes were compared in females of 2 inbred strains given either 2 or 4 Gy of acute X-rays 16.5 days prior to sampling. The data are summarized in Table 2.

b) Females of the F₁ hybrid type C3H/HeH x 101/H were given 1 Gy of acute X-rays shortly before ovulation. They were mated to tester males of the genotype Rb(8.19)1ct *ru*/Rb(9.19)163H *ru* and their offspring screened for the exceptional occurrence of the *ru* phenotype which occurs when an oocyte nullisomic for chromosome 19 is fertilized by a sperm with disomy for chromosome 19. The results of this experiment are summarized in Table 3.

Since only a proportion of induced chromosome 19 events are actually complemented by paternal disomy, the actual incidence of chromosome loss has to be estimated using the rate of recovery of *ru* exceptions and the frequency of nondisjunction in spermatogenesis. The latter was determined by cytogenetic analysis of metaphase II stage spermatocytes from a group of 5 males from the tester stock. In a sample of 500 secondary spermatocytes,

14.3% were found to have disomy for chromosome 19. Using these data and those from Table 2, 1 Gy of X-rays to immediately pre-ovulatory oocytes resulted in loss of chromosome 19 from an estimated 1.68% of cells (95% confidence limits: 0.64% - 3.39%).

Table 2

Strain	Dose (Gy)	Aberration type				Total aberrations	Total number of cells
		Interchanges	Fragments	Gaps/breaks	Isochromatid gaps		
C3H/HeH	0	1 (0.5)	4 (2.1)	1 (0.5)	0	6 (3.1)	195
	2	22 (12.2)	31 (17.2)	5 (2.8)	3 (1.7)	61 (33.9)	180
	4	97 (50.3)	122 (63.2)	43 (22.3)	8 (4.1)	270 (139.9)	193
101/H	0	1 (0.5)	1 (0.5)	0	0	2 (0.9)	221
	2	28 (12.1)	27 (11.6)	6 (2.6)	3 (1.3)	64 (27.6)	232
	4	93 (43.1)	88 (40.7)	32 (14.8)	6 (2.8)	219 (101.4)	216

() average/100 cells

Table 3

Treatment group	Number of offspring classified	Number of <i>ru/ru</i> offspring	Dominant mutations
Control	1603	0	0
1 Gy	1674	6	4

4. In situ hybridisation

Following introduction of this novel technique to the laboratory, a small experiment was initiated using the X chromosome repeat sequence probe, 70-38, which hybridises to a locus, DXWas70, at bands XA1/XA2. Two reciprocal translocations and an inversion are known to have breakpoints within this region and an analysis of the relative positions of the breakpoints of these 3 rearrangements and the DXWas70 locus was undertaken.

The hybridisation patterns in chromosome preparations from mice carrying one or other rearrangement showed that the locus DXWas70 was distal to the breakpoints of the translocation T(X.11)38H and the inversion In(X)1H but proximal to that of another translocation T(X.4)37H. These observations indicated the linear order of centromere: T(X.11)38H/In(X)1H : DXWas70 : T(X.4)37H. It was not possible using this probe to determine which of T(X.11)38H or In(X)1H has the more proximal breakpoint.

Publications

- Cattanach, B.M., Rasberry, C. and Beechey, C.V. Factors affecting mutation-induction by X-rays in the spermatogonial stem cells of mice of strain 101/H. Banbury Report, No 34: Biology of Mammalian Germ Cell Mutagenesis: Cold Spring Harbor Laboratory Press pp 209-220 (1990).
- Zsebo, K., Williams, D.A., Geissler, E.N., Broudy, V.C., Martin, F.H., Atkins, H.L., Hsu, R.Y., Birkett, N.C., Okino, K.H., Murdock, D.C., Jacobsen, F.W., Langley, K.E., Smith, K.A., Takeishi, T., Cattanach, B.M., Gall, S.J. and Suggs, S.V. Stem cell factor is encoded at the *Sl* locus of the mouse and is the ligand for the c-kit tyrosine kinase receptor. *Cell*, 63:213-224 (1990).
- Cattanach, B.M., Rasberry, C., Evans, E.P. and Avner, P. Genetic and molecular evidence of an X-chromosome deletion spanning the tabby (*Ta*) and testicular feminization (*Tfm*) loci in the mouse. *Cytogenet. Cell Genet.* (In press).
- Brockdorf, N., Kay, G., Cattanach, B.M. and Rastan, S. Molecular analysis of the *Ta^{2H}* deletion: evidence for additional deleted loci. *Mammalian Genome*, (In press).
- Evans, E.P., Burtenshaw, M. and Cattanach, B.M. Deletions at the *Sl* locus. *Mouse Genome*, 86:230 (1990).
- Jones, J., Peters, J., Ball, S., Cattanach, B.M. and Kwon, B.S. Molecular analysis of germline mutations at the albino locus of the mouse. *Mutagenesis*, 5:90 (1990).
- Rasberry, C., Cattanach, B.M., Burtenshaw, M. and Evans, E.P. Three new translocation. *Mouse Genome*, 89(3):550-551 (1991).
- Cattanach, B.M., Rasberry, C., Burtenshaw, M. and Evans, E.P. Detection of large autosomal deletions. *Mouse Genome*, 89(3): p550 (1991).
- Tease, C. Radiation and chemically induced chromosome aberrations in mouse oocytes: a comparison with effects in males. *Mutation Research* (In press).
- Fisher, G. and Tease C. *T^{2H}*: a radiation-induced deletion affecting the *T*, *qk* and *Tme* loci. *Mouse Genome*, 90:209-210 (1992).



RADIATION-INDUCED GENETIC EFFECTS IN GERM CELLS OF MAMMALS

Contract Bi6-166 - Sector B14

1) *Van Buul*, Univ. Leiden Sylvius Lab.

Summary of project global objectives and achievements

The project is aimed at gaining information on the effects of ionizing radiation on germ cells of rodents and primates as measured by induced chromosomal translocations or DNA breaks. Such information will facilitate a better use of animal data to estimate genetic risks due to exposure of human populations.

1. Translocations in stem cell spermatogonia of the rhesus monkey and the mouse

For the rhesus monkey we could demonstrate that, under the experimental conditions chosen, the ratio of spermatogonial stem cell killing and the induction of chromosomal translocations was comparable to that observed for the mouse. This suggests that the well documented differences in translocation induction patterns between mouse and monkey probably originate from else.

The recorded meiotic delay of translocation carrying spermatocytes seems not to exist at the lowest dose level of 2 Gy that we studied. This finding increases the reliability of the genetic risks associated with structural chromosomal aberrations as estimated by the UNSCEAR. Although the so far obtained yields of translocations in steel (SL^{con}/SL^{con}) and dominant spotting ($W^+/+$) mice with 'primate type' of spermatogenesis are lower than observed in normal mice, they are much higher than those found in the rhesus monkey. Thus the mutants seem no suitable primate model for studying X-ray induced genetic damage.

2. Induction of DNA breaks in mouse oocytes

Dose response relationships for the induction of DNA single strand breaks for mouse oocytes as measured with a single cell gel electrophoresis technique turned out to be steeper than similar curves obtained for human peripheral blood lymphocytes or Chinese Hamster Ovary fibroblast cultures. This probably reflexes differences in chromatin structure between meiotic stages and diploid somatic cells.

Project 1

Head of project: *Dr. Van Buul*

Objectives for the reporting period

During the reporting period we constructed a dose response curve for the induction of translocations in spermatogonial stem cells of Steel ($S1^{con}/S1^{con}$) and Dominant spotting ($W^v/+$) mouse mutants with a primate type of spermatogenesis. So far for Steel doses of 0, 1, 2, 3, 4, 6 and 8 Gy have been analysed, for Dominant spotting doses of 0, 1, 3, 5 and 7 Gy and for normal mice 0, 1, 3, 6 and 9 Gy. In addition cell killing, measured as loss of testis weight, and repopulation after 4 Gy irradiation was studied. Furthermore, we developed a technique to measure the induction (and repair) of DNA strand breaks in individual oocytes of the mouse.

Progress achieved including publications

The results obtained on the mouse mutants indicate (a) no differences in cell killing between normal mice and both mutants; (b) a lower recovery rate of full spermatogenesis in the mutants, and (c) lower frequencies of induced translocations in both mutants. The oocyte data suggested higher induction rates of DNA single strand breaks in maturing oocytes than in human peripheral blood lymphocytes or in in vitro Chinese Hamster Ovary fibroblast cultures.

Publications 1991

- Buul, P.P.W. van, J.H. Goudzwaard and M.C.J. Seelen (1991) Meiotic delay of translocation carrying spermatocytes responsible for reduced transmission, In: *New developments in fundamental & applied radiobiology* (eds. Seymour and Mothersill). Proceedings of the 23rd Meeting of the ESRB, Taylor & Francis Ltd., London, p. 24-28.
- Buul, P.P.W. van and M.C.J. Seelen (1991) The relationship between induced reciprocal translocations and cell killing of rhesus monkey spermatogonial stem cells after combined treatments with follicle-stimulating hormone and X-rays, *Mutation Res.*, 263, 1-8.
- Buul, P.P.W. van, J.H. Goudzwaard and C.M.J. Seelen (1991) On the origin of differences in chromosomal radiosensitivity of male premeiotic germ cells of mouse and rhesus monkey, In: *Radiation Research; A Twentieth-Century Perspective*, Vol. I, ICRP Meeting Toronto (eds. Chapman et al.), ISBN 0-12-168561-6 (v,1) Academic Press N.Y., p. 409 (abstract).
- Buul, P.P.W. van and M.C.J. Seelen (1991) Differences in genetic radiation response between mouse and rhesus monkey caused by differences in post irradiation proliferation and differentiation patterns of surviving stem cell spermatogonia, *Int. J. Rad. Biol.*, 60, 725 (abstract).
- Buul, P.P.W. van (1991) X-ray induced translocations in premeiotic germ cells of monkeys, *Mutation Res.*, 251, 31-39.
- Buul, P.P.W. van, A. Tuinenburg-Bol Raap, H.J. Goudzwaard, C.M.J. Seelen, C.V. Beechey, A.T. Natarajan and A.G. Searle (1991) Cytogenetic characterization of radiosensitive mouse mutants, *Mutation Res.*, 251, 171-179.

RADIATION-INDUCED GENETIC EFFECTS IN GERM CELLS OF MAMMALS

Contract Bi6-069 - Sector B14

1) *Jacquet*, CEN-SCK

Summary of project global objectives and achievements

This project was mainly concentrated on the radiosensitivity of the "resting" oocytes, which represent some 90% of the total population of oocytes in the ovary and are the most important female germ cells from the genetic point of view, since they receive the largest part of the genetically significant lifetime dose of radiation.

Up to now, most studies on radiosensitivity of the mammalian germ cells have been carried out on mice, for which inbred strains and genetic markers are available. However, the extreme sensitivity of the mouse resting oocytes to killing by radiation renders their study very difficult and has stimulated additional studies on other mammalian species, in order to obtain a better picture of the potential genetic hazard of radiation for man.

For such studies, it has been suggested that the guinea-pig could constitute one of the best models, due to the apparently high resistance of its resting oocytes to cell killing which could be comparable to that of humans resting oocytes. In addition, this species shows an interesting feature, i.e. the presence of two distinct populations of resting oocytes at diplotene : an oocyte with a large nucleus, comparable to that of man, and another with a contracted nucleus, which appears a few days after birth and which predominates as the animal ages. Up to now, studies have been concentrated on the contracted resting oocyte, typical of the adult animal.

The two years of the present project were devoted to a comparison of the radiosensitivity of the resting oocyte of the guinea-pig at its two different nuclear states. The study was completed by an evaluation of the radiosensitivity of the immature oocyte at earlier stages of oogenesis, that is during embryonic life in utero.

Several parameters can be used to assess the radiosensitivity of the germ cells : our project was mainly concentrated on long-term reproductive effects.

For this purpose, female guinea-pigs were exposed during intra-uterine life, early postnatal life or adult life to different doses of X-rays. 6 and 12 months after treatment, the fertility of the females was tested by mating them with untreated males. The studied parameters included : number of pregnant animals, number of dead embryos, weight and normality of the life embryos, effects on oocyte populations in the ovaries. These studies confirmed the extreme radioresistance of the guinea-pig oocytes at their different stages of oogenesis and the suitability of this species for further studies on the genetic effects of radiation : even a dose of 4 Gy administered to the ovaries of the newborn animal allowed still normal reproduction one year after treatment, although the stage tested here (resting oocyte at diplotene) had been found to be very sensitive to the killing effects of radiation in other rodents.

On the other hand, we developed techniques for culturing guinea-pig oocytes to the first meiotic metaphase and preparing their chromosomes for cytogenetic analysis. This was completed by preliminary studies on the effects of radiation on the induction of chromosome aberrations in resting oocytes of this species.

Project 1

Head of project: *Dr. Jacquet*

Objectives for the reporting period

- For about 10 years, our laboratory has accumulated a considerable experience with respect to the sensitivity of the mouse oocyte and preimplantation embryo to radiation and chemicals. This experience had now to be transposed to the guinea-pig, and this supposed some preliminary work in order to : 1) acquire an expertise in the basic manipulations of guinea-pigs (mating, estrus control, vaginal smears etc...); 2) determine the doses of X-rays which could be used for the long term reproductive study; 3) adapt some techniques used in the mouse to the guinea pig : fixation and staining of the ovaries, identification of the various stages of oogenesis and their chronology, culture of the oocytes and preparation of their meiotic chromosomes for cytogenetic analysis.
- According to the results of the preliminary studies, we intended to irradiate females at three different times (corresponding to different stages of oogenesis), and with two different doses of X-rays. The effects of the various treatments on the reproductive capacity of the animals would be followed 6 and 12 months after irradiation, and this would be completed by detailed histological studies of the ovaries from a number of animals, in order to have a precise idea of the killing effects of radiation on the various stages of oogenesis.
- The last part of our work would be devoted to preliminary investigations on the cytogenetic effects of radiation in the resting oocytes of the guinea-pig.

Progress achieved including publications

1. Histological study of oogenesis in the untreated guinea-pig

For this study, ovaries fixed with Bouin were cut at 3μ and stained with the "triple staining of A. Prenant" (Heidenhain's iron hematoxylin + Erythrosin + light green). Ovaries which were examined were derived from a number of control embryos and fetuses aged 26, 32 and 41 days post coitum (p.c.) (total duration of pregnancy : \pm 68 days), and from control animals aged 0-1 days, and 1,3,8,14 and 18 months.

The first results of this study were in general agreement with those reported earlier by Ioannou. Ovaries of embryos aged 26 days contained only oogonia, either in interphase or in mitotic prophase or metaphase. Ovaries of 32 days showed the additional presence of oocytes in the first stages of meiotic prophase (leptotenes + a few zygotenes), while those of 41 days showed oogonia and all stages of meiotic prophase, with a great majority of zygotenes and pachytenes and very few diplotenes. Newborn animals (0 - 1 days) possessed only diplotene oocytes of the "large" type, plus low numbers of maturing oocytes. Some of them were already invested in Graafian follicles (five or more layers of granulosa cells surrounding an antrum). In adult animals (from 4 months p.p.), the "large" diplotenes were generally replaced by those of the "contracted" type (85-95% of the total population of resting oocytes).

However, in animals aged one year or more, the mean proportion of "large" diplotenes again raised, to reach about 50% of the total population of resting oocytes. These results contrast somewhat with those reported by Ioannou, but large variations between the animals clearly appear in the

results given by this author. In fact, our own results clearly suggested that this proportion was depending on some physiological factors : for example, animals which were killed in the course of the experiment because of illness exhibited a majority of "large" resting oocytes, while pregnancy was generally associated with a high percentage of "contracted" resting oocytes.

2. Development of a method for obtaining chromosome preparations of metaphase I oocytes of the guinea-pig

In the guinea-pig, the only possibility to dispose of sufficient numbers of oocytes for cytogenetic studies is to induce their maturation in vitro. Up to now the techniques which were found to give the most satisfactory results were derived from that of Yanagimachi for the culture of guinea-pig oocytes and from those of Tarkowski and of Morrison for the fixation of the meiotic preparations.

Oocytes were obtained by puncturing the large follicles, and they were cultured in Yamada's medium, a medium which is used in our laboratory for the culture of mouse oocytes and preimplantation embryos. Like for the mouse and the rat, it was experimented that oocytes must have reached a certain critical size to be able to resume meiosis in culture. Such meiotically competent oocytes were incubated in culture medium for 6 hours, to obtain first meiotic metaphases. At the end of the culture, oocytes are still surrounded by the cumulus cells. Removal of these cells and of the very thick zona pellucida is difficult and represents the most critical step of the techniques, since oocytes without their zona pellucida may become very fragile and easily burst when placed on the slide for fixation, unless appropriate modifications are made to hypotonic treatment. The cytoplasm of the guinea-pig oocyte contains a great amount of yolk globules which may also considerably interfere with the spreading of the chromosomes and the quality of the preparations, if they cannot be discarded during fixation. Using this method, very good chromosome preparations could be obtained. However, the results still suffer some variability, so that we will try to further improve it.

3. Studies on the effects of radiation on the reproductive capacity of the female guinea-pig

3.1. Choice of the doses to be used.

Restricted numbers of female guinea-pigs were irradiated at various times of pregnancy with either 2 or 6 Gy of X-rays, and the influence of this treatment on delivery and subsequent fertility 4 months after treatment was examined. At the end of this short experiment, ovaries were taken from a few animals of each group, and processed for histological examination. On the basis of the results of this preliminary experiment, doses of 2 and 4 Gy were chosen for the long term reproductive study. These doses were administered to adult (6-8 months) pregnant and not pregnant animals, fetuses (32 days post conception) in utero, and newborn (0-1 days post partum) animals. According to our histological study, the target cells were, respectively, the "contracted" resting oocytes (adult animals), the oogonia + oocytes at beginning of meiotic prophase (fetuses in utero) and the "large" resting oocytes (newborn animals). For each of the treated groups and their corresponding controls, 25 female animals were used.

3.2. Results obtained

The dose of 4 Gy revealed highly lethal for fetuses irradiated in utero, so that only one female animal was obtained at birth in this group. Other groups could be normally tested from their reproductive capacity, 6 and 12 months after irradiation. Among those, no clear effect of radiation could be evidenced, whatever the dose given or the stage of oogenesis tested : even

one year after irradiation, treated animals were still even fertile as control ones, and this was generally true for the different tested parameters (percentage of females giving embryos; number of living and dead embryos / female; normality and weight of the embryos). On the other hand, a clear decrease in the number of oocytes was observed in the ovaries of all the treated groups, 12 months after irradiation. This effect was dose-dependent but was less pronounced in animals treated at birth, when all resting oocytes were of the "large" type. This clearly demonstrated the high radioresistance of this most important stage of oogenesis.

4. Cytogenetic effects of radiation in the guinea-pig

For the preliminary experiments, a dose of 1 Gy was chosen. 20 females were irradiated on the day of birth (target cells : "large" resting oocytes) and 20 others at 6 months (target cells : "contracted" resting oocytes). Animals were killed at the age of one year, their oocytes were cultured to the first meiotic metaphase and examined for the presence of chromosomal anomalies. These experiments have to be completed, since the number of cultured oocytes which could be analyzed was rather low. However, these first results showed that irradiation is able to induce chromosome translocations in the resting oocytes of the guinea-pig, confirming the results obtained very recently in the mouse by Strumane et al. (Mutat. Res. 248, 123-133, 1991).

Publications

P. Jacquet and S. Grinfeld, Influence of some methodological factors on the radiosensitivity of the mouse zygote. Teratology, 42, 453-462 (1990).

In preparation :

P. Jacquet and J. Vankerkom, Comparative effects of irradiation at various stages of oogenesis on the reproductive capacity and oocyte killing in the guinea pig.

P. Jacquet and J. Vankerkom, Preliminary results on the induction of translocations by radiation in the resting oocytes of the guinea-pig.

P. Jacquet and J. Vankerkom, Influence of physiological factors on the nuclear morphology of the guinea-pig resting oocyte.

RADIATION-INDUCED GENETIC EFFECTS IN GERM CELLS OF MAMMALS

Contract B16-077 - Sector B14

1) *Streffer*, Universitätsklinikum Essen

Summary of project global objectives and achievements

The possibility of the induction of malformations after radiation exposure during pregnancy is a serious radiation hazard. Numerous studies have shown that teratogenic effects are primarily induced, when radiation exposure has taken place during organogenesis. However, there have also been reports from animal experiments on an increased frequency of abnormal fetuses after exposure during the preimplantation stage. This result is strongly dependent on the mouse strain.

From the point of view of radiation risk, it may be even more important to look for a potential teratogenic risk after radiation exposure of germ cells, because they are at risk over the whole reproductive life time. That such a teratogenic risk actually exists has been demonstrated for mice by Nomura (e.g. *Nature* 296 (1982) 575-577) and by Kirk and Lyon (*Mutation Research* 106 (1982) 73-83 and *Mutation Research* 125 (1984) 75-85).

Studies in our institute during recent years have shown that one of our mouse strains ("Heiligenberger", NMRI like) does respond with a higher frequency of malformations after radiation exposure during the preimplantation stage. The fact that malformations, which are observed on day 19, are inducible even in the one-cell stage suggests, that there is an effect on the genetic material and that this effect is inherited over a number of cell generations. It is conceivable that such an effect on the genetic material can also result from the irradiation of germ cells.

Thus, the global objectives of the project refer to radiation exposure of germ cell stages with different radiation qualities (X- or gamma-rays) and different dose rates (1 Gy/min and below 0.01 Gy/min in order to avoid lethal effects on the sensitive immature female germ cells). The uterine content is examined on day 19 of gestation with regard to early and late resorptions, dead and malformed fetuses, and fetal weights.

The global achievements are as follows. It was possible, indeed, to induce malformations in 19 days old fetuses by radiation exposure of oocytes. As has already been characteristic for radiation exposure of preimplantation stages in previous experiments, the major type of malformation was that one of a gastroschisis. Usage of high dose rates (1 Gy/min, X-rays) showed a marked extent of lethal effects on mature stages (between 4 weeks and 1 week before conception) and limited the studies to these most mature stages of oogenesis, because less mature oocytes were completely killed even after comparatively low doses (0.5 Gy). Exposure with a lower dose rate (0.28 Gy/h, gamma-rays of a ^{137}Cs source) avoided the lethal effects on the mature stages, whereas induction of malformations was still observed. Also lethality in immature stages was somewhat reduced, so that oocytes up to 5 weeks before conception could be studied; however, less mature stages could not be checked for the induction of malformations, because of the lethal effects even after this low dose rate.

Project 1

Head of project: *Prof. Streffer*

Objectives for the reporting period

1. Impact of X-rays (dose rate 1 Gy/min; dose range 0.5-3 Gy) on fetal damage, in particular lethal effects and macroscopically visible malformations, after exposure of oogenesis stages.
2. Impact of gamma-rays (^{137}Cs ; dose rate 0.28 Gy/h = 0.0046 Gy/min; dose range 0.7-2.7 Gy) on fetal damage, in particular lethal effects and macroscopically visible malformations, after exposure of oogenesis stages.
3. Protein patterns of malformed and normal fetuses.

Progress achieved including publications

1. Introduction

Previous experiments have shown that one of the mouse strains kept in our Institute (Heiligenberger mice; inbred strain; similar to NMRI-mice) does respond with a higher frequency of malformations after radiation exposure of preimplantation stages. From the point of view of radiation risk, exposure of germ cell stages may be even more important, because these cells are at risk over the whole reproductive life time, whereas the preimplantation period lasts only a couple of days. Therefore, we studied the impact of X-rays (with high dose rate) or gamma-rays (with low dose rate) on various stages of oogenesis in mice.

2. Methodology

Female mice were irradiated either with X-rays (dose rate 1 Gy/min), gamma-rays (^{137}Cs ; dose rate 4.6 mGy/min) or sham-irradiated. Mating started immediately after radiation exposure or, in some cases, after a delay of some weeks. Plug control was carried out every morning and those females with a vaginal plug (unequivocal sign of copulation) were singled out. 19 days after copulation (day of copulation = day 1), the mice were killed by cervical dislocation and the uterine content checked for early resorptions, late resorptions, late fetal death, surviving fetuses, and fetuses with macroscopically visible malformations. Protein patterns were established by extraction of liver proteins and two-dimensional gel electrophoresis.

3. Results

3.1 Exposure to X-rays (high dose rate experiments)

Even after the lowest dose (0.5 Gy) used in the experiments pregnant females were obtained only during the first four weeks after radiation exposure, irrespective of whether mating started immediately after radiation exposure or with a delay of two weeks. This result is in line with previous observations reported in the literature and reflects the high radiation sensitivity of oocytes after high dose rate exposures.

Tab. 1 summarizes the results of the X-ray experiments. In this table, the data are pooled for the first four weeks. This was done despite the fact that some fluctuation was seen within the weeks. Whether this fluctuation was simply due to statistics or whether a real time dependence was responsible, was not checked, because considerably higher numbers of mice would have been necessary for a decision. As the major question was whether malformations can be induced by exposure of oocytes, and the answer was a clear "yes", we omitted further, more detailed experiments.

Tab. 1 shows that total litter loss is very pronounced in the controls. This fact presumably depends on the inbreeding of the strain, because in previous years, when we used colony-bred mice, the amount of total litter loss never exceeded 10%. Only after the highest dose (3 Gy) a significant increase is observed. The number of early resorptions is enhanced after doses of 2 and 3 Gy, whereas late resorptions and late fetal deaths are not affected by radiation exposure of oocytes.

Similar to our experience with preimplantation stages, a significant increase of malformed fetuses was found after 2 and 3 Gy and, also comparable to preimplantation exposure, gastroschises were seen almost exclusively. Radiation sensitivity of oogenesis is somewhat lower than that of 1-cell embryos, but comparable to preimplantation stages succeeding the 1-cell stage.

Table 1: Fetal damage after radiation exposure of oocytes to X-rays (copulation within the first four weeks after radiation exposure)

Dose (Gy)	Total litter loss	Impl./Mice checked	Early ^a resorpt.	Late ^a resorpt.	Late ^a deaths	Malfor- mations ^b
0	23.2%	864/109	6.5% (56)	1.0%(9)	0.7%(6)	4.9% (39)
0.5	22.7%	227/ 34	7.1% (16)	0.9%(2)	1.3%(3)	3.4% (7)
1	26.5%	530/ 75	9.6% (51)	1.5%(8)	0.8%(4)	6.4% (30)
1.5	29.5%	236/ 31	9.3% (22)	1.3%(3)	0.9%(2)	6.2% (13)
2	25.0%	514/ 75	18.5%*(95)	1.4%(7)	0.4%(2)	9.0%*(37)
3	55.6%*	292/ 48	29.5%*(86)	3.1%(9)	0.3%(1)	17.3%*(34)

^a Per implantation site

^b Per living fetus

* Significantly different from control at P<0.01

3.2 Exposure to gamma-rays (low dose rate experiments)

The first conclusion that could be drawn from the low dose rate experiments was that also those oocytes stages that were exposed five weeks (instead of four in the high dose rate experiments) before copulation could be checked for malformations, because some of the fetuses survived. Tab. 2 also shows that the lethal effects for oocytes exposed 1 to 5 weeks before conception were markedly smaller than in the X-ray series. Again, the data for the various weeks were pooled for the sake of brevity, although some information is obscured by this procedure.

Table 2: Fetal damage after radiation exposure of oocytes to gamma-rays (copulation within the first five weeks after radiation exposure)

Dose (Gy)	Total litter loss	Impl./Mice checked	Early ^a resorpt.	Late ^a resorpt.	Late ^a deaths	Malfor- mations ^b
0	31.4%	950/109	5.6% (53)	0.9%(9)	0.6%(6)	2.5% (22)
0.7	39.5%	355/ 46	6.2% (22)	0.3%(1)	0.3%(1)	5.4% (18)
2.7	35.6%	725/ 87	9.4% (68)	2.1%(15)	1.0%(7)	6.0%*(38)

^a Per implantation site

^b Per living fetus

* Significantly different from control at P<0.01

As in the high dose rate experiments, a significant increase in the number of malformed fetuses was observed after 2.7 Gy. The 0.7 Gy result was significant only at the P<0.05 level and, even more important, the difference to the control was entirely

due to a high number of malformed fetuses (10 out of 53 living fetuses) in week number 5 before conception. All the other weeks did not show any deviation from the control frequency.

3.3 Protein patterns

An important question in the context of these studies is that of the mechanism that leads to the observed effects. Irradiation is done on oocytes (one cell with just one genome!) and the effects are observed many cell generations later. Lethal effects on the exposed cells (a common mechanism for many teratogenic effects after exposure during organogenesis) can definitely be ruled out, so that one must assume that the damage is transmitted over several cell generations and finally expressed. For such a transmission DNA is the most probable candidate. As even nowadays with the sophisticated methods to study DNA it is still difficult to look for specific damage on the DNA level, we decided to monitor the protein patterns in malformed and non-malformed fetuses. As the amount of work is considerable, we also decided to study the protein pattern in these fetuses after exposure of 1-cell embryos, in order to get information also for preimplantation embryos. For the 1-cell embryo the same considerations apply as for oocytes (no lethal effects applicable as explanation for the observed effects).

Analysis of almost 250 protein patterns revealed that exposed fetuses with gastroschisis had a markedly higher number of alterations in the protein pattern of liver cells than various control groups, although no specific change characteristic for all fetuses with gastroschisis was observed. In non-exposed normal fetuses 6.3% (4/64) had an altered protein pattern, in exposed (1 Gy) normal fetuses 16.7% (12/72), in non-exposed gastroschisis fetuses 20.0% (7/35), and in exposed (1 Gy) gastroschisis fetuses 32.1% (25/78). We interpret these results as an indication that by radiation exposure some labilization of the genome occurs which is responsible for a higher risk to end up as a malformed fetus.

Publications

Müller, W.-U. and Streffer, C.

Lethal and teratogenic effects after exposure to X-rays at various times of early murine gestation.

Teratology 42 (1990) 643-650

Hillebrandt, S.; Streffer, C.; Müller, W.-U.

Increased protein variants levels in liver from gastroschisis fetuses.

Radiation Research: A twentieth-century perspective; J.D.

Chapman, W.C. Dewey, G.F. Whitmore (eds.), Academic Press, San Diego (1991), page 223

Schotten, H.; PhD thesis, submitted 1992

RADIATION-INDUCED GENETIC EFFECTS IN GERM CELLS OF MAMMALS

Contract Bi7-048 - Sector B14

1) *Van der Schans* , TNO-Medical Biological Lab.

Summary of Project Global Objectives and Global Achievements

The project aims at a better understanding of the fundamental principles that determine the radiation sensitivity in humans, with specific attention for the role of DNA repair in germ cells. Such knowledge is important for assessing relative radiation risk of individual persons, because people may exhibit considerable differences in their response to ionizing radiation. In this project, the induction and repair of damage in DNA of germ cells of the Syrian golden hamster exposed to ionizing radiation is studied at biologically relevant doses. These studies require the development of more sensitive and advanced techniques for determining radiosensitivity within the normal dose range, which approach therefore will be pursued. We shall also investigate which aspects of DNA sequence or chromosomal organisation are important with respect to their influence on the reparability of DNA damage.

The project is part of the ongoing programme of the Department of Genetic Toxicology of TNO Medical Biological Laboratory. The three main topics of this department are:

a) Assessment of the induction and repair of DNA damage *in vitro* and *in vivo* in cells exposed to genotoxic agents, in relation to genetic and/or phenotypic effects, b) Establishment of reliable procedures for biological monitoring of man potentially exposed to genotoxic agents, c) Development of methods for the dosimetry of exposure to ionizing radiation on the basis of biological effects, e.g. induction of lesions in DNA of blood cells.

This project is part of a project coordinated by Dr Favor, Neuherberg, Germany.

Project 1

Head of project: *Dr. Van der Schans*

Objectives for the reporting period

i: Detection of the induction and repair of base damage in DNA of germ cells of the Syrian golden hamster exposed to ionizing radiation at different stages of the spermatogenesis.

ii: Development of a method to detect single-strand DNA breaks at the single-cell level by means of quantitative immunofluorescence microscopy.

Progress achieved, including publications

1. Induction and repair of damage

Exposure of cells to ionizing radiation results in damage to the DNA. This damage comprises strand breaks and base modifications. These damages may lead to mutagenesis and carcinogenesis or, when induced into germ cells, to genetic abnormalities and other hereditary effects in the offspring. It is important, therefore, to inventory and quantify the various damages to get information about their relative contribution and persistency. To this purpose we are developing sensitive immunochemical and biochemical methods to quantify single-strand breaks, alkali-labile sites and base damages. These methods make use of the property of double-stranded DNA to unwind when exposed to alkali, thereby becoming single-stranded at a rate depending on the pH. The immunochemical method is based on the binding of a monoclonal antibody to single-stranded DNA. The technique is based upon the determination of the percentage single-strandedness resulting from the partial unwinding of cellular DNA under strictly controlled alkaline conditions. Strand breaks and alkali-labile sites form initiation points for the unwinding. The extent of unwinding is a measure of the number of such sites. The results are compared with those obtained with "alkaline elution", which assays the extent of unwinding on the basis of the rate at which the DNA passes through the pores of a membrane filter in an alkaline elution fluid. The usefulness of these approaches to detect single-strand breaks, without the requirement to pre-label radioactively the cellular DNA, was demonstrated by detection of damage and its repair in DNA-containing cells of the human blood after *in vitro* and *in vivo* exposure to ionizing radiation. Single-strand breaks (SSB) could be assayed with both techniques down to doses as low as 0.5 Gy.

2. Male germ cells

Subsequently, the attention was focused on male germ cells of the Syrian golden hamster exposed to ionizing radiation at different stages of spermatogenesis. Until now, five stages of the spermatogenesis were investigated, the mid and late spermatocytes, the early and mid spermatids and the elongated spermatids. With both methods the induction and repair was investigated of SSB introduced by $^{60}\text{Co-}\gamma$ -rays. The high sensitivity of the assays permitted to study these processes in the successive stages after exposure of the cells to biologically relevant radiation doses (0 - 8 Gy). With the alkaline elution the germ cells were studied after *in vitro* irradiation, and compared to bone marrow cells of the same animal. As to SSB induction, an essentially linear increase with dose was observed in all 5 stages. With respect to removal, spermatocytes, round spermatids and bone marrow cells showed the normal fast repair when compared to data reported for cultured rodent cells or human lymphocytes. In contrast, in the elongated spermatids, the last stage before the differentiation into spermatozoa, hardly any SSB removal occurred.

With the immunochemical method comparable studies were performed. However, also *in vivo* irradiations were included ($^{137}\text{Cs-}\gamma$ -rays). Both the *in vitro* and the *in vivo* results confirmed the above mentioned observations: exceptional behaviour of the elongated spermatids which did not show removal of SSB up to 90 min after exposure.

In principle, the methods developed also can be used to detect base damages. These, too, can be quantitated via alkaline unwinding provided it is preceded by treatment of the DNA with damage-

oriented endonucleases (*i.c.* a *Micrococcus luteus* extract). These enzymes recognize base damages (BD) in the DNA, upon which they will introduce a break, or remove the modified base thereby leaving an alkali-labile site. This break or alkali-labile site can be detected by means of "alkaline elution". In the experiments performed up to now, BD could be detected after *in vitro* irradiation of human blood in the dose range of 1.5 to 25 Gy. After 5 Gy, measurable BD was still present at 1.5 h after exposure. Also leukemia patients undergoing chemo- and radiotherapy were investigated. These patients were exposed to the cytostatic drug Endoxan followed by total body irradiation. BD induced by doses of 4.5 to 8.6 Gy could be detected, even at 90 min after irradiation.

We also applied this technique on germ cells of the Syrian golden hamster after γ -irradiation.

The initial rate of repair of BD in spermatocytes and bone-marrow cells was in the same range as that for SSB, but only 60-70 % of the initial BD were repaired within 1 h, whereas after that period SSB no longer were detectable. The round spermatids hardly repaired any BD within the first hour after irradiation, but after 7 h only a few BD could be detected.

The results show substantial loss of repair capacity during passage through the different stages of spermatogenesis which appears to be manifest in an earlier stage for the more complicated repair of BD than for the repair of SSB. Because DNA is the major target for mutation induction, the assay applied may be useful for assessment of the genetic risk involved in exposure of male germ cells to ionizing radiation, in relation to the stage of development.

Spermatozoa, which are easily obtainable from male morning urine, probably could provide a biological indicator of radiation damage or injury that is well suited for practical application. So far it was not possible, however, to apply the above mentioned detection methods on spermatozoa, because the DNA stays in the condensed nucleus when the cells are brought into the alkaline solution. Therefore, modifications of the methods had to be introduced, in order to make these cells accessible to investigation of DNA-damage induction and repair. Recently, it appeared to be possible to release and unwind the DNA of bovine and human spermatozoa under adapted controlled alkaline conditions, *i.e.* in the presence of urea, dithiothreitol and a detergent, Triton X100, but in the absence of salt. Under these conditions a much slower unwinding is achieved than in the presence of salt. It appeared that the DNA of both the bovine and human spermatozoa contained an extremely high level of breaks (or alkali-labile sites), in the order of magnitude corresponding to 100-500 Gy γ -irradiation. Probably, this damage is not induced during the alkali-treatment itself since the same treatment applied on human WBC did show the normal low level of damage. Apparently, the previously observed absence of repair in elongated spermatids is continued in the final stage of spermatogenesis resulting in a strong accumulation of, presumably, oxidative damage.

3. Female germ cells

In the TNO Medical Biological Laboratory a technique has been developed to detect DNA damages at the single-cell level. This technique uses monoclonal antibodies directed against specific DNA damages. The antibodies have a fluorescent label which can be detected by making use of a laser-scan microscope. The intensity of fluorescence is a measure for the amount of damage in the cell. It was possible to detect DNA adducts in cultured cells (V79, CHO and HeLa cells) as well as in human skin biopsies that had been exposed to genotoxic chemical agents or to UV light. Because little is known about DNA damage-processing in oocytes, we wish to collect more information about the induction of damage and the repair mechanisms operating in these germ cells. The immunofluorescence method appears to be very suited for the study of DNA-damage induction and repair in oocytes, since it has the advantage that only a few cells are required which is a prerequisite when a study of mammalian oocytes is intended (mice and monkey).

So far, immunofluorescence microscopy was not applied to detect damage in DNA in cells exposed to ionizing radiation. In attempts to use this technique with such cells, an approach was followed analogous to that of the immunochemical assay for the detection of single-strand breaks. We treated γ -irradiated human WBC, after fixation on microscope slides, with 70% formamide in 0.14 M NaCl +0.01 M sodium citrate, at 80°C for 15 min. Treatment with formamide resulted in a more reproducible unwinding under these conditions than treatment with alkali. In a dose range of 0 to 2 Gy a linear dose-response relationship was observed between the single-strand DNA specific fluorescence and the radiation dose. After higher radiation doses the fluorescence leveled off or even decreased, presumably due to loss of single-stranded DNA fragments.

Publications

- Boer, P.J.den, A.A.W.M. van Loon, P. Mackenbach, G.P. van der Schans and J.A. Grootegoed (1990) Effect of glutathione depletion on cytotoxicity of peroxides, xenobiotics and the induction of single-strand DNA breaks by ionizing radiation in isolated hamster round spermatids. *J. of Reproduction and Fertility* 88, 259-269.
- Lehmann, A.R, J.H.J. Hoeijmakers, A.A. van Zeeland, C.M.P. Backendorf, B.A. Bridges, A. Collins, R.P.D. Fuchs, G.P. Margison, R. Montesano, E. Moustacchi, A. T. Natarajan, M. Radman, A. Sarasin, E. Seeberg, C.A. Smith, M. Stefanini, L.H. Thompson, G.P. Van der Schans, C.A. Weber, and M.Z. Zdzienicka (1992) Workshop on DNA repair. Noordwijkerhout, The Netherlands, April 1991. *Mutation Research* 273, 1-28.
- Loon, A.A.W.M. van, G.P. van der Schans, A.J. Timmerman, F.J.A. Kouwenberg, R.H. Groenendijk, P.H.M. Lohman and R.A. Baan (1991) Single-strand breaks and base damage in DNA of human white blood cells in full blood exposed to ionizing radiation detected at biologically relevant doses. *Proceedings NATO Advanced Research workshop: The early effects of radiation on DNA*, San Miniato, Italy, May 1990, Eds. M. Fielden and P. O'Neill. Springer-Verlag Berlin, London, pp 105-106.
- Loon, A.A.W.M. van, G.P. van der Schans and P.H.M. Lohman (1991) Detection of DNA damage in human white blood cells after in vitro or in vivo exposure to ionizing radiation, with alkaline elution and an immunochemical assay. In: *Proc. 23rd Ann. Meeting Eur. Soc. Rad. Biol.*, Dublin, Sep 1990. pp. 107-112.
- Loon, A.A.W.M. van, R.H. Groenendijk, G.P. van der Schans, P. Mackenbach, J.A. Grootegoed, R.A. Baan and P.H. M. Lohman (1991) Immunochemical detection of DNA damage induction and repair at different cellular stages of spermatogenesis of the hamster after in vitro or in vivo exposure to ionizing radiation. *Exp. Cell Res.*, 193, 303-309.
- Loon, A.A.W.M. van, R.H. Groenendijk, A.J. Timmerman, G.P. van der Schans, P.H.M. Lohman and R.A. Baan (1992) Quantitative detection of DNA damage after exposure to ionizing radiation by means of an improved immunochemical assay. *Mutation Res.*, 274, 19-27.
- Loon, A.A.W.M. van, R.H. Groenendijk, G.P. van der Schans, P.H.M. Lohman and R.A. Baan (1990) Detection of base damage in DNA in human blood exposed to ionizing radiation at biologically relevant doses. *Int. J. Radiat. Biol.*, 59, 651-660.
- Loon, A.A.W.M. van, (1992) Radiation induced DNA lesions and their repair in mammalian somatic and germ cells. Thesis, State University Leiden, the Netherlands.
- Loon, A.A.W.M. van, A.J. Timmerman, G.P. van der Schans, P.H.M. Lohman and R.A. Baan (1992) Different repair kinetics of radiation-induced DNA lesions in human and murine white blood cells. *Carcinogenesis*, 13, 457-462.
- Loon, A.A.W.M. van, F.C. Raadsheer, A.J. Timmerman, C. Haanen, J. Wessels, G.P. van der Schans, P.H.M. Lohman and R.A. Baan (1992) Detection of single-strand breaks and base damage in DNA of blood cells from leukemia patients receiving chemo- and radiotherapy. *Int. J. Radiation Biology*, 62, 33-43.
- Schans, G.P. van der (1991) Effect of dose modifiers on radiation-induced cellular DNA damage. *Proceedings NATO Advanced Research workshop: The early effects of radiation on DNA*, San Miniato, Italy, May 1990, Eds. M. Fielden and P. O'Neill. Springer-Verlag Berlin, London, pp 347-362.
- Schans, G.P. van der (1990) Hoe radiotherapie het DNA van tumorcellen beschadigt. *Tijdschrift Kanker*, 14, 128-131.
- Schans, G.P. van der, A.A.W.M. van Loon, P. Boekema, J.C.M. Wessels, P.H.M. Lohman en R.A. Baan (1992) Een gevoelige en snelle immunochemische methode voor biologische stralingsdosimetrie gebaseerd op de detectie van DNA-schade. *Nederlands Militair Geneeskundig Tijdschrift* (in press).

Short communications, abstracts...

- Loon, A.A.W.M. van, G.P. van der Schans, R.H. Groenendijk, P. den Boer, A.J. Grootegoed, P.H.M. Lohman and R.A. Baan (1989) Induction and repair of DNA-damage in different stages of the spermatogenesis of the Syrian goldhamster as detected with an immunochemical assay. *Abstract Ned.Ver. Rad. Biol. meeting*, March 1990, Utrecht, *Int.J. Radiat. Biol.* 55, 1040, and *Book of abstracts 22nd meeting Eur. Soc. Radiation Biology*, September 1989, Brussels, p. 93

(abstract).

- Loon, A.A.W.M. van, F.C. Raadsheer, A.J. Timmerman, P. Muus, G.P. van der Schans, R.A. Baan, P.H.M. Lohman, 1990. Detection of single-strand breaks and base damage in DNA of human white blood cells after *in vitro* or *in vivo* exposure to ionizing radiation at biologically relevant doses. Abstract Ned.Ver. Rad. Biol. meeting, March 1990, Utrecht, Int.J. Radiat. Biol. 58, 1046.
- Loon, A.A.W.M. van, G.P. van der Schans, A.J. Timmerman, F.J.A. Kouwenberg, R.H. Groenendijk, P.H.M. Lohman and R.A. Baan (1990) Single-strand breaks and base damage in DNA of human white blood cells in full blood exposed to ionizing radiation detected at biologically relevant doses. NATO Advanced Research workshop: the early effects of radiation on DNA, San Miniato, Italy, May 1990 p. 40 (abstract)
- Loon, A.A.W.M. van, G.P. van der Schans, P.H.M. Lohman and R.A. Baan. (1990) New methods to detect DNA damage induction and repair in somatic cells. abstracts book Retraite MW-Dwarsverband Gerontologie, Egmont aan Zee, Oct. 1990.
- Loon, A.A.W.M. van, M. Item-Affentranger, W. Burkart, P.H.M. Lohman and G.P. van der Schans (1990) Detection of DNA damage at the single cell level with monoclonal antibodies after exposure to ionizing radiation. Book of abstracts , 23rd Ann. Meet. Eur. Soc Rad. Biol., Dublin, Sep 1990.
- Loon, A.A.W.M. van, G.P. van der Schans, P.H.M. Lohman and R.A. Baan. (1991), Different repair kinetics of radiation-induced DNA lesions between man and mice, determined with alkaline elution and an immunochemical assay. Book of Abstracts 9th ICRR, Toronto, July 1991.
- Schans, G.P. van der, A.A.W.M. van Loon, A.J. Timmerman, F.J.A. Kouwenberg, R.H. Groenendijk and R.A. Baan, 1990, Immunochemical and biochemical detection of single-strand breaks and base-damage in DNA of human white blood cells in full blood exposed to ionizing radiation at biologically relevant doses. J. Cellular Biochem., 14A, 79 (abstract)
- Schans, G.P. van der, A.A.W.M. van Loon, A.J. Timmerman, F.J.A. Kouwenberg, R.H. Groenendijk, P.H.M. Lohman and R.A. Baan, 1991, Single-strand breaks and base damage in DNA of human white blood cells in full blood; Detection after *in vitro* and *in vivo* exposure to ionizing radiation at biologically relevant doses. Book of abstracts of "Workshop on DNA repair with emphasis on eukaryotic systems. Noordwijkerhout, The Netherlands, April 1991.
- Baan, R.A., J.H.M. van Delft, A.A.W.M. van Loon, L. Roza, G.P. van der Schans (1992) Detection of DNA damage induced by radiation and genotoxic chemicals by use of sensitive immunochemical, physicochemical and biochemical techniques. Mutagenesis (in press).
- Schans, G.P. van der, (1991) Induction and repair of single-strand breaks and DNA base damage at different stages of spermatogenesis of the hamster after *in vitro* exposure to ionizing radiation. EC Concerted Action Programme on DNA repair and cancer. Meeting, Oct. 1991, London (abstract 5C).
- Schans, G.P. van der, A.A.W.M. van Loon, A.J. Timmerman, F.J.A. Kouwenberg, R.H. Groenendijk, P.H.M. Lohman and R.A. Baan, 1991, Detection of radiation-induced single-strand breaks and base damage in DNA of human white blood cells in full blood after *in vitro* and *in vivo* exposure. Book of abstracts 9th ICRR, Toronto July 1991.
- Schans, G.P. van der, A.A.W.M. van Loon, A.J. Timmerman, F.J.A. Kouwenberg, R.H. Groenendijk, P.H.M. Lohman and R.A. Baan, 1991, Single-strand breaks and base damage in DNA of human white blood cells in full blood; Detection after *in vitro* and *in vivo* exposure to ionizing radiation at biologically relevant doses. Book of abstracts of "Workshop on DNA repair with emphasis on eukaryotic systems. Noordwijkerhout, The Netherlands, April 1991.
- Schans, G.P. van der, A.A.W.M. van Loon, A.J. Timmerman, F.J.A. Kouwenberg, R.H. Groenendijk, P.H.M. Lohman and R.A. Baan, 1992, Differences in repair kinetics of radiation-induced DNA lesions between man and mice, and between radioprotection *in vitro* and *in vivo*. Abstract Ned.Ver. Rad. Biol. meeting, March 1992, Leiden, Int.J. Radiat. Biol. (in press)
- Schans, G.P. van der, A.J. Timmerman, R.H. Mars-Groenendijk and R.A. Baan (1992) *In vivo* induction and repair of single-strand breaks and base damage in DNA of blood cells and germ cells exposed to ionizing radiation. Abstract Joint Meeting of the Association for Radiation Research, Netherlands Radiobiology Society, Swedish Radiobiology Society, St Andrews, (UK), April 1992, Int. J. Radiat. Biol. (in press).

RADIOBIOLOGICAL PROPERTIES OF SPERMATOGONIAL STEM CELLS IN C3H/101 HYBRID MICE AND EVALUATION OF THE MODEL FOR INDUCTION OF GENETIC DAMAGE IN SPERMATOGONIAL STEM CELLS

Contract Bi7-052 - Sector B14

1) *De Rooij*, Univ. Utrecht

Summary of project global objectives and achievements

In 1981, Leenhouts and Chadwick published a theoretical model which fitted most of the data on the induction of translocations by ionizing radiation in mouse spermatogonial stem cells. In this model it was assumed that there are radiosensitive and radioresistant spermatogonial stem cells, for both cell killing and the induction of translocations, although no D_0 values for killing of the different types of stem cells were known at that time.

In recent years it has become clear that both the radiosensitivity for cell killing and the proliferative activity of the spermatogonial stem cells, varies during the cycle of the seminiferous epithelium. In CBA mice it was found that when the stem cells are actively proliferating (epithelial stages IX-III), they have a D_0 value for X-rays of approximately 2.4 Gy and when these cells are quiescent (stages VI-VII) the D_0 is 1.0 Gy. This relation between proliferative activity and cell killing is closely similar to that found earlier in Cpb-N mice after fission neutron irradiation. Hence, quiescent spermatogonial stem cells are highly sensitive to the cell killing effect of irradiation and they are much more resistant during active proliferation.

Unfortunately, only few data on the induction of genetic damage in the above mentioned strains of mice are available. Therefore, we now study C3H/101 F1 (3H1) hybrid mice, which are the most widely used type of mice in radiation genetic studies. Answers to the following questions have been sought:

1. What are the D_0 values for killing of proliferating and quiescent stem cells by X-irradiation in 3H1 mice?

It was found that the largely proliferating stem cell population in epithelial stage IX up to stage III has a D_0 value of 2.5 Gy and 1.1 Gy for the largely quiescent stem cells in stages VII and VIII.

2. How many stem cells are present per 3H1 testis and what is the density of these cells during the epithelial cycle?

Cell counts and image analysis techniques revealed that there are about 35,000 spermatogonial stem cells in each 3H1 testis. The average density of the stem cells during the epithelial cycle is 11.8 per 1000 Sertoli cells with a low of 9.0 in stage I and a high of 14.4 in stage VI.

3. What are the approximate numbers of proliferating and quiescent stem cells in a 3H1 mouse testis?

The results of the cell counts indicate that the undifferentiated spermatogonia, including the stem cells, proliferate actively from stage XII to stage III. Consequently, the numbers of proliferating and quiescent stem cells per testis can be estimated to be about 15,000 and 20,000, respectively. These numbers will be compared with the numbers of radioresistant and radiosensitive stem cells per testis as will be determined in a dose-response experiment with fission neutron irradiation, the cell counts of which are presently taking place.

Project 1

Head of project: *Dr. De Rooij*

Objectives for the reporting period

The objectives for the reporting period were:

1. To finish the cell counts for the dose-response experiment with graded doses of X irradiation.
2. To determine the number of spermatogonial stem cells during the cycle of the seminiferous epithelium, and the total number of these cells per 3H1 mouse testis by way of cell counts in whole-mounts of seminiferous tubules and image analysis techniques.
3. To perform cell counts for a dose-response experiment with fission neutron irradiation and to determine D_0 values for stem cell killing and the numbers of repopulating colonies after graded doses of irradiation. As the dose effect relationship after fission neutron irradiation gives no shoulder these data should enable us to calculate the approximate numbers of radioresistant and radiosensitive stem cells per testis.

Progress achieved including publications

1. Dose-response experiment with graded doses of X-irradiation

The cell counts for this experiment have been completed now. However, the statistical analysis of the data is not finished yet. Nevertheless, although many more data have been gathered it has become clear that they are not significantly different from the preliminary data reported previously.

2. Quantitative study of spermatogonial multiplication in the 3H1 mouse

Counts have been performed of all types of spermatogonia throughout the cycle of the seminiferous epithelium (Table 1). The average number of stem cells (A_s spermatogonia) was found to be 11.8 per 1000 Sertoli cells, the numbers in each epithelial stage fluctuating between 9.0 (stage I) and 14.4 (stage VI).

The data further show that at first in stages IX-XI the number of A_{s1} spermatogonia is low, only chains of 4 being present. Thereafter, the numbers of both A_{pr} and A_{s1} spermatogonia start to increase and during the ensuing stages more and more A_{s1} spermatogonia are formed of increasing chain length. In stages VII-VIII virtually all A_{s1} and many A_{pr} spermatogonia differentiate and become the first generation of the so-called differentiating spermatogonia, the $A1$ spermatogonia.

The $A1$ spermatogonia start a series of divisions ultimately rendering preleptotene spermatocytes via $A2$, $A3$, $A4$, In and B spermatogonia. From the numbers of these cells per 1000 Sertoli cells it can be inferred that many differentiating type A spermatogonia degenerate during these divisions. In fact only 39 % of the maximally possible number of preleptotene spermatocytes is formed, each epithelial cycle.

The course of the numbers of undifferentiated spermatogonia during the cycle of the seminiferous epithelium (Figure 1) indicates that these cells proliferate actively from about stage XII up to stage III and that they are largely quiescent from stage IV to stage XI.

Table 1: Numbers of spermatogonia per 1000 Sertoli cells in the different stages of the cycle of the seminiferous epithelium of 3H1-mice (\pm SEM; n=5).

Stage	Undifferentiated spermatogonia				Differentiating spermatogonia
	A _s	A _{pr}	A _{al-4}	A _{al-3+}	
IX	13.0 \pm 0.6	13.0 \pm 1.6	2.8 \pm 0.9	0	207 \pm 7 (A1)
XI	9.6 \pm 0.9	11.6 \pm 1.7	2.6 \pm 1.5	0	301 \pm 11 (A2)
I	9.0 \pm 0.3	23.2 \pm 1.7 ^a	18.2 \pm 2.3 ^a	1.4 \pm 0.7	445 \pm 9 (A3)
II	12.0 \pm 0.3 ^a	29.0 \pm 0.8 ^b	54.8 \pm 3.0 ^a	34.0 \pm 3.4 ^a	704 \pm 4 (A4)
IV	13.0 \pm 0.3	36.2 \pm 2.4	59.2 \pm 5.2	84.0 \pm 4.2 ^a	1368 \pm 14 (In)
VI	14.4 \pm 0.7	35.2 \pm 2.9	55.8 \pm 5.9	132.2 \pm 12.9 ^b	2694 \pm 18 (B)
IX	13.0 \pm 0.6	13.0 \pm 1.6	2.8 \pm 0.9	0	5137 \pm 69 (Pl)

a, b: significant changes between previous stage and indicated stage, as determined by the student t-test (a: $p < 0.01$, b: $p < 0.05$).

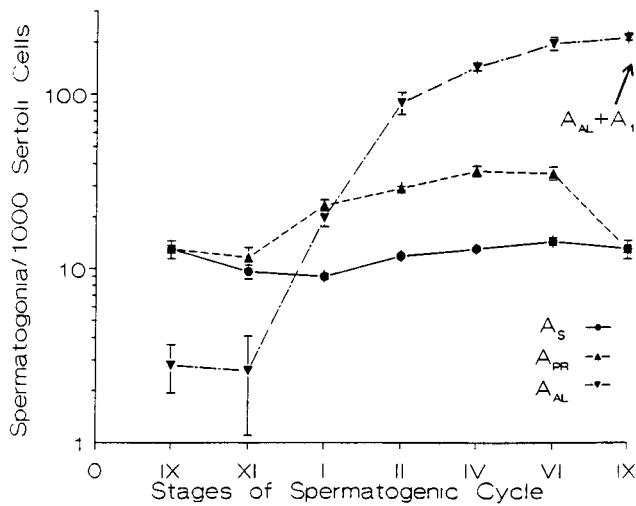


Figure 1: The numbers of the various types of undifferentiated spermatogonia (A_s, A_{pr} and A_{al} spermatogonia) in various epithelial stages of the 3H1 mouse.

Using the disector method as described by Sterio (J. Microsc. 184, 127-136, 1984) and image analysis, the number of Sertoli cells was determined and found to be $3.0 \pm 0.2 \cdot 10^6$ per testis. As the average number of A₁ spermatogonia throughout the epithelial cycle was found to be 11.8 ± 0.4 per 1000 Sertoli cells the number of stem cells per testis can be calculated to be about $35,000 \pm 500$ per testis. As the proliferative activity of the stem cells largely follows that of the undifferentiated spermatogonia being active in stages XII-IV and mostly quiescent in stages IV-XI, it can be roughly estimated that in each testis there are 15,000 proliferating and 20,000 quiescent stem cells.

3. Dose-response experiment with graded doses of fission neutron irradiation

A dose-response experiment has been carried out in which 3H1 mice received graded doses of 1MeV fission neutron irradiation ranging from 0.25 to 3 Gy. Mice were killed 6 or 10 days after irradiation and whole mounts of seminiferous tubules were prepared. D₀ values for stem cell killing and the size of the repopulating colonies will be determined as described earlier (Van Beek et al. 1986. Radiation Res. 108, 282-295). As the dose effect relationship after fission neutron irradiation gives no shoulder, these data will enable the calculation of the approximate numbers of radioresistant and radiosensitive stem cells per testis.

The cell counts for this experiment are presently being carried out. At present no data on D₀ values or colony size are available.

Publications

- Van der Meer, Y., Tegelenbosch, R.A.J., Cattanach, B.M., and De Rooij, D.G. 1992. Proliferative activity and radiosensitivity of spermatogonial stem cells in C3H/101 F1 hybrid mice. Int. J. Radiat. Biol. In press. Abstract.
- Van der Meer, Y., Cattanach, B.M., and De Rooij, D.G. The radiosensitivity of spermatogonial stem cells in C3H/101 F1 hybrid mice. In preparation.
- Tegelenbosch, R.A.J., and De Rooij, D.G. A quantitative study of spermatogonial multiplication and stem cell renewal in the C3H/101 F1 hybrid mouse. In preparation.

STUDIES ON SPONTANEOUSLY-ARISING GENETIC AND PARTIALLY GENETIC DISORDERS IN MAN WITHIN THE FRAMEWORK OF THE EVALUATION OF GENETIC RADIATION HAZARDS

Contract Bi6-226 - Sector B14

1) *Lohman* , Univ. Leiden, Sylvius Labor.

Summary of project global objectives and achievements

This project is aimed at (i) making detailed analyses of the naturally-occurring multifactorial, Mendelian and chromosomal diseases in man in order to assess the validity of the estimates of prevalence and of assumptions currently used in the context of the evaluation of genetic radiation hazards in man; (ii) making use of the data on prevalences and those that bear on the severity of these diseases to arrive at estimates of detriment and (iii) exploring and devising methods that can be used for making quantitative estimates of risk of multifactorial diseases associated with exposure to ionizing radiation.

The work completed during 1990, 1991 and the first few months of 1992 include, first, a thorough re-examination of the concepts and assumptions used in genetic risk estimation and a critical analysis of the impact of knowledge on the nature of mutations (spontaneous and radiation-induced) on the estimation of risk of Mendelian disease due to radiation exposures and second, analysis of the data (epidemiological and aetiological aspects) on severe visual and hearing defects in Hungarian school-age children and their use in estimating detriment associated with these conditions; this part of the work was carried out in close collaboration with Dr. A. Czeizel, National Institute of Hygiene, Budapest, Hungary. Additionally, a beginning has been made to analyse the existing information on multifactorial diseases.

Project 1

Heads of project: *Prof. Lohman, Prof. K. Sankaranarayanan*

Objectives for the reporting period

For the period (1990, 1991 and the first few months of 1992) covered by this final report, the main objectives have been (1) a re-examination of the concepts and assumptions used in genetic risk estimation and a critical analysis of the impact of advances on the nature of mutations (spontaneous and radiation-induced) on the estimation of the risk of Mendelian disease due to exposures to ionizing radiation; (2) an analysis of the data (epidemiological and aetiological aspects) on severe visual and hearing defects in Hungarian school-age children and their use in estimating detriment associated with these conditions and (3) to begin compiling and analysing data on multifactorial diseases in man with emphasis on prevalences, recurrence risks, the aetiological factors and models that have so far been used to explain their prevalences and recurrence risks; this information is essential for the development of mathematical models that can be used for estimating risk of these conditions in an irradiated population.

Progress achieved including publications

1. Re-examination of concepts and assumptions used in genetic risk estimation and analysis of the impact of knowledge on the nature of mutations to the estimation of radiation risk of Mendelian disease. Some of the principal conclusions from this part of the work are the following: (i) about 50% of naturally-occurring Mendelian diseases are due to point mutations (base-pair changes in the DNA) while the remainder are due to deletions or other gross changes; (ii) point mutations do not appear to be distributed at random throughout the gene; likewise, the breakpoints of deletions are also non-randomly distributed; (iii) in mouse germ cells, most radiation-induced mutations are DNA deletions and this is also generally true of radiation-induced mutations in mammalian somatic cell systems studied in vitro; (iv) on the basis of chromatin and DNA organization in cells and the biophysical and microdosimetric properties of ionizing radiation, one can qualitatively explain the predominance of deletions; for spontaneously-arising and radiation-induced point mutations, there may be common elements in mechanisms, but for spontaneously-arising and induced deletions, the extent of overlap in mechanisms is difficult to discern at present.

On the basis of these and other findings, arguments were advanced to support the thesis that (i) ionizing radiation is probably not efficient in inducing the very specific molecular changes that are known to underlie spontaneous mutations which cause naturally-occurring Mendelian diseases; (ii) the doubling dose estimate of 1 Gy that is currently used to estimate risk for these diseases is conservative; (iii) the 1% prevalence figure for these diseases that is used for this purpose may be too high; (iv) if arguments (ii) and (iii) mentioned above are valid, the current estimate of risk of dominant and X-linked diseases may need to be revised downwards; (v) the choice of an overall doubling dose for genetic risk estimation (which takes into account the numerically very large class of multifactorial diseases and for which there is no simple relationship between mutation and disease) depends on what

indicators are perceived to be relevant in the human context and is largely judgemental and (vi) since, among radiation-induced mutations, recessives predominate, adverse genetic effects of radiation exposure are primarily those associated with induced recessives in the heterozygous condition.

2. Severe visual and hearing handicaps in Hungary. In Hungary, the school-age (7-14 years) prevalences of severe visual handicaps and of profound childhood deafness have been estimated to be about 6/10⁴ and 10/10⁴, respectively. Most of these conditions have onset at birth or in early childhood and are aetiologically heterogeneous.

Severe visual handicaps have been grouped under 11 aetiological categories, their relative contributions to the prevalence being, perinatal damage syndrome (20%; half of this is due to retinopathy of premature infants), cataracts (15%), choroidoretinal degenerations (15%), congenital abnormalities of the eye (15%), syndromes (10%), high myopia with or without retinal detachment (7%), postnatal causes (5%), nystagmus (5%), optic atrophy (4%), bilateral retinoblastoma (2%) and prenatal causes (2%). Overall, Mendelian conditions (included under many of the above) account for about 50% with relatively more autosomal dominant than autosomal recessive and X-linked entities, and acquired causes, for about 40% of the cases studied. No aetiology could be assigned in 10% of the cases.

For profound childhood deafness, the rank order of the aetiological categories is: autosomal recessive entities (34%), postnatal causes (22%), perinatal causes (19%), autosomal dominant entities (17%), prenatal causes (5%) and unknown causes (3%).

Severe childhood visual handicaps are responsible for about 60 years of loss of life per 10⁴ livebirths and about 400 years of impaired life per 10⁴ livebirths. Genetic causes account for one-quarter of lost life years and three-quarters of impaired life years. The comparable estimates for profound childhood deafness are: about 240 years of life loss per 10⁴ livebirths (again, about one-quarter due to genetic causes) and about 640 years of impaired life 10⁴ livebirths (about one-half due to genetic causes). In all these calculations, it has been assumed that the average life expectancy at birth for an individual in the population is 70 years.

3. Multifactorial diseases. A beginning has been made to compile data on the prevalence of congenital abnormalities (CAs) in man and comparisons between the results of different studies. The salient conclusions are the following: (i) the prevalence estimates in the different studies vary over a wide range, from about 1% in livebirths to a high of about 8.5% in total (still + livebirths) depending on, among others, definition, classification and diagnostic criteria, entities included, method of ascertainment, duration of follow-up of liveborn children, sample sizes etc; (ii) a comparison of the estimates of prevalence in Hungary (A. Czeizel and K. Sankaranarayanan, Mutation Res 128, 73-103, 1984) with those in the Canadian province of British Columbia (P. Baird et al, Am. J. Hum. Genet. 42, 677-693, 1988) shows that under conditions of good ascertainment, the overall prevalences are similar and are of the order of about 6-7%; (iii) the CAs are aetiologically heterogeneous and can result from diverse causes; considered as a whole, the relative proportions of isolated CAs due to single gene mutations, chromosomal anomalies and environmental (including maternal) factors are about 6%, 5% and 6%, respectively; for about two-thirds of the remaining 80%, twin and family studies suggest a complex aetiology depending on polygenic predisposition and environmental factors that may also be multiple; (iv) for the well-studied isolated CAs, the proportion of affected first-degree relatives is many times (from about 5 to 50-fold) that in the general population, depending on the

birth frequency of the particular CA in the general population; (v) there is a sharp decrease in the proportion affected as one passes from first to second to third-degree relatives; (vi) the recurrence risks depend on the number of affected family members, severity of the index case and whether one sex is more frequently affected and (vi) the Multifactorial Threshold Model (MTM) provides a satisfactory explanation for the inheritance patterns observed, and a useful framework to estimate recurrence risks.

The MTM rests on the assumptions that (i) all environmental and genetic causes can be combined into a single continuous variable termed "liability"; (ii) the distribution of liability is normal (Gaussian) and the affected individuals are those for whom the liability falls beyond a certain threshold value; (iii) liability is determined by a combination of genetic and environmental factors and the genetic factors are polygenic i.e., numerous acting additively without dominance or epistasis, each contributing a small amount of liability and (iv) environmental contributions to the aetiology of the disorder are due to many events whose effects are additive.

Publications 1990-1992

- Czeizel, A., K. Sankaranarayanan, M. Szondy (1990) The load of genetic and partially genetic diseases in man. III. Mental retardation. *Mutation Res* 232, 291-303.
- Lohman, P. H. M., K. Sankaranarayanan and J. Ashby (1992) Choosing the limits to life. *Nature* 357, 185-186.
- Sankaranarayanan, K (1990a) Genetic risks to man from exposure to long-lived radionuclides. *J. Radioanalytical and Nuclear Chemistry, Articles*, 138, 271-291.
- Sankaranarayanan, K (1990b). Some problems and considerations in the assessment of genetic risks of exposure to ionizing radiation. *In Mutation and the Environment* (M. L. Mendelsohn and R. J. Albertini, Eds), Part C, Wiley-Liss Inc, N. Y., pp 233-245.
- Sankaranarayanan, K (1990c). How healthy or sick are we, genetically speaking? *Proc. Workshop on Genetic Effects of Ionizing Radiation* (D. J. TerMarsch and N. E. Gentner, Eds), AECL Res, Chalk River Laboratories, Chalk River, Canada, AECL-10230, pp 11-12.
- Sankaranarayanan, K (1990d) Genetic effects of ionizing radiation: 1988 UNSCEAR estimates and future perspectives. *Proc. Workshop on Genetic Effects of Ionizing Radiation* (D. J. TerMarsch and N. E. Gentner, Eds) AECL Res, Chalk River laboratories, Chalk River, Canada, AECL-10230, pp 21-22.
- Sankaranarayanan, K (1991a) Ionizing radiation and genetic risks. I. Epidemiological, population genetic, biochemical and molecular aspects of Mendelian diseases. *Mutation Res* 258, 3-49.
- Sankaranarayanan, K (1991b) Ionizing radiation and genetic risks. II. Nature of radiation-induced mutations in experimental mammalian in vivo systems. *Mutation Res* 258, 51-73.
- Sankaranarayanan, K (1991c) Ionizing radiation and genetic risks. III. Nature of spontaneous and radiation-induced mutations in mammalian in vitro systems and mechanisms of induction of mutations by radiation. *Mutation Res* 258, 75-97.
- Sankaranarayanan, K (1991d) Ionizing radiation and genetic risks. IV. Current methods, estimates of risk of Mendelian disease, human data and lessons from biochemical and molecular studies of mutations. *Mutation Res* 258, 99-122.
- Sankaranarayanan, K (1991e) Genetic effects of ionising radiation in man. *Annals of the ICRP* 22, 75-94.

Sankaranarayanan, K and A. Czeizel (1991) Disease Spectrum, Chapter XII, In Genetics of the Hungarian Population (A. Czeizel et al, Eds), Akademiai Kiado, Budapest and Springer-Verlag, Heidelberg, 1991, pp 237-280.

In press 1992

Baverstock, K. F., and K. Sankaranarayanan. Alpha particles and human leukaemia. *Nature*.

Czeizel, A., K. Skirpeczky, E. Mester and K. Sankaranarayanan. The load of genetic and partially genetic diseases in man. IV. Severe visual handicaps and profound childhood deafness in Hungarian school-age children. *Mutation Res.*

Sankaranarayanan, K. Risk estimates for hereditary effects of ionizing radiation. In Proc. Int. Workshop on Recent Advances in Radiobiology, (19 September 1991) Ferrara, Italy.

Sankaranarayanan, K. Ionizing radiation, genetic risks and radiation protection. In Proc. Int. Conf. on Radiation Effects and Protection, (March 18-20, 1992) Mito, Japan.

Sankaranarayanan, K. Estimates of genetic risks of exposure to ionizing radiation and their use in radiation protection: the 1992 status. *J. Radiation Protection*.

MOLECULAR BIOLOGY OF PATERNAL ONCOGENESIS

Contract Bi7-068 - Sector B14

1) *Höfler* , GSF Neuherberg

Summary of project global objectives and achievements

The tumor suppressor genes have been identified as key loci that are inactivated during carcinogenesis. Molecular and cytogenetic analysis has established that inactivation of both alleles (two hit model) at a tumor suppressor locus is required for inactivation and the resulting propensity to carcinogenesis. The Knudson hypothesis predicts that in offspring of individuals where one allele at a tumor suppressor locus has already been mutated or lost in the germ line only a single inactivational event at the tumor suppressor locus will be required for inactivation. Consequently an F1 generation inheriting a mutated allele at a tumor suppressor locus will show a much greater sensitivity to radiation-induced carcinogenesis compared with a population inheriting two normal alleles. This model has direct parallels in human populations where multiple generations are exposed to environmental agents capable of inactivating tumor suppressor genes.

Our goal is to investigate the molecular basis for such increased sensitivity, and to use this knowledge to identify at risk populations. We have designed an animal model whereby parental germ-line mutations are introduced by chemical carcinogenesis, and the sensitivity of the F1 generation is assessed by administration of a low dose of an alpha-emitting radionuclide.

We have demonstrated that the chemical carcinogen ethylnitrosourea (ENU) induced germ-line mutations that were transmitted to the F1 offspring. These offspring, when challenged with low dose irradiation, showed the anticipated increased sensitivity to ionizing radiation, with a highly significant increase in the incidence of osteosarcoma formation. Tissue samples have been collected from the experimental animals and will be used in future studies to determine the inheritance pattern of mutations at tumor suppressor loci.

Project 1

Head of project: *Dr. Höfler*

Objectives for the reporting period

For this reporting period the objective of the project is to establish an experimental animal model of germline-induced increased sensitivity according to the Knudson hypothesis. Such a model will allow the molecular-genetic tracing of the inheritance of mutations in tumor-relevant genes.

Progress achieved

1. Chemical mutagenesis of the male parental germ line

To efficiently introduce quantifiable mutations into the paternal germ line we treated male mice with the chemical carcinogen ethylnitrosourea. Male mice, 80 days old C3Hx102/F1, received a single i.p. injection of the chemical mutagen 160 mg ethylnitrosourea (ENU)/ kg body weight or a placebo injection of physiological saline solution. After allowing a 5 month recovery these males were mated with T-stock females.

In order to check the efficiency of the induced mutation the frequency of recessive specific locus mutations was determined in the F1-generation. There were 0.5% (5/955) phenotypically identifiable mutations in the F1-generation offspring of ENU treated males and 0% (0/1057) in the F1-generation of saline treated males ($p=0.024$). We are thus able to infer that the ENU-treated male parents have indeed passed mutations to the F1 generation. Consequently this F1 generation will serve as a valid model for assessing increased tumourigenic risk after exposure to ionizing radiation.

2. Osteosarcomagenesis in F1 offspring of ENU treated male parents after exposure to a low-dose alpha-emitting bone seeking radionuclide

One half of the F1 generation born of ENU treated or saline treated males received a single i.p. injection of 37 kBq ²²⁷Thorium/kg at the age of about 100 days. This activity of the short-lived (18.7 days half life) alpha-emitting bone-seeking radionuclide corresponds to a mean skeletal dose of 2 Gy. In an untreated mouse population this would be expected to lead to a lifetime osteosarcoma expectancy of about 20%. After 13,5 months of the experiment the number of osteosarcomas observed after incorporation are significantly higher amongst the offspring of ENU-treated male

parents compared to the offspring of control animals (Table). This confirms that the parental exposure has indeed led to an increased sensitivity of the osteogenic tissue of the F1 generation to alpha-irradiation-induced carcinogenesis.

3. Molecular analysis of inherited mutations in F1 offspring of ENU-treated male parents

Our own studies have shown that mutation of the p53 tumour supresor locus is very frequent in radiation-induced murine osteosarcomas, where inactivation of both p53 alleles is associated with carcinogenesis. Evidence from clinical genetics predicts that parental transmission of a mutated p53 allele will predispose the F1 generation to tumor formation (Knudson Hypothesis). Consequently we intend to analyse the frequency of p53 mutations in the F1 and parental generations, and observe if tumour incidence in the F1 generation is associated with inheritance of a mutated p53 allele. At the same time this study will allow us to compare the mutation rate of the p53 locus determined by DNA sequencing, to that identified by phenoytpic characterisation in the specific locus test. The experimental hypothesis is that that complete sequencing of a tumor-relevant target-gene might be a more sensitive mutagenicity test . Consequently we have collected tissue samples for DNA analysis from the experimental animals in the study. In the group with ENU-treated males maternal was collected from 24 parent couples and 66 female and 72 male F1 animals. In the group with saline-treated males material was collected from 23 parent couples and 57 female and 46 male F1 animals.

Table: Osteosarcoma induction 13,5 months after incorporation of 37 kBq 227Th/kg in 100 days old offspring of [Tx(C3Hx102)F1] mice. Comparison of groups with ENU-treated (160 mg/kg 5 months before mating) and saline treated fathers.

F1 group	Paternal exposure	Treatment	Females	Males	Females + Males
PO KO	saline	saline	0% (0/69)	0% (0/72)	0% (0/141)
PO T	saline	227Th	2% (1/65)	0% (0/66)	1% (1/131)
PE KO	ENU	saline	0% (0/70)*	0% (0/68)	0% (0/138)**
PET	ENU	227Th	6% (4/66)*	2% (1/66)	4% (4/132)**

*p=0.053

**p=0.027

OSTEOSARCOMA AND TUMOURS OF THE HAEMOPOIETIC SYSTEM BY LOW-DOSE IRRADIATION

Contract Bi7-002 - Sector B15

- 1) Höfler , GSF Neuherberg - 2) Höfler , Univ. München - Technische
3) Erfle , GSF Neuherberg - 4) Skou Pedersen , Aarhus Universitet
5) Schoeters , CEN - SCK - 6) Bentvelzen , TNO - ITRI

Summary of project global objectives and achievements

The objective of this project is to facilitate the more precise quantification and understanding of the risk of radiation-induced carcinogenesis. Exposure to low doses of alpha-emitting bone seeking radionuclides has been selected as an experimental model. Previous studies under the radiation protection programme have shown that human exposure to bone-seeking radium and thorium radionuclides results in osteosarcoma. Animal modelling has already broadly defined the dose-response relationship.

Although therapeutic use of alpha-emitting radionuclides has been largely discontinued, human exposure may still occur in the environment from the use of nuclear energy, disposal of radioactive waste and exposure to radon and its daughters. This pattern of exposure may be anticipated to result in a low-dose irradiation of sensitive tissues, particularly the physiologically interrelated bone and bone marrow cell populations. Thus, protection of the general population by definition of carcinogenic dose levels, and identification of at risk individuals remain the necessary objectives of radiation protection.

Identification of the radiation-induced molecular lesions that directly lead to cancerogenesis will allow a more accurate assessment of the dose-effect relationship, and will permit a monitoring of at risk individuals. Our experimental goal is to use a range of model systems to identify those molecular mechanisms involved in radiation-induced tumorigenesis. We have adopted an integrated approach to this problem, combining animal studies with *in vitro* cell culture systems and molecular biological analysis.

Global objectives

- 1) Identification of the bone cell population at risk from exposure to bone-seeking alpha-emitting radionuclides.
- 2) Analysis of the molecular events leading to osteosarcomagenesis

Achievements

1. Identification of the cell population at risk

The osteoprogenitor population of the murine bone marrow represents a potential target for transforming effects of irradiation. We have succeeded in partly characterizing a marrow stromal cell population responsible for production of cells committed to the osteoblast lineage. This cell population has shown a high degree of radiosensitivity in vivo and in vitro (3 mGy/day) when bone-seeking alpha emitters were used. In contrast X ray doses above 4Gy were required to influence osteogenesis by these cells.

Bone seeking radionuclides are rapidly bound to the bone mineralized matrix where they may irradiate the sensitive marrow population indirectly. We have developed an alternative model whereby the radionuclide may accumulate within the sensitive cell population. Using a highly differentiated rat osteosarcoma cell line we have been able to demonstrate that ²²³radium is taken up via the transferrin-transferrin receptor system and incorporated into the iron-sequestering protein ferritin.

2. Analysis of the molecular events leading to osteosarcomagenesis

Molecular events that can initiate or sustain carcinogenesis have been observed in transformed cell populations derived from radiation-induced murine osteosarcoma. these are mutation of the tumour suppressor locus p53, activation of endogenous retroviral elements and insertional mutagenesis.

Alterations in the p53 locus were identified in a great majority of cultured murine osteosarcoma cell lines. These have been characterized and our investigations reveals that the mutational events are highly varied. thus, point mutations, small intragenic deletions and loss of the entire locus have all been observed. The fos oncogene is present in osteosarcoma-inducing retroviruses, and is implicated in

bone tumour development . Our investigations have shown that there is not a direct link between irradiation and transient alterations in fos expression associated with bone cell proliferation. Thus, an acute effect of fos can be excluded from the cascade of radiation-induced events leading to transformation. A potential effect for fos can however be demonstrated in the induction of transcription from retroviral LTRs. These regulatory elements have been shown to possess the ability to regulate expression of both retroviral and adjacent genes. Thus, a radiation-induced fos-mediated activation of LTR transcriptional activity may be involved in the retroviral-mediated transformational events.

Continued investigation of the consequences of endogenous retroviral activation for cell transformation has revealed that the prior infection with active retrovirus can enhance the proliferative consequences of irradiation in a sensitive bone progenitor cell population. Thus we present evidence that not only can irradiation induce retroviral activation, but also the presence of pre-activated retrovirus can potentiate transforming potential of irradiation.

A novel mutational event in radiation-induced tumour formation has been observed. In one osteosarcoma line an endogenous retrotransposon has become inserted into the p53 gene. The resultant disruption of the coding sequence results in a loss of p53 expression. This event has great mechanistic similarity to the retroviral activation event already described, but shows a different pathway for tumorigenic consequences.

In order to detect regions of the genome that are specifically damaged by irradiation the genomic subtraction technique of Straus and Ausubel was applied to radiation-induced tumour material. Using this powerful screening approach a potential target site of radiation-induced gene deletion has been defined, indicative of a potential new tumour suppressor locus.

Project 1

Head of project: *Dr. Höfler*

Objectives for the reporting period

The research completed during this period has been focused upon two areas.:-

Firstly we have completed a series of animal studies to determine the risk of osteosarcomagenesis following acute and transient exposure to a short lived bone-seeking radionuclide (Thorium 227) coinciding with a chronic background exposure to low levels of a long-lived isotope.

Secondly we have investigated the possibility that cellular ferritin may capture and accumulate radioactive bone seeking metals within the sensitive osteoblastic cell population.

Progress achieved Including publications

Low-level long term exposure was produced in three month old female NMRI mice by injecting 1.85 kBq/kg of ²²⁷Actinium (mean skeletal dose 100 cGy per 600 days). The long-term exposure results from the production of the ²²⁷Thorium decay product. Acute exposures were then made at 4 or 12 months using the short-lived alpha-emitter ²²⁷Thorium. (mean skeletal alpha dose burden of 50 cGy and 200cGy at doses of 9.25 and 37 kBq/kg ²²⁷Thorium respectively)

In the lower dose range (Thorium 9.25 kBq/kg or Actinium plus Thorium 9.25 kBq/kg) a similar (i.e. not significantly different) osteosarcoma rate was observed in animals treated at either 4 or 12 months of age. The older age of the animals presumably compensates for the later incorporation of the ²²⁷Thorium. At the higher dose (Thorium 37 kBq/kg or Actinium plus Thorium 37 kBq/kg) the osteosarcoma rate in the older age groups was significantly lower than in those groups receiving Thorium at a young age. Despite this fact, low level background irradiation by ²²⁷Actinium seems to unmask the promoting efficiency of the older age. An increase of the osteosarcoma risk by incorporation of the additional activity of ²²⁷Thorium in animals with a low

activity background burden of ^{227}Ac was significant only for the groups older at the time of ^{227}Th incorporation and is seen at both levels of ^{227}Th activity.

We have determined that osteoblastic cells express considerable levels of the iron-sequestering protein ferritin. The isoform of the protein found in the osteoblasts possesses a preponderance of light-chain ferritin monomers, consistent with a depot / storage function. This bone isoform is comparable to that seen in blood-forming tissues and the kidney. As ferritin is known to be a highly promiscuous metal-binding substrate, we have measured intracellular deposition of bone-seeking ^{223}Ra in osteoblastic ferritin in vitro.

The key step in the uptake of radionuclides into the intracellular environment will be passage across the cell membrane. It is already known that osteoblasts express cell surface receptors for the iron-transport protein transferrin. We have confirmed that a fully functional iron-storage pathway exists in osteoblasts ^{59}Fe -labelled transferrin was readily taken up by osteoblasts, and the ^{59}Fe transferred into the ferritin molecule. We prepared ^{223}Ra -transferrin and used this to determine the uptake of radium into osteoblastic cells. 24 hours after adding ^{223}Ra -transferrin to the culture medium a single radiolabelled protein, co-migrating with native ferritin, was identified by non-denaturing polyacrylamide gel electrophoresis (PAGE) of cell lysates. Immunoprecipitation of the lysate with an anti-ferritin antiserum, followed by non-denaturing PAGE, confirmed the identity of the ^{223}Ra -labelled protein as ferritin. Thus, we have demonstrated that the intracellular metal-storage protein ferritin can serve as a site of intracellular deposition of the bone-seeking radionuclide radium in osteoblasts. The intracellular localization may dramatically influence the dose received by individual cells, and could explain cell-specific carcinogenic actions attributed to bone-seeking nuclides.

Publications

Luz, A., Erfle, V., Strauss, P. G., Müller, K., Schmidt, J., Müller, W. A., Linzner, U., Gössner, W., Höfler, H.: The role of age and genetic background as cofactors in the pathogenesis of radiation-induced osteosarcoma. In: Joint Bone Radiobiology Workshop, Toronto, Canada, July 12-13, 1991 (Ed.: N. J. Parks). University of California, Davis, USA: USDOE Report UCD-472-136, 30-33 (1991)

Luz, A., Müller, W. A., Linzner, U., Strauß, P. G., Schmidt, J., Müller, K., Atkinson, M. J., Murray, A. B., Gössner, W., Erfle, V., Höfler, H.: Bone tumor induction after incorporation of short-lived radionuclides. *Radiat. Environ. Biophys.* 30, 225-227 (1991)

Luz, A., Murray, A. B., Schmidt, J.: Osteoma, spontaneous and virus-induced, mouse. In: ILSI Monographs on Pathology of Laboratory Animals - Cardiovascular and Musculoskeletal Systems (Eds.: T. C. Jones et al.). Berlin: Springer, 182-190 (1991)

Müller, W. A.: Transmission of leukaemia. *Nature* 345, 483-484 (1990)

Müller, W. A., Luz, A., Linzner, U., Murray, A. B.: The combined effect of two different bone-seeking radionuclides on the induction of osteosarcomas in mice. In: *New Developments in Fundamental and Applied Radiobiology* (Eds.: C. B. Seymour and C. Mothersill). London: Taylor & Francis, 64-71 (1991)

Müller, W. A., Luz, A., Linzner, U., Murray, A. B.: The oncogenic risk of alpha doses from osteotropic radionuclides down to the milligray range and the role of the reverse protraction factor. In: *Joint Bone Radiobiology Workshop, Toronto, Canada, July 12-13, 1991* (Ed.: N. J. Parks). University of California, Davis, USA: USDOE Report UCD-472-136, 2-5 (1991)

Müller, W. A., Luz, A., Murray, A. B., Linzner, U.: Induction of lymphoma and osteosarcoma in mice by single and protracted low α doses. *Health Phys.* 59, 305-310 (1990)

Müller, W. A., Murray, A. B., Linzner, U., Luz, A.: Osteosarcoma risk after simultaneous incorporation of the long-lived radionuclide ^{227}Ac and the short-lived radionuclide ^{227}Th . *Radiat. Res.* 121, 14-20 (1990)

Project 2

Head of project: *Dr. Höfler*

Objectives for the reporting period

Our overall objective has been to develop a molecular biological assay system for the quantification of genetic alterations in radiation-induced osteosarcoma. The p53 tumour suppressor locus was selected for analysis as this represents a clinically relevant mutational event in a wide range of human tumours.

We have developed Polymerase Chain Reaction (PCR) techniques for the amplification of short nucleic acid segments of defined loci in tumour materials. Initially the method was established using the retinoblastoma locus (RB1) using formalin-fixed and paraffin-embedded tumour material. Small deletions in the amplified DNA were detectable using high-resolution polyacrylamide gel electrophoresis. This technique proved ideal for the detection of similar deletions in radiation-induced osteosarcomas.

In order to detect the presence of point mutations in tumour material, which are undetectable by conventional electrophoresis, we developed a direct sequencing technique for the sequencing of PCR amplified DNA. This was established and tested using a panel of human tumour materials where mutations in the p53 locus were expected. Using these techniques we have now analyzed mutational events in the p53 locus in radiation-induced osteosarcomas.

Progress achieved including publications

We have analyzed alterations in the murine p53 locus in a number of cell lines established from radiation-induced murine osteosarcomas, provided by partner 01 and partner 03. RNA were isolated from 6 osteosarcoma cell lines established from osteosarcomas arising in 227Th-treated mice and from 2 osteosarcomas arising in control untreated animals. The RNA was reverse transcribed into cDNA and amplified in the PCR. The entire coding region of the p53 cDNA was amplified using primers located in Exon 1 and Exon 11. By careful selection of the Exon 11 primer sequence amplification of the processed p53 pseudogene was avoided. The presence of mutations was determined by direct sequencing of the PCR amplification product, targeting exon 5 and 8 which are mutational hot-spots with a high frequency of mutation in a variety of different human and murine tumours.

In six of the cell lines tested mutations affecting the p53 locus were detectable. In one case both alleles had been deleted from the genome, in three cases small intragenic deletions were seen (ranging from loss of 1 base to deletion of the entire exons 8 and 9). One case showed a single point mutation resulting in an amino acid substitution within an evolutionary conserved domain. In the final case a phenomenon was observed that has significant implications for future research in radiation-induced tumorigenesis.

In this case the expressed p53 mRNA was shown to have contain non-p53 DNA sequences spliced into the middle of the normal normal sequence. This insertional event introduced a premature stop codon into the p53 open reading frame, and is responsible for inactivation of the p53 gene. More detailed analysis of the mutation revealed that the insertion of an endogenous retrotransposon into the p53 gene had taken place. The resulting mRNA transcript is processed incorrectly due to the presence of consensus splice sites present in the retrotransposon. The final mRNA transcript thus contains retrotransposon sequences spliced into the p53 sequence.

Our collaborative partners 03 and 04 have already demonstrated that the activation of endogenous retroviral elements in the genome of irradiated mice results in tumourigenic alteration of the cell phenotype. We now are able to provide a direct link between activation of mobile genetic elements and inactivation of a specific tumour suppressor locus involved in radiation-induced carcinogenesis. We cannot yet determine if the retrotransposon insertion was directly provoked by irradiation or was facilitated as a consequence of the activation of other mobile elements.

Publications

Lohmann, D., Horsthemke, B., Gillessen-Kaesbach, G., Stefani, F. H., Höfler, H.: Detection of small RB1 gene deletions in retinoblastoma by multiplex PCR and high-resolution gel electrophoresis. Hum. Genet. (in press)

Strauss, P. G., Mitreiter, K., Zitzelsberger, H., Luz, A., Schmidt, J., Erfle, V., Höfler, H.: Elevated p53 RNA expression correlates with incomplete osteogenic differentiation of radiation-induced murine osteosarcomas. Int. J. Cancer 50, 252-258 (1992)

Project 3

Head of project: *Dr. Erfle*

Objectives for the reporting period

Radiation-induction of osteosarcomas in mice is associated with a dose-dependent activation and expression of endogenous retroviral sequences. Radiation-activated retroviruses exert significant effects on the mouse skeleton, ranging from excessive new bone formation together with the development of benign bone tumours to the induction of osteosarcomas after infection of newborn mice. Our studies are aimed at the analysis of the role of radiation-activated endogenous retroviruses in the initiation, fixation, enhancement and/or acceleration of radiation-induced genomic alterations as well as at possible cooperative effects of α -irradiation and retrovirus infection on osteogenic differentiation and neoplastic transformation. These objectives are implemented by:

- a) characterization of cooperating effects of α -irradiation and retrovirus infection on cell proliferation in mandibular condyles;
- b) pathogenicity studies of treated tissues and cell lines established therefrom, and
- c) expression studies of transcription factors and growth control genes in treated tissues

Progress achieved including publications

Endogenous retroviruses are activated both in the early latent period of radiation-induced osteosarcomas and in the radiation-induced tumors. "In vitro" and "in vivo" studies have shown, that activated endogenous retroviruses induce significant effects on skeletal cells of the mouse, including induction of osteogenic differentiation and new bone formation as well as induction of benign and malignant bone tumors in infected newborn mice. In order to study a cooperative effect of α -irradiation (^{224}Ra) and retroviral infection on neoplastic transformation of skeletal cells and tissue, mandibular condyles of newborn mice were irradiated with doses ranging between 0.007 kBq/ml and 7.4 kBq/ml ^{224}Ra for 3.5, 7, 10.5, 14, and 21 days in the presence and absence of infectious retroviruses (RFB MuLV). It has been shown that continuous irradiation of mice in this dose range, over a period of 36 weeks, induces osteosarcomas in 10% to 95%. Control tissues were infected with RFB MuLV or not treated. After the end of the treatment period the tissues

were transplanted into syngeneic mice (1 to 4 condyles/mouse). Within an observation period of 3 months after transplantation no tumour development was observed, suggesting, that under these conditions the above doses or the irradiation period are not sufficient to induce malignant transformation of osteogenic tissue cultured "in vitro". To study the effect of irradiation and retrovirus infection on cell growth, the cell number in mandibular condyles was determined after various treatments: irradiation (7 days) was followed by RFB MuLV infection (14 days) and vice versa; controls were either irradiated (21 days) or infected with RFB MuLV or not treated. The highest cell number was observed in tissues which were irradiated for 7 days and infected thereafter with RFB MuLV and cultured further for 14 days. These data suggest that irradiation increases the susceptibility of skeletal cells to the proliferation-inducing effects of RFB MuLV.

Irradiated and/or retrovirus infected mandibular condyles were dissociated by collagenase and single cell suspensions were used to establish monolayer cell lines. The highest cell proliferation was found in cell lines established from tissue which had been irradiated and infected, indicating a cooperative effect of α -irradiation and RFB MuLV infection on growth of skeletal cells.

The *c-fos* protooncogene plays a significant role in osteogenic differentiation, in transdifferentiation of cartilage cells to bone cells, and in terminal differentiation processes of bone cells in osteosarcomas. The *v-fos* oncogene, on the other hand, is a potent inducer of osteosarcomas. Further, "in vivo" studies with *c-fos* transgenic mice indicated that endogenous retroviruses cooperate with cellular oncogenes in bone tumor development.

Northern blot analysis of irradiated mandibular condyles showed a high transient expression of the *c-fos* protooncogene between 30 min and 2 hours after start of the culture and down regulation of *c-fos* after 6 hours similar to that observed in non-irradiated control condyles. In contrast to published reports on fibroblast cell lines using toxic doses of γ -irradiation, increased expression of *c-jun* or *c-myc* was not found in ^{224}Ra -irradiated condyles.

These data suggest that the observed stimulation of cell proliferation is not a result of enhanced transcriptional activity of the growth control genes *c-fos*, *c-jun*, or *c-myc*. Irradiated condyles, however, showed an enhanced RNA level of the T1 gene. T1 is a gene stimulated by the oncogene *Ha-ras* and was isolated from *Ha-ras* transformed NIH3T3 cells. T1 expression was analysed by reverse transcription of total cellular RNA from irradiated condyles and sequence-specific amplification of a 400 bp sequence by PCR. In contrast to non-irradiated tissues, irradiated tissues showed expression of T1 at

2 hours after start of the culture, suggesting that T1 is activated by ^{223}Ra . Further in situ hybridization analysis will be carried out to study the cell type specific expression of genes, which are sensitive to ^{223}Ra in irradiated mandibular condyles.

During the reporting period ^{224}Ra was no longer commercially available. As an alternative, ^{223}Ra was obtained from the GSF-Institute of Pathology, Neuherberg, and subsequent experiments were carried out with ^{223}Ra . For future experiments this radionuclide will be available on request.

Summary

- α -irradiation followed by retrovirus infection increases cell proliferation, suggesting that irradiation enhances the susceptibility of skeletal cells to proliferation-inducing effects of bone-pathogenic retroviruses;
- enhancement of proliferation in low dose-irradiated mandibular condyles is not due to enhanced transcriptional activity or significant induction of the growth control genes *c-fos*, *c-jun* or *c-myc*;
- short term irradiation and/or retrovirus infection are not sufficient for the induction of neoplastic transformation of skeletal tissue "in vitro".

Publications

Goralczyk, R., Closs, E.I., R  ther, U., Wagner, E.F., Strau  , P.G., Erfle, V., Schmidt, J. Characterization of fos-induced osteogenic tumours and tumour-derived murine cell lines. *Differentiation* 44:122-131 (1990).

Closs, E.I., Murray, A.B., Schmidt, J., Sch  n, A., Erfle, V., Strauss, P.G. C-fos expression precedes osteogenic differentiation of cartilage cells in vitro. *J. Cell Biol.* 111:1313-1323 (1990).

Strauss, P.G., Closs, E.I., Schmidt, J., Erfle, V. Osteogenic differentiation of cartilage cells in vitro. *J. Cell Biol.* 110:1369-1378 (1990).

Leib-M  sch, C., Brack-Werner, R., Salmons, B., Schmidt, J., Strau  , P.G., Hehlmann, R., Erfle, V. The significance of retroviruses in oncology. *Onkologie* 13:405-414 (1990).

Pedersen, L., Strauss, P.G., Schmidt, J., Luz, A., Erfle, V., J  rgensen, P., Kjeldgaard, N.O., Pedersen, F.S. Pathogenicity of Balb/c-derived N-tropic murine leukemia viruses. *Virology* 179:931-935 (1990).

Aresu, O., Nicolo, G., Allavena, G., Melchiori, A., Schmidt, J., Kopp, J.B., d'Amore, E., Chader, G., Albini, A. Invasive activity, spreading on and chemotactic response to laminin are properties of high but not low metastatic mouse osteosarcoma cells. *Invasion and Metastasis*. 11:2-13 (1991).

Hallberg, B., Schmidt, J., Luz, A., Pedersen, F.S., Grundström, T. SEF1 transcriptional activators are required for tumour formation by SL3-3 murine leukemia virus. *J. Virol.* 65:4177-4181 (1991).

Luz, A., Müller, W.A., Linzner, U., Strauss, P.G., Schmidt, J., Müller, K., Atkinson, M., Murray, A.B., Gössner, W., Erfle, V., Höfler, H. Bone tumour induction after incorporation of short-lived radionuclides. *Radiat. Environ. Biophys.* 30:225-227 (1991).

Strauss, P.G., Müller, K., Zitzelsberger, H., Luz, A., Schmidt, J., Erfle, V., Höfler, H. Elevated p53 RNA expression correlates with incomplete osteogenic differentiation of radiation-induced murine osteosarcomas. *Int. J. Cancer* 50:252-258, 1992.

Goralczyk, R., Luz, A., Erfle, V., Schmidt, J. Metastatic growth of v-fos-induced osteosarcoma following in vitro cultivation. *Zentralbl. Pathol.* 138:97-102 (1992).

Pedersen, L., Strauss, P.G., Schmidt, J., Luz, A., Pedersen, F.S., Erfle, V. Molecular cloning confirms that the bone-pathogenic RFB virus is a replication-competent MuLV. Submitted.

Project 4

Head of project: *Dr. F. Skou Pedersen*

Objectives for the reporting period

Endogenous retroviruses are frequently activated in association with radiation-induced osteosarcomagenesis in laboratory strains of mice. Our work addresses the following questions of interest for understanding of immediate and late effects of ionizing radiation: How are endogenous proviruses activated? Are the activated viruses pathogenic? What features in a retroviral genome may affect its pathogenicity for bone tissues? What molecular mechanisms may contribute to the effect of a retrovirus on bone cells?

Two approaches are followed in the analysis of proviral genes as targets for radiation carcinogenesis:

- 1) To study the possibility of indirect activation of proviruses through a cellular stress response following radiation
- 2) To analyze genetic alterations in tumour DNA caused by proviral insertion

Progress achieved including publications

ad 1) The protooncogene *c-fos* may be activated as part of the stress response that is an immediate consequence of irradiation. *c-fos* also plays a role in normal osteogenic differentiation, and potential interactions between this protooncogene and a virus are therefore of major interest for understanding the role of activated viruses in the effects of radiation on bone tissues. Our recent transient expression studies indicate that the *c-fos* product can specifically trans-regulate expression from virus LTRs in an osteogenic cell line. This effect is stimulatory at lower levels of *c-fos* expression and inhibitory at higher levels. We have identified a smaller region of the LTR which seems to be responsible for the inhibitory effect of Fos on the transcriptional activity of the LTR. Such regulatory interactions may be involved in both early and late effects of radiation on bone tissue.

ad 2) Our studies of genetic alterations in tumour DNA caused by proviral integrations in DNA from virus-induced and radiation-induced tumours use both Southern hybridization techniques and polymerase chain reaction techniques. Several prototype viruses are included in these studies. The viruses are available as molecular clones and all are closely related to the prototype endogenous ecotropic murine leukemia virus, Akv. The viruses induce lymphomas, osteopetrosis, and osteomas in NMRI mice, but differ in potency of disease induction. In CBA mice, on the other hand the effects are frequent osteomas and rare lymphomas. The pathogenicity data in Table I illustrate the differences between these two mouse strains by results obtained with our most bone-pathogenic isolate, RFB MLV.

TABLE 1

PATHOGENICITY OF RFB AND SL3-3 VIRUSES.

Virus	Mouse strain	Mean latent period (days±SEM)	Osteope-trosis	Osteoma	Osteomas per mouse	Malignant Lymphomas
RFB-14	CBA	363 ±37	0/14	14/14 (100%)	4.4	1/14 (7%)
RFB-18	CBA	386 ±50	0/11	11/12 (92%)	6.5	1/12 (8%)
SL3-3	CBA	189 ±58	0/15	0/15		13/15 (87%)
NIH 3T3 (Neg. control)	CBA	429 ±11	0/16	0/16		0/16
RFB-14	NMRI	233 ±85	5/14 (36%)	2/14 (14%)	5.5	13/14 (93%)
RFB-18	NMRI	221 ±51	8/15 (53%)	1/15 (7%)	1.0	15/15 (100%)
SL3-3	NMRI	126 ±28	2/27 (7%)	0/27		27/27 (100%)
NIH 3T3 (Neg. control)	NMRI	550	0/13	0/13		5/13 (38%)

Among the newly integrated proviruses in radiation induced osteosarcomas, we have focussed upon OTS25, a newly integrated provirus from a radiation-induced osteosarcoma of a BALB/c mouse. In NMRI mice viruses derived from OTS25 induced high incidences of malignant lymphomas (60%) and a lower incidence of osteopetrosis (20%) within a long latency period (496 ± 106 days) (Pedersen et al., 1990). Ongoing pathogenicity studies of OTS25 viruses in CBA mice indicate no lymphoma induction and no osteoma induction in 21 injected mice after an observation period of 781 days. Therefore OTS25 is an optimal candidate as the negative control in recombinant studies with the highly bone-pathogenic RFB MLV (Table I), in order to map its osteoma-inducing potential in CBA mice. Another experiment to map the bone-pathogenic determinant has been initiated using RFB MLV as one parent and SL3-3 as the other parent. SL3-3 is strongly lymphomagenic but has no or little pathogenic effect on bone tissues (Table I). Our long-term goal behind these mapping studies is to locate nucleotide positions on the viral genome that may affect bone-pathogenicity

The LTR region represents a region of significance for viral pathogenicity and a major affecter of functional alterations in tumour DNA caused by proviral insertion. The nucleotide sequence of the LTR regions of RFB-14 and RFB-18 are identical and unique, although highly related to that of Akv MLV. The activity of the RFB LTR defines a new transcriptional phenotype. In contrast to the LTRs of other leukemogenic and bone-pathogenic viruses, the RFB LTR is highly transcribed in all cell lines tested (osteogenic, fibroblastic and T-lymphocytic cells). In a parallel study (Hallberg et al., 1991) of SL3-3 MLV we have identified single nucleotide positions in the U3 region of the viral genome that are crucial both for expression in cultured T-lymphoma cells and for lymphomagenicity in the animals, thus directly linking in vivo and in vitro results.

All studies are carried out in close collaboration with Institut für Molekulare Virologie, GSF-München (FRG).

Publications:

Dai, H.Y., Etzerodt, M., Bækgaard, A.J., Lovmand, S., Jørgensen, P., Kjeldgaard, N.O., and Pedersen, F.S.: Multiple sequence elements in the U3 region of the leukemogenic murine retrovirus SL3-2 contribute to cell-dependent gene expression. *Virology* 175, 581-585 (1990).

Pallisgaard, N., Pedersen, F.S., Kjeldgaard, N.O., and Jørgensen, P.: Cloning of cDNAs for proteins binding to the MuLV enhancer region. In *Gene Regulation, Oncogenesis, and AIDS* (T.S. Papas, ed.), pp. 87-94, Portfolio Publishing Company, The Woodlands, Texas, 1990.

Lovmand, S., Kjeldgaard, N.O., Jørgensen, P., and Pedersen, F.S.: Enhancer functions in U3 of Akv virus: A role for cooperativity of a tandem repeat unit and its flanking DNA sequences. *J. Virol.* 64, 3185-3191 (1990).

Olsen, H.S., Lovmand, S., Lovmand, J., Jørgensen, P., Kjeldgaard, N.O., and

- Pedersen, F.S.: Involvement of Nuclear Factor I binding sites in control of Akv virus gene expression. *J. Virol.* 64, 4152-4161 (1990).
- Duch, M., Paludan, K., Pedersen, L., Jørgensen, P., Kjeldgaard, N.O., and Pedersen, F.S.: Determination of transient or stable neo-expression levels in mammalian cells. *Gene.* 95, 285-288 (1990).
- Pedersen, L., Strauss, P.G., Schmidt, J., Luz, A., Erfle, V., Jørgensen, P., Kjeldgaard, N.O., and Pedersen F. S.: Pathogenicity of endogenous N-tropic BALB/c viruses. *Virology* 179, 931-935 (1990).
- Pedersen, F.S., Paludan, K., Dai, H.Y., Duch, M., Jørgensen, P., Kjeldgaard, N.O., Hallberg, B., Grundström, T., Schmidt, J., and Luz, A. The murine leukemia virus LTR in oncogenesis: Effect of point mutations and integration sites. *Rad. Environ. Biophys.* 30, 195-198 (1991).
- Morrison, H.L., Dai, H.Y., Pedersen, F.S., and Lenz, J.: Analysis of the significance of two single base-pair differences in the SL3-3 and Akv virus long terminal repeats. *J. Virol.* 65, 1019-1022 (1991).
- Hallberg, B., Schmidt, J., Luz, A., Pedersen, F.S., and Grundström, T.: SL3-3 Enhancer Factor 1 transcriptional activators are required for tumor formation by SL3-3 murine leukemia virus. *J. Virol.* 65, 4177-4181 (1991).
- Jørgensen, P., Mikkelsen, T., Pedersen, K., Pedersen, F.S., and Kjeldgaard, N.O.: Tagging the genome of the murine leukemia retrovirus SL3-3 by a bacterial lac operator sequence. *Gene* 109, 243-248 (1991).
- Sørensen, M.S., Duch, M., Paludan, K., Jørgensen, P., and Pedersen, F.S.: Measurement of hygromycin B phosphotransferase activity in mammalian cell extracts by a simple dot-assay. *Gene* 112, 257-260 (1992).
- Pedersen, K., Lovmand, S., Jørgensen, E.C.B., Pedersen, F.S., and Jørgensen, P.: Efficient expression and replication of murine leukemia virus with major deletions in the enhancer region of U3. *Virology* 187, 821-824 (1992).
- Jørgensen, E.C.B., Pedersen, F.S., and Jørgensen, P.: Matrix protein of Akv murine leukemia virus: Genetic mapping of regions essential for particle formation. *J. Virol.* 66, 4479-4487 (1992).
- Nielsen, A.L., Pallisgaard, N., Pedersen, F.S., and Jørgensen, P.: Murine helix-loop-helix transcriptional activator proteins binding to the E-box motif of the Akv murine leukemia virus enhancer identified by cDNA cloning. *Mol. Cell. Biol.* 12, in press (Aug. 1992)
- Pedersen, L., Behnisch, W., Schmidt, J., Luz, A., Pedersen, F.S., Erfle, V. and Strauss, P.G.: Molecular cloning of osteoma-inducing replication-competent murine leukemia virus from the RFB osteoma virus stock. *J. Virol.* 66, in press (Oct. 1992)

Project 5

Head of project: *Dr. Schoeters*

Objectives for the reporting period

The goals of our contribution are the identification of cells at risk for bone tumor development, and their response after incorporation of low doses of bone-seeking radionuclides. This information should allow more accurate estimations of osteosarcomogenic doses and detection of early events related to subsequent development of bone cancers.

The primary objectives at this stage are :

- Phenotypic characterization of precursor cells for bone cells among bone marrow.
- Determination of radiosensitivity of the bone progenitor cells after in vivo contamination of Balb/c mice with ^{241}Am .
- Radiation induced changes after in vitro alpha-irradiation of osteogenic bone marrow cultures with ^{223}Ra .

Progress achieved including publications

1. Characterization of bone precursor cells among bone marrow

The ability of bone marrow to express under well defined in vitro conditions osteogenic characteristics is used to screen for osteogenic precursor cells among the marrow after various cell separation techniques. It has been shown that proliferating cells contribute to osteogenic differentiation : incorporation of $^3\text{HTdr}$ with high specific activity reduces the mineralization capacity of bone marrow fragments. The osteogenic cells belong to the adherent bone marrow stromal cells as they are cultured in long-term bone marrow cultures. Irradiation with high X-ray doses of confluent bone marrow stromal cell layers does not impair the mineralization capacity, this indicates that haemopoietic stem cells which are killed on these stroma are not involved in the mineralization.

5-Fluorouracyl treatment of mice, 5 days prior to initiation of mineralizing bone marrow cultures indicates that the osteoprogenitor cells belong to a non-cycling cell population in vivo. Cell density separation on percoll gradient showed that osteogenic cells belong to the low density fraction.

2. Radiosensitivity of the osteoprogenitor cells

Adult BALB/c mice, injected with osteosarcomogenic amounts of ^{241}Am (between 40 and 500 Bq/g mouse) showed an impaired mineralization capacity of their femoral bone marrow. This effect persisted until at least 1 year after ^{241}Am injection and was expressed after incubation of bone marrow cells in vitro in conditions allowing osteogenic differentiation. The mineralization capacity of marrow in vitro was evaluated by measuring ^{85}Sr uptake from the tissue culture medium. Two osteogenic assays were used: in marrow cultured as an intact organ (marrow organ cultures), reduced mineralization was observed after 149 Bq ^{241}Am injected per g mouse or more

(skeletal dose rate of 25 mGy/day), in stromal marrow cells cultured from adherent layers and subsequently brought into a three-dimensional (3D) mineralizing condition (stromal 3D cultures), reduced ^{85}Sr uptake was observed from the lowest dose level tested (42 Bq ^{241}Am /g mouse, skeletal dose rate of 7 mGy/day). Taking into account that only a fraction of the skeletal α -dose reached the marrow of the femoral diaphyses, marrow organ cultures and stromal 3D cultures exhibited high radiosensitivity to α -irradiation in vivo. However, after acute X-irradiation of marrow in vivo or in vitro prior to initiation of the marrow organ cultures, X-ray doses of 4 Gy or higher were needed to significantly impair the mineralization capacity.

3. Radiation induced changes after in vitro alpha-radiation of osteogenic bone marrow cultures with ^{223}Ra

To learn about the changes induced by continuous alpha-irradiation on a target tissue, marrow fragments were cultured for 10 days in the presence of $^{223}\text{RaCl}_2$ (up to 400 Bq/ml tissue culture medium). Preliminary results show that at 400 Bq/ml the mineralization capacity was diminished compared to control cultures. This model will be further explored for the cellular and molecular nature of the damage.

4. Conclusions

Cell separation and selective culture techniques showed that osteogenic cells among murine bone marrow belong to the adherent bone marrow stromal cell population. The in vitro osteogenic marrow assay we developed can be used to detect radiation induced changes at osteosarcomogenic doses of ^{241}Am . Impaired mineralization persisted until at least one year after injection of 42 ^{241}Am Bq/g mouse (calculated initial marrow dose rate of 3 mGy/day).

Continuous in vitro irradiation of osteogenic marrow cultures with ^{223}Ra seems an appropriate model for the study of by α -irradiation induced changes in target tissue.

Publications

1. MATHIEU E., SCHOETERS G., VANDERPLAETSE F., MERREGAERT J. Establishment of an osteogenic cell line derived from adult mouse bone marrow stroma by use of a recombinant retrovirus. *Calcified Tissue International* (1992) 50:562-371.
2. SCHOETERS G.E.R., MAISIN J.R., VANDERBORCHT O.L.J. Toxicity of ^{241}Am in male C57Bl mice, relative risk versus ^{226}Ra . *Radiation Research* (1991) 126: 198-205.
3. SCHOETERS G.E.R., MAISIN J.R., VANDERBORCHT O.L.J. Protracted treatment of C57Bl mice with Zn-DTPA after ^{241}Am injection reduces the long-term radiation effects. *Int. J. Radiat. Biol.* (1991) 59: 1027-1038.
4. SCHOETERS G.E.R., VANDER PLAETSE F., VAN DEN HEUVEL R.L. High radiosensitivity of the mineralization capacity of adult murine bone marrow in vitro to continuous α -irradiation compared to acute X-irradiation. *Int. J. Radiat. Biol.* (in press) 1992.
5. SCHOETERS G.E.R., LEPPENS H., VAN GORP U., VAN DEN HEUVEL R. Haemopoietic long-term bone marrow cultures from adult mice show osteogenic capacity in vitro on 3-dimensional collagen sponges. *Cell and Tissue Kinetics* (in press) 1992.

Project 6

Head of project: *Dr. Bentvelzen*

Objectives for the reporting period

To devise new molecular biological methods for the detection of chromosomal deletions, which are not microscopically observable. This might lead to the detection of new tumour suppressor genes, which are inactivated (in a homozygous state) in radiation-induced tumours

Progress achieved

DNA from radiation-induced rat tumours was sheared and then biotinylated photochemically. This was hybridized with a restricted amount of normal rat DNA of the same inbred strain. Heteroduplexes and unhybridized tumour DNA was removed by incubation with beads conjugated with streptavidine. This subtraction hybridization procedure was repeated two times. The remaining DNA was ligated to adaptors containing the *Sau* IIIA restriction site and then used as substrate for a so-called sequence-independent PCR. In a model experiment in which a plasmid with the MMTV-LTR was used as a putative deleted sequence, this subtraction hybridization PCR method yielded the expected products. With regard to tumour DNA, this procedure yielded five different PCR products in the range of 1.2 to 0.35kb. The different PCR products were cloned in the M13 phage. The 1.2 kb product proved to contain a moderate repeat, which as demonstrated by *in situ* hybridization is present at localized spots in several rat chromosomes. Southern blot hybridization with this sequence revealed that several radiation-induced pulmonary tumours and rhabdomyosarcomas of rats lack sequences containing this repeat as compared to normal rat DNA. Although some high molecular weight fragments were lacking in all tested radiation-induced tumours, additional deletions were found in the various tumour lines. The southern blot pattern differed from one tumour to the other.

THE DOSIMETRY AND METABOLISM OF INCORPORATED RADIONUCLIDES

Contract Bi6-089 - Sector B15

1) Harrison, NRPB

Summary of project global objectives and achievements

A comparative study to examine the differences in biokinetics and toxicity of the three bone-seeking radionuclides ^{239}Pu , ^{241}Am and ^{233}U is in progress with the objective of relating differences in the distribution of dose within the skeleton and the extent of irradiation of the different cell types, with the observed incidence and distribution of osteosarcoma and myeloid leukaemia.

Studies of distribution and skeletal retention of ^{239}Pu , ^{241}Am and ^{233}U have been completed. Results show that the skeleton accounted for 85%, 88% and 97% of retained activity of ^{239}Pu , ^{241}Am and ^{233}U , respectively, from 56 days after injection. Within the skeleton, inhomogeneity of the distribution between individual bones was in the order $^{239}\text{Pu} > ^{241}\text{Am} > ^{233}\text{U}$ with greatest concentrations in the main body of the spine, limb girdles and ribs and lowest concentrations in the lower limbs, paws and caudal vertebrae. The distribution became more homogeneous with time particularly for ^{239}Pu . Autoradiography showed that plutonium was deposited fairly evenly on endosteal bone surfaces and to a lesser extent on periosteal surfaces. At later times, some burial in the form of lines of activity was apparent as well as areas with more diffuse activity indicative of redeposition during bone remodelling. Progressive accumulation of plutonium in marrow was also observed. Americium deposited more evenly on all bone surfaces and also in the internal surfaces of vascular canals in the cortical bone. With time, some burial occurred at the growth plate and some accumulation of americium in marrow macrophages was also seen but less than that observed for plutonium. Uranium deposited on both periosteal and endosteal bone surfaces but not evenly, concentrating preferentially on some parts of the surface. Small amounts of diffuse activity were seen throughout the bone marrow and bone mineral.

The toxicity study comparing osteosarcoma and leukaemia incidence is not yet complete. Three dose levels of each radionuclide were used with administered activities adjusted to give equal average bone doses for the three radionuclides. The incidence of identified bone tumours in mice given ^{239}Pu , expressed in terms of the total time since administration for animals in each group (incidence per 10^5 days), is currently 4, 9 and 25 for the low medium and high groups, respectively. For ^{241}Am , the corresponding incidences are 0, 4 and 9, respectively, and for ^{233}U , 3, 5 and 3, respectively. The incidences of myeloid leukaemia to date are 3, 5 and 2% for ^{239}Pu for the low, medium and high groups respectively with corresponding values of 3, 2.6 and 0% for ^{241}Am and 5, 8.3 and 4% for ^{233}U . The results to date suggest a greater incidence of myeloid leukaemia in mice exposed to ^{233}U than in those exposed to ^{239}Pu and ^{241}Am .

Studies to determine the distribution and retention of ^{210}Po in the skeleton of rats after intraperitoneal injection of either ^{210}Po or ^{210}Pb are in progress with the objective of assessing alpha doses and leukaemic risk from these naturally-occurring radionuclides. Studies of the distribution of ^{238}Pu and ^{210}Po in the marmoset skeleton have also been undertaken. Results show that for systemic administration of ^{210}Po citrate, the skeleton retains about 10% of injected activity in rats and marmosets. Autoradiography showed that the activity is confined to the marrow. The ICRP model for Po will be modified to take account of skeletal (ICRP Publication 56). Experiments to determine the behaviour of ^{210}Pb after administration of ^{210}Po are in progress.

Project 1

Head of project: *Dr. Harrison*

Objectives for the reporting period

To continue with studies of the distribution of ^{239}Pu , ^{241}Am and ^{233}U in mice, their retention in individual bones of the skeleton, and micro-distribution within bone. To continue with studies to examine the comparative toxicity of the three bone-seeking radionuclides ^{239}Pu , ^{241}Am and ^{233}U , with the objective of relating differences in the distribution of dose within the skeleton, and the extent of irradiation of the different cell types, with the observed incidence and distribution of osteosarcoma and myeloid leukaemia.

To undertake studies to determine the distribution and retention of ^{210}Po in the skeleton of rats after intraperitoneal injection of ^{210}Po or ^{210}Pb and comparisons of the distribution of ^{238}Pu and ^{210}Po in marmoset bones.

Progress achieved including publications

1. Biokinetics and toxicity of ^{239}Pu , ^{241}Am and ^{233}U in mice

The study of the behaviour and toxicity of ^{239}Pu , ^{241}Am and ^{233}U in CBA/H mice can be considered as consisting in four parts: radiochemical measurements of the distribution of the nuclides between the skeleton and soft tissues at times up to 448 days after intraperitoneal injection as their citrate complexes; radiochemical measurements of the retention of the nuclides in individual bones of the skeleton over the same period; autoradiographic studies of the distribution of the nuclides within bone; and comparisons of osteosarcoma induction in groups of mice given intraperitoneal injections of ^{239}Pu , ^{241}Am and ^{233}U activity to deliver equivalent average skeletal doses.

1.1 Tissue distribution and retention of ^{239}Pu , ^{241}Am and ^{233}U

The study of the distribution and retention of the nuclides in the skeleton and soft tissues after systemic injection of 40 kBq kg^{-1} at times up to 448 days is complete. Intraperitoneal injection was used after first establishing that differences in distribution after intravenous and intraperitoneal administration were negligible. Groups of mice were killed 1, 7, 14, 28, 56, 112, 224 and 448 days after the injection of the radionuclides in citrate solution. Five animals were dissected for separate analysis of liver, kidneys, adrenals, spleen, gastrointestinal tract, gonads, femora, humeri and remaining carcass. Groups of male and female mice were used but no significant differences in distribution and retention between the sexes was observed.

The whole-body retention of ^{239}Pu and ^{241}Am were similar with values of about 80% and 70% respectively, after 1 day, falling to about 50% and 45% after 4 weeks and about 25% and 20% after 448 days. The total retention of ^{233}U was considerably lower, falling from about 15% after 1 day to about 5% after 4 weeks and about 3% after 448 days. For each nuclide, the skeleton was the major site of long-term retention. At one day after injection of ^{239}Pu , about 50% of retained activity was in the liver and about 24% in the skeleton. With time, the level of activity present in the liver decreased while retention in bone increased over the first month after injection and subsequently decreased. The distribution of americium in mouse tissues was very similar to that of plutonium. The initial uptake of americium in the skeleton was less than for plutonium (13% cf. 24%) while uptake in the liver was similar. As for plutonium, the level of activity in the liver decreased rapidly while retention in bone increased over the first month and subsequently decreased. The maximum retention in the skeleton, at 28 days after injection, accounted for 30% of administered americium compared with 37% of plutonium. For uranium, total retention at one day accounted for 16% of administered activity, about 10% in the skeleton and about 5% in the kidneys. Retention in the kidneys decreased rapidly while skeletal retention decreased progressively. As a percentage of whole body activity, the skeleton initially accounted for 30%, 18% and 65% of retained ^{239}Pu , ^{241}Am and

^{233}U , respectively, increasing to 85%, 88% and 97% respectively, after 56 days; the corresponding values after 448 days were 86%, 94% and 99% respectively. Average doses to the skeleton to 448 days after injection of 40 kBq kg^{-1} were calculated as about 0.6 Gy for both ^{239}Pu and ^{241}Am and about 0.1 Gy for ^{233}U .

1.2 Distribution of ^{239}Pu , ^{241}Am and ^{233}U between individual bones

The second study examining the retention and distribution of ^{239}Pu , ^{241}Am and ^{233}U in the individual bones of the skeleton after systemic injection of 40 kBq kg^{-1} at times up to 448 days is complete. The skeletons were cleaned in a colony of *Dermestes* beetles and radiochemical analysis was undertaken separately for the skull, mandibles, groups of cervical, thoracic, lumbar, sacral and caudal vertebrae, sternum, ribs, scapular, humeri, radii, ulnae, pelvis, femorae, fibiae, tibiae, patellae and paws.

The nuclides deposited preferentially in the main body of the spine, limb girdles and ribs with lower concentrations in the lower limbs, paws and caudal vertebrae. The distribution pattern was similar to that observed in rats by other workers. The relative concentrations of the individual bones compared with the whole skeleton have been calculated. Those with the highest relative concentrations at 1 day were the thoracic vertebrae, lumbar vertebrae and sternum (2.0, 2.2 and 2.0 respectively at 1 day following injection). The bones with the lowest values were the caudal vertebrae, paws and mandibles (0.5, 0.3 and 0.5 respectively at 1 day following injection).

The differences in the relative concentrations of the nuclides in the individual bones reduced with time as bone remodelling occurred, leading to a more homogeneous distribution. The inhomogeneity function, which describes the deviation of the relative concentration of the individual bones from the concentration of the whole skeleton, was also calculated. Inhomogeneity was greatest for plutonium and least for americium. The decrease in inhomogeneity with time was more pronounced for plutonium and uranium than americium.

1.3 Autoradiography of ^{239}Pu , ^{241}Am and ^{233}U in mouse bone

Detailed studies on the radionuclide distribution within two bones (femur and lumbar vertebrae) after systemic injection of 40 kBq kg^{-1} of either ^{239}Pu , ^{241}Am or ^{233}U citrate using autoradiographic techniques have been undertaken. Following difficulties with the preparation of conventional autoradiographs on sections of femora and lumbar vertebrae, an additional experiment was initiated to study the distribution of the radionuclides in the more readily processed mandibular condyle and rib.

Alpha-track autoradiographs of femur using the plastic detector, CR39, have been examined to qualitatively determine the gross distribution of each radionuclide at 1, 7, 28, 112, 224 and 448 days after intraperitoneal injection. These studies have shown that ^{239}Pu was deposited fairly evenly on endosteal bone surfaces and to a lesser extent on periosteal surfaces. At later times, some burial in the form of lines of activity was apparent as well as areas with more diffuse activity indicative of redeposition during bone remodelling. Progressive accumulation of plutonium in marrow was also observed. ^{241}Am deposited more evenly on all bone surfaces and also in the internal surfaces of vascular canals in the cortical bone. With time, some burial occurred at the growth plate and some accumulation of americium in marrow macrophages was also seen but less than that observed for plutonium. ^{233}U deposited on both periosteal and endosteal bone surfaces but not evenly, concentrating preferentially on some parts of the surface. Small amounts of diffuse activity were seen throughout the bone marrow and bone mineral.

To quantify the distribution of alpha activity within the bone, fission track autoradiographs of femur sections have been produced. Track counts on random areas of sections have been used to make preliminary estimates of dose. The initial calculations show that while the doses to endosteal surfaces from ^{239}Pu and ^{241}Am were greater than average bone doses at both 1 day and 224 days after administration, the dose from ^{233}U was greater than the average bone dose initially but lower at 224 days. The bone marrow dose from ^{239}Pu was about the same as the average bone dose at 1 day and slightly higher at 224 days. Marrow doses from ^{241}Am and ^{233}U were lower than those for ^{239}Pu . Further calculations are being undertaken to take account of doses to bone surfaces and marrow from activity near but not on bone surfaces.

1.4 Induction of osteosarcoma and leukaemia by ^{239}Pu , ^{241}Am and ^{233}U

On the basis of the average bone doses calculated from the distribution studies, it was estimated that the ratios of ^{239}Pu : ^{241}Am : ^{233}U to give the same doses were 1: 1.05: 5.25. Three dose levels of ^{239}Pu were used, 5, 15 and 25 kBq kg^{-1} , with the expectation that the incidence of osteosarcoma in these groups would be about 7%, 15% and 30% respectively. The corresponding activities of ^{241}Am and ^{233}U were 6, 17, and 29 kBq kg^{-1} and 40, 120 and 200 kBq kg^{-1} , respectively. To avoid chemical damage to the kidneys from U, the administration of activity was fractionated over a 3 week period. Groups of mice (50 - 100) were therefore given 9 intraperitoneal injection of the radionuclides in citrate over a 3 month period and a control group was similarly injected with inactive solution.

Approximately 90% of the animals have now died, the incidence of osteosarcoma and leukaemia for the different radionuclides are given in the table. A total of 24 bone tumours have been identified to date by X-ray examination of the skeleton at death. Confirmation by histological examination is in progress and further suspected tumours are being evaluated histologically. In animals given ^{239}Pu , the bone tumour incidences are 3, 6.7 and 14% for the low, medium and high groups respectively. The incidences for ^{241}Am are 0, 3.5 and 6% and for ^{233}U are 2, 3.3 and 2% (low, medium and high groups). The incidence of identified bone tumours in mice given ^{239}Pu , expressed in terms of the total time since administration for animals in each group (incidence per 10^5 days), is currently 4, 9 and 25 for the low, medium and high groups, respectively. For ^{241}Am , the corresponding incidences are 0, 4 and 9, respectively, and for ^{233}U , 3, 5 and 3, respectively (see table).

The myeloid leukaemias are confirmed by blood counts, analysis of blood smears for abnormal cells and by passing the spleen homogenate into untreated mice to look for myeloid leukaemia development. Under CEC Contract B170037 a number of the leukaemias have been karyotyped and have shown chromosome 2 rearrangements characteristic of acute myeloid leukaemia. Cells from future suspected leukaemias will be karyotyped in the same way.

Twenty-four myeloid leukaemias have been confirmed to date and evaluation of several additional suspected myeloid leukaemias is currently underway. In animals given ^{239}Pu the incidences are 3, 5 and 2% for the low, medium and high groups respectively. The incidences for ^{231}Am are 3, 2.7 and 0% and for ^{233}U are 5, 8.3 and 4% (low, medium and high groups). The confirmation of several suspected myeloid leukaemias by passing is underway. The results to date suggest a greater incidence of myeloid leukaemia in mice exposed to ^{233}U than in those exposed to ^{239}Pu and ^{241}Am .

2. Biokinetics of ^{210}Po in rats and marmosets

Uncertainties in doses to the red bone marrow from ^{210}Po as the daughter of ^{222}Ra and ^{210}Po have recently been highlighted and controversial suggestions have been made concerning the importance these natural alpha-emitters in the induction of leukaemia. One uncertainty is the behaviour of ^{210}Po entering the bone marrow from the circulation or after decay from ^{210}Pb in mineral bone.

A study of the distribution and retention of ^{210}Po in the skeleton of rats is in progress. Tissue distribution results showed a skeletal retention of about 10% of administered activity at 7 days after intravenous injection as ^{210}Po citrate. Autoradiographs of femurs and vertebrae showed a fairly uniform distribution of activity throughout the marrow at 7 and 200 days after administration; the values for tissue retention at later times are not yet available. Studies of the distribution and retention of ^{210}Po in the rat skeleton after administration of ^{210}Pb are planned.

A study of the distribution and retention of ^{239}Pu and ^{210}Po in the marmoset has been undertaken.

References

Ellender M and Haines J W. The retention and distribution of ^{233}U , ^{239}Pu and ^{241}Am in the CBA mouse. EULEP Newsletter, 52 14-15 (1989).

Ellender M, Haines J W and Harrison J D. A comparison of the biokinetics and toxicity of ^{239}Pu , ^{241}Am and ^{233}U in CBA/H mice. EULEP Newsletter, 57 26-27 (1990).

Ellender, M, Haines, J W, Cragg, T A, and Harrison, J D. Distribution and toxicity of ^{239}Pu , ^{241}Am and ^{233}U in the mouse skeleton. EULEP Newsletter, 62 26-27 (1991).

Ellender, M, Robbins, L, Bouffler, S D, and Harrison, J D. Induction of osteosarcoma and leukaemia by ^{239}Pu , ^{241}Am and ^{233}U in CBA/H mice. EULEP Newsletter, 67 25-26 (1992).

Haines, J W, Ellender, M, Talbot, R J, and Harrison, J D. Autoradiographic studies and dose estimates for ^{239}Pu , ^{241}Am , ^{233}U and ^{210}Po in animal bone. EULEP Newsletter, 62 28-29 (1991).

Haines J W. A technique to embed undecalcified bone samples for the detection of alpha-emitters using vacuum impregnation of Spurr's resin. Biotechnic and Histochemistry, 67 45-49 (1992).

Priest N D, Haines J W, Humphreys J A M, Metivier H and Kathren R L. The bone volume effect on the dosimetry of plutonium-239 and americium-241 in the skeleton of man and baboon. Journal of Radiological and Nuclear Chemistry, 156 33-53 (1992).

Tanner R J and Haines J W. Solid state nuclear track detectors and their applications in radiological protection. Radiol. Prot. Bull., 122 14-19 (1991).

Table - Incidence of osteosarcoma and myeloid leukaemia in CBA/H mice following the administration of ²³⁹Pu, ²⁴¹Am and ²³³U

²³⁹Pu

Dose kBq kg ⁻¹	0	5	15	25
Average bone dose at 500 days (Gy)	0	0.1	0.3	0.5
No of mice entered	100	100	60	50
No of mice dead	93	95	57	48
Myeloid leukaemia	0	3	3	1
Osteosarcoma	0	3	4	7
Mouse days exposure	61331	69937	39845	31764
10 ⁵ x Myeloid leukaemia days ⁻¹	0	4.3	7.5	3.1
10 ⁵ x Osteosarcoma days ⁻¹	0	4.3	8.5	25.2

²⁴¹Am

Dose kBq kg ⁻¹	0	6	17	29
Average bone dose at 500 days (Gy)	0	0.1	0.3	0.5
No of mice entered	100	100	75	50
No of mice dead	93	94	73	49
Myeloid leukaemia	0	3	2	0
Osteosarcoma	0	0	2	3
Mouse days exposure	61331	66756	48983	34175
10 ⁵ x Myeloid leukaemia days ⁻¹	0	4.5	4.1	0
10 ⁵ x Osteosarcoma days ⁻¹	0	0	4.1	8.8

²³³U

Dose kBq kg ⁻¹	0	40	120	200
Average bone dose at 500 days (Gy)	0	0.1	0.5	0.5
No of mice entered	100	100	60	50
No of mice dead	93	96	54	47
Myeloid leukaemia	0	5	5	2
Osteosarcoma	0	2	2	1
Mouse days exposure	61331	68618	40631	31894
10 ⁵ x Myeloid leukaemia days ⁻¹	0	7.3	12.3	6.3
10 ⁵ x Osteosarcoma days ⁻¹	0	2.9	4.9	3.1

STUDIES ON MYELOID LEUKAEMIA AND OSTEOSARCOMA INDUCED IN MICE BY RA-224

Contract Bi6-064 - Sector B15

1) *Humphreys*, MRC Radiobiological Unit

Summary of project global objectives and achievements

The potential contamination of the environment by α -particle emitting radionuclides is a continuing spur to the experimental investigation of their toxicity. Animal experiments (Vaughan 1973, Müller et al 1978) and human experience (Rowland et al 1983, Mays et al 1986) have shown osteosarcoma to be the major late effect of bone-seeking α -particle emitters but, more recently, it has been shown in CBA/H mice that myeloid leukaemia is also induced by ^{224}Ra and that there may be a range of injected activity in which more myeloid leukaemia than osteosarcoma is induced (Humphreys et al 1985).

An early series of experiments also demonstrated conclusively, in NMRI mice, that multiple administrations of ^{224}Ra to mice was more effective than a single administration of the same total amount in inducing osteosarcoma (Müller et al 1978). This was shown also to be true in a reanalysis of epidemiological data from humans exposed to ^{224}Ra (Chmelevsky et al 1990).

The aim of the present series of experiments was to confirm the earlier findings on the relative yields of myeloid leukaemia and osteosarcoma in a larger series of animals and to investigate the effects of protracted administration of ^{224}Ra on the incidence of myeloid leukaemia.

In an experiment in which 1600 mice were given amounts of ^{224}Ra in the range 69 - 555 Bq g⁻¹ and a further 400 mice were given diluting solution only, all as single injections, it has now been confirmed that the yield of each tumour type was related to the amount administered and that the overall ratio myeloid leukaemia:osteosarcoma is 2.4.

A further experiment was carried out in which groups of 200 mice were given either diluting solution (controls) or totals of 32, 64 or 128 Bq g⁻¹ ^{224}Ra in sixteen injections spaced at equal intervals over an eight week period. It was shown that whereas only one myeloid leukaemia was seen in each of the groups given 32 and 64 Bq g⁻¹, nine were observed in the group given 128 Bq g⁻¹. This has been interpreted to indicate that an effect of protraction may have been seen at 128 Bq g⁻¹ but not at the smaller total administrations. This falls in line with observations made on osteosarcoma (Müller et al 1983) although the incidence of myeloid leukaemia induced by 128 Bq g⁻¹ administered in sixteen injections has not yet been shown to be significantly greater than that seen following an injection of the same amount in a single injection.

Four further groups of 200 CBA/H mice have now been exposed to continuous administrations of ^{224}Ra throughout their lifespans by the paratibial injection of ^{228}Th in colloidal suspension shown to act as a source of ^{224}Ra . This experiment is at a much earlier stage but has already shown incidences of myeloid leukaemia and of osteosarcoma (both at the site of injection and in other regions of the skeleton). It is

not yet known, however, whether or not this continuous administration of ^{224}Ra has had a greater effect on the incidence of myeloid leukaemia than either multiple injections over an eight week period or single injections.

Chronic myeloid leukaemia has recently been identified as radiation-induced in an epidemiological study of patients given small amounts of ^{224}Ra in the treatment of ankylosing spondylitis (Wick and Gössner 1989). There is sufficient agreement, therefore, between the present results and those from human experience to suggest that persons exposed to amounts of α -particle emitters previously thought to pose an acceptable risk from osteosarcoma, may instead be at risk from myeloid leukaemia. Further work using data from the multiple injection and continuous exposure experiments may provide information on the effectiveness of protracted administration on the incidence of myeloid leukaemia and therefore provide more relevant information on the effects of environmental contamination.

Project 1

Head of project: *Dr. Humphreys*

Objectives for the reporting period

To continue the studies of the leukaemogenic and osteosarcomagenic effects of small amounts of ^{224}Ra on male CBA/H mice in lifespan experiments and particularly to investigate the effects of protracting the administration of the radionuclide in time.

Progress achieved including publications

^{224}Ra was obtained from Amersham Buchler, Braunschweig, Germany via Amersham International, Amersham, United Kingdom as a solution of the chloride in sterile physiological saline.

1. Single injection experiment

The delivered solution of ^{224}Ra was diluted with sterile physiological saline containing $100\mu\text{gcm}^{-3}\text{Ca}^{2+}$ to give injection solutions containing 4, 8, 16 or 32kBqg^{-1} .

Male CBA/H mice (84 ± 5) days old at injection were introduced into the experiment over a period of 34 months. Each was injected intraperitoneally with 0.5cm^3 of the appropriate injection solution; control mice were injected with 0.5cm^3 diluting solution. The amounts injected and the main findings in the different groups are shown in table 1.

Table 1
Single injection experiment
(Mean values \pm S.E.M)

^{224}Ra Bq g^{-1}	0	69	139	280	550
Mice entered	400	400	400	400	400
Mice excluded *	6	6	1	5	1
Mean age at entry (days)	84.9 \pm 0.1	84.5 \pm 0.1	84.2 \pm 0.2	83.8 \pm 0.2	85.1 \pm 0.1
Mean survival (days)	710 \pm 9	689 \pm 10	669 \pm 10	677 \pm 10	658 \pm 9
Mouse days exposure	279603	271382	266908	267501	262671
Number of mice with:					
Myeloid leukaemia	1	6	11	17	18
10^{-5} mouse-days	0.36	2.21	4.12	6.36	6.85
Osteosarcoma	1	1	4	6	10
10^{-5} mouse-days	0.36	0.36	1.50	2.24	3.81

* Two mice escaped; the remainder were excluded because autolysis made diagnoses unreliable.

These results confirm the earlier indications that, in the range of injected amounts of ^{224}Ra between 69 and 550Bq g^{-1} , more myeloid leukaemia than osteosarcoma is induced. Overall the ratio is 2.4

although the table shows a variation between groups. It is also clear that the incidence of each tumour depends upon the amount of ^{224}Ra injected.

2. Multiple injection experiment

Since it was necessary to introduce the mice into the experiment over several weeks, the solutions were obtained in weekly batches to limit the build-up of the long-lived contaminants stated by the manufacturers to be present at a nominal approximate concentration of 10^{-5} of the stated activity. Each solution was diluted with sterile physiological saline containing $100\mu\text{gcm}^{-3}\text{Ca}^{2+}$ to give injection solutions containing 3.2, 6.4 or 12.8kBqg^{-1} at each of the two times of injection for that batch. Duplicate standards were prepared from each injection solution and their gamma-activities determined (using an LKB Compugamma scintillation counter) in a closely-defined region of the gamma energy spectrum which included the 240keV gamma rays from ^{212}Pb .

Male CBA/H mice (84 ± 5) days old at injection were weighed and injected with one-hundredth of the body mass of the appropriate injection solution; the control mice were similarly injected with diluting solution. The setup of the experiment and main findings are shown in table 2.

Table 2
Multiple injection experiment
(Mean values \pm S.E.M)

^{224}Ra Bq g^{-1}	0	32	64	128
Mice entered	200	200	200	200
Mice excluded *	8	3	1	0
Mean age at entry (days)	82.6+0.1	87.3+0.1	86.3+0.1	84.9+0.2
Mean survival (days)	701+14	671+14	671+15	666+16
Mouse days exposure	134677	132161	133551	133262
Number of mice with:				
Myeloid leukaemia	0	1	1	9
10^{-5} mouse days	0	0.77	0.75	6.75

* Two mice escaped; the remainder were excluded because autolysis made diagnoses unreliable.

These results show a very marked increase in the incidence of myeloid leukaemia when the total amount injected is increased from 64 to 128Bq g^{-1} ; the yields in the groups given 32, 64 and 128Bq g^{-1} ^{224}Ra are 0.77, 0.75 and 6.75 myeloid leukaemias per 10^5 mouse days exposure respectively. The yield of myeloid leukaemia in those animals given 128Bq g^{-1} in sixteen injections spaced over eight weeks is greater than the corresponding interpolated value for the animals given the same amount in a single injection (approximately 4 myeloid leukaemias per 10^5 mouse days exposure - table 1) although this difference has not yet been shown to be statistically significant.

3. Continuous exposure experiment

^{228}Th was obtained from AEA Technology, Harwell, UK as a solution of either the chloride or the nitrate in HCl or HNO₃, respectively. This was very carefully neutralized, as an unbuffered solution, with decreasing concentrations of NaOH to give colloidal suspensions containing appropriate concentrations of ^{228}Th so that injections of 50 μl into preweighed mice gave either 3.45, 6.9, 13.8 or 27.6 Bq g⁻¹. A total of 200 male CBA/H mice were injected in each of the four groups; each mouse was injected under halothane anaesthesia into the gastrocnemius muscle of the left leg so that the tip of the needle just touched the tibia. The setup of the experiment and preliminary findings are shown in table 3.

Table 3
Continuous exposure experiment
(Mean values \pm S.E.M)

^{228}Th Bq g ⁻¹	3.45	6.9	13.8	27.6
Mice entered	200	200	200	200
Mean age at entry (days)	84.8 \pm 0.2	83.7 \pm 0.2	83.6 \pm 0.2	84.6 \pm 0.2
No. of mice dead	28	48	79	85
Mouse days exposure	102861	109144	111701	99282
Number of mice with:				
Myeloid leukaemia	1	0	0	1
Osteosarcoma	1	2	2	3

This experiment (paratibial injection of ^{228}Th) is at a very much earlier stage and, although it can be seen that both myeloid leukaemia and osteosarcoma have been induced, these do not yet give any guidance on the final pattern of induction.

The techniques and procedures involved in housing the mice and in diagnosing myeloid leukaemia and osteosarcoma are fully described in Humphreys et al (1989).

Publications arising from work carried out under this contract

Humphreys, E.R. and Stones, V.A. (1991)

The induction of myeloid leukaemia in CBA/H mice by alpha-particle emitters.

Joint Bone Radiobiology Workshop, Toronto, Canada 12 - 13 July 1991, EULEP/DOE

Humphreys, E.R., Loutit, J.F., Major, I.R. and Stones, V.A. (1988)

Experiments using alpha-emitters in mice and their relevance to humans
Forum on alpha-emitters in bone and leukaemia. Committee on the effects of ionizing radiation. International Journal of Radiation Biology 53
521 - 539 pp 527 - 529

Humphreys, E.R., Major, I.R. and Stones, V.A. (1989)

Myeloid leukaemia/osteosarcoma ratio in CBA/H mice given ^{224}Ra - interim results.

Risks from Radium and Thorotrast (Edited by D.M.Taylor, C.W.Mays, G.B.Gerber and R.G.Thomas) British Institute of Radiology Report 21 Butterworths, Sevenoaks, Kent, England; Stoneham, Mass. USA pp 36 - 39

Humphreys,E.R., Major,I.R. and Stones,V.A. (1990)
The effects of protracted alpha-particle-emitting radionuclides on mice.
International Journal of Radiation Biology 58 874 - 875

Other references

Chmelevsky,D., Spiess,H., Mays,C.W. and Kellerer,A.M. (1990)
The reverse protraction factor in the induction of bone sarcomas in radium-224 patients.
Radiation Research 124 S69 - S79

Humphreys,E.R., Loutit,J.F., Major,I.R. and Stones,V.A. (1985)
The induction by ^{224}Ra of myeloid leukaemia and osteosarcoma in male CBA mice.
International Journal of Radiation Biology 47 239 - 247

Mays,C.W., Spiess,H., Chmelevsky,D. and Kellerer,A. (1986)
Bone sarcoma cumulative tumor rates in patients injected with ^{224}Ra .
In:"The radiobiology of radium and thorotrast" Edited by Gössner,W., Gerber,G.B., Hagen,U. and Luz,A. Supplement to Strahlentherapie Vol. 80. Urban and Schwartzenberg Munich Wien Baltimore pp 27 - 31

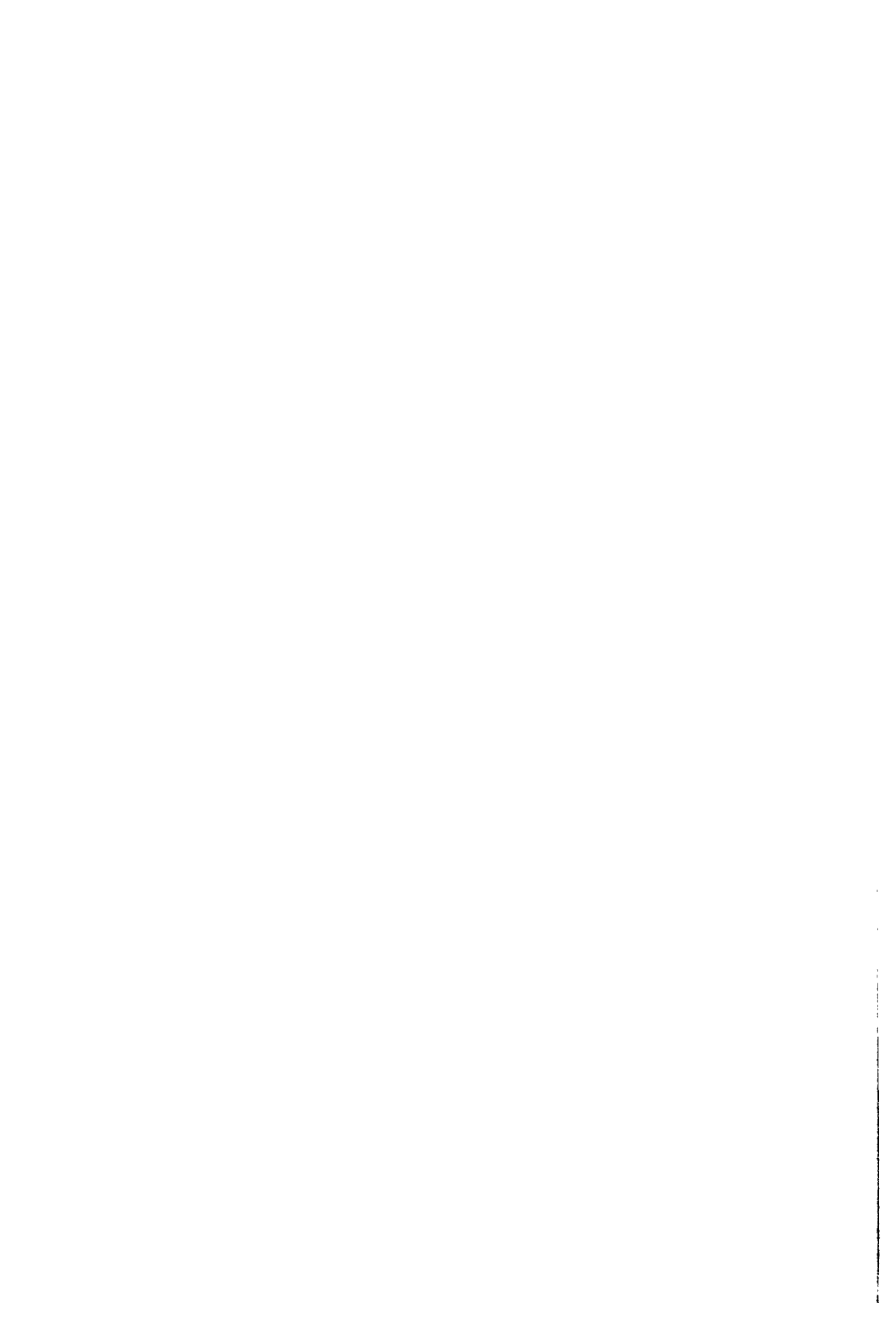
Müller,W.A., Gössner,W., Hug,O. and Luz,A. (1978)
Late effects after incorporation of the short-lived alpha-emitters ^{224}Ra and ^{227}Th in mice.
Health physics 35 33 - 55

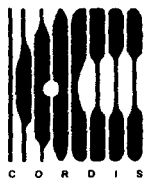
Müller,W.A., Luz,A. Schaffer,E.H. and Gössner,W. (1983)
The role of time-factor and RBE for the induction of osteosarcoma by incorporated short-lived bone-seekers.
Health Physics 44 Suppl.1 203 - 212

Rowland,R.E., Stehney,A.F. and Lucas,H.F. (1983)
Dose-response relationships for radium induced bone sarcomas
Health Phys. 44 Suppl.1 15 - 31

Vaughan,J.M. (1973)
The effects of irradiation on the skeleton.
Clarendon Press, Oxford.

Wick,R.R. and Gössner,W. (1989)
Recent results of the follow-up of radium-224-treated ankylosing spondylitis patients.
Risks from Radium and Thorotrast (Edited by Taylor,D.M, Mays,C.W., Gerber,G.B. and Thomas,R.G.) British Institute of Radiology Report No. 21 pp 25 - 28





**The Communities research and development
information service**

C O R D I S

**A vital part of your programme's
dissemination strategy**

CORDIS is the information service set up under the VALUE programme to give quick and easy access to information on European Community research programmes. It is available free-of-charge online via the European Commission host organization (ECHO), and now also on a newly released CD-ROM.

CORDIS offers the European R&D community:

- a comprehensive up-to-date view of EC R&TD activities, through a set of databases and related services,
- quick and easy access to information on EC research programmes and results,
- a continuously evolving Commission service tailored to the needs of the research community and industry,
- full user support, including documentation, training and the CORDIS help desk.

The CORDIS Databases are:

**R&TD-programmes – R&TD-projects – R&TD-partners – R&TD-results
R&TD-publications – R&TD-comdocuments – R&TD-acronyms – R&TD-news**

Make sure your programme gains the maximum benefit from CORDIS

- Inform the CORDIS unit of your programme initiatives,
- contribute information regularly to CORDIS databases such as R&TD-news, R&TD-publications and R&TD-programmes,
- use CORDIS databases, such as R&TD-partners, in the implementation of your programme,
- consult CORDIS for up-to-date information on other programmes relevant to your activities,
- inform your programme participants about CORDIS and the importance of their contribution to the service as well as the benefits which they will derive from it,
- contribute to the evolution of CORDIS by sending your comments on the service to the CORDIS Unit.

**For more information about contributing to CORDIS,
contact the DG XIII CORDIS Unit**

Brussels

Ms I. Vounakis

Tel. +(32) 2 299 0464

Fax +(32) 2 299 0467

Luxembourg

M. B. Niessen

Tel. +(352) 4301 33638

Fax +(352) 4301 34989

To register for online access to CORDIS, contact:

ECHO Customer Service

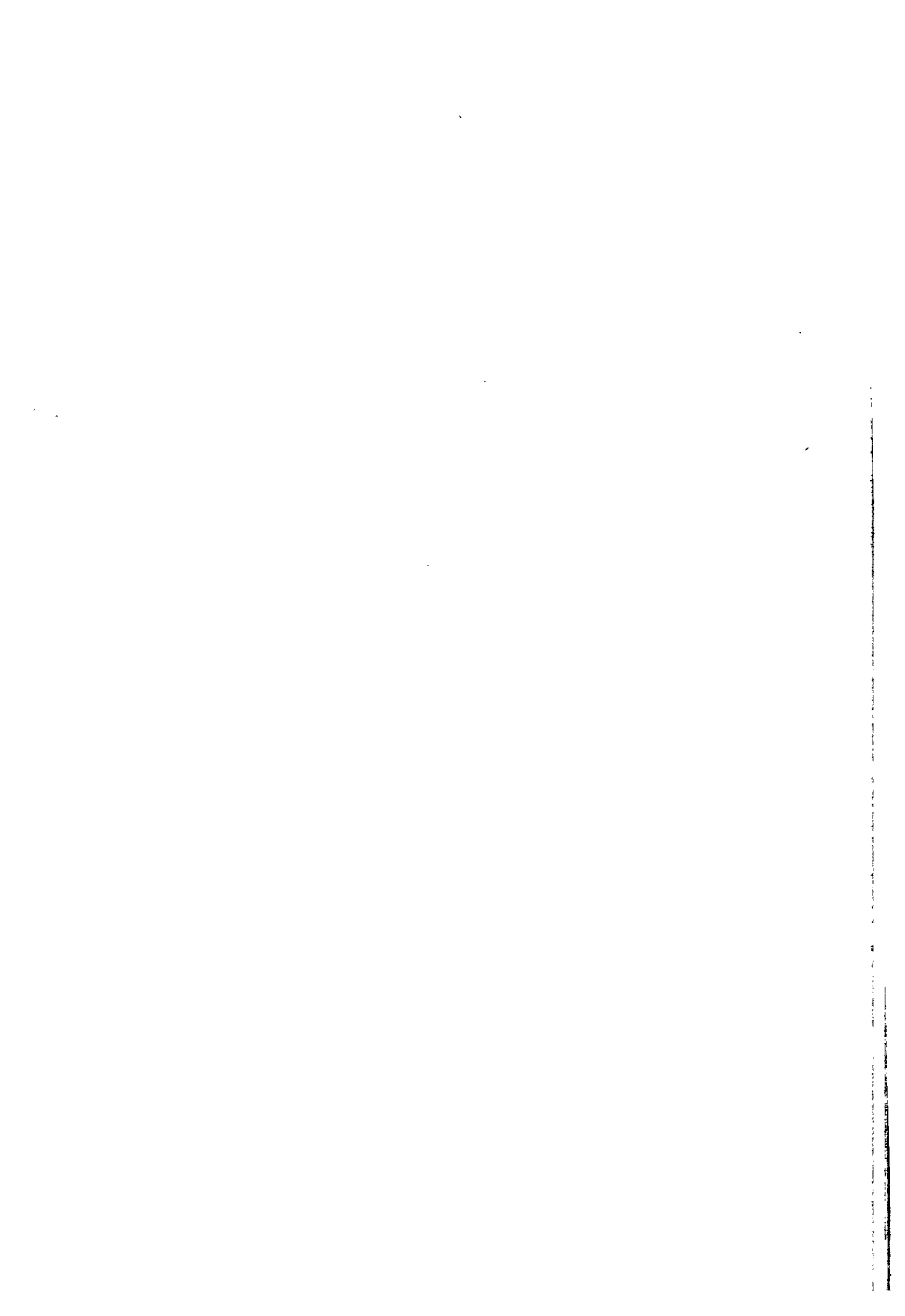
BP 2373

L-1023 Luxembourg

Tel. +(352) 3498 1240

Fax +(352) 3498 1248

If you are already an ECHO user, please mention your customer number.



Europäische Kommission
European Commission
Commission européenne

EUR 15295 – Radiation protection programme 1990-91 (Volume 1)

Luxembourg: Office for Official Publications of the European Communities

1994 – XXX, 1096 pp. – num. tab., fig. – 16.2 × 22.9 cm

Radiation protection series

ISBN 92-826-8683-3 (Volume 1)

ISBN 92-826-8682-5 (Volumes 1 and 2)

Preis in Luxemburg (ohne MwSt.): ECU 89

Price (excluding VAT) in Luxembourg: ECU 89

Prix au Luxembourg, TVA exclue: ECU 89

1990-91 – Final report

The final report of the 1990-91 period of the radiation protection programme outlines the research work carried out during the whole contractual period under all contracts between the European Commission and research groups in the Member States. More than 450 scientists collaborated on this programme.

Results of more than 350 projects are reported. They are grouped into three sectors:

1. Human exposure to radiation and radioactivity, which includes:
 - 1.1. Measurement of radiation dose and its interpretation.
 - 1.2. Transfer and behaviour of radionuclides in the environment.
2. Consequences of radiation exposure to man: assessment, prevention and treatment, which includes:
 - 2.1. Stochastic effects of radiation.
 - 2.2. Non-stochastic effects of radiation.
 - 2.3. Radiation effects on the developing organism.
3. Risks and management of exposure, which includes:
 - 3.1. Assessment of human exposure and risks.
 - 3.2. Optimization and management of radiation protection.

Within the framework programme, the aim of this scientific research is to improve the conditions of life with respect to work and protection of man and his environment and to assure safe production of energy, i.e.:

- (i) to improve methods necessary to protect workers and the population by updating the scientific basis for appropriate standards,
- (ii) to prevent and counteract harmful effects of radiation;
- (iii) to assess radiation risks and provide methods to cope with the consequences of radiation accidents.

Vertical line of text or artifacts on the right edge of the page.

Venta y suscripciones • Sale and subscriptions • Verkauf und Abonnements • Vendita e abbonamenti • Verkoop en abonneringen • Verkoop en abonneringen • Verkoop en abonneringen

BELGIQUE / BELGIË
 Wapsteen België /
 Wapsteen established
 Rue de Louvain 42 / Louvainweg 42
 1300 Bruxelles / 1300 Brussel
 Tel. (02) 512 06 26
 Fax (02) 511 01 64

Jean De Lannoy
 Avenue du Roi 202 / Koningslaan 202
 1050 Bruxelles / 1050 Brussel
 Tel. (02) 538 51 69
 Telex 43229 UNBOOK B
 Fax (02) 538 06 41
Juana Distributors /
Joanna verkooptuist
 Avenida de la Libertad
 1000 Bruxelles / 1000 Brussel
 Tel. (02) 221 94 35
 Fax (02) 229 06 20

DANMARK
J.V. Schmidt, Importører A/S
 Hørslevvej 48-52
 2625 Albertslund
 Tel. 43 83 23 00
 Fax (Bokst) 43 83 19 89
 Fax (Annoncer) 43 83 19 49

DEUTSCHLAND
Wissenschaftliche Verlag
 Berlin Straße 28-30
 Postfach 19 99 34
 10007 Berlin
 Tel. (030 21) 20 29 0
 Fax (030 21) 20 29 78

GREENE/ITALIA
R.C. International S.p.A.
 Via Venezia 10
 40138 Bologna
 Tel. 051 261 21 29
 Fax 051 261 21 29

ESPAÑA
Subido Oficial del Estado
 Trafalgar, 27-29
 28071 Madrid
 Tel. (91) 538 22 95
 Fax. (91) 538 29 48

Raport-Praxis Libro, SA
 Casallo, 37
 28001 Madrid
 Tel. (91) 421 29 56 (Línea)
 491 38 22 (Reservación)
 491 38 37 (Directivo)
 Telex 493754 LJ 2
 Fax (91) 576 09 98

Suizaa
Libreria Internazionale Editrice
 Casella de Ceres, 391
 69039 Casertola
 Tel. (071) 455 51 69
 Fax (071) 455 51 69

Libreria de la Universidad
 de Salamanca
 Ronda del Estadio, 118 (Pab. 118a)
 36002 Salamanca
 Tel. (93) 202 89 35
 Tel. (93) 202 84 52
 Fax (93) 202 12 59

FRANCE
Journal officiel
 Service des publications
 des Communautés européennes
 29, rue Desaix
 75727 Paris Cedex 15
 Tel. (1) 40 58 77 01/51
 Fax (1) 40 58 77 00

IRELAND
Government Supplies Agency
 4-5 Harcourt Road
 Dublin 2
 Tel. (1) 85 13 111
 Fax (1) 47 80 645

ITALIA
Liesse SpA
 Via Dada di Collette 1/1
 Casella postale 552
 50125 Firenze
 Tel. (055) 54 54 15
 Fax 54 15 57
 Telex 570486 LICOSA I

GRAND-QUICRIE DE LUXEMBOURG
Magasinerie du Nord
 5, rue Raiffeisen
 1011 Luxembourg
 Tel. 43 10 20
 Fax 46 46 51

NEEDHAM
ONE Communications
 (Boston Postoffice)
 5225 BA, 3 (Franklin)
 Tel. (617) 37 88 80
 Fax (617) 37 88 788

PORTUGAL
Imprensa Nacional
 Casa do Minho, EP
 Rua C. Francisco Manuel de Melo, 2
 1000 Lisboa Centro
 Tel. (011 351 21) 53055 65 25
 Fax (011 351 21) 53 01 32

Stichting voor de Liberij
 Buitenvoort 1
 1017 CA Amsterdam, NL
 Grijze Sintjans 2A
 Postbus Verreke des Vrees, 4-6
 1017 CA Amsterdam, NL
 Tel. (020) 693 8000
 Telex 30000 UNIBOOK
 Fax (020) 693 8000

LA BIBLIOTECA
Libreria Internazionale Editrice
 Casella de Ceres, 391
 69039 Casertola
 Tel. (071) 455 51 69
 Fax (071) 455 51 69

OLIMPIA
Magasinerie du Nord
 5, rue Raiffeisen
 1011 Luxembourg
 Tel. 43 10 20
 Fax 46 46 51

SCHENKER AG
Abteilung International
 Kesselstraße 1
 D-53002 Bonn
 Tel. (0228) 121 41
 Fax (0228) 121 44 41

NOBIS
Magasinerie du Nord
 5, rue Raiffeisen
 1011 Luxembourg
 Tel. 43 10 20
 Fax 46 46 51

SVENSK
BFA AB
 Traktorvägen 13
 22103 Lund
 Tel. (040) 18 00 00
 Fax (040) 18 01 25
 30 79 47

ICELAND
SKOJARU
LARUSAR BÚNDIÐ
 Skólavörðug. 2
 101 Reykjavík
 Tel. 11 58 50
 Fax 12 55 60

SCHWIZ / SUISSE / SVIZZERA
OSPC
 Spiezstrasse 65
 3000 Spiez
 Tel. (071) 865 91 69
 Fax (071) 355 54 11

SALGERS
Magasinerie du Nord
 5, rue Raiffeisen
 1011 Luxembourg
 Tel. 43 10 20
 Fax 46 46 51

REPÚBLICA
Mag. SA
 Avenida 22
 1000 Lisboa
 Tel. (011 351 21) 53055 65 25
 Fax (011 351 21) 53 01 32

SRBIJA
Magasinerie du Nord
 5, rue Raiffeisen
 1011 Luxembourg
 Tel. 43 10 20
 Fax 46 46 51

MINISTERSTVO
Magasinerie du Nord
 5, rue Raiffeisen
 1011 Luxembourg
 Tel. 43 10 20
 Fax 46 46 51

ROMANIA
Magasinerie du Nord
 5, rue Raiffeisen
 1011 Luxembourg
 Tel. 43 10 20
 Fax 46 46 51

RUSSIA
Magasinerie du Nord
 5, rue Raiffeisen
 1011 Luxembourg
 Tel. 43 10 20
 Fax 46 46 51

SLOVENIA
Magasinerie du Nord
 5, rue Raiffeisen
 1011 Luxembourg
 Tel. 43 10 20
 Fax 46 46 51

SPAIN
Magasinerie du Nord
 5, rue Raiffeisen
 1011 Luxembourg
 Tel. 43 10 20
 Fax 46 46 51

SWEDEN
BFA AB
 Traktorvägen 13
 22103 Lund
 Tel. (040) 18 00 00
 Fax (040) 18 01 25
 30 79 47

TURKEY
Press AS
 İhtilal Caddesi 469
 80060 Tuzlakent/İstanbul
 Tel. 00120 852 81 41 - 251 91 96
 Fax 0212) 251 91 97

ISRAEL
BOY International
 PO Box 13058
 41 Bnei Brak/Petach Tikva
 Tel Aviv 61130
 Tel. 3 488 136
 Fax. 3 648 60 38

EGYPT / MIDDLE EAST
Magasinerie du Nord
 5, rue Raiffeisen
 1011 Luxembourg
 Tel. 43 10 20
 Fax 46 46 51

UNITED STATES OF AMERICA / CANADA
UNIPUB
 4011-F Assembly Drive
 Lanham, MD 20158-0001
 Tel. Toll Free (800) 274-1888
 Fax (301) 434-0288

CANADA
Subscriptions only
 Unipub subscriptions
 4011-F Assembly Drive
 Lanham, MD 20158-0001
 Tel. Toll Free (800) 274-1888
 Fax (301) 434-0288

REPOBLICA
Mag. SA
 Avenida 22
 1000 Lisboa
 Tel. (011 351 21) 53055 65 25
 Fax (011 351 21) 53 01 32

ALBANIA
Magasinerie du Nord
 5, rue Raiffeisen
 1011 Luxembourg
 Tel. 43 10 20
 Fax 46 46 51

ARGENTINA
Magasinerie du Nord
 5, rue Raiffeisen
 1011 Luxembourg
 Tel. 43 10 20
 Fax 46 46 51

AUSTRALIA
Magasinerie du Nord
 5, rue Raiffeisen
 1011 Luxembourg
 Tel. 43 10 20
 Fax 46 46 51

BELGIUM
Magasinerie du Nord
 5, rue Raiffeisen
 1011 Luxembourg
 Tel. 43 10 20
 Fax 46 46 51

BELGIUM
Magasinerie du Nord
 5, rue Raiffeisen
 1011 Luxembourg
 Tel. 43 10 20
 Fax 46 46 51

BELGIUM
Magasinerie du Nord
 5, rue Raiffeisen
 1011 Luxembourg
 Tel. 43 10 20
 Fax 46 46 51

NOTICE TO THE READER

All scientific and technical reports published by the European Commission are announced in the monthly periodical 'euro abstracts'. For subscription (1 year: ECU 80) please write to the address below.

Price (excluding VAT) in Luxembourg:
(Volume 1) ECU 89
(Volumes 1 and 2) ECU 148

ISSN 0264-3758-3

OFFICE FOR OFFICIAL PUBLICATIONS
OF THE EUROPEAN COMMUNITIES

L-2985 Luxembourg



9 789262 684339